Green Synthetic Strategies for the C-H Chalcogenative Annulation of 2-Alkynyl Biaryls and C-H Chalcogenation of Alkenes

THESIS

Submitted in partial fulfillment

of the requirements for the degree of

DOCTOR OF PHILOSOPHY

By

Nilanjana Mukherjee

ID. No. 2018PHXF0411H

Under the Supervision of

Dr. Tanmay Chatterjee

BIRLA INSTITUTE OF TECHNOLOGY AND SCIENCE, PILANI

2023

BIRLA INSTITUTE OF TECHNOLOGY AND SCIENCE, PILANI

CERTIFICATE

This is to certify that the thesis titled "**Green Synthetic Strategies for the C-H Chalcogenative Annulation of 2-Alkynyl Biaryls and C-H Chalcogenation of Alkenes**" submitted by **NILANJANA MUKHERJEE**, ID No. **2018PHXF0411H** for an award of a Ph.D. from the Institute, embodies original work done by her under my supervision.

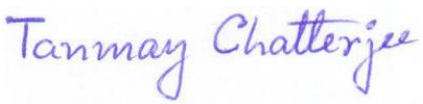

Signature of the Supervisor:

Name in capital letters: TANMAY CHATTERJEE

Designation : Assistant Professor

Date : 4th September 2023

Acknowledgment

The present piece of work would not have been possible without the assistance of several people for whom I am eternally grateful.

First and foremost, praises and thanks to the Almighty, for showering blessings throughout my research work which enabled me to successfully complete the research. I would like to express my deepest and sincere gratitude and respect to my supervisor Dr. Tanmay Chatterjee, Assisstant Professor, Department of Chemistry, Birla Institute of Technology & Science (BITS), Pilani, Hyderabad Campus, Jawahar Nagar, Kapra Mandal, Hyderabad - 500078, Telangana, India, for his constant and invaluable support, since I ever started working with him. It is a great privilege to work with him. He has introduced me to the fascinating field of "Synthetic Organic Chemistry". I am immensely grateful to him for channeling my thought process in science in the right direction and making me realize the true meaning of the words "Strive for Excellence". His dynamism, vision, sincerity, and motivation have deeply inspired me.

I would like to extend my gratitude to Prof. Vamsi Krishna Venuganti, Associate Dean, Academic-Graduate Studies and Research Division (AGSRD), BITS Pilani, Hyderabad Campus for helping me to complete the procedure of my thesis submission. I want to thank Mr. Praveen, AGSRD, BITS Pilani, Hyderabad campus, for the informative assistance in completing the course procedures within the prescribed time. I would like to express my gratitude to former DRC Convener Prof. Durba Roy, Department of Chemistry, BITS Pilani, Hyderabad Campus for initiating the process of submitting my thesis. I am very much thankful to Prof. Sounak Roy, head of the chemistry department, BITS Pilani, Hyderabad Campus, for creating a student friendly environment in the department.

I am also grateful to the laboratory technicians of Central Analytical Laboratory (CAL), BITS Pilani, Hyderabad campus, for their constant help in the laboratories.

I would not have reached anywhere near where I am now if it had not been for my respected teachers. My sincere gratitude goes out to all professors in our department for their support, wise criticism, and challenging inquiries that helped to illuminate my thesis.

I am lucky to have some lab mates like Mr. Appanapalli Nagavenkata Satyanarayana, Ms. Paramita Pattanayak, Mr. Ainala Naresh, and Ms. Sai Keerthana H. They helped me wholeheartedly in different academic and non-academic work during my research.

It is high time to acknowledge my gratitude to Dr. Banchhanidhi Prusti for being an elder brother to me and helping me in various ways throughout my research work. I want to convey my heartiest thanks to Dr. Sayantan Halder for lending me his helping hand as an elder brother and for his kind assistance in some future collaborations. I acknowledge Mr. Milan Paul and Ms. Madhuparna Chakraborty for helping me in various aspects and for being with me in this wonderful period starting from my journey to my Ph.D. I want to thank Dr. Soumitra Patra and Dr. Dinabandhu Patra for being such wonderful friends and assisting me in exploring and understanding many academic and non-academic fields. I want to give special thanks to Ms. Shalini Dyagala for her helping hands in some future collaborative works. I would like to thank my labmates Leela, Radha, Shankha, Rohan, Bandana, Neha, Niharika, Joel, Sayan, Soumen, Shalini, Saurav, and Animesh for creating such a wonderful environment in the lab.

I would like to sincerely acknowledge Chancuex Labs LLP, Hyderabad and Extra Mural Researchof the Councilof Scientific and Industrial Research (CSIR).

Finally, I take this opportunity to acknowledge my family that has been my pillar of strength in the truest sense. It will never be enough to say thanks to my parents Late Gautam Mukherjee and Mrs. Suniti Mukherjee, for her unconditional love, support, and sacrifices I would like to convey my heartiest respect to my maternal uncle, Mr. Madhusudan Thakur, Mr. Raghunath Thakur, and Mr. Jadunath Thakur for taking care of me and standing beside me in every situation of my life. Finally, I want to express my heartiest gratitude to my husband, Dr. Rajesh Goswami, who always inspired me throughout my career and stood beside me.

Place: BITS-Pilani, Hyderabad Campus

NILANJANA MUKHERJEE

ABSTRACT

The primary objective of this research work is to develop green synthetic strategies for the synthesis of potential organic molecules *via* C-H annulation or C-H functionalization reactions.

Chapter 1: This chapter describes the general introduction to green chemistry and its twelve guiding principles. Reagents including catalysts, solvents, and generated wastes in an organic transformation are the major concerns of green chemistry. This chapter briefly specifies the choice of a solvent and catalyst and the utility of iodine as a catalyst in developing a metal-free green organic reaction. Moreover, the advantages of the electrochemical approach over the traditional chemical approach in designing and developing an organic transformation avoiding the requirement of a catalyst and stoichiometric reagents is also discussed.

Chapter 2: This chapter describes iodine-catalyzed various organic transformations (**Section-I**), synthesis of phenanthrenes by annulation reactions with alkynes (**Section-II**), synthesis of 9-sulfenylphenanthrenes *via* sulfenylative annulation of 2-alkynyl biaryls (**Section-III**), and our metal-free approach to access 9-sulfenylphenanthrenes under iodine-catalysis (**Section-IV**). We developed a sustainable and cost-effective synthetic methodology to access a wide variety of valuable sulfenylphenanthrenes and polycyclic heteroaromatics in moderate to high yield through electrophilic sulfenylative annulation of 2-alkynyl biaryls (6-*endo*-dig cyclization) using methyl sulfoxides such as dimethyl sulfoxide (DMSO) as the sulfur source. The transformation requires only iodine in a catalytic amount and trifluoroacetic anhydride. Notably, DMSO played multiple roles such as methylthiolating reagent, oxidant, and solvent in this reaction. The last section (**Section-V**) of this chapter describes the application of one of our synthesized molecules *i.e.*, methyl(10-phenylphenanthren-9-yl)sulfane (MPPS) as a fluorescent molecule to probe the aggregation properties (micellization) of various ionic and non-ionic surfactants and also the binding isotherm of a protein (bovine serum albumin).

Chapter 3: This chapter details the iodine-catalyzed cyclization reactions in water (**Section-I**), and our iodine-catalyzed synthetic strategy for the synthesis of 9-sulfenylphenanthrenes and polycyclic heteroaromatics in water (**Section-II**). We developed a green synthetic method for the sulfenylative annulation of 2-alkynyl biaryls and 2-heteroaryl substituted alkynyl benzenes with disulfides in water to access a wide variety of sulfenyl phenanthrenes and polycyclic heteroaromatics. The substrate scope, scalability, and green chemistry metrics of the developed protocol were found good to excellent.

Chapter 4: This chapter enlightens the synthesis of organoselenides by selenylative annulation/cyclization reactions (**Section-I**), previously developed non-catalytic methods for the C-H selenylative annulations of 2-alkynyl biaryls to access 9-selenylphenanthrenes (**Section-II**), and our metal-free, catalytic approach for the C-H selenylative annulation of 2-alkynyl biaryls for the synthesis of selanyl polycyclic aromatic hydrocarbons (PAHs) including phenanthrenes and polycyclic heteroaromatics (**Section-III**). We developed a metal-free, iodine-catalyzed, highly atom-economic, cost-effective, scalable, and sustainable synthetic strategy for the selenylative annulation of 2-alkynyl biaryls or 2-heteroaryl-substituted alkynyl benzenes with readily available diselenides in water, for the first time. The organic transformation required only a couple of inexpensive reagents, such as iodine as a catalyst and H_2O_2 as a green oxidant only in sub-stoichiometric amounts (0.3 equiv). The catalyst, iodine was recovered after the reaction during the column chromatography stage and recycled without any compromization in reaction outcome. Experimental and computational studies supported a radical pathway over the ionic pathway for this reaction. The scalability and green metrics of the protocol were found excellent.

Chapter 5: This chapter elucidates various electrochemical selenylative annulation reactions for the synthesis of organoselenides (**Section-I**) and our approach for the development of highly atom-economic and efficient electrochemical selenylative annulation of 2-alkynyl biaryls (**Section-II**). We developed a catalyst- and oxidant-free, scalable, and sustainable synthetic method for the selenylative annulation of 2-alkynyl biaryls or 2-heteroaryl-substituted alkynyl benzenes with readily available diselenides under electrochemical conditions to synthesize a wide variety of selanyl polycyclic aromatic hydrocarbons and polycyclic heteroaromatics in high to excellent yield up to 99% at room temperature in a short time (2-5 h). The transformation required only electricity as a green reagent and produced hydrogen gas as the only innocuous byproduct. The efficiency, scalability, and majority of the green metrics of the electrochemical protocol were found superior as compared to our previously developed iodine-catalyzed conventional protocol.

Chapter 6: This chapter outlines iodine-catalyzed C-H chalcogenation reactions of heterocycles (**Section-I**), general C-H chalcogenation reactions of alkenes (**Section-II**), and our approach to developing a recyclable iodine-catalyzed oxidative C-H chalcogenation of 1,1-diarylethenes in water for the green synthesis of trisubstituted vinyl sulfides and selenides selenides including some aggregation-induced-emission (AIE) active molecules. (**Section-III**). The scalability and green metrics of the protocol were found excellent.

Table of Contents

Contents	Page No.
Certificate	i
Acknowledgment	ii-iii
Abstract	iv-v
Table of contents	v-ix
List of Tables	x-xii
List of Figures	xii-xiv
List of Abbreviations	xv-xviii
Chapter 1 **General Introduction**	1-5
Chapter 2: **Section-I: Iodine-Catalyzed Organic Transformations** 2.1.1. Introduction 2.1.2. Review 2.1.3. Conclusion **Section-II: Synthesis of Phenanthrenes by Annulation Reactions with Alkynes** 2.2.1. Introduction 2.2.2. Review 2.2.3. Conclusion **Section-III: Synthesis of 9-Sulfenylphenanthrenes *via* Sulfenylative Annulation of 2-Alkynyl Biaryls** 2.3.1. Introduction 2.3.2. Review 2.3.3. Conclusion **Section-IV: Iodine Catalyzed Methylthiolative Annulation of 2-Alkynyl Biaryls with DMSO: A Metal-Free Approach to 9-Sulfenylphenanthrenes** Present Work	6-87 9 9 17 19 20 24 26 27 28

2.4.1. Introduction	30
2.4.2. Results and Discussion	31
2.4.3. Conclusion	42
2.4.4. Experimental Section	43
2.4.5. ^{1}H and ^{13}C NMR Spectra of Some Selected 10-Phenylphenanthren-9-yl)(methyl)sulfanes	55
Section-V Applications of Methyl(10-phenylphenanthren-9-yl)sulfane (MPPS) As a Fluorescence Probe	
2.5.1. Introduction	76
2.5.2. Results and Discussion	76
2.5.3. Conclusion	87
Chapter 3: **Section-I: Iodine-Catalyzed Cyclization ReacTions in Water**	88-138
3.1.1. Introduction	90
3.1.2. Review	90
3.1.3. Conclusion	92
Section-II: Iodine-Catalyzed, Highly Atom-Economic Synthesis of 9-Sulfenylphenanthrenes and Polycyclic Heteroaromatics in Water	
3.2.1. Introduction	94
3.2.2. Results and Discussion	95
3.2.3. Conclusion	108
3.2.4. Experimental Section	109
3.2.5. ^{1}H and ^{13}C NMR Spectra of Some Selected 9-Sulfenylphenanthrenes	117
Chapter 4: **Section I: Synthesis of Organoselenides by Selenylative Annulation/Cyclization Reactions**	139-232
4.1.1. Introduction	141
4.1.2. Review	141
4.1.3. Conclusion	148

Section-II: C-H Selenylative Annulations of 2-Alkynyl Biaryls for the Synthesis of 9-Selenylphenanthrenes	
4.2.1. Introduction	150
4.2.2. Review	150
4.2.3. Conclusion	152
Section-III: Recyclable Iodine-Catalyzed Radical Selenylative Annulation of 2- Alkynyl Biaryls with Diselenides in Water: A Green Approach to Selanyl Polycyclic Aromatic Hydrocarbons and Polycyclic Heteroaromatics	
4.3.1. Introduction	154
4.3.2. Results and Discussion	155
4.4.3. Conclusion	186
4.4.4. Experimental Section	187
4.4.5. ^{1}H , ^{13}C and ^{77}Se NMR Spectra of Some 9-Selanyl-Phenanthrenes and Polycyclic Heteroaromatics	198
Chapter 5:	233-287
Section-I: Electrochemical Selenylative Annulation for the Synthesis of Organoselenides	
5.1.1. Introduction	236
5.1.2. Review	237
5.1.3. Conclusion	241
Section-II: Highly Atom-Economic and Efficient Electrochemical Selenylative Annulation of 2-Alkynyl Biaryls	
5.2.1. Introduction	243
5.2.2. Results and Discussion	244
5.2.3. Conclusion	257
5.2.4. Experimental Section	258
5.2.5. ^{1}H , ^{13}C and ^{77}Se NMR Spectra of Some 9-Selanyl-Phenanthrenes and Polycyclic Heteroaromatics	269
Chapter 6	289-365

Section-I: Iodine-Catalyzed C-H Chalcogenation of Heterocycles	
	290
6.1.1. Introduction	290
61.2. Review	294
6.1.3 Conclusion	
Section-II: C-H Chalcogenation Reactions of Alkenes	
6.2.1. Introduction	296
6.2.2. Review	297
6.2.3. Conclusion	299
Section-III: Recyclable Iodine-catalyzed Oxidative C-H Chalcogenation of 1,1-Diarylethenes in Water: Green Synthesis of Trisubstituted Vinyl Sulfides and Selenides	
6.3.1. Introduction	301
6.3.2. Results and Discussion	301
6.3.3. Conclusion	319
6.3.4. Experimental Section	320
6.3.5. ^{1}H and ^{13}C NMR Spectra of Some Diphenylvinyl Sulfane and Selane	336
Future scope of work	366
References	367-402
Appendix	
List of publications and presentations	A-D
Biography of candidate	E
Biography of supervisor	F

List of Tables

Table No.	Title	Page No.
2.4.1.	Optimization of the Reaction Conditions	42
2.4.2.	Substrate Scope	44
2.4.3.	Selected crystal data for compounds **3ca**, **3da**, **3ea**, **3fa**, **3ha** and **3ab**	48
2.3.4.	Optimization of the Reaction Conditions for the Synthesis of **11** and **12**	53
2.5.1.	Photophysical Properties of MPPS	89
3.2.1.	Optimization of Reaction Conditions	108
3.2.2.	Substrate Scope	109
3.2.3.	Evaluation of Green Chemistry Metrics for the Synthesis of **3aa**	111
3.2.4.	Calculation of EcoScale Score for the I_2 Catalyzed Synthetic Process in Water to Synthesize Phenyl(10-phenylphenanthren-9-yl)sulfane (**3aa**) from 2-(Phenylethynyl)-1,1'-biphenyl (1a) and Diphenyl diselenide (**2a**)	112
3.2.5.	Calculation of Green Metrics for the Pd-Catalyzed Synthetic Process to Synthesize Phenyl(10-phenylphenanthren-9-yl)sulfane (3aa) from 2-(Phenylethynyl)-1,1'-biphenyl (**1a**) and Diphenyl Disulfide (**2a**)	113
3.2.6**.**	Calculation of EcoScale Score for the Pd-Catalyzed Synthetic Process to Synthesize Phenyl(10-phenylphenanthren-9-yl)sulfane (**3aa**) from 2-(Phenylethynyl)-1,1'-biphenyl (**1a**) and Diphenyl Diselenide (**2a**)	114
3.2.7.	Calculation of Green Metrics for the I_2-Catalyzed Synthetic Process to Synthesize Phenyl(10-phenylphenanthren-9-yl)sulfane (**3aa**) from 2-(Phenylethynyl)-1,1'-biphenyl (**1a**) and (Methylsulfinyl)benzene (**2a′**)	115
3.2.8.	Calculation of EcoScale Score for the I_2-Catalyzed Synthetic Process to Synthesize Phenyl(10-phenylphenanthren-9-yl)sulfane (**3aa**) from 2-(Phenylethynyl)-1,1'-biphenyl (**1a**) and (Methylsulfinyl)benzene (**2a′**)	116
3.2.9.	Detailed Comparison of the Previously Developed Synthetic Methodologies with This Work to Synthesize **3aa** from **1a**	117
4.3.1.	Optimization of reaction conditions	170
4.3.2.	Substrate Scope	172

4.3.3.	Selected Crystal Data for Compounds **3ba**, **3ea**, **3la**	175
4.3.4	Synthetic Diversification of **3aa, 3ab**, and **3ca** to Access **5, 6**, and **7** Respectively	177
4.3.5.	Evaluation of Green Chemistry Metrics for the Synthesis of **3aa.**	178
4.3.6.	Calculation of EcoScale Score for the I_2-Catalyzed Synthetic Process to Synthesize Phenyl(10-phenylphenanthren-9-yl)selane (**3aa**) from 2-(Phenylethynyl)-1,1'-biphenyl (**1a**) and Diphenyl Diselenide (**2a**)	179
4.3.7.	The Bond Dissociation Energies (kcal/mol) of the Se-X bond (X = Cl, Br, I) at the M06-2X/LanL2DZ Level of Theory in Water as an Implicit Solvent	181
4.3.8.	Radical Quenching Experiments	182
5.2.1.	Optimization of the Reaction Conditions	246
5.2.2.	Substrate Scope and A Direct Comparison of the Scope of the Electrochemical Approach with that of Chemical Approach (I_2-Catalysis)	249
5.2.3.	Selected Crystal Data for Compounds **3da**, **3ha**	250
5.2.4.	Evaluation of Green Chemistry Metrics for the Synthesis of **3aa**.	253
5.2.5.	Calculation of EcoScale Score for the I_2-Catalyzed Synthetic Process to Synthesize Phenyl(10-phenylphenanthren-9-yl)selane (**3aa**) from 2-(Phenylethynyl)-1,1'-biphenyl (1a) and Diphenyl Diselenide (**2a**)	254
5.2.6.	Photophysical Data of Synthesized Compound 6	255
6.3.1.	Optimization of Reaction Conditions	311
6.3.2.	Scope of C-H Sulfenylation of 1,1-Diarylethenes with Dioraganyl Disulfides	312
6.3.3.	Crystal Data of **3bi**	314
6.3.4.	Scope of C-H Selenation of Alkenes with Dioraganyl Diselenides	317
6.3.5.	Evaluation of Green Chemistry Metrics for the Synthesis of **3aa**	320
6.3.6.	Calculation of EcoScale Score of the Developed Protocol for the Synthesis of (2,2-Diphenylvinyl)(phenyl)sulfane **3aa**	321
6.3.7.	Evaluation of Green Chemistry Metrics for the Synthesis of **6aa**	322
6.3.8.	Calculation of EcoScale Score of the Developed Protocol for the Synthesis of (2,2-Diphenylvinyl)(phenyl)selane **6aa**	323

List of Figures

Figure No	Title	Page No.
Fig. 2.1.1.	Pictorial Presentation of the Biological Role of Iodine	11
Figure 2.1.2	Pictorial Diagram of the Molecular Iodine	11
Figure 2.2.1.	Some Examples Biologically-active of Phenanthrenes	26
Figure 2.3.1.	Some Examples of Biologically Active Organosulfides	36
Figure 2.4.1	X-ray Crystal Structure of **3ca** (Thermal Ellipsoids Shown at 50% Probability) including Atomic Numbering	45
Figure 2.4.2.	X-ray Crystal Structure of **3da** (Thermal Ellipsoids Shown at 50% Probability) including Atomic Numbering	46
Figure 2.4.3.	X-ray Crystal Structure of **3ea** (Thermal Ellipsoids Shown at 50% Probability) Including Atomic Numbering	46
Figure 2.4.4.	X-ray crystal structure of **3ha** (thermal ellipsoids shown at 50% probability) including atomic numbering	47
Figure 2.4.6.	X-ray crystal structure of **3ab** (thermal ellipsoids shown at 50% probability) including atomic numbering	47
Figure 2.4.7.	*In situ* detection of MeSI by the base peak of the MS spectrum at m/z = 174	52
Figure 2.5.1.	Absorption Spectra of MPPS in Different Solvents	89
Figure 2.5.2.	Emission Spectra of MPPS in Different Solvents	90
Figure 2.5.3.	Fluorescence Intensities of MPPS at Different Concentrations of DTAB	90
Figure 2.5.4.	Fluorescence intensities of MPPS at Different Concentrations of SDS	91
Figure 2.5.5.	Fluorescence Intensities of MPPS at Different Concentrations of Triton X-100	91
Figure 2.5.6.	Fluorescence Intensities of MPPS at Different Concentrations of 12-6-12,2Br$^-$.	92
Figure 2.5.7.	Fluorescence Spectra of MPPS (5 μM) as a Function of Concentrations of BSA	93
Figure 2.5.8.	Fluorescence Intensities of MPPS at Different Concentrations of BSA. [MPPS] = 5 μM, λ_{ex} = 330 nm, λ_{em} = 395 nm	93
Figure 2.5.9.	Benesi-Hildebrand Plot for the Binding of MPPS with BSA	94

Figure 2.5.10.	F/F_O Plot of MPPS in Presence of BSA along with Increasing Concentration of 12-6-12,2Br$^-$. [MPPS] = 5 μM, [BSA] = 5.0 μM. (λ_{ex} = 330 nm, λ_{em} = 395 nm)	95
Figure 2.5.11.	λ_{max}^{fl} of MPPS in Presence of BSA along with Increasing concentration of 12-6-12,2Br$^-$. [MPPS] = 5 μM, [BSA] = 5.0 μM. (λ_{ex} = 330 nm)	96
Figure 3.2.1.	Mass Spectrum of the Reaction Mixture of Diphenyl Disulfide and I_2	118
Figure 4.1.1.	Some Examples of Biologically Active Unsymmetrical Diaryl or Aryl-heteroaryl Selenides.	152
Figure 4.3.1	^{77}Se NMR of (A) Ph_2Se_2; (B) Ph_2Se_2 + H_2O_2 (5 equiv), 100 ^oC, 12 h; (C) Ph_2Se_2 + H_2O_2 (0.5 equiv), 100 ^oC, 12 h; recorded in DMSO-d_6	171
Figure 4.3.2.	X-ray Crystal Structure of **3ba** (Thermal Ellipsoids Shown at 50% Probability) Including Hetero-atom Numbering	173
Figure 4.3.3.	X-ray Crystal Structure of **3ea** (Thermal Ellipsoids Shown at 50% Probability) including Hetero-atom Numbering	174
Figure 4.3.4.	X-ray Crystal Structure f **3la** (Thermal Ellipsoids Shown at 50% Probability) Including Hetero-atom Numbering	174
Figure 4.3.5.	Mass Spectrum of the Reaction Mixture of Diphenyl Diselenide and I_2.	180
Figure 4.3.6.	Mass Spectrum of the Reaction Mixture of **1a** and Diphenyl Diselenide **2a** in the Presence of Radical Quencher, Ethene-1,1-diyldibenzene under Standard Reaction Conditions	183
Figure 4.3.7.	Free Energy Profile for the Conversion of **1a** and PhSeI **6**, Formed *in situ* from Diphenyl Diselenide **2a** and I_2, to **3aa** through the Radical Pathway in Water as Implicit Solvent at LanL2DZ/M06-2X Level of Theory	184
Figure 4.3.8.	Free Energy Profile for the Initial Step for the Conversion of **1a** and PhSeI to **3aa** through the Polar Pathway in Water	185
Figure 5.1.1.	Schematic representation of a general electrochemical organic transformation and its advantages over traditional chemical methods involving expensive and toxic reagents and catalysts	235
Figure 5.2.1.	X-ray Crystal Structure of **3da** (Thermal Ellipsoids Shown at 50% Probability) Including Hetero-atom Numbering	250

Figure 5.2.2.	X-ray Crystal Structure of **3ha** (Thermal Ellipsoids Shown at 50% Probability) Including Hetero-atom Numbering	250
Figure 5.2.3.	Reaction Kinetics Studies for the Synthesis of **3aa** from **1a** and **2a** under Electrochemical and Chemical (I_2-catalyzed) Standard Conditions	252
Figure 5.2.4	(A) Gram-scale Synthesis of **3aa** under Electrochemical Conditions; (B) Comparison of the Outcome of the Scale-up Experiment of **1a** with **2a** under Electrochemical and Chemical Conditions	252
Figure 5.2.5.	Mass Spectrum of the Reaction Mixture of **1a** and Diphenyl Diselenide **2a** in the Presence of Radical quencher, Ethene-1,1-diyldibenzene under Standard Reaction	256
Figure 5.2.6.	Cyclic Voltammograms	256
Figure 5.2.7.	Cyclic Voltammograms of Radical Quenchers	258
Figure 6.1.1.	Schematic Representation of C-H Functionalization Reaction	292
Figure 6.2.1.	Examples of valuable vinyl sulfides and selenides	300
Figure 6.3.1.	X-ray Crystal Structure of **3bi** (Thermal Ellipsoids Shown at 50% Probability) Including Hetero-Atom Numbering	313
Figure 6.3.2.	(A) ^{1}H-NMR Spectrum of **3fa**, (B) NOE Difference Spectrum, with Irradiation at 6.79 ppm	312
Figure 6.3.3.	Mass Spectrum of the Reaction Mixture of Ethene-1,1-diyldibenzene, I_2 and 1,2-Di-*tert*-butyldisulfane	313
Figure 6.3.4.	Mass Spectrum of the Reaction Mixture of Ethene-1,1-diyldibenzene, I_2 and 1,2-Di-tert-butyldisulfane	313
Figure 6.3.5.	(A) ^{1}H-NMR Spectrum of **6fa**, (B) NOE Difference Spectrum, with Irradiation at 6.95 ppm	315

LIST OF ABBREVIATIONS AND SYMBOLS

Abbreviation/Symbol	Full Form of the Abbreviation/Symbol
EPA	The Environmental Protection Agency
I^-	Iodide
IO_3^-	Iodate
I_2	Iodine
NH_4OAC	Ammonium Acetate
DMSO	Dimethyl Sulfoxide
O_2	Oxygen
KOH	Potassium Hydroxide
PIDA	Poly(diiododiacetylene)
MeOH	Methanol
DBU	1,8-Diazabicyclo[5.4. 0]undec-7-ene
rt	Room Temperature
TFA	Trifluoroacetic Acid
TMSCN	Trimethylsilyl Cyanide
TBHP	*tert*-Butyl Hydroperoxide
K_2CO_3	Potassium carbonate
MeCN	Acetonitrile
h	Hour
^oC	Degree Celsius
BPO	Benzoyl peroxide
PhCl	Chlorobenzene
THF	Tetrahydrofuran
DMF	Dimethylformamide
TBAI	Tetrabutylammonium iodide
S_8	Sulfur
Na_2SO_4	Sodium Sulfate
NH_2NH_2	Hydrazine
EtOH	Ethanol
DCE	1,2-Dichlorethane

AIE	Aggregation-induced Emission
PAHs	Polycyclic Aromatic Hydrocarbons
HIV	Human Immunodeficiency Virus
^{t}BuONO	*tert*-Butyl Nitrite
fac-Ir(ppy)$_3$	*fac*-Tris(2-phenylpyridine)iridium(III)
LED	Light-emitting diode
[C_p*RhCl$_2$]$_2$	Pentamethylcyclopentadienyl rhodium dichloride dimer
Cu(OAC)$_2$	Copper(II) Acetate
AIBN	Azobisisobutyronitrile
Bu_3SnH	Tributyltin hydride
[IrCl(cod)$_2$]	Cyclooctadiene Iridium Chloride Dimer
P(*t*-Bu)$_3$	Tri-*tert*-butylphosphine
Fe(acac)$_3$	Tris(acetylacetonato) Iron(III)
dtbpy	4,4'-Di-tert-butyl-2,2'-bipyridine
Pd(OAc)$_2$	Palladium(II) Acetate
Ag_2CO_3	Silver Carbonate
Fe(OTf)$_3$	Iron(III) Trifluoromethanesulfonate
AuCl	Gold(I) Chloride
$PtCl_2$	Platinum(II) Chloride
NaOAc	Sodium Acetate
LiCl	Lithium Chloride
H	Hydrogen
Me	Methyl
$PdCl_2$	Palladium(II) Chloride
SMe	Thiomethyl
TM	Transition-metal
MeSI	Methyl Hypoiodothioite
TFAA	Trifluoroacetic Anhydride
MeSH	Thiomethanol
HCHO	Formaldehyde
HI	Hydroiodic Acid
Pd(PPh$_3$)$_4$	Tetrakis(triphenylphosphine)palladium(0)

PhMe	Toluene
$Pd(PPh_3)Cl_2$	Bis(triphenylphosphine)palladium(II) Dichloride
CuI	Copper Iodide
Et_3N	Triethylamine
PTSA	*p*-Toluenesulfonic Acid
KI	Potassium Iodide
$NaNO_2$	Sodium Nitrite
ε	Dielectric Constant
λ	Wavelength
DTAB	Dodecyltrimethylammonium Bromide
SDS	Sodium dodecyl sulfate
CMC	Critical Micelle Concentration
BSA	Bovine serum albumin
MPPS	Methyl(10-phenylphenanthren-9-yl)sulfane
NH_4OAc	Ammonium Acetate
LDG	Lysosome Directing Groups
BTEAC	Benzyltriethylammonium chloride
$NaHCO_3$	Sodium Bicarbonate
H_2O_2	Hydrogen Peroxide
PAHs	Polycyclic Aromatic Hydrocarbons
AE	Atom-efficiency
CE	Carbon-efficiency
RME	Reaction Mass Efficiency
m-CPBA	*meta*-Perchlorobenzoic Acid
$K_2S_2O_8$	Potassium Pursulfate
$MeNO_2$	Nitromethane
US	Ultrasound
DABSO	1,4-Diazabicyclo[2.2.2]octane bis(sulfur dioxide)
$FeCl_3$	Ferric Chloride
$CuCl_2$	Copper (II) Chloride
CsOAc	Caesium acetate

$AgNO_2$	Silver Nitrate
Tf_2O	Trifluoromethanesulfonic anhydride
TEMPO	2,2,6,6-Tetramethylpiperidinyloxy
BHT	Butylated Hydroxytoluene
DFT	Density Functional Theory
TS	Transition State
CPE	Constant Potential Electrolysis
CCE	Constant Current Electrolysis
gr	Graphite
Pt	Platinum
$^{n}Bu_4PF_6$	Tetrabutylammonium hexafluorophosphate
$TBAClO_4$	Tetrabutylammonium Perchlorate
$^{n}Bu_4NBF_4$	Tetrabutylammonium Tetrafluoroborate
KBr	Potassium Bromide
$LiClO_4$	Lithium Perchlorate
TFE	Tetrafluoroethylene
$^{n}Bu_4NI$	Tetrabutylammonium Iodide
TLC	Thin Layer Chromatography
Ar	Aryl
S	Sulfur
Se	Selenium
CS_2	Carbon Disulfide
ADA	Adenosine Deaminase
$Cu(OTf)_2$	Copper(II) Triflate
Py	Pyridine
$Na_2S_2O_8$	Sodium Persulfate
PhSH	Thiophenol
$(PhS)_2$	Diphenyl Disulphide
$(PhSe)_2$	Diphenyl Diselenide

Chapter 1

General Introduction

1.1. Introduction.

Green chemistry [1] appeared from several pre-existing ideas and research efforts (such as atom economy and catalysis) in the period preceding the 1990s, in the context of growing concern about chemical pollution and resource depletion. Green chemistry's development in Europe and the United States coincided with a shift in environmental problem-solving strategies: a shift away from command and control regulation and mandated reductions in industrial emissions at the "end of the pipe" and towards active pollution prevention through the innovative design of production technologies themselves. [2] The set of concepts now known as green chemistry came together in the mid-to-late 1990s, along with broader acceptance of the term (which won out over competing terms like"clean" and "sustainable" chemistry).[3]

The Environmental Protection Agency (EPA) in the United States was a pioneer in promoting green chemistry through pollution prevention programs, funding, and professional coordination. At the same time, researchers at the University of York contributed to the formation of the Royal Society of Chemistry's Green Chemistry Network and the publication of the journal Green Chemistry.[4]

Green chemistry, also known as sustainable chemistry,[5] is a branch of chemical engineering and chemistry that focuses on developing green methods that reduce the use and production of hazardous substances.[6] Green chemistry is the design of chemical products and processes that reduce or eliminate the use or production of hazardous substances to humans, animals, plants, and the environment. The goal of sustainable chemistry is to minimize or eliminate the usage as well as production of any hazardous materials in a chemical process. In 1998, Paul Anastas (who then directed the Green Chemistry Program at the US EPA) and John C. Warner (then of Polaroid Corporation) published a set of principles to guide the practice of green chemistry.[7] The twelve principles address a range of ways to lower the environmental and health impacts of chemical production and also indicate research priorities for the development of green chemistry technologies.

According to one definition, "green chemistry" means:

"The creation of chemical products and methods to reduce or end the use and manufacture of hazardous substances."

In recent years, the study of green synthesis[8] has emerged as a fresh and exciting area of study in organic chemistry. The popularity of green synthesis has increased substantially in recent years due to its many benefits, including the fact that it is straightforward, economical, environmentally benign, and readily scaled up for large-scale synthesis.

The twelve principles of green chemistry are:

1. **Prevention:** Waste prevention is preferable to waste treatment or cleanup after production. It should be kept in mind that the prevention of waste must be prioritized rather than cleaning up and treating waste after it has been created.

2. **Atom economy:** The ratio of the number of atoms needed in the reactant to the number of atoms wasted is used to determine how effective a synthetic approach is. Waste must be reduced at the molecular level by maximizing the number of atoms from all reagents that are incorporated into the final product. Hence atom economy is used to evaluate the reaction efficiency.

3. **Less hazardous chemical synthesis:** Green chemistry is a strategy that tries to stop the production and use of dangerous substances by improving the way chemicals are made. Chemical reactions and synthetic routes should be designed safely and healthily by considering the hazards of substances handled, during the reaction, including waste.

4. **Designing safer chemicals:** We must develop all chemicals to be less hazardous by designing them in addition to making them effective for their intended use. Toxicity must be minimized directly by molecular design. Physical properties, toxicity, and environmental fate should be predicted and evaluated throughout the design process.

5. **Safer solvents and auxiliaries:** Ingredients in formulations may not be essential to the product's functionality but improve it for the user. The safest solvent available must be chosen for any given step to minimize the total amount of solvents and auxiliary substances used, as these make up a large percentage of the total waste created.

6. **Design for energy efficiency:** Synthetic procedures are to be carried out at room temperature and pressure. The least energy-intensive chemical route must be chosen in such a way that one can avoid heating, cooling, as well as pressurized and vacuum conditions (*i.e.* ambient pressure and temperature are optimal).

7. **Use of renewal feedstocks:** In contrast to depleting feedstocks, which take significantly longer to replenish and are consumed at a faster pace by human activity, renewable feedstocks can be replenished on a human timeline. Chemicals made from renewable (*i.e.* plant-based) sources, rather than other, equivalent chemicals originating from petrochemical sources must be used.

8. **Reduce derivatives:** Protecting groups and derivatives should be used less frequently when synthesizing target compounds. The use of temporary derivatives such as protecting groups must be minimized to avoid reaction steps, resources required and waste created.

9. **Catalysis:** Stoichiometric reagents should not be used in place of catalytic reagents. Catalysts must be chosen in such a way that can increase selectivity, minimize waste and reduce reaction time and energy demands.

10. **Design for degradation:** Chemical should be made so that when they have served their purpose, they disintegrate into harmless degradation products and molecules that are safe for use around people, pets, and the environment. Chemicals should be designed to degrade discard easily by ensuring both the chemicals and their degradation product should not be toxic, bioaccumulative, or environmentally persistent.

11. **Real-Time Pollution Prevention:** To serve societal needs, scientific activity in general, and the analytical technique in particular, must avoid mistakes in chemical processes that could result in acts that endanger ecosystems and human health. Chemical reactions in real-time must be monitored to prevent the formation and release of any potentially hazardous and polluting substances.

12. **Safer Chemistry for accident prevention:** Reaction substances shouldn't provide too many risks. Chemical procedures must be chosen and developed in such a way that the process must be safer and inherently minimize the risk of accidents. One should know the possible risks and assess them beforehand.

The solvent is an important component of an organic reaction and it is always a matter of concern in the context of green chemistry as they are used in large quantities and mostly inflammable chemicals. Most of the organic solvents have negative effects on health and the environment as it leads to the production of organic wastes, and also pollute the air. Water is regarded as the most environmentally friendly solvent. However, it is generally regarded as the enemy of many organic transformations because of the sensitivity of many reagents towards water and their immiscibility. Thus use of water as a solvent in an organic reaction is a challenge. Hence, developing an organic transformation in water, the greenest solvent is always challenging but desirable in the context of green chemistry.

Several advantages of catalysis include the lowering of the activation energy barrier of an organic reaction thus enhancing its efficiency and the use of catalytic rather than stoichiometric amounts of ingredients lowering the generation of stoichiometric wastes. The feasibility of a reaction depends heavily on the catalyst. Scientists are developing new procedures to conduct molecular iodine-catalyzed reactions [9] for the preparation of organic molecules in response to the enormous demand for catalytic procedures. For more

than a century, molecular iodine, an easy-to-handle solid, has been used as a catalyst in various organic transformations. Even though it is active in very small amounts, the origin of this remarkable catalytic effect is unknown. Iodine-catalyzed C-H annulation [10] and C-H functionalization reactions[11] have recently been achieved in an atom-economic, cost-effective, and sustainable manner.

In the area of synthetic organic chemistry, there is always a strong drive to develop challenging organic transformations such as C-H annulation and functionalization reactions in a cost-effective, sustainable, and practical manner.[12] In recent times, electrochemical organic synthesis, where electricity plays the role of an oxidizing/reducing reagent to generate reactive species has regained significant attention of synthetic chemists in enabling a challenging organic transformation under transition-metal- and reagent-free conditions. Under electrochemical conditions, radical ions or free radicals are formed from easily accessible starting materials through anodic oxidation or cathodic reduction leading to the formation of desired product *via* C-C or C-X (X = heteroatom) bond formation. It offers several advantages and green features as compared to the other chemical technologies.[13]

This thesis deals with the design and development of several metal-free green approaches under iodine-catalysis or electrochemical conditions for the chalcogenylative C-H annulation and C-H chalcogenation reactions to access novel polycyclic aromatic hydrocarbons (PAHs), polycyclic heteroaromatics and olefins bearing a sulfenyl/selenyl functional group.

Chapter 2

Section-I

Iodine-Catalyzed Organic Transformations

2.1.1. Introduction.

Iodine

Iodine is a chemical element with the atomic number 53 and the symbol I. At standard conditions, it exists as a semi-lustrous, non-metallic solid that melts to form a deep violet liquid at 114 °C and boils to form a violet gas at 184 °C. Iodine can exist in a variety of oxidation states, including iodide (I^-), iodate (IO_3^-), and various periodate anions. It is the sixty-first most abundant element in the universe and the least abundant of the stable halogens. Iodine, as the heaviest essential mineral nutrient, is required for the synthesis of thyroid hormones.

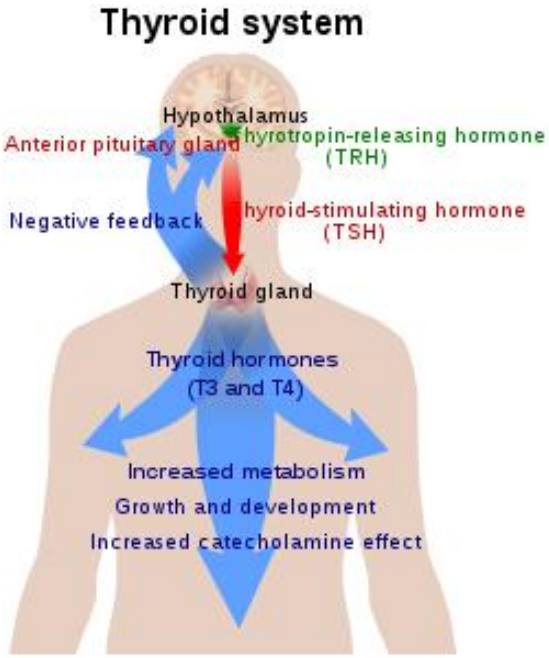

Fig. 2.1.1. Pictorial Presentation of the Biological Role of Iodine.

Fig. 2.1.2. Pictorial Diagram of the Molecular Iodine.

2.1.2. Iodine in Organic Synthesis.

Metal-free, catalytic organic transformations are of high importance in the context of green chemistry. Molecular iodine, being a cheap and non-toxic chemical, is found to replace toxic and highly expensive transition metals in various types of organic transformations including annulation or cyclization reactions.[1] With iodine as a catalyst, one can not only avoid the requirement of toxic metals and ligands in an organic reaction but also avoid the requirement of hazardous stoichiometric reagents thus making the process more sustainable and cost-effective.

In recent years, iodine-catalyzed annulation reactions have attracted wide attention of synthetic organic chemists in synthesizing carbo- and heterocyclic molecules.[2] Consequently, several iodine-–catalyzed annulation reactions have been developed for the synthesis of heterocyclic compounds having potential applications in pharmaceutical synthesis, agrochemicals, materials science, dyes, etc. The state-of-the-art of iodine-catalyzed organic transformations, in particular annulation or cyclization reactions, are reviewed.

2.1.3. Review.

In 2023, Yao and his co-workers developed an iodine-catalyzed cascade cyclization of *ortho*-formylarylketones with indoles in dichloromethane at 0^{o}C to access a wide variety of indolyl benzo*[b]*carbazoles with high functional group tolerance (Scheme 2.1.1).[3] The reaction was initiated in the presence of iodine by two successive nucleophilic additions of indoles with an aldehyde group of *ortho*-formylarylketones. The developed protocol could be scaled up to a gram-scale without any appreciable loss in product yield.

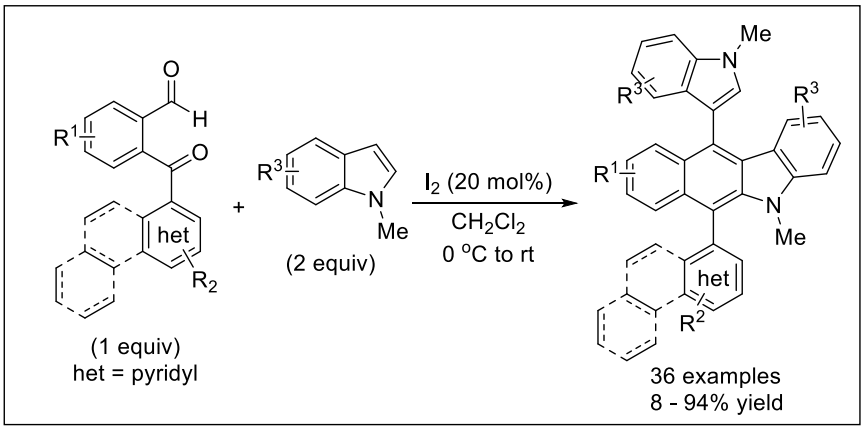

Scheme 2.1.1. Iodine-Catalyzed Synthesis of Indolylbenzo[*b*]carbazoles.

In 2022, Sharghi and his coworkers reported an iodine-catalyzed cascade cyclization of catechols using ammonium acetate in DMSO at 150^{o}C for the synthesis of a biologically-active class of molecules,

2-(hetero)arylbenzoxazoles[4] involving the coupling of catechols, ammonium acetate, alkenes, alkynes, and ketones (Scheme 2.1.2).[5] The reaction mechanism revealed the presence of acetophenone (confirmed by the GC-MS analysis of the reaction mixture of aryl alkenes or aryl acetylenes with iodine in DMSO).

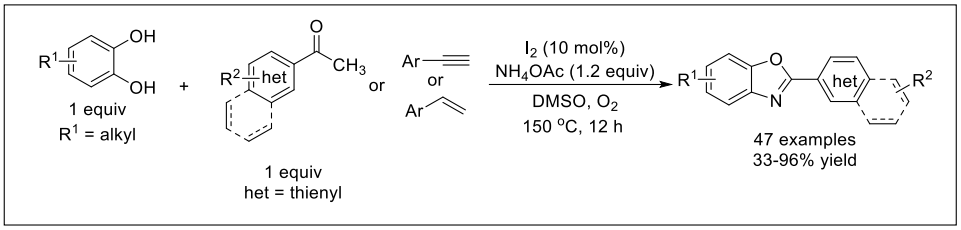

Scheme 2.1.2. Iodine-Catalyzed Synthesis of Benzoxazoles.

In 2022, Dong *et al* developed an iodine-catalyzed one-pot synthesis of medicinally potential chromones with moderate yields using readily available starting materials *i.e*. aryl isocyanates, alcohols, and enaminones in the presence of PIDA as an oxidant and KOH as a base (Scheme 2.1.3). [6] The reactions were carried out in a one-pot, two steps process where in the first step 1 equiv of phenyl isocyanate was treated with 1 equiv of KOH in methanol at room temperature followed by the addition of 1.2 equiv of enaminones, 25 mol% I_2, and 1 equiv of PIDA in the second step.

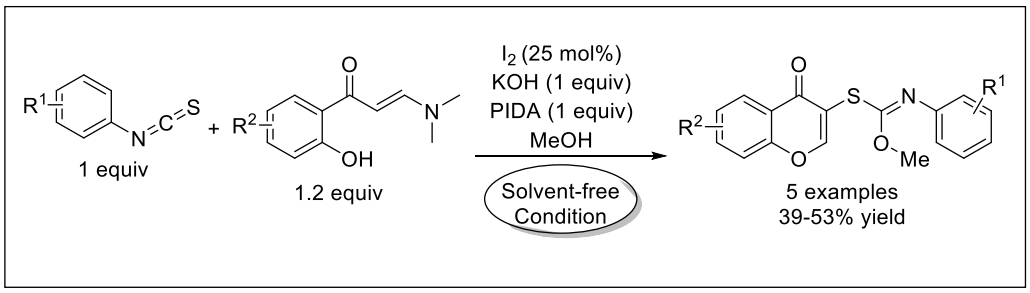

Scheme 2.1.3. Iodine-Catalyzed Synthesis of Chromones.

In 2022, Hao and coworkers disclosed a novel iodine-catalyzed tandem cyclization of *o*-alkynylphenyl isothiocyanates with organophosphorus esters *via* C_{sp}^2 –P bond formation of *o*-alkynylphenyl isothiocyanates to afford 4*H*-benzo[*d*][1,3]thiazin-2-ylphosphonate (Scheme 2.1.4).[7]

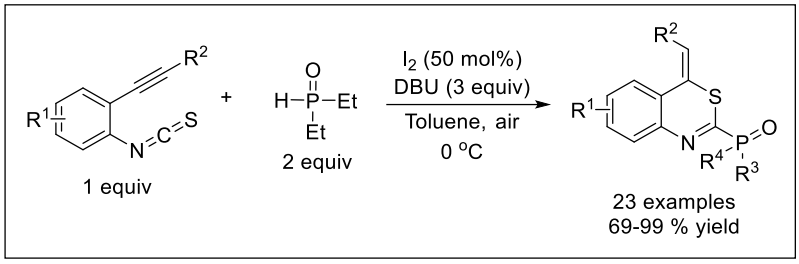

Scheme 2.1.4. Iodine-Catalyzed Tandem Cyclization of *o*-Alkynyl phenyl isothiocyanates.

In 2021, the Nguyen group disclosed an iodine-catalyzed intramolecular cyclization of dihydropyrans, dihydrofurans, and furans from various *β*-diketo carbonyl compounds bearing either alkenyl or alkyne substituents under neat condition (Scheme 2.1.5).[8] Experimental and computational density functional theory (DFT) studies revealed that the reaction proceeded *via* a carbocation intermediate being assisted by iodine.

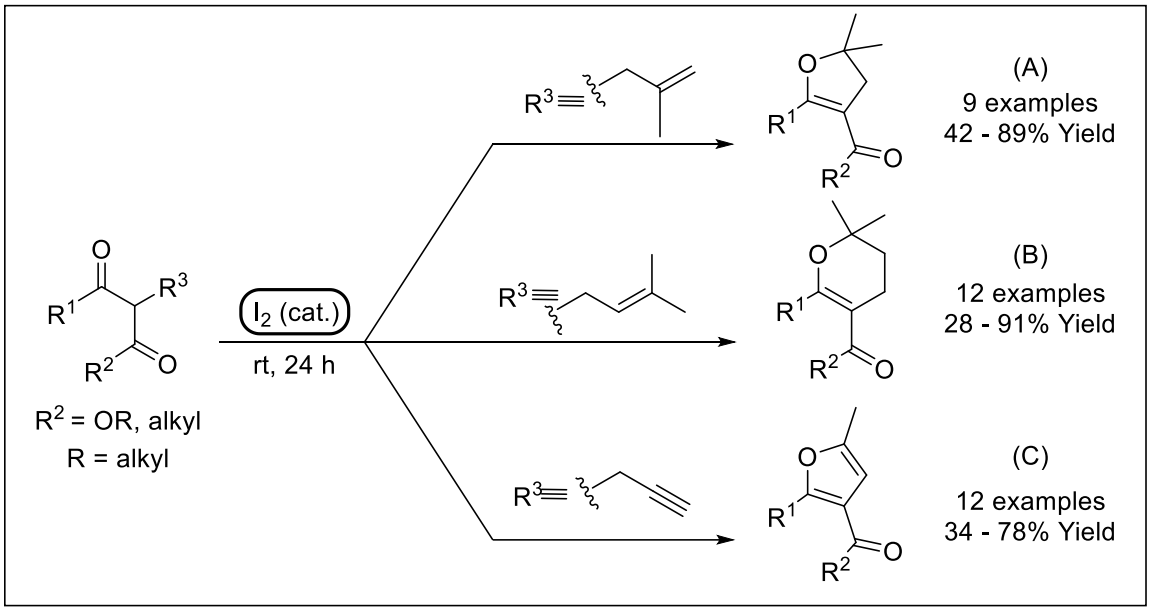

Scheme 2.1.5. Iodine-Catalyzed Synthesis of Substituted Furans and Pyrans.

In 2021, the Zhu group developed an iodine-catalyzed domino cyclization (formation of two C-C and one C-O bonds in one-pot) of methyl azaarene with 5-alkyl-2-aryl-2,4-dihydro-3*H*-pyrazol-3-ones in DMSO at room temperature *via* Csp^3-H functionalization to access a fused seven-membered oxa-heterocycles with broad functional group tolerance in moderate to high yield (Scheme 2.1.6).[9]

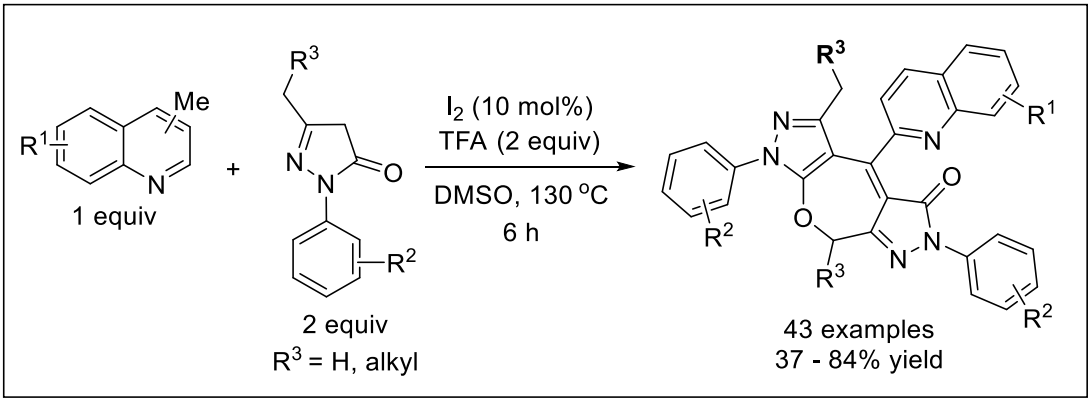

Scheme 2.1.6. Iodine-Catalyzed Synthesis of Pyrazolooxepinopyrazolones *via* Methyl azaarene Csp^3-H functionalization.

In 2020, He and coworkers disclosed iodine-catalyzed, highly regio- and chemoselective synthesis of cyanopyrrolines using alkene, TMSCN, and *N*, *N*-disubstituted formamides in an aerobic atmosphere without using any transition metal and solvent (Scheme 2.1.7).[10]

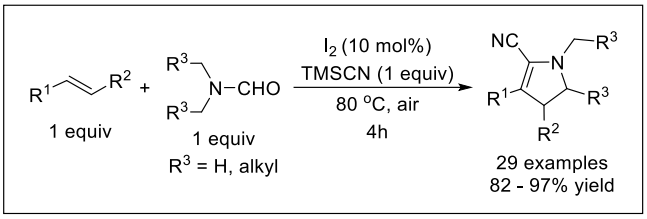

Scheme 2.1.7. Iodine-Catalyzed Synthesis of α-Cyanopyrrolines.

In 2020, Prabhu *et al* developed an iodine-catalyzed annulation of cyclopentene-dione with benzamidine hydrochloride *via* a double C-H functionalization strategy which paves an excellent way for synthesizing a wide variety of substituted fused imidazole derivatives in moderate to good yield (Scheme 2.1.8).[11]

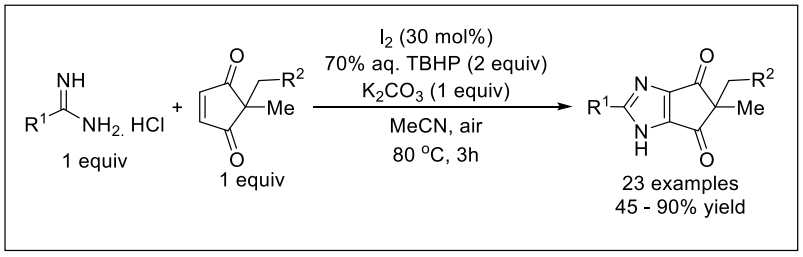

Scheme 2.1.8. Iodine-Catalyzed Synthesis of Fused Imidazoles.

In 2019, Zhao and co-workers developed an iodine-catalyzed regioselective synthesis of substituted dihydro pyrazoles *via* an oxidative cyclization strategy of aldehyde hydrazones with electron-deficient olefins. The reaction was supposed to proceed *via* a cascade C-H functionalization, C-N bond formation, and oxidation (Scheme 2.1.9).[12] The synthetic application of the developed protocol was demonstrated by synthesizing a herbicide safener, *i.e.*, Mefenpyr-Diethyl.

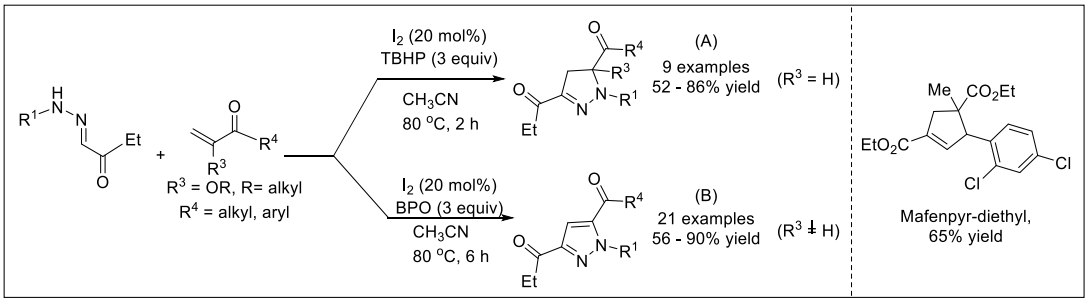

Scheme 2.1.9. Iodine-Catalyzed Regioselective Oxidative Cyclization of Aldehyde hydrazones with Olefins.

In 2019, Anilkumar and his co-workers first disclosed an iodine-catalyzed Ortoleva-King type protocol in which they synthesized a library of imidazo[1,2-*a*]pyridines, a "drug prejudice" possessing a various applications in medicinal chemistry,[13 21]in moderate to excellent yield (Scheme 2.1.10).[14] A gastro-protective drug, Zolimidine was synthesized by the developed protocol.

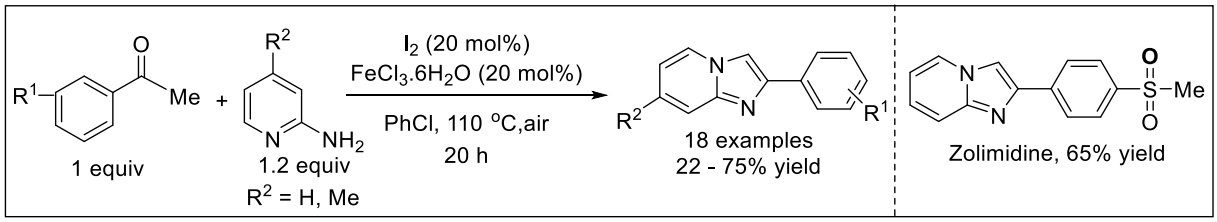

Scheme 2.1.10. Iodine-Catalyzed Synthesis of Imidazo[1,2-*a*]pyridines.

In 2019, Li and his co-workers developed an iodine-catalyzed synthesis of pyrrolidine-2-carboxylates *via* a one-pot cycloaddition of an aldehyde, an amino acid ester, and a chalcone in the presence of K_2CO_3 as a base in tetrahydrofuran at 80 °C resulting in good to excellent yield (scheme 2.1.11).[15]

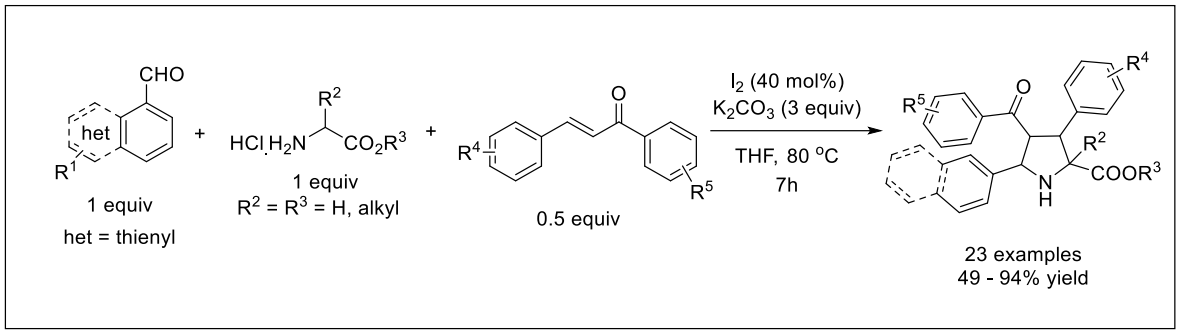

Scheme 2.1.11. Iodine-Catalyzed Synthesis of Multi-substituted Pyrrolidine-2-carboxylates.

In 2019, Maiti group developed an I_2-catalyzed intermolecular cyclization of primary aliphatic amines with 1,2-diketone analogues under aerobic conditions in 1,4-dioxane to afford some new classes of molecules such as oxazoles, oxazines, and oxazinone (Scheme 2.1.12).[16] The reaction involved α-Csp^3-H functionalization of primary amine leading to the formation of 5, 6- intermolecular cyclized product in good to high yield. The newly synthesized compounds are reported to be effective organic nano-building blocks to achieve valuable organic nanomaterials for smart devices.

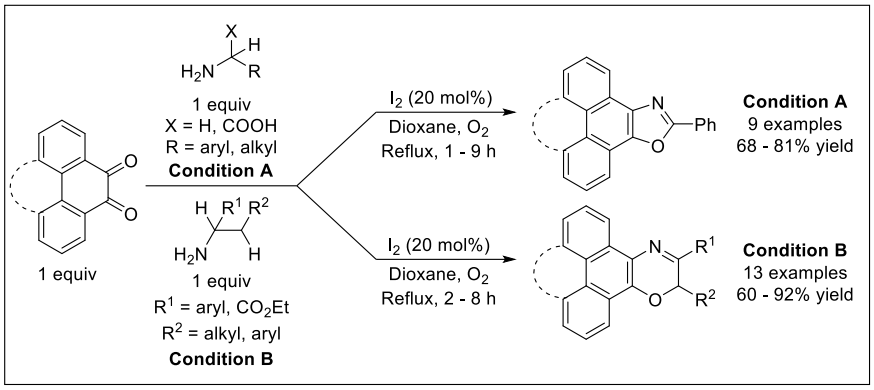

Scheme 2.1.12. Iodine-Catalyzed Functionalization of Primary Aliphatic Amines.

In 2018, Wen and his co-workers reported an iodine-catalyzed ethyl-lactate-mediated synthesis of *N*,*S*-containing heterocyclic compounds such as 1,4-benzothiazines *via* cascade C-N bond transamination and C(sp^2)-H sulfenylation (Scheme 2.13).[17]

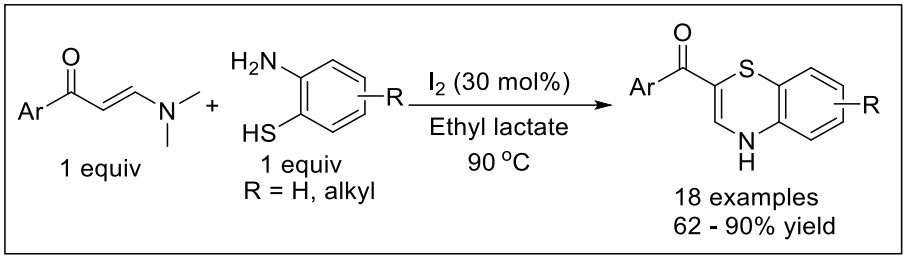

Scheme 2.1.13. Iodine-Catalyzed Synthesis of 1,4-Benzothiazine.

In 2018, Liu and his co-workers developed an iodine-catalyzed oxidative annulation of 3-cyanoacetylindoles with benzylamines to synthesize a variety of biologically-active bi-heteroaryls (Scheme 2.14) [18] *i.e.*, 5-(3-indolyl)oxazoles with high functional group tolerance.

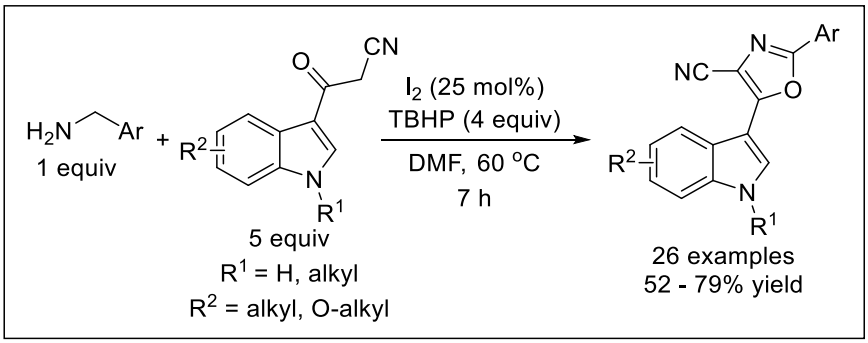

Scheme 2.1.14. Iodine-Catalyzed Synthesis of 5-(3- Indolyl)oxazoles.

In 2018, Wang and his co-workers developed an iodine-catalyzed domino cyclization reaction of 5-benzoyl-8*H*-phthalazino[1,2-*b*]quinazolin-8-ones from 2-aminobenzohydrazides and 2-alkynyl benzaldehydes (Scheme 2.15).[19] This strategy followed a tandem pathway involving the following three

key steps: (a) condensation between 2-alkynylbenzaldehyde and 2- aminobenzohydrazide, (b) addition of iodine to the triple bond *via* sequential intra-molecular hydroamination and aromatization, and (c) noteworthy oxidation of active methylene group by oxygen under metal-catalyst-free conditions.

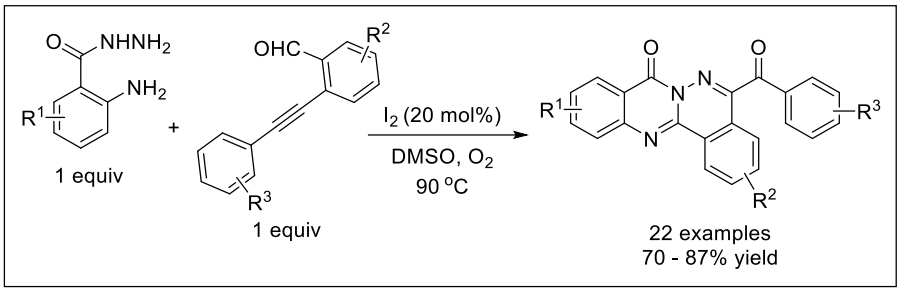

Scheme 2.1.15. Iodine-Catalyzed Synthesis of 5-Benzoyl-8*H*-phthalazino[1,2-*b*] quinazolin-8-one.Derivatives.

In 2018, Chen and his co-workers developed an iodine-catalyzed three component protocol for the synthesis of 2-aryl benzothiazoles *via* sequential C–S and C–N bond formation followed by C(CO) – C bond cleavage using readily available starting materials like substituted acetophenones, anilines with naphthalenamine and elemental sulfur (Scheme 2.16).[20]

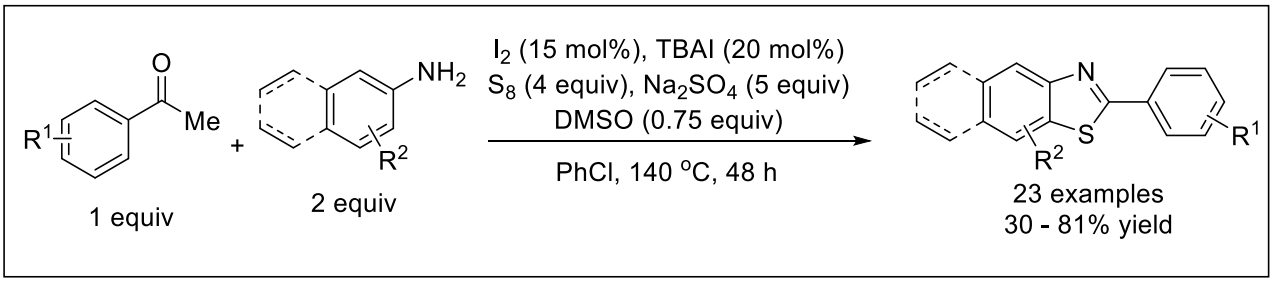

Scheme 2.1.16. Iodine-Catalyzed Synthesis of 2-Aryl benzothiazole.

In 2018, Shivashankar *et al.* disclosed an iodine-catalyzed multicomponent tandem cyclization to synthesize a library of furo[2,3-*b*] pyrrole and thieno[2,3-*b*]pyrrole derivatives *via* a Fischer-type cyclization (scheme 2.17).[21] This single-step protocol overcome the limitations of previously reported multistep routes.[22]

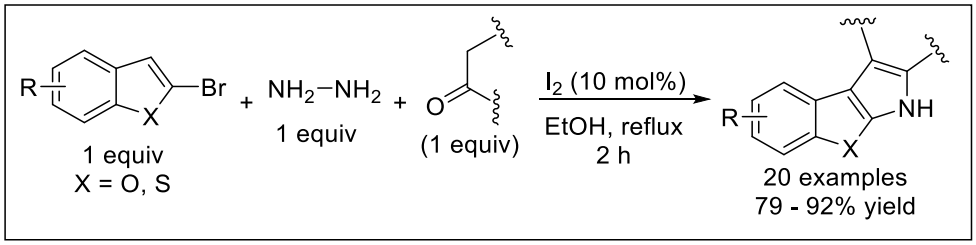

Scheme 2.1.17. Iodine-Catalyzed Synthesis of Benzofuran/thieno[2,3-*b*]pyrrole Motifs.

In 2018, Guo and his co-workers reported an iodine-catalyzed one-pot annulation of alkynes with *o*-phenylenediamines in DMSO at 130 °C to rt to access quinoxalines, a bioactive class of *N*-heterocycle possessing a wide range of biological activities such as antitumors,[23]antibacterials,[24] anti-inflammatories, [25] antivirals,[26] activities and kinase inhibition property.[27], in good to excellent yield (Scheme 2.18).[28]

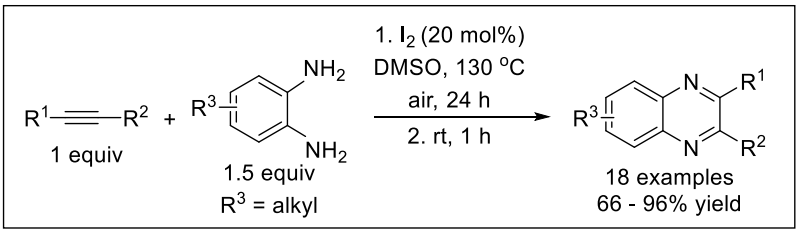

Scheme 2.1.18. Iodine-Catalyzed Synthesis of Quinoxalines.

Iodine-Catalyzed Sulfenylative Annulation

In 2019, the Pramanik group disclosed an iodine-catalyzed regioselective sulfenylative annulation of 2-iminothiazoline with 2-bromo-arylethanone using thiol and DMSO as an oxidant in DCE at 80 °C to access diversely substituted 5-sulfenyl-2-iminothiazoline derivatives up to 82% yield Scheme 2.1.19). [29]This reaction involved the following key steps: (a) cross-dehydrogenative coupling (b) sp^2 C-H functionalization, (c) C-5 sulfenylation, (d) generation of dimethyl sulfide as a by-product (confirmed by GC-MS). Mechanistic studies revealed that the reaction proceeded *via* an ionic pathway.

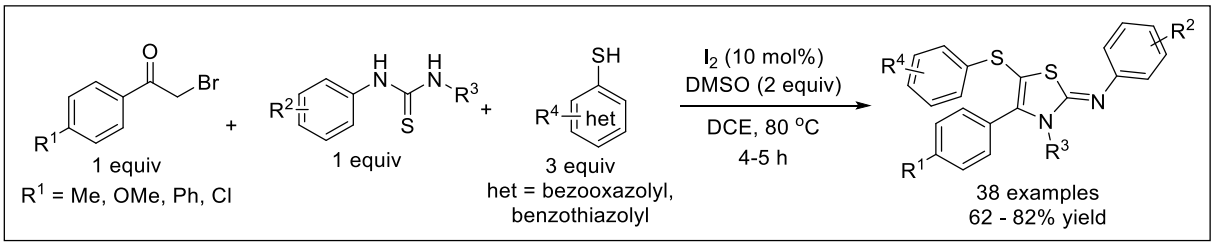

Scheme 2.1.19. Iodine-Catalyzed Synthesis of 5-Sulfenyl-2-iminothiazolines by Cross-dehydrogenative C−S Coupling.

In 2017, the Wang group reported an iodine-catalyzed domino multicomponent cyclocondensation reaction (MCR) of 1,3-diketones with hydrazine and thiol in DMSO at 70 °C to afford a wide variety of biologically active sulfenylated pyrazoles in good to excellent yield (Scheme 2.1.20). [30] Some of the key features of this reaction is as follows: (a) formation of two C-N bonds and one C-N bond in a one-pot reaction, (b) C-4 sulfenylation. The drawback of this reaction is that only aryl thiols can take part in this reaction.

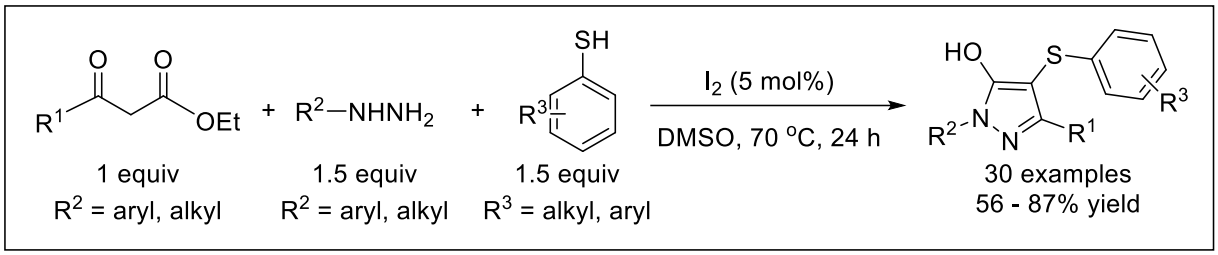

Scheme 2.1.20. Iodine-Catalyzed Cyclocondensation to Synthesize C-4 Sulfenylated pyrazoles.

2.1.4. Conclusion.

In summary, the reliability and feasibility of iodine has endowed the metal-free access to potential heterocyclic molecules through C-C, C-N, and C-O bond formation *via* radical or ionic pathway. This review demonstrated the potential utilization of molecular iodine in various organic transformations, in particular, cyclization reactions for the synthesis of useful heterocycles. However, the iodine-catalyzed carbannulation strategy for the synthesis of potential carbocyclic molecules such as polycyclic aromatic hydrocarbons (PAHs) is rarely explored or underdeveloped, to the best of our knowledge.

SECTION – II

Synthesis of Phenanthrenes by Annulation Reactions with Alkynes

2.2.1. Introduction.

Phenanthrenes, one of the most important classes of polycyclic aromatic hydrocarbons, are found in a wide variety of biologically active compounds, including natural products, [1] and exhibit a wide range of biological activities such as antiviral, [2] antimicrobial, [3] anticancer,[4] antitumor, [5] and anti-HIV [6] activity (Figure 2.2.1.). Furthermore, phenanthrene derivatives have attractive electronic[7] (Figure 2.2.1.) and optical[8] properties and are used in a variety of useful materials, including organic field-effect transistors[9] and solar cells[10].

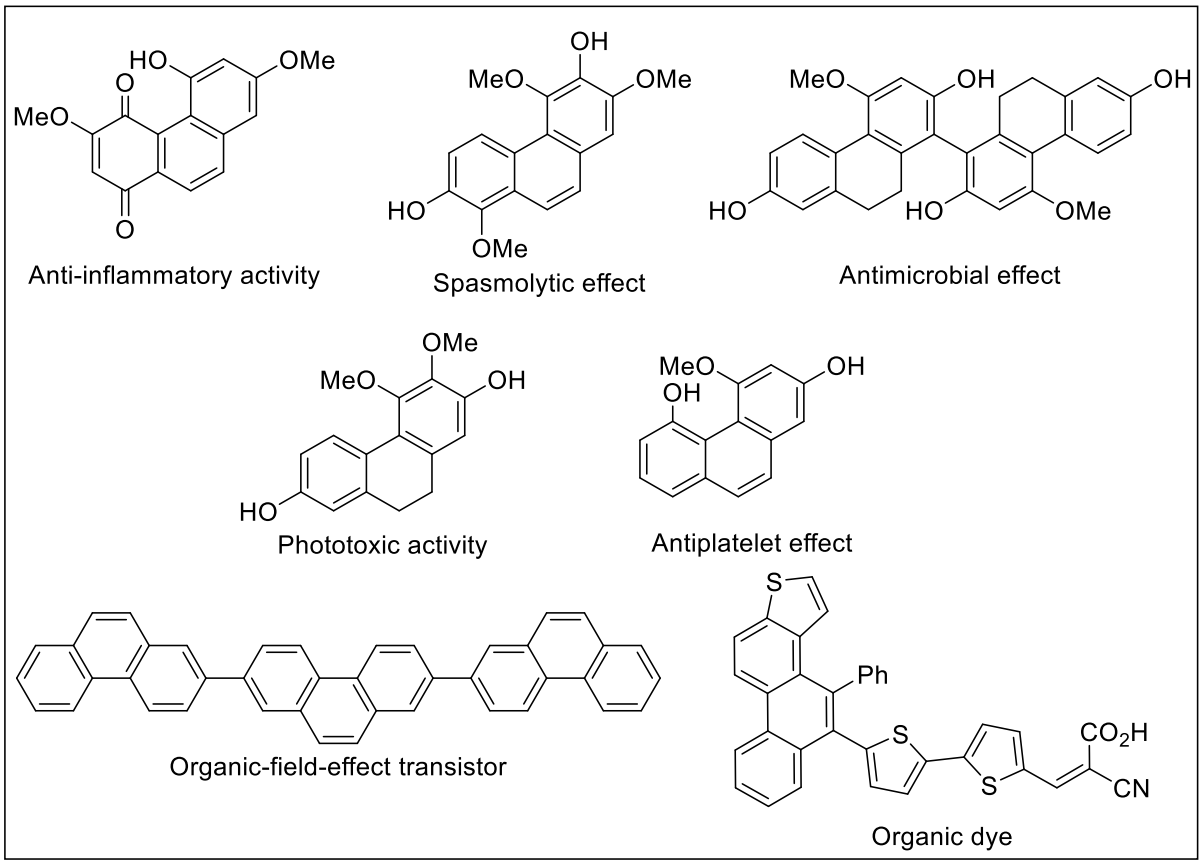

Figure 2.2.1. Some Examples of Phenanthrene-based Biologically-active Molecules and Useful Materials.

Consequently, several synthetic strategies have been developed so far for the synthesis of phenanthrenes.[11,12] Among them, two synthetic strategies, *i.e.*, transition-metal (TM) (Pd, Ir, Rh, and Fe)-catalyzed or visible-light photocatalyzed [4+2]-benzannulation of 2- functionalized 1,1′-biaryls with alkynes [13] and transition-metal (Pt, Au, Ga, Ir, Ru, Fe, and Sn)-catalyzed/mediated intramolecular carbocyclization or electrophilic annulation of 2-alkynyl biaryls (6-endo-dig cyclization) are widely employed, perhaps because of their high atom-economical feature and the requirement of relatively less functionalized starting materials.[14]

2.2.2. Review.

In 2017, Cho *et al.* reported a regioselective [4+2]-benzannulation of 2-(hetero)aryl-substituted anilines with alkynes by visible light photocatalysis using ^{t}BuONO as a diazotizing agent and *fac*-Ir(ppy)$_3$ as a photocatalyst at room temperature to afford a wide variety of 9,10-disubstituted polycyclic (hetero)aromatic compounds, including phenanthrenes, in moderate to high yields (Scheme 2.2.1).[15]

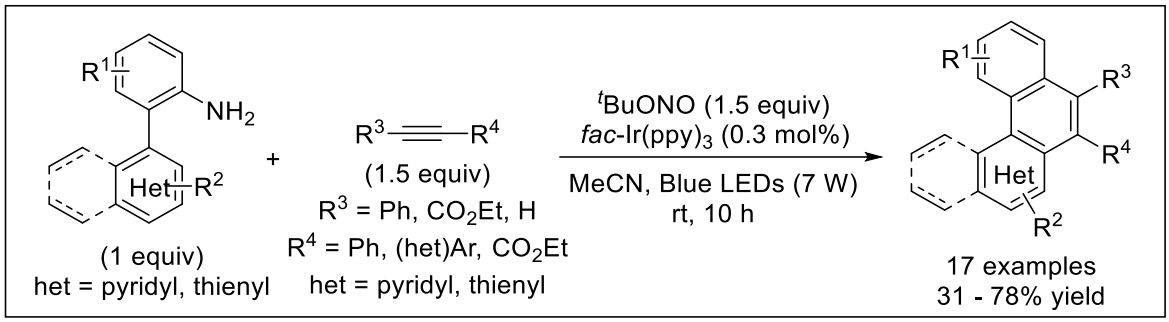

Scheme 2.2.1. Synthesis of Polycyclic (hetero)aromatics by Visible-light-induced Photocatalytic [4 + 2] Benzannulation.

In 2016, the Miura group disclosed a Rh-catalyzed annulation of (2-arylphenyl)boronic acids with alkynes using oxygen as the terminal oxidant to afford a wide variety of 9, 10–disubstituted phenanthrenes *via* the formation of a 5-membered rhodacycle intermediate, as evident by the mechanistic studies (Scheme 2.2.3).[16]

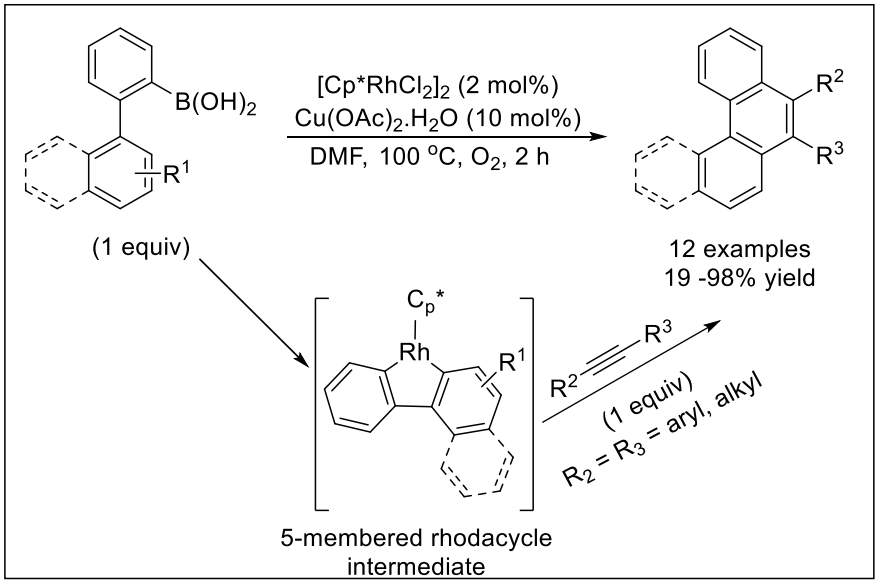

Scheme 2.2.3. Rh-catalyzed Oxidative Annulation of (2-Arylphenyl)boronic Acids with Alkynes.

In 2015, Alabugin and co-workers disclosed a Sn-mediated radical cascade oxidative cycloisomerization of 2-(arylethynyl)-biphenyls using AIBN and Bu_3SnH system in toluene at 110 ^{o}C to

access 9- substituted phenanthrenes in good to excellent yield (Scheme. 2.2.4).[17] The mechanism of the reaction involved the formation of a central ring of phenanthrene *via* regioselective vinyl radical formation followed by a 6-endo-dig cyclization to afford Sn-substituted phenanthrenes which finally underwent protonation by HCl (3M) to afford 9- substituted phenanthrenes.

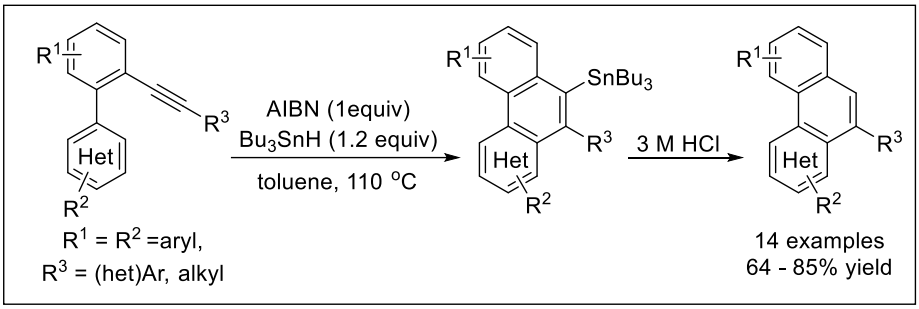

Scheme 2.2.4. Synthesis of Phenanthrenes *via* Regioselective Oxidative Radical Cyclization.

In 2014, Miura *et al.* reported an Ir-catalyzed annulation of 2-arylbenzoyl chlorides treated with internal alkynes using P(*t*-Bu)$_3$ as ligand *via* the elimination of carbon monoxide and hydrogen chloride to afford a library of 9,10-disubstituted phenanthrene derivatives (Scheme 2.2.5).[18] Deuterium-labeling experiments using 2-(d_5-phenyl)benzoyl chloride suggested that the rate-determining step does not involve the C_2'−H bond cleavage. Mechanistic studies revealed that the reaction proceeded through the formation of a [(*t*-Bu)$_3$PH][(biphenyl-2,2′-diyl)Ir(CO)Cl$_2$] complex dimer as the active catalytic system (Scheme 2.2.5) which supported that the C-H bond cleavage was promoted by the phosphine ligand P(*t*-Bu)$_3$.

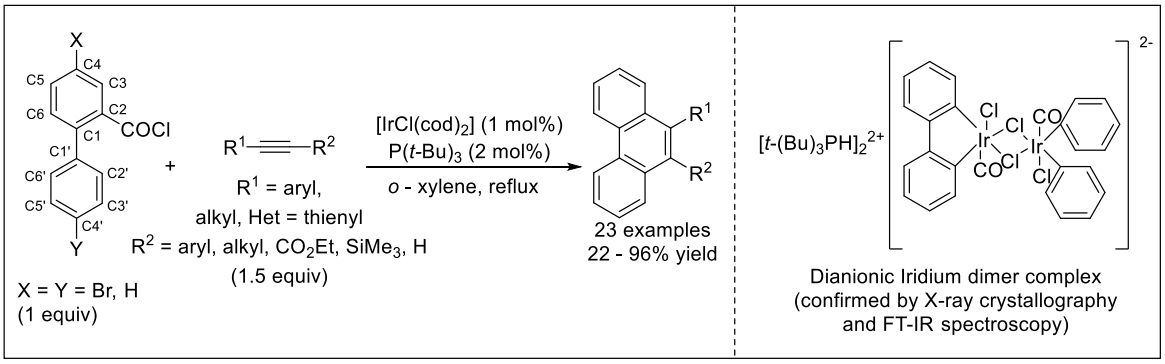

Scheme 2.2.5. Iridium-catalyzed Annulative Coupling of 2-Arylbenzoyl Chlorides with Alkynes.

In 2011, the Nakamura group disclosed an Fe-catalyzed [4 + 2] benzannulation between alkyne and 2-alkenylphenyl Grignard reagents in the presence of Fe(acac)$_3$, 4,4' -di-*tert*-butyl-2,2' -bipyridyl, and 1,2-dichloro-2-methylpropane at room temperature in 1 h to afford a wide variety of 9-substituted or 9,10-disubstituted phenanthrenes with a high functional group in moderate to excellent yield (Scheme 2.2.6).[19]

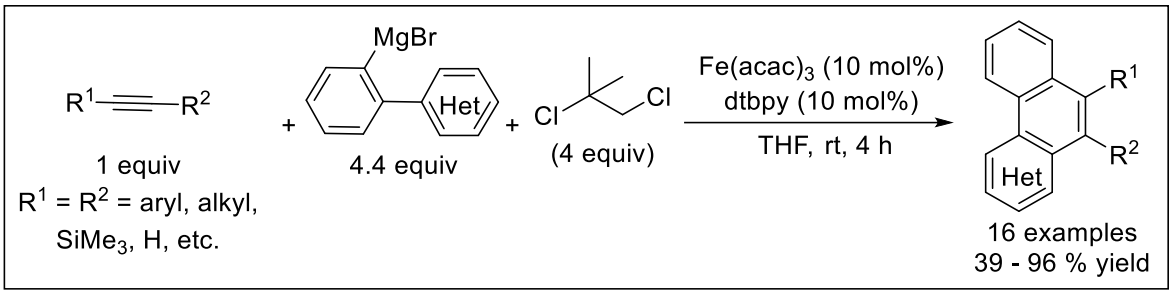

Scheme 2.2.6. Iron-catalyzed [4+2] Benzannulation between Alkyne and Biaryl or 2-Alkenylphenyl Grignard Reagent.

In 2010, the Glorius group developed a palladium-catalyzed intermolecular decarboxylative [4 + 2] benzannulation of 2-phenylbenzoic acids with alkynes using acridine, and Ag_2CO_3 in DMF to afford a wide variety of 9,10-disubstituted phenanthrenes in moderate to good yield (Scheme 2.2.7).[20]

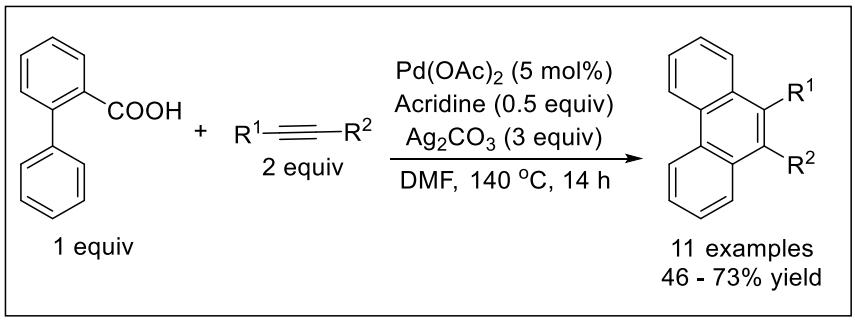

Scheme 2.2.7. Palladium-catalyzed Intermolecular Decarboxylative Coupling of 2-Phenylbenzoic Acids with Alkynes.

In 2010, Takaki *et al.*developed an $Fe(OTf)_3$-catalyzed intramolecular hydroarylation of 2-arylethynyl biaryls in DCE at 80 °C to access substituted phenanthrenes with broad functional group in good to high yield (Scheme 2.2.8).[21]

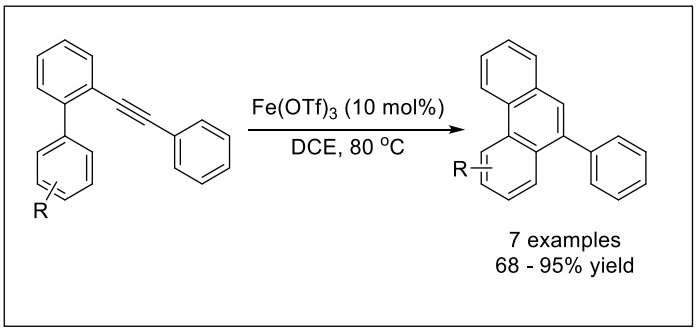

Scheme 2.2.8. Iron-catalyzed Intramolecular Alkyne-hydroarylation.

In 2004, Furstner and co-workers disclosed transition-metal catalyzed cycloisomerization reactions of 2-halo- or aryl/alkyl-substituted ethynyl biaryls in toluene at 80 °C to afford 9-halophenanthrenes or 10-

halo or aryl/alkylphenanthrenes selectively based on the nature of transition-metal (Scheme 2.2.9).[22] When 2-haloethynyl biaryls were treated with AuCl in toluene at 80 ^{o}C, 9-halophenanthtrenes (8 examples) were obtained in 7-95% yield. However, when 2-halo- or aryl/alkylethynyl biaryls were treated with MX (where MX= $PtCl_2$, $AuCl_3$, $GaCl_3$, $InCl_3$) in toluene at 80 ^{o}C, the other regioisomeric product, *i.e.*, 10-halo or aryl/alkyl-substituted phenanthrenes (24 examples) were obtained in moderate to high yield (55 – 96% yield).

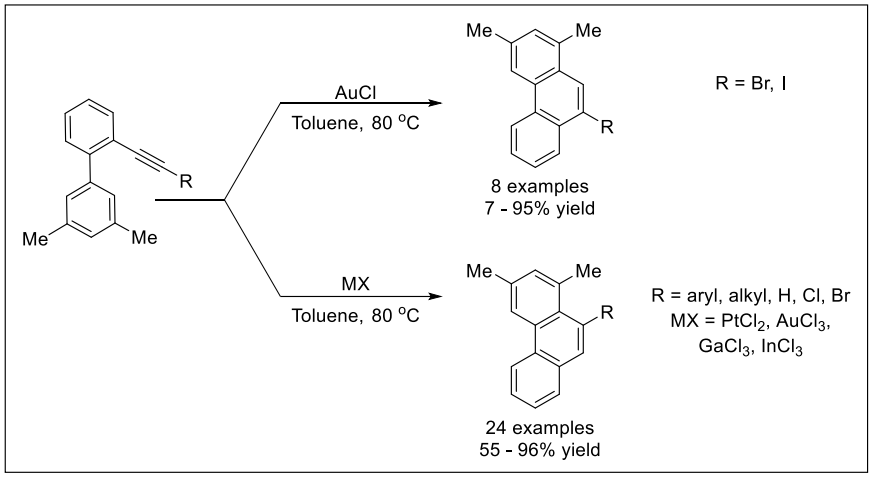

Scheme 2.2.9. Synthesis of Phenanthrenes and Polycyclic Heteroarenes by Transition-metal Catalyzed Cycloisomerization Reactions.

In 2002, the Mamane group reported a $PtCl_2$-catalyzed cycloisomerization reaction of biaryl alkynes *via* a 6-*endo*-dig cyclization through initial π-coordination of the alkyne unit followed by interception of the resulting η^2-metal complex by the adjacent arene ring to afford 9-substituted phenanthrenes in good yields(Scheme 2.2.10).[23]

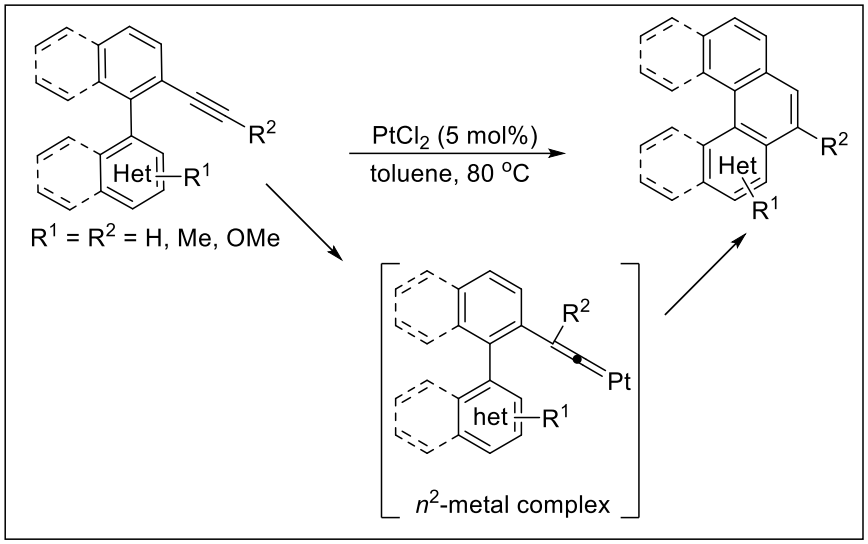

Scheme 2.2.10 Synthesis of Phenanthrenes by Pt-catalyzed Cycloisomerization Reaction.

In 1997, the Zenner group disclosed a palladium-catalyzed carbo-annulation of 2-iodobiaryls with internal alkynes using NaOAc, LiCl in DMF to afford a wide variety of 9,10-disubstituted phenanthrenes (Scheme 2.2.11).[24]

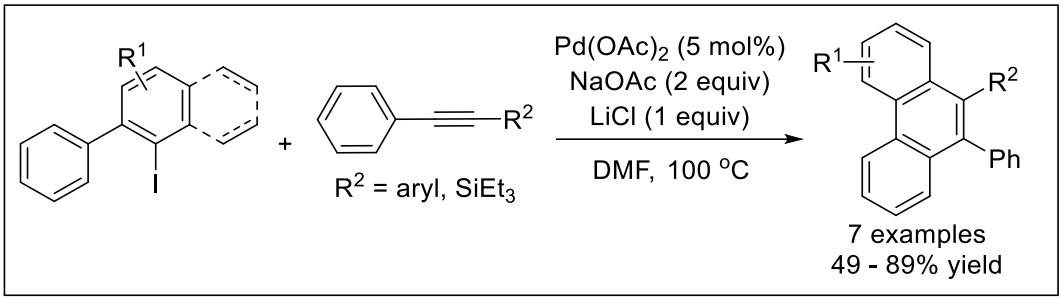

Scheme 2.2.11. Synthesis of Polycyclic Aromatic Hydrocarbons by the Pd-catalyzed Annulation of Alkynes.

2.2.3. Conclusion.

Phenanthrene is a nucleus of the poly aromatic hydrocarbon family consisting of three fused benzene rings. They are of great importance in the field of medicine and materials science. This short review revealed several metal-catalyzed annulation strategies for the synthesis of phenanthrenes in the recent few years. Despite significant advancement, the abovementioned synthetic methods suffer from at least one of the following serious limitations, (a) the requirement of expensive and toxic transition-metal salts or complexes in catalytic or (sub)stoichiometric amounts, (b) the use of expensive and hazardous ligand and reagents, (c) harsh or critical reaction conditions, and (d) a limited substrate scope. Hence, the development of metal-free general synthetic strategy for the construction of a phenanthrenes core is highly desirable.

SECTION-III

Synthesis of 9-Sulfenylphenanthrenes via Sulfenylative Annulation of 2-Alkynyl Biaryls

2.3.1. Introduction.

Organosulfides or sulfur-containing molecules, in particular, unsymmetrical diaryl or aryl-heteroaryl sulfides are ubiquitous in numerous pharmaceuticals,[1] natural products, [2] and valuable materials (Figure 3.2.1.).[3] Hence, several synthetic strategies and techniques have been developed for the synthesis of valuable organosulfides through a C-S bond formation.[4] Among them, the transition-metal-catalyzed cross-coupling reaction is the most widely employed strategy and a powerful tool for constructing organosulfides.[5] However, those methods suffer from several limitations such as the requirement of highly expensive, toxic, and air-sensitive transition-metal catalysts, ligands and reagents, harsh reaction conditions, the requirement of pre-functionalized starting materials, low atom-economy, generation of hazardous wastes, etc. which are not desirable in the context of green chemistry. Hence the development of metal-free and environmentally benign synthetic methodologies without using any toxic/hazardous reagents or solvents is always desirable.

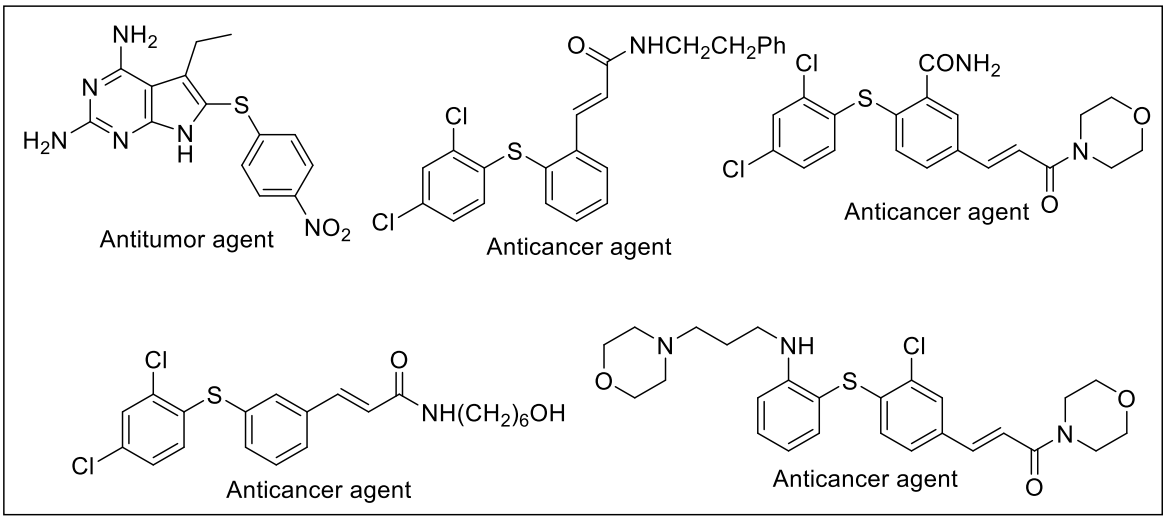

Figure 2.3.1. Some Examples of Biologically Active Organosulfides.

Considering the numerous potential applications of organosulfides and phenanthrenes in medicinal chemistry as well as materials science, the synthesis of sulfenyl-phenanthrenes is obviously of great importance. However, only a couple of general synthetic strategies are found in the literature for the synthesis of 9-sulfenylphenanthrenes which are presented below.

2.3.2. Review.

In 2005, Larock et al. reported a transition-metal-free, electrophilic 6-endo-dig cyclization of 2-alkynyl biaryls with *p*-$NO_2C_6H_4SCl$ to synthesize 9-(4-nitrophenyl)sulfenylphenanthrenes (Scheme 3.2.1). [6] However, the requirement of a highly electrophilic arylsulfenyl chloride, *p*-$NO_2C_6H_4SCl$, and its commercial non-availability eventually limited this method's scope to access a wide variety of 9-sulfenyl phenanthrenes.

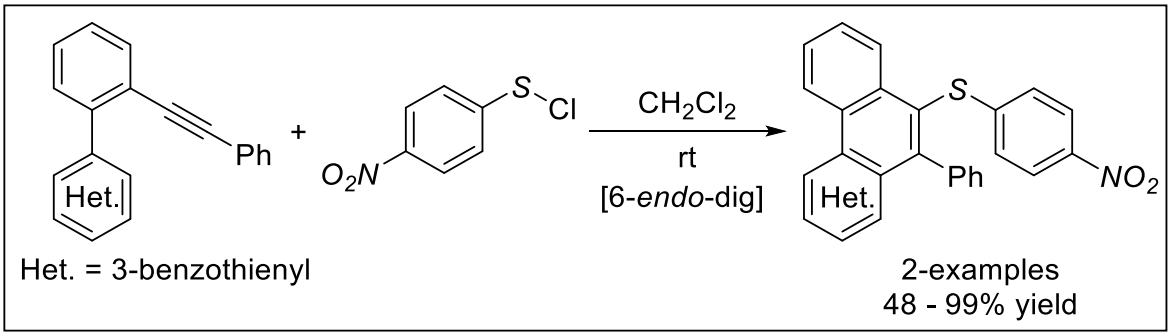

Scheme 2.2.1. Synthetic Strategy to Access 9-(4-Nitrophenyl)sulfenyl Phenanthrenes.

The Qian and Zhang group first disclosed a general synthetic strategy for synthesizing 9-sulfenylphenanthrenes from 2-alkynyl biaryls and disulfides by using 10 mol% $Pd(OAc)_2$ as a catalyst, 2 equiv iodine as a reagent, and THF as solvent at 80 ^oC (Scheme 3.2.2).[7] Despite good substrate scope, this method suffers from several serious limitations such as the requirement of a highly expensive and toxic rare-earth transition-metal catalyst in sub-stoichiometric amounts, requirement of over-stoichiometric iodine, low atom economy of the reaction since only half equivalent of disulfide was utilized and the other half equivalent was wasted.

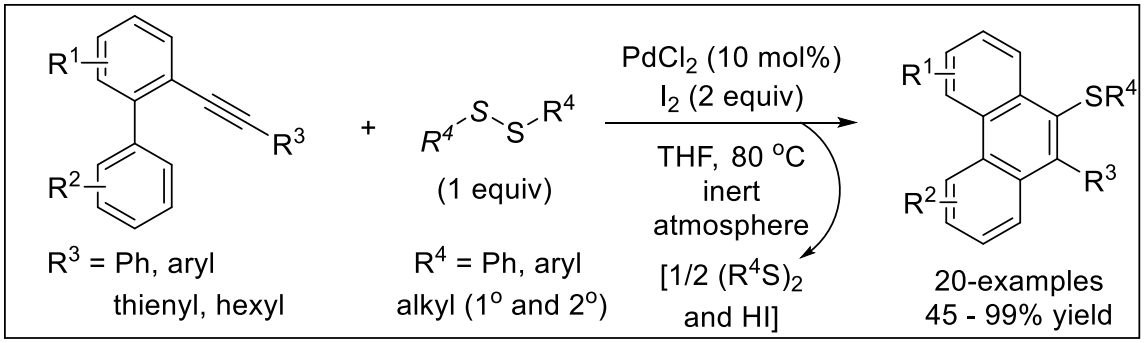

Scheme 2.2.2. Palladium-catalyzed Electrophilic Annulation of 2-(1-Alkynyl)biphenyls with Disulfides.

2.3.3. Conclusion.

The available synthetic methods to access 9-sulfenyl phenanthrenes are very limited and those methods also suffer from many serious issues. Moreover, no metal-free general synthetic strategy has been developed so far to access a wide variety of 9-sulfenylphenanthrenes. Hence, the development of a metal-free synthetic strategy for the general construction of 9-sulfenylphenanthrenes is highly desirable.

SECTION-IV

Iodine Catalyzed Methylthiolative Annulation of 2-Alkynyl Biaryls with DMSO: A Metal-Free Approach to 9-Sulfenylphenanthrenes

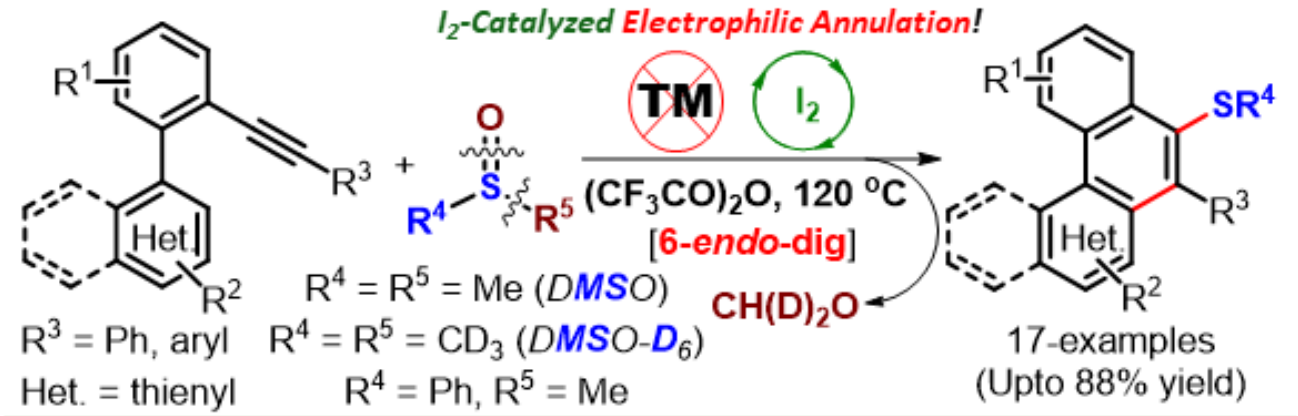

- ✓ Transition-metal-free, sustainable, cost-effective, and atom-economical protocol
- ✓ Multiple roles of DMSO such as methylthiolating reagent, oxidant, and solvent
- ✓ Evidence of *in situ* decomposition of DMSO by $(CF_3CO)_2O$ to CH_2O and MeSH
- ✓ Synthesis of a wide variety of sulfenyl-phenanthrenes and naphthothiophenes

2.4. Present Work.

2.4.1. Introduction.

In recent times, DMSO has been utilized as the source of a thiomethyl (−SMe) group in developing a few transition-metal (TM) catalyzed C−H methylthiolation reactions [1] and radical coupling reactions under TM-free conditions.[2] We designed and developed a TM-free, sustainable, and cost-effective synthetic strategy for the methylthiolative annulation of 2-alkynyl biaryls by using inexpensive and commercially available methyl sulfoxides such as DMSO as the source of thiomethyl group (−SMe), iodine (I_2) as the catalyst, and TFAA as a reagent to synthesize a wide variety of 9-sulfenylphenanthrenes and polycyclic heteroaromatics, *i.e.*, naphthothiophenes (Scheme 2.3.1). DMSO played multiple roles in the reaction such as methylthiolating reagent, oxidant, and solvent in the reaction. We hypothesized that in the presence of iodine, an electrophilic species, *i.e.*, methyl sufenyl iodide (MeSI), could be generated through the *in situ* decomposition of DMSO by an electrophilic reagent such as TFAA into formaldehyde and thiomethanol.[3,4] Subsequently, the electrophilic methylthiolative annulation of 2-alkynyl biaryls with MeSI would furnish the desired product, 9-sulfenyl phenanthrenes, *via* the formation of intermediate **A**[3] During the reaction, HI will be formed, which will be oxidized by DMSO under the reaction conditions to regenerate iodine in the catalytic cycle.[5] The unique feature of this protocol is the synthesis of a wide variety of 9-sulfenyl phenanthrenes and polycyclic heteroaromatics from readily available 2-alkynyl biaryls and DMSO in a metal-free, cost-effective, and sustainable manner.

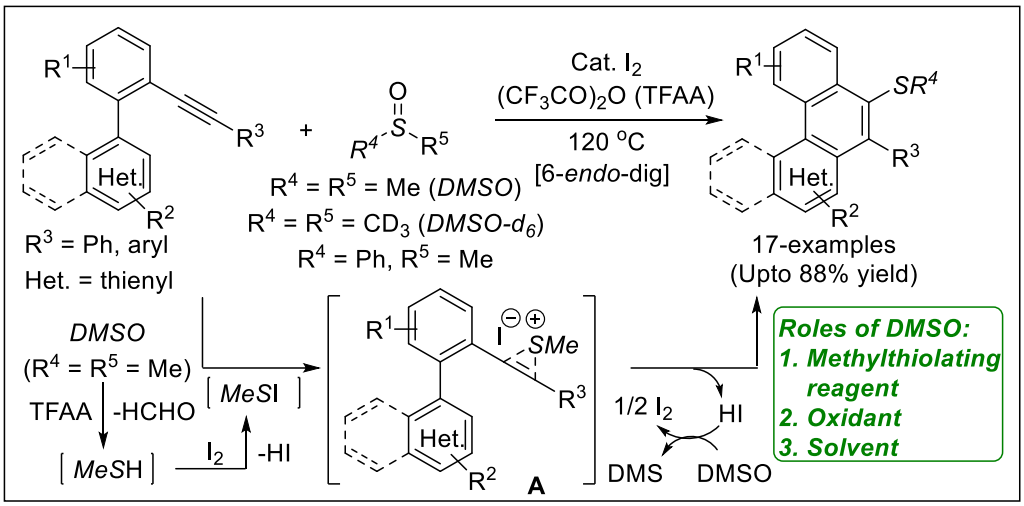

Scheme 2.4.1. Schematic Presentation of Iodine-Catalyzed Methylthiolative Annulation of 2-Alkynyl Biaryls with DMSO.

2.4.2. Results and discussions.

We commenced our investigation of methylthiolative annulation of 2-(phenylethynyl)-1,1′-biphenyl **1a** with 10 equiv DMSO **2a** using iodine and TFAA at 120 °C under an aerobic atmosphere. To our delight, when the reaction was conducted using 20 mol% of I_2 and 3 equiv of TFAA for 3 h, 91% of the desired product, methyl(10-phenylphenanthren-9- yl)sulfane **3aa** was formed along with a trace amount of 9-iodo-10-phenylphenanthrene **4a** (entry 1, Table 2.3.1).

Table 2.4.1. Optimization of the Reaction Conditions[a]

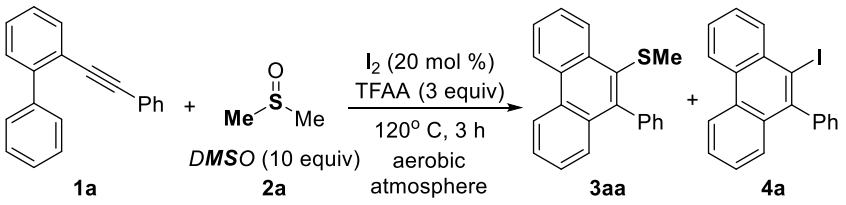

1a **2a** **3aa** **4a**

entry	variation in condition from scheme	yield (%)[b]	
		3aa	**4a**
1.	none	91	trace
2.	10 mol% of I_2	50	trace
3.	20 mol% of TBAI was used instead of I_2	65	trace
4.	4 equiv of TFAA was used	90	8
5.	4 equiv of Ac_2O was used instead of TFAA	0	0
6.	4 equiv of CF_3SO_2Cl was used instead of TFAA	60	-
7.	4 equiv of *p*-NO_2-C_6H_4-SO_2Cl were used instead of TFAA	20	trace
8.	2 equiv of TFAA was used	55	trace
9.	reaction was conducted at 100 °C	30	trace
10.	reaction was conducted at room temperature (25 °C)	0	0
11.	5 equiv of DMSO was used	40	0
12.	3 equiv of Na_2CO_3 was used	7	trace
13.	3 equiv of K_3PO_4 was used	trace	trace
14.	3 equiv of Et_3N was used	trace	trace
15.	reaction was conducted without I_2 (blanck experiment)	0	0
16.	reaction was conducted without TFAA (blanck experiment)	0	trace
17.	reaction was conducted under Ar-atmosphere	trace	trace
18.	**reaction was conducted for 1.5 h (*condition A*)**	**91**	**trace**
19.	reaction was conducted in toluene (0.4 M) using 2 equiv of DMSO for 22 h	60	trace
20.	**reaction was conducted in toluene (0.4 M) using 3 equiv of DMSO for 22 h (*condition B*)**	**92**	**trace**
21.	reaction was conducted in *m*-xylene (0.4 M) using 3 equiv of DMSO for 22 h	60	15
22.	reaction was conducted in DMF (0.4 M) using 3 equiv of DMSO for 22 h	trace	trace

[a]All the reactions were conducted in 0.1 mmol scale; [b]yield of products were determined by ^{1}H-NMR of the crude using 1,3,5-trimethoxybenzene as the internal standard

However, only 50% **3aa** was formed using 10 mol % of I_2 (entry 2, Table 2.3.1). When 20 mol% of tetrabutylammonium iodide (TBAI) was used instead of I_2, 65% of **3aa** was formed (entry 3, Table 2.3.1).

Among various electrophilic reagents such as TFAA, acetic anhydride, CF_3SO_2Cl, and *p*-$NO_2C_6H_4SO_2Cl$, TFAA was found to be the best (entries 5−7 vs entry 1, Table 2.3.1).

The use of 3 equiv of TFAA was found optimum for the reaction (entries 4 and 8 vs entry 1, Table 1). Lowering of reaction temperature from 120 °C had a negative impact on the reaction outcome; no product was formed at room temperature (entries 9 and 10 vs entry 1, Table 2.3.1). Lowering the stoichiometry of DMSO also negatively impacted the reaction outcome (entry 11, vs entry 1, Table 2.3.1). The use of inorganic and organic bases such as Na_2CO_3, K_3PO_4, and Et_3N also harmed the reaction's outcome (entries 12−14, Table 2.3.1). The blank experiments revealed the essential roles of iodine and TFAA in this reaction (entries 15 and 16, Table 2.3.1). Notably, a trace amount of **3aa** was formed when the reaction was conducted under an argon atmosphere (entry 17, Table 2.3.1). Thus, heating the reaction mixture of **1a** with 10 equiv of DMSO **2a** in the presence of 20 mol% I_2 and 3 equiv of TFAA at 120 °C under aerobic atmosphere for 1.5 h (conditions **A**) was found as the optimum conditions to furnish **3aa** in 91% yield (entry 18, Table 2.3.1). To decrease the methyl sulfoxide loading, which would be useful for the reactions with other methyl sulfoxides, particularly the ones with a high melting point, we conducted several experiments using another solvent and DMSO. Among various solvents such as toluene, m-xylene, and DMF, toluene was found to be the best (entries 19−22, Table 2.3.1), and by using the same, the stoichiometry of DMSO could be lowered to 3 equiv. The reaction of **1a** with 3 equiv of **2a** in the presence of 20 mol % I_2 and 3 equiv of TFAA in toluene (0.4 M) at 120 °C under aerobic atmosphere (conditions B) furnished **3aa** in 92% yield (entry 20, Table 2.3.1).

Next, we explored the scope of 2-(arylethynyl)-1,1′-biaryls for the methythiolative annulation reaction with DMSO under conditions **A** or **B** (Scheme-2.3.2). Various electron-withdrawing and -donating group substituted 2-(phenylethynyl)-1,1′-biaryls participated in the reaction with DMSO smoothly under conditions A to furnish 10-phenyl-9-sulfenylphenanthrenes (**3ba**−**3ha**) in moderate to high yield. Notably, various halogens (Br, Cl, and F) were found intact in the various positions of phenanthrenes, which could further be utilized for the products' synthetic diversification via cross-coupling reaction. Moreover, electron-donating and -withdrawing group substituted 2-(arylethynyl)-1,1′-biphenyls also underwent methythiolative annulation reaction with DMSO under conditions **A** or **B** to furnish 10-aryl-9-sulfenylphenantheres (**3ia**−**3la**) in moderate to high yield except 2-(4-cyanophenylethynyl)-1,1′-biphenyl, which furnished the corresponding product, 4-(10-(methylthio)phenanthren-9-yl)benzonitrile (**3la**) in 31% yield.

Table 2.4.2. Substrate Scope

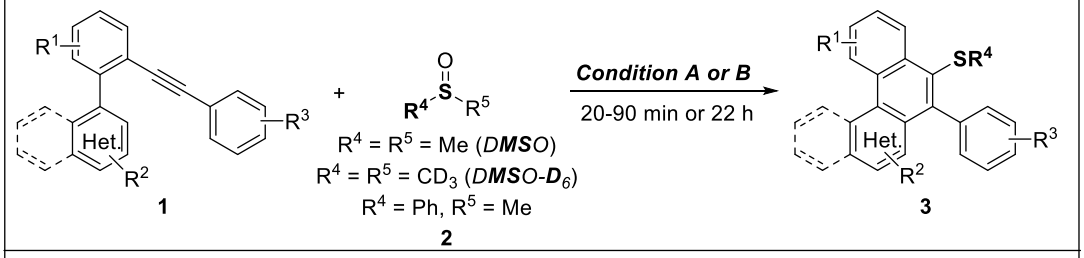

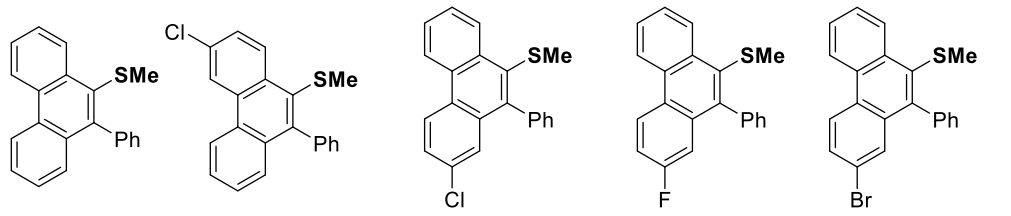

3aa (88%)[a] **3ba** (60%)[a] **3ca** (69%)[a] ***CCDC:2052187*** **3da** (82%)[a] ***CCDC:2041730*** **3ea** (67%)[a] ***CCDC:2033891***

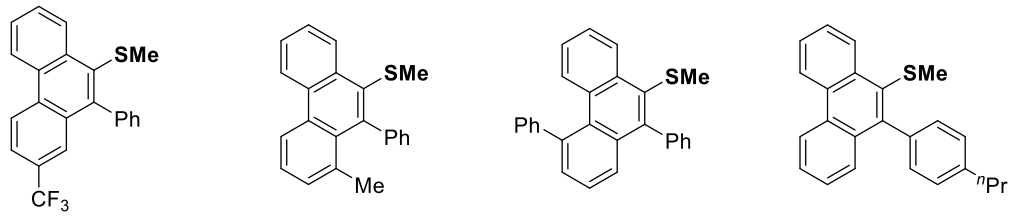

3fa (70%)[a] ***CCDC:2041729*** **3ga** (54%)[a] **3ha** (80%)[a] ***CCDC:2052186*** **3ia** (71%)[b]

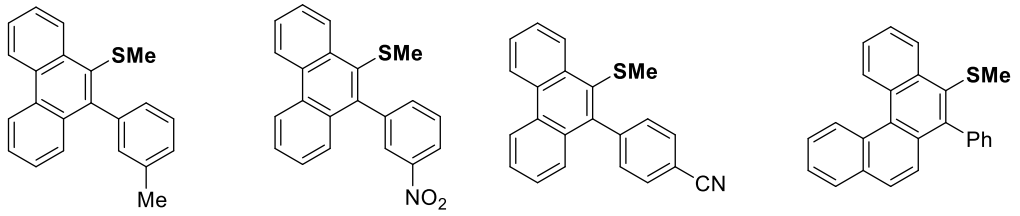

3ja (81%)[a] **3ka** (62%)[a] **3la** (31%)[a] **3ma** (35%)[a]

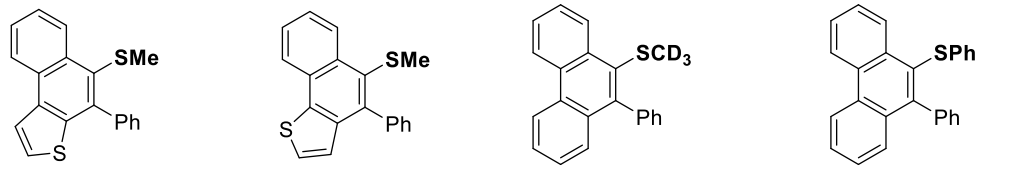

3na (60%)[a] **3oa** (25%)[a] **3ab** (80%)[a] ***CCDC:2044602*** **3ac** (81%)[b]

[a]Reaction condition A: 1 (0.5 mmol), 2 (10 equiv), I_2 (20 mol%), TFAA (3 equiv), 120 °C; [b]reaction condition B: 1 (0.5 mmol), 2 (3 equiv), I_2 (20 mol%), TFAA (3 equiv), toluene (0.4 M), 120 °C; [c]yield of product was reported in parentheses.

When 1-(2-(phenylethynyl)phenyl)- naphthalene was subjected to reaction with DMSO under conditions A, 6-phenyl-5-sulfenyl benzo[*c*]phenanthrene **3ma** was formed in low yield (35%). The 2-

heteroaryl-substituted phenylethynylbenzenes also participated in the reaction with DMSO to furnish the corresponding polycyclic heteroaromatics such as naphthothiophenes (**3na** and **3oa**). Significantly, the methylthiolative annulation was found to be highly regioselective since only one regioisomer, 5-(methylthio)-4-phenylnaphtho[2,1-*b*]thiophene **3na** was formed from 3-(2-(phenylethynyl)phenyl)thiophene 1n, which also supported the electrophilic annulation reaction. The reaction of 2-(phenylethynyl)-1,1′-biphenyl **1a** with DMSO-d6 **2b** under conditions A furnished (methyl-d_3)(10- phenylphenanthren-9-yl)sulfane **3ab** in 80% yield, which further supported that the source of the thiomethyl group is DMSO. When methyl phenyl sulfoxide **2c** was subjected to reaction with **1a** under conditions **B**, 81% of phenyl(10- phenylphenanthren-9-yl)sulfane 3ac was formed. The structures of **3ca**, **3da**, **3ea**, **3fa**, **3ha**, and **3ab** were confirmed by Xray crystallographic structure determination (Figures 2.3.1-2.3.6 and Table 2.3.3).

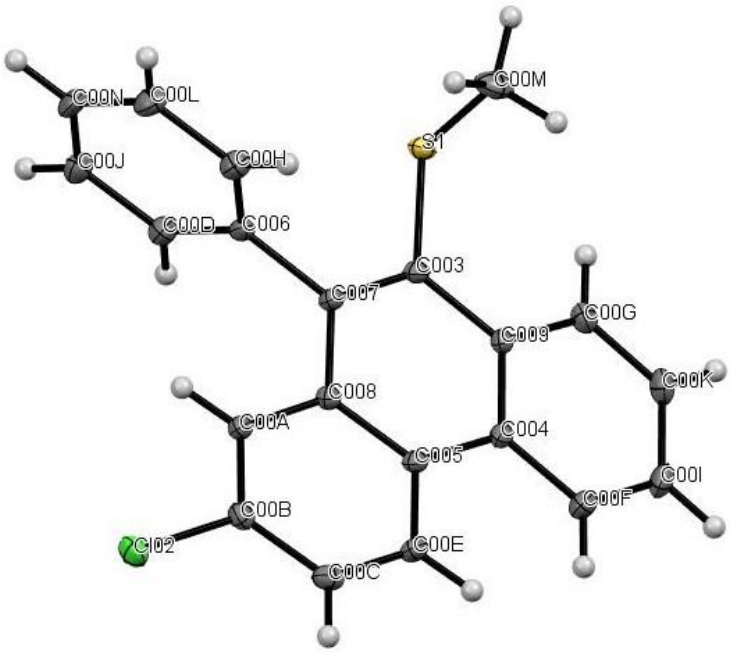

Figure *2.4.1.* X-ray Crystal Structure of **3ca** (Thermal Ellipsoids Shown at 50% Probability) including Atomic Numbering.

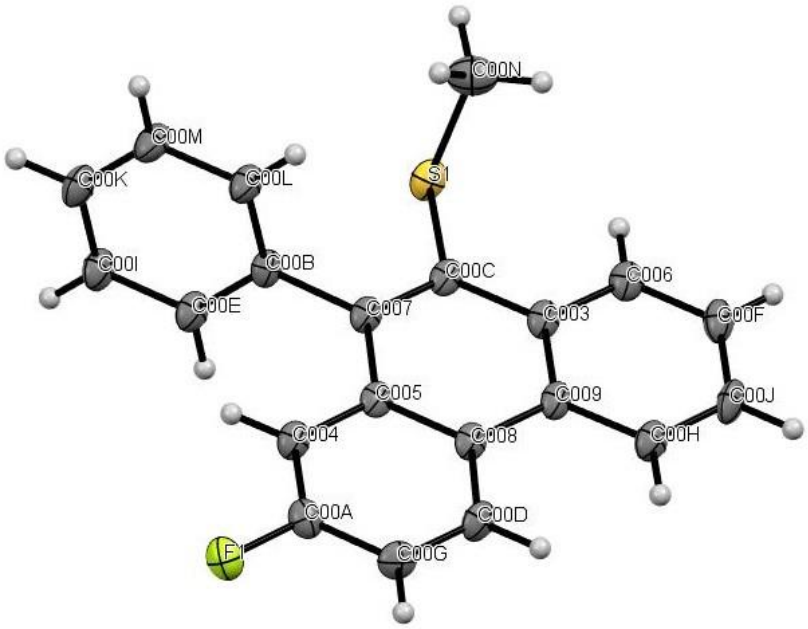

Figure 2.4.2. X-ray Crystal Structure of **3da** (Thermal Ellipsoids Shown at 50% Probability) Including Atomic Numbering.

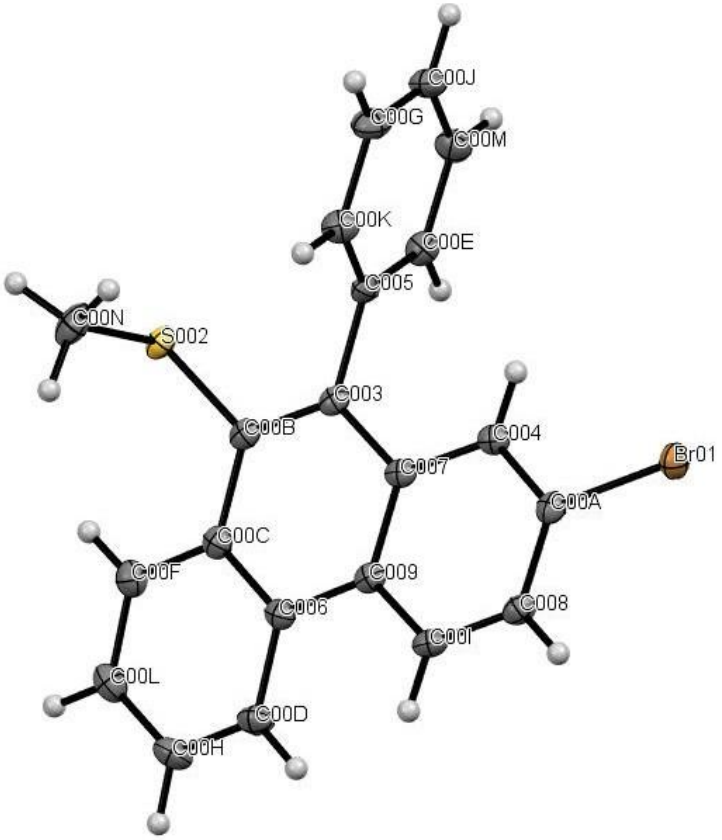

Figure 2.4.3. X-ray Crystal Structure of **3ea** (Thermal Ellipsoids Shown at 50% Probability) Including Atomic Numbering.

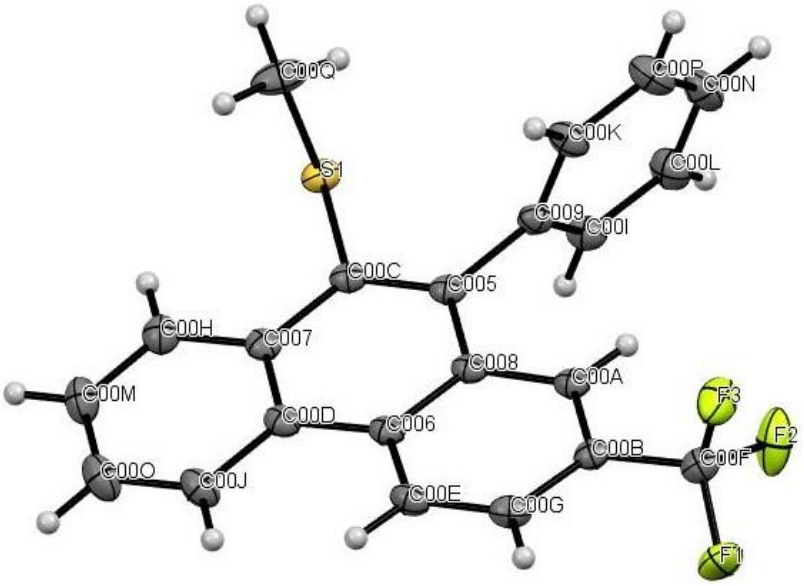

Figure 2.4.4. X-ray Crystal Structure of **3fa** (Thermal Ellipsoids Shown at 50% Probability) Including Atomic Numbering.

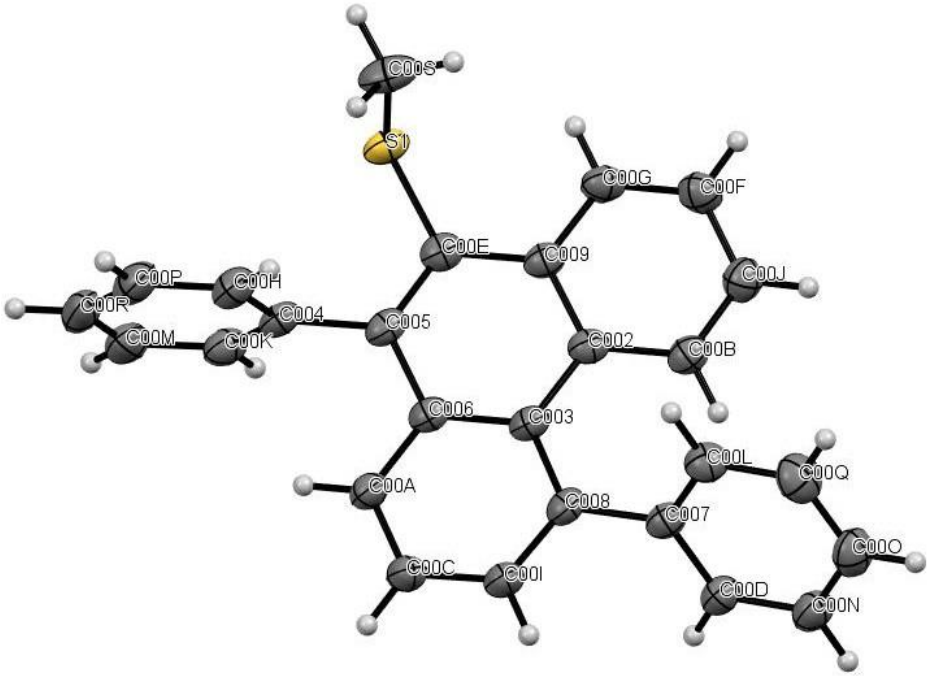

Figure 2.4.5. X-ray Crystal Structure of **3ha** (Thermal Ellipsoids Shown at 50% Probability) Including Atomic Numbering.

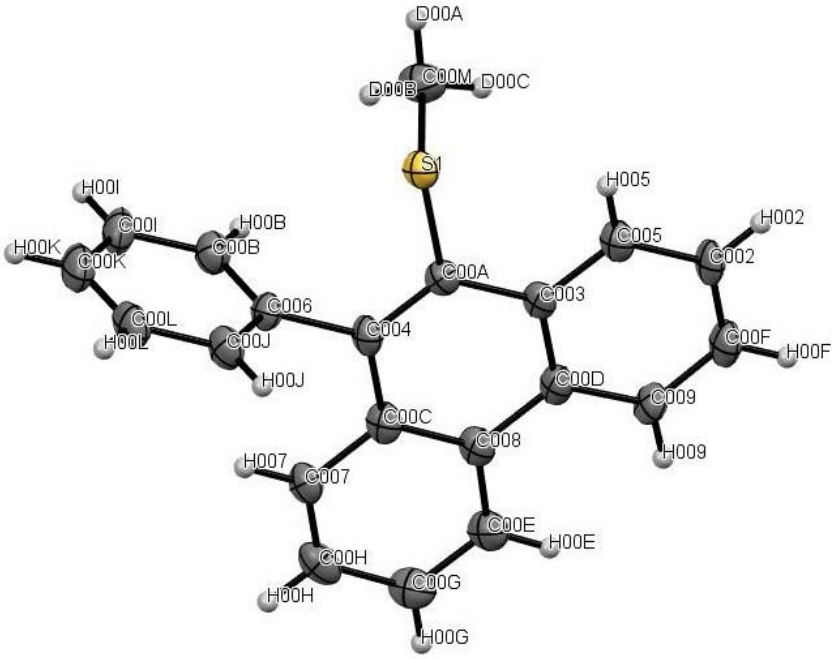

Figure 2.4.6. X-ray Crystal Structure of **3ab** (Thermal Ellipsoids Shown at 50% Probability) Including Atomic Numbering.

Table-2.4.3. Selected crystal data for compounds **3ca**, **3da**, **3ea**, **3fa**, **3ha** and **3ab.**

Parameters	**3ca**	**3da**	**3ea**	**3fa**	**3ha**	**3ab**
Empirical formula	$C_{21}H_{15}ClS$	$C_{21}H_{15}FS$	$C_{21}H_{15}BrS$	$C_{22}H_{15}F_3S$	$C_{27}H_{20}S$	$C_{21}H_{13}D_3S$
Formula weight	191.34	181.94	216.74	196.48	188.24	202.28
Temperature/K	293(2)	293(2)	293(2)	293(2)	293(2)	293
Crystal system	orthorhombic	monoclinic	orthorhombic	orthorhombic	triclinic	monoclinic
Space group	P b c a	P 1 21/c 1	P b c a	P b c a	P -1	P 1 21 1
a/Å	17.1061(3)	9.5122(6)	17.1503(2)	17.3252(2)	10.3879(5)	9.3352(4)
b/Å	9.8468(2)	20.3790(12)	9.94820(10)	10.15760(10)	10.6688(6)	7.6102(2)

c/Å	18.8077(3)	8.0902(7)	18.8746(2)	19.4281(3)	11.1966(4)	11.3177(4)
α (°)	90	90	90	90	94.935(4)	90
β (°)	90	98.616(7)	90	90	114.042(4)	105.900(4)
γ(°)	90	90	90	90	115.081(5)	90
Volume/Å³	3167.98(10)	1550.58(19)	3220.28(6)	3419.00(7)	974.87(9)	773.28(5)
Z	14	7	14	15	4	3
μ/mm^{-1}	3.310	1.900	4.638	1.978	1.520	1.776
D_x [g cm^{-3}]	1.404	1.364	1.565	1.431	1.283	1.303
F(000)	1392	664	1536	1520	396	316
2Θ range for data collection (°)	5.3810 - 79.5520	5.9700 - 78.9390	4.6630 - 79.4670	4.5320 - 79.3650	4.5870 - 78.4120	7.0740 - 79.1830
Index ranges	-19≤ h ≤ 21, -11 ≤ k ≤ 12, -23 ≤ l ≤ 15	-11≤ h ≤ 12, -19 ≤ k ≤ 25, -10 ≤ l ≤ 9	-20≤ h ≤ 21, -6 ≤ k ≤ 12, -22 ≤ l ≤ 23	-11≤ h ≤ 21, -12 ≤ k ≤ 7, -24 ≤ l ≤ 23	-12≤ h ≤ 13 -13 ≤ k ≤ 7, -13 ≤ l ≤ 14	-11≤ h ≤ 10 -4 ≤ k ≤ 9, -14 ≤ l ≤ 14
Reflections measured	10930	7901	11955	13776	9191	3636
Unique reflections	3379	3255	3428	3644	4080	1911
Parameters /restraints/	209/0	210/0	209/0	236/0	254/0	201/1
Goodness-of-fit on F2	1.054	1.106	1.114	1.128	1.103	0.883

R_1 [$I \geq 2\sigma$ (I)]	0.0647	0.0682	0.0368	0.0367	0.0714	0.0575
wR_2 (all data)	0.1814	0.2078	0.1146	0.1297	0.2150	0.1548
Largest diff. peak/hole/e Å^{-3}	0.454/-1.010	0.576/-0.833	0.450/-1.179	0.282/-0.321	0.505/-0.833	0.695/
CCDC	**2052187**	**2041730**	**2033891**	**2041729**	**2052186**	**2044602**

To shed light on the reaction mechanism, we carried out few reactions, as outlined in Scheme 2.3.3. The reaction of **1a** with diphenyl sulfoxide did not furnish **3ac** (Scheme 2.3.3A), which revealed the requirement of methyl sulfoxides to synthesize 9-sulfenyl phenanthrenes from 2-alkynyl biaryls.**Scheme 2.3.2.** Mechanistic Studies.

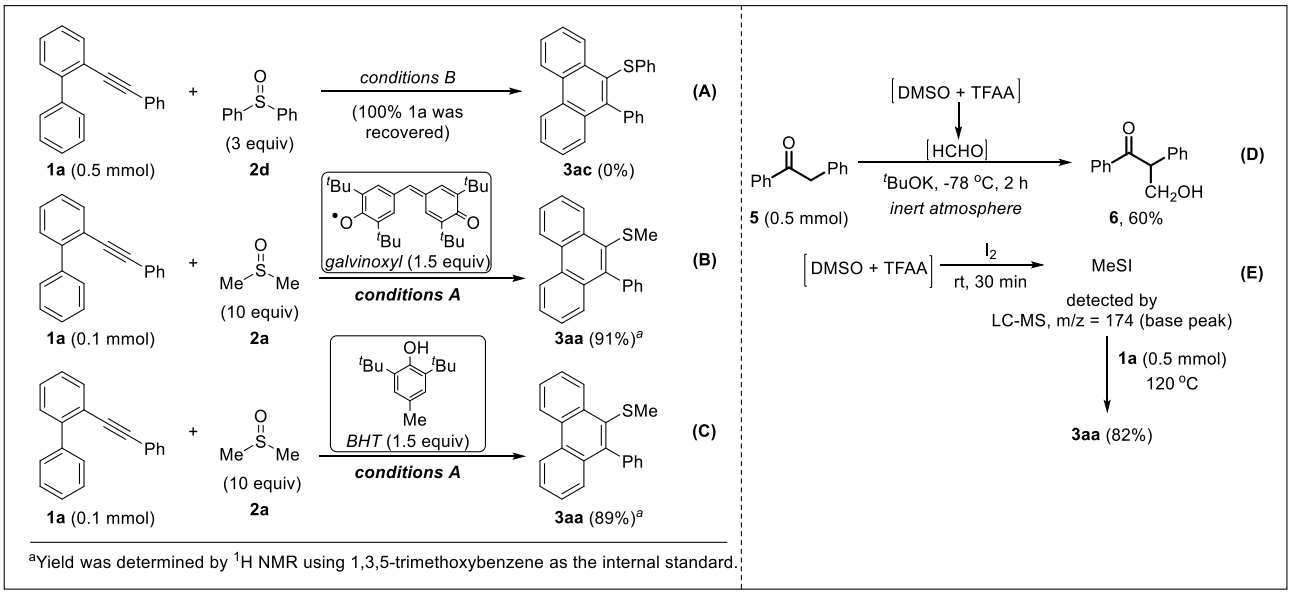

A couple of radical quenching experiments of the model reaction in between **1a** and DMSO **2a** in the presence of a radical quencher such as galvinoxyl (Scheme 2.3.3B) and butylated hydroxytoluene (BHT) (Scheme 2.3.3C) were conducted, and **3aa** was formed in 91% and 89% yield, respectively, revealing the non-involvement of free-radicals in the reaction. To prove the in situ decomposition of DMSO to MeSH and HCHO by TFAA, we probe a reaction for the in situ detection of formaldehyde, as outlined in Scheme 2.3.3D. The nucleophilic addition of the enolate of 2-phenylacetophenone (**5**) to the *in situ* formed formalde-hyde from DMSO and TFAA furnished 3-hydroxy-1,2-diphenylpropan-1-one in 60%

yield. When the mixture of DMSO and TFAA was treated with I_2 and stirred at room temperature for a while, MeSI was formed in situ, as evident by the LC-MS analysis (base peak at *m/z* = 174) of the reaction mixture (Figure 2.3.7).

Scheme 2.4.3. Plausible Reaction Mechanism.

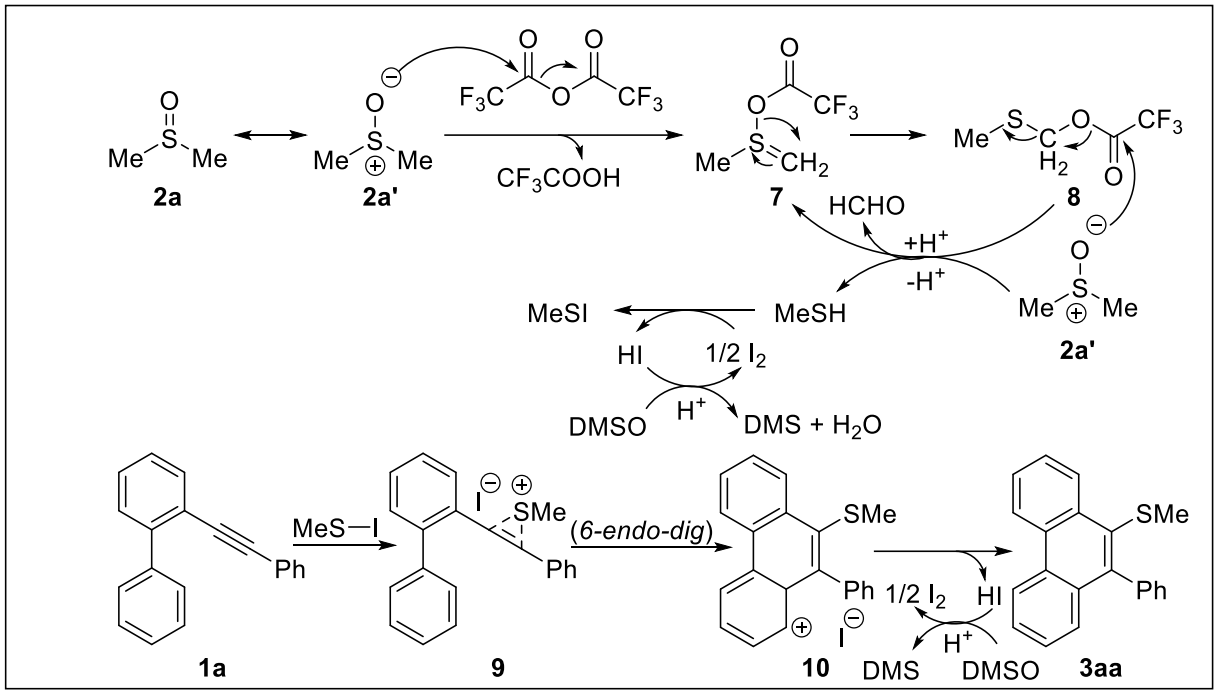

After 30 min, when **1a** was added to the reaction mixture and it was heated at 120 ^oC for 1.5 h, **3aa** was produced in 82% yield (Scheme 2.3.3E) which supported the fact that the intermediate MeSI is the active electrophilic species for the methylthiolative annulation of 2-alkynyl biaryls.

Based on the mechanistic studies and the previous literature reports,[3] we proposed a plausible mechanism for the methylthiolative annulation reaction of 2-alkynyl biaryls with DMSO as outlined in Scheme 4. Nucleophilic acyl substitution of TFAA by DMSO followed by deprotonation produced a sulfur ylide **7** along with the formation of trifluoroacetic acid (TFA). A rearrangement of the ylide (**7**) through the intramolecular migration of trifluoroacetate group from the *S*-centre to more electrophilic *C*-centre furnished **8**. Next, *in situ* generated acid (TFA)-catalyzed nucleophilic acyl substitution of **8** by another DMSO molecule (**2a′**) reproduced the sulfur ylide **7** along with the formation of MeSH and HCHO through C-O and C-S bond cleavage. The *in situ* formed MeSH then immediately reacted with iodine to form the active electrophilic species, MeSI, along with the formation of HI. Finally, the electrophilic annulation of **1a** (6-*endo*-dig cyclization) with MeSI furnished **3aa** along with the formation of HI again, which was finally oxidized by DMSO under acidic conditions to regenerate iodine in the catalytic cycle.[5]

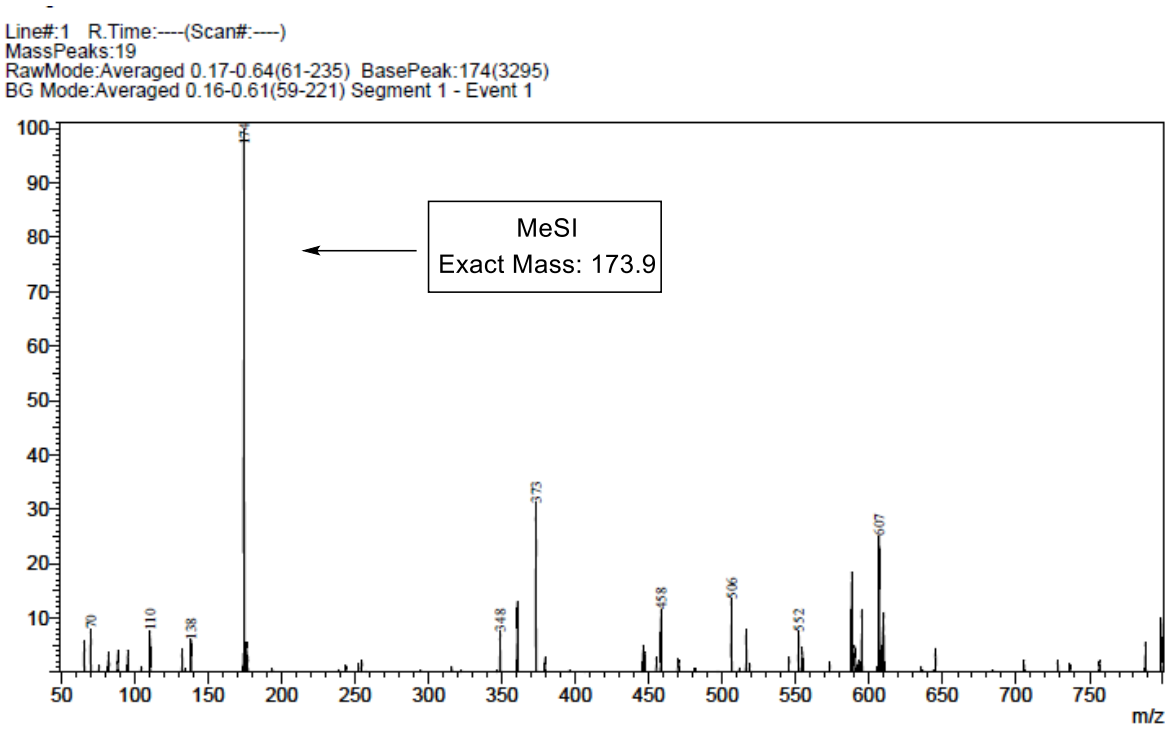

Figure 2.4.7. *In situ* Detection of MeSI by the Base Peak of the MS Spectrum at m/z = 174

The synthetic diversification of the product, 10-phenyl-9-sulfenyl phenanthrene **3aa** was demonstrated through sustainable and selective oxidation reactions using oxone as the oxidant to the corresponding sulfoxide and sulfone (Scheme 2.3.4). When **3aa** was heated with 0.6 equiv of oxone in ethanol at 60 °C, 91% of the corresponding sulfoxide **11** was formed selectively.[6] However, when 3 equivalent of oxone was used in ethanol, 83% of the corresponding sulfone **12** was formed (Table 2.3.4).

Scheme 2.4.4. Synthetic Diversification of Sythesized Product, 10-phenyl-9-sulfenyl phenanthrene 3aa.[a]

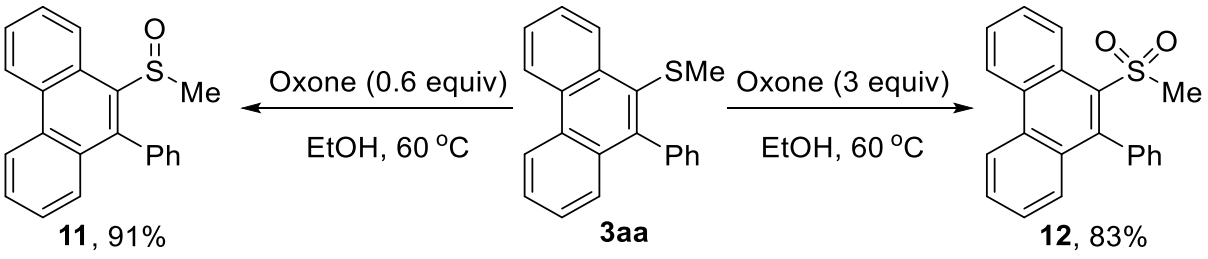

[a]Reactions were performed on a 0.3 mmol scale

Table-*2.4.4.* Optimization of the Reaction Conditions for the Synthesis of **11** and **12**.

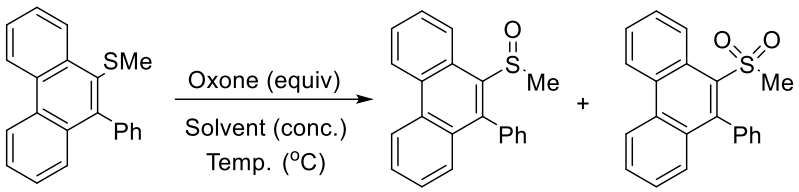

3aa **11** **12**

Entry	Oxone (equiv)	Solvent (conc.)	Temperature (°C)	Yield (%)[b]	
				11	**12**
1	0.6	EtOH (0.067 M)	60	95	0
2	1.5	H_2O (0.067 M)	60	0	0
3	3	H_2O (0.067 M)	60	0	0
4	1.5	EtOH:H_2O (1:1) (0.1 M)	60	0	0
5	3	EtOH:H_2O (1:1) (0.1 M)	60	60	40
6	6	EtOH:H_2O (1:1) (0.1 M)	60	60	40
7	3	EtOH (0.2)	60	0	83
8	6	EtOH (0.2)	60	0	82
9	3	EtOH (0.2)	100	0	83

[a]Reaction conditions: **3aa** (0.3 mmol). [b]Yield of isolated product is reported.

2.4.3. Conclusion

In conclusion, we have developed an iodine-catalyzed sustainable, cost-effective, and atom-economic synthetic methodology for the methylthiolative annulation of 2-alkynyl biaryls with DMSO to synthesize a wide variety of sulfenyl-phenanthrenes and polycyclic heteroaromatics, i.e., naphthothiophenes (15 new molecules) in moderate to good yields under transition-metal-free, aerobic, and simple reaction conditions. The mechanistic studies revealed that the reaction proceeded through the *in situ* decomposition of DMSO by TFAA to formaldehyde and MeSH, facilitated under the *in situ* formed acid catalytic conditions. Notably, DMSO played multiple roles in the methylthiolative annulation reaction, such as the methylthiolating reagent, oxidant, and solvent. The synthetic utility of the synthesized product, 10-phenyl-9-sulfenylphenanthrene **3aa**, was demonstrated by preparing other new but potential molecules, 9-(methylsulfinyl)-10-phenylphenanthrene and 9-(methylsulfonyl)-10-phenylphenanthrene through selective and sustainable oxidation of **3aa** by using oxone. To the best of our knowledge, this is the first report of iodine catalyzed methylthiolative annulation reaction using DMSO as the sulfur-source. We believe this

cost-effective, sustainable, atom-economic, and simple strategy will be further explored in synthesizing various potential classes of organic molecules.

2.4.4. Experimental Section.

Experimental Procedure for the Synthesis of 2-(Phenylethynyl)-1,1'-biaryls (1a -1k).

Reperesentative Experimental Procedure for the Synthesis of 5-Chloro-2-(phenylethynyl)-1,1'-biphenyl (1b):

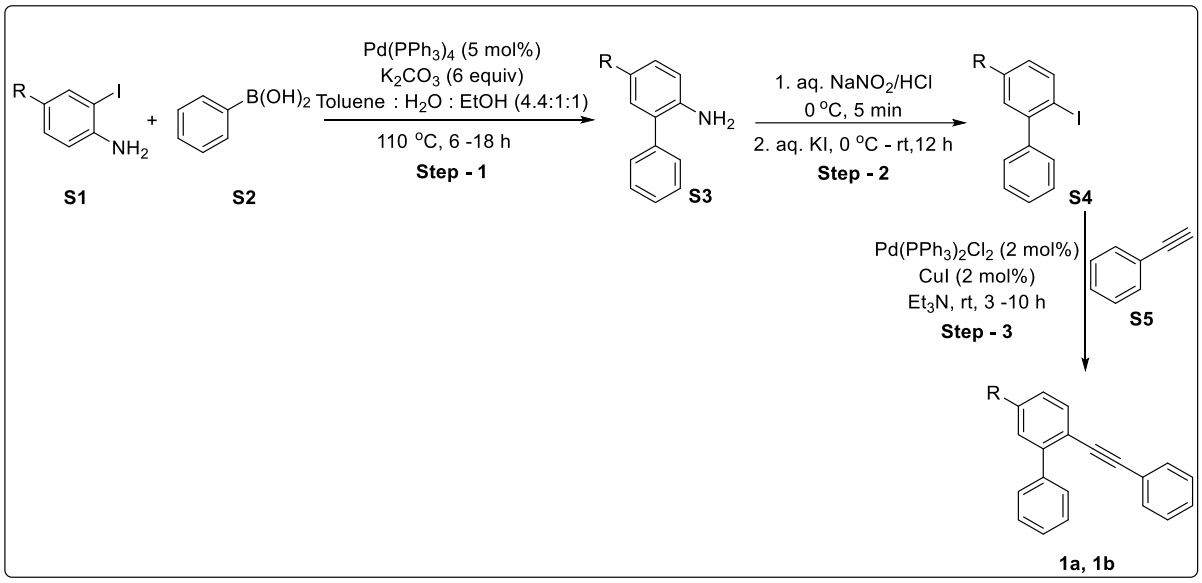

Step-1:[7] 4-chloro-2-iodoaniline ***S1*** (2.54 g, 10 mmol, 1 equiv), phenyl boronic acid (0.403 g, 10 mmol), $Pd(PPh_3)_4$ (0.578 g, 0.5 mmol), K_2CO_3 (8.3 g, 60 mmol) and solvent (320 mL, PhMe : H_2O : EtOH = 4.4:1:1) were taken in a 250 mL round-bottom flask (RBF). The reaction mixture was refluxed and the progress of the reaction was monitored by thin layer chromatography until the completion of the reaction. The mixture was cooled to room temperature and extracted with ethyl acetate (30x3 mL) three times. The combined organic layer was further washed with brine (30 mL) and subsequently dried over anhydrous Na_2SO_4. Finally the solvent was evaporated under reduced pressure to get the crude product which was purified by flash column chromatography on silica gel to afford 4-chloro-[1,1'-biphenyl]-2-amine ***S3*** (1.98 g, 9.7 mmol) in 97% yield.

The corresponding analytical data also matched with the reported literature.[7]

Step-2:[7] 4-chloro-[1,1'-biphenyl]-2-amine ***S3*** (1.6 g, 8 mmol, 1 equiv) was added to a solution of aqueous HCl (4.16 mL in 13 mL H_2O) and cooled to 0 ^oC and was added gradually to aqueous solution of $NaNO_2$ (0.672 g in 13.28 mL H_2O) and KI (2 g in 13.28 mL H_2O) at 0 ^oC. The reaction mixture was stirred for 10-

15 min at 0 ^{o}C and further stirring was continued at room temperature for 12 h. After the completion of the reaction, saturated $Na_2S_2O_3$ solution was added. The crude reaction mixture was extracted with ethyl acetate (30x3 mL) and washed with water (30x2 mL) twice and purified through silica-gel coloumn chromatography to provide 5-chloro-2-iodo-1,1'-biphenyl ***S4*** (1.58 g, 5 mmol) in 64% yield.
The corresponding analytical data also matched with the reported literature.[7]

Step-3:[8] 5-Chloro-2-iodo-1,1'-biphenyl ***S4*** (1.58 g, 5 mmol, 1 equiv), $Pd(PPh_3)_2Cl_2$ (0.07 g, 0.2 mmol), CuI (0.038 g, 0.2 mmol) and Et_3N (13 mL) were added in a flame-dried two neck RBF under N_2 atmosphere in a standard Schlenk-line process and stirred for 5 min at room temperature. Then phenylacetylene ***S2*** (659 µL, 6 mmol, 1.2 equiv) was added to the reaction mixture under nitrogen atmosphere. The reaction mixture was stirred for 3 h at room temperature. After the completion of the reaction, the solvent was evaporated under reduced pressure. The crude reaction mixture was diluted with ethyl acetate (30 mL) and washed with water three times (3 x 10 mL). The crude product was purified through silica gel column chromatography to provide 2-chloro-5-(phenylethynyl)-1,1'-biphenyl **1b** (1.275 g, 4.4 mmol) in 88.5% yield.

The corresponding analytical data also matched with the reported literature.[8]

1a was also synthesized from commercially available [1,1'-biphenyl]-2-amine by following the **step-2** and **step-3** as mentioned above. The corresponding analytical data also matched with the reported literature.[8]

General Experimental Procedure for the Synthesis of 2- (phenylethynyl)-1,1'-biaryls (1c-1k and 1m-1o):

Reperesentative Experimental Procedure for the Synthesis of 4'-Chloro-2-(phenylethynyl)-1,1'-biphenyl (1c):

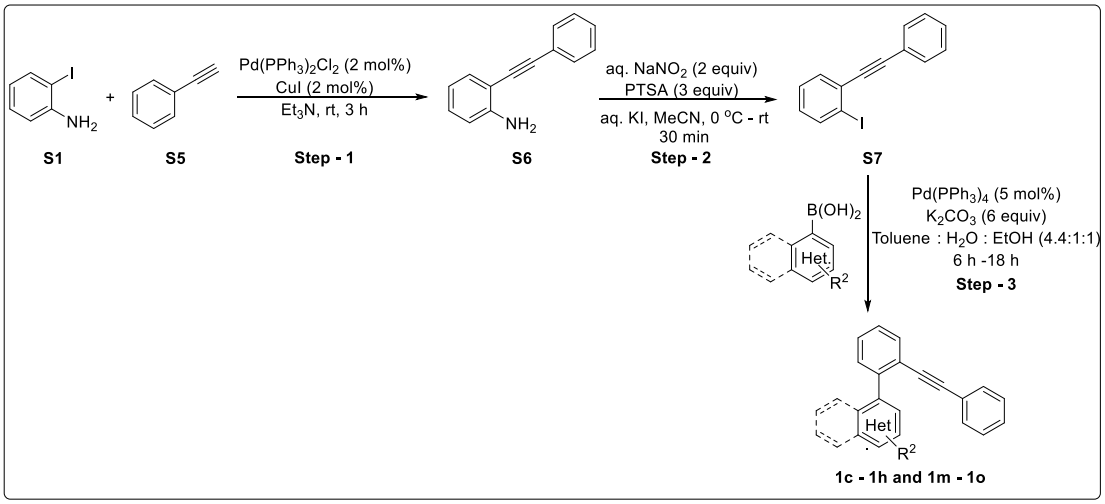

Step-1:[9] 2-Iodoaniline ***S1*** (2.19 g, 10 mmol, 1 equiv), $Pd(PPh_3)_2Cl_2$ (0.14 g, 0.4 mmole), CuI (0.076 g, 0.4 mmol) and Et_3N (26 mL) were taken in a flame-dried two neck RBF in a standard Schlenk-line process under N_2 atmosphere and the solution was stirred at room temperature for 5 minutes. Phenylacetylene ***S5*** (1318 μL, 12 mmol, 1.2 equiv) was added to the RBF and the reaction mixture was stirred for 3 h at room temperature. After the completion of the reaction, the solvent was evaporated. The crude reaction mixture was diluted with ethyl acetate (100 mL) and washed with water three times (3 x 10 mL). The crude product was purified through silica gel column chromatography to provide 2-(phenylethynyl)aniline ***S6*** (1.62 g, 8.4 mmole) in 84% yield as yellow solid.

The corresponding analytical data also matched with the reported literature.[9]

Step-2:[10] 2-(phenylethynyl)aniline ***S6*** (1.55 g, 8 mmol) was added to a solution of *p*-TsOH.H_2O (4.57 g, 24 mmol) dissolved in MeCN (48 mL). The resulting suspension of ammonium salt was cooled to 0 ^oC and was added gradually to a solution of $NaNO_2$ (1.11 g, 16 mmol) and KI (3.32 g, 20 mmol) in water (4.8 mL). The reaction mixture was stirred for 10-15 min at 0 ^oC. After the completion of the reaction, saturated $NaHCO_3$ and $Na_2S_2O_3$ solution was added. The crude reaction mixture was extracted with ethyl acetate (100 mL) and washed with water (30x3 mL) three times and purified through silica-gel coloumn chromatography to provide 1-iodo-2-(phenylethynyl)benzene ***S7*** in 50% yield as yellow liquid.

The corresponding analytical data also matched with the reported literature.[10]

Step-3 [11] 1-iodo-2-(phenylethynyl)benzene ***S4*** (0.913 g, 3 mmol), phenyl boronic acid (0.403 g, 3.3 mmol), $Pd(PPh_3)_4$ (0.174 g, 0.15 mmol), K_2CO_3 (2.5 g, 18 mmol) and solvent (96 mL, PhMe : H_2O : EtOH = 4.4:1:1) were added subsequently in a 250 mL round-buttom flask. The resulting mixture was refluxed and the progress of the reaction was monitored by thin layer chromatography up to completion. The mixture was cooled to room temperature and extracted with ethyl acetate. The combined organic layer was dried over anhydrous Na_2SO_4. The solvent was evaporated under reduced pressure to get the crude product which was purified by flash column chromatography on silica gel to afford 4'-chloro-2-(phenylethynyl)-1,1'-biphenyl **1c** (0.704 g, 2.1 mmol) in 70% yield.

The corresponding analytical data also matched with the reported literature.[11]

The other starting materials **1d-1h** and **1m-1o** were also synthesized by following the above mentioned protocol.

Reperesentative Experimental Procedure for the Synthesis of 2-(*m*-tolylethynyl)-1,1'-biphenyl (1j):

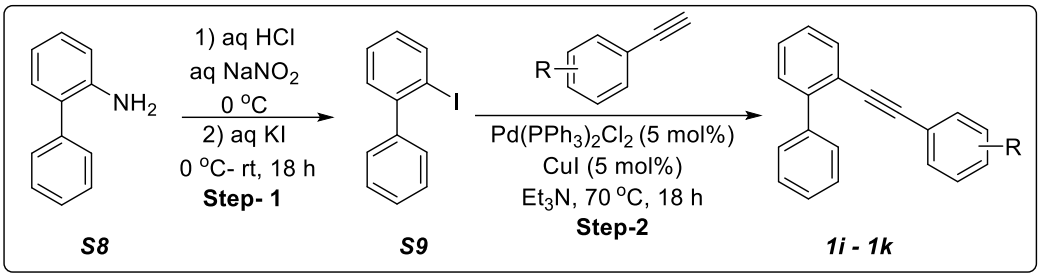

Step-1:[12] [1,1'-biphenyl]-2-amine ***S8*** (1.70 g, 10 mmol) was taken to aqueous HCl (5.2 mL, H_2O 16.6 mL) solution. The reaction mixture was cooled to 0-5 °C. After 5 min aqueous $NaNO_2$ solution (0.84 g in 16.6 mL H_2O) was added dropwise at 0-5 °C. The resulting solution turns yellow after the addition of aqueous KI solution (2.50 g in 16.6 mL H_2O). The reaction mixture was stirred vigorously for 18 h. After the completion of the reaction the solution was quenched by the addition of aqueous $Na_2S_2O_3$ solution. The resulting solution was extracted by ethyl acetate (30 x 3 mL) and washed with water (30 mL). The combined organic layer was dried over anhydrous Na_2SO_4. The solvent was evaporated under reduced pressure to get the crude product which was purified by flash column chromatography on silica gel to afford 2-iodo-1,1'-biphenyl (2.38 g, 8.5 mmol) ***S9*** in 85% yield.

The corresponding analytical data also matched with the reported literature.[12]

Step-2:[13] In a RBF, $PdCl_2(PPh_3)_2$ (0.105 g , 0.15 mmole) and CuI (0.028 g, 0.15 mmol) were added to a solution of 2-iodo-1,1'-biphenyl ***S9*** (2.80 g, 3 mmol) in Et_3N (9 mL) under nitrogen atmosphere in a standard Schlenk-line process. The reaction mixture was stirred for 5 min. Then, 1-ethynyl-3-methylbenzene (465 µL, 3.6 mmol, 1.2 equiv) was added to the RBF. The resulting mixture was then heated under nitrogen atmosphere at 70 °C for 18 h. The reaction mixture was allowed to cool to room temperature. Then, solvent was evaporated under reduced pressure. The crude reaction mixture was extracted with ethyl acetate thrice (3 x 30 mL). The combined organic layer was washed with water three times (3 x 30 mL) and concentrated under reduced pressure to get the crude product which was purified by column chromatography through silica gel to afford 2-(*m*-tolylethynyl)-1,1'-biphenyl **1j** (0.52 g, 1.94 mmol) in 63% yield.

The corresponding analytical data matched with the reported literature.[13]

The other starting materials **1g** and **1k** were also synthesized by following the above mentioned protocol.

Experimental Procedure for the Synthesis of 4-([1,1'-Biphenyl]-2-ylethynyl)benzonitrile(1l):

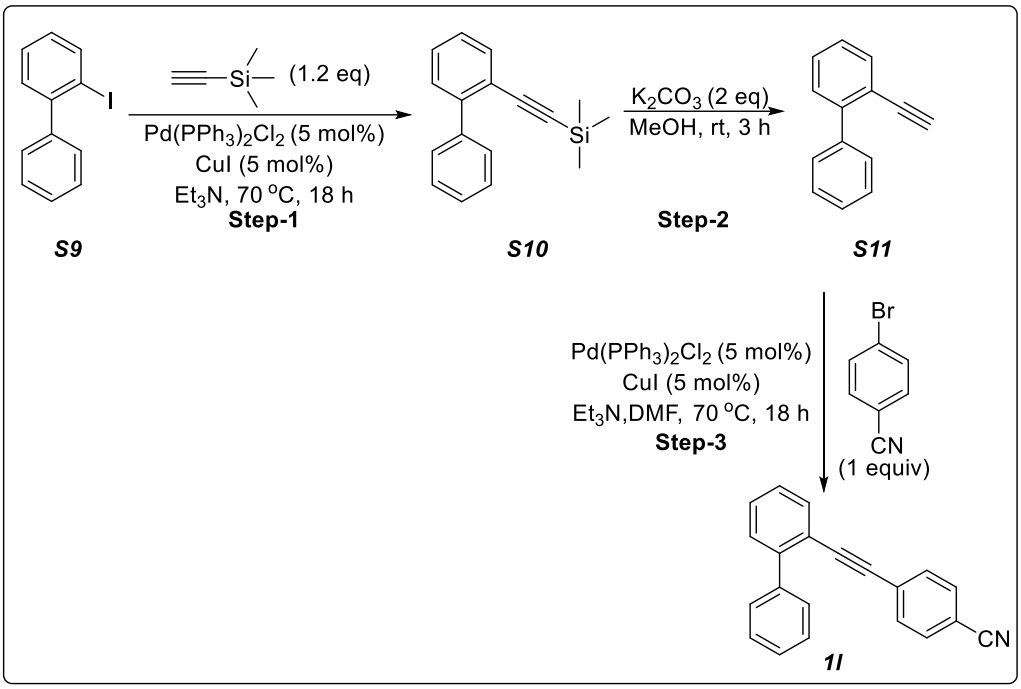

Step-1:[14] $PdCl_2(PPh_3)_2$ (0.14 g , 0.4 mmole) and CuI (0.076 g, 0.4 mmol) were added to a solution of 2-iodo-1,1'-biphenyl ***S9*** (2.80 g, 10 mmol) in Et_3N (26 mL) under nitrogen atmosphere in a standard Schlenk-line process. The reaction mixture was stirred for 5 min. Then, trimethylsilylacetylene (1709 µL, 12 mmol, 1.2 equiv) was added to the RBF. The resulting mixture was heated under an nitrogen atmosphere at 70 °C for 18 h. The mixture was allowed to cool to room temperature. The solvent was removed under reduced pressure. The crude reaction mixture was extracted with ethyl acetate thrice (3 x 30 mL). The combined organic layer was washed with brine (30 mL) and concentrated under reduced pressure. The crude product was purified by column chromatography through silica gel to afford the corresponding product, ([1,1'-biphenyl]-2-ylethynyl)trimethylsilane ***S10*** (1.0464 g, 4.2 mmole) in 42% yield.

The corresponding analytical data matched with the reported literature. [14]

Step-2:[15] K_2CO_3 (1.104 g, 8 mmol) was added into the solution of ([1,1'-biphenyl]-2-ylethynyl)trimethylsilane ***S7*** (1.001 g, 4 mmol) dissolved in MeOH (8.37 mL). The reaction mixture was stirred for 3 h at room temperature. After the completion of the reaction, solvent was evaporated under reduced pressure. The crude reaction mixture was extracted with ethyl acetate thrice (3 x 30 mL). The combined organic layer was washed with brine (30 mL) and concentrated under reduced pressure. The crude product was purified by column chromatography to get pure 2-ethynyl-1,1'-biphenyl ***S11*** in 99 % yield (0.704 g, 3.95 mmol).

The corresponding analytical data matched with the reported literature.[15]

Step-3:[16] To a solution of 4-bromobenzonitrile (231µL, 2 mmol, 1 equiv) in Et_3N (20 mL) and DMF (6 mL) were added $PdCl_2(PPh_3)_2$ (0.070 g , 0.1 mmol) and CuI (0.019 g, 0.1 mmol) under nitrogen atmosphere in a standard Schlenk-line process. The reaction mixture was stirred for 5 min under N_2 atmosphere. Then, 2-ethynyl-1,1'-biphenyl ***S11*** (337 µL, 2 mmol, 1 equiv) was added to the reaction mixture. The resulting mixture was then heated under an nitrogen atmosphere at 70 °C for 18 h. The mixture was allowed to cool to room temperature. The solvent was removed under reduced pressure. The crude reaction mixture was extracted with ethyl acetate thrice (3 x 30 mL). The combined organic layer was washed with brine solution (30 mL) and concentrated under reduced pressure. The crude product was purified by flash column chromatography through silica gel to afford the product 4-([1,1'-biphenyl]-2-ylethynyl)benzonitrile **1l** (0.2 g, 0.72 mmol) in 36% yield.

The corresponding analytical also matched with the literature report.[16]

Representative Experimental Procedure for the Synthesis of 10-aryl-9-sulfenyl phenanphrenes or naphthothiophenes (3aa - 3oa and 3ab - 3ac).

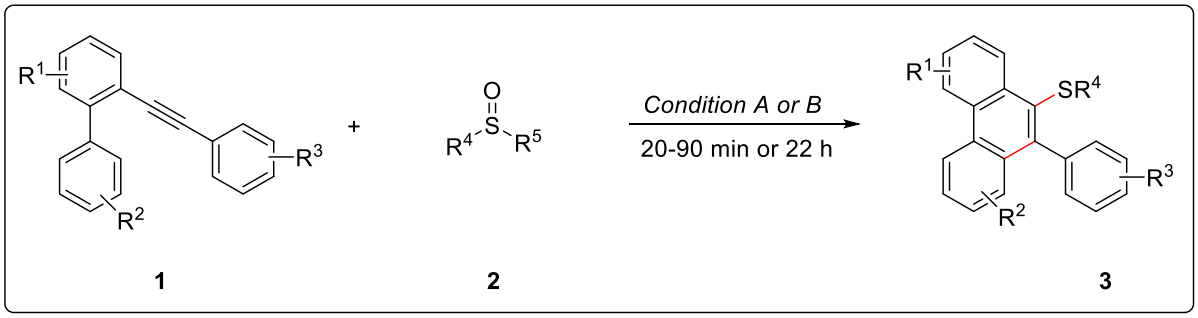

Condition A: To a solution of 2-(phenylethynyl)-1,1':2',1''-terphenyl **1h** (0.165 g, 0.5 mmol, 1 equiv) in DMSO **2a** (0.36 mL, 5 mmol, 1.4 M), I_2 (0.0254 g, 0.1 mmol) was added in a flame-dried RBF. Then, TFAA (0.212 mL, 1.5 mmol) was added to the RBF and the reaction mixture was stirred at 120 ^oC under aerobic atmosphere. The progress of the reaction was monitored by TLC. After completion of the reaction, the resulting solution was extracted with ethyl acetate thrice (3 x 10 mL) and the combined organic layer was washed with water (3 x 10 mL). The solvent was evaporated under reduced pressure to afford the crude product which was purified by flash column chromatography through silica gel to afford the product, (4,10-diphenylphenanthren-9-yl)(methyl)sulfane **3ha** (0.151 g, 0.401 mmol) in yield 80.3%.

Condition B: To a solution of 2-(phenylethynyl)-1,1'-biphenyl **1a** (0.127 g, 0.5 mmol, 1 equiv), (methylsulfinyl)benzene **2c** (0.21 g, 1.5 mmol, 3 equiv) in toluene (1.25 mL, 0.4 M), I_2 (0.0254 g, 0.1 mmol) was added in a flame-dried RBF. Then TFAA (0.212 mL, 1.5 mmol) was added to the RBF and the reaction

mixture was stirred at 120 °C under aerobic atmosphere. The progress of the reaction was monitored by TLC. After completion of the reaction the resulting solution was extracted with ethyl acetate thrice (3 x 10 mL). The combined organic layer was washed with water (3 x 10 mL) and evaporated under reduced pressure. The crude product was purified by flash column chromatography through silica gel to afford pure phenyl(10-phenylphenanthren-9-yl)sulfane **3ac** (0.147 g, 0.405 mmol) in 81.2% yield .

2.4.5. Analytical Data of the Synthesized Starting Materials and Products.

Analytical Data of Some Selected Starting Materials, 2-Alkynylbiaryls (1e – 1o)

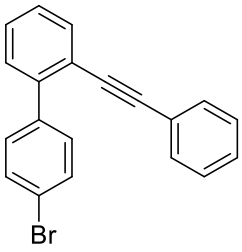

4'-Bromo-2-(phenylethynyl)-1,1'-biphenyl (1e): White solid; m.p.= 64 - 66 °C; **^{1}H NMR (400 MHz, $CDCl_3$)** δ 7.67 (d, *J* = 7.4 Hz, 1H), 7.58 (q, *J* = 8.7 Hz, 4H), 7.44 – 7.29 (m, 8H); **^{13}C NMR (100 MHz, $CDCl_3$)** δ 142.5, 139.4, 133.0, 131.3, 131.0, 129.3, 128.6, 128.3, 128.3, 127.4, 123.2, 121.8, 121.5, 92.6, 88.9 (overlapping peak present); **HRMS** (**ESI**), m/z: calcd for $C_{20}H_{13}Br$ $[M]^+$: 332.0201; found: 332.0203.

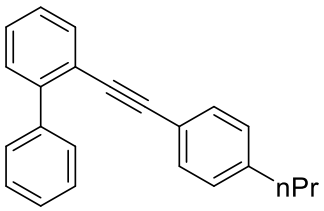

2-((4-Propylphenyl)ethynyl)-1,1'-biphenyl (1i): Yellow viscous liquid; **^{1}H NMR (400 MHz, $CDCl_3$)** δ 7.72 – 7.58 (m, 3H), 7.48 – 7.28 (m, 6H), 7.25 – 7.23 (m, 2H), 7.09 (d, *J* = 8.2 Hz, 2H), 2.59 – 2.53 (t, 2H), 1.61 (m, *J* = 7.5 Hz, 2H), 0.91 (t, *J* = 7.3 Hz, 3H); **^{13}C NMR (100 MHz, $CDCl_3$)** δ 143.8, 143.0, 140.6, 132.8, 131.2, 129.4, 128.42, 128.3, 127.8, 127.4, 127.0, 121.8, 120.6, 92.5, 88.7, 37.9, 24.3, 13.7 (overlapping peaks present); **HRMS** (ESI) m/z: calcd for $C_{23}H_{20}$ $[M]^+$: 296.1565; found: 296.1508.

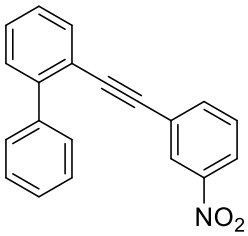

2-((3-Nitrophenyl)ethynyl)-1,1'-biphenyl (1k): Yellow solid; m.p.= 68 – 70 °C; **^{1}H NMR (400 MHz, $CDCl_3$)** δ 8.21 – 8.14 (m, 1H), 8.11 (ddd, *J* = 8.2, 2.3, 1.1 Hz, 1H), 7.70 – 7.65 (m, 3H), 7.60 – 7.56 (m, 1H), 7.52 (m, 2H), 7.49 – 7.45 (m, 3H), 7.44 – 7.35 (m, 2H); **^{13}C NMR (100 MHz, $CDCl_3$)** δ 148.0, 144.3, 140.2, 136.7, 132.8, 129.5, 129.2, 129.2, 127.9, 127.7, 127.1, 126.0, 125.1, 122.6, 120.5, 92.0, 89.6 (Overlapping peak present); **Anal** calcd for $C_{20}H_{13}NO_2$: C, 80.25; H, 4.38; N, 4.68; found C, 80.75; H, 4.18; N, 5.08.

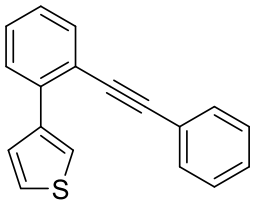

3-(2-(Phenylethynyl)phenyl)thiophene (1n): Colourless liquid; **^{1}H NMR (400 MHz, $CDCl_3$)** δ 7.71 (d, *J* = 2.9 Hz, 1H), 7.65 (d, *J* = 7.6 Hz, 1H), 7.55 (d, *J* = 5.0 Hz, 1H), 7.51 (d, *J* = 7.1 Hz, 1H), 7.47 – 7.43 (m, 2H), 7.42 – 7.37 (m, 2H), 7.37 – 7.28 (m, 5H); **^{13}C NMR (100 MHz, $CDCl_3$)** δ 141.0, 138.2, 133.2, 131.4, 129.0, 128.7, 128.6, 128.3, 128.2, 126.9, 124.7, 123.6, 123.4, 121.1, 92.6, 89.6; **Anal** calcd for $C_{18}H_{12}S$: C, 83.04; H, 4.65; S, 12.31; found C, 83.25; H, 4.78; S, 12.01.

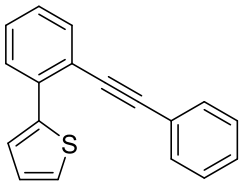

2-(2-(Phenylethynyl)phenyl)thiophene (1o): Colourless liquid; **^{1}H NMR (400 MHz, $CDCl_3$)** δ 7.63 (ddd, *J* = 8.9, 8.0, 1.6 Hz, 3H), 7.54 – 7.49 (m, 2H), 7.36 (ddd, *J* = 6.5, 5.8, 1.2 Hz, 5H), 7.29 (td, *J* = 7.6, 1.3 Hz, 1H), 7.14 (dd, *J* = 5.1, 3.7 Hz, 1H); **^{13}C NMR (100 MHz, $CDCl_3$)** δ 142.6, 136.0, 133.7, 131.4, 129.0, 128.6, 128.3, 127.1, 127.1, 126.8, 125.9, 123.4, 120.6, 93.7, 89.5 (Overlapping peak present); **HRMS (ESI)** m/z: calcd for $C_{18}H_{12}S$ $[M]^+$: 260.0660; found: 260.0607.

Analytical Data of the Synthesized Products, 9-Sulfenyl phenanthrenes or Naphthothiophenes (3aa – 3ac).

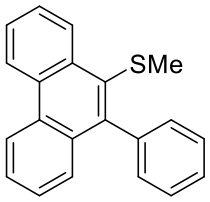

Methyl(10-phenylphenanthren-9-yl)sulfane (3aa):[3] Yellow liquid; **^{1}H NMR (400 MHz, $CDCl_3$)** δ 8.89 (dd, *J* = 7.5, 1.9 Hz, 1H), 8.81 – 8.74 (m, 2H), 7.78 – 7.70 (m, 2H), 7.66 (m, 1H), 7.58 – 7.50 (m, 3H), 7.49 – 7.41 (m, 2H), 7.36 (dd, *J* = 7.9, 1.6 Hz, 2H), 2.20 (s, 3H); **^{13}C NMR (100 MHz, $CDCl_3$)** δ 145.2, 140.8, 132.1, 132.0, 131.6, 130.8, 130.5, 129.9, 128.4, 128.1, 127.7, 127.4, 127.3, 127.1, 126.9, 126.6, 123.0, 122.5, 20.0.

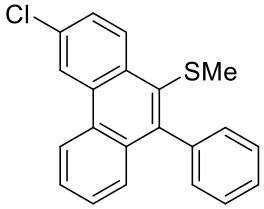

(6-Chloro-10-phenylphenanthren-9-yl)(methyl)sulfane (3ba): Yellow liquid; **^{1}H NMR (400 MHz, $CDCl_3$)** δ 8.83 (d, *J* = 8.9 Hz, 1H), 8.73 (d, *J* = 2.1 Hz, 1H), 8.64 (d, *J* = 8.3 Hz, 1H), 7.71 – 7.64 (m, 2H), 7.58 – 7.43 (m, 5H), 7.35 (dd, *J* = 7.7, 1.6 Hz, 2H), 2.18 (s, 3H); **^{13}C NMR (100 MHz, $CDCl_3$)** δ 145.5, 140.4, 133.1, 132.5, 131.9, 131.2, 130.43, 129.8, 129.5, 129.4, 128.5, 128.1, 127.8, 127.4, 127.2, 122.6, 122.5, 20.0; **HRMS (ESI)** m/z: calcd for $C_{21}H_{15}ClS$ $[M]^+$: 334.0583; found: 334.0567.

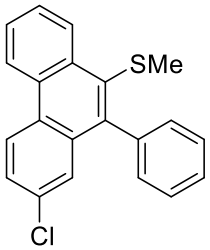

(2-Chloro-10-phenylphenanthren-9-yl)(methyl)sulfane (3ca): Off white crystalline solid; m.p.= 185 - 187 ^{o}C; **^{1}H NMR (400 MHz, $CDCl_3$)** δ 8.86 (dd, *J* = 7.6, 2.0 Hz, 1H), 8.73 – 8.68 (d, *J*= 8.9 Hz, 1H), 8.66 (d, *J* = 8.9 Hz, 1H), 7.80 – 7.69 (m, 2H), 7.62 – 7.49 (m, 4H), 7.39 (d, *J* = 2.2 Hz, 1H), 7.32 (dd, *J* = 7.8, 1.6 Hz, 2H), 2.19 (s, 3H); **^{13}C NMR (100 MHz, $CDCl_3$)** δ 144.2, 140.0, 133.3, 132.7, 131.9, 130.3, 129.8, 128.9, 128.3, 127.9, 127.7, 127.6, 127.4, 127.2, 124.2, 122.9, 20.0; **Anal** calcd for $C_{21}H_{15}ClS$: C, 75.32; H, 4.52; S, 9.57; found C, 75.43; H, 4.55; S, 8.84; ***CCDC* 2052187**.

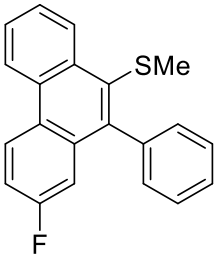

(2-Fluoro-10-phenylphenanthren-9-yl)(methyl)sulfane (3da): White crystalline solid, m.p. = 156 - 158 °C; **^{1}H NMR (400 MHz, CDCl$_3$)** δ 8.91 (dd, *J* = 7.6, 1.9 Hz, 1H), 8.74 – 8.65 (m, 2H), 7.80 – 7.70 (m, 2H), 7.58 – 7.54 (m, 3H), 7.44 – 7.31 (m, 3H), 7.10 (dd, *J* = 10.8, 2.7 Hz, 1H), 2.22 (s, 3H); **^{13}C NMR (100 MHz, CDCl$_3$)** δ 161.1 (d, $^1J_{C\text{-}F}$ = 245 Hz), 144.4, 144.3, 140.1, 133.4 (d, $^3J_{C\text{-}F}$ = 8.15 Hz), 133.1, 131.4, 130.4, 129.7, 128.2, 127.8, 127.5, 127.2, 127.2, 127.1, 124.8 (d, $^3J_{C\text{-}F}$ = 8.59 Hz), 122.7, 116.0 (d, $^2J_{C\text{-}F}$ = 23.63 Hz), 112.7, 19.9; **Anal** calcd for $C_{21}H_{15}FS$: C, 82.08; H, 4.50; S, 8.43; found C, 81.54; H, 4.80; S, 8.30; ***CCDC* 2041730**.

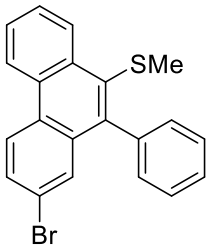

(2-bromo-10-phenylphenanthren-9-yl)(methyl)sulfane (3ea): White crystalline solid; m.p.= 202 - 204 °C; **^{1}H NMR (400 MHz, CDCl$_3$)** δ 8.87 (dd, *J* = 7.5, 1.9 Hz, 1H), 8.70 (d, *J* = 7.8 Hz, 1H), 8.58 (d, *J* = 8.9 Hz, 1H), 7.81 – 7.68 (m, 3H), 7.55 (dd, *J* = 6.8, 2.3 Hz, 4H), 7.32 (dd, *J* = 7.7, 1.7 Hz, 2H), 2.19 (s, 3H); **^{13}C NMR (100 MHz, CDCl$_3$)** δ 144.1, 139.9, 133.6, 133.2, 131.9, 130.5, 130.2, 129.8, 129.2, 128.3, 127.8, 127.6, 127.2, 124.3, 122.8, 120.9, 20.0; **Anal** calcd for $C_{21}H_{15}BrS$: C, 66.50; H, 3.99; S, 8.45; found C, 66.66; H, 3.91; S, 7.86; ***CCDC* 2033891**.

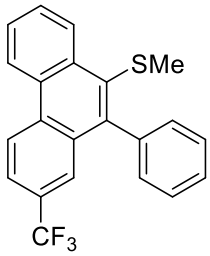

Methyl(10-phenyl-2-(trifluoromethyl)phenanthren-9-yl)sulfane (3fa): Yellowish white crystalline solid, m.p. = 124 - 126 °C; **^{1}H NMR (400 MHz, CDCl$_3$)** δ 8.91 (d, *J* = 7.8 Hz, 1H), 8.84 (d, *J* = 8.9 Hz, 1H), 8.79 (d, *J* = 8.0 Hz, 1H), 7.86 – 7.76 (m, 3H), 7.73 (d, *J* = 6.7 Hz, 1H), 7.60 – 7.52 (m, 3H), 7.34 (d, *J* = 7.9 Hz, 2H), 2.20 (s, 3H); **^{13}C NMR (100 MHz, CDCl$_3$)** δ 144.9, 139.6, 133.5, 132.7, 132.5, 131.6, 130.0, 129.8, 129.6, 128.5, 128.3, 128.2, 127.9, 127.7, 127.3, 125.5, 125.5, 123.4, 122.9, 19.9; **Anal** calcd for $C_{22}H_{15}F_3S$: C, 71.72; H, 4.10; S, 8.70; found C, 71.48; H, 4.24; S, 8.10; ***CCDC* 2041729.**

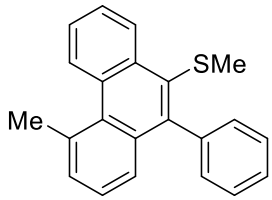

Methyl(4-methyl-10-phenylphenanthren-9-yl)sulfane (3ga): White semi-solid; **^{1}H NMR (400 MHz, CDCl$_3$)** δ 8.99 (d, *J* = 8.1 Hz, 1H), 8.91 (d, *J* = 7.9 Hz, 1H), 7.79 – 7.75 (m, 1H), 7.73 – 7.69 (m, 1H), 7.57 – 7.53 (m, 4H), 7.37 – 7.53 (m, 4H), 3.19 (s, 3H), 2.23 (s, 3H); **^{13}C NMR (100 MHz, CDCl$_3$)** δ 145.5, 141.5, 134.8, 133.6, 132.8, 131.9, 131.7, 131.5, 130.8, 129.9, 128.0, 127.9, 127.4, 127.1, 126.9, 126.7, 125.6, 125.4, 27.2, 19.9; **HRMS** (**ESI**) m/z: calcd for $C_{22}H_{18}S$ $[M]^+$: 314.1129; found: 314.1133.

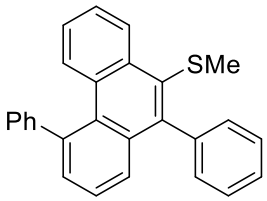

(4,10-Diphenylphenanthren-9-yl)(methyl)sulfane (3ha): White crystsalline solid; m.p.= 143 – 145 ^{o}C; **^{1}H NMR (400 MHz, CDCl$_3$)** δ 8.83 (d, *J* = 7.3 Hz, 1H), 7.86 (d, *J* = 7.9 Hz, 1H), 7.59 – 7.37 (m, 14H), 7.14 (ddd, *J* = 8.5, 6.9, 1.4 Hz, 1H), 2.22 (s, 3H); **^{13}C NMR (100MHz, CDCl$_3$)** δ 145.4, 145.0, 141.2, 140.1, 133.6, 132.9, 132.1, 131.4, 130.8, 130.0, 129.2, 129.1, 128.1, 127.9, 127.3, 127.1, 127.1, 126.8, 125.6, 124.7, 20.0; **Anal** calcd for $C_{27}H_{20}S$: C, 86.13; H, 5.35; S, 8.51; found C, 85.84; H, 5.43; S, 9.21; ***CCDC* 2052186**.

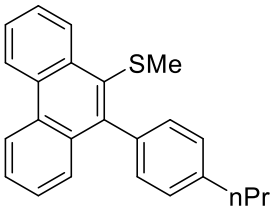

Methyl(10-(4-propylphenyl)phenanthren-9-yl)sulfane (3ia): Off white crystalline solid; m.p.= 134 – 136 ^{o}C; **^{1}H NMR (400 MHz, CDCl$_3$)** δ 8.90 (dd, *J* = 7.6, 1.9 Hz, 1H), 8.79 (dd, *J* = 7.7, 1.8 Hz, 1H), 8.76 (d, *J* = 8.6 Hz, 1H), 7.78 – 7.71 (m, 2H), 7.68 – 7.64 (m, 1H), 7.52 – 7.44 (m, 2H), 7.37 (d, *J* = 8.1 Hz, 2H), 7.28 (d, *J* = 2.4 Hz, 2H), 2.82 – 2.70 (m, 2H), 2.21 (s, 3H), 1.85 – 1.79 (m, 2H), 1.08 (t, *J* = 7.3 Hz, 3H); **^{13}C NMR (100 MHz, CDCl$_3$)** δ 145.3, 141.6, 137.9, 129.7, 128.5, 128.1, 127.7, 127.4, 127.1, 126.7, 126.6, 122.9, 122.4, 38.0, 24.5, 20.0, 14.03; **HRMS** (**ESI**) m/z: calcd for $C_{24}H_{22}S$ $[M]^+$: 342.1442; found: 342.1447.

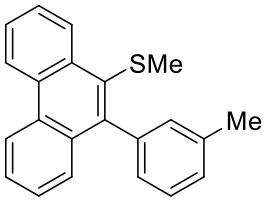

Methyl(10-(*m*-tolyl)phenanthren-9-yl)sulfane (3ja): Yellowish white crystalline solid, m.p.= 205 – 207 ^{o}C; **^{1}H NMR (400 MHz, CDCl$_3$)** δ 8.86 (dd, *J* = 7.6, 1.9 Hz, 1H), 8.82 – 8.69 (m, 2H), 7.76 – 7.67 (m, 2H), 7.66 – 7.59 (m, 1H), 7.46 – 7.38 (m, 3H), 7.33 – 7.29 (m, 1H), 7.15 (d, *J* = 0.6 Hz, 2H), 2.46 (s, 3H), 2.20 (s, 3H); **^{13}C NMR (100 MHz, CDCl$_3$)** δ 145.4, 140.8, 137.6, 132.2, 132.0, 131.4, 130.8, 130.5, 128.5, 128.0, 127.9, 127.7, 127.4, 127.1, 126.9, 126.8, 126.6, 123.0, 122.4, 21.6, 20.1; **Anal** calcd for $C_{22}H_{18}S$: C, 84.03; H, 5.77; S, 10.20; found C, 83.83; H, 6.17; S, 9.82.

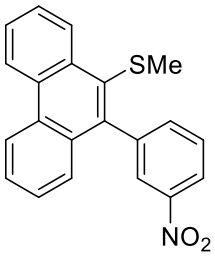

Methyl(10-(3-nitrophenyl)phenanthren-9-yl)sulfane (3ka): Yellow viscous liquid; **^{1}H NMR (400 MHz, CDCl$_3$)** δ 8.85 (dd, *J* = 6.4, 3.1 Hz, 1H), 8.81 – 8.77 (m, 2H), 8.39 – 8.36 (m, 1H), 8.25 (t, *J* = 1.7 Hz, 1H), 7.77 (dd, *J* = 6.3, 3.3 Hz, 2H), 7.73 – 7.67 (m, 3H), 7.51 – 7.46 (m, 2H), 7.30 (dd, *J* = 8.3, 0.9 Hz, 1H), 2.19 (s, 3H); **^{13}C NMR (100 MHz, CDCl$_3$)** δ 148.2, 142.6, 142.4, 136.3, 132.3, 131.6, 131.3, 131.0, 130.7, 129.1, 127.7, 127.6, 127.5, 127.0, 125.0, 123.1, 122.8, 122.4; **HRMS** (**ESI**) m/z: calcd for $C_{21}H_{15}NO_2S$ $[M]^+$: 345.0823; found: 345.0796.

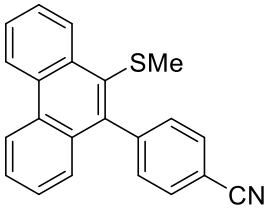

4-(10-(Methylthio)phenanthren-9-yl)benzonitrile (3la): Yellow solid, m.p.=155 – 157 °C; **^{1}H NMR (400 MHz, CDCl$_3$)** δ 8.89 (dd, *J* = 7.5, 1.9 Hz, 1H), 8.81 – 8.74 (m, 2H), 7.78 – 7.70 (m, 2H), 7.66 (ddd, *J* = 8.3, 6.4, 1.9 Hz, 1H), 7.58 – 7.50 (m, 3H), 7.49 – 7.41 (m, 2H), 7.36 (dd, *J* = 7.9, 1.6 Hz, 2H), 2.20 (s, 3H); **^{13}C NMR (100 MHz, CDCl$_3$)** δ 145.8, 143.3, 132.0, 131.7, 131.6, 131.2, 131.0, 130.9, 130.6, 127.7, 127.6, 127.5, 127.4, 127.0, 123.1, 122.8, 120.0, 111.3, 20.0; **HRMS** (**ESI**) m/z: calcd for $C_{22}H_{15}NS$ $[M]^+$: 325.0925; found: 325.099.

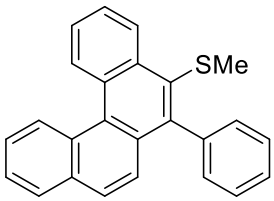

Methyl(6-phenylbenzo[*c*]phenanthren-5-yl)sulfane (3ma): White solid, m.p. = 134 – 136 °C; **^{1}H NMR (400 MHz, CDCl$_3$)** δ 9.08 (dd, *J* = 12.9, 8.2 Hz, 2H), 8.97 (d, *J* = 8.0 Hz, 1H), 7.98 (d, *J* = 7.8 Hz, 1H), 7.81 – 7.71 (m, 3H), 7.71 – 7.61 (m, 2H), 7.59 – 7.52 (m, 3H), 7.39 (dd, *J* = 8.4, 6.9 Hz, 3H), 2.23 (s, 3H); **^{13}C NMR (100 MHz, CDCl$_3$)** δ 144.4, 140.8, 133.4, 133.1, 130.6, 130.3, 128.8, 128.7, 128.2, 128.1, 127.4 127.2, 127.0, 126.9, 126.4, 126.2, 126.1, 125.4, 20.1; **HRMS** (**ESI**) m/z: calcd for $C_{25}H_{18}S$ $[M]^+$: 350.1129; found: 350.1138.

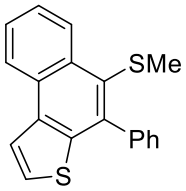

5-(Methylthio)-4-phenylnaphtho[2,1-*b*]thiophene (3na): White solid, m.p.= 109 -111 °C; **^{1}H NMR (400 MHz, CDCl$_3$)** δ 8.90 – 8.83 (m, 1H), 8.44 – 8.36 (m, 1H), 8.04 (d, *J* = 5.5 Hz, 1H), 7.71 – 7.65 (m, 2H), 7.60 (d, *J* = 5.4 Hz, 1H), 7.54 – 7.49 (m, 5H), 2.19 (s, 3H); **^{13}C NMR (100 MHz, CDCl$_3$)** δ 142.2, 140.7, 138.3, 138.0, 131.6, 129.7, 129.2, 129.1, 128.1, 128.0, 127.4, 126.8, 126.7, 125.9, 124.6, 124.3, 20.2; **HRMS (ESI)** m/z: calcd for $C_{19}H_{14}S_2$ $[M]^+$: 306.0537; found: 306.0494.

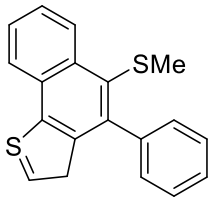

5-(Methylthio)-4-phenyl-3*H*-1λ^3-naphtho[1,2-*b*]thiophene (3oa): Colourless liquid; **^{1}H NMR (400 MHz, CDCl$_3$)** δ 8.84 (d, *J* = 7.7 Hz, 1H), 8.21 (d, *J* = 7.3 Hz, 1H), 7.65 (m, 2H), 7.55 – 7.47 (m, 3H), 7.44 – 7.37 (m, 3H), 6.99 (d, *J* = 5.4 Hz, 1H), 2.17 (s, 3H); **^{13}C NMR (100 MHz, CDCl$_3$)** δ 142.2, 140.7, 138.3, 138.0, 131.6, 129.7, 129.2, 129.1, 128.1, 128.0, 127.4, 126.8, 126.7, 125.9, 124.6, 124.3, 20.2; **HRMS** (**ESI**) m/z: calcd for $C_{19}H_{14}S_2$ $[M]^+$: 306.0537; found: 306.0535.

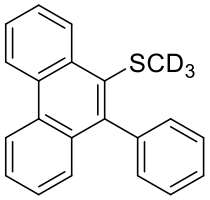

(Methyl-*d*$_3$)(10-phenylphenanthren-9-yl)sulfane (3ab): White crystalline solid; m.p.=178 -180 ^{o}C; **^{1}H NMR (400 MHz, CDCl$_3$)** δ 8.94 (d, *J* = 7.6 Hz, 1H), 8.82 – 8.76 (m, 2H), 7.82 – 7.72 (m, 2H), 7.70 – 7.66 (m, 1H), 7.63 – 7.44 (m, 5H), 7.40 (d, *J* = 6.2 Hz, 2H); **^{13}C NMR (100 MHz, CDCl$_3$)** δ 145.2, 140.8, 132.1, 132.0, 130.7, 130.5, 129.9, 128.4, 128.0, 127.6, 127.4, 127.2, 127.1, 126.8, 126.6, 122.9, 122.4; **Anal** calcd for $C_{21}H_{13}D_3S$: C, 83.12; H, 6.31; S, 10.57; found C, 83.02; H, 6.85; S, 10.43; ***CCDC*** **2044602.**

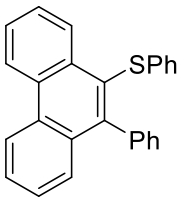

Phenyl(10-phenylphenanthren-9-yl)sulfane (3ac):[3] Yellow liquid; **^{1}H NMR (400 MHz, CDCl$_3$)** δ 8.80 (dd, *J* = 8.3, 3.9 Hz, 2H), 8.65 (d, *J* = 7.3 Hz, 1H), 7.76 – 7.67 (m, 2H), 7.60 (ddd, *J* = 8.2, 7.0, 1.2 Hz, 1H), 7.54 – 7.49 (m, 2H), 7.47 – 7.40 (m, 3H), 7.29 – 7.26 (m, 2H), 7.16 – 6.98 (m, 3H), 6.93 (dd, *J* = 8.3, 1.2 Hz, 2H); **^{13}C NMR (100 MHz, CDCl$_3$)** δ 146.8, 140.2, 139.0, 134.2, 132.3, 132.1, 131.1, 130.9, 130.0, 129.5, 128.7, 128.7, 128.5, 128.3, 128.1, 128.0, 127.6, 127.6, 127.4, 127.1, 127.1, 126.7, 126.4, 124.7, 122.8, 122.6 (Overlapping peaks present).

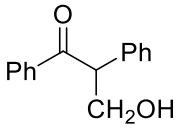

3-Hydroxy-1,2-diphenylpropan-1-one (6):[17] White solid, **^{1}H NMR (400 MHz, CDCl$_3$)** δ 7.86 (dd, *J* = 8.4, 1.3 Hz, 2H), 7.40 (ddd, *J* = 6.8, 4.0, 1.3 Hz, 1H), 7.32 – 7.16 (m, 7H), 4.72 (dd, *J* = 8.4, 4.8 Hz, 1H), 4.20 (dd, *J* = 11.4, 8.4 Hz, 1H), 3.81 (dd, *J* = 11.4, 4.8 Hz, 1H); **^{13}C NMR (100 MHz, CDCl$_3$)** δ 200.0, 136.2, 136.1, 133.2, 129.2, 128.9, 128.5, 128.4, 127.6, 65.2, 56.4.

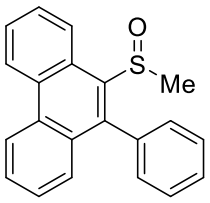

9-(Methylsulfinyl)-10-phenylphenanthrene (11): White solid; m.p.= 183 – 185 ^{o}C. **^{1}H NMR (400 MHz, CDCl$_3$)** δ 9.55 (dd, *J* = 7.6, 2.0 Hz, 1H), 8.80 (d, *J* = 9.6 Hz, 1H), 8.73 (d, *J* = 8.3 Hz, 1H), 7.79 – 7.67 (m, 3H), 7.60 – 7.39 (m, 6H), 7.12 (d, *J* = 6.5 Hz, 1H), 3.03 (s, 3H); **^{13}C NMR (100 MHz, CDCl$_3$)** δ 140.3, 136.8, 134.9, 131.4, 131.2, 130.6, 129.7, 129.6, 128.8, 128.7, 128.5, 128.1, 128.0, 127.4, 127.3, 127.0, 125.1, 123.4, 122.5, 38.7 (Overlapping peaks present); **HRMS (ESI)** m/z: calcd for $C_{21}H_{16}OS$ $[M]^+$: 316.0922; found: 316.0893.

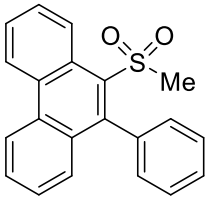

9-(Methylsulfonyl)-10-phenylphenanthrene (12): White solid; m.p. = 172-174 ^{o}C; **^{1}H NMR (400 MHz, CDCl$_3$)** δ 9.10 (dd, *J* = 7.5, 2.2 Hz, 1H), 8.83 (dd, *J* = 7.5, 2.3 Hz, 1H), 8.76 (d, *J* = 8.3 Hz, 1H), 7.81 – 7.74 (m, 3H), 7.51 (ddd, *J* = 8.2, 5.4, 1.2 Hz, 4H), 7.42 (dd, *J* = 8.4, 1.0 Hz, 1H), 7.38 – 7.33 (m, 2H), 3.14 (s, 3H); **^{13}C NMR (100 MHz, CDCl$_3$)** δ 143.0, 137.9, 133.0, 132.1, 131.6, 131.1, 129.8, 129.7, 127.9, 127.9, 127.8, 127.6, 127.4, 126.8, 126.5, 123.4, 122.5, 46.1 (One 1C Peak missing); **HRMS (ESI)** m/z: calcd for $C_{21}H_{16}0_2S$ $[M]^+$: 332.0871; found: 332.0781.

^{1}H and ^{13}C NMR Spectra of Some Selected 10-Phenylphenanthren-9-yl)(methyl)sulfanes

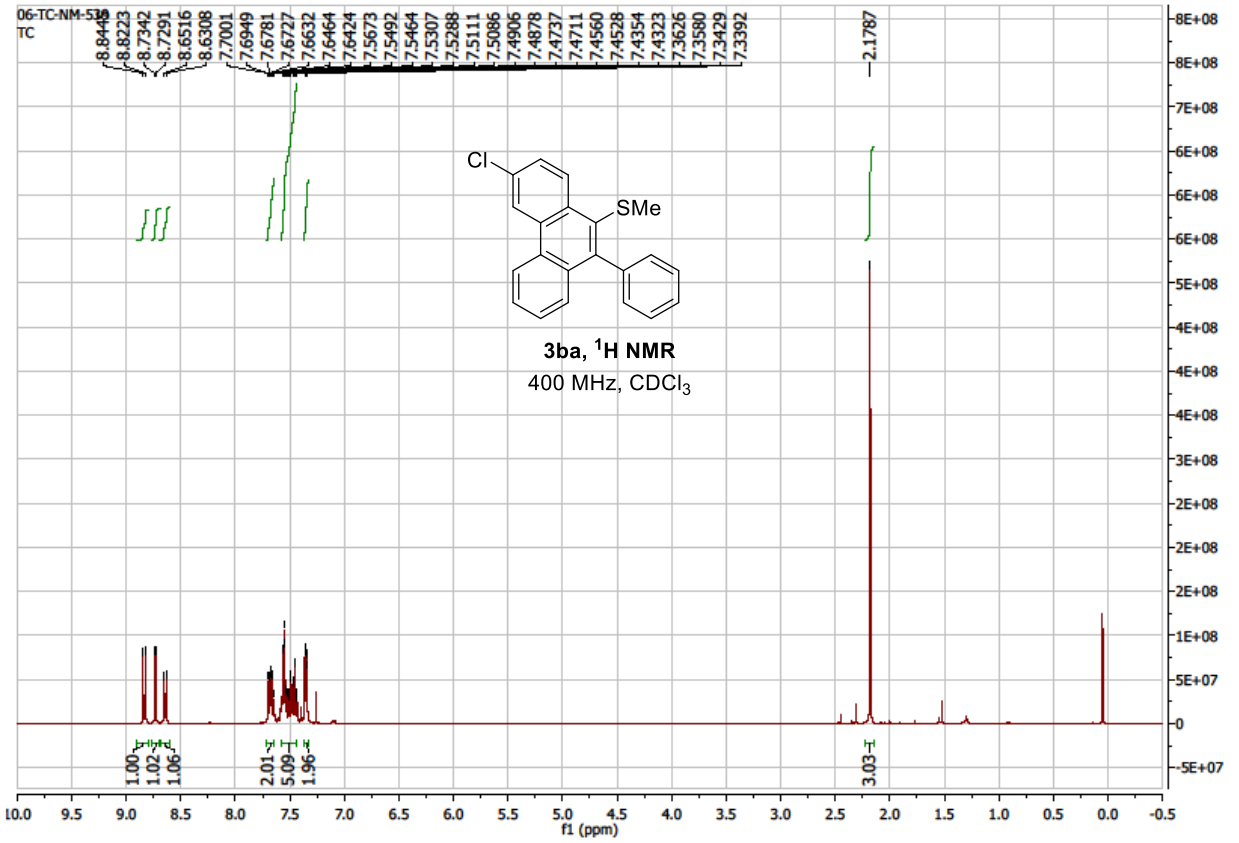

3ba, ^{1}H NMR

400 MHz, $CDCl_3$

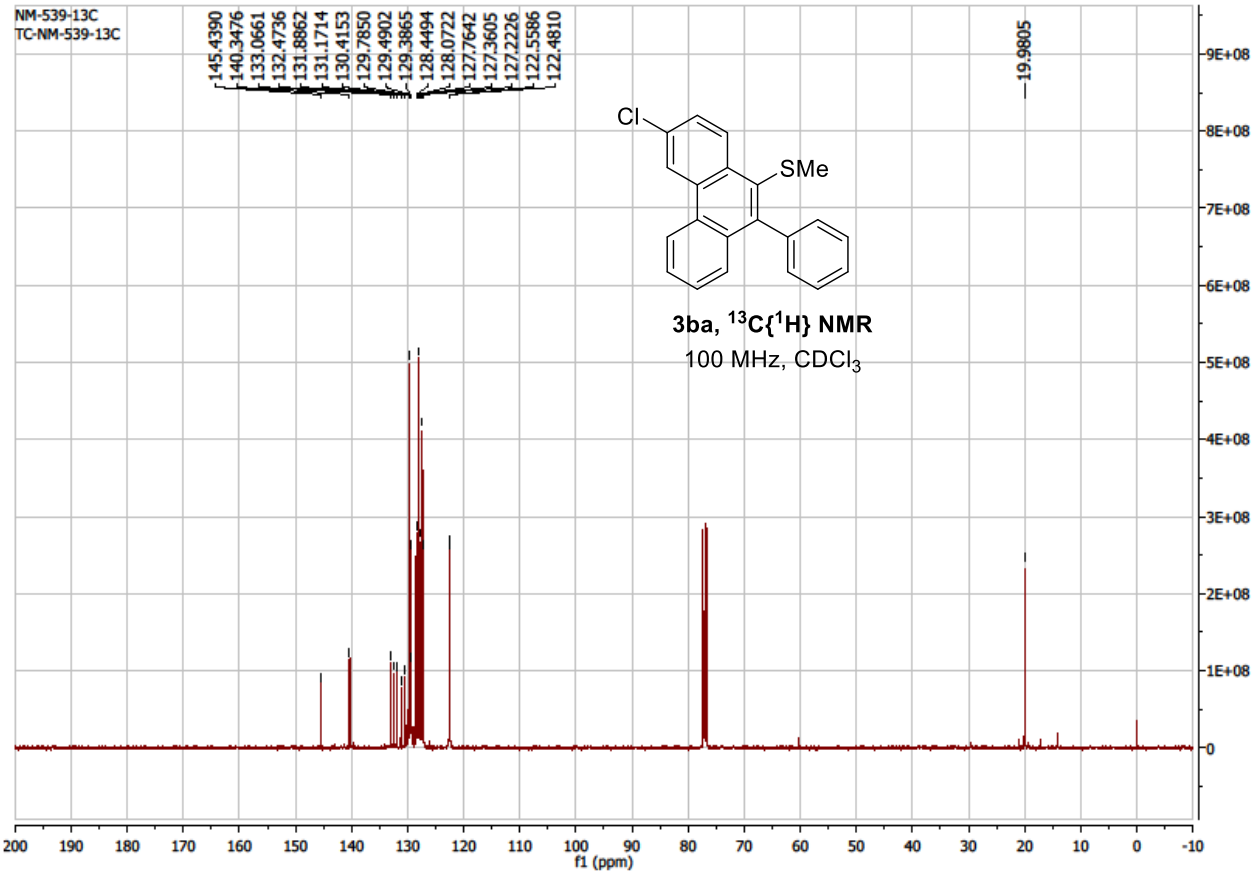

3ba, ^{13}C{^{1}H} NMR

100 MHz, $CDCl_3$

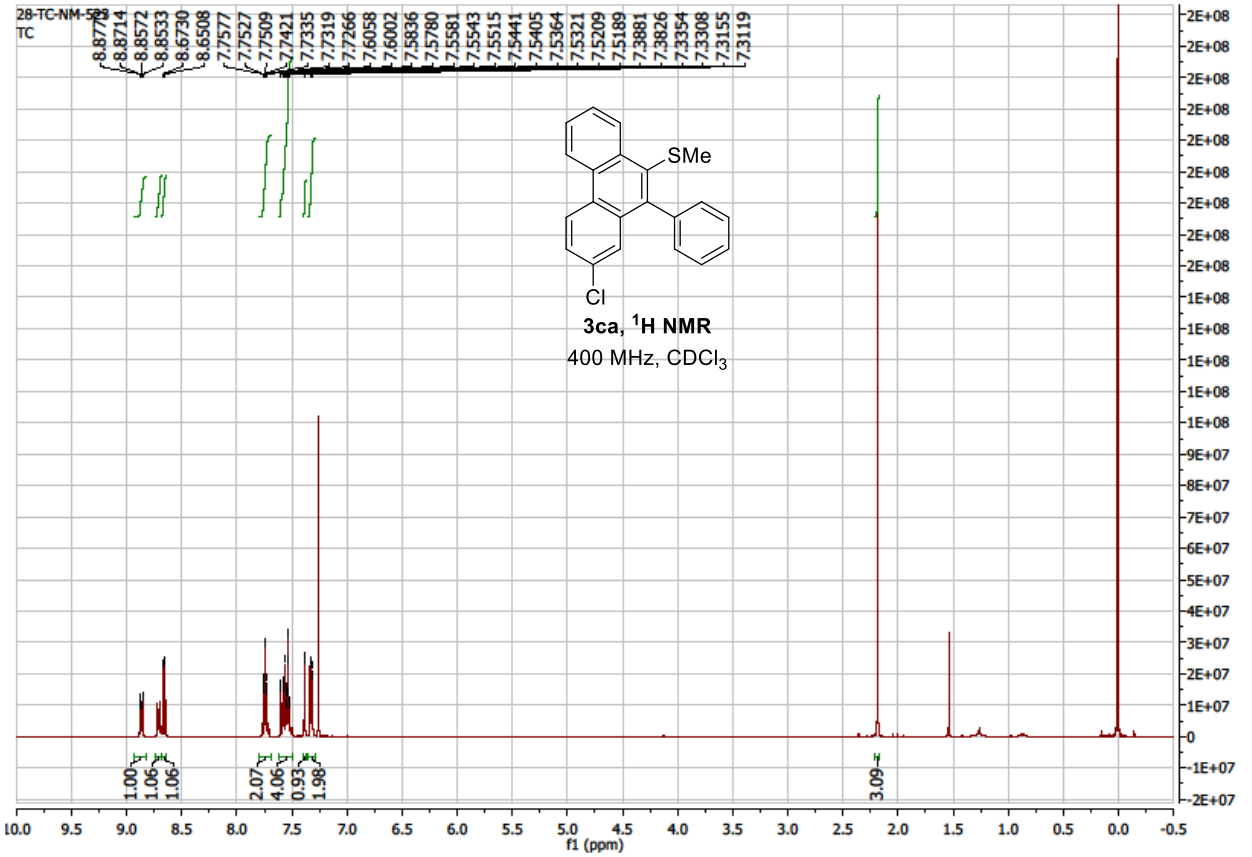
28-TC-NM-523
TC
SMe
Cl
3ca, ^{1}H NMR
400 MHz, $CDCl_3$
f1 (ppm)

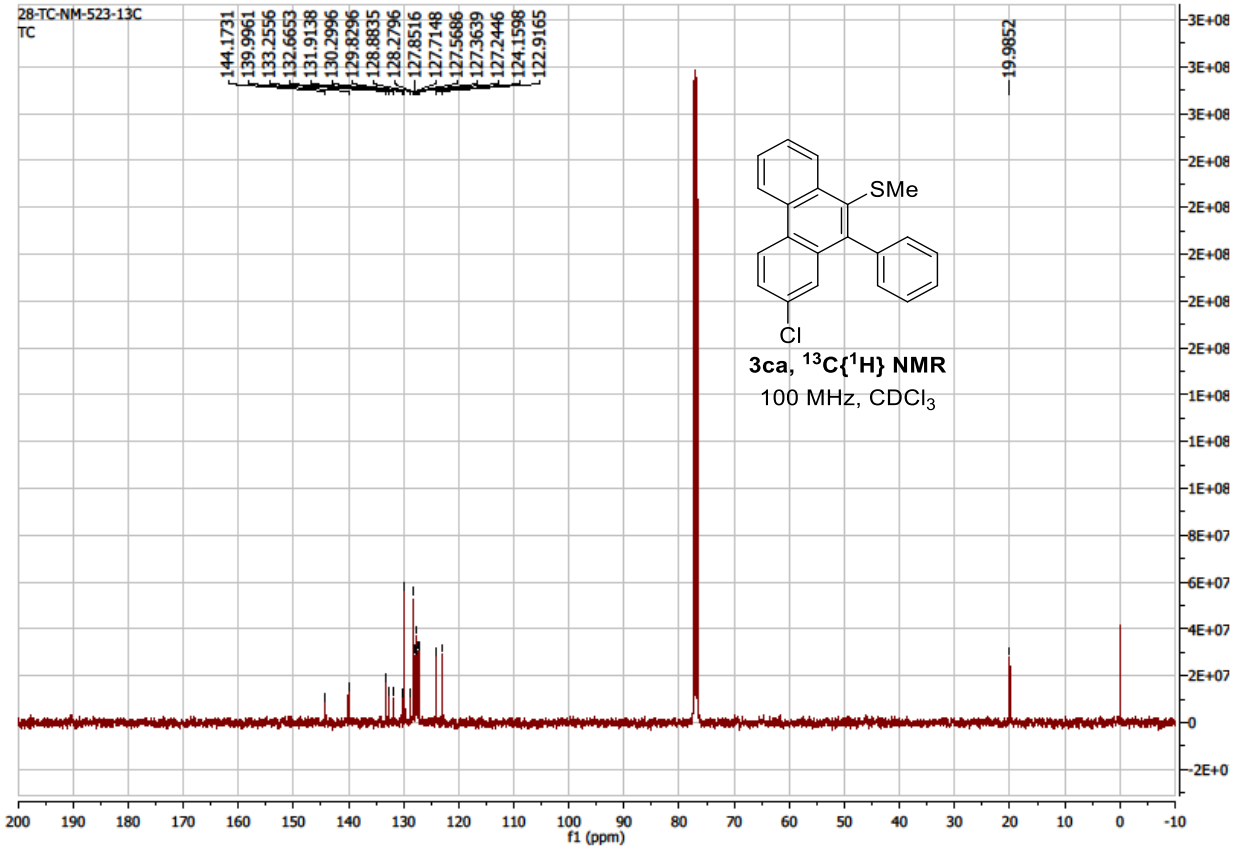
28-TC-NM-523-13C
TC
SMe
Cl
3ca, $^{13}C\{^{1}H\}$ NMR
100 MHz, $CDCl_3$
f1 (ppm)

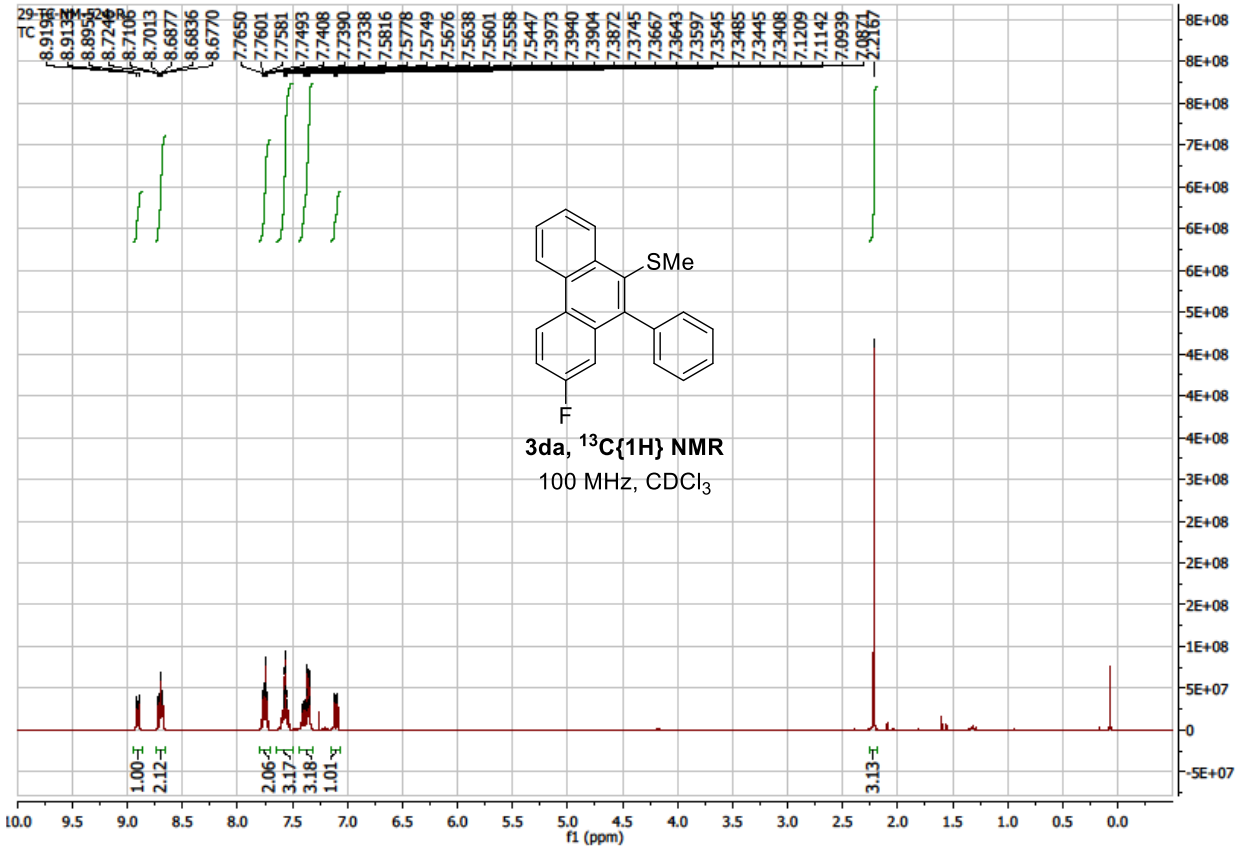
SMe
F
3da, ^{13}C{1H} NMR
100 MHz, CDCl$_3$
f1 (ppm)

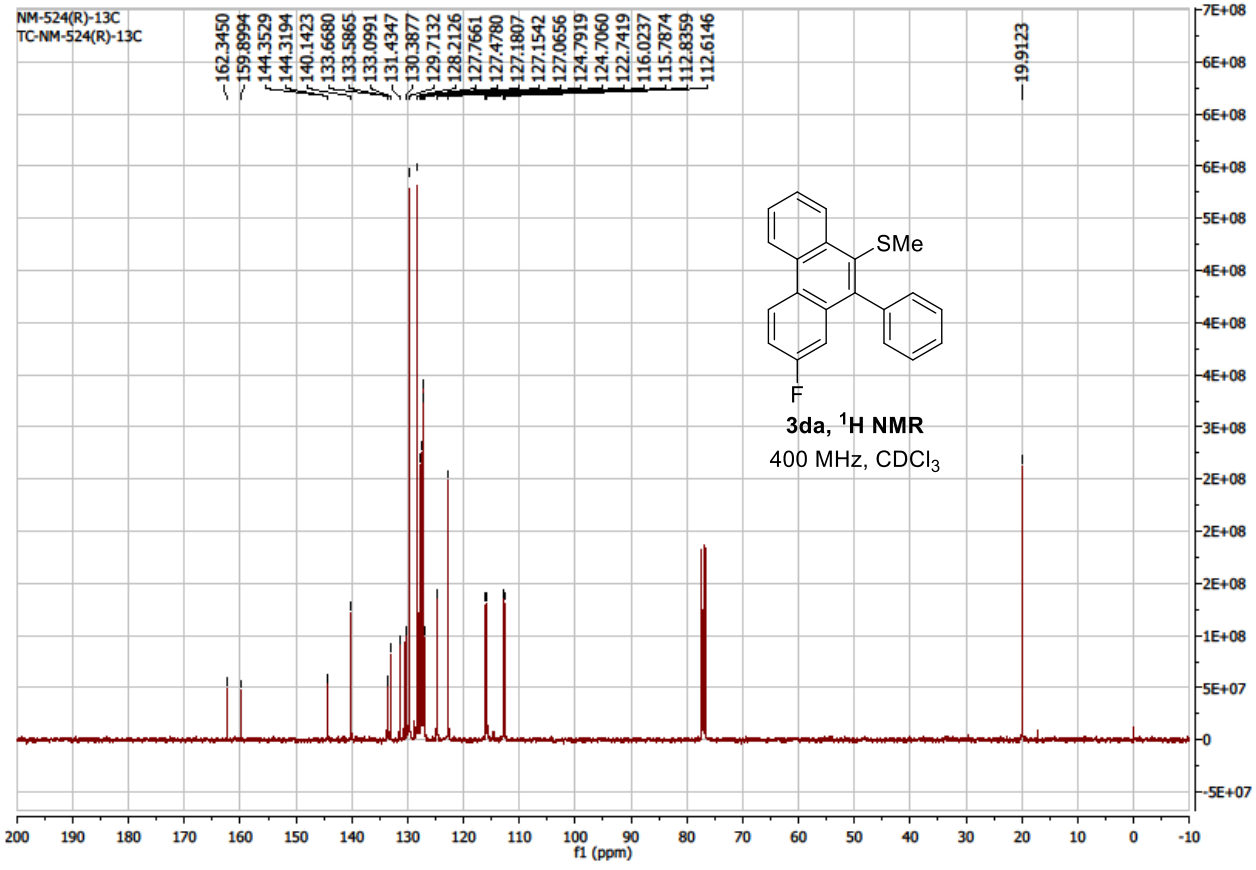
NM-524(R)-13C
TC-NM-524(R)-13C
SMe
F
3da, ^{1}H NMR
400 MHz, CDCl$_3$
f1 (ppm)

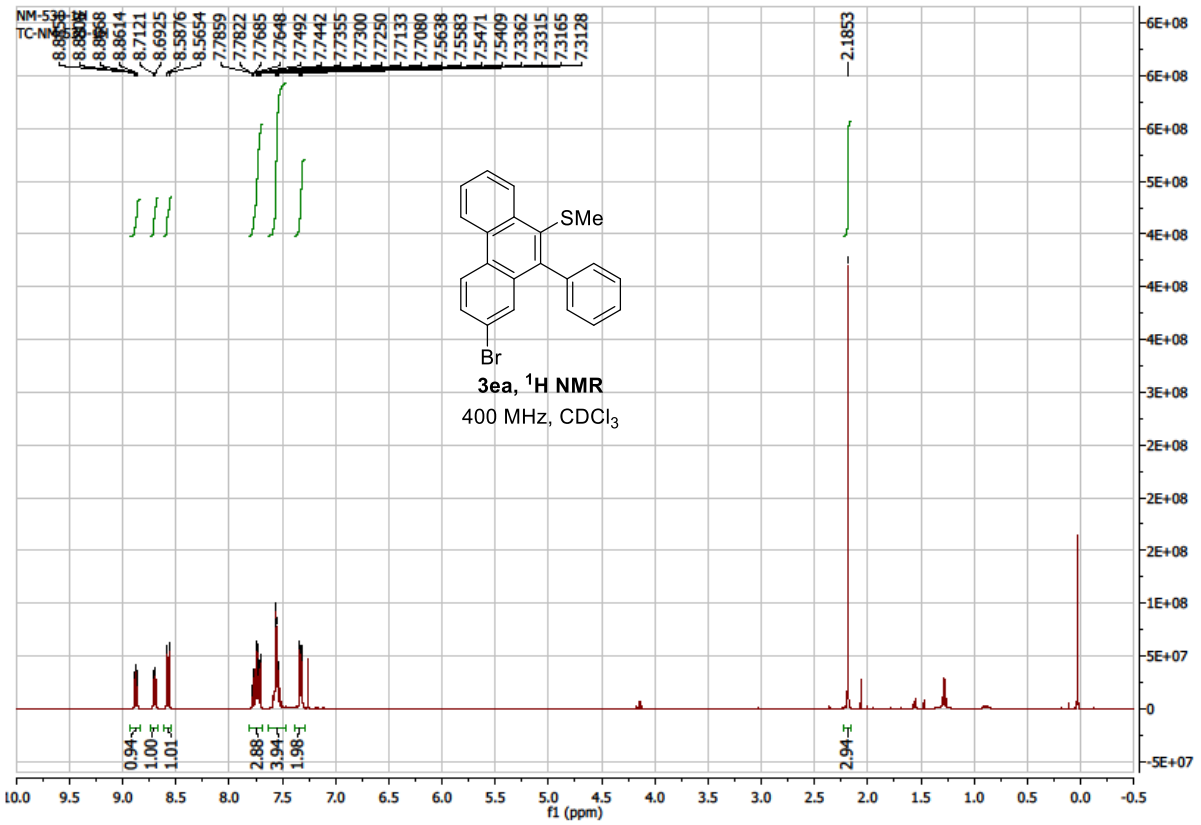
SMe
Br
3ea, ^{1}H NMR
400 MHz, $CDCl_3$
f1 (ppm)

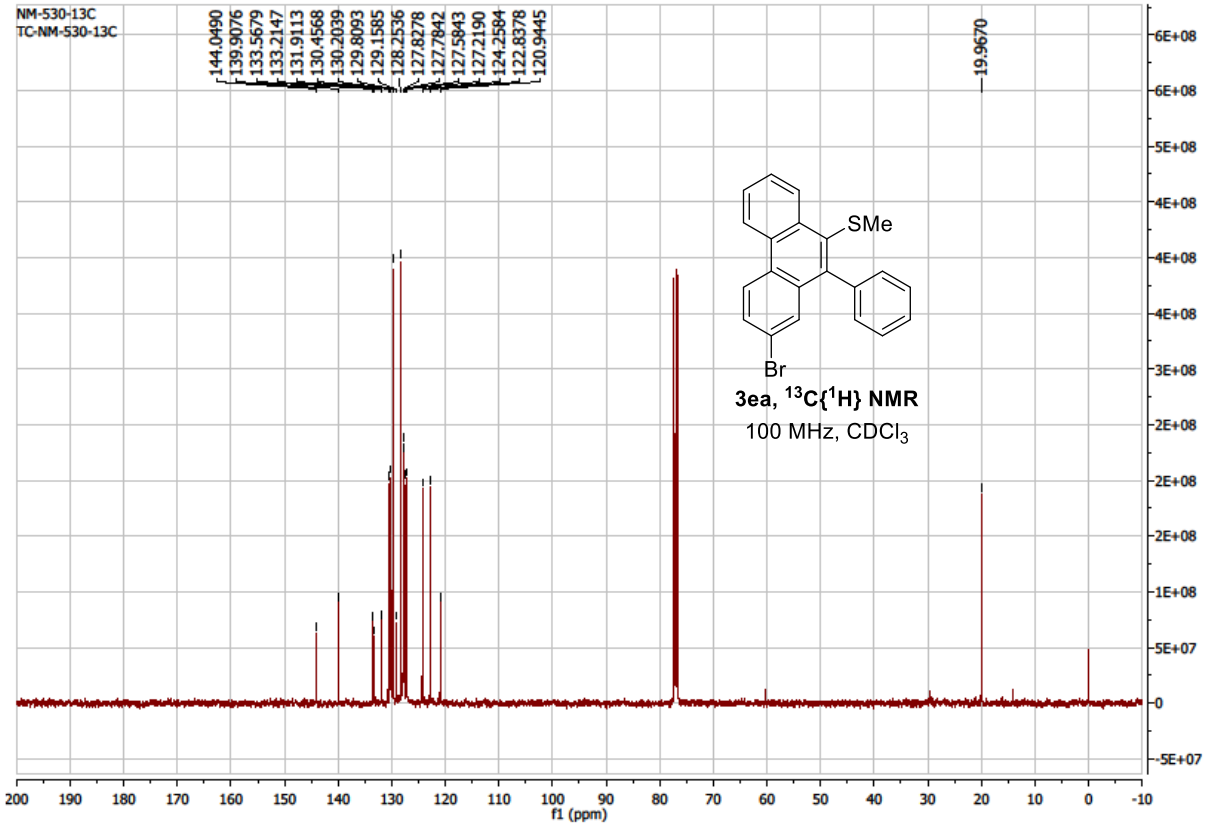
NM-530-13C
TC-NM-530-13C
SMe
Br
3ea, ^{13}C{^{1}H} NMR
100 MHz, $CDCl_3$
f1 (ppm)

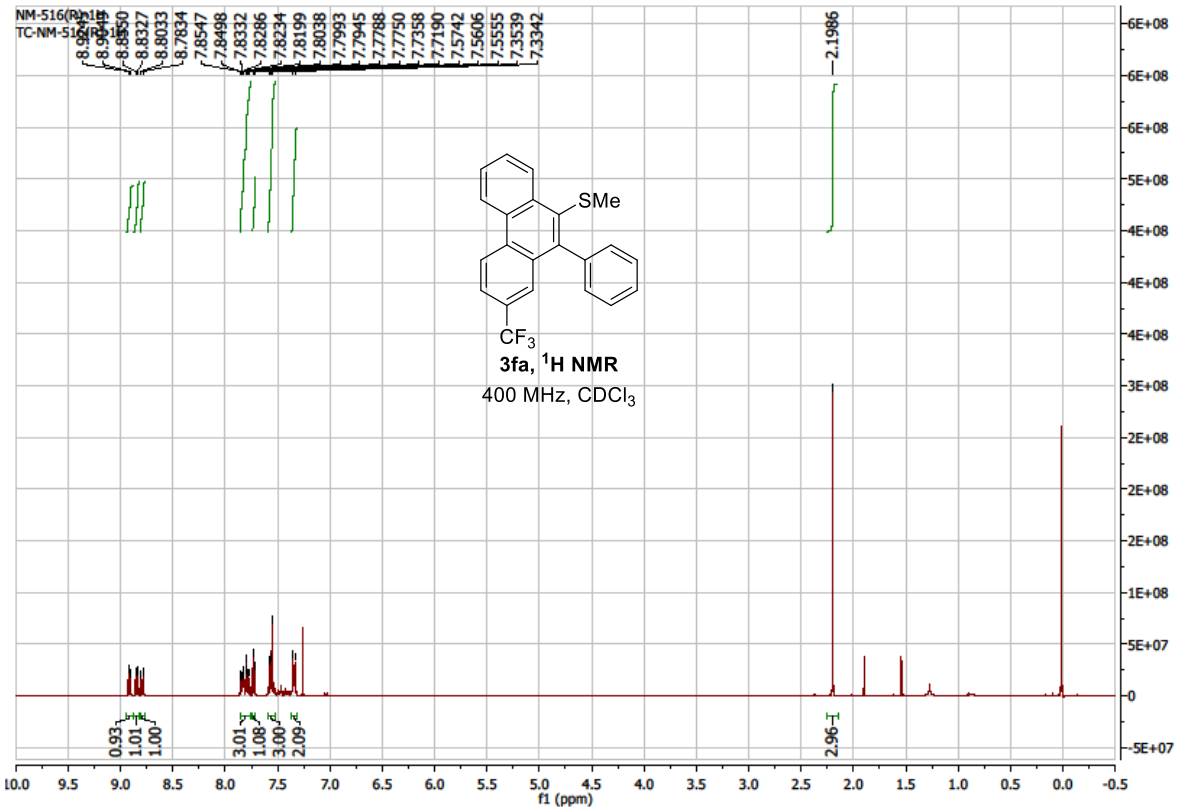
SMe
CF3
3fa, 1H NMR
400 MHz, CDCl3
f1 (ppm)

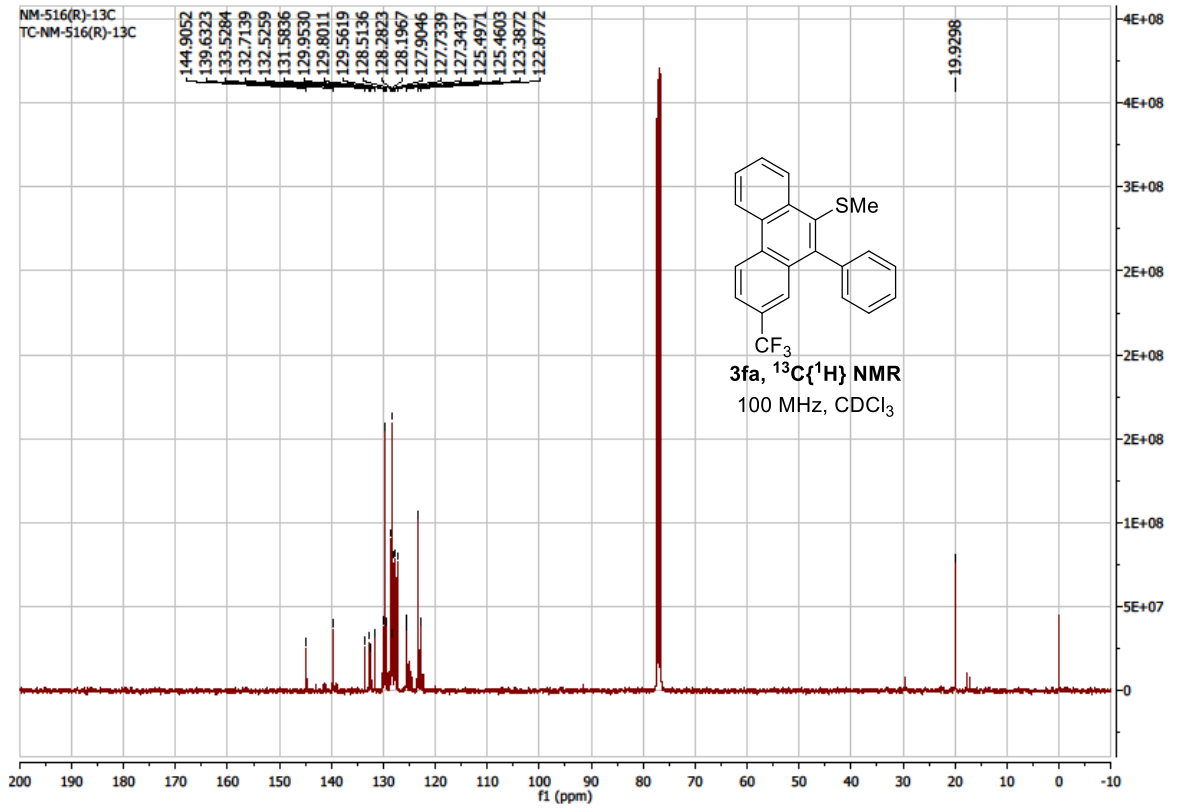
SMe
CF3
3fa, 13C{1H} NMR
100 MHz, CDCl3
f1 (ppm)

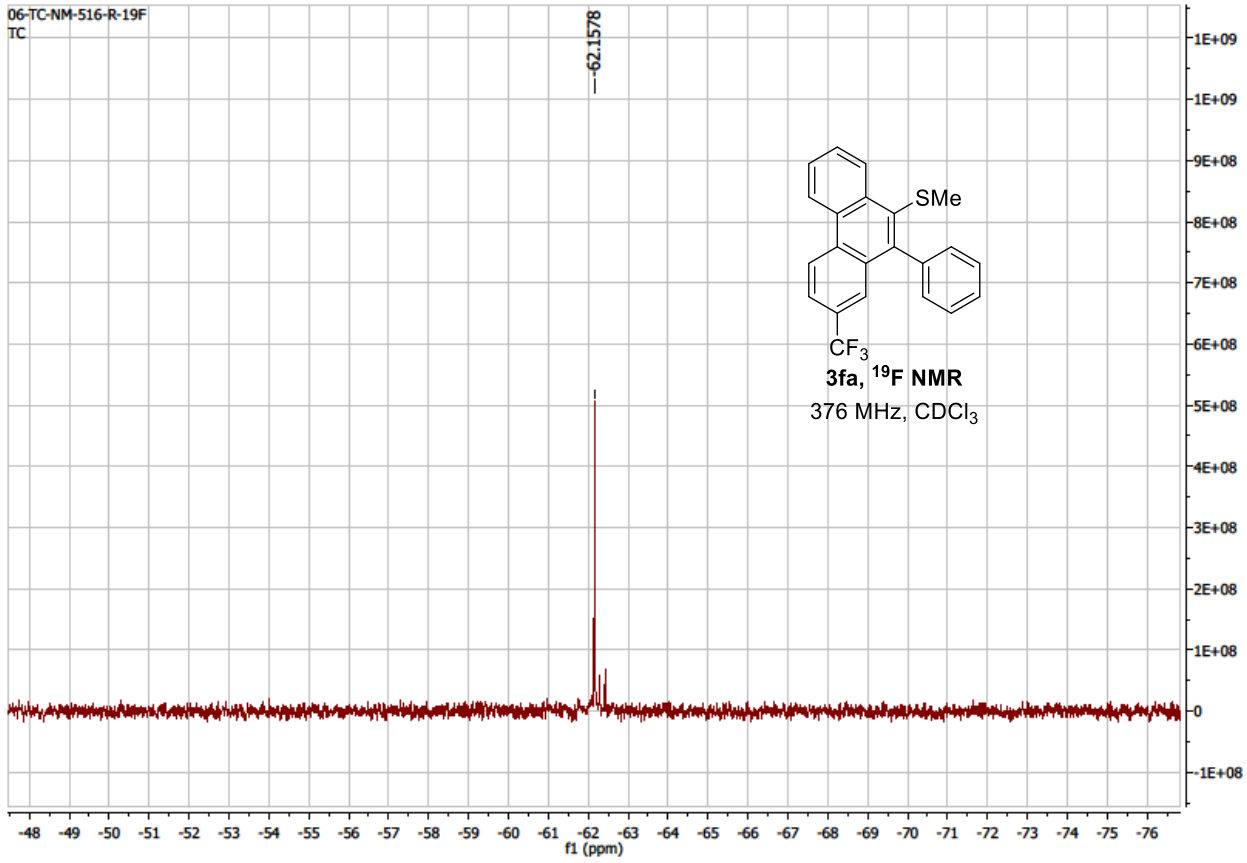

3fa, ^{19}F NMR

376 MHz, $CDCl_3$

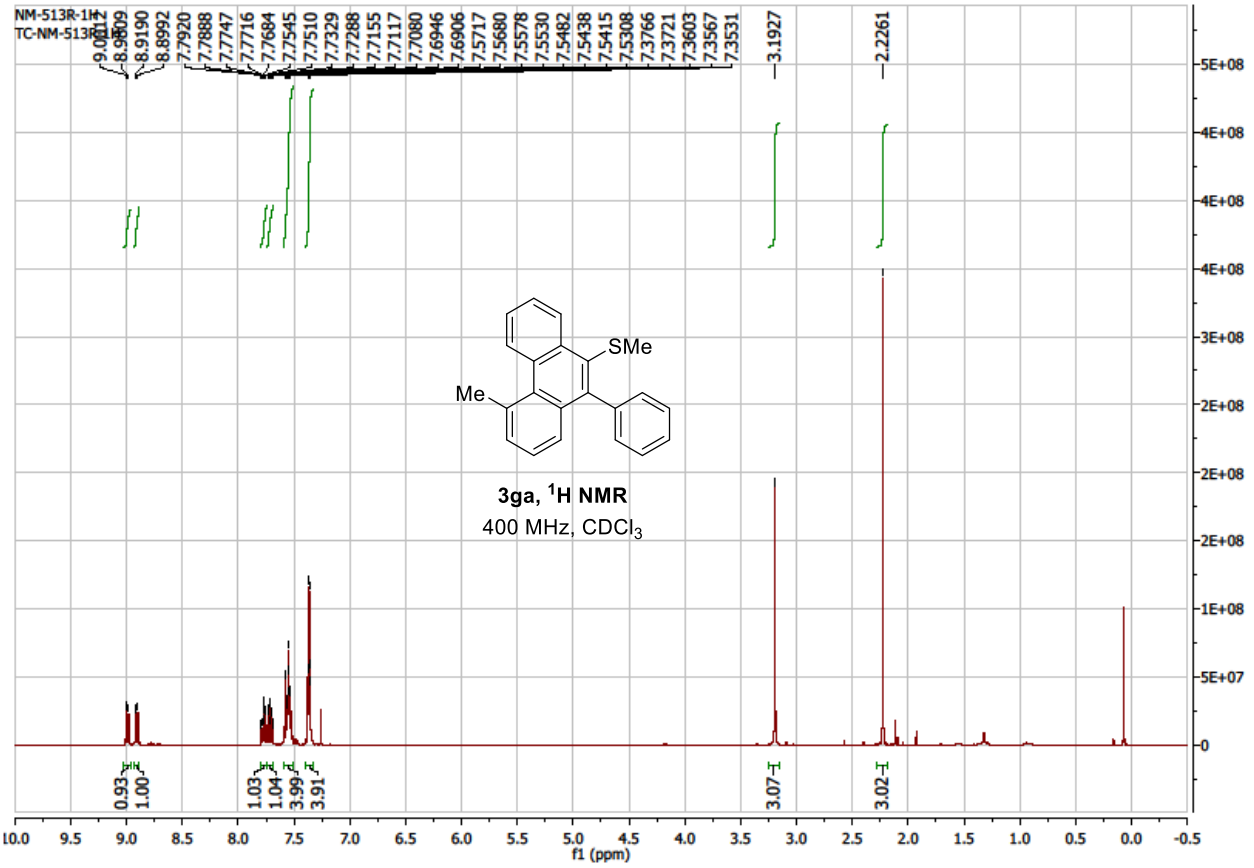

3ga, ^{1}H NMR

400 MHz, $CDCl_3$

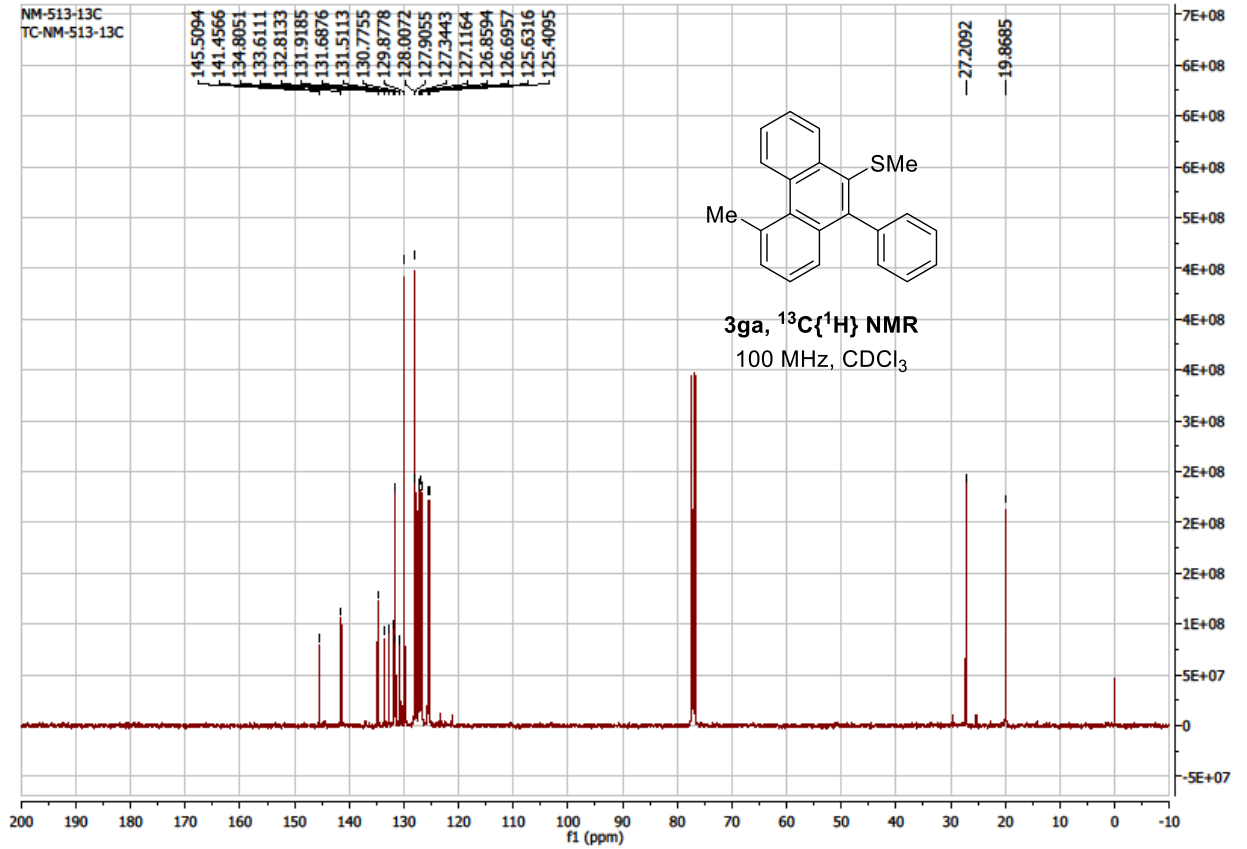

3ga, $^{13}C\{^{1}H\}$ NMR
100 MHz, $CDCl_3$

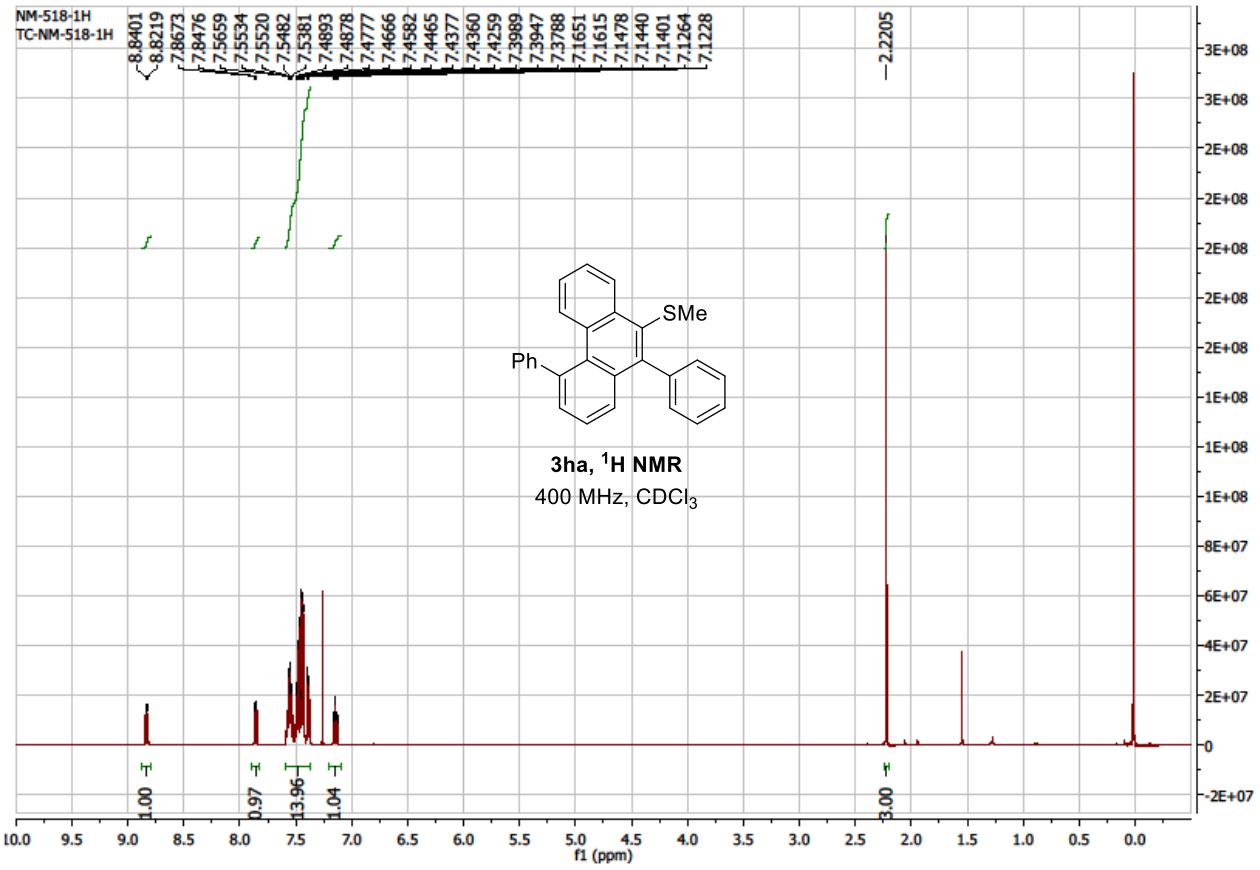

3ha, ^{1}H NMR
400 MHz, $CDCl_3$

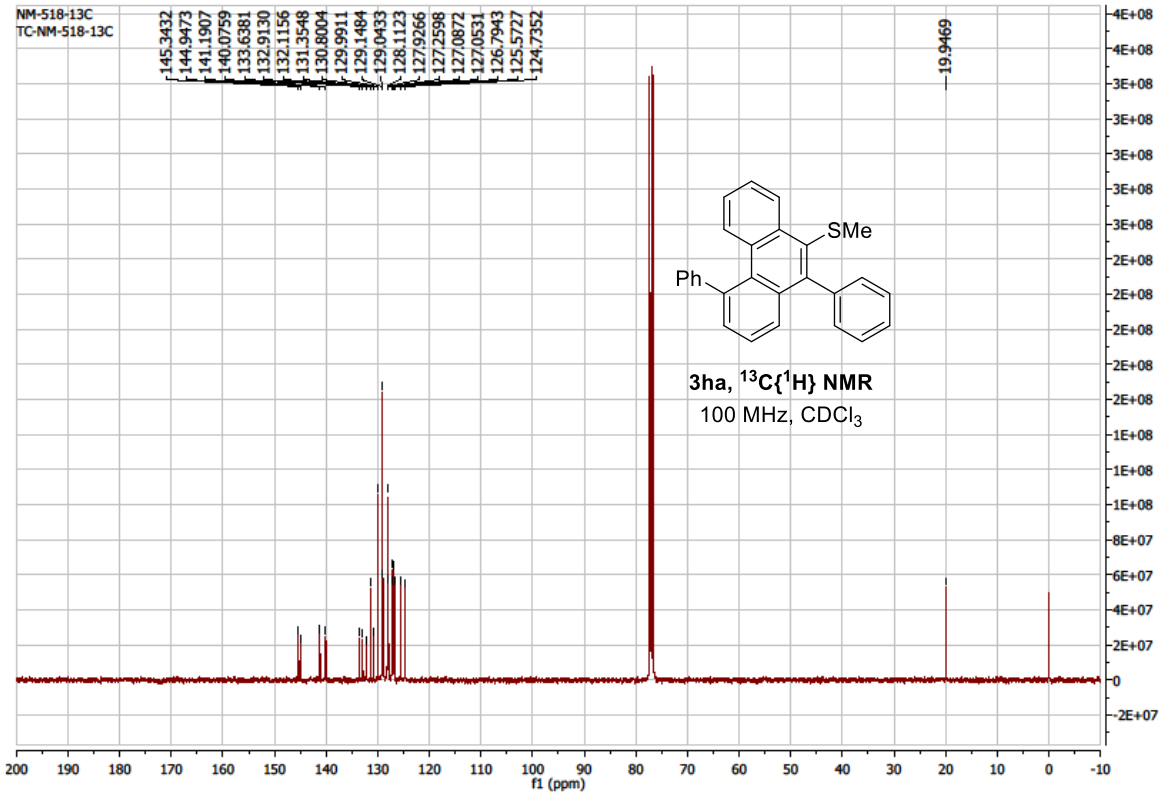
NM-518-13C
TC-NM-518-13C
SMe
Ph
3ha, $^{13}C\{^{1}H\}$ NMR
100 MHz, $CDCl_3$
f1 (ppm)

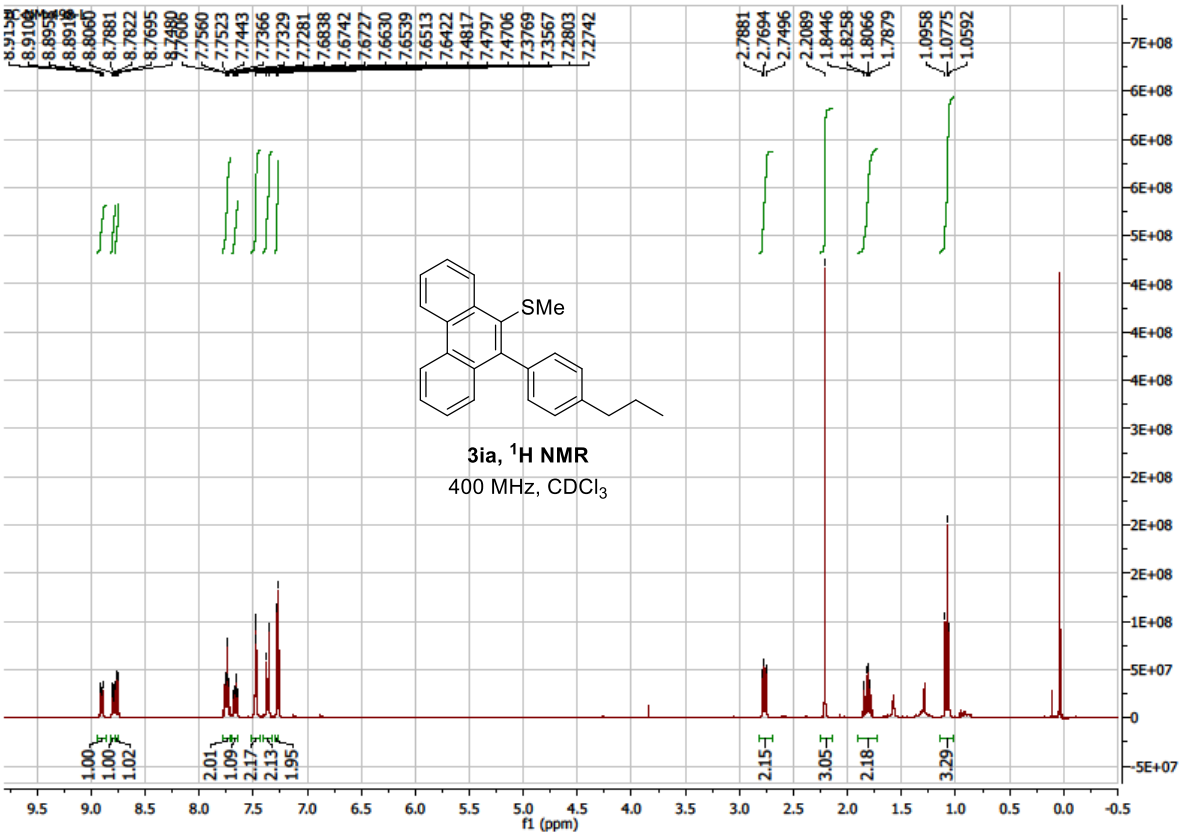
SMe
3ia, ^{1}H NMR
400 MHz, $CDCl_3$
f1 (ppm)

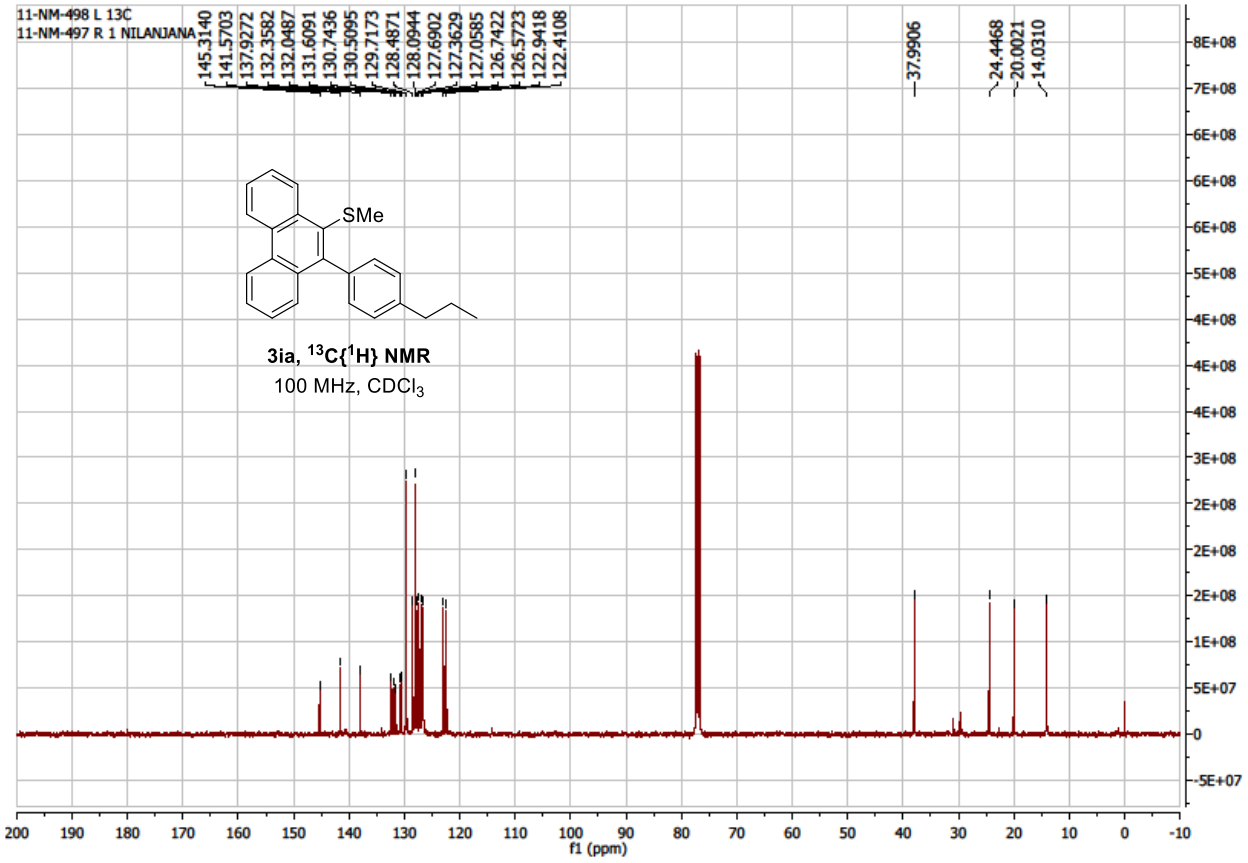
11-NM-498 L 13C
11-NM-497 R 1 NILANJANA
SMe
3ia, $^{13}C\{^{1}H\}$ NMR
100 MHz, $CDCl_3$
f1 (ppm)

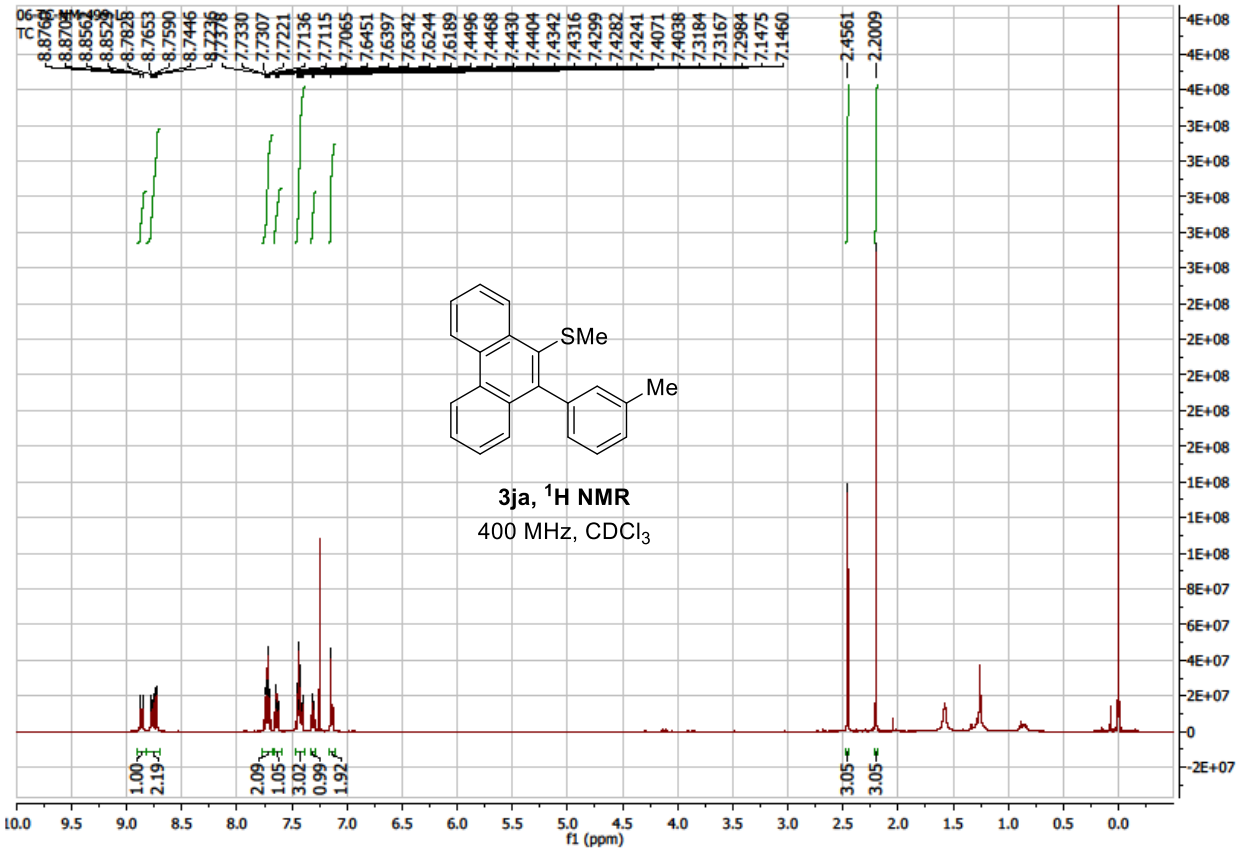
SMe
Me
3ja, ^{1}H NMR
400 MHz, $CDCl_3$
f1 (ppm)

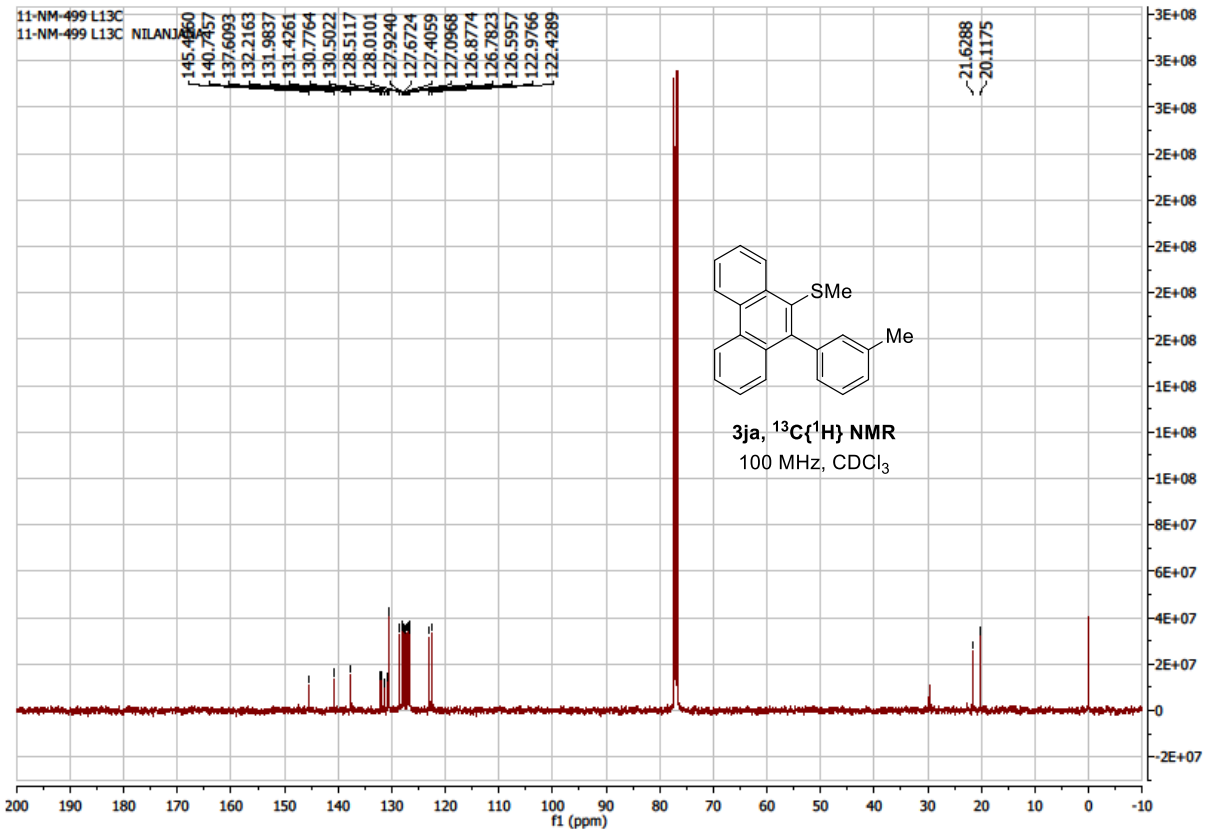

3ja, $^{13}C\{^{1}H\}$ NMR
100 MHz, $CDCl_3$

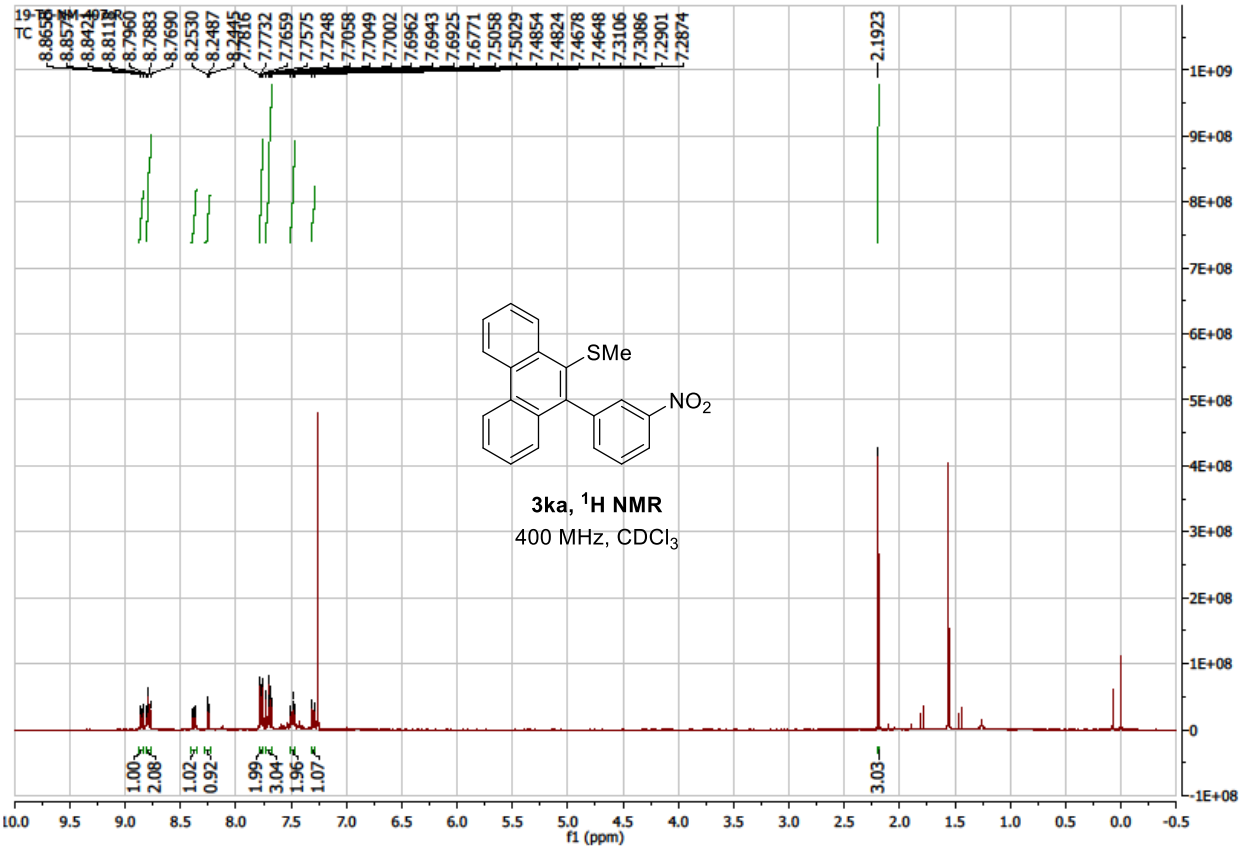

3ka, ^{1}H NMR
400 MHz, $CDCl_3$

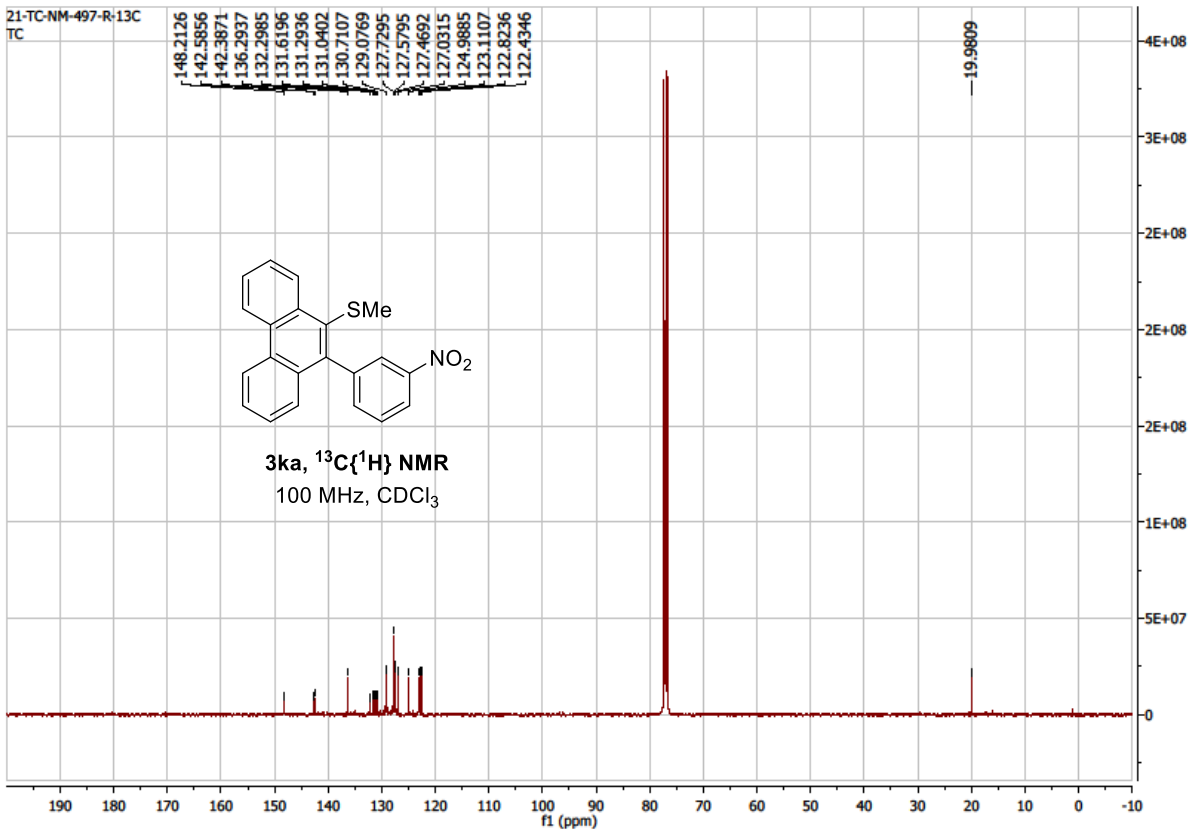

3ka, $^{13}C\{^{1}H\}$ NMR
100 MHz, $CDCl_3$

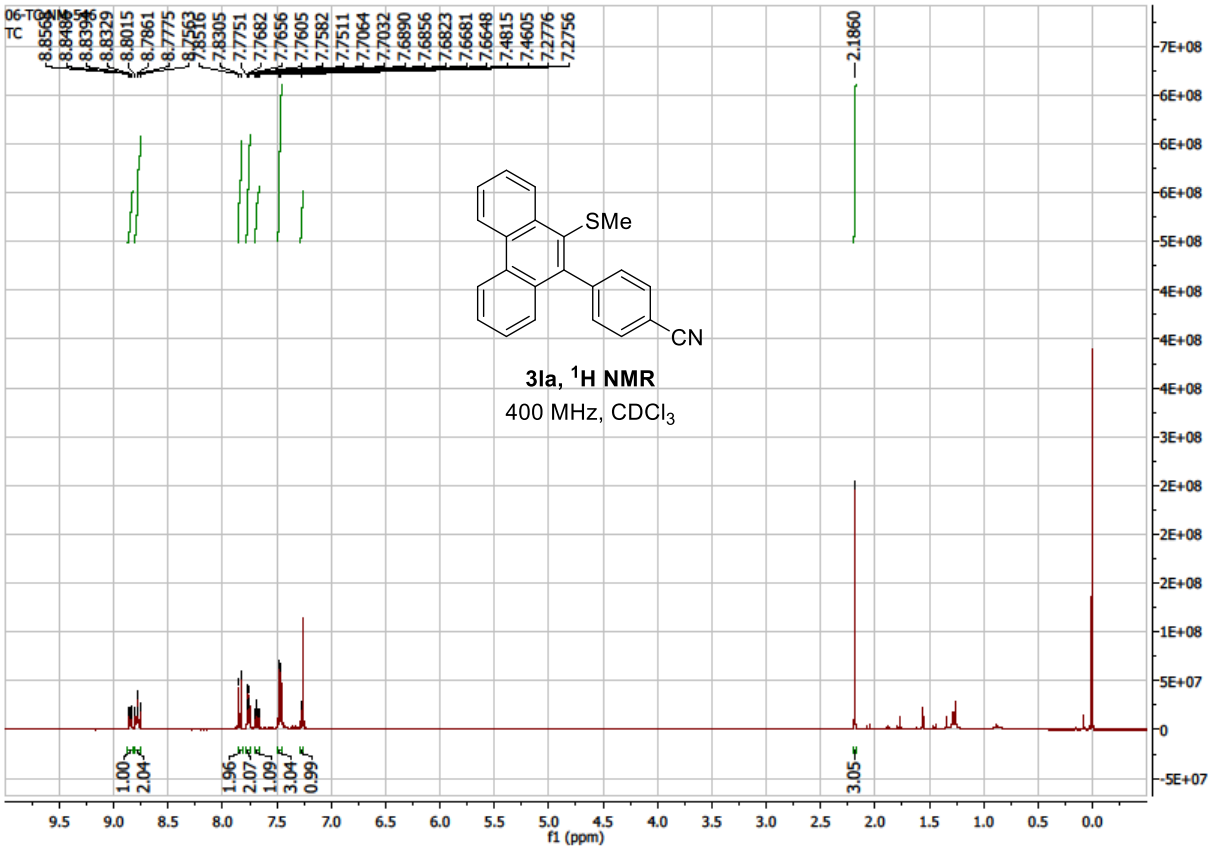

3la, ^{1}H NMR
400 MHz, $CDCl_3$

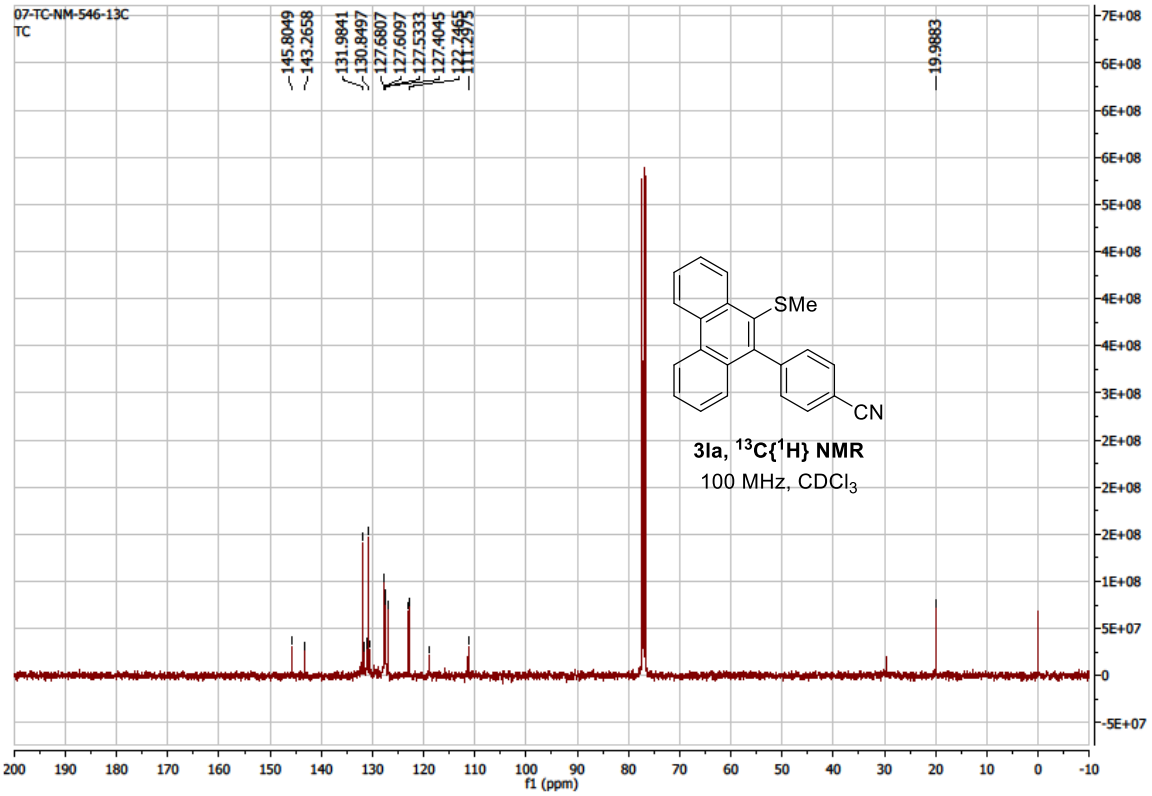
07-TC-NM-546-13C
TC
SMe
CN
3la, $^{13}C\{^{1}H\}$ NMR
100 MHz, $CDCl_3$
f1 (ppm)

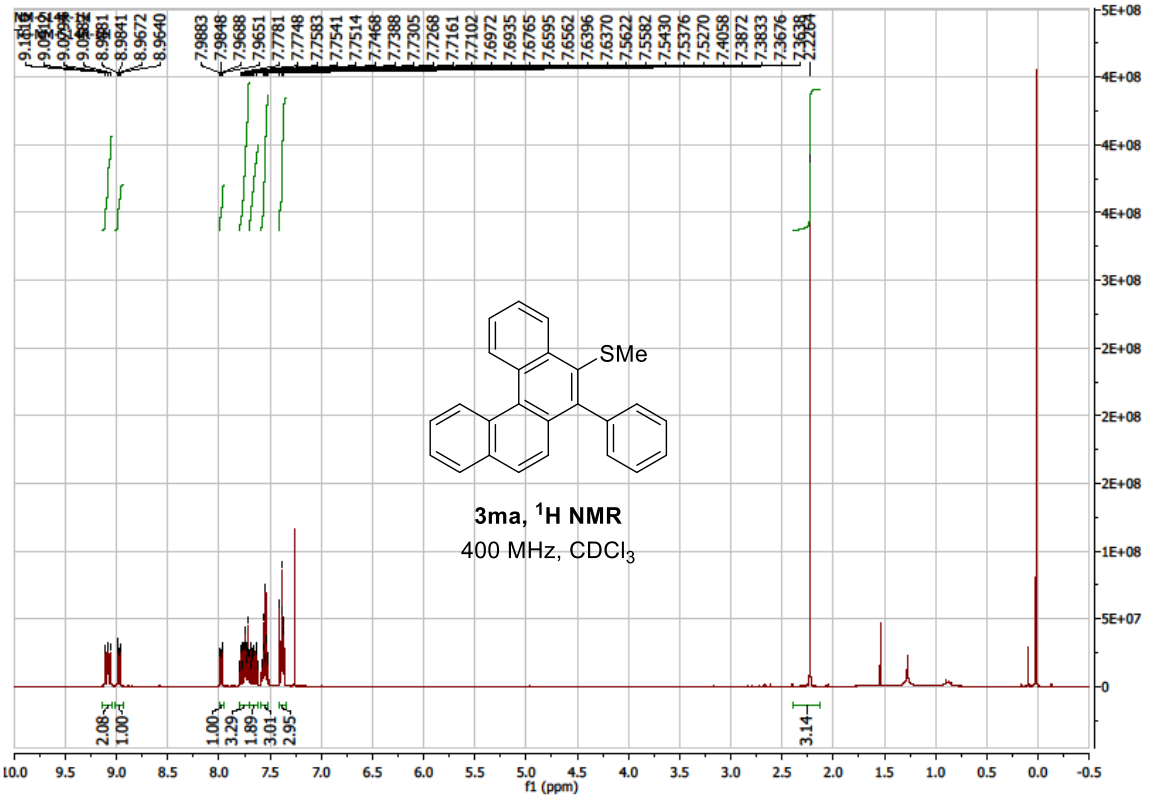
SMe
3ma, ^{1}H NMR
400 MHz, $CDCl_3$
f1 (ppm)

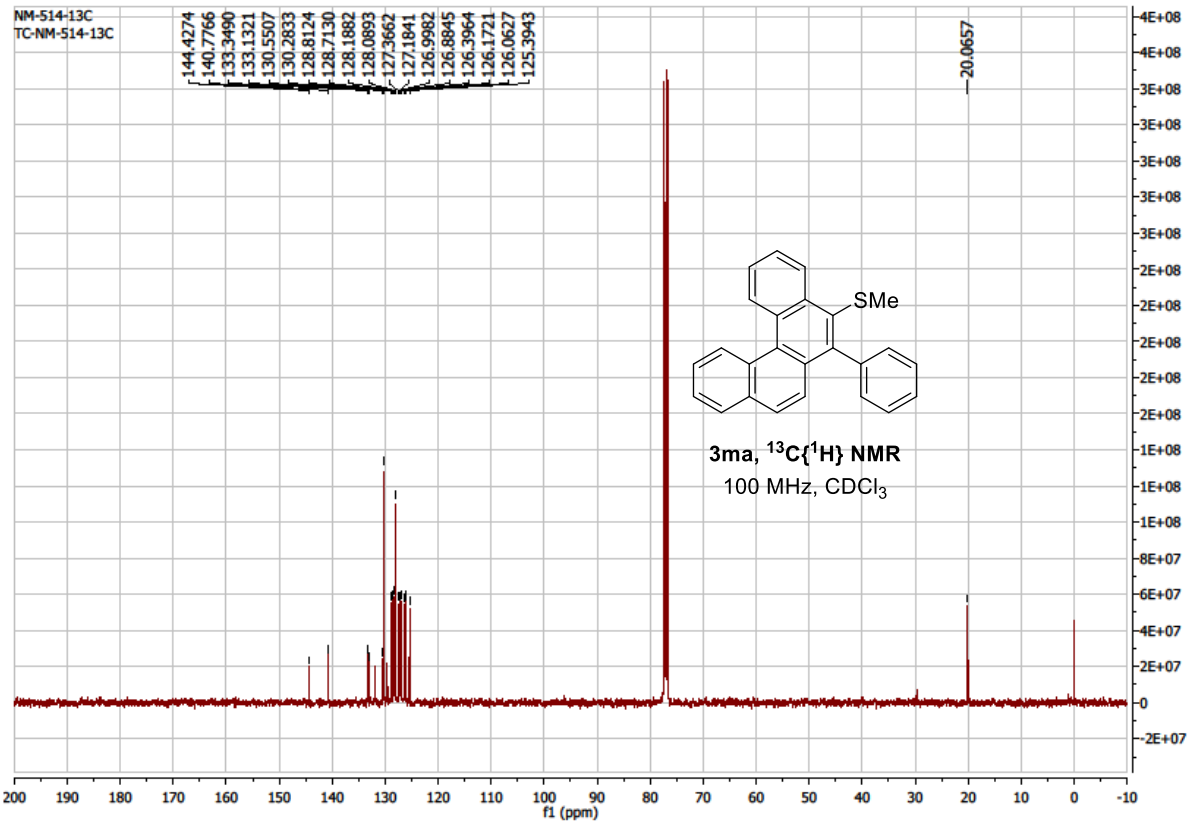
NM-514-13C
TC-NM-514-13C
144.4274
140.7766
133.3490
133.1321
130.5507
130.2833
128.8124
128.7130
128.1882
128.0893
127.3662
127.1841
126.9982
126.8845
126.3964
126.1721
126.0627
125.3943
20.0657
SMe
3ma, $^{13}C\{^{1}H\}$ NMR
100 MHz, $CDCl_3$
f1 (ppm)

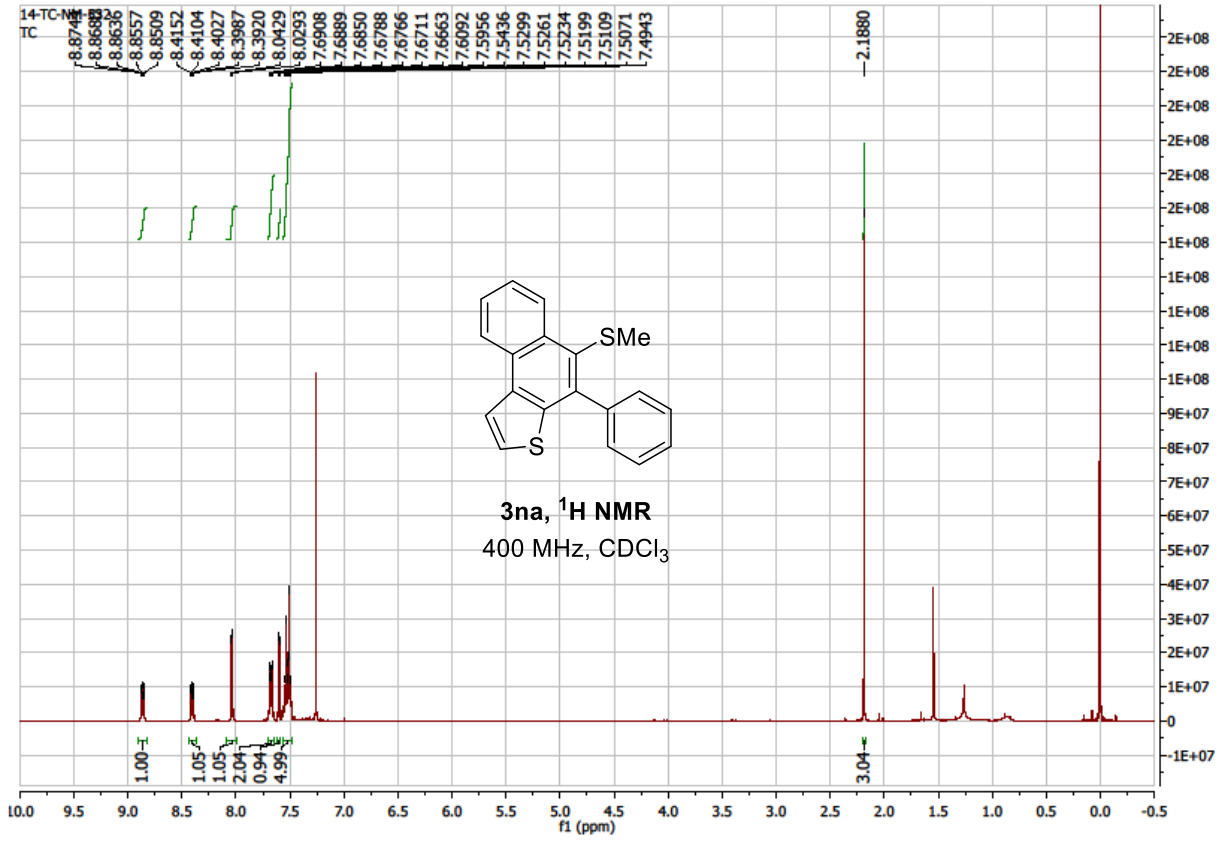
14-TC-NM-532
TC
8.8509
8.4152
8.4104
8.4027
8.3987
8.3920
8.0429
8.0293
7.6908
7.6889
7.6850
7.6788
7.6766
7.6711
7.6663
7.6092
7.5956
7.5436
7.5299
7.5261
7.5234
7.5199
7.5109
7.5071
7.4943
2.1880
SMe
S
3na, ^{1}H NMR
400 MHz, $CDCl_3$
1.00
1.05
1.05
2.04
0.94
4.99
3.04
f1 (ppm)

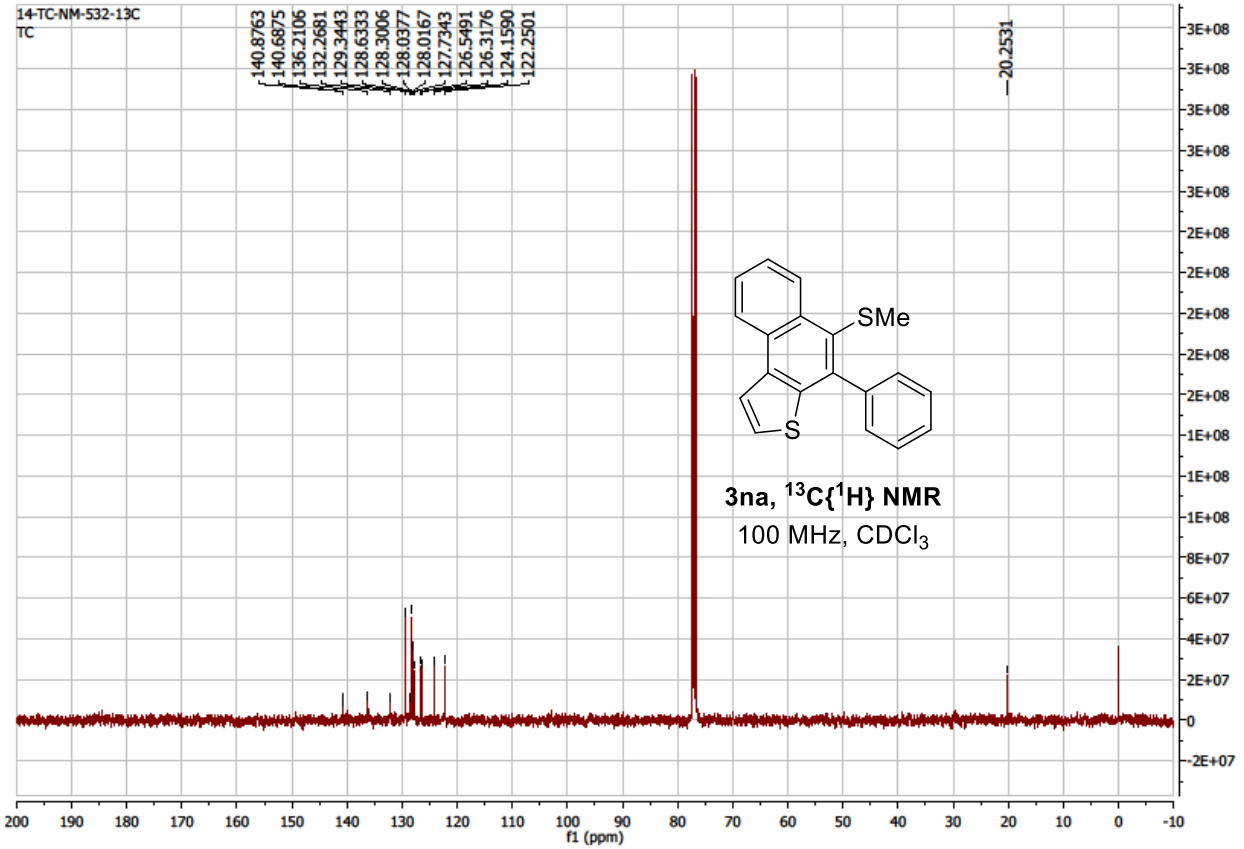
14-TC-NM-532-13C
TC
140.8763
140.6875
136.2106
132.2681
129.3443
128.6333
128.3006
128.0377
128.0167
127.7343
126.5491
126.3176
124.1590
122.2501
20.2531
SMe
S
3na, $^{13}C\{^{1}H\}$ NMR
100 MHz, $CDCl_3$
f1 (ppm)

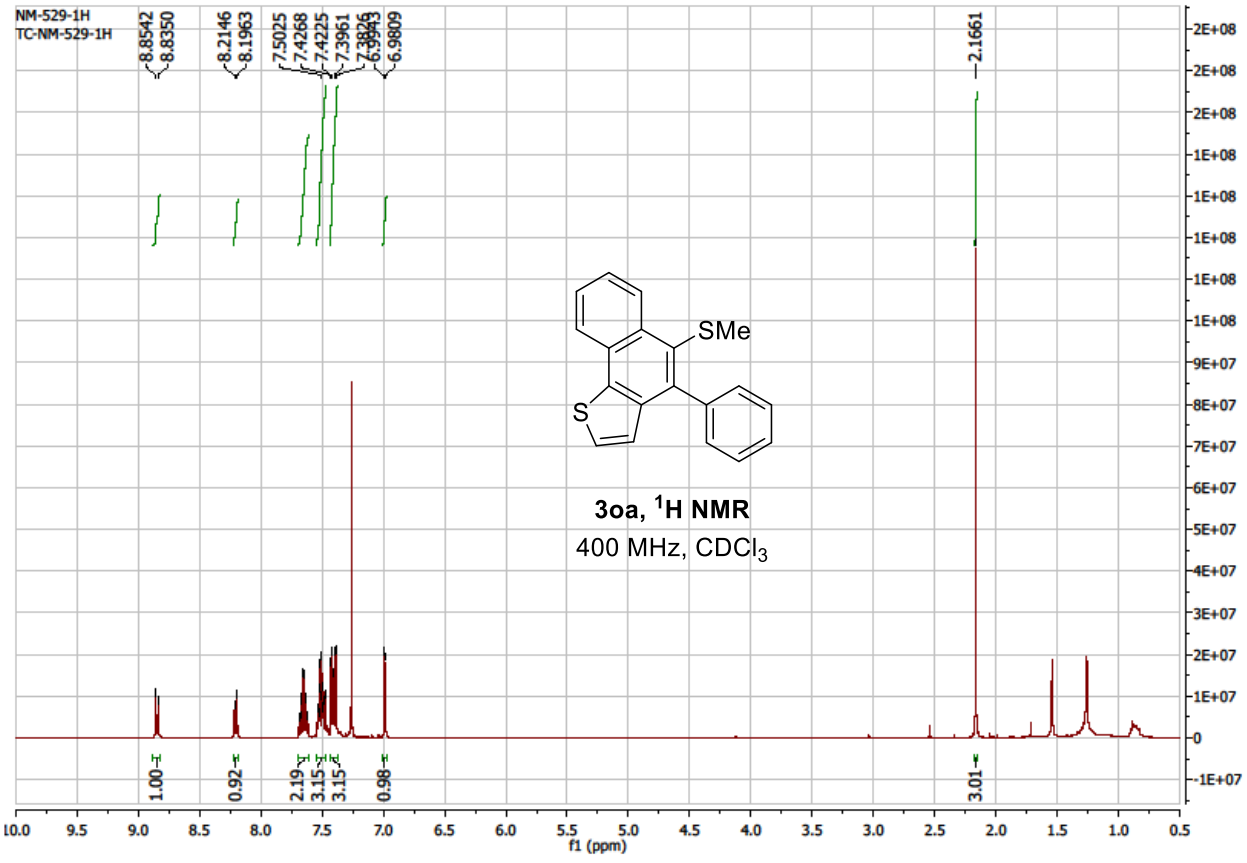
NM-529-1H
TC-NM-529-1H
8.8542
8.8350
8.2146
8.1963
7.5025
7.4268
7.4225
7.3961
7.3826
6.9943
6.9809
2.1661
SMe
S
3oa, ^{1}H NMR
400 MHz, $CDCl_3$
1.00
0.92
2.19
3.15
3.15
0.98
3.01
f1 (ppm)

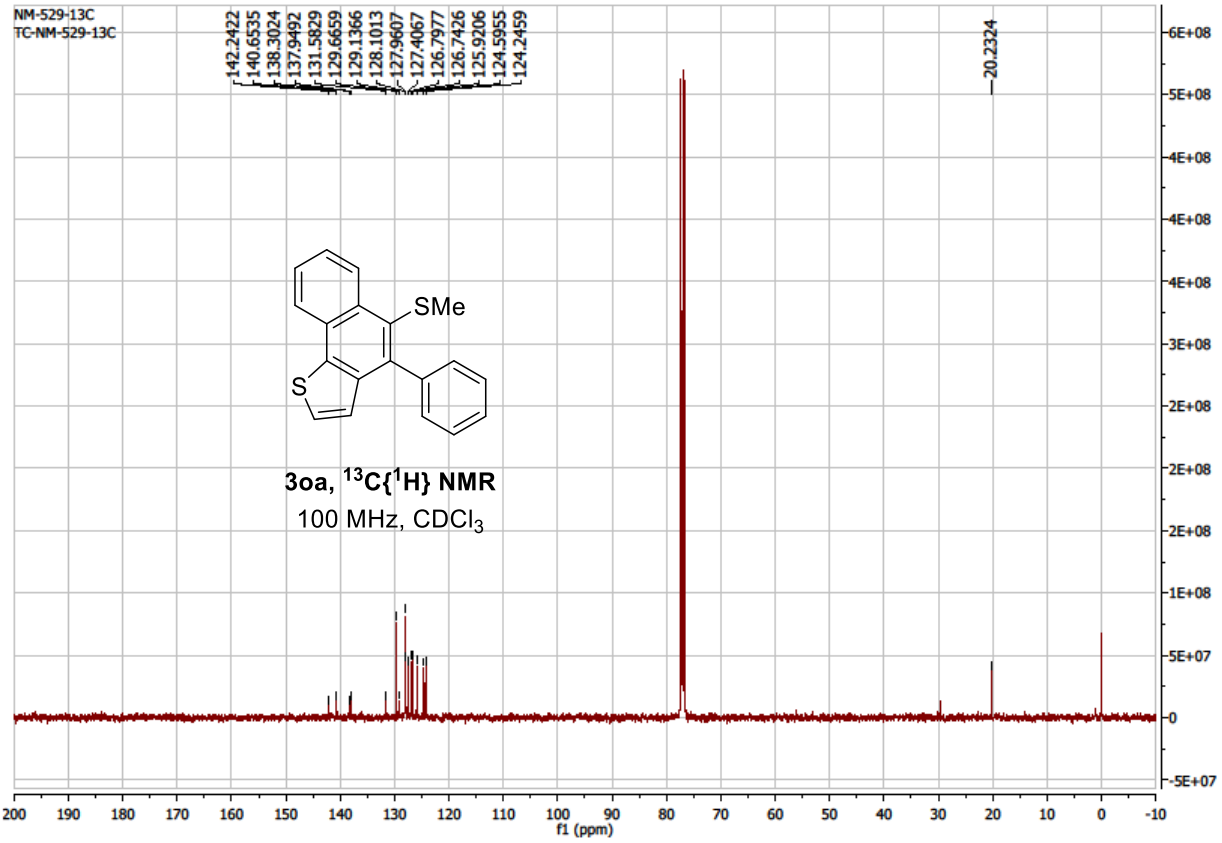

3oa, $^{13}C\{^{1}H\}$ NMR

100 MHz, $CDCl_3$

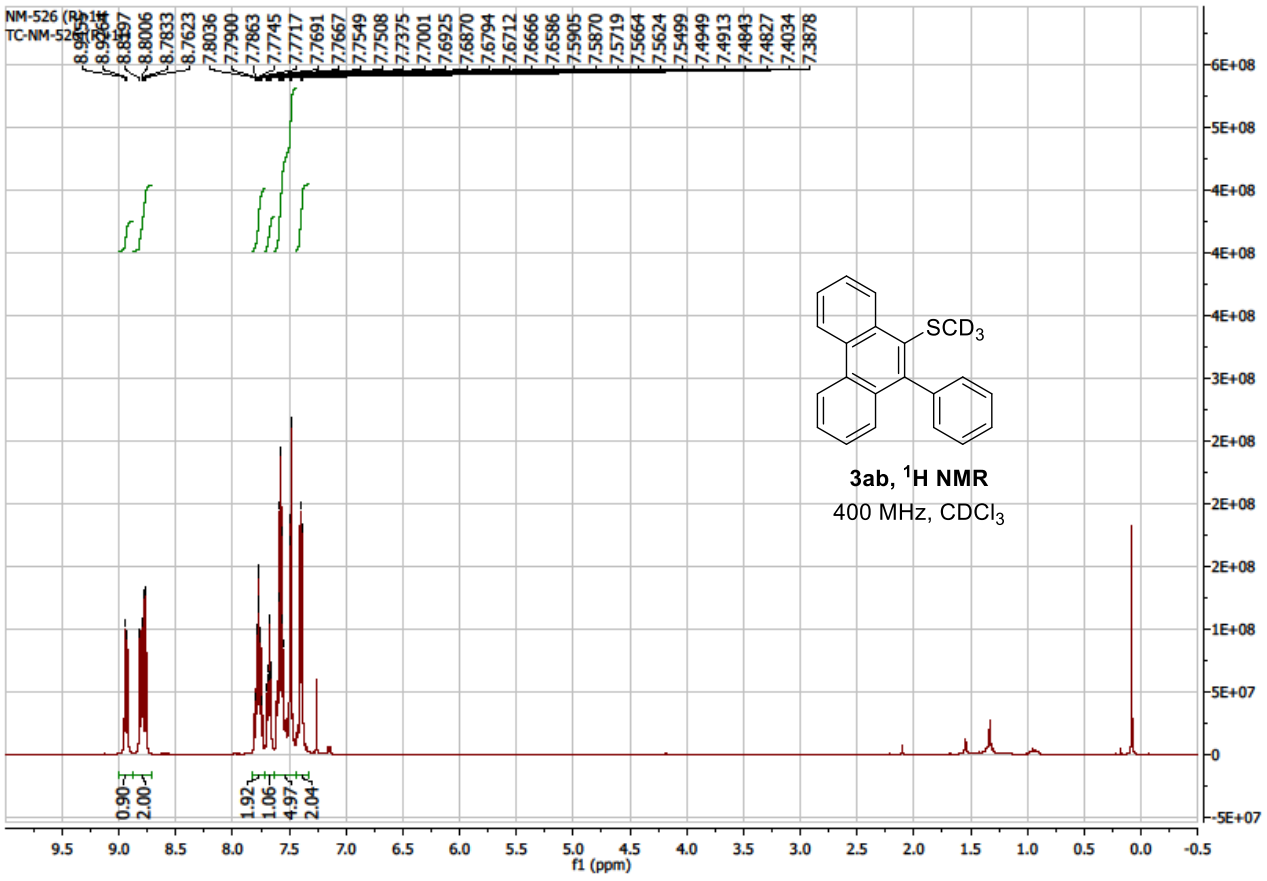

3ab, ^{1}H NMR

400 MHz, $CDCl_3$

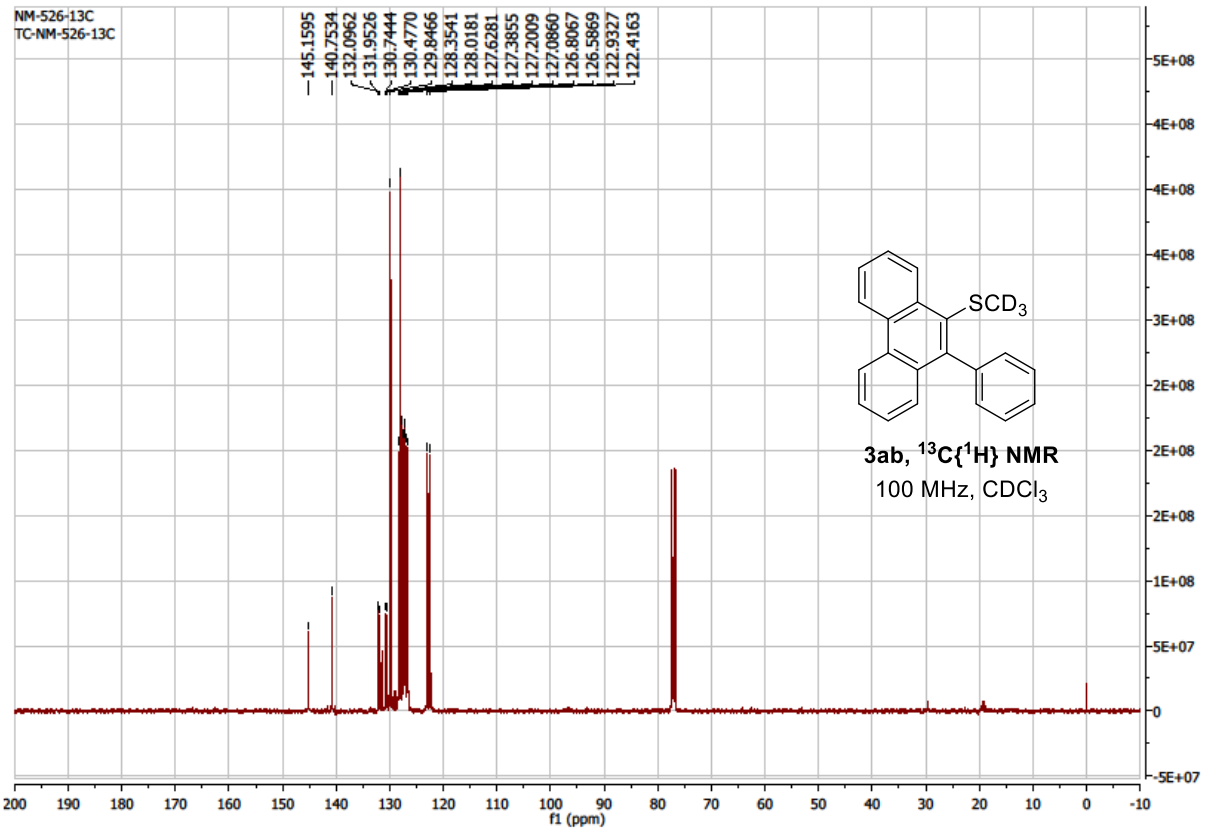

3ab, $^{13}C\{^{1}H\}$ NMR
100 MHz, $CDCl_3$

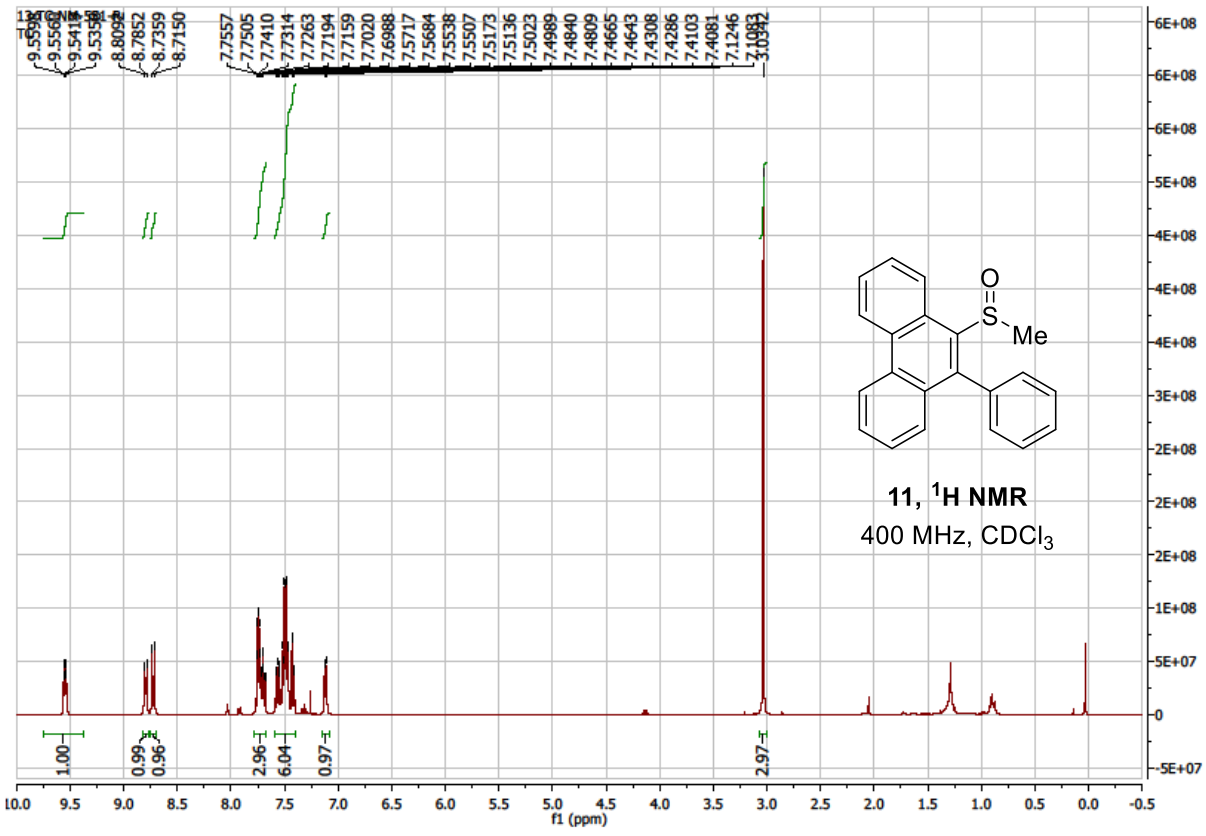

11, ^{1}H NMR
400 MHz, $CDCl_3$

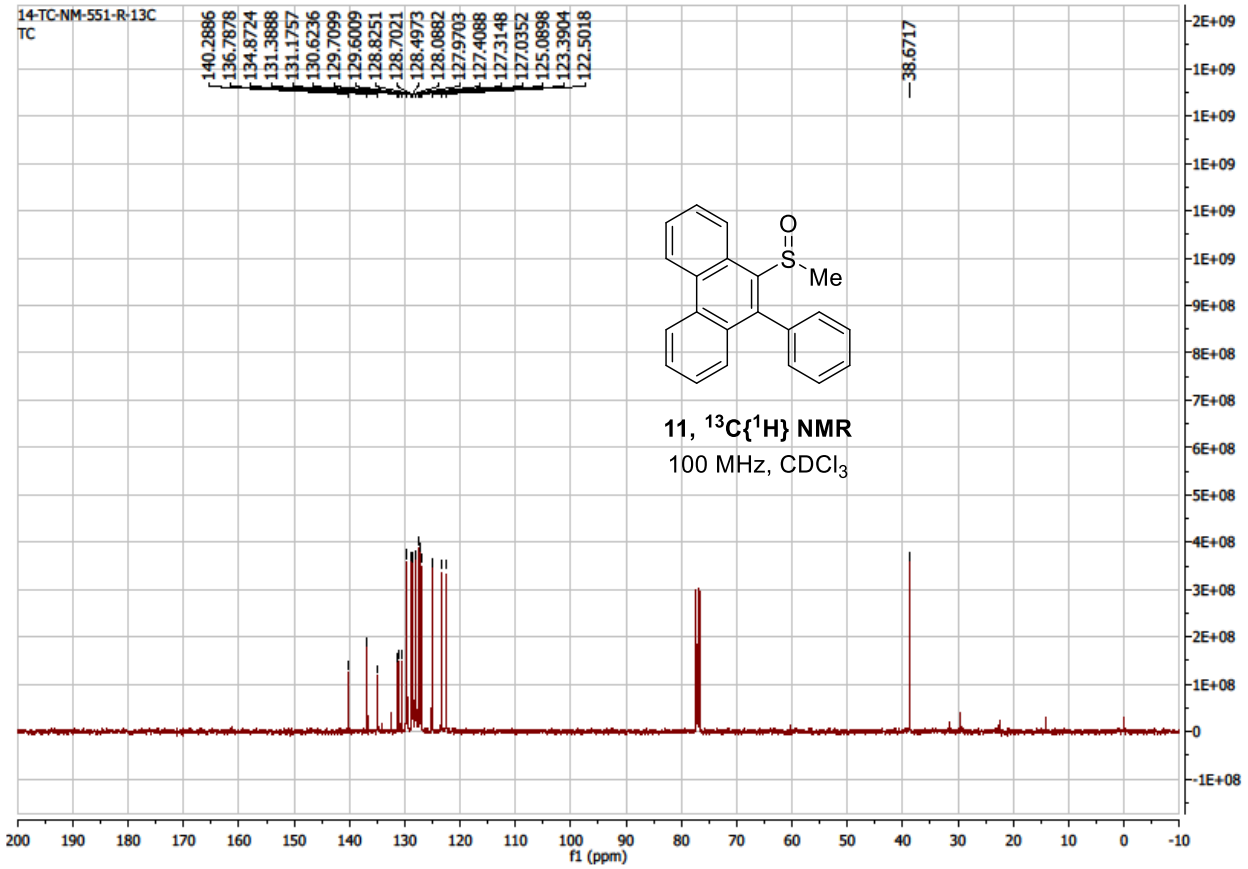

11, $^{13}C\{^{1}H\}$ NMR

100 MHz, $CDCl_3$

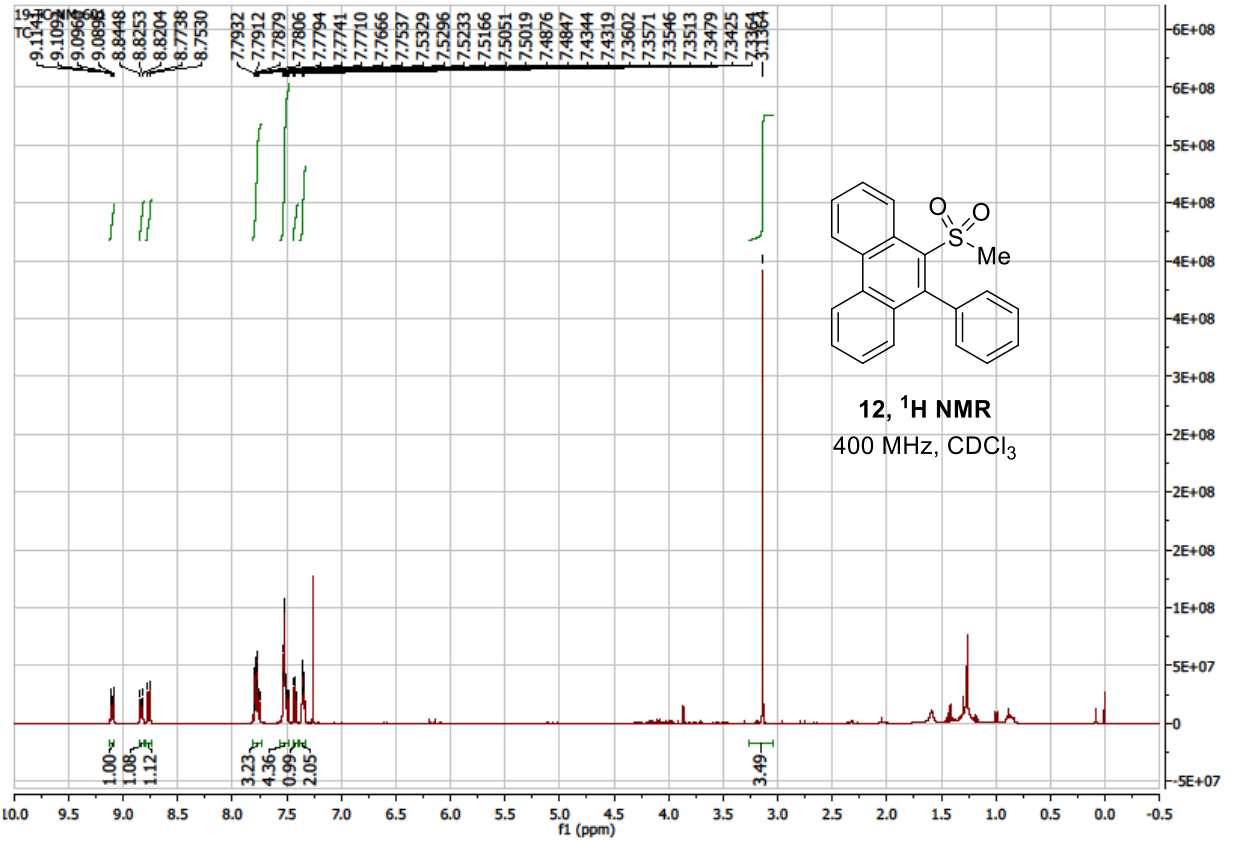

12, ^{1}H NMR

400 MHz, $CDCl_3$

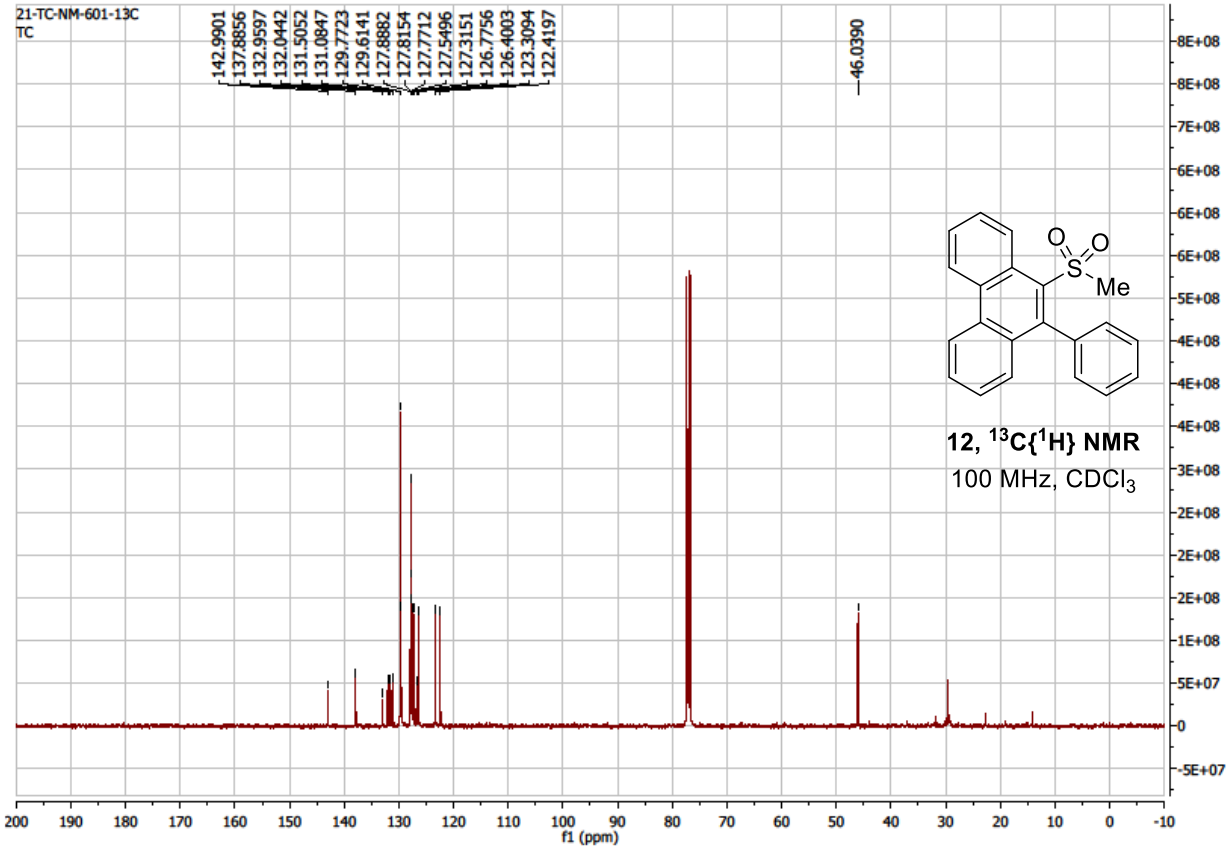
21-TC-NM-601-13C
TC
142.9901
137.8856
132.9597
132.0442
131.5052
131.0847
129.7723
129.6141
127.8882
127.8154
127.7712
127.5496
127.3151
126.7756
126.4003
123.3094
122.4197
46.0390
O
O
S
Me
12, 13C{1H} NMR
100 MHz, CDCl3
f1 (ppm)

JOC The Journal of Organic Chemistry

pubs.acs.org/joc Note

Iodine-Catalyzed Methylthiolative Annulation of 2-Alkynyl Biaryls with DMSO: A Metal-Free Approach to 9-Sulfenylphenanthrenes

Nilanjana Mukherjee and Tanmay Chatterjee*

Cite This: J. Org. Chem. 2021, 86, 7881−7890 Read Online

ACCESS | Metrics & More | Article Recommendations | Supporting Information

ABSTRACT: An iodine-catalyzed sustainable, cost-effective, and atom-economic synthetic methodology is developed to synthesize a wide variety of valuable sulfenylphenanthrenes and polycyclic heteroaromatics in moderate to high yield through electrophilic thiolative annulation of 2-alkynyl biaryls (6-*endo*-*dig* cyclization) using methyl sulfoxides such as dimethyl sulfoxide (DMSO) as the sulfur source under transition-metal-free conditions. The transformation requires only iodine in a catalytic amount and trifluoroacetic anhydride. Notably, DMSO played multiple roles such as methylthiolating reagent, oxidant, and solvent in this reaction.

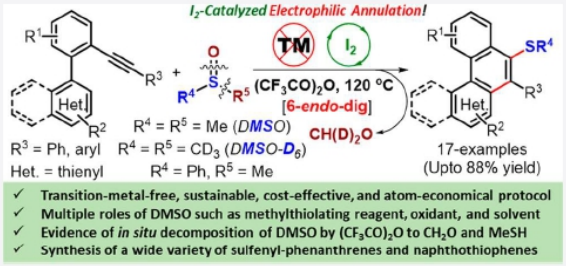

Phenanthrenes, one of the important classes of polycyclic aromatic hydrocarbons, are ubiquitous in numerous biologically active compounds including natural products[1] and exhibit a broad spectrum of biological activities such as antiviral,[2] antimicrobial,[3] anticancer,[4] antitumor,[5] and anti-HIV[6] activity. Moreover, phenanthrene derivatives also exhibit interesting electronic[7] and optical[8] properties and are utilized in various useful materials, such as organic field-effect transistors[9] and solar cells.[10] Consequently, several synthetic strategies have been developed so far for the synthesis of phenanthrenes.[11,12] Among them, two synthetic strategies, i.e., transition-metal (TM) (Pd, Ir, Rh, and Fe)-catalyzed or visible-light photocatalyzed [4 + 2]-benzannulation of 2-functionalized 1,1′-biaryls with alkynes[13] and transition-metal (Pt, Au, Ga, Ir, Ru, Fe, and Sn)-catalyzed/mediated intramolecular carbocyclization or electrophilic annulation of 2-alkynyl biaryls (6-*endo*-*dig* cyclization) are widely employed, perhaps because of their high atom-economical feature and the requirement of relatively less prefunctionalized starting materials.[14] Despite significant advancement, the above-mentioned synthetic methods suffer from at least one of the following severe limitations, such as the requirement of (a) expensive and toxic transition-metal salts or complexes in catalytic or (sub)stoichiometric amounts, (b) expensive and hazardous ligand and reagents, (c) harsh or critical reaction conditions, and (d) limited substrate scope. In 2005, Larock et al. disclosed a transition-metal-free, electrophilic 6-*endo*-*dig* cyclization of 2-alkynyl biaryls with ICl, *N*-bromosuccinimide (NBS), and *p*-$O_2NC_6H_4SCl$ to synthesize 9-halo (I and Br)- and 9-(4-nitrophenyl)sulfenylphenanthrenes, respectively (Scheme 1 A).[15]

However, the requirement of a highly electrophilic arylsulfenyl chloride, *p*-$O_2NC_6H_4SCl$, and its commercial

Scheme 1. General Synthetic Strategies to 9-Sulfenylphenanthrenes

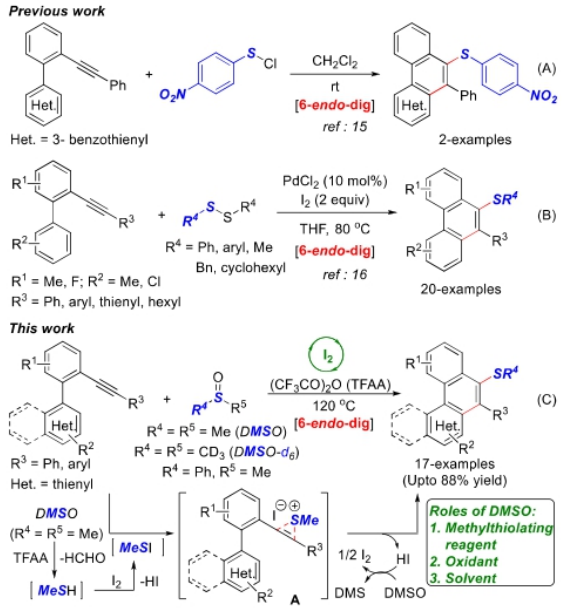

Received: April 14, 2021
Published: May 24, 2021

SECTION-V

Applications of Methyl(10-phenylphenanthren-9-yl)sulfane (MPPS) As a Fluorescence Probe

2.5.1. Introduction.

Being motivated by the useful applications of phenanthrenes, as discussed in Section II, we became interested in exploring one of our synthesized molecules, *i.e.*, methyl(10-phenylphenanthren-9-yl)sulfane (MPPS). To understand whether MPPS could be utilized as a fluorescent probe, we first studied its photophysical properties in collaboration with Prof. Subit Saha's group at BITS Pilani, Hyderabad Campus.

2.5.2. Results and Discussion.

UV-Vis Absorption and Fluorescence Study: UV-Vis absorption spectra of MPPS in solvents of different polarities are recorded and displayed in Figure 2.5.1. The values of peak maxima for longer wavelength absorption bands are calculated and tabulated in Table 2.5.1. along with the dielectric constant (ε) of solvents. The general trend is that the absorption peak maxima are blue-shifted with increasing polarity of the solvents. It depicts that the ground state dipole moment is greater than that of the excited state dipole moment. The fluorescence spectra of MPPS in different solvents have been recorded by excitation at corresponding absorption peak maxima and are presented in Figure 2.5.2. The fluorescence peak maxima values are given in Table 2.5.1. The fluorescence peak maxima are red-shifted with increasing polarity of the solvents. It indicates that the emitting state is more polar than the ground state. The fluorescence intensities in polar solvents are found to be much lower than that in non-polar solvents. It could be due to the fact that the polar emitting state gets stabilized in a polar solvent and as a result, the state becomes energetically close to the triplet state as well as the ground state. Therefore, the rates of intersystem crossing and internal conversion increase leading to reduced quantum yields.

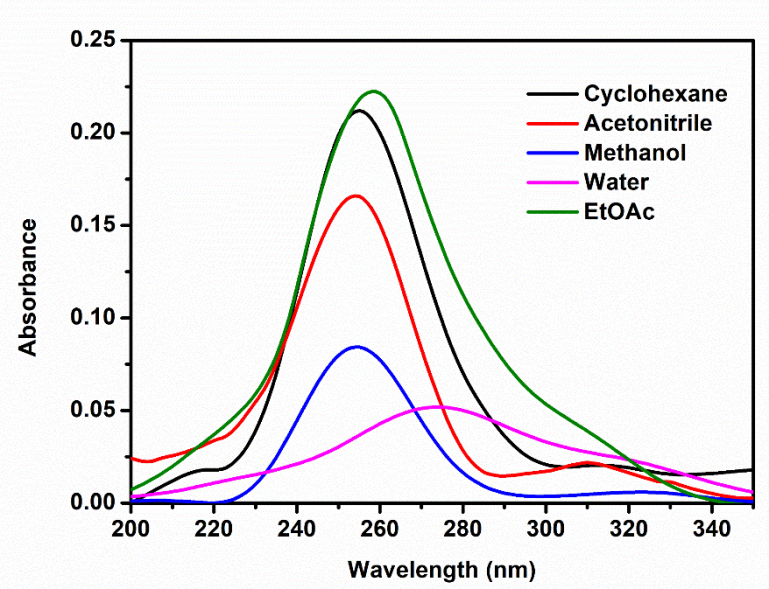

Figure 2.5.1. Absorption Spectra of MPPS in Different Solvents.

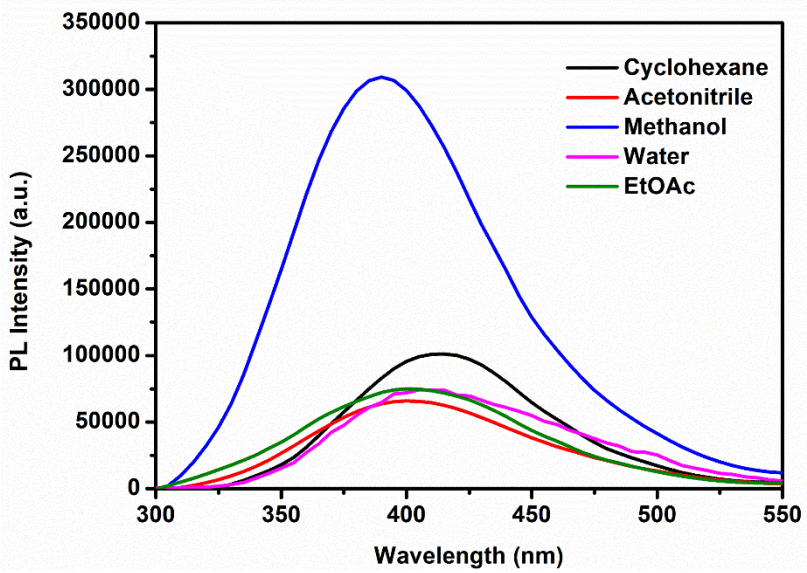

Figure 2.5.2. Emission Spectra of MPPS in Different Solvents.

Table 2.5.1: Photophysical Properties of MPPS

Solvents	Solution (nm) λ_{abs}	λ_{em}	Stoke's Shift (cm^{-1})	ε
Cyclohexane	255, 314	415	99,010	2.02
Ethyl Acetate	258, 311	404	68,493	6.0
Methanol	254, 327	390	1,58,730	32.66
Acetonitrile	255, 311	401	1,11,111	35.94
Water	273, 323	413	71,428	78.36

In order to present the molecule MPPS as a potential fluorescent probe, the molecule has been explored to characterize the micelles of different surfactants (both conventional and gemini surfactants) and protein, bovine serum albumin (BSA).

Binding of MPPS with micelles of surfactants

Cationic surfactant, DTAB

Figure 2.5.3 displays the fluorescence intensities of MPPS at different concentrations of a conventional cationic surfactant, dodecyl trimethylammonium bromide (DTAB). It can be seen that the fluorescence intensity decreases, reaches a minimum, and then increases with increasing concentration of the surfactant. The minimum appears at [DTAB] = 14.5 mM, which is the CMC of DTAB, and the value is close to the reported CMC value of DTAB as 14.7 mM.[1,2]

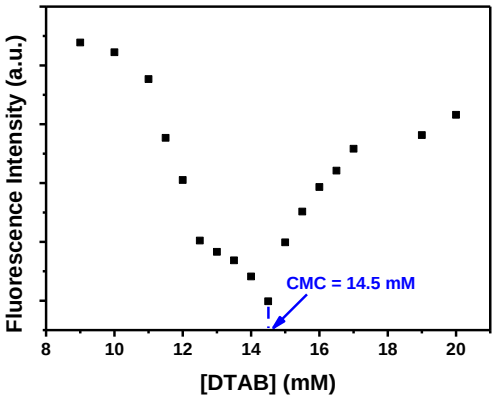

Figure 2.5.3. Fluorescence Intensities of MPPS at Different Concentrations of DTAB.

[MPPS] = 5 μM, λ_{ex} = 330 nm and λ_{em} = 395 nm.

Anionic surfactant, SDS

Figure 2.5.4 presents the variations of fluorescence intensities of MPPS with changing the concentrations of a conventional anionic surfactant, sodium dodecyl sulfate (SDS). With increasing concentrations of SDS, the fluorescence intensity first decreases, and after reaching a minimum, it increases. The concentration of SDS at which the minimum appears is 8.02 mM, almost the same as the CMC value of SDS found in the literature i.e. 8.2 mM [1]

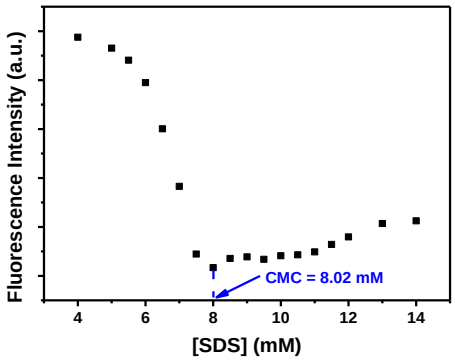

Figure 2.5.4, Fluorescence Intensities of MPPS at Different Concentrations of SDS.

[MPPS] = 5 μM, λ_{ex} = 330 nm and λ_{em} = 395 nm.

Non-ionic surfactant, Triton-X 100

The variation of fluorescence intensities of MPPS with increasing concentration of a conventional non-ionic surfactant, Triton X-100 has been shown by Figure 2.5.5. Like the other two cases, here also, the fluorescence intensity of MPPS decreases, gives a minimum fluorescence intensity value at [Triton X-100] = 0.21 mM, and then increases with increasing concentrations of Triton X-100. The minimum corresponds to the CMC of Triton X-100, which is almost the same as the reported CMC value of Triton X-100.[3]

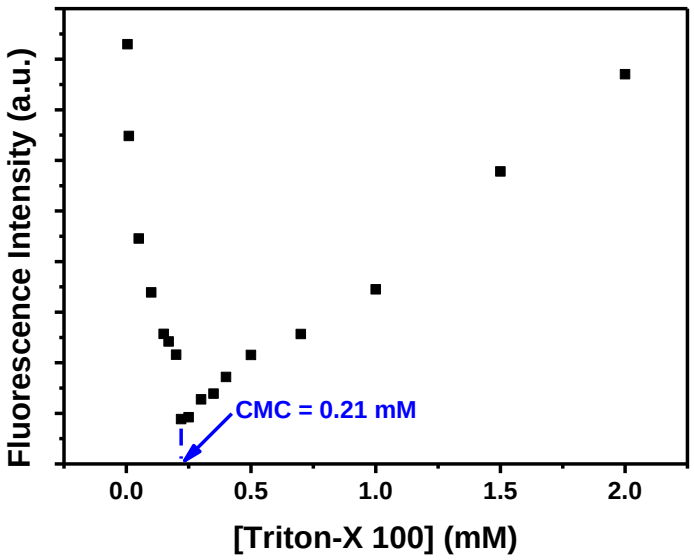

Figure 2.5.5. Fluorescence Intensities of MPPS at Different Concentrations of Triton X-100. [MPPS] = 5 μM, λ_{ex} = 330 nm and λ_{em} = 395 nm.

Cationic gemini surfactant, 12-6-12,2Br$^-$

To study how the fluorescence property of MPPS responds to the changes in the concentrations of a gemini surfactant, 12-6-12,2Br$^-$ in the solution, the fluorescence spectra of MPPS have been recorded at different concentrations of the gemini surfactant and the fluorescence intensity at λ_{em} = ??? are plotted against the [12-6-12,2Br$^-$] as shown by Figure 2.5.6. The fluorescence intensities change in the same way as discussed for the other three surfactants. The minimum fluorescence intensity of MPPS is noted at 0.95 mM of 12-6-12,2Br$^-$ which is the CMC of this surfactant. The literature reports the CMC of 12-6-12,2Br$^-$ as 1.03 mM [4]

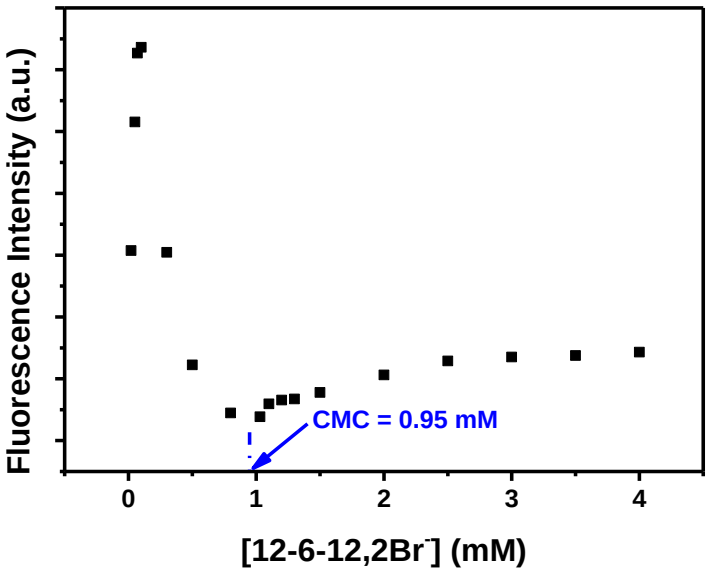

Figure 2.5.6. Fluorescence Intensities of MPPS at Different Concentrations of 12-6-12,2Br$^-$.

[MPPS] = 5 μM, λ_{ex} = 330 nm and λ_{em} = 395 nm.

The results presented above show that the CMC value determined based on the changes in fluorescence intensities of MPPS with increasing surfactant concentrations is very close to the reported CMC for each surfactant. It depicts that the fluorescence property of MPPS is very sensitive to the changes in the microenvironment around it. In the pre-micellar region, each ionic surfactant acts as a strong electrolyte, therefore, with increasing concentration of the surfactant the number of ions gradually increases resulting-in increasing polarity of the medium. In this region, the fluorescence intensity of MPPS decreases with increasing concentration of a surfactant. The result is supported by the above mentioned solvatochromic data wherein the fluorescence intensity of MPPS is found to be decreased with increasing polarity of the solvent. However, once the micelles start to form above the CMC, the fluorescence intensity of MPPS increases. It has been discussed above that the fluorescence intensity of MPPS increases with decreasding polarity of the medium. Thus in the post micellar region the increase in fluorescence intensity of MPPS says that the molecules are going from the polar bulk to the non-polar sites of the micelles. as the polarity of the microenvironment around MPPS decreases due to the solubilisation of the MPPS in micelles.

Binding of MPPS with Protein, Bovine Serum Albumin (BSA)

To study the binding of MPPS with BSA, the fluorescence spectra of native BSA (λ_{ex} = 295 nm) have been recorded at different concentrations of MPPS (0 to 25 μM) and shown by Figure 2.5.7. Notably, the excitation of BSA at 295 nm results in fluorescence from the Trp residues of the protein. It can be seen in Figures 2.5.7 that with increasing comcentration of MPPS, the fluorescence intensity of BSA decreases and that of MPPS increases. Therefore, MPPS acts as a quencher. As MPPS also has an absorption at 295 nm, thus fluorescence from both BSA and MPPS are seen in this figure. While the fluorescence peak maximum of BSA appears at ~350 nm, the same for a fluorescence band of MPPS is seen at ~363 nm. Figure 8 displays the changes in flurescence intensity ratios, F_o/F (where F_o and F are fluorescence intensities of BSA in the absence and presence of MPPS, respectively) of BSA with increasing concentration of MPPS. This Stern-Volmer plot (Fig. 2.5.8) shows a downward curvature incating the fact of fractional accesibilty of Trp residues of BSA to the quencher, MPPS. Two different fractions of Trp residues, Trp-213 and Trp-134 do exist in BSA.[5] Trp-213 is located in a hydrophobic pocket, and Trp-134 resides in a hydrophilic environment i. e. near to the surface of the protein.[5] Docking results (Fig. 2.5.10) show that MPPS binds to the hydrophobic region of the BSA. Therefore, it is expected that MPPS is more accessible to Trp-213 than to Trp-134. In our earlier study, a blue shift in fluorescence peak maximum of BSA has been noted with increasing concentration of a probe, dimethylaminopstyryl benzothiazole (DMASBT).[5] It is due to the accessibility of Trp-134 to DMASBT, as the latter binds to the hydrophilic sites of BSA. As the fluorescence from Trp-134 occurs slightly at a longer wavelength than that of Trp-213, thus with the quenching of

fluorescence from Trp-134, the overall peak maximum of BSA gets blue shifted. However, in the present case the blue shift in BSA fluorescence peak maximum with increasing concentration of MPPS is not seen, supporting the fact that MPPS quenches fluorescene from Trp-213 not from Trp 134.

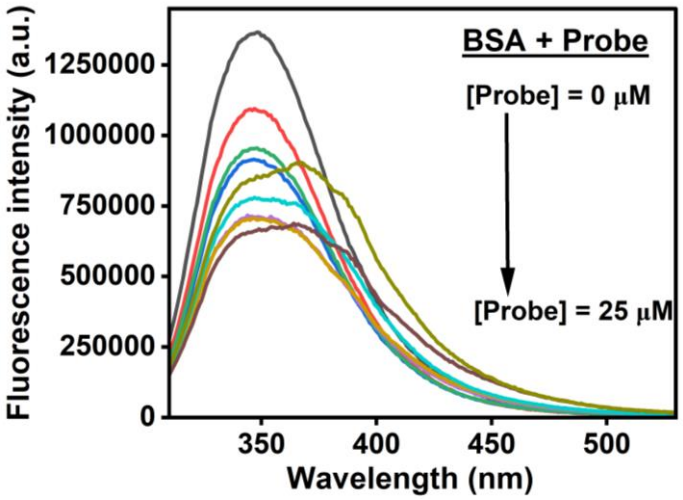

Figure 2.5.7. Fluorescence Spectra of MPPS (5 μM) as a Function of Concentrations of BSA. [Inset: Variation in Fluorescence Peak Maxima of the Synthesized Probe as a Function of Concentrations of BSA (λ_{ex} = 330 nm)].

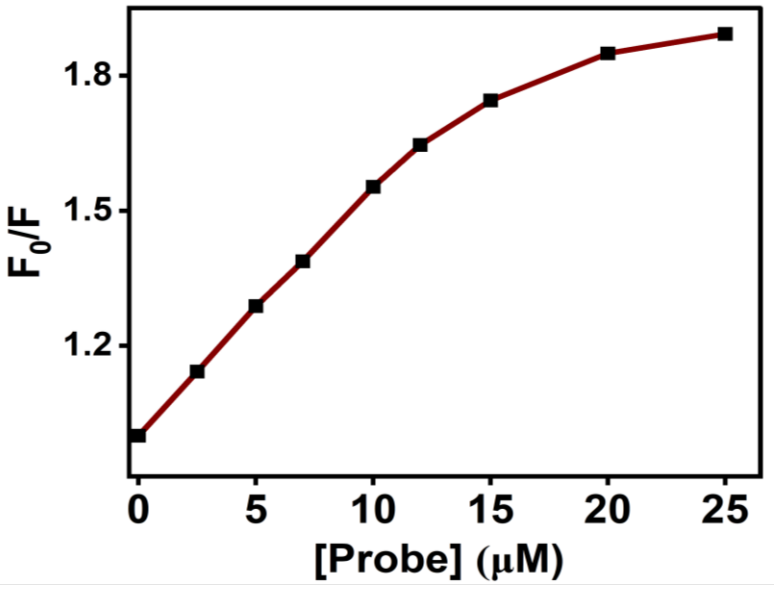

Figure 2.5.8. Stern-Volmer plot for the quenching of fluorescence of BSA by MPPS. λ_{ex} = 295 nm.

To estimate the fractional accessibility of Trp residues to MPPS in native BSA, and to calculate the value of fraction of Trp residues accessible to MPPS (f_a) in the native protein, the modified Stern-Volmer plot (Fig. 2.5.9) based on the Equation 1[5] has been made and shown by Figure 9:

$$\frac{F_o}{(F_o - F)} = \frac{1}{f_a K_a [APSM]} + \frac{1}{f_a} \quad (1)$$

where F_o and F are the total fluorescence intensities of Trp residues in BSA in the absence and presence of MPPS at its concentration, [MPPS], respectively. K_a is the Stern-Volmer constant for the quenching of accessible fraction. f_a is the fraction of Trp residues accessible to MPPS. f_a can be written as:

$$f_a = \frac{F_{0a}}{F_{0b} + F_{0a}} \quad (2)$$

where the subscript 0 refers to the fluorescence intensity in the absence of quencher. Thus, F_{0a} denotes the fluorescence intensity from the accessible fraction, while F_{0b} refers to the fluorescence intensity from the inaccessible fraction in BSA in the absence of quencher. The correlation coefficient of this modified Stern-Volmer plot is found to be 0.999. f_a and K_a values calculated from the intercept and the slope of the modified Stern-Volmer plot after linear fitting of the data are found to be 0.68 and 1.63×10^8 M^{-1}. Thus, 68 % of Trp residues are only accessible to the MPPS in native BSA. The Stern-Volmer quenching constant of accessible fraction, $K_a = k_q \tau_o = 1.63\times10^8$ M^{-1}. The τ_o value for BSA protein is reported to be ~10^{-8} s. [5] Thus, the bimolecular quenching rate constant (k_q) value is calculated to be 1.63×10^{16} M^{-1} s^{-1}. However, the maximum value of k_q for a diffusion-controlled fluorescence quenching process with a biopolymer is reported to ~ 2.0×10^{10} M^{-1} s^{-1}.[5] It depicts that the fluorescence quenching mechanism of accessible fraction of Trp residues is static in nature

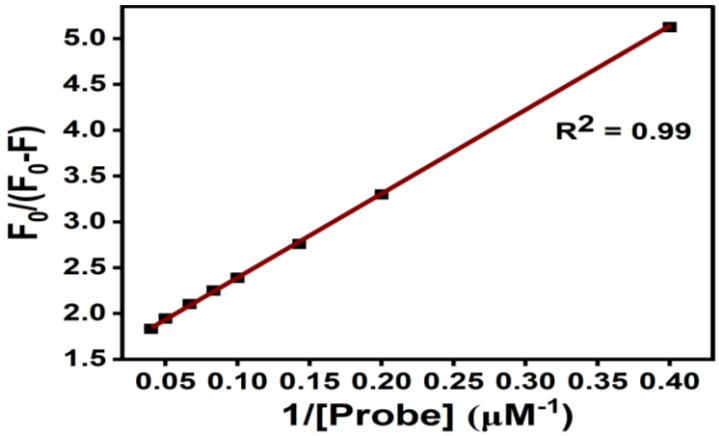

Figure 2.5.9. Modified Stern-Volmer plot for the Quenching of Trp residues in Native BSA by MPPS. λ_{ex} = 295 nm.

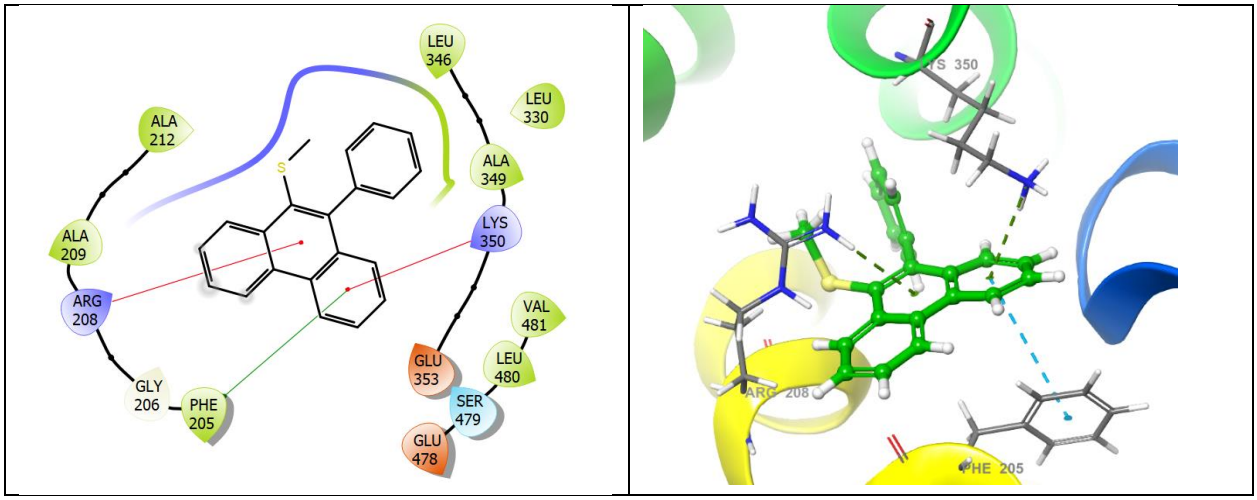

Figure 2.5.10. Molecular Docking Studies.

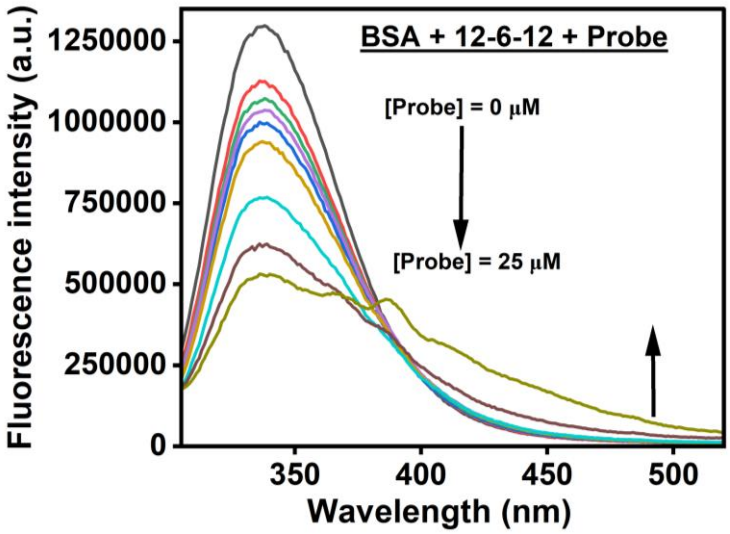

Figure 2.5.11. Fluorescence spectra of BSA with increasing concentrations of MPPS in the presence of 0.3 mM of 12-6-12,2Br$^-$. λ_{ex} = 295 nm.

The fluorescence quenching of BSA by MPPS has also been studied in denatured protein. The denaturation of BSA has been done by using 0.3 mM of 12-6-12,2Br$^-$. It has been discussed below that at 0.3 mM concentration of 12-6-12,2Br$^-$, BSA exists in denatured form. Figure 2.5.11 displays the fluorescence bands of BSA at varying concentrations of MPPS (0 to 25 µM) in the presence of 0.3 mM of 12-6-12,2Br$^-$. The Stern-Volmer plot obtained using fluorescence quenching data is shown by Figure 2.5.12. The correlation coefficient of this plot = 0.99. Interestingly, no downward curvature is noted in this Stern-Volmer plot depicting the fact of equal accesibilty of all Trp residues of BSA to the quencher, MPPS. It is expected because in the presence of surfactant the BSA gets unfolded, and therefore, both Trp residues

are exposed to the bulk. The Stern-Volmer constant calculated from the slope of the plot after linear fitting of the data = 5.67×10^{3} M^{-1}. Therefore, the bimolecular quenching rate constant, $k_q = 5.67\times10^{11}$ M^{-1} S^{-1}.

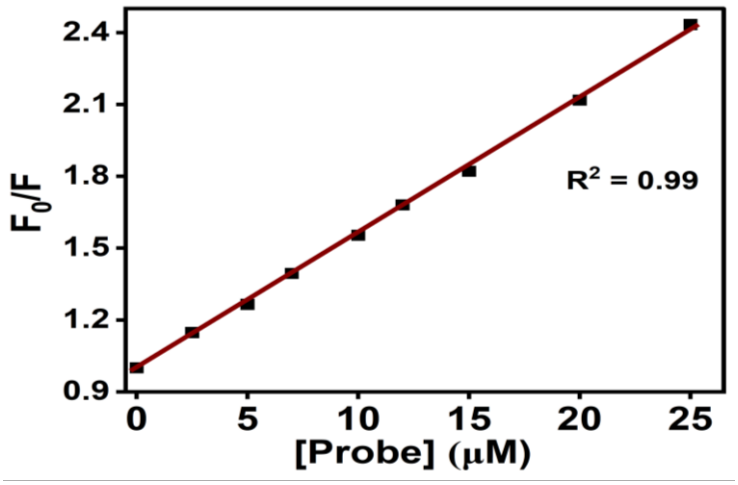

Figure 2.5.12. Stern-Volmer plot for the quenching of fluorescence of BSA by MPPS in the presence of 0.3 mM of 12-6-12,2Br^{-}. λ_{ex} = 295 nm.

The binding constant (K') of MPPS and the number of binding sites (n) for both native and denatured BSA have been calculated from the linear fitting of the data in Figures 2.5.13a and 2.5.13b based on Equation 3 (given below), respectively. For a static quenching mechanism with the assumption that the protein has the same and independent binding sites, the following equation (Equation 3) can be used to determine the binding constant (K') and the number of binding sites (n).[5]

$$\log[(F_o - F)/F] = n \log K' - n \log(1/([\text{MPPS}] - (F_o - F)[\text{P}]/F_o)) \qquad (3)$$

where F_o and F are fluorescence intensities of BSA in the absence and presence of quencher, respectively, [MPPS] and [P] are total concentrations of quencher and protein, respectively. For native BSA, the K' and n values are noted to be 2.75×10^{5} M^{-1} and 0.57, respectively. Whereas for denatured BSA, the K' and n values are found to be 4.41×10^{4} M^{-1} and 0.91, respectively. As compared to native BSA, the binding constant value is decreased and the number of binding sites is increased for denatured BSA. This is due to the fact that in denatured state of the protein, the binding strength of MPPS molecules is reduced as the hydrophobic area of the protein is decreased.[5] It is evidenced by the fluorescence peak maximum values of MPPS in two systems: λ = ~363 nm in the presence of native BSA and λ = ~375 nm in the presence of BSA and the gemini surfactant, 12-6-12,2Br^{-}. The red-shift in band position of MPPS in case of denatured BSA is because of its exposure to comparatively more polar environment. Also, the possibility of binding sites may increase with unfolding of the protein as noted.

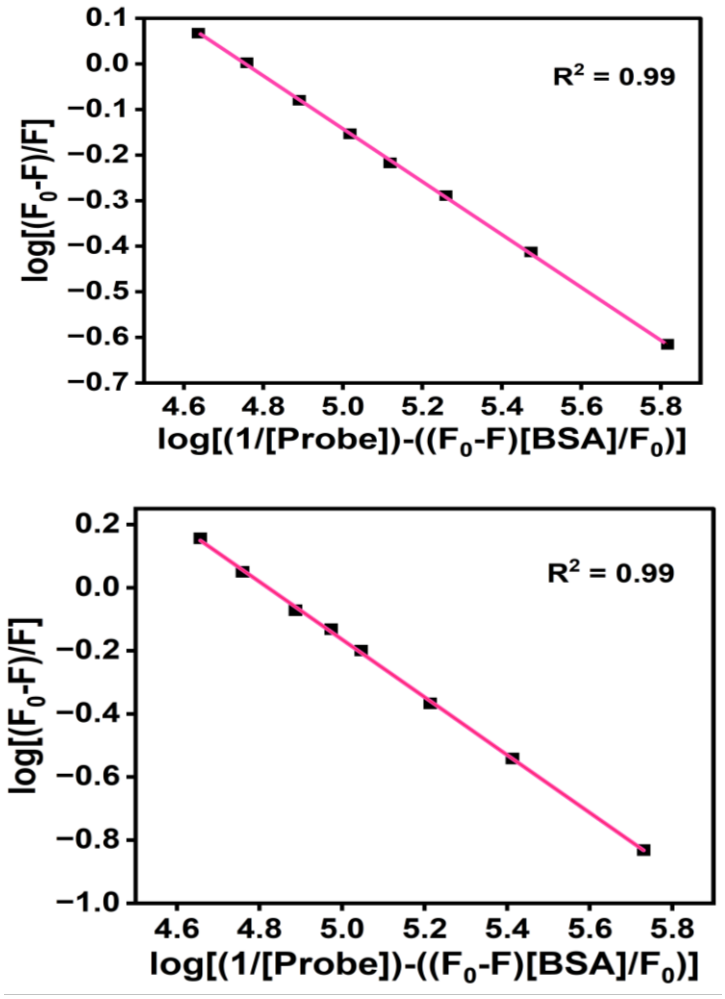

Figure 2.5.13. Plots of log[(F_o – F)/F] versus log(1/([MPPS] – (F_o – F)[BSA]/F_o)) in case of (a) native BSA, and (b) BSA + 0.3 mM 12-6-12,2Br$^-$. [BSA] = 5 μM. λ_{ex} = 295 nm.

Binding Isotherm of Gemini Surfactant, 12-6-12 with BSA

Steady-state Fluorescence

Looking into the fact that the fluorescence properties of MPPS responding well with the changes in the microenvironment because of what the CMC of different surfactants could be measured accurately, the molecule is explored to demonstrate the binding isotherm of a gemini surfactant, 12-6-12,2Br$^-$ with BSA. The fluorescence spectra of MPPS in 5 μM of BSA have been recorded in the presence of different concentrations of 12-6-12,2Br$^-$ at λ_{ex} = 330 nm. No absorbance for BSA at λ = 330 nm ensures that the fluorescence occurs from MPPS only. The fluorescence intensity ratios, F/F_o (where, F and F_o are fluorescence intensities of MPPS in the presence and absence of surfactant at λ_{em} = 395nm) at different concentrations of 12-6-12,2Br$^-$ have been calculated and plotted in Figure 2.5.14 The different regions of the binding isotherm have been depicted by letters *a, b, c* and *d*. The Region *a* represents the high energy specific binding of the surfactant with BSA due to coulombic attractive interactions between positive

charges of surfactants' headgroups and negative charges on the protein. As because the BSA becomes more compact in this region,[5] the MPPS feels more non-polar environment and as a result the fluorescence intensity is increased. It also shows that atleast some proportion of MPPS molecules can be located to the hydrophobic pocket of the BSA. In this region, a maximum appears at [12-6-12,2Br$^-$] = 0.01 mM. As a result of compaction, the % α-helix is increased. With further increasing concentration of 12-6-12,2Br$^-$, the fluorescence intensity starts decreasing before reaching a minimum at 0.06 mM of 12-6-12,2Br$^-$ (Region *b*). The Region *b* represents competitive binding between the surfactant and BSA. In this region, the hydrophobic interactions between the surfactant's tails and the non-polar part of the protein mostly play a role. The protein molecule gets unfolded with decrease in % α-helix (Figure 2.5.14) due to these interactions and as a result, the probe, MPPS gets exposed to the polar environment. Thus , the fluorescence intensity is quenched. Beyond 0.06 mM of 12-6-12,2Br$^-$, the fluorescence intensity of MPPS increases (Region *c*) before reaching a maximum at 0.13 mM of the surfactant. The Region *c* exists due to the cooperative binding wherein the micelles formed by surfactants bind along the protein chain. [6]

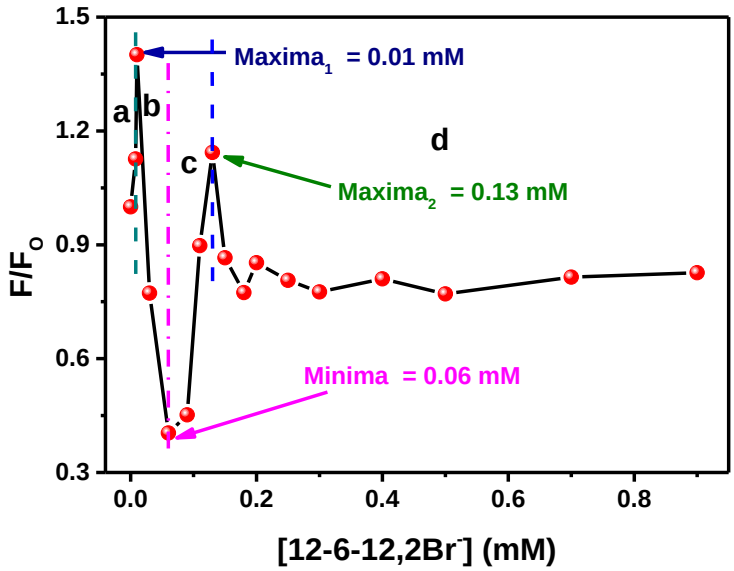

Figure 2.5.14. $^{F}/_{F_0}$ Plot of MPPS in Presence of BSA along with Increasing Concentration of 12-6-12,2Br$^-$. [MPPS] = 5 μM, [BSA] = 5.0 μM. (λ_{ex} = 330 nm, λ_{em} = 395 nm).

However, the probe molecules, MPPS experience a non-polar environment of hydrophobic microdomain created by micelles of surfactants, [6,7] The hydrophobic microdomain that is created within the protein molecule results in the compaction of the protein structure [6,7] that is supported by the increase in the % of α-helix [8] It is noteworthy that micelles formation starts at 0.06 mM concentration of 12-6-12,2Br$^-$ is much less than its CMC value for a solution without BSA. Similar results were obtained in our earlier work with the gemini surfactants, 12-4-12,2Br$^-$ and 12-8-12,2Br$^-$ utilizing some other fluorescent probe molecule [9] Thus, 0.06 mM is the critical aggregation concentration (CAC) of 12-6-12,2Br$^-$ in the

HEPES buffer solution (pH = 7.4, 10 mM) in the presence of 5 μM of BSA. In Region *d*, due to the massive binding of surfactants with the protein, the protein molecules get unfolded and as a consequence of that the fluorescence intensity of MPPS is once again decreased due to its exposure to the polar medium with a decrease in % of α-helix. With further increase in the concentration of 12-6-12,2Br^-, no change in the fluorescence intensity occurs as no sites of the protein chain are left for binding and saturation of surfactant binding occurs.

2.5.3. Conclusion.

The synthesized molecule, methyl(10-phenylphenanthren-9-yl)sulfane (MPPS) can be used as a fluorescent molecule to probe the aggregation properties of various ionic and non-ionic surfactants and also the binding isotherm of protein.

Chapter 3

SECTION – I

Iodine-Catalyzed Cyclization Reactions in Water

3.1.1. Introduction.

Iodine-catalyzed C-H heteroannulation reactions[1] have gained special attention in synthetic organic chemistry over the last decades due to the inexpensiveness, tolerance, and environmentally benign nature of iodine. The notable advantage associated with this strategy is the synthesis of potential heterocyclic molecules[2] avoiding the requirement of highly expensive and toxic rare-earth metal catalysts. However, in many iodine-catalyzed cyclization reactions, hazardous/toxic solvents like dimethyl sulfoxide (DMSO), dimethyl formamide (DMF), dichloromethane (DCM), acetonitrile (MeCN), 1,4-dioxane, etc. are used which is a major concern in the context of green chemistry. Water is generally regarded as the best non-toxic, safe, and environmentally-friendly solvent among all solvents.[3] It has always been the best choice as a solvent for an organic transformation in the context of green chemistry.[4] Hence several iodine-catalyzed synthetic methods have been developed so far for the synthesis of novel heterocyclic molecules using water as the green solvent. The state-of-the-art of this particular area of research is presented below.

3.1.2. Review.

In 2023, Mukhopadhyay *et al*. disclosed an iodine-catalyzed cascade C-N coupling followed by C-C coupling to afford a wide variety of 5*H*-pyrazino[*2,3-b*]indoles in an aqueous medium (Scheme 3.1.1).[5] This transformation proceeded through two consecutive oxidative cross-coupling reactions involving $C_\alpha(sp^3)$-H of benzyl amines followed by intramolecular cyclization to afford the desired products in water in the presence of air.

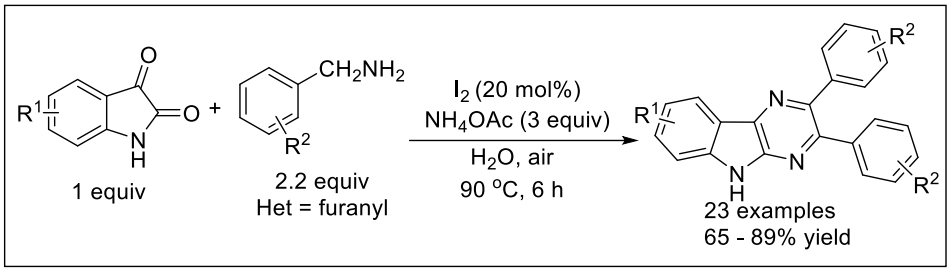

Scheme 3.1.1. Iodine-Catalyzed Synthesis of 5*H*-Pyrazino[2,3-*b*]indoles in Aqueous Medium.

In 2020, the Banerji group reported an iodine-catalyzed cyclization strategy of different primary amines or aldehydes with 1,2-diketones using K_2CO_3 as base *via* C-N bond formation in water at 70 °C to access a wide variety of polysubstituted imidazoles (Scheme 3.1.2).[6] Mechanistic studies revealed that the reaction proceeded *via* the radical pathway. Some of the imidazole derivatives acted as fluorophores both in the solid and solution phase, which was successfully applied for live-cell imaging (LysoTracker molecules). It was shown that lysosome-directing groups (LDG) were incorporated in two synthesized imidazoles to track intracellular lysosomes (Scheme 3.1.2).[6] These LDG-incorporated imidazole

derivatives furthermore showed bright blue fluorescence while detecting lysosomes in human or murine cells and were considered to be rapid lysosome-staining probes.

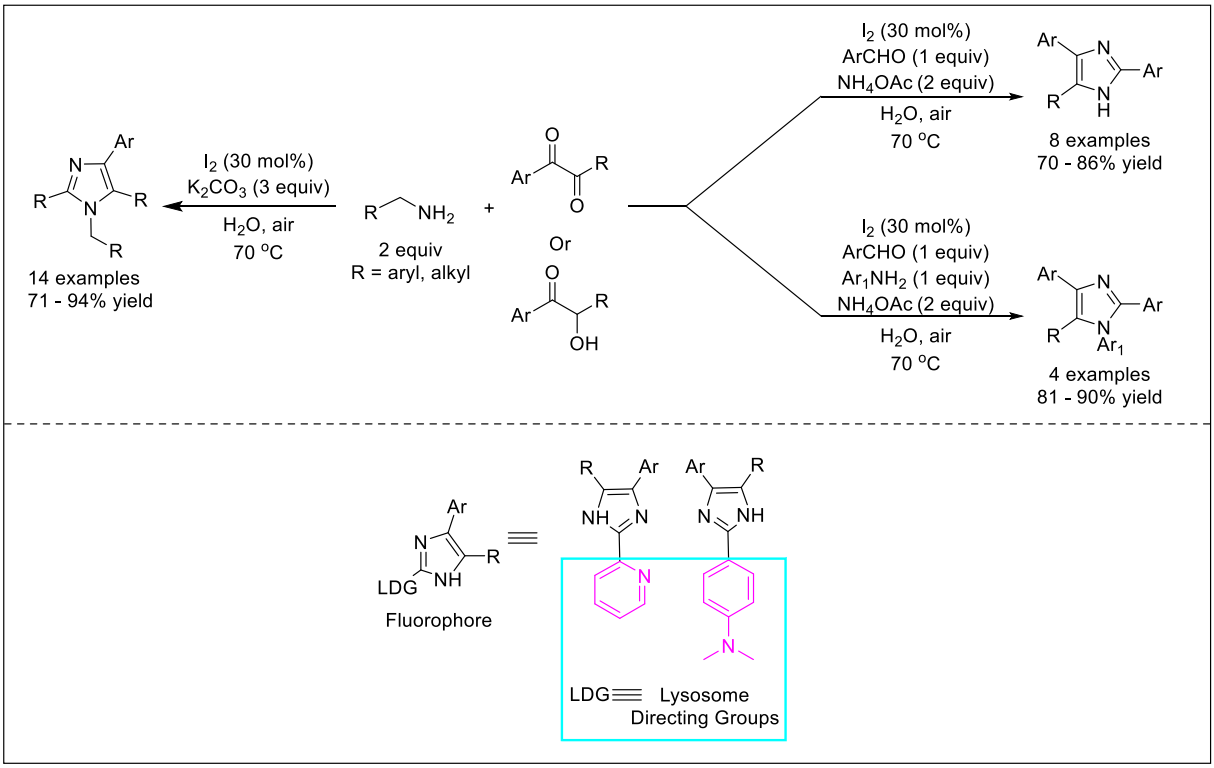

Scheme 3.1.2. Synthesis of Iodine-Catalyzed Polysubstituted Imidazoles.

In 2019, Ghosh and his co-workers developed an iodine-catalyzed oxidative Csp^3-H functionalization of primary amines from readily available starting materials such as 1,2- diketones and acyloins (alpha hydroxyl ketones) to provide specific regioisomer of polysubstituted oxazoles in water (Scheme 3.1.3).[7] The utility of this methodology was demonstrated by preparing a natural product, texaline. Furthermore, these highly substituted oxazole molecules could be utilized as fluorescent probes in medicinal chemistry as well as in material science.

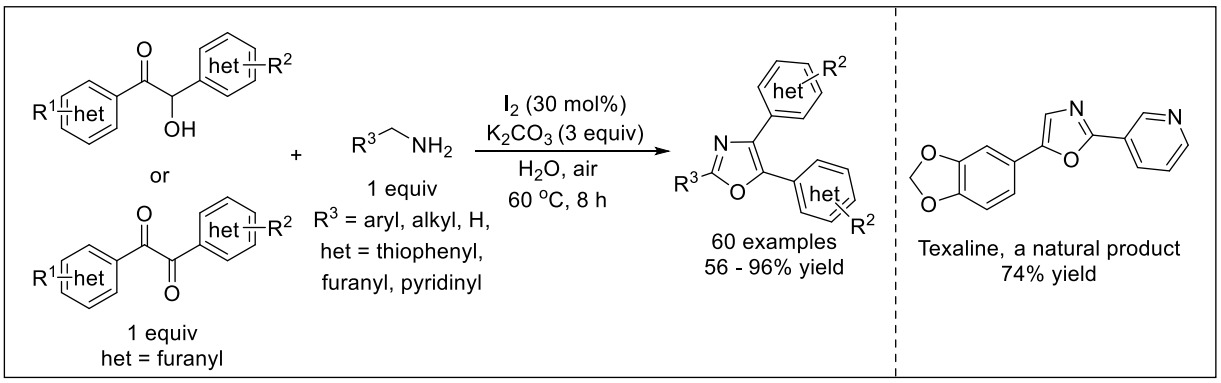

Scheme 3.1.3. Iodine-Catalyzed Synthesis of Polyarylated Oxazoles in Water.

In 2019, Rai *et al*. disclosed a facile iodine-catalysed enal-based *cis*-selective construction of aziridine-2-aldehyde in water using Chloramine-T as nitrogen transfer agent and BTEAC as phase-transfer catalyst to access a wide variety of tosylaziridines in high to excellent yield (84 –93%), excellent diastereoselectivity (95-99%) in favor of *cis*-isomer (Scheme 3.1.4).[8] Mechanistic studies revealed that the reaction proceeded through an ionic pathway.

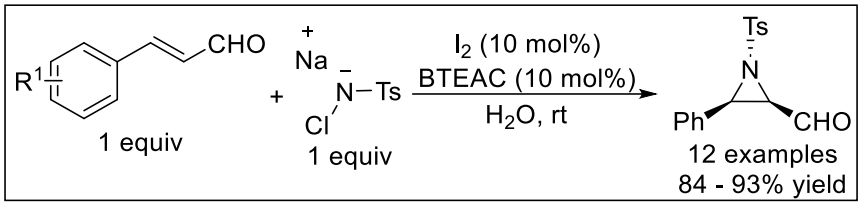

Scheme 3.1.4. Iodine-Catalyzed Enals-Based Cis-Selective Construction of Aziridine-2-aldehyde in Water.

In the same year, the Wan group developed an iodine-catalyzed cascade reaction between NH_2-functionalized enaminones and sulfonyl hydrazines in the presence of TBHP as oxidant and $NaHCO_3$ as a base in water *via* C-N bond cleavage (which was confirmed by ^{15}N-labeled experiment) to access substituted pyrazoles (Scheme 3.1.5).[3a] Mechanistic studies revealed that the reaction proceeded through a radical pathway.

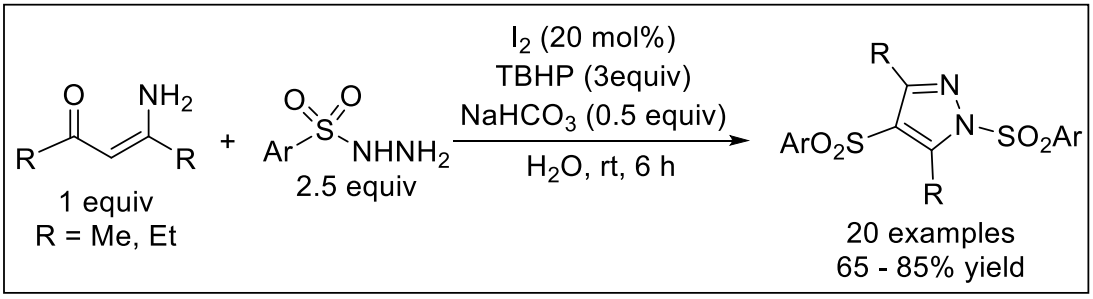

Scheme 3.1.5. Iodine-Catalyzed Cyclization Reaction of Substituted Pyrazoles in Water.

3.1.3. Conclusion.

This short review enlightens the organic transformations, particularly, iodine-catalyzed oxidative cyclization reactions involving carbon-heteroatom bond formation using water as the solvent. The use of water as a solvent accord with the goal of sustainability of the developed synthetic methods. The iodine-catalyzed cyclization reactions in water enabled the synthesis of biologically-active heterocyclic molecules in a cost-effective and sustainable fashion. However, the development of iodine-catalyzed oxidative cyclization or annulation reactions involving carbon-carbon bond formation in water has rarely been explored to the best of our knowledge.

SECTION-II

Iodine-Catalyzed, Highly Atom-Economic Synthesis of 9-Sulfenylphenanthrenes and Polycyclic Heteroaromatics in Water

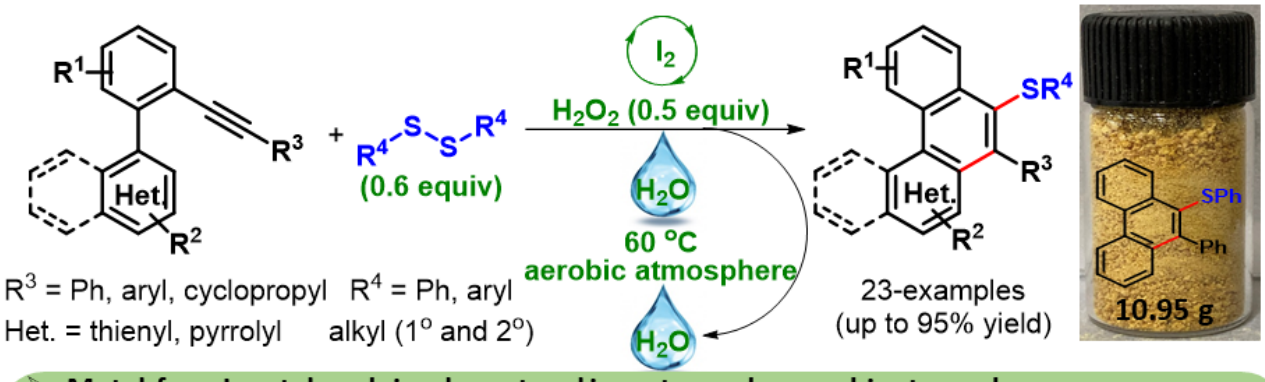

- Metal-free, I_2-catalyzed simple protocol in water under aerobic atmosphere
- Highly atom-economic (90.09%) and carbon-efficient (95.59%) reaction
- Low E-factor (2.25) and high EcoScale score (67)
- Generation of water as the major waste
- Straight-forward scale-up process up to 10 g scale, revealing the practicality of the protocol
- Access to various 9-sulfenylphenanthrenes and polycyclic heteroaromatics with broad substrate scope and high functional group tolerance

3.2.1. Introduction.

The most important goal of sustainable chemistry[1] is to reduce the adverse consequences of the substances that we use and generate. Moreover, one of the most attractive concepts in chemistry for sustainability is "Green Chemistry" [2] which is the utilization of a set of principles that reduces or eliminates the use or generation of hazardous substances in the design, manufacture, and applications of chemical products. It should be noted that the rapid development of Green Chemistry is due to the recognition that environmentally friendly products and processes will be economical in the long term.

As specified in the previous chapter, we developed a metal-free, iodine-catalyzed methylthiolative annulation of 2-alkynyl biaryls using DMSO as the source of –SMe group, oxidant, and solvent.[3] Despite notable features of the developed protocol, it suffered from some serious limitations in the context of green chemistry such as (a) the requirement of over-stoichiometric trifluoroacetic anhydride (3 equiv) for the decomposition of DMSO (10 equiv) or methyl sulfoxides (3 equiv), (b) limited substrate scope, (c) generation of hazardous carbon-wastes such as formaldehyde, trifluoroacetic acid, and dimethyl sulfide (DMS), (d) low atom-economy, (e) limitation of the protocol with the substrates bearing acid-sensitive group owing to the generation of the strong acidic (TFA) medium and, (f) high temperature. Herein, we disclosed a highly atom-economical, sustainable, cost-effective, and practical synthetic methodology for synthesizing 9-sulfenylphenanthrenes and polycyclic heteroaromatics through iodine-catalyzed sulfenylative annulation of 2-alkynyl biaryls with disulfides in water at 60 ^{o}C (Scheme 3.2.1). The notable advantages of the current protocol are (a) transition-metal-free, simple and mild reaction conditions, (b) highly atom-economic reaction, (c) utilization of a couple of inexpensive reagents such as iodine as a catalyst and H_2O_2 as a green oxidant, (d) use of a natural resource, water as the green reaction medium (e) generation of water as the major green-waste (g) broad substrate scope with high functional group tolerance.

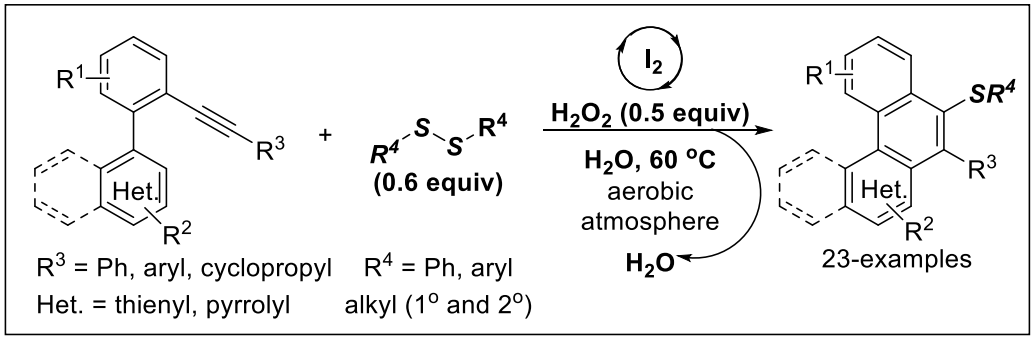

Scheme 3.2.1. Synthetic Strategy for the Synthesis of 9-Sulfenylphenanthrenes in Water.

3.2.2. Results and Discussion.

We commenced our investigation of thiolative annulation of 2-(phenylethynyl)-1,1′-biphenyl **1a** using 1.5 equiv diphenyl disulfide **2a** as the *S*-source, iodine as the catalyst, and DMSO as the oxidant as well as solvent. When the said reaction was conducted in the presence of 20 mol% iodine and 10 equiv DMSO at 120 ^{o}C under aerobic atmosphere, it took 14 hours for the reaction to be completed, and 89% phenyl(10-phenylphenanthren-9-yl)sulfane **3aa** was formed along with 6% 9-iodo-10-phenylphenanthrene **4a** (entry 1, Table 3.2.1). Notably, the use of DMSO (3 equiv) as the only oxidant in the presence of water (1.6 M) as solvent furnished **3aa** in 90% yield along with 8% **4a** (entry 2, Table 3.2.1). Further lowering of the stoichiometry of DMSO to 1.2 equiv did not affect the yield of **3aa** (entry 3, Table 3.2.1). When H_2O_2 (1.2 equiv), a green oxidant, was used instead of DMSO, gratifyingly **3aa** was formed in 92% yield along with a trace amount of **4a** (entry 4, Table 3.2.1).

Among various oxidants (1.2 equiv.) such as H_2O_2, tert-butyl hydroperoxide (TBHP), oxone, *m*-CPBA, $Na_2S_2O_8$, and $K_2S_2O_8$, H_2O_2, the most non-toxic or green oxidant was found the best (entry 4 vs. entries 5–9, Table 3.2.1). Notably, further lowing of the stoichiometry of H_2O_2 to 0.5 equiv. positively impacted the outcome of the reaction as **3aa** was formed in 94% yield along with a trace amount of **4a** (entry 10 vs. entry 4, Table 3.2.1). The stoichiometry of diphenyl disulfide was also optimized to 0.6 equiv., which revealed that both the units of disulfide are reactive and nothing is getting lost (entry 12 vs. entries 10, 11, and 13, Table 3.2.1). Next, the temperature of the reaction was optimized, and 60 °C was found to be the best; however, 73% **3aa** was formed at room temperature (entry 15 vs. entries 12, 14, and 16, Table 3.2.1). The presence of a base harmed the outcome of the reaction (entries 17 and 18, Table 3.2.1). Interestingly, water was found the best among various solvents such as water, toluene, methanol, DMF, THF, and MeCN (entries 19–23 vs. 15, Table 3.2.1). Further, increasing the reaction concentration to 1 M, lowering the reaction time to 10 h, and lowering the catalyst loading to 10 mol% had a negative impact on the reaction outcome (entries 24–26 vs. entry 15, Table 3.2.1). The blank experiment without using iodine did not furnish **3aa**, which revealed iodine's essential role in this reaction (entry 27, Table 3.2.1). However, in the blank experiment in the absence of H_2O_2, 55% of **3aa** was formed, which revealed the partial role of aerial oxygen on the reaction outcome (entry 28, Table 3.2.1). Hence the thiolative annulation reaction of **1a** with **2a** (0.6 equiv.) was optimum in the presence of 20 mol% iodine and 0.5 equiv. H_2O_2 in water (1.67 M) at 60 °C under aerobic conditions.

Among various oxidants (1.2 equiv) such as H_2O_2, *tert*-butyl hydroperoxide (TBHP), oxone, *m*-CPBA, $Na_2S_2O_8$, and $K_2S_2O_8$, H_2O_2, the most non-toxic or green oxidant was found the best (entry 4 *vs* entries 5-9, Table 3.2.1). Notably, further lowing of the stoichiometry of H_2O_2 to 0.5 equiv positively

impacted the outcome of the reaction as **3aa** was formed in 94% yield along with a trace amount of **4a** (entry 10 *vs* entry 4, Table 3.2.1). The stoichiometry of diphenyl disulfide was also optimized to 0.6 equiv, which revealed that both the disulfide units are reactive and nothing is getting lost (entry 12 *vs* entries 10, 11, and 13, Table 3.2.1). Next, the temperature of the reaction was optimized, and 60 ^{o}C was found to be the best; however, 73% **3aa** was formed at room temperature (entry 15 *vs* entries 12, 14, and 16, Table 3.2.1). The presence of a base harmed the outcome of the reaction (entries 17 and 18, Table 3.2.1). Interestingly, water was found the best among various solvents such as water, toluene, methanol, DMF, THF, and MeCN (entries 19-23 *vs* 15, Table 3.2.1). Further, increasing the reaction concentration to 1 M, lowering the reaction time to 10 h, and lowering the catalyst loading to 10 mol% had a negative impact on the reaction outcome (entry 24-26 *vs* entry 15, Table 3.2.1). The blank experiment without using iodine did not furnish **3aa**, which revealed iodine's essential role in this reaction (entry 27, Table 3.2.1). However, in the blank experiment in the absence of H_2O_2, 55% of **3aa** was formed, which revealed the partial role of aerial oxygen on the reaction outcome (entry 28, Table 3.2.1). Hence the thiolative annulation reaction of **1a** with **2a** (0.6 equiv) was optimum in the presence of 20 mol% iodine and 0.5 equiv H_2O_2 in water (1.67 M) at 60 ^{o}C under aerobic conditions.

With the optimized conditions in hand, we started exploring the scope of the thiolative annulation reaction of 2-alkynyl biaryls with disulfides. The results are presented in Table 2.

At first, the scope of the thiolative annulation of 2-(phenylethynyl)-1,1′-biphenyl **1a** was explored with various disulfides. Under the optimized conditions, **1a** reacted with diphenyl disulfide **2a** to furnish phenyl(10-phenylphenanthren-9-yl)sulfane **3aa** in 92% isolated yield. Both electron-withdrawing (Br, Cl, F, and NO_2) and donating- (Me and NHCOPh) group substituted diaryl disulfides reacted smoothly with **1a** to afford the corresponding aryl(10-phenylphenanthren-9-yl)sulfanes (**3ab** – **3ag**) in good to excellent yield except **3ae** (36%). Notably, an acid-sensitive functional group (NHCOPh) was found intact under the reaction conditions, which was not feasible in our previously developed synthetic strategy[3] using 3 equiv trifluoroacetic anhydride since trifluoroacetic acid was formed *in situ* resulting in the reaction medium being highly acidic. Various dialkyl disulfides such as dibenzyl disulfide, dipropyl disulfide, 4,4′-dithiobutyric acid, bis(2-hydroxyethyl) disulfide, and dicyclohexyl disulfide also participated in the reaction with **1a** to furnish the corresponding 9-alkylsulfenyl phenanthrenes (**3ah** – **3al**), which was also difficult to access in our previously developed synthetic strategy due to the non-availability of the corresponding methyl sulfoxides. Interestingly, the oxidizable group (-CH_2OH) in **2k** was found intact in the product (**3ak**) under the optimized reaction conditions.

Table 3.2.1. Optimization of Reaction Conditions[a].

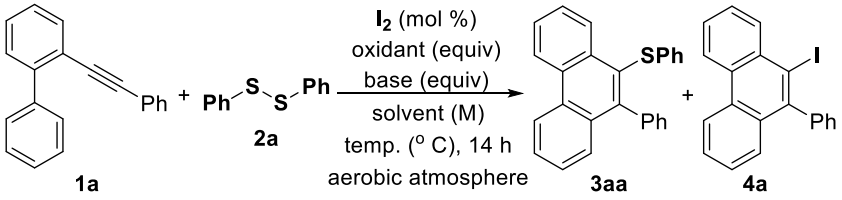

1a 3aa 4a

entry	I_2 (mol %)	**2a** (equiv)	oxidant (equiv)	solvent (M)	temp. (°C)	yield (%)[b]	
						3aa	**4a**
1	20	1.5	DMSO (10)	-	120	89	6
2	20	1.5	DMSO (3)	H_2O (1.6)	120	90	8
3	20	1.5	DMSO (1.2)	H_2O (1.6)	120	90	7
4	20	1.5	H_2O_2 (1.2)	H_2O (1.6)	120	92	trace
5	20	1.5	TBHP (1.2)	H_2O (1.6)	120	85	6
6	20	1.5	oxone (1.2)	H_2O (1.6)	120	53	6
7	20	1.5	*m*-CPBA (1.2)	H_2O (1.6)	120	45	5
8	20	1.5	$Na_2S_2O_8$ (1.2)	H_2O (1.6)	120	75	5
9	20	1.5	$K_2S_2O_8$ (1.2)	H_2O (1.6)	120	70	5
10	20	1.5	H_2O_2 (0.5)	H_2O (1.6)	120	94	trace
11	20	1	H_2O_2 (0.5)	H_2O (1.6)	120	94	trace
12	20	0.6	H_2O_2 (0.5)	H_2O (1.6)	120	94	trace
13	20	0.5	H_2O_2 (0.5)	H_2O (1.6)	120	75	trace
14	20	0.6	H_2O_2 (0.5)	H_2O (1.6)	100	94	trace
15	**20**	**0.6**	**H_2O_2 (0.5)**	**H_2O (1.6)**	**60**	**94**	**trace**
16	20	0.6	H_2O_2 (0.5)	H_2O (1.6)	rt	73	9
17[c]	20	0.6	H_2O_2 (0.5)	H_2O (1.6)	60	trace	trace
18[d]	20	0.6	H_2O_2 (0.5)	H_2O (1.6)	60	trace	trace
19	20	0.6	H_2O_2 (0.5)	toluene (1.6)	60	20	trace
20	20	0.6	H_2O_2 (0.5)	methanol (1.6)	60	20	5
21	20	0.6	H_2O_2 (0.5)	DMF (1.6)	60	30	5
22	20	0.6	H_2O_2 (0.5)	THF (1.6)	60	90	6
23	20	0.6	H_2O_2 (0.5)	MeCN (1.6)	60	60	20
24	20	0.6	H_2O_2 (0.5)	H_2O (1)	60	73	4
25[e]	20	0.6	H_2O_2 (0.5)	H_2O (1.6)	60	75	trace
26	10	0.6	H_2O_2 (0.5)	H_2O (1.6)	60	40	trace
27	-	0.6	H_2O_2 (0.5)	H_2O (1.6)	60	trace	trace
28	20			H_2O (1.6)	60	55	trace

[a]Reactions were conducted in 0.1 mmol scale; [b]yield was determined by the ^{1}H NMR of the crude reaction mixture using 1,3,5-trimethoxybenzene as internal standard; [c]K2CO3 (1.2 equiv) was used; [d]K3PO4 (1.2 equiv) was used; ereaction was conducted for 10 h.

Next, the scope of the reaction for 2-(phenylethynyl)-1,1′-biaryls was explored. Various electron-withdrawing (Cl, Br, and Ph) and -donating (Me) group substituted 2-(phenylethynyl)-1,1′-biaryls smoothly reacted with diphenyl disulfide **2a** to produce the corresponding 10-phenyl-9-phenylsulfenyl phenanthrenes (**3ba**–**3fa**).

Table 3.2.2. Substrate Scope.

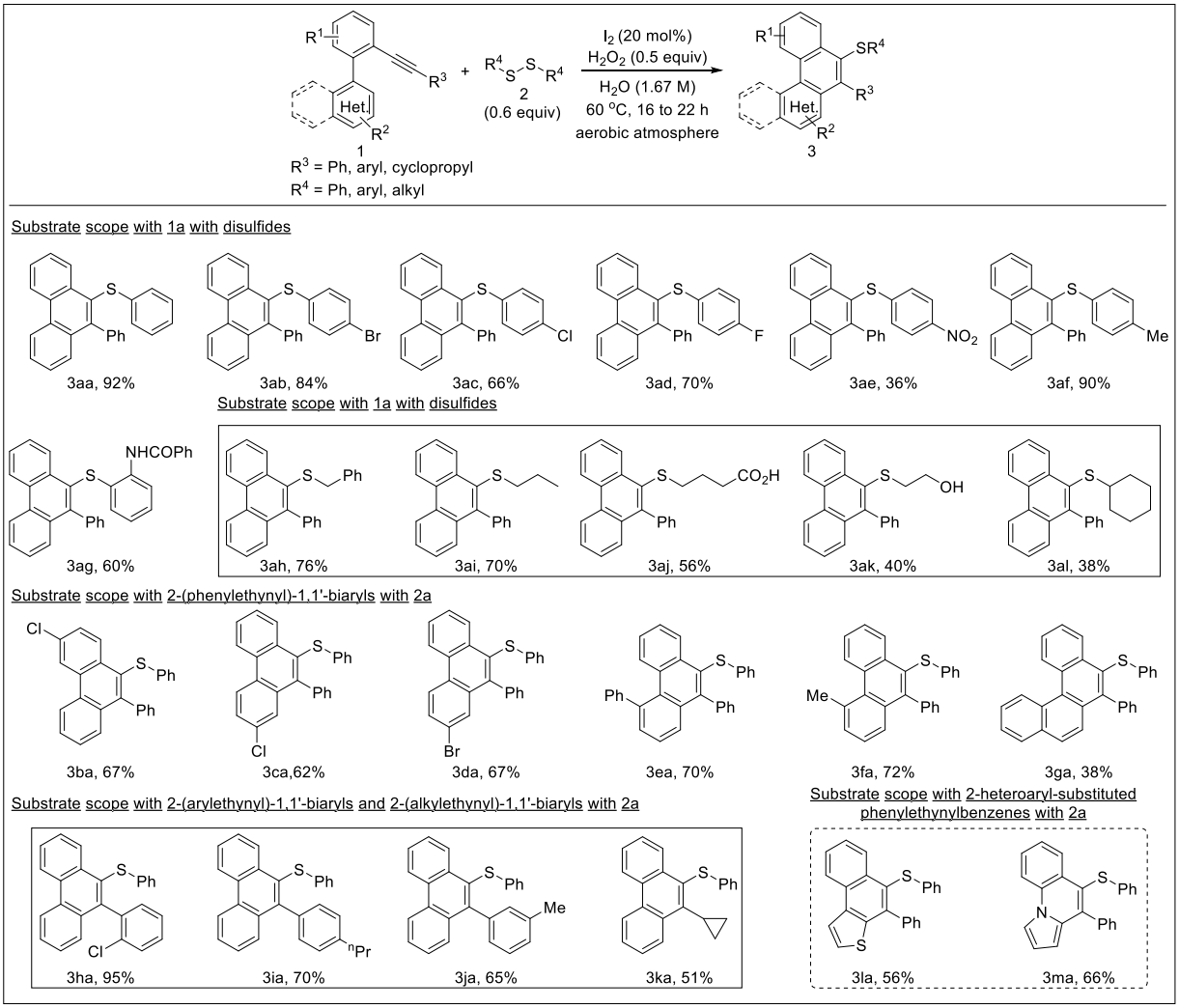

The electronic nature of the substituents and their position did not significantly affect the related product's yield (**3ba** *vs* **3ca** and **3da**–**3fa**). When 1-(2-(phenylethynyl)phenyl)naphthalene **1g** was treated with **2a**, phenyl(6-phenylbenzo[*c*]phenanthren-5-yl)sulfane **3ga** was formed, albeit low yield. Next, the scope of the reaction for electron-withdrawing (Cl) and –donating (^{n}-Pr, Me) group substituted 2-(arylethynyl)-1,1′-biphenyls was explored with **2a**, and the corresponding 10-phenyl-9-arylsulfenyl phenanthrenes (**3ha** – **3ja**) were produced in high to excellent yield. Alkyl group substituted ethynyl biphenyl, i.e., 2-(cyclopropylethynyl)-1,1'-biphenyl also participated in the reaction with **2a** to furnish (10-cyclopropylphenanthren-9-yl)(phenyl)sulfane **3ka** in 51% yield. Finally, we explored the scope of the reaction for 2-heteroaryl-substituted phenylethynylbenzenes for the synthesis of sulfenyl polycyclic heteroaromatics. 3-(2-(Phenylethynyl)phenyl)thiophene **1l** and 1-(2-(phenylethynyl)phenyl)-1*H*-pyrrole **1m** underwent the phenylthiolative annulation reaction with **2a** to produce two different classes of polycyclic heteroaromatics, i.e., 4-phenyl-5-(phenylthio)naphtho[2,1-*b*]thiophene **3la** and 4-phenyl-5-(phenylthio)pyrrolo[1,2-*a*]quinoline, respectively. In general, the scope of the reaction was found to be

broad with high functional group tolerance. When thiophenol **5** (1.2 equiv) was used instead of diphenyl disulfide **2a** to react with **1a** in the presence of 20 mol% I_2 and 2 equiv of H_2O_2 in water at 60 °C, 80% **3aa** was formed, which revealed that the use of disulfides is more advantageous than the corresponding toxic and foul-smelling thiols (Scheme 3.2.3).

Scheme 3.2.3. Phenylthiolative Annulation of **1a** with Thiophenol.

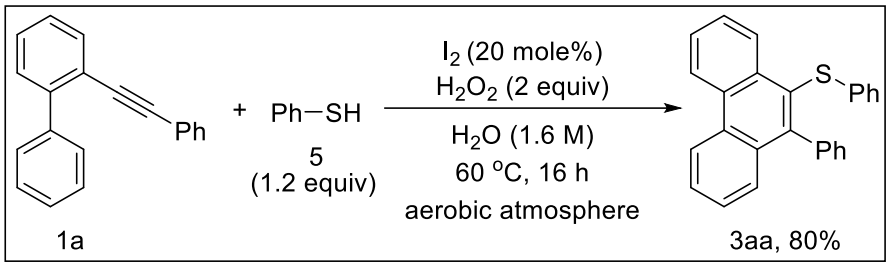

In order to demonstrate the practicality of the developed green synthetic method, we performed a multigram-scale reaction of **1a** (10.17 g, 40 mmol) with **2a** (5.24 g, 24 mmol, 0.6 equiv) under the optimized reaction conditions. Gratifyingly, **3aa** was formed in 75.52% isolated yield (10.95 g, 30.2 mmol), which revealed that the scale-up process for this reaction is straight-forward (Scheme 3.2.4).

Scheme 3.2.4. Multigram-scale Synthesis of **3aa.**

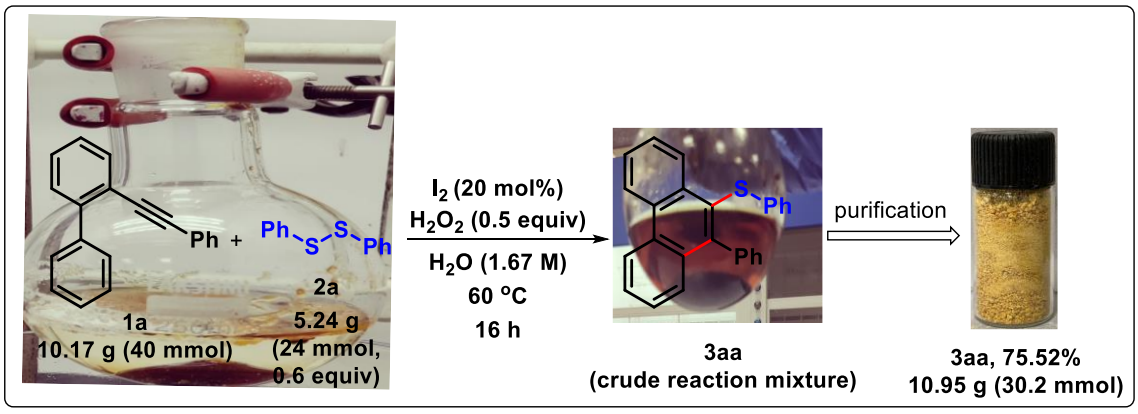

In order to measure the greenness of the developed method and compare the same with the previously developed methods quantitatively, we evaluated the green chemistry metrics such as atom economy, atom efficiency (AE), carbon efficiency (CE), reaction mass efficiency (RME), E-factor and EcoScale score for this method by following reported protocol.[4-6] The results are presented in Table 3. Significantly, the developed synthetic method is found 90.09% atom-economic, 82.88% atom-efficient, 95.59% carbon-efficient, and 77.96% reaction-mass efficient. Moreover, E-factor (the total waste in Kg/total product in Kg), an essential green parameter to quantify the quality of an organic process based on the generated waste, is found to have the value of 2.25 for the synthesis of **3aa** and majority of the generated waste is water. The

EcoScale score, another crucial green parameter based on an organic process's safety, economic, and ecological features, has a higher value (67) for this method.

Table 3.2.3. Evaluation of Green Chemistry Metrics for the Synthesis of **3aa**.

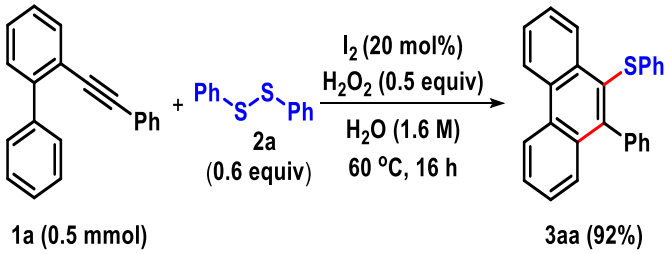

1a (0.5 mmol) 3aa (92%)

Yield of desired product (3aa) = 92%

$$\text{Atom Economy (\%)} = \frac{\text{mass of desired product}}{\text{total mass of all reactants}} \times 100 = \frac{362.49}{254.33 + (0.6 \times 218.33) + (0.5 \times 34.015)} \times 100 = 90.09\%$$

$$\text{Atom Efficiency (\%)} = (\%\text{yield of product} \times \%\text{atom economy}) \times 100 = (92\% \times 90.09\%) \times 100 = 82.88\%$$

$$\text{Carbon Efficiency (\%)} = \frac{\text{amount of carbon in desired product}}{\text{total amount of carbon presented in all reactants}} \times 100 = \frac{26}{20 + (0.6 \times 12)} \times 100 = 95.59\%$$

$$\text{Reaction Mass Efficiency (\%)} = \frac{\text{mass of isolated product}}{\text{mass of all reactants}} \times 100 = \frac{0.167}{0.127 + 0.065 + 0.0222} \times 100 = 77.96\%$$

Reactant 1:	2-(Phenylethynyl) 1,1'-biphenyl (1a)	0.127 g	0.5 mmol	FW 254.332
Reactant 2:	1,2-Diphenyldisulfane (2a)	0.065 g	0.3 mmol	FW 218.332
Catalyst:	Iodine	0.025 g	0.1 mmol	FW 253.8089
Reagent (oxidant):	Hydrogen peroxide (30% in water)	0.0222 g	0.25 mmol	FW 34.0147
Solvent:	Water	0.304 g	16.89 mmol	FW 18
Product:	Phenyl(10-phenylphenanthren-9-yl)sulfane	0.167 g	0.46 mmol	FW 362.49

$$\text{E-factor} = \frac{\text{total waste (Kg)}}{\text{total product (Kg)}} = \frac{(0.127 + 0.065 + 0.025 + 0.0222 + 0.304) - 0.167}{0.167} = 2.25 \text{ Kg waste/Kg pdt}$$

Eco Scale = 100 - Sum of individual penalties
Score on Eco Scale: > 75, Excellent; >50, acceptable; <50, Inadequate

EcoScale score = (100 - 33[a]) = 67 (>50; So, it is an acceptable synthesis)

Table 3.2.4. Calculation of EcoScale Score for the I_2 Catalyzed Synthetic Process in Water to Synthesize Phenyl(10-phenylphenanthren-9-yl)sulfane (**3aa**) from 2-(Phenylethynyl)-1,1'-biphenyl (**1a**) and Diphenyl diselenide (**2a**) (This Work).

EcoScale Calculation:

Eco Scale = 100 - Sum of individual penalties
Score on Eco Scale: > 75, Excellent; >50, acceptable; <50, Inadequate

A. Calculation of Penalty Points :

Parameters		Penalty Points
1. Yield:	(100 - % of yield)/2 = (100 - 92)/2	4
2. Price of reaction components (To obtain 10 mmol of end product, **3aa**)		
a. 2-(Phenylethynyl)-1,1'-biphenyl = 10.87 mmole		
[Synthesis cost : Required Chemicals :		
i) [1,1'-biphenyl]-2-amine = 2.74 g = USD 7.85		
ii) HCl = 8.32 mL= USD 0.264		
iii) $NaNO_2$ = 1.344 g = USD 0.0062		
i**v)** KI = 4 g = USD 1.272		
v) Bis(triphenyl phosphine)Pd(II) dichloride= 0.095 g = USD 1.81		
vi) CuI = 0.025 g = USD 0.0083		
vii) Phenyl acetylene = 1.79 mL = USD 0.765		
viii) Triethylamine = 35.36 mL = USD 0.375		
b. 1,2-Diphenyldisulfane = 6.5 mmole = 1.423 g = USD 0.911		
c. Iodine (As catalyst) = 2.17 mmole = 0.552 g = USD 0.163		
d. Hydrogen Peroxide (30% aqueous solution) = 0.42 mL = USD 0.11		
Total cost of synthesis of **3aa** = (13.84 + 0.911 + 0.163 + 0.11) = USD 15.024 Thus expensive, since \$10<(total cost of synthesis of 10 mmol of **3aa**) < \$50:		3
3. Safety		
1,2-Diphenyldisulfane (T)		5
Iodine (T)		5
4. Technical Setup		
Common Setup		0
5. Temperature/ Time		
60 ^{o}C, 14 h (Heating, > 1h)		3
6. Work up and purification :		
a. Adding solvent		0
b. Liquid-Liquid extraction		3
c. Classical Chromatography		10
	Total penalty points:	33

B. Ecoscale calculation:

EcoScale score: **(100 - 33) = 67 (>50; it is an acceptable synthesis)**

Table 3.2.5. Calculation of Green Metrics for the Pd-Catalyzed Synthetic Process to Synthesize Phenyl(10-phenylphenanthren-9-yl)sulfane (**3aa**) from 2-(Phenylethynyl)-1,1'-biphenyl (**1a**) and Diphenyl Disulfide (**2a**).

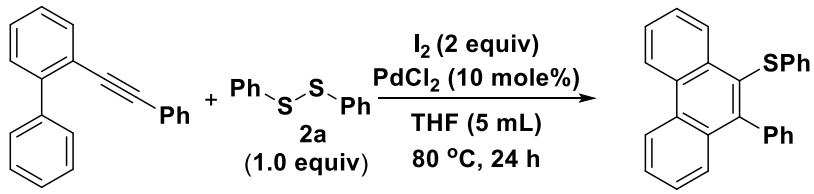

1a (0.5 mmol) **3aa (92%)**

Yield of desired product (3aa) = 95%

$$\text{Atom Economy (\%)} = \frac{\text{mass of atoms in desired product}}{\text{mass of atoms in all reactants}} \times 100 = \frac{362.49}{254.33 + 218.33 + (2*253.8089)} \times 100 = \mathbf{36.98\%}$$

$$\text{Atom Efficiency (\%)} = (\%\text{yield of product} \times \%\text{atom economy}) \times 100 = (95\% \times 36.98\%) \times 100 = \mathbf{35.13\%}$$

$$\text{Carbon Efficiency (\%)} = \frac{\text{number of carbon atoms in desired product}}{\text{number of carbon atoms in all reactants}} \times 100 = \frac{26}{20 + 12} \times 100 = \mathbf{81.3\%}$$

$$\text{Reaction Mass Efficiency (\%)} = \frac{\text{mass of isolated product}}{\text{mass of all reactants}} \times 100 = \frac{0.172}{0.127 + 0.109 + 0.253} \times 100 = \mathbf{35.17\%}$$

Reactant 1:	**2-(Phenylethynyl) 1,1'-biphenyl (1a)**	0.127 g	0.5 mmol	FW 254.332
Reactant 2:	**1,2-Diphenyldisulfane (2a)**	0.109 g	0.5 mmol	FW 218.332
Catalyst 1:	**Iodine**	0.253 g	1.0 mmol	FW 253.8089
Catalyst 2:	**palladium(II) chloride**	0.008 g	0.05 mmol	FW 177.32
Solvent:	**THF**	4.44 g	61.57 mmol	FW 72.11
Product:	**Phenyl(10-phenylphenanthren-9-yl)sulfane**	0.172 g	0.47 mmol	FW 362.49

$$\text{E-factor} = \frac{\text{total waste (Kg)}}{\text{total product (Kg)}} = \frac{(0.127 + 0.109 + 0.253 + 0.008 + 4.44) - 0.172}{0.172} = \mathbf{27.7}\ \text{Kg waste/Kg pdt}$$

Table 3.2.6. Calculation of EcoScale Score for the Pd-Catalyzed Synthetic Process to Synthesize Phenyl(10-phenylphenanthren-9-yl)sulfane (**3aa**) from 2-(Phenylethynyl)-1,1'-biphenyl (**1a**) and Diphenyl Diselenide (**2a**).

Eco Scale Calculation:

Eco Scale = 100 - Sum of individual penalties

Score on Eco Scale: > 75, Excellent; >50, acceptable; <50, Inadequate

A. Calculation of Penalty Points :

Parameters		Penalty Points
1. Yield:	(100 - % of yield)/2 = (100 - 95)/2 = 2.5	**2.5**
2. Price of reaction components (To obtain 10 mmol of end product, **3aa**)		
a. 2-(Phenylethynyl)-1,1'-biphenyl = 10.64 mmole = 2.94 g = USD 13.55		
[Synthesis cost : Required Chemicals :		
i) [1,1'-biphenyl]-2-amine = 2.65 g = USD 7.71		
ii) HCl = 8.13 mL= USD 0.26		
iii) $NaNO_2$ = 1.31 g = USD 0.059		
i**v)** KI = 3.91 g = USD 1.24		
v) Bis(triphenyl phosphine)Pd(II) dichloride= 0.093 g = USD 1.77		
vi) CuI = 0.025 g = USD 0.0083		
vii) Phenyl acetylene = 1.75 mL = USD 2.19		
viii) Triethylamine = 31.90 mL = USD 0.316		
b. 1,2-Diphenyldisulfane = 10.64 mmole = 2.32 g = USD 1.49		
c. Iodine = 21.28 mmole = 5.40 g = USD 1.60		
d. Palladium(II) chloride (As catalyst) = 0.188 g = USD 13.35		
e. THF = 106.4 mL = USD 8.34		
Total cost of synthesis of **3aa** = (13.55 + 1.49 + 1.60 + 13.35 + 8.34) = USD 38.33 Thus expensive, since \$10<(total cost of synthesis of 10 mmol of **3aa**) < \$50:		**3**
3. Safety		
1,2-Diphenyldisulfane (T)		**5**
Iodine (T)		**5**
Palladium(II) chloride (T)		**5**
THF (T, F)		**10**
4. Technical Setup		
Common Setup		**0**
Inert gas atmosphere		**1**
5. Temperature/ Time		
80 ^{o}C, 14 h (Heating, > 1h)		**3**
6. Work up and purification :		
a. Adding solvent		**0**
b. Liquid-Liquid extraction		**3**
c. Classical Chromatography		**10**
Total penalty points:		**47.5**

B. Ecoscale calculation:

Eco-scale Score: (100 - 47.5) = 52.5 (>50; it is an acceptable synthesis)

Table 3.2.7. Calculation of Green Metrics for the I_2-Catalyzed Synthetic Process to Synthesize Phenyl(10-phenylphenanthren-9-yl)sulfane (**3aa**) from 2-(Phenylethynyl)-1,1'-biphenyl (**1a**) and (Methylsulfinyl)benzene (**2a′**).

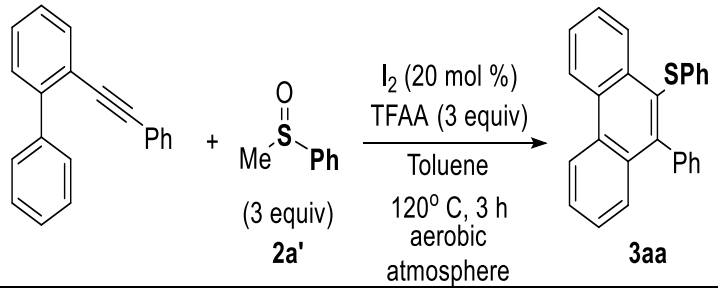

Yield of desired product (3aa) = 81%

$$\text{Atom Economy (\%)} = \frac{\text{mass of atoms in desired product}}{\text{mass of atoms in all reactants}} \times 100 = \frac{362.49}{254.33 + [(2*140.2)\text{ as oxidant}] + 140\text{ (as Reactant)} + (210.3*3)} \times 100 = \mathbf{27.76\%}$$

$$\text{Atom Efficiency (\%)} = (\%\text{yield of product} \times \%\text{atom economy}) \times 100 = (81\% \times 27.76\%) \times 100 = \mathbf{22.48\%}$$

$$\text{Carbon Efficiency (\%)} = \frac{\text{number of carbon atoms in desired product}}{\text{number of carbon atoms in all reactants}} \times 100 = \frac{24}{20 + 7} \times 100 = \mathbf{88.89\%}$$

$$\text{Reaction Mass Efficiency (\%)} = \frac{\text{mass of isolated product}}{\text{mass of all reactants}} \times 100 = \frac{0.147}{0.127 + 0.210 + 0.315} \times 100 = \mathbf{22.55\%}$$

Reactant 1:	**2-(Phenylethynyl) 1,1'-biphenyl (1a)**	0.127 g	0.5 mmol	FW 254.332
Reactant 2:	**Methyl Phenyl Sulfoxide**	0.210 g	1.5 mmol	FW 140.2
Catalyst:	**Iodine**	0.025 g	0.1 mmol	FW 253.8089
Reagent :	**TFAA**	0.315 g	1.5 mmol	FW 210.3
Solvent:	**Toluene**	1.083 g	11.75 mmol	FW 92.14
Product: phenyl(10-phenylphenanthren-9-yl)sulfane (3aa)		0.147 g	0.405 mmol	FW 362.49

$$\text{E-factor} = \frac{\text{total waste (Kg)}}{\text{total product (Kg)}} = \frac{(0.127 + 0.210 + 0.025 + 0.315 + 1.083) - 0.147}{0.147} = \mathbf{10.97}\text{ Kg waste/Kg pdt}$$

Table 3.2.8. Calculation of EcoScale Score for the I_2-Catalyzed Synthetic Process to Synthesize Phenyl(10-phenylphenanthren-9-yl)sulfane (**3aa**) from 2-(Phenylethynyl)-1,1'-biphenyl (**1a**) and (Methylsulfinyl)benzene (**2a′**).

Eco Scale Calculation:

Eco Scale = 100 - Sum of individual penalties

Score on Eco Scale: > 75, Excellent; >50, acceptable; <50, Inadequate

A. Calculation of Penalty Points :

Parameters		Penalty Points
1. Yield:	(100 - % of yield)/2 = (100 - 81)/2	**9.5**
2. Price of reaction components (To obtain 10 mmol of end product, **3aa**)		
a. 2-(Phenylethynyl)-1,1'-biphenyl = 12.35 mmol = 3.14 g = USD 15.72		
[Synthesis cost : Required Chemicals :		
i) [1,1'-biphenyl]-2-amine = 3.07 g = USD 8.93		
ii) HCl = 9.44 mL= USD 0.30		
iii) $NaNO_2$ = 1.53 g = USD 0.07		
i**v)** KI = 4.54 g = USD 1.44		
v) Bis(triphenyl phosphine)Pd(II) dichloride= 0.108 g = USD 2.06		
vi) CuI = 0.029 g = USD 0.0097		
vii) Phenyl acetylene = 2.034 mL = USD 2.54		
viii) Triethylamine = 37.06 mL = USD 0.37		
b. Methyl Phenyl Sulfoxide = 37.05 mmol = 5.19 g = USD 28.65		
c. Iodine (As catalyst) = 2.47 mmol = 0.627 g = USD 0.19		
d. TFAA = 5.16 mL = USD 0.97		
e. Toluene = 30.88 mL = USD 1.13		
Total cost of synthesis of **3aa** = (13.67 + 28.74 + 0.186 + 0.967 + 1.136) = USD 46.66 Thus expensive, since \$10<(total cost of synthesis of 10 mmol of **3aa**) < \$50:		**3**
3. Safety		
Methyl Phenyl Sulfoxide (T)		**5**
Iodine (T)		**5**
TFAA		**5**
Toluene (F,T)		**10**
4. Technical Setup Common Setup		**0**
5. Temperature/time: 120 ^oC, 3 h (Heating, > 1h)		**3**
6. Work-up and purification:		
Adding of solvents		**0**
Liquid-liquid Extraction		**3**
Column Chromatography		**10**
Total penalty points:		**53.5**

B. Ecoscale calculation:

Eco-scale Score: (100 - 53.5) = 46.5 (<50, it is an inadequate synthesis)

A detailed comparison of this method with the previously reported ones for the synthesis of **3aa** from **1a** with respect to various parameters, including those green chemistry parameters, is given in Table 3.2.8. The analysis of these data quantitatively revealed that this method is much greener than those previously reported ones concerning all the green parameters.

Table 3.2.9. Detailed Comparison of the Previously Developed Synthetic Methodologies with This Work to Synthesize **3aa** from **1a.**

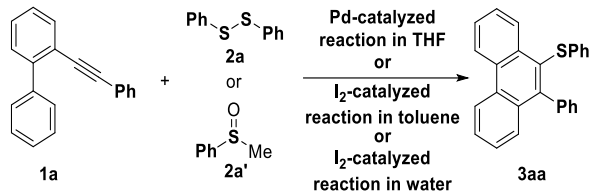

entry	catalyst (mol%)	**2a/2a'** (equiv)	reagent (equiv)	solvent (M)	temp. (°C)	%yield of **3aa**	%atom economy	%atom efficiency	%carbon efficiency	%reaction-mass efficiency	E-factor	EcoScale score	ref.
1	$PdCl_2$ (10)	$(PhS)_2$ (1)	I_2 (2)	THF (0.1)	80	95	36.98	35.13	81.3	35.17	27.7	52.5	7
2	I_2 (20)	PhSOMe (3)	TFAA (3)	Toluene (0.4)	120	81	27.76	22.48	45.28	22.55	10.97	46.5	**3**
3	**I_2 (20)**	**$(PhS)_2$ (0.6)**	**H_2O_2 (0.5)**	**H_2O (1.6)**	**60**	**92**	**90.09**	**82.88**	**95.59**	**77.96**	**2.25**	**67**	this work

To shed light on the reaction mechanism, we performed several experiments as outlined in Scheme 4. When diphenyl disulfide **2a** was subjected to react with I_2 in water at 60 °C, and the mass spectrum of the reaction mixture was recorded after 1.5 h, a peak at m/z = 236 was found, which supported the *in situ* formation of phenyl sulfenyl iodide **6** (m/z = 236) as the intermediate of the reaction (Scheme 3.2.5).

Next, several radical quenching experiments of the model reaction between **1a** and **2a** were carried out under optimized reaction conditions in the presence of a radical quencher such as butyloxy hydroxytoluene (BHT), galvinoxyl radical, and TEMPO. In the presence of BHT (1.5 equiv), the reaction was not quenched at all, and 91% of **3aa** was formed (Scheme 3.2.5.B). However, in the presence of galvinoxyl radical (1.5 equiv), the reaction was found to be quenched to a certain extent as **3aa** was formed in 71% yield. When the stoichiometry of the galvinoxyl radical was increased to 3 equiv, the yield of **3aa** further decreased to 36%, indicating a sharp quenching of the reaction by galvinoxyl radical. Notably, in the presence of TEMPO (1.5 equiv), the reaction was found to be fully quenched since **3aa** was not detected at all and **1a** was found to remain as such after the reaction (Scheme 3.2.5.D). However, we could not detect any radical adduct formation with either galvinoxyl radical or TEMPO by LC-MS.

Scheme 3.2.5. Mechanistic Studies.

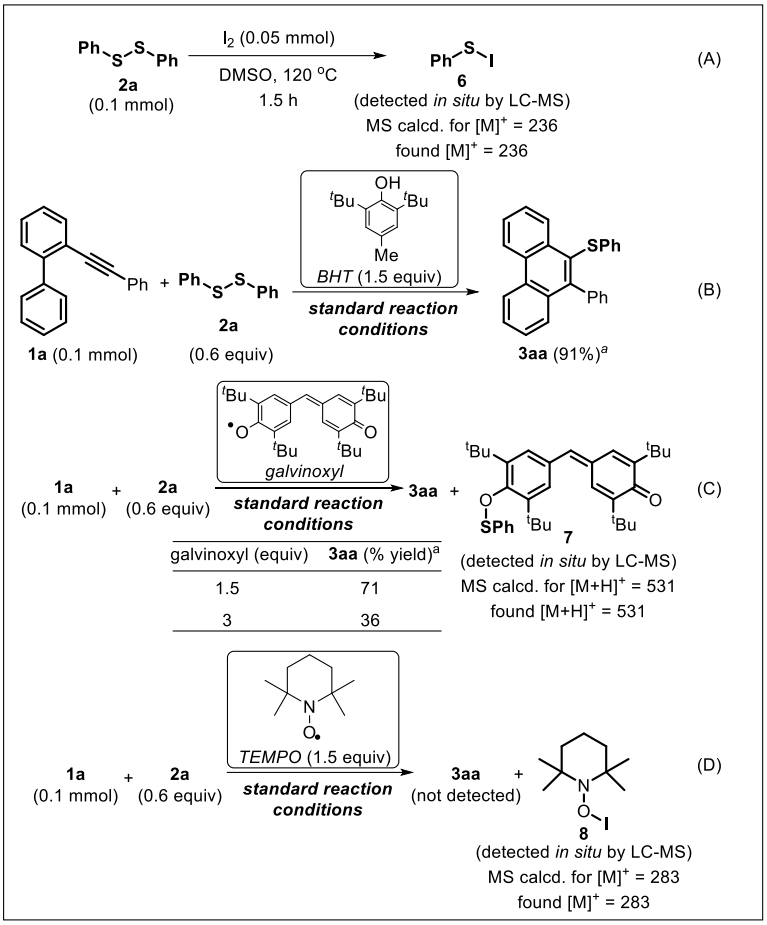

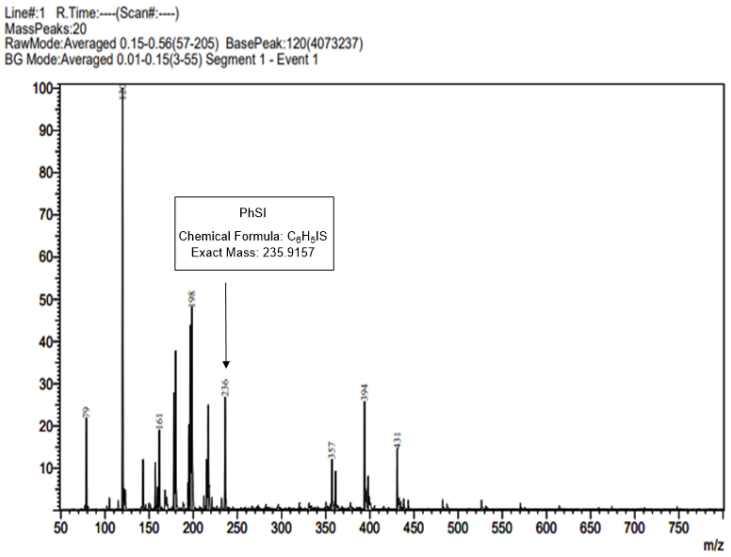

Figure 3.2.1. Mass Spectrum of the Reaction Mixture of Diphenyl Disulfide and I_2.

Based on the mechanistic studies, we propose a plausible reaction mechanism for the synthesis of 3aa as outlined in Scheme 3.2.6. Diphenyl disulfide **2a** reacted with iodine to form phenyl sulfenyl iodide (PhSI) **6**,[8] which underwent homolytic cleavage to form PhS· **7** (*path A*). Radical addition of **7** to the -C≡C- bond of **1a** furnished the corresponding vinyl radical **8**. Intramolecular radical cyclization of **8** furnished **9**, which eventually gets converted to the desired product **3aa** through oxidation by iodine followed by deprotonation. In the final step, HI was formed, which was immediately oxidized by H_2O_2 or aerobic oxygen to regenerate I_2, and H_2O was formed as the only waste in the reaction. Although we proposed a radical mechanism, we cannot rule out the electrophilic annulation of **1a** with PhSI **6** for the synthesis of **3aa** via the formation of intermediates **10** and **11** (*path B*).[7, 3]

Scheme 3.2.6. Mechanism.

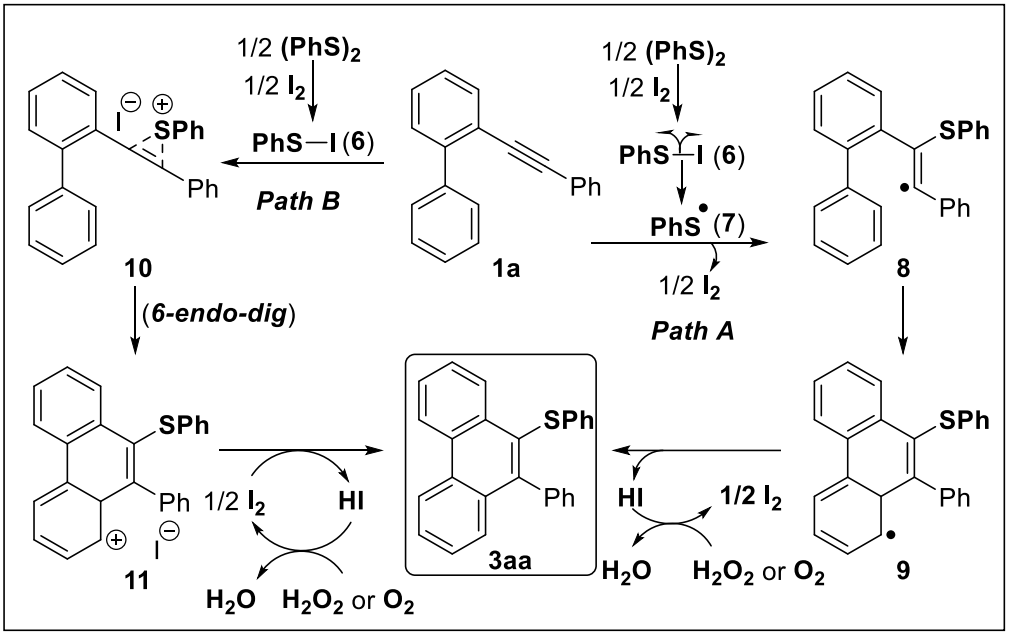

3.2.3. Conclusions.

We have developed an iodine-catalyzed, highly atom-economic, and green synthetic methodology for the thiolative annulation of 2-alkynyl biaryls or 2-heteroaryl substituted alkynyl benzenes with disulfides in water. A wide variety of sulfenyl phenanthrenes and polycyclic heteroaromatics such as 4-phenyl-5-(phenylthio)naphtho[2,1-*b*]thiophene and 4-phenyl-5-(phenylthio)pyrrolo[1,2-*a*]quinoline have been synthesized in moderate to excellent yield. Various functional groups, in particular, the acid-sensitive functional group (–NHCOPh), the oxidizable functional group (-CH_2OH), were found intact under the reaction conditions. The notable advantages of this protocol are a) transition-metal-free protocol, b) use of water as a solvent, c) use of iodine as a catalyst, d) use of H_2O_2 and aerial oxygen as the green oxidant, e)

water as the waste, f) straight-forward scale-up process up to 10 g scale, g) excellent green chemistry parameters such as high atom-economy (90.09%), high atom-efficiency (82.88%), high reaction-mass-efficiency (77.96%), high carbon-efficiency (95.59%), low E-factor (2.25) and high EcoScale score (67). Moreover, all the green parameters of this method for the synthesis of phenyl(10-phenylphenanthren-9-yl)sulfane (**3aa**) from 2-(phenylethynyl)-1,1'-biphenyl (**1a**) are found superior with respect to those of the previously reported Pd-catalyzed or iodine-catalyzed methods. We believe this green strategy of oxidative annulation will find useful applications in synthesizing various potential classes of molecules.

3.2.4. Experimental Section.

Experimental Procedure for the Synthesis of 2-(Cyclopropylethynyl)-1,1'-biphenyl (1k).

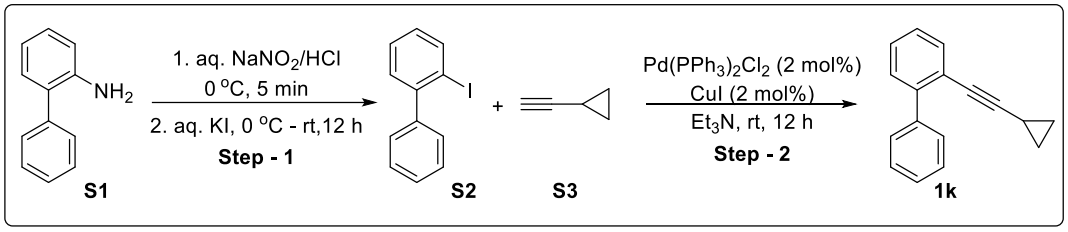

Step-1: 2-Iodo-1,1'-biphenyl **S2** was synthesized from [1,1'-biphenyl]-2-amine **S1** by following a reported protocol.[5]

Step-2: 2-iodo-1,1'-biphenyl **S2** (1.4 g, 5 mmol, 1 equiv), $Pd(PPh_3)_2Cl_2$ (0.07 g, 0.1 mmol), CuI (0.019 g, 0.1 mmol) and Et_3N (13 mL) were added in a flame-dried two neck round bottomed flask (RBF) under N_2 atmosphere in a standard Schlenk-line process and stirred for 5 min at room temperature. Cyclopropylacetylene **S2** (508 µL, 6 mmol, 1.2 equiv) was then added to the reaction mixture under nitrogen atmosphere. The reaction mixture was stirred for 12 h at room temperature. After the completion of the reaction, Et_3N was evaporated under reduced pressure. The crude reaction mixture was diluted with ethyl acetate (30 mL) and washed with water three times (3 x 10 mL). The solvent was evaporated under reduced pressure and the crude product was purified through silica gel column chromatography to provide 2-(cyclopropylethynyl)-1,1'-biphenyl **1k** (0.436 g, 2 mmol) in 40% yield.

General Experimental Procedure for the Synthesis of 9-Sulfenylphenanthrenes and Polycyclic Heteroaromatics (3aa-3al and 3ba−3ma). Representative Experimental Procedure for the Synthesis of Phenyl(10-phenylphenanthren-9-yl)sulfane (3aa):

Phenyl(10-phenylphenanthren-9-yl)sulfane **1a** (0.127 g, 0.5 mmol, 1 equiv), 1,2-diphenyldisulfane **2a** (0.065 g, 0.3 mmol, 0.6 equiv) and I_2 (0.0254 g, 0.1 mmol) were taken in a RBF and H_2O (0.3 mL, 1.6 M) was added to it. Then H_2O_2 (0.02 mL, 0.25 mmol, 0.5 equiv) was added to the RBF and the reaction mixture

was stirred in an oil bath at 60 °C under aerobic atmosphere. The progress of the reaction was monitored by TLC. After completion of the reaction, iodine was quenched with saturated sodium thiosulfate solution and ethyl acetate (30 mL) was added to the reaction mixture. The whole solution was then transferred to a separating funnel for extraction. The reaction mixture was extracted with ethyl acetate twice (2 X 10 mL) and the combined organic layer was washed with water (3 X 10 mL). The solvent was evaporated under reduced pressure to afford the crude product which was purified by flash column chromatography through silica gel to afford the pure product, phenyl(10-phenylphenanthren-9-yl)sulfane **3aa** (0.167 g, 0.46 mmol) in 92% yield.

3.2.5. Analytical Data of All Synthesized Products (3aa-3al and 3ba -3ma).

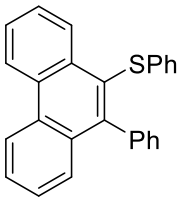

Phenyl(10-phenylphenanthren-9-yl)sulfane (3aa).[7] White crystalline solid (0.167 g, 92%); eluent hexane; mp = 125−127 °C; **^{1}H NMR (400 MHz, CDCl$_3$)** δ 8.83 (dd, *J* = 8.2, 3.1 Hz, 2H), 8.72 (d, *J* = 8.2 Hz, 1H), 7.77 – 7.71 (m, 2H), 7.64 (dd, *J* = 8.0, 7.2 Hz, 1H), 7.60 – 7.53 (m, 2H), 7.51 – 7.46 (m, 3H), 7.36 – 7.32 (m, 2H), 7.13 (dd, *J* = 8.0, 7.0 Hz, 2H), 7.09 – 7.03 (m, 1H), 7.00 (d, *J* = 7.9 Hz, 2H). **^{13}C NMR (100 MHz, CDCl$_3$)** δ 146.82, 140.15, 138.97, 132.21, 132.04, 131.08, 130.87, 129.48, 128.70, 128.63, 128.02, 127.93, 127.61, 127.57, 127.34, 127.09, 127.05, 126.71, 126.33, 124.63, 122.74, 122.55.

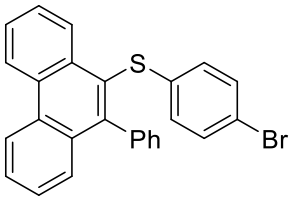

(4-Bromophenyl)(10-phenylphenanthren-9-yl)sulfane (3ab) : White solid (0.185 g, 84%); eluent hexane; mp = 166−168 °C; **^{1}H NMR (400 MHz, CDCl$_3$)** δ 8.69 (dd, *J* = 18.2, 8.2 Hz, 2H), 8.63 (d, *J* = 8.9 Hz, 1H), 7.78 (dd, *J* = 8.9, 2.1 Hz, 1H), 7.73 – 7.59 (m, 3H), 7.50 – 7.44 (m, 3H), 7.28 – 7.24 (m, 2H), 7.11 (t, *J* = 7.6 Hz, 2H), 7.07 – 7.02 (m, 1H), 6.93 (d, *J* = 8.1 Hz, 2H). **^{13}C NMR (100 MHz, CDCl$_3$)** δ 145.63, 139.34, 138.61, 133.68, 132.02, 130.76, 130.70, 130.41, 129.74, 129.46, 128.88, 128.71, 128.23, 128.16, 127.94, 127.70, 127.44, 126.51, 124.86, 124.38, 122.64, 121.06. **Anal** calcd for $C_{26}H_{17}BrS$: C, 70.75; H, 3.88; S, 7.26; found C, 70.91; H, 3.56; S, 7.41.

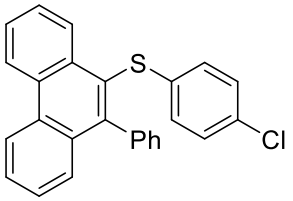

(4-Chlorophenyl)(10-phenylphenanthren-9-yl)sulfane (3ac):[7] White solid (0.131 g, 66%); eluent hexane; mp = 115−117 °C; **^{1}H NMR (400 MHz, CDCl$_3$)** δ 8.81 – 8.78 (m, 2H), 8.58 (dd, *J* = 8.3, 1.0 Hz, 1H), 7.71 (m, 2H), 7.64 – 7.59 (m, 1H), 7.51 – 7.48 (m, 2H), 7.44 (dd, *J* = 4.9, 1.7 Hz, 3H), 7.24 (dd, *J* = 6.6, 3.0 Hz, 2H), 7.04 (d, *J* = 8.7 Hz, 2H), 6.82 (d, *J* = 8.7 Hz, 2H). **^{13}C NMR (100 MHz, CDCl$_3$)** δ 147.04, 140.01, 137.54, 132.17, 131.80, 131.17, 130.97, 130.47, 129.43, 128.78, 128.03, 127.82, 127.79, 127.71, 127.55, 127.50, 127.21, 126.84, 126.66, 122.87, 122.60.

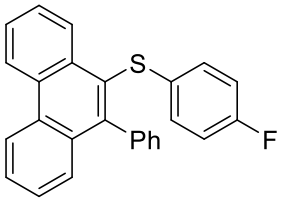

(4-Fluorophenyl)(10-phenylphenanthren-9-yl)sulfane (3ad) : [7]White crystalline solid (0.144 g, 76%); eluent hexane; mp = 118−120 °C; **^{1}H NMR (400 MHz, $CDCl_3$)** δ 8.81 (d, *J* = 8.4 Hz, 2H), 8.72 – 8.69 (m, 1H), 7.73 (ddd, *J* = 8.2, 5.9, 1.7 Hz, 2H), 7.65 (ddd, *J* = 8.2, 5.6, 1.2 Hz, 1H), 7.53 (ddd, *J* = 5.1, 3.6, 2.2 Hz, 2H), 7.48 (dd, *J* = 4.3, 2.1 Hz, 3H), 7.31 – 7.28 (m, 2H), 6.95 – 6.90 (m, 2H), 6.85 – 6.80 (m, 2H). **^{13}C NMR (100 MHz, $CDCl_3$)** δ 161.91, 159.48, 146.68, 140.04, 133.87, 133.84, 132.16, 131.93, 131.05, 130.93, 129.86, 129.55, 128.66, 128.35, 128.27, 127.97, 127.87, 127.68, 127.59, 127.55, 127.39, 127.21, 127.11, 126.78, 122.95, 122.81, 122.55, 122.43, 115.84, 115.63.

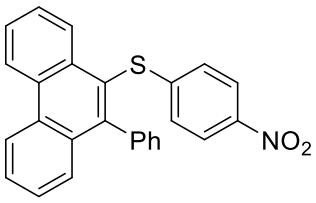

(4-Nitrophenyl)(10-phenylphenanthren-9-yl)sulfane (3ae) : Yellow crystalline solid (0.082 g, 40%); eluent hexane/EtOAc (10:1); mp = 188−190 oC; **^{1}H NMR (400 MHz, $CDCl_3$)** δ 8.74 (d, J = 7.8 Hz, 2H), 8.37 (d, J = 8.1 Hz, 1H), 7.90 – 7.80 (m, 2H), 7.67 (dd, J = 6.7, 1.6 Hz, 2H), 7.60 – 7.49 (m, 2H), 7.43 (d, J = 2.1 Hz, 2H), 7.35 (d, J = 3.8 Hz, 2H), 7.15 – 7.11 (m, 2H), 6.91 – 6.84 (m, 2H). **^{13}C NMR (100 MHz, $CDCl_3$)** δ 148.95, 147.78, 144.81, 139.61, 132.05, 131.41, 131.33, 131.07, 129.14, 128.96, 128.32, 128.16, 128.00, 127.80, 127.56, 127.18, 127.06, 125.60, 124.69, 123.89, 123.12, 122.71, 77.00.

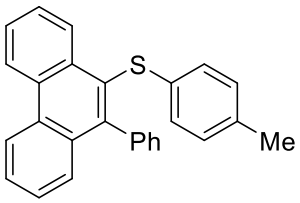

(10-Phenylphenanthren-9-yl)(p-tolyl)sulfane (3af) : [7] Yellow solid (0.170 g, 90%); eluent hexane; mp = 105−107 °C; **^{1}H NMR (400 MHz, $CDCl_3$)** δ 8.82 (dd, *J* = 8.2, 4.4 Hz, 2H), 8.72 (dd, *J* = 8.3, 0.9 Hz, 1H), 7.76 – 7.70 (m, 2H), 7.66 – 7.61 (m, 1H), 7.59 – 7.52 (m, 2H), 7.51 – 7.48 (m, 3H), 7.37 – 7.31 (m, 2H), 6.92 (dd, *J* = 21.3, 8.3 Hz, 4H), 2.26 (s, 3H). **^{13}C NMR (100 MHz, $CDCl_3$)** δ 146.63, 140.25, 135.34, 134.38, 132.23, 132.07, 131.04, 130.88, 129.55, 129.44, 128.68, 128.12, 127.94, 127.52, 127.30, 126.98, 126.68, 126.47, 122.71, 122.54, 20.82.

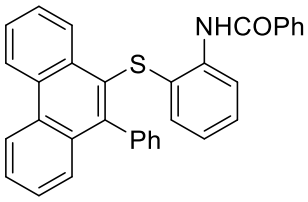

***N*-(2-(10-Phenylphenanthren-9-yl)phenyl)benzamide (3ag)** : Off White solid (0.145 g, 60%); eluent hexane/EtOAc (20:1); mp = 155−157 °C; **^{1}H NMR (400 MHz, $CDCl_3$)** δ 8.40 (dd, *J* = 7.8, 1.7 Hz, 1H), 8.36 – 8.27 (m, 2H), 7.78 (d, *J* = 8.0 Hz, 1H), 7.61 (s, 1H), 7.28 (s, 1H), 7.24 (d, *J* = 1.6 Hz, 1H), 7.21 (ddd, *J* = 8.3, 5.1, 1.6 Hz, 1H), 7.09 – 7.04 (m, 1H), 7.00 – 6.94 (m, 3H), 6.88 (dd, *J* = 8.3, 0.9 Hz, 1H), 6.78 (dd, *J* = 5.3, 2.1 Hz, 3H), 6.72 – 6.66 (m, 1H), 6.58 – 6.53 (m, 2H), 6.43 (dd, *J* = 7.9, 1.4 Hz, 1H), 6.31 (m, 1H**).**

^{13}C NMR (100 MHz, $CDCl_3$) δ 164.93, 146.03, 139.65, 136.45, 134.60, 132.76, 132.20, 131.64, 130.78, 130.71, 130.57, 129.41, 128.63, 128.50, 128.22, 128.16, 128.08, 127.83, 127.70, 127.45, 127.38, 127.27, 127.16, 127.11, 126.80, 124.65, 122.85, 122.53, 121.10. **HRMS (ESI)** m/z calcd for $C_{33}H_{24}NOS$ $[M + H]^+$: 482.1573; found: 482.1553.

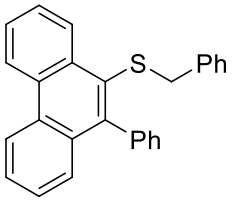

Benzyl(10-phenylphenanthren-9-yl)sulfane (3ah) : White crystalline solid (0.143 g, 76%); eluent hexane; mp = 185−187 °C; **^{1}H NMR (400 MHz, $CDCl_3$)** δ 8.90 (dd, *J* = 6.2, 3.3 Hz, 1H), 8.82 – 8.73 (m, 2H), 7.74 (dd, *J* = 6.3, 3.3 Hz, 2H), 7.68 – 7.63 (m, 1H), 7.42 (d, *J* = 6.9 Hz, 3H), 7.37 (d, *J* = 8.2 Hz, 1H), 7.10 (d, *J* = 7.3 Hz, 3H), 6.97 (dd, *J* = 7.5, 1.7 Hz, 2H), 6.82 (d, *J* = 6.4 Hz, 2H), 3.83 (s, 2H). **^{13}C NMR (100 MHz, $CDCl_3$)** δ 146.22, 140.35, 137.72, 132.22, 132.10, 130.70, 130.60, 130.11, 128.95, 128.53, 128.19, 127.80, 127.40, 127.17, 127.03, 126.84, 126.57, 122.98, 122.45, 40.84. **HRMS (ESI)** m/z calcd for $C_{27}H_{20}S$ $[M + H]^+$: 377.1358; found: 377.1285.

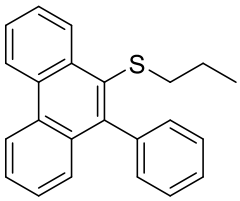

(10-Phenylphenanthren-9-yl)(propyl)sulfane (3ai) : White crystalline solid (0.115 g, 70%); eluent hexane; mp = 100−102 °C; **^{1}H NMR (400 MHz, $CDCl_3$)** δ 8.97 (d, *J* = 7.6 Hz, 1H), 8.79 (dd, *J* = 12.8, 8.0 Hz, 2H), 7.80 – 7.72 (m, 2H), 7.67 (ddd, *J* = 8.3, 5.8, 2.4 Hz, 1H), 7.60 – 7.49 (m, 5H), 7.40 (dd, *J* = 7.8, 1.3 Hz, 2H), 2.66 (t, *J* = 7.3 Hz, 2H), 1.45 (dd, *J* = 14.7, 7.3 Hz, 2H), 0.84 (t, *J* = 7.3 Hz, 3H). **^{13}C NMR (100 MHz, $CDCl_3$)** δ 145.39, 140.64, 132.53, 132.10, 130.65, 130.45, 130.35, 128.32, 127.93, 127.87, 127.20, 127.11, 126.98, 126.74, 126.56, 122.85, 122.41, 38.67, 22.87, 13.41 (Overlapping peaks present). **HRMS (ESI)** m/z calcd for $C_{23}H_{21}S$ $[M + H]^+$: 329.1358; found: 329.1292.

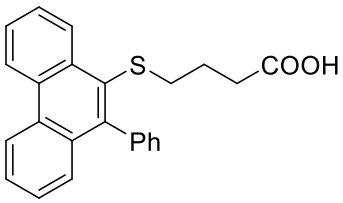

4-((10-Phenylphenanthren-9-yl)thio)butanoic acid (3aj) : Yellow crystalline solid (0.104 g, 56%); eluent hexane/EtOAc (20:1); mp = 130−132 °C; **^{1}H NMR (400 MHz, $CDCl_3$)** δ 8.90 (dd, *J* = 6.9, 2.6 Hz, 1H), 8.77 (dd, *J* = 12.4, 7.9 Hz, 2H), 7.77 – 7.71 (m, 2H), 7.67 (ddd, *J* = 8.3, 5.9, 2.4 Hz, 1H), 7.56 – 7.48 (m, 5H), 7.37 (dd, *J* = 7.8, 1.5 Hz, 2H), 2.71 (t, *J* = 6.9 Hz, 2H), 2.24 (t, *J* = 7.4 Hz, 2H), 1.72 – 1.65 (m, 2H). **^{13}C NMR (100 MHz, $CDCl_3$)** δ 179.33, 145.69, 140.38, 132.23, 131.97, 130.71, 130.53, 130.40, 129.42, 128.38, 127.94, 127.69, 127.32, 127.26, 127.15, 126.83, 126.63, 122.94, 122.42, 77.00, 35.54, 32.55, 24.04. **HRMS (ESI)** m/z calcd for $C_{24}H_{21}O_2S$ [M]: 373.1257; found: 373.1180.

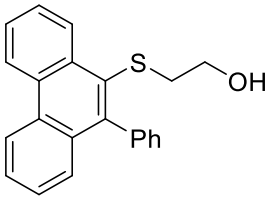

2-(10-Phenylphenanthren-9-yl)ethan-1-ol (3ak) : Yellow solid (0.066g, 40%); eluent hexane/EtOAc (25:1); mp = 123−125 °C; **^{1}H NMR (400 MHz, CDCl$_3$)** δ 8.84 (dd, *J* = 7.5, 2.1 Hz, 1H), 8.79 (dd, *J* = 7.5, 2.0 Hz, 1H), 8.75 (d, *J* = 8.4 Hz, 1H), 7.77 – 7.71 (m, 2H), 7.67 (ddd, *J* = 8.3, 5.0, 3.3 Hz, 1H), 7.60 – 7.55 (m, 2H), 7.53 (dd, *J* = 5.1, 3.6 Hz, 1H), 7.49 – 7.45 (m, 2H), 7.39 – 7.35 (m, 2H), 3.38 (t, *J* = 5.6 Hz, 2H), 2.87 (t, *J* = 5.6 Hz, 2H). **^{13}C NMR (100 MHz, CDCl$_3$)** δ 146.03, 140.35, 131.80, 130.89, 130.63, 130.38, 128.50, 128.28, 127.60, 127.50, 127.37, 126.99, 126.80, 123.13, 122.48, 59.78, 39.77. **Anal** calcd for $C_{22}H_{18}OS$: C, 79.97; H, 5.49; S, 9.70; found C, 79.81; H, 5.61; S, 9.86.

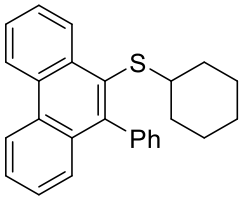

Cyclohexyl(10-phenylphenanthren-9-yl)sulfane (3al) :[7] Off White solid (,0.074 g, 38%); eluent hexane; mp = 129−131 °C; **^{1}H NMR (400 MHz, CDCl$_3$)** δ 8.92 (dd, *J* = 7.2, 2.5 Hz, 1H), 8.76 (dd, *J* = 10.5, 7.8 Hz, 2H), 7.72 (ddd, *J* = 4.6, 2.4, 0.6 Hz, 2H), 7.65 (m, 1H), 7.55 – 7.52 (m, 1H), 7.52 – 7.46 (m, 2H), 7.45 (d, *J* = 3.6 Hz, 2H), 7.35 (d, *J* = 1.6 Hz, 1H), 7.33 (d, *J* = 1.4 Hz, 1H), 2.83 (tt, *J* = 10.7, 3.7 Hz, 1H), 1.69 (dd, *J* = 13.3, 3.0 Hz, 2H), 1.51 – 1.45 (m, 1H), 1.33 – 1.18 (m, 4H), 1.09 (ddd, *J* = 16.7, 10.3, 3.1 Hz, 3H). **^{13}C NMR (100 MHz, CDCl$_3$)** δ 145.47, 140.62, 133.16, 132.17, 130.69, 130.56, 130.44, 129.85, 128.36, 128.25, 127.78, 127.10, 127.05, 126.94, 126.70, 126.57, 122.77, 122.42, 48.55, 33.46, 26.03, 25.63.

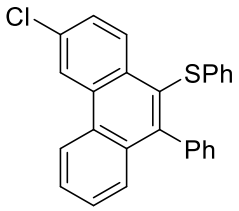

(6-Chloro-10-phenylphenanthren-9-yl)(phenyl)sulfane (3ba) : Yellow crystalline solid (0.133 g, 67%); eluent hexane; mp = 155−157 °C; **^{1}H NMR (400 MHz, CDCl$_3$)** δ 8.72 (d, *J* = 2.1 Hz, 1H), 8.69 (d, *J* = 8.4 Hz, 1H), 8.63 (d, *J* = 8.9 Hz, 1H), 7.71 (ddd, *J* = 8.3, 6.2, 2.1 Hz, 1H), 7.51 (dd, *J* = 3.0, 1.6 Hz, 1H), 7.49 (dd, *J* = 1.9, 1.0 Hz, 2H), 7.45 (d, *J* = 2.0 Hz, 2H), 7.44 (d, *J* = 1.8 Hz, 1H), 7.25 (d, *J* = 2.0 Hz, 1H), 7.24 – 7.22 (m, 1H), 7.06 (ddd, *J* = 4.9, 3.3, 1.9 Hz, 3H), 7.04 – 7.01 (m, 2H). **^{13}C NMR (100 MHz, CDCl$_3$)** δ 147.04, 141.63, 133.87, 133.28, 132.45, 132.36, 131.80, 130.86, 130.09, 129.61, 129.20, 129.03, 128.03, 127.93, 127.72, 127.47, 127.39, 127.14, 125.72, 122.63, 122.32. **HRMS (ESI)** m/z calcd for $C_{26}H_{17}ClS$ [M]: 396.0739; found: 396.0717.

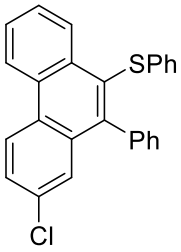

(2-Chloro-10-phenylphenanthren-9-yl)(phenyl)sulfane (3ca):[7] White crystalline solid (0.129 g, 65%); eluent hexane; mp = 145−147 °C; **^{1}H NMR (400 MHz, CDCl$_3$)** δ 9.68 – 9.57 (m, 3H), 8.66 – 8.61 (m, 1H), 8.60 – 8.50 (m, 2H), 8.47 – 8.34 (m, 4H), 8.23 – 8.17 (m, 2H), 8.08 – 8.00 (m, 2H), 8.00 – 7.95 (m, 1H), 7.93 – 7.79 (m, 2H). **^{13}C NMR (100 MHz, CDCl$_3$)** δ 145.69, 139.37, 138.60, 133.31, 132.76, 131.96, 130.36, 129.44, 128.87, 128.70, 128.20, 128.15, 128.00, 127.83, 127.67, 127.61, 127.42, 126.49, 124.85, 124.24, 122.68.

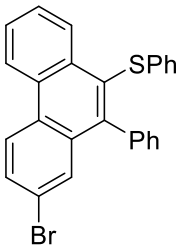

(2-Bromo-10-phenylphenanthren-9-yl)(phenyl)sulfane (3da) : White solid (0.155 g, 70%); eluent hexane; mp = 166−168 °C; **^{1}H NMR (400 MHz, CDCl$_3$)** δ 8.69 (dd, *J* = 18.2, 8.2 Hz, 2H), 8.63 (d, *J* = 8.9 Hz, 1H), 7.78 (dd, *J* = 8.9, 2.1 Hz, 1H), 7.73 – 7.59 (m, 3H), 7.50 – 7.44 (m, 3H), 7.28 – 7.25 (m, 2H), 7.11 (t, *J* = 7.6 Hz, 2H), 7.07 – 7.02 (m, 1H), 6.93 (d, *J* = 8.1 Hz, 2H). **^{13}C NMR (100 MHz, CDCl$_3$)** δ 145.63, 139.34, 138.61, 133.68, 132.02, 130.76, 130.70, 130.41, 129.74, 129.46, 128.88, 128.71, 128.23, 128.16, 127.94, 127.70, 127.44, 126.51, 126.37, 124.86, 124.38, 122.64, 121.06. **Anal** calcd for $C_{26}H_{17}BrS$: C, 70.75; H, 3.88; S, 7.26 found C, 70.96; H, 3.61; S, 7.10.

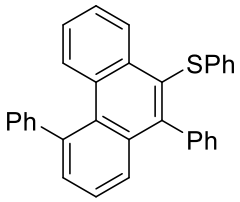

(4,10-Diphenylphenanthren-9-yl)(phenyl)sulfane (3ea) :White crystalline solid (0.154 g, 70%); eluent hexane; mp = 200−202 °C; **^{1}H NMR (400 MHz, CDCl$_3$)** δ 8.63 (d, *J* = 8.2 Hz, 1H), 7.88 (d, *J* = 8.5 Hz, 1H), 7.48 (d, *J* = 14.7 Hz, 12H), 7.31 (d, *J* = 3.0 Hz, 2H), 7.12 (dd, *J* = 11.6, 7.3 Hz, 3H), 7.00 (dd, *J* = 31.2, 7.3 Hz, 3H). **^{13}C NMR (100 MHz, CDCl$_3$)** δ 146.71, 145.25, 140.62, 140.23, 138.90, 133.74, 133.06, 131.89, 130.89, 129.60, 129.09, 129.03, 128.89, 128.66, 128.28, 128.00, 127.77, 127.47, 127.35, 127.12, 126.94, 126.53, 125.68, 124.97, 124.71. **Anal** calcd for $C_{32}H_{22}S$: C, 87.63; H, 5.06; S, 7.31; found C, 87.76; H, 5.18; S, 7.18.

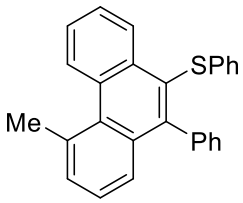

(4-Methyl-10-phenylphenanthren-9-yl)(phenyl)sulfane (3fa) : Yellow solid (0.135 g, 72%); eluent hexane; mp = 188−190 °C; **^{1}H NMR (400 MHz, CDCl$_3$)** δ 8.92 (d, *J* = 8.2 Hz, 1H), 8.77 (dd, *J* = 8.2, 1.4 Hz, 1H), 7.69 (ddd, *J* = 8.5, 7.0, 1.6 Hz, 1H), 7.65 – 7.59 (m, 2H), 7.46 (dd, *J* = 4.1, 2.4 Hz, 3H), 7.44 – 7.38 (m, 2H), 7.31 – 7.27 (m, 2H), 7.14 – 7.09 (m, 2H), 7.06 – 7.02 (m, 1H), 6.98 (d, *J* = 1.4 Hz, 1H), 6.96 (s, 1H), 3.23 (s, 3H). **^{13}C NMR (100 MHz, CDCl$_3$)** δ 147.23, 140.88, 138.94, 134.98, 133.71, 132.94, 132.23, 132.03, 131.33, 129.50, 128.62, 127.92, 127.71, 127.23, 127.11, 126.84, 126.39, 125.75, 125.64, 124.61, 27.29. **HRMS (ESI)** m/z calcd for $C_{27}H_{21}S$ $[M + H]^+$: 377.1358; found: 377.1286.

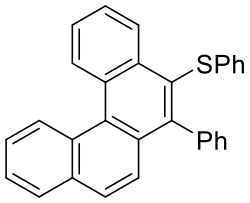

Phenyl(6-phenylbenzo[*c*]phenanthren-5-yl)sulfane (3ga) : Yellow solid (0.083 g, 40%); eluent hexane; mp = 145−147 °C; **^{1}H NMR (400 MHz, CDCl$_3$)** δ 9.15 (d, *J* = 8.0 Hz, 2H), 8.83 (dd, *J* = 8.3, 1.0 Hz, 1H), 8.03 (d, *J* = 7.7 Hz, 1H), 7.80 – 7.67 (m, 5H), 7.49 (dd, *J* = 5.5, 3.4 Hz, 4H), 7.37 – 7.29 (m, 2H), 7.12 (dd, *J* = 11.4, 4.3 Hz, 2H), 7.05 (d, *J* = 7.1 Hz, 1H), 7.00 – 6.94 (m, 2H). **^{13}C NMR (100 MHz, CDCl$_3$)** δ 146.03, 140.21, 138.98, 133.52, 133.31, 130.64, 130.40, 129.84, 129.53, 129.15, 128.83, 128.65, 128.58, 128.21, 127.95, 127.46, 127.40, 127.12, 127.04, 126.64, 126.25, 126.22, 125.47, 124.74. **HRMS (ESI)** m/z calcd for $C_{30}H_{21}S$ $[M + H]^+$: 413.1358; found: 413.1327.

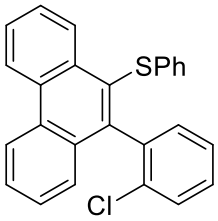

(10-(2-Chlorophenyl)phenanthren-9-yl)(phenyl)sulfane (3ha) : White crystalline solid (0.188g, 95%); eluent hexane; mp = 130−132 °C; **^{1}H NMR (400 MHz, CDCl$_3$)** δ 8.74 (d, *J* = 2.0 Hz, 1H), 8.69 (d, *J* = 8.4 Hz, 1H), 8.58 (d, *J* = 8.9 Hz, 1H), 7.72 (ddd, *J* = 8.3, 5.2, 3.1 Hz, 1H), 7.55 – 7.51 (m, 3H), 7.45 (dd, *J* = 4.9, 1.7 Hz, 3H), 7.30 – 7.26 (m, 2H), 7.14 – 7.09 (m, 2H), 7.04 (ddd, *J* = 7.3, 3.6, 1.2 Hz, 1H), 6.94 – 6.90 (m, 2H). **^{13}C NMR (100 MHz, CDCl$_3$)** δ 147.03, 139.80, 138.57, 133.31, 132.59, 132.05, 130.47, 130.08, 129.78, 129.45, 128.82, 128.75, 128.01, 127.97, 127.89, 127.50, 127.37, 126.80, 126.40, 124.89, 122.63, 122.42. **Anal** calcd for $C_{26}H_{17}ClS$: C, 78.67; H, 4.32; S, 8.08; found C, 78.56; H, 4.48; S, 8.21.

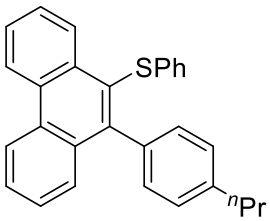

Phenyl(10-(4-propylphenyl)phenanthren-9-yl)sulfane (3ia) : Off White crystalline solid (0.142 g, 70%); eluent hexane; mp = 150−152 °C; **^{1}H NMR (400 MHz, CDCl$_3$)** δ 8.81 (dd, *J* = 8.2, 3.4 Hz, 2H), 8.67 (dd, *J* = 8.3, 1.0 Hz, 1H), 7.72 (dtd, *J* = 8.3, 6.7, 1.5 Hz, 2H), 7.62 (ddd, *J* = 8.2, 7.0, 1.2 Hz, 1H), 7.57 (dd, *J* = 8.3, 1.2 Hz, 1H), 7.54 – 7.50 (m, 1H), 7.28 (s, 1H), 7.20 (d, *J* = 8.1 Hz, 2H), 7.14 – 7.08 (m, 2H), 7.06 – 7.01 (m, 1H), 6.99 – 6.94 (m, 2H), 2.75 – 2.70 (m, 2H), 1.78 (dd, *J* = 15.1, 7.5 Hz, 2H), 1.06 (t, *J* = 7.3 Hz, 3H). **^{13}C NMR (100 MHz, CDCl$_3$)** δ 146.96, 141.68, 139.11, 137.36, 132.44, 132.12, 131.09, 130.86, 129.35, 128.82, 128.61, 128.06, 127.99, 127.55, 127.52, 127.24, 126.95, 126.67, 126.49, 124.62, 122.73, 122.52, 37.91, 24.40, 13.96. **Anal** calcd for $C_{29}H_{24}S$: C, 86.10; H, 5.98; S, 7.92; found C, 86.46; H, 5.66; S, 7.82.

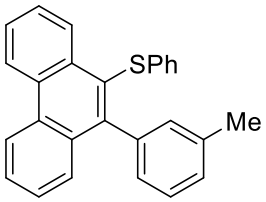

Phenyl(10-(*m*-tolyl)phenanthren-9-yl)sulfane (3ja) : Yellow crystalline solid (0.132 g, 70%); eluent hexane; mp = 165−167 °C; **^{1}H NMR (400 MHz, CDCl$_3$)** δ 8.83 (d, *J* = 8.4 Hz, 2H), 8.74 (dd, *J* = 8.3, 1.1 Hz, 1H), 7.74 (m, 2H), 7.65 (ddd, *J* = 8.2, 7.0, 1.2 Hz, 1H), 7.60 (dd, *J* = 8.3, 1.3 Hz, 1H), 7.54 (ddd, *J* = 8.2, 6.8, 1.1 Hz, 1H), 7.39 (t, *J* = 7.5 Hz, 1H), 7.31 (d, *J* = 7.6 Hz, 1H), 7.14 (ddd, *J* = 9.5, 5.0, 1.3 Hz, 4H), 7.08 (dd, *J* = 4.9, 3.6 Hz, 1H), 7.03 – 6.99 (m, 2H), 2.41 (s, 3H). **^{13}C NMR (100 MHz, CDCl$_3$)** δ 146.93, 140.05, 139.11, 137.39, 132.28, 132.15, 131.05, 130.83, 130.26, 128.76, 128.58, 128.07, 128.03, 127.81, 127.53, 127.15, 126.96, 126.66, 126.53, 124.65, 122.72, 122.51, 21.48. **HRMS (ESI)** m/z calcd for $C_{27}H_{21}S$ $[M + H]^+$: 377.1358; found: 377.1324.

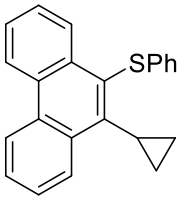

(10-Cyclopropylphenanthren-9-yl)(phenyl)sulfane (3ka) : Yellow liquid (0.083 g, 51%); eluent hexane; **^{1}H NMR (400 MHz, CDCl$_3$)** δ 7.47 – 7.42 (m, 2H), 7.40 – 7.34 (m, 3H), 7.32 – 7.27 (m, 2H), 7.25 – 7.23 (m, 1H), 7.21 – 7.14 (m, 2H), 7.13 – 7.08 (m, 1H), 6.94 (dd, *J* = 8.3, 1.2 Hz, 2H), 1.85 (tt, *J* = 8.2, 5.2 Hz, 1H), 0.76 – 0.64 (m, 2H), 0.64 – 0.56 (m, 1H), 0.44 – 0.32 (m, 1H). **^{13}C NMR (100 MHz, CDCl$_3$)** δ 142.56, 140.88, 140.51, 138.79, 136.39, 130.03, 129.37, 128.95, 128.55, 128.35, 127.79, 127.11, 127.00, 125.53, 107.14, 22.63, 9.54, 8.62. **Anal** calcd for $C_{26}H_{17}ClS$: C, 84.62; H, 5.56; S, 9.82; found C, 84.71; H, 5.36; S, 9.92.

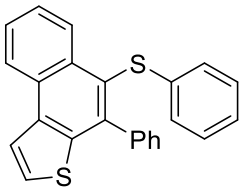

4-Phenyl-5-(phenylthio)naphtho[2,1-b]thiophene (3la) : Yellow solid (0.103 g, 56%); eluent hexane; mp =80−82 °C; **^{1}H NMR (400 MHz, CDCl$_3$)** δ 8.68 (d, *J* = 8.4 Hz, 1H), 8.47 – 8.38 (m, 1H), 8.09 (d, *J* = 5.5 Hz, 1H), 7.73 – 7.64 (m, 2H), 7.58 (ddd, *J* = 8.1, 7.1, 1.2 Hz, 1H), 7.52 – 7.38 (m, 5H), 7.14 – 7.08 (m, 2H), 7.07 – 7.01 (m, 1H), 6.95 (dd, *J* = 7.2, 1.3 Hz, 2H). **^{13}C NMR (100 MHz, CDCl$_3$)** δ 142.35, 140.14, 139.92, 139.21, 137.14, 132.50, 129.45, 128.96, 128.76, 128.66, 128.15, 128.00, 126.74, 126.60, 126.31, 124.70, 123.98, 123.73, 122.35. **HRMS (ESI)** m/z calcd for $C_{24}H_{17}S_2$ [M]: 369.0766; found: 369.0732.

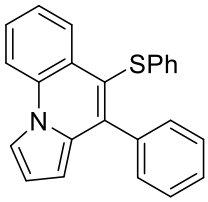

4-Phenyl-5-(phenylthio)pyrrolo[1,2-*a*]quinoline (3ma) : Yellow solid (0.127 g, 72%); eluent hexane; mp = 56−58 °C; **^{1}H NMR (400 MHz, CDCl$_3$)** δ 8.19 – 8.09 (m, 1H), 7.56 (s, 1H), 7.49 (d, *J* = 1.8 Hz, 1H), 7.47 (dd, *J* = 5.9, 1.6 Hz, 3H), 7.43 (dd, *J* = 4.9, 3.6 Hz, 2H), 7.36 – 7.33 (m, 1H), 7.33 – 7.27 (m, 5H), 7.14 (s, 1H), 6.94 – 6.87 (m, 1H). **^{13}C NMR (100 MHz, CDCl$_3$)** δ 140.31, 138.97, 138.85, 137.31, 136.06, 135.97, 130.21, 130.03, 129.93, 128.78, 128.63, 128.49, 127.88, 127.80, 127.74, 127.70, 126.53, 126.48, 126.25, 126.13, 125.92, 125.83, 123.89, 119.96, 101.08, 100.76. **Anal** calcd for $C_{24}H_{17}NS$: C, 82.02; H, 4.88; N, 3.99; S, 9.12; found C, 82.26; H, 4.36; N, 4.07; S, 9.31.

^{1}H and ^{13}C NMR Spectra of Some Selected 9-Sulfenylphenanthrenes

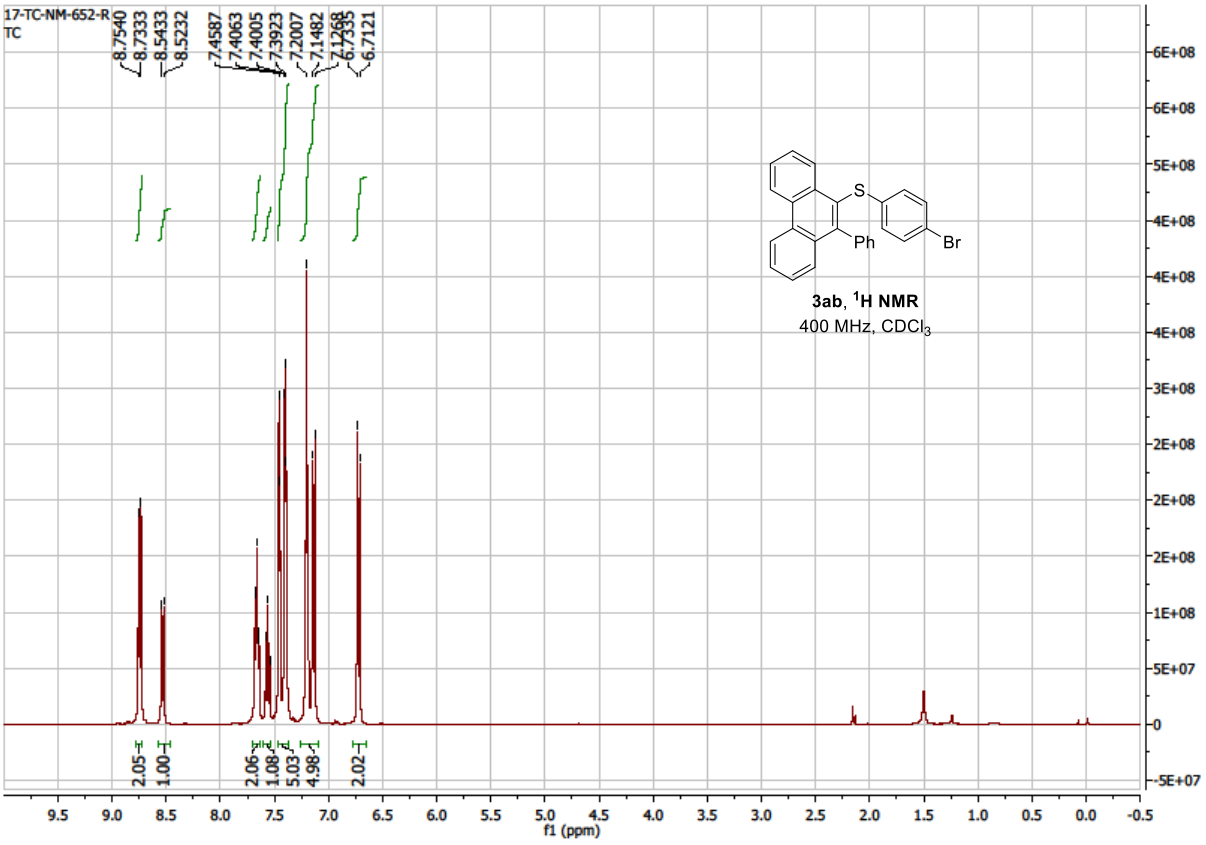
17-TC-NM-652-R
TC
8.7540
8.7333
8.5433
8.5232
7.4587
7.4063
7.4005
7.3923
7.2007
7.1482
7.1268
6.7335
6.7121
2.05
1.00
2.06
1.08
5.03
4.98
2.02
S
Ph
Br
3ab, 1H NMR
400 MHz, CDCl3
f1 (ppm)

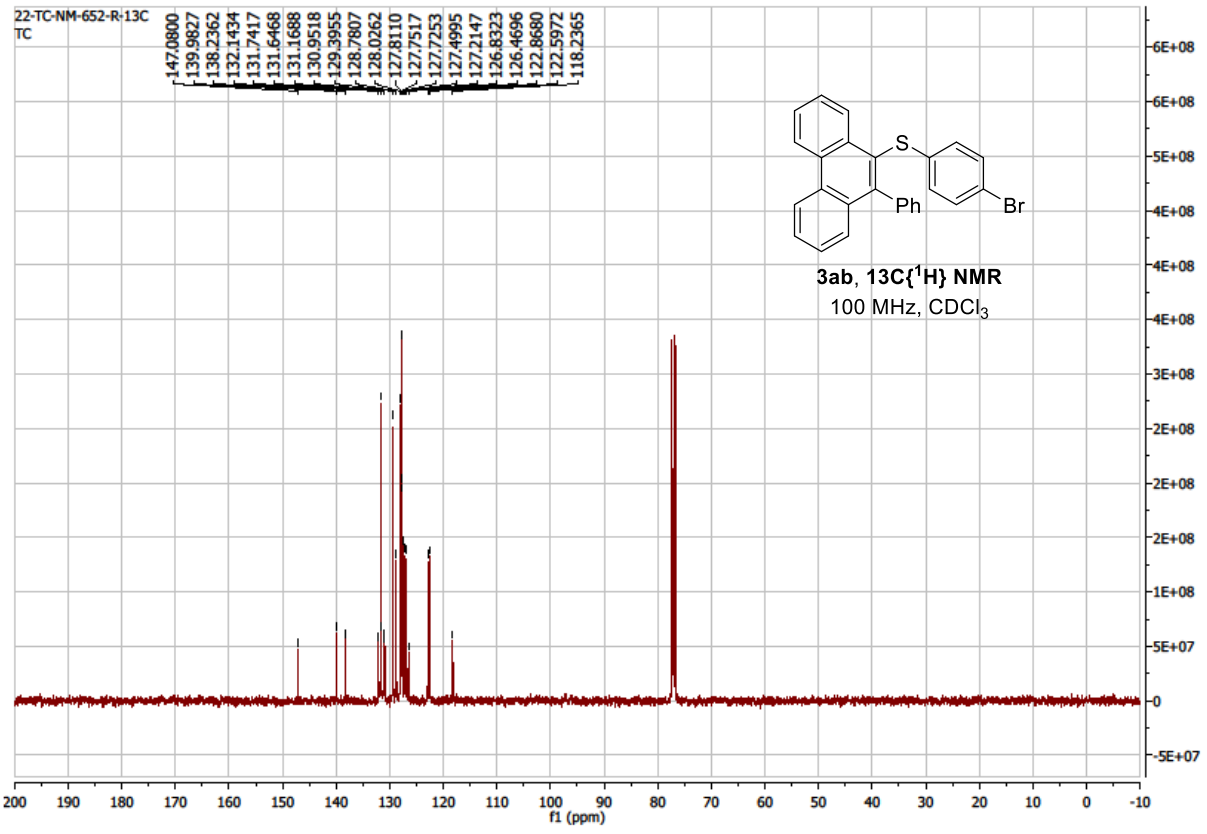
22-TC-NM-652-R-13C
TC
147.0800
139.9827
138.2362
132.1434
131.7417
131.6468
131.1688
130.9518
129.3955
128.7807
128.0262
127.8110
127.7517
127.7253
127.4995
127.2147
126.8323
126.4696
122.8680
122.5972
118.2365
S
Ph
Br
3ab, 13C{1H} NMR
100 MHz, CDCl3
f1 (ppm)

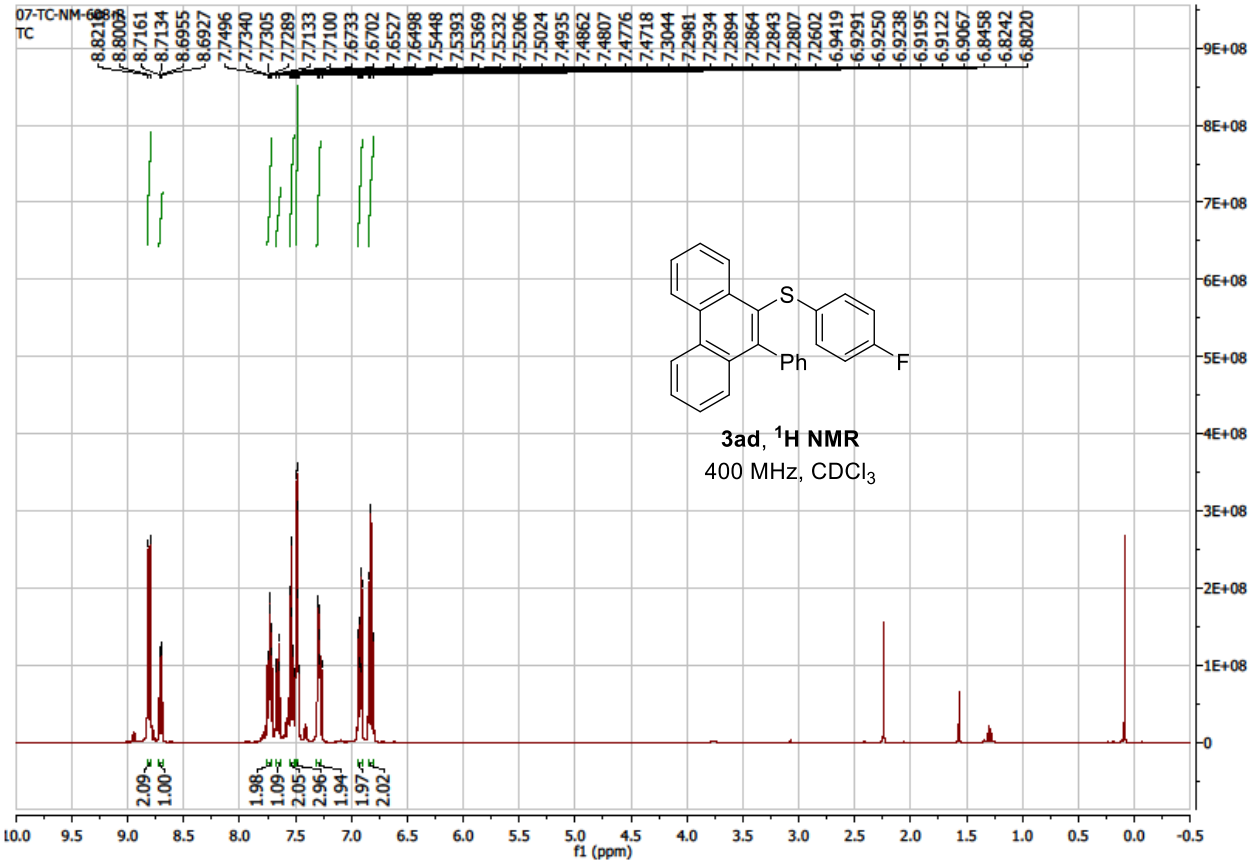
07-TC-NM-608-R
TC
S
Ph
F
3ad, ^{1}H NMR
400 MHz, $CDCl_3$
f1 (ppm)

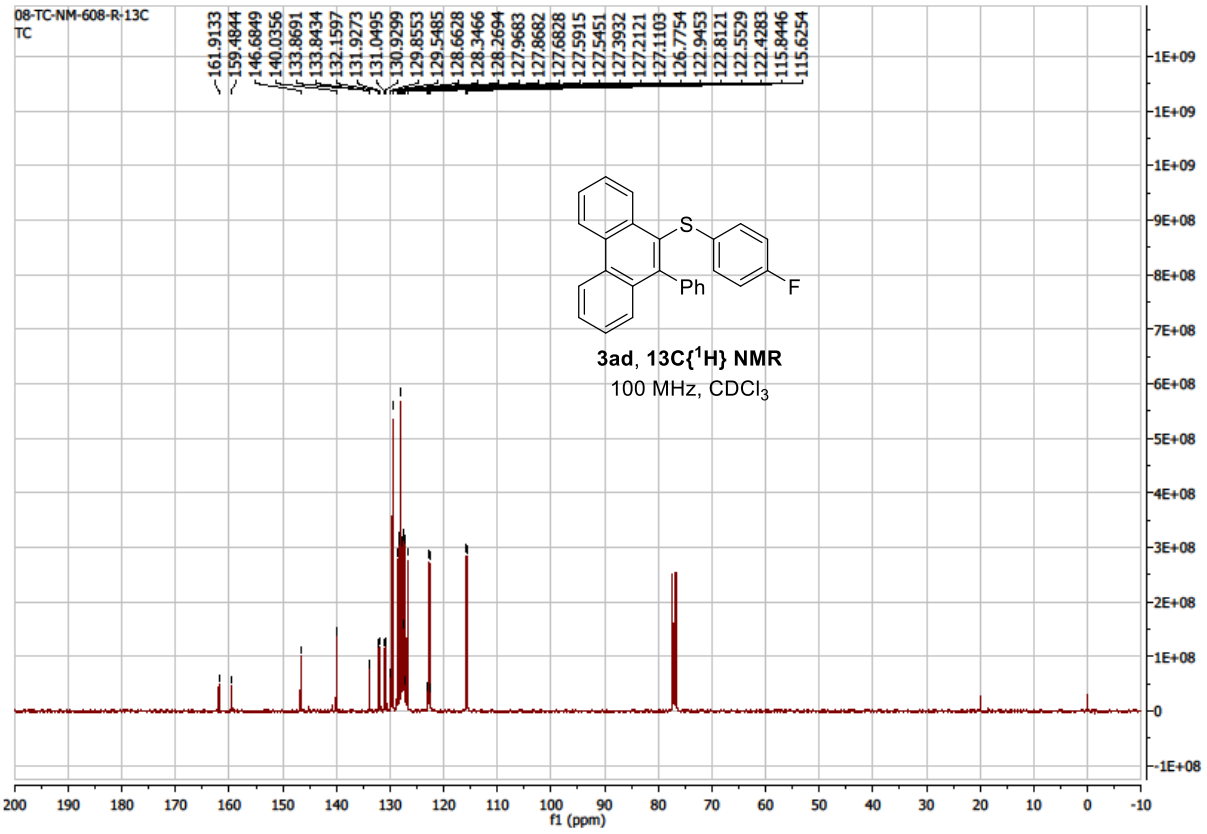
08-TC-NM-608-R-13C
TC
S
Ph
F
3ad, 13C{^{1}H} NMR
100 MHz, $CDCl_3$
f1 (ppm)

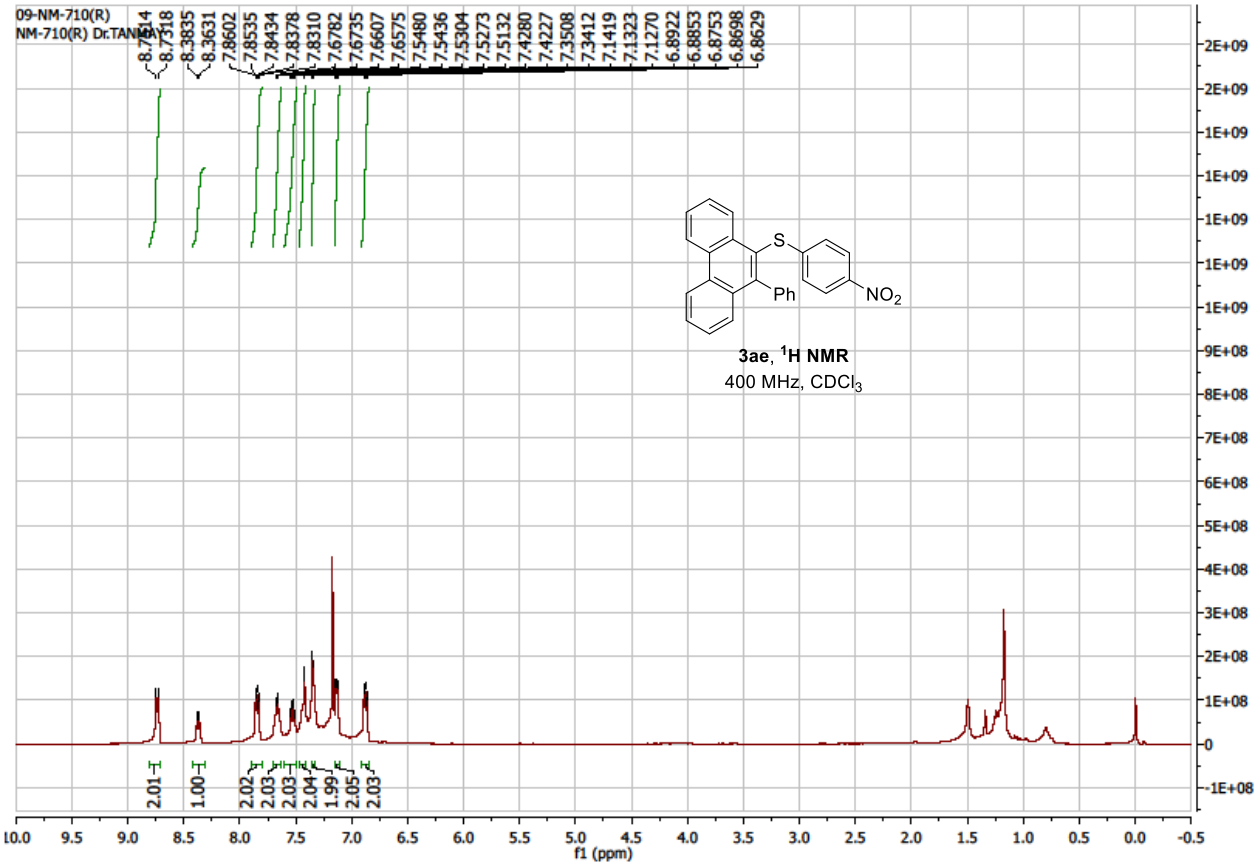
09-NM-710(R)
NM-710(R) Dr.TANMAY
8.7364
8.7318
8.3835
8.3631
8.8602
7.8535
7.8434
7.8378
7.8310
7.6782
7.6735
7.6607
7.6575
7.5480
7.5436
7.5304
7.5273
7.5132
7.4280
7.4227
7.3508
7.3412
7.1419
7.1323
7.1270
6.8922
6.8853
6.8753
6.8698
6.8629
S
Ph
NO2
3ae, 1H NMR
400 MHz, CDCl3
2.01
1.00
2.02
2.03
2.03
2.04
1.99
2.05
2.03
f1 (ppm)

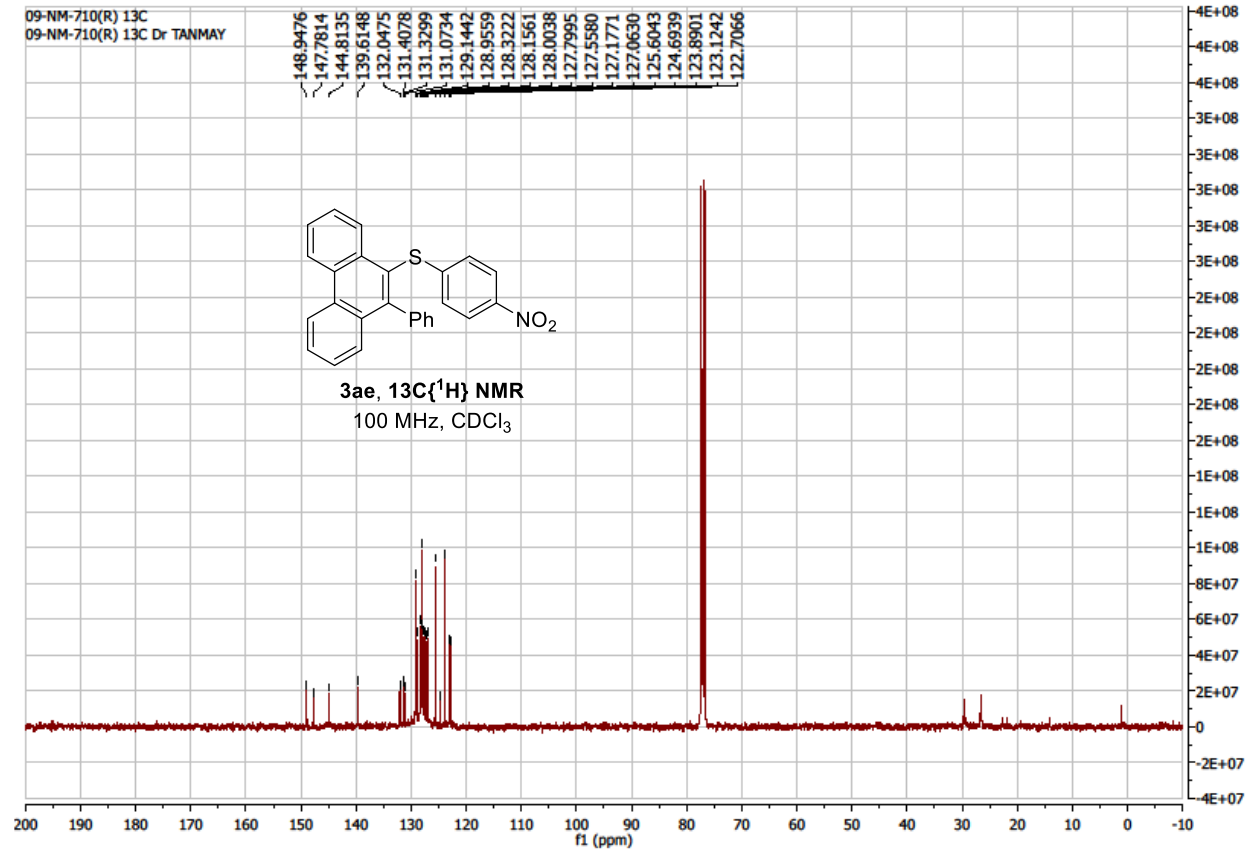
09-NM-710(R) 13C
09-NM-710(R) 13C Dr TANMAY
148.9476
147.7814
144.8135
139.6148
132.0475
131.4078
131.3299
131.0734
129.1442
128.9559
128.3222
128.1561
128.0038
127.7995
127.5580
127.1771
127.0630
125.6043
124.6939
123.8901
123.1242
122.7066
S
Ph
NO2
3ae, 13C{1H} NMR
100 MHz, CDCl3
f1 (ppm)

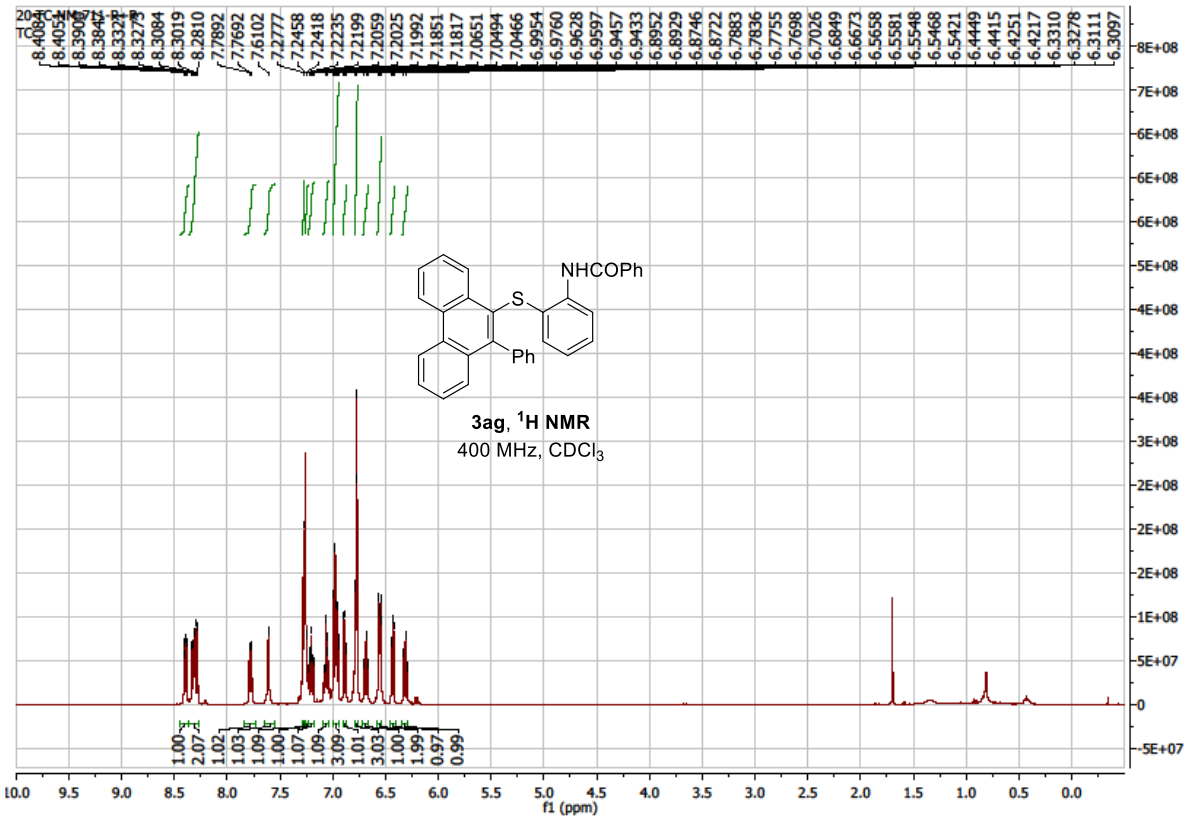
NHCOPh
S
Ph
3ag, 1H NMR
400 MHz, CDCl3
f1 (ppm)

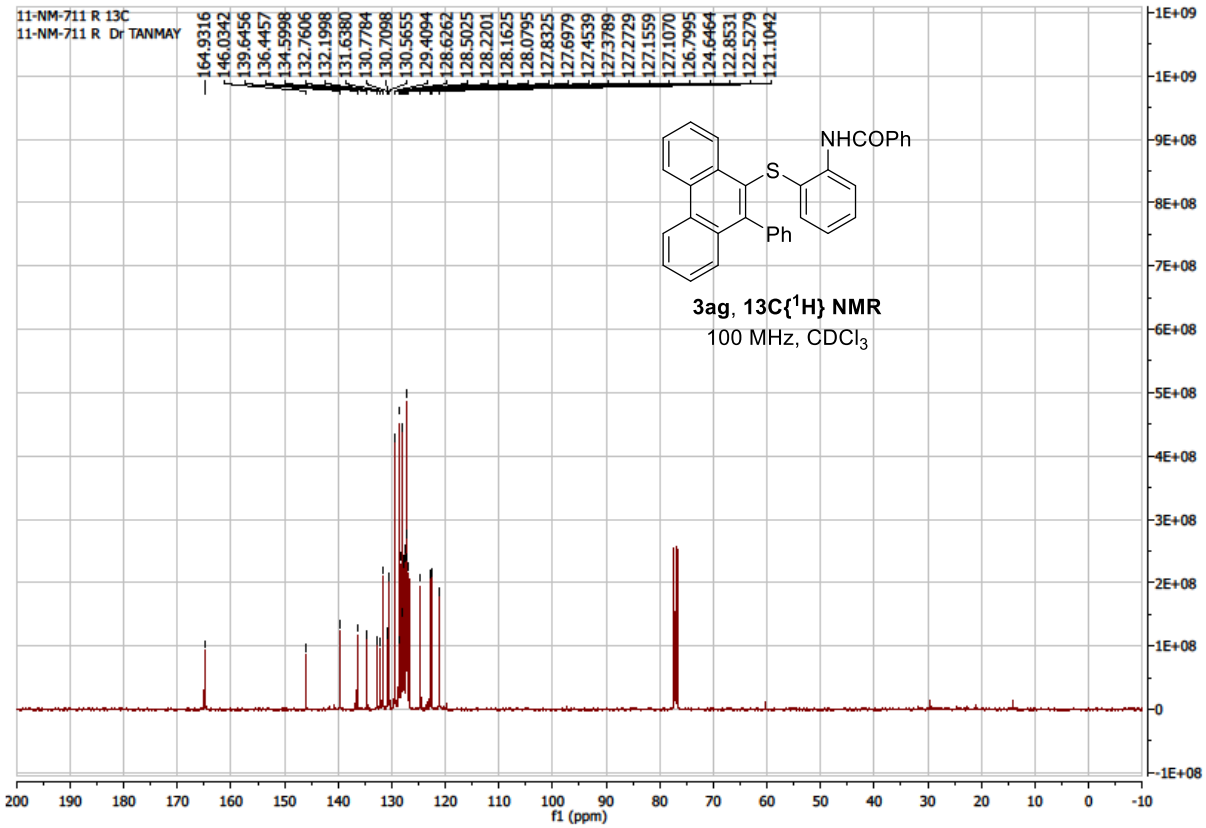
11-NM-711 R 13C
11-NM-711 R Dr TANMAY
NHCOPh
S
Ph
3ag, 13C{1H} NMR
100 MHz, CDCl3
f1 (ppm)

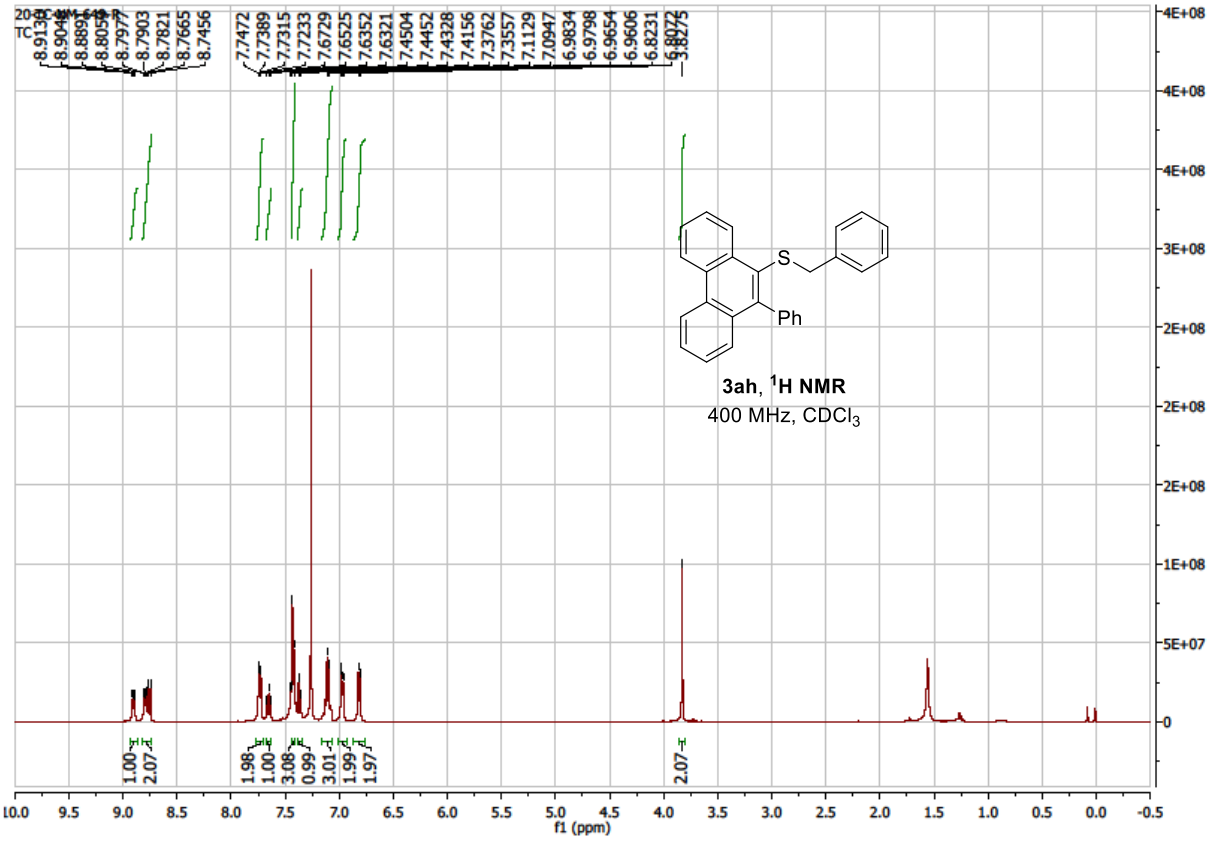
S
Ph
3ah, ^{1}H NMR
400 MHz, $CDCl_3$
f1 (ppm)

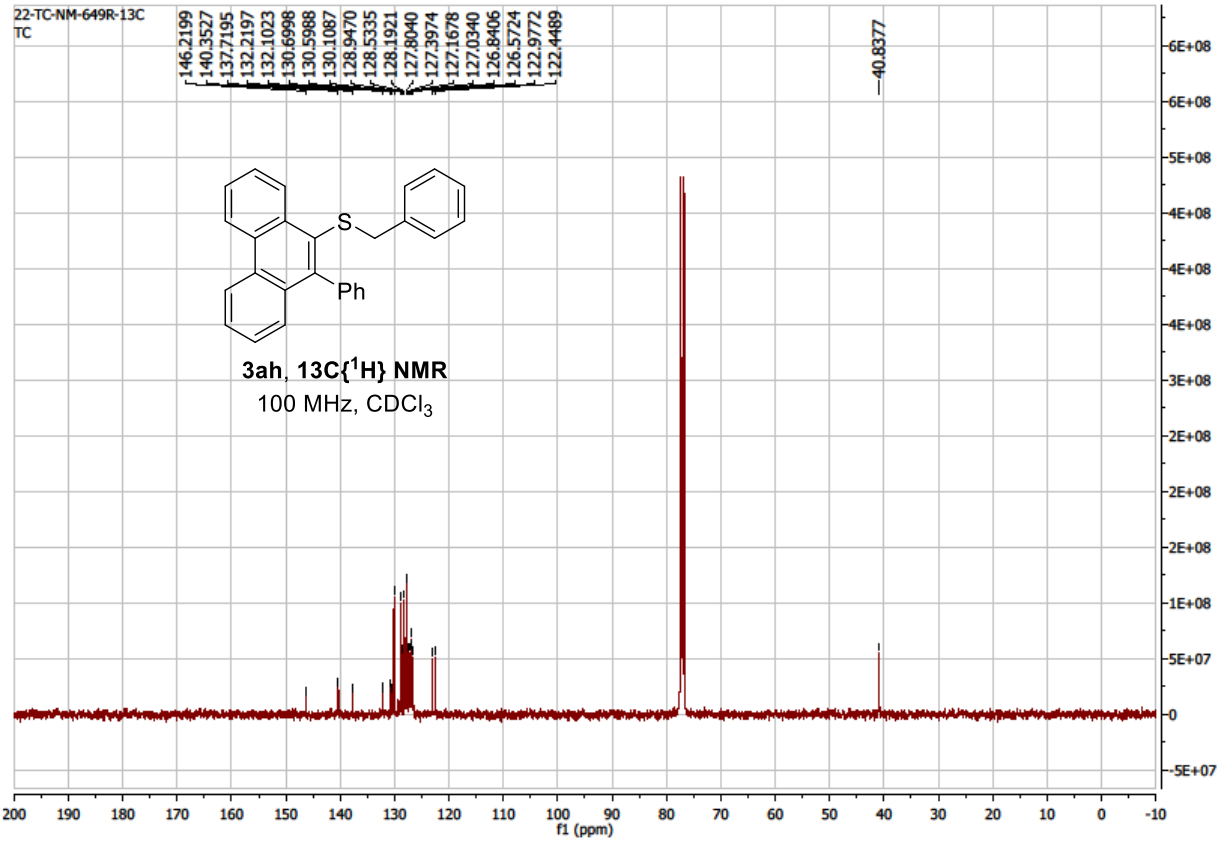
22-TC-NM-649R-13C
TC
S
Ph
3ah, 13C{^{1}H} NMR
100 MHz, $CDCl_3$
f1 (ppm)

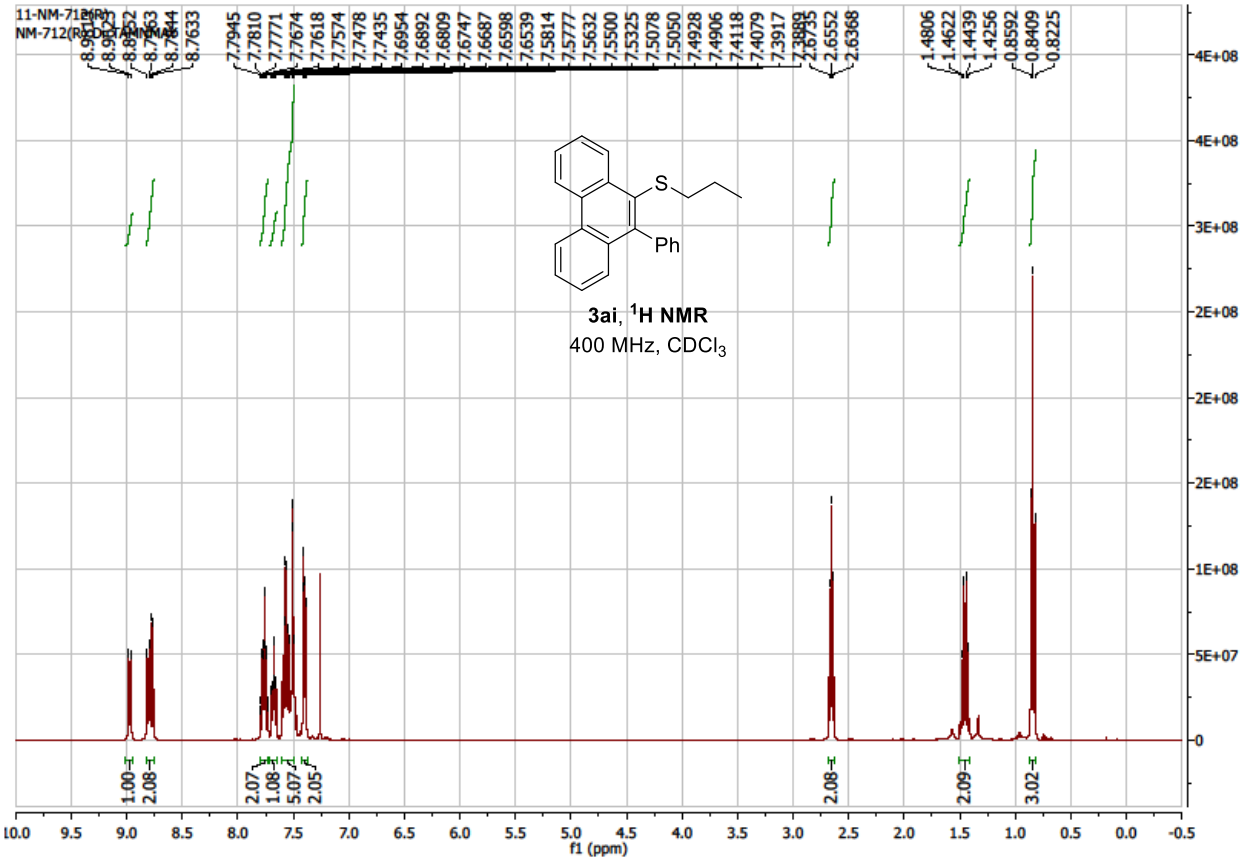
S
Ph
3ai, ^{1}H NMR
400 MHz, $CDCl_3$
f1 (ppm)

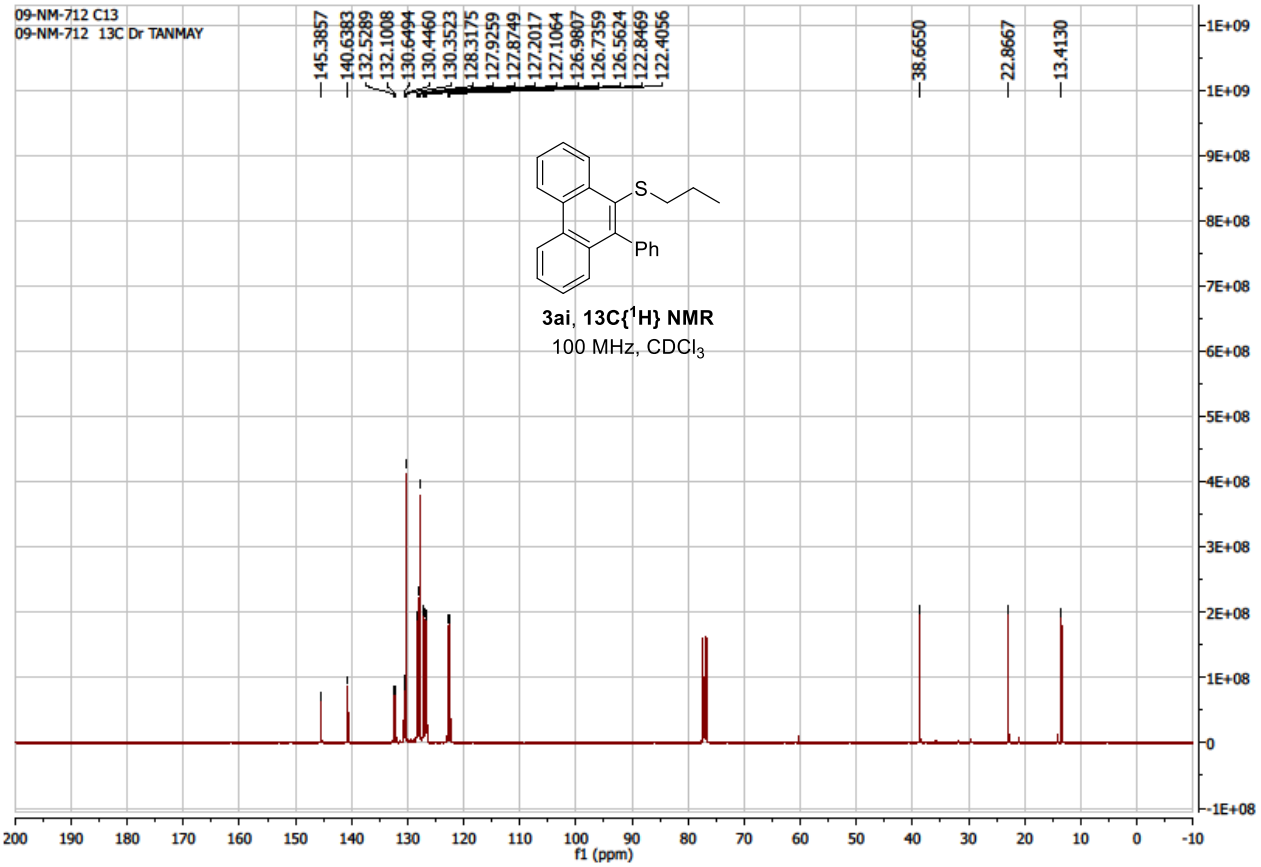
09-NM-712 C13
09-NM-712 13C Dr TANMAY
S
Ph
3ai, 13C{^{1}H} NMR
100 MHz, $CDCl_3$
f1 (ppm)

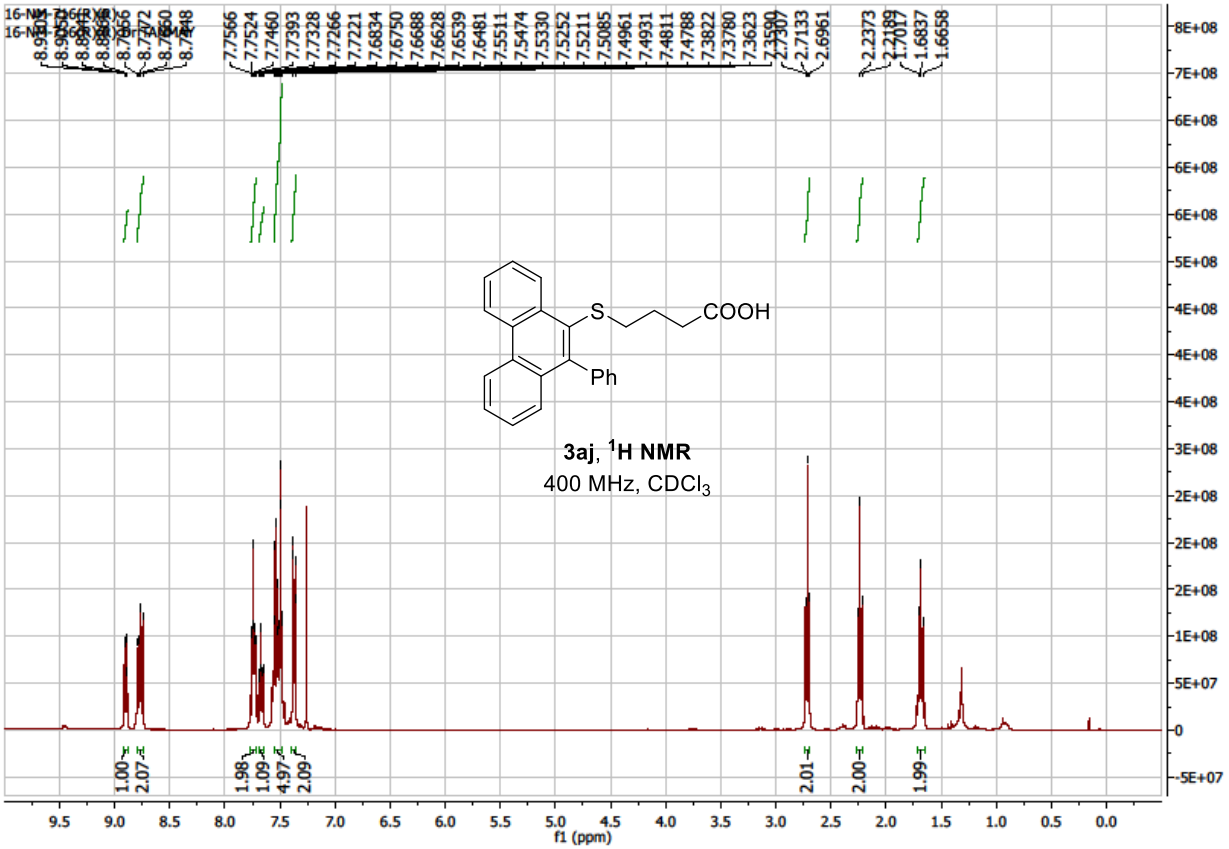
S
COOH
Ph
3aj, ^{1}H NMR
400 MHz, CDCl$_3$
f1 (ppm)

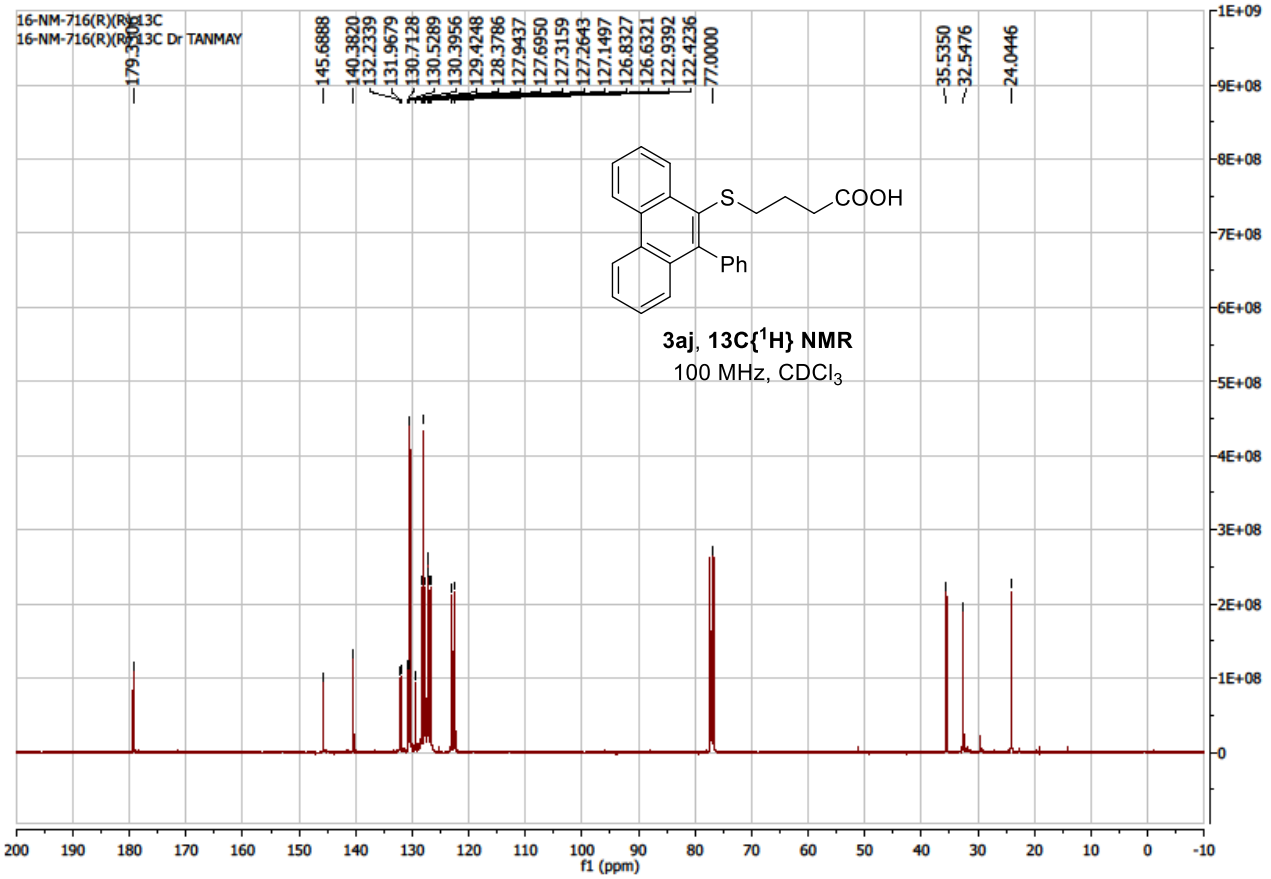
S
COOH
Ph
3aj, 13C{^{1}H} NMR
100 MHz, CDCl$_3$
f1 (ppm)

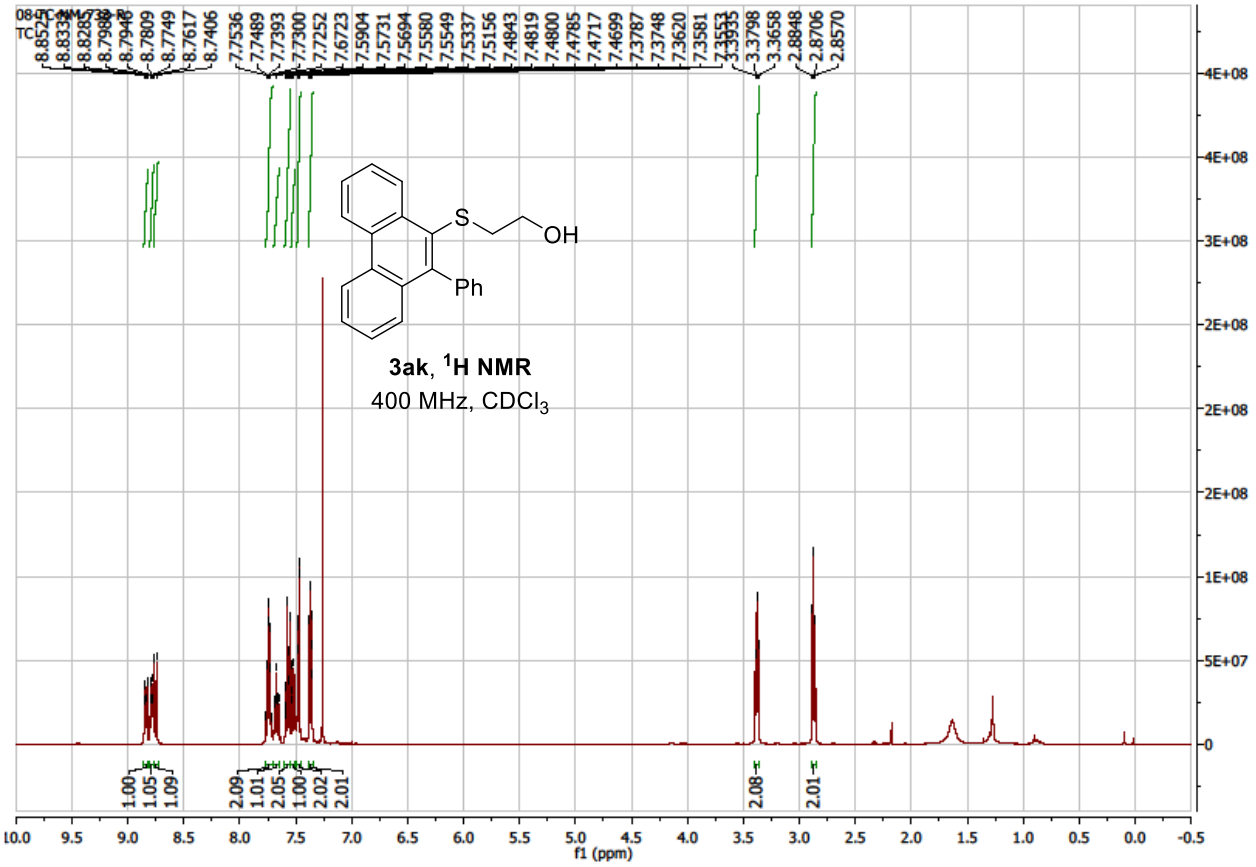
S
OH
Ph
3ak, ^{1}H NMR
400 MHz, $CDCl_3$
f1 (ppm)

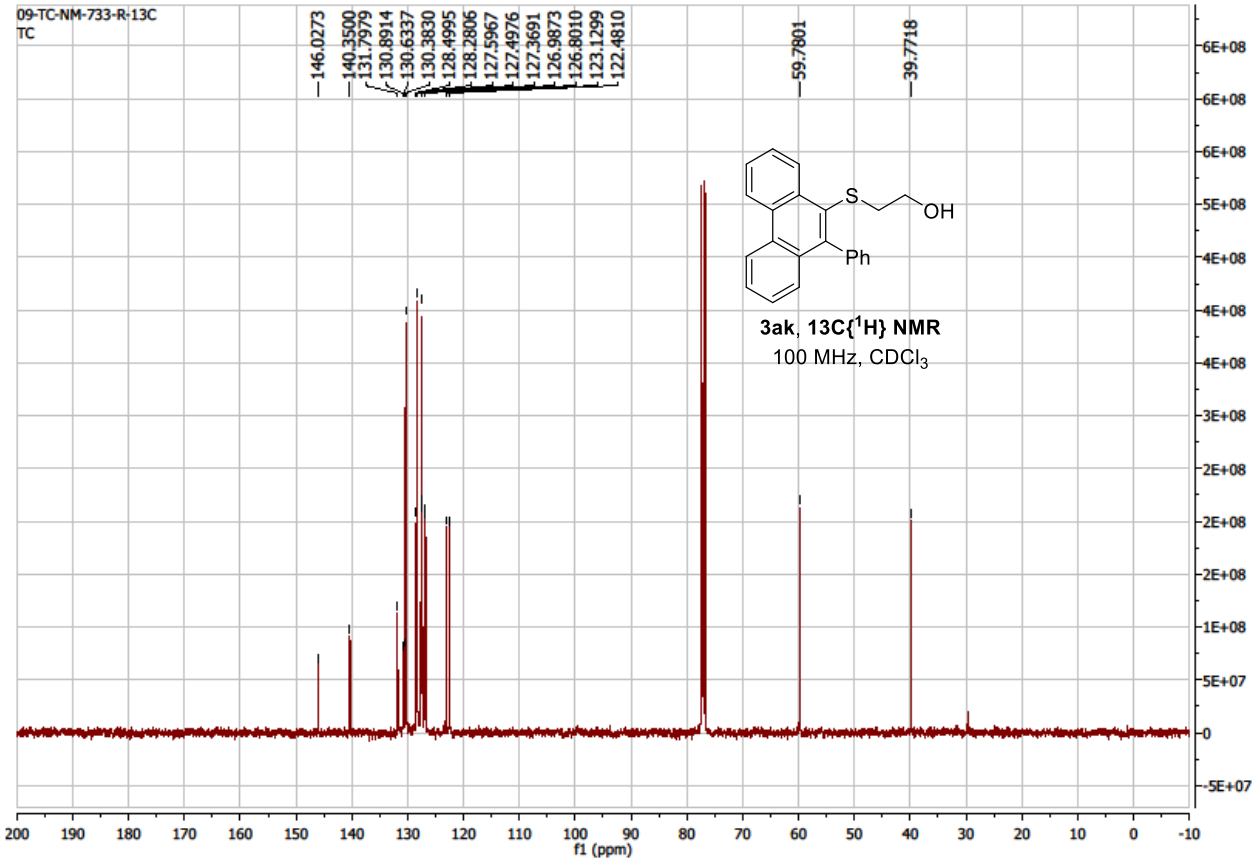
09-TC-NM-733-R-13C
TC
S
OH
Ph
3ak, 13C{^{1}H} NMR
100 MHz, $CDCl_3$
f1 (ppm)

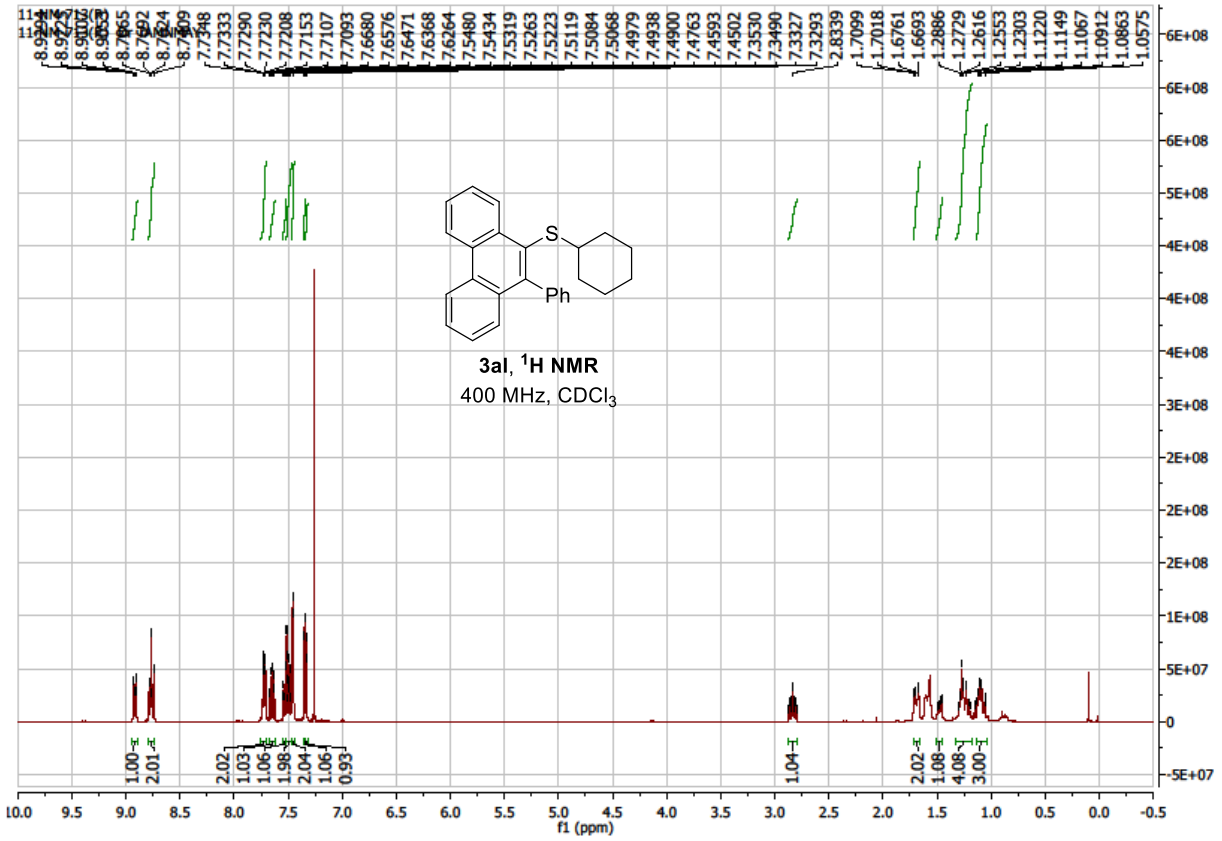
S
Ph
3al, ^{1}H NMR
400 MHz, $CDCl_3$
f1 (ppm)

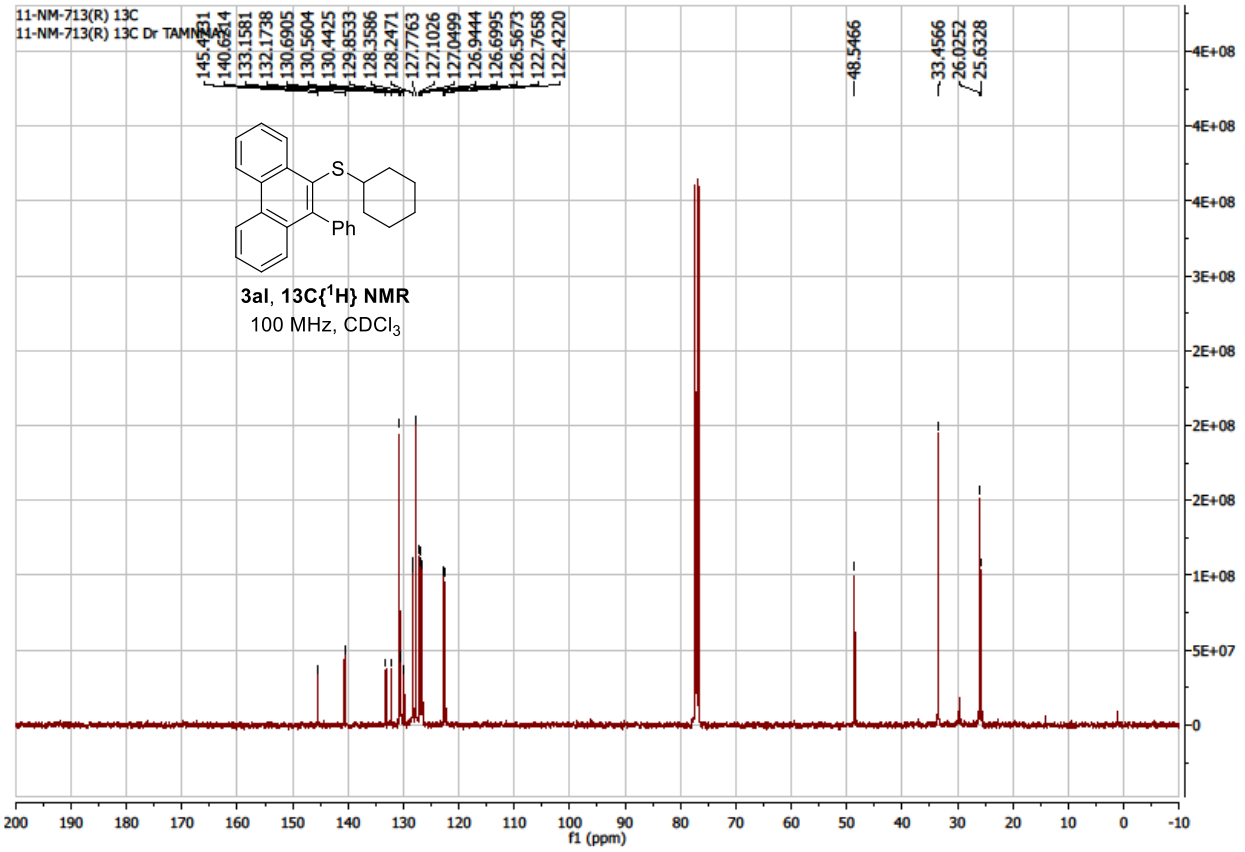
11-NM-713(R) 13C
11-NM-713(R) 13C Dr TAMNNA
S
Ph
3al, 13C{^{1}H} NMR
100 MHz, $CDCl_3$
f1 (ppm)

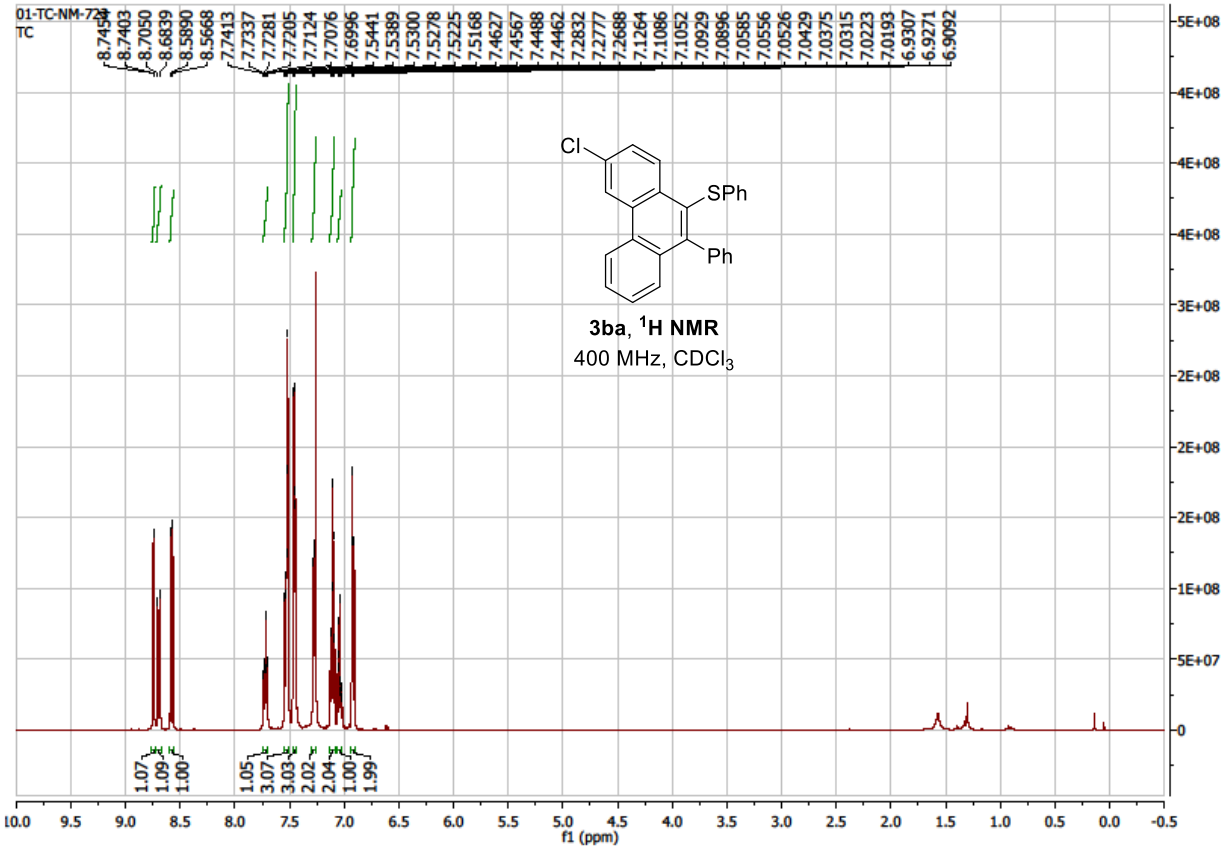
01-TC-NM-723
TC
Cl
SPh
Ph
3ba, 1H NMR
400 MHz, CDCl3
f1 (ppm)

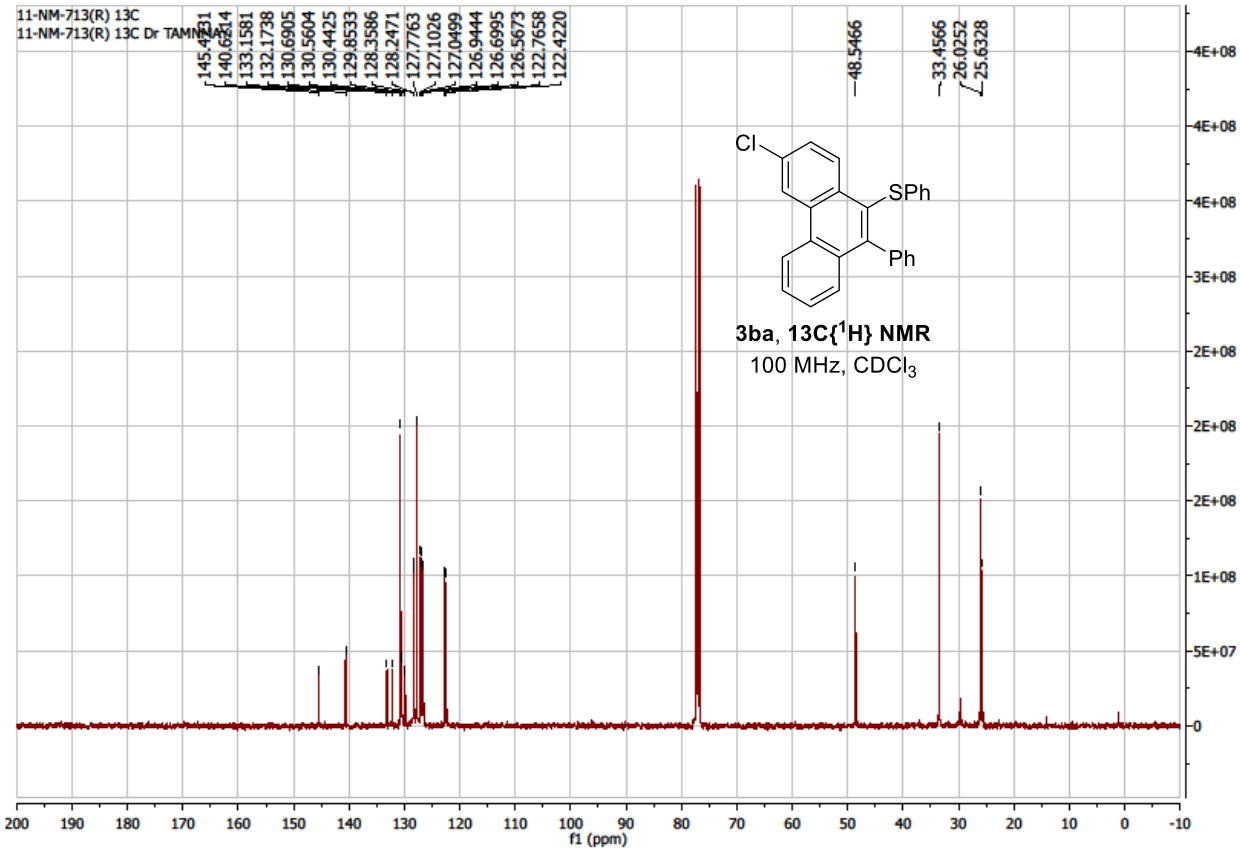
11-NM-713(R) 13C
11-NM-713(R) 13C Dr TAMNA
Cl
SPh
Ph
3ba, 13C{1H} NMR
100 MHz, CDCl3
f1 (ppm)

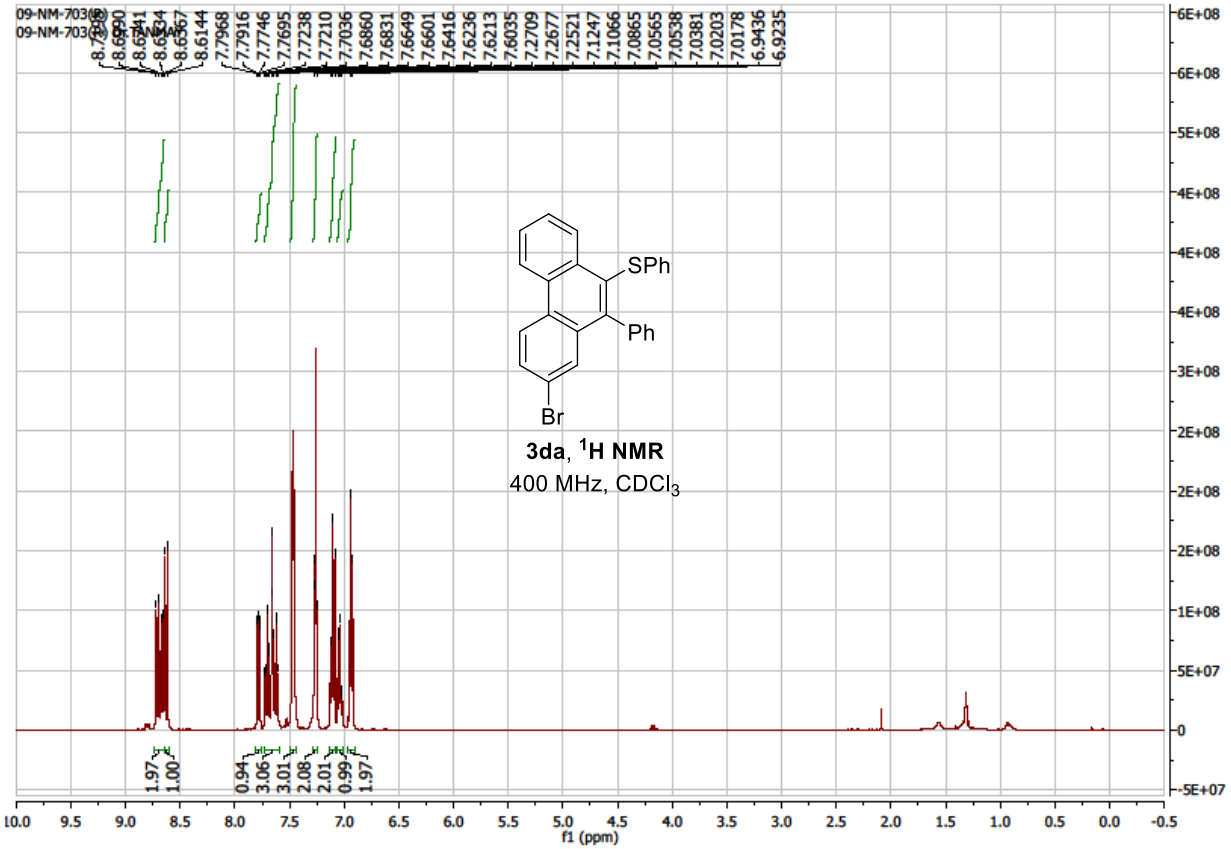
SPh
Ph
Br
3da, ^{1}H NMR
400 MHz, $CDCl_3$
f1 (ppm)

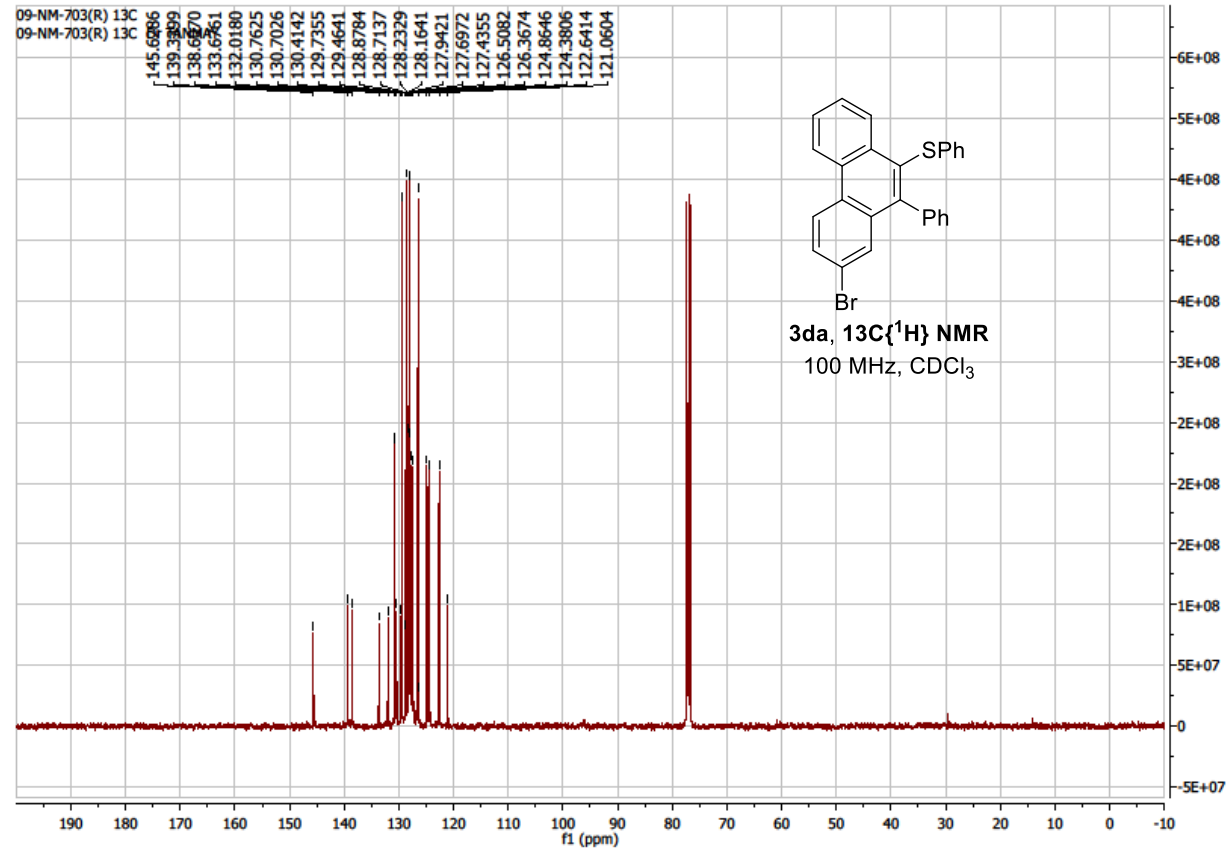
SPh
Ph
Br
3da, 13C{^{1}H} NMR
100 MHz, $CDCl_3$
f1 (ppm)

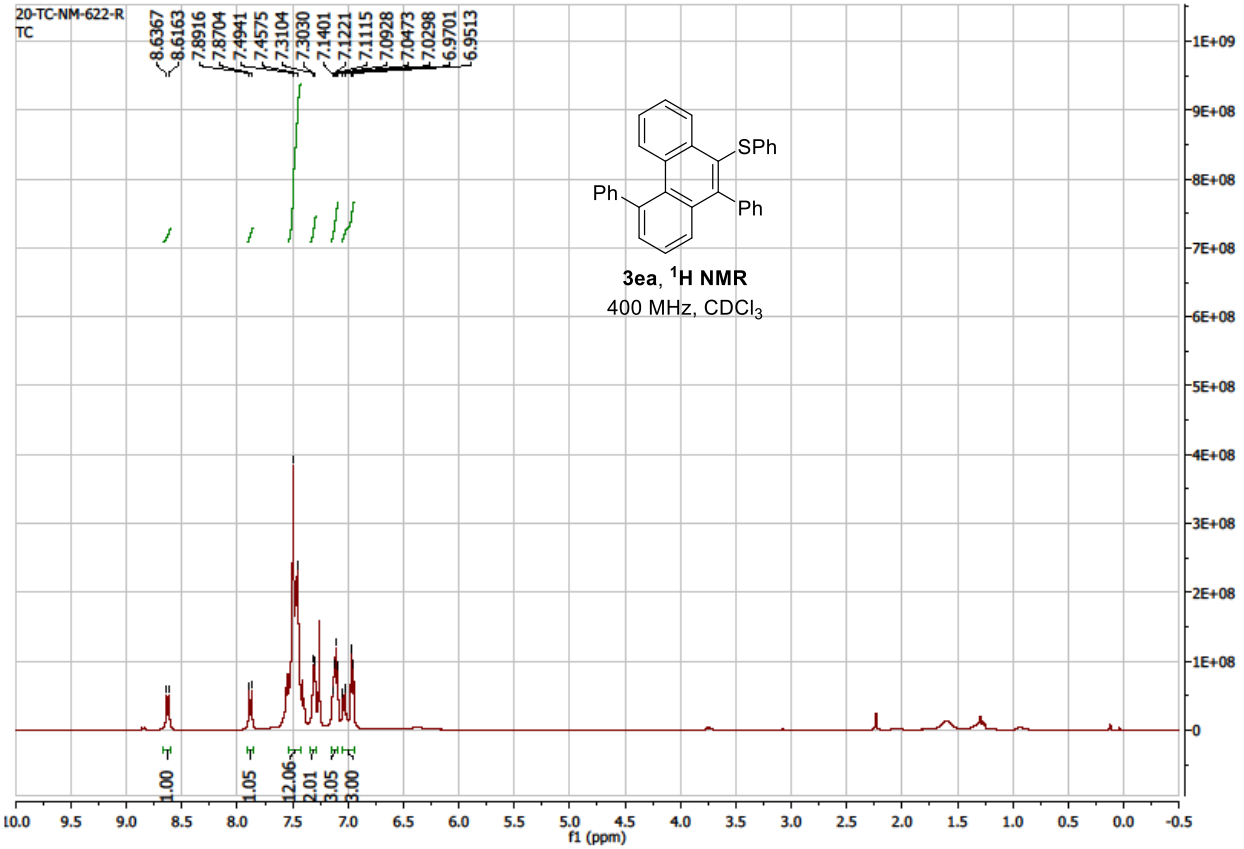
20-TC-NM-622-R
TC
8.6367
8.6163
7.8916
7.8704
7.4941
7.4575
7.3104
7.3030
7.1401
7.1221
7.1115
7.0928
7.0473
7.0298
6.9701
6.9513
SPh
Ph
Ph
3ea, 1H NMR
400 MHz, CDCl3
1.00
1.05
12.06
2.01
3.05
3.00
f1 (ppm)

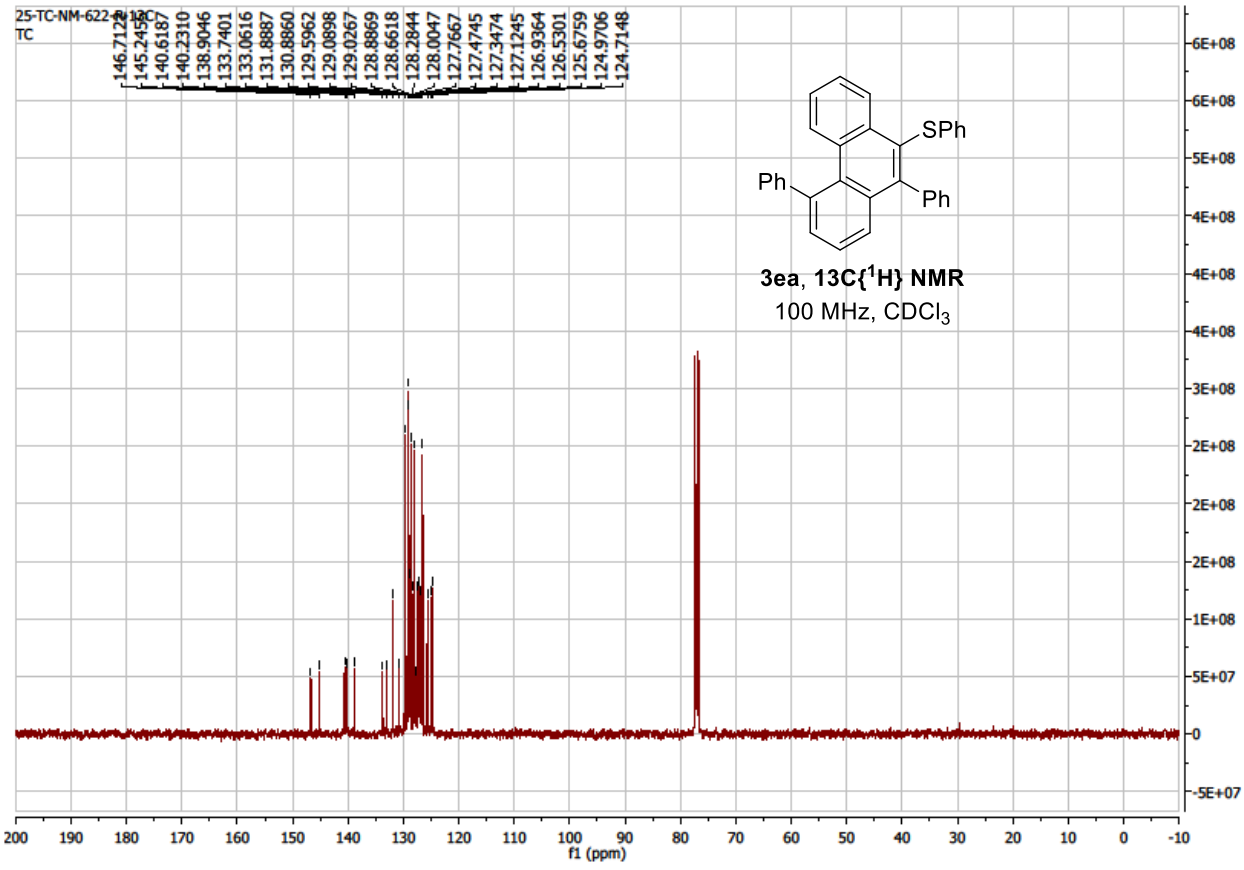
25-TC-NM-622-R 13C
TC
146.7128
145.2455
140.6187
140.2310
138.9046
133.7401
133.0616
131.8887
130.8860
129.5962
129.0898
129.0267
128.8869
128.6618
128.2844
128.0047
127.7667
127.4745
127.3474
127.1245
126.9364
126.5301
125.6759
124.9706
124.7148
SPh
Ph
Ph
3ea, 13C{1H} NMR
100 MHz, CDCl3
f1 (ppm)

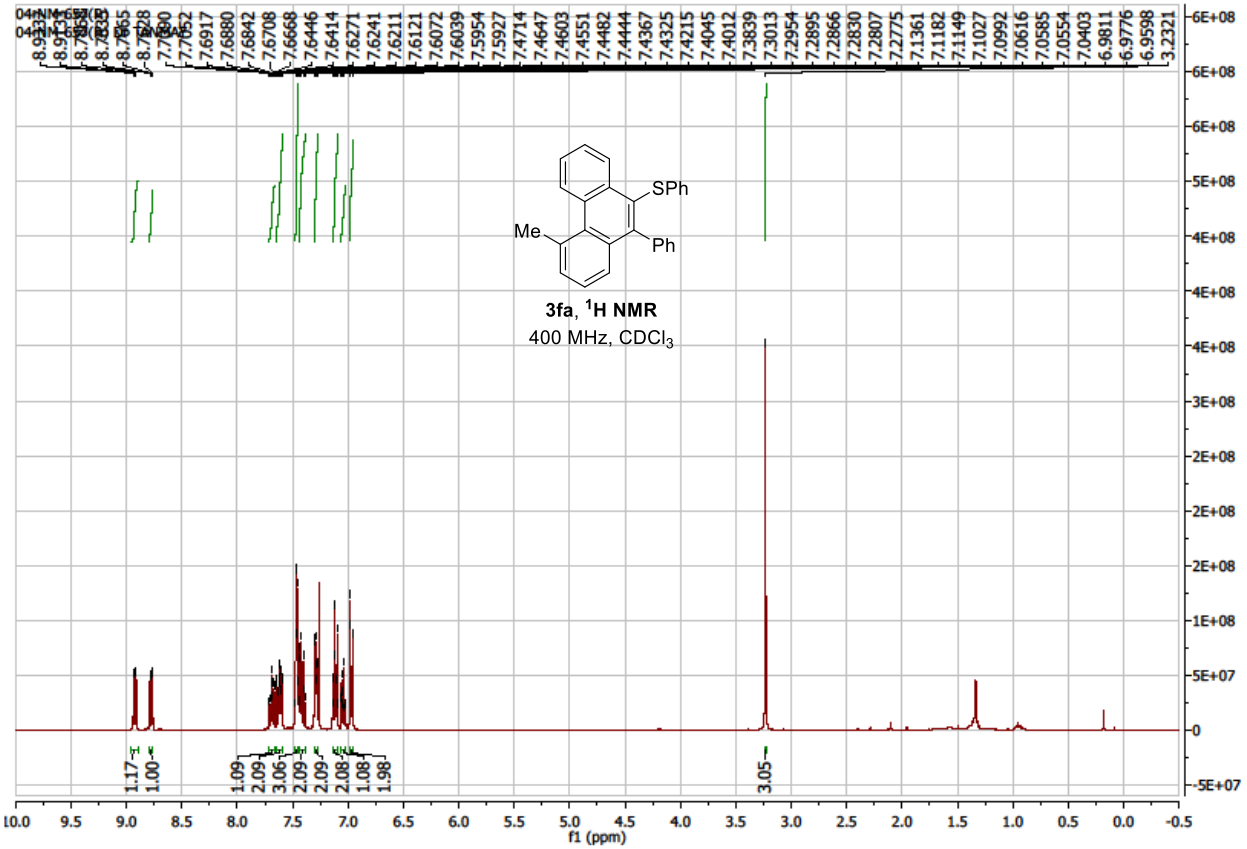
SPh
Me
Ph
3fa, ^{1}H NMR
400 MHz, $CDCl_3$
f1 (ppm)

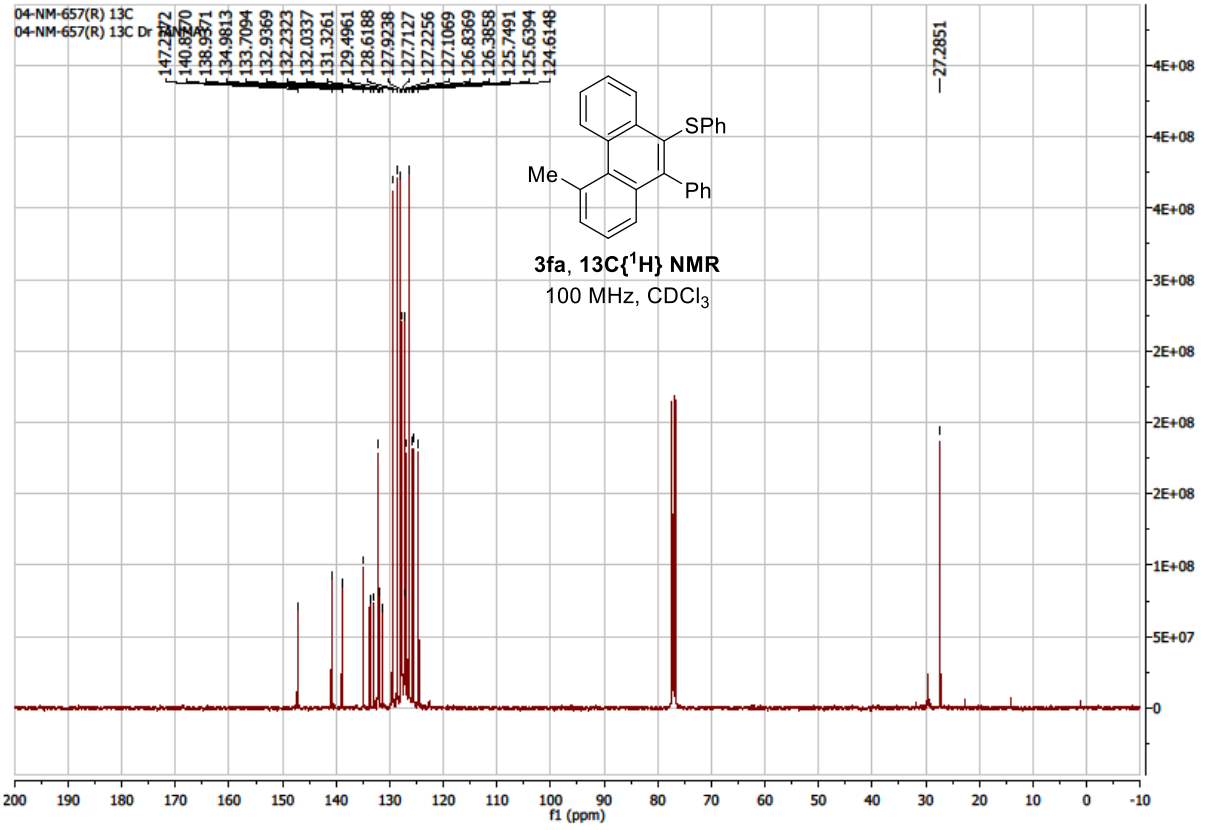
04-NM-657(R) 13C
SPh
Me
Ph
3fa, 13C{^{1}H} NMR
100 MHz, $CDCl_3$
f1 (ppm)

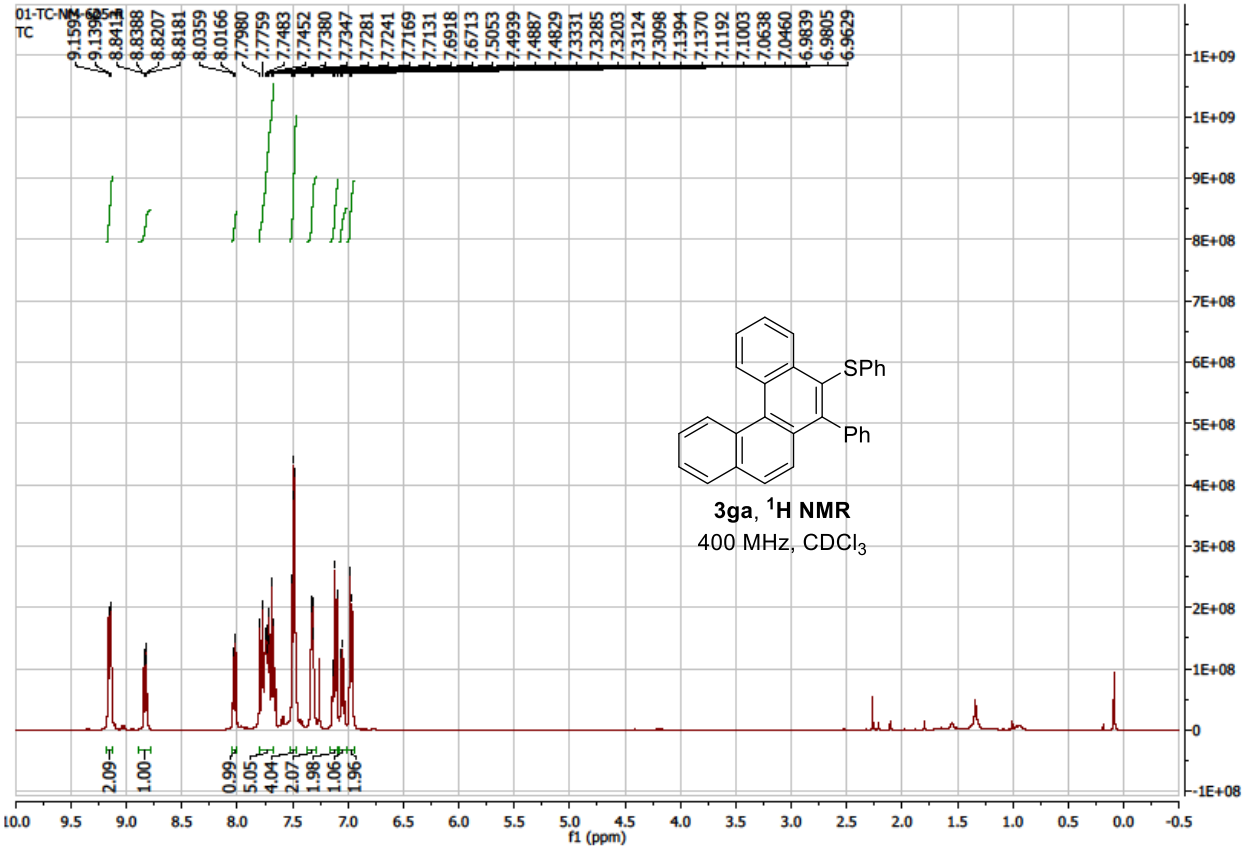
SPh
Ph
3ga, ^{1}H NMR
400 MHz, $CDCl_3$
f1 (ppm)

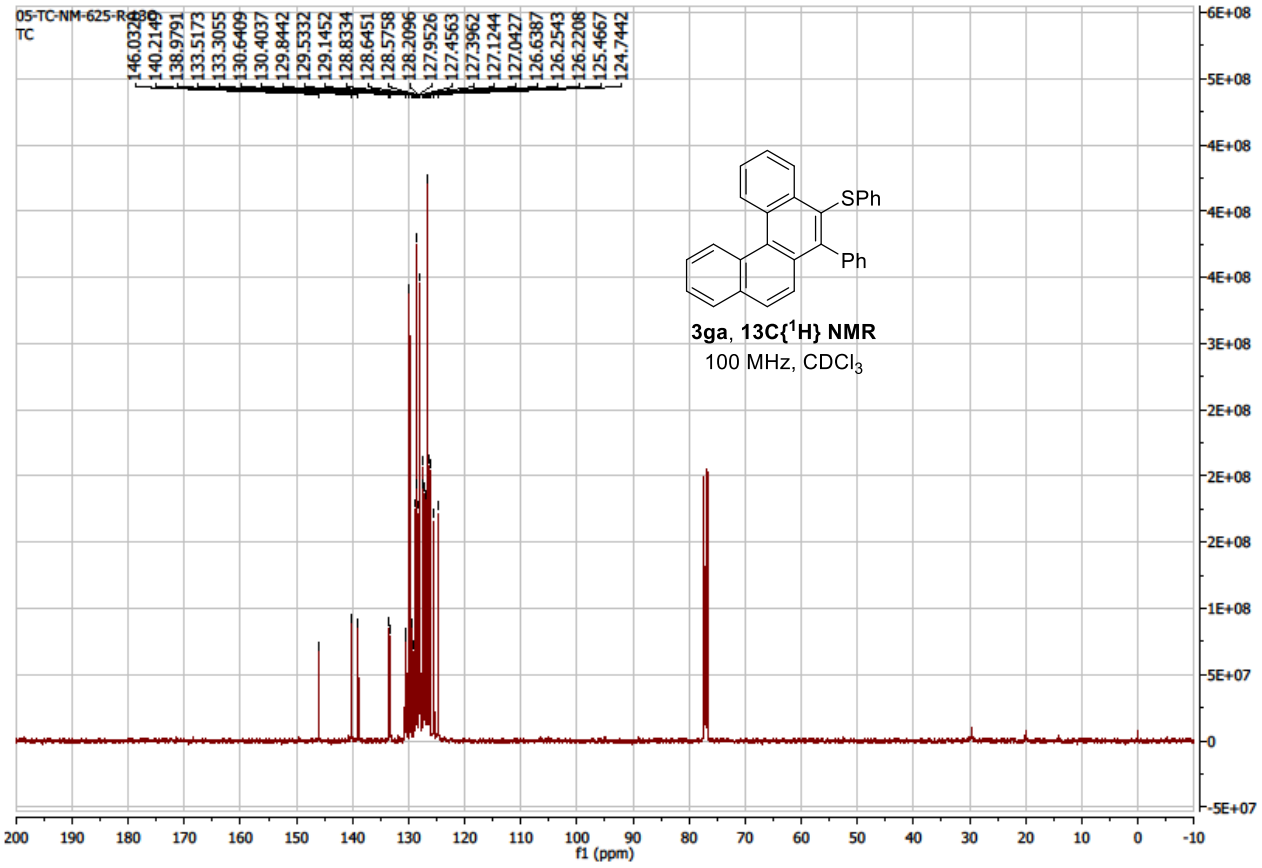
SPh
Ph
3ga, 13C{^{1}H} NMR
100 MHz, $CDCl_3$
f1 (ppm)

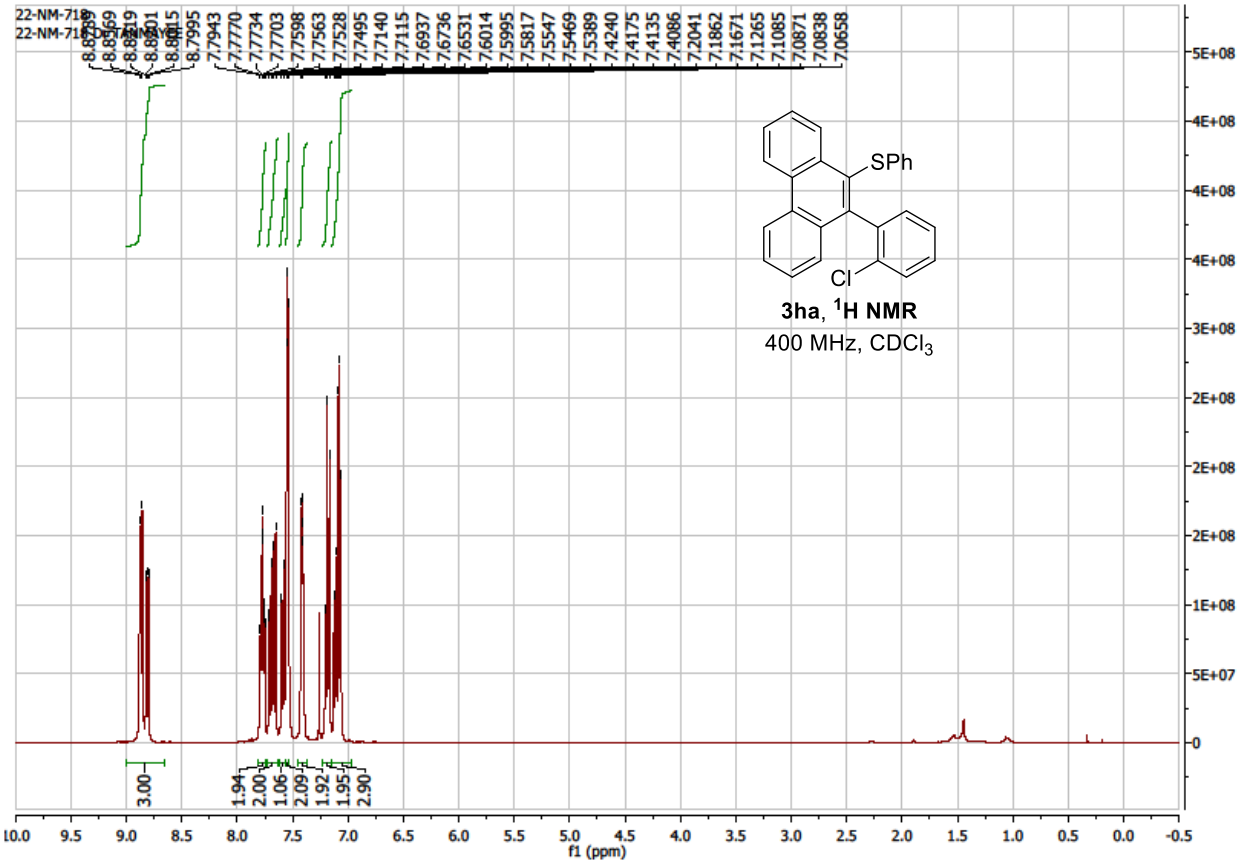
SPh
Cl
3ha, ^{1}H NMR
400 MHz, $CDCl_3$
f1 (ppm)

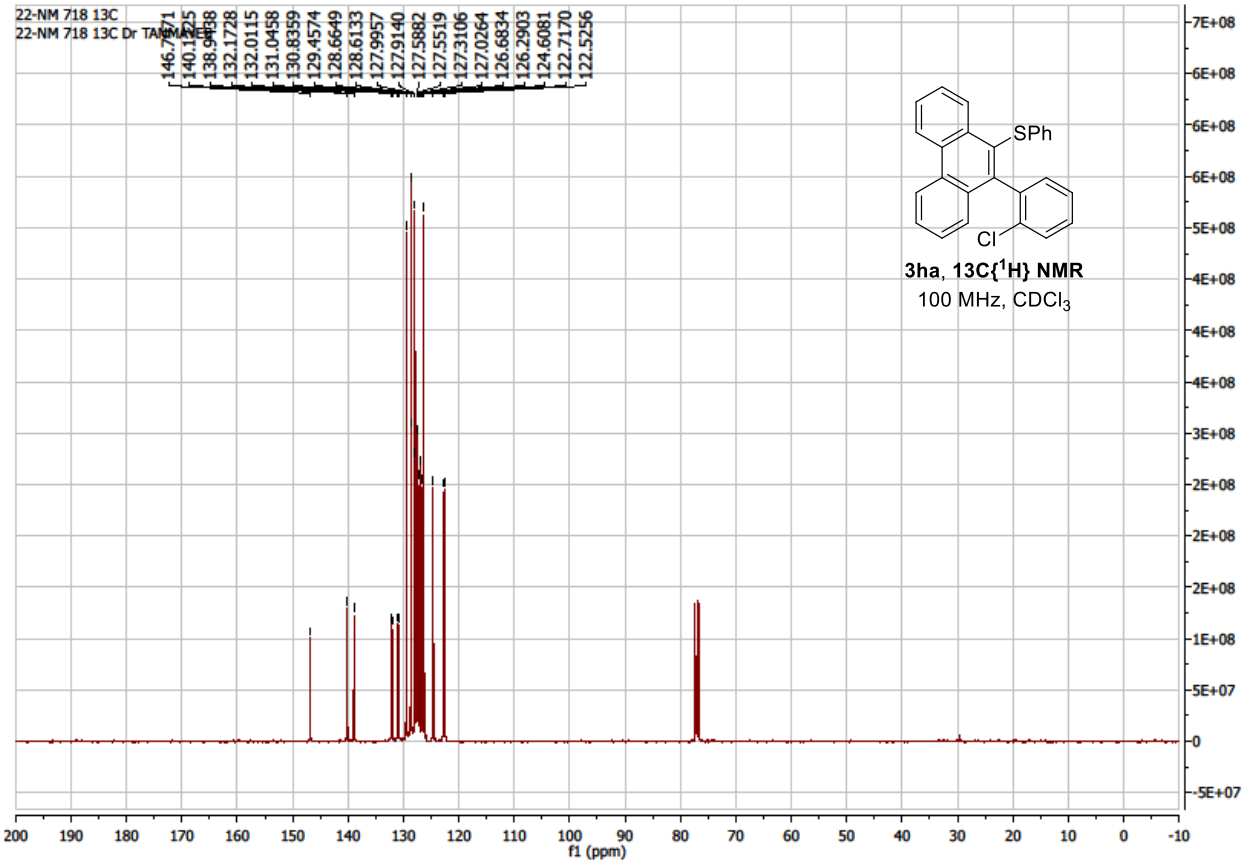
SPh
Cl
3ha, 13C{^{1}H} NMR
100 MHz, $CDCl_3$
f1 (ppm)

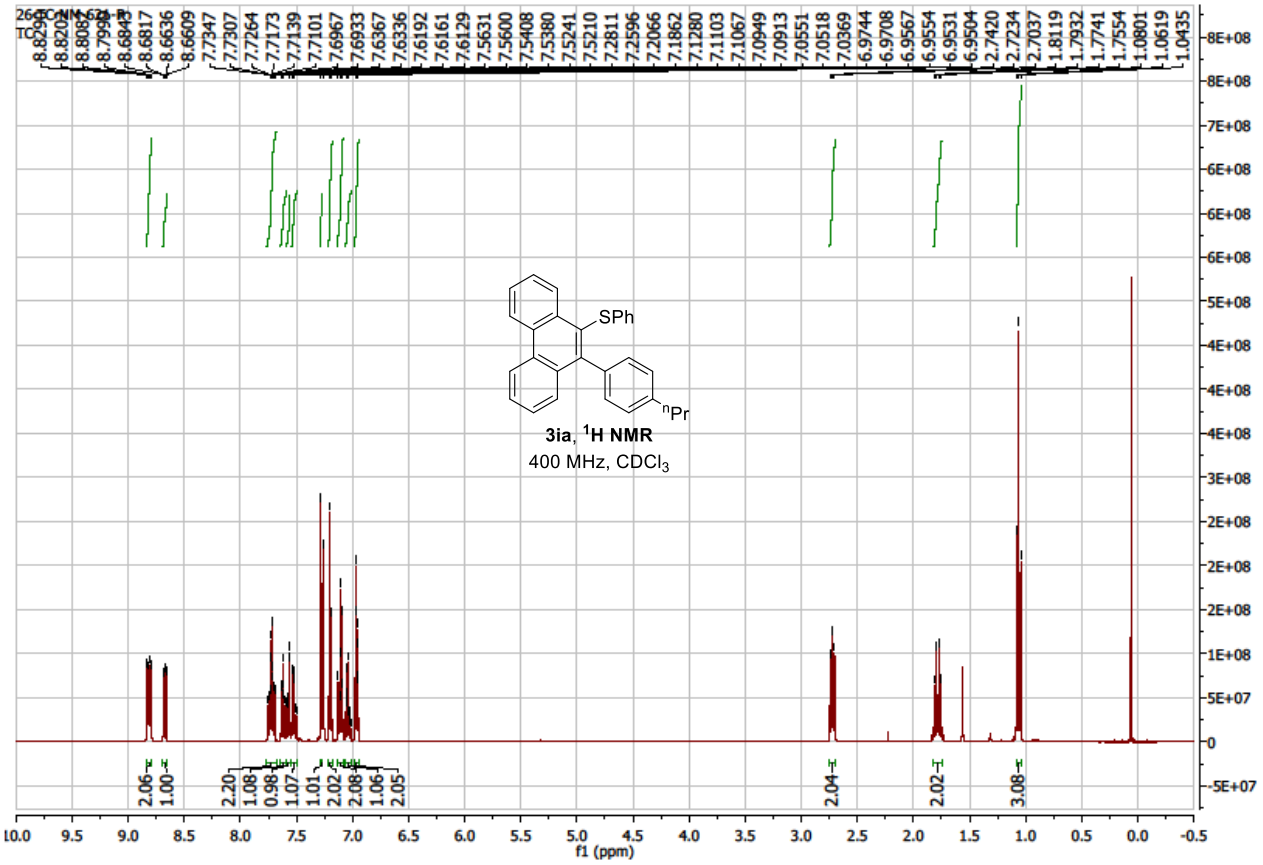
SPh
nPr
3ia, 1H NMR
400 MHz, CDCl3
f1 (ppm)

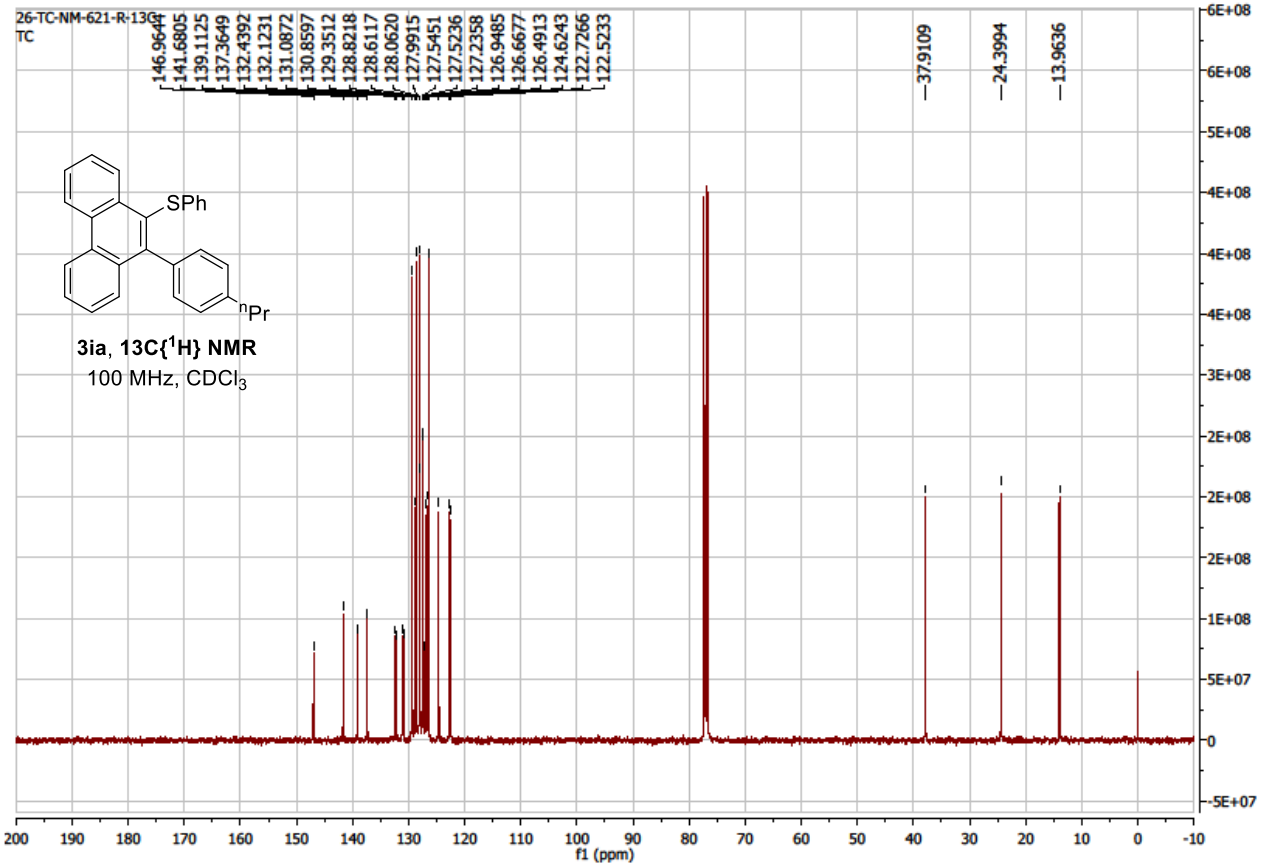
SPh
nPr
3ia, 13C{1H} NMR
100 MHz, CDCl3
f1 (ppm)

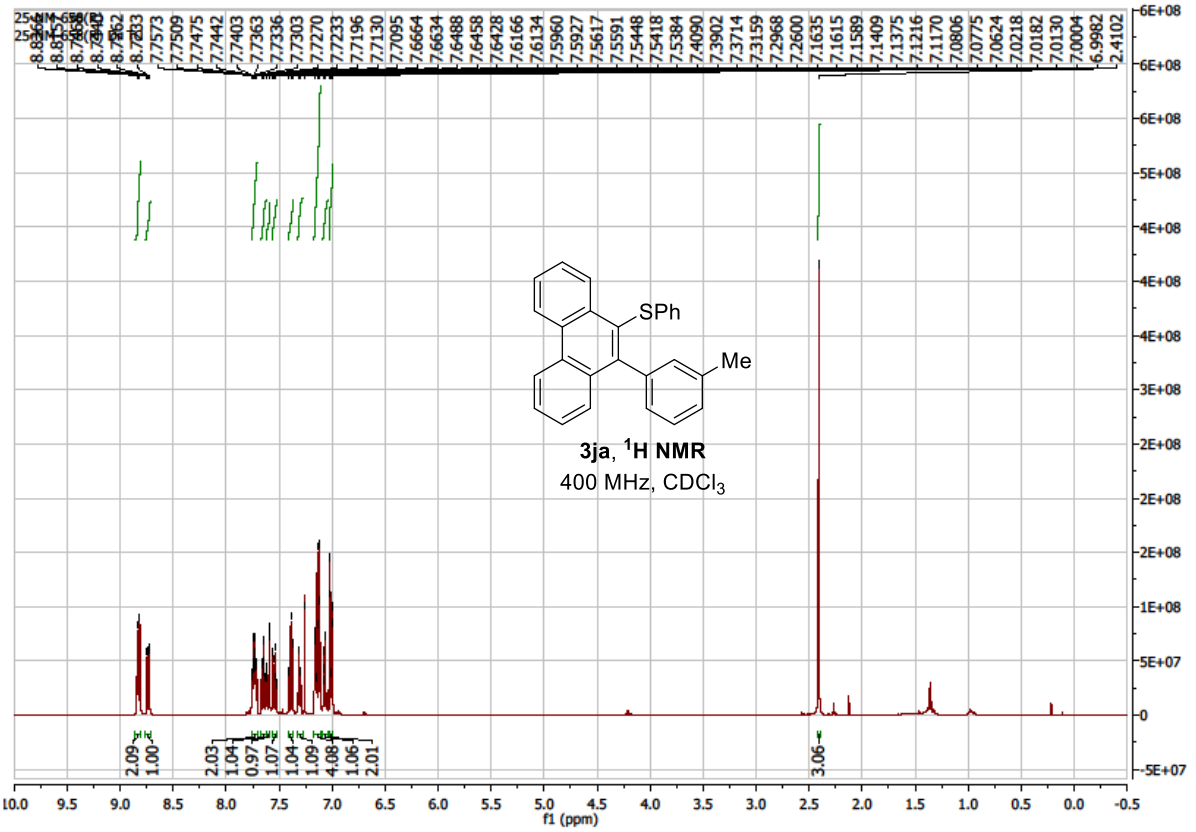
SPh
Me
3ja, ^{1}H NMR
400 MHz, $CDCl_3$
f1 (ppm)

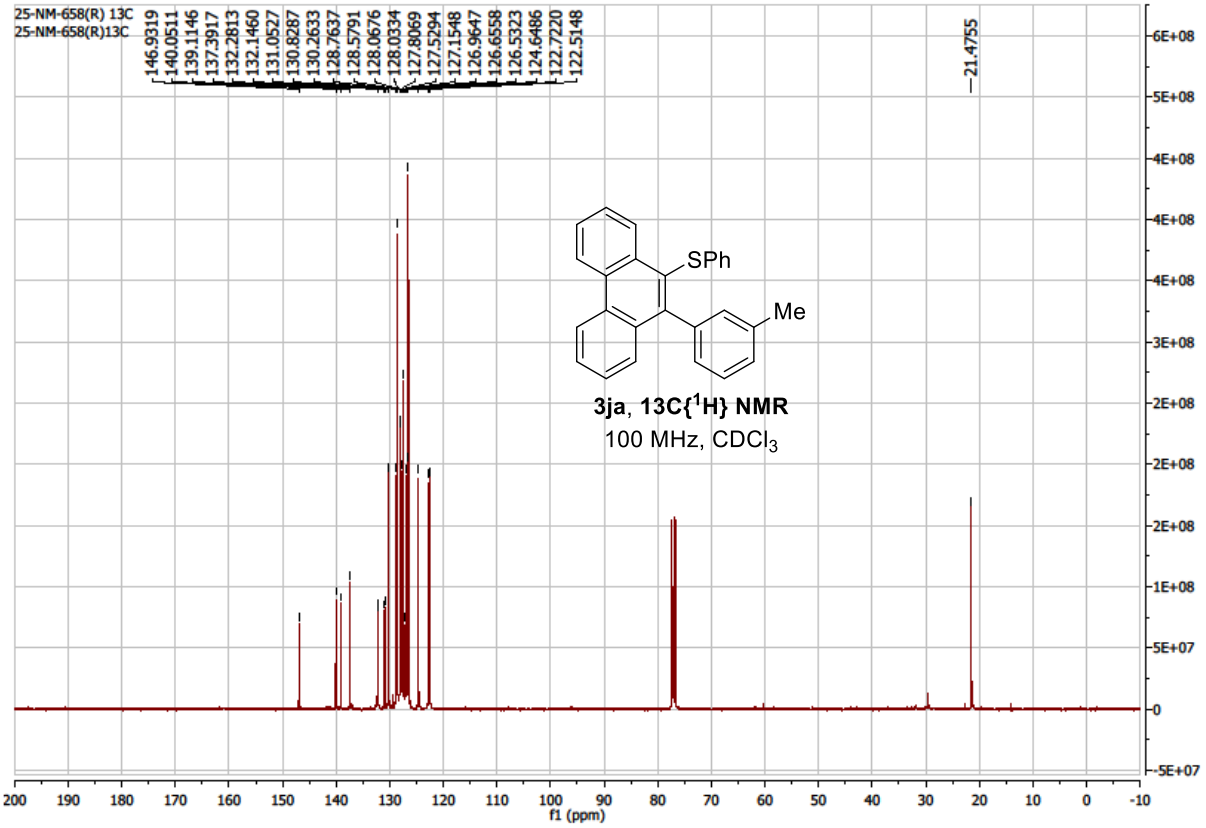
SPh
Me
3ja, 13C{^{1}H} NMR
100 MHz, $CDCl_3$
f1 (ppm)

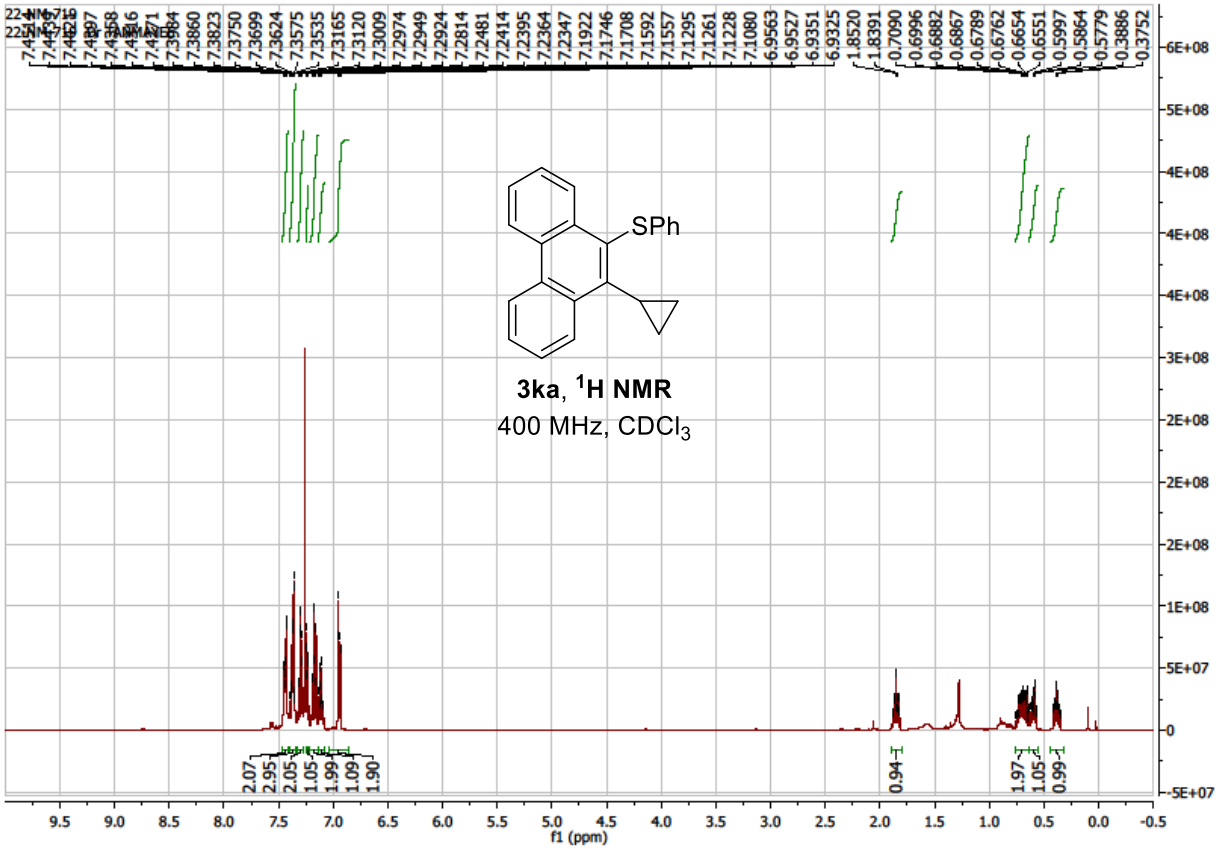
SPh
3ka, 1H NMR
400 MHz, CDCl3
f1 (ppm)

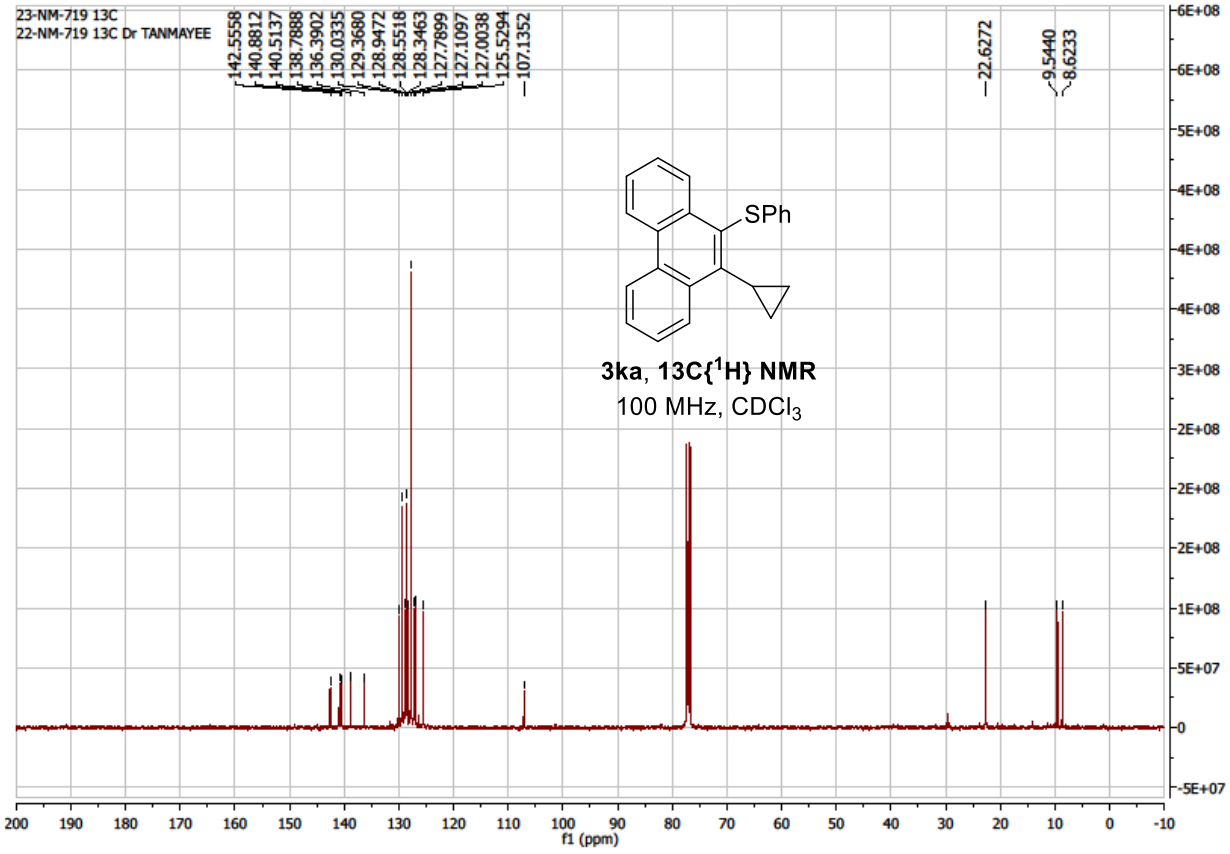
23-NM-719 13C
22-NM-719 13C Dr TANMAYEE
SPh
3ka, 13C{1H} NMR
100 MHz, CDCl3
f1 (ppm)

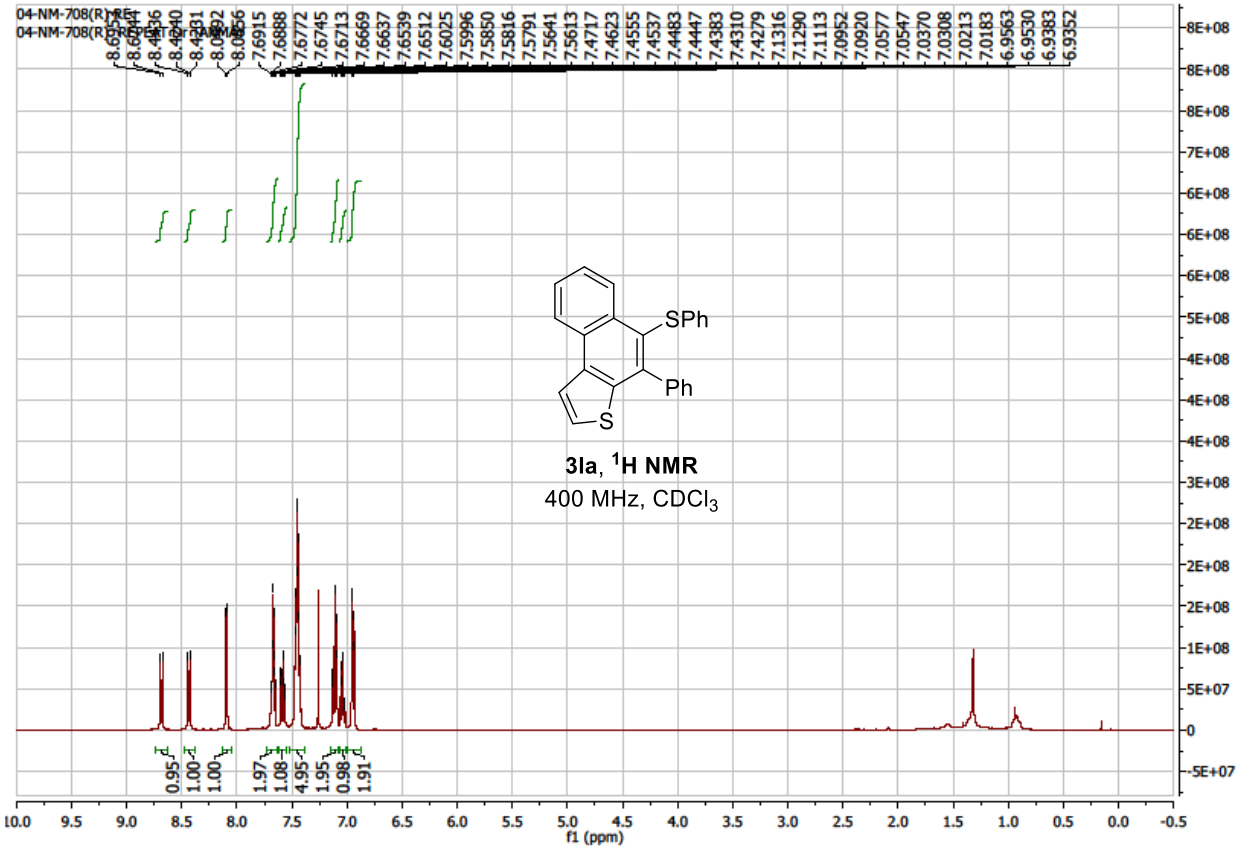
SPh
Ph
S
3la, ^{1}H NMR
400 MHz, $CDCl_3$
f1 (ppm)

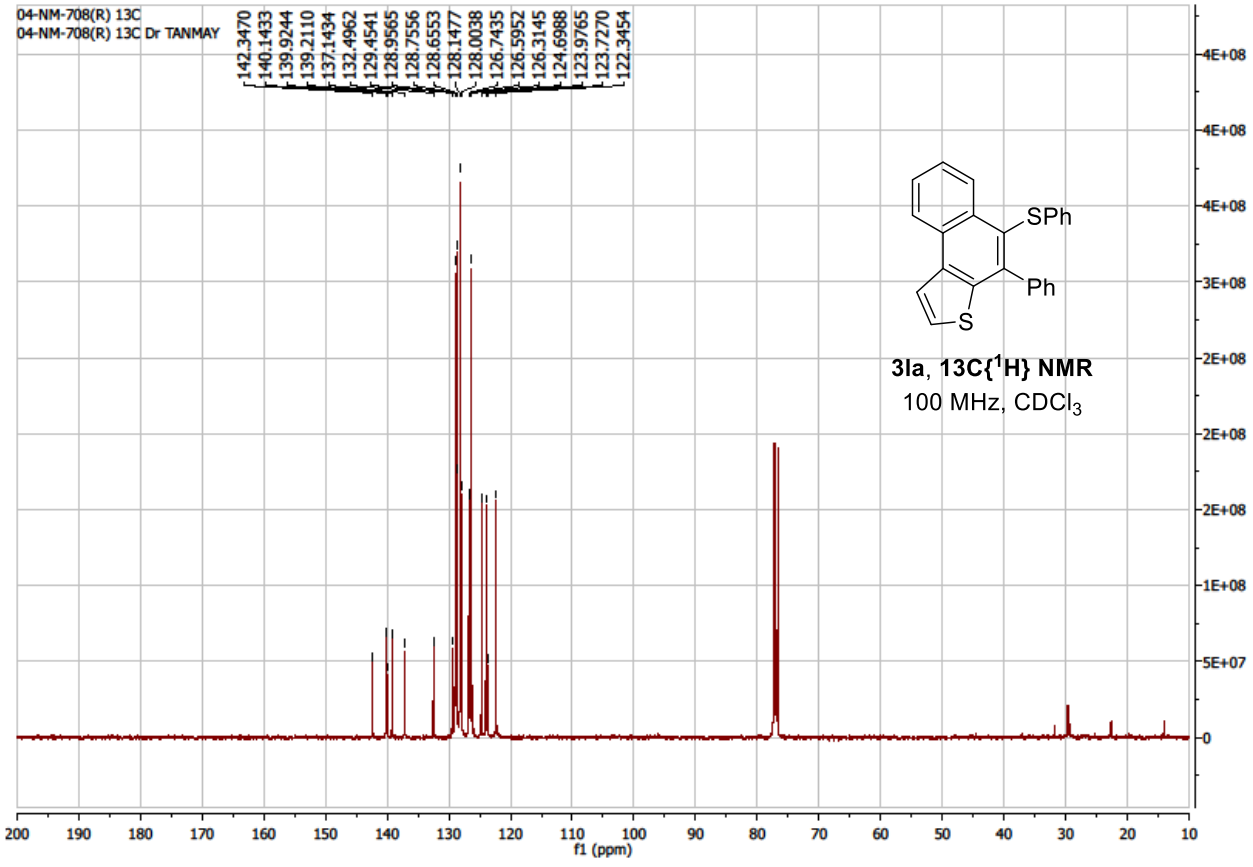
04-NM-708(R) 13C
04-NM-708(R) 13C Dr TANMAY
SPh
Ph
S
3la, 13C{^{1}H} NMR
100 MHz, $CDCl_3$
f1 (ppm)

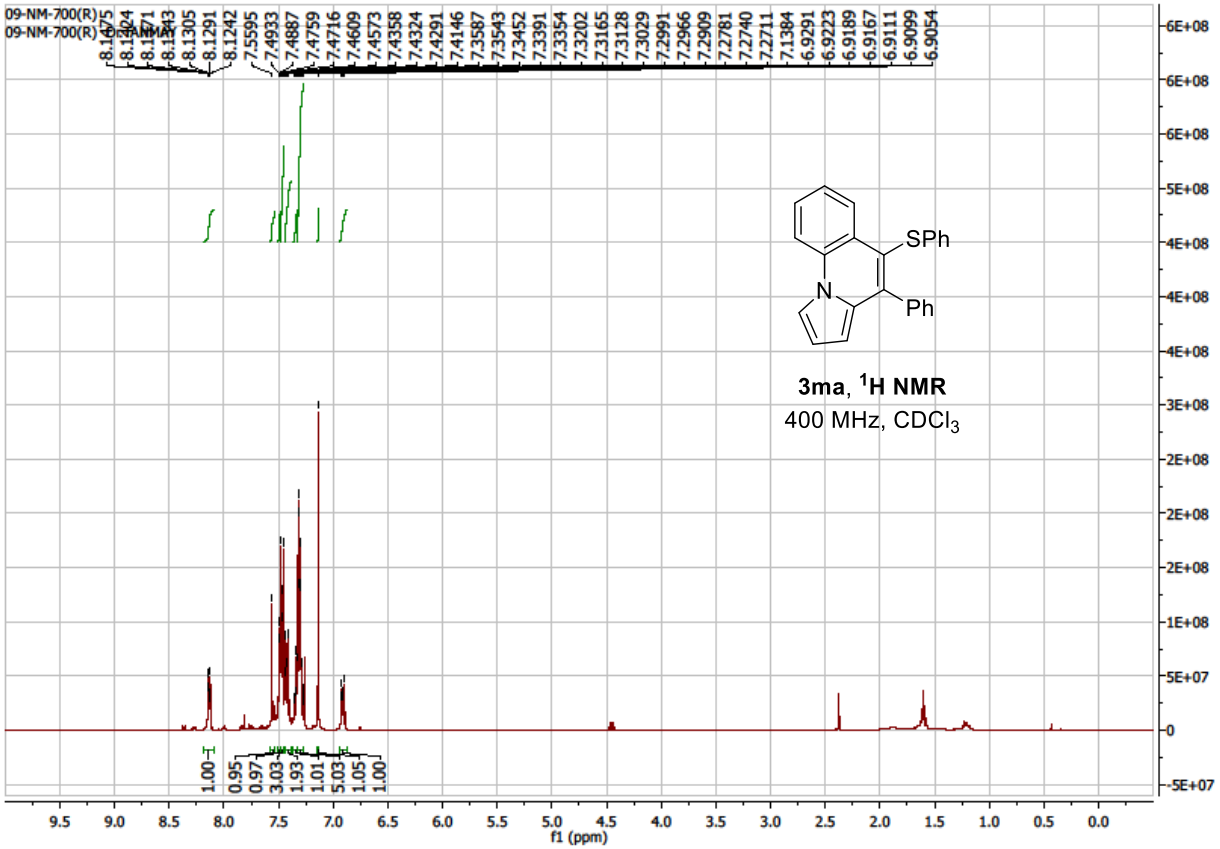
SPh
N
Ph
3ma, ^{1}H NMR
400 MHz, $CDCl_3$
f1 (ppm)

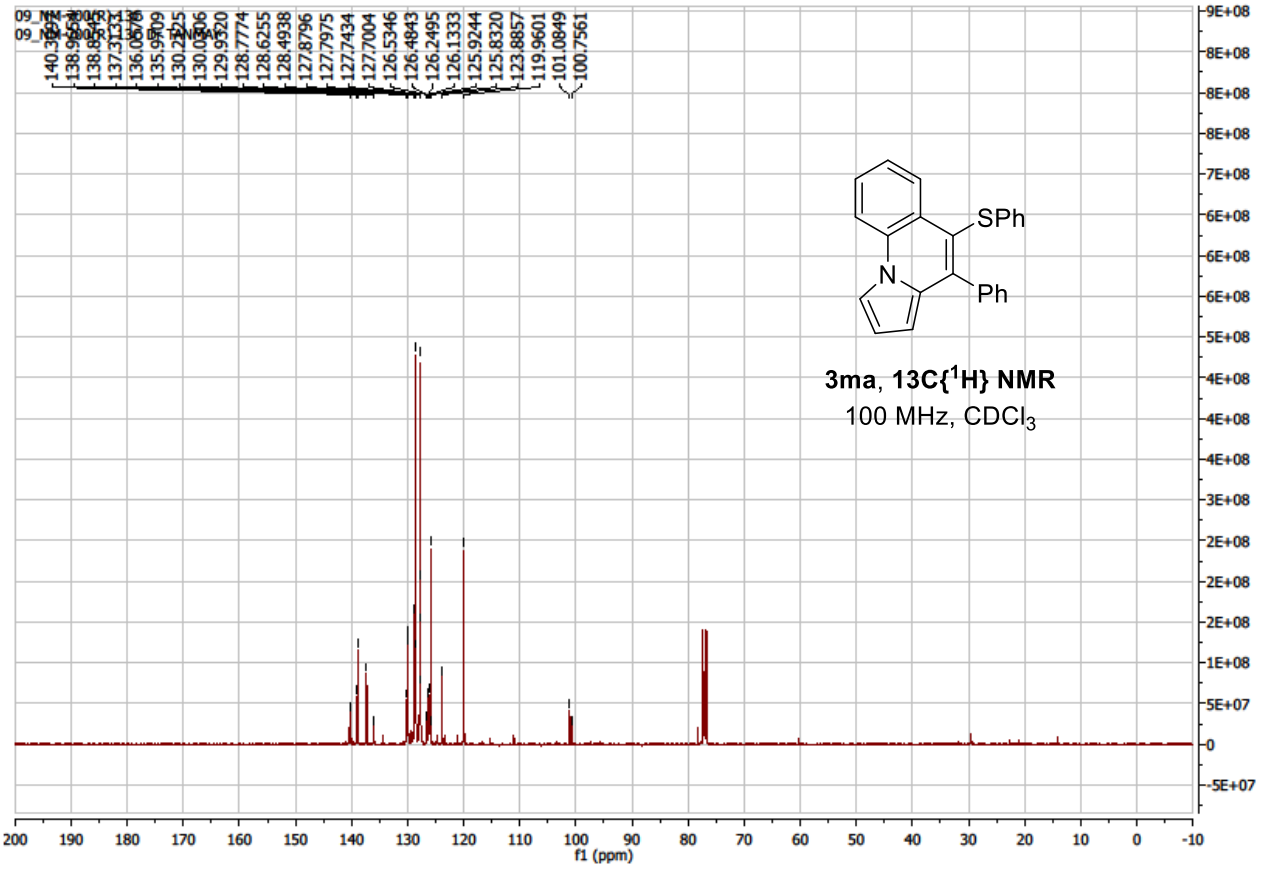
SPh
N
Ph
3ma, 13C{^{1}H} NMR
100 MHz, $CDCl_3$
f1 (ppm)

Green Chemistry

ROYAL SOCIETY OF CHEMISTRY

PAPER

View Article Online
View Journal | View Issue

Cite this: *Green Chem.*, 2021, **23**, 10006

Iodine-catalyzed, highly atom-economic synthesis of 9-sulfenylphenanthrenes and polycyclic heteroaromatics in water†

Nilanjana Mukherjee and Tanmay Chatterjee *

Received 9th September 2021,
Accepted 11th November 2021

DOI: 10.1039/d1gc03305k

rsc.li/greenchem

A highly atom-economical and green synthetic method is developed for the oxidative thiolative annulation of 2-alkynyl biaryls with disulfides to synthesize a wide variety of 9-sulfenylphenanthrenes and polycyclic heteroaromatics in water. The transformation requires only a couple of inexpensive reagents, *i.e.*, iodine as a catalyst and hydrogen peroxide (H_2O_2) as a green oxidant, to furnish the desired products in good to excellent yield. The notable advantages of this protocol over the previously developed synthetic methods are a metal-free, cost-effective, and highly atom economic (>90%) protocol, use of inexpensive reagents as the catalyst and green oxidant, use of water as the reaction medium, very high (>95%) carbon efficiency (water as the major waste), broad substrate scope, high functional group tolerance, high yields of products up to 95%, straight-forward scale-up process upto 10 g scale and significantly, low *E*-factor (2.25) and high EcoScale score (67).

Introduction

Organosulfides or sulfur-containing molecules are ubiquitous in numerous pharmaceuticals,[1] natural products,[2] and valuable materials.[3] Hence, several synthetic strategies and techniques have been developed to construct a C–S bond to synthesize valuable organosulfides.[4] Among them, transition-metal-catalyzed cross-coupling reaction is the most widely employed strategy and a powerful tool for constructing organosulfides.[5] However, those methods suffer from several limitations such as the requirement of highly expensive, toxic and air-sensitive transition-metal catalyst, ligand and reagents, harsh reaction conditions, requirement of pre-functionalized starting materials, low atom-economy, generation of toxic waste *etc*. which are not desirable in the context of green chemistry. Hence the development of metal-free synthetic methodologies without using any toxic/hazardous reagents or solvent is always desirable.

On the other hand, phenanthrenes are one of the important polycyclic aromatic hydrocarbons (PAHs) possessing plenty of biological activities such as anticancer,[6] antiviral,[7] antimicrobial,[8] and anti-HIV[9] activity. Consequently, phenanthrene core moiety is found in numerous biologically active molecules, including pharmaceuticals[6–9] and natural products.[10] Moreover, they also exhibit interesting optical and electronic properties and are thus used to develop various valuable materials such as solar cells[11] and organic field-effect transistors.[12] Owing to their broad applications in a diverse area, several synthetic strategies, primarily based on transition-metal-catalyzed/mediated reactions, have been developed so far to construct a phenanthrene core.[13,14]

However, a very few strategies are focused on the synthesis of 9-sulfenylphenanthrenes,[15,16] a much more potential class of PAHs considering the known properties or activities of phenanthrenes, organosulfides and also the easy synthetic diversification of 9-sulfenylphenanthrenes to their corresponding potential derivatives, *i.e.*, sulfoxides and sulfones.[16] Only a couple of general synthetic strategies have been found in the literature to synthesize 9-sulfenylphenanthrenes (Scheme 1A and B). The Qian and Zhang group first disclosed a general synthetic strategy for synthesizing 9-sulfenylphenanthrenes from 2-alkynyl biaryls and disulfides by using 10 mol% Pd $(OAc)_2$ as a catalyst, 2 equiv. iodine as a reagent, and THF as solvent at 80 °C (Scheme 1A).[15] Despite good substrate scope, this method suffers from several serious limitations such as the requirement of highly expensive and toxic rare-earth transition-metal catalyst in sub-stoichiometric amounts, use of excess iodine, low atom economy of the reaction since only half equivalent of disulfide was utilized and the other half equivalent was wasted. Recently, our group reported a transition-metal-free synthetic strategy for the synthesis of 9-sulfe-

Department of Chemistry, Birla Institute of Technology and Science, Pilani, Hyderabad Campus, Jawahar Nagar, Hyderabad – 500078, India.
E-mail: tanmay@hyderabad.bits-pilani.ac.in

† Electronic supplementary information (ESI) available: Experimental procedure, calculation of green parameters, analytical data, and NMR spectra of the synthesized compounds. See DOI: 10.1039/d1gc03305k

Chapter 4

SECTION – I

Synthesis of Organoselenides by Selenylative Annulation/Cyclization Reactions

4.1.1. Introduction.

Organoselenides, in particular, unsymmetrical diaryl selenides are prevalent in numerous biologically active molecules, including pharmacologically active molecules, for example, thyroxin receptor (TR) or glucocorticoid receptor (GR) inhibitor, 5-lipoxygenase (LOX) inhibitor, human breast cancer cell growth inhibitor, antitumor agent or retinoic acid (RAR) agonist (Fig 4.1.1).[1] The electron donor, halogen-bond, and hydrogen-bond acceptor attributes of the selenium atom help an organoselenide to interact and alter the characteristics of enzymes' active sites. Thus, incorporating a selenium atom into an organic molecule often significantly enhances its pharmacological and physical properties.[2]

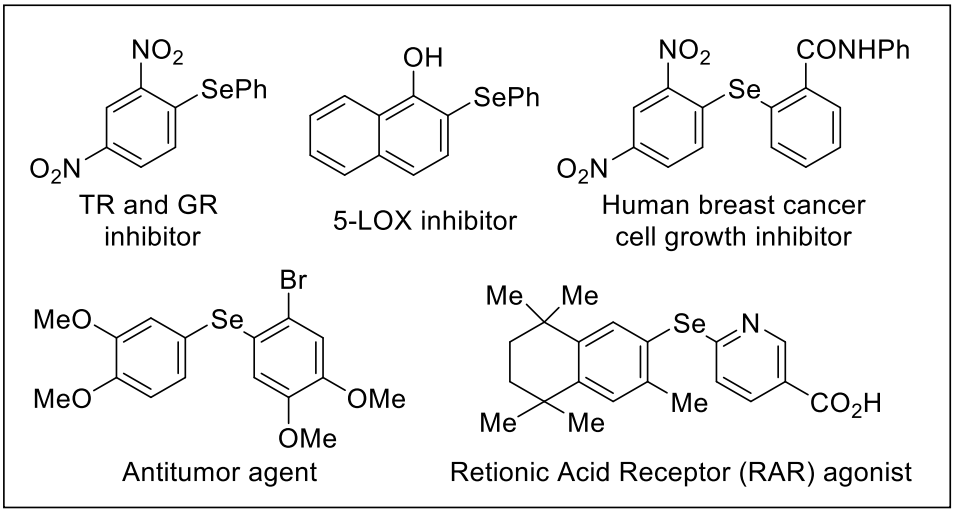

Figure 4.1.1. Some Examples of Biologically Active Unsymmetrical Diaryl or Aryl-heteroaryl Selenides.

Owing to the importance of organoselenides, several synthetic strategies have been developed so far for the synthesis of this class of molecules.[3] Among them, selenylative carbannulation or hetero-annulation[4] is perhaps the most frequently employed strategy for the construction of selenium-incorporated carbocyclic or heterocyclic compounds. The state-of-art of this research is described below.

4.1.2. Review.

4.1.2.1. Iodine-Catalyzed Selenylative Annulation

In 2022, the Sun group disclosed an iodine-catalyzed cascade electrophilic selenylative cyclization of a diene (*N*-allyl-2-(1-phenylvinyl)-aniline) with diaryl diselenides in nitromethane as solvent at 40 ^{o}C for 10 h. The reaction proceeded *via* regioselective selenylation followed by 7-*exo*-trig cyclization for the synthesis of seleno-benzo[*b*]azepines (Scheme 4.1.1).[5] The scalability of the developed protocol was straight-forward and the synthetic utility was demonstrated by synthetic diversification of the product, seleno-benzo[*b*]azepines. Mechanistic studies revealed that the reaction proceeded through ionic pathway.

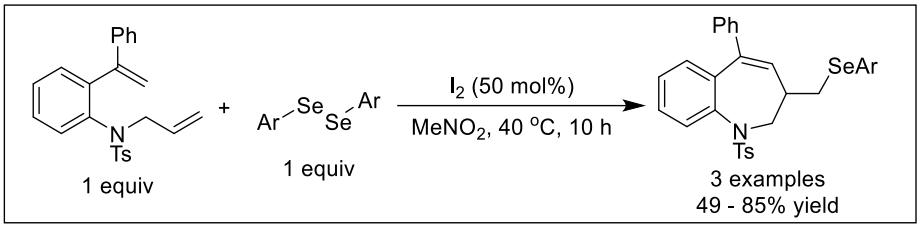

Scheme 4.1.1. Iodine-Catalyzed Electrophilic Selenylative Cyclization to Access Seleno-Benzo[*b*]azepines.

4.1.2.2. Selenylative Annulation in Water

In 2018, Roehrs and co-workers reported an unltrasound-promoted selenylative annulation of alkynols using diorganyl diselenides using oxone as an oxidant in water to synthesize a wide variety of 2-organoselanyl naphthalenes in moderate to excellent yield (Scheme 4.1.2).[6] The reaction proceeded *via* the oxidative electrophilic selenylative annulation of 2-organoselanyl naphthalenes.

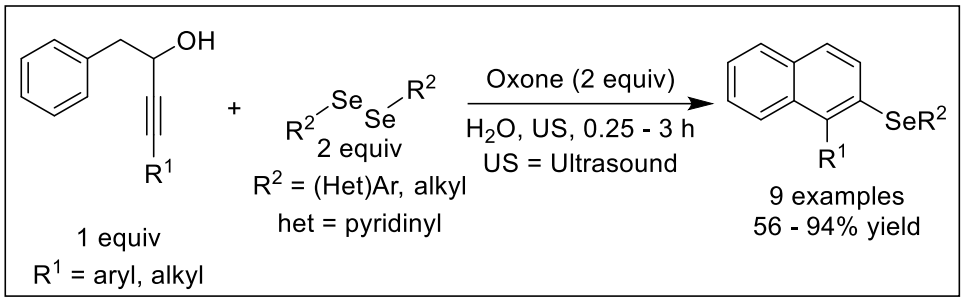

Scheme 4.1.2. Ultrasound-promoted Selenylative Annulation of 2-Organoselanyl naphthalenes.

4.1.2.3. Selenylative Annulation of Alkynes

In 2022, Volla *et al.* developed a highly regio- and diastereoselective cascade radical selenylative Giese cyclization of alkynyl cyclohexadienones using diaryl diselenides, aryl diazonium salts as aryl partners and DABSO as a benign SO_2 source and also a redox mediator *via* the formation of four new bonds *i.e.* C-Se, C-S, C-C, and C-H bonds for the synthesis of highly functionalized dihydrochromenones (Scheme 4.1.3).[7]

Scheme 4.1.3. Selenylative Cyclization for The Synthesis of Dihydrochromenones.

In 2021, the Zhu group disclosed a selenylative cyclization of 1,6-enynes with diaryl diselenides under visible-light irradiation in an inert atmosphere at room temperature (Scheme 4.1.4). [8] The reaction proceeded *via* a radical addition/ cyclization/ selenation sequence being initiated by the formation of selenyl radical followed by the atom transfer radical coupling (ATRC) process. Both the terminal and internal alkynes were suitable for this reaction.

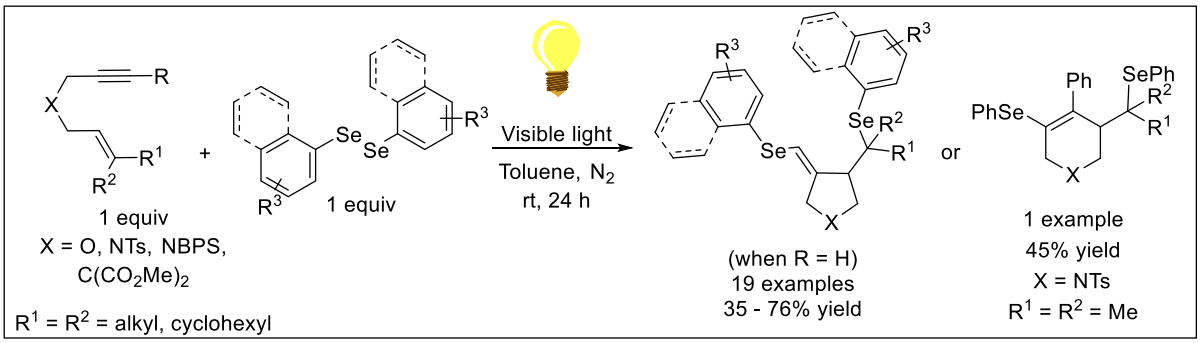

Scheme 4.1.4. Visible-light Mediated Di-arylselenylative Cyclization.

In 2020, the Ji group disclosed iron(III) chloride-promoted selenylative cyclization of *α,β*-alkynic tosylhydrazones using diselenides in DCE for 12 h at room temperature to afford a library of 4-(arylselanyl)-1*H*-pyrazole derivatives (Scheme 4.1.5). [9] The reaction was a one-pot process that involved the formation of C-N and C-Se bonds.

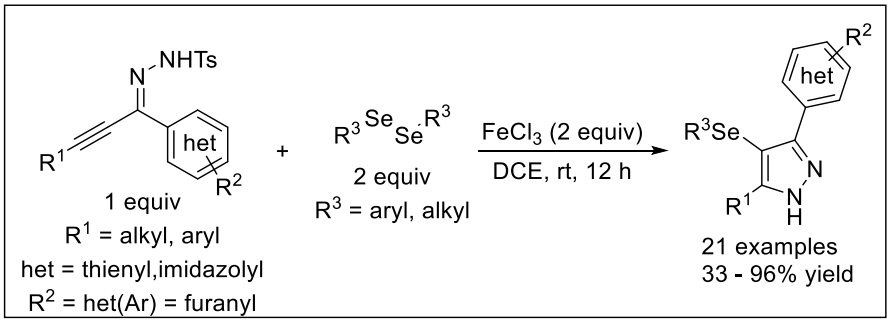

Scheme 4.1.5. $FeCl_3$-Promoted Selenylative Cyclization for The Synthesis of 4-(Arylselanyl)-1*H*-pyrazoles.

In 2020, Koketsu and his co-workers disclosed an Fe(III)-promoted electrophilic selenylative cyclization of arylethynyl quinazoline with diorganyl diselenides for the synthesis of isoquinoline-fused quinazolinones (Scheme 4.1.6).[10] Some of the synthesized isoquinoline-fused quinazolinone derivatives (Scheme 4.1.6) showed notable fluorescence properties.

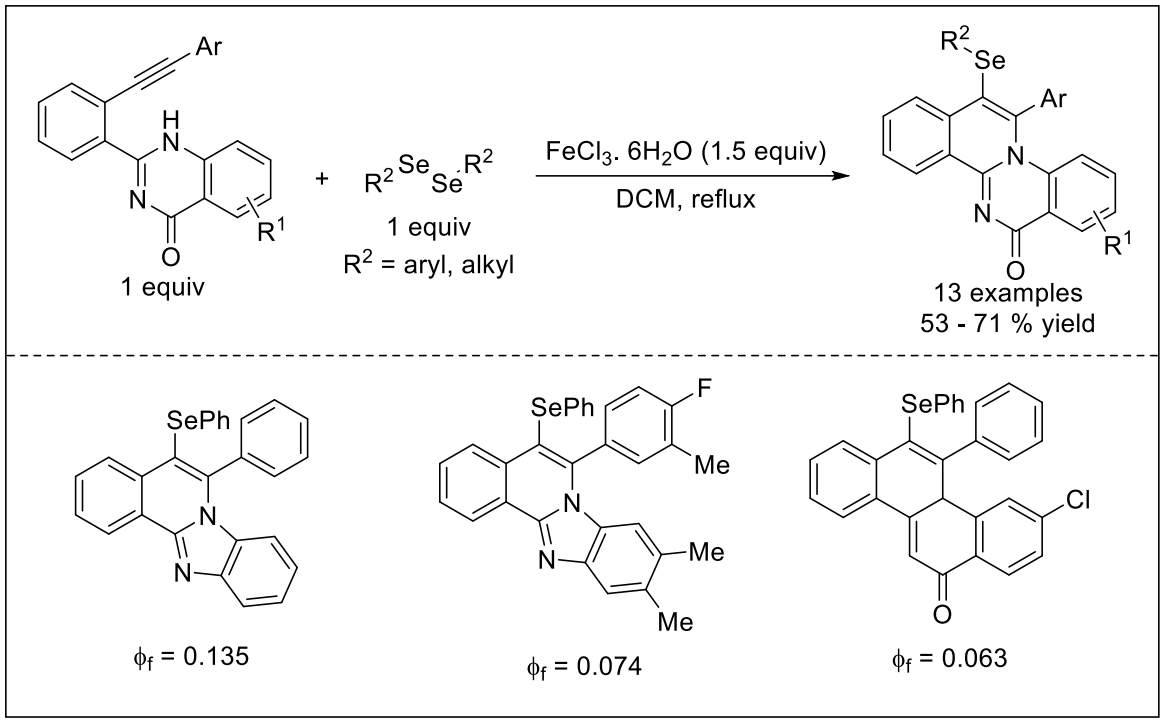

Scheme 4.1.6. Iron (III)- Promoted Selenylative Cyclization of Isoquinoline-Fused Quinazolinones.

In 2020, Wang and his co-workers developed a visible light-promoted regio- and chemoselective radical selenylative cyclization of 1,6-enynes with diaryl diselenides in acetone using 34 W blue LEDs to synthesize substituted pyrrolidines through the formation C-SO_2, C-C, and C-Se bonds (Scheme 4.1.7). [11]

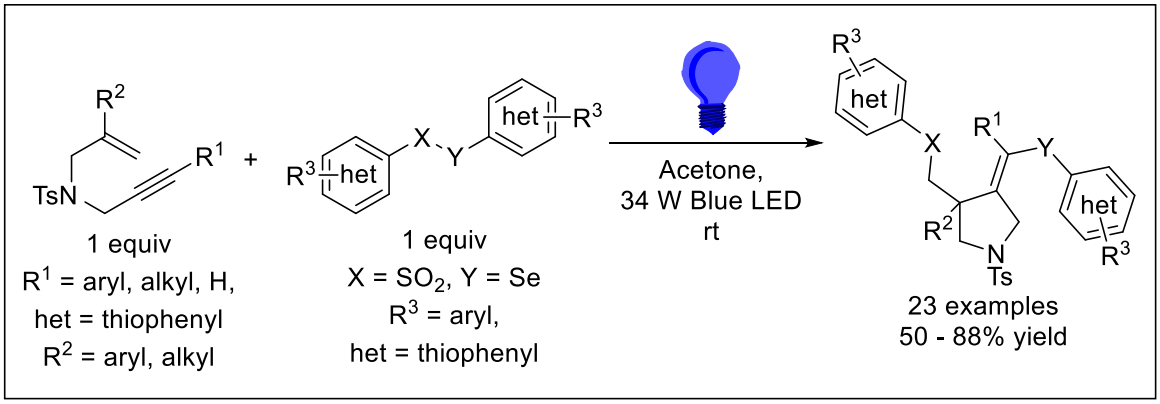

Scheme 4.1.7. Regio- and Chemoselective Radical Selenylative Cyclization of 1,6-enynes.

In the same year, the Xu group disclosed a visible light-induced radical selenylative spirocyclization of indolylynones with diaryl diselenides at room temperature in THF using 30 W white LEDs to access a wide variety of 3-selenospiroindolenines (Scheme 4.1.8).[12] Some of the synthesized compounds exhibited potent inhibitory activities by MTT assay against different cell-lines such as Hela and MGC-803 cell lines with notable IC_{50} values.

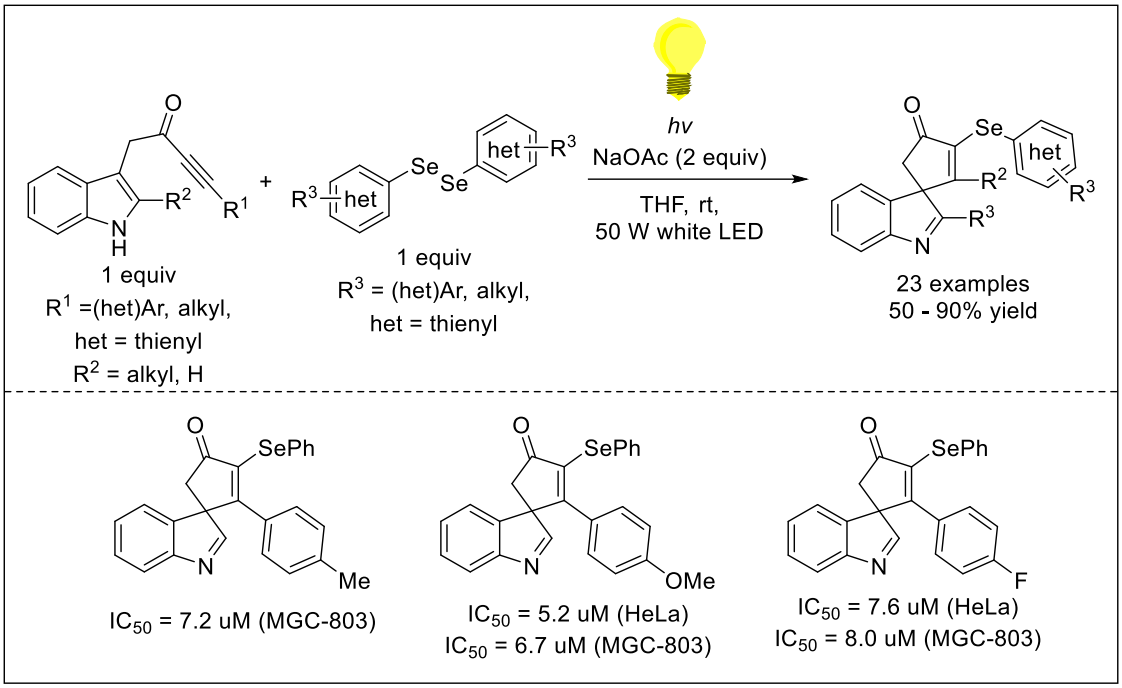

Scheme 4.1.8. Visible Light-Promoted Selenylative Spirocyclization of Indolylynones.

In 2020, Sahoo *et al*. developed an unconventional radical selenylative annulation of yne-tethered-ynamides using diorganyl diselenides and arylthiol at 70 °C for 36 h (Scheme 4.1.9).[13] The experimental and theoretical (DFT) studies revealed the formation of RSe· over RS· followed by the regioselective attack of RSe· to alkynes over ynamides followed by 5-*exo*-dig cyclization to access 4-selenyl pyrrole derivatives.

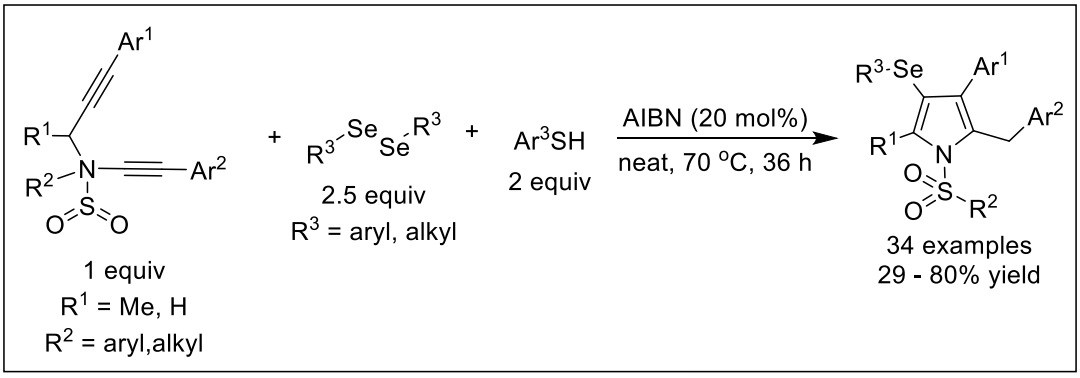

Scheme 4.1.9. Regio- and Chemoselective Cyclization of Yne-Ynamides.

In 2019, Reddy *et al*. developed a copper-catalyzed intramolecular selenoamination of enynyl azides using diorganyl diselenides in MeCN to synthesize a library of 5-selenyl nicotinates *via aza*-annulation of enyl azides (Scheme 4.1.10).[14] This method involved regioselective intramolecular chalcogenoamination of alkynes to provide substituted 5-chalcogenyl nicotinates in good to excellent yields. The synthetic utility of the protocol was demonstrated by further transformations of nicotinates to their corresponding oxides, sulfones, and acid derivatives.

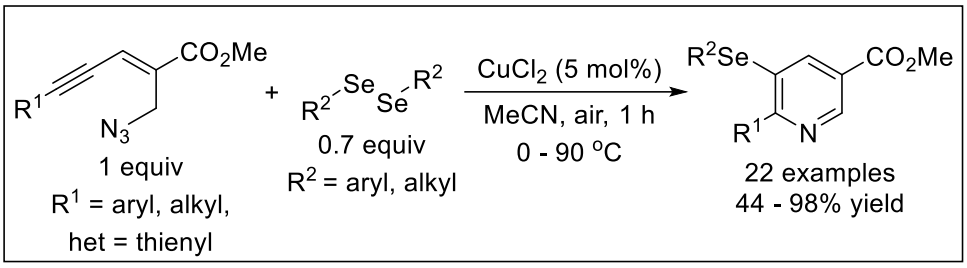

Scheme 4.1.10. Copper-Catalyzed Intramolecular Selenoamination of Enynyl Azides.

In 2019, the Xu group disclosed Se-radical triggered cascade cyclization of alkyne-tethered cyclohexadienones *via* the formation of 3,5-diselenyl-4a,8a-dihydro-2*H*-chromen-6(5*H*)-one followed by the hydrolysis in presence of CsOAc to afford 5-hydroxy-3-selenyl-4a,8a-dihydro-2*H*-chromen-6(5*H*)-ones (Scheme 4.1.11).[15] Some of the synthesized compounds exhibited potent inhibitory activities by MTT assay against different cell-lines with notable IC_{50} values.

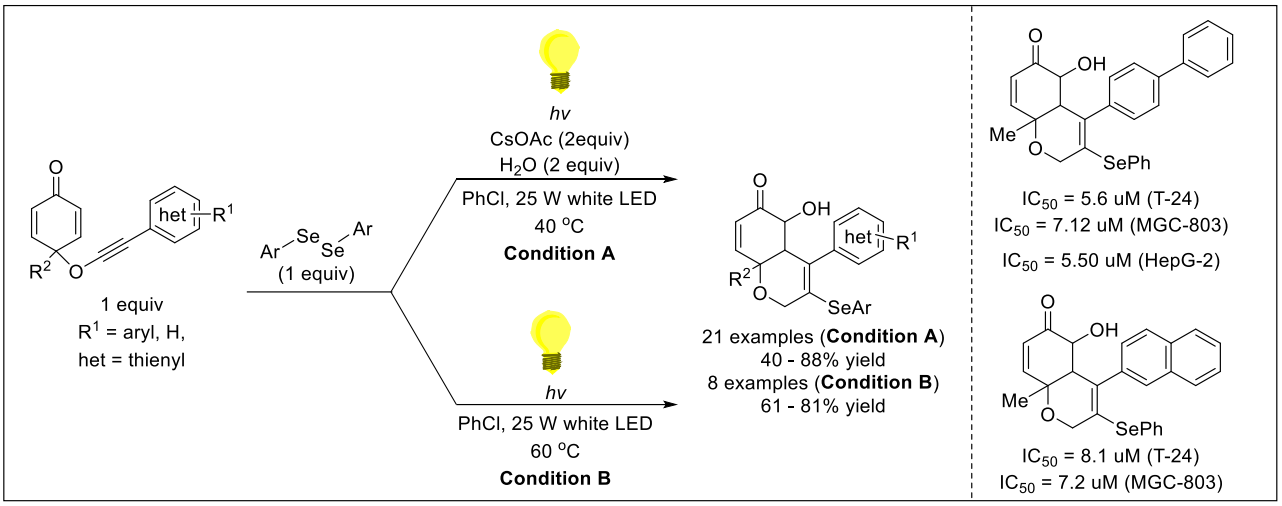

Scheme 4.1.11. Visible-light Mediated Selenylative Cyclization to Synthesize 5-hydroxy-3-selenyl-4*a*,8*a*-dihydro-2*H*-chromen-6(5*H*)-ones.

In 2019, Perin *et al*. disclosed a consecutive electrophilic selenylative intramolecular cyclization of 1,3-ynes with diorganyl diselenides using Oxone to access 5*H*-selenopheno[3,2-*c*]isochromen-5-ones in moderate to good yield (Scheme 4.1.12).[16]

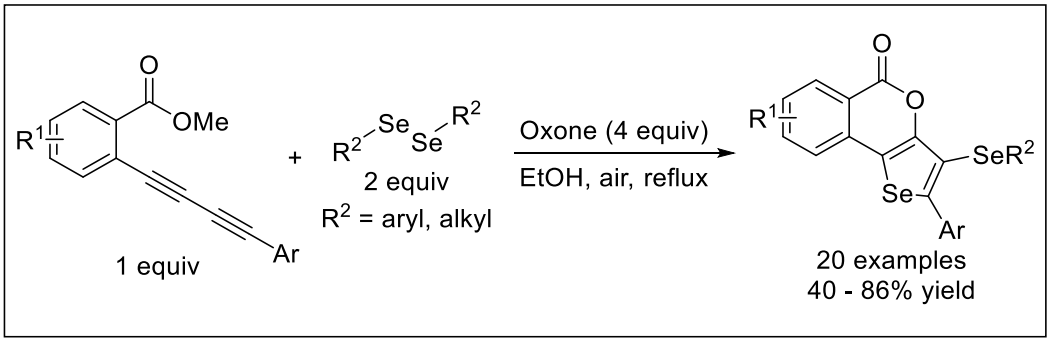

Scheme 4.1.12. Selenylative Cyclization to Synthesize of 5*H*-Selenopheno[3,2-*c*]isochromen-5-ones Promoted by Diorganyl Diselenides and Oxone.

In 2019, Lenardao and his co-workers developed an electrophilic cyclization of 2-functionalized chalcogenoalkynes promoted by Oxone to afford a library of 2,3-bis organochalcogenyl-benzo[*b*]chalcogenophenes in good to excellent yield (Scheme 4.1.13).[17]

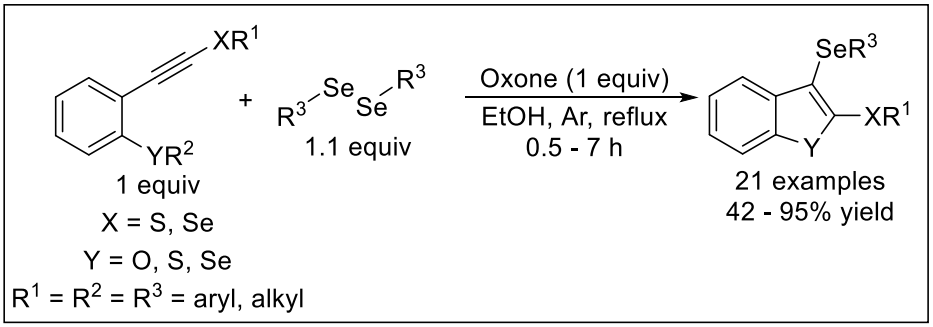

Scheme 4.1.13. Selenylative Cyclization Synthesis of 2,3-Bis-organochalcogenyl-benzo[*b*]chalcogenophenes promoted by Oxone.

In 2019, Perin *et al*. reported an Oxone-mediated electrophilic selenylative cyclization of *α,β* – alkynyl hydrazones with diorganyl diselenides in ethanol as solvent at 70 ^{o}C to afford a wide varieties of 4-organoselanyl-1*H*-pyrazoles in moderate to excellent yield (Scheme 4.1.14).[18] The selenyl cation intermediate obtained from the reaction of diorganyl diselenides and Oxone was characterised by ^{77}Se NMR spectroscopy and high-resolution mass spectroscopy (HRMS).

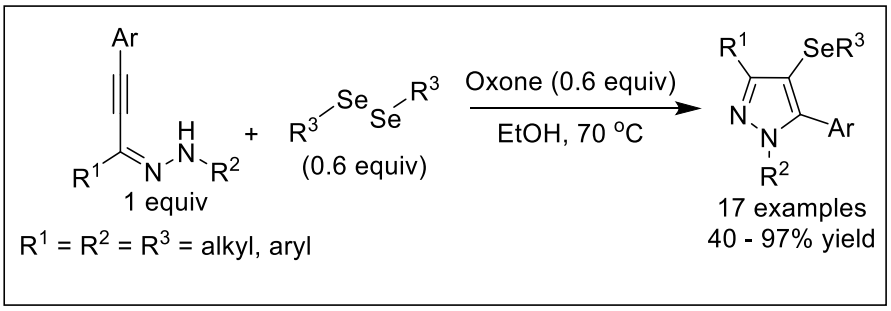

Scheme 4.1.14. Selenylative Cyclization to Synthesize of 4-Organoselanyl-1*H*-pyrazoles

In 2019, Baidya and co-workers disclosed a radical based switchable *ortho*/*ipso* oxidative cyclization of N-aryl alkynamides with readily available diaryl diselenides and $K_2S_2O_8$ as an oxidant in DCE at 80 ^{o}C to access 3-selenyl quinolin-2-ones and 3-selenospiro [*4,5*]trienones in moderate to high yield

through the formation of a spirocyclic intermediate formed *via* an intramolecular *ipso*-cyclization route (Scheme 4.1.15).[19]

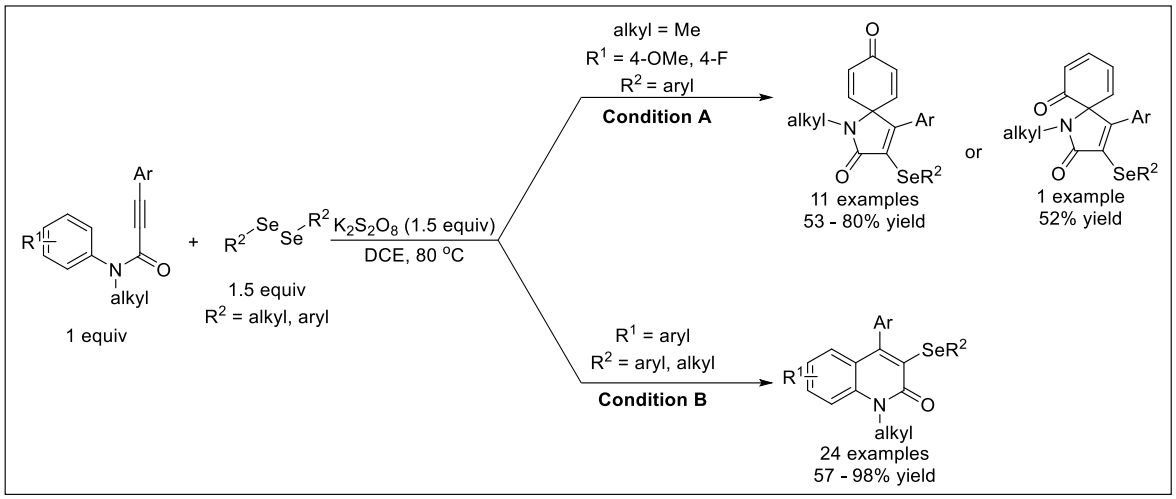

Scheme 4.1.15. Selenylative Cyclization to Synthesize 4-Organoselanyl-1*H*-pyrazoles.

In the same year, Wu *et al*. developed an $AgNO_2$-catalyzed one-pot radical cyclization of 2-alkynylanisoles or 2-alkynylthioanisoles using Se powder and aryl boronic acids in DMSO under aerobic atmosphere at 100 °C *via* the formation of two C−Se bonds, and a C−O(S) bond as well as the cleavage of a C−O(S) bond in a single step through the aryl selenium radical intermediate to afford a wide variety of selenated benzofurans or benzothiophenes in moderate to excellent yield (Scheme 4.1.16).[20]

Scheme 4.1.16. Selenylative Cyclization to Synthesize Benzothiophenes.

4.1.3. Conclusion.

This short review revealed that selenylative annulation strategy is widely employed for the synthesis of selenyl heterocyclic compounds except for a couple of examples where selenyl carbocycles were synthesized. However, most of the developed protocols require either a metal catalyst or over-stoichiometric hazardous reagents. Hence the development of a metal-free, catalytic green synthetic strategy for the synthesis of organoselenides is highly desirable in the context of green chemistry.

SECTION-II

C-H Selenylative Annulations of 2-Alkynyl Biaryls for the Synthesis of 9-Selenylphenanthrenes

4.2.1. Introduction.

Considering the numerous potential applications of organoselenides and phenanthrenes in medicinal chemistry[1, 2] as well as materials science,[3,4] as described in the previous chapters (Chapters 2 and 3), the synthesis of selenylphenanthrenes is obviously of great importance. However, a literature survey revealed that only three synthetic methods have been developed so far which are based on the C-H annulation strategy of 2-alkynyl biaryls for the synthesis of selenyl phenanthrenes or polycyclic aromatic hydrocarbons (PAHs).[5]

4.2.2. Review.

In 2016, the Zeni group first developed a $FeCl_3$-mediated electrophilic selanylative annulation of 2-alkynyl biaryls with diaryl diselenides (1.1 equiv) in dry DCM under inert atmosphere to synthesize 9-arylselanyl-10-aryl-phenanthrenes in moderate to good yield (Scheme 4.2.1).[6] However, the method suffered from several limitations such as low atom economy, the requirement of iron salt in over stoichiometric amounts, hazardous chlorinated solvent (DCM) and inert atmosphere, generation of iron complex, and aryl selenols as waste, and limited substrate scope.

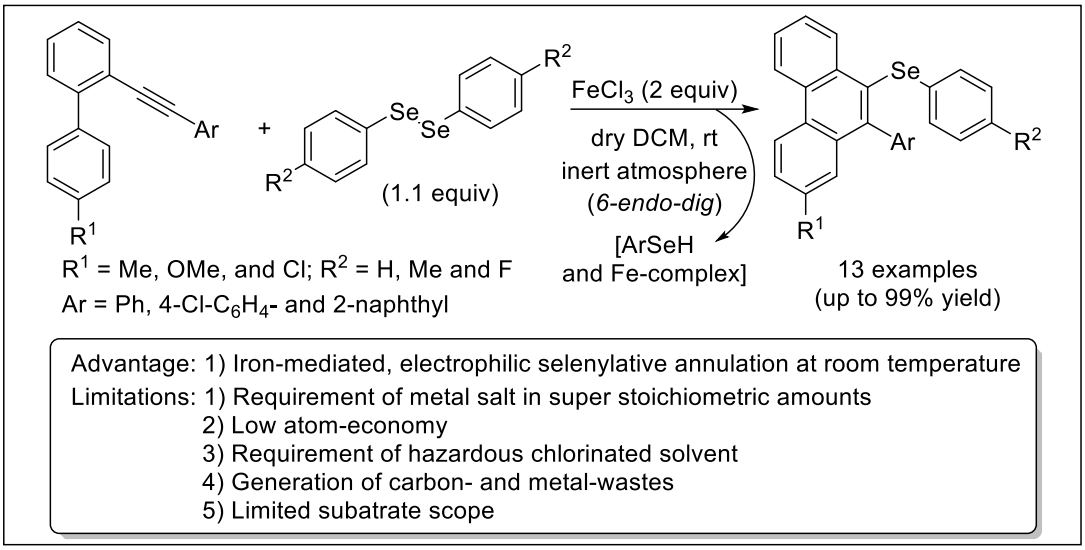

Scheme 4.2.1. $FeCl_3$-Mediated Electrophilic Selanylative Annulation of 2-Alkynyl Biaryls with Diaryl Diselenides.

In 2021, Arsenyan *et. al.* reported a metal-free, oxidative selenylative annulation of 2-alkynyl biaryls with diphenyl diselenide (2 equiv) in dry MeCN under aerobic atmosphere to synthesize 9-phenylselanylphenanthrenes in good yield.[7] This method also suffered from several severe limitations such as very low atom-economy, the requirement of super stoichiometric diphenyl

diselenide (2 equiv), and a hazardous oxidant, *m*-CPBA (5 equiv), toxic solvent, MeCN, high temperature (100 ^{o}C), generation of hazardous wastes, and limited substrate scope.

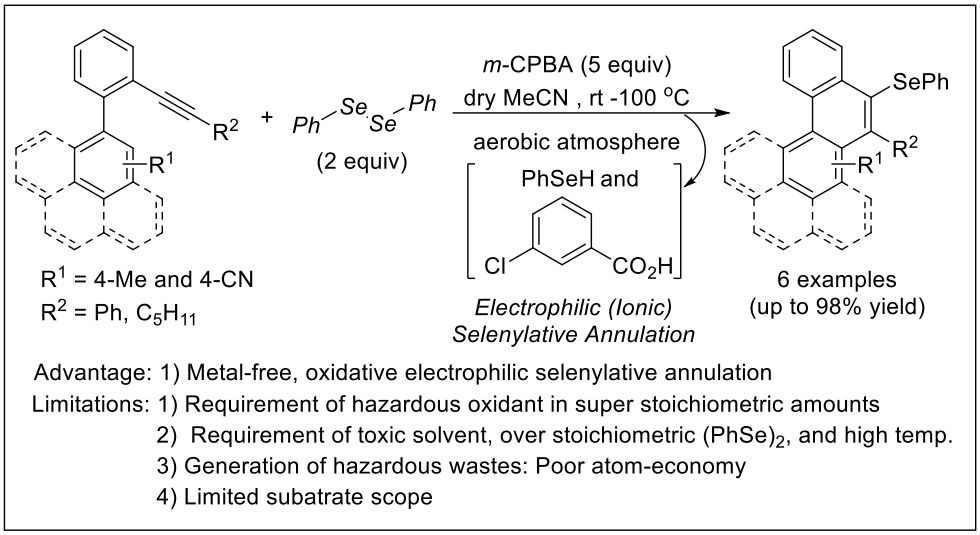

Scheme 4.2.2. Oxidative Selenylative Annulation of 2-Alkynyl Biaryls with Diphenyl Diselenides.

The Li-group reported an electrophilic cyclization of alkynes with triflic anhydride-activated methyl selenoxides and only 9-phenylselanyl-10-phenyl-phenanthrene was synthesized in 68% yield from 2-(phenylethynyl)-1,1′-biphenyl and phenyl methyl selenoxide.[8] The serious limitations associated with this method are the requirement of hazardous reagents in stoichiometric or super stoichiometric amounts, toxic solvent, specific reaction conditions (-78 ^{o}C), moderate yield of product, very low atom-economy, generation of hazardous wastes and the requirement of two-step synthesis of phenyl methyl selenoxide from diphenyl diselenide involving hazardous reagents, thus limiting the substrate scope of this method in accessing selanyl PAHs.

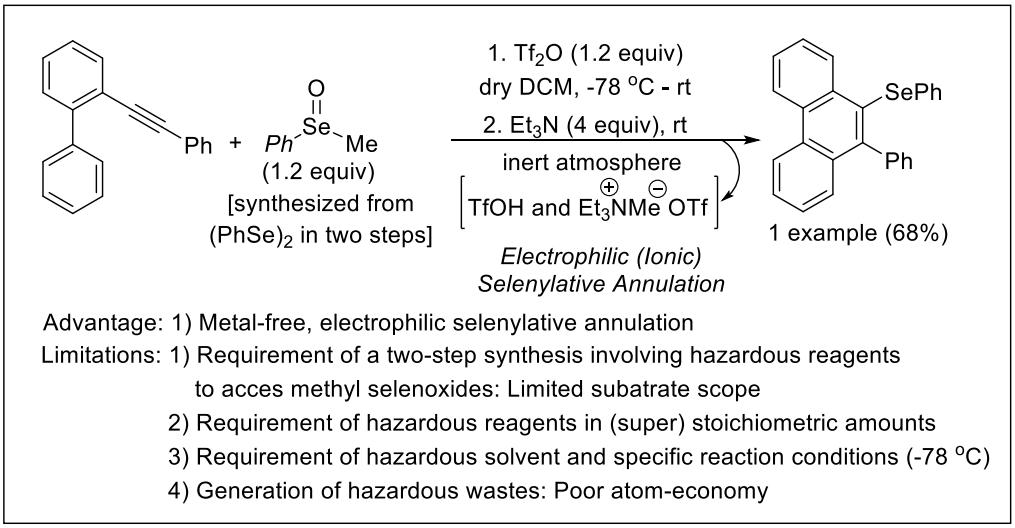

Scheme 4.2.3. Electrophilic Selenylative Cyclization of Alkynes with Triflic Anhydride-activated Methyl Selenoxides.

4.2.3. Conclusion.

This review revealed that none of the three synthetics methods is catalytic in nature for the synthesis 9-selenyl phenanthrenes. Moreover, all of them suffer from some serious limitations, as described above, in the context of green chemistry. Hence the development of a metal-free, catalytic, and sustainable synthetic method for the general synthesis of selenyl-phenanthrenes, PAHs, and polycyclic heteroaromatics is highly desirable.

SECTION-III

Recyclable Iodine-Catalyzed Radical Selenylative Annulation of 2- Alkynyl Biaryls with Diselenides in Water: A Green Approach to Selanyl Polycyclic Aromatic Hydrocarbons and Polycyclic Heteroaromatics

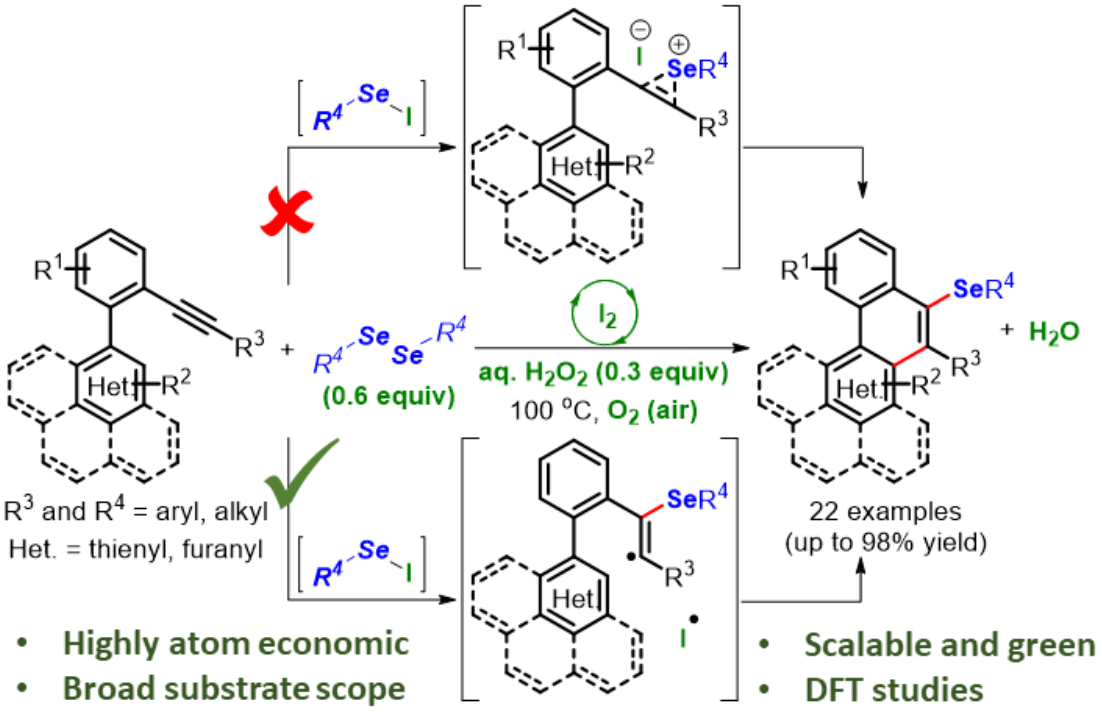

4.3.1. Introduction.

The most important goal of sustainable chemistry is to reduce the adverse consequences of the substances that we use and generate. Moreover, one of the most attractive concepts in chemistry for sustainability is "Green Chemistry" which is the utilization of a set of principles that reduces or eliminates the use of generation of hazardous substances in the design, manufacture, and applications of chemical products. It should be noted that the rapid development of Green Chemistry is due to the recognition that environmentally friendly products and processes will be economical in the long term.

As a part of our continued interest in developing iodinecatalyzed oxidative annulation reactions,[1,2] we developed a recyclable iodine-catalyzed, highly atom-economic oxidative radical selenylative annulation of 2- alkynyl biaryls with diselenides through the *in situ* formation of selenyl iodides to synthesize a wide variety of selanyl PAHs and polycyclic heteroaromatics in water using only a substoichiometric amount (0.3 equiv) of H_2O_2 as the green oxidant under aerobic atmosphere (Scheme 4.3.1). The notable advantages of this protocol over the previously developed synthetic methods are metal-free, highly atom-economic protocol, the requirement of inexpensive reagents such as iodine as a recyclable catalyst and H_2O_2 as a green oxidant only in sub-stoichiometric amounts, use of water as the green reaction medium and generation of water as the only major waste, broad substrate scope in accessing a wide variety of selanyl PAHs and polycyclic heteroaromatics, straight-forward scale-up process up to gram scale, high atom-efficiency, carbon-efficiency, reaction-mass-efficiency, EcoScale score, and low *E*-factor. The only limitation associated with our developed method was the requirement of high temperature (100 ^oC).

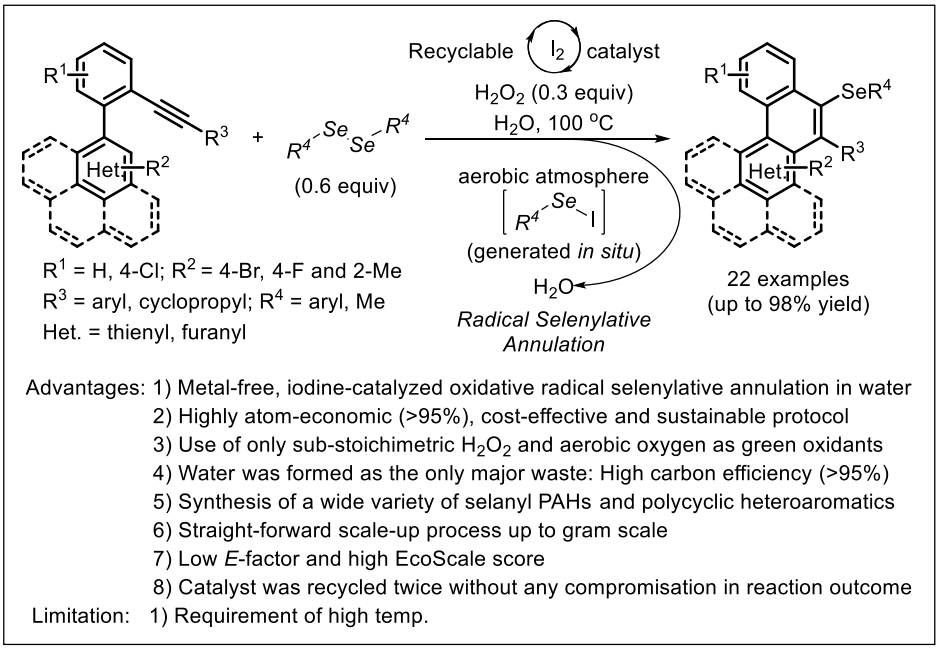

Scheme 4.3.1. Synthetic Strategies to Selanyl PAHs and Polycyclic Heteroaromatics in Water.

The notable advantages of this protocol over the previously developed synthetic methods are metal-free, highly atom-economic protocol, the requirement of inexpensive reagents such as iodine as a recyclable catalyst and H_2O_2 as a green oxidant only in sub-stoichiometric amounts, use of water as the green reaction medium and generation of water as the only major waste, broad substrate scope in accessing a wide variety of selanyl PAHs and polycyclic heteroaromatics, straight-forward scale-up process up to gram scale, high atom-efficiency, carbon-efficiency, reaction-mass-efficiency, EcoScale score, and low E-factor. The only limitation associated with our developed method was the requirement of high temperature (100 ^oC).

4.3.2. Results and Discussion.

We started our investigation of oxidative selenylative annulation with 2-(phenylethynyl)-1,1′-biphenyl **1a** using 0.6 equiv diphenyl diselenide **2a**, 20 mol% iodine, and 0.6 equiv H_2O_2 (30% aqueous v/v solution) in water (0.06 mL) at 60 ^oC under aerobic atmosphere which furnished the desired product, phenyl(10-phenylphenanthren-9-yl)selane **3aa** in 65% yield along with trace amount of 9-iodo-10-phenylphenanthrene **4a** (entry 1, Table 4.3.1). The yield of **3aa** increased gradually with the gradual increase in temperature up to 100 ^oC, which was found as the optimum temperature for the selenylative annulation reaction (entry 3 vs. entries 1–4, Table 4.3.1). The stoichiometry of **2a** was then optimized, and the usage of 0.6 equiv of **2a** furnished the best result (entry 3 vs. entries 5–6, Table 4.3.1), which revealed that both the units of 2a are reactive. Notably, the use of sub-stoichiometric (0.3 equiv) H_2O_2 (30% aqueous v/v solution) was found to be optimum, furnishing only the desired product in almost quantitative yield (99%) (entry 7 vs. entries 3 and 8, Table 4.3.1). Among other oxidants such as TBHP, $Na_2S_2O_8$, $K_2S_2O_8$, *m*-CPBA, and oxone, only TBHP furnished **3aa** in 98% yield (entry 7 vs. entries 9–13, Table 4.3.1). Although the reaction outcome was comparable using either H_2O_2 or TBHP as oxidant (entry 7 vs. 9, Table 1), we chose H_2O_2 for our further study as it is a greener oxidant than TBHP. When DMSO (10 equiv) was used as oxidant as well as solvent, 60% **3aa** was formed (entry 14, Table 4.3.1). Among other solvents (0.06 mL), such as methanol, 1,4-dioxane, DMF, MeCN, toluene, and DCM, **3aa** was formed almost quantitatively (99%) only in toluene (entry 19 vs. entries 15–20, Table 4.3.1). Although the reaction outcome was the same using either water (0.06 mL) or toluene (0.06 mL) as solvent (entry 7 vs. 19, Table 4.3.1), we chose water as the reaction medium for our further study as it is a green solvent. The use of either inorganic bases (K_2CO_3 and K_3PO_4) or an organic base (Et_3N) harmed the reaction outcome (entry 7 vs. entries 21–23, Table 4.3.1). Lowering the catalyst loading to 10 mol% also negatively impacted the reaction outcome (entry 24, Table 4.3.1). The use of 0.06 mL water was found optimum (entry 7 vs. entries 25–26, Table 4.3.1). The blank experiments revealed the essential roles of iodine, H_2O_2, and a combination of both

of them (entry 7 vs. entries 27–29, Table 4.3.1). Notably, 42% 3aa was formed in the absence of H_2O_2, which revealed the participation of aerobic oxygen as another green oxidant too in the reaction (entry 28, Table 4.3.1).

Table 4.3.1. Optimization of reaction conditions[a,b]

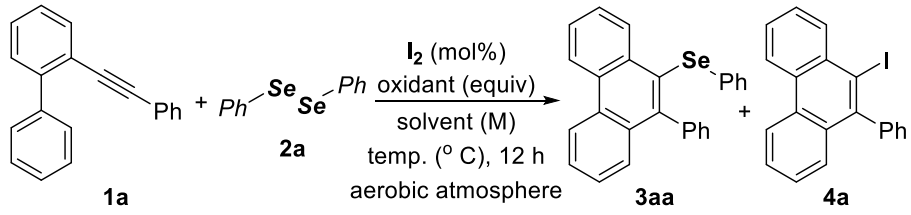

1a 3aa 4a

entry	I_2 (mol%)	2a (equiv)	oxidant (equiv)	solvent (mL)	temp. (°C)	yield (%)[c]	
						3aa	4a
1	20	0.6	H_2O_2 (0.6)	H_2O (0.06)	60	65	trace
2	20	0.6	H_2O_2 (0.6)	H_2O (0.06)	80	85	trace
3	20	0.6	H_2O_2 (0.6)	H_2O (0.06)	100	96	trace
4[d]	20	0.6	H_2O_2 (0.6)	H_2O (0.06)	120	91	trace
5	20	1.2	H_2O_2 (0.6)	H_2O (0.06)	100	87	trace
6	20	0.5	H_2O_2 (0.6)	H_2O (0.06)	100	76	trace
7	**20**	**0.6**	**H_2O_2 (0.3)**	**H_2O (0.06)**	**100**	**99**	**ND**
8	20	0.6	H_2O_2 (0.15)	H_2O (0.06)	100	37	trace
9	20	0.6	TBHP (0.3)	H_2O (0.06)	100	98	ND
10	20	0.6	$Na_2S_2O_8$ (0.3)	H_2O (0.06)	100	64	20
11	20	0.6	$K_2S_2O_8$ (0.3)	H_2O (0.06)	100	70	trace
12	20	0.6	*m-CPBA* (0.3)	H_2O (0.06)	100	43	26
13	20	0.6	Oxone (0.3)	H_2O (0.06)	100	29	trace
14	20	0.6	DMSO (10)	-	100	60	-
15	20	0.6	H_2O_2 (0.3)	methanol (0.06)	100	28	trace
16	20	0.6	H_2O_2 (0.3)	1,4-dioxane (0.06)	100	60	-
17	20	0.6	H_2O_2 (0.3)	DMF (0.06)	100	86	trace
18	20	0.6	H_2O_2 (0.3)	MeCN (0.06)	100	80	16
19	20	0.6	H_2O_2 (0.3)	toluene (0.06)	100	99	ND
20	20	0.6	H_2O_2 (0.3)	DCM (0.06)	60	21	trace
21[e]	20	0.6	H_2O_2 (0.3)	H_2O (0.06)	100	8	trace
22[f]	20	0.6	H_2O_2 (0.3)	H_2O (0.06)	100	8	trace
23[g]	20	0.6	H_2O_2 (0.3)	H_2O (0.06)	100	10	trace
24	10	0.6	H_2O_2 (0.3)	H_2O (0.06)	100	32	trace
25	20	0.6	H_2O_2 (0.3)	H_2O (0.1)	100	85	ND
26	20	0.6	H_2O_2 (0.3)	H_2O (0.03)	100	82	ND
27	-	0.6	H_2O_2 (0.3)	H_2O (0.06)	100	7	ND
28	20	0.6	-	H_2O (0.06)	100	42	trace
29	-	0.6	-	H_2O (0.06)	100	0	0

[a]Reactions were conducted in 0.1 mmol scale; [b]concentration of H_2O_2 used, wherever applicable, was 30% aqueous solution (v/v); [c]yield was determined by the ^{1}H NMR of the crude reaction mixture using 1,3,5-trimethoxybenzene

as the internal standard; [d]reaction mixture was refluxed using cold-water circulation; [e]K_2CO_3 (1.2 equiv) was used; [f]K_3PO_4 (1.2 equiv) was used; [g]Et_3N (1.2 equiv) was used.

The participation of aerobic oxygen as an oxidant eventually lowered the required stoichiometry of 30% aqueous solution (v/v) of H_2O_2 (0.3 equiv for **1a** and 0.5 equiv for **2a**), leading to the higher atom economy of the reaction. The use of sub-stoichiometric H_2O_2 is found to be indispensable for the higher atom-economy of the reaction as the use of super-stoichiometric H_2O_2 may cause the higher loading of diphenyl diselenide **2a** owing to its favourable oxidation to phenyl selenic acid ($PhSeO_3H$) by super-stoichiometric H_2O_2.[3] Notably, it has been found that the use of excess H_2O_2 (5 equiv) oxidized diphenyl diselenide **2a** to phenyl selenic acid ($PhSeO_3H$) quantitatively,[3] but the same reaction was not effective at all when only 0.5 equiv of H_2O_2 was used, as evident by the ^{77}Se NMR spectrum of the corresponding reaction mixtures (Fig 4.3.1).

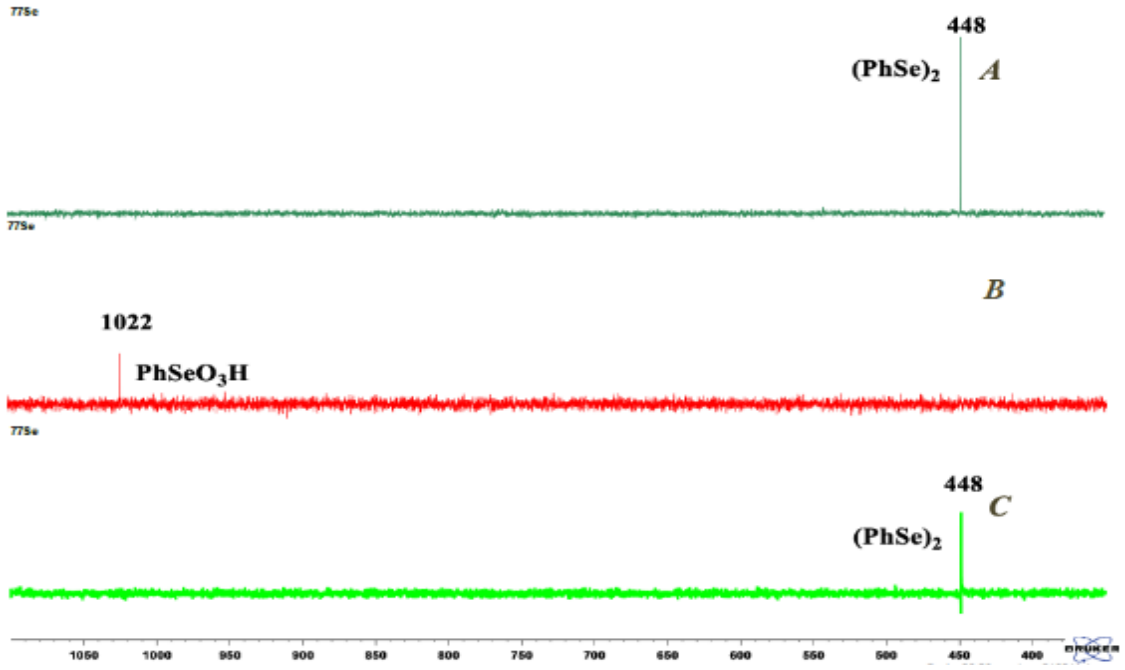

Figure 4.3.1. ^{77}Se NMR of (A) Ph_2Se_2; (B) Ph_2Se_2 + H_2O_2 (5 equiv), 100 ^oC, 12 h; (C) Ph_2Se_2 + H_2O_2 (0.5 equiv), 100 ^oC, 12 h; recorded in DMSO-d_6.

Next, the scope of the selenylative annulation reaction was explored with respect to both the substrates under the optimized reaction conditions, and the results are presented in Table 4.3.2. At first, the scope of diselenides was explored with 2-(phenylethynyl)-1,1-biphenyl **1a**. Diphenyl diselenide **2a** furnished the desired product **3aa** in 98% isolated yield. Various diaryl diselenides such as electron-withdrawing (Br, Cl, F, CF_3, and NO_2) and electron-donating (Me) group substituted diaryl diselenides participated in the reaction with **1a** smoothly to furnish the corresponding aryl(10-phenylphenanthren-9-yl)selanes (3ab–3ag)

in moderate to good yield. Notably, one dialkyl diselenide, i.e., dimethyl diselenide, reacted with **1a** without any difficulties and afforded methyl(10-phenylphenanthren-9-yl)selane **3ah** in 76% yield.

Table 4.3.2. Substrate Scope[a,b].

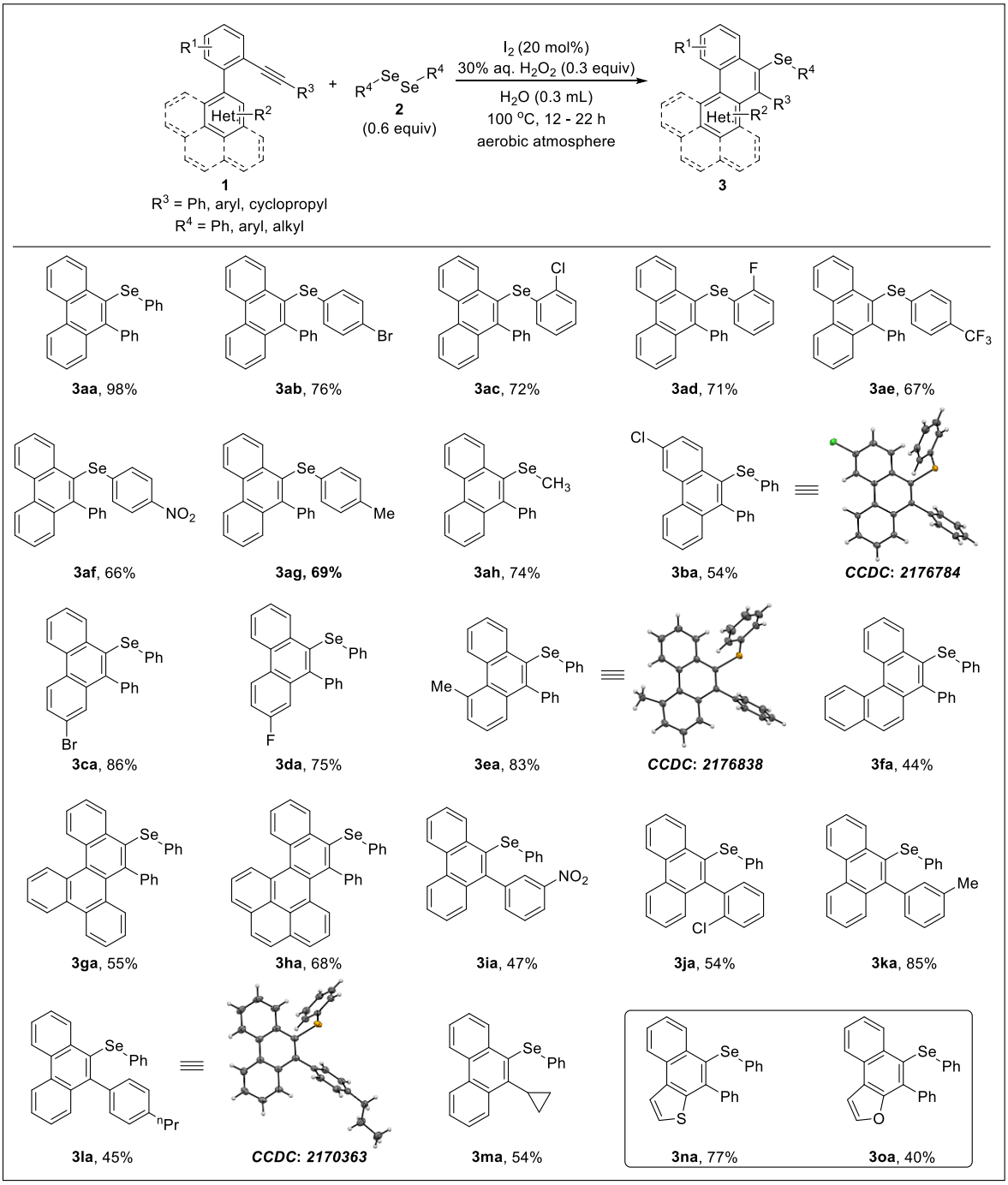

[a]Reaction conditions: **1** (0.5 mmol), **2** (0.3 mmol), I_2 (0.1 mmol), 30% aq. solution (v/v) of H_2O_2 (0.15 mmol), H_2O (0.3 mL), 100 °C. bIsolated yield of product was reported.

Next, the scope of 2-(phenylethynyl)-1,1-biaryls was explored with diphenyl diselenide **2a**. Halogen (Cl, Br, and F) substituted and electron-donating (Me) group substituted 2-(phenylethynyl)-1,1-biaryls (**1b-1e**) smoothly reacted with **2a** to produce the corresponding phenyl(10-phenylphenanthren-9-yl)selanes (**3ba**–**3ea**) in good yield except **3ba**. PAHs such as naphthalene, phenanthrene and pyrene-substituted 2-phenylethynyl benzenes (**1f** – **1h**) also underwent selenylative annulation with **2a** under the optimized reaction conditions to furnish highly fused PAHs such as phenyl(6-phenylbenzo[*c*]phenanthren-5-yl)selane **3fa**, phenyl(5-phenylbenzo[*g*]chrysen-6-yl)selane **3ga**, and phenyl(14-phenyldibenzo[*ij*,*no*]tetraphen-13-yl)selane **3ha** respectively in moderate yield. Next, the scope of 2-(arylethynyl)-1,1′-biphenyls was explored with **2a** and both electron-withdrawing (NO_2, Cl) and electron-donating (Me, *i*-Pr) group substituted 2-(arylethynyl)-1,1′-biphenyls (**1i**–**1l**) afforded the corresponding phenyl(10-arylphenanthren-9-yl)selanes (**3ia**–**3la**). 2-(Cyclopropylethynyl)-1,1′-biphenyl **1m** also participated in the reaction with **2a** to furnish (10-cyclopropylphenanthren-9-yl)(phenyl)selane **3ma** in 54% yield. Finally, we employed a few 2-heteroaryl-substituted phenylethynylbenzenes, *i.e.,* 3-(2-(phenylethynyl)phenyl)thiophene **1n** and 3-(2-(phenylethynyl)phenyl)furan **1o** which also underwent selenylative annulation with **2a** under the optimized reaction conditions and produced two different classes of polycyclic heteroaromatics, i.e., 4-phenyl-5-(phenylselanyl)naphtho[2,1-*b*]thiophene **3na** and 4-phenyl-5-(phenylselanyl)naphtho[2,1-*b*]furan **3oa**, respectively.

In general, the scope of the reaction was found to be broad with respect to both substrates. The structures of **3ba**, **3ea**, and **3la** were confirmed by X-ray crystallographic structure determination (Fig. 4.3.2−4.3.4 and Table 4.3.3). The reactions were relatively more clean and efficient with diselenides compared to disulfides,[2] since the by-product, 9-iodo-10-phenylphenanthrene **4a** was hardly formed in most of the reactions. Unfortunately, the annulation of 1a did not work with diphenyl ditelluride, $(PhTe)_2$.

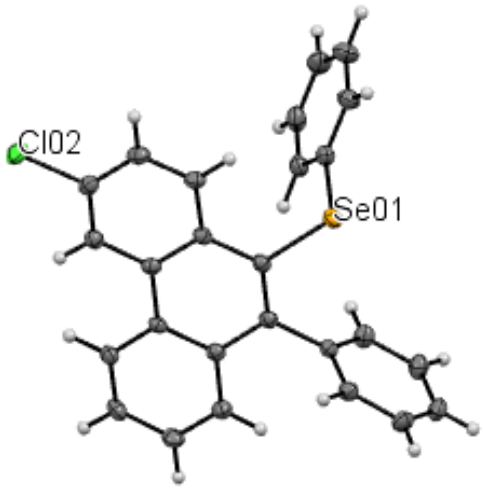

Figure 4.3.2. X-ray Crystal Structure of **3ba** (Thermal Ellipsoids Shown at 50% Probability) Including Hetero-atom Numbering.

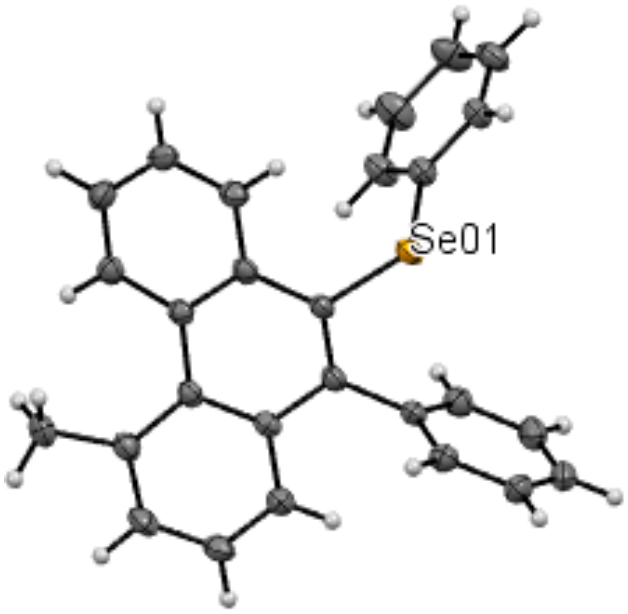

Figure 4.3.3. X-ray Crystal Structure of **3ea** (Thermal Ellipsoids Shown at 50% Probability) including Hetero-atom Numbering.

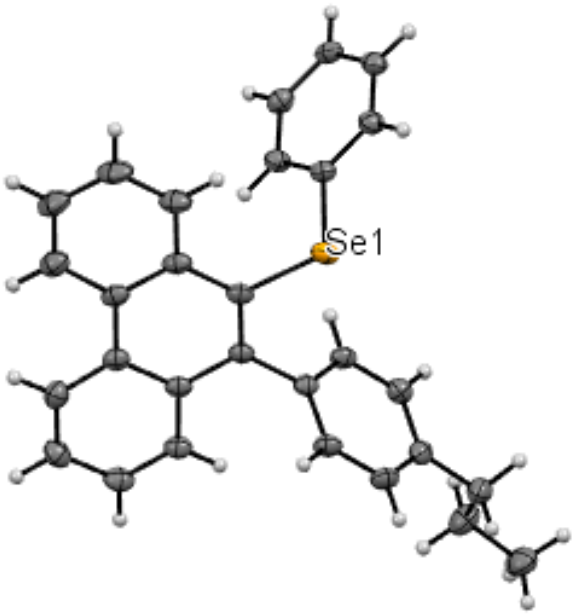

Figure 4.3.4. X-ray Crystal Structure f **3la** (Thermal Ellipsoids Shown at 50% Probability) Including Hetero-atom Numbering.

Table- 4.3.3. Selected Crystal Data for Compounds **3ba**, **3ea**, **3la**.

Parameters	3ba	3ea	3la
Empirical formula	$C_{26}H_{17}ClSe$	$C_{27}H_{20}Se$	$C_{29}H_{24}Se$
Formula weight	443.80	423.419	451.47
Temperature/K	100	100	100
Crystal system	monoclinic	monoclinic	triclinic
Space group	P 1 21/c 1	P 1 21/c 1	P -1
a/Å	15.3921(2)	11.2182(3)	9.9628(2)
b/Å	10.18330(10)	10.3531(3)	10.1107(2)
c/Å	13.1358(2)	17.3831(5)	12.9334(2)
α (°)	90	90	71.458(2)
β (°)	107.7750(10)	100.258(3)	73.161(2)
γ(°)	90	90	63.999(2)
Volume/Å^3	1960.65(4)	1986.66(10)	1092.75(4)
Z	4	4	2
μ/mm^{-1}	3.894	2.605	2.402
D_x [g cm^{-3}]	1.503	1.416	1.372
F(000)	896	862.989	463.6
2Θ range for data collection (°)	5.5900-79.1990	4.0480-79.2670	5.0300-79.4120
Index ranges	-19≤ h ≤ 19, -12 ≤ k ≤ 12, -16 ≤ l ≤ 13	-13≤ h ≤ 14, -11 ≤ k ≤ 12, -16 ≤ l ≤ 21	-12≤ h ≤ 9, -12 ≤ k ≤ 12, -16 ≤ l ≤ 16
Reflections measured	7962	5183	12419
Unique reflections	4133	4136	4610
Parameters /restraints/	321/0	254/0	285/0
Goodness-of-fit on F2	1.149	1.085	1.027
R_1 [I ≥ 2σ (I)]	0.075	0.100	0.0309
wR_2 (all data)	0.0882(4133)	0.1256 (4136)	0.0814(4610)
Largest diff. peak/hole/e Å^{-3}	0.548/-0.523	0.6378/-0.9648	0.5256/-0.6478
CCDC	***2176784***	***2176838***	***2170363***

Scheme 4.3.2. Recovery and Recyclability of the Catalyst, Iodine.

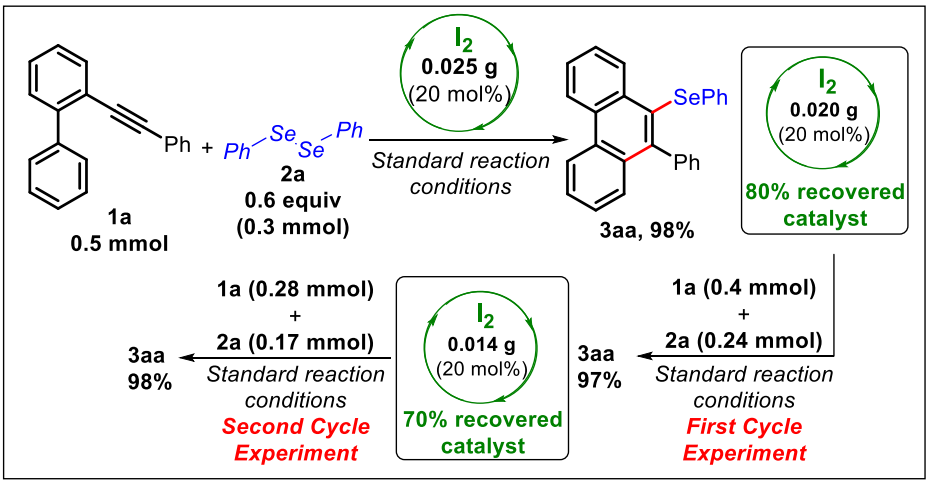

Next, we checked the feasibility of the recovery and recyclability the catalyst (iodine) after the reaction. Gratifyingly, we were able to recover 80% of the catalyst after the reaction of **1a** with **2a**, during the column chromatography stage and recycled the catalyst for the next (first) cycle experiment. After the first cycle experiment, we were able to recover 70% of the catalyst again and recycled the same for the second cycle experiment. In the recycling process of the catalyst the reaction outcome was found to be uncompromised in each time (Scheme 4.3.2). The little loss of the catalyst after each reaction could be because of the sublimation nature of iodine.

To demonstrate the practicality of the developed synthetic method, a gram-scale reaction was conducted between **1a** (1.017 g, 4 mmol) and **2a** (0.749 g, 2.4 mmol) under the optimized reaction conditions, and **3aa** was isolated in 80.6% yield (1.32 g, 3.224 mmol) which revealed that the scale-up process is straight-forward (Scheme 4.3.3).

Scheme 4.3.3. Gram-scale Synthesis of **3aa**.

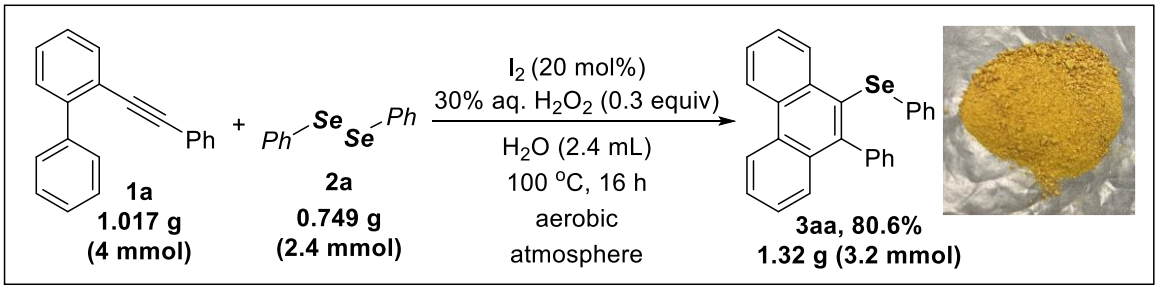

The synthesized product, **3aa**, was further synthetically diversified through simple oxidation using *m*-CPBA to the corresponding selenoxide, 9-phenyl-10-(phenylseleninyl)phenanthrene **5** in

86% yield (Scheme 4.3.4.A). Moreover, the halogen, in particular, bromine (Br) which was intact in a couple of synthesized products (**3ab** and **3ca**), was further utilized for synthetic diversification of **3ab** and **3ca** by a cross-coupling, i.e., Suzuki cross-coupling reaction using phenylboronic acid to afford **6** and **7** respectively in moderate yield (Scheme 4.3.4.B and 4.3.4.C).

Table 4.3.4. Synthetic Diversification of **3aa, 3ab**, and **3ca** to Access **5, 6**, and **7** Respectively.

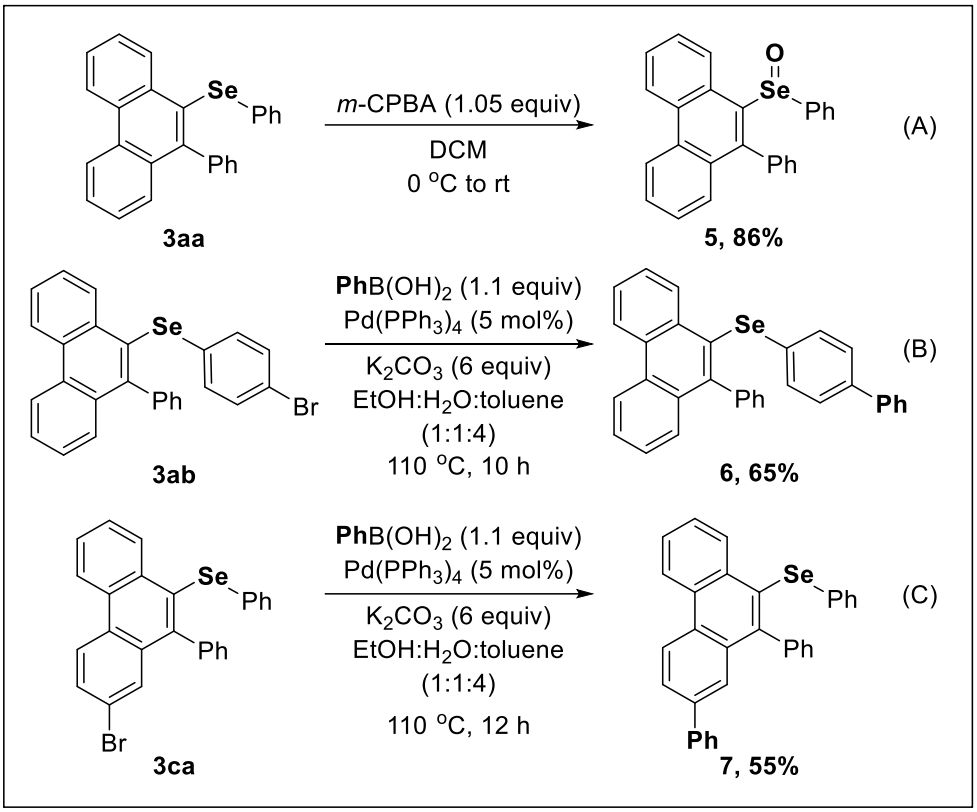

In order to measure the greenness of our developed method quantitatively, we evaluated the green chemistry metrics [4] for the synthesis of **3aa**. The data is tabulated in Table 4.3.5. Notably, our method is found to be 95.8% atom economical, 93.9% atom efficient, 95.01% carbon-efficient, and 86.7% reaction mass efficient. In addition, an essential parameter to quantify the quality of an organic process based on the generated waste, i.e., *E*-factor, [4] is found to have a low value of 1.68 for the synthesis of **3aa**, and the majority of the generated waste is water. Another crucial green parameter, i.e., EcoScale score, [4] which is based on an organic process's safety, economic, and ecological features, is also evaluated, and it showed a high value of 70 for the synthesis of **3aa** (Table 4.3.6).

Table 4.3.5. Evaluation of Green Chemistry Metrics for the Synthesis of **3aa.**

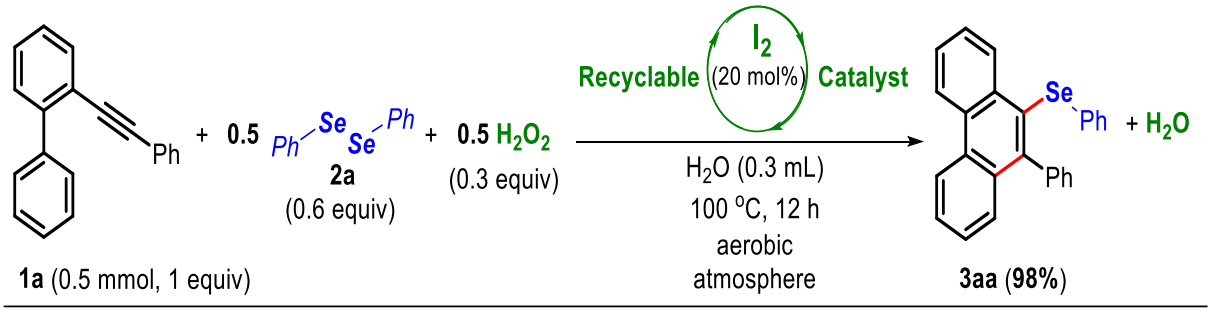

1a (0.5 mmol, 1 equiv) **3aa** (**98%**)

Yield of desired product (3aa) = 98%

$$\text{Atom Economy (\%)} = \frac{\text{Mol. wt. of product}}{\text{Mol. wt. of all reactants}} \times 100 = \frac{409.39}{254.33 + (0.5 \times 312.13) + (0.3 \times 34.015)} \times 100 = 97.3\%$$

Atom Efficiency (%) = (%yield of product x %atom economy) x 100 = (98% x 97.3%) x 100 = **95.4%**

$$\text{Carbon Efficiency (\%)} = \frac{\text{(moles of 3aa x no. of carbons in 3aa) x 100}}{\text{(moles of 1a x carbons in 1a) + (moles of 2a x carbons in 2a)}} = \frac{(0.497 \times 26) \times 100}{(0.5 \times 20) + (0.3 \times 12)} = 95.01\%$$

$$\text{Reaction Mass Efficiency (\%)} = \frac{\text{mass of isolated product}}{\text{mass of all reactants}} \times 100 = \frac{0.202}{0.127 + 0.093 + 0.013} \times 100 = 86.7\%$$

Reactant 1:	**2-(Phenylethynyl)-1,1'-biphenyl (1a)**	0.127 g	0.5 mmol	FW 254.33
Reactant 2:	**1,2-Diphenyldiselane (2a)**	0.093 g	0.3 mmol	FW 312.13
Catalyst:	**Iodine**	0.025 g	0.1 mmol	FW 253.81
Reagent (oxidant):	**Hydrogen peroxide (30% aq. sol. v/v)**	0.013 g	0.25 mmol	FW 34.02
Solvent:	**Water**	0.304 g	16.89 mmol	FW 18
Recovered and recycled catalyst:	**Iodine**	0.020 g	0.079 mmol	FW 312.13
Product:	**Phenyl(10-phenylphenanthren-9-yl)selane (3aa)**	0.202 g	0.495 mmol	FW 409.39

$$\text{E-factor} = \frac{\text{total waste (g)}}{\text{total product (g)}} = \frac{(0.127 + 0.093 + 0.025 + 0.013 + 0.304) - (0.202 + 0.02)}{0.202} = 1.68 \text{ g waste/g product}$$

Eco Scale = 100 - Sum of individual penalties
Score on Eco Scale: > 75, Excellent; >50, acceptable; <50, Inadequate

EcoScale score = (100 - 30[a]) = 70 (>50; So, it is an acceptable synthesis)

Table 4.3.6. Calculation of EcoScale Score for the I_2-Catalyzed Synthetic Process to Synthesize Phenyl(10-phenylphenanthren-9-yl)selane (**3aa**) from 2-(Phenylethynyl)-1,1'-biphenyl (**1a**) and Diphenyl Diselenide (**2a**).

EcoScale Calculation:

EcoScale = 100 - Sum of individual penalties
Score on EcoScale: > 75, Excellent; >50, acceptable; <50, Inadequate

Parameters		Penalty Points
1. Yield:	(100 - % of yield)/2 = (100 - 98)/2 = 1	**1**
2. Price of reaction components (To obtain 10 mmol of end product, **3aa**)		
A. Calculation of Penalty Points :		
a. 2-(Phenylethynyl)-1,1'-biphenyl = 10.2 mmol = 2.59 g = USD 13.84		
[Synthesis cost : Required Chemicals :		
i) [1,1'-biphenyl]-2-amine = 2.54 g = USD 7.39		
ii) HCl = 7.8 mL= USD 0.25		
iii) $NaNO_2$ = 1.26 g = USD 0.056		
i**v)** KI = 3.75 g = USD 1.192		
v) Bis(triphenyl phosphine)Pd(II) dichloride= 0.089 g = USD 1.70		
vi) CuI = 0.024 g = USD 0.008		
vii) Phenyl acetylene = 1.68 mL = USD 2.35		
viii) Triethylamine = 33.15 mL = USD 0.343		
b. 1,2-diphenyldiselane = 6.12 mmol = 1.92 g = USD 7.68		
c. Iodine (As catalyst) = 2.02 mmol = 0.517 g = USD 0.152		
d. Hydrogen Peroxide (30% aqueous solution) = 0.24 mL = USD 0.063		
Total cost of synthesis of **3aa** = (13.30 + 7.68 + 0.152 + 0.063) = USD 21.195 Thus expensive, since \$10<(total cost of synthesis of 10 mmol of **3aa**) < \$50:		**3**
3. Safety		
1,2-diphenyldiselane (T)		**5**
Iodine (T)		**5**
4. Technical Setup		
Common Setup		**0**
5. Temperature/ Time		
100 ^oC, 12 h (Heating, > 1h)		**3**
6. Work up and purification :		
a. Adding solvent		**0**
b. Liquid-Liquid extraction		**3**
c. Classical Chromatography		**10**
Total penalty points:		**30**

B. EcoScale calculation:

EcoScale score: (100 - 30) = 70 (>50; it is an acceptable synthesis)

To get insights into the reaction mechanism, several experiments were conducted. When diphenyl diselenide **2a** reacted with iodine in DCM at room temperature, phenylselenyl iodide, PhSeI (**6**), was formed *in situ*, as evident by the LC-MS (Fig. 4.3.5) analysis (Scheme 4.3.5.A). However, we could not detect the *in situ* formation of **6** in water may be because of relatively less life-time of PhSeI in water in comparison to DCM. When the reaction of **1a** was

conducted with 1.2 equiv of phenylselenyl bromide, PhSeBr **7** (Scheme 4.3.5.B) and phenylselenyl chloride, PhSeCl **8** (Scheme 4.3.5.C) in the presence of 0.3 equiv H_2O_2 (30% aq. sol. v/v) in water at 100 ^oC, **3aa** was formed in 85% and 70% yield respectively. Hence, these observations revealed that the *in situ* formed PhSeI is not only the active intermediate for the iodine-catalyzed selenylative annulation of 2-alkynyl biaryls, but also a better reagent than its other halo-anlogues, i.e., PhSeBr and PhSeCl as the corresponding product 3aa was formed in relatively higher yield (99%) under similar reaction conditions (Scheme 4.3.5.D). Eventually, the order of reactivity of phenylselenyl halides (PhSeX where X = I, Br, and Cl) for the selenylative annulation of 2-alkynyl biaryls is found to be PhSeI (6) > PhSeBr (7) > PhSeCl (8) and that could be because of the opposite order of bond dissociation energies (BDE) of PhSe-X, i.e., PhSe-I (6) < PhSe-Br (7) < PhSe-Cl (8) which were calculated using the following equation: BDEX = EPhSe• + EX• – EPhSeX [where, EPhSeX represents Gibb's free energy for PhSeX, EPhSe• represents Gibb's free energy for PhSe• radical, and EX• is Gibb's free energy for halogen radical] (Table 4.3.7).

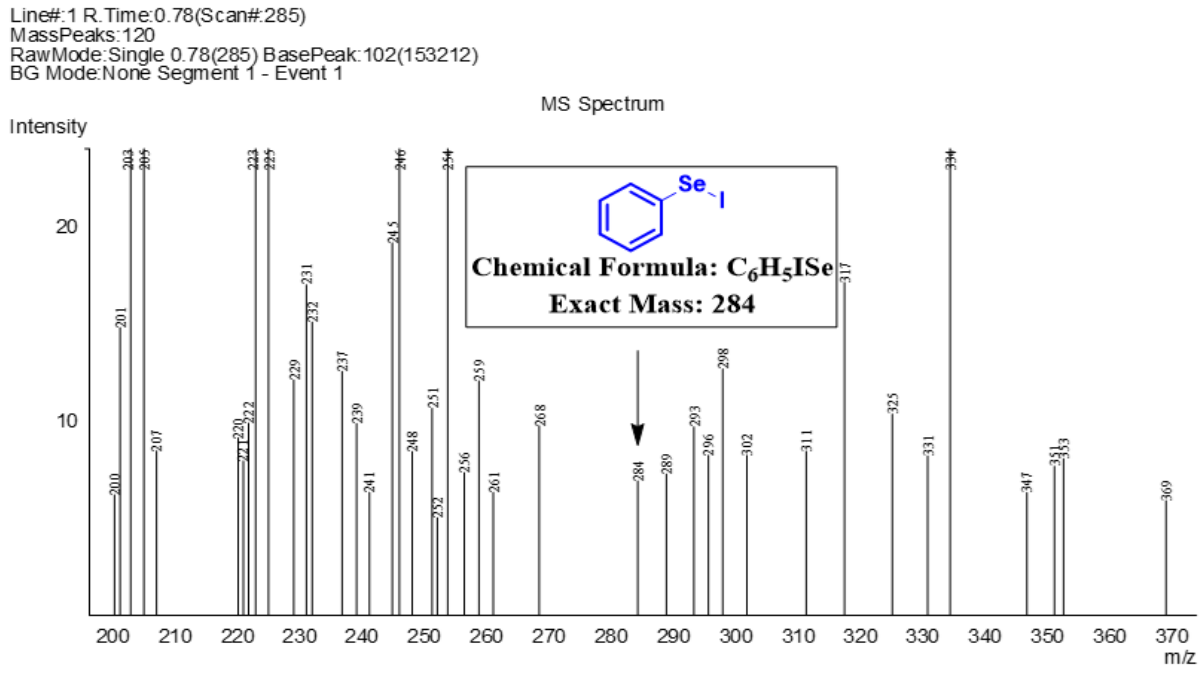

Figure 4.3.5. Mass Spectrum of the Reaction Mixture of Diphenyl Diselenide and I_2.

Scheme 4.3.5. *In situ* Detection of PhSeI and The Reactions of **1a** with PhSeBr, PhSeCl and *in situ* Formed PhSeI.

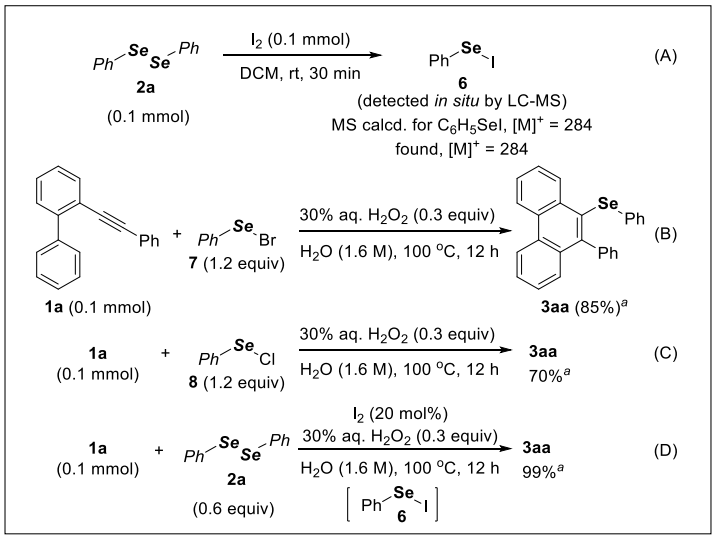

[a]Yield was determined by the ^{1}H NMR of the crude reaction mixture using 1,3,5-trimethoxybenzene as the internal standard.

Calculation of the Bond Dissociation Energies (BDE) for PhSe-X (X = Cl, Br, and I)

The bond dissociation energies (BDE) for PhSe-X (X=Cl, Br, and I) were calculated using the following equation: $BDE_X = E_{PhSe^\bullet} + E_{X^\bullet} - E_{PhSeX}$

where, E_{PhSeX} represents Gibb's free energy for PhSeX (X= Cl, Br, I), $E_{PhSe^\bullet}$ represents Gibb's free energy for $PhSe^\bullet$ radical, and $E_{X^\bullet}$ is Gibb's free energy for halogen radical.

Table 4.3.7. The Bond Dissociation Energies (kcal/mol) of the Se-X bond (X = Cl, Br, I) at the M06-2X/LanL2DZ Level of Theory in Water as an Implicit Solvent.

System	Bond dissociation energy (Se-X bond, X=Cl, Br, I)
PhSeCl	47.53
PhSeBr	39.57
PhSeI	34.40

Next, to figure out the involvement of any free radical, the reaction of **1a** with **2a** was conducted in the presence of various radical quenchers such as TEMPO, BHT, galvinoxyl radical, and ethene-1,1-diyldibenzene. In all cases, the yield of **3aa** gradually decreased along with the increment of the stoichiometry of the corresponding quencher (Table 4), revealing the involvement of free radicals in the reaction. Moreover, (2,2-diphenylvinyl)(phenyl)selane **9**

was detected in situ by LC-MS (Fig. 4.3.6) in the radical quenching experiment using ethene-1,1-diyldibenzene as the quencher which revealed that the reaction involved the *in situ* formation of phenylselenyl radical from **2a** (Scheme 4.3.6).[5]

Table 4.3.8. Radical Quenching Experiments[a].

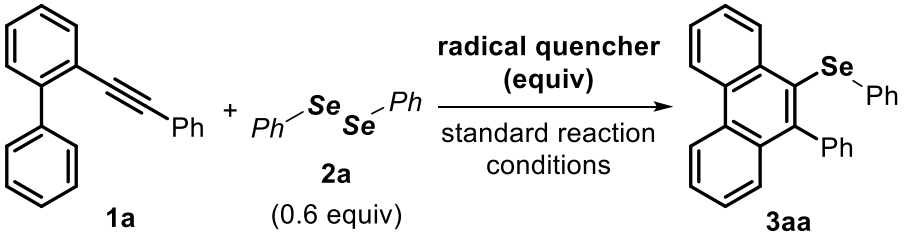

1a **2a** (0.6 equiv) **3aa**

entry	radical quencher (equiv)	yield (%)
1	TEMPO (1.5)	90
2	TEMPO (3.0)	25
3	TEMPO (6.0)	trace
4	BHT (1.5)	87
5	BHT (3.0)	50
6	galvinoxyl (1.5)	36
7	galvinoxyl (3.0)	20
8	ethene-1,1-diyldibenzene (1.5)	80
9	ethene-1,1-diyldibenzene (3.0)	30

[a]Reactions were conducted in 0.1 mmol scale; [b]yield was determined by the ^{1}H NMR of the crude reaction mixture using 1,3,5-trimethoxybenzene as the internal standard.

Scheme 4.3.6. Radical Quenching Experiment using ethene-1,1-diyldibenzene and *in situ* Detection of **9**.

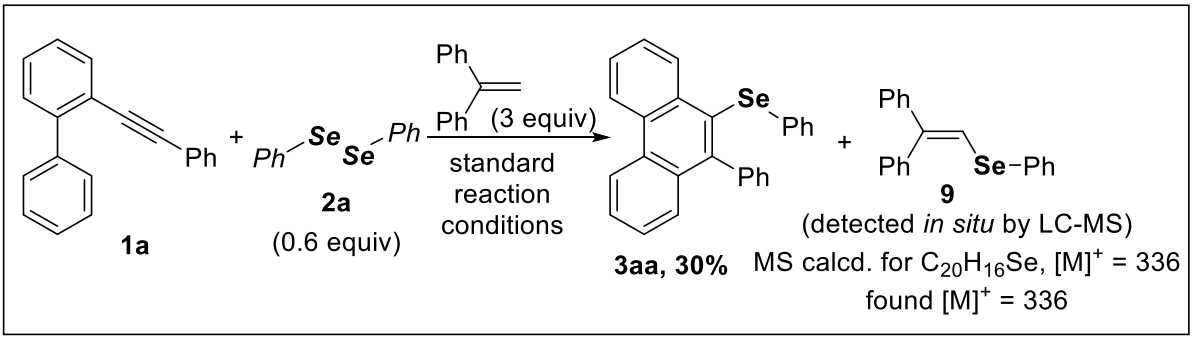

1a **2a** (0.6 equiv) **3aa, 30%** **9**

(detected *in situ* by LC-MS)

MS calcd. for $C_{20}H_{16}Se$, $[M]^+$ = 336

found $[M]^+$ = 336

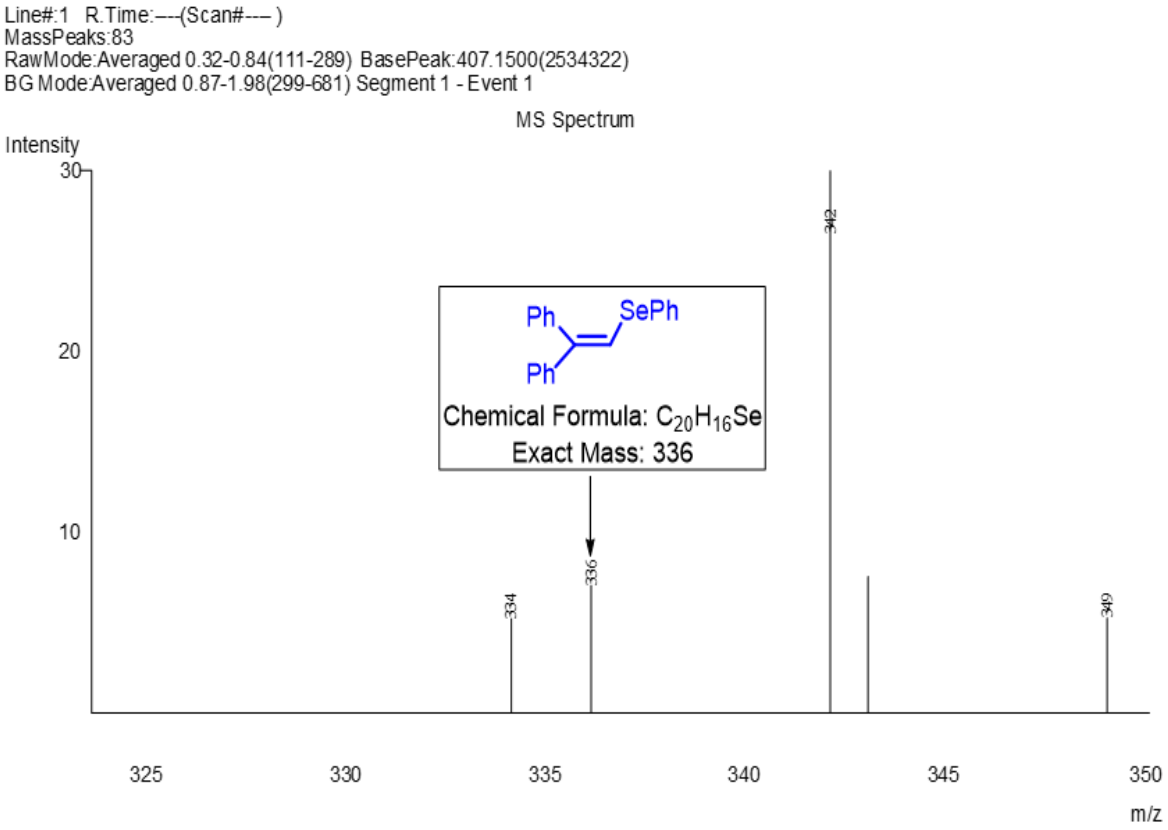

Figure 4.3.6. Mass Spectrum of the Reaction Mixture of **1a** and Diphenyl Diselenide **2a** in the Presence of Radical Quencher, Ethene-1,1-diyldibenzene under Standard Reaction Conditions.

To further validate the radical pathway for the oxidative selenylative annulation of 2-alkynyl biaryls, particularly to investigate any possibility of the involvement of the polar (ionic) pathway in the reaction, we conducted computational studies. Specifically, to investigate the minimum energy pathway for forming **3aa** from **1a** and 6, formed in situ from **2a** and iodine, we employed Density Functional Theory (DFT) calculations using Gaussian09 package[5] with water as the implicit solvent (Fig 4.3.7). We investigated both the radical and polar pathways. We noted that the free energy barrier for the initial step for the polar pathway is highly energy demanding (ΔG# = 31.75 kcal/mol, Fig. 4.3.8), suggesting that the polar pathway is not likely to be operative under reaction conditions (at 100 ºC). The radical mechanism entails homolytic cleavage of phenylselenyl iodide (PhSeI) to phenylselenyl radical (PhSe$^{\bullet}$), **11**, and iodine radical (I$^{\bullet}$). The conversion of the PhSeI (singlet) → PhSe$^{\bullet}$ + I$^{\bullet}$ (triplet) is endergonic (ΔG = 15.98 kcal/mol). In the first step after the formation of radicals, PhSe• and I$^{\bullet}$ interact with the triple bond of 2-(phenylethynyl)-1,1′-biphenyl, **1a** to from intermediate A (our reference point

for free energy profile) (Figure 3). Subsequently, **A** transforms to **10** with a low free energy barrier of 8.91 kcal/mol through the transition state $\mathbf{TS_{1a}}$. In the next step, **10** undergoes C-C bond rotation to form 10′. We noticed π – π interaction between phenyl rings of the phenylethynyl and phenylselenyl groups during these conformational arrangements. The transformation from **10′→11** (new C-C bond formation) through $\mathbf{TS_b}$ required high activation free energy (19.45 kcal/mol) due to loss in the aromaticity of a phenyl ring of the biphenyl group. However, intermediate **11** is stabilized by the delocalization of the radical over the remaining double bonds of the phenanthrenyl ring. Due to such stabilization over previous vinyl radical (**10**), **11** is almost thermoneutral to **A** (ΔG = 1.39 kcal/mol). Subsequently, the formation of **3aa** from **11** involves the abstraction of a proton from the phenyl ring. This step is energetically demanding with an activation free energy barrier of 21.02 kcal/mol through $\mathbf{TS_c}$.

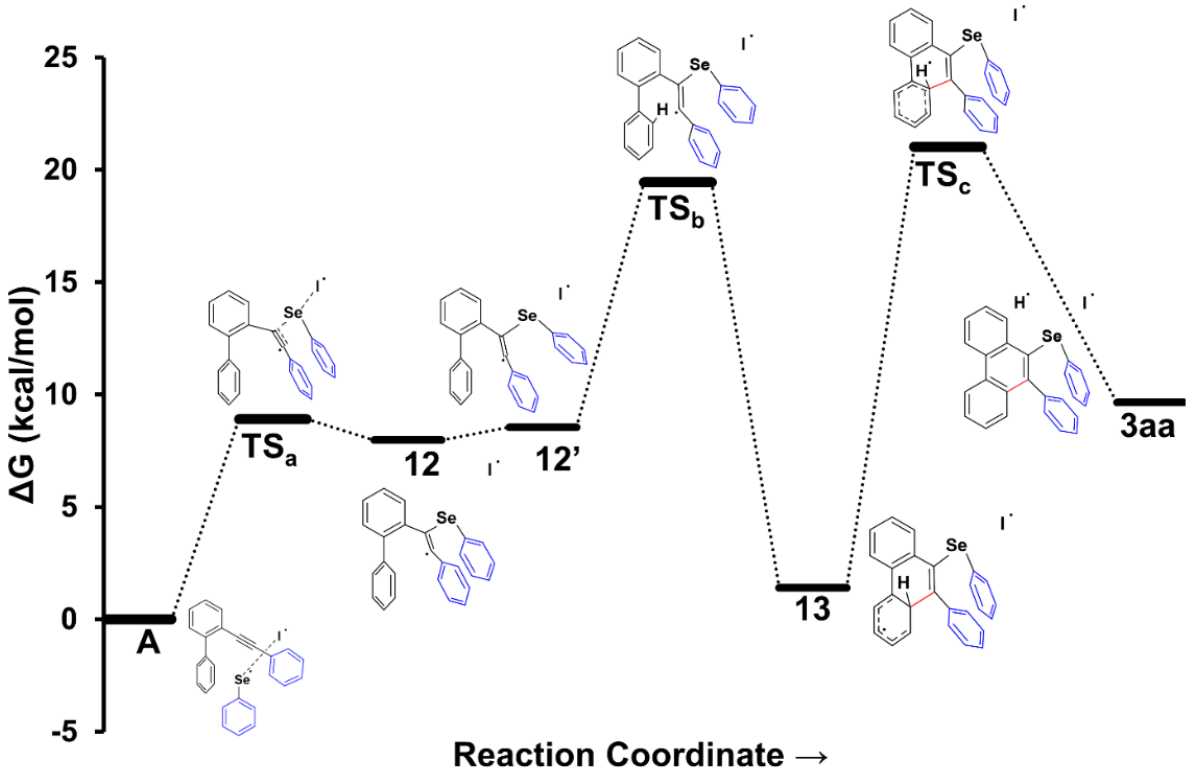

Figure 4.3.7. Free Energy Profile for the Conversion of **1a** and PhSeI **6**, Formed *in situ* from Diphenyl Diselenide **2a** and I_2, to **3aa** through the Radical Pathway in Water as Implicit Solvent at LanL2DZ/M06-2X Level of Theory. Free Energies are Referenced to the Intermediate **A**.

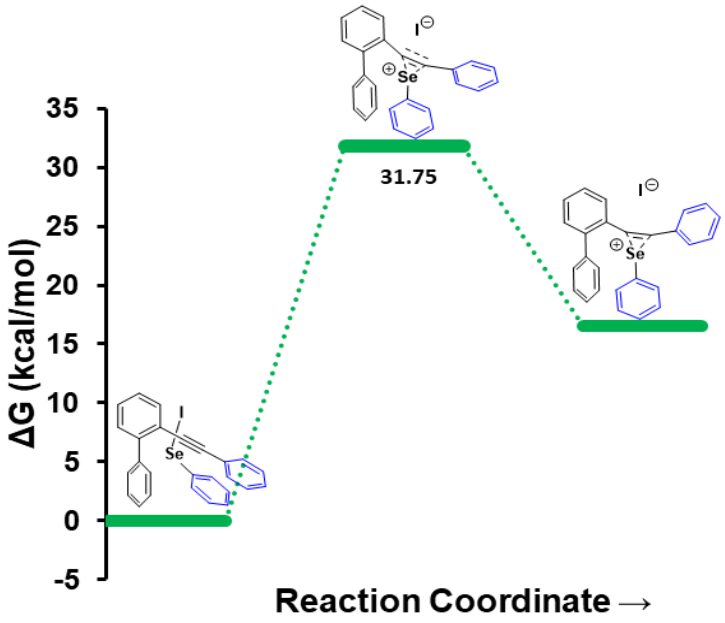

Figure 4.3.8. Free Energy Profile for the Initial Step for the Conversion of **1a** and PhSeI to **3aa** through the Polar Pathway in Water.

Scheme 4.3.7. Proposed Reaction Mechanism.

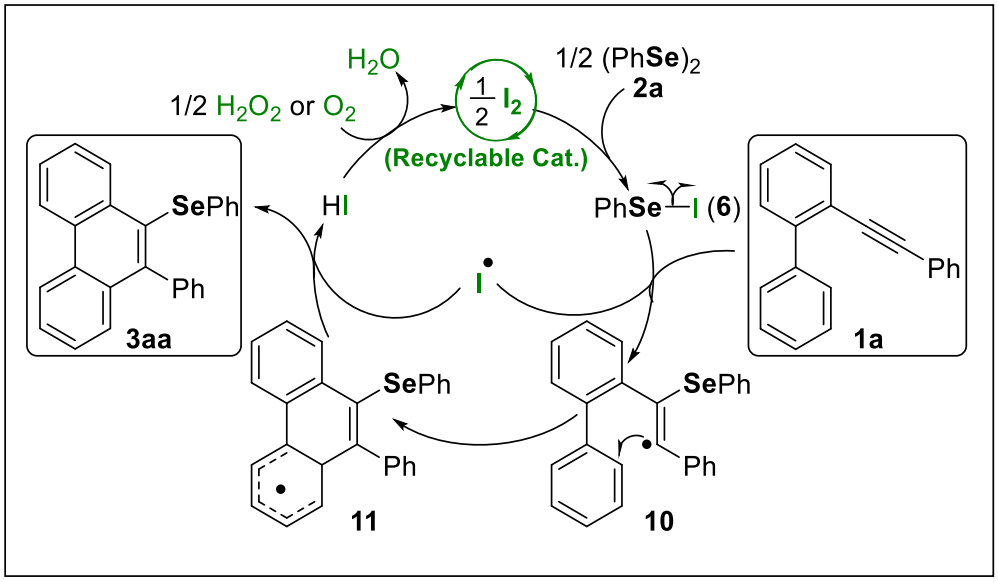

Based on the experimental and computational studies we proposed a reaction mechanism for synthesizing **3aa** from **1a** and **2a** as outlined in Scheme 4.3.7. At first, phenylselenyl iodine, PhSeI **6** was formed in situ from **1a** and **2a**.[6] Then, PhSeI underwent homolytic cleavage under

the reaction conditions to form iodine radical ($I^{\bullet}$) and phenylselenyl radical ($PhSe^{\bullet}$), which immediately added to **1a** to form the corresponding vinyl radical **10**. Intramolecular cyclization of the vinyl radical **10** with the tethered phenyl ring furnished highly stable phenanthrenyl radical **11**. Abstraction of a hydrogen atom by the iodine radical, driven by the aromatic stabilization energy, furnished the desired product **3aa** along with the generation of HI, which subsequently underwent oxidation by H_2O_2 or aerobic oxygen to regenerate molecular iodine in the catalytic cycle.

4.3.3. Conclusions.

We have developed a metal-free, highly atom-economic, cost-effective, scalable, and sustainable synthetic strategy of oxidative selenylative annulation of 2-alkynyl biaryls or 2-heteroaryl-substituted alkynyl benzenes with ready available diselenides in water, for the first time, through the *in situ* formation of the corresponding selenyl iodides. The organic transformation required only a couple of inexpensive reagents, such as iodine as a catalyst and H_2O_2 as a green oxidant only in sub-stoichiometric amounts (0.3 equiv). A wide variety of selanyl PAHs such as phenanthrenes, benzo[*c*]phenanthrene, benzo[*g*]chrysene, and dibenzo[*ij*,*no*]tetraphene and also selanyl polycyclic heteroaromatics such as naphtho[2,1-b]thiophene and naphtho[2,1-b]furan were synthesized in moderate to excellent yield. In contrast to the previously reported electrophilic (ionic) selenylative annulations of 2-alkynyl biaryls,[3,6,7] we unveiled and proposed that the reaction mechanism operates through a radical pathway but not through a polar (ionic) pathway, as supported by both experimental and computational studies. The in situ formed phenylselenyl iodide (PhSeI) was found to be more reactive than the commercially available PhSeBr or PhSeCl for the synthesis of selanyl PAHs or polycyclic aromatic hydrocarbons. Several synthesized products, such as **3aa**, **3ab**, and **3ac** were further synthetically diversified to some interesting new molecules. The notable advantages of this radical selenylative annulation over the previously reported electrophilic (ionic) annulations of 2-alkynyl biaryls are a) transition-metal-free protocol, b) use of iodine as a catalyst, c) use of sub-stoichiometric H_2O_2 and aerial oxygen as the green oxidants, d) use of water as a solvent, e) broad substrate scope in accessing a wide variety of selanyl PAHs, f) water was formed as the only major waste, f) straight-forward scale-up process, g) excellent green chemistry parameters such as high atom-economy (95.8%), high atom-efficiency (93.9%), high carbon-efficiency (95.01%), high reaction-mass-efficiency (86.7%), low E-

factor (1.68) and high EcoScale score (70). All the green parameters of this radical selenylative annulation strategy in synthesizing selanyl PAHs would obviously be superior to those of the previously reported electrophilic (ionic) annulation strategies. Moreover, selanyl polycyclic heteroaromatics were also successfully synthesized in water by this protocol for the first time, to the best of our knowledge. Significantly, the catalyst, iodine was recovered after the reaction during column chromatography stage and recycled twice successfully without any compromisation in the yield of the product. Hence, we believe this green strategy of radical selenylative annulation will find practical applications in synthesizing other classes of valuable or challenging molecules.

4.3.4. Experimental Section.

General Experimental Procedure for the Synthesis of 9-Selenylphenanthrenes (3aa-3ah and 3ba−3ma) and Selenyl Polycyclic Heteroaromatics (3na and 3oa).

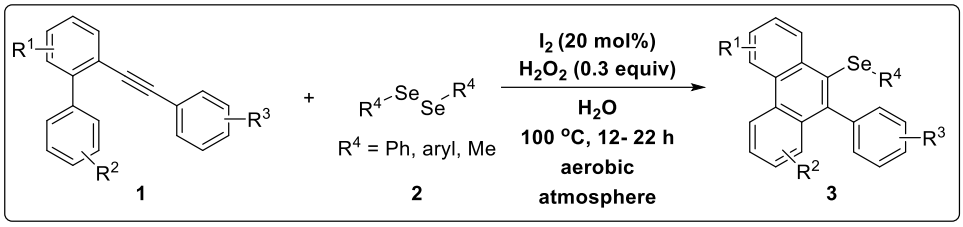

Representative Experimental Procedure for the Synthesis of Phenyl(10-phenylphenanthren-9-yl)selane (3aa): 2-(phenylethynyl)-1,1'-biphenyl **1a** (0.127 g, 0.5 mmol, 1 equiv), 1,2-diphenyldiselane **2a** (0.094 g, 0.3 mmol, 0.6 equiv) and I_2 (0.0254 g, 0.1 mmol) were taken in a round-bottomed flask (RBF) and H_2O (0.3 mL) was added to it. Then 30% aqueous H_2O_2 (v/v) (0.012 mL, 0.15 mmol, 0.3 equiv) was added to the RBF and the reaction mixture was stirred in an oil bath at 100 ^oC under aerobic atmosphere. The progress of the reaction was monitored by TLC. The solution was then transferred to a separating funnel for extraction. The reaction mixture was extracted with ethyl acetate twice (2 X 20 mL) and the combined organic layer was washed with water (3 X 10 mL). The solvent was evaporated under reduced pressure and iodine was recovered from the reaction mixture first by column chromatography using pentane as eluent. The column chromatography process was further continued to afford the pure product, phenyl(10-phenylphenanthren-9-yl)selane **3aa** (0.202 g, 0.495 mmol) in 98% yield using hexane as eluent.

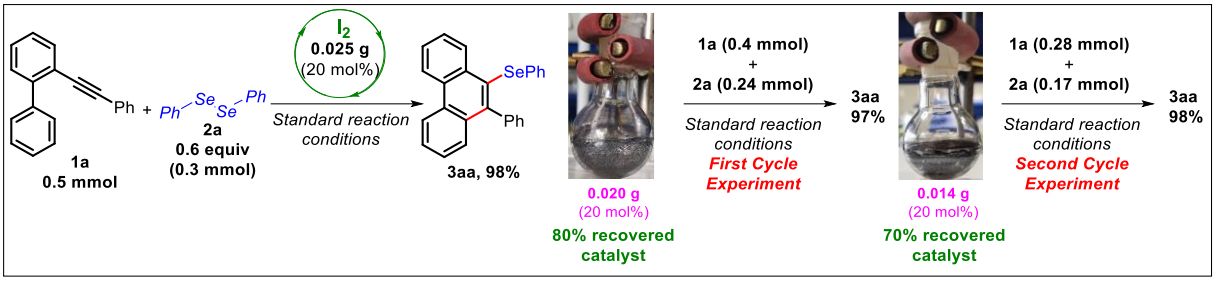

Experimental Procedure for the Synthesis of 9-Phenyl-10-(phenylseleninyl)phenanthrene.

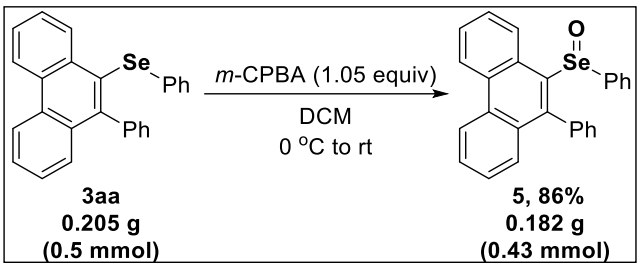

3-Chloroperoxybenzoic acid, *m*-CPBA (purity: 65-70%) (0.140 g, 0.525 mmol) was added to a solution of phenyl(10-phenylphenanthren-9-yl)selane **3aa** (0.205 g, 0.5 mmol) dissolved in dichloromethane (2.5 mL) at 0 °C. The reaction mixture was cooled at 0 °C. Then, the reaction mixture was stirred vigorously for 2 h. After the completion of the reaction the solvent was evaporated under reduced pressure. The crude reaction mixture was extracted with dichloromethane thrice (3 x 10 mL). The combined organic layer was washed with water (3 x 10 mL) and evaporated under reduced pressure. The crude product was purified by flash column chromatography through silica gel to afford the 9-phenyl-10-(phenylseleninyl)phenanthrene ***5*** in (0.182 g, 0.43 mmol) in 86% yield.

Experimental Procedure of Suzuki Coupling Reaction of 4-Bromophenyl)(10-phenylphenanthren-9-yl)selane 3ab and (2-Bromo-10-phenylphenanthren-9-yl)(phenyl)selane 3ca.

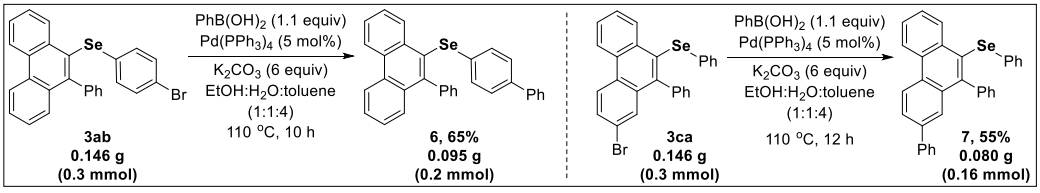

Representative Experimental Procedure for the Suzuki Reaction with 3ab: 4-Bromophenyl)(10-phenylphenanthren-9-yl)selane **3ab** (0.146 g, 0.3 mmol, 1 equiv), phenyl boronic acid (0.040 g, 0.33 mmol), $Pd(PPh_3)_4$ (0.017 g, 0.015 mmol), K_2CO_3 (0.248 g, 1.8

mmol) and solvent (0.96 mL, EtOH : H_2O : PhMe = 1:1:4.4) were taken in a 25 mL round-bottom flask (RBF). The reaction mixture was refluxed at 110 ^oC and the progress of the reaction was monitored by thin layer chromatography. The mixture was cooled to room temperature and extracted with ethyl acetate (30x3 mL) three times. The combined organic layer was further washed with brine (30 mL) and subsequently dried over anhydrous Na_2SO_4. Finally the solvent was evaporated under reduced pressure to get the crude product which was purified by flash column chromatography on silica gel to afford [1,1'-biphenyl]-4-yl(10-phenylphenanthren-9-yl)selane **6** (0.0958 g, 0.2 mmol) in 65% yield.

4.3.5. Analytical Data of All Aynthesized Products (3aa - 3ah, 3ba - 3oa and 5, 6, 7).

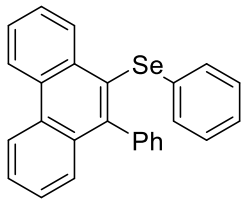

Phenyl(10-phenylphenanthren-9-yl)selane (3aa):[3] Yellow solid (0.201 g, 98%); eluent hexane; mp = 82−84 ^oC; **^{1}H NMR (400 MHz, $CDCl_3$)** δ 8.85 – 8.74 (m, 3H), 7.72 (m, 2H), 7.62 (ddd, *J* = 8.2, 7.0, 1.2 Hz, 1H), 7.56 – 7.50 (m, 2H), 7.50 – 7.46 (m, 3H), 7.33 – 7.27 (m, 2H), 7.10 (d, *J* = 1.5 Hz, 5H). **^{13}C NMR (100 MHz, $CDCl_3$)** δ 146.81, 141.95, 134.23, 132.42, 132.13, 131.07, 130.70, 130.62, 129.65, 129.13, 128.90, 127.94, 127.61, 127.57, 127.43, 127.29, 127.02, 126.72, 125.47, 122.68, 122.55 (Overlapping peaks are present). **^{77}Se NMR (76 MHz, DMSO-d_6)** δ 318.29 (s).

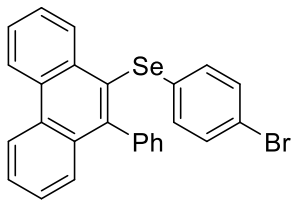

4-Bromophenyl)(10-phenylphenanthren-9-yl)selane (3ab): Yellow solid (0.185 g, 76%); eluent hexane; mp = 127−129 ^oC; **^{1}H NMR (400 MHz, $CDCl_3$)** δ 8.61 (t, *J* = 7.4 Hz, 2H), 8.50 (dd, *J* = 8.3, 1.0 Hz, 1H), 7.56 – 7.50 (m, 2H), 7.43 (ddd, *J* = 8.2, 7.0, 1.2 Hz, 1H), 7.37 – 7.27 (m, 5H), 7.10 – 7.06 (m, 2H), 7.02 – 6.96 (m, 2H), 6.78 – 6.70 (m, 2H). **^{13}C NMR (100 MHz, $CDCl_3$)** δ 146.99, 141.75, 133.18, 132.11, 132.02, 131.88, 131.09, 130.74, 130.59, 130.31, 129.54, 128.91, 127.99, 127.68, 127.61, 127.40, 127.14, 126.81, 122.78, 122.55, 119.35 55 (Overlapping peaks are present).**^{77}Se NMR (76 MHz, $CDCl_3$)** δ 323.21 (s). **HRMS (ESI)** m/z calcd for $C_{26}H_{17}BrSe$ [M]: 487.9679; found: 487.9665.

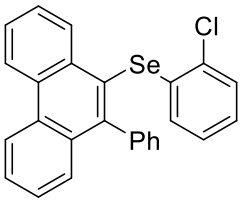

(2-Chlorophenyl)(10-phenylphenanthren-9-yl)selane (3ac): Yellow solid (0.160 g, 72%); eluent hexane; **^{1}H NMR (400 MHz, CDCl$_3$)** δ 8.84 (t, *J* = 8.8 Hz, 2H), 8.70 (dd, *J* = 8.3, 1.0 Hz, 1H), 7.75 (ddd, *J* = 15.7, 7.7, 1.3 Hz, 2H), 7.67 – 7.60 (m, 2H), 7.58 – 7.53 (m, 1H), 7.52 – 7.47 (m, 3H), 7.33 (ddd, *J* = 6.0, 3.4, 1.5 Hz, 3H), 7.03 (td, *J* = 7.7, 1.5 Hz, 1H), 6.85 (td, *J* = 7.8, 1.3 Hz, 1H), 6.70 (dd, *J* = 8.0, 1.5 Hz, 1H). **^{13}C NMR (100 MHz, CDCl$_3$)** δ 147.63, 141.55, 134.67, 132.31, 132.12, 132.09, 131.21, 130.70, 130.27, 129.45, 129.25, 129.07, 128.97, 127.98, 127.76, 127.69, 127.44, 127.19, 127.04, 126.77, 126.71, 126.20, 122.74, 122.56. **^{77}Se NMR (76 MHz, CDCl$_3$)** δ 321.32 (s). **HRMS (ESI)** m/z calcd for $C_{26}H_{17}ClSe$ [M]: 444.0184; found: 444.0191.

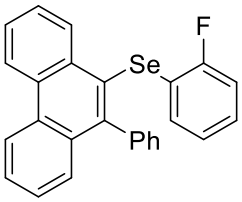

(2-Fluorophenyl)(10-phenylphenanthren-9-yl)selane (3ad): Yellow solid (0.151 g, 71%); eluent hexane; **^{1}H NMR (400 MHz, CDCl$_3$)** δ 8.81 (d, *J* = 8.8 Hz, 2H), 8.65 (dd, *J* = 8.3, 1.0 Hz, 1H), 7.74 – 7.68 (m, 2H), 7.61 – 7.57 (m, 1H), 7.51 – 7.49 (m, 2H), 7.47 – 7.43 (m, 3H), 7.27 (s, 1H), 7.25 – 7.24 (m, 1H), 7.05 (dtd, *J* = 6.4, 5.4, 2.7 Hz, 1H), 6.98 – 6.93 (m, 1H), 6.77 – 6.72 (m, 1H), 6.70 – 6.65 (m, 1H). **^{13}C NMR (100 MHz, CDCl$_3$)** δ 159.79 (d, $^{1}J_{C\text{-}F}$ = 241 Hz), 147.50, 141.68, 132.22 (d, $^{3}J_{C\text{-}F}$ = 18 Hz), 131.18, 130.72, 130.32, 129.50, 128.92, 128.01, 127.68, 127.63, 127.45, 127.28, 127.15, 127.08, 126.79, 125.81, 125.53, 124.68, 124.66, 122.67 (d, $^{3}J_{C\text{-}F}$ = 17 Hz), 120.96 (d, $^{2}J_{C\text{-}F}$ = 22 Hz), 115 (d, $^{2}J_{C\text{-}F}$ = 22 Hz). **^{77}Se NMR (76 MHz, CDCl$_3$)** δ 321.26 (s). **^{19}F NMR (377 MHz, CDCl$_3$)** δ -106.16 (s). **HRMS (ESI)** m/z calcd for $C_{26}H_{17}FSe$ [M]: 428.0480; found: 428.0483.

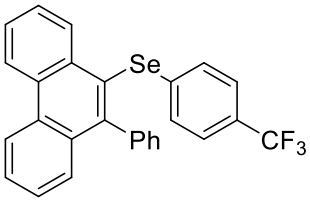

(10-Phenylphenanthren-9-yl)(4-(trifluoromethyl)phenyl)selane (3ae): Yellow solid (0.16 g, 67%); eluent hexane; mp = 190−192 °C; **^{1}H NMR (400 MHz, CDCl$_3$)** δ 8.78 – 8.73 (m, 2H), 8.58 (d, *J* = 8.2 Hz, 1H), 7.66 (m, 2H), 7.56 (dd, *J* = 11.2, 4.0 Hz, 1H), 7.48 – 7.38 (m, 5H), 7.26 – 7.18 (m, 4H), 7.07 (d, *J* = 8.2 Hz, 2H). **^{13}C NMR (100 MHz, CDCl$_3$)** δ 147.40, 141.71, 139.69, 132.07, 131.24, 130.82, 130.17, 129.45, 129.03, 128.61, 128.05, 127.84, 127.82, 127.67, 127.52, 127.30, 126.91, 126.47, 125.61, 125.58, 122.89, 122.62, 120.10. **^{77}Se NMR (76 MHz, CDCl$_3$)** δ 333.47 (s). **^{19}F NMR (76 MHz, CDCl$_3$)** δ -62.44 (s). **HRMS (ESI)** m/z calcd for $C_{27}H_{17}F_3Se$ [M]: 478.0448; found: 478.0447.

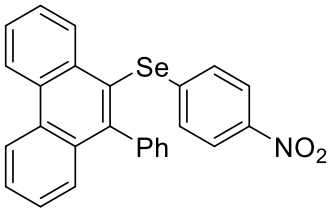

(4-Nitrophenyl)(10-phenylphenanthren-9-yl)selane (3af): Yellow solid (0.151 g, 66%); eluent hexane; mp = 170−172 °C; **^{1}H NMR (400 MHz, CDCl$_3$)** δ 8.74 (d, *J* = 4.0 Hz, 2H), 8.49 (d, *J* = 7.8 Hz, 1H), 7.82 (d, *J* = 8.0 Hz, 2H), 7.67 (d, *J* = 5.6 Hz, 2H), 7.58 – 7.53 (m, 1H), 7.44 (d, *J* = 26.3 Hz, 5H), 7.19 (s, 2H), 7.06 (d, *J* = 7.9 Hz, 2H). **^{13}C NMR (100 MHz, CDCl$_3$)** δ 147.74, 145.61, 145.13, 141.50, 131.99, 131.79, 131.35, 130.93, 129.79, 129.29, 129.12, 128.39, 128.13, 128.09, 127.99, 127.71, 127.49, 127.05, 125.82, 123.79, 123.04, 122.68. **^{77}Se NMR (76 MHz, CDCl$_3$)** δ 350.20 (s). **HRMS (ESI)** m/z calcd for $C_{26}H_{18}NO_2Se$ $[M + H]^+$: 456.0497; found: 456.0499.

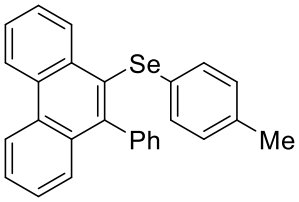

(10-Phenylphenanthren-9-yl)(*p*-tolyl)selane (3ag):[8] White solid (0.146 g, 69%); eluent hexane; mp = 110−112 °C; **^{1}H NMR (400 MHz, CDCl$_3$)** δ 8.85 – 8.74 (m, 3H), 7.71 (m, 2H), 7.61 (m, 1H), 7.57 – 7.44 (m, 5H), 7.36 – 7.28 (m, 2H), 7.01 (d, *J* = 8.2 Hz, 2H), 6.91 (d, *J* = 8.0 Hz, 2H), 2.24 (s, 3H). **^{13}C NMR (100 MHz, CDCl$_3$)** δ 146.62, 142.03, 135.26, 132.45, 132.13, 131.02, 130.69, 130.32, 129.73, 129.28, 128.85, 127.93, 127.51, 127.34, 127.25, 126.94, 126.68, 122.65, 122.52, 20.8855 (Overlapping peaks are present).

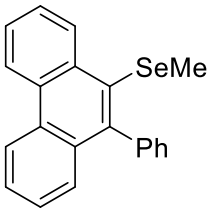

Methyl(10-phenylphenanthren-9-yl)selane (3ah): Yellow solid (0.129 g, 74%); eluent hexane; mp = 150−152 °C; **^{1}H NMR (400 MHz, CDCl$_3$)** δ 8.77 (d, *J* = 7.5 Hz, 1H), 8.66 (t, *J* = 7.7 Hz, 2H), 7.62 (dd, *J* = 6.3, 2.5 Hz, 2H), 7.56 – 7.53 (m, 1H), 7.44 – 7.42 (m, 2H), 7.36 – 7.33 (m, 2H), 7.23 (dd, *J* = 5.4, 1.5 Hz, 2H), 7.15 (d, *J* = 2.4 Hz, 1H), 1.96 (s, 3H). **^{13}C NMR (100 MHz, CDCl$_3$)** δ 145.44, 142.42, 132.32, 131.92, 130.55, 130.35, 129.94, 129.37, 128.53, 128.01, 127.68, 127.43, 127.21, 126.99, 126.81, 126.64, 122.91, 122.44, 10.04. **^{77}Se NMR (76 MHz, CDCl$_3$)** δ 118.24 (s). **Anal** calcd for $C_{21}H_{16}Se$: C, 72.62; H, 4.64; found C, 72.26; H, 4.92.

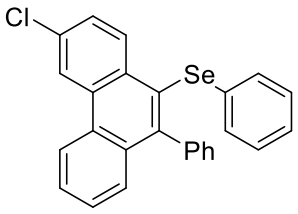

(6-Chloro-10-phenylphenanthren-9-yl)(phenyl)selane (3ba): Off White solid (0.120 g, 54%); eluent hexane; mp = 163−165 °C; **^{1}H NMR (400 MHz, CDCl$_3$)** δ 8.72 (d, *J* = 2.1 Hz, 1H), 8.69 (d, *J* = 8.4 Hz, 1H), 8.63 (d, *J* = 8.9 Hz, 1H), 7.71 (m, 1H), 7.53 – 7.43 (m, 6H),

7.25 – 7.22 (m, 2H), 7.10 – 7.00 (m, 5H). **^{13}C NMR (100 MHz, $CDCl_3$)** δ 147.04, 141.63, 133.87, 133.28, 132.45, 132.36, 131.80, 130.86, 130.09, 129.61, 129.20, 129.03, 128.03, 127.93, 127.72, 127.47, 127.39, 127.14, 125.72, 122.63, 122.32 55 (Overlapping peaks are present). **^{77}Se NMR (76 MHz, $CDCl_3$)** δ 325.10 (s). **HRMS (ESI)** m/z calcd for $C_{26}H_{17}ClSe$ [M]: 444.0184; found: 444.0190; the assignment is also supported by an X-ray crystallographic structure determination (**CCDC 2176784**).

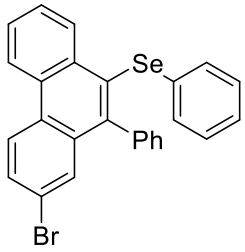

(2-Bromo-10-phenylphenanthren-9-yl)(phenyl)selane (3ca): Yellowish viscous solid (0.210 g, 86%); eluent hexane; mp = 190−192 °C; **^{1}H NMR (400 MHz, $CDCl_3$)** δ 9.03 – 8.89 (m, 2H), 8.85 – 8.75 (m, 1H), 7.95 – 7.82 (m, 3H), 7.81 – 7.77 (m, 1H), 7.66 (dd, *J* = 4.5, 2.2 Hz, 4H), 7.49 – 7.43 (m, 2H), 7.26 (s, 4H). **^{13}C NMR (100 MHz, $CDCl_3$)** δ 146.76, 145.53, 141.89, 141.06, 133.89, 133.44, 132.30, 130.84, 130.75, 130.45, 130.12, 129.56, 129.21, 128.93, 128.11, 127.59, 126.98, 126.68, 125.62, 124.31, 122.52, 121.01. **^{77}Se NMR (76 MHz, $CDCl_3$)** δ 328.34 (s). **HRMS (ESI)** m/z calcd for $C_{26}H_{17}BrSe$ $[M]^+$: 487.9679; found: 487.9707.

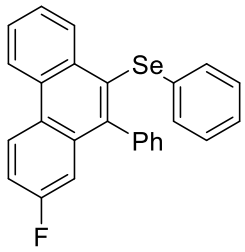

(2-Fluoro-10-phenylphenanthren-9-yl)(phenyl)selane (3da): Yellow solid (0.161 g, 75%); eluent hexane; mp = 140−142 °C; **^{1}H NMR (400 MHz, $CDCl_3$)** δ 8.79 – 8.75 (m, 1H), 8.74 – 8.71 (m, 1H), 8.68 (d, *J* = 8.1 Hz, 1H), 7.69 (m, 1H), 7.58 (m, 1H), 7.46 (dd, *J* = 5.0, 1.9 Hz, 3H), 7.45 – 7.41 (m, 1H), 7.26 – 7.22 (m, 2H), 7.14 (dd, *J* = 10.8, 2.7 Hz, 1H), 7.07 (s, 5H). **^{13}C NMR (100 MHz, $CDCl_3$)** δ 161.18 (d, $^{1}J_{C\text{-}F}$ = 245 Hz), 145.98, 141.40, 133.97, 133.64 (d, $^{3}J_{C\text{-}F}$ = 8 Hz), 131.97, 130.79, 130.34, 129.56, 129.30, 129.23, 128.97, 128.16, 127.67, 127.58, 127.38, 125.66, 124.90 (d, $^{3}J_{C\text{-}F}$ = 9 Hz) 122.52, 116.3 (d, $^{2}J_{C\text{-}F}$ = 24 Hz), 113.27 (d, $^{2}J_{C\text{-}F}$ = 22 Hz) (Overlapping peaks are present). **^{77}Se NMR (76 MHz, $CDCl_3$)** δ 327.35 (s). **^{19}F NMR (377 MHz, $CDCl_3$)** δ -113.38 (s). **HRMS (ESI)** m/z calcd for $C_{26}H_{17}FSe$ $[M]^+$: 428.0480; found: 428.0506.

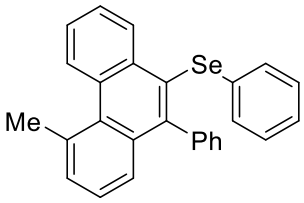

(4-Methyl-10-phenylphenanthren-9-yl)(phenyl)selane (3ea): Off White solid (0.176 g, 83%); eluent hexane; mp = 130−132 °C; **^{1}H NMR (400 MHz, $CDCl_3$)** δ 8.79 (d, *J* = 8.0 Hz, 1H), 8.75 (dd, *J* = 8.2, 1.4 Hz, 1H), 7.52 (m, 3H), 7.42 – 7.34 (m, 4H), 7.28 (dd, *J* = 8.1, 7.1 Hz, 1H), 7.19 (dd, *J* = 6.4, 3.1 Hz, 2H), 7.05 – 6.94 (m, 5H), 3.11 (s, 3H). **^{13}C NMR (100 MHz, $CDCl_3$)** δ 147.13, 142.61, 134.85, 134.21, 133.58, 133.28, 132.00, 131.82, 131.29, 130.31, 129.65, 129.13, 128.87, 127.90, 127.74, 127.62, 127.30, 127.17, 126.81, 125.73, 125.55, 125.42, 27.22. **^{77}Se NMR (76 MHz, $CDCl_3$)** δ 324.16 (s). The assignment is supported by an X-ray crystallographic structure determination (**CCDC 2176838).**

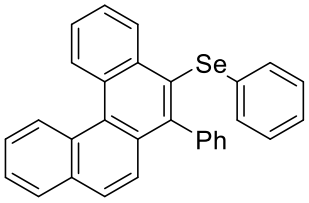

Phenyl(6-phenylbenzo[*c*]phenanthren-5-yl)selane (3fa):[7] Off White solid (0.102 g, 44%); eluent hexane; mp = 122−124 °C; **^{1}H NMR (400 MHz, $CDCl_3$)** δ 9.11 (t, *J* = 8.3 Hz, 2H), 8.84 (d, *J* = 8.2 Hz, 1H), 8.01 (d, *J* = 7.6 Hz, 1H), 7.81 – 7.58 (m, 6H), 7.47 (m, 4H), 7.28 (dd, *J* = 7.2, 2.2 Hz, 2H), 7.08 (s, 5H). **^{13}C NMR (100 MHz, $CDCl_3$)** δ 146.01, 141.94, 134.24, 133.65, 133.45, 130.51, 130.26, 130.02, 129.55, 129.44, 129.09, 128.93, 128.86, 128.57, 128.19, 127.98, 127.40, 127.12, 127.03, 126.56, 126.22, 126.18, 125.70, 125.60.

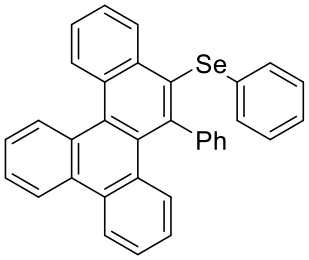

Phenyl(5-phenylbenzo[*g*]chrysen-6-yl)selane (3ga):[7] Off White solid (0.140 g, 55%); eluent hexane; mp = 210−212 °C; **^{1}H NMR (400 MHz, $CDCl_3$)** δ 8.81 – 8.66 (m, 4H), 8.58 (d, *J* = 8.0 Hz, 1H), 7.71 (m, 2H), 7.63 – 7.53 (m, 3H), 7.50 – 7.34 (m, 6H), 7.06 (s, 6H). **^{13}C NMR (100 MHz, $CDCl_3$)** δ 144.55, 143.37, 134.51, 133.77, 131.40, 131.29, 130.67, 130.25, 130.09, 129.93, 129.84, 129.54, 129.27, 129.14, 128.90, 128.67, 128.10, 127.88, 127.57, 127.23, 126.95, 126.49, 126.21, 125.97, 125.70, 125.61, 123.54, 123.03.

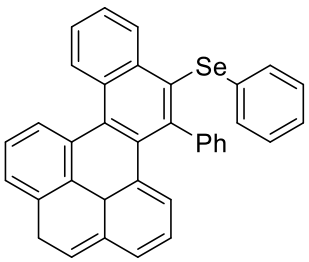

Phenyl(14-phenyldibenzo[*ij*,*no*]tetraphen-13-yl)selane (3ha):[7] Brown solid (0.182 g, 68%); eluent hexane; mp = 220−222 °C; **^{1}H NMR (400 MHz, $CDCl_3$)** δ 9.37 (d, *J* = 9.3 Hz, 1H), 9.16 (d, *J* = 8.2 Hz, 1H), 8.87 (dd, *J* = 8.2, 1.1 Hz, 1H), 8.32 (d, *J* = 9.3 Hz, 1H), 8.27 (d, *J* = 7.6 Hz, 1H), 8.16 (d, *J* = 7.2 Hz, 1H), 8.13 (s, 1H), 8.05 (t, *J*

= 7.6 Hz, 1H), 7.98 (d, *J* = 9.0 Hz, 1H), 7.90 (d, *J* = 9.0 Hz, 1H), 7.78 – 7.73 (m, 1H), 7.68 (dd, *J* = 11.1, 4.1 Hz, 1H), 7.58 – 7.52 (m, 3H), 7.40 – 7.36 (m, 2H), 7.15 (dd, *J* = 6.5, 3.3 Hz, 2H), 7.12 – 7.06 (m, 3H). **^{13}C NMR (100 MHz, $CDCl_3$)** δ 146.39, 142.01, 134.17, 133.06, 131.65, 130.95, 130.59, 130.22, 129.97, 129.55, 129.40, 128.98, 128.12, 128.03, 127.85, 127.57, 127.33, 127.19, 127.13, 126.75, 126.40, 126.26, 126.13, 125.65, 125.19, 124.97, 124.76, 124.33.

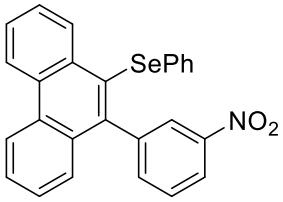

(10-(3-Nitrophenyl)phenanthren-9-yl)(phenyl)selane (3ia): Yellow crystal (0.107 g, 47%); eluent hexane; mp = 150−152 °C; **^{1}H NMR (400 MHz, $CDCl_3$)** δ 8.85 – 8.78 (m, 3H), 8.32 – 8.24 (m, 1H), 8.03 – 7.98 (m, 1H), 7.74 (d, *J* = 8.0 Hz, 2H), 7.66 (d, *J* = 1.2 Hz, 1H), 7.60 – 7.49 (m, 5H), 7.33 (dd, *J* = 8.4, 1.0 Hz, 1H), 7.06 – 7.04 (m, 2H), 6.98 (d, *J* = 1.6 Hz, 1H). **^{13}C NMR (100 MHz, CDC_3)** δ 147.84, 143.16, 136.07, 133.50, 131.40, 131.16, 130.82, 130.58, 129.53, 129.10, 128.89, 128.63, 127.93, 127.89, 127.83, 127.68, 127.11, 126.14, 125.04, 122.92, 122.83, 122.35. **^{77}Se NMR (76 MHz, $CDCl_3$)** δ 352.1 (s). **HRMS (ESI)** m/z calcd for $C_{26}H_{17}NO_2Se$ [M]: 455.0425; found: 455.0436.

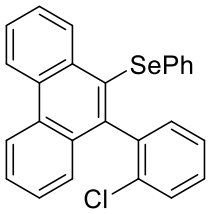

(10-(2-Chlorophenyl)phenanthren-9-yl)(phenyl)selane (3ja) : Yellow crystal (0.120 g, 54%); eluent hexane; **^{1}H NMR (400 MHz, $CDCl_3$)** δ 8.84 (t, *J* = 8.8 Hz, 2H), 8.70 (dd, *J* = 8.3, 1.0 Hz, 1H), 7.75 (m, 2H), 7.67 – 7.60 (m, 2H), 7.58 – 7.53 (m, 1H), 7.52 – 7.47 (m, 3H), 7.33 (ddd, *J* = 6.0, 3.4, 1.5 Hz, 3H), 7.03 (td, *J* = 7.7, 1.5 Hz, 1H), 6.85 (m, 1H), 6.70 (dd, *J* = 8.0, 1.5 Hz, 1H). **^{13}C NMR (100 MHz, $CDCl_3$)** δ 147.63, 141.55, 134.67, 132.31, 132.12, 132.09, 131.21, 130.70, 130.27, 129.45, 129.25, 129.07, 128.97, 127.98, 127.76, 127.69, 127.44, 127.19, 127.04, 126.77, 126.71, 126.20, 122.74, 122.56. **^{77}Se NMR (76 MHz, $CDCl_3$)** δ 322.65 (s). **HRMS (ESI)** m/z calcd for $C_{26}H_{17}ClSe$ [M]: 444.0184; found: 444.0191.

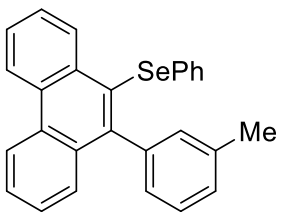

Phenyl(10-(m-tolyl)phenanthren-9-yl)selane (3ka): Yellow solid (0.180 g, 85%); eluent hexane; mp = 140−142 °C; **^{1}H NMR (400 MHz, $CDCl_3$)** δ 8.82 (t, *J* = 7.4 Hz, 3H), 7.73 (m, 2H), 7.68 – 7.59 (m, 2H), 7.57 – 7.51 (m, 1H), 7.41 (t, *J* = 7.5 Hz, 1H), 7.33 (d, *J* = 7.6 Hz, 1H), 7.14 (ddd, *J* = 14.6, 6.8, 2.6 Hz, 7H), 2.43 (s, 3H). **^{13}C NMR (100 MHz, $CDCl_3$)** δ 146.91,

141.82, 137.39, 134.37, 132.48, 132.17, 131.02, 130.61, 130.40, 129.28, 128.92, 128.84, 127.99, 127.80, 127.63, 127.51, 127.36, 126.92, 126.67, 125.47, 122.66, 122.50, 21.50. **^{77}Se NMR (76 MHz, $CDCl_3$)** δ 323.31 (s). **HRMS (ESI)** m/z calcd for $C_{27}H_{20}Se$ [M]: 424.0730; found: 424.0728.

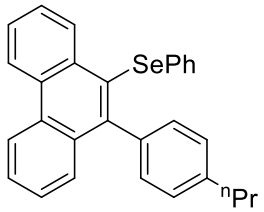

Phenyl(10-(4-propylphenyl)phenanthren-9-yl)selane (3la) : Reddish Brown solid (0.102 g, 45%); eluent hexane; mp = 125−127 °C; **^{1}H NMR (400 MHz, $CDCl_3$)** δ 8.67 (t, *J* = 8.6 Hz, 2H), 8.59 (dd, *J* = 8.3, 1.0 Hz, 1H), 7.61 – 7.55 (m, 2H), 7.49 – 7.45 (m, 1H), 7.42 (dd, *J* = 8.2, 1.4 Hz, 1H), 7.40 – 7.36 (m, 1H), 7.14 (d, *J* = 9.5 Hz, 3H), 7.04 (d, *J* = 8.1 Hz, 2H), 6.95 (s, 4H), 2.63 – 2.58 (m, 2H), 1.66 (dd, *J* = 15.1, 7.5 Hz, 2H), 0.93 (t, *J* = 7.3 Hz, 3H). **^{13}C NMR (100 MHz, $CDCl_3$)** δ 146.93, 141.66, 139.17, 134.35, 132.48, 132.34, 131.06, 130.65, 129.51, 129.28, 128.98, 128.88, 127.98, 127.81, 127.50, 127.36, 126.91, 126.68, 125.47, 122.67, 122.51, 37.92, 24.43, 13.95. **^{77}Se NMR (76 MHz, $CDCl_3$)** δ 323.50 (s). **HRMS (ESI)** m/z calcd for $C_{29}H_{24}Se$ [M]: 452.1043; found: 452.1046; the assignment is supported by an X-ray crystallographic structure determination (CCDC **2170363**).

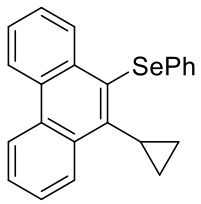

(10-Cyclopropylphenanthren-9-yl)(phenyl)selane (3ma): Brown Viscous liquid(0.101 g, 54%); eluent hexane; **^{1}H NMR (400 MHz, $CDCl_3$)** δ 7.49 – 7.45 (m, 2H), 7.38 – 7.36 (m, 3H), 7.33 – 7.29 (m, 2H), 7.18 – 7.13 (m, 4H), 7.10 – 7.08 (m, 2H), 1.75 (ddd, *J* = 8.2, 5.2, 3.0 Hz, 1H), 0.75 – 0.67 (m, 2H), 0.64 – 0.57 (m, 1H), 0.43 – 0.35 (m, 1H). **^{13}C NMR (100 MHz, $CDCl_3$)** δ 143.49, 140.84, 140.44, 138.06, 134.34, 132.27, 130.95, 130.08, 129.57, 129.46, 129.37, 129.08, 128.85, 128.49, 128.43, 127.81, 127.18, 127.05, 126.43, 104.39, 24.23, 10.38, 9.41. **^{77}Se NMR (76 MHz, $CDCl_3$)** δ 410.69 (s). **Anal** calcd for $C_{23}H_{18}Se$: C, 73.99; H, 4.86; found C, 73.26; H, 4.49.

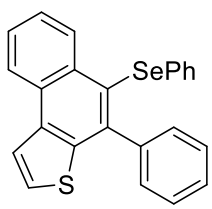

4-Phenyl-5-(phenylselanyl)naphtho[2,1-*b*]thiophene (3na): Yellow solid (0.160 g, 77%); eluent hexane; mp = 95−97 °C; **^{1}H NMR (400 MHz, $CDCl_3$)** δ 8.76 (d, *J* = 8.3 Hz, 1H), 8.42 (dd, *J* = 8.1, 0.6 Hz, 1H), 8.08 (d, *J* = 5.5 Hz, 1H), 7.69 – 7.63 (m, 2H), 7.60 – 7.56 (m, 1H), 7.49 – 7.45 (m,

3H), 7.42 – 7.39 (m, 2H), 7.08 (s, 5H). **^{13}C NMR (100 MHz, $CDCl_3$)** δ 142.45, 141.77, 139.71, 137.00, 134.24, 132.82, 130.45, 129.10, 129.07, 128.89, 128.47, 128.10, 128.02, 126.78, 126.68, 126.56, 125.52, 123.91, 123.86, 122.24. **^{77}Se NMR (76 MHz, $CDCl_3$)** δ 306.69 (s). **HRMS (ESI)** m/z calcd for $C_{24}H_{16}SSe$ [M]: 416.0138; found: 416.0139.

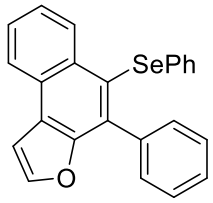

4-Phenyl-5-(phenylselanyl)naphtho[2,1-*b*]furan (3oa): Brown solid (0.080 g, 40%); eluent hexane; **^{1}H NMR (400 MHz, $CDCl_3$)** δ 8.73 (d, *J* = 8.4 Hz, 1H), 8.21 (dd, *J* = 8.1, 0.7 Hz, 1H), 7.77 (d, *J* = 2.1 Hz, 1H), 7.63 (dt, *J* = 4.2, 2.3 Hz, 1H), 7.55 – 7.51 (m, 1H), 7.46 – 7.43 (m, 3H), 7.39 (ddd, *J* = 3.6, 2.4, 1.7 Hz, 2H), 7.36 (d, *J* = 2.1 Hz, 1H), 7.08 – 7.00 (m, 5H). **^{13}C NMR (100 MHz, $CDCl_3$)** δ 150.75, 145.54, 137.38, 134.71, 134.38, 132.19, 131.50, 130.69, 130.05, 129.11, 128.94, 127.98, 127.79, 126.63, 126.01, 125.57, 124.53, 124.14, 123.76, 105.81. **^{77}Se NMR (76 MHz, $CDCl_3$)** δ 302.58 (s). **HRMS (ESI)** m/z calcd for $C_{24}H_{16}OSe$ [M]: 400.0366; found: 400.0359.

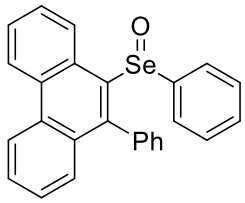

9-Phenyl-10-(phenylseleninyl)phenanthrene (5): Orange crystal (0.182 g, 86%); eluent hexane; mp = 172−175 °C; **^{1}H NMR (400 MHz, $CDCl_3$)** δ 8.99 (d, *J* = 8.2 Hz, 1H), 8.66 (dd, *J* = 14.6, 8.3 Hz, 2H), 7.71 – 7.64 (m, 3H), 7.62 – 7.57 (m, 2H), 7.53 (m, 5H), 7.46 – 7.40 (m, 2H), 7.32 (m, 3H). **^{13}C NMR (100 MHz, $CDCl_3$)** δ 143.71, 141.87, 137.15, 135.40, 131.64, 131.23, 130.59, 130.36, 130.31, 130.15, 129.20, 129.08, 128.59, 128.35, 127.31, 127.23, 127.05, 126.59, 126.11, 122.65, 122.59 (Overlapping peaks are present). **^{77}Se NMR (76 MHz, $CDCl_3$)** δ 895.08 (s). **HRMS (ESI)** m/z calcd for $C_{26}H_{18}OSe$ [M]: 426.0523; found: 426.0656.

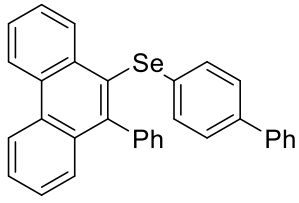

[1,1'-biphenyl]-4-yl(10-phenylphenanthren-9-yl)selane (6): Yellow liquid (0.095 g, 65%); eluent hexane; **^{1}H NMR (400 MHz, $CDCl_3$)** δ 8.86 – 8.76 (m, 3H), 7.72 (dd, *J* = 3.2, 1.8 Hz, 2H), 7.63 (d, *J* = 1.2 Hz, 1H), 7.54 – 7.53 (m, 1H), 7.52 – 7.47 (m, 6H), 7.40 (dd, *J* = 8.2, 6.8 Hz, 2H), 7.34 – 7.30 (m, 5H), 7.17 – 7.12 (m, 2H). **^{13}C NMR (100 MHz, $CDCl_3$)** δ 146.89, 141.94, 140.40, 138.37, 133.41, 132.43, 132.15, 131.10, 130.73, 130.62, 129.67, 129.44, 128.91, 128.69, 127.98, 127.66, 127.53, 127.50, 127.33, 127.09, 127.07, 126.76, 126.66, 122.73, 122.57(Overlapping peaks are present). **^{77}Se NMR**

(76 MHz, $CDCl_3$) δ 319.82 (s). **Anal** calcd for $C_{32}H_{22}Se$: C, 79.17; H, 4.57; found C, 79.84; H, 4.06.

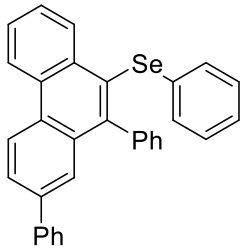

(2,10-diphenylphenanthren-9-yl)(phenyl)selane (7): Yellow solid (0.080 g, 55%); eluent hexane; mp = 73-75 °C; **^{1}H NMR (400 MHz, $CDCl_3$)** δ 8.76 (ddd, *J* = 18.5, 9.3, 4.8 Hz, 3H), 7.95 (dd, *J* = 8.6, 2.0 Hz, 1H), 7.71 – 7.67 (m, 2H), 7.60 – 7.57 (m, 1H), 7.57 – 7.49 (m, 3H), 7.45 – 7.38 (m, 5H), 7.35 (dd, *J* = 4.9, 3.6 Hz, 1H), 7.28 (d, *J* = 2.4 Hz, 1H), 7.23 (s, 1H), 7.05 (d, *J* = 4.2 Hz, 4H). **^{13}C NMR (101 MHz, $CDCl_3$)** δ 144.05, 141.82, 140.65, 140.57, 139.36, 134.25, 132.53, 130.72, 130.58, 130.23, 130.23, 129.71, 129.22, 128.94, 128.85, 128.20, 128.04, 127.60, 127.45, 127.30, 127.15, 126.95, 126.68, 125.54, 123.20, 122.76. **^{77}Se NMR (76 MHz, $CDCl_3$)** δ 324.04 (s). **Anal** calcd for $C_{32}H_{22}Se$: C, 79.17; H, 4.57; found C, 79.95; H, 4.04.

^{1}H ,^{13}C and ^{77}Se NMR Spectra of Some Selected 9-Selanylphenanthrenes and Polycyclic Heteroaromatics

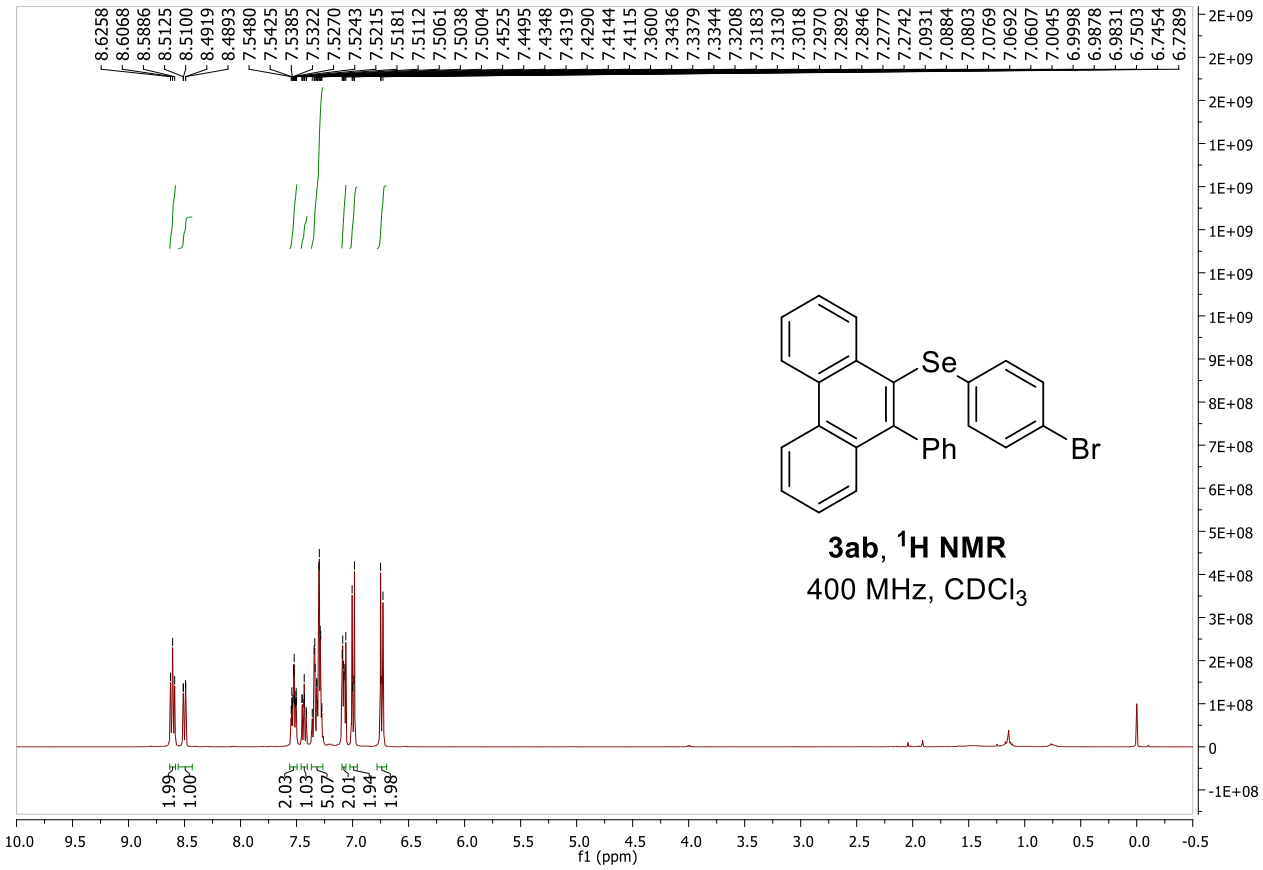
Se
Ph
Br
3ab, 1H NMR
400 MHz, CDCl3
f1 (ppm)

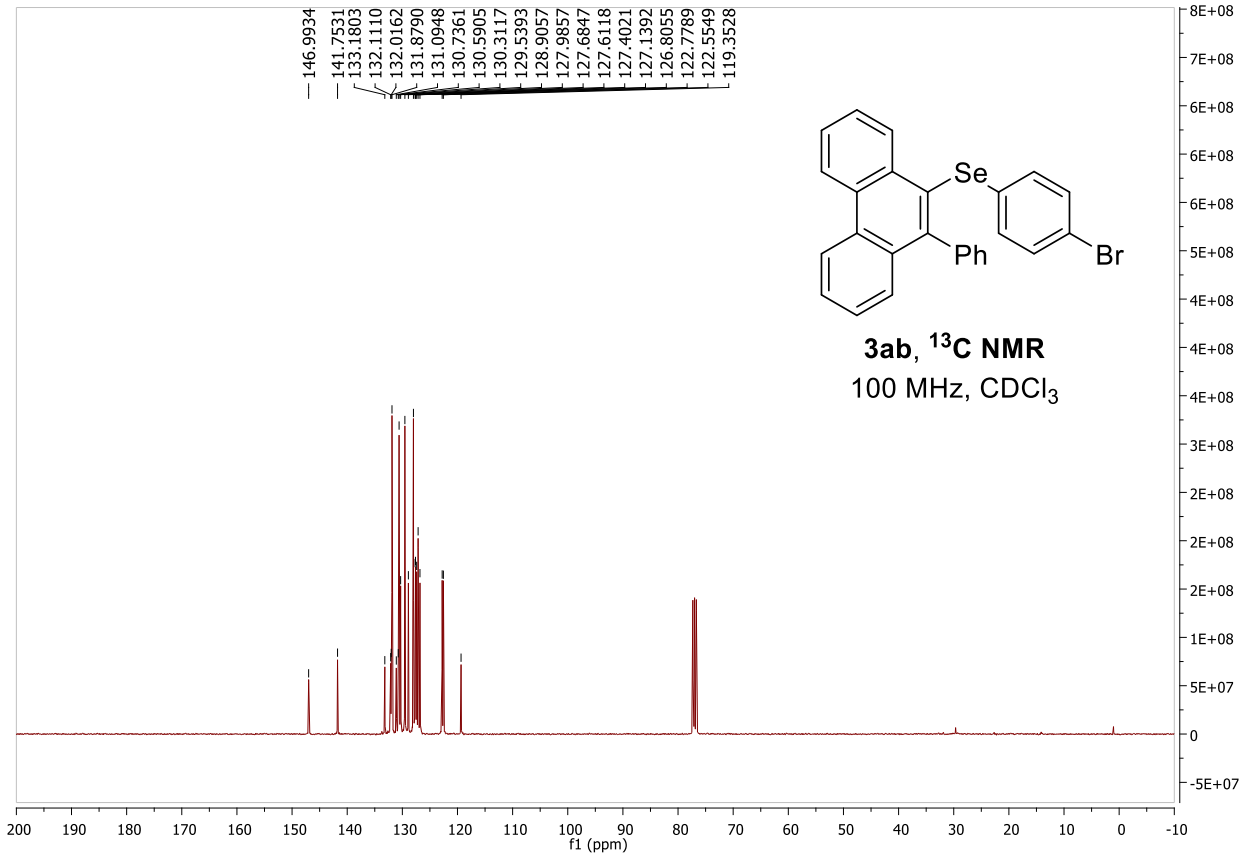
Se
Ph
Br
3ab, 13C NMR
100 MHz, CDCl3
f1 (ppm)

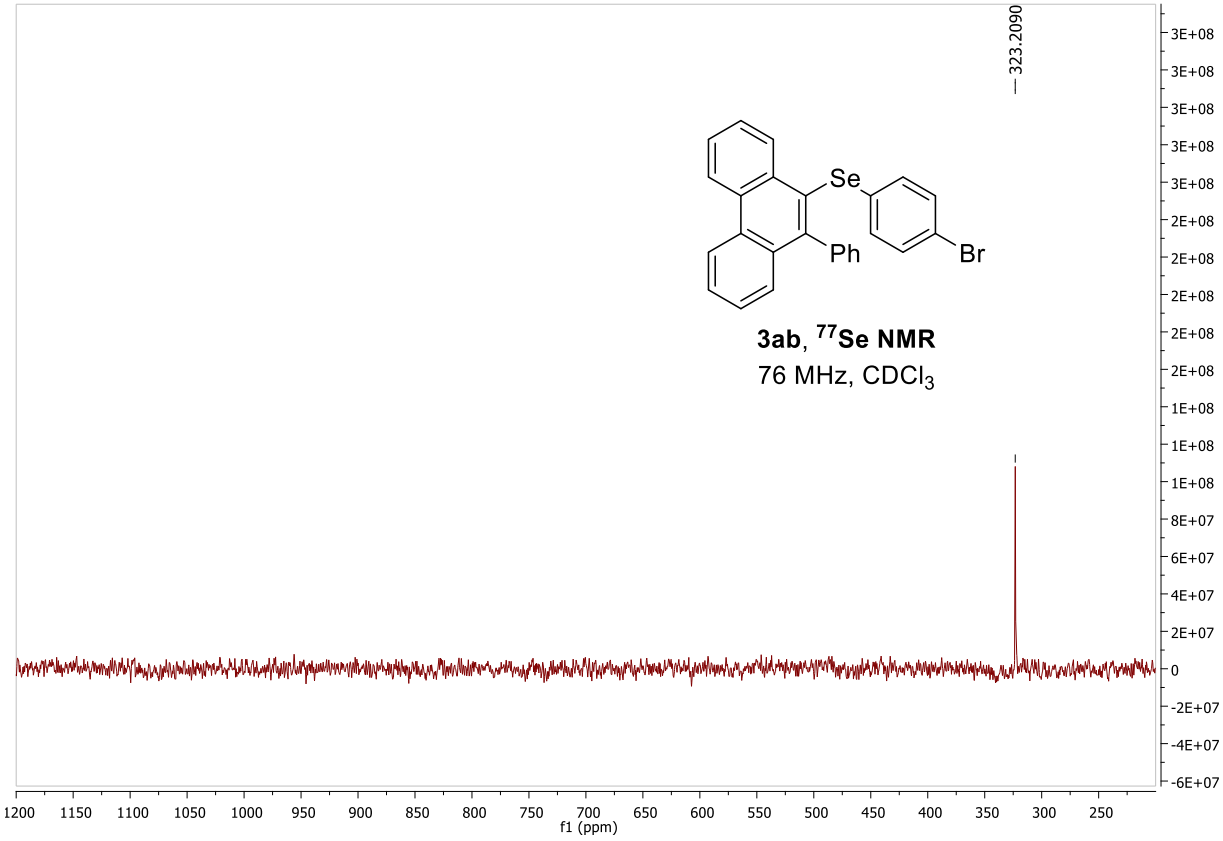

3ab, **^{77}Se NMR**

76 MHz, $CDCl_3$

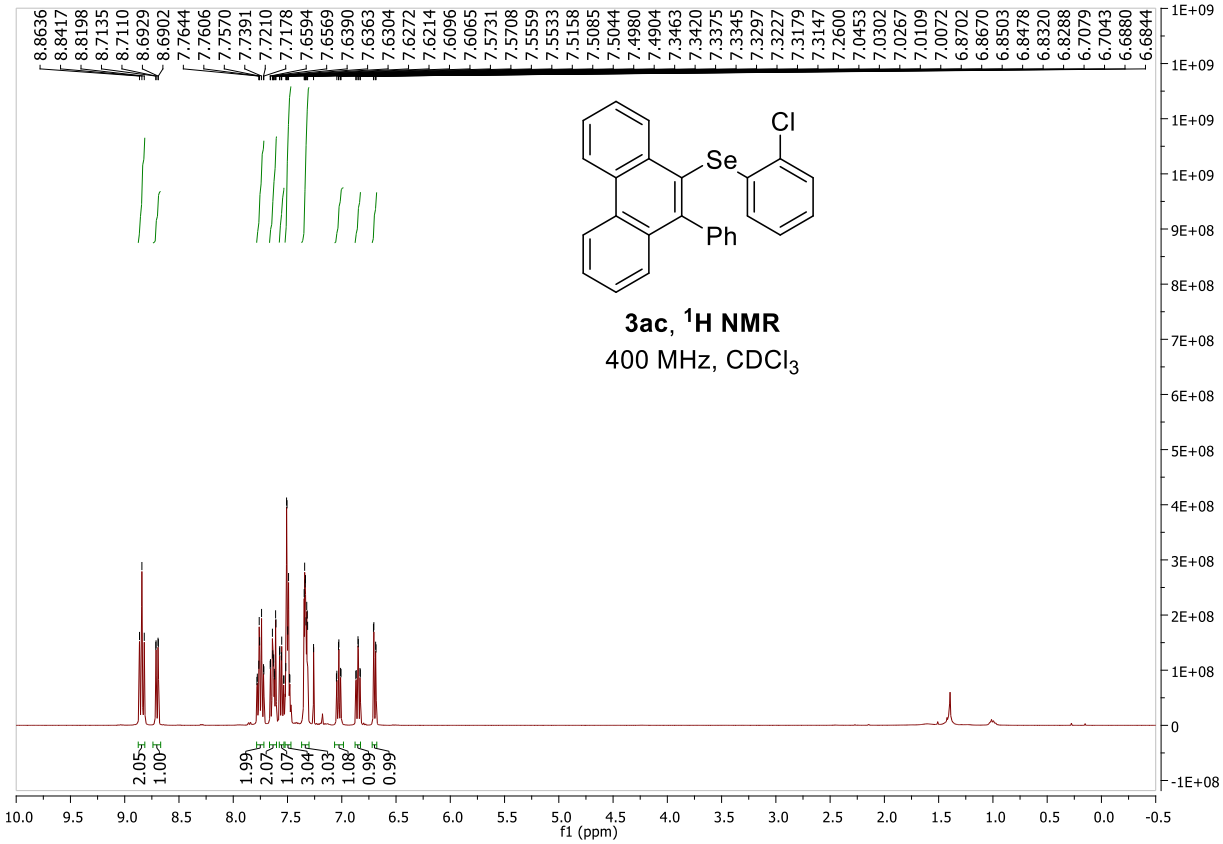

3ac, **^{1}H NMR**

400 MHz, $CDCl_3$

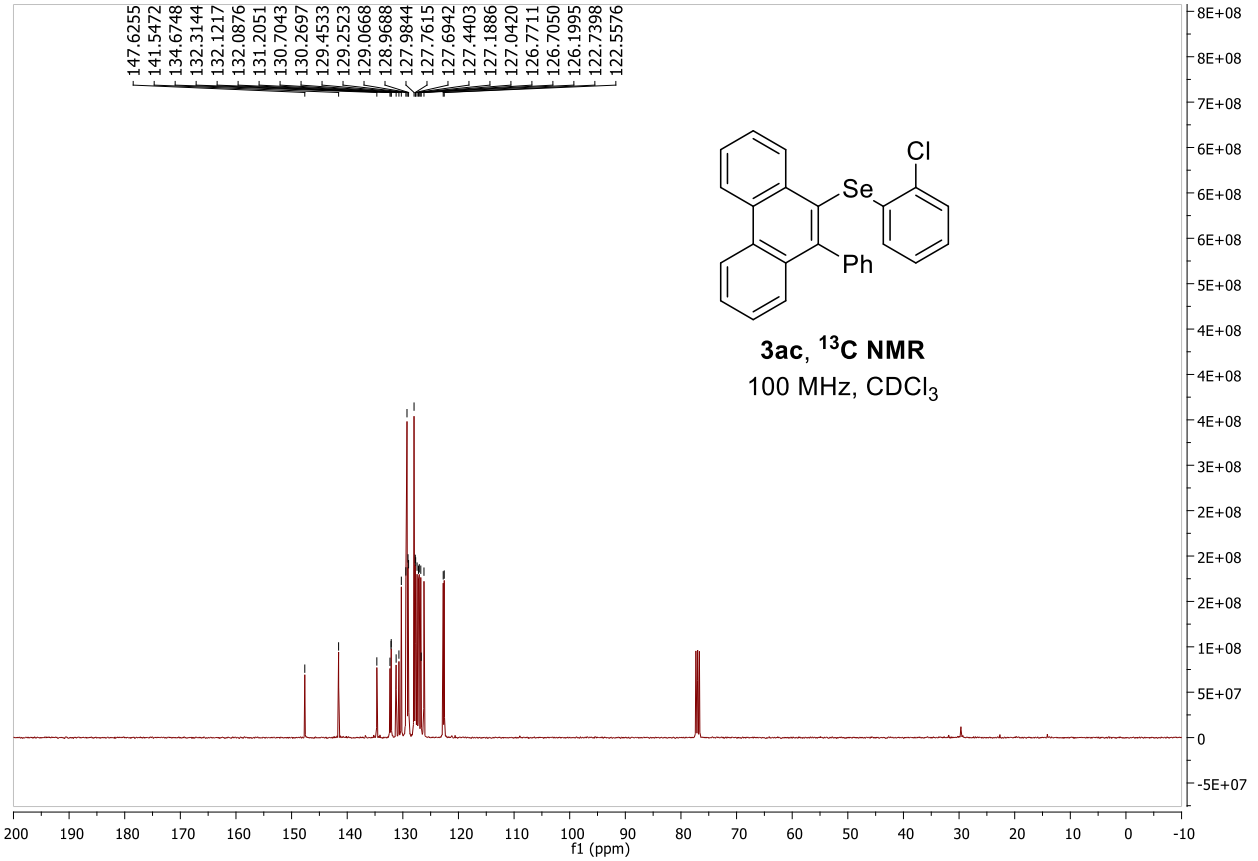
147.6255
141.5472
134.6748
132.3144
132.1217
132.0876
131.2051
130.7043
130.2697
129.4533
129.2523
129.0668
128.9688
127.9844
127.7615
127.6942
127.4403
127.1886
127.0420
126.7711
126.7050
126.1995
122.7398
122.5576
Cl
Se
Ph
3ac, 13C NMR
100 MHz, CDCl3
f1 (ppm)

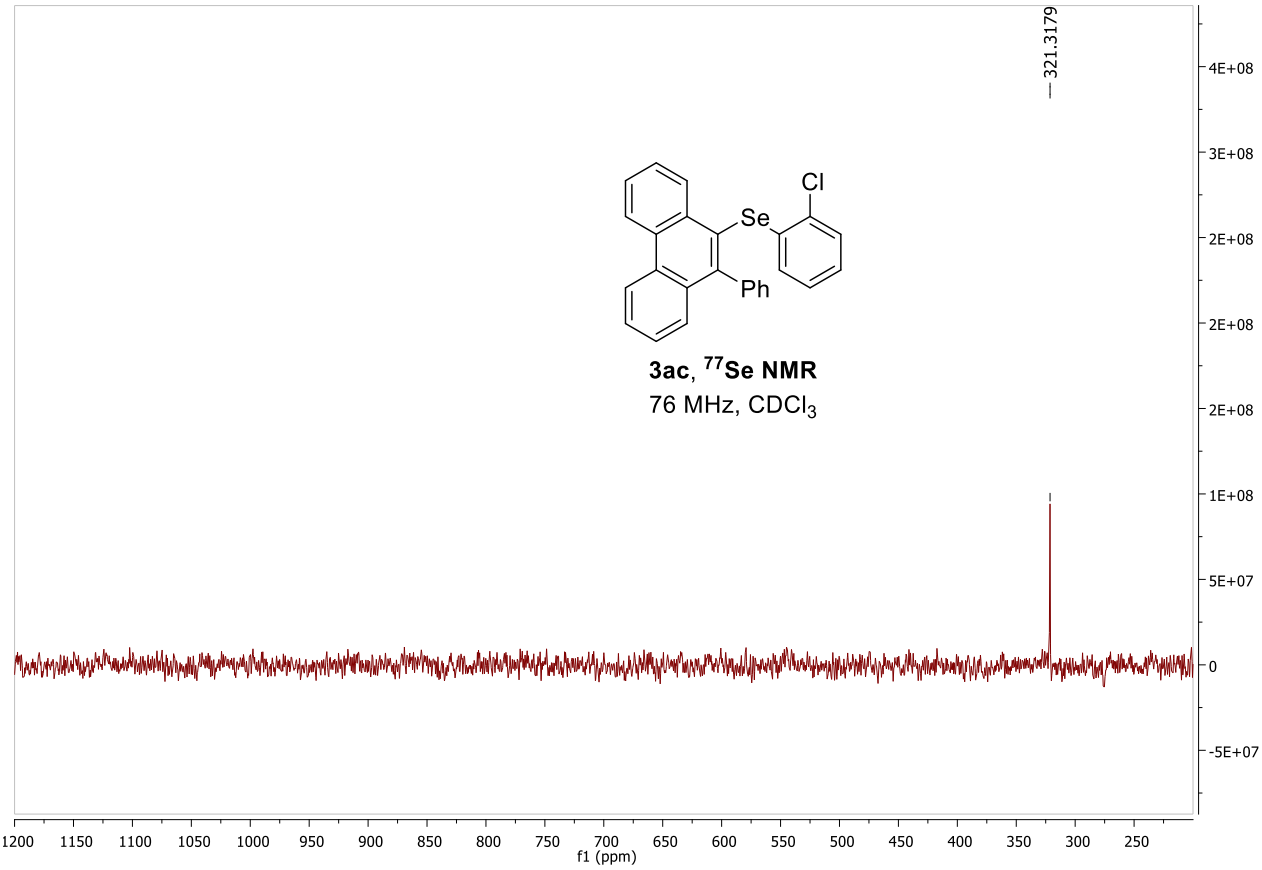
321.3179
Cl
Se
Ph
3ac, 77Se NMR
76 MHz, CDCl3
f1 (ppm)

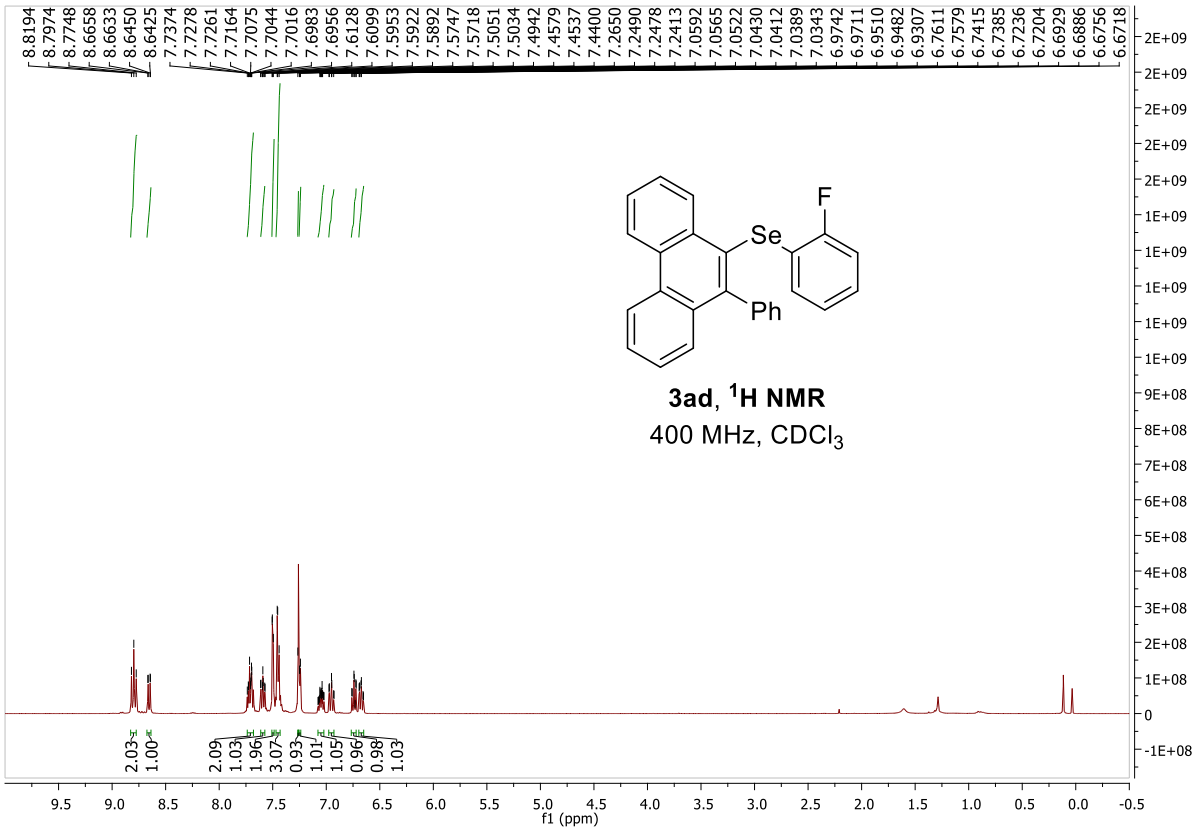
F
Se
Ph
3ad, 1H NMR
400 MHz, CDCl3
f1 (ppm)

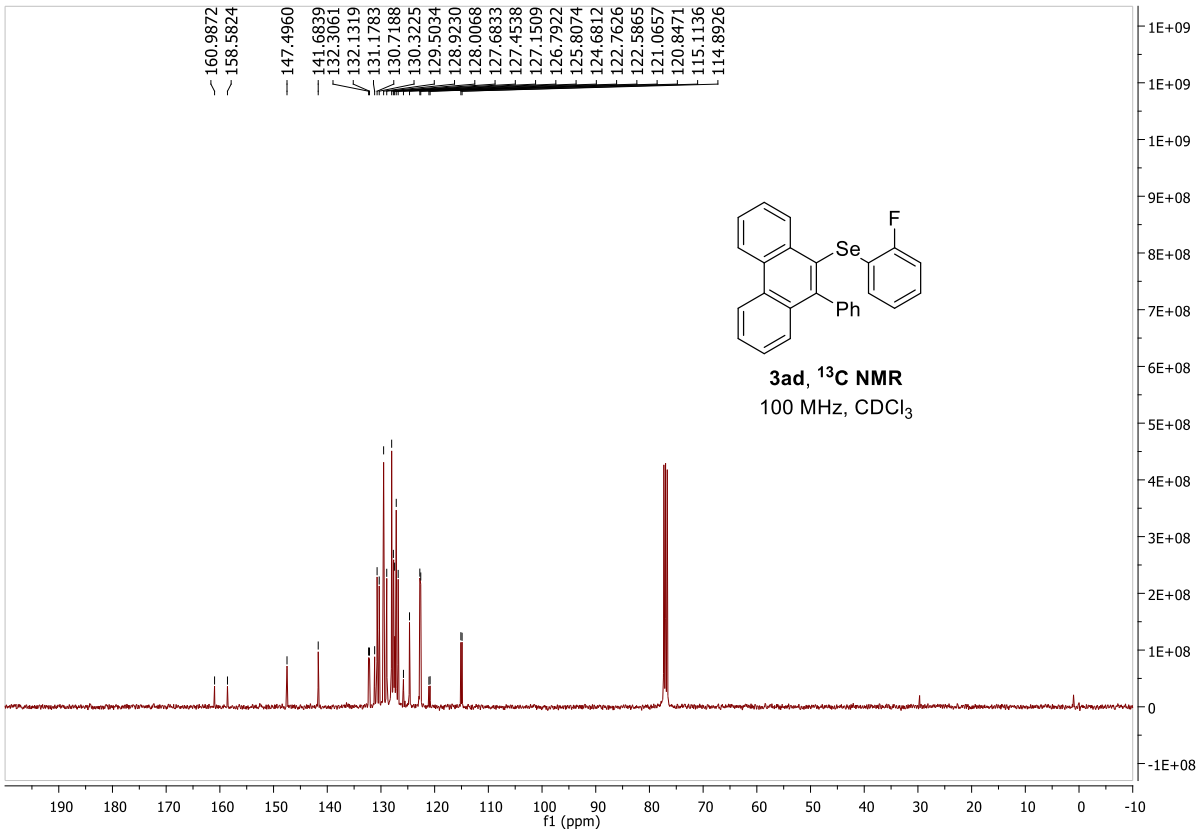
F
Se
Ph
3ad, 13C NMR
100 MHz, CDCl3
f1 (ppm)

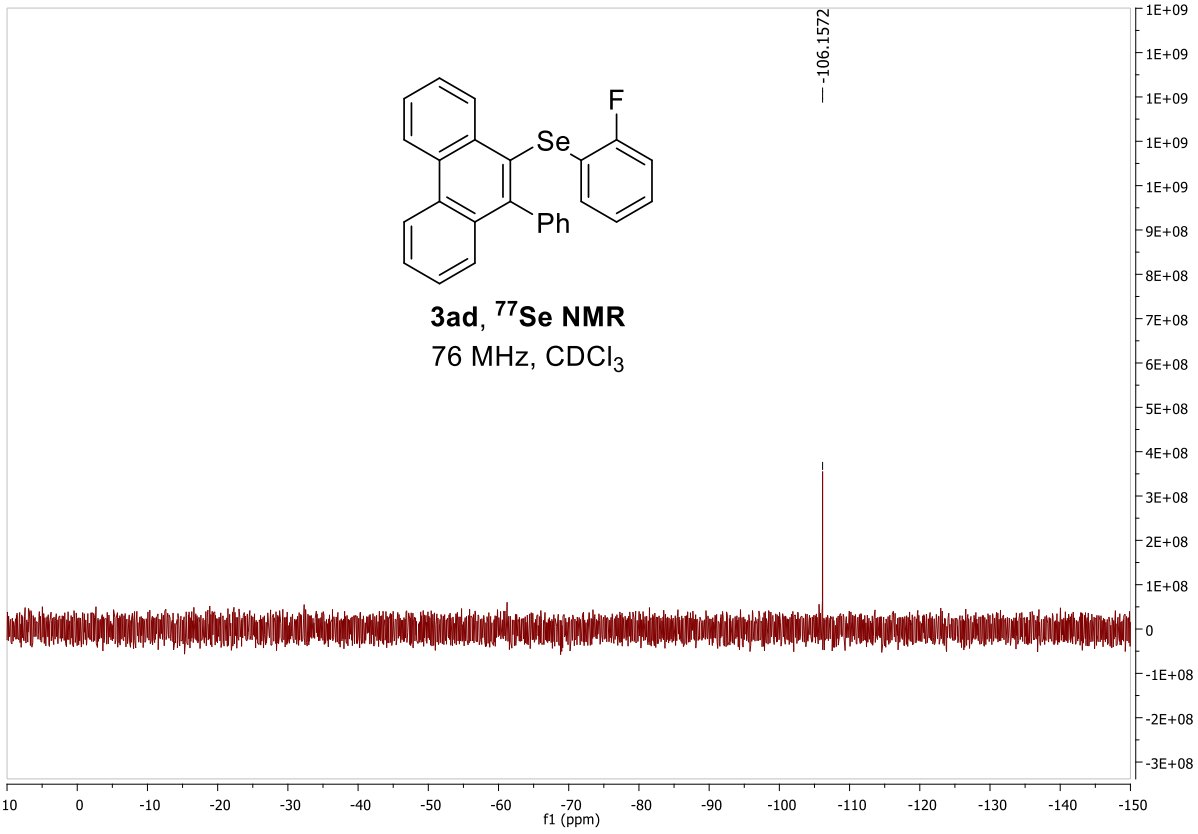
-106.1572
F
Se
Ph
3ad, 77Se NMR
76 MHz, CDCl3
f1 (ppm)

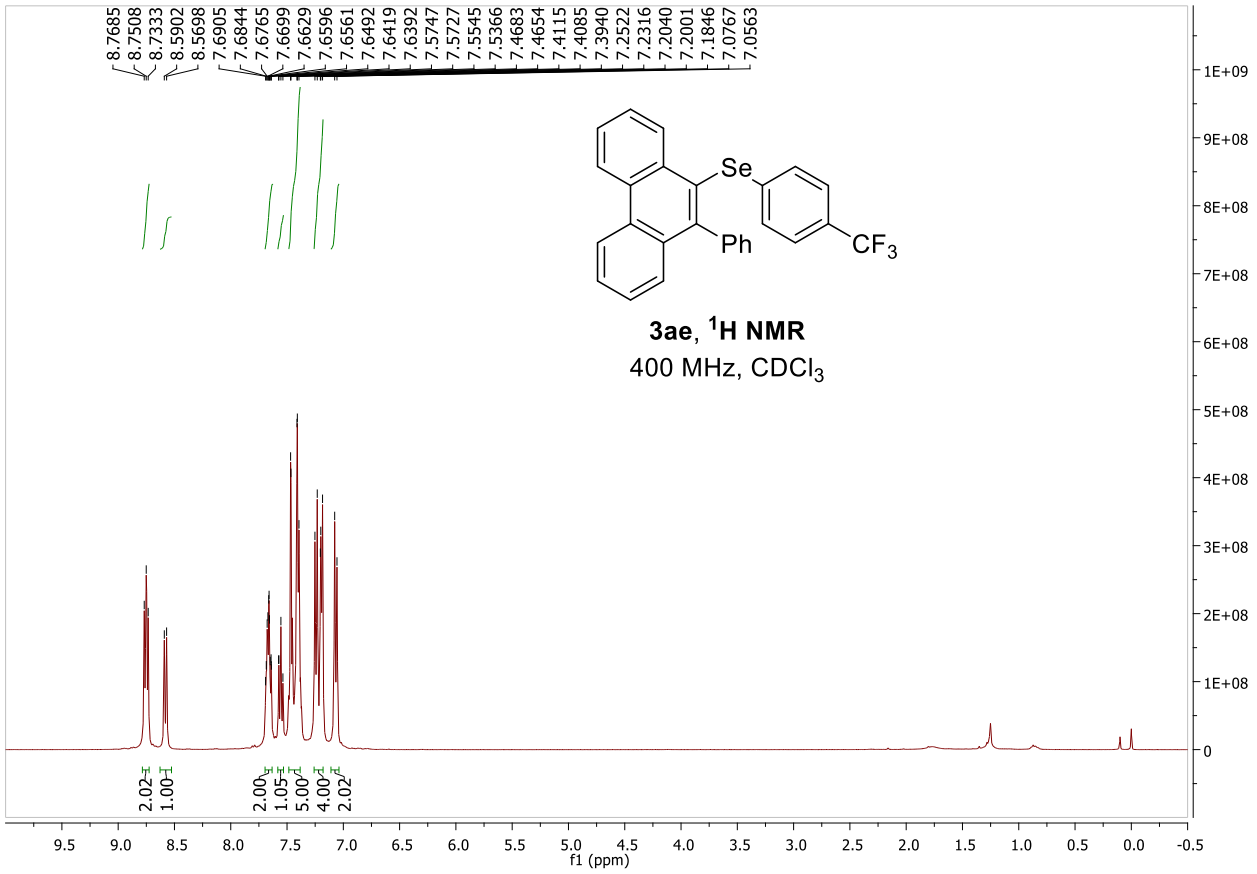
8.7685
8.7508
8.7333
8.5902
8.5698
7.6905
7.6844
7.6765
7.6699
7.6629
7.6596
7.6561
7.6492
7.6419
7.6392
7.5747
7.5727
7.5545
7.5366
7.4683
7.4654
7.4115
7.4085
7.3940
7.2522
7.2316
7.2040
7.2001
7.1846
7.0767
7.0563
Se
Ph
CF3
3ae, 1H NMR
400 MHz, CDCl3
2.02
1.00
2.00
1.05
5.00
4.00
2.02
f1 (ppm)

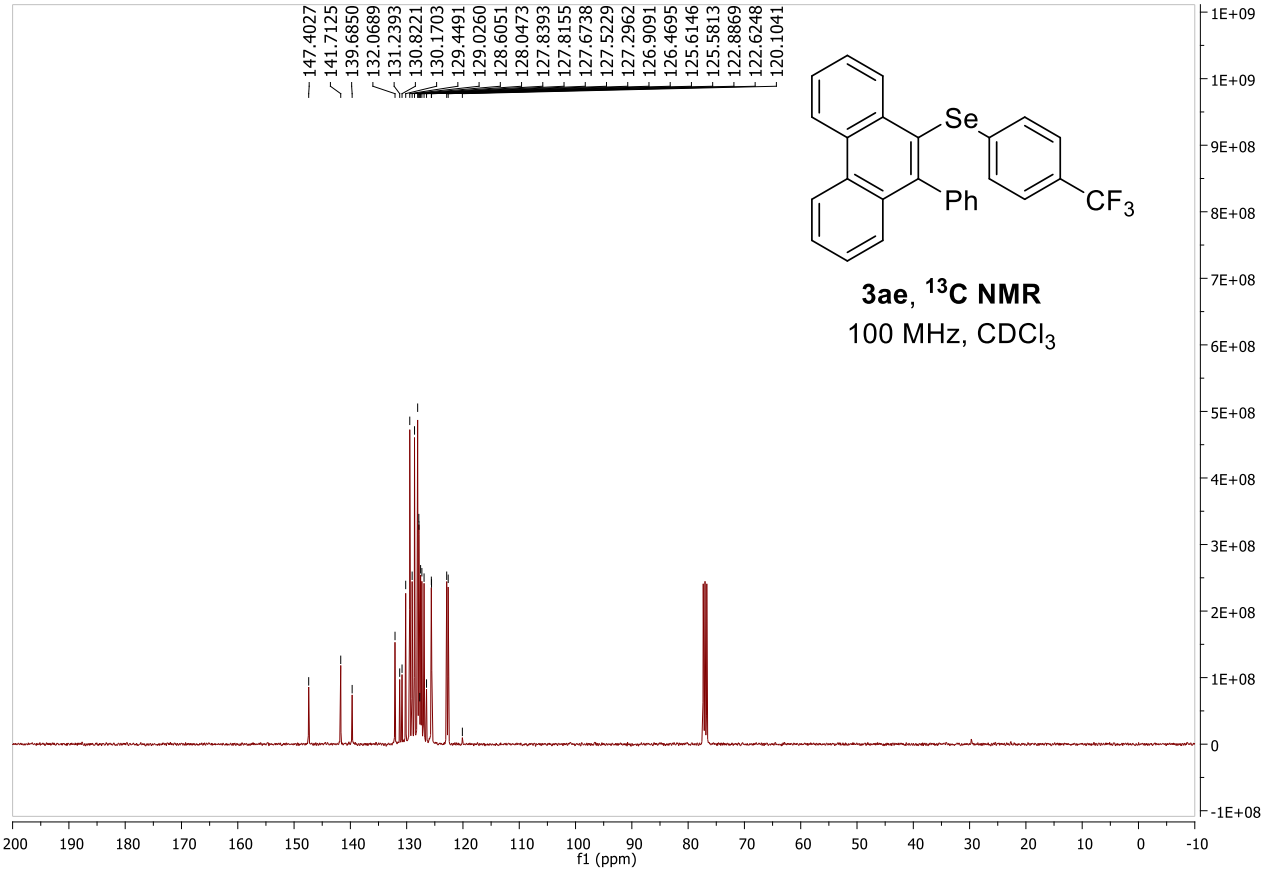
147.4027
141.7125
139.6850
132.0689
131.2393
130.8221
130.1703
129.4491
129.0260
128.6051
128.0473
127.8393
127.8155
127.6738
127.5229
127.2962
126.9091
126.4695
125.6146
125.5813
122.8869
122.6248
120.1041
Se
Ph
CF3
3ae, 13C NMR
100 MHz, CDCl3
f1 (ppm)

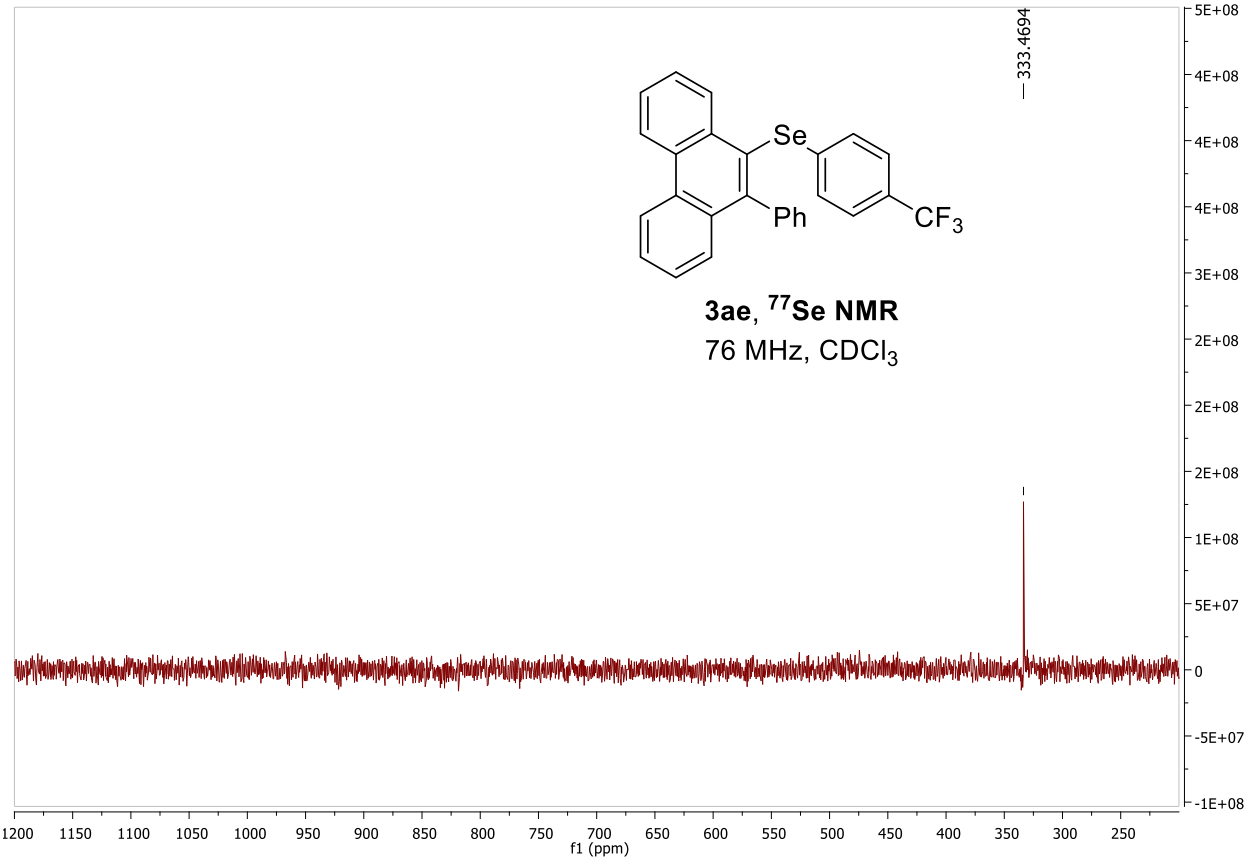
333.4694
Se
Ph
CF3
3ae, 77Se NMR
76 MHz, CDCl3
f1 (ppm)

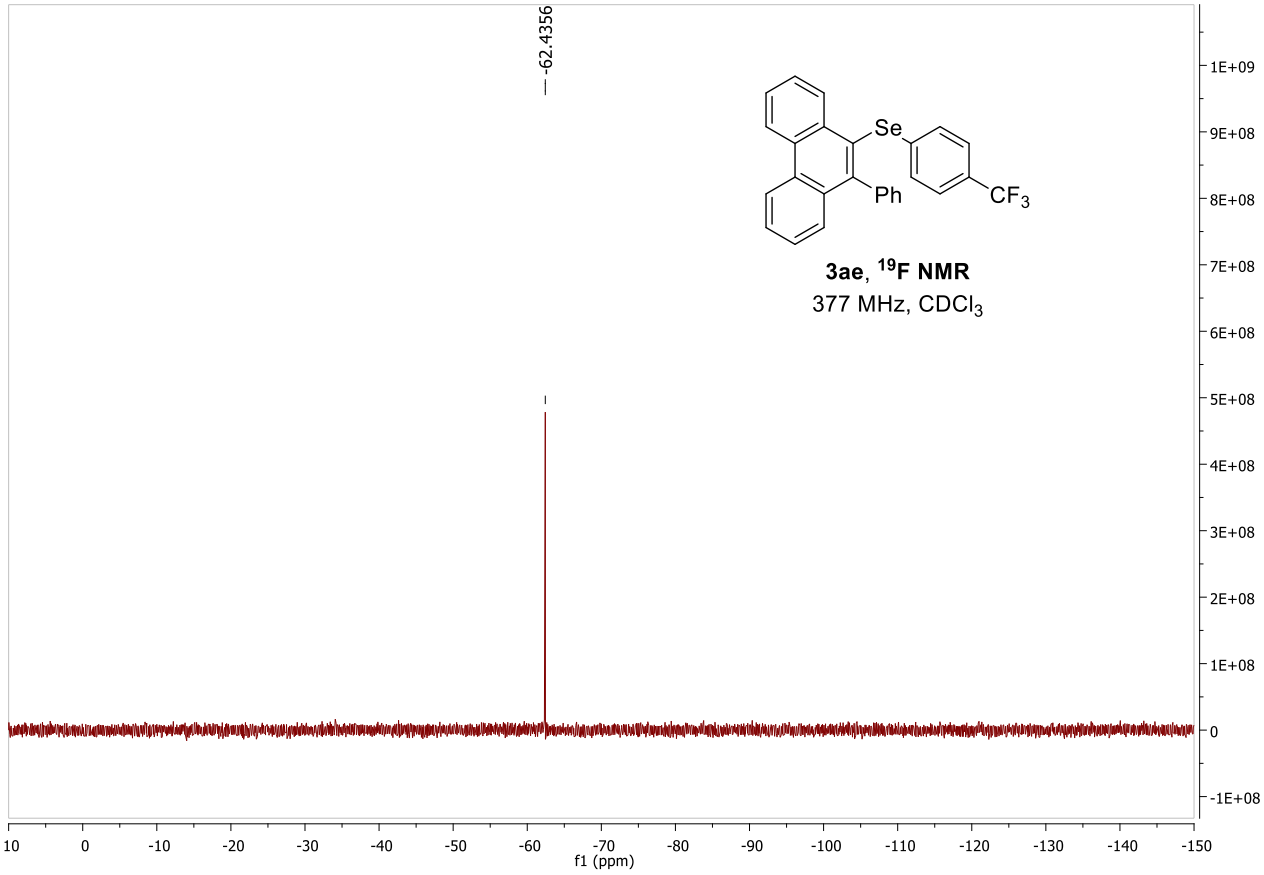
-62.4356
Se
Ph
CF3
3ae, 19F NMR
377 MHz, CDCl3
f1 (ppm)

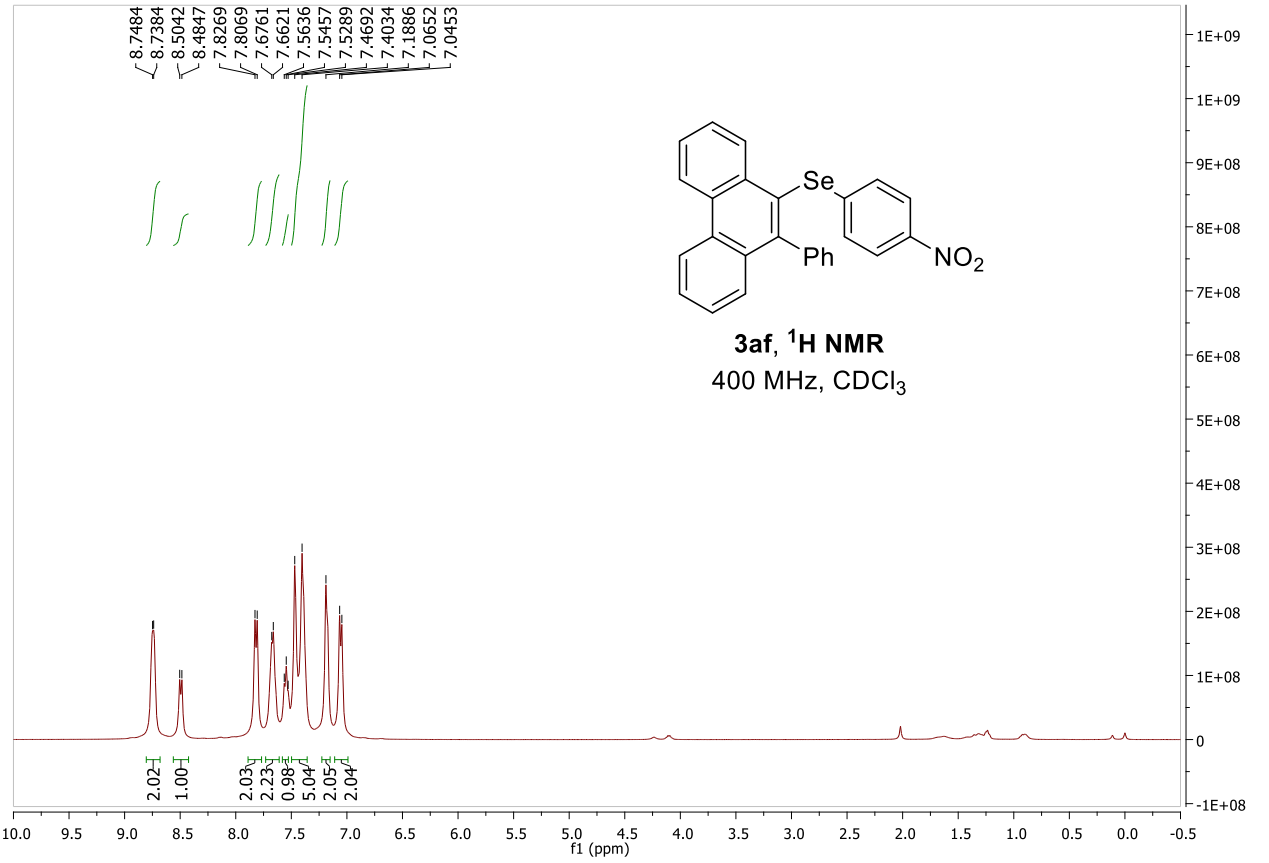
8.7484
8.7384
8.5042
8.4847
7.8269
7.8069
7.6761
7.6621
7.5636
7.5457
7.5289
7.4692
7.4034
7.1886
7.0652
7.0453
Se
Ph
NO2
3af, 1H NMR
400 MHz, CDCl3
2.02
1.00
2.03
2.23
0.98
5.04
2.05
2.04
f1 (ppm)

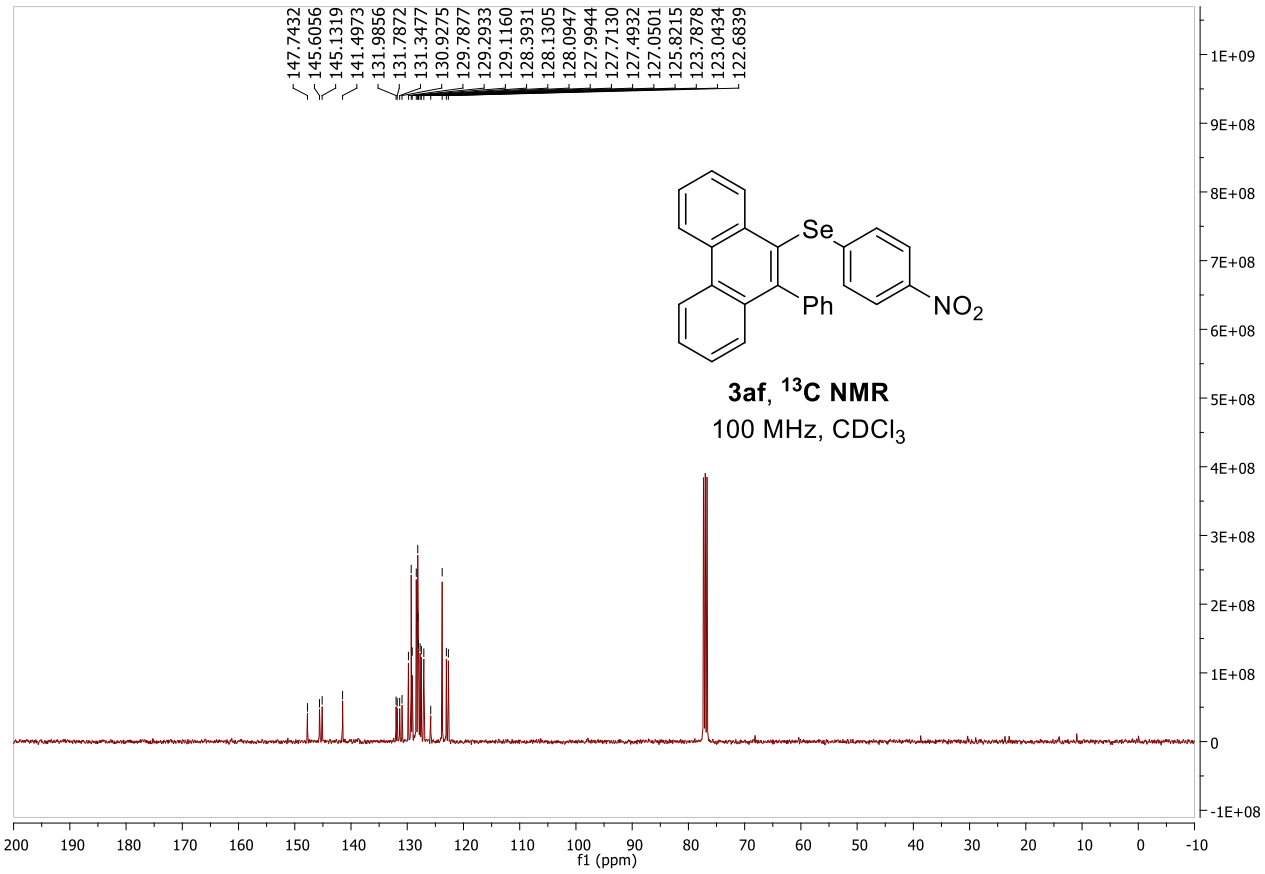
147.7432
145.6056
145.1319
141.4973
131.9856
131.7872
131.3477
130.9275
129.7877
129.2933
129.1160
128.3931
128.1305
128.0947
127.9944
127.7130
127.4932
127.0501
125.8215
123.7878
123.0434
122.6839
Se
Ph
NO2
3af, 13C NMR
100 MHz, CDCl3
f1 (ppm)

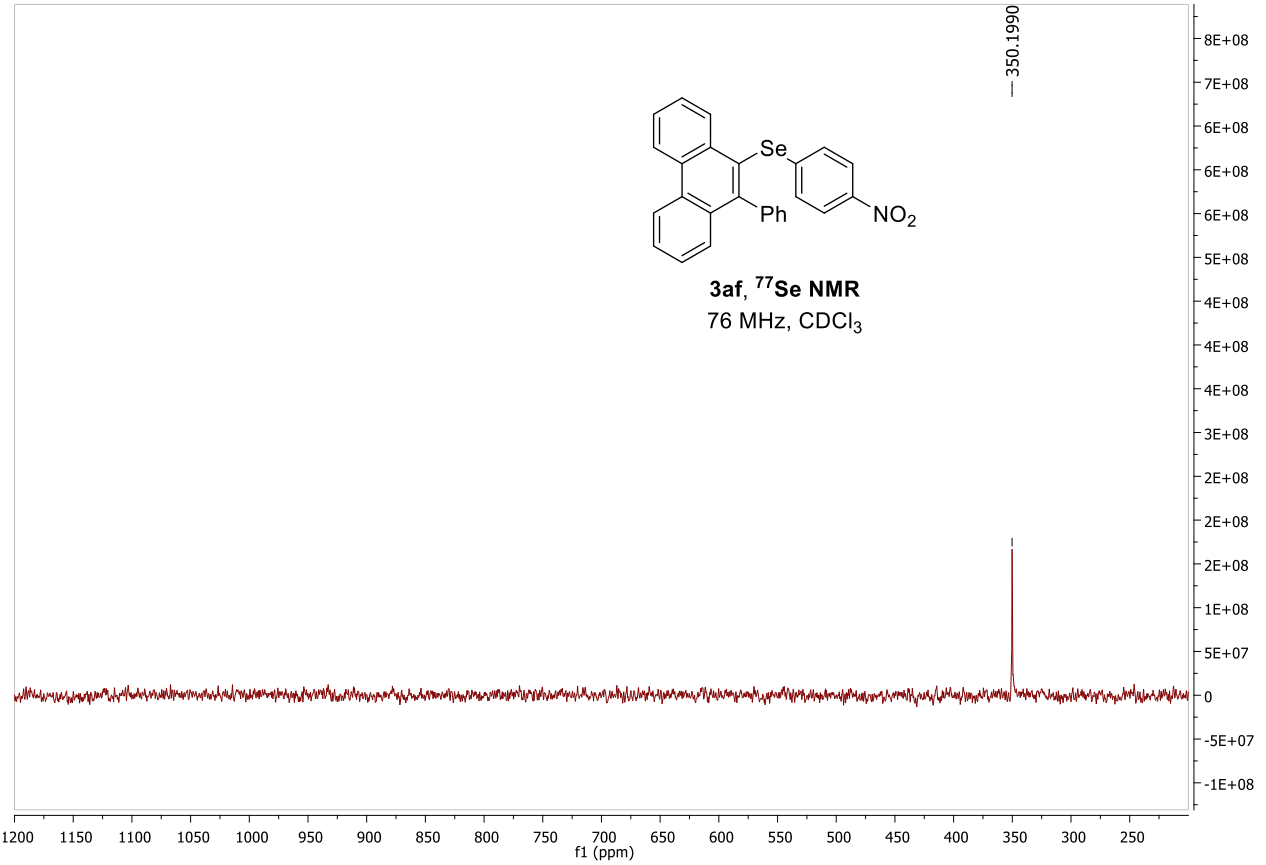
350.1990
Se
Ph
NO2
3af, 77Se NMR
76 MHz, CDCl3
f1 (ppm)

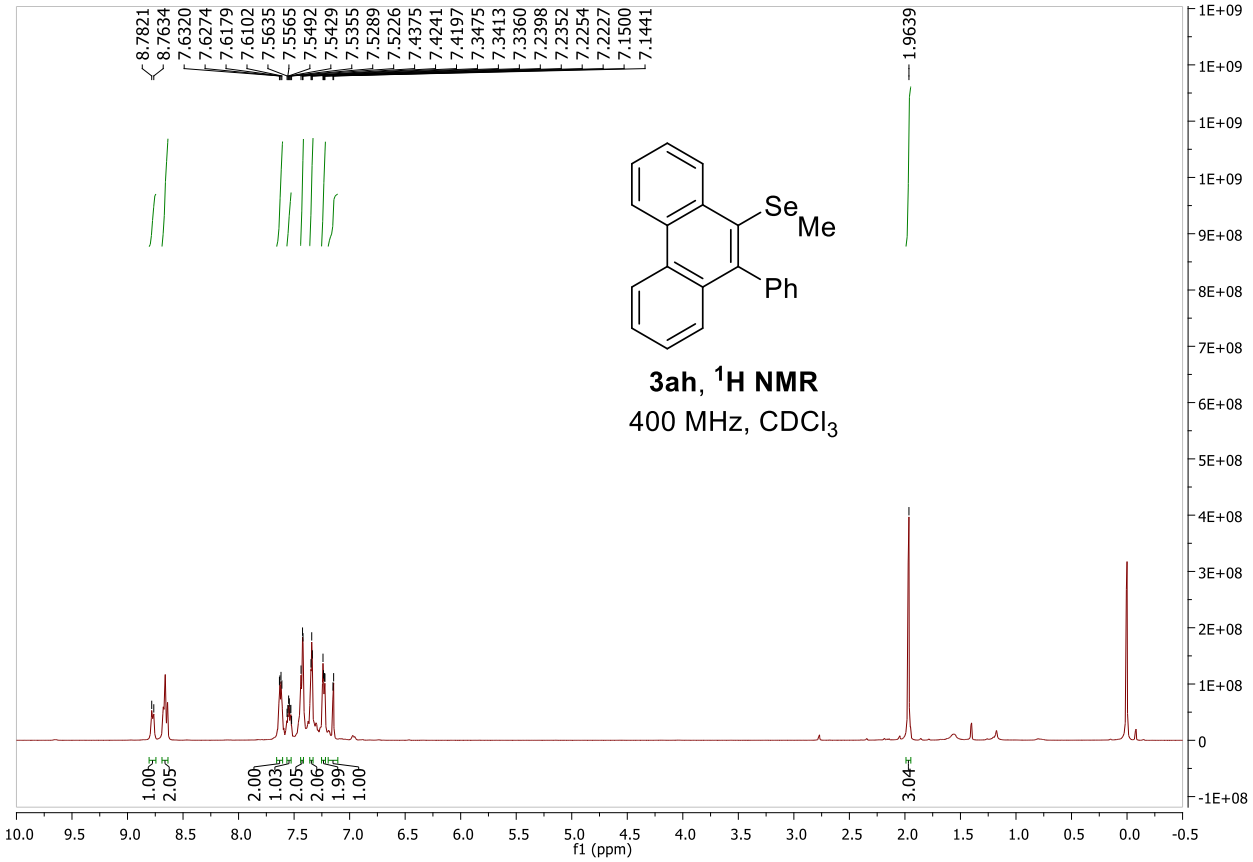
8.7821
8.7634
7.6320
7.6274
7.6179
7.6102
7.5635
7.5565
7.5492
7.5429
7.5355
7.5289
7.5226
7.4375
7.4241
7.4197
7.3475
7.3413
7.3360
7.2398
7.2352
7.2254
7.2227
7.1500
7.1441
1.9639
Se
Me
Ph
3ah, 1H NMR
400 MHz, CDCl3
1.00
2.05
2.00
1.03
2.05
2.06
1.99
1.00
3.04
f1 (ppm)

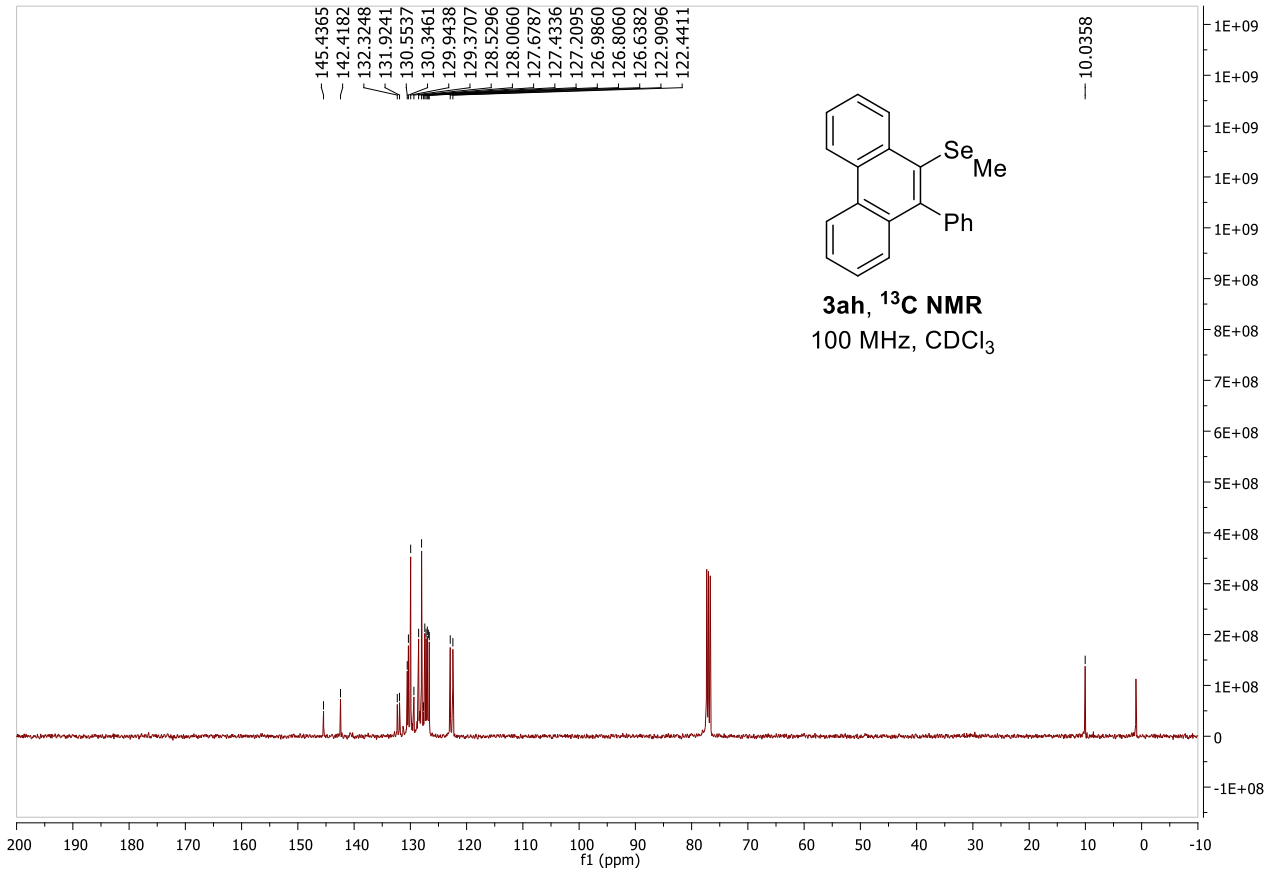
145.4365
142.4182
132.3248
131.9241
130.5537
130.3461
129.9438
129.3707
128.5296
128.0060
127.6787
127.4336
127.2095
126.9860
126.8060
126.6382
122.9096
122.4411
10.0358
Se
Me
Ph
3ah, 13C NMR
100 MHz, CDCl3
f1 (ppm)

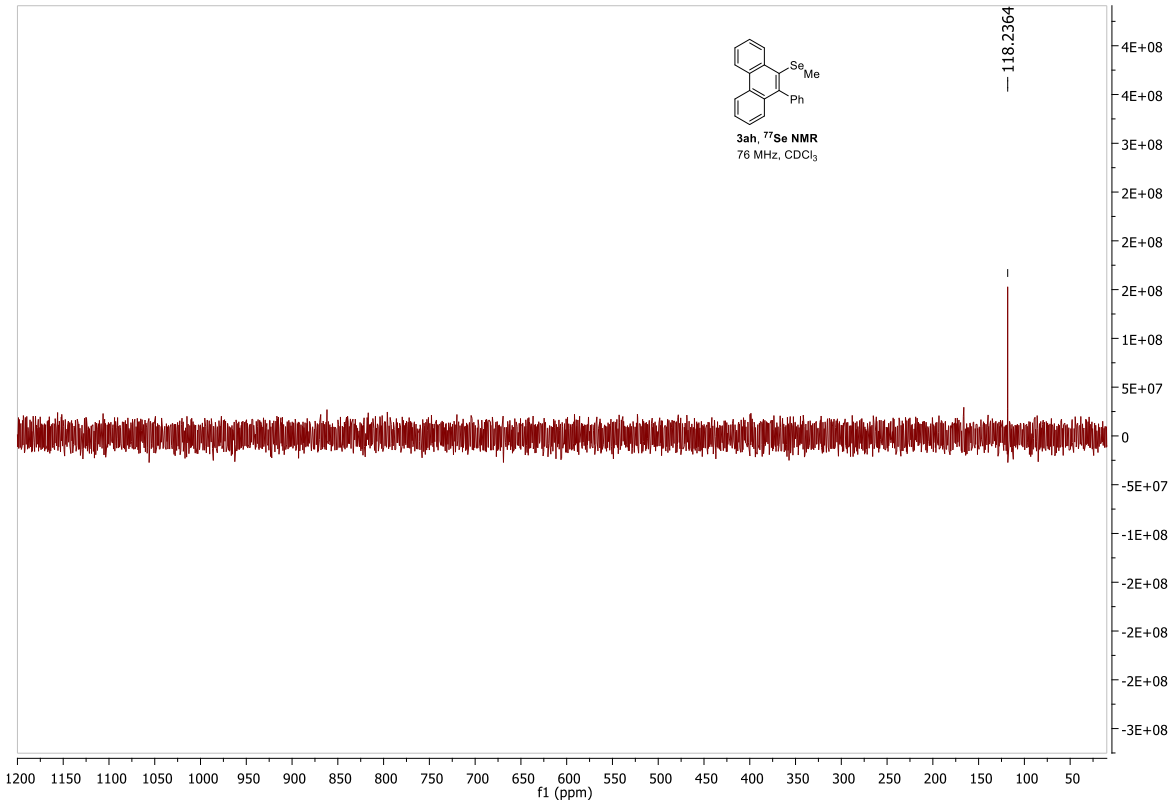
118.2364
Se
Me
Ph
3ah, 77Se NMR
76 MHz, CDCl3
f1 (ppm)

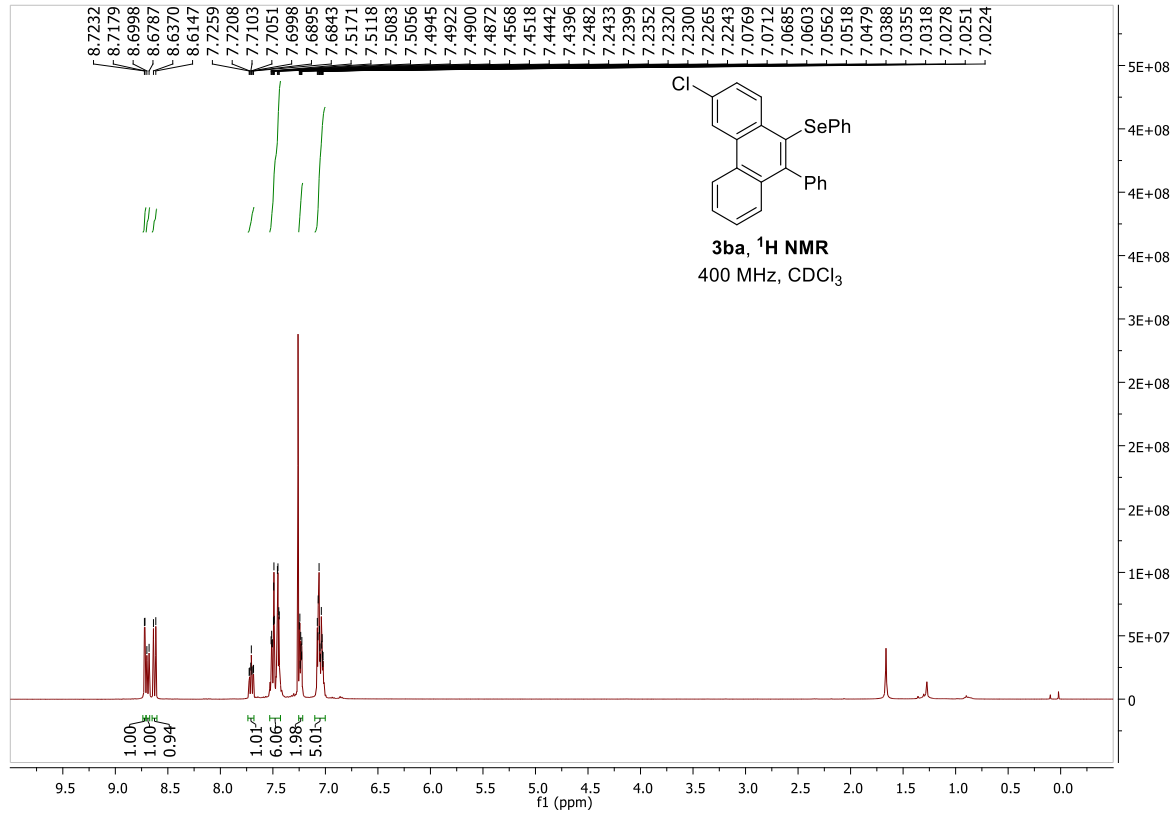
Cl
SePh
Ph
3ba, 1H NMR
400 MHz, CDCl3
f1 (ppm)

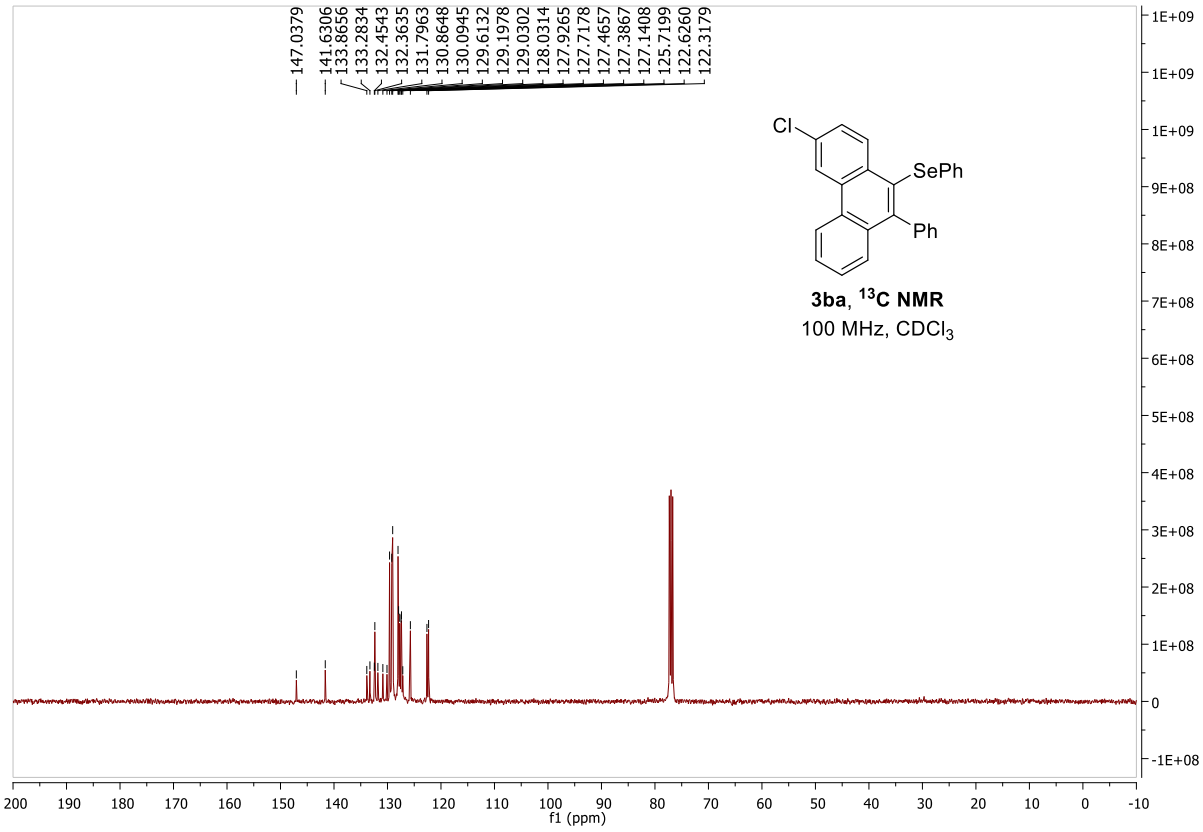
147.0379
141.6306
133.8656
133.2834
132.4543
132.3635
131.7963
130.8648
130.0945
129.6132
129.1978
129.0302
128.0314
127.9265
127.7178
127.4657
127.3867
127.1408
125.7199
122.6260
122.3179
Cl
SePh
Ph
3ba, 13C NMR
100 MHz, CDCl3
f1 (ppm)

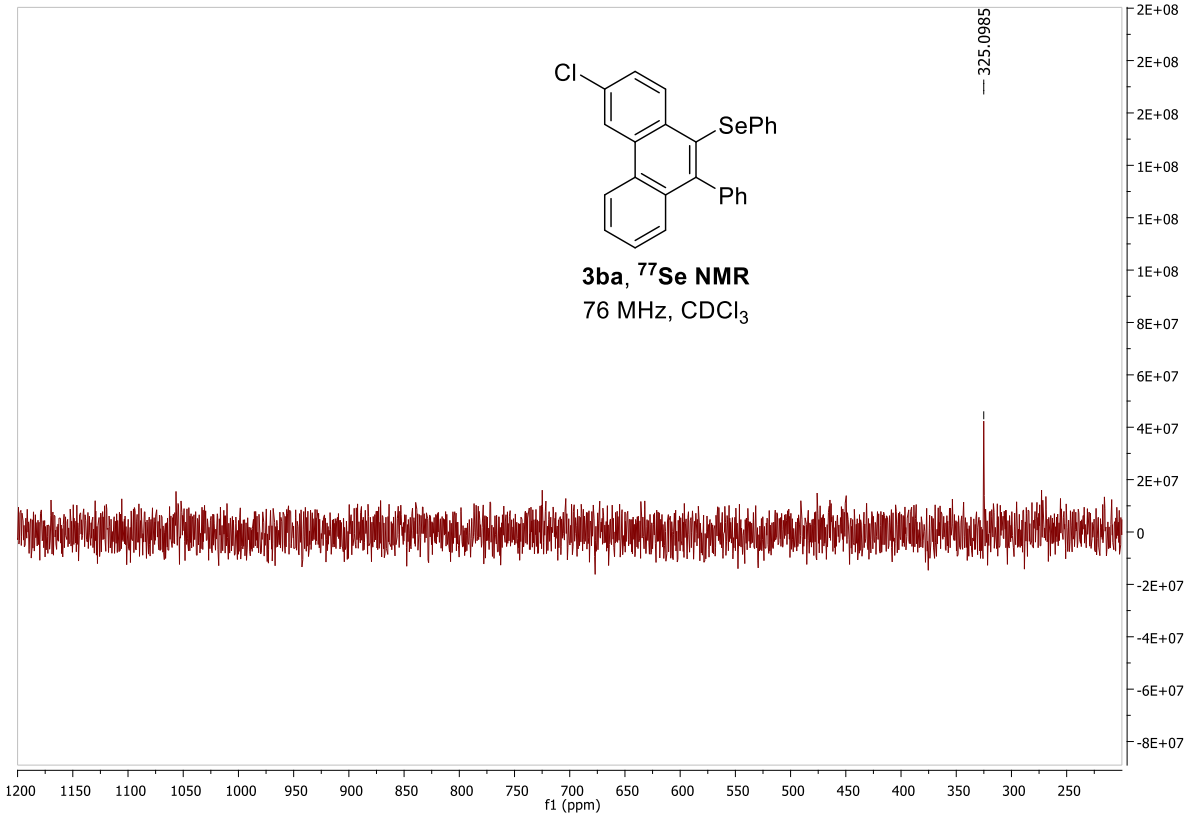
325.0985
Cl
SePh
Ph
3ba, 77Se NMR
76 MHz, CDCl3
f1 (ppm)

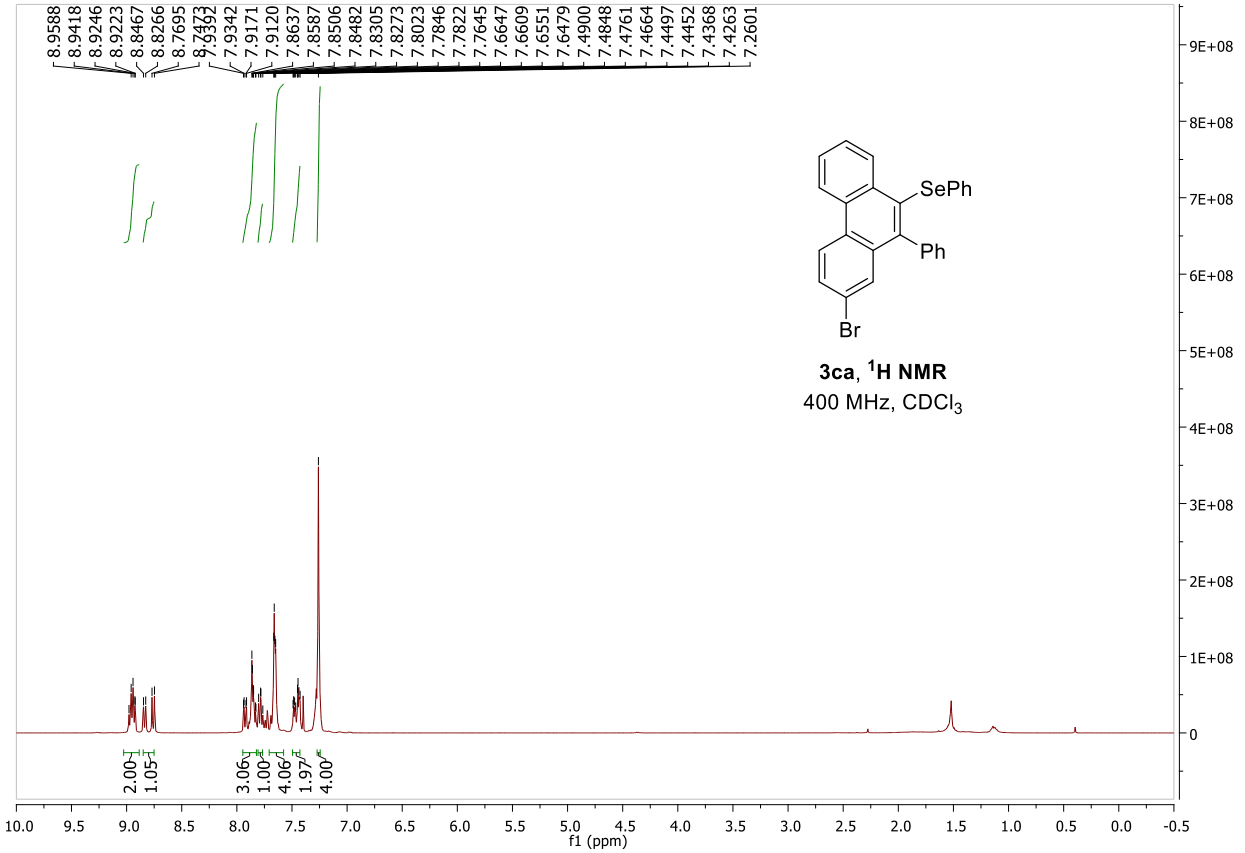
8.9588
8.9418
8.9246
8.9223
8.8467
8.8266
8.7695
8.7473
7.9392
7.9342
7.9171
7.9120
7.8637
7.8587
7.8506
7.8482
7.8305
7.8273
7.8023
7.7846
7.7822
7.7645
7.6647
7.6609
7.6551
7.6479
7.4900
7.4848
7.4761
7.4664
7.4497
7.4452
7.4368
7.4263
7.2601
SePh
Ph
Br
3ca, 1H NMR
400 MHz, CDCl3
2.00
1.05
3.06
1.00
4.06
1.97
4.00
f1 (ppm)

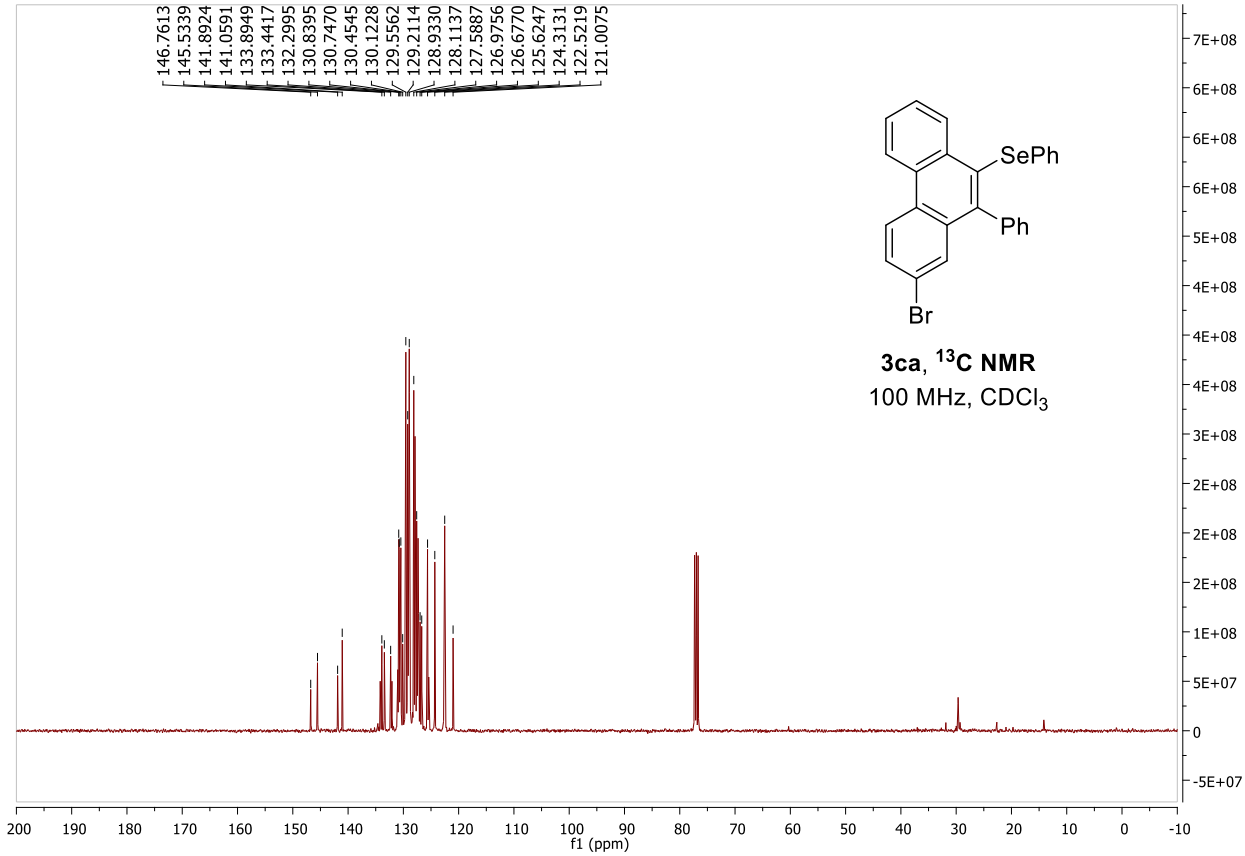
146.7613
145.5339
141.8924
141.0591
133.8949
133.4417
132.2995
130.8395
130.7470
130.4545
130.1228
129.5562
129.2114
128.9330
128.1137
127.5887
126.9756
126.6770
125.6247
124.3131
122.5219
121.0075
SePh
Ph
Br
3ca, 13C NMR
100 MHz, CDCl3
f1 (ppm)

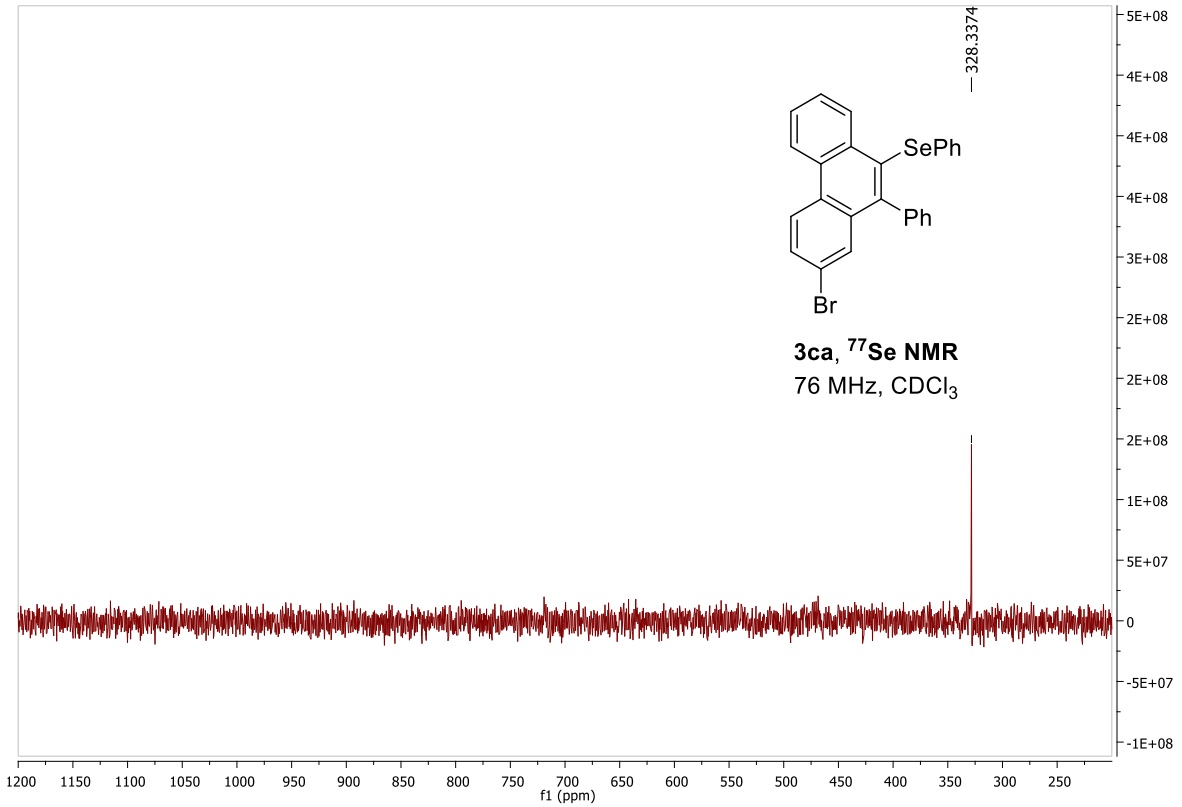
328.3374
SePh
Ph
Br
3ca, 77Se NMR
76 MHz, CDCl3
f1 (ppm)

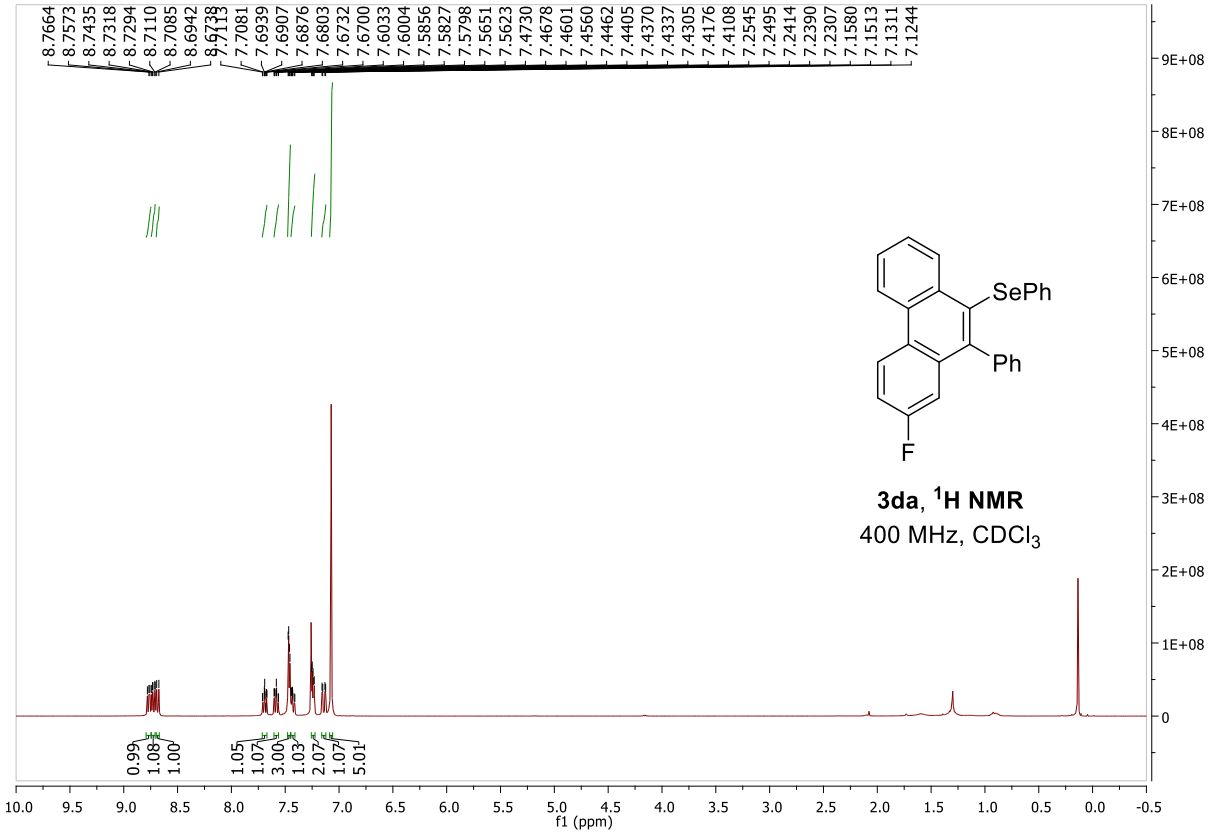
SePh
Ph
F
3da, 1H NMR
400 MHz, CDCl3
f1 (ppm)

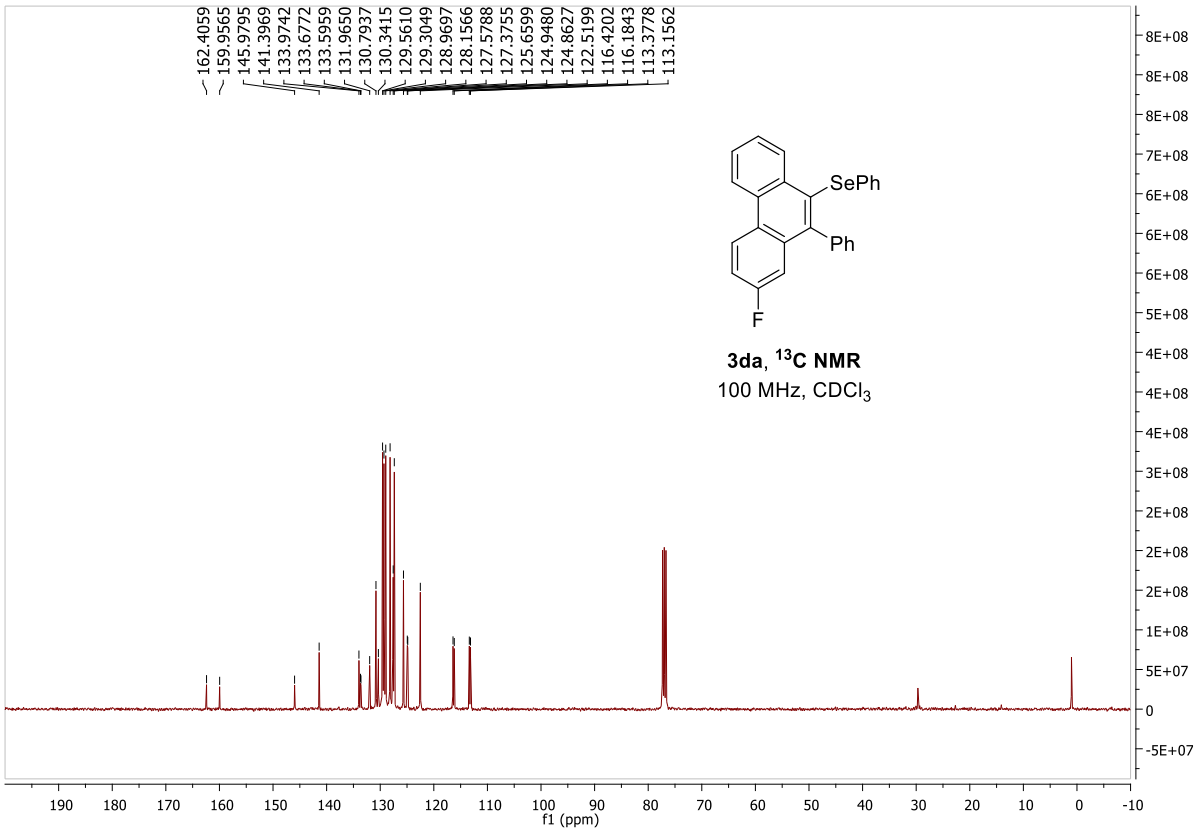
162.4059
159.9565
145.9795
141.3969
133.9742
133.6772
133.5959
131.9650
130.7937
130.3415
129.5610
129.3049
128.9697
128.1566
127.5788
127.3755
125.6599
124.9480
124.8627
122.5199
116.4202
116.1843
113.3778
113.1562
SePh
Ph
F
3da, 13C NMR
100 MHz, CDCl3
f1 (ppm)

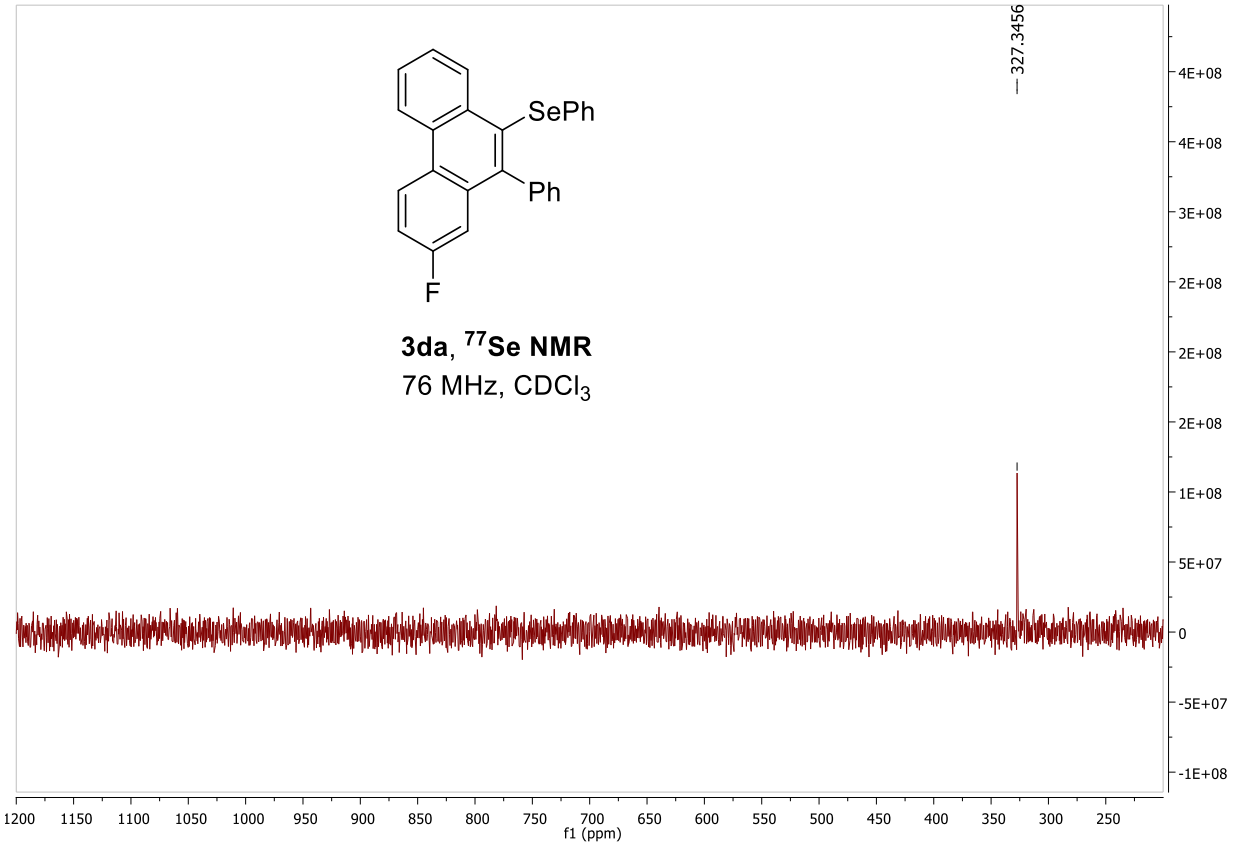
327.3456
SePh
Ph
F
3da, 77Se NMR
76 MHz, CDCl3
f1 (ppm)

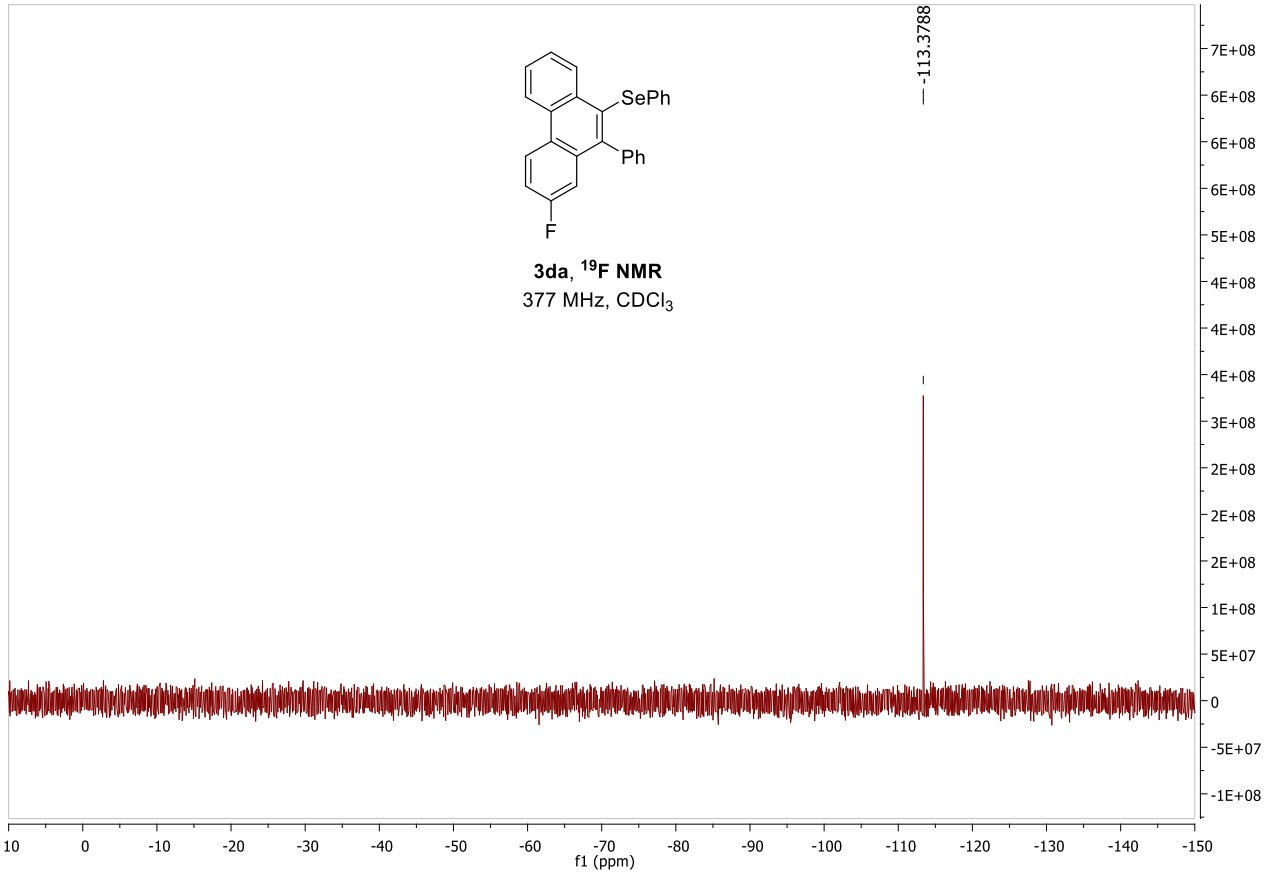
-113.3788
SePh
Ph
F
3da, 19F NMR
377 MHz, CDCl3
f1 (ppm)

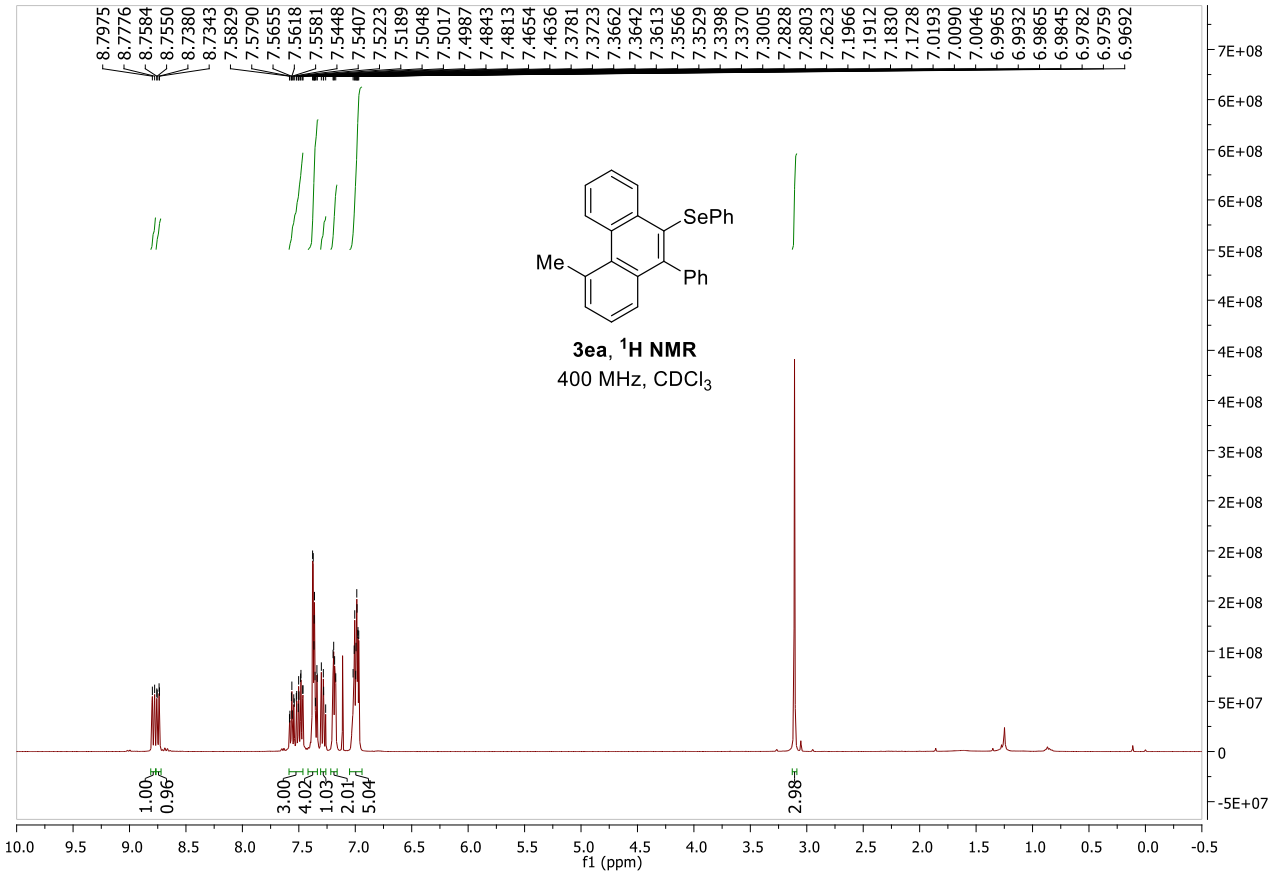
8.7975
8.7776
8.7584
8.7550
8.7380
8.7343
7.5829
7.5790
7.5655
7.5618
7.5581
7.5448
7.5407
7.5223
7.5189
7.5048
7.5017
7.4987
7.4843
7.4813
7.4654
7.4636
7.3781
7.3723
7.3662
7.3642
7.3613
7.3566
7.3529
7.3398
7.3370
7.3005
7.2828
7.2803
7.2623
7.1966
7.1912
7.1830
7.1728
7.0193
7.0090
7.0046
6.9965
6.9932
6.9865
6.9845
6.9782
6.9759
6.9692
SePh
Me
Ph
3ea, 1H NMR
400 MHz, CDCl3
1.00
0.96
3.00
4.02
1.03
2.01
5.04
2.98
f1 (ppm)

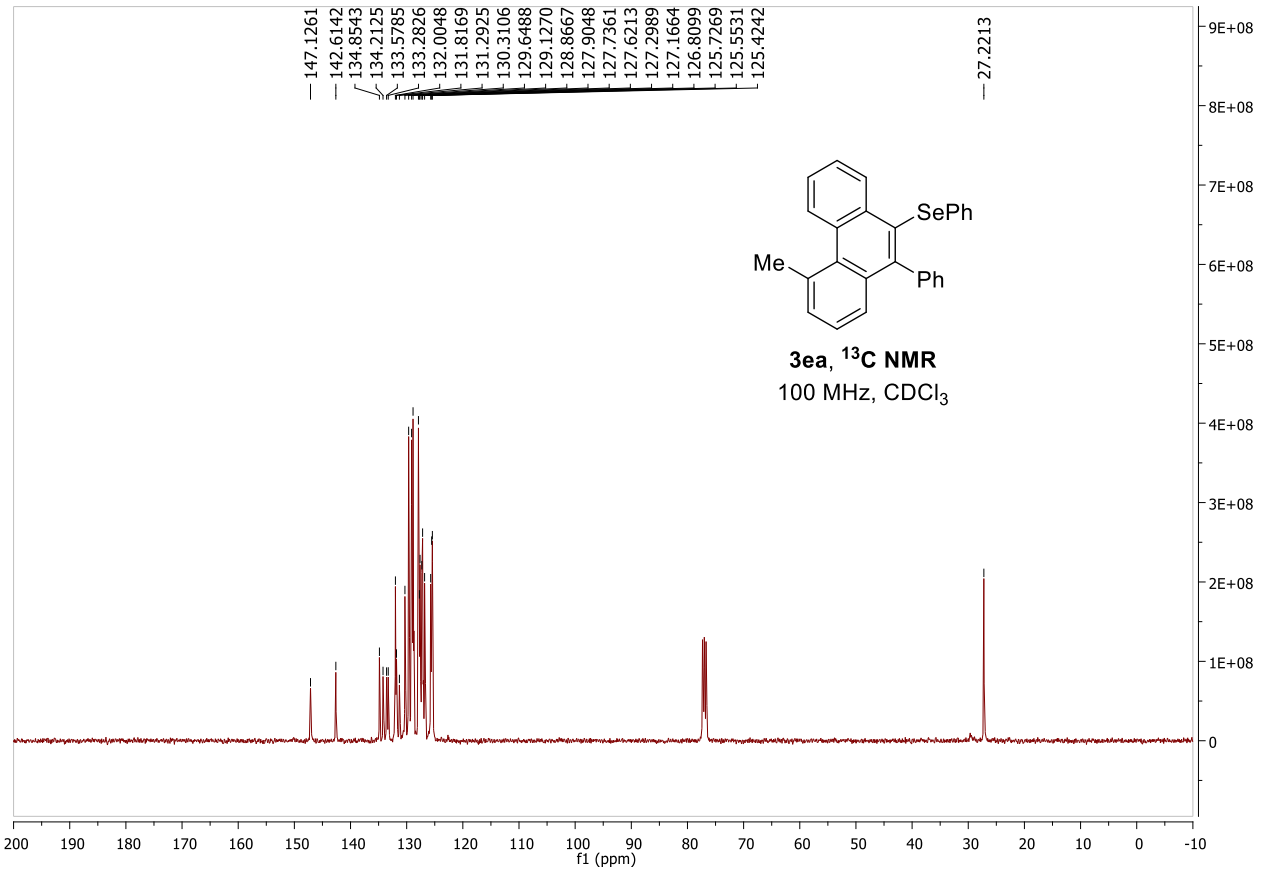
147.1261
142.6142
134.8543
134.2125
133.5785
133.2826
132.0048
131.8169
131.2925
130.3106
129.6488
129.1270
128.8667
127.9048
127.7361
127.6213
127.2989
127.1664
126.8099
125.7269
125.5531
125.4242
27.2213
SePh
Me
Ph
3ea, 13C NMR
100 MHz, CDCl3
f1 (ppm)

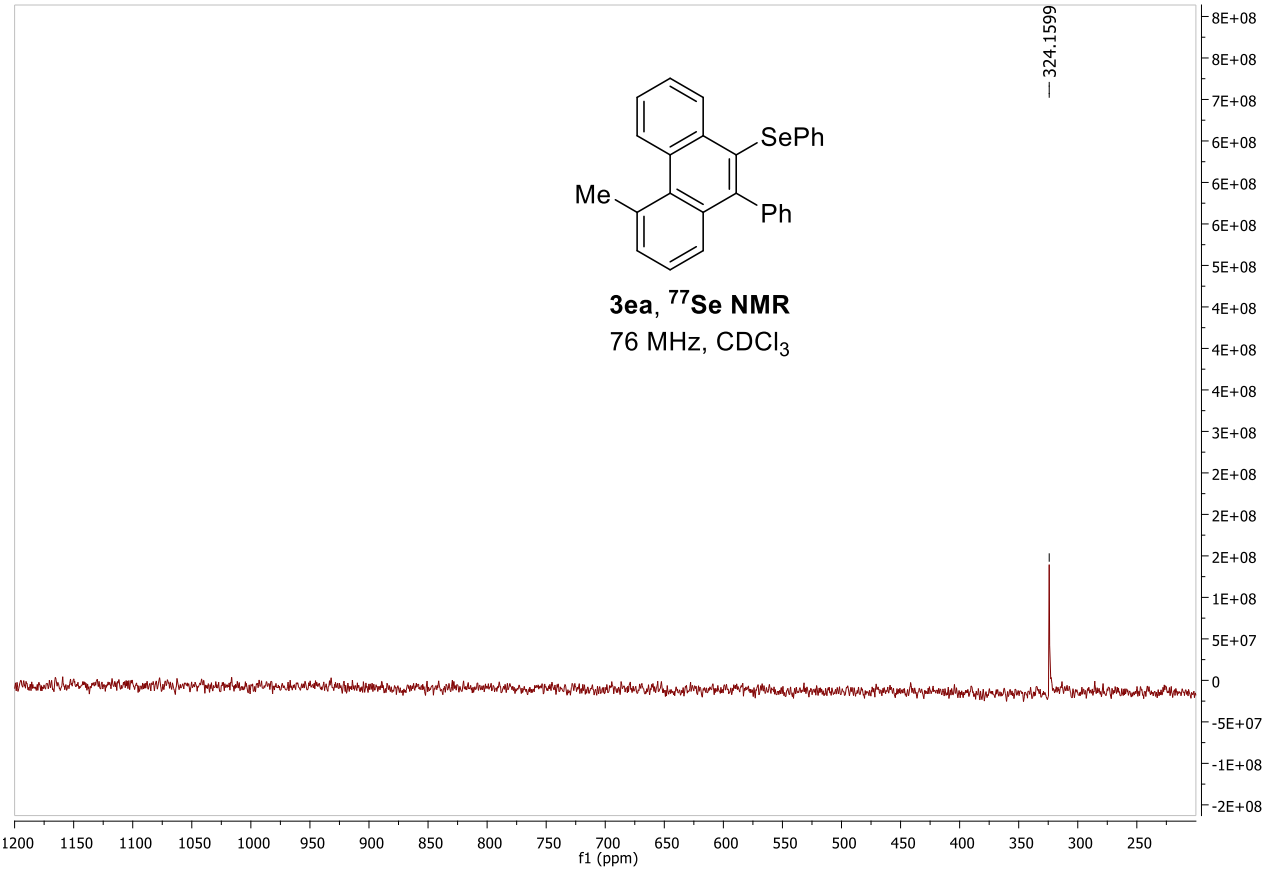
324.1599
SePh
Me
Ph
3ea, 77Se NMR
76 MHz, CDCl3
f1 (ppm)

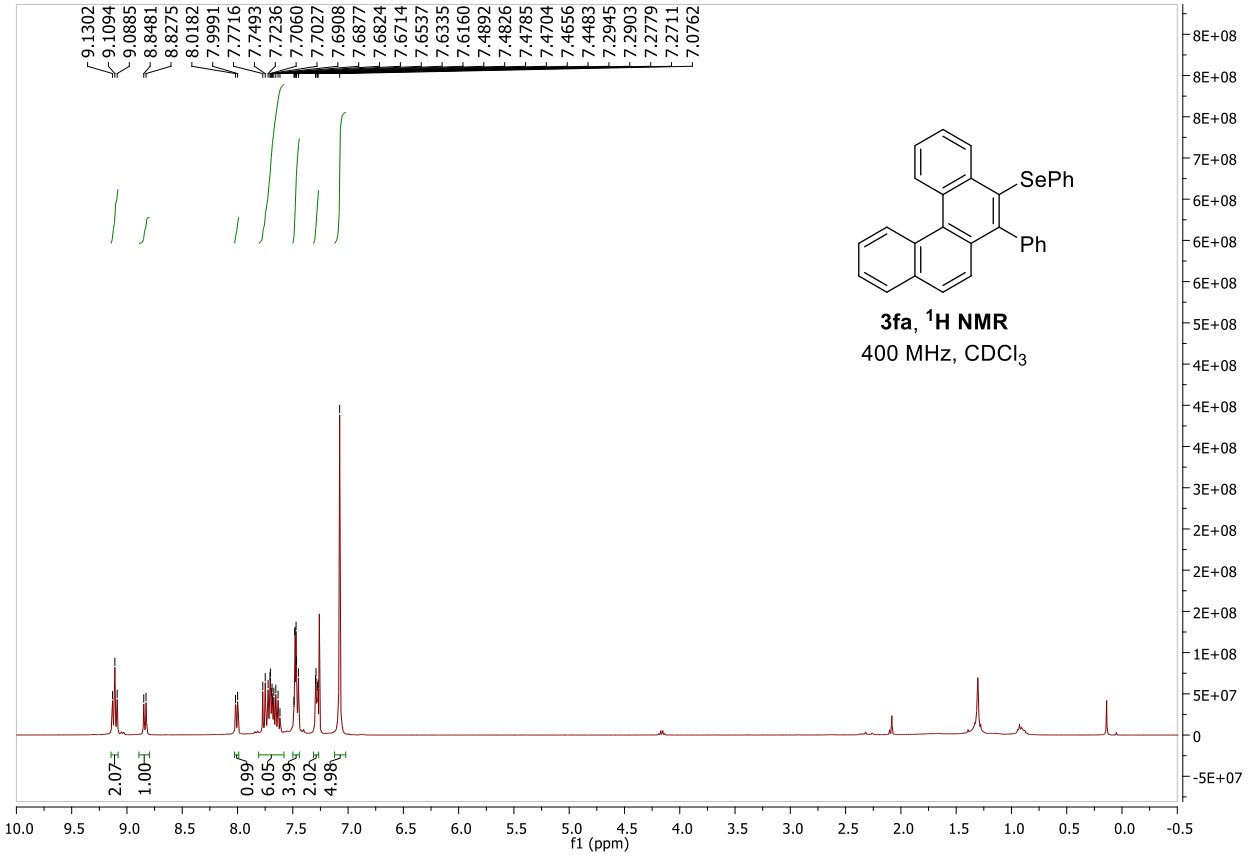

3fa, **^{1}H NMR**
400 MHz, $CDCl_3$

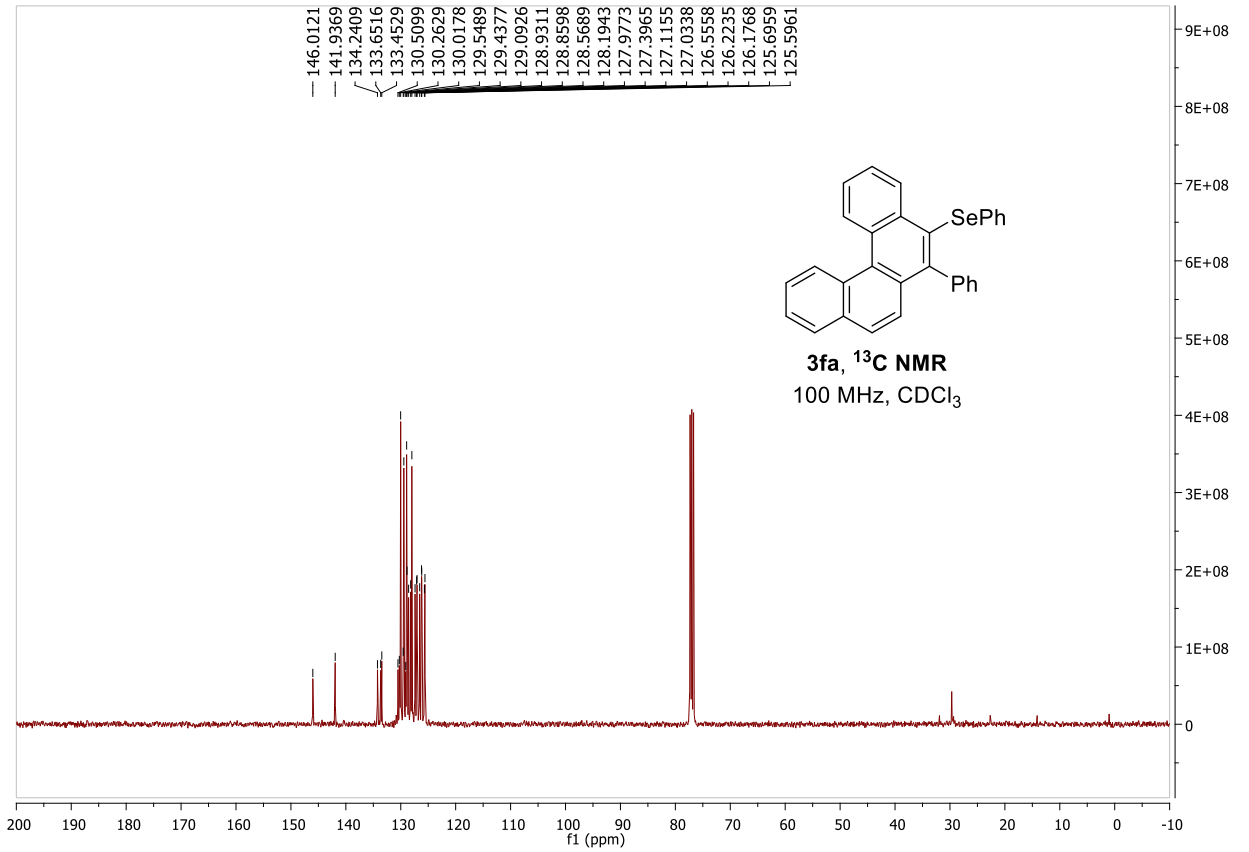

3fa, **^{13}C NMR**
100 MHz, $CDCl_3$

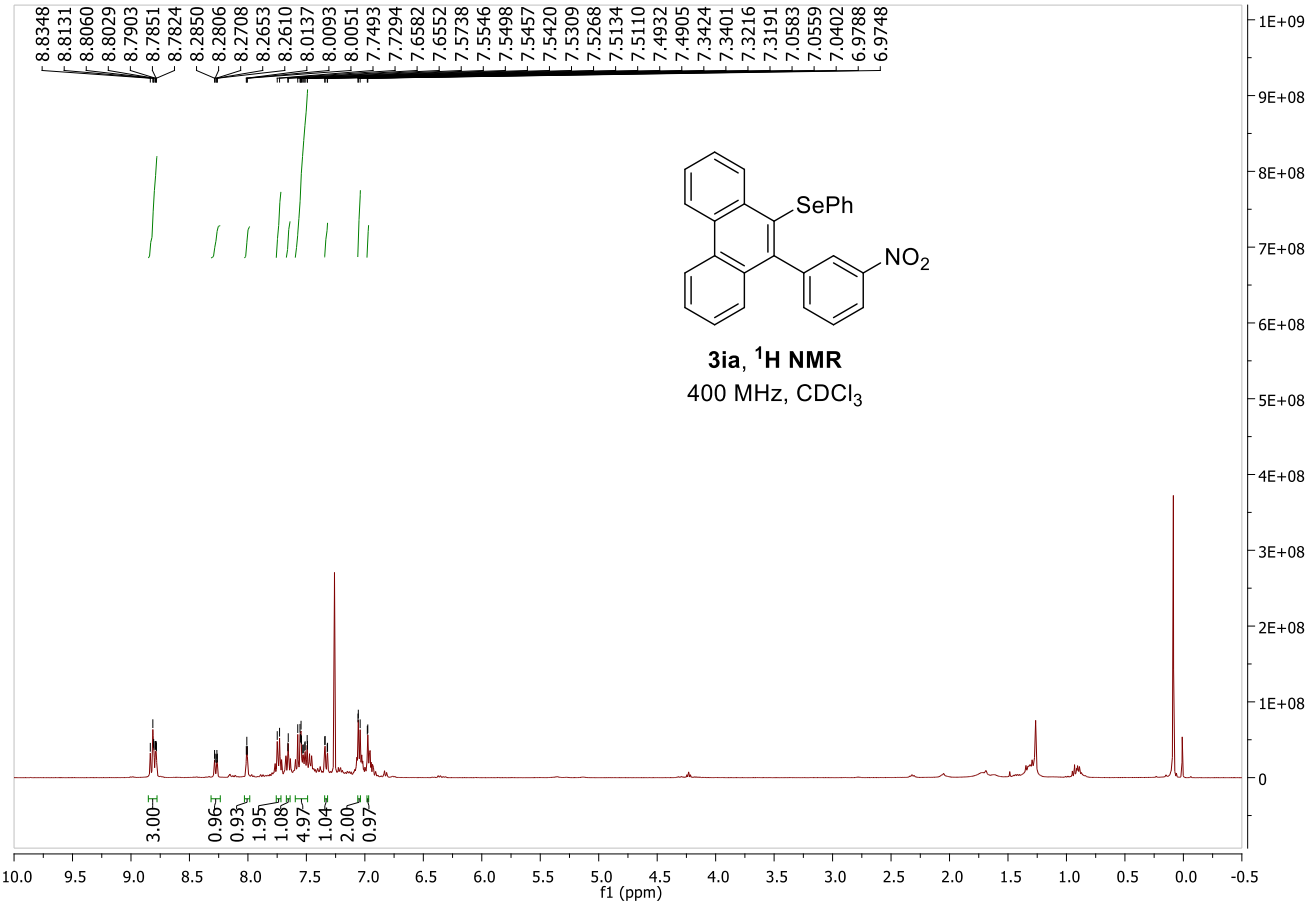

3ia, **^{1}H NMR**

400 MHz, $CDCl_3$

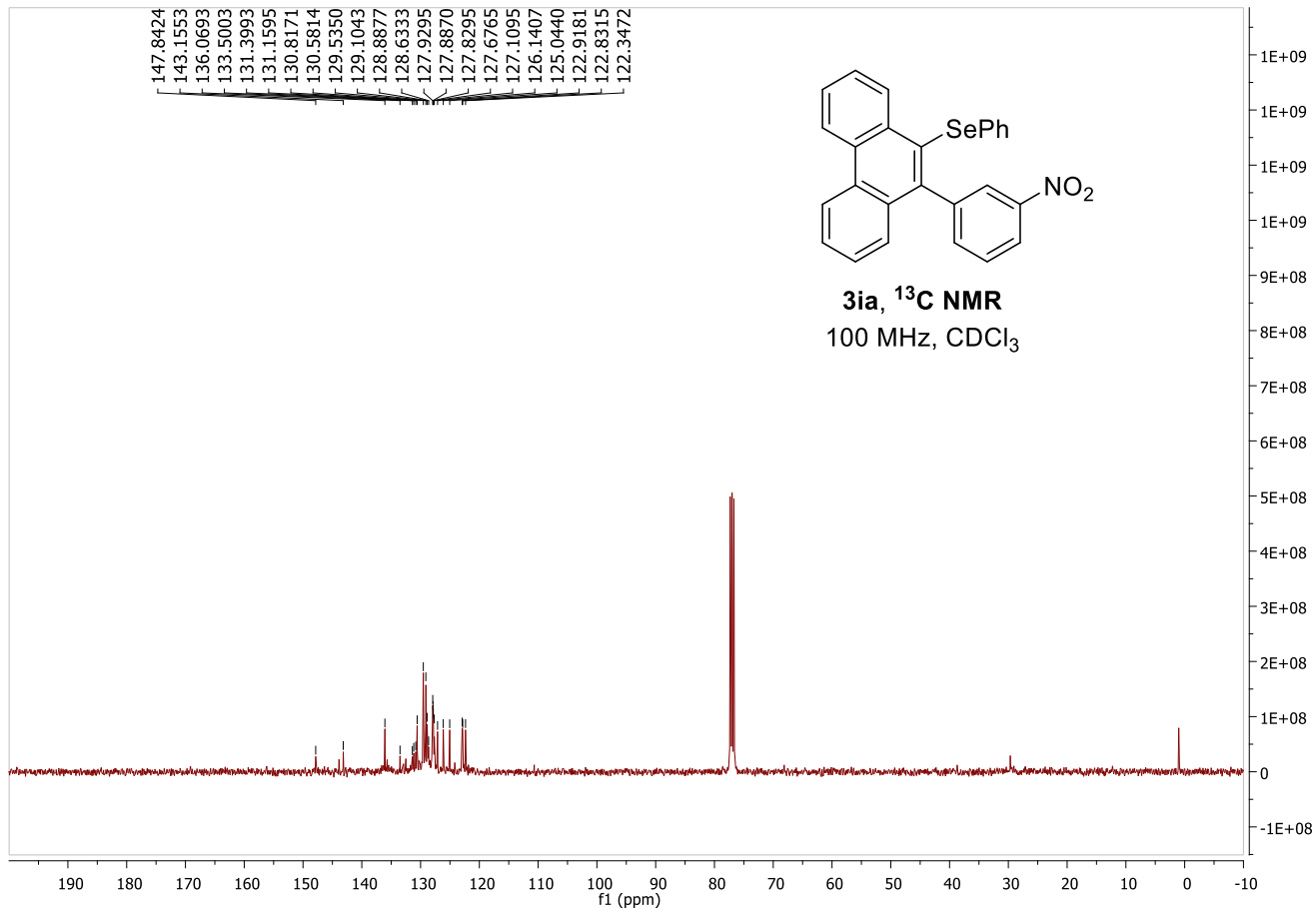

3ia, **^{13}C NMR**

100 MHz, $CDCl_3$

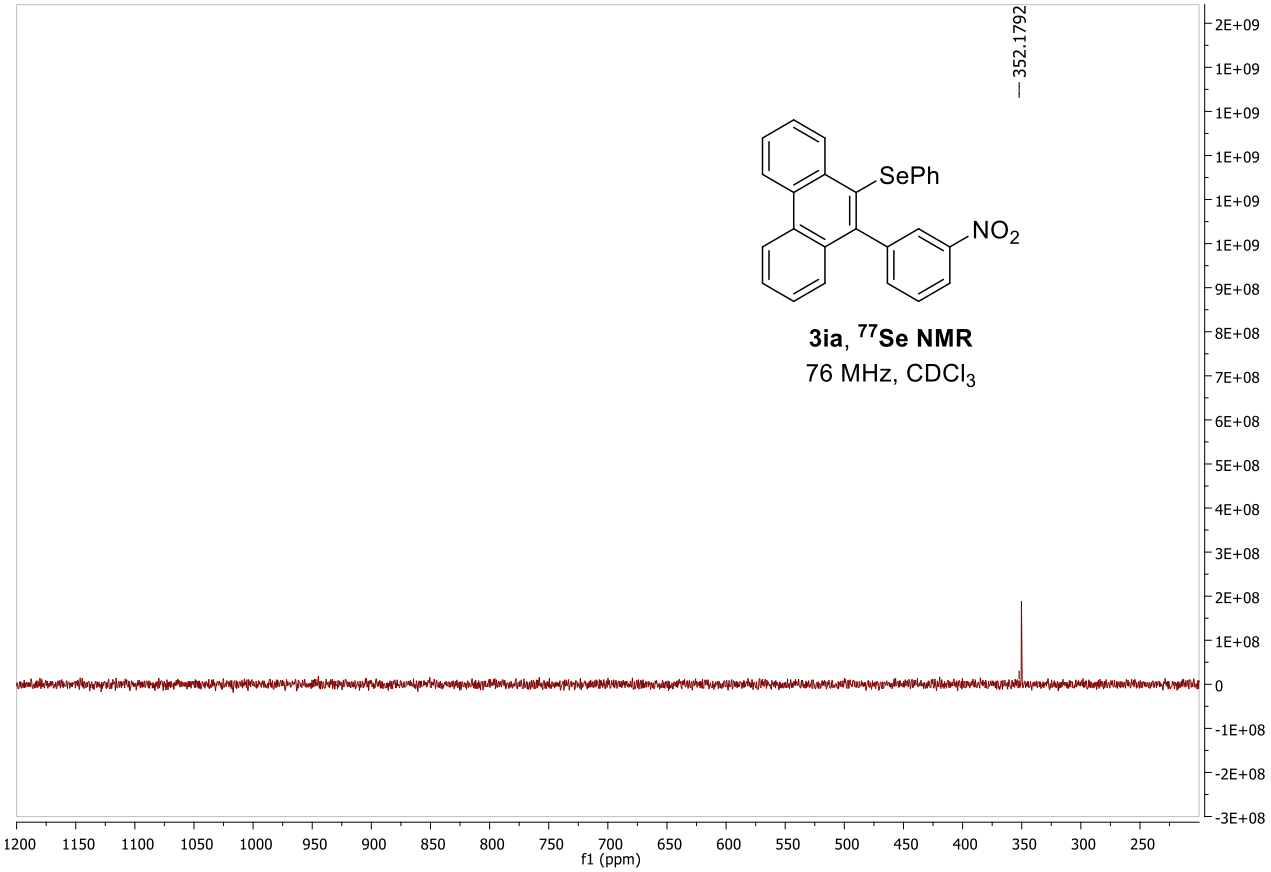
352.1792
SePh
NO2
3ia, 77Se NMR
76 MHz, CDCl3
f1 (ppm)

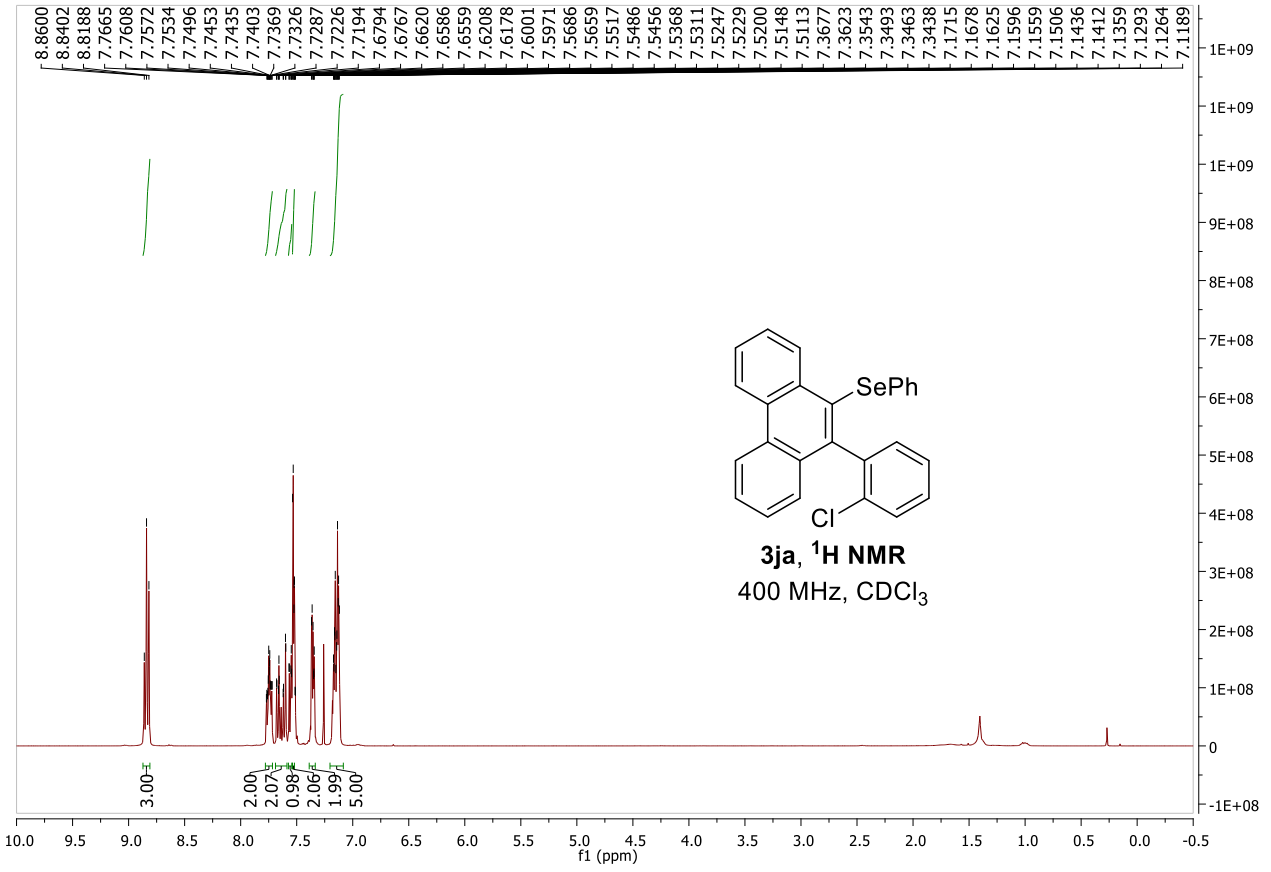
SePh
Cl
3ja, 1H NMR
400 MHz, CDCl3
3.00
2.00
2.07
0.98
2.06
1.99
5.00
f1 (ppm)

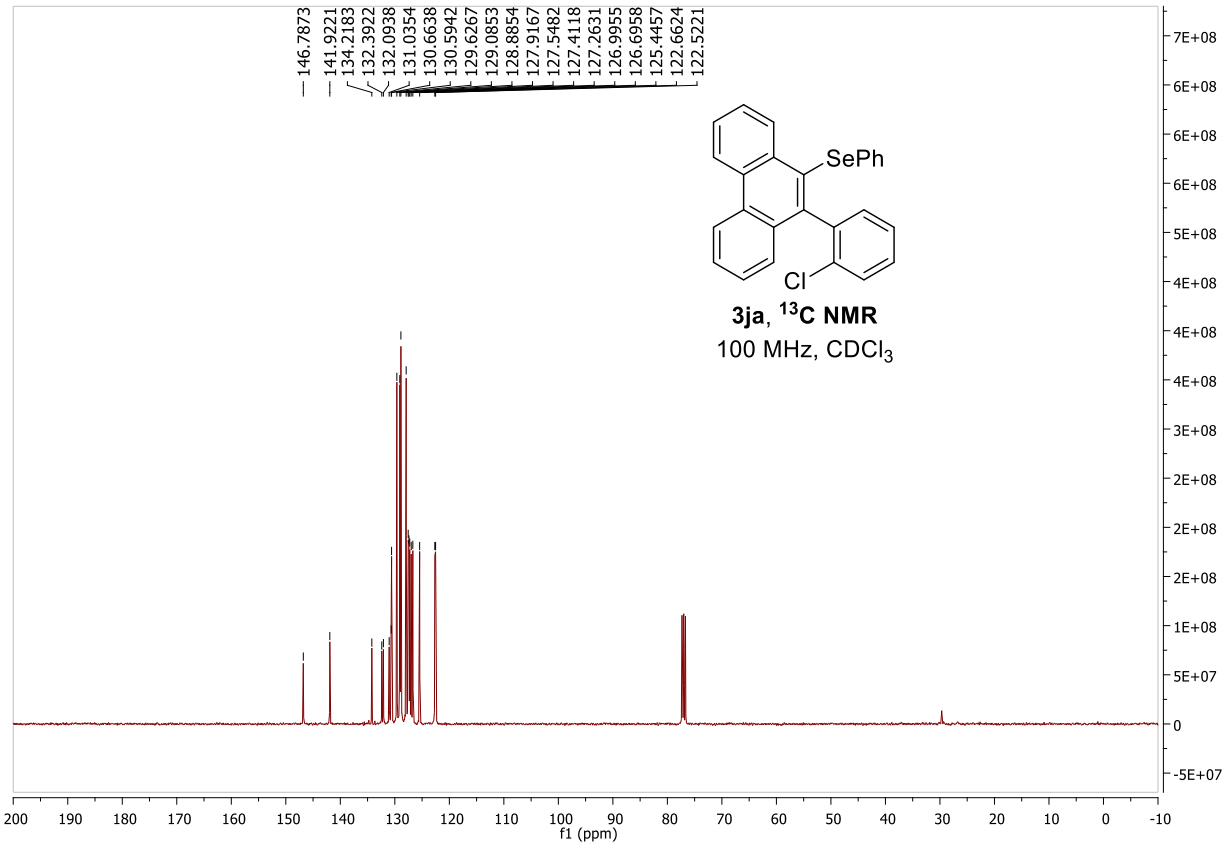
146.7873
141.9221
134.2183
132.3922
132.0938
131.0354
130.6638
130.5942
129.6267
129.0853
128.8854
127.9167
127.5482
127.4118
127.2631
126.9955
126.6958
125.4457
122.6624
122.5221
SePh
Cl
3ja, 13C NMR
100 MHz, CDCl3
f1 (ppm)

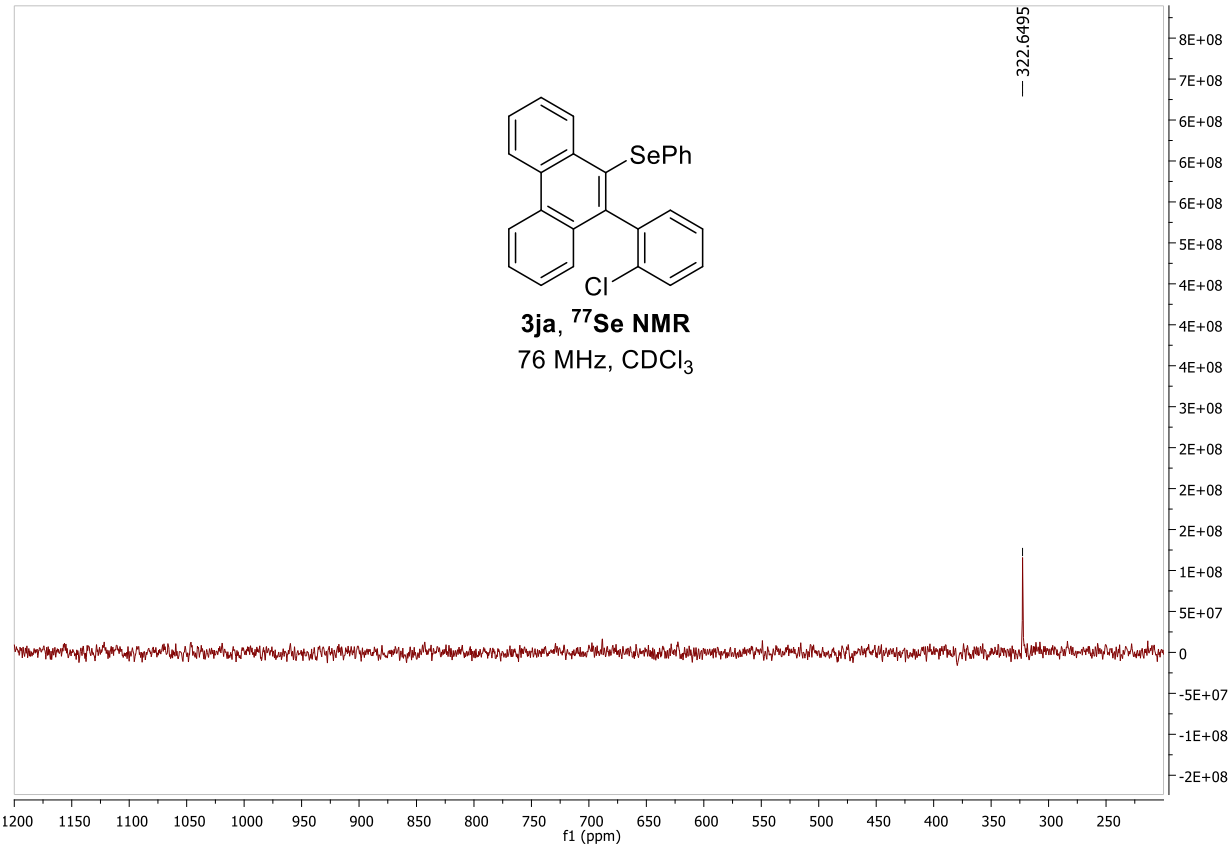
322.6495
SePh
Cl
3ja, 77Se NMR
76 MHz, CDCl3
f1 (ppm)

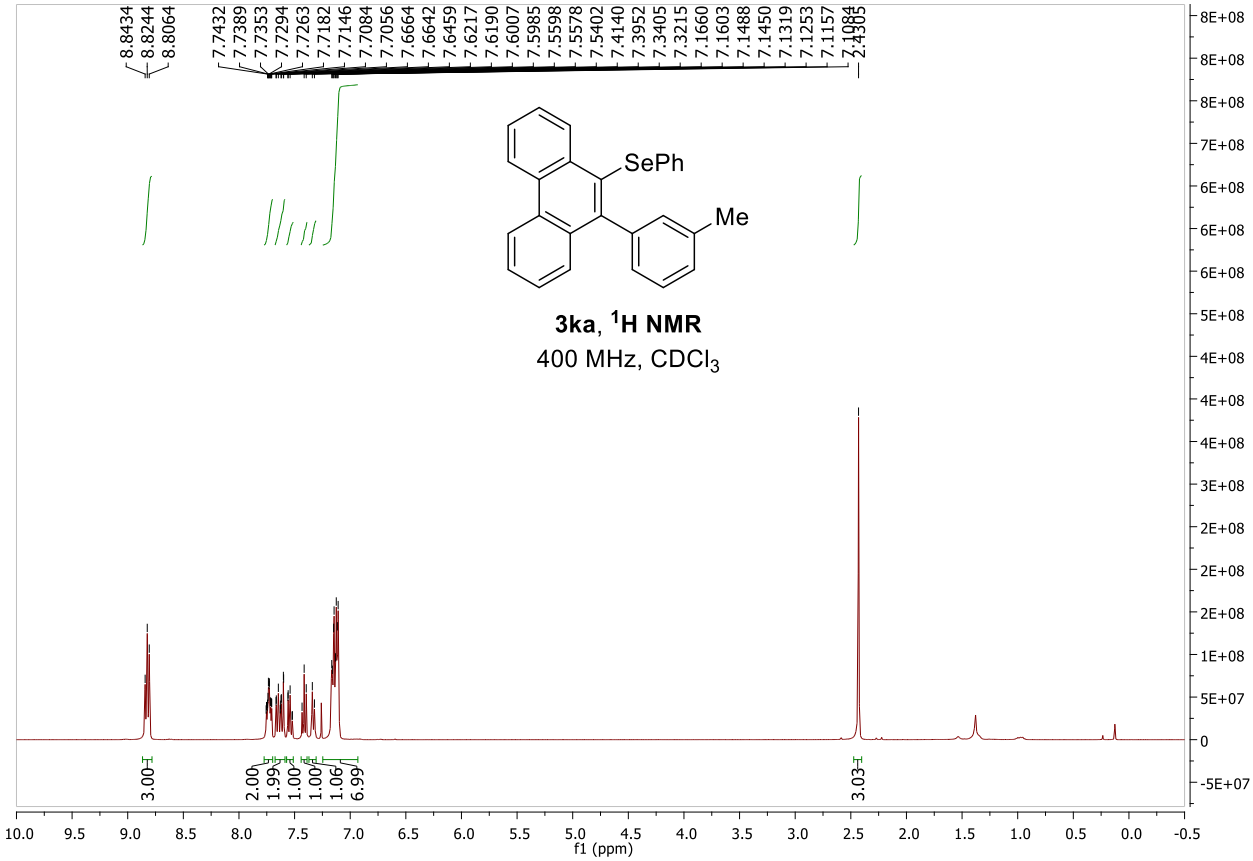

3ka, **^{1}H NMR**
400 MHz, $CDCl_3$

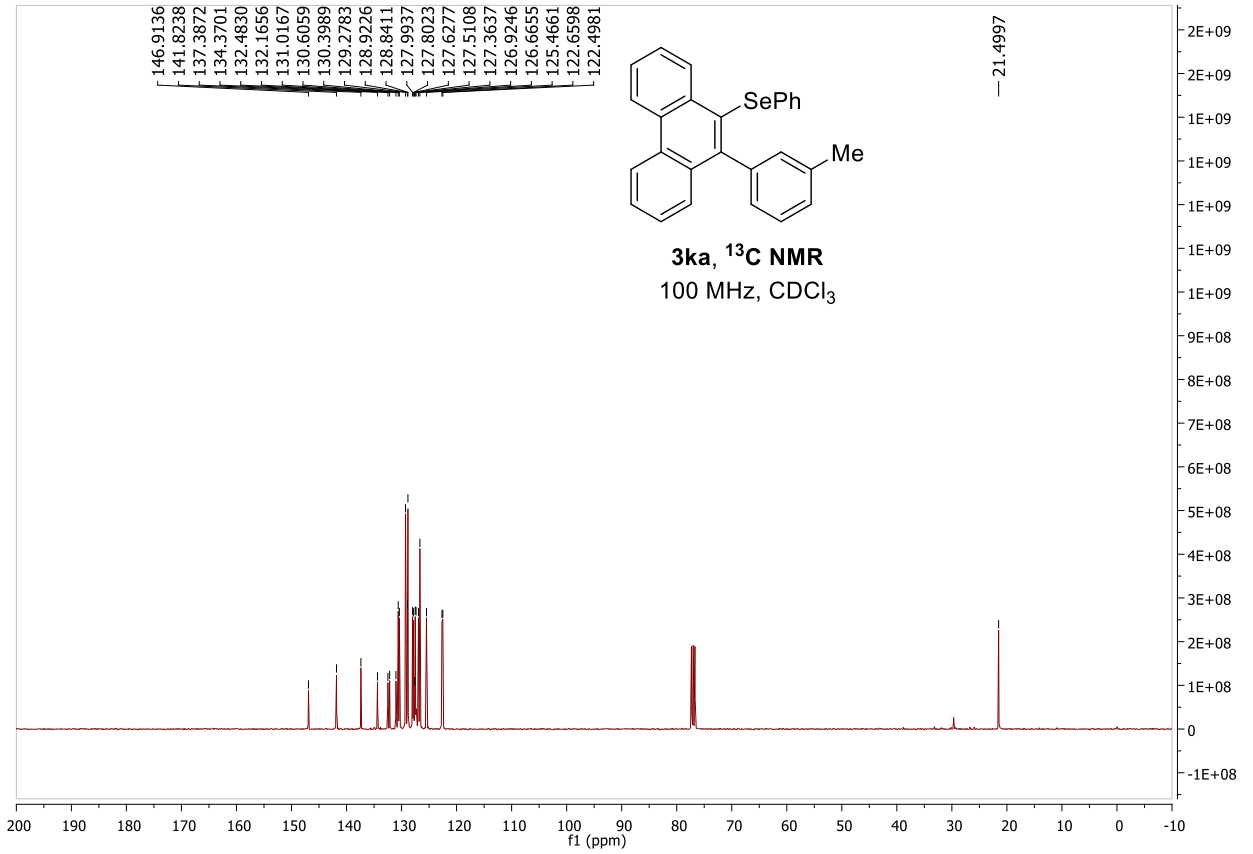

3ka, **^{13}C NMR**
100 MHz, $CDCl_3$

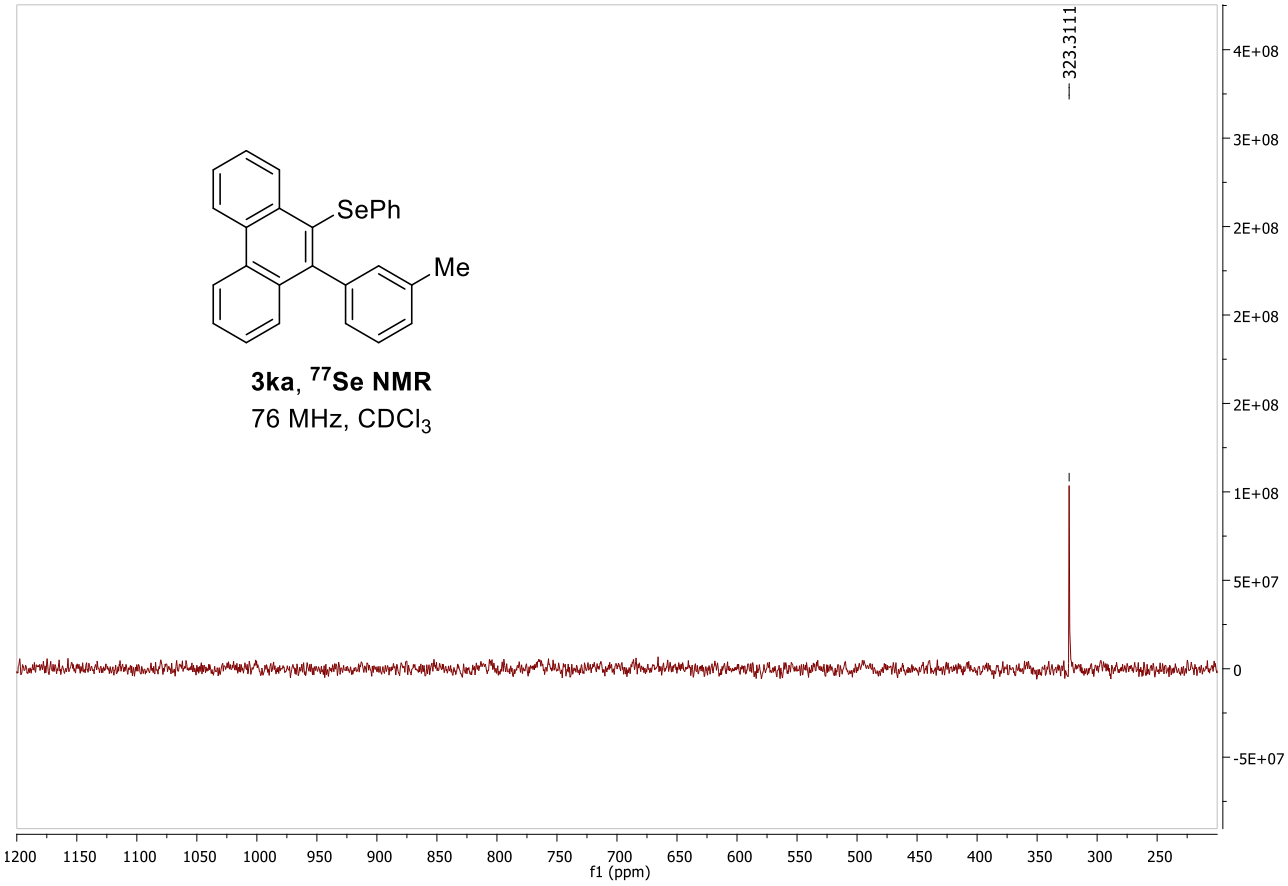
323.3111
SePh
Me
3ka, 77Se NMR
76 MHz, CDCl3
f1 (ppm)

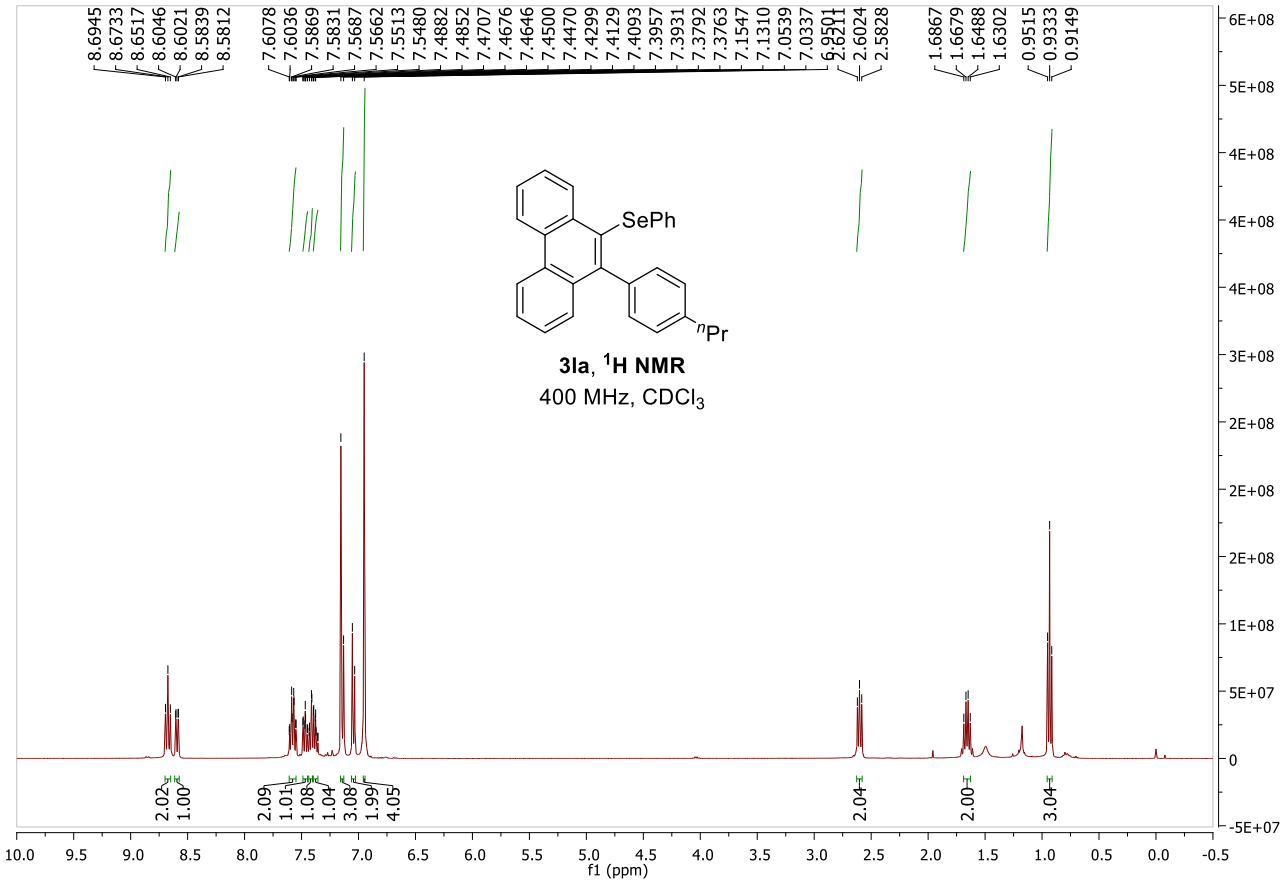
8.6945
8.6733
8.6517
8.6046
8.6021
8.5839
8.5812
7.6078
7.6036
7.5869
7.5831
7.5687
7.5662
7.5513
7.5480
7.4882
7.4852
7.4707
7.4676
7.4646
7.4500
7.4470
7.4299
7.4129
7.4093
7.3957
7.3931
7.3792
7.3763
7.1547
7.1310
7.0539
7.0337
6.9501
2.6211
2.6024
2.5828
1.6867
1.6679
1.6488
1.6302
0.9515
0.9333
0.9149
SePh
nPr
3la, 1H NMR
400 MHz, CDCl3
2.02
1.00
2.09
1.01
1.08
1.04
3.08
1.99
4.05
2.04
2.00
3.04
f1 (ppm)

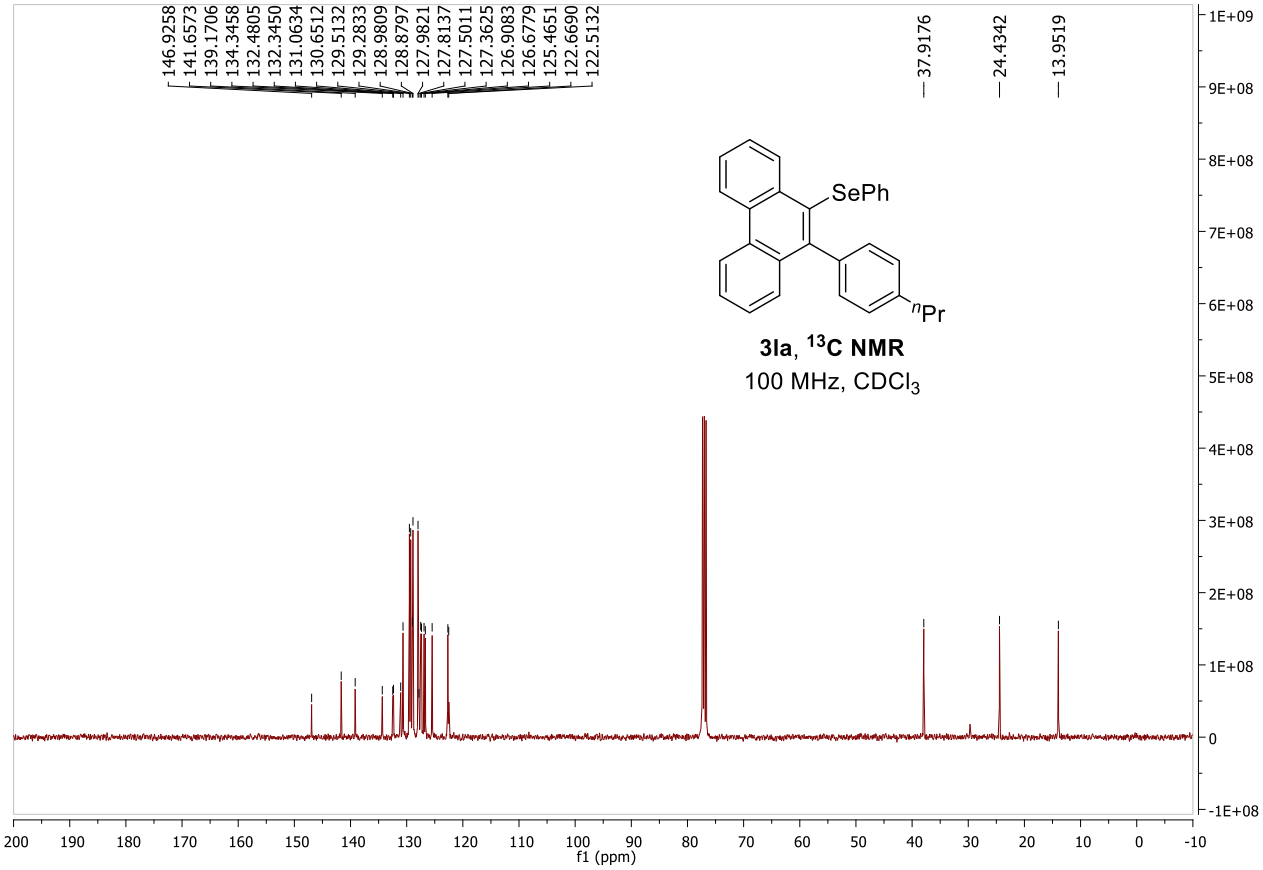
146.9258
141.6573
139.1706
134.3458
132.4805
132.3450
131.0634
130.6512
129.5132
129.2833
128.9809
128.8797
127.9821
127.8137
127.5011
127.3625
126.9083
126.6779
125.4651
122.6690
122.5132
37.9176
24.4342
13.9519
SePh
nPr
3la, 13C NMR
100 MHz, CDCl3
f1 (ppm)

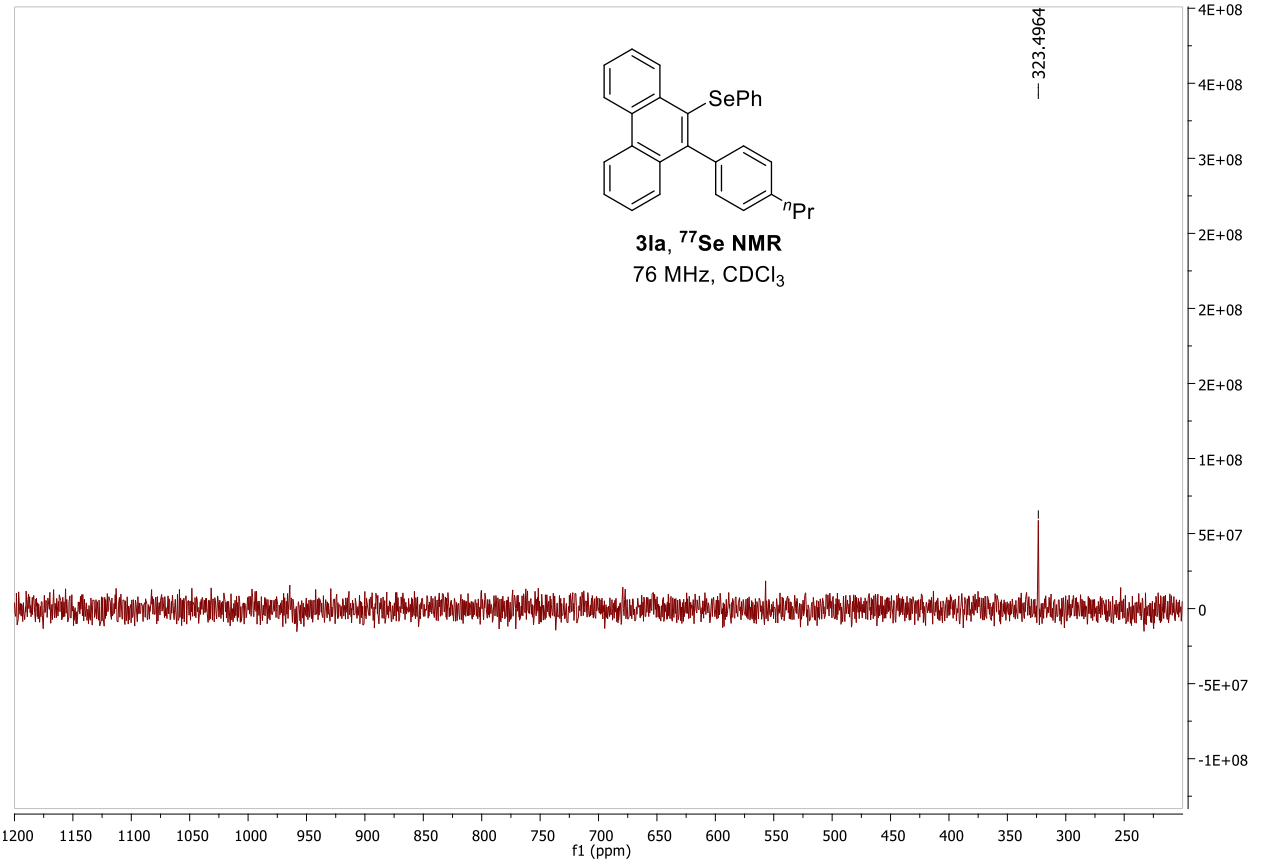
323.4964
SePh
nPr
3la, 77Se NMR
76 MHz, CDCl3
f1 (ppm)

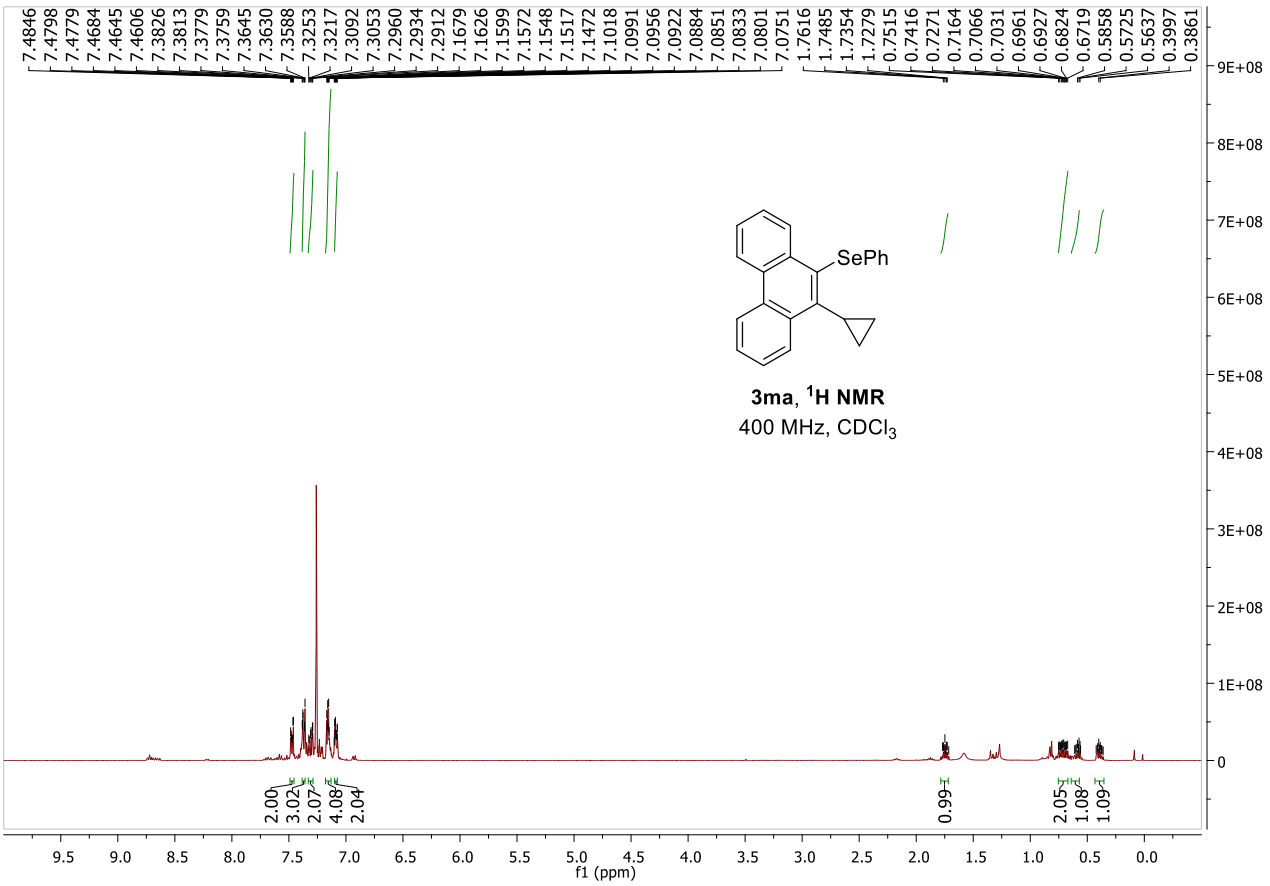
SePh
3ma, 1H NMR
400 MHz, CDCl3
f1 (ppm)

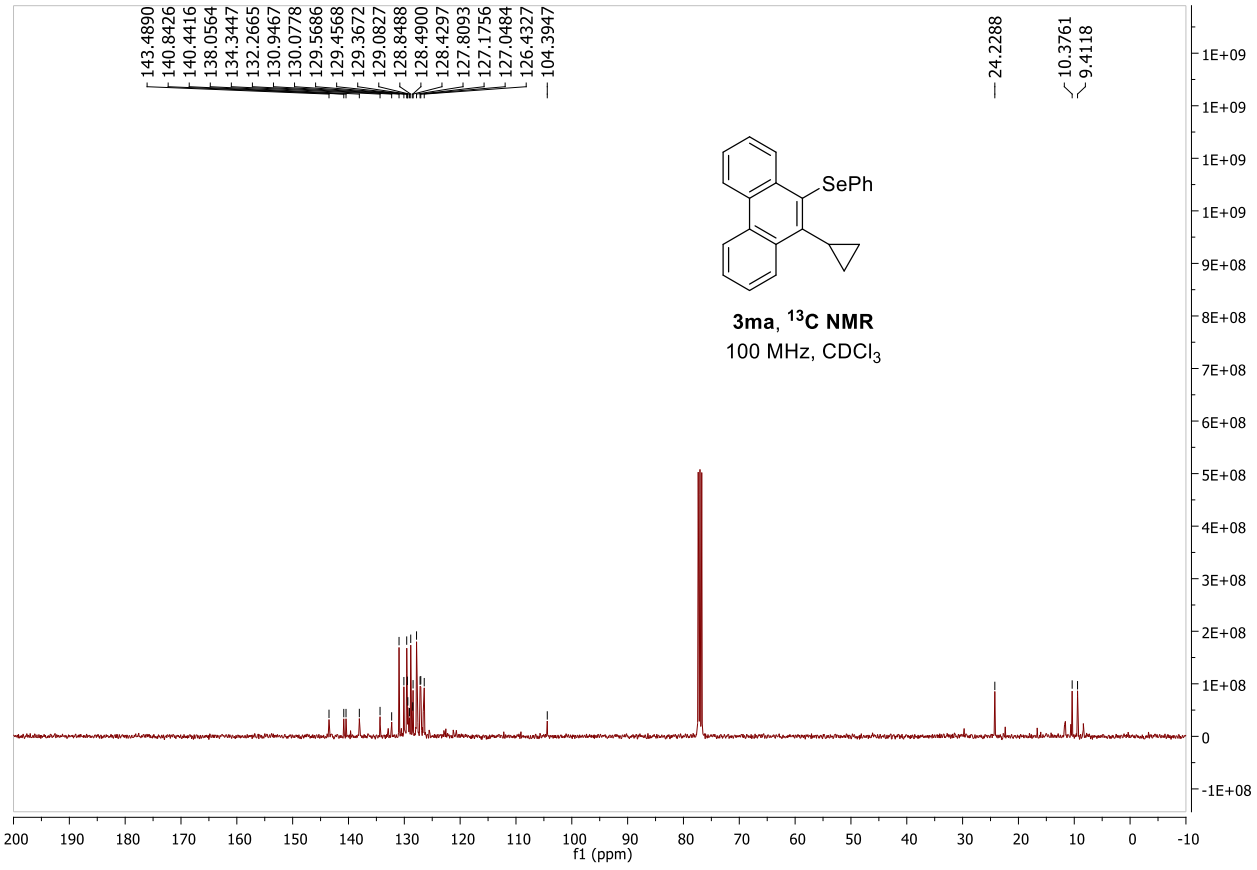
SePh
3ma, 13C NMR
100 MHz, CDCl3
f1 (ppm)

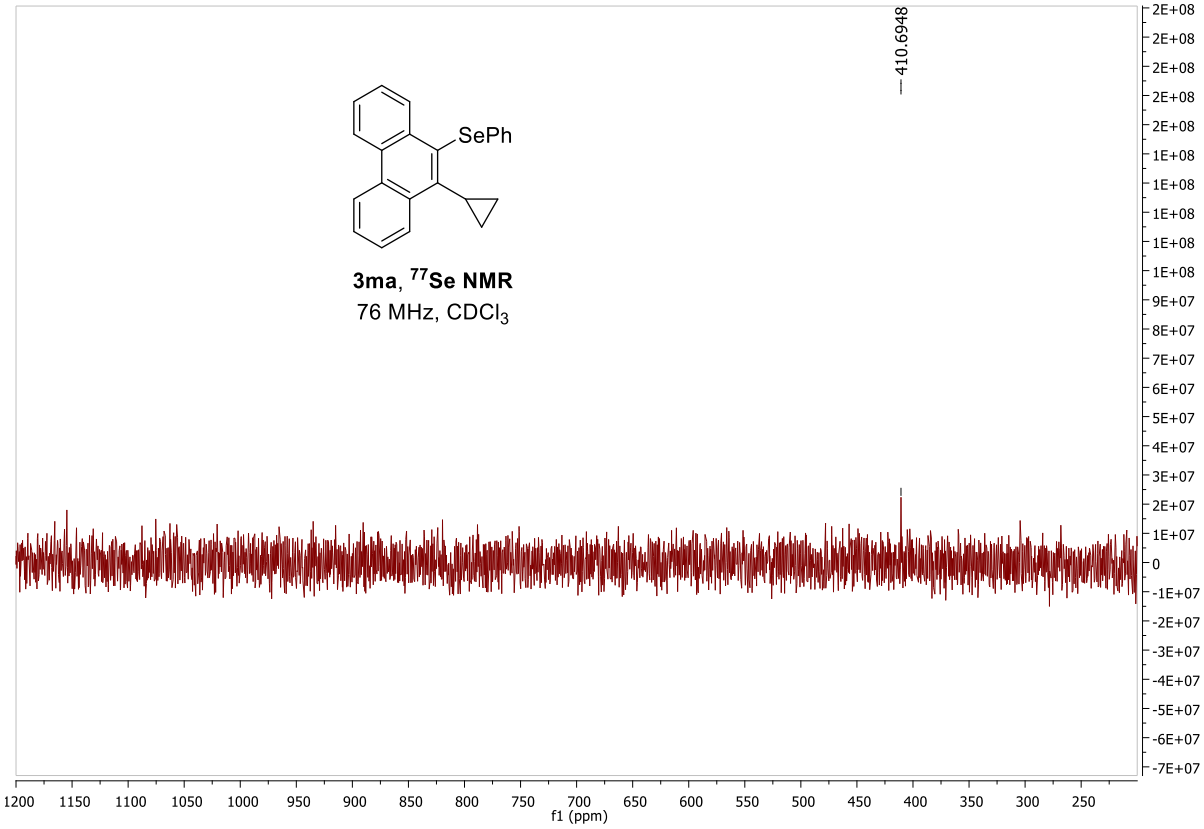
410.6948
SePh
3ma, 77Se NMR
76 MHz, CDCl3
f1 (ppm)

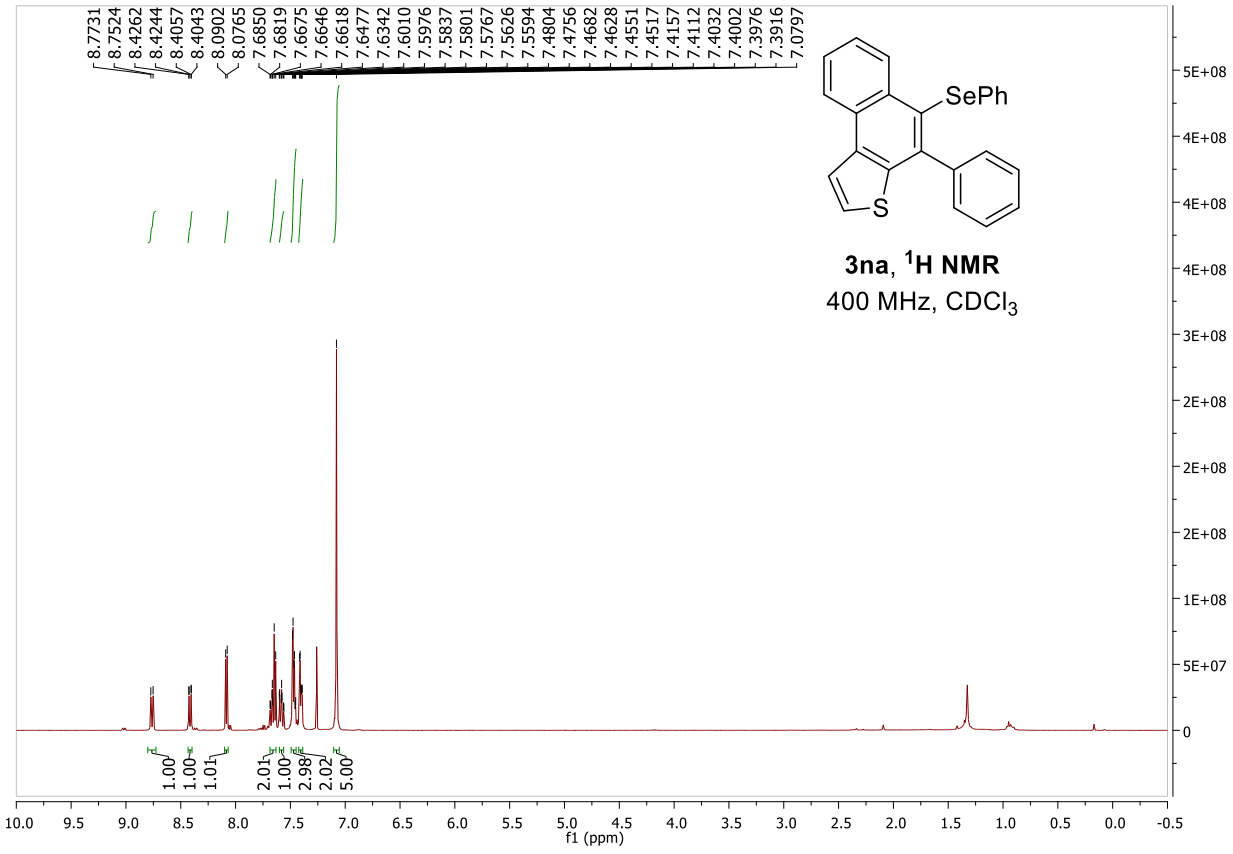
8.7731
8.7524
8.4262
8.4244
8.4057
8.4043
8.0902
8.0765
7.6850
7.6819
7.6675
7.6646
7.6618
7.6477
7.6342
7.6010
7.5976
7.5837
7.5801
7.5767
7.5626
7.5594
7.4804
7.4756
7.4682
7.4628
7.4551
7.4517
7.4157
7.4112
7.4032
7.4002
7.3976
7.3916
7.0797
SePh
S
3na, 1H NMR
400 MHz, CDCl3
1.00
1.00
1.01
2.01
1.00
2.98
2.02
5.00
f1 (ppm)

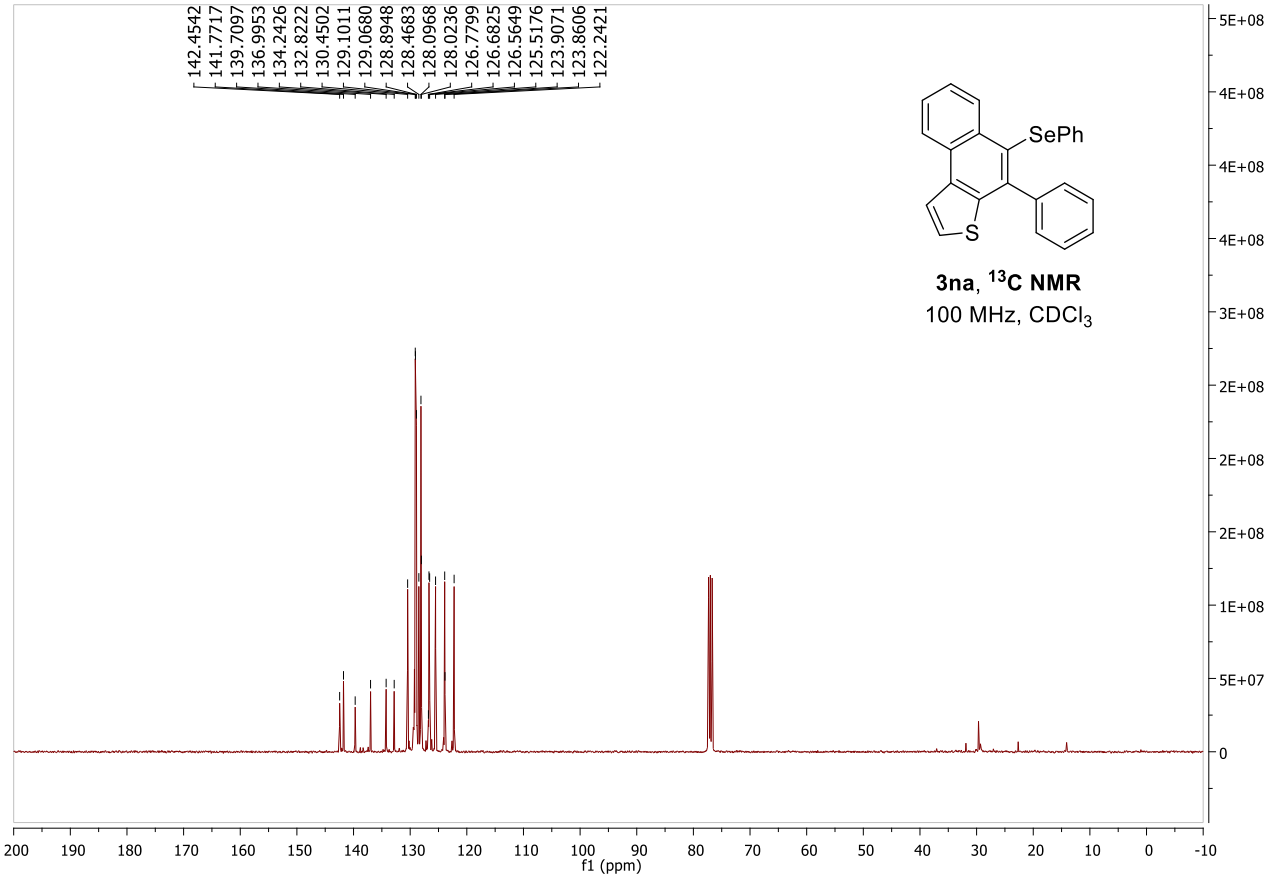
142.4542
141.7717
139.7097
136.9953
134.2426
132.8222
130.4502
129.1011
129.0680
128.8948
128.4683
128.0968
128.0236
126.7799
126.6825
126.5649
125.5176
123.9071
123.8606
122.2421
SePh
S
3na, 13C NMR
100 MHz, CDCl3
f1 (ppm)

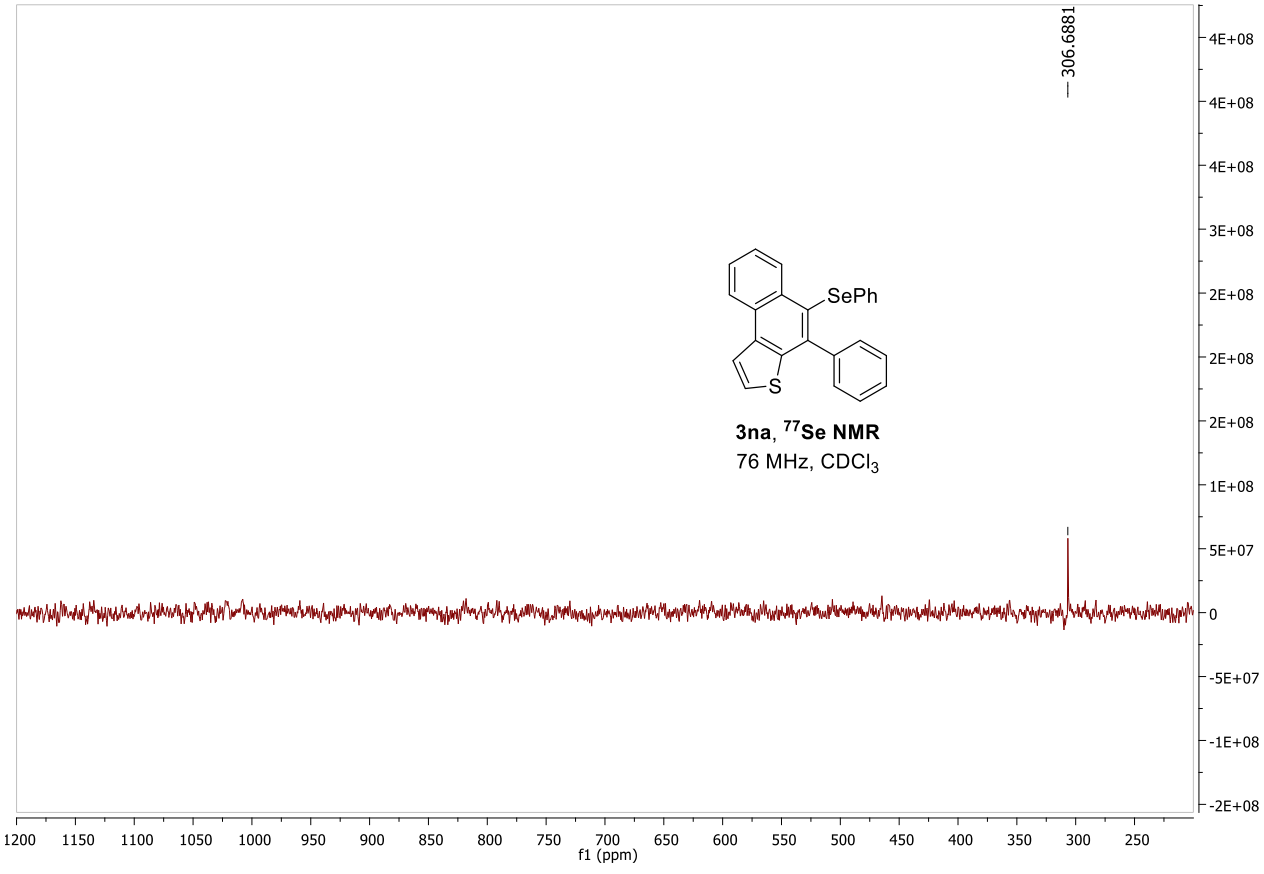
306.6881
SePh
S
3na, 77Se NMR
76 MHz, CDCl3
f1 (ppm)

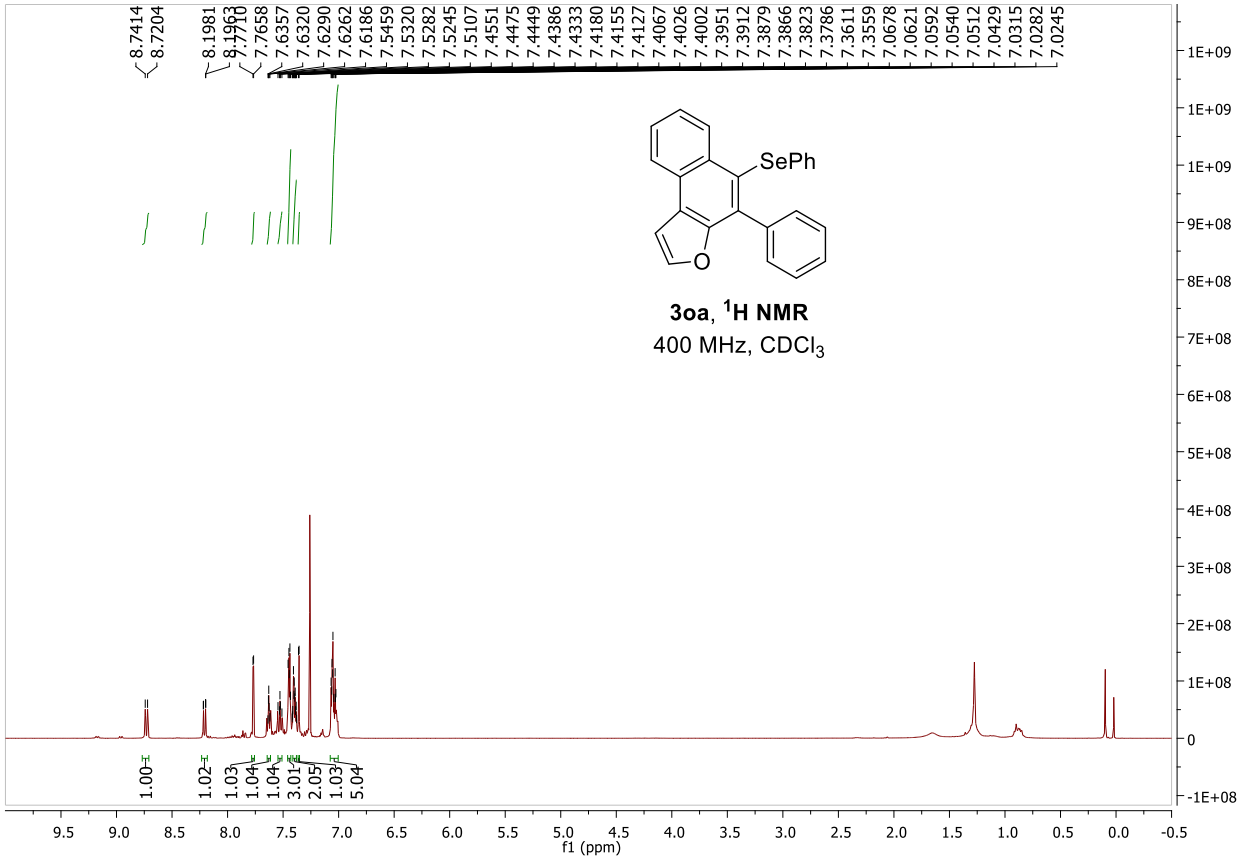

3oa, ^{1}**H NMR**
400 MHz, $CDCl_3$

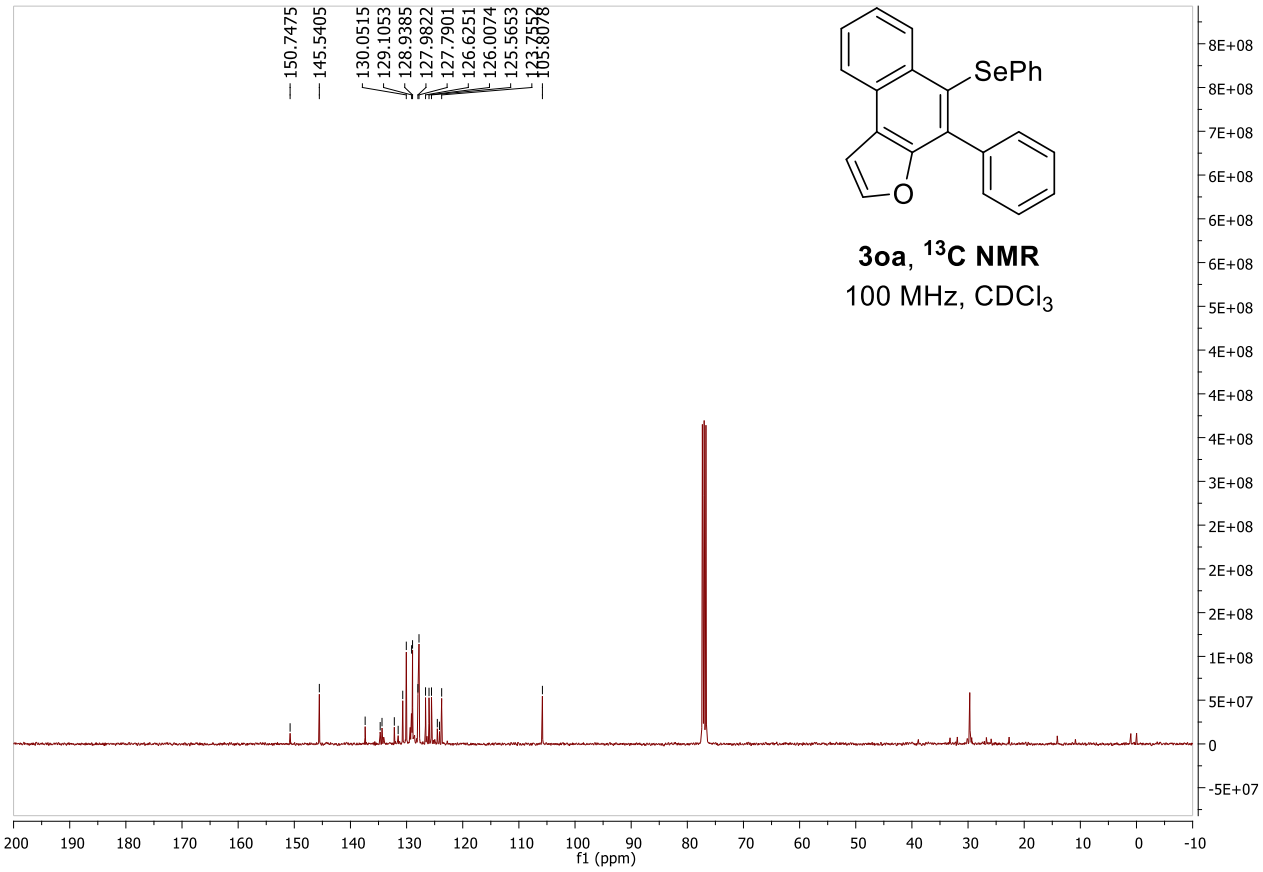

3oa, ^{13}**C NMR**
100 MHz, $CDCl_3$

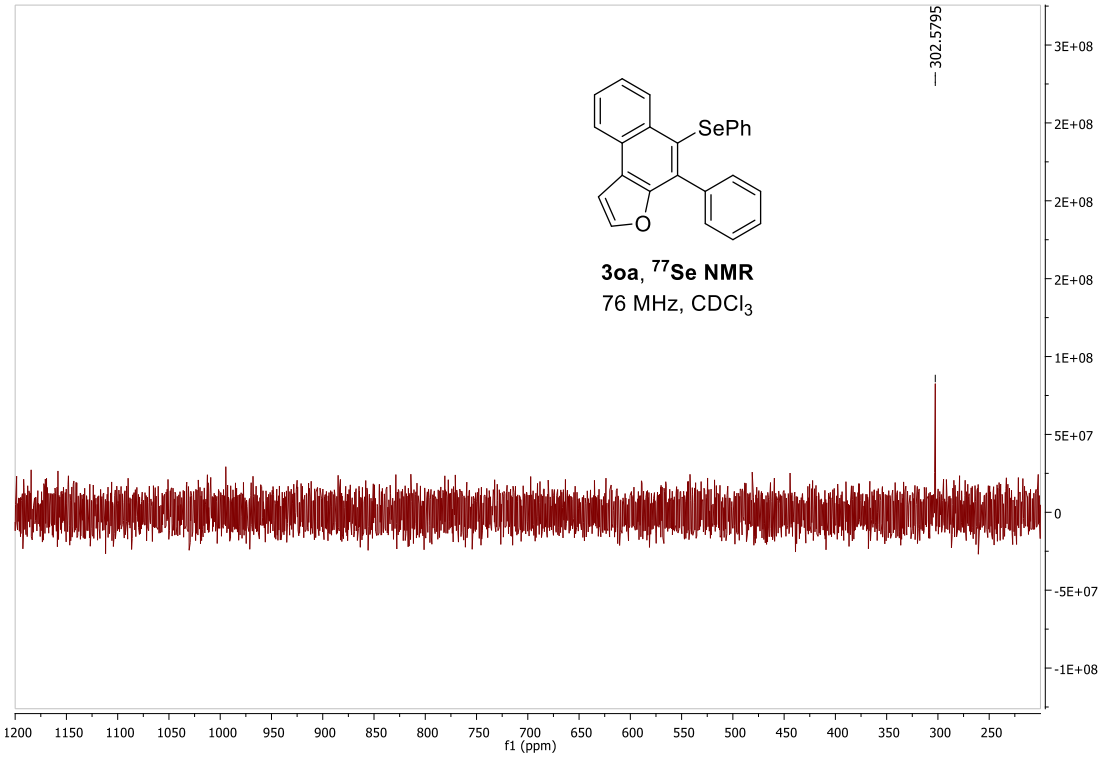
302.5795
SePh
O
3oa, 77Se NMR
76 MHz, CDCl3
f1 (ppm)

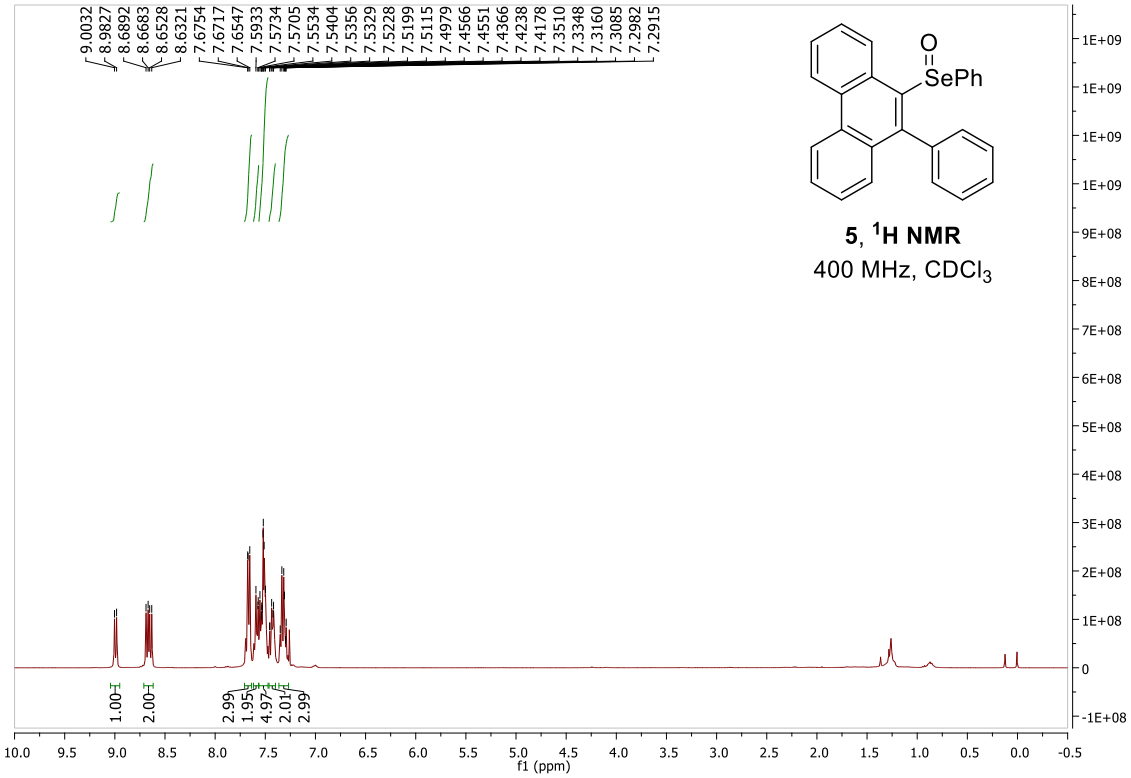
9.0032
8.9827
8.6892
8.6683
8.6528
8.6321
7.6754
7.6717
7.6547
7.5933
7.5734
7.5705
7.5534
7.5404
7.5356
7.5329
7.5228
7.5199
7.5115
7.4979
7.4566
7.4551
7.4366
7.4238
7.4178
7.3510
7.3348
7.3160
7.3085
7.2982
7.2915
O
SePh
5, 1H NMR
400 MHz, CDCl3
1.00
2.00
2.99
1.95
4.97
2.01
2.99
f1 (ppm)

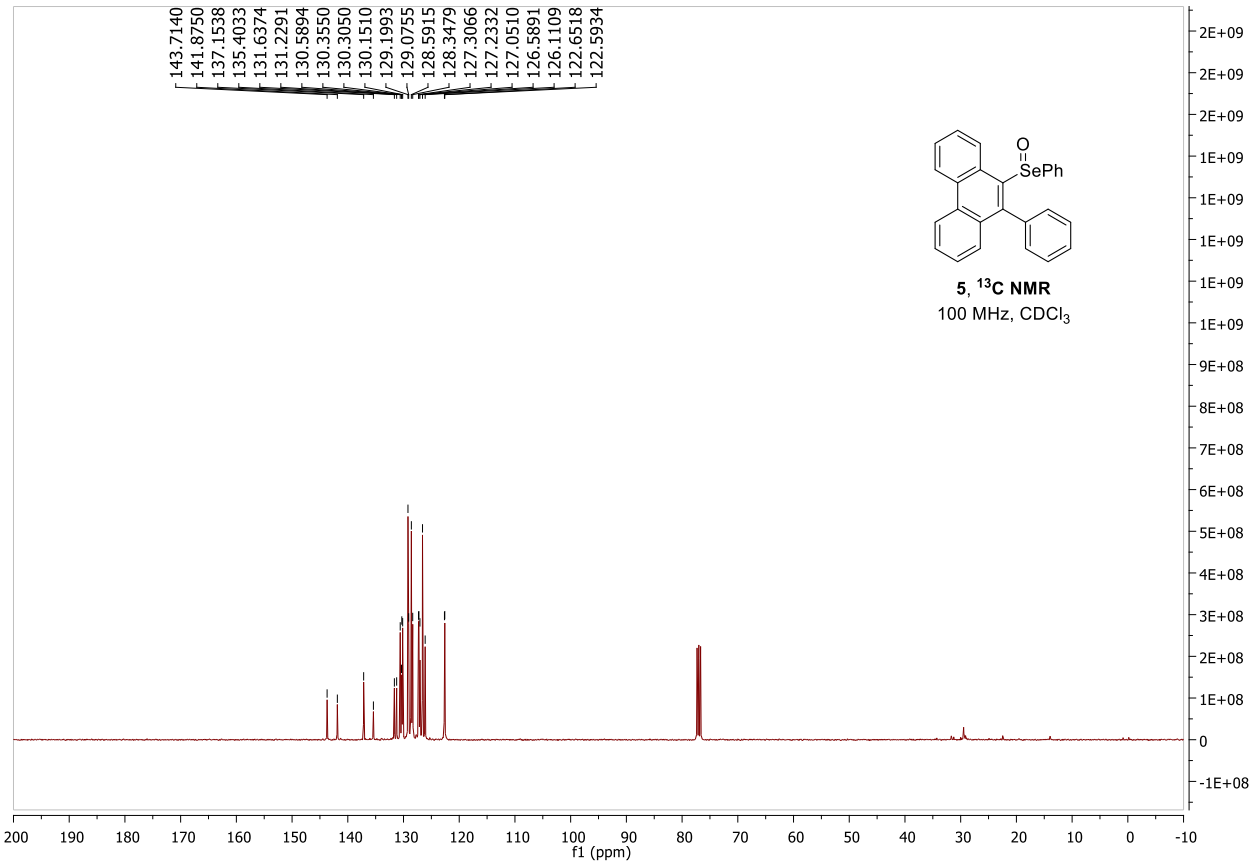

5, **^{13}C NMR**
100 MHz, $CDCl_3$

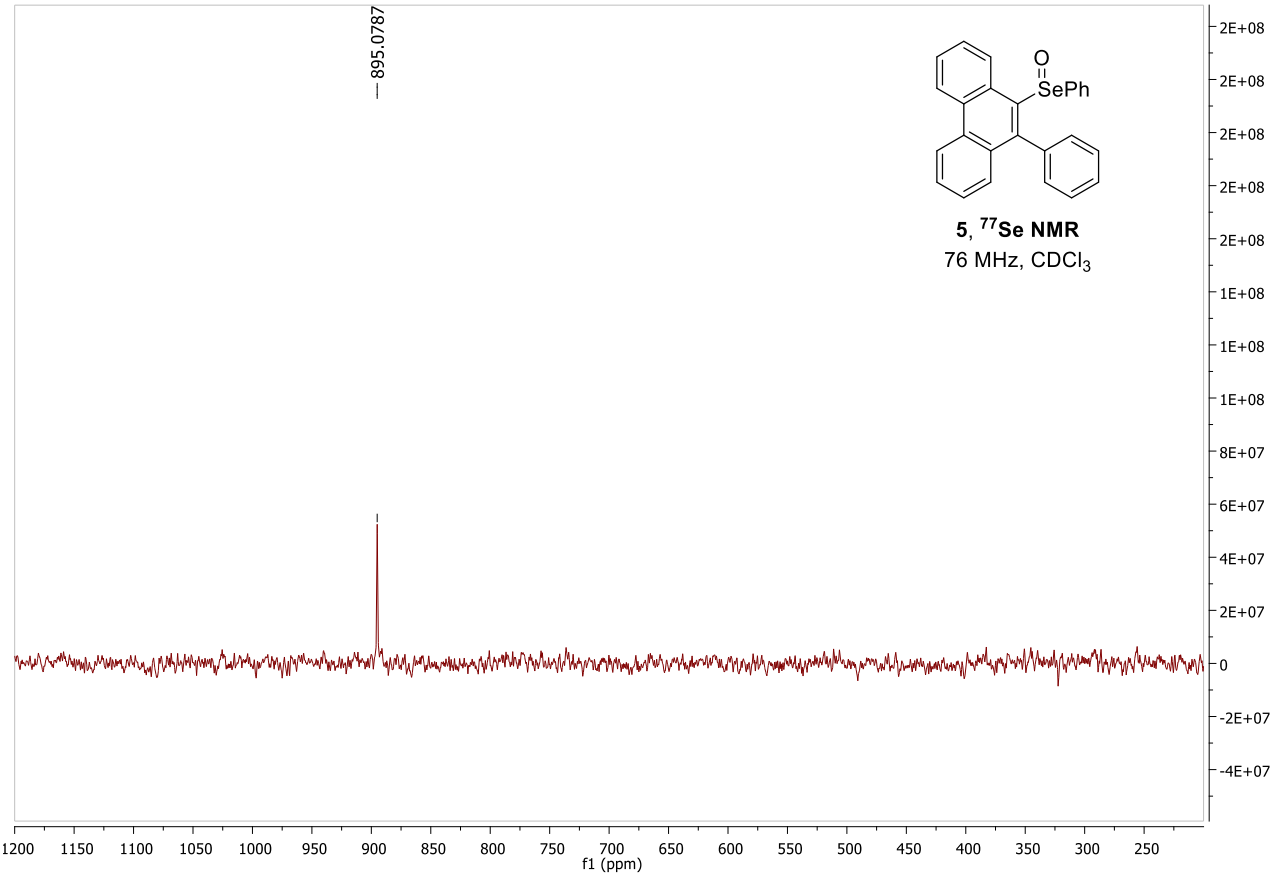

5, **^{77}Se NMR**
76 MHz, $CDCl_3$

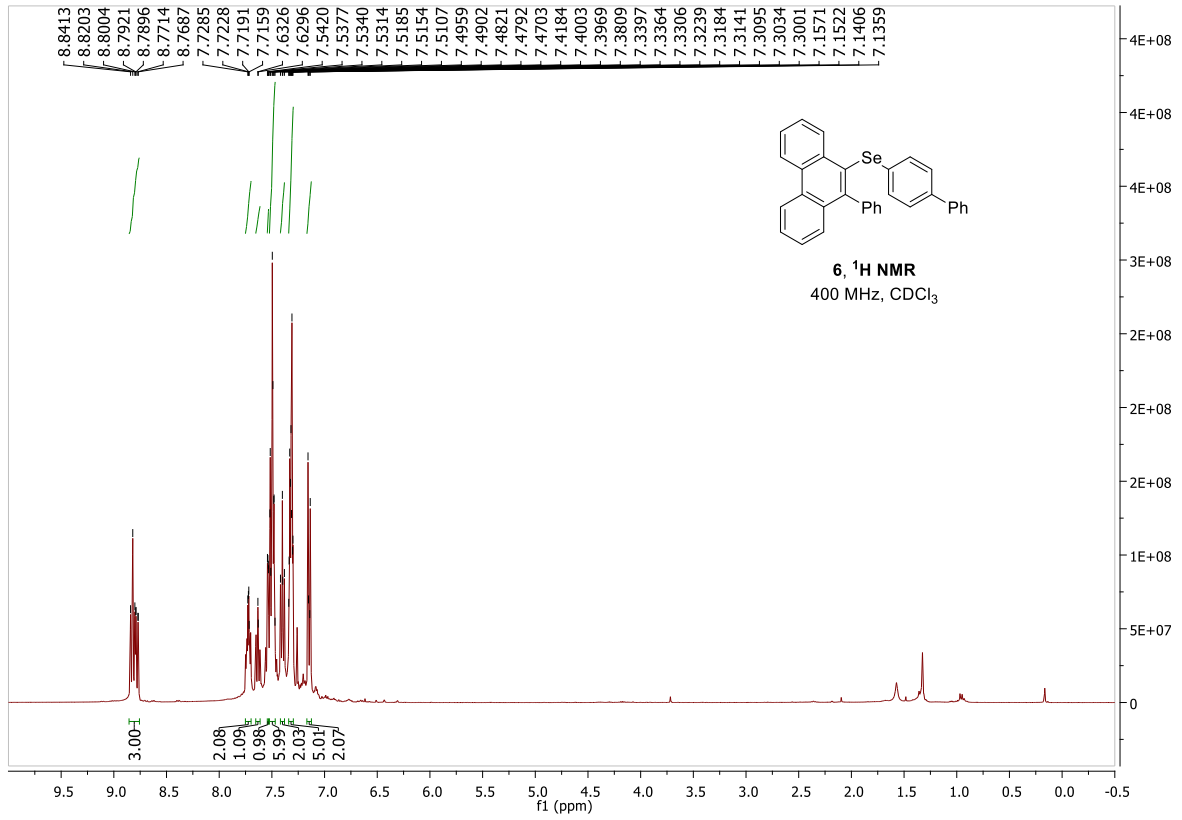
8.8413
8.8203
8.8004
8.7921
8.7896
8.7714
8.7687
7.7285
7.7228
7.7191
7.7159
7.6326
7.6296
7.5420
7.5377
7.5340
7.5314
7.5185
7.5154
7.5107
7.4959
7.4902
7.4821
7.4792
7.4703
7.4184
7.4003
7.3969
7.3809
7.3397
7.3364
7.3306
7.3239
7.3184
7.3141
7.3095
7.3034
7.3001
7.1571
7.1522
7.1406
7.1359
Se
Ph
Ph
6, 1H NMR
400 MHz, CDCl3
3.00
2.08
1.09
0.98
5.99
2.03
5.01
2.07
f1 (ppm)

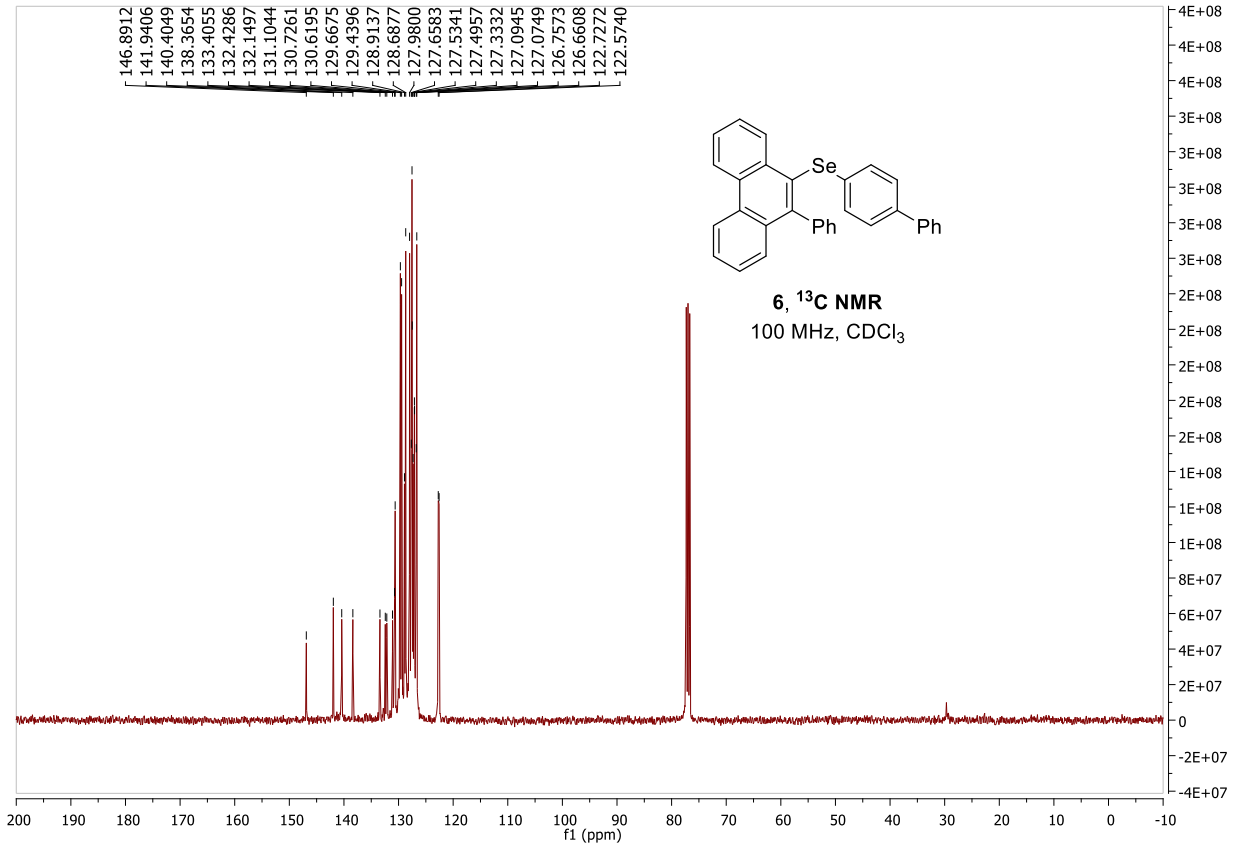
146.8912
141.9406
140.4049
138.3654
133.4055
132.4286
132.1497
131.1044
130.7261
130.6195
129.6675
129.4396
128.9137
128.6877
127.9800
127.6583
127.5341
127.4957
127.3332
127.0945
127.0749
126.7573
126.6608
122.7272
122.5740
Se
Ph
Ph
6, 13C NMR
100 MHz, CDCl3
f1 (ppm)

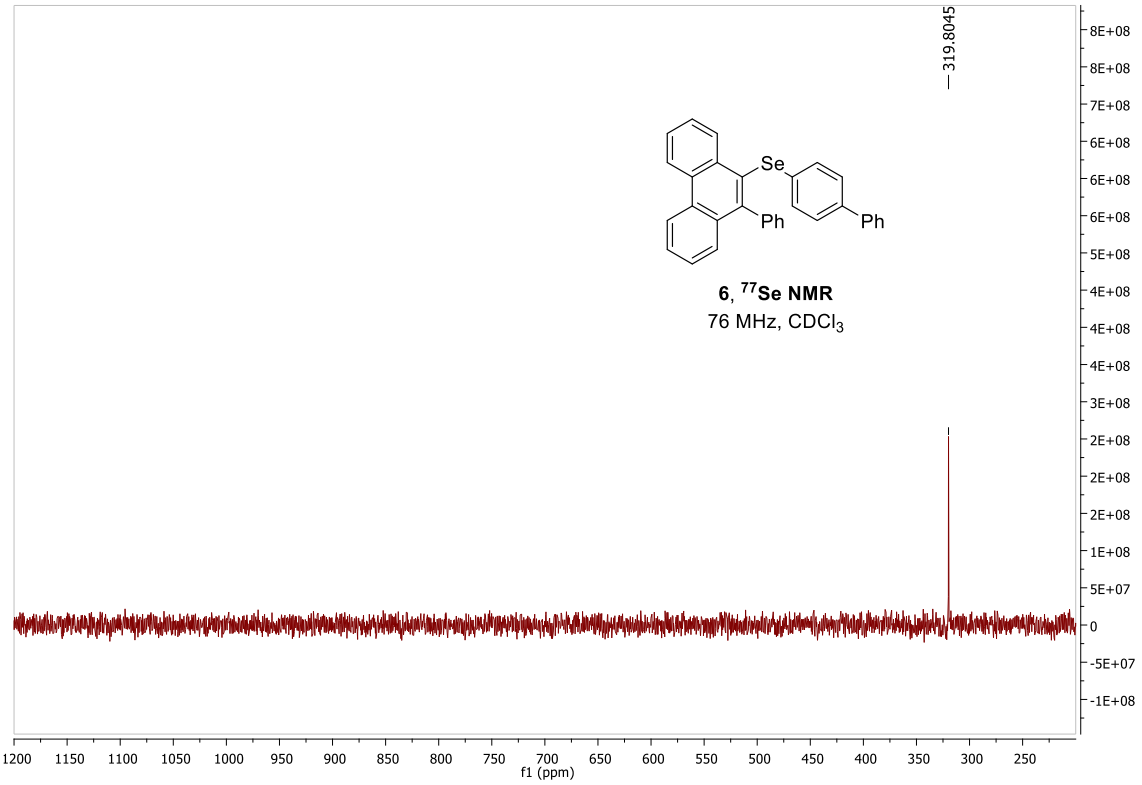

6, **^{77}Se NMR**
76 MHz, $CDCl_3$

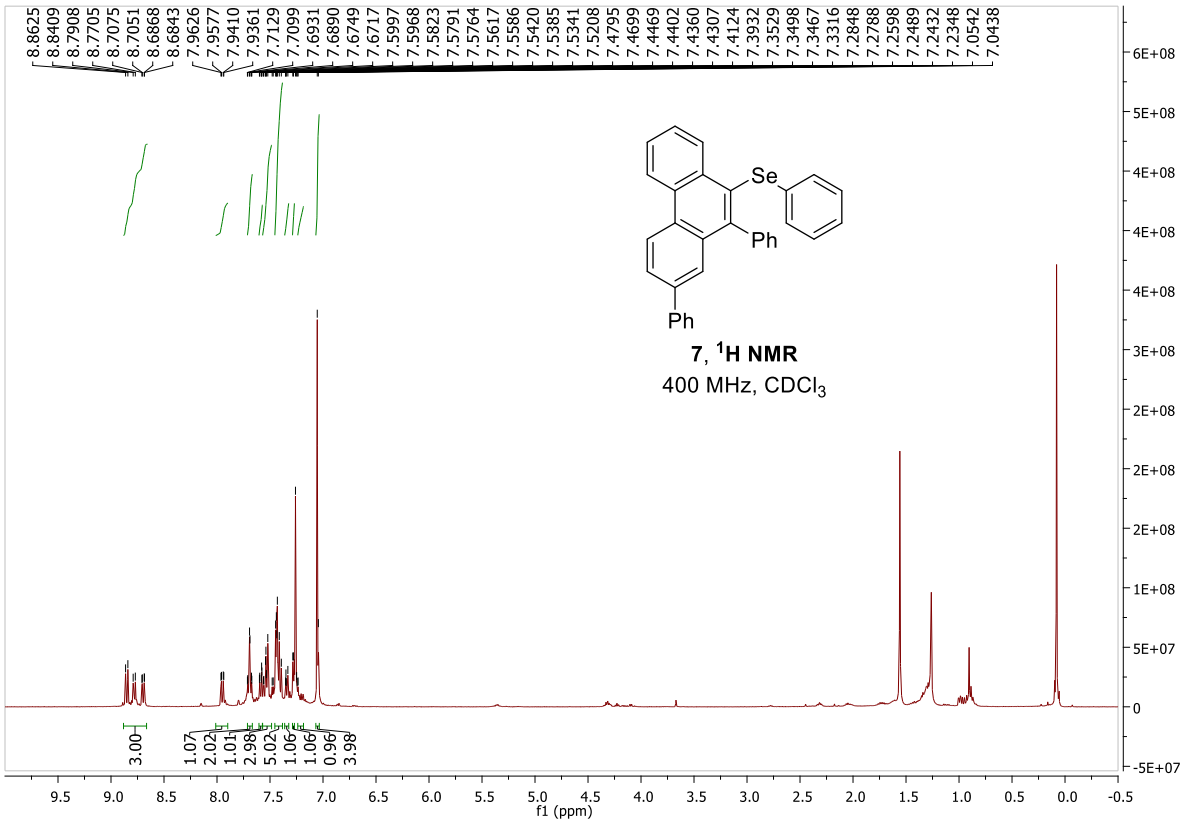

7, **^{1}H NMR**
400 MHz, $CDCl_3$

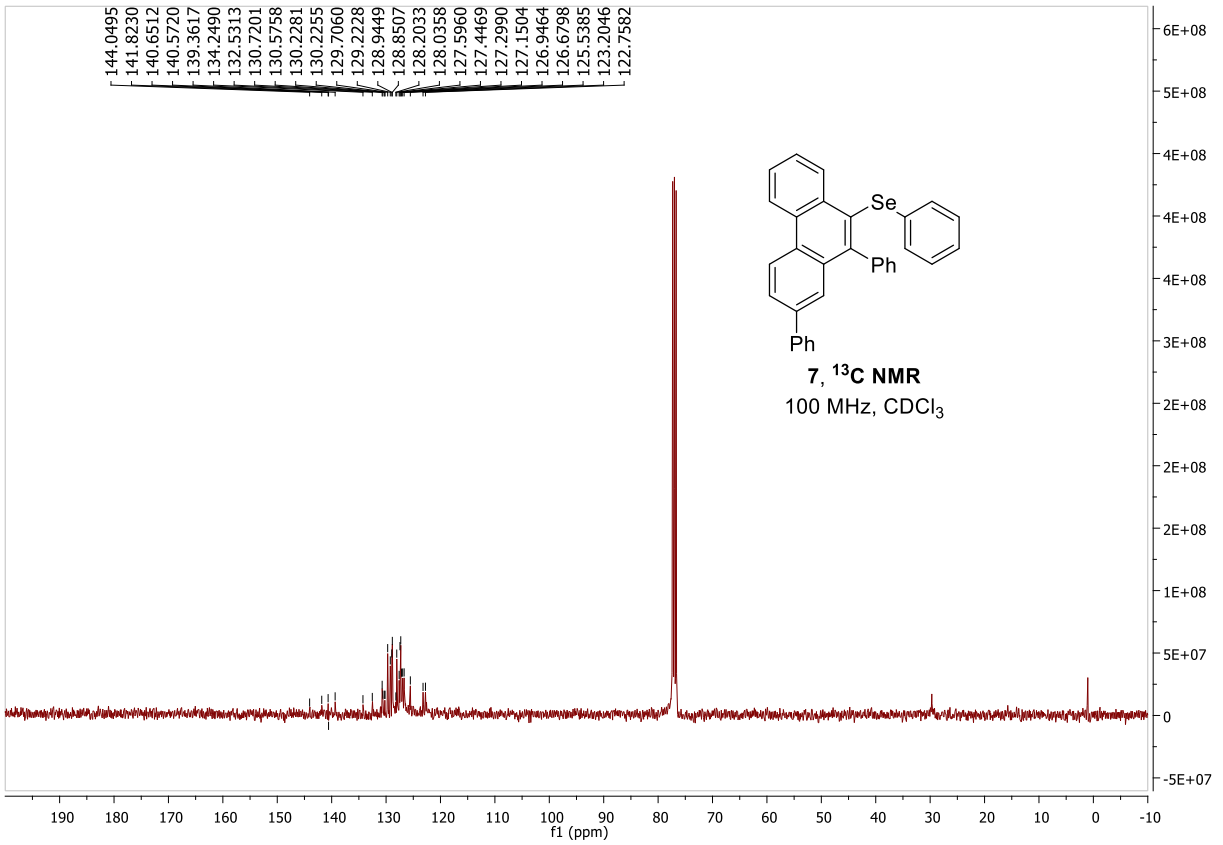
144.0495
141.8230
140.6512
140.5720
139.3617
134.2490
132.5313
130.7201
130.5758
130.2281
130.2255
129.7060
129.2228
128.9449
128.8507
128.2033
128.0358
127.5960
127.4469
127.2990
127.1504
126.9464
126.6798
125.5385
123.2046
122.7582
Se
Ph
Ph
7, 13C NMR
100 MHz, CDCl3
f1 (ppm)

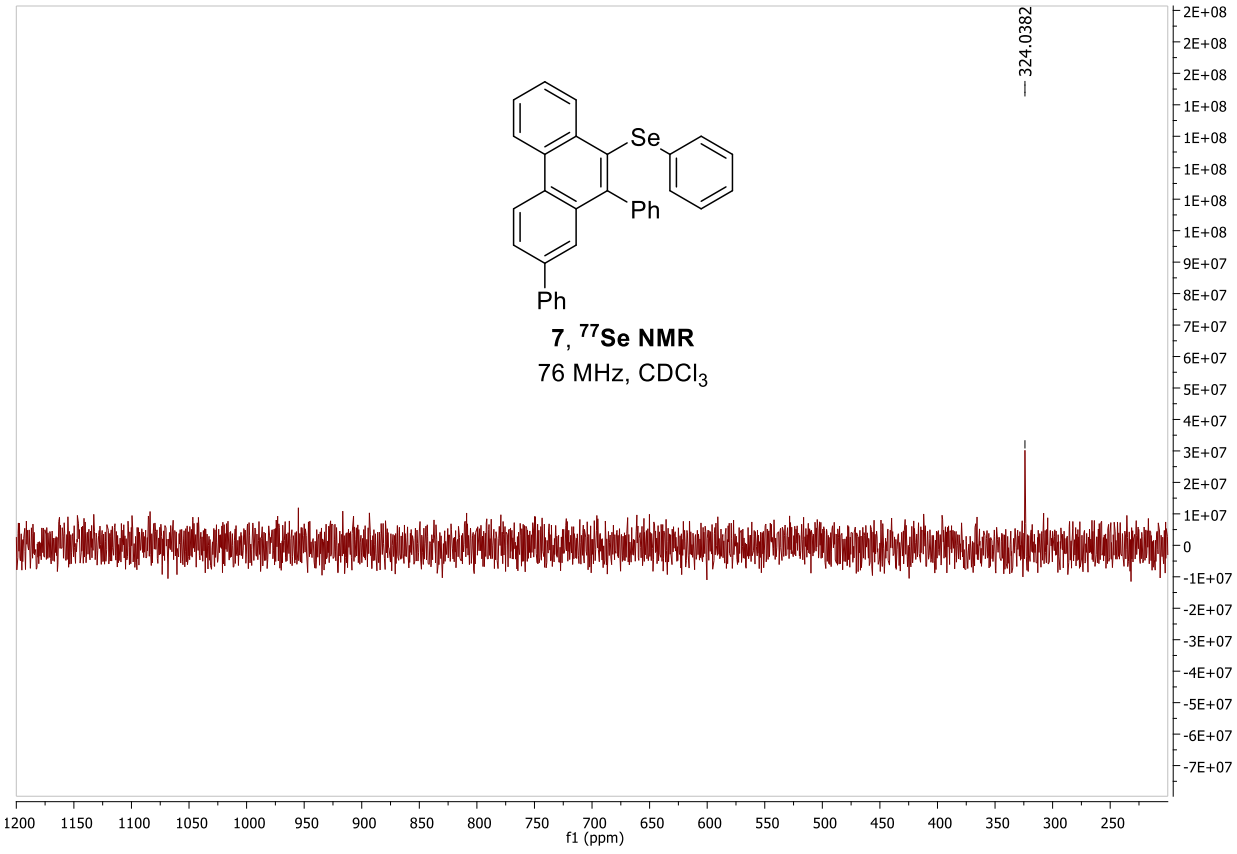
324.0382
Se
Ph
Ph
7, 77Se NMR
76 MHz, CDCl3
f1 (ppm)

Green Chemistry

PAPER

View Article Online
View Journal | View Issue

Cite this: *Green Chem.*, 2022, **24**, 7029

Recyclable iodine-catalyzed radical selenylative annulation of 2-alkynyl biaryls with diselenides in water: a green approach to selanyl polycyclic aromatic hydrocarbons and polycyclic heteroaromatics†

Nilanjana Mukherjee, Appanapalli N. V. Satyanarayana, Priti Singh, Mudit Dixit and Tanmay Chatterjee *

Received 14th June 2022,
Accepted 9th August 2022

DOI: 10.1039/d2gc02256g

rsc.li/greenchem

Herein, we disclose a metal-free, recyclable iodine-catalyzed, highly atom-economical, cost-effective, scalable, and sustainable oxidative selenylative annulation of 2-alkynyl biaryls and 2-heteroaryl-substituted alkynyl benzenes with diselenides in water for the synthesis of a wide variety of selanyl polycyclic aromatic hydrocarbons (PAHs) and polycyclic heteroaromatics, respectively, through the *in situ* formation of the corresponding selenyl iodide intermediates. The phenylselenyl iodide (PhSeI), formed *in situ* from $(PhSe)_2$ and I_2, is found to be more reactive than its other halo-analogues (commercially available), *i.e.*, PhSeBr and PhSeCl, for the selenylative annulation of 2-alkynyl biaryls. Several synthesized products, *i.e.*, selanyl phenanthrenes were further synthetically diversified to various new classes of interesting molecules. Both experimental and computational studies supported the radical pathway over the polar (ionic) pathway for the oxidative selenylative annulation of 2-alkynyl biaryls. Notably, 70–80% of the catalyst (iodine) was recovered after the reaction during the column chromatography stage and further the same was recycled for two successive runs without any compromise in the reaction outcome.

Introduction

Organoselenides, in particular, unsymmetrical diaryl selenides are prevalent in numerous biologically active molecules, including pharmacologically active molecules (Fig. 1).[1] The electron donor, halogen-bond, and hydrogen-bond acceptor attributes of the selenium atom help an organoselenide to interact and alter the characteristics of enzymatic active sites. Thus, incorporating a selenium atom into an organic molecule often significantly enhances its pharmacological and physical properties.[2]

On the other hand, polycyclic aromatic hydrocarbons (PAHs) such as phenanthrenes, anthracenes, perylenes, and pyrenes are ubiquitous in the universe. They are well-known because of their attractive physical, chemical, and biological properties.[3] Among them, phenanthrenes are found in numerous natural products[4] and pharmaceuticals[5–8] possessing valuable biological activities such as antimicrobial,[5] antiviral,[6] anticancer,[7] and anti-HIV[8] activities. Furthermore, PAHs are found to be promising candidates for developing valuable materials such as electronic and optical materials, and thus, PAHs have received significant attention in materials science.[9] For example, phenanthrene derivatives are widely utilized in developing various useful materials such as organic semiconductors,[10] organic light-emitting diodes,[11] fluorescence

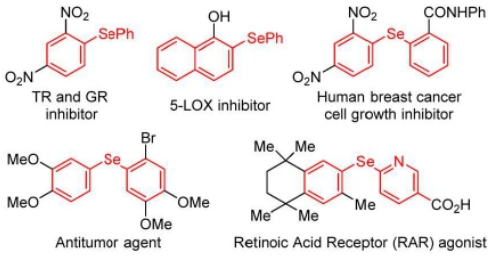

Fig. 1 Some examples of biologically active unsymmetrical diaryl or aryl–heteroaryl selenides.

Department of Chemistry, Birla Institute of Technology and Science, Pilani (BITS-Pilani), Hyderabad Campus, Jawahar Nagar, Hyderabad – 500078, Telangana, India. E-mail: tanmay@hyderabad.bits-pilani.ac.in

† Electronic supplementary information (ESI) available: Experimental procedure, X-ray data, LC-MS spectra, DFT studies, calculation of the EcoScale score, analytical data, and NMR spectra of the synthesized compounds. CCDC 2170363, 2176784 and 2176838. For ESI and crystallographic data in CIF or other electronic format see DOI: https://doi.org/10.1039/d2gc02256g

Chapter 5

SECTION-I

Electrochemical Selenylative Annulation for the Synthesis of Organoselenides

5.1.1. Introduction.

In the past few years, electrochemical organic synthesis (electrosynthesis) has become very attractive in terms of the economical, ecological, and green aspects of organic synthesis.[1] Electrosynthesis involves transferring charge between two electrodes to promote chemical reactions either by applying potential (Constant Potential Electrolysis) or current (Constant Current Elecytolysis). During an electrochemical reaction, there is no net consumption of electrons: the electrons gained at the anode (during oxidation) or supplied at the cathode (during reduction) are consumed or obtained, respectively, at another electrode in the reaction cell.[2] Generally, one of these reactions is the reaction of interest and the electrode at which it occurs is called the working electrode. The counter-reaction occurs at another electrode, called the auxiliary or counter electrode, to maintain electron neutrality in the solution.[3] This transfer of electrons from the working to the counter electrode turns electrosynthesis into a no-reagent approach. In electrochemical organic synthesis, a challenging organic transformation could be designed and developed *via* the *in situ* formation of radical ion or free radical from easily accessible starting materials through anodic oxidation or cathodic reduction followed by subsequent C-C or C-X (X = heteroatom) bond formation resulting desired product (Fig. 5.1.1).[4] Electrochemical organic synthesis where electricity plays the role of an oxidizing/reducing reagent to generate reactive species in a controlled fashion under mild conditions offers several advantages over other chemical technologies or traditional organic synthesis such as cost-effective and sustainable protocol avoiding the requirement of expensive and hazardous metallic or non-metallic reagents in catalytic or stoichiometric amounts, energy-efficient and mild reaction conditions, high functional group tolerance and generation minimum and inoffensive waste such as H_2.

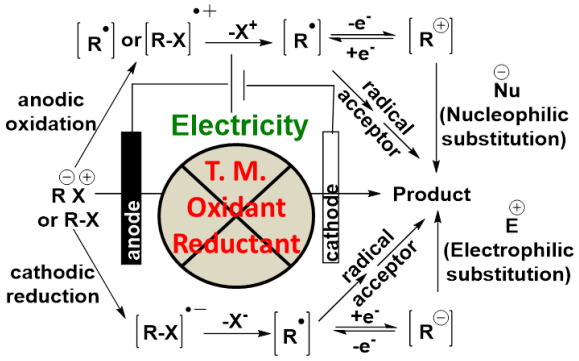

Advantages of Electrochemical Organic Synthesis:

- Cost-effective, sustainable and practical approach
- Tarnsition-metal-free protocol
- Stoichiometric oxidant/reductant-free protocol
- High functional group tolerance
- Generation of minimal and inoffensive waste e.g., H_2
- Straight forward scale-up process
- Wide scope in designing and developing radical C-H functionalization, cascade cyclization reactions without the requirement of prefunctionalized substrates

Figure 5.1.1. Schematic representation of a general electrochemical organic transformation and its advantages over traditional chemical methods involving expensive and toxic reagents and catalysts.

In recent years, several electrochemical selenylative annulation/cyclization reactions are developed for the synthesis of organoselenides. The state-of-the-art of electrochemical selenylative annulation is discussed below.

5.1.2. Review.

In 2023, Zhang and his co-workers reported an electrochemical cascade cyclization of dienes with diselenides in an undivided cell using graphite rod as anode and platinum plate as cathode through constant current electrolysis (5 *m*A) under N_2 atmosphere at room temperature to access a wide variety of seleno-benzo[*b*]azepines, an important class of biologically active molecules[5] (Scheme 5.1.1).[6]

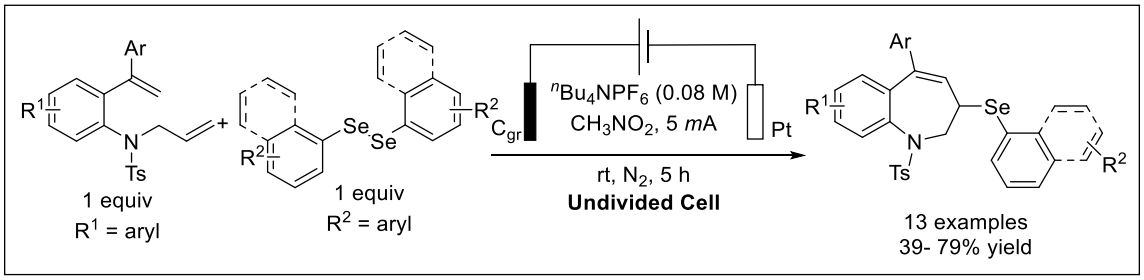

Scheme 5.1.1. Electrochemical Cyclization of Dienes with Diselenides to Access Seleno-Benzo[*b*]azepines.

In 2022, Braga *et al*. disclosed an electrochemical oxidative intramolecular cyclization of 2-alkynylphenol with diorganyl diselenides in an undivided cell using platinum as both anode and cathode under a constant current of 10 *m*A at room temperature under aerobic atmosphere to access a wide variety of selenylbenzo[*b*]furan derivatives in moderate to excellent yield (Scheme 5.1.2).[7] Mechanistic studies revealed that the reaction proceeded *via* ionic pathway.

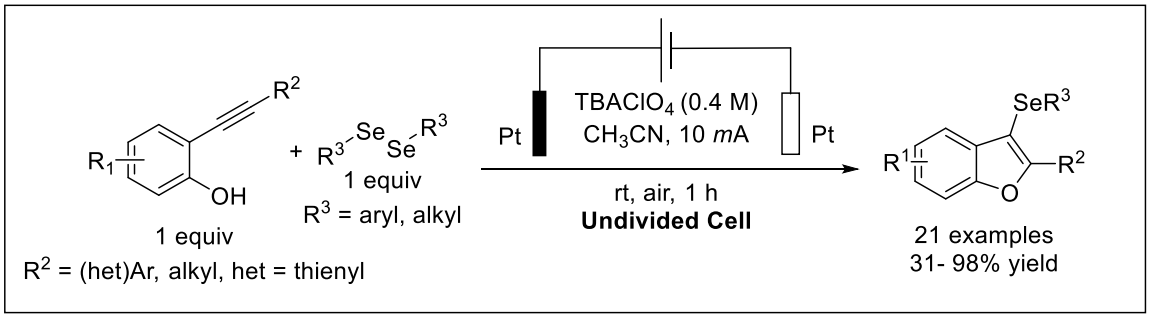

Scheme 5.1.2. Electrochemical Synthesis of Selenylbenzo[*b*]furan Derivatives through the Cyclization of 2-Alkynylphenols

In 2022, Lei group reported an electrochemical oxidative selenocyclization of olefinic amides with diphenyl diselenides in an undivided cell through constant current electrolysis (30 *m*A) using carbon rod as anode and platinum plate as cathode in CH_3CN at 40 ^oC under argon atmosphere to synthesize a library of iminoisobenzofurans in moderate to excellent yield (Scheme 5.13).[8] This method was found to be scalable without the compromisation of the yield. Mechanistic studies revealed that the reaction proceeded *via* a radical pathway.

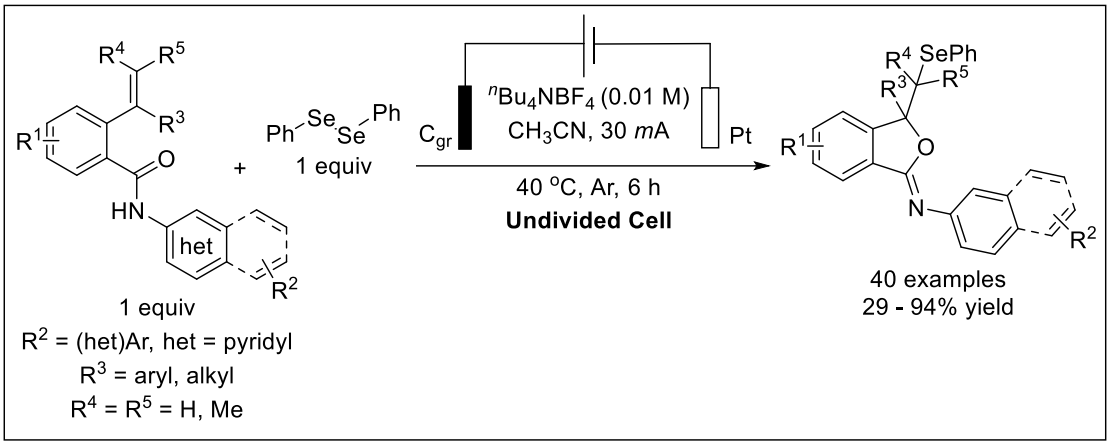

Scheme 5.1.3. Electrochemical Oxidative Selenocyclization of Olefinic Amides towards the Synthesis of Iminoisobenzofurans.

In 2022, Liu *et al*. developed electrochemical oxidative three-component cyclization of allylic alcohols, boronic acids, and diaryl diselenides under a constant current of 5 *m*A at room temperature to access chalcogenated boronic esters in moderate to good yield (Scheme 5.1.4). [9] The synthetic utility of this protocol was demonstrated by further conversion of selenated boronic esters into their corresponding 1,3-diols.

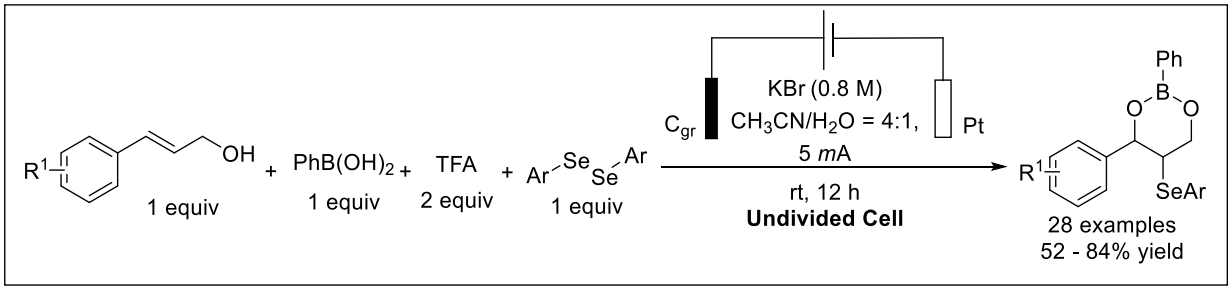

Scheme 5.1.4. Electrochemical Oxidative Cyclization of Alkenes, Boronic Acids, and Dichalcogenides to Access Chalcogenated Boronic Esters and 1,3-Diols.

In 2021, Sarkar and his co-workers disclosed an electrochemical selenocyclization of homopropargylic alcohols with diaryl diselenides in mixed solvent, CH_3CN/TFE = 20:1 using platinum as both anode and cathode through constant current electrolysis (8 *m*A) at room temperature under argon atmosphere in an undivided cell to synthesize polysubstituted furans in moderate to good yield (Scheme 5.1.5).[10]

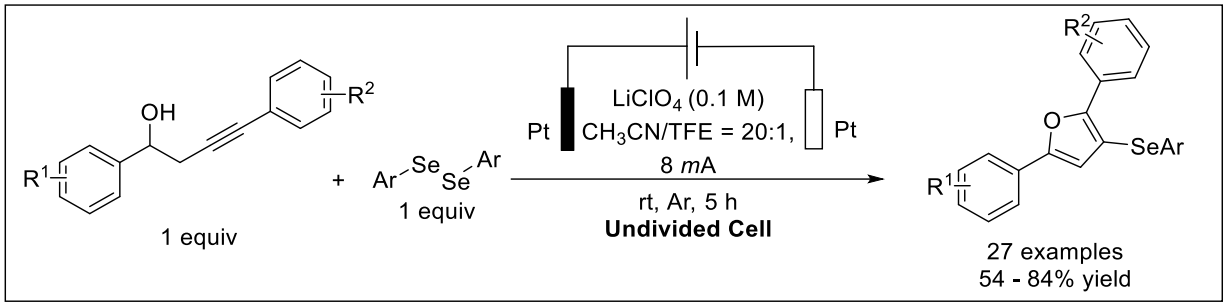

Scheme 5.1.5. Synthesis of Polysubstituted Furans through Electrochemical Selenocyclization of Homopropargylic Alcohols.

In 2021, the Ruan group developed an electrochemical selenylative cyclization of alkene-tethered benzoic acids/amides with diorganyl diselenides through constant current electrolysis (8 *m*A) using platinum as both anode and cathode at room temperature to access iminoisobenzofuran and lactones (Condition **A**). When *N*-aryl acrylamides were employed as substrate to react with diselenides under similar conditions but higher temperature (50 – 70 ^{o}C), a library of oxindoles and quinolinones were obtained (Condition **B)**. The gram-scale reactions were found to be straight-forward furnishing the desired products in high yield (Scheme 5.1.6).[11]

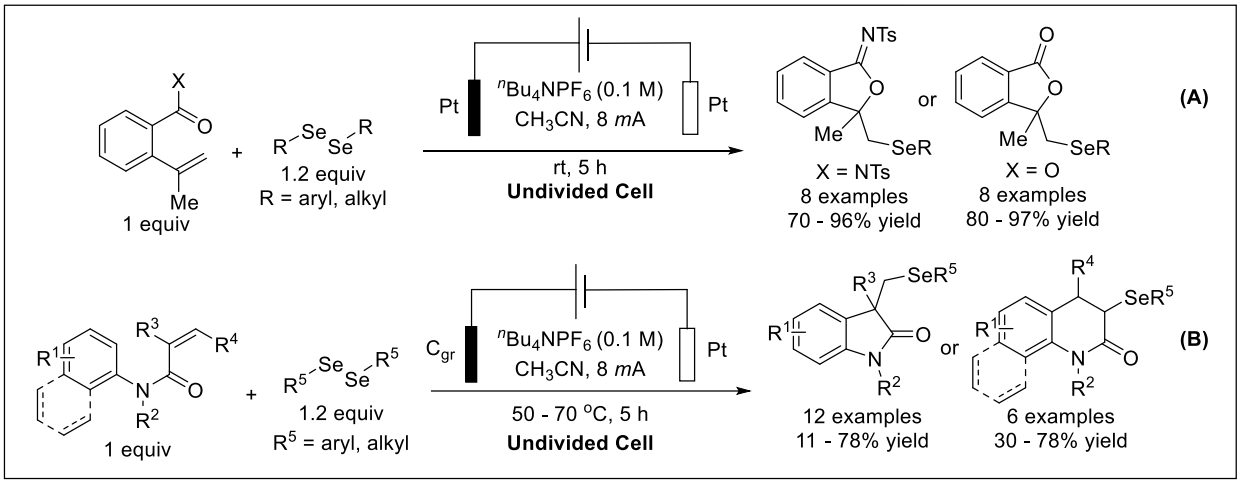

Scheme 5.1.6. Electrochemical Selenoyclization of Alkenes to Access Functionalized Benzheterocycles.

In 2021, Reddy *et al*. disclosed selenylative carbannulation (6-*endo*-dig cyclization; when X≠ OMe) and dearomative *ipso*-annulation (when X = OMe) of biaryl ynones with diphenyl diselenide using graphite electrode as anode and platinum electrode as cathode in an undivided cell under constant current of 15 *m*A at room temperature to access a wide variety of seleno-dibenzocycloheptenones and spiro[*5.5*]trienones, respectively (Scheme 5.1.7).[12]

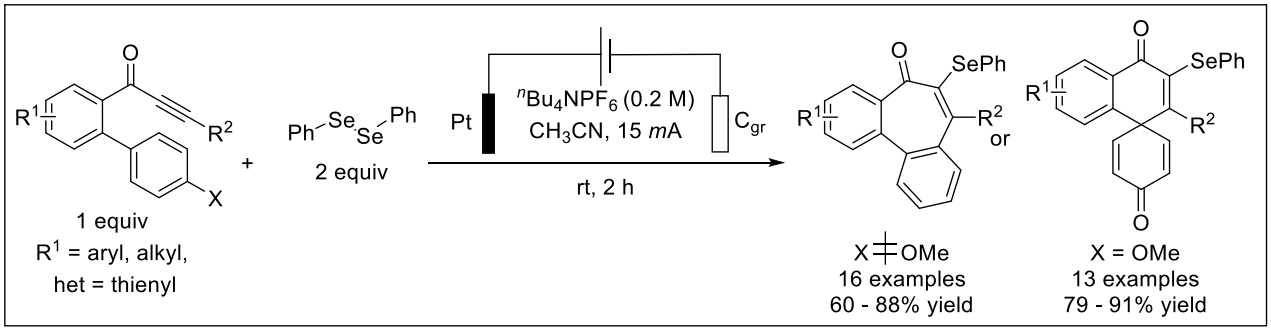

Scheme 5.1.7. Electrochemical Selenylative Carbannulation of Biaryl Ynones to Seleno-Dibenzocycloheptenones/Spiro[5.5]Trienones.

In 2020, Junior *et al*. disclosed an electrochemical oxidative selenation of quinones with diaryl diselenides in CH_3CN as solvent at room temperature for only 1 h an undivided cell through constant current electrolysis (15 *m*A) using platinum as both cathode and anode to access a library of quinonoid compounds (Scheme 5.1.8).[13] Some of the synthesized compounds showed anticancer activity against different cell lines with notable IC_{50} values.

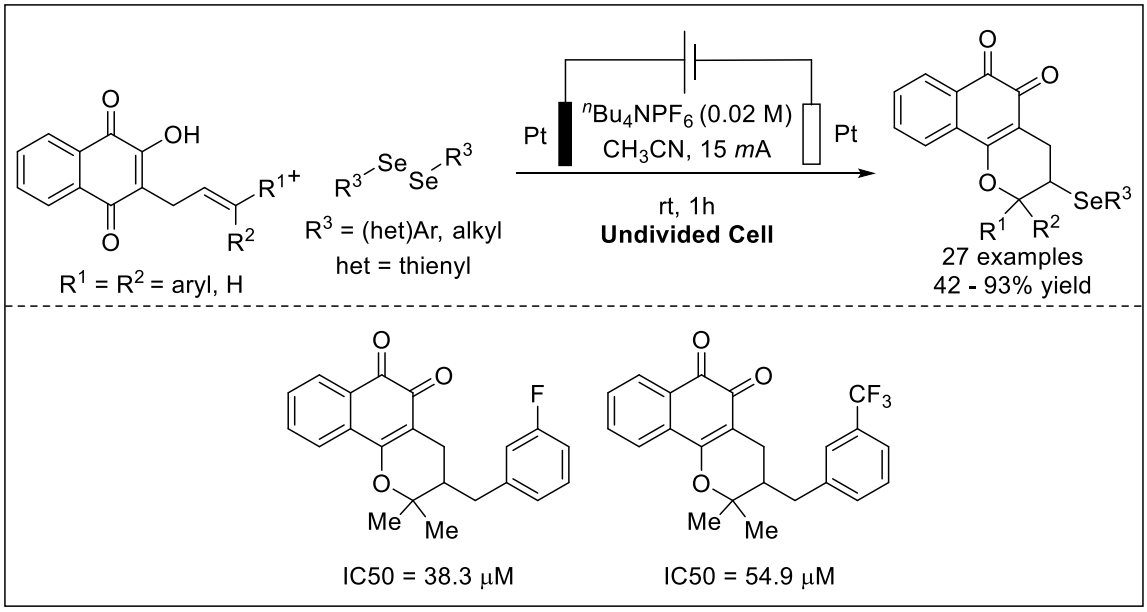

Scheme 5.1.8. Electrochemical Selenocyclization of Quinones.

In 2020, Weisi group developed an electrochemical selenylative cyclization of *N*-allylthioamides with diorganyl diselenides to access a wide variety of selenium containing 2-thiazolines in an undivided cell using graphite electrode as both cathode and anode under constant current of 2 *m*A at room temperature (Scheme 5.1.9).[14]

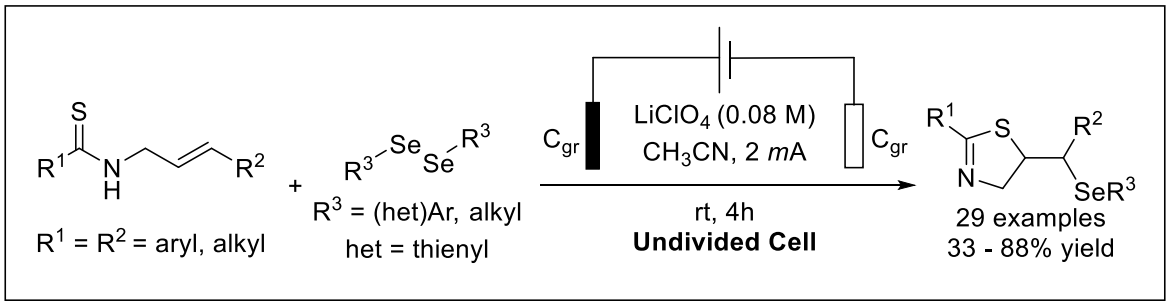

Scheme 5.1.9. Electrochemical Selenocyclization of *N*-Allylthioamides to Access 2-Thiazolines.

In 2020, Braga and his co-workers reported an electrochemical oxyselenylation of allyl-naphthol/phenol derivatives in an undivided cell in CH_3CN as solvent through constant current electrolysis (5 *m*A) using platinum as both cathode and anode to access a library of selenyl-dihydrofuran in good to excellent yield (Scheme 5.1.10). [15] Notably, several synthesized products exhibited a high percentage of acetylcholinesterase (AChE) inhibition highlighting their potential *anti*-Alzheimer activity.

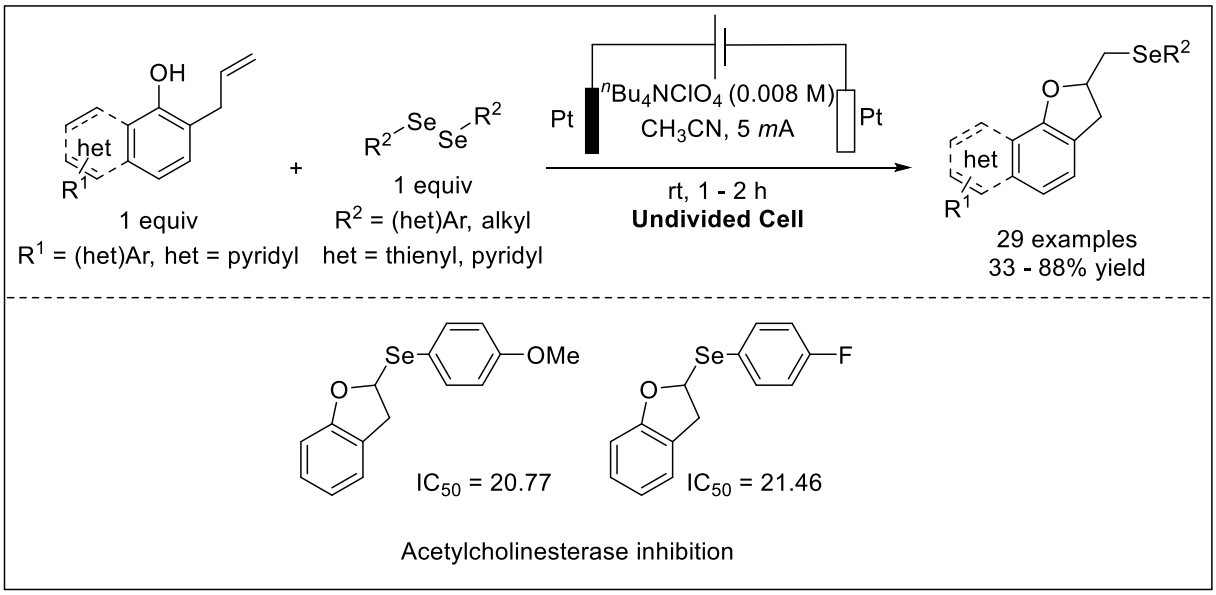

Scheme 5.1.10. Electrochemical Selenocyclization of of Allylnaphthol/phenol Derivatives to Access Selenyl-dihydrofurans.

In 2019, Guo and his co-workers developed an electrochemical selenylative cyclization of alkynoates and alkynamides with diselenides for the synthesis of Se-containing coumarins and quinolinones in moderate to good yield under constant current of 15 *m*A using graphite rod as anode and platinum plate as anode at room temperature for 2 h in an undivided cell (Scheme 5.1.11). [16] This method was scalable without the compromisation of the yield of the product.

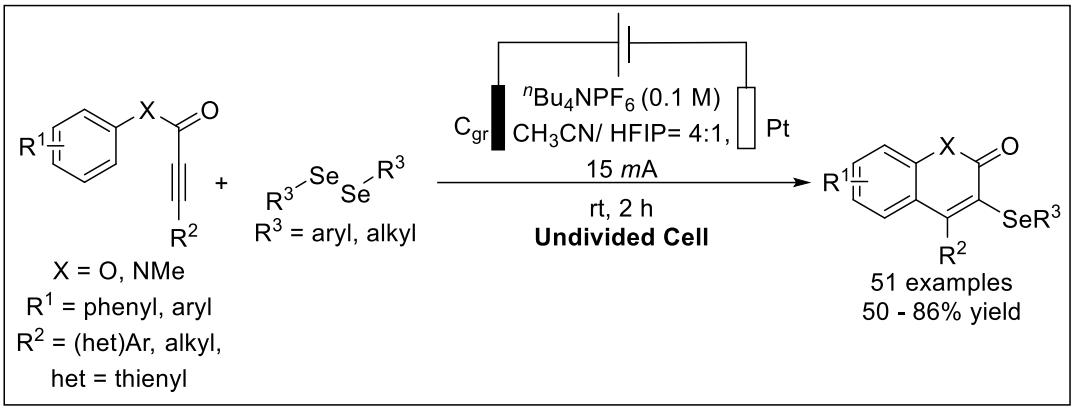

Scheme 5.1.11. Electrochemical Selenocyclization of Activated Alkynes with Diselenides.

5.1.3. Conclusion.

During the past two decades, electrochemistry has experienced increased popularity as a versatile method in organic synthesis, especially for the generation of highly reactive intermediates in a controlled way under mild conditions. This review revealed the recent developments of selenylative annulation reactions under electrochemical conditions for the synthesis of organoselenides, in particular, selenyl heterocyclic compounds. However, very few electrochemical selenylative annulation reactions have been developed so far for the synthesis of selenyl polycyclic aromatic hydrocarbons (PAHs) and polycyclic heteroaromatics. Hence, the development of electrochemical selenylative annulation reactions to access selenyl PAHs and polycyclic heteroaromatics is an unexplored area of research.

SECTION-II

Highly Atom-Economic and Efficient Electrochemical Selenylative Annulation of 2-Alkynyl Biaryls

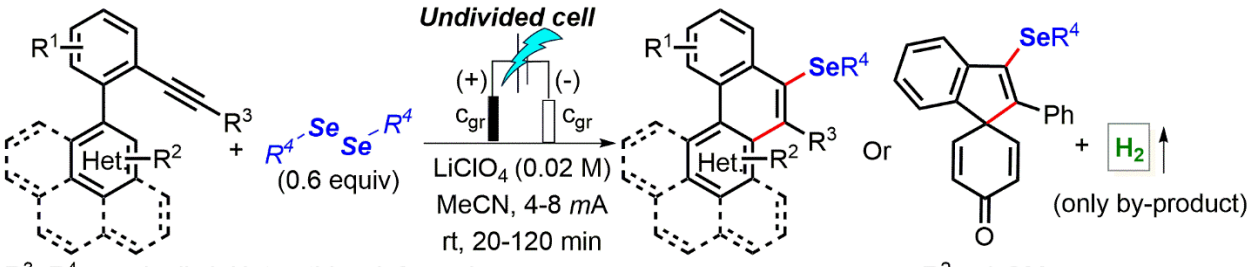

5.2.1. Introduction

As discussed in the previous chapter, we developed a metal-free, catalytic method for the oxidative selenylative annulation of 2-alkynyl biaryls with diselenides (0.6 equiv) using iodine as a catalyst and H_2O_2 as the oxidant in water at 100 ^oC for the synthesis of selanyl PAHs including phenanthrens and polycyclic heteroaromatics through the *in situ* generation of the corresponding selenyl iodide intermediate followed by its thermal activation.[1] Despite the notable green features of the protocol, it still requires a couple of reagents, *i.e.*, iodine as a catalyst, and H_2O_2 as an oxidant at high temperature (100 ^oC) for a prolonged period of time (12-22 h). Moreover, the protocol was found unsuccessful or inefficient in some cases furnishing the desired product in poor yield and also generating 9-iodophenanthrene or iodo-PAHs or polycyclic heteroaromatics in small quantities as byproduct. In this context, the development of a catalyst- and oxidant-free, highly efficient, and practical synthetic strategy for the selenylative annulation of 2-alkynyl biaryls under mild reaction conditions is highly desirable.

Being motivated by the advantages of the electrochemical approach over conventional approach, we planned to develop a catalyst- and oxidant-free selenylative annulation of 2-alkynyl biaryls under electrochemical conditions wherein a direct electrochemical activation of diselenide would furnish the corresponding selenyl radical for the radical selenylative annulation of 2-alkynyl biaryls at room temperature and thus making the protocol highly energy-efficient. Moreover, under this electrochemical strategy, the only by-product that would form will be nothing but the innocuous hydrogen gas, making the protocol more sustainable (Scheme 5.2.1).

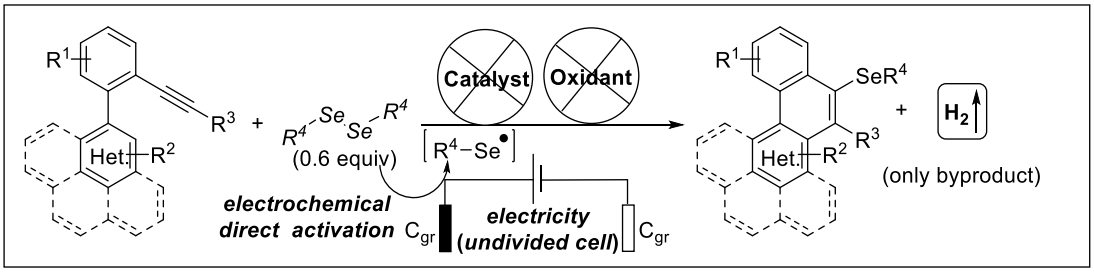

Scheme 5.2.1. Synthetic Strategy for the Radical Selenylative Annulation to Access Selanyl PAHs and Polycyclic Heteroaromatics under Electrochemical Conditions.

5.2.2. Results and discussions

With the abovementioned plan in mind, we performed a reaction between 2-(phenylethynyl)-1,1'-biphenyl **1a** and diphenyl diselenide **2a** (0.6 equiv) in an undivided electrochemical cell equipped with carbon cloths both as anode and cathode under constant current electrolysis (CCE) at 10 mA using 0.02 M electrolyte ($LiClO_4$) in MeCN, and to our delight, the desired product **3aa** was formed in 99% yield in 20 min at room temperature (entry 1, Table 5.2.1).

Table 5.2.1. Optimization of the Reaction Conditions.[a]

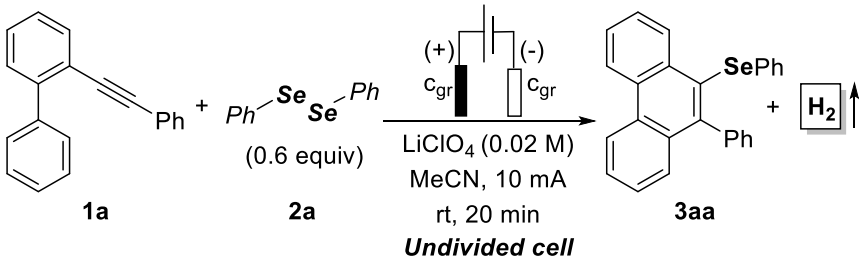

entry	variation from the standard conditions	yield[b] (%)
1	**none**	**99**
2	Pt as anode instead of carbon	90
3	Pt as cathode instead of carbon	96
4	Pt as both anode and cathode instead of carbon	40
5	0.1 M $LiClO_4$ was used instead of 0.02 M	96
6	0.25 M $LiClO_4$ was used instead of 0.02 M	45
7	DMSO instead of CH_3CN	ND
8	DMF instead of CH_3CN	ND
9	$^nBu_4NClO_4$ instead of $LiClO_4$	45
10	$^nBu_4NPF_6$ instead of $LiClO_4$	53
11	$^nBu_4NI$ instead of $LiClO_4$	trace
12	$^nBu_4NBr$ instead of $LiClO_4$	trace
13	Et_4NBr instead of $LiClO_4$	trace
14	15 *m*A instead of 10 mA	96
15	5 *m*A instead of 10 mA	54
16	0.5 equiv of **2a** was used instead of 0.6 equiv	75
17	reaction was conducted for 10 min	75
18	no electrolyte	ND
19	no electricity	ND

[a]Reaction conditions: **1a** (0.1 mmol), **2a** (0.06 mmol), $LiClO_4$ (0.05 mmol), CH_3CN (3 mL), carbon cloth (1 x 1.5 cm^2) anode, carbon cloth (1 x 1.5 cm^2) cathode, constant current, I = 10 mA, 20 min, rt,

aerobic atmosphere. Q = 12 C, 0.000124 F. [b]Yield was determined by the ^{1}H NMR of the crude reaction mixture using 1,3,5-trimethoxybenzene as the internal standard.

The yield of **3aa** was slightly reduced when Pt was used either as anode or cathode instead of carbon (entry 1 *vs* entries 2-4, Table 5.2.1). Increasing the concentration of $LiClO_4$ had a negative impact on the reaction outcome (entry 1 *vs* entries 5 and 6, Table 5.2.1). No product formation was detected when dimethyl sulfoxide (DMSO) and dimethyl formamide (DMF) were used as solvent (entries 7 and 8, Table 5.2.1). While the yield of **3aa** greatly reduced in the presence of organic electrolytes such as tetrabutylammonium perchlorate (^{n}Bu$_4$NClO$_4$), tetrabutylammonium hexafluorophosphate (^{n}Bu$_4$NPF$_6$), only trace amount of **3aa** was formed in the presence of tetrabutylammonium iodide (^{n}Bu$_4$NI), tetrabutylammonium bromide (^{n}Bu$_4$NBr) and tetraethylammonium bromide (Et$_4$NBr) (entries 9-13, Table 5.2.1). While with the increase of the current to 15 mA furnished **3aa** in 96%, with decrease of the same to 5 mA the yield of **3aa** reduced to 54% (entries 14-15, Table 5.2.1). Lowering the stoichiometry of diphenyl diselenide **2a** to 0.5 equiv and lowering the reaction time to 10 min had a negative impact on the reaction outcome (entries 16 and 17, Table 5.2.1). The blank experiments revealed the essential requirements of an electrolyte and electricity for the selenylative annulation of **1a** to access **3aa** (entries 18 and 19, Table 5.2.1).

With the optimized conditions in hand, we started exploring the scope of the reaction under electrochemical condition and also compared the outcome of the same with that of our previously developed iodine-catalyzed chemical conditions.[1] The results are presented in Table 5.2.2. At first, the scope of diselenides with **1a** was explored. Diphenyl diselenide **2a** furnished the desired product **3aa** in 99% yield in 2 h at room temperature under electrochemical conditions while the same was produced in 98% yield in 12 h under iodine-catalysis at 100 ^{o}C. Halogen (Cl, and F) substituted diaryl diselenides (**2b** and **2c**) reacted smoothly with **1a** under electrochemical conditions furnishing the desired products **3ab** and **3ac** in relatively higher yield (88% and 92% respectively) within shorter time (3 h) as compared to that under iodine-catalysis. Strongly electron-withdrawing group (CF_3 and NO_2) substituted diaryl diselenides (**2d** and **2e**) afforded the desired products (**3ad** and **3ae**) in 70% and 66% yield within 2 h, whereas to obtain the similar results 12-13 h of heating of the reaction mixture at 100 ^{o}C was required under iodine catalysis. Electron-donating group (Me) substituted diaryl diselenide *i.e.*, *p*-tolyldiselenide **2f** and dialkyl diselenides *i.e.*, dimethyl diselenide **2g** and dibenzyl diselenide **2h** furnished the desired products (**3af**–**3ah**) in much higher yield (60-85%) within shorter time (3-4 h) as compared to the iodine catalysis. Next, we explored the scope of 2-(phenylethynyl)-

1,1′-biaryls under electrochemical conditions. Various halo (Br, Cl, and F), electron-withdrawing (Ph and CF_3), and electron-donating (Me) group substituted 2-(phenylethynyl)-1,1′-biaryls (**1b**-**1h**) smoothly reacted with **2a** irrespective to the position of the substituents to furnish the desired products (**3ba**–**3ha**) in good to excellent yield. In all the cases, the desired products were formed in a much higher yield within shorter time under electrochemical conditions in comparison to that under chemical approach (iodine catalysis). Notably, three substrates, *i.e.*, **1d**, **1f**, and **1h** which were unsuccessful to react with **2a** under iodine-catalytic conditions, furnished the desired products **3da**, **3fa**, and **3ha** in 85%, 70%, and 80% yield respectively under electrochemical conditions. The structures of **3da** and **3ha** were confirmed by X-ray crystallographic structure determination (Fig. 5.2.1 and 5.2.2 and Table 5.2.3).

PAH-substituted 2-phenylethynyl benzenes (**1i**–**1k**) also furnished the desired highly fused selenyl PAHs, *i.e.*, phenyl(6-phenylbenzo[*c*]phenanthren-5-yl)selane **3ia**, phenyl(5-phenylbenzo[*g*]chrysen-6-yl)selane **3ja**, and phenyl(14-phenyldibenzo[*ij*,*no*]tetraphen-13-yl)selane **3ka** in better yield within shorter time under electrochemical conditions as compared to the conventional iodine-catalytic conditions. Next, the scope of 2-(arylethynyl)-1,1′-biphenyls (**1l**–**1r**) was explored with **2a**, and both electron-withdrawing (Cl, CN, and NO_2) and electron-donating (*i*-Pr, Me and OMe) group substituted substrates, irrespective to their position, afforded the desired products **3la**–**3ra** in much higher yield within shorter time under electrochemical conditions in comparison to that under iodine-catalyzed conditions. 2-(Cyclopropylethynyl)-1,1′-biphenyl **1s** also reacted smoothly with **2a** to furnish (10-cyclopropylphenanthren-9-yl)(phenyl)selane **3sa** in relatively higher yield under electrochemical conditions as compared to the iodine-catalyzed conditions. Finally, the scope of 2-heteroaryl-substituted phenylethynylbenzenes was explored and both thiophene and furan substituted substrates furnished the desired products (**3ta**–**3va**) in much higher yield within shorter time as compared to the chemical approach. Notably, 2-(2-(phenylethynyl)phenyl)thiophene (**1t**) which did not react with **2a** under iodine catalysis, afforded the desired product **3ta** in 62% yield under electrochemical conditions.

While the dearomative *ipso*-annulation of 4'-methoxy-2-(phenylethynyl)-1,1'-biphenyl **4a** with diphenyl diselenide **2a** and dimethyl diselenide **2g** was found inefficient under iodine-catalyzed conditions (chemical approach) furnishing the desired products **5aa** and **5ag** in poor yield (20-30%), the same was found highly efficient under electrochemical conditions affording **5a** and **5g** in 82% and 85% yield respectively in 2 h at room temperature (Scheme 5.2.2).

Table 5.2.2. Substrate Scope and A Direct Comparison of the Scope of the Electrochemical Approach with that of Chemical Approach (I_2-Catalysis) [a, b, c]

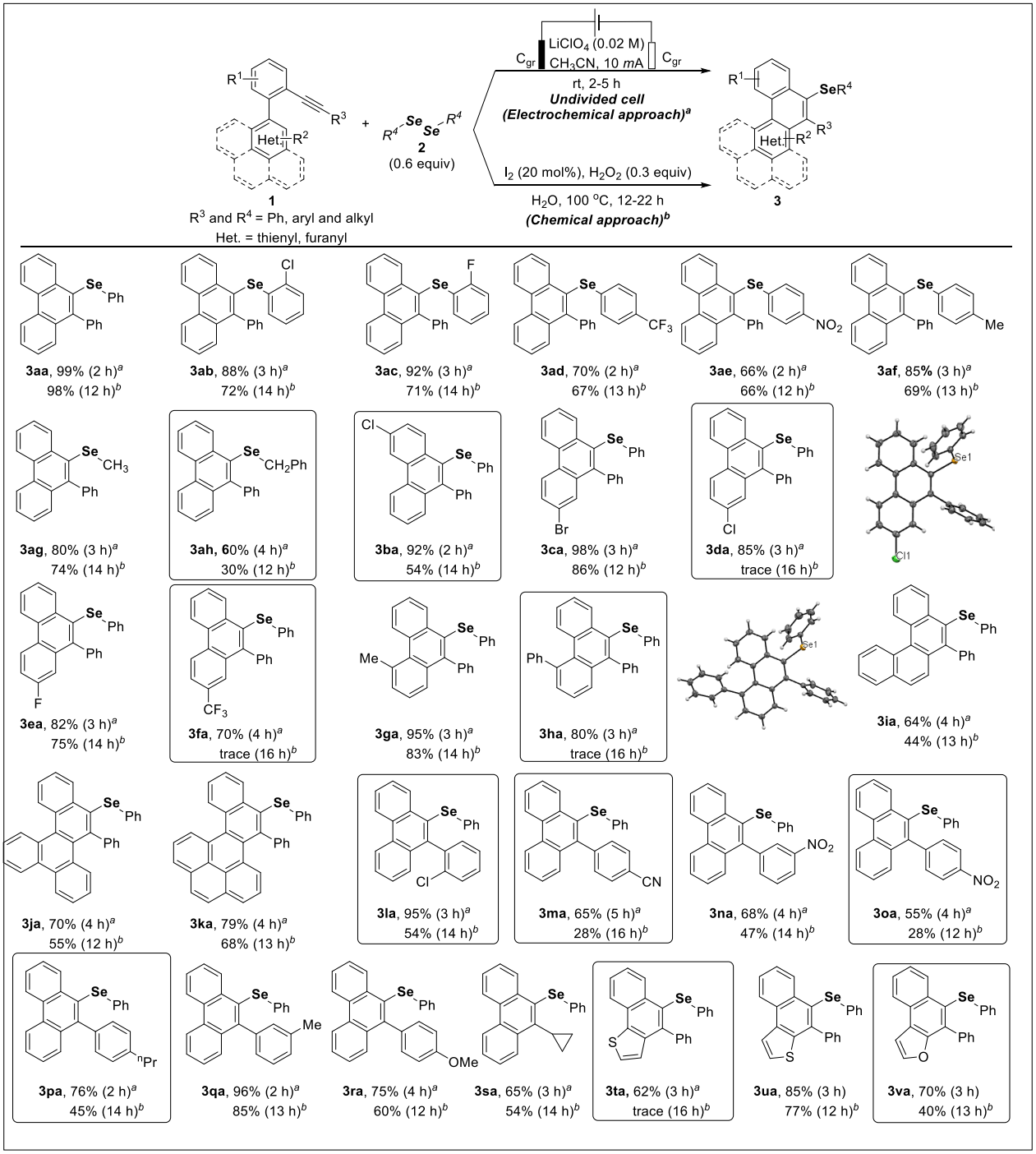

[a]Reaction conditions of electrochemical approach: **1** (0.5 mmol, 1 equiv), **2** (0.3 mmol, 0.6 equiv), $LiClO_4$ (0.25 mmol, 0.5 equiv), CH_3CN (15 mL), carbon cloth (1 x 1.5 cm^2) anode, carbon cloth (1 x 1.5 cm^2) cathode, constant current, I = 10 *m*A, rt, aerobic atmosphere; [b]Reaction conditions of chemical approach: 1 (0.5 mmol, 1 equiv), **2** (0.3 mmol, 0.6 equiv), I_2 (0.1 mmol, 0.2 equiv), 30% aq. solution (v/v) of H_2O_2 (0.15 mmol, 0.3 equiv), H_2O (0.3 mL), 100 °C. [c]Isolated yield of product was reported.

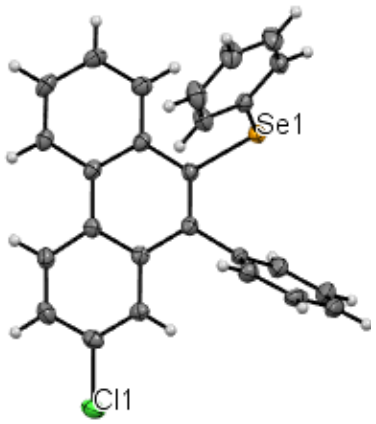

Figure 5.2.1 X-ray Crystal Structure of **3da** (Thermal Ellipsoids Shown at 50% Probability) Including Hetero-atom Numbering.

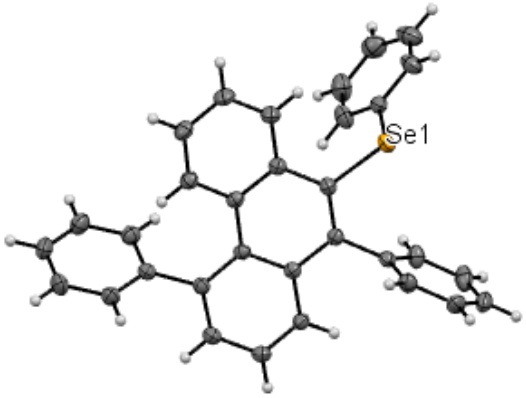

Figure 5.2.2. X-ray Crystal Structure of **3ha** (Thermal Ellipsoids Shown at 50% Probability) Including Hetero-atom Numbering.

Table-5.2.3. Selected Crystal Data for Compounds **3da, 3ha**

Parameters	3da	3ha
Empirical formula	$C_{26}H_{17}ClSe$	$C_{32}H_{22}Se$
Formula weight	443.837	485.491
Temperature/K	298	298
Crystal system	monoclinic	triclinic
Space group	P 1 21/c 1	P -1
a/Å	15.7518(2)	9.7916(2)
b/Å	7.7471(1)	10.1862(2)
c/Å	16.8615(2)	12.1187(2)
α (°)	90	91.214(1)
β (°)	107.619(1)	106.997(2)

$\gamma(°)$	90	95.940(1)
$Volume/Å^3$	1961.10(4)	1148.02(4)
Z	4	2
μ/mm^{-1}	3.893	2.333
$D_x\ [g\ cm^{-3}]$	1.503	1.404
$F(000)$	896.443	495.687
2Θ range for data collection (°)	5.40-79.94	3.82-79.55
Index ranges	-19≤ h ≤ 20, -9 ≤ k ≤ 9, -21 ≤ l ≤ 21	-12≤ h ≤ 11, -11 ≤ k ≤ 12, -15 ≤ l ≤ 15
Reflections measured	11660	9396
Unique reflections	4168	4815
Parameters /restraints	253/0	298/0
Goodness-of-fit on F2	0.7037	0.9336
$R_1\ [I \geq 2\sigma(I)]$	0.184	0.098
wR_2 (all data)	0.0908	0.0875
Largest diff. peak/hole/e $Å^{-3}$	0.3794/-0.5859	0.3441/-0.5393
CCDC	2234652	2235895

The reaction kinetics for the synthesis of **3aa** from **1a** and **2a** was studied under electrochemical conditions as well as under iodine-catalyzed chemical conditions which certainly revealed that electrochemical selenylative annulation is much faster than that of the iodine-catalysed chemical conditions (Figure 5.2.3).

To demonstrate the practicality of the electrochemical protocol, a gram-scale reaction of **1a** (1.27 g, 5 mmol) with **2a** (0.936 g, 3 mmol, 0.6 equiv) was conducted under constant current electrolysis (CCE) at 30 mA using 0.08 M $LiClO_4$ and gratifyingly the desired product, **3aa** was formed in 95% yield (1.95 g, 4.76 mmol) in 7 h at room temperature (Figure 5.2.4A). This result revealed that the electrochemical process is more practical as it could be scaled-up efficiently up to gram-scale without any considerable compromisation in the reaction outcome whereas the same is associated with a certain loss of yield of **3aa** (81%) under iodine-catalyzed (chemical approach) selenylative annulation of **1a** with **2a** (Figure 5.2.4B).

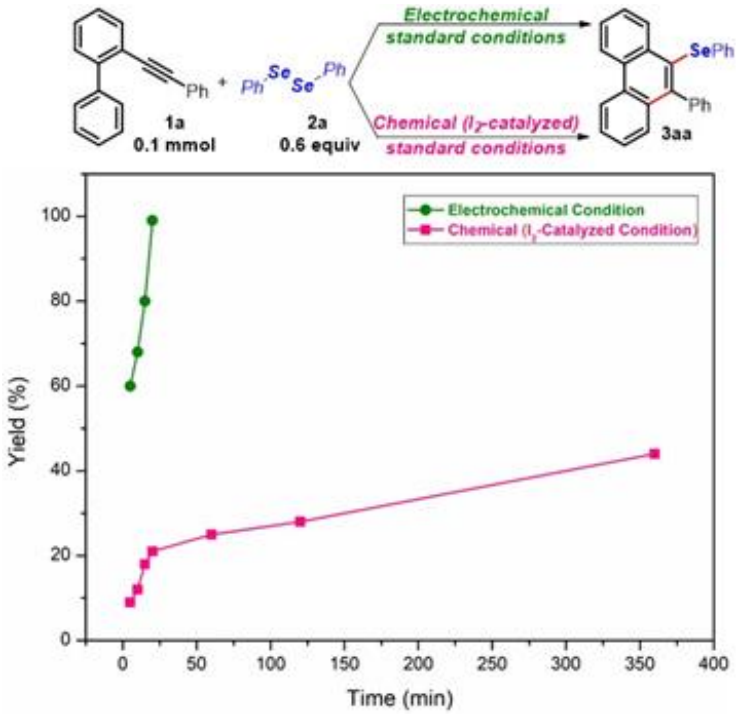

Figure 5.2.3. Reaction Kinetics Studies for the Synthesis of **3aa** from **1a** and **2a** under Electrochemical and Chemical (I_2-catalyzed) Standard Conditions.

Scheme 5.2.2. Selenylative *Ipso*-Annulation of 4'-Methoxy-2-(phenylethynyl)-1,1'-biphenyl **4** with Diselenides to Access Spiro[cyclohexane-1,1'-indene]-2,5-dien-4-ones.

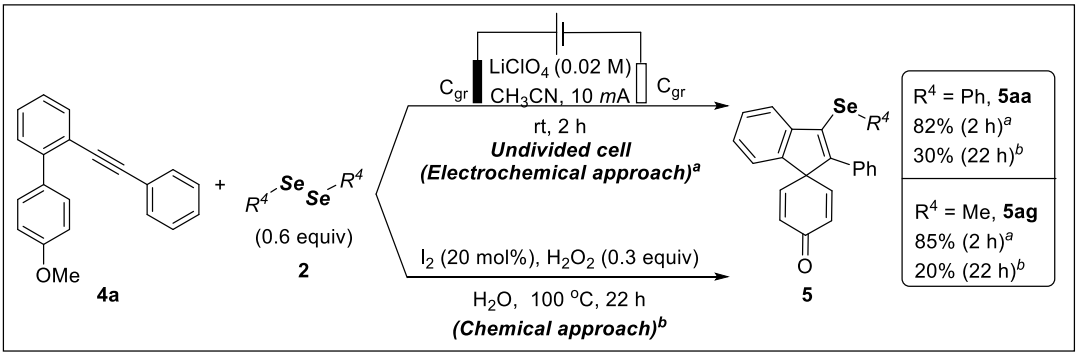

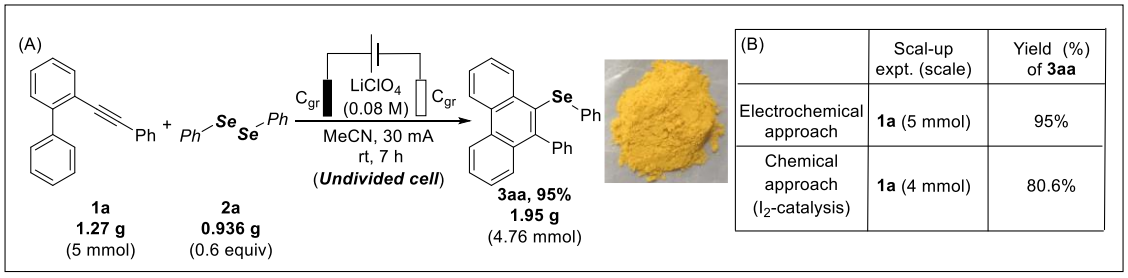

Figure 5.2.4. (A) Gram-scale Synthesis of **3aa** under Electrochemical Conditions; (B) Comparison of the Outcome of the Scale-up Experiment of **1a** with **2a** under Electrochemical and Chemical Conditions.

Table 5.2.4. Evaluation of Green Chemistry Metrics for the Synthesis of **3aa**.

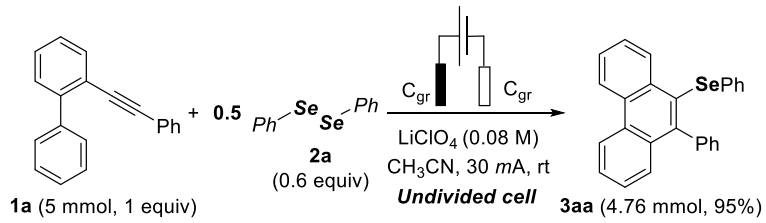

1a (5 mmol, 1 equiv) **3aa** (4.76 mmol, 95%)

Yield of desired product (**3aa**) = 95%

Atom Economy (%) = $\frac{\text{Mol. wt. of product}}{\text{Mol. wt. of all reactants}} \times 100 = \frac{409.39}{254.33 + (0.5 \times 312.13)} \times 100 =$ **99.8%**

Atom Efficiency (%) = (%yield of product x %atom economy) x 100 = (95% x 99.8%) x 100 = **94.8%**

Carbon Efficiency (%) = $\frac{\text{(moles of 3aa x no. of carbons in 3aa) x 100}}{\text{(moles of 1a x no. of carbons in 1a) + (moles of 2a x no. of carbons in 2a)}} = \frac{(4.76 \times 26) \times 100}{(5 \times 20) + (3 \times 12)} =$ **91%**

Reaction Mass Efficiency (%) = $\frac{\text{mass of isolated product}}{\text{mass of all reactants}} \times 100 = \frac{1.95}{1.27 + 0.93} \times 100 =$ **88.6%**

Reactant 1:	2-(phenylethynyl)-1,1'-biphenyl (**1a**)	1.27 g	5.0 mmol	FW 254.33
Reactant 2:	1,2-diphenyldiselane (**2a**)	0.93 g	3.0 mmol	FW 312.13
Electrolyte:	Lithium perchlorate	0.27 g	2.5 mmol	FW 106.39
Solvent:	Acetonitrile	24 g	585 mmol	FW 41.05
Recovered and recycled solvent:	Acetonitrile	22 g	536 mmol	FW 41.05
Product:	Phenyl(10-phenylphenanthren-9-yl)selane (**3aa**)	1.95 g	4.76 mmol	FW 409.39

E-factor = $\frac{\text{total waste (g)}}{\text{total product (g)}} = \frac{(1.27 + 0.93 + 0.27 + 24) - (1.95 + 22)}{1.95} =$ **1.29** g waste/g pdt

Eco Scale = 100 - Sum of individual penalties
Score on Eco Scale: > 75, Excellent; >50, acceptable; <50, Inadequate

EcoScale score = (100 - 30.5) = **69.5** (>50; So, it is an acceptable synthesis)

To quantify the greenness of the electrochemical protocol, various green chemistry metrics[2] were evaluated for the gram-scale synthesis of **3aa** from **1a** and **2a** under electrochemical conditions (Table 5.2.4). Significantly, atom-economy of the protocol was found to be almost quantitative (99.8%) and other parameters such as atom-efficiency (94.8%), carbonefficiency (91%), reaction-mass-efficiency (88.6%) were also excellent. Moreover, E-factor, [2b] an essential green chemistry parameter of an organic process based on the generated waste, is calculated to have a low value of 1.29 for the electrochemical synthesis of **3aa**. In addition, another crucial green parameter based on an organic process's safety, economic, and ecological features, i.e., EcoScale score, [2c] is also found to have a high value of 69.5 for the synthesis of **3aa** (Table 5.2.5).

Table 5.2.5. Calculation of EcoScale Score for the I_2-Catalyzed Synthetic Process to Synthesize Phenyl(10-phenylphenanthren-9-yl)selane (**3aa**) from 2-(Phenylethynyl)-1,1'-biphenyl (**1a**) and Diphenyl Diselenide (**2a**).

Eco Scale Calculation:

Eco Scale = 100 - Sum of individual penalties
Score on Eco Scale: > 75, Excellent; >50, acceptable; <50, Inadequate

Parameters	Penalty Points
1. Yield: (100 - % of yield)/2 = (100 - 99)/2 = 0.5	0.5
2. Price of reaction components (To obtain 10 mmol of end product, **3aa**)	
A. Calculation of Penalty Points :	
a. 2-(Phenylethynyl)-1,1'-biphenyl = 10.04 mmole = 2.55 g = USD 12.64	
[Synthesis cost : Required Chemicals :	
i) [1,1'-biphenyl]-2-amine = 2.50 g = USD 7.27	
ii) HCl = 7.68 mL= USD 0.25	
iii) $NaNO_2$ = 1.24 g = USD 0.055	
iv) KI = 3.69 g = USD 1.173	
v) Bis(triphenyl phosphine)Pd(II) dichloride= 0.088 g = USD 1.68	
vi) CuI = 0.024 g = USD 0.008	
vii) Phenyl acetylene = 1.34 mL = USD 1.87	
viii) Triethylamine = 32.63mL = USD 0.338	
b. 1,2-diphenyldiselane = 6.02 mmole = 1.88 g = USD 7.55	
c. $LiClO_4$ = 2.5 mmol = 0.27 g = USD = 1.04	
d. Acetonitrile = 30 mL = USD 3.62	
Total cost of synthesis of **3aa** = (12.64 + 7.55 + 1.04 + 3.62) = USD 24.85 Thus expensive, since \$10<(total cost of synthesis of 10 mmol of **3aa**) < \$50:	**3**
3. Safety	
1,2-diphenyldiselane (T)	**5**
Solvent: MeCN	
Toxic (T)	**5**
Highly Flammable (F)	**5**
4. Technical Setup	
Common Setup	**0**
5. Temperature/ Time	**0**
6. Work up and purification :	
a. Adding solvent	**0**
b. Removal of solvent with bp < 150°C	0
c. Classical Chromatography	**10**
Total penalty points:	**28.5**

B. Ecoscale calculation:

EcoScale score: (100 - 28.5) = 71.5>50; it is an acceptable synthesis)

The product **3aa** was further synthetically diversified to a new class of molecule, *i.e.*, benzo[*b*]phenanthro[9,10-*d*]selenophene **6** through a Pd-catalyzed, dephenylative C-H selenation reaction in the presence of $Pd(OAc)_2$ as a catalyst and 2,6-dimethylbenzoic acid as a ligand in toluene at 140 °C (Scheme 5.2.4).[3] The photophysical properties of **6** were evaluated in THF by UV-VIS and fluorescence spectroscopy. It showed absorbance at 330 nm, and emission at 440 nm (stoke shift = 110 nm) with a fluorescence quantum yield of 20.26% (Table 5.2.6).

Table 5.2.6. Photophysical Data of Synthesized Compound **6.**

Title of the Compound : 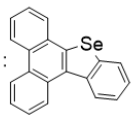

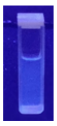

Λ_{abs} (nm)	Λ_{em} (nm)	Stoke's shift (nm)	ϕ_F (%)
330	440	110	20.26

Scheme 5.2.4. Synthetic Diversification of **3aa** to **6** *via* a Pd-Catalyzed C-H Selenation Reaction.

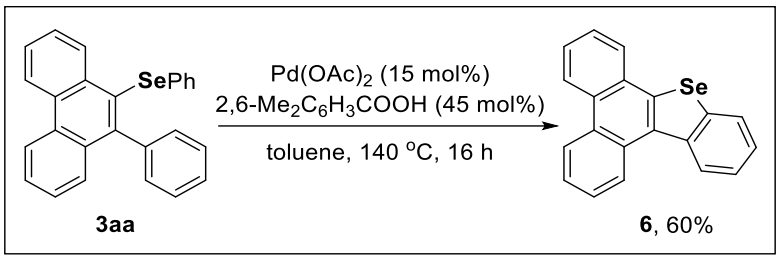

To get insights into the reaction mechanisms, several control experiments were conducted including radical quenching experiments and cyclic voltammetry. In the presence of various radical quenchers such as BHT, 1,1-diphenylethene, and TEMPO, the selenylative annulation of **1a** with **2a** was quenched to considerable extent furnishing **3aa** in 40%, 35%, and 10% respectively (Scheme 5.2.5). These results revealed a radical pathway for the reaction which was further supported by the *in situ* detection of the adduct of phenylselenyl radical and the quencher, 1,1-diphenylethene, *i.e.*, (2,2-diphenylvinyl)(phenyl)selane **7**, by LC-MS (Fig. 5.2.5).

Scheme 5.2.5. Radical Quenching Experiments.

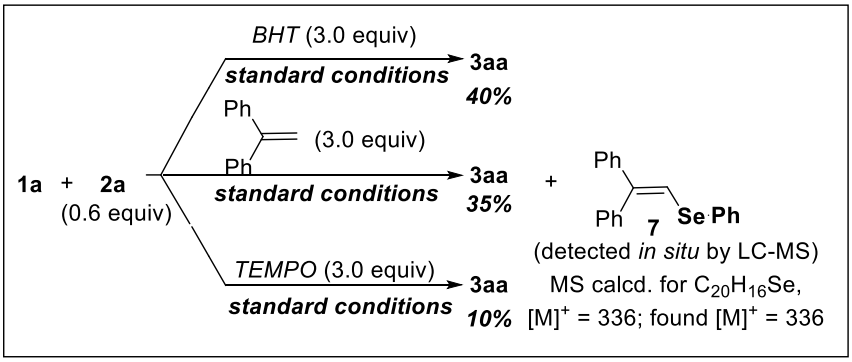

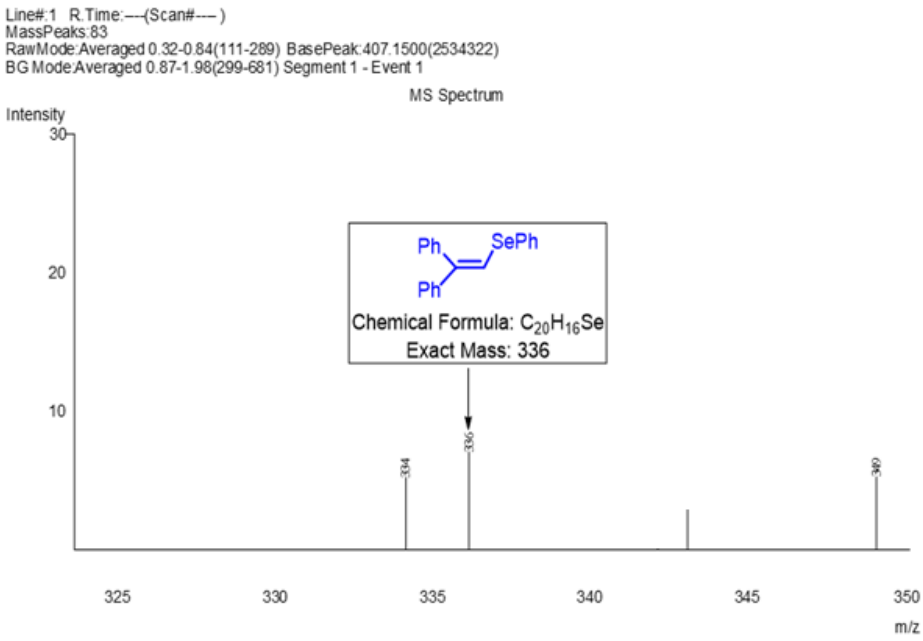

Figure 5.2.5. Mass Spectrum of the Reaction Mixture of **1a** and Diphenyl Diselenide **2a** in the Presence of Radical quencher, Ethene-1,1-diyldibenzene under Standard Reaction.

Next, the cyclic voltammetry (CV) experiments were carried out in order to analyze the redox potential of the substrates wherein the diphenyl diselenide (**2a**) showed an oxidation peak at 1.35 V and **1a** showed an oxidation peak at 1.61 V (Figure 5.2.6). The CV analysis revealed that diphenyl diselenide (**2a**) having a lower oxidation potential (1.35 V) in comparison to that of **1a** (1.61 V) would undergo preferential oxidation at anode.

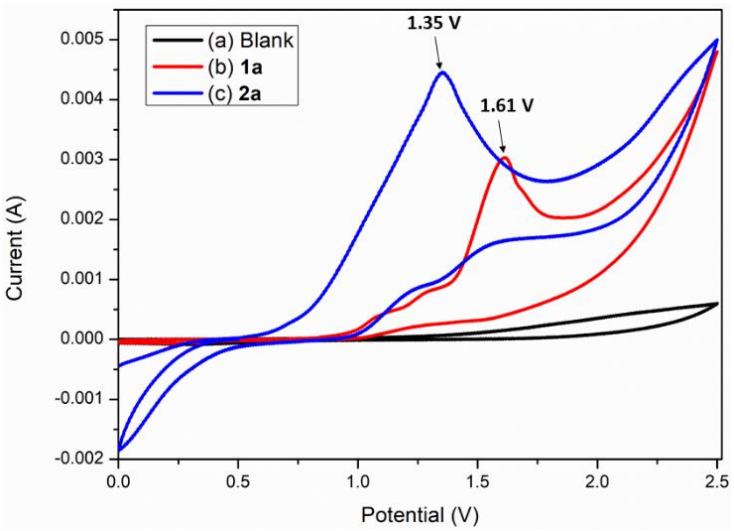

Figure 5.2.6. Cyclic Voltammograms. Conditions: a Pt-working electrode, a Ag/Ag^{+} (1 M $AgNO_3$) reference electrode, and a carbon-cloth counter electrode, $LiClO_4$ (0.1 M in MeCN), scan rate = 100 mV/s with (a) blank; (b) **1a** (0.02 M); (c) **2a** (0.02 M).

Scheme 5.2.6. Proposed Reaction Mechanism.

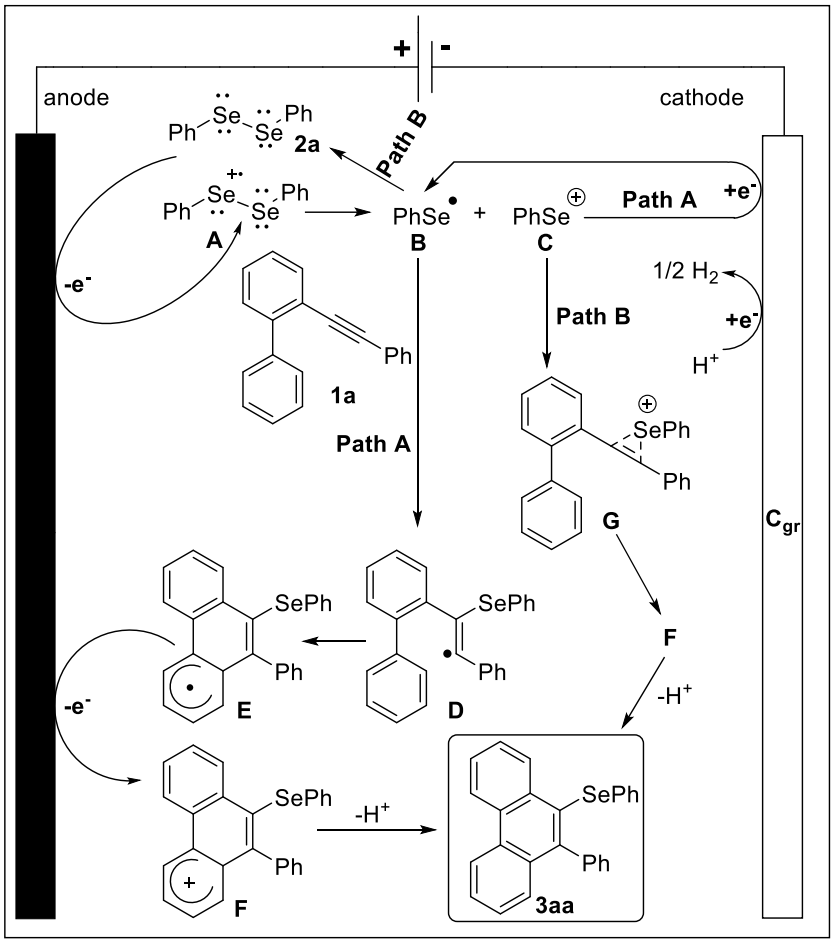

Based on the experimental results and the previous literature reports[4,5] we proposed a plausible mechanism for the synthesis of **3aa** from **1a** and **2a** under electrochemical conditions (Scheme 5). Preferential oxidation of **2a** over **1a** at anode furnishes a radical cation **A** which immediately dissociates to form a phenyl selenyl radical **B** and phenyl selenyl cation **C**. The phenyl selenyl cation **C** gets reduced at cathode to furnish the phenyl selenyl radical **B** (Path A). Thus **B** is formed effectively under electrochemical conditions which then adds to **1a** to form the corresponding vinyl radical **D**. Then **D** undergoes radical cyclization with the tethered phenyl ring to form the phenanthrenyl radical **E** which after one electron oxidation at anode followed by deprotonation furnished the desired product **3aa**. Although we proposed a radical mechanism for the synthesis of **3aa**, we cannot fully rule out the ionic pathway wherein **1a** could undergo electrophilic selenylative annulation with the *in situ* generated phenyl selenyl cation (**C**) followed by deprotonation to afford **3aa** (Path B). The liberated proton gets reduced at the cathode to form hydrogen gas as the only byproduct.[5]

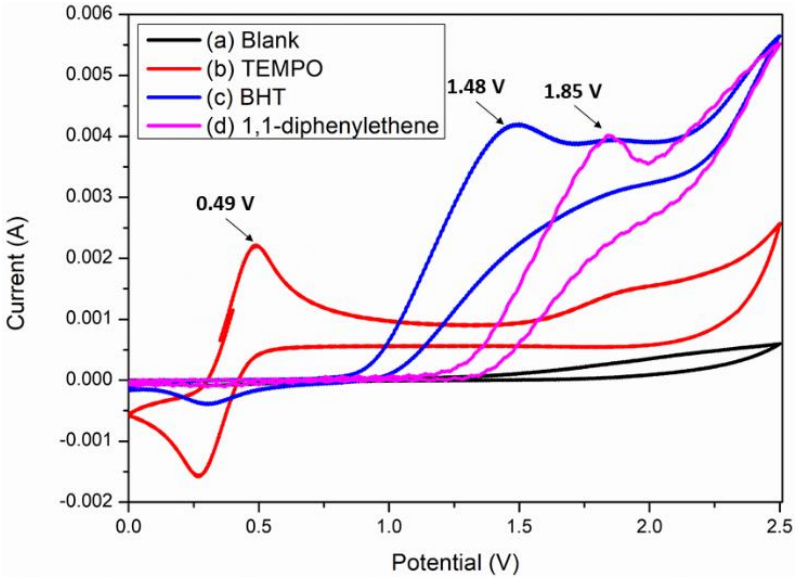

Figure 5.2.7. Cyclic Voltammograms of Radical Quenchers. Conditions: a Pt-working electrode, a Ag/Ag^+ (1 M $AgNO_3$) reference electrode, and a carbon-cloth counter electrode, $LiClO_4$ (0.1 M in MeCN), scan rate = 100 mV/s with (a) blank; (b) TEMPO (0.02 M); (c) BHT (0.02 M); (d) 1,1-diphenylethene (0.02 M).

To understand the quenching mechanisms of the reaction of 1a with 2a in the presence of various radical quenchers under electrochemical conditions, we conducted the CV experiments of the radical quenchers. While BHT (E_{ox} = 1.48 V) and 1,1-diphenylethene (E_{ox} = 1.85 V) showed higher oxidation potentials than that of diphenyl diselenide 2a (E_{ox} = 1.35 V), TEMPO showed a relatively lower reversible oxidation potential (E_{ox} = 0.49 V) than that of 2a (Figure 5.2.7).

Scheme 5.2.7. Plausible Quenching Mechanism with TEMPO.

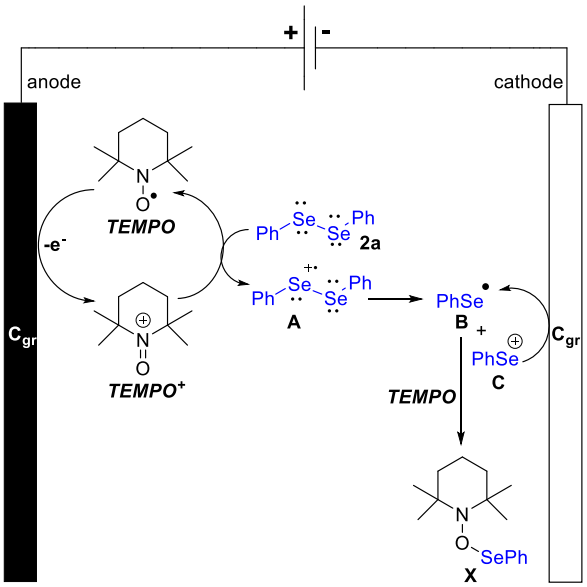

Hence, we speculate that in the presence of BHT and 1,1-diphenylethene, the *in situ* generated phenyl selenyl radical B, formed *via* direct electrolysis, was quenched by the respective radical quenchers. However, TEMPO having much lower and reversible oxidation potential than 2a, underwent preferential oxidation at the anode to form the oxidized $TEMPO^+$ which then oxidized 2a to form A *via* indirect electrolysis and regenerated TEMPO (Scheme 5.2.7).[6] The phenyl selenyl radical B, generated from A, was then quenched by TEMPO and thus the formation of 3aa was prohibited to a considerable extent. However, we couldn't detect the formation of phenyl selenyl radical adduct of TEMPO (Scheme 5.2.7) by LC-MS may be because of its instability.

5.2.3. Conclusion.

In conclusion, we have developed a catalyst- and oxidant-free but highly efficient synthetic protocol under electrochemical conditions using electricity as the only green reagent for the selenylative annulation of 2-alkynyl biaryls or 2-heteroayl-substituted alkynyl benzenes to access a wide variety of selenyl PAHs, spiro[cyclohexane-1,1'-indene]-2,5-dien-4-ones and polycyclic heteroaromatics. The transformation required only electricity as the green reagent and obviates the need for any catalyst and external chemical oxidant and produces hydrogen gas as the only inoffensive byproduct. Notably, it has been found that the developed electrochemical selenylative annulation furnished all the desired products in higher yield within a much shorter time at room temperature in comparison to that of our previously developed iodine-catalyzed chemical conditions at high temperature (100 ^oC) which certainly revealed that electrochemical process is more energy-efficient.[1] Moreover, the scope of the selenylative annulation reactions of 2-alkynyl biaryls under electrochemical conditions was found wider in comparison to that under iodine-catalyzed chemical conditions since some substrates such as 1d, 1f, 1h, and 1t which were unsuccessful under iodine-catalyzed chemical conditions, furnished the desired products (3da, 3fa, 3ha and 3ta) in moderate to high yield under electrochemical conditions. Significantly, the electrochemical scale-up process is found to be highly efficient up to gram scale furnishing the desired product in 95% yield. The electrochemical process was found 99.8% atom-economic, 94.8% atom-efficient, 91% carbon-efficient, 88.6% reaction-mass-efficient having a low E-factor (1.29) and high EcoScale score (69.5). Overall, the electrochemical approach for the selenylative annulation of 2-alkynyl biaryls is highly energy efficient, cost-effective, high-yielding, efficiently scalable, and

sustainable. We believe this highly-efficient and practical electrochemical protocol will be useful for the synthesis of various valuable selanyl PAHs and polycyclic heteroaromatics.

5.2.4. Experimental Section.

General Experimental Procedure for the Synthesis of Selenyl PAHs (3aa-3ah and 3ba−3ma) and Selenyl Polycyclic Heteroaromatics (3na and 3oa). Representative Experimental Procedure for the Synthesis of 3aa.

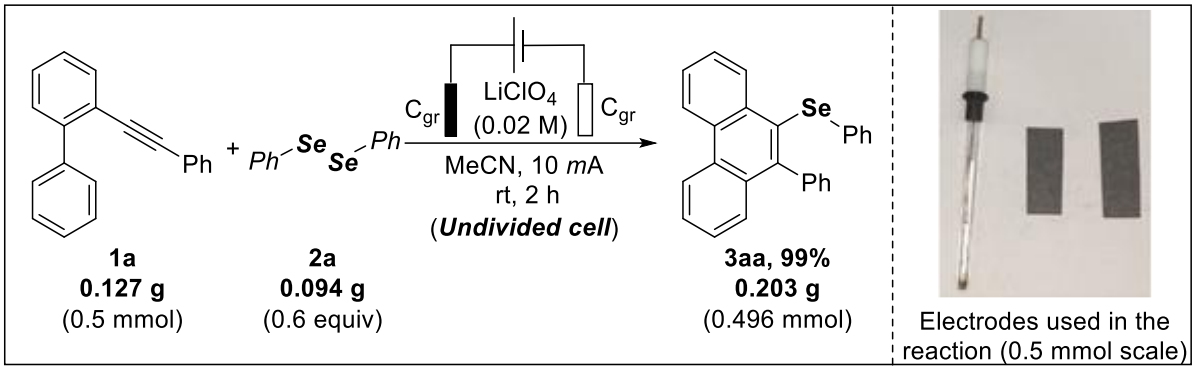

2-(Phenylethynyl)-1,1'-biphenyl 1a (0.127 g, 0.5 mmol, 1 equiv), 1,2-diphenyldiselane **2a** (0.094 g, 0.3 mmol, 0.6 equiv), lithium perchlorate (27 mg, 0.25 mmol, 0.5 equiv) and CH_3CN (15 mL) were taken into an electrochemical undivided cell. The cell was equipped with a Ag/Ag+ reference electrode and two carbon cloth (1 X 1.5 cm^2) electrodes as the working (anode) and counter (cathode) respectively. The reaction mixture was stirred and electrolyzed at a constant current of 10 mA at room temperature under aerobic atmosphere. The progress of the reaction was monitored by TLC until full conversion of **1a** to **3aa**. The solvent was evaporated and recovered under reduced pressure. The crude product was extracted with ethyl acetate twice (2 X 20 mL) and the combined organic layer was washed with water (3 X 10 mL). The solvent was evaporated under reduced pressure and the crude product was purified by column chromatography using hexane as eluent to afford the pure product, phenyl(10-phenylphenanthren-9-yl)selane **3aa** (0.203 g, 0.496 mmol) in 99% yield.

Experimental Procedure for the Synthesis of 3'-(Methylselanyl)-2'-phenylspiro[cyclohexane-1,1'-indene]-2,5-dien-4-one (5ag)

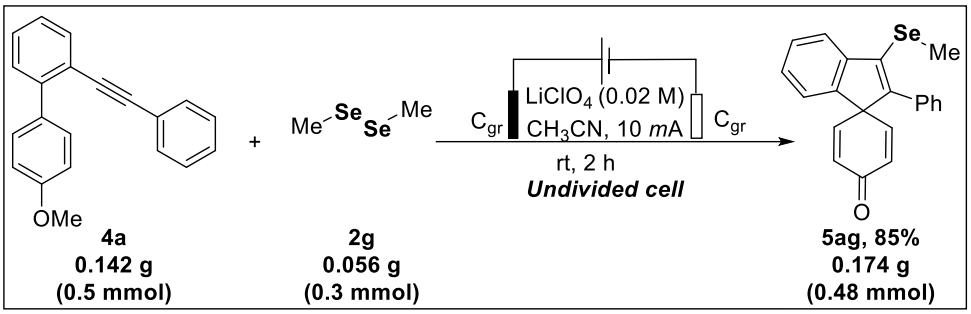

4'-Methoxy-2-(phenylethynyl)-1,1'-biphenyl **4a** (0.140 g, 0.5 mmol, 1 equiv), 1,2-diphenyldiselane **2a** (0.054 mL, 0.3 mmol, 0.6 equiv), lithium perchlorate (27 mg, 0.25 mmol, 0.5 equiv), CH_3CN (15 mL) were combined and taken into an electrochemical cell. The cell was equipped with a Ag/Ag^+ reference electrode two carbon cloth (1 X 1.5 cm^2) as the working (anode) and counter (cathode). The reaction mixture was stirred and electrolyzed at a constant current of 10 mA at room temperature under aerobic atmosphere. The progress of the reaction was monitored by TLC until full conversion of **1a** to **5ag** (120 min). The solvent was evaporated and recovered under reduced pressure. The crude product was extracted with ethyl acetate twice (2 X 20 mL) and the combined organic layer was washed with water (3 X 10 mL). The column chromatography process was further continued to afford the pure product, 3'-(methylselanyl)-2'-phenylspiro[cyclohexane-1,1'-indene]-2,5-dien-4-one **5ag** (0.174 g, 0.48 mmol) in 85% yield using hexane as eluent.

5.2.5. Analytical Data of All Synthesized Products (3aa - 3ah, 3ba – 3va and 5aa, 5ag, 6).

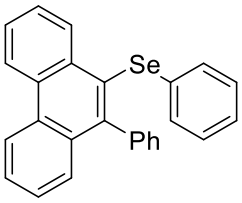

Phenyl(10-phenylphenanthren-9-yl)selane (3aa):[1] Yellow solid (0.203 g, 99%); eluent hexane; **^{1}H NMR (400 MHz, $CDCl_3$)** δ 8.72 (t, *J* = 8.6 Hz, 2H), 8.67 (dd, *J* = 8.3, 1.0 Hz, 1H), 7.66 – 7.61 (m, 2H), 7.53 (td, *J* = 7.0, 3.5 Hz, 1H), 7.47 – 7.42 (m, 2H), 7.40 (dd, *J* = 5.0, 1.7 Hz, 3H), 7.23 – 7.20 (m, 2H), 7.01 (d, *J* = 1.5 Hz, 5H). **^{13}C NMR (100 MHz, $CDCl_3$)** δ 146.8, 142.0, 134.2, 132.4, 132.1, 131.1, 130.7, 130.6, 129.7, 129.1, 128.9, 127.9, 127.6, 127.6, 127.4, 127.3, 127.0, 126.7, 125.5, 122.7, 122.5. (Overlapping peaks present).

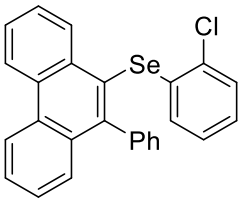

(2-Chlorophenyl)(10-phenylphenanthren-9-yl)selane (3ab):[1] Yellow solid (0.196 g, 88%); eluent hexane; **^{1}H NMR (400 MHz,** δ 8.84 (t, *J* = 8.8 Hz, 2H), 8.70 (dd, *J* = 8.3, 1.0 Hz, 1H), 7.75 (ddd, *J* = 15.7, 7.7, 1.3 Hz, 2H), 7.66 – 7.60 (m, 2H), 7.57 – 7.53 (m, 1H), 7.52 – 7.47 (m, 3H), 7.33 (ddd, *J* = 6.0, 3.4, 1.5 Hz, 3H), 7.03 (td, *J* = 7.7, 1.5 Hz, 1H), 6.85 (td, *J* = 7.8, 1.3 Hz, 1H), 6.70 (dd, *J* = 8.0, 1.5 Hz, 1H). **^{13}C NMR (100 MHz, CDCl$_3$)** δ 147.6, 141.6, 134.7, 132.3, 132.1, 132.1, 131.2, 130.7, 130.3, 129.5, 129.3, 129.1, 129.0, 128.0, 127.8, 127.7, 127.4, 127.2, 127.0, 126.8, 126.7, 126.2, 122.7, 122.6.

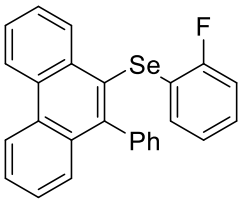

2-Fluorophenyl)(10-phenylphenanthren-9-yl)selane (3ac): [1] Yellow solid (0.197 g, 92%); eluent hexane; **^{1}H NMR (400 MHz)** δ 8.81 (d, *J* = 8.8 Hz, 2H), 8.65 (dd, *J* = 8.3, 1.0 Hz, 1H), 7.74 – 7.68 (m, 2H), 7.61 – 7.57 (m, 1H), 7.51 – 7.49 (m, 2H), 7.47 – 7.43 (m, 3H), 7.26 (s, 1H), 7.25 – 7.24 (m, 1H), 7.05 (dtd, *J* = 6.4, 5.4, 2.7 Hz, 1H), 6.98 – 6.93 (m, 1H), 6.77 – 6.72 (m, 1H), 6.69 – 6.65 (m, 1H). **^{13}C NMR (100 MHz, CDCl$_3$)** δ 159.8 (d, $^{1}J_{C\text{-}F}$ = 240 Hz), 147.5, 141.7, 132.2 (d, $^{3}J_{C\text{-}F}$ = 17 Hz), 131.2, 130.7, 130.3, 129.5, 128.9, 128.0, 127.7, 127.6, 127.5, 127.3, 127.2, 127.1, 126.8, 125.8, 125.5, 124.68, 124.66, 122.7 (d, $^{3}J_{C\text{-}F}$ = 17 Hz), 121.0 (d, $^{2}J_{C\text{-}F}$ = 22 Hz), 115.0 (d, $^{2}J_{C\text{-}F}$ = 22 Hz).

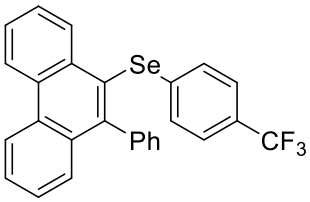

(10-Phenylphenanthren-9-yl)(4-(trifluoromethyl)phenyl)selane (3ad): [1] Yellow solid (0.168 g, 70%); eluent hexane; **^{1}H NMR (400 MHz, CDCl$_3$** δ 8.81 – 8.75 (m, 2H), 8.60 (d, *J* = 8.2 Hz, 1H), 7.69 (tdd, *J* = 6.8, 4.8, 1.8 Hz, 2H), 7.58 (dd, *J* = 11.2, 4.0 Hz, 1H), 7.51 – 7.41 (m, 5H), 7.28 – 7.20 (m, 4H), 7.09 (d, *J* = 8.2 Hz, 2H). **^{13}C NMR (100 MHz, CDCl$_3$)** δ 147.4, 141.7, 139.7, 132.1, 131.2, 130.8, 130.2, 129.4, 129.0, 128.6, 128.0, 127.8, 127.81, 127.51, 127.50 (q, $^{2}J_{C\text{-}F}$ = 36 Hz), 127.3, 126.9, 126.5, 125.6, 125.6, 122.9, 122.6, 121.4 (q, $^{1}J_{C\text{-}F}$ = 270 Hz).

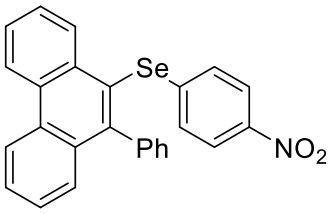

(4-Nitrophenyl)(10-phenylphenanthren-9-yl)selane (3ae):[1] Yellow solid (0.150 g, 66%); eluent hexane; **^{1}H NMR (400 MHz, $CDCl_3$)** δ 8.69 (d, *J* = 4.0 Hz, 2H), 8.44 (d, *J* = 7.8 Hz, 1H), 7.76 (d, *J* = 8.0 Hz, 2H), 7.62 (d, *J* = 5.6 Hz, 2H), 7.53 – 7.47 (m, 1H), 7.38 (d, *J* = 26.3 Hz, 5H), 7.14 (s, 2H), 7.00 (d, *J* = 7.9 Hz, 2H). **^{13}C NMR (100 MHz, $CDCl_3$** δ 147.7, 145.6, 145.1, 141.50, 132.0, 131.8, 131.4, 130.9, 129.8, 129.3, 129.1, 128.4, 128.1, 128.1, 128.0, 127.7, 127.5, 127.1, 125.8, 123.8, 123.0, 122.7.

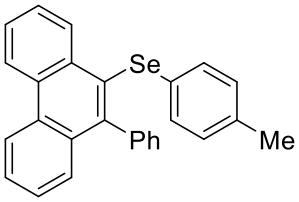

(10-Phenylphenanthren-9-yl)(*p*-tolyl)selane (3af):[1] White solid (0.180g, 85%); eluent hexane; **^{1}H NMR (400 MHz, $CDCl_3$)** δ 8.67 – 8.57 (m, 3H), 7.53 (dddd, *J* = 8.3, 7.0, 5.0, 1.7 Hz, 2H), 7.44 (ddd, *J* = 8.2, 7.0, 1.3 Hz, 1H), 7.40 – 7.27 (m, 5H), 7.19 – 7.10 (m, 2H), 6.84 (d, *J* = 8.2 Hz, 2H), 6.74 (d, *J* = 8.0 Hz, 2H), 2.07 (s, 3H). **^{13}C NMR (100 MHz, $CDCl_3$)** δ 146.6, 142.0, 135.3, 132.5, 132.1, 131.0, 130.7, 130.3, 129.7, 129.3, 128.9, 127.9, 127.5, 127.3, 127.3, 126.9, 126.7, 122.6, 122.5, 20.9. (Overlapping peaks present).

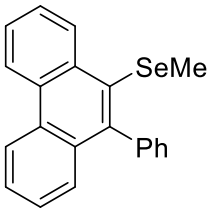

Methyl(10-phenylphenanthren-9-yl)selane (3ag):[1] Yellow solid (0.139 g, 80%); eluent hexane; **^{1}H NMR (400 MHz, $CDCl_3$)** δ 8.89 – 8.86 (m, 1H), 8.79 – 8.75 (m, 2H), 7.73 (ddd, *J* = 4.8, 2.4, 0.8 Hz, 2H), 7.67 – 7.63 (m, 1H), 7.55 – 7.51 (m, 3H), 7.46 – 7.44 (m, 2H), 7.35 – 7.32 (m, 2H), 2.07 (s, 3H). **^{13}C NMR (100 MHz, $CDCl_3$)** δ 145.5, 142.4, 132.3, 131.9, 130.6, 130.4, 130.0, 129.4, 128.6, 128.3, 128.2, 128.0, 127.5, 127.2, 127.0, 126.8, 126.7, 122.9, 122.5, 10.0.

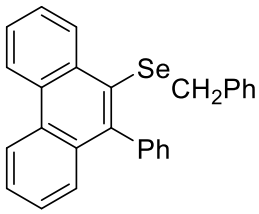

Methyl(10-phenylphenanthren-9-yl)selane (3ah): White solid (0.127 g, 60%); eluent hexane; ; mp = 158−160 °C; **^{1}H NMR (400 MHz, $CDCl_3$)** δ 8.94 – 8.84 (m, 1H), 8.83 – 8.73 (m, 2H), 7.76 – 7.70 (m, 2H), 7.65 (s, 1H), 7.45 – 7.35 (m, 5H), 7.14 – 6.97 (m, 4H), 6.92 – 6.90 (m, 1H), 6.79 (d, *J* = 5.8 Hz, 1H), 3.86 (s, 2H). **^{13}C NMR (10 MHz, $CDCl_3$)** δ 146.6, 142.1, 138.8, 132.6, 132.0, 130.7, 130.5, 130.4, 130.1, 128.7, 128.7, 128.2, 128.1, 127.8, 127.5, 127.1, 127.0, 126.8, 126.6, 126.5, 122.9, 122.5, 32.9. **^{77}Se NMR (76 MHz, $CDCl_3$)** δ 289.1 (s). **Anal** calcd for $C_{27}H_{20}Se$: C, 76.59; H, 4; found C, 76.26; H, 4.92.

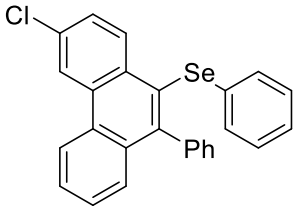

6-Chloro-10-phenylphenanthren-9-yl)(phenyl)selane (3ba):[1] Off White solid (0.205 g, 92%); **^{1}H NMR (400 MHz, CDCl$_3$)** δ 8.70 (dd, *J* = 11.0, 5.2 Hz, 2H), 8.62 (d, *J* = 8.9 Hz, 1H), 7.70 (ddd, *J* = 8.3, 6.4, 1.9 Hz, 1H), 7.52 – 7.43 (m, 6H), 7.25 – 7.21 (m, 2H), 7.08 – 7.00 (m, 5H). **^{13}C NMR (100 MHz, CDCl$_3$)** δ 147.1, 141.6, 133.9, 133.3, 132.5, 132.4, 131.8, 130.9, 130.1, 129.6, 129.2, 129.0, 128.0, 127.9, 127.7, 127.5, 127.4, 127.2, 125.7, 122.6, 122.3 (Overlapping peaks present).

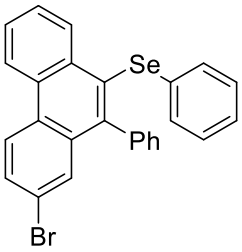

(2-Bromo-10-phenylphenanthren-9-yl)(phenyl)selane (3ca):[1] Yellow viscous liquid (0.240 g, 98%); **^{1}H NMR (400 MHz, CDCl$_3$)** δ 8.59 – 8.47 (m, 2H), 8.43 (d, *J* = 8.9 Hz, 1H), 7.59 (dd, *J* = 8.9, 2.1 Hz, 1H), 7.54 – 7.47 (m, 2H), 7.44 (dd, *J* = 8.2, 1.1 Hz, 1H), 7.33 – 7.27 (m, 3H), 7.10 – 7.05 (m, 2H), 6.90 (s, 5H). **^{13}C NMR (100 MHz, CDCl$_3$)** δ 145.6, 141.1, 133.9, 133.5, 132.4, 130.9, 130.8, 130.5, 130.2, 129.7, 129.6, 129.3, 129.1, 129.0, 128.1, 127.9, 127.6, 127.4, 125.7, 124.3, 122.6, 121.0.

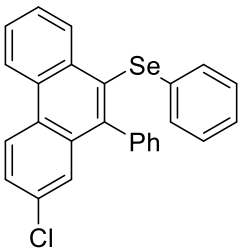

(2-chloro-10-phenylphenanthren-9-yl)(phenyl)selane (3da): White crystalline solid (0.188 g, 85%); mp = 161−163 °C; **^{1}H NMR (400 MHz, CDCl$_3$)** δ 8.50 (d, *J* = 8.1 Hz, 1H), 8.39 (d, *J* = 8.9 Hz, 2H), 7.38 (dt, *J* = 27.8, 7.2 Hz, 3H), 7.31 – 7.14 (m, 4H), 7.01 (dd, *J* = 6.1, 2.6 Hz, 2H), 6.83 (s, 5H). **^{13}C NMR (100 MHz, CDCl$_3$)** δ 145.6, 141.1, 133.9, 133.1, 132.7, 132.3, 130.73, 130.1, 129.6, 129.3, 129.2, 128.9, 128.1, 127.8, 127.7, 127.6, 127.3, 125.6, 124.2, 122.6 (Overlapping peaks present). **^{77}Se NMR (76 MHz, CDCl$_3$)** δ 327.8 (s). Anal calcd for $C_{26}H_{17}ClSe$: C, 70.36; H, 3.86; found C, 70.74; H, 3.15.

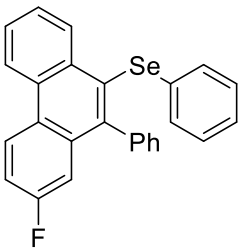

2-Fluoro-10-phenylphenanthren-9-yl)(phenyl)selane (3ea): [1] Yellow solid (0.176 g, 82%); eluent hexane; **^{1}H NMR (400 MHz, CDCl$_3$)** δ 8.64 (dd, *J* = 9.2, 5.5 Hz, 1H), 8.61 – 8.54 (m, 2H), 7.57 (m, 1H), 7.45 (m, 1H), 7.36 – 7.28 (m, 4H), 7.14 – 7.08 (m, 2H), 7.00 (dd, *J* = 10.8, 2.7 Hz, 1H), 6.95 (t, *J* = 2.5 Hz, 5H). **^{13}C NMR (100 MHz, CDCl$_3$)** δ 161.2 (d, $^{1}J_{C\text{-}F}$ =

245 Hz), 146.0, 141.4, 134.0, 133.6 (d, $^{3}J_{C\text{-}F}$ = 8 Hz), 132.0, 130.8, 130.4, 129.6, 129.3, 129.2, 129.0, 128.7, 128.2, 127.7, 127.4, 127.4, 125.7, 125.0 (d, $^{3}J_{C\text{-}F}$ = 8 Hz), 122.5, 116.3 (d, $^{2}J_{C\text{-}F}$ = 23 Hz), 113.3 (d, $^{2}J_{C\text{-}F}$ = 23 Hz).

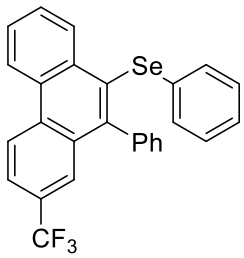

Phenyl(10-phenyl-2-(trifluoromethyl)phenanthren-9-yl)selane (3fa): Viscous liquid (0.167 g, 70%); eluent hexane; **^{1}H NMR (400 MHz, CDCl$_3$)** δ 8.89 (d, *J* = 8.8 Hz, 1H), 8.79 – 8.73 (m, 2H), 7.88 (dd, *J* = 8.7, 1.7 Hz, 1H), 7.77 (s, 1H), 7.73 (ddd, *J* = 8.3, 7.0, 1.4 Hz, 1H), 7.65 (ddd, *J* = 8.2, 7.0, 1.2 Hz, 1H), 7.48 – 7.44 (m, 3H), 7.24 (m, 2H), 7.06 (d, *J* = 2.9 Hz, 5H). **^{13}C NMR (100 MHz, CDCl$_3$)** δ 146.5, 140.9, 133.8, 133.2, 133.1, 131.6, 130.9, 129.9, 129.7, 129.4, 129.2, 129.0, 128.9, 128.7, 128.2, 127.95, 128.0 (q, $^{1}J_{C\text{-}F}$ = 269 Hz), 127.7 (q, $^{2}J_{C\text{-}F}$ = 28 Hz), 127.4 (q, $^{3}J_{C\text{-}F}$ = 14 Hz), 126.7, 123.6, 123.2, 122.6 (q, $^{3}J_{C\text{-}F}$ = 14 Hz). **^{77}Se NMR (76 MHz, CDCl$_3$)** δ 328.2 (s). **^{19}F NMR (377 MHz, CDCl$_3$)** δ -62.2 (s). **Anal** calcd for $C_{27}H_{17}F_3Se$: C, 67.93; H, 3.59; found C, 67.56; H, 4.06.

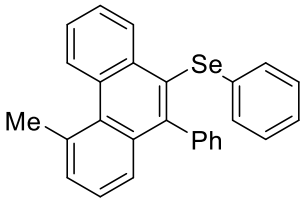

(4-Methyl-10-phenylphenanthren-9-yl)(phenyl)selane (3ga):[1] Off White solid (0.202 g, 95%); eluent hexane; **^{1}H NMR (400 MHz, CDCl$_3$)** δ 8.93 (d, *J* = 8.0 Hz, 1H), 8.89 (dd, *J* = 8.2, 1.4 Hz, 1H), 7.71 (m, 1H), 7.67 – 7.61 (m, 2H), 7.53 – 7.48 (m, 4H), 7.45 – 7.41 (m, 1H), 7.36 – 7.31 (m, 2H), 7.18 – 7.11 (m, 5H), 3.26 (s, 3H). **^{13}C NMR (100 MHz, CDCl$_3$)** δ 147.1, 142.6, 134.9, 134.2, 133.6, 133.3, 132.0, 131.8, 131.3, 129.7, 129.1, 128.9, 127.9, 127.7, 127.6, 127.5, 127.3, 127.2, 126.8, 125.7, 125.6, 125.4, 27.2.

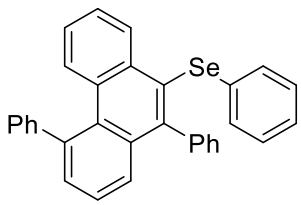

(4,10-diphenylphenanthren-9-yl)(phenyl)selane (**3ha):** White crystalline solid (0.194 g, 80%); eluent hexane; ; mp = 185−187 ºC **^{1}H NMR (400 MHz, CDCl$_3$)** δ 8.53 (dd, *J* = 8.3, 0.9 Hz, 1H), 7.75 – 7.69 (m, 1H), 7.36 – 7.33 (m, 2H), 7.32 – 7.24 (m, 9H), 7.23 – 7.19 (m, 1H), 7.14 – 7.10 (m, 2H), 6.96 – 6.86 (m, 6H). **^{13}C NMR (100 MHz, CDCl$_3$)** δ 146.6, 145.3, 142.4, 140.1, 134.2, 133.6, 133.4, 131.7 130.7, 130.1, 129.7, 129.6, 129.3, 129.0, 129.0, 128.9, 128.9, 128.4, 128.3, 128.0, 127.3, 127.1, 126.9, 125.7, 125.5, 124.9. **^{77}Se NMR (76 MHz, CDCl$_3$)** δ 325.8 (s). Anal calcd for $C_{32}H_{22}Se$: C, 79.17; H, 4.57; found C, 79.54; H, 4.15.

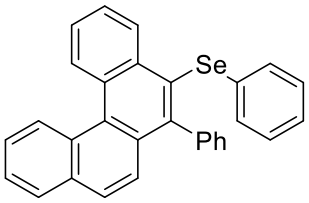

Phenyl(6-phenylbenzo[*c*]phenanthren-5-yl)selane (3ia):[1] Off White solid (0.147 g, 64%); eluent hexane; **^{1}H NMR (400 MHz, $CDCl_3$)** δ 8.97 (t, *J* = 8.3 Hz, 2H), 8.70 (d, *J* = 8.2 Hz, 1H), 7.87 (d, *J* = 7.6 Hz, 1H), 7.62 (d, *J* = 8.9 Hz, 1H), 7.59 – 7.53 (m, 3H), 7.49 (s, 1H), 7.33 (m, 4H), 7.14 (dd, *J* = 7.2, 2.2 Hz, 2H), 6.94 (s, 5H). **^{13}C NMR (100 MHz, $CDCl_3$)** δ 146.0, 141.9, 134.2, 133.7, 133.5, 130.5, 130.3, 130.0, 129.6, 129.4, 129.1, 128.9, 128.9, 128.57, 128.2, 128.0, 127.4, 127.1, 127.0, 126.6, 126.2, 126.2, 125.7, 125.6.

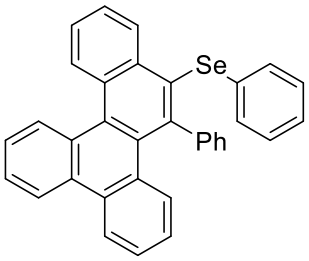

Phenyl(5-phenylbenzo[*g*]chrysen-6-yl)selane (3ja):[1] Off White solid (0.178 g, 70%); eluent hexane; **^{1}H NMR (400 MHz, $CDCl_3$)** δ 8.76 (dd, *J* = 15.5, 8.0 Hz, 2H), 8.69 (t, *J* = 6.8 Hz, 2H), 8.57 (d, *J* = 8.0 Hz, 1H), 7.71 (dt, *J* = 14.8, 6.9 Hz, 2H), 7.63 – 7.52 (m, 3H), 7.49 – 7.32 (m, 6H), 7.06 (s, 6H). **^{13}C NMR (100 MHz, $CDCl_3$)** δ 144.6, 143.4, 134.5, 133.8, 131.4, 130.7, 130.3, 130.1, 129.9, 129.8, 129.3, 129.1, 128.9, 128.7, 128.1, 127.9, 127.6, 127.2, 127.0, 126.5, 126.2, 126.0, 125.7, 125.6, 123.5, 123.0.

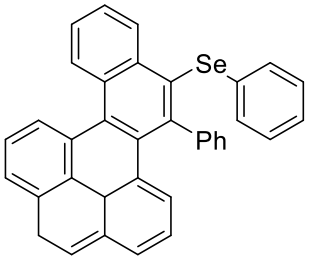

Phenyl(14-phenyldibenzo[*ij*,*no*]tetraphen-13-yl)selane (3ka):[1] Brown solid (0.211 g, 79%); eluent hexane; **^{1}H NMR (400 MHz, $CDCl_3$)** δ 9.36 (d, *J* = 9.3 Hz, 1H), 9.16 (d, *J* = 8.2 Hz, 1H), 8.87 (dd, *J* = 8.2, 1.1 Hz, 1H), 8.32 (d, *J* = 9.3 Hz, 1H), 8.27 (d, *J* = 7.6 Hz, 1H), 8.21 – 8.10 (m, 2H), 8.05 (t, *J* = 7.6 Hz, 1H), 7.98 (d, *J* = 9.0 Hz, 1H), 7.90 (d, *J* = 9.0 Hz, 1H), 7.78 – 7.72 (m, 1H), 7.68 (dd, *J* = 11.1, 4.1 Hz, 1H), 7.60 – 7.48 (m, 3H), 7.42 – 7.33 (m, 2H), 7.15 (dd, *J* = 6.5, 3.3 Hz, 2H), 7.13 – 7.00 (m, 3H). **^{13}C NMR (100 MHz, $CDCl_3$)** δ 146.4, 142.0, 134.2, 133.1, 131.7, 131.0, 130.6, 130.2, 130.0, 129.6, 129.4, 129.0, 128.1, 128.0, 127.9, 127.6, 127.3, 127.2, 127.1, 126.7, 126.4, 126.3, 126.1, 125.7, 125.2, 125.0, 124.8, 124.3.

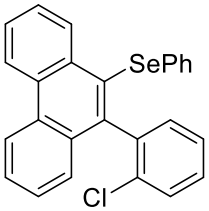

(10-(2-Chlorophenyl)phenanthren-9-yl)(phenyl)selane (3la) :[1]Yellow crystalline solid (0.210 g, 95%); eluent hexane; **^{1}H NMR (400 MHz, $CDCl_3$)** δ 8.64 (t, *J* = 8.6 Hz, 2H), 8.59 (dd, *J* = 8.3, 1.0 Hz, 1H), 7.57 – 7.51 (m, 2H), 7.47 – 7.42 (m, 1H), 7.36 (dd, *J* = 3.6, 1.3 Hz, 1H), 7.31 (dd, *J* = 5.0, 1.8 Hz, 3H), 7.15 – 7.10 (m, 2H), 6.95 – 6.89 (m, 5H). **^{13}C NMR (100 MHz, $CDCl_3$)** δ

146.8, 142.0, 134.2, 132.4, 132.1, 131.1, 130.7, 130.6, 129.7, 129.1, 128.9, 127.9, 127.61, 127.57, 127.4, 127.3, 127.0, 126.7, 125.5, 122.7, 122.5 (Overlapping peaks present).

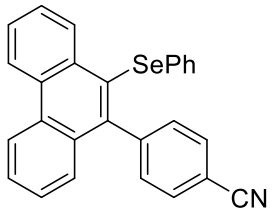

4-(10-(Phenylselanyl)phenanthren-9-yl)benzonitrile (3ma) : Yellow viscous liquid (0.143 g, 65%); eluent hexane; **^{1}H NMR (400 MHz, $CDCl_3$)** δ 8.85 – 8.76 (m, 3H), 7.77 – 7.68 (m, 4H), 7.67 – 7.63 (m, 1H), 7.54 – 7.50 (m, 1H), 7.37 – 7.30 (m, 3H), 7.12 – 7.04 (m, 3H), 7.05 – 6.97 (m, 2H).**^{13}C NMR (100 MHz, $CDCl_3$)** δ 146.5, 144.7, 133.6, 132.2, 131.7, 131.2, 131.0, 130.7, 130.5, 130.4, 129.1, 129.0, 127.9, 127.8, 127.7, 127.5, 127.0, 125.8, 122.8, 122.7, 118.8, 111.1. **^{77}Se NMR (76 MHz, $CDCl_3$)** δ 351.0 (s). **Anal** calcd for $C_{27}H_{17}NSe$: C, 74.65; H, 3.94; N, 3.22; found C, 74.85; H, 3.00; N, 3.60.

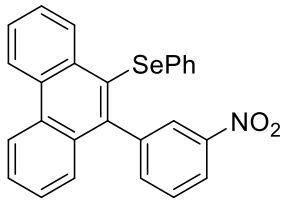

10-(3-Nitrophenyl)phenanthren-9-yl)(phenyl)selane (3na):[1] Yellow solid (0.155 g, 68%); eluent hexane; **^{1}H NMR (400 MHz, $CDCl_3$) ^{1}H NMR (400 MHz, $CDCl_3$)** δ 8.89 – 8.78 (m, 3H), 8.35 – 8.27 (m, 1H), 8.13 – 8.07 (m, 1H), 7.75 (m, 2H), 7.68 (m, 1H), 7.61 – 7.56 (m, 2H), 7.55 – 7.50 (m, 1H), 7.41 (dd, *J* = 8.3, 0.9 Hz, 1H), 7.13 – 7.02 (m, 5H). **^{13}C NMR (100 MHz, $CDCl_3$)** δ 147.7, 143.8, 143.0, 136.0, 133.4, 132.4, 131.3, 131.0, 130.7, 130.5, 129.4, 129.0, 128.8, 128.7, 127.80, 127.78, 127.7, 127.6, 127.0, 126.0, 124.9, 122.8, 122.8, 122.2.

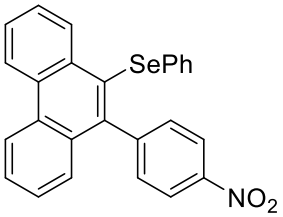

(10-(4-Nitrophenyl)phenanthren-9-yl)(phenyl)selane (3oa): Semi Yellow solid (0.125 g, 55%); eluent hexane; mp = 159−161 °C **^{1}H NMR (400 MHz, $CDCl_3$)** δ 8.86 – 8.74 (m, 3H), 8.33 – 8.19 (m, 2H), 7.79 – 7.70 (m, 2H), 7.68 – 7.61 (m, 1H), 7.53 – 7.47 (m, 1H), 7.42 – 7.35 (m, 2H), 7.34 – 7.29 (m, 1H), 7.11 – 7.03 (m, 3H), 7.03 – 6.94 (m, 2H). **^{13}C NMR (100 MHz, $CDCl_3$)** δ 148.6, 147.1, 144.4, 133.6, 132.3, 131.2, 131.2, 130.8, 130.5, 129.1, 128.0, 127.9, 127.7, 127.1, 126.0, 123.3, 122.9, 122.8. **^{77}Se NMR (76 MHz, $CDCl_3$)** δ 352.8 (s). **Anal** calcd for $C_{26}H_{17}NO_2Se$: C, 68.73; H, 3.77; N, 3.08; found C, 68.90; H, 3.65; N, 3.16.

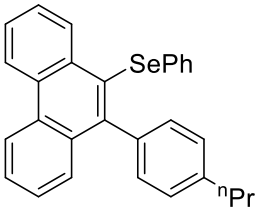

Phenyl(10-(4-propylphenyl)phenanthren-9-yl)selane (3pa) :[1] Reddish Brown solid (0.172 g, 76%); eluent hexane; **^{1}H NMR (400 MHz, $CDCl_3$)** δ 8.77 (t, *J* = 8.6 Hz, 2H), 8.68 (dd, *J* = 8.3, 1.0 Hz, 1H), 7.68 (dt, *J* = 8.0, 6.7 Hz, 2H), 7.59 – 7.55 (m, 1H), 7.52 (s, 2H), 7.23 (d, *J* = 8.0 Hz, 2H), 7.15 – 7.12 (m, 2H), 7.05 (s, 5H), 2.72 – 2.67 (m, 2H), 1.75 (dd, *J* = 15.1, 7.5 Hz, 2H), 1.03 (t, *J* = 7.3 Hz, 3H). **^{13}C NMR (100 MHz, $CDCl_3$)** δ 146.9, 141.7, 139.2, 134.4, 132.5, 132.4, 131.1, 130.7, 129.5, 129.3, 129.0, 128.9, 128.0, 127.8, 127.5, 127.4, 126.9, 126.7, 125.5, 122.7, 122.5, 37.9, 24.4, 14.0(Overlapping peaks present).

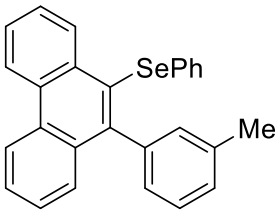

Phenyl(10-(*m*-tolyl)phenanthren-9-yl)selane (3qa):[1] Yellow solid (0.204 g, 96%); eluent hexane; **^{1}H NMR (400 MHz, $CDCl_3$)** δ 8.82 (t, *J* = 7.4 Hz, 3H), 7.73 (m, 2H), 7.68 – 7.58 (m, 2H), 7.57 – 7.51 (m, 1H), 7.41 (t, *J* = 7.5 Hz, 1H), 7.33 (d, *J* = 7.6 Hz, 1H), 7.14 (m, 7H), 2.43 (s, 3H). **^{13}C NMR (100 MHz, $CDCl_3$)** δ 146.9, 141.8, 137.4, 134.4, 132.5, 132.2, 131.0, 130.6, 130.4, 129.3, 128.9, 128.8, 128.0, 127.8, 127.6, 127.5, 127.4, 126.9, 126.7, 125.5, 122.7, 122.5, 21.5.

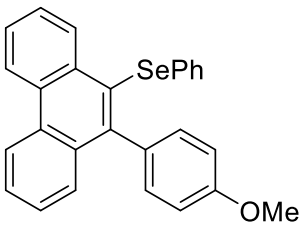

Phenyl(10-(*m*-tolyl)phenanthren-9-yl)selane (3ra): Yellow solid (0.165 g, 75%); eluent hexane; mp = 137−139 °C; **^{1}H NMR (400 MHz, $CDCl_3$)** δ 8.57 (m, 3H), 7.54 – 7.51 (m, 1H), 7.48 (dd, *J* = 8.1, 1.3 Hz, 1H), 7.43 – 7.38 (m, 2H), 7.32 (m, 1H), 7.01 (d, *J* = 8.7 Hz, 2H), 6.95 – 6.86 (m, 5H), 6.82 (d, *J* = 8.7 Hz, 2H), 3.71 (s, 3H). **^{13}C NMR (100 MHz, $CDCl_3$)** δ 158.7, 146.5, 134.3, 132.4, 131.0, 130.7, 130.6, 129.0, 128.9, 128.1, 127.5, 127.3, 126.9, 126.6, 125.4, 122.6, 122.5, 113.3, 55.1 (Overlapping peaks present)**. ^{77}Se NMR (76 MHz, $CDCl_3$)** δ 322.7 (s). **Anal** calcd for $C_{27}H_{20}OSe$ C, 73.80; H, 4.59; found C, 73.92; H, 4.36.

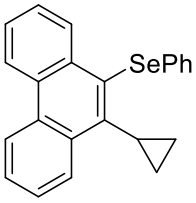

(10-Cyclopropylphenanthren-9-yl)(phenyl)selane (3sa):[1] Brown Viscous liquid (0.122 g, 65%); eluent hexane; **^{1}H NMR (400 MHz, $CDCl_3$)** δ 7.43 (dd, *J* = 6.5, 3.2 Hz, 2H), 7.36 (dd, *J* = 5.0, 2.0 Hz, 3H), 7.29 (dd, *J* = 2.5, 1.1 Hz, 2H), 7.22 (dd, *J* = 9.4, 8.9 Hz, 2H), 7.17 (d, *J* = 1.4 Hz, 1H), 7.12 (dd, *J*

= 4.9, 3.7 Hz, 1H), 6.96 – 6.92 (m, 2H), 1.84 (m, 1H), 0.74 – 0.65 (m, 2H), 0.59 (m, 1H), 0.41 – 0.34 (m, 1H). **^{13}C NMR (100 MHz, $CDCl_3$)** δ 143.4, 140.8, 140.4, 138.0, 134.3, 132.2, 130.8, 130.0, 129.5, 129.4, 129.3, 129.0, 128.8, 128.4, 128.4, 127.7, 127.7, 127.5, 127.1, 127.0, 126.5, 126.4, 104.3, 24.2, 10.3, 9.3.

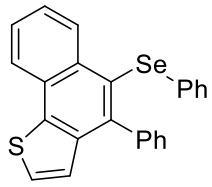

4-Phenyl-5-(phenylselanyl)naphtho[1,2-*b*]thiophene (3ta): Colourless liquid (0.129 g, 62%); eluent hexane; **^{1}H NMR (400 MHz, $CDCl_3$)** δ 8.68 (dd, *J* = 8.4, 0.5 Hz, 1H), 8.20 (dd, *J* = 8.1, 0.7 Hz, 1H), 7.60 (ddd, *J* = 8.1, 7.0, 1.2 Hz, 1H), 7.55 – 7.51 (m, 1H), 7.41 (dd, *J* = 3.4, 2.2 Hz, 3H), 7.28 (dd, *J* = 6.6, 3.0 Hz, 2H), 7.07 – 7.00 (m, 7H). **^{13}C NMR (100 MHz, $CDCl_3$)** δ 143.8, 141.8, 139.3, 138.0, 134.3, 132.1, 130.9, 129.4, 129.1, 128.9, 128.0, 127.8, 127.5, 127.0, 127.0, 126.3, 125.5, 124.7, 124.6, 124.0. **^{77}Se NMR (76 MHz, $CDCl_3$)** δ 304.5 (s). **Anal** calcd for $C_{27}H_{20}OSe$ C, 69.39; H, 3.88; found C, 69.48; H, 3.76.

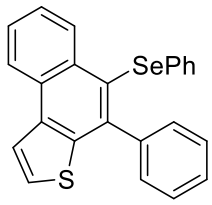

4-Phenyl-5-(phenylselanyl)naphtho[2,1-*b*]thiophene (3ua):[1] Yellow solid (0.177 g, 85%); eluent hexane; **^{1}H NMR (400 MHz, $CDCl_3$)** δ 8.73 (dd, *J* = 8.5, 0.6 Hz, 1H), 8.42 (d, *J* = 0.8 Hz, 1H), 8.08 (d, *J* = 5.5 Hz, 1H), 7.68 – 7.63 (m, 2H), 7.58 – 7.54 (m, 1H), 7.48 – 7.43 (m, 3H), 7.40 – 7.36 (m, 2H), 7.09 – 7.02 (m, 5H). **^{13}C NMR (100 MHz, $CDCl_3$)** δ 142.485, 141.8, 139.7, 137.0, 134.3, 132.9, 130.5, 129.3, 129.14, 129.1, 128.9, 128.5, 128.1, 128.1, 126.7, 126.6, 125.5, 123.9, 122.3 (Overlapping peaks present).

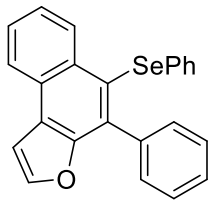

4-Phenyl-5-(phenylselanyl)naphtho[2,1-*b*]furan (3va): [1] Brown solid (0.140 g, 70%); eluent hexane; **^{1}H NMR (400 MHz, $CDCl_3$)** δ 8.73 (d, *J* = 8.4 Hz, 1H), 8.21 (dd, *J* = 8.1, 0.7 Hz, 1H), 7.77 (d, *J* = 2.1 Hz, 1H), 7.63 (dd, *J* = 3.2, 2.1 Hz, 1H), 7.55 – 7.51 (m, 1H), 7.45 (dd, *J* = 3.8, 2.8 Hz, 3H), 7.41 – 7.38 (m, 2H), 7.36 (d, *J* = 2.1 Hz, 1H), 7.08 – 7.01 (m, 5H). **^{13}C NMR (100 MHz, $CDCl_3$)** δ 150.8, 145.5, 137.4, 134.7, 132.2, 131.5, 130.7, 130.1, 129.1, 129.0, 128.0, 127.8, 126.6, 126.0, 125.6, 124.5, 124.1, 123.8, 105.8.

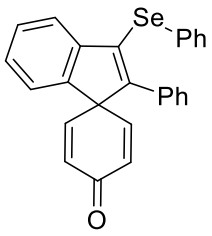

2'-Phenyl-3'-(phenylselanyl)spiro[cyclohexane-1,1'-indene]-2,5-dien-4-one (5a): Yellow solid (0.174 g, 82%); eluent hexane; mp = 175−177 °C; **^{1}H NMR (400 MHz, CDCl$_3$)** δ 7.27 – 7.13 (m, 10H), 7.12 – 7.04 (m, 4H), 6.52 (d, *J* = 10.1 Hz, 2H), 6.41 (d, *J* = 10.1 Hz, 2H). **^{13}C NMR (100 MHz, CDCl$_3$)** δ 186.0, 151.6, 148.0, 145.3, 140.7, 134.3, 132.1, 130.9, 129.8, 129.3, 128.8, 128.7, 128.5, 128.1, 127.2, 126.8, 123.5, 123.0, 62.2. **^{77}Se NMR (76 MHz, CDCl$_3$)** δ 280.43 (s). **Anal** calcd for $C_{26}H_{18}OSe$ C, 73.4; H, 4.27; found C, 73.65; H, 4.02.

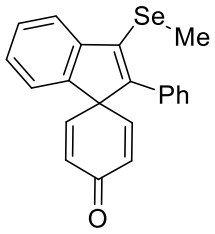

3'-(Methylselanyl)-2'-phenylspiro[cyclohexane-1,1'-indene]-2,5-dien-4-one (5ag): Yellow solid (0.154g, 85%); eluent hexane; mp = 165−167 °C; **^{1}H NMR (400 MHz, CDCl$_3$)** δ 7.59 (d, *J* = 7.6 Hz, 1H), 7.45 (td, *J* = 7.5, 1.1 Hz, 1H), 7.41 – 7.37 (m, 2H), 7.33 (qd, *J* = 3.7, 1.6 Hz, 3H), 7.29 (dd, *J* = 7.5, 1.1 Hz, 1H), 7.15 (d, *J* = 7.4 Hz, 1H), 6.54 (d, *J* = 10.1 Hz, 2H), 6.46 (d, *J* = 10.1 Hz, 2H), 2.07 (s, 3H). **^{13}C NMR (100 MHz, CDCl$_3$)** δ 186.1, 148.4, 147.6, 145.9, 140.4, 134.7, 133.3, 130.9, 128.9, 128.6, 128.5, 128.2, 127.2, 123.6, 122.2, 62.3, 7.3. **^{77}Se NMR (76 MHz, CDCl$_3$)** δ 86.3 (s). **Anal** calcd for $C_{21}H_{16}OSe$ C, 69.42; H, 4.44; found C, 69.58; H, 4.07.

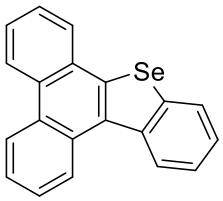

Benzo[*b*]phenanthro[9,10-d]selenophene (6):[5] White solid (0.060 g, 60%); eluent hexane; mp = 130−132 °C; **^{1}H NMR (400 MHz, CDCl$_3$)** δ 9.10 – 9.02 (m, 1H), 8.87 – 8.79 (m, 2H), 8.72 (dd, *J* = 8.4, 0.9 Hz, 1H), 8.07 (dd, *J* = 7.9, 0.7 Hz, 1H), 8.04 – 7.98 (m, 1H), 7.76 (ddd, *J* = 8.4, 7.0, 1.5 Hz, 1H), 7.73 – 7.64 (m, 3H), 7.59 (ddd, *J* = 8.4, 7.2, 1.3 Hz, 1H), 7.46 – 7.42 (m, 1H). **^{13}C NMR (100 MHz, CDCl$_3$)** δ 141.5, 140.5, 139.8, 130.7, 130.1, 129.2, 127.5, 127.4, 127.2, 126.6, 126.3, 125.6, 125.4, 125.2, 124.1, 123.9, 123.3. **^{77}Se NMR (76 MHz, CDCl$_3$)** δ 446.1 (s). **Anal** calcd for $C_{20}H_{12}Se$ C, 72.51; H, 3.65; found C, 72.38; H, 3.82.

^{1}H ,^{13}C and ^{77}Se NMR Spectra of Some Selected 9-Selanylphenanthrenes and Polycyclic Heteroaromatics

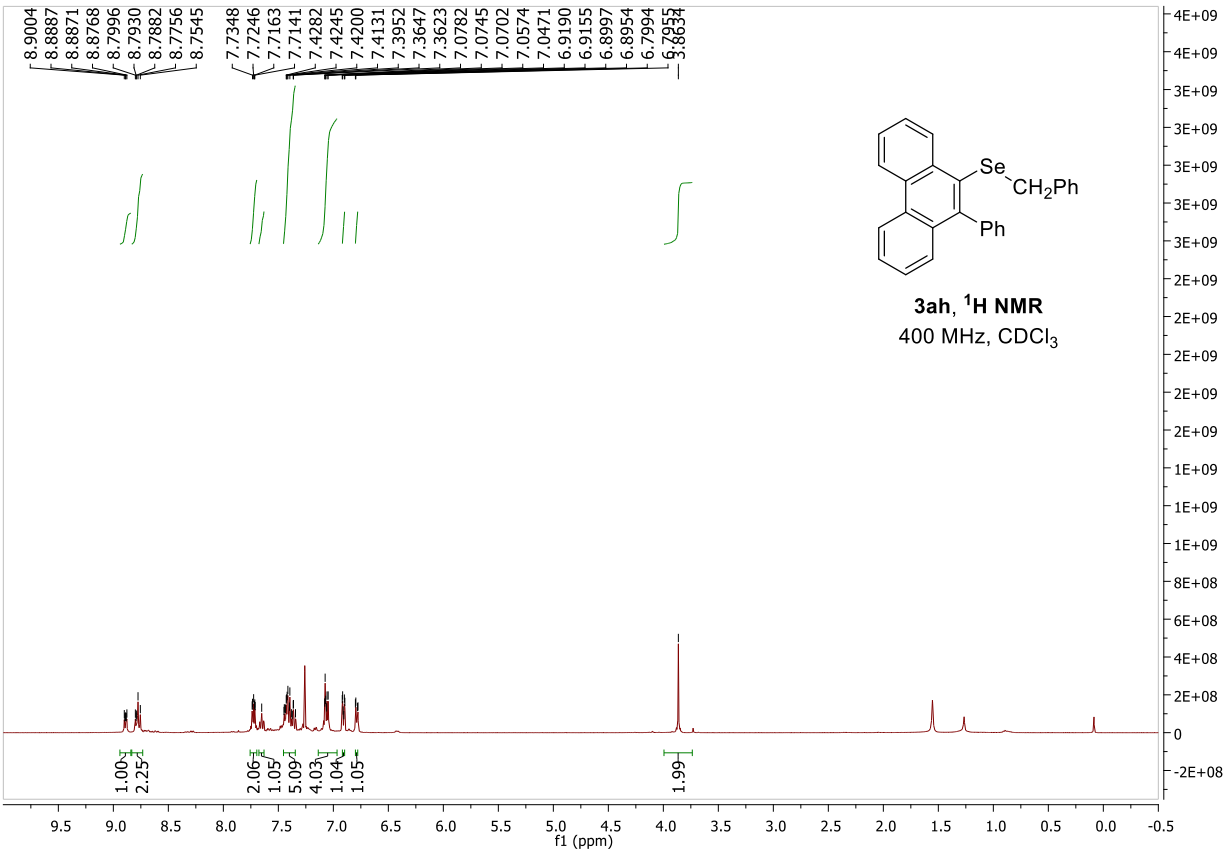
8.9004
8.8887
8.8871
8.8768
8.7996
8.7930
8.7882
8.7756
8.7545
7.7348
7.7246
7.7163
7.7141
7.4282
7.4245
7.4200
7.4131
7.3952
7.3647
7.3623
7.0782
7.0745
7.0702
7.0574
7.0471
6.9190
6.9155
6.8997
6.8954
6.7994
6.7955
3.8834
Se
CH2Ph
Ph
3ah, 1H NMR
400 MHz, CDCl3
1.00
2.25
2.06
1.05
5.09
4.03
1.04
1.05
1.99
f1 (ppm)

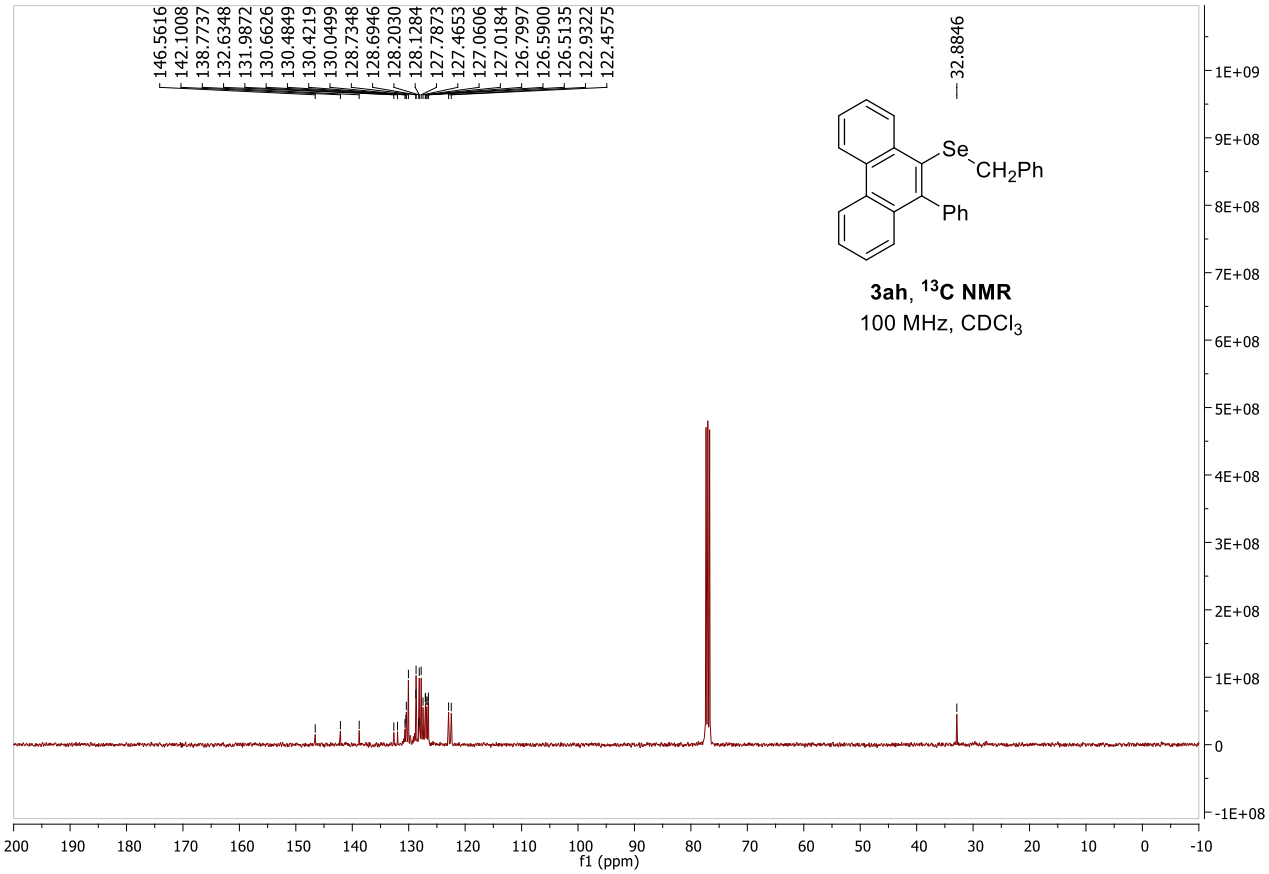
146.5616
142.1008
138.7737
132.6348
131.9872
130.6626
130.4849
130.4219
130.0499
128.7348
128.6946
128.2030
128.1284
127.7873
127.4653
127.0606
127.0184
126.7997
126.5900
126.5135
122.9322
122.4575
32.8846
Se
CH2Ph
Ph
3ah, 13C NMR
100 MHz, CDCl3
f1 (ppm)

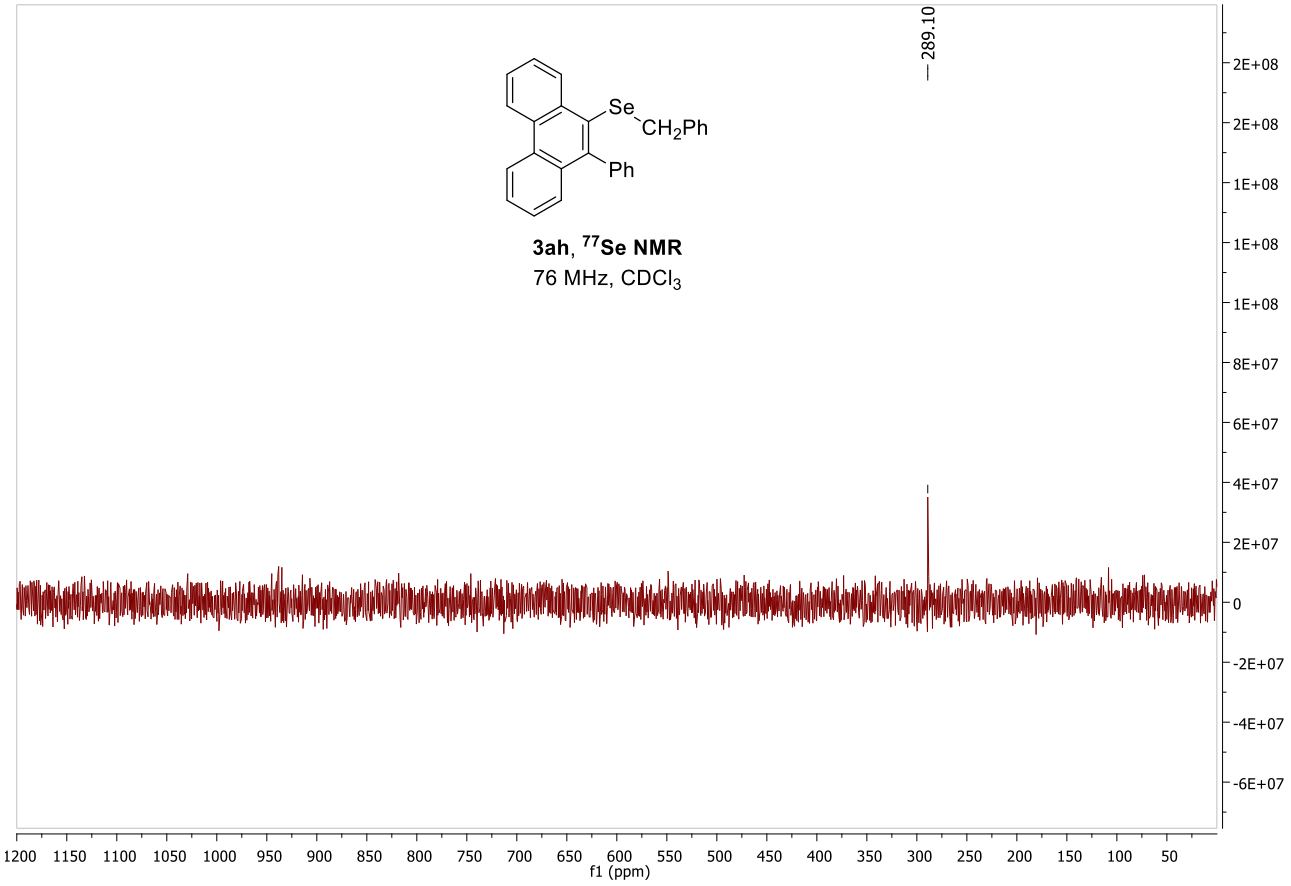
289.10
Se
CH2Ph
Ph
3ah, 77Se NMR
76 MHz, CDCl3
f1 (ppm)

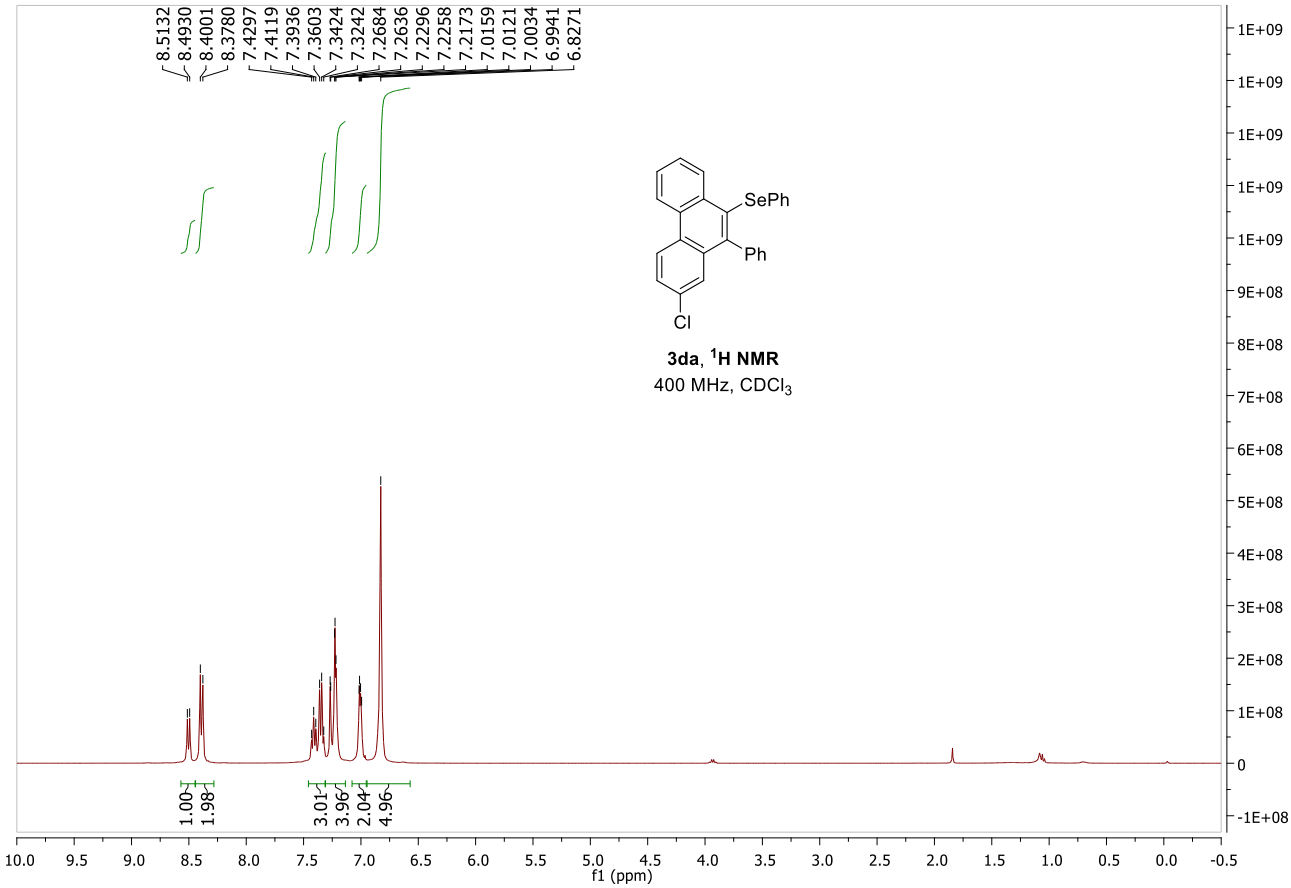
8.5132
8.4930
8.4001
8.3780
7.4297
7.4119
7.3936
7.3603
7.3424
7.3242
7.2684
7.2636
7.2296
7.2258
7.2173
7.0159
7.0121
7.0034
6.9941
6.8271
SePh
Ph
Cl
3da, 1H NMR
400 MHz, CDCl3
1.00
1.98
3.01
3.96
2.04
4.96
f1 (ppm)

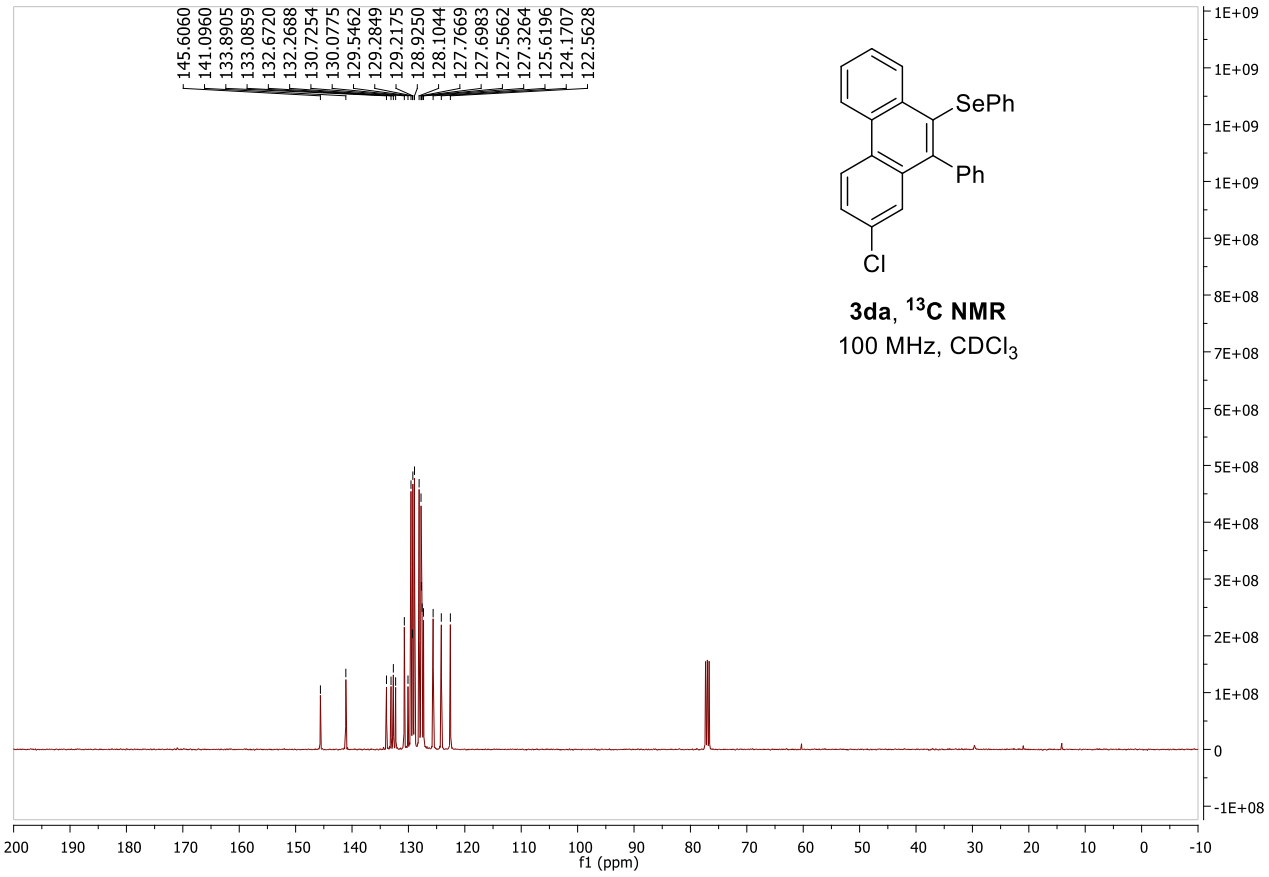

3da, ^{13}**C NMR**
100 MHz, $CDCl_3$

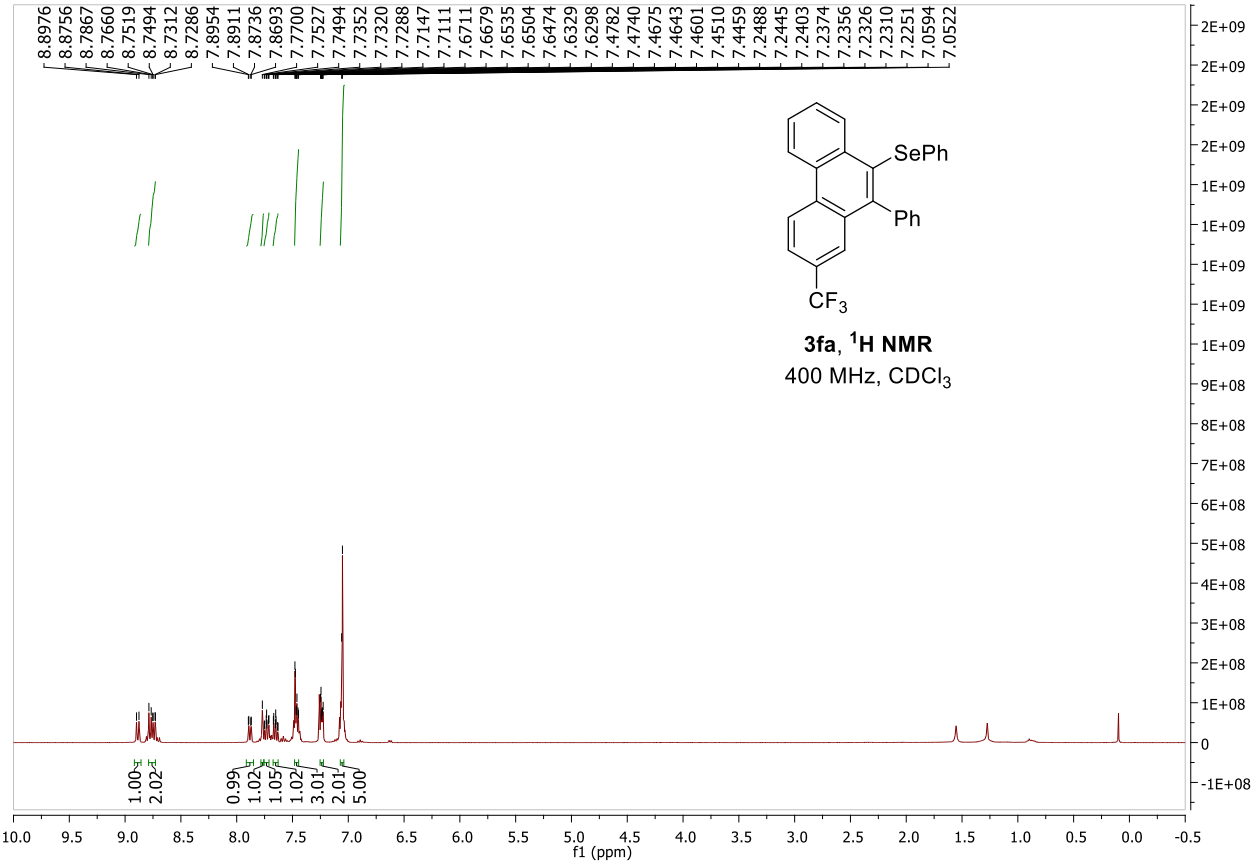

3fa, ^{1}**H NMR**
400 MHz, $CDCl_3$

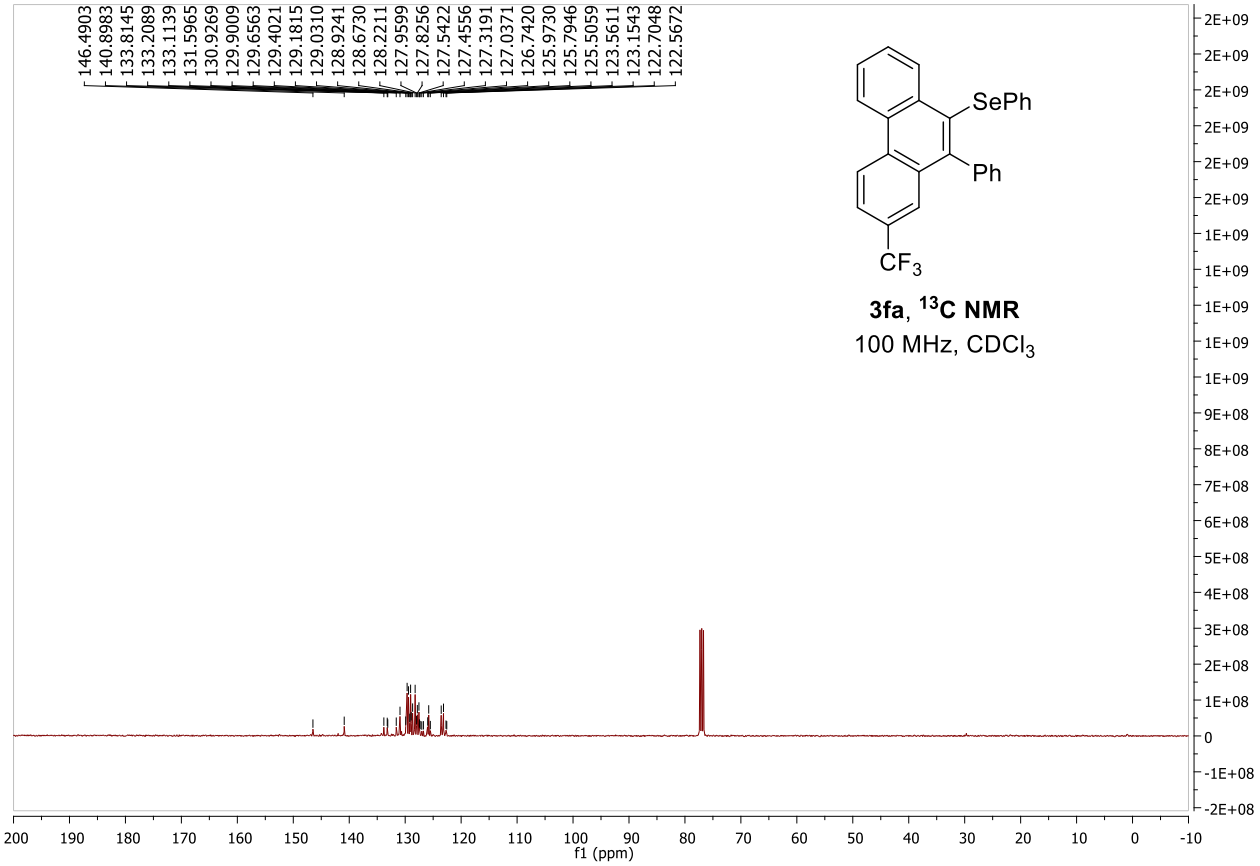
146.4903
140.8983
133.8145
133.2089
133.1139
131.5965
130.9269
129.9009
129.6563
129.4021
129.1815
129.0310
128.9241
128.6730
128.2211
127.9599
127.8256
127.5422
127.4556
127.3191
127.0371
126.7420
125.9730
125.7946
125.5059
123.5611
123.1543
122.7048
122.5672
SePh
Ph
CF3
3fa, 13C NMR
100 MHz, CDCl3
f1 (ppm)

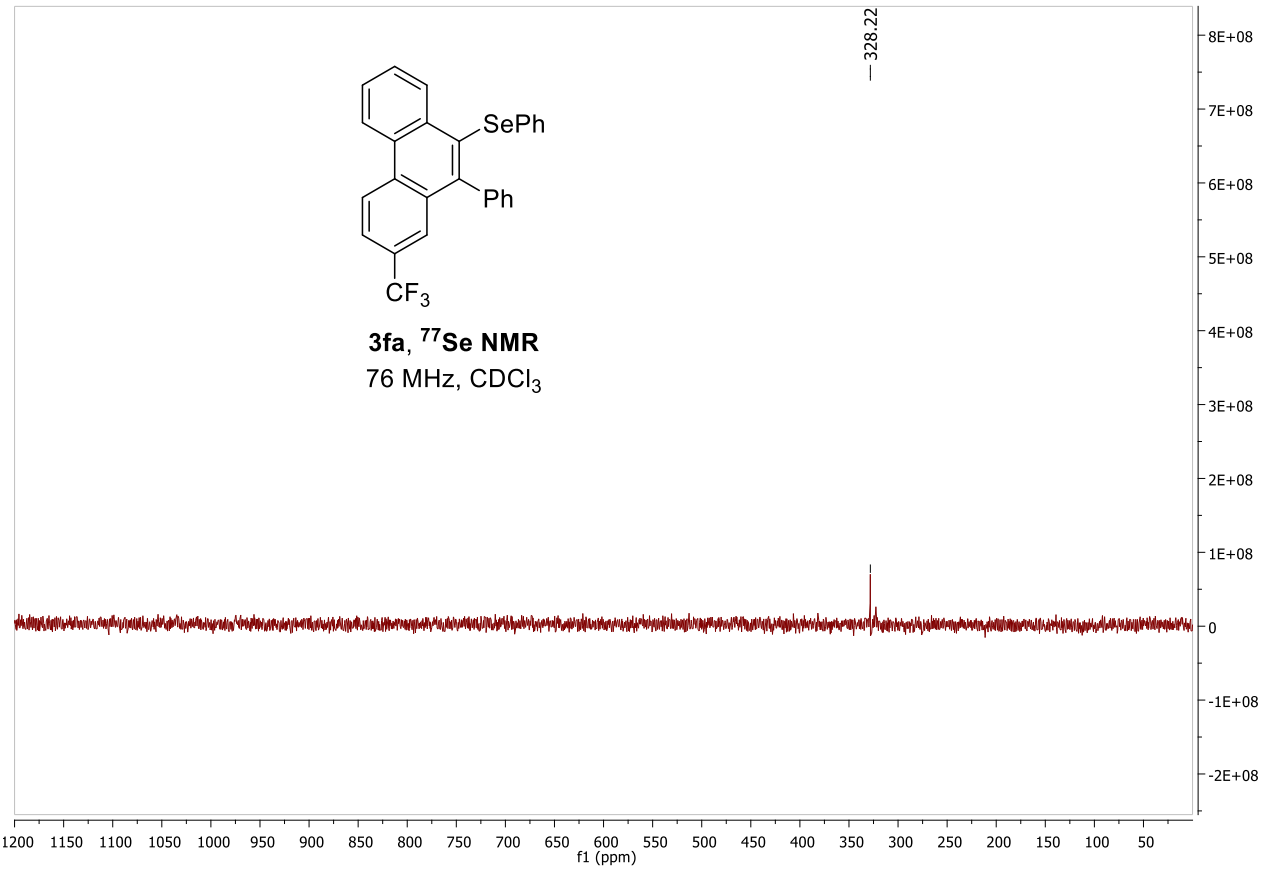
328.22
SePh
Ph
CF3
3fa, 77Se NMR
76 MHz, CDCl3
f1 (ppm)

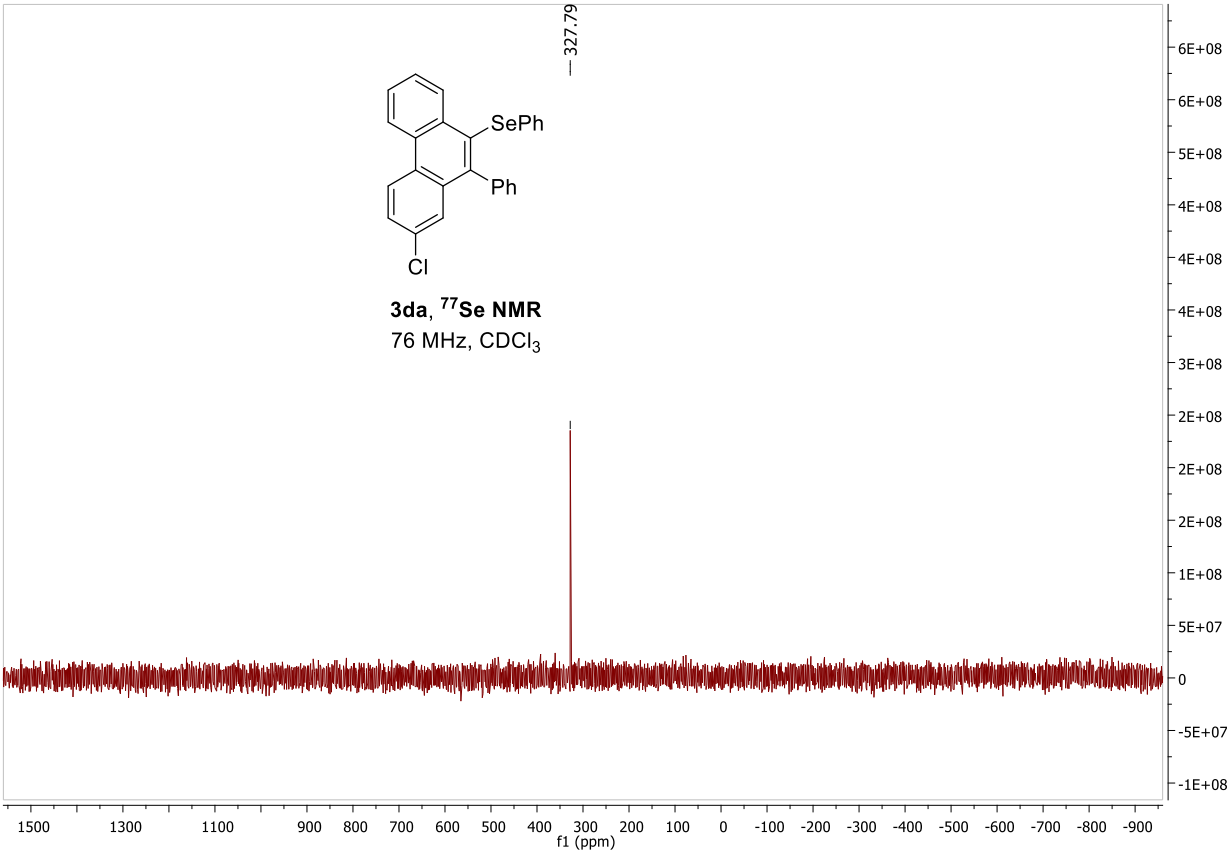
327.79
SePh
Ph
Cl
3da, 77Se NMR
76 MHz, CDCl3
f1 (ppm)

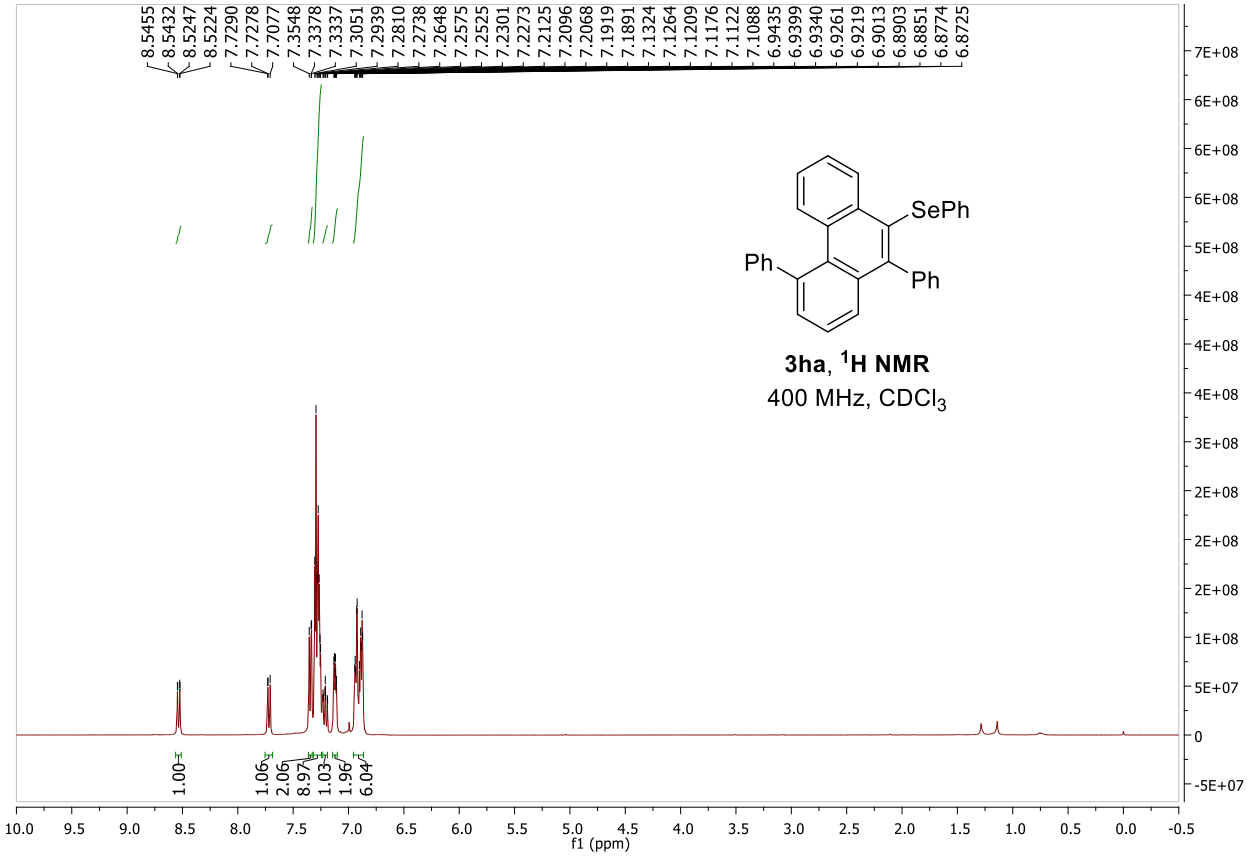
8.5455
8.5432
8.5247
8.5224
7.7290
7.7278
7.7077
7.3548
7.3378
7.3337
7.3051
7.2939
7.2810
7.2738
7.2648
7.2575
7.2525
7.2301
7.2273
7.2125
7.2096
7.2068
7.1919
7.1891
7.1324
7.1264
7.1209
7.1176
7.1122
7.1088
6.9435
6.9399
6.9340
6.9261
6.9219
6.9013
6.8903
6.8851
6.8774
6.8725
SePh
Ph
Ph
3ha, 1H NMR
400 MHz, CDCl3
1.00
1.06
2.06
8.97
1.03
1.96
6.04
f1 (ppm)

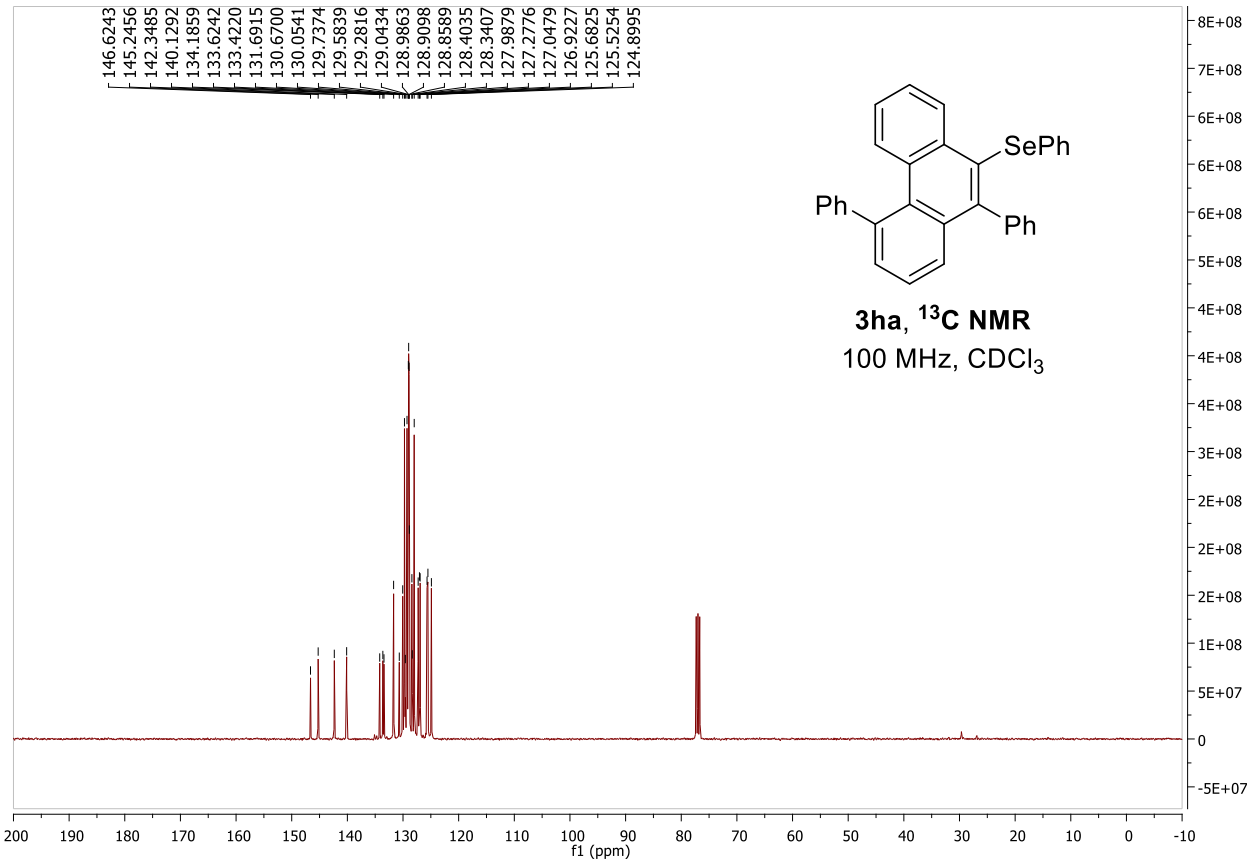
146.6243
145.2456
142.3485
140.1292
134.1859
133.6242
133.4220
131.6915
130.6700
130.0541
129.7374
129.5839
129.2816
129.0434
128.9863
128.9098
128.8589
128.4035
128.3407
127.9879
127.2776
127.0479
126.9227
125.6825
125.5254
124.8995
SePh
Ph
Ph
3ha, 13C NMR
100 MHz, CDCl3
f1 (ppm)

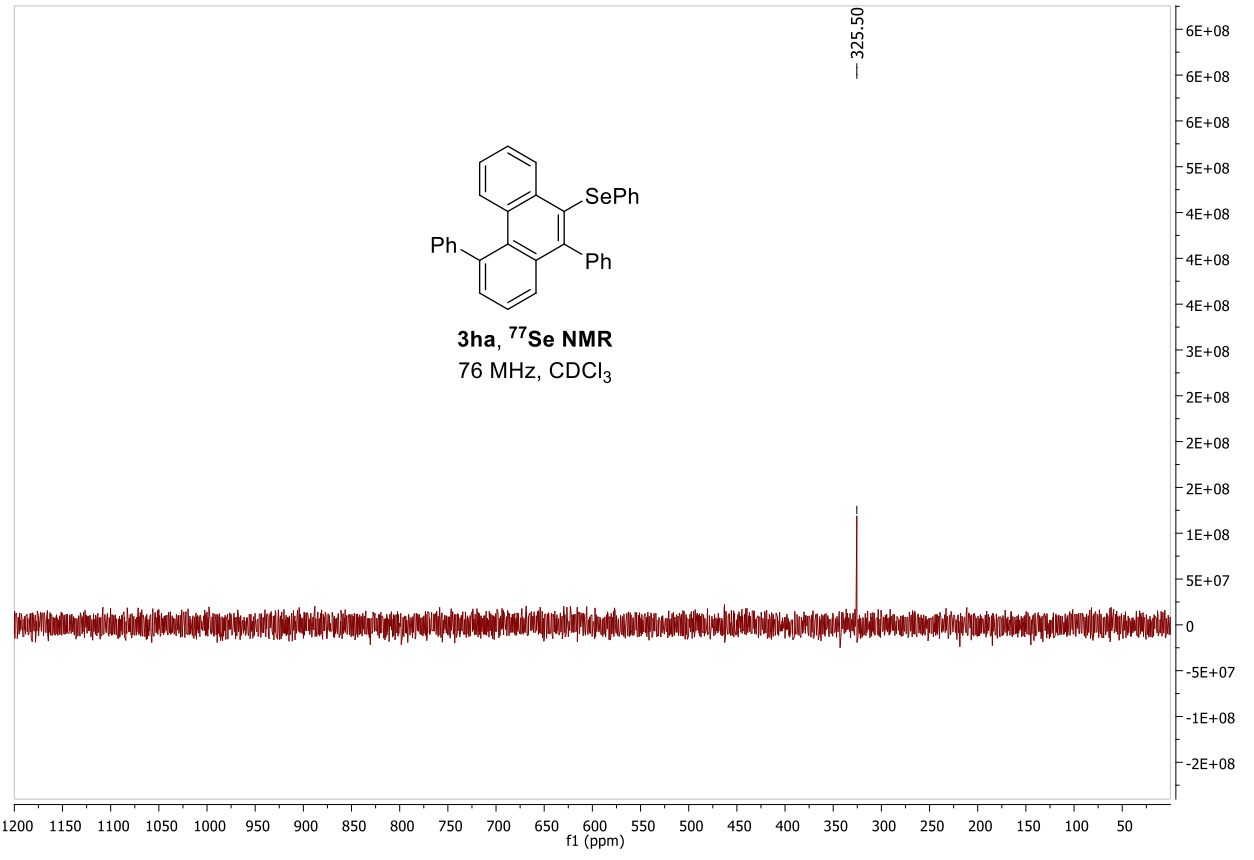
325.50
SePh
Ph
Ph
3ha, 77Se NMR
76 MHz, CDCl3
f1 (ppm)

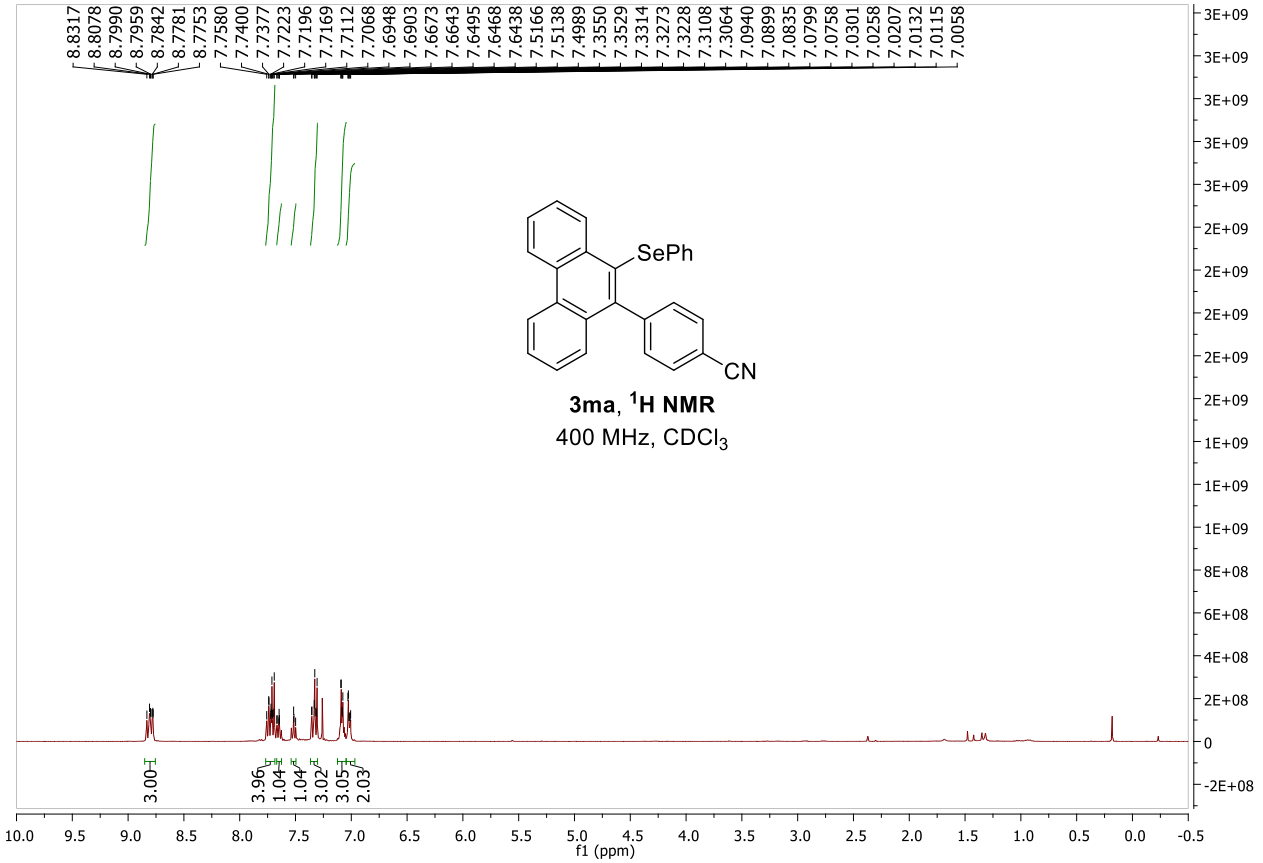

3ma, **^{1}H NMR**

400 MHz, $CDCl_3$

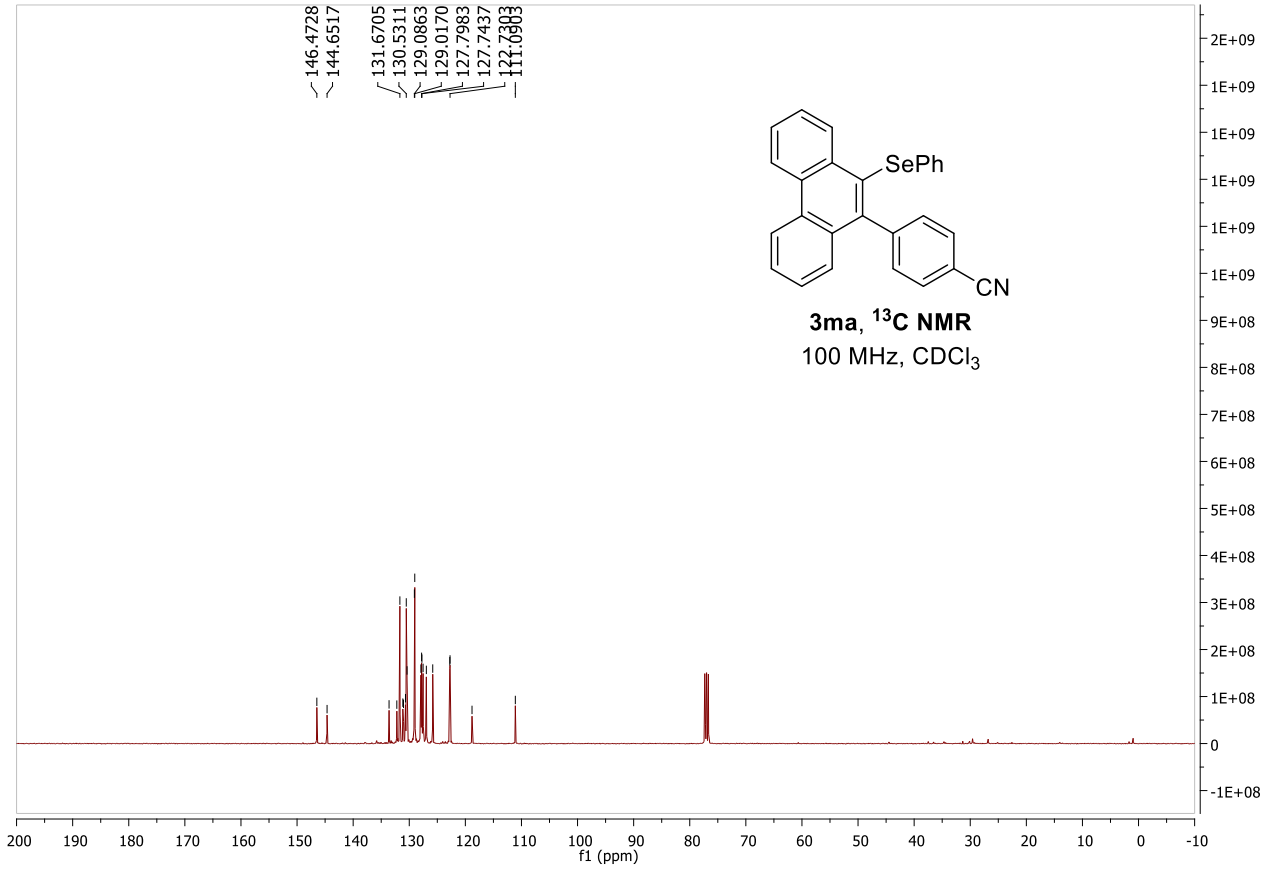

3ma, **^{13}C NMR**

100 MHz, $CDCl_3$

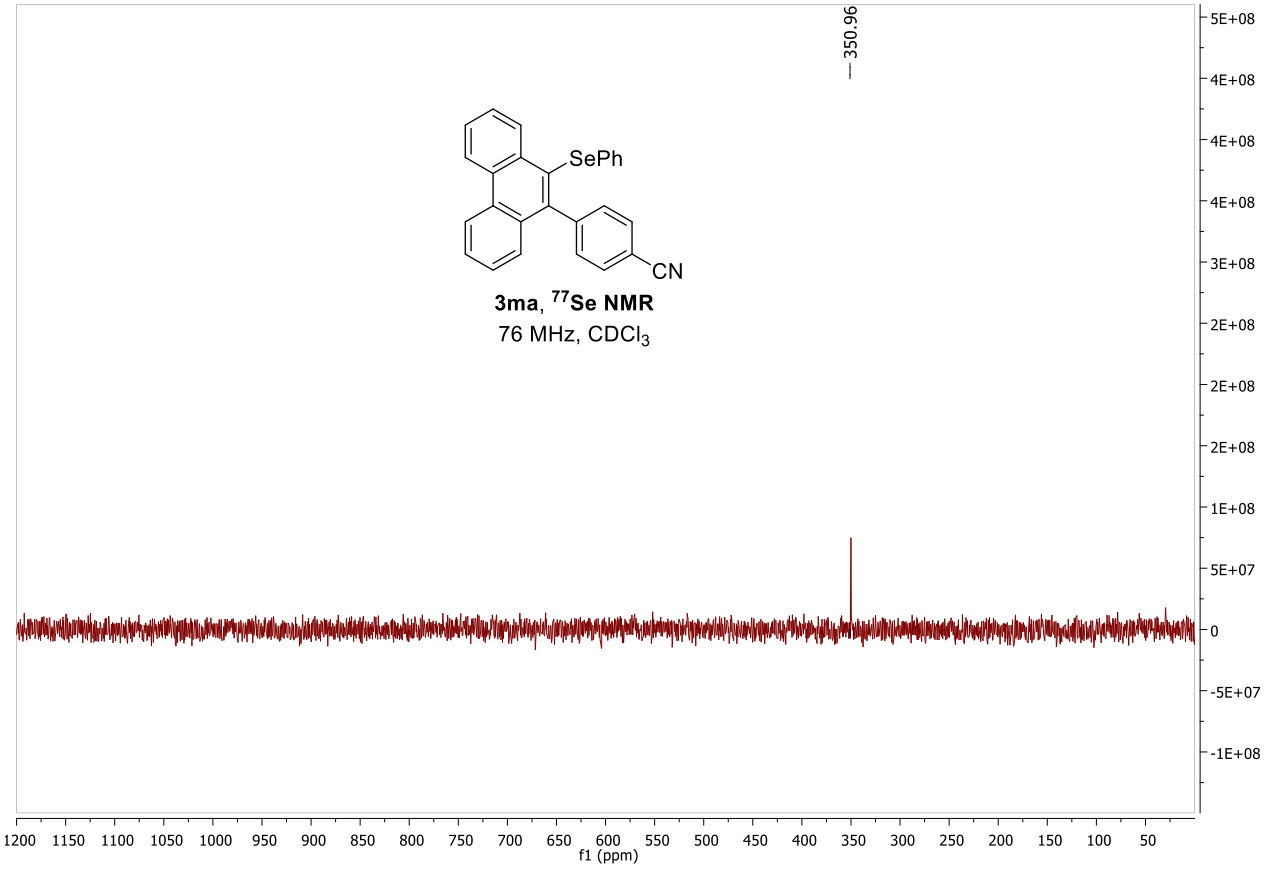
350.96
SePh
CN
3ma, 77Se NMR
76 MHz, CDCl3
f1 (ppm)

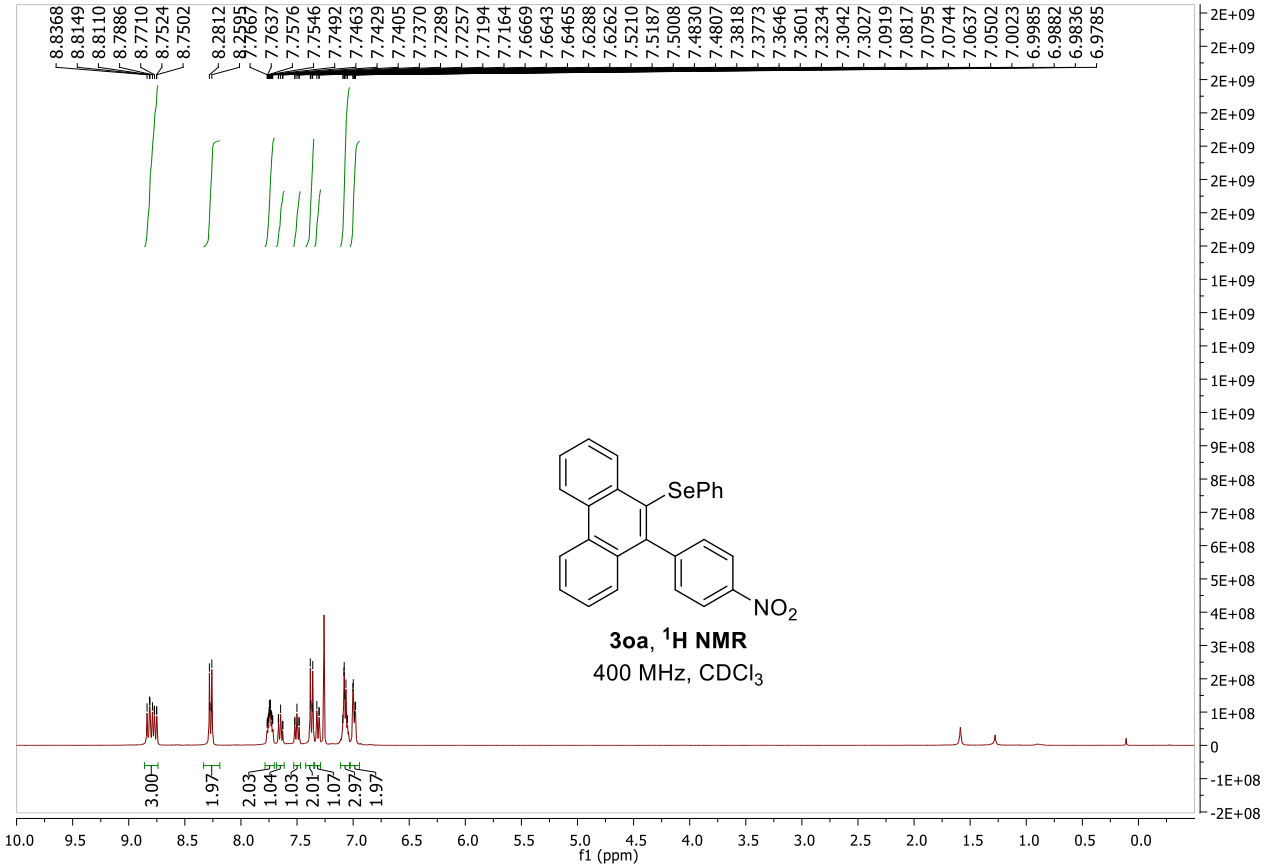
8.8368
8.8149
8.8110
8.7886
8.7710
8.7524
8.7502
8.2812
7.7637
7.7576
7.7546
7.7492
7.7463
7.7429
7.7405
7.7370
7.7289
7.7257
7.7194
7.7164
7.6669
7.6643
7.6465
7.6288
7.6262
7.5210
7.5187
7.5008
7.4830
7.4807
7.3818
7.3773
7.3646
7.3601
7.3234
7.3042
7.3027
7.0919
7.0817
7.0795
7.0744
7.0637
7.0502
7.0023
6.9985
6.9882
6.9836
6.9785
SePh
NO2
3oa, 1H NMR
400 MHz, CDCl3
3.00
1.97
2.03
1.04
1.03
2.01
1.07
2.97
1.97
f1 (ppm)

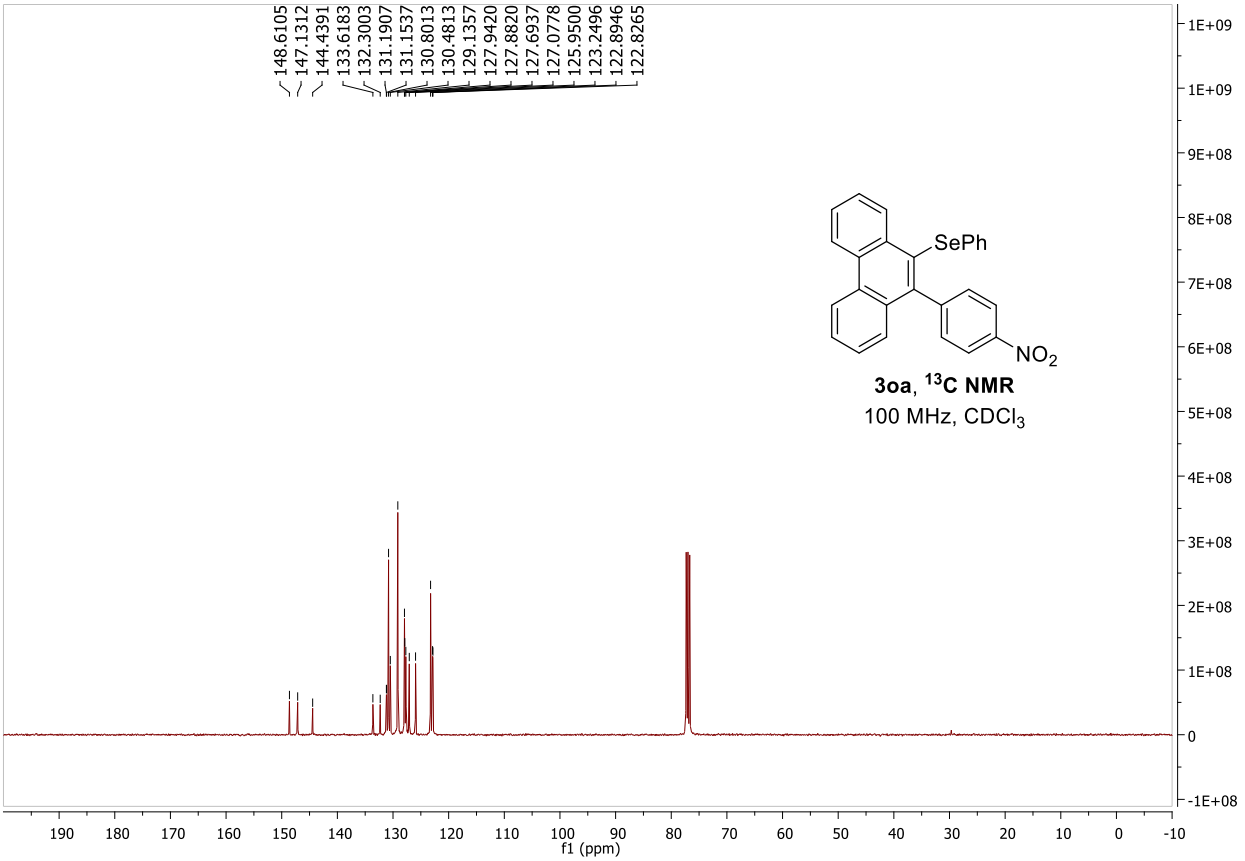
148.6105
147.1312
144.4391
133.6183
132.3003
131.1907
131.1537
130.8013
130.4813
129.1357
127.9420
127.8820
127.6937
127.0778
125.9500
123.2496
122.8946
122.8265
SePh
NO2
3oa, 13C NMR
100 MHz, CDCl3
f1 (ppm)

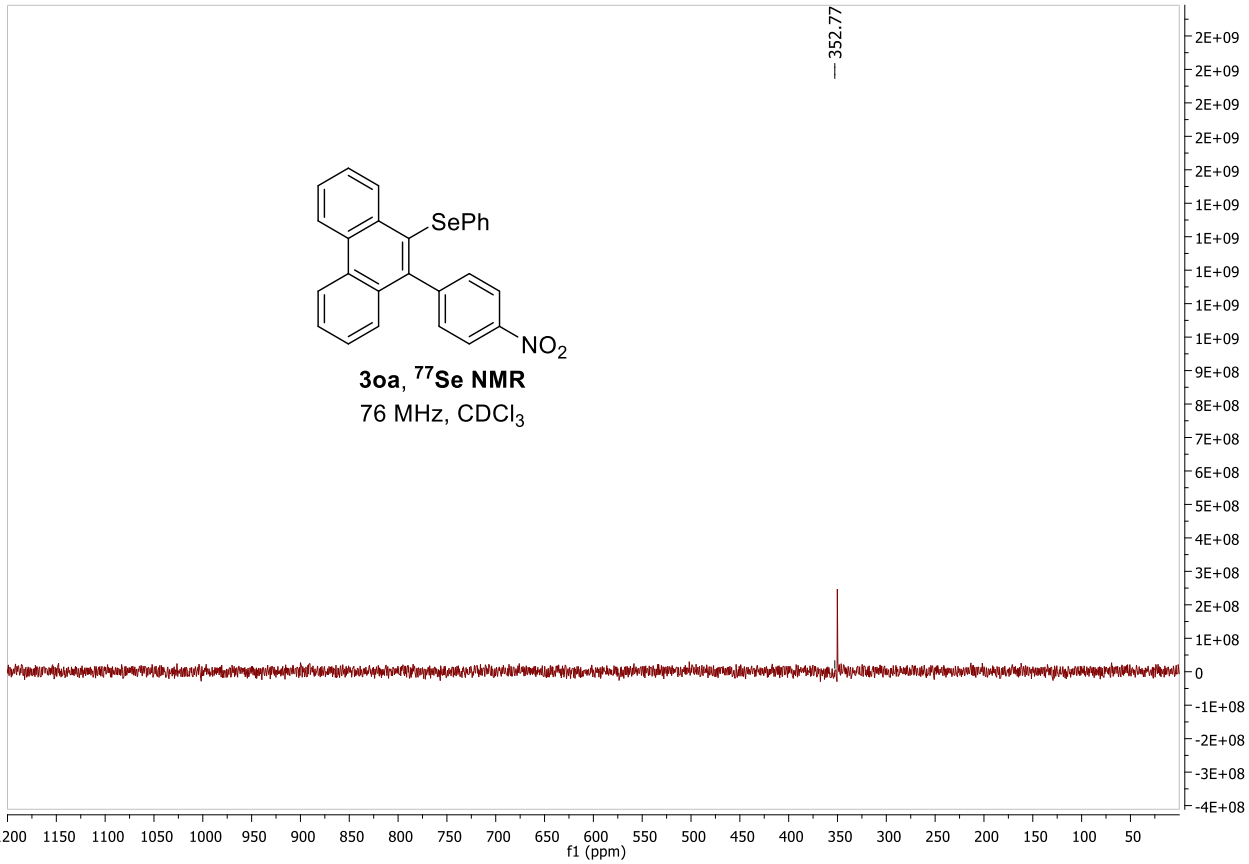
352.77
SePh
NO2
3oa, 77Se NMR
76 MHz, CDCl3
f1 (ppm)

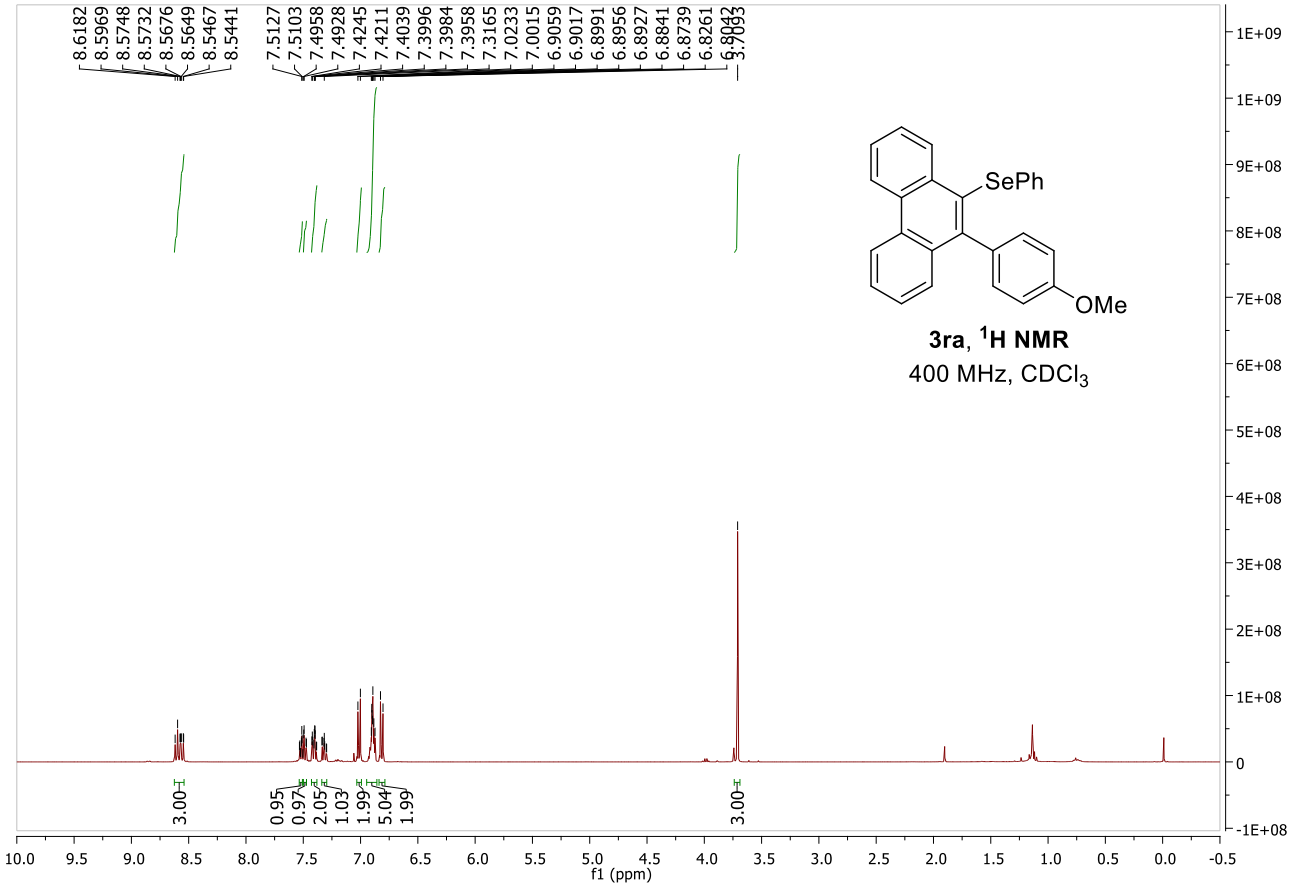
8.6182
8.5969
8.5748
8.5732
8.5676
8.5649
8.5467
8.5441
7.5127
7.5103
7.4958
7.4928
7.4245
7.4211
7.4039
7.3996
7.3984
7.3958
7.3165
7.0233
7.0015
6.9059
6.9017
6.8991
6.8956
6.8927
6.8841
6.8739
6.8261
3.7093
SePh
OMe
3ra, 1H NMR
400 MHz, CDCl3
3.00
0.95
0.97
2.05
1.03
1.99
5.04
1.99
3.00
f1 (ppm)

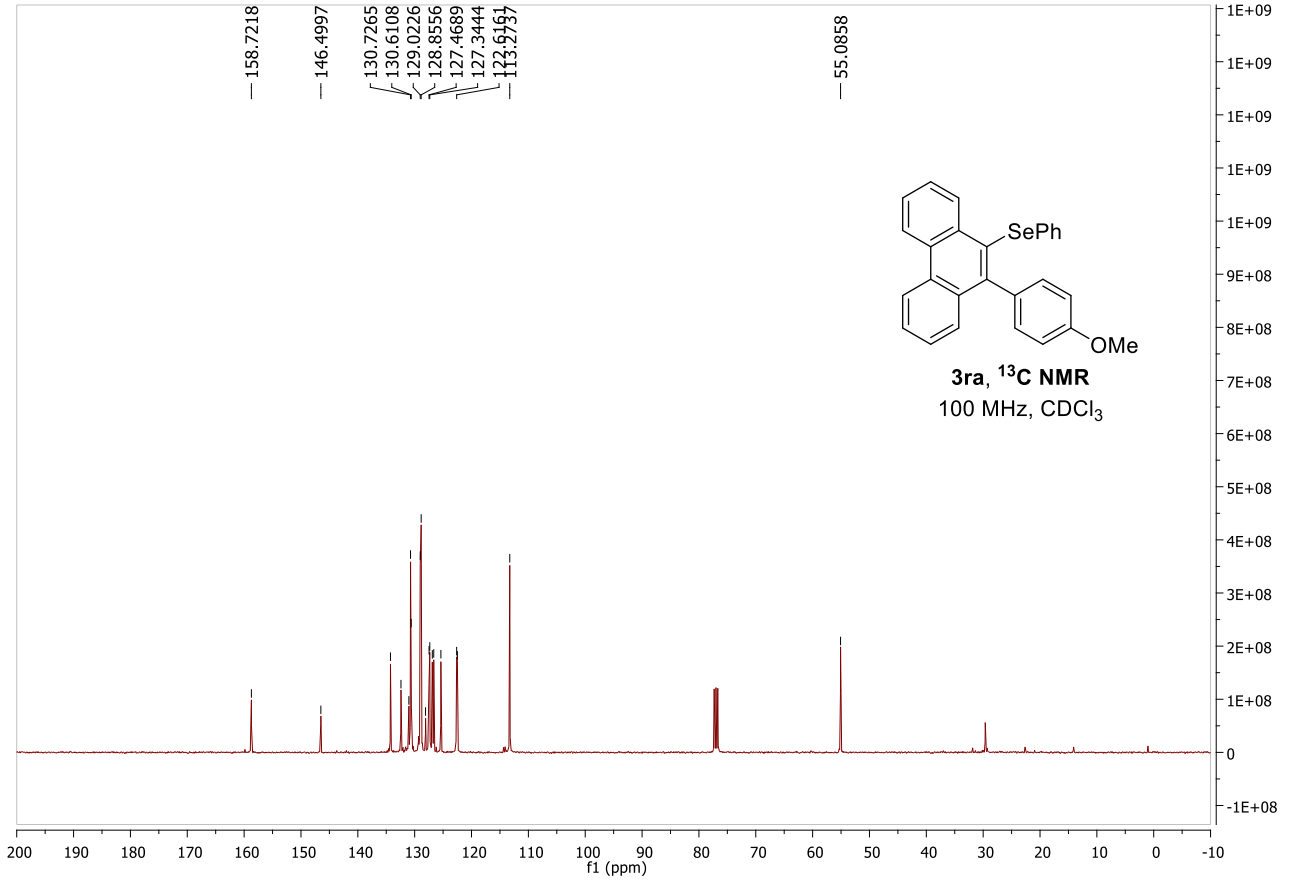
158.7218
146.4997
130.7265
130.6108
129.0226
128.8556
127.4689
127.3444
55.0858
SePh
OMe
3ra, 13C NMR
100 MHz, CDCl3
f1 (ppm)

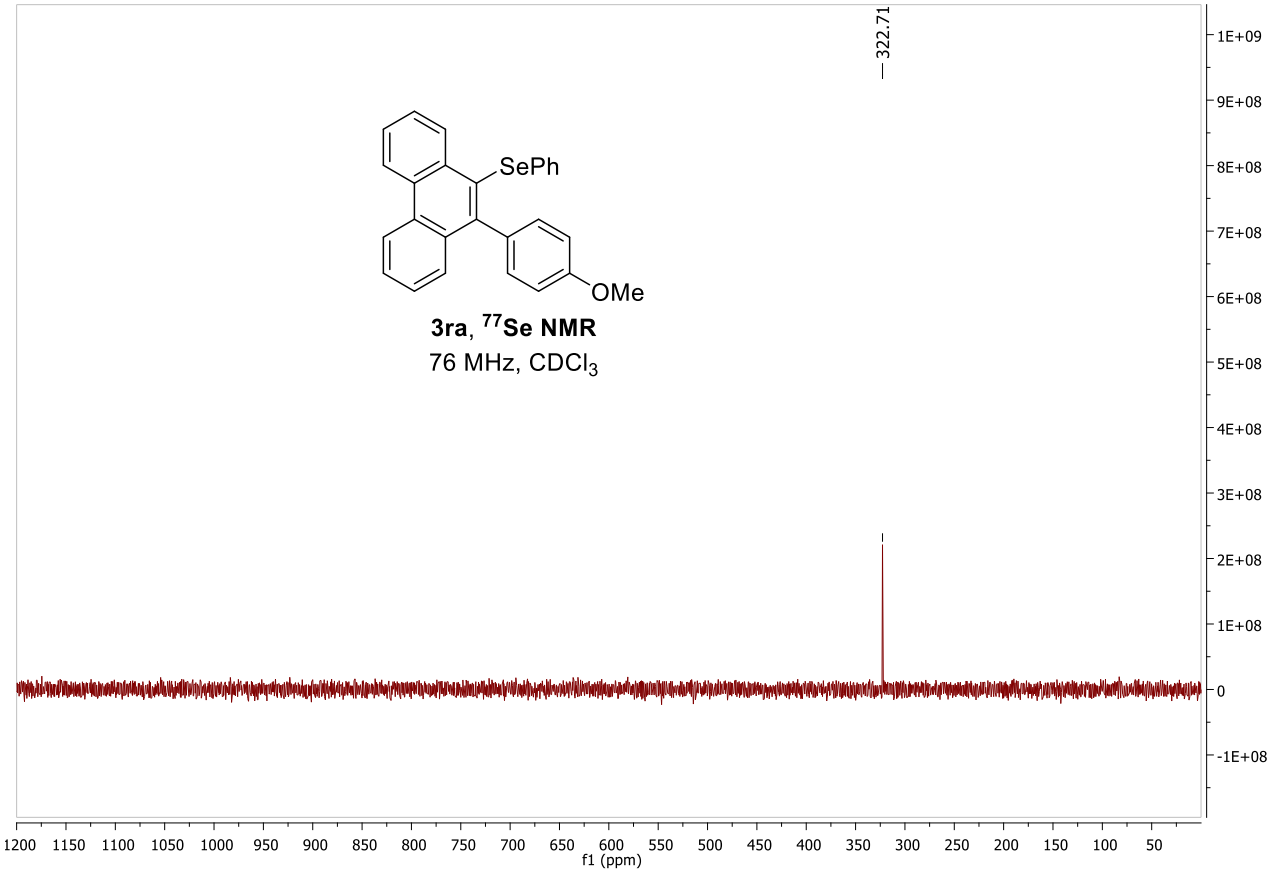

3ra, **^{77}Se NMR**

76 MHz, $CDCl_3$

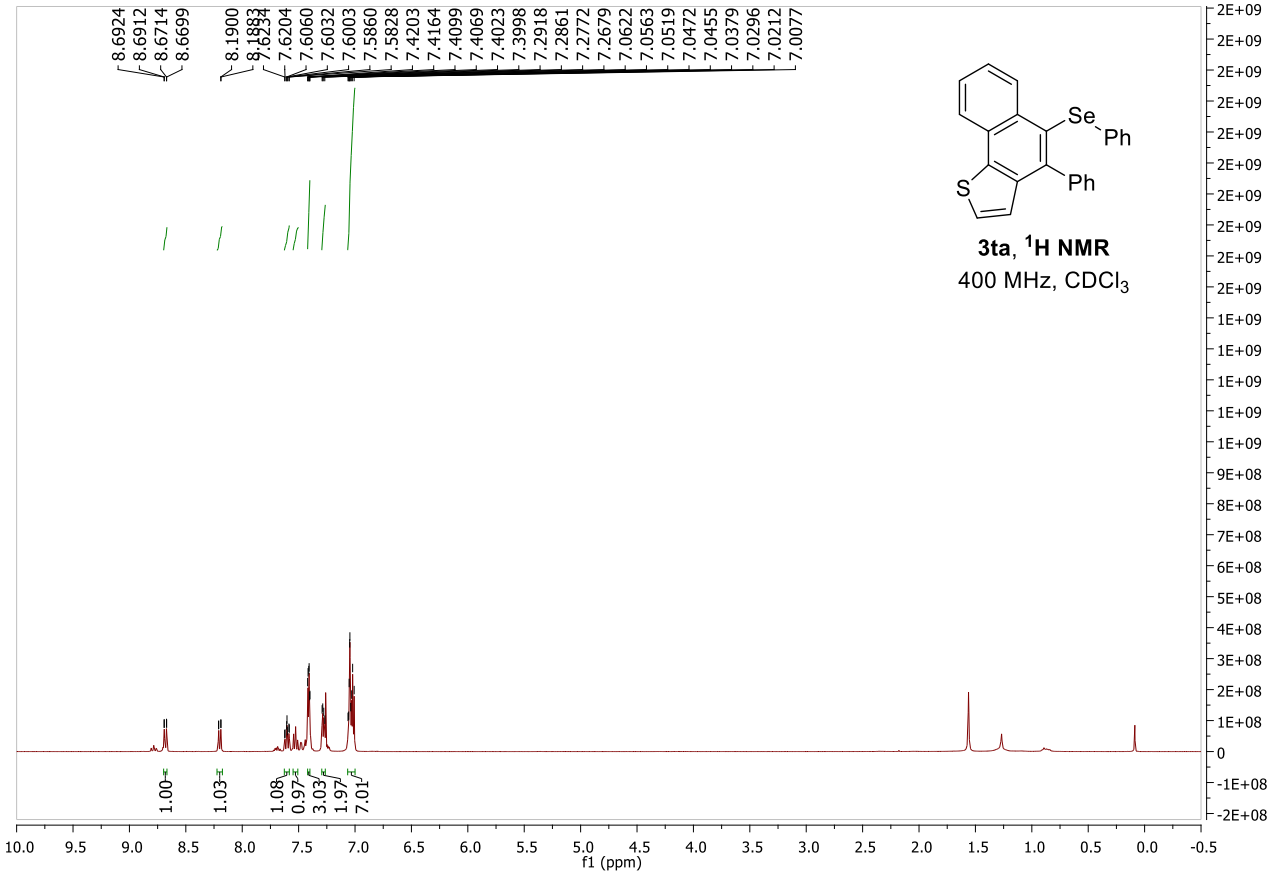

3ta, **^{1}H NMR**

400 MHz, $CDCl_3$

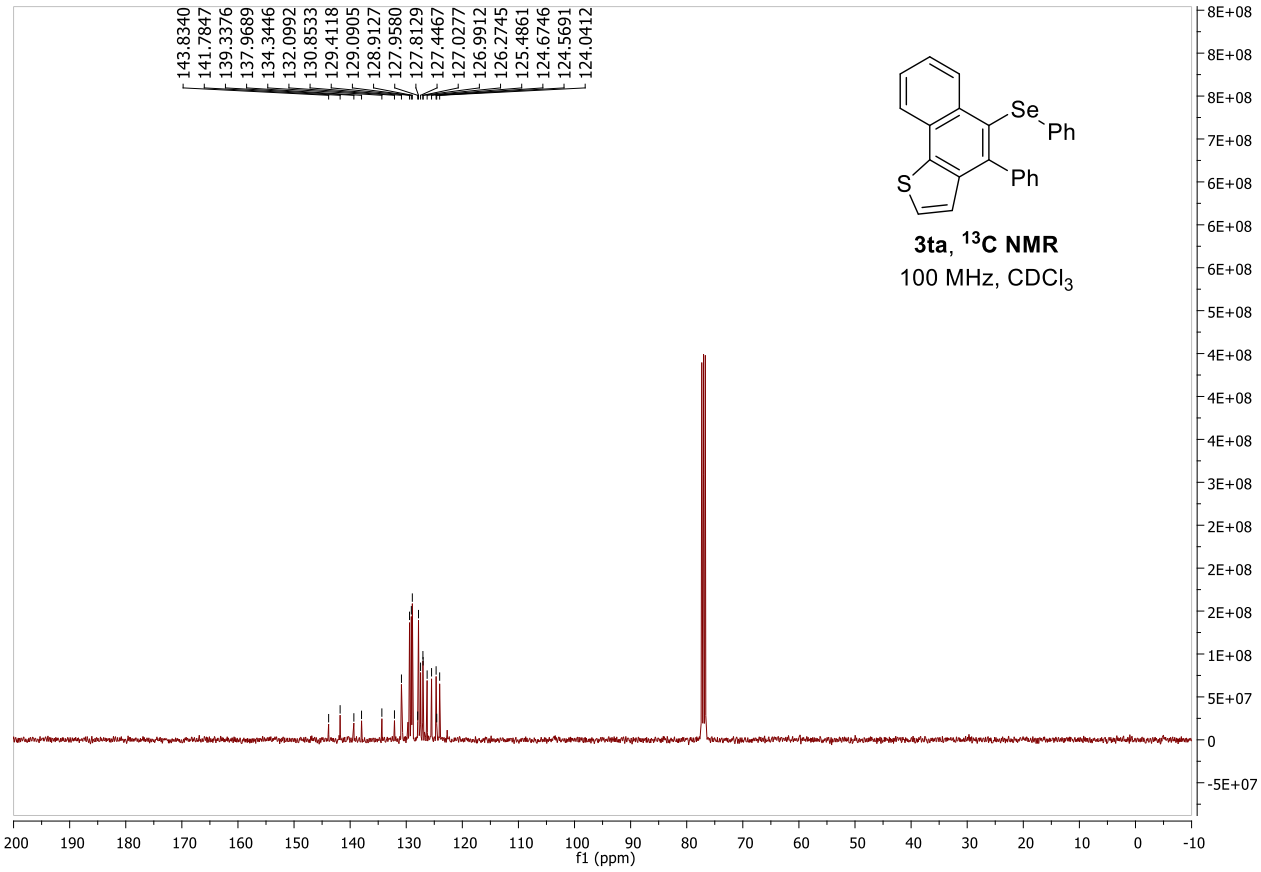
143.8340
141.7847
139.3376
137.9689
134.3446
132.0992
130.8533
129.4118
129.0905
128.9127
127.9580
127.8129
127.4467
127.0277
126.9912
126.2745
125.4861
124.6746
124.5691
124.0412
Se
Ph
Ph
S
3ta, 13C NMR
100 MHz, CDCl3
f1 (ppm)

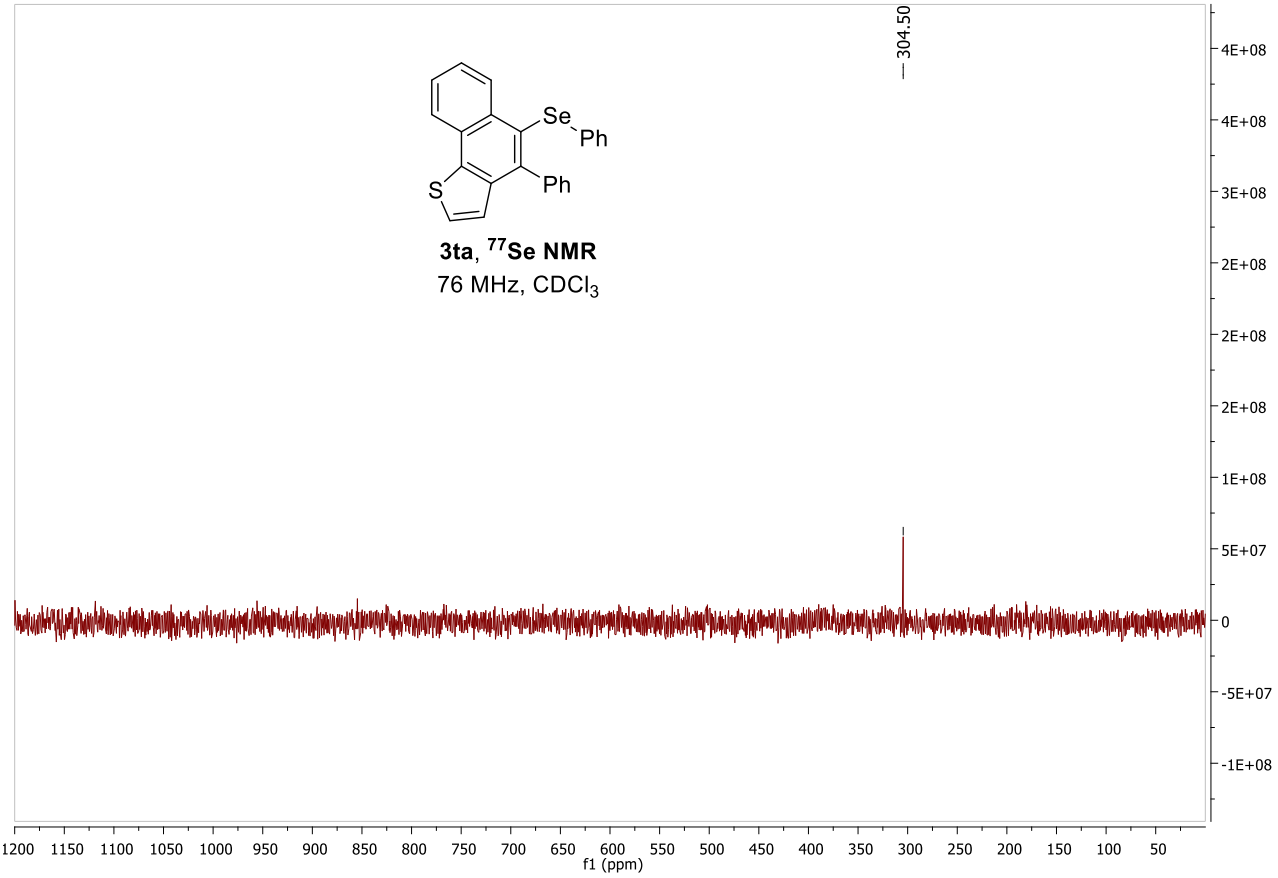
304.50
Se
Ph
Ph
S
3ta, 77Se NMR
76 MHz, CDCl3
f1 (ppm)

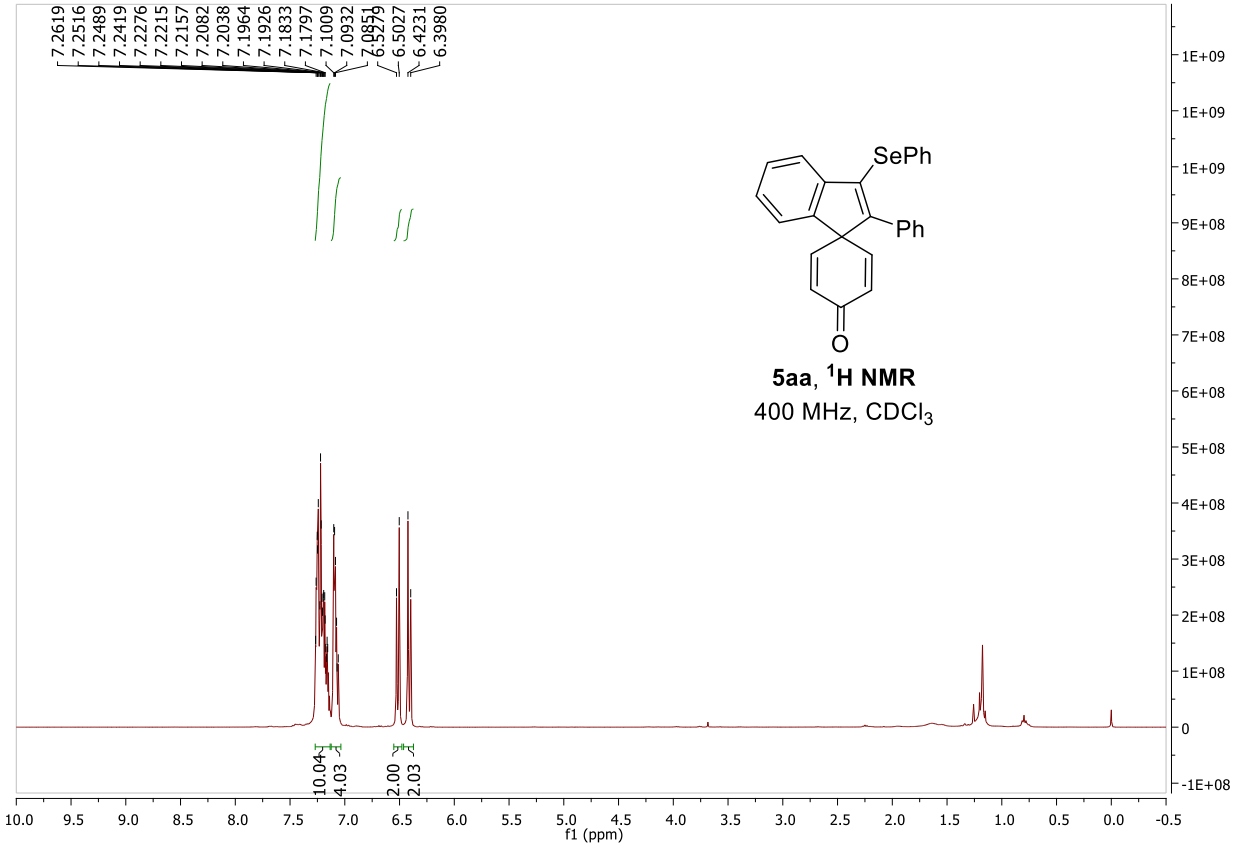
7.2619
7.2516
7.2489
7.2419
7.2276
7.2215
7.2157
7.2082
7.2038
7.1964
7.1926
7.1833
7.1797
7.1009
7.0932
6.5279
6.5027
6.4231
6.3980
SePh
Ph
O
5aa, 1H NMR
400 MHz, CDCl3
10.04
4.03
2.00
2.03
f1 (ppm)

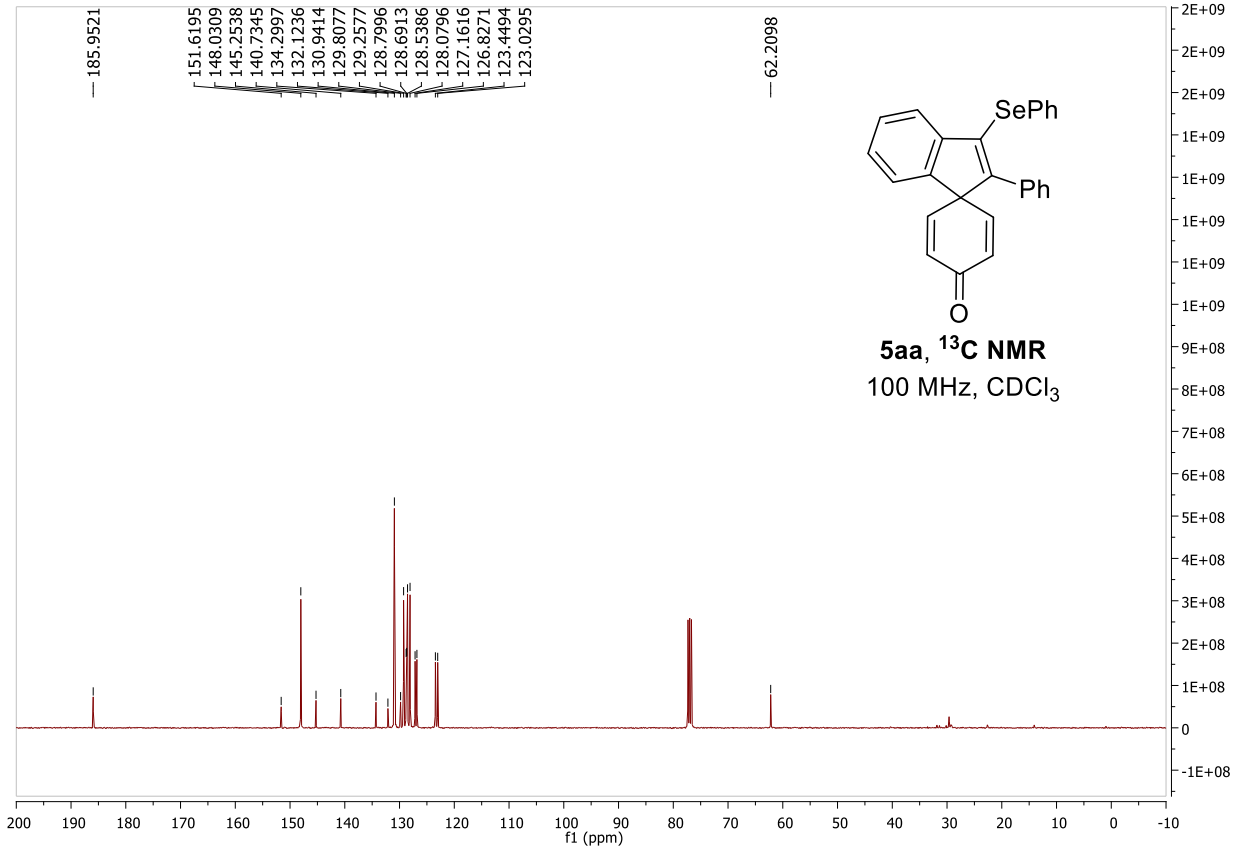
185.9521
151.6195
148.0309
145.2538
140.7345
134.2997
132.1236
130.9414
129.8077
129.2577
128.7996
128.6913
128.5386
128.0796
127.1616
126.8271
123.4494
123.0295
62.2098
SePh
Ph
O
5aa, 13C NMR
100 MHz, CDCl3
f1 (ppm)

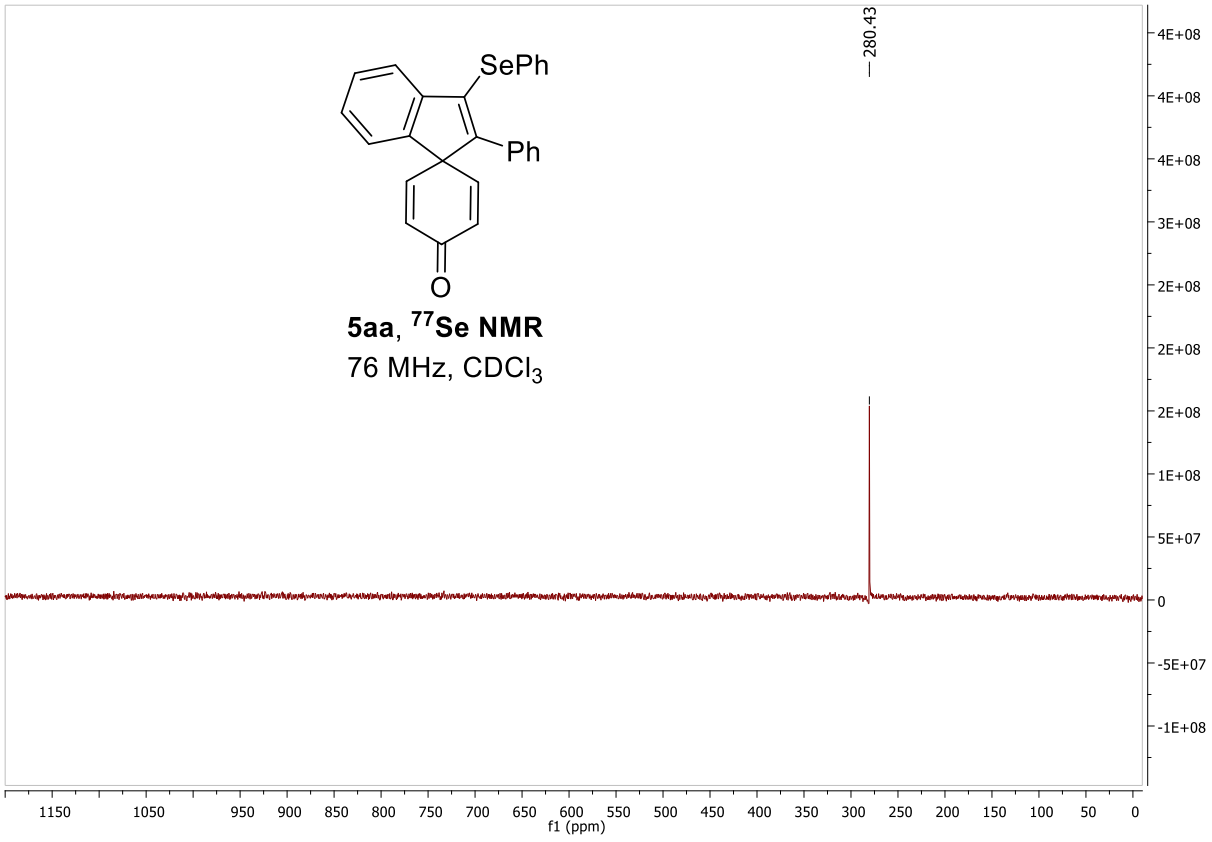

5aa, **^{77}Se NMR**

76 MHz, $CDCl_3$

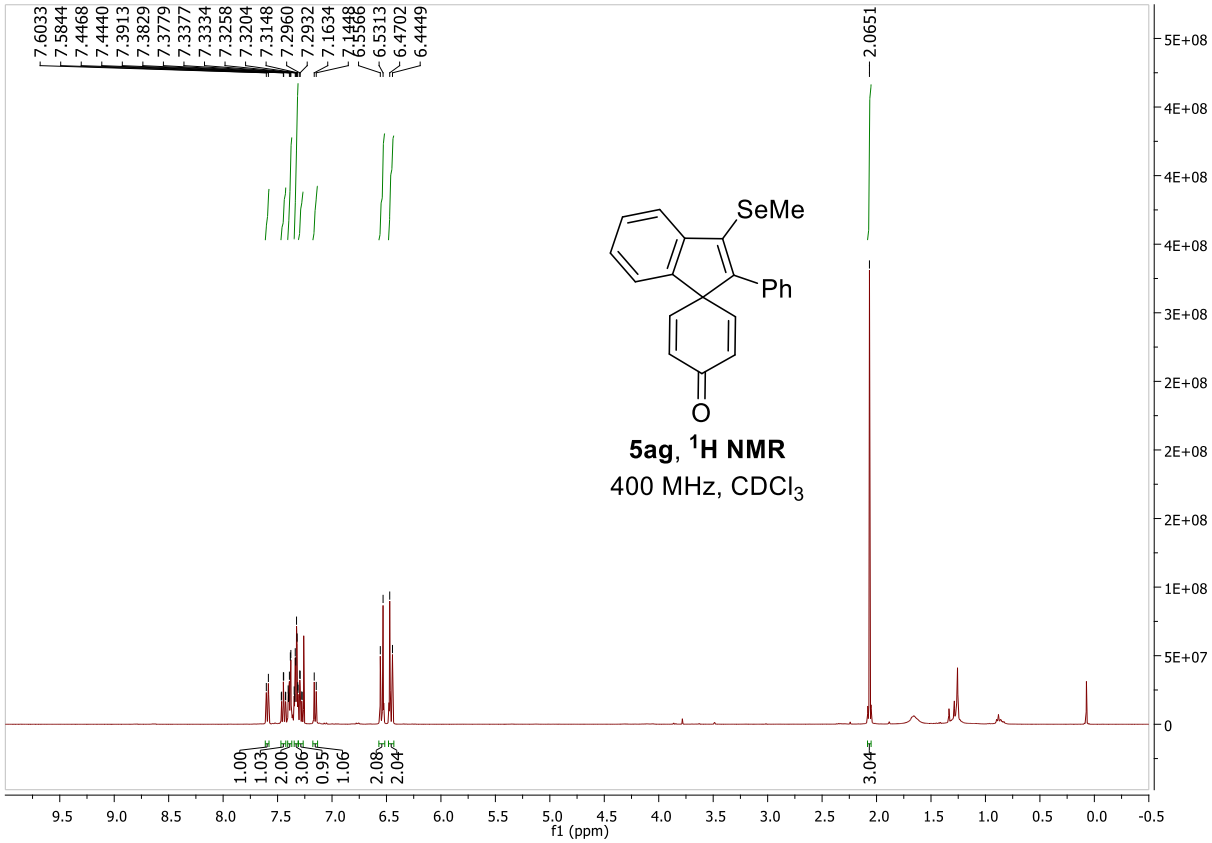

5ag, **^{1}H NMR**

400 MHz, $CDCl_3$

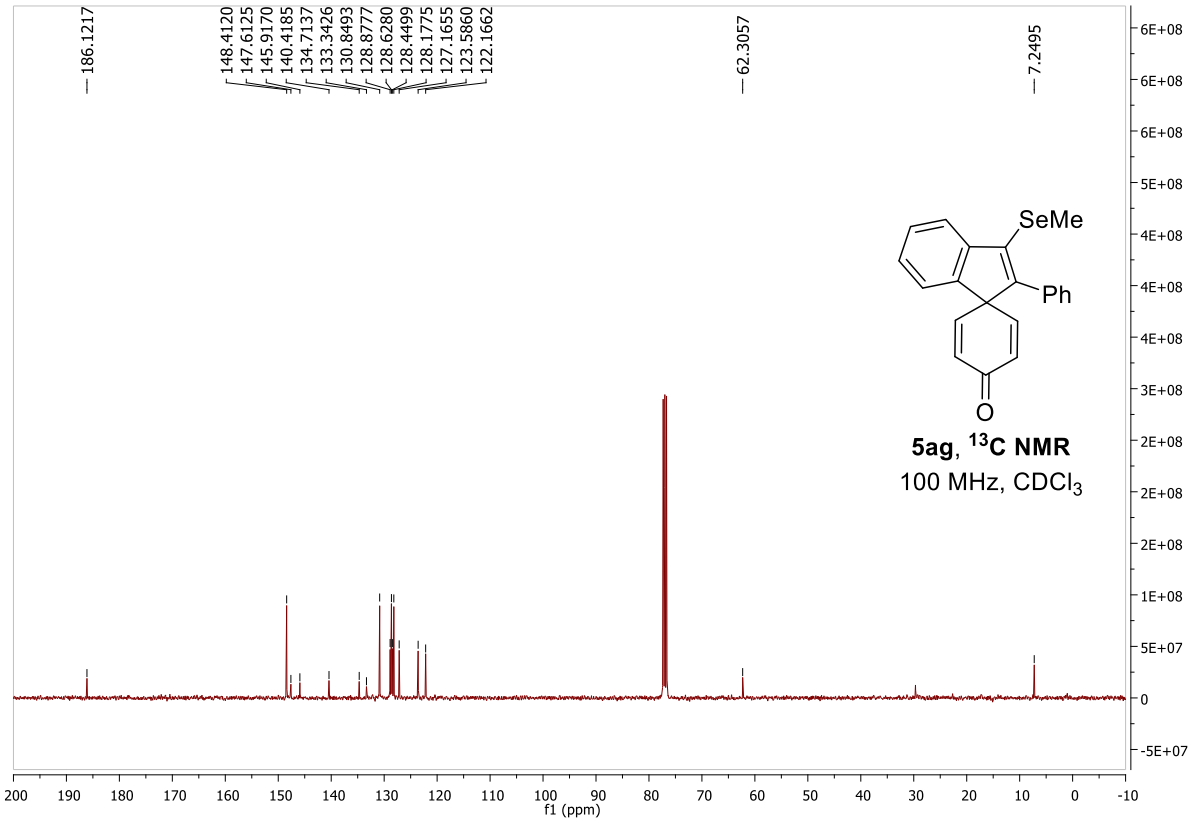
186.1217
148.4120
147.6125
145.9170
140.4185
134.7137
133.3426
130.8493
128.8777
128.6280
128.4499
128.1775
127.1655
123.5860
122.1662
62.3057
7.2495
SeMe
Ph
O
5ag, 13C NMR
100 MHz, CDCl3
f1 (ppm)

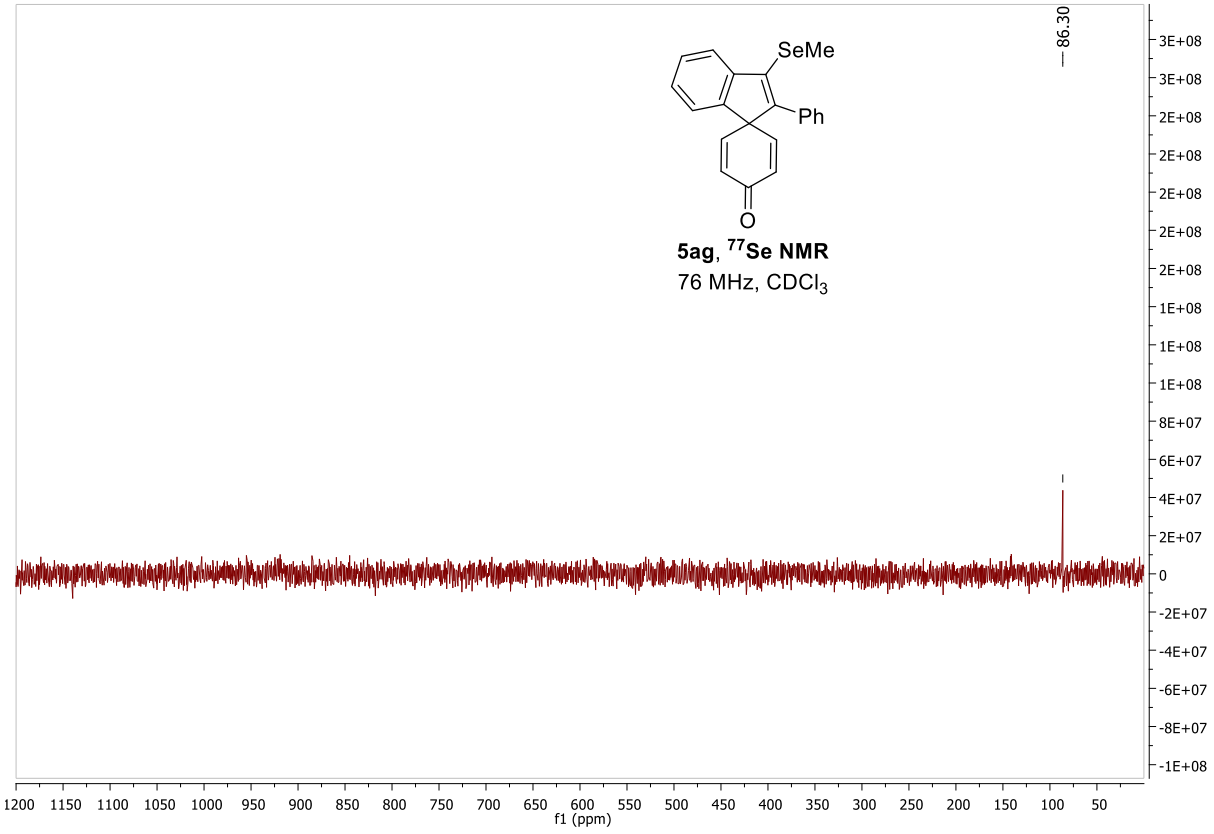
86.30
SeMe
Ph
O
5ag, 77Se NMR
76 MHz, CDCl3
f1 (ppm)

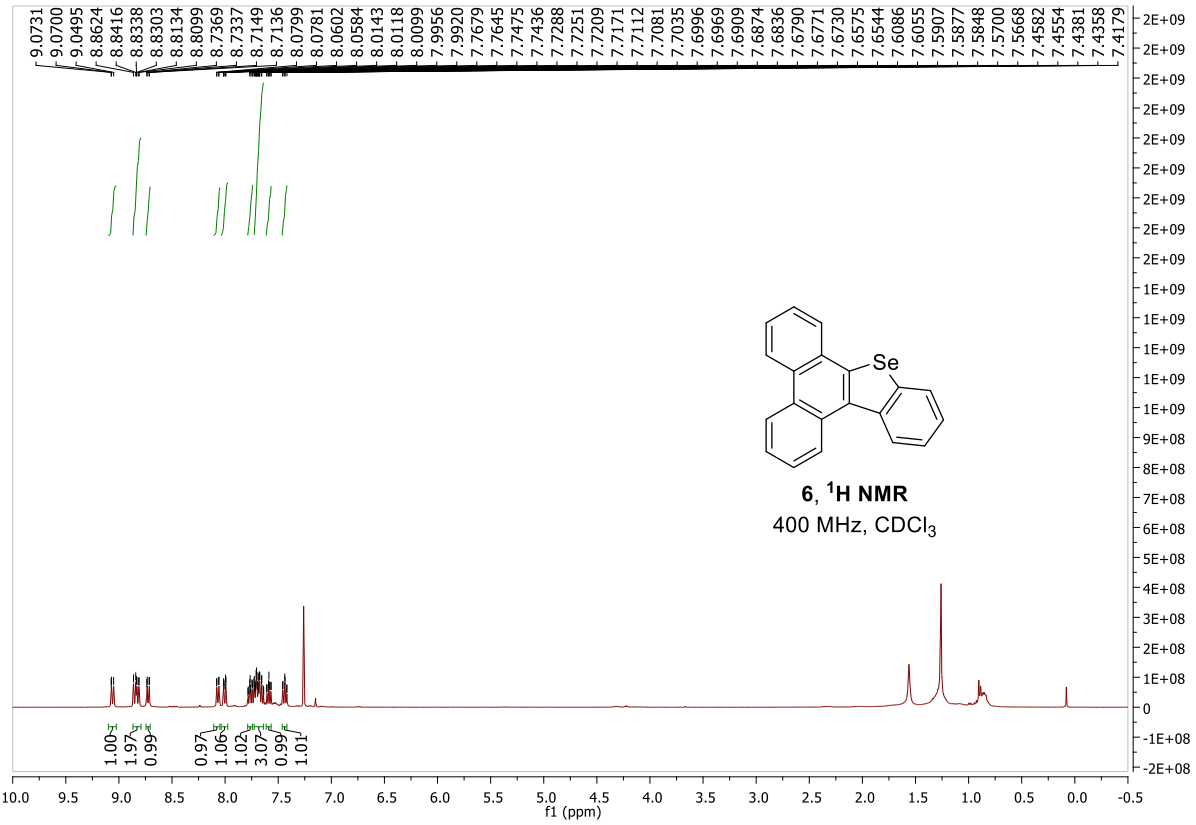
Se
6, 1H NMR
400 MHz, CDCl3
f1 (ppm)

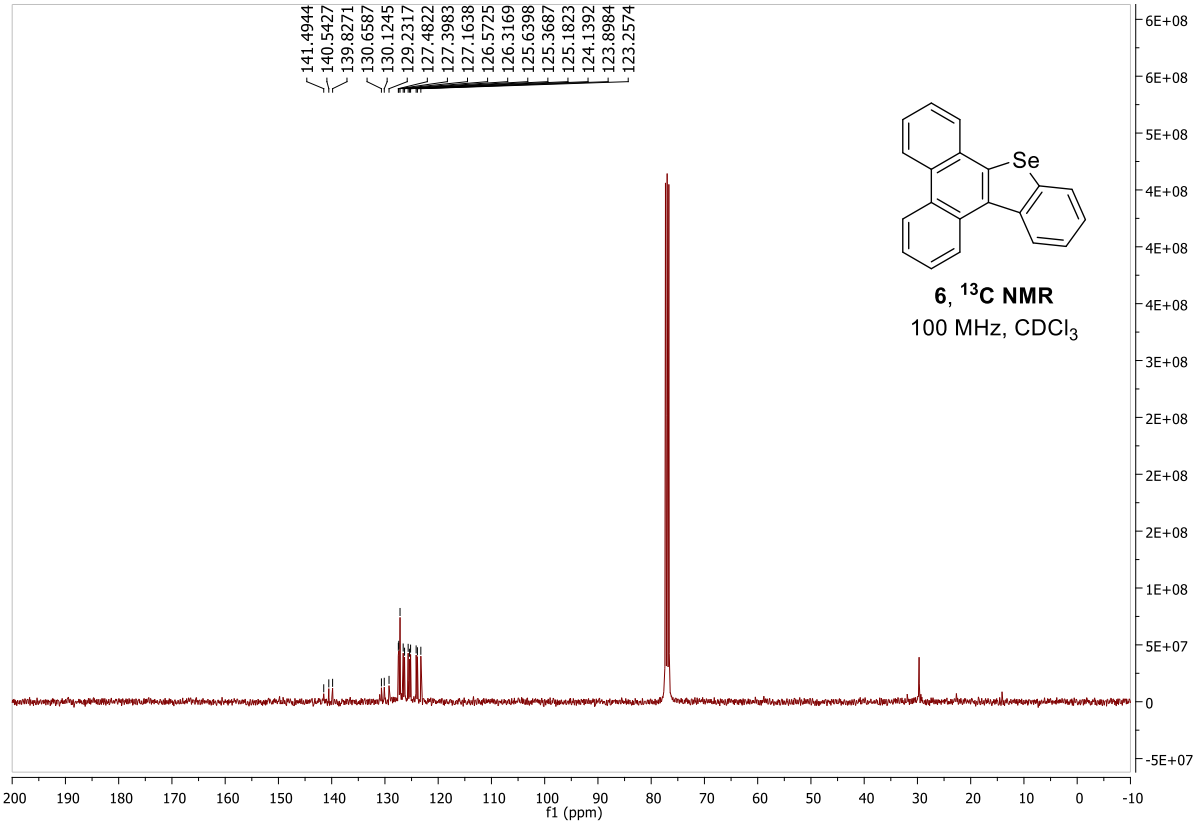
Se
6, 13C NMR
100 MHz, CDCl3
f1 (ppm)

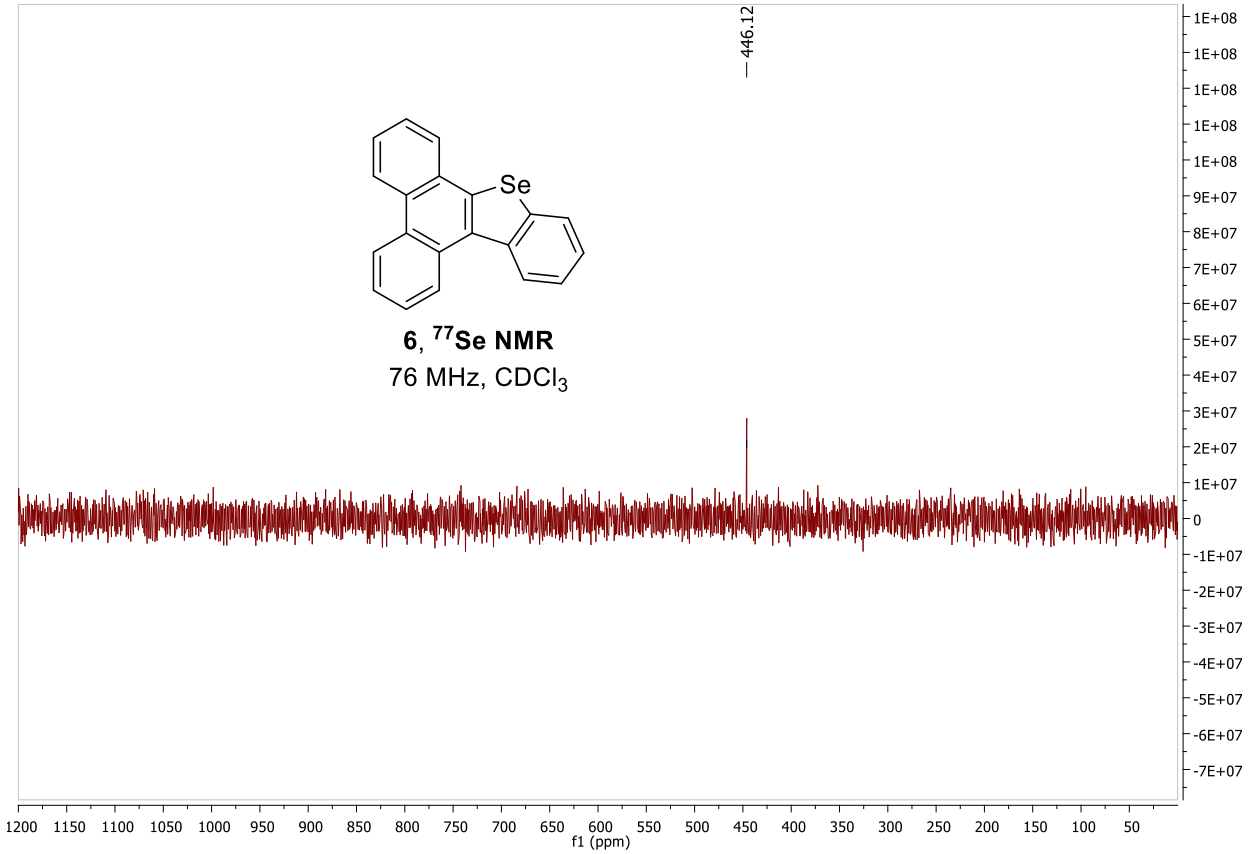
446.12
Se
6, 77Se NMR
76 MHz, CDCl3
1E+08
1E+08
1E+08
1E+08
1E+08
9E+07
8E+07
7E+07
6E+07
5E+07
4E+07
3E+07
2E+07
1E+07
0
-1E+07
-2E+07
-3E+07
-4E+07
-5E+07
-6E+07
-7E+07
1200 1150 1100 1050 1000 950 900 850 800 750 700 650 600 550 500 450 400 350 300 250 200 150 100 50
f1 (ppm)

UPDATES doi.org/10.1002/adsc.202300333 Advanced Synthesis & Catalysis

Highly Atom-Economic and Efficient Electrochemical Selenylative Annulation of 2-Alkynyl Biaryls

Nilanjana Mukherjee[a] and Tanmay Chatterjee[a,*]

[a] Department of Chemistry, Birla Institute of Technology and Science, Pilani, Hyderabad Campus, Jawahar Nagar, Hyderabad – 500078, India
E-mail: tanmay@hyderabad.bits-pilani.ac.in

Manuscript received: April 7, 2023; Revised manuscript received: May 4, 2023;
Version of record online: June 12, 2023

Supporting information for this article is available on the WWW under https://doi.org/10.1002/adsc.202300333

Abstract: A catalyst- and oxidant-free, highly efficient, scalable, and sustainable synthetic method is developed for the selenylative annulation of 2-alkynyl biaryls or 2-heteroaryl-substituted alkynyl benzenes with readily available diselenides under electrochemical conditions to synthesize a wide variety of selanyl polycyclic aromatic hydrocarbons and polycyclic heteroaromatics in high to excellent yield up to 99% at room temperature in a short time (2-5 h). The transformation required only electricity as a green reagent and produces hydrogen gas as the only innocuous byproduct. Notably, the green chemistry metrics of the protocol are found excellent. Mechanistic studies revealed a radical pathway being initiated by the *in situ* generation of the corresponding selenyl radical from diselenides under electrochemical conditions. Significantly, a direct comparison of the electrochemical approach with that of our previously developed iodine-catalyzed chemical approach revealed that the electrochemical approach is not only catalyst- and oxidant-free, but also more energy-efficient, high-yielding, sustainable, and practical.

Keywords: Annulation; Electrochemical; Atom economy; Phenanthrenes; Selenium; Efficient

Polycyclic aromatic hydrocarbons (PAHs), in particular, phenanthrenes, have attracted significant interest from both synthetic organic and material chemists due to their occurrence in several biologically active natural products exhibiting a wide range of biological activities such as antiviral,[1] antimicrobial,[2] anticancer,[3] antitumor,[4] and anti-HIV[5] activity and also having interesting materials applications such as organic-light-emitting-diodes (OLEDs), organic field-effect transistors[6] and solar cells.[7] On the other hand, selenium atom incorporation into an organic molecule often leads to the significant enhancement of pharmacological and physical properties owing to the electron donor, halogen-bond, and hydrogen-bond acceptor attributes.[8,9] Hence, the development of highly efficient and novel synthetic methods for the synthesis of selanyl PAHs, including phenanthrenes and polycyclic heteroaromatics, is highly desirable. However, only a few synthetic strategies are developed so far for the synthesis of selanyl phenanthrenes. In 2016, Zeni and co-workers first reported a Fe-mediated electrophilic selanylative annulation of 2-alkynyl biaryls with diaryl diselenides (1.1 equiv.) using 2 equiv. of $FeCl_3$.[10] The Arsenyan group developed a metal-free, oxidative selenylative annulation of 2-alkynyl biaryls with diphenyl diselenide (2 equiv.) using super-stoichiometric hazardous oxidant, *m*-CPBA to synthesize 9-phenylselanylphenanthrenes and selanyl PAHs.[11] Li *et al.* reported the synthesis of only 9-phenylselanyl-10-phenylphenanthrene (1 example) through electrophilic cyclization of 2-(phenylethynyl)-1,1′-biphenyl with triflic anhydride-activated (methylseleninyl)benzene which was synthesized from diphenyl diselenide in two steps using hazardous reagents in stoichiometric or over-stoichiometric amounts.[12] Despite notable advancement, these non-catalytic methods suffered from some serious limitations, such as the requirement of over-stoichiometric selenide counterpart (diaryl diselenide) and other reagents, thus generating over-stoichiometric metallic or non-metallic hazardous wastes, poor atom-economy of the reaction and limited substrate scope. Recently, we developed a metal-free, catalytic method for the oxidative selenylative annulation of 2-alkynyl biaryls with diselenides (0.6 equiv.) using iodine as a catalyst and H_2O_2 as the oxidant in water at 100 °C for the synthesis of selanyl PAHs including phenanthrens and polycyclic heteroaromatics through the *in situ* gener-

Chapter 6

SECTION-I

Iodine-Catalyzed C-H Chalcogenation of Heterocycles

6.1.1. Introduction

Owing to the high atom-economic feature, the C-H functionalization reaction (Figure 6.1.1.) has become one of the important strategies in organic synthesis in the context of green chemistry.[1] With an appropriate catalyst, C-H bond functionalization can be performed enabling the efficient synthesis of potential organic molecules including drug-molecules and natural products.[2] Although a huge number of C-H functionalization strategies have been developed under transition-metal-catalysis or metal-free approach,[3] a few are developed under iodine-catalysis.[4] As a part of our continued interest in developing iodine-catalyzed organic transformations, we intend to develop C-H functionalization, in particular, C-H chalcogenation reactions under iodine catalysis. A thorough literature survey revealed that a few iodine-catalyzed C-H chalcogenation reactions, in particular, C-H chalcogenation of heterocycles have been developed so far which are described below.

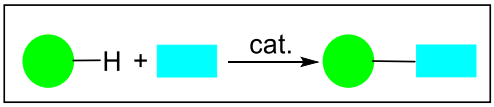

Figure 6.1.1. Schematic Representation of C-H Functionalization Reaction.

6.1.2. Review.

In 2021, Das group reported a C-H chalcogenation of 4*H*-pyrido[1,2-*a*]pyrimidin-4-ones with diaryl dichalcogenides using potassium pursulfate ($K_2S_2O_8$) as an oxidant in CH_3CN at 70 ^oC to synthesize a variety of 3-chalcogenyl 4*H*-pyrido[1,2-*a*]pyrimidin-4-ones in moderate to excellent yield (Scheme 6.1.1).[5] Mechanistic studies revealed a radical pathway involving the *in situ* formation of aryl chalcogenyl radical (Ar-X•), formed *via* the homolytic cleavage of the active intermediate, Ar-X-I (X= S/Se), followed by radical-addition, oxidation and proton elimination steps to form the desired products.

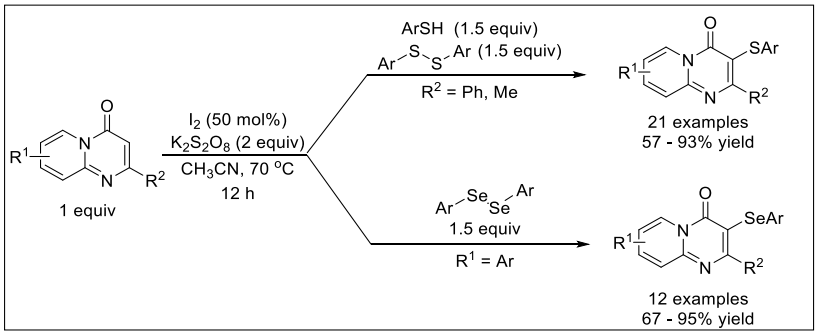

Scheme 6.1.1. C-H Chalcogenation of 4*H*-Pyrido[1,2-*a*]pyrimidin-4-ones.

In 2020, Singh and his co-workers disclosed an iodine-catalyzed regioselective C-H sulfenylation of indoles using 1-aryltriazene/CS_2 as a new sufenylating reagent for the synthesis of 3-arylthioindoles in good yield (Scheme 6.1.2).[6] 1-Aryltriazene **A** reacted with iodine to form B which after the elimination of *N*-iodopyrrolidine **C** furnished arene diazonium intermediate **D**. The diazonium ion **D** was then reduced by the iodide ion to form the aryl radical **E**. Carbon disulphide was then reacted with **E** to form the radical intermediate **F**. After the loss of carbon monosulfide, F gets converted to thiyl radical **G** which immediately was captured by iodine radical to form aryl selenyl iodide **H**. Finally, the substrate indole **I** underwent electrophilic substitution with **H** (ArSI) to afford the sulfenylated product **J**.

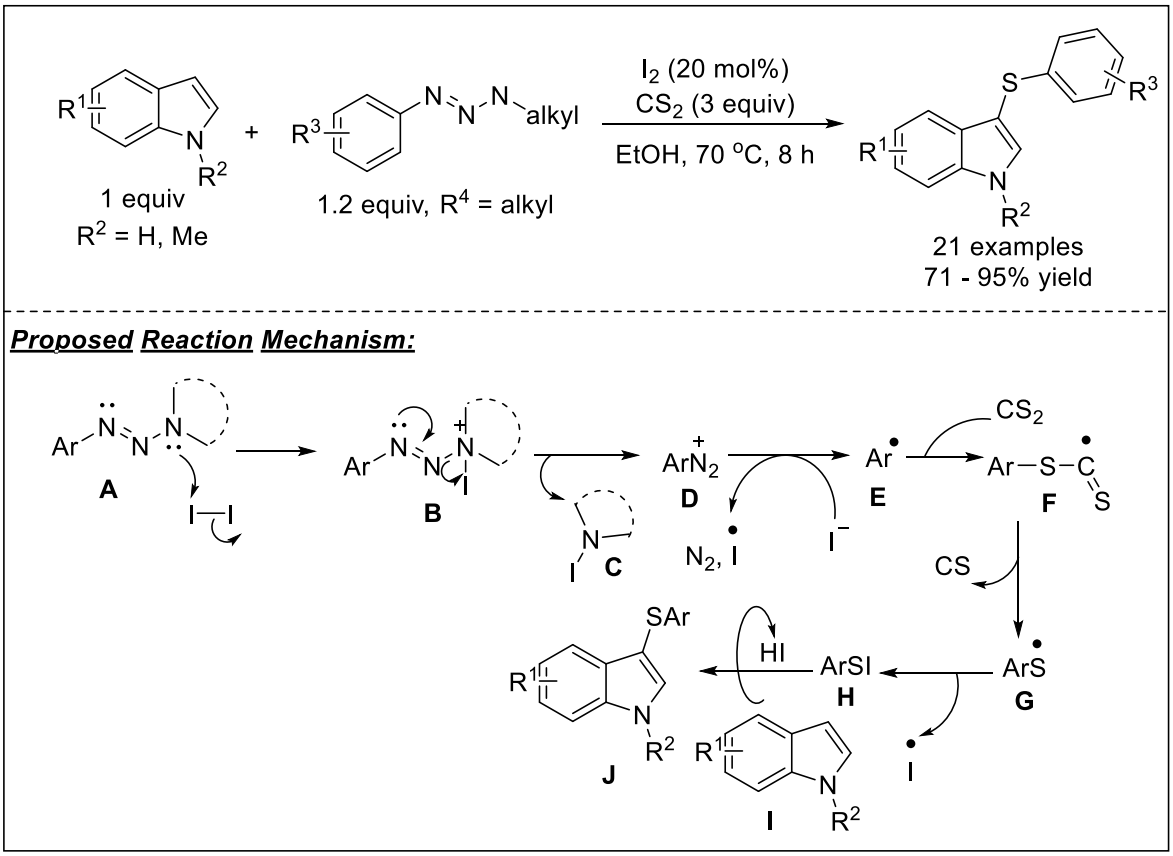

Scheme 6.1.2. Iodine-Catalyzed Synthesis of 3-Arylthioindoles Employing a 1-Aryltriazene/CS_2 as a New Arylsulfenyl (ArS-) Source.

In 2020, Song *et al.* reported an iodine-catalyzed, C-3 chalcogenation of imidazopyridines using KXCN (X = S, Se) and PIDA in aqueous medium at 110 °C for the synthesis of a library of chalcogenated imidazopyridines (Scheme 6.1.3).[7] Iodine reacted with KXCN in the presence of PIDA to generate electrophilic iodochalcogenocyanate IXCN[8]

Subsequently, 2-phenylimidazo[1,2-*a*]pyridine **A** underwent Friedel−Crafts reaction with IXCN to affords intermediate **B**. Intermediate **B** underwent HI elimination to afford chalcogenocyanated product **C**. Homolytical cleavage of **C** afforded selenium radical **D**, which immediately reacted with **A** to form intermediate **E**. Intermediate **E** formed the final product **G** along with the loss of HI (Scheme 6.1.3). This protocol is scalable up to gram-scale without compromising the yield of the product.

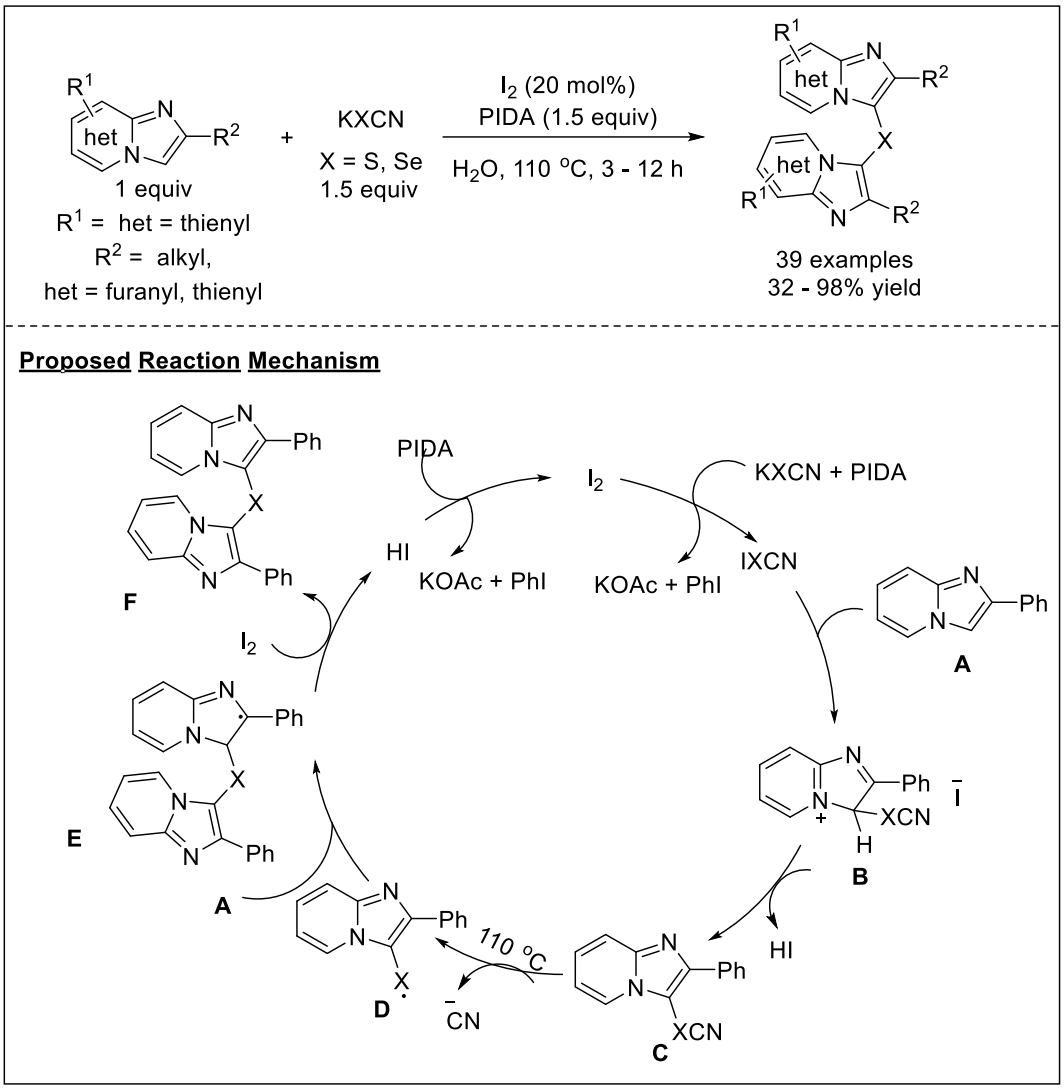

Scheme 6.1.3. C-H Chalcogenation of Imidazopyridines in Water.

In 2019, Hazra and his co-workers developed an iodine-catalyzed C-3 aryl-selenation of 2*H*-indazole with diaryl diselenides under the neat condition at room temperature to access a wide variety of 3-(phenylselanyl)-2*H*-indazoles with wide functional group tolerance in good yield (Scheme 6.1.4).[9] Mechanistic studies revealed that the reaction proceeded through an ionic pathway.

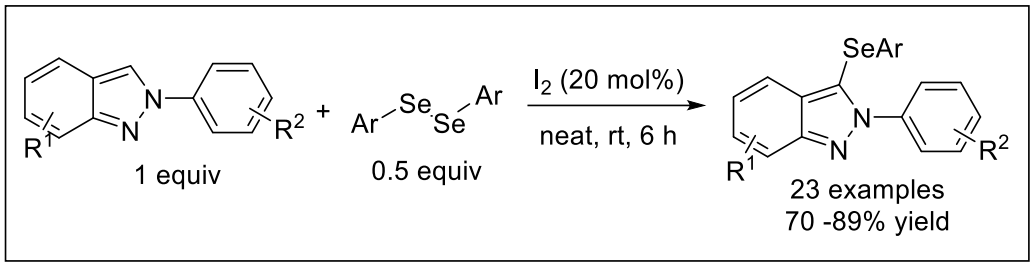

Scheme 6.1.4. Iodine-Catalyzed Selenylation of 2*H*-Indazole.

In the same year, Saha group reported a regioselective C-5 chalcogenation of 8-aminoquinoline analogues with diorganyl dichalcogenides using TBHP (^{t}BuOOH) at room temperature to access a library of chalcogenated quinolines in moderate to good yield (Scheme 6.1.5).[16] The reaction went well with various disulfides and diselenides irrespective of the nature and position of various substituents. The protocol is scalable up to gram-scale without any appreciable loss in product's yield. The further diversification of the developed protocol was demonstrated by synthesizing *N*-Boc premaquine derivatives, an antimalarial drug. Mechanistic studied revealed that the reaction proceeded through an ionic pathway (Scheme 6.1.6).[10]

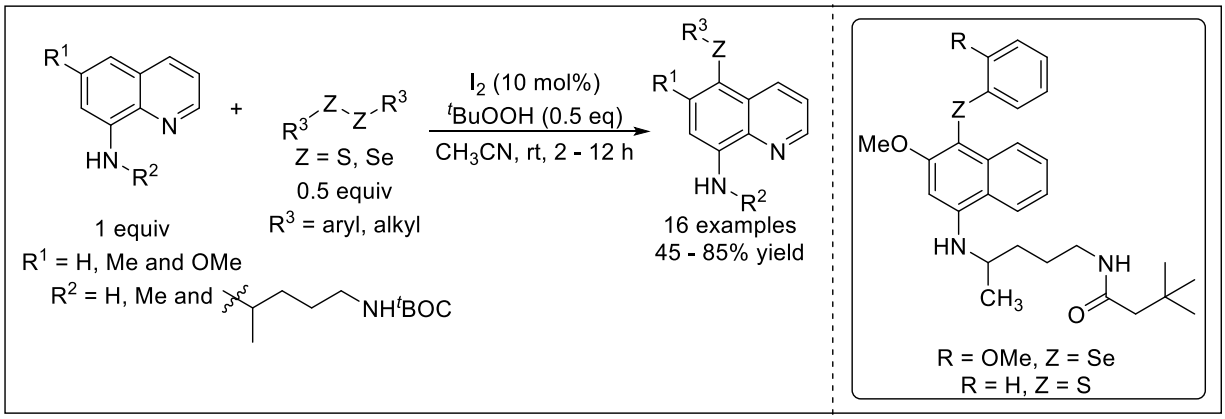

Scheme 6.1.5. Iodine-Catalyzed C-5 Chalcogenation of 8-Aminoquinolines.

In 2019, Yang *et al*. disclosed an regioselective iodine-catalyzed deoxygenative C-H chalcogenation of 7-azindole-*N*-oxides with diaryl diselenides in PEG-200 at 110 ^{o}C under aerobic atmosphere to afford a wide variety of 7-azaindoles with broad substrate scope in good to excellent yield (Scheme 6.1.6).[11]

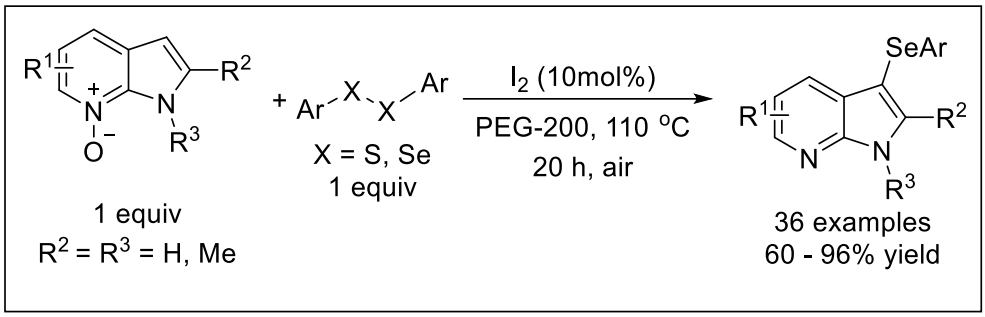

Scheme 6.1.6. I_2-Catalyzed Chalcogenation of 7-Azindole-*N*-oxides.

In 2018, Ohkado *et al*. disclosed a tandem flavin-iodine-catalyzed aerobic oxidative sulfenylation of imidazo[1,2-*a*]pyridines with thiols to afford a library of biologically active 3-sulfenylimidazo[1,2-*a*]pyridines in moderate to excellent yield and H_2O as the only by-product (Scheme 6.1.7).[12] The reaction proceeded *via* the oxidation of thiol to disulphide under aerobic atmosphere followed by the *in situ* formation of PhSI. Mechanistis studied revealed that the the reaction proceeded through ionic pathway.

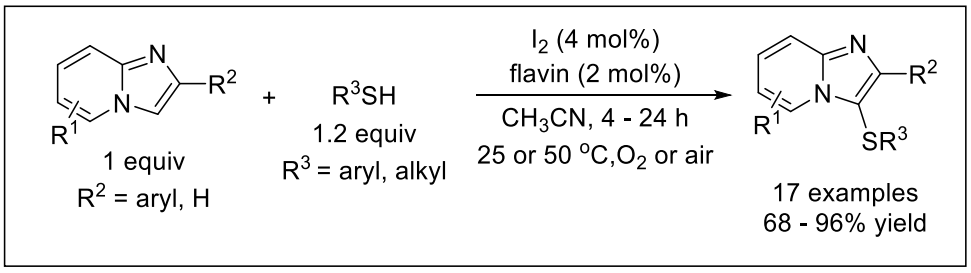

Scheme 6.1.7. Iodine-Catalyzed Aerobic Oxidative Sulfenylation of Imidazo[1,2-*a*]Pyridines with Thiols.

6.1.3. Conclusion.

Although there are several iodine-catalyzed C-H chalcogenation reactions developed so far, most of them are focused on the development of C-H chalcogenation of heterocyclic molecules. Most of the reactions proceeded through the formation of. However, this strategy of C-H chalcogenation of alkenes through the formation of chalcogenyl iodide intermediates is hardly explored so far. Hence, the development of iodine-catalyzed C-H chalcogenation of alkenes is a research topic of interest that we intend to explore.

SECTION-II

C-H Chalcogenation Reactions of Alkenes

6.2.1. Introduction.

Vinyl sulfides[1] and selenides[2] are valuable structural units in numerous biologically active compounds including drug molecules such as antibiotics and proliferation-inhibitor (Fig. 6.2.1). Moreover, these classes of molecules also find useful applications as versatile intermediates or valuable building blocks in organic syntheses such as Michael acceptor,[3] olefin metathesis, [4] enol substitutes,[5] and vinyl or ethylene derivatives.[6] Vinyl sulfides possess various applications in materials science, such as aggregation-induced emission (AIE),[7] luminogens,[7b] polymers,[8] and molecular electronics (Fig. 1).[9]

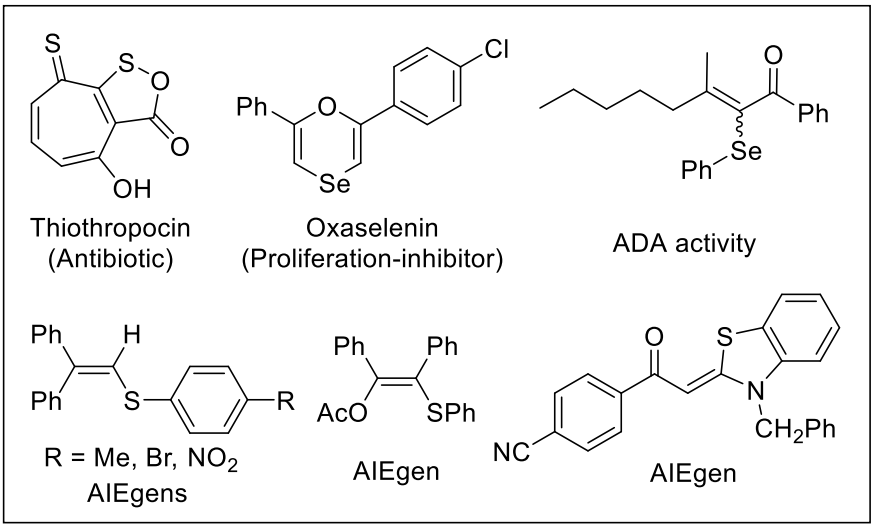

Figure 6.2.1. Examples of valuable vinyl sulfides and selenides.

Consequently, several synthetic strategies have been developed to synthesize vinyl sulfides[10] and selenides,[11] and among them, the following two are employed most frequently *i.e.*, (a) transition-metal-catalyzed cross-coupling of vinyl halides or boronic acids with various organochalcogenides such as thiols/disulfides and selenols/diselenides[12] and (b) hydrothiolation/hydroselenation of alkynes.[13] However, these strategies suffered from one of the following limitations such as (a) the requirement of expensive and/or hazardous metallic or non-metallic reagents and/or ligands in catalytic or stoichiometric amounts, thus producing considerable waste, (b) the requirement of prefunctionalized starting materials leading to the generation of stoichiometric waste and resulting in poor atom-economy and (c) poor stereoselectivity.

Since the last few decades, developing the C-H functionalization strategy for synthesizing valuable classes of molecules has received tremendous attention from synthetic organic chemists owing to its high atom-economic feature and non-requirement of

prefunctionalized substrates.[14] Consequently, several C-H chalcogenation strategies have also been developed to synthesize vinyl sulfides and selenides. The traditional approaches of C-H chalcogenation, particularly C-H sulfenylation, involved deprotonating a vinylic proton by organolithium reagent followed by quenching with disulfides.[15] However, these strategies also suffered from some limitations, such as the requirement of hazardous and harsh reagents such as organolithium reagent and poor atom economy since one part of the disulfide is lost during the reaction. A couple of transition-metal-catalyzed/mediated, directing group-assisted alkenyl C-H sulfenylation/selenylation of enamides[16] and *N*-tosyl acrylamides[17] have been developed which relied on the requirement of various expensive and hazardous transition-metal salts/ complexes in either catalytic or (sub)stoichiometric amounts. Recently, some other synthetic strategies for C-H chalcogenation were also developed. The state-of-art of area of research is given below.

6.2.2. Review.

Zhang and co-workers reported a Cu-catalyzed and iodine-mediated oxidative C-H sulfenylation of alkenes with diaryl disulfides for the stereoselective synthesis of alkenyl sulfides (Scheme 6.2.1). [18]

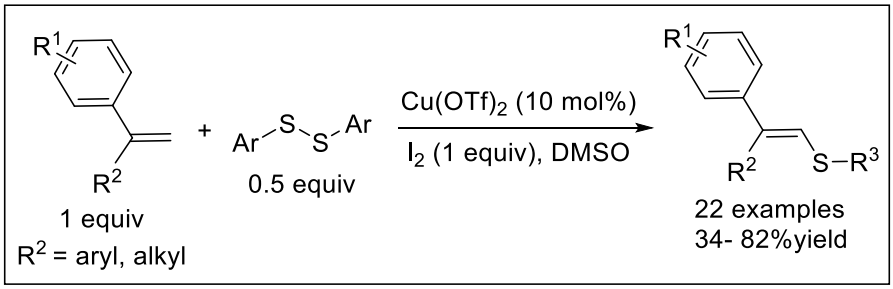

Scheme 6.2.1. Copper-Mediated Stereospecific C–H Oxidative Sulfenylation of Terminal Alkenes with Disulfides.

The Zeng group reported a pyridinium chloride-mediated tandem sulfenylation and elimination strategy with 1,1-disubstituted alkenes for synthesizing 1,1-disubstituted vinyl sulfides using *N*-thiosuccinimide as the source of sulfenyl group (Scheme 6.2.2).[19]

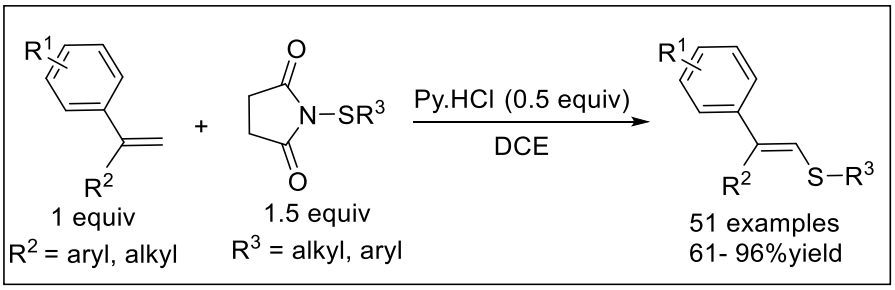

Scheme 6.2.2. Pyridine Hydrochloride-Catalyzed Thiolation of Alkenes to Access Allyl and Vinyl Sulphides.

Wang and Jiang *et al.* reported HI-mediated C-H sulfenylation of 1,1-diarylethenes with sodium arylsulfinates using over stoichiometric (3 equiv) HI (Scheme 6.2.3). [7b]

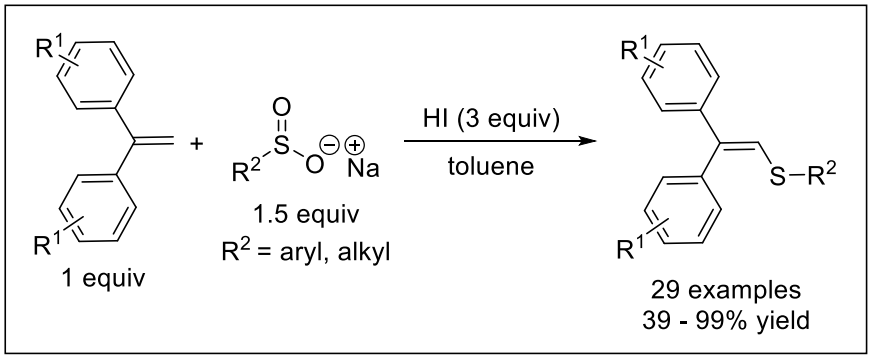

Scheme 6.2.3. C-H Sulfenylation of 1,1-Diphenylvinylsulfide.

The Zhou and Liu group reported a Cu-catalyzed radical C-H selenation of 1,1-diarylethenes to synthesize vinyl selenides using aryl boronic acids as the source of the aryl group of arylselenyl unit and selenium powder as the source of Se (Scheme 6.2.4).[20]

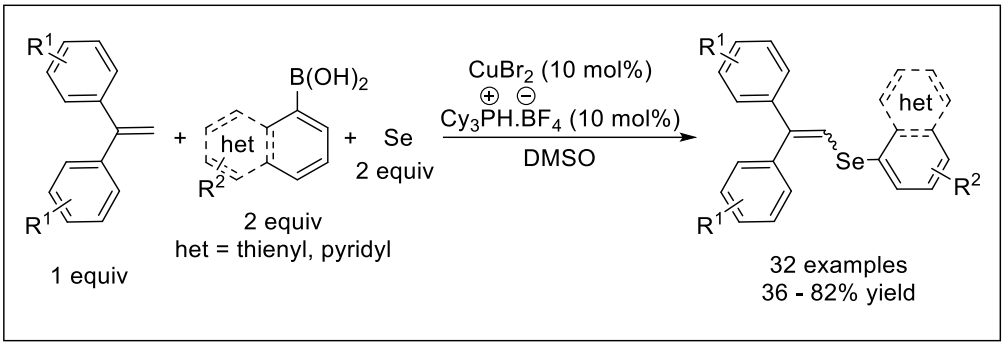

Scheme 6.2.4. Cu-Catalyzed Radical Selenylation of Olefin: A Direct Access to Vinyl Selenides.

6.2.3. Conclusion.

Although several synthetic strategies have been developed for oxidative C-H sulfenylation, C-H selenation is relatively underdeveloped. Despite significant advancement, these methods suffer from at least one of the following limitations (a) the requirement of metal catalyst, (b) over stoichiometric hazardous reagents, (c) hazardous solvent, (d) poor atom economy, and (e) generation of hazardous wastes. Hence, the development of a metal-free, highly atom-economic, and sustainable synthetic strategy for both vinylic C-H sulfenylation and selenation is highly desirable in the context of green chemistry.

SECTION-III

Recyclable Iodine-catalyzed Oxidative C-H Chalcogenation of 1,1-Diarylethenes in Water: Green Synthesis of Trisubstituted Vinyl Sulfides and Selenides

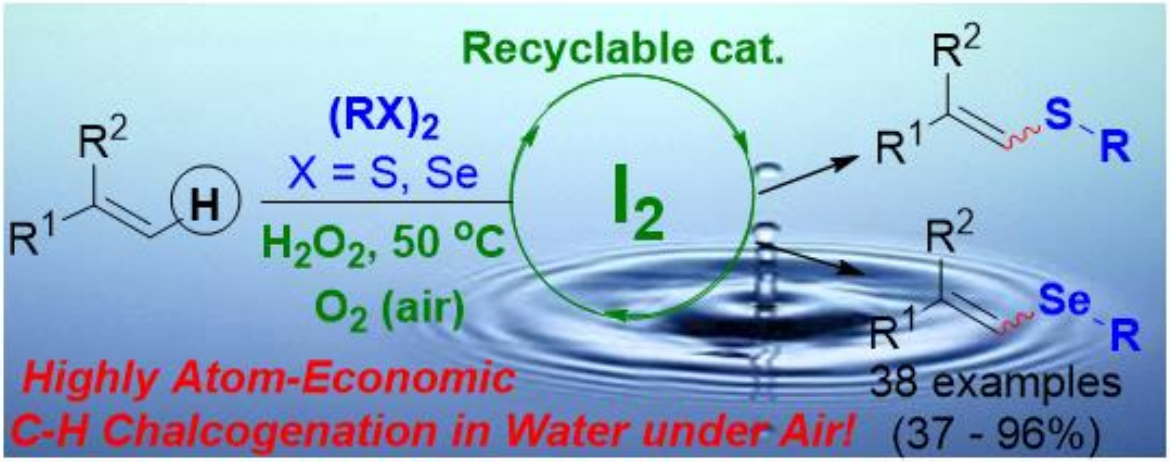

6.3.1. Introduction.

As a part of our continued interest in developing iodine-catalyzed/mediated sustainable synthetic methodologies,[1] herein we report a recyclable iodine-catalyzed, oxidative C-H sulfenylation and selenation of 1,1-diarylethenes with diorganyl dichalcogenides using catalytic amounts of iodine in water which exhibits several advantages with respect to the previous reports in the context of green chemistry (Scheme 6.3.1).

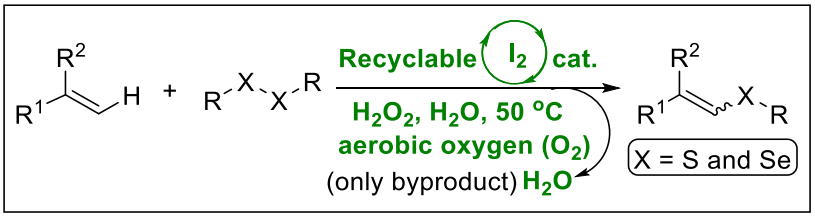

Scheme 6.3.1. Iodine-Catalyzed C-H Functionalization of Alkenes in Water.

6.3.2. Results and Discussion.

We commenced our investigation of optimization of the reaction conditions using 1,1-diphenyl ethene **1a** and diphenyl disulfide **2a** (0.6 equiv) as the model substrates and the results are summarized in Table 6.3.1. When the reaction was conducted using iodine (20 mol%) as the catalyst, 30% (v/v) aqueous H_2O_2 (0.5 equiv) as the oxidant in DMSO (0.06 mL) at 120 ^oC under aerobic atmosphere, gratifyingly, the desired product, *i.e.*, (2,2-diphenylvinyl)(phenyl)sulfane **3aa** was formed in 90% yield in 4 h (entry 1, Table 6.3.1). The blank experiment without H_2O_2 also furnished the same result (entry 2, Table 6.3.1), which revealed that DMSO could play the role of an oxidant. However, it leads to the formation of hazardous dimethyl sulfide (DMS) in stoichiometric amounts and that is not desirable in the context of green chemistry. Hence we screened various other solvents such as toluene, 1,4-dioxane, DMF, MeCN, DCM, EtOH, and H_2O using H_2O_2 (0.5 equiv) as oxidant. Gratifyingly, **3aa** was formed in 78% yield in EtOH and in 75% yield in H_2O (entries 4-10, Table 6.3.1). Next, we continued our optimization studies in water. The change of oxidant from H_2O_2 to TBHP, Oxone, and $Na_2S_2O_8$ had a negative impact on the reaction outcome which revealed that the green oxidant, H_2O_2 is the best (entry 10 vs entries 11-13, Table 6.3.1). Notably, when the loading of iodine was reduced to 10 mol%, the yield of **3aa** increased to 93% (entry 15, Table 6.3.1). However, further lowering of the loading of iodine to 5 mol% lowered the yield of **3aa** to 66% (entry 16, Table 6.3.1). Lowering the stoichiometry of **2a** and H_2O_2 to 0.5 equiv and 0.3 equiv respectively had no impact on the reaction outcome (entries 17 and 18, Table

6.3.1) revealing the higher atom economy of the reaction. Next, we optimized the temperature, and 50 ^{o}C was found the optimum (entry 18 vs entries 19-21, Table 6.3.1). The blank experiment without using H_2O_2 furnished **3aa** in 55% yield which revealed that aerobic oxygen is also playing the role of another oxidant (entry 22, Table 6.3.1). When the reaction was performed under an argon atmosphere, only 30% of **3aa** was formed which further revealed the essential role of aerobic oxygen for the efficient synthesis of **3aa** (entry 23, Table 6.3.1). When the reaction was performed under a pure oxygen atmosphere without using H_2O_2, 66% of **3aa** was formed which revealed that pure molecular oxygen cannot fully replace the requirement of H_2O_2 (entry 24, Table 6.3.1). When NaI or $PhI(OAc)_2$ was used instead of I_2, only a trace amount of **3aa** was formed in both cases (entries 25 and 26, Table 6.3.1). The blank experiment without iodine did not furnish **3aa** (entry 27, Table 6.3.1), which revealed the essential role of iodine for this reaction. Hence, heating the reaction mixture of **1a** with **2a** (0.5 equiv) in the presence of only 10 mol% I_2 and 0.3 equiv H_2O_2 in water at 50 ^{o}C under air is found to be the optimum reaction conditions for the synthesis of **3aa**.

Table 6.3.1. Optimization of Reaction Conditions[a].

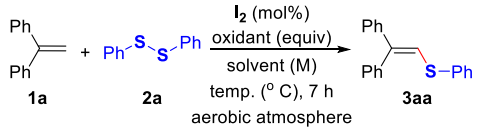

entry	I_2 (mol%)	**2a** (equiv)	oxidant (equiv)	solvent (mL)	temp. (^{o}C)	time (h)	yield (%)[b]
1	20	0.6	H_2O_2 (0.5)	DMSO (0.06)	120	4	90
2	20	0.6	-	DMSO (0.06)	120	4	90
3	20	0.6	-	DMSO (0.06)	100	4	84
4	20	0.6	H_2O_2 (0.5)	toluene (0.06)	100	4	70
5	20	0.6	H_2O_2 (0.5)	1,4-dioxane (0.06)	100	4	65
6	20	0.6	H_2O_2 (0.5)	DMF (0.06)	100	4	60
7	20	0.6	H_2O_2 (0.5)	MeCN (0.06)	100	4	74
8	20	0.6	H_2O_2 (0.5)	DCM (0.06)	60	4	21
9	20	0.6	H_2O_2 (0.5)	EtOH (0.06)	80	4	78
10	20	0.6	H_2O_2 (0.5)	H_2O (0.06)	100	4	75
11	20	0.6	TBHP (0.5)	H_2O (0.06)	100	4	45
12	20	0.6	Oxone (0.5)	H_2O (0.06)	100	4	38
13	20	0.6	$Na_2S_2O_8$ (0.5)	H_2O (0.06)	100	4	42
14	20	0.6	H_2O_2 (0.5)	H_2O (0.06)	100	7	82
15	10	0.6	H_2O_2 (0.5)	H_2O (0.06)	100	7	93
16	5	0.6	H_2O_2 (0.5)	H_2O (0.06)	100	7	66
17	10	0.5	H_2O_2 (0.5)	H_2O (0.06)	100	7	96
18	10	0.5	H_2O_2 (0.3)	H_2O (0.06)	100	7	95
19	10	0.5	H_2O_2 (0.3)	H_2O (0.06)	80	7	95
20	**10**	**0.5**	**H_2O_2 (0.3)**	**H_2O (0.06)**	**50**	**7**	**96**
21	10	0.5	H_2O_2 (0.3)	H_2O (0.06)	rt	7	66
22	10	0.5	-	H_2O (0.06)	50	7	55
23[c]	10	0.5	H_2O_2 (0.3)	H_2O (0.06)	50	7	30
24[d]	10	0.5	H_2O_2 (0.3)	H_2O (0.06)	50	7	66
25[e]	10	0.5	H_2O_2 (0.3)	H_2O (0.06)	50	7	trace
26[f]	10	0.5	H_2O_2 (0.3)	H_2O (0.06)	50	7	trace
27	-	0.5	H_2O_2 (0.3)	H_2O (0.06)	50	7	trace
28	10	0.5	H_2O_2 (0.3)	H_2O (0.12)	50	7	96

[a]The reactions were carried out on a 0.1 mmol scale; [b]yield of **3aa** was determined by the ^{1}H NMR of the crude reaction mixture using 1,3,5-trimethoxybenzene as the internal standard; [c]the reaction was performed under argon atmosphere; [d]the reaction was performed under oxygen atmosphere without using H_2O_2; [e]NaI was used instead of I_2; [f]$PhI(OAc)_2$ was used instead of I_2.

Table 6.3.2. Scope of C-H Sulfenylation of 1,1-Diarylethenes with Dioraganyl Disulfides[a,b].

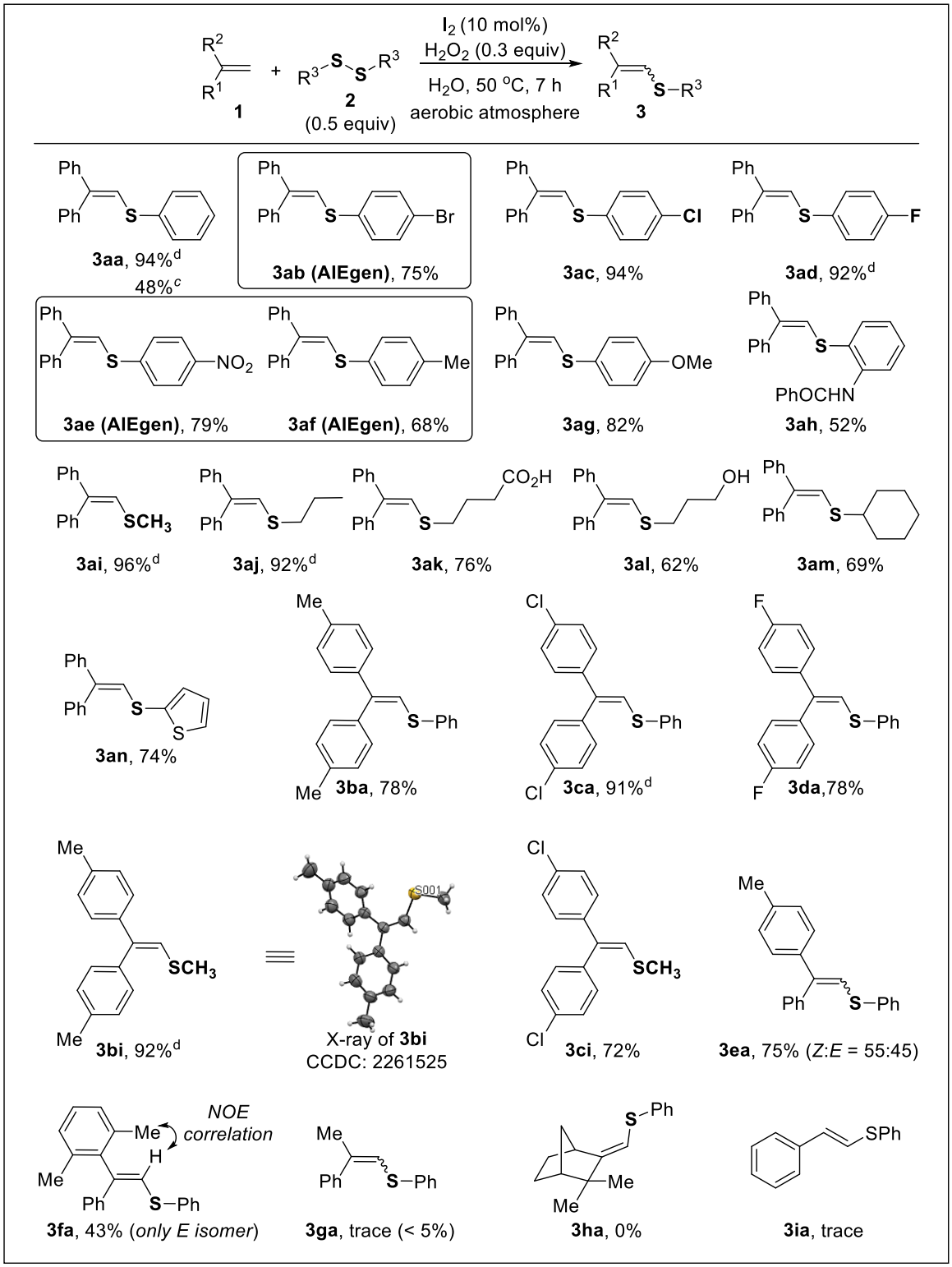

[a]Reaction conditions: **1** (0.5 mmol), **2** (0.25 mmol), I_2 (0.05 mmol), 30% (v/v) aqueous H_2O_2 (0.3 equiv), H_2O (0.3 mL), 50 °C; [b]Yield of isolated products was reported; [c]reaction was conducted in the presence of 1.2 equiv of PhSH instead of $(PhS)_2$ **2a**; [d]100% conversion of the reactants to product, which was purified by only work-up avoiding column chromatography.

With the optimized conditions in hand, we started exploring the scope of C-H sulfenylation of 1,1-disubstituted alkenes in a 0.5 mmol scale and the results are summarized in Table 2. At first, the scope of diaryl disulfides was explored with 1,1-diphenylethene **1a**. Diphenyl disulfide **2a** reacted with **1a** to furnish the desired product, (2,2-diphenylvinyl)(phenyl)sulfane **3aa** in 94% yield. The reaction of **1a** with thiophenol (1.2 equiv) under the standard reaction conditions furnished **3aa** in 48% yield which revealed that the reaction is more efficient with disulfide as compared to thiol. Both halogen (4-Br, 4-Cl, and 4-F) and strong electron-withdrawing (4-NO_2) group-substituted diaryl disulfides (**2b** – **2e**) reacted smoothly with **1a** to furnish the desired trisubstituted alkenyl sulphides (**3ab** – **3ae**) in good to excellent yield (75% – 94%). Electron-donating (4-Me and 4-OMe) group substituted diaryl disulfides also reacted with **1a** to furnish the desired products **3af** and **3ag** in 68% and 82% yield respectively. Notably, three molecules, i.e., **3ab**, **3ae**, and **3af** which are known as AIEgens (Chapter-6, Section-II, Fig 6.2.1),**7b** were synthesized in moderate to good yields. A base-sensitive functional group (NHCOPh) was tolerated under the optimized reaction conditions while **2h** was employed as the disulfide to react with **1a** furnishing **3ah**. Next, the scope of dialkyl disulfides was explored and various **1o** and **2o** dialkyl disulfides smoothly reacted with **1a** to furnish the desired products (**3ai** – **3al**) in moderate to excellent yield (62% – 96%) wherein some sensitive functional groups such as –COOH and –OH were tolerated.

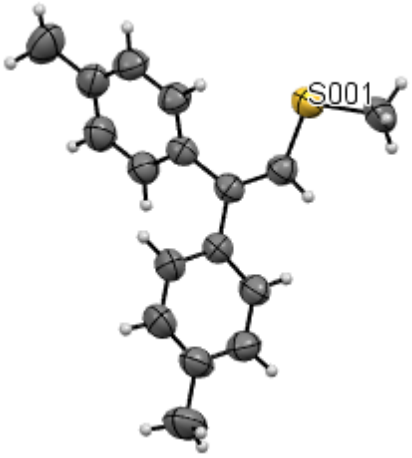

Figure 6.3.1. X-ray Crystal Structure of **3bi** (Thermal Ellipsoids Shown at 50% Probability) Including Hetero-Atom Numbering.

Table-6.3.3. Crystal Data of **3bi**.

Parameters	***3bi***
Empirical formula	$C_{17}H_{18}S$
Formula weight	*254.37*
Temperature/K	*295*
Crystal system	*orthorhombic*
Space group	*P 21 21 21*
a/Å	*9.4617(5)*
b/Å	*11.8672(7)*
c/Å	*13.2190(8)*
α (°)	*90*
β (°)	*90*
γ(°)	*90*
Volume/Å^3	*1484.28(15)*
Z	*4*
μ/mm^{-1}	*1.754*
D_x [g cm^{-3}]	*1.138*
F(000)	*544*
2Θ range for data collection (°)	*5.008-79.763*
Index ranges	*-11≤ h ≤ 12, -10 ≤ k ≤ 14, -16 ≤ l ≤ 15*
Reflections measured	*2648*
Unique reflections	*5041*
Parameters /restraints	*209/0*
Goodness-of-fit on F2	*1.084*
R_1 [I ≥ 2σ (I)]	*0.0419*
wR_2 (all data)	*0.1226*
Largest diff. peak/hole/e Å^{-3}	*0.204/-0.264*
CCDC	***2261525***

A diheteroaryl disulfide, *i.e.*, 1,2-di(thiophen-2-yl)disulfane **2n** also reacted with **1a** without any difficulties and furnished the desired product **3an** in 74% yield. Finally, the scope of 1,1- diarylethene was explored and both electron-donating (4-Me) and electron-withdrawing (4-Cl and 4-F) group substituted symmetrical 1,1-diarylethenes (**1b** – **1d**) reacted with **2a** to furnish the desired products (**3ba**-**3da**) in moderate to high yield. Dimethyl disulfide (**2i**) also reacted with 1,1-diarylethenes (**1b** and **1c**) to afford the corresponding products, *i.e.*, **3bi** in

92% yield and **3ci** in 72% yield respectively. The structure of **3bi** was confirmed by X-ray crystallographic structure determination (Fig. 6.3.1 and Table 6.3.3). When unsymmetrical 1,1-diarylethene, *i.e.*, 1-methyl-4-(1-phenylvinyl)benzene (**1e**) was subjected to react with **2a**, the desired product **3ea** was formed in 75% yield but with poor stereoselectivity (Z:E= 55:45). However, when 1,3-dimethyl-2-(1-phenylvinyl)benzene (**1f**) was subjected to react with **2a**, the reaction was highly stereoselective furnishing only (*E*)-(2-(2,6-dimethylphenyl)-2-phenylvinyl)(phenyl)sulfane **3fa** in 43% yield. The stereochemistry of **3fa** was confirmed by NOE difference spectroscopy (Fig. 6.3.2). The reaction of 1-aryl-1-alkyl-substituted ethene, *i.e.*, *α*-methylstyrene with **2a** was ineffective while 1,1-dialkyl-sustututed ethene, *i.e.*, camphene and styrene were unsuccessful. Notably, for the synthesis of **3aa**, **3ac**, **3ad**, **3ai**, **3aj**, **3ca** and 3**bi**, no column chromatographic purification was required.

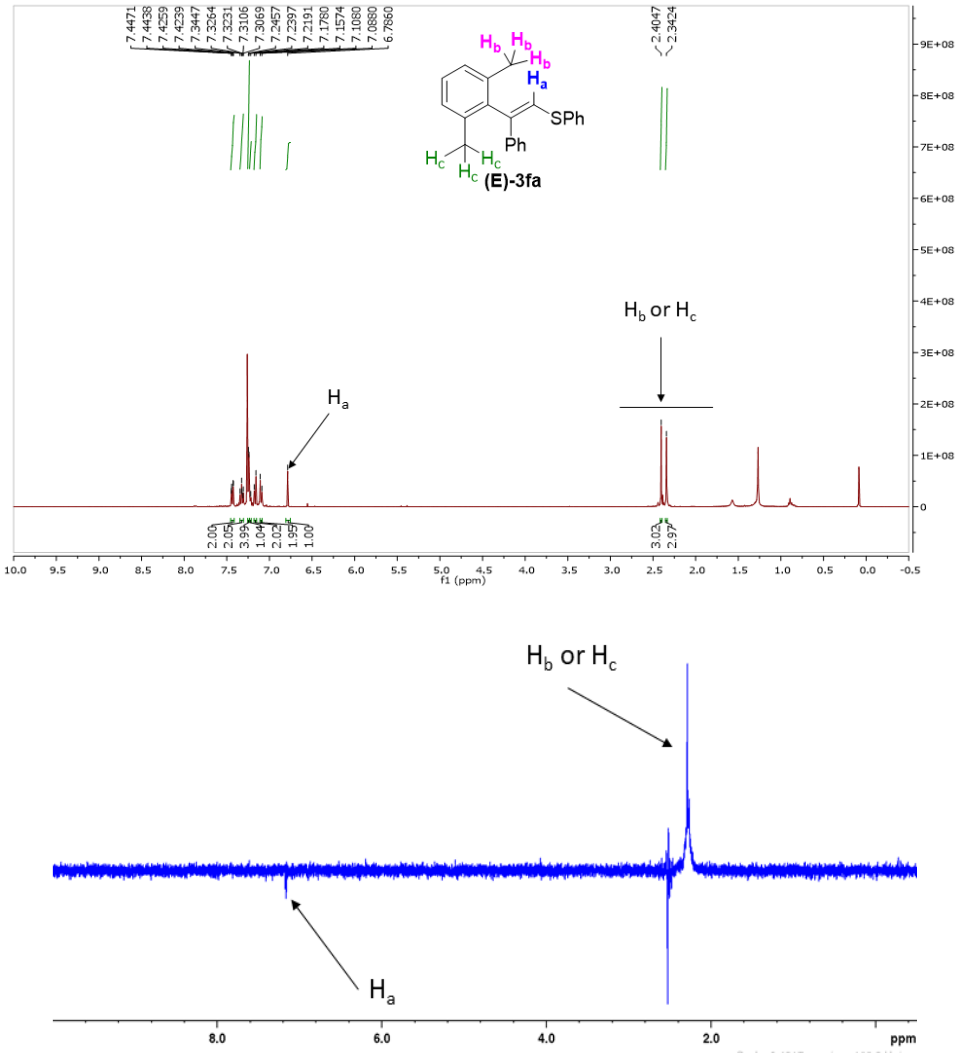

Figure 6.3.2: (A) ^{1}H-NMR Spectrum of **3fa**, (B) NOE Difference Spectrum, with Irradiation at 6.79 ppm.

When the reaction of **1a** was conducted with di-tert-butyl disulfide **2o**, interestingly an unprecedented product, *i.e.*, 1,2-bis(2,2-diphenylvinyl)disulfane **4** was formed and the desired C-H sulfenylated product, i.e., 3ao was not obtained (Scheme 6.3.2). However, **3ao** was detected in situ by LC-MS (Fig. 6.3.3). We speculate that the protonation of **3ao** at the α-carbon furnishes a stable carbocation A. However, it is a reversible process as the intermediate A could not lead to the formation of any stable compound through C-C or C-S bond cleavage. On the other hand, protonation at the β-carbon of **3ao** leads to the formation of carbocation **A**' which leads to the formation of intermediate **B** through C-S bond cleavage along with the elimination of isobutene. Next, **B** undergoes tautomerism immediately to form a more stable 2,2-diphenylethene-1-thiol (**C**) which is also detected in situ by LC-MS (Fig. 6.3.4). Finally, under the oxidative conditions, intermediate **C** is dimerized to 1,2-bis(2,2-diphenylvinyl)disulfane (**4**).

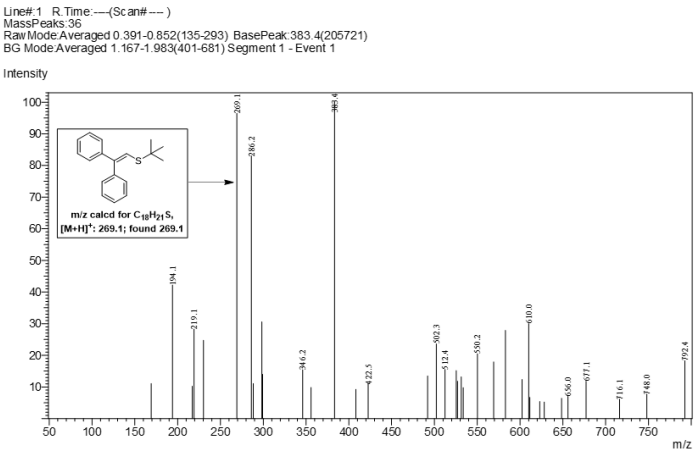

Figure 6.3.3. Mass Spectrum of the Reaction Mixture of Ethene-1,1-diyldibenzene, I_2 and 1,2-Di-tert-butyldisulfane.

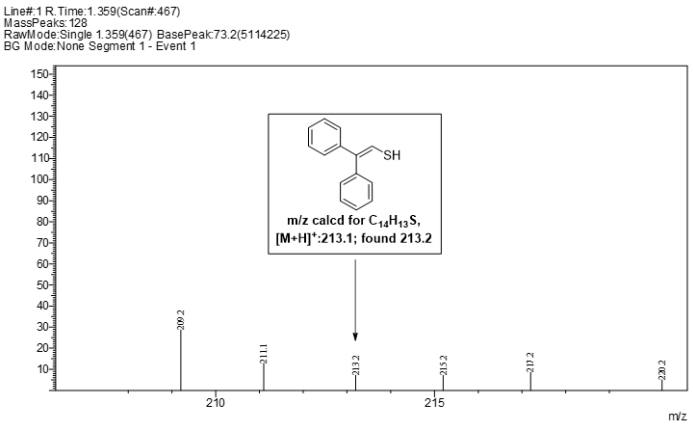

Figure 6.3.4. Mass Spectrum of the Reaction Mixture of Ethene-1,1-diyldibenzene, I_2 and 1,2-Di-tert-butyldisulfane.

Scheme 6.3.2. Unprecedented Synthesis of 1,2-Bis(2,2-diphenylvinyl)disulfane.

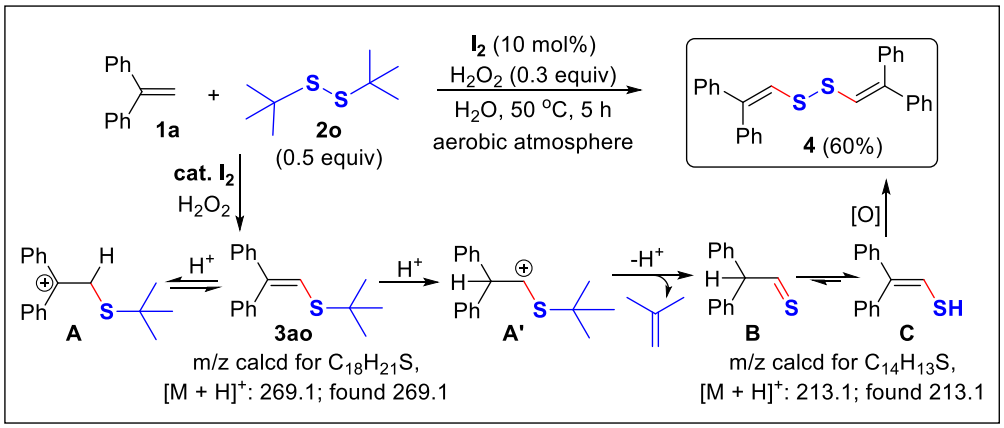

Next, we explored the scope of C-H selanation of alkenes with diselenides under the optimized reaction conditions, and the results are summarized in Table 6.3.4.

Table 6.3.4. Scope of C-H Selenation of Alkenes with Dioraganyl Diselenides[a,b].

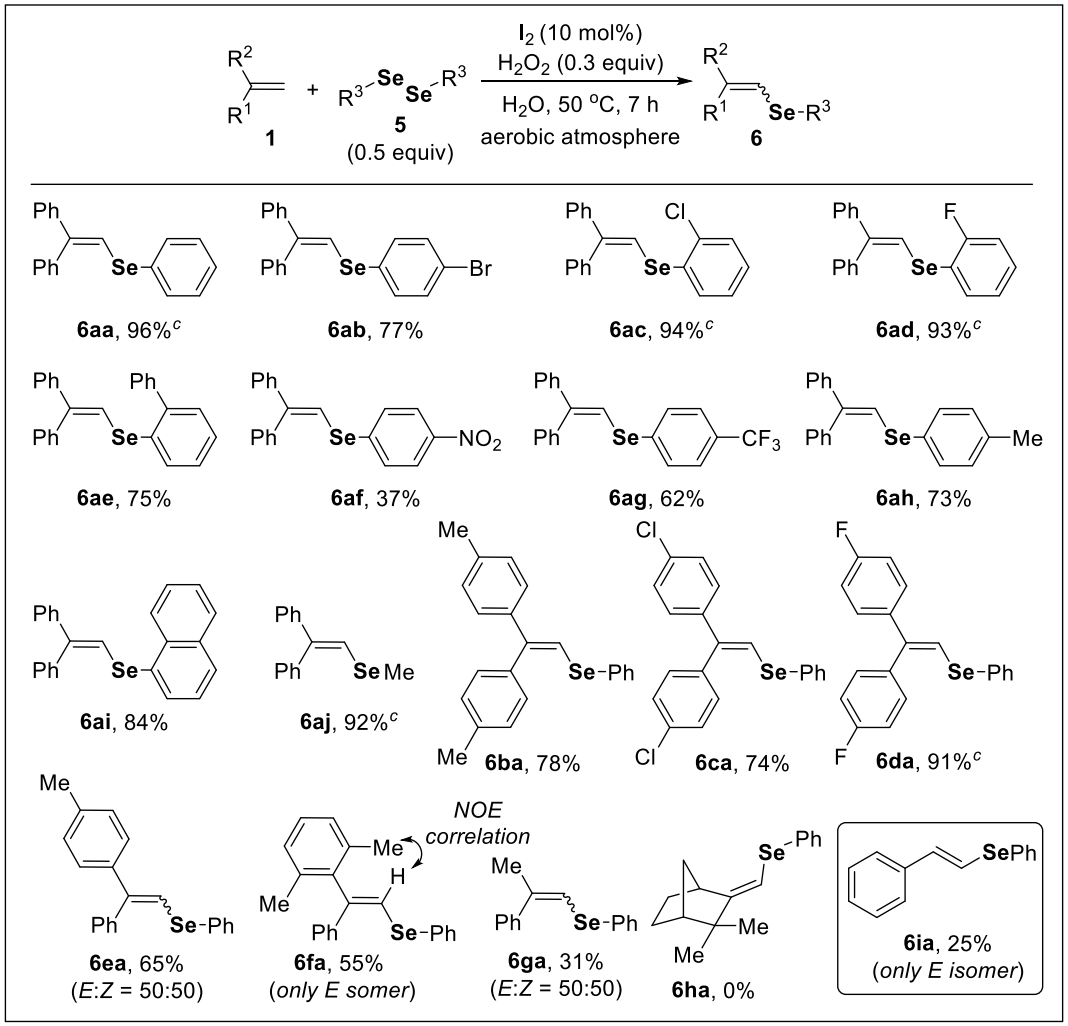

[a]Reaction conditions: **1** (0.5 mmol), **2** (0.25 mmol), I_2 (0.05 mmol), 30% (v/v) aqueous H_2O_2 (0.3 equiv), H_2O (0.3 mL), 50 °C; [b]Yield of isolated products was reported; [c]100% conversion of the reactants to product, which was purified by only work-up avoiding column chromatography.

The reaction of **1a** with diphenyl diselenide **5a** afforded (2,2-diphenylvinyl)(phenyl)selane 6aa in 96% yield. Both halogen (4-Br, 2-Cl, 2-F), electron-withdrawing (2-Ph, 4-NO_2, 4-CF_3), and electron-donating (4-Me) groups substituted diaryl diselenides reacted smoothly with **1a** to afford the desired products (**6ab** – **6ah**) in 37-94% yield. 1,2-Di(naphthalen-1-yl)diselane furnished the desired product, **6ai** in 84% yield upon reaction with **1a**. Dialkyl diselenide, in particular, dimethyl diselenide also furnished the desired product **6aj** in 92% yield. *p*-Me, *p*-Cl, and *p*-F-substituted symmetrical 1,1-diarylethene smoothly reacted with **5a** to afford the desired products, **6ba**, **6ca**, and **6da** respectively in high yield (74% - 91%).

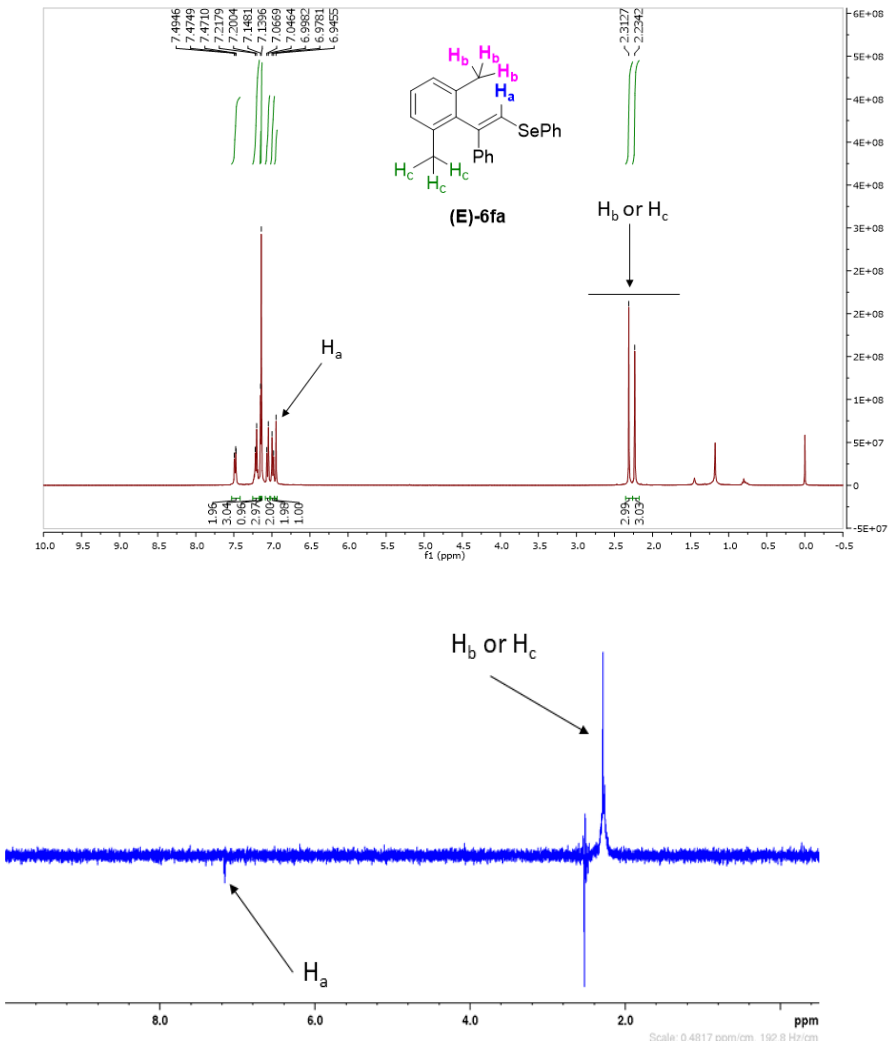

Figure 6.3.5: (A) ^{1}H-NMR Spectrum of **6fa**, (B) NOE Difference Spectrum, with Irradiation at 6.95 ppm.

While the reaction of unsymmetrical 1,1-diarylethene, i.e., **1e** with **5a** was non-stereoselective furnishing **6ea** in 65% yield with *E*:*Z* = 50:50, the same with 1f was highly stereoselective furnishing only (*E*)-(2-(2,6-dimethylphenyl)-2-phenylvinyl)(phenyl)selane **6fa** in 55% yield. The stereochemistry of **6fa** was confirmed by NOE difference spectroscopy (Fig. 6.3.5). Although, C-H sulfenylation did not work with *α*-methylstyrene (**1g**) and styrene (**1i**) under the optimized reaction conditions, C-H selenation of the same with diphenyl diselenide **5a** furnished the desired products *i.e.*, phenyl(2-phenylprop-1-en-1-yl)selane **6ga** in 31% yield (*E*:*Z* = 50:50) and (*E*)-phenyl(styryl)selane **6ia** in 25% yield respectively. However, the C-H selenation did not work with camphene **1h**. Notably, for the synthesis of **6aa**, **6ac**, **6ad**, **6aj**, and **6da**, no column chromatographic purification was required.

Scheme 6.3.3. Explanation of Stereoselectivity of C-H Chalcogenation Reactions with Unsymmetrical Alkenes.

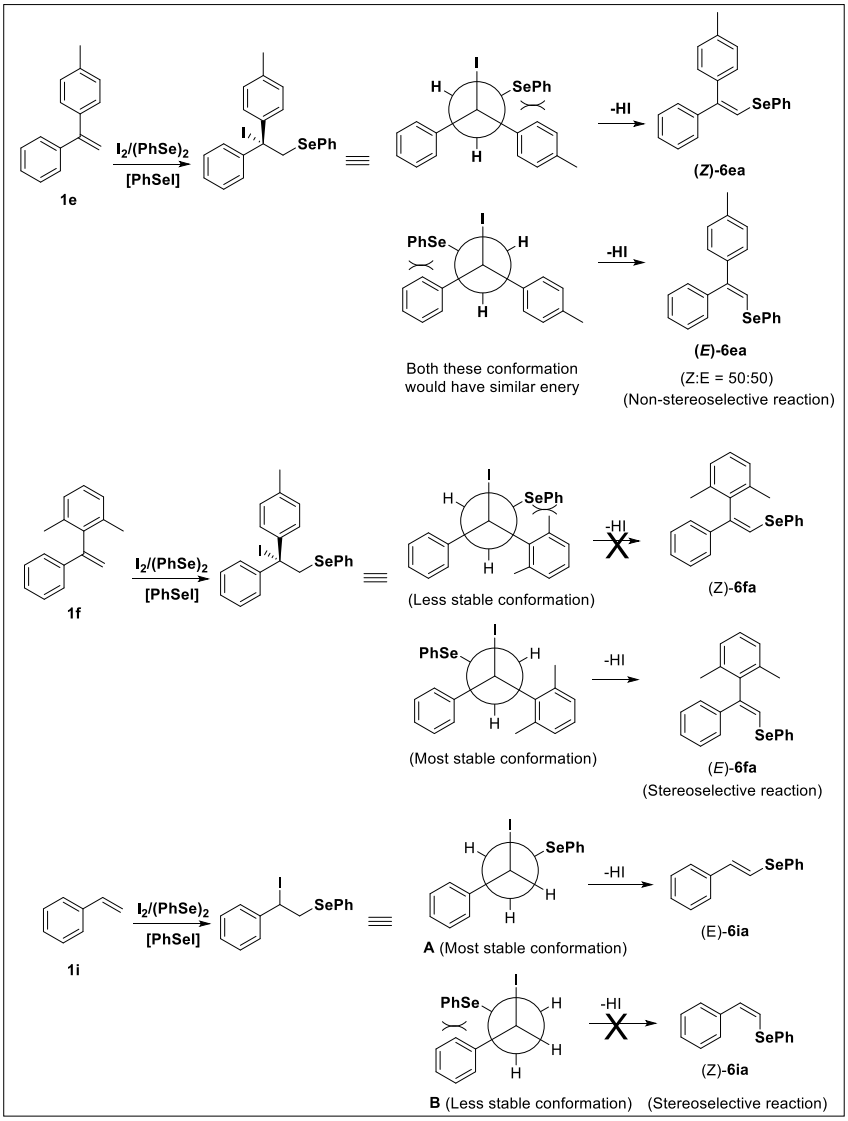

We speculate that the stereoselectivity of C-H chalcogenation of unsymmetrical alkenes depends on the difference in stability of the two different conformations of alkyl iodides from which HI elimination (E2) could happen leading to the formation of (*E*) and (*Z*) alkenes. If there is a certain difference in stability, the reaction is stereoselective, otherwise not. Hence the reactions with 1,3-dimethyl-2-(1-phenylvinyl)benzene (**1f**) and styrene (**1i**) were found highly stereoselective while the same with 1-methyl-4-(1-phenylvinyl)benzene (**1e**) was not (Scheme 6.3.3).

To check the practicality of the developed method, we conducted the gram-scale experiments of **1a** with both diphenyl disulfide **2a** and diphenyl diselenide **5a**, and to our delight, the desired products **3aa** and **6aa** were formed in 90% and 96% yields (no appreciable loss in yields) respectively which certainly revealed that the protocol is efficiently scalable (Scheme 6.3.4).

In order to measure the greenness of our developed method quantitatively, we evaluated the green chemistry metrics[3] for the synthesis of **3aa** and **6aa** from **1a** on a gram scale and the results are tabulated in Tables 6.3.5 - 6.3.8. Notably, for the synthesis of **3aa**, the method was found to be 96.3% atom-economic, 87% atom-efficient, 88.3% carbon-efficient, 81% reaction-mass-efficient having low E-factor (4.52 g waste as water/g product formation), and very high EcoScale score (82) while for the synthesis of 6aa, the method was found to be 97% atom-economic, 93% atom-efficient, 96.3% carbon-efficient 89% reaction-mass-efficient having a low E-factor (3.5 g waste as water/g product formation), and very high EcoScale score (85), which revealed that the developed method is excellent in the context of green chemistry.

Scheme 6.3.4. Gram-Scale Synthesis of **3aa** and **6aa.**

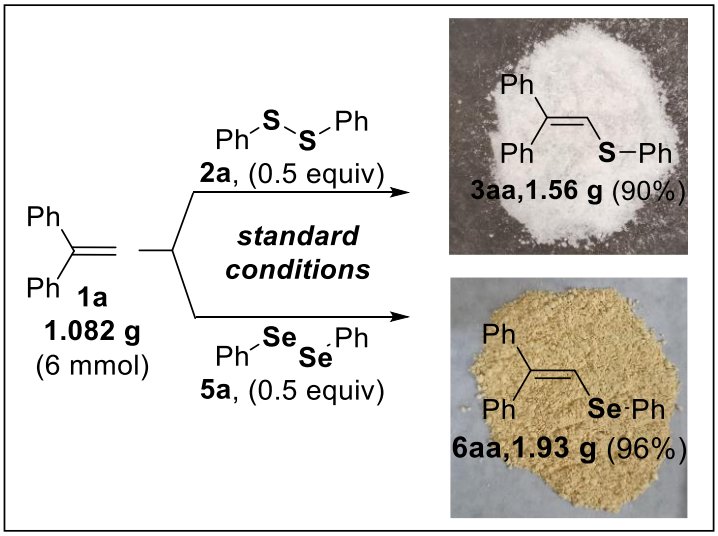

Table 6.3.5. Evaluation of Green Chemistry Metrics for the Synthesis of **3aa.**

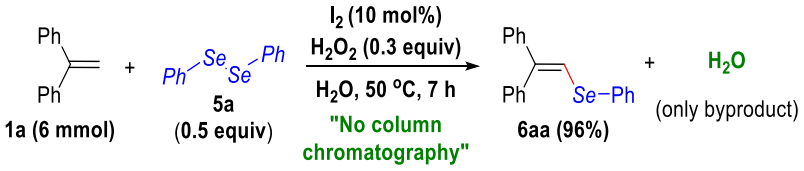

Yield of desired product (6aa) = 96%

$$\text{Atom Economy (\%)} = \frac{\text{Mol. wt. of desired product}}{\text{Mol. wt. of all reactants}} \times 100 = \frac{335.31}{180.25 + (0.5 \times 312.13) + (0.3 \times 34.02)} \times 100 = 97\%$$

Atom Efficiency (%) = (%yield of product x %atom economy) x 100 = (96% x 97%) x 100 = **93%**

$$\text{Carbon Efficiency (\%)} = \frac{\text{mmols of 3aa x no. of carbons in 3aa x 100}}{\text{(mmols of 1a x no. of carbons in 1a) + (mmols of 2a x no. of carbons in 2a)}} = \frac{(5.78 \times 20)}{(6 \times 14) + (3 \times 12)} \times 100 = 96.3\%$$

$$\text{Reaction Mass Efficiency (\%)} = \frac{\text{mass of isolated product}}{\text{mass of all reactants}} \times 100 = \frac{1.94}{(1.08 + 0.94 + 0.16)} \times 100 = 89\%$$

Reactant 1:	ethene-1,1-diyldibenzene (1a)	1.08 g	6 mmol	FW 180.25
Reactant 2:	1,2-diphenyldiselane (2a)	0.94 g	3 mmol	FW 312.13
Catalyst:	Iodine	0.15 g	0.6 mmol	FW 253.81
Reagent (oxidant):	30% aq H_2O_2 (v/v)	0.16 g	1.8 mmol	FW 34.02
Solvent:	Water	3.6 g	0.2 mmol	FW 18
Iodine quenching reagent	$Na_2S_2O_3$	0.095 g	0.6 mmol	FW 158.11
Solvent used for the extraction of product:	EtOAc	67.65 g (75 mL)	7.7 mmol	FW 88.11
Recovered solvent after extraction:	EtOAc	64.94 g (72 mL)	7.4 mmol	FW 88.11
Product:	(2,2-diphenylvinyl)(phenyl)selane (6aa)	1.94 g	5.78 mmol	FW 335.31

$$\text{E-factor} = \frac{\text{total waste (g)}}{\text{total product (g)}} = \frac{(1.08 + 0.94 + 0.15 + 0.16 + 3.6 + 0.095 + 67.65) - (64.94 + 1.94)}{1.94} = 3.5 \text{ g waste/g pdt}$$

EcoScale score = (100 - 15[a]) = 85 (>75; So, it is an excellent synthesis)

Table 6.3.6. Calculation of EcoScale Score of the Developed Protocol for the Synthesis of (2,2-Diphenylvinyl)(phenyl)sulfane (**3aa**). [3]

Eco Scale Calculation:

Eco Scale = 100 - Sum of individual penalties
Score on Eco Scale: > 75, Excellent; >50, acceptable; <50, Inadequate

Parameters		Penalty Points
1. Yield:	(100 - % of yield)/2 = (100 - 96)/2 = 2	2
2. Price of reaction components (To obtain 10 mmol of end product, **6aa**)		
A. Calculation of Penalty Points :		
a. ethene-1,1-diyldibenzene = 10.42 mmol = 1.88 g = USD 6.49		
b. 1,2-diphenyldiselane = 5.21 mmol = 1.63 g = USD 2.45		
c. Iodine (As catalyst) = 1.04 mmol = 0.264 g = USD 0.091		
d. Hydrogen Peroxide (30% of aqueous solution) = 0.31 mL = USD 0.082		
Total cost of synthesis of **6aa** = (6.49 + 2.45 + 0.091 + 0.082) = USD 9.113 Thus expensive, since < $10 (total cost of synthesis of 10 mmol of **6aa**):		0
3. Safety		
ethene-1,1-diyldibenzene		0
1,2-diphenyldiselane (T)		**5**
Iodine (T)		**5**
4. Technical Setup		
Common Setup		**0**
5. Temperature/ Time		
50 ^{o}C, 7 h (Heating, > 1h)		**3**
6. Work up and purification :		
a. Adding solvent		**0**
b. No classical chromatography		0
Total penalty points:		**15**

B. Ecoscale calculation:

EcoScale score: (100 - 15) = 85 (>75; it is an excellent synthesis)

Table 6.3.7. Evaluation of Green Chemistry Metrics for the Synthesis of **6aa.**

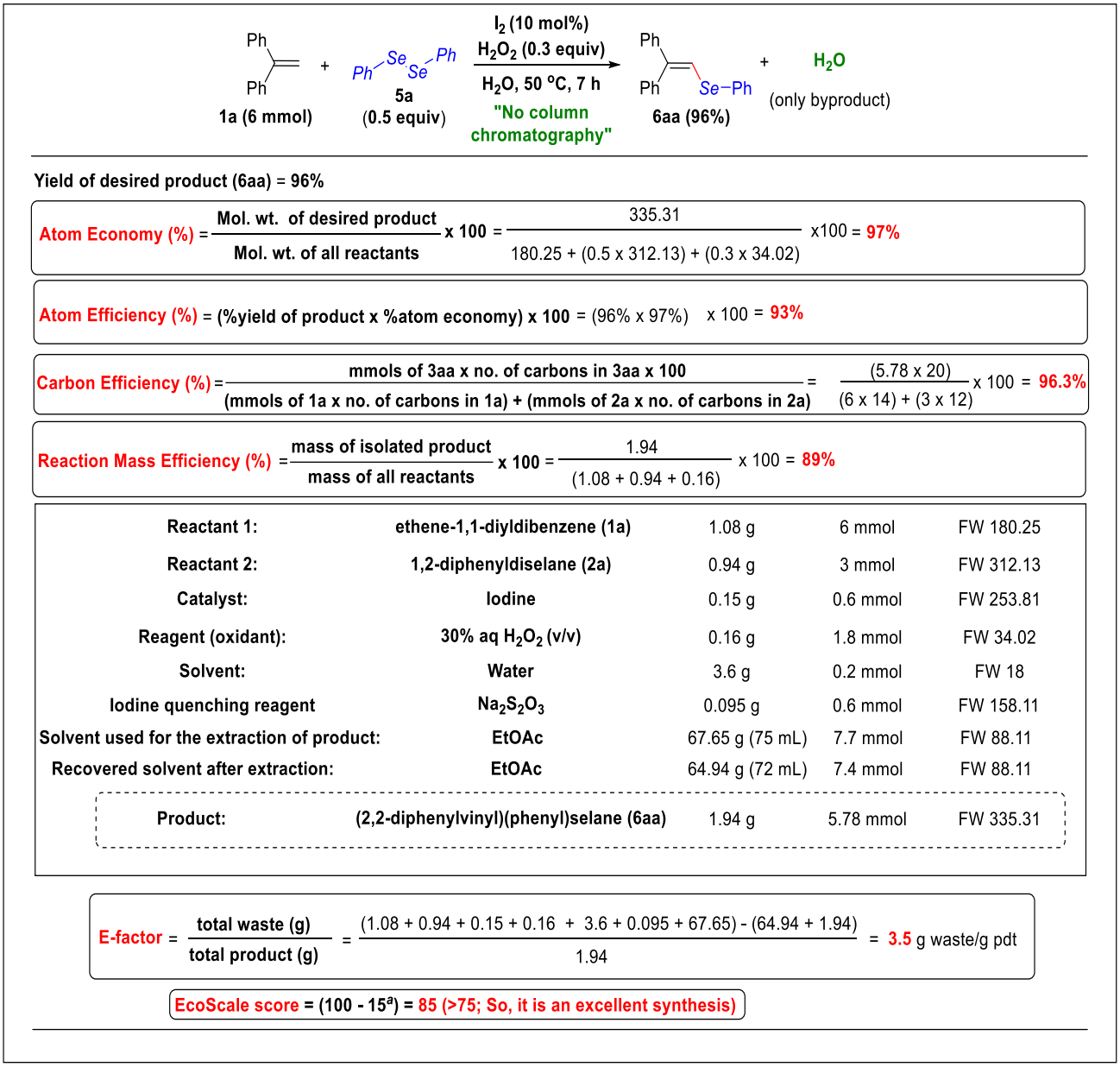

Table 6.3.8. Calculation of EcoScale Score of the Developed Protocol for the Synthesis of (2,2-Diphenylvinyl)(phenyl)selane (**6aa**).[3]

Eco Scale Calculation:

Eco Scale = 100 - Sum of individual penalties
Score on Eco Scale: > 75, Excellent; >50, acceptable; <50, Inadequate

Parameters		Penalty Points
1. Yield:	(100 - % of yield)/2 = (100 - 90)/2 = 5	5
2. Price of reaction components (To obtain 10 mmol of end product, **3aa**)		
A. Calculation of Penalty Points :		
a. ethene-1,1-diyldibenzene = 11.37 mmol = 2.05 g = USD 7.08		
b. 1,2-diphenyldisulfane = 5.69 mmol = 1.24 g = USD 0.64		
c. Iodine (As catalyst) = 1.14 mmol = 0.289 g = USD 0.099		
d. Hydrogen Peroxide (30% of aqueous solution) = 0.33 mL = USD 0.087		
Total cost of synthesis of **3aa** = (6.49 + 0.64 + 0.099 + 0.087) = USD 7.32		
Thus inexpensive, since <$10(total cost of synthesis of 10 mmol of **3aa**) :		0
3. Safety		
ethene-1,1-diyldibenzene		0
1,2-diphenyldisulfane (T)		**5**
Iodine (T)		**5**
4. Technical Setup		
Common Setup		**0**
5. Temperature/ Time		
50 ^{o}C, 7 h (Heating, > 1h)		**3**
6. Work up and purification :		
a. Adding solvent		**0**
b. No classical chromatography		0
Total penalty points:		**18**

B. Ecoscale calculation:

EcoScale score: (100 - 18) = 82 (>75; it is an excellent synthesis)

Next, we checked the feasibility of recovery and recyclability of the catalyst, iodine. After the completion of the reaction of **1a** with **2a** in a 6 mmol scale, 80% iodine was recovered during the column chromatography stage and recycled in the next run, *i.e.*, the first-cycle experiment in a 4.8 mmol scale (Scheme 6.3.5). After the first-cycle experiment, we were able to recover 67% of iodine which was further reused in the next run, *i.e.*, the second-cycle experiment in a 3.2 mmol scale. Notably, in each cycle of the experiment, the reaction outcome remained uncompromised which revealed that the developed protocol is highly sustainable, cost-effective, and practical.

Scheme 6.3.5. Recovery and Recyclability of the Catalyst, Iodine.

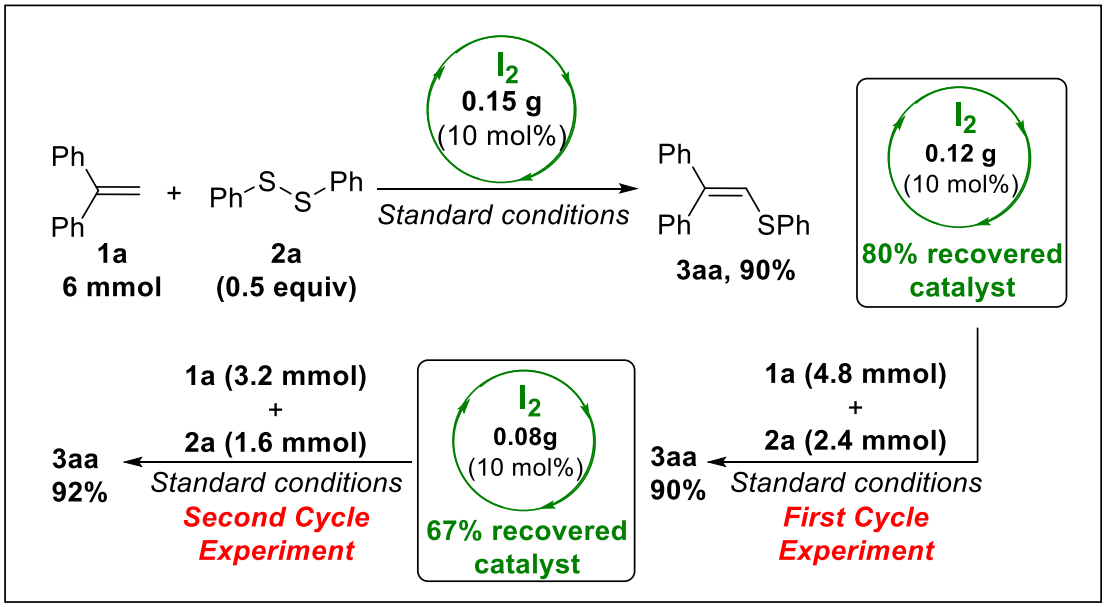

To demonstrate the synthetic utility of the method, the products such as **3aa**, **3ab** and **6aa** were further synthetically diversified to different classes of potential molecules. The results are summarized in Scheme 6.3.6.

At first, **3aa** was synthetically diversified to corresponding sulfoxide **7** and sulfone **8** by simple and controlled oxidation using *m*-CPBA or Oxone (Scheme 6.3.6). When **3aa** was treated with chloramine T, a new class of molecule, *i.e.*, **9** was formed in 78% yield. Notably, a biologically active heterocyclic scaffold *i.e.*, benzo[*b*]thiophene,[4] in particular, 3-phenylbenzo[*b*]thiophene **10** was synthesized through a sulfur-directed, Pd-catalyzed, C-H sulfenylation of **3aa** (Scheme 6.3.6).[5] The AIEgen, (4-Bromophenyl)(2,2-diphenylvinyl)sulfane **3ab** was also synthetically diversified to access **11** and **12** by Suzuki and Sonogashira cross-coupling reactions respectively.

Scheme 6.3.6. Synthetic Diversification of **3aa, 3ab** and **6aa**.

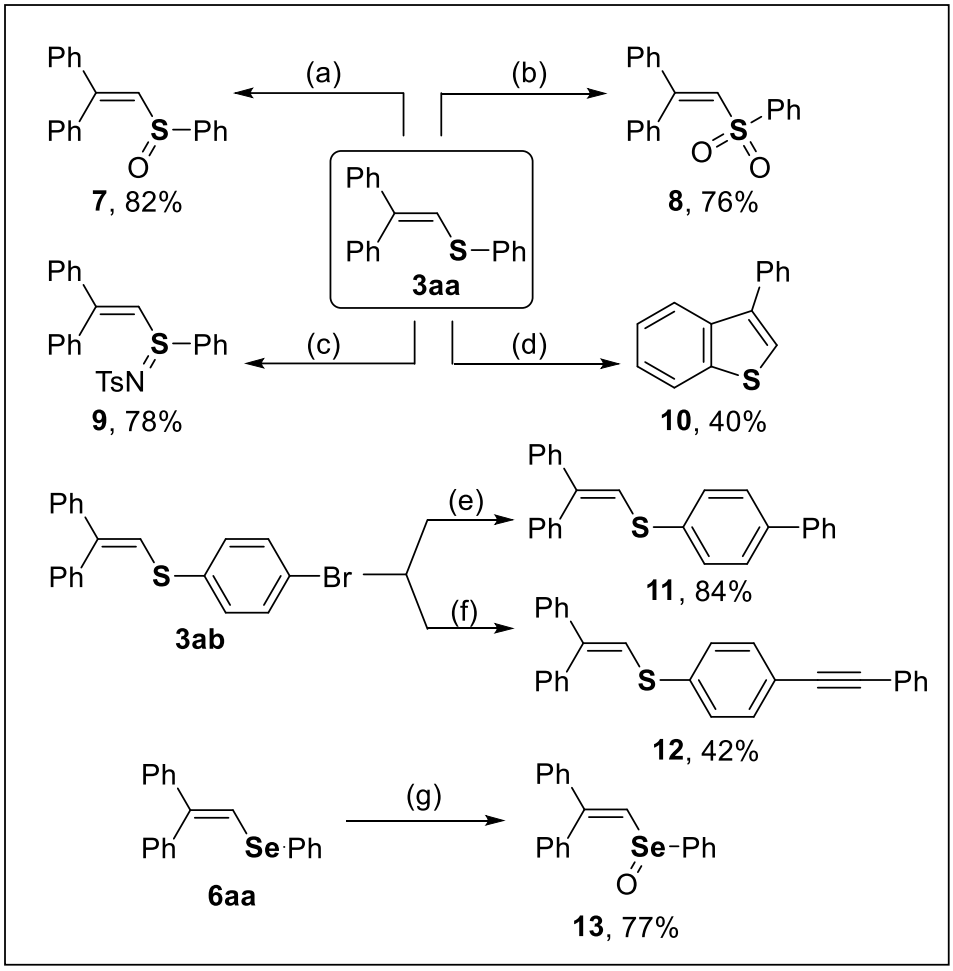

Reaction conditions: (a) *m*-CPBA (1.05 equiv), DCM, 0-5 ^{o}C; (b) Oxone (6 equiv), EtOH, 60 ^{o}C; (c) Chloramin T (2.1 equiv), AcOH (20 mol%), MeCN, 80 ^{o}C; (d) $Pd(OAc)_2$ (15 mol%), 2,6-$Me_2C_6H_3CO_2H$ (45 mol%), toluene, 140 ^{o}C; (e) $PhB(OH)_2$ (1.1 equiv), $Pd(PPh_3)_4$ (5 mol%); K_2CO_3 (3 equiv), EtOH:H_2O:toluene (1:1:3); (f) Phenyl acetylene (1.2 equiv), $Pd(PPh_3)_2Cl_2$ (3 mol%), CuI (3 mol%), Et_3N, 80 ^{o}C (g) *m*-CPBA (1.05 equiv), DCM, 0-5 ^{o}C.

To shed light on the reaction mechanism, several control experiments were conducted which are summarized in Scheme 6.3.7 When the reaction of **1a** with **2a** was conducted in the presence of 1 equiv of iodine, **3aa** was formed in 50% yield along with the formation of (2-iodoethene-1,1-diyl)dibenzene **14** in 20% yield (Scheme 6.3.7.A), which revealed that the use of stoichiometric iodine had a negative impact on the reaction outcome. In the absence of **2a**, **14** was formed in 91% yield using 1 equiv iodine, however, **14** was formed in trace amount when only 10 mol% iodine was used. When **14** was treated with **2a** under the standard reaction condition, **3aa** was not formed at all which revealed that **14** is not an intermediate of the reaction.

Scheme 6.3.7. Control Experiments.

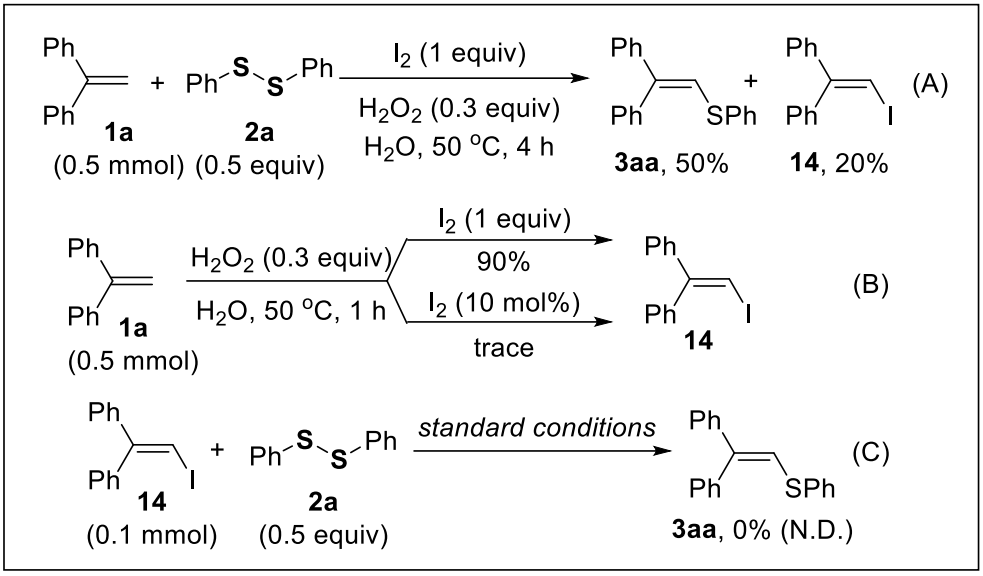

Next, we conducted the reaction of **1a** with **2a** and **5a** in the presence of various radical quenchers such as BHT, galvinoxyl radical, and TEMPO. The results are summarized in Table 6.3.9.

Table 6.3.9. Radical Quenching Experiments.

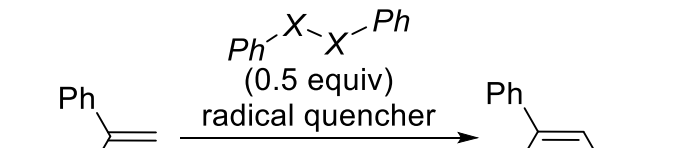

entry	radical quencher (equiv)	yield (%)[a] 3aa	6aa
1	BHT (3)	38	54
2	galvinoxyl radical (3)	35	78
3	TEMPO (3)	0	0

[a]Yield of **3aa/6aa** was determined by the ^{1}H NMR of the crude reaction mixture using 1,3,5-trimethoxybenzene as the internal standard.

While in the presence of BHT, the formation of **3aa** and **6aa** quenched to a certain extent, in the presence of TEMPO it was quenched fully which suggested a radical pathway for these reactions.

Based on the radical quenching experiments and the previous literature reports[1b, 1c] we proposed a plausible mechanism for the synthesis of **3aa**/**6aa** from **1a** (Scheme 6.3.8). Diphenyl disulfide (**3a**) or diphenyl diselenide (**5a**) reacted with iodine to form the corresponding phenyl chalcogenyl iodide (**D**) *in situ* which underwent hemolytic cleavage to form phenyl chalcogenyl radical (**E**) and iodine radical.[6]

Scheme 6.3.8. Plausible Reaction Mechanism.

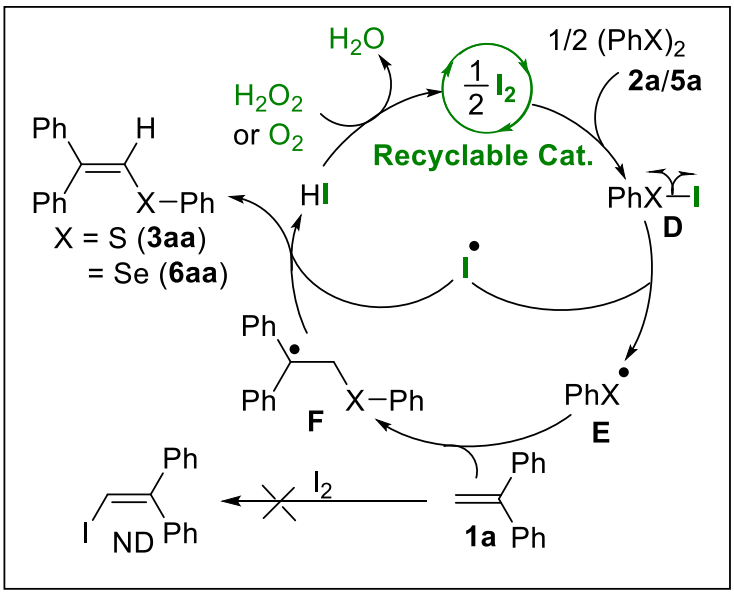

Then phenyl chalcogenyl radical **E** was added to the terminal carbon of **1a** to furnish a relatively more stable radical **F**. The radical **F** captured the iodine radical which underwent the elimination of HI under the reaction conditions to furnish the desired product **3aa**/**6aa**. Finally, HI was oxidized by H_2O_2 and/or aerobic oxygen to regenerate iodine in the catalytic cycle along with the formation of water as the only byproduct.

6.3.3. Conclusions.

In conclusion, we have developed a metal-free, iodine-catalyzed oxidative C-H chalcogenation of 1,1-diaryl ethenes in water for the highly atom-economic, cost-effective, and sustainable synthesis of a wide variety of valuable trisubstituted vinyl sulfides and selenides including some AIEgens (**3ab**, **3ae** and **3af**). The transformation required only 10 mol% iodine as a catalyst and 0.3 equiv of a green oxidant, H_2O_2, and proceeded under mild conditions, *i.e.*, 50

^{o}C and an aerobic atmosphere. The gram-scale reactions were found straightforward revealing the practicality of the developed method. Significantly, the green metrics, *i.e.*, atom-economy, atom-efficiency, carbon-efficiency, reaction-mass efficiency, E-factor and EcoScale score of the developed protocol for the synthesis of **3aa** and **6aa** from **1a** in a gram scale were found excellent. Notably, the catalyst, iodine could be recovered after the reaction during the column chromatography stage and recycled for two successive runs without any compromization in the reaction outcome, revealing the high sustainability of the developed protocol. To the best of our knowledge, this is the first report on both C-H sulfenylation and selenation of alkenes under metal-free, mild conditions in water. We believe this green strategy of C-H chalcogenation will find useful applications in preparing valuable molecules including vinyl chalcogenides in a cost-effective, sustainable, and practical manner.

6.3.4. Experimental Section.

General Experimental Procedure for the Synthesis of Vinyl Sulfanes (3aa-3an, 3bi, 3ci and 3ba−3fa) and Vinyl Selanes (6aa-6aj and 6ba−6ia).

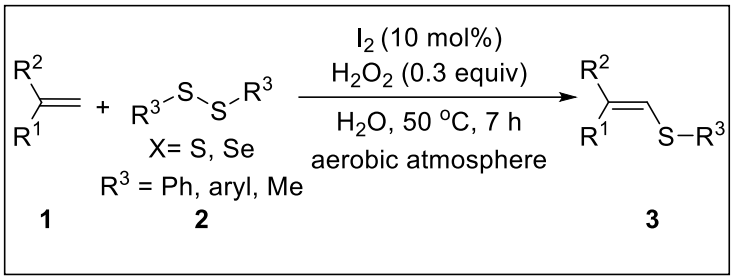

Representative Experimental Procedure for the Synthesis of (2,2-Diphenylvinyl)(phenyl)sulfane (3aa):

Ethene-1,1-diyldibenzene 1a (0.088 mL, 0.5 mmol, 1 equiv), I_2 (0.013 g, 0.05 mmol) and 1,2-diphenyldisulfane 2a (0.055 g, 0.25 mmol, 0.5 equiv) in a round-bottom flask (RBF) and H_2O (0.3 mL). was added to it. Then 30% aqueous H_2O_2 (v/v) (0.015 mL, 0.15 mmol, 0.3 equiv) was added and the reaction mixture was stirred at 50 ^{o}C under aerobic atmosphere. The progress of the reaction was monitored by TLC and after 7 h both the starting materials were found to be fully converted to product. To avoid the huge-solvent-consuming column chromatographic technique, we first quenched the iodine by saturated $Na_2S_2O_8$ solution and then the product was separated from the reaction mixture by simple work-up using EtOAc (3 x 25 mL). The organic layers were combined and washed with water and evaporated to dryness which furnished the pure product, (2,2-diphenylvinyl)(phenyl)sulfane 3aa (0.135 g, 0.47 mmol) in 94% yield. The

reactions were staring materials were not fully consumed, column chromatographic purification were conducted to obtain the pure product.

Experimental Procedure for the Synthesis of 2-(Phenylsulfinyl)ethene-1,1-diyl)dibenzene 7 and (2-(Phenylsulfonyl)ethene-1,1-diyl)dibenzene 8.

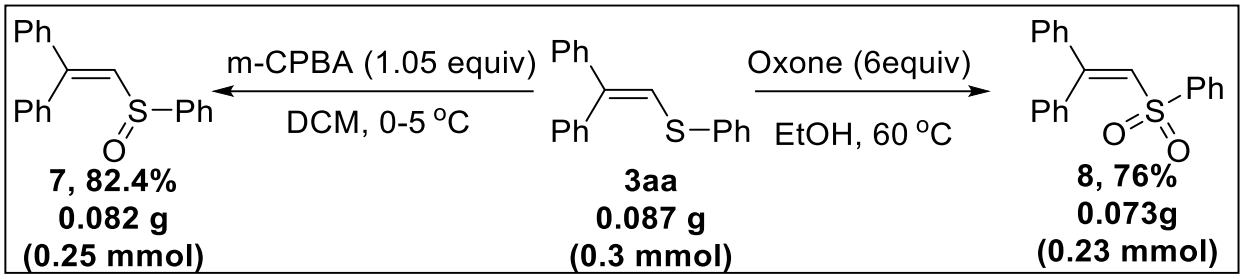

Experimental Procedure for the Synthesis of 2-(Phenylsulfinyl)ethene-1,1-diyl)dibenzene 7:

3-Chloroperoxybenzoic acid, *m*-CPBA (purity: 65-70%) (0.140 g, 0.32 mmol) was added to the solution of (2,2-diphenylvinyl)(phenyl)sulfane **3aa** (0.087 g, 0.3 mmol, 1 equiv) dissolved in dichloromethane, DCM (2.5 mL) at 0 °C. Then, the reaction mixture was stirred vigorously for 2 h at room temperature. The progress of the reaction was monitored by TLC and after the completion of the reaction the solvent was evaporated under reduced pressure. The crude reaction mixture was extracted with DCM thrice (3 x 10 mL). The combined organic layer was washed with water (3 x 10 mL) and evaporated under reduced pressure. The crude product was purified by flash column chromatography through silica gel to afford the (2-(phenylsulfinyl)ethene-1,1-diyl)dibenzene **7** in (0.082 g, 0.25 mmol) in 82% yield.

Experimental Procedure for the Synthesis of (2-(Phenylsulfonyl)ethene-1,1-diyl)dibenzene 8:

Oxone (1.11 g, 1.8 mmol) was added to the solution of (2,2-diphenylvinyl)(phenyl)sulfane **3aa** (0.091 g, 0.3 mmol, 1 equiv) in ethanol (1.5 mL). The reaction mixture was stirred at 60 °C. The progress of the reaction was monitored by TLC until completion. After the completion of the reaction, the solvent was evaporated under reduced pressure. The crude reaction mixture was extracted with ethyl acetate thrice (3 x 10 mL). The combined organic layer was washed with water (3 x 10 mL) and evaporated under reduced pressure. The crude product was purified by flash column chromatography through silica gel to afford (2-(phenylsulfonyl)ethene-1,1-diyl)dibenzene **8** in (0.073 g, 0.23 mmol) 76% yield.

Experimental Procedure for the Synthesis of *N*-((2,2-Diphenylvinyl)(phenyl)-λ_4-sulfanylidene)-4-methylbenzenesulfonamide (9):

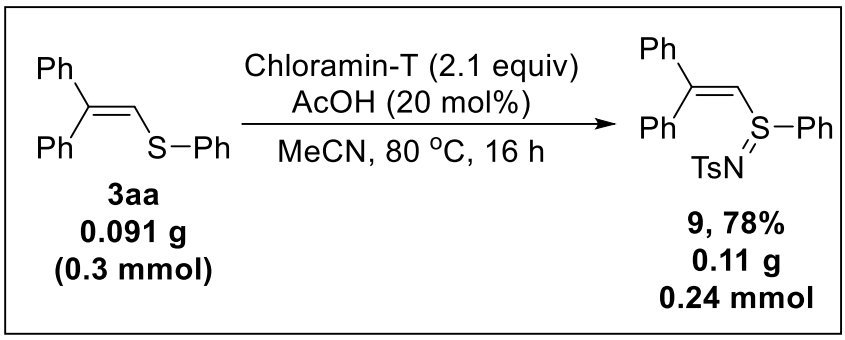

To a solution of (2,2-Diphenylvinyl)(phenyl)sulfane 3aa (0.091 g, 0.3 mmol) in MeCN (0.1 M) was added Chloramin-T trihydrate (0.18 g , 0.63 mmol) and glacial acetic acid (3 μL, 0.06 mmol). The reaction mixture was then refluxed at 80 °C for 16 h. The mixture was allowed to cool to room temperature. The solvent was removed under reduced pressure. The crude reaction mixture was extracted with ethyl acetate thrice (3 x 30 mL). The combined organic layer was washed with brine solution (30 mL) and concentrated under reduced pressure. The crude product was purified by flash column chromatography through silica gel to afford N-((2,2-diphenylvinyl)(phenyl)-λ_4-sulfanylidene)-4-methylbenzenesulfonamide 9 (0.11 g, 0.24 mmol) in 78% yield.

Experimental Procedure for the Synthesis of 3-Phenylbenzo[*b*]thiophene [5]

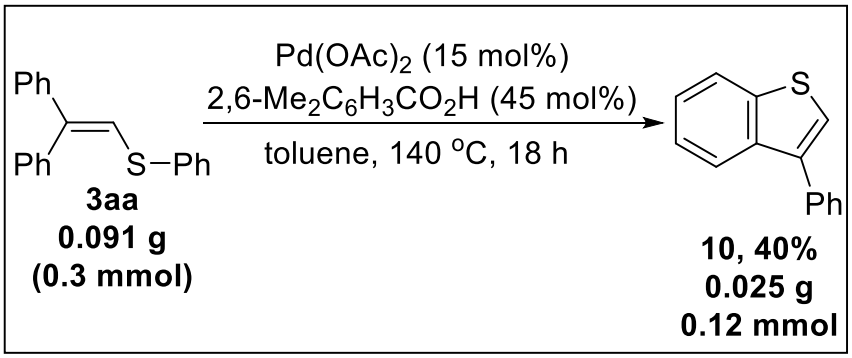

(2,2-diphenylvinyl)(phenyl)sulfane **3aa** (0.091 g, 0.3 mmol), diacetoxypalladium (0.010 g, 0.045 mmol, 1 equiv) , 2,6-dimethylbenzoic acid (0.021 g, 0.135 mmol) in toluene (1.5 M) were taken in a 10 mL RBF. The reaction mixture was refluxed at 140 °C for 16 h. The mixture was cooled to room temperature and extracted with ethyl acetate (30x3 mL) three times. The combined organic layer was further washed with brine (30 mL) and subsequently dried over anhydrous Na_2SO_4. Finally, the solvent was evaporated under reduced pressure to get the crude

product which was purified by flash column chromatography on silica gel to afford 3-phenylbenzo[*b*]thiophene **10** (0.025 g, 0.12 mmol) in 40% yield.

Experimental Procedure for the Synthesis of [1,1'-Biphenyl]-4-yl(2,2-diphenylvinyl)sulfane (11):

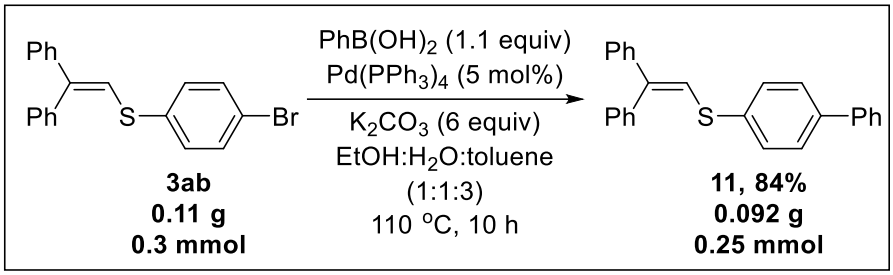

4(4-Bromophenyl)(2,2-diphenylvinyl)sulfane 3ab (0.11 g, 0.3 mmol, 1 equiv), phenyl boronic acid (0.040 g, 0.33 mmol), $Pd(PPh_3)_4$ (0.017 g, 0.015 mmol), K_2CO_3 (0.124 g, 0.9 mmol) and solvent (1 mL, EtOH : H_2O : PhMe = 1:1:3) were taken in a 25 mL RBF. The reaction mixture was refluxed at 110 °C and the progress of the reaction was monitored by thin layer chromatography. The mixture was cooled to room temperature and extracted with ethyl acetate (30x3 mL) three times. The combined organic layer was further washed with brine (30 mL) and subsequently dried over anhydrous Na_2SO_4. Finally the solvent was evaporated under reduced pressure to get the crude product which was purified by flash column chromatography on silica gel to afford [1,1'-biphenyl]-4-yl(2,2-diphenylvinyl)sulfane 11 (0.092 g, 0.25 mmol) in 84% yield.

Experimental Procedure for The Synthesis of (2,2-diphenylvinyl)(4-(phenylethynyl)phenyl)sulfane (12):

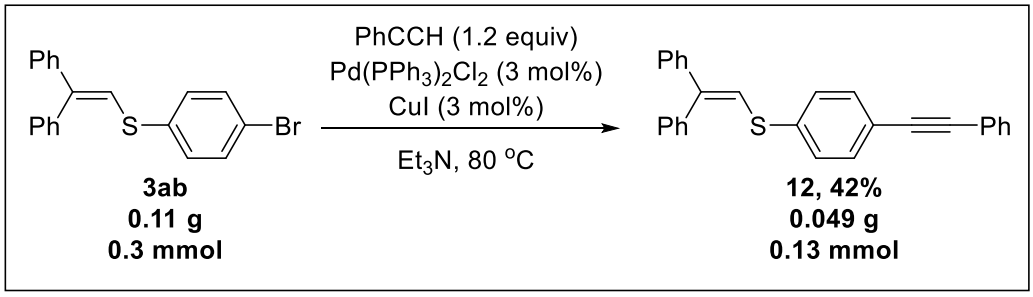

To a solution of 4(4-Bromophenyl)(2,2-diphenylvinyl)sulfane 3ab (0.11 g, 0.3 mmol, 1 equiv) in Et_3N (3 mL) were added $PdCl_2(PPh_3)_2$ (0.006 g , 0.009 mmol) and CuI (0.0017 g, 0.009 mmol) under nitrogen atmosphere in a standard Schlenk-line process. The reaction mixture was stirred for 5 min under an inert atmosphere. Then, 2-phenyl acetylene (40 µL, 0.36 mmol, 1.2

equiv) was added to the reaction mixture. The resulting mixture was then heated under an inert atmosphere at 80 °C for 18 h. The mixture was allowed to cool to room temperature. The solvent was evaporated under reduced pressure. The crude reaction mixture was extracted with ethyl acetate thrice (3 x 30 mL). The combined organic layer was washed with brine solution (30 mL) and concentrated under reduced pressure. The crude product was purified by flash column chromatography through silica gel to afford the product (2,2-diphenylvinyl)(4-(phenylethynyl)phenyl)sulfane 12 (0.049 g, 0.13 mmol) in 42% yield.

Experimental Procedure for the Synthesis of (2-(Phenylseleninyl)ethene-1,1-diyl)dibenzene (13):

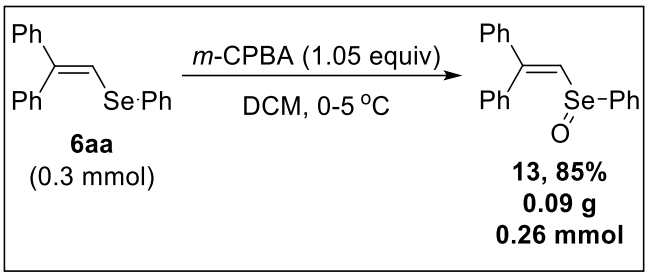

3-Chloroperoxybenzoic acid, *m*-CPBA (purity: 65-70%) (0.140 g, 0.32 mmol) was added to a solution of (2,2-diphenylvinyl)(phenyl)selane **6aa** (0.168 g, 0.3 mmol) dissolved in dichloromethane (2.5 mL) at 0 °C. The reaction mixture was cooled at 0 °C. Then, the reaction mixture was stirred vigorously for 2 h. After the completion of the reaction the solvent was evaporated under reduced pressure. The crude reaction mixture was extracted with dichloromethane thrice (3 x 10 mL). The combined organic layer was washed with water (3 x 10 mL) and evaporated under reduced pressure. The crude product was purified by flash column chromatography through silica gel to afford the (2-(phenylseleninyl)ethene-1,1-diyl)dibenzene **13** in (0.09 g, 0.26 mmol) in 85% yield.

6.3.5. Analytical Data of All Synthesized Products (3aa - 3an, 3ba – 3fa, 3bi, 3ci and 4, 6aa - 6aj, 6ba – 6ia, 7 - 14).

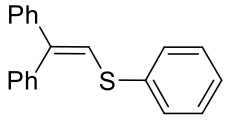

(2,2-Diphenylvinyl)(phenyl)sulfane (3aa):[2] White solid (0.135 g, 94%); eluent hexane; **^{1}H NMR (400 MHz, $CDCl_3$)** δ 7.54 – 7.48 (m, 4H), 7.45 (m, 3H), 7.42 – 7.36 (m, 3H), 7.35 (d, *J* = 2.9 Hz, 3H), 7.32 (m, 2H), 6.95

(s, 1H). **^{13}C{^{1}H} NMR (100 MHz, CDCl$_3$)** δ 141.4, 141.0, 139.1, 136.5, 129.7, 129.5, 129.1, 128.3, 128.3, 127.7, 127.3, 127.2, 126.7, 124.1.

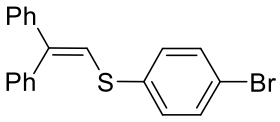

(4-Bromophenyl)(2,2-diphenylvinyl)sulfane (3ab):[2] White solid (0.138 g, 75%); eluent hexane; **^{1}H NMR (400 MHz, CDCl$_3$** δ 7.39 – 7.07 (m, 14H), 6.68 (s, 1H). **^{13}C{^{1}H} NMR (100 MHz, CDCl$_3$)** δ 142.1, 141.2, 138.9, 135.7, 132.1, 130.8, 129.7, 128.4, 128.3, 127.9, 127.5, 127.2, 122.9, 120.6.

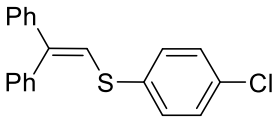

(4-Chlorophenyl)(2,2-diphenylvinyl)sulfane (3ac):[2] White solid (0.15 g, 94%); eluent hexane; **^{1}H NMR (400 MHz, CDCl$_3$**) δ 7.49 – 7.44 (m, 2H), 7.43 – 7.37 (m, 5H), 7.36 – 7.29 (m, 7H), 6.83 (s, 1H). **^{13}C NMR (100 MHz, CDCl$_3$)** δ 141.9, 141.2, 138.9, 135.0, 132.7, 130.6, 129.7, 129.2, 128.4, 128.3, 127.9, 127.5, 127.2, 123.2.

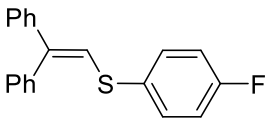

2,2-Diphenylvinyl)(4-fluorophenyl)sulfane (3ad):[2] White solid (0.14 g, 92%); eluent hexane; **^{1}H NMR (400 MHz, CDCl$_3$**) δ 7.30 (m, 4H), 7.23 (m, 3H), 7.17 – 7.10 (m, 5H), 6.94 – 6.85 (m, 2H), 6.65 (s, 1H). **^{13}C{^{1}H} NMR (100 MHz, CDCl$_3$)** δ 162.1 (d, $^{1}J_{C\text{-}F}$ = 246 Hz), 141.3, 140.8, 139.0, 132.0 (d, $^{3}J_{C\text{-}F}$ = 8 Hz), 131.5 (d, $^{4}J_{C\text{-}F}$ = 4 Hz), 129.7, 128.4, 128.2, 127.8, 127.3, 127.1, 124.6, 116.2(d, $^{2}J_{C\text{-}F}$ = 22 Hz) (Overlapping peaks present). **^{19}F NMR (376 MHz, CDCl$_3$)** δ -114.45 (s).

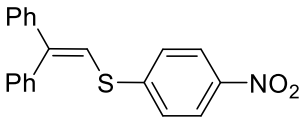

(2,2-Diphenylvinyl)(4-nitrophenyl)sulfane (3ae):[2] Yellow solid (0.13 g, 79%); eluent hexane; **^{1}H NMR (400 MHz, CDCl$_3$**) δ 8.17 (d, *J* = 9.0 Hz, 2H), 7.48 (d, *J* = 9.0 Hz, 2H), 7.45 – 7.42 (m, 2H), 7.36 – 7.30 (m, 8H), 6.87 (s, 1H). **^{13}C{^{1}H} NMR (100 MHz, CDCl$_3$)** δ 146.61, 146.33, 145.70, 140.77, 138.56, 129.57, 128.47, 128.32, 128.19, 128.12, 127.42, 127.21, 124.13, 118.51.

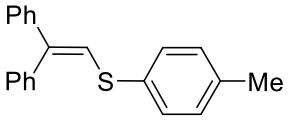

(2,2-Diphenylvinyl)(p-tolyl)sulfane (3af):[2] White solid (0.103 g, 68%); eluent hexane; **^{1}H NMR (400 MHz, CDCl$_3$**) δ 7.27 (s, 1H), 7.27 – 7.18 (m, 6H), 7.13 – 7.06 (m, 5H), 6.99-6.97 (m, 2H), 6.70 (s, 1H), 2.18 (s, 3H). **^{13}C{^{1}H} NMR (100 MHz, CDCl$_3$)** δ 141.5, 140.1, 139.2, 136.9, 132.8, 130.0, 129.8, 129.7, 128.3, 128.2, 127., 127.1, 125.2, 21.0 (overlapping peaks are present).

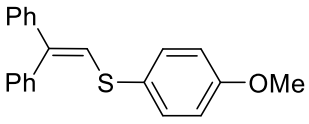

(2,2-Diphenylvinyl)(4-methoxyphenyl)sulfane (3ag):[2] Colourless liquid (0.13 g, 82%); eluent hexane; **^{1}H NMR (400 MHz, CDCl$_3$)** δ 7.29-7.24 (m, 6H), 7.22 (s, 1H), 7.11-7.10 (m, 5H), 6.76-6.73 (m, 2H), 6.65 (s, 1H), 3.64 (s, 3H). **^{13}C{^{1}H} NMR (100 MHz, CDCl$_3$)** δ 159.2, 141.4, 139.1, 132.5, 129.7, 128.3, 128.2, 127.6, 127.03, 126.99, 126.7, 126.5, 114.7, 55.3 (overlapping peaks are present).

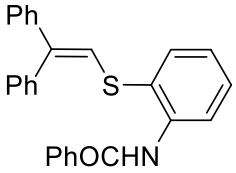

***N*-(2-((2,2-Diphenylvinyl)thio)phenyl)benzamide (3ah):** Yellow liquid (0.11 g, 52%); eluent hexane; **^{1}H NMR (400 MHz, CDCl$_3$)** δ 8.92 (brS, 1H), 8.62 (dd, *J* = 8.3, 1.1 Hz, 1H), 7.90 – 7.78 (m, 2H), 7.67 (dd, *J* = 7.7, 1.4 Hz, 1H), 7.57 – 7.52 (m, 1H), 7.49 – 7.41 (m, 6H), 7.32 (dd, *J* = 8.0, 1.5 Hz, 2H), 7.23 (dd, *J* = 5.1, 1.8 Hz, 3H), 7.18 – 7.10 (m, 3H), 6.49 (s, 1H). **^{13}C{^{1}H} NMR (100 MHz, CDCl$_3$)** δ 165.2, 142.4, 140.7, 139.3, 138.6, 134.8, 134.6, 132.0, 130.5, 129.6, 128.8, 128.5, 128.3, 128.2, 127.6, 127.2, 127.1, 124.4, 124.0, 123.2, 120.8. **HRMS (ESI)**, m/z calcd for $C_{27}H_{22}NOS$ $[M + H]^+$: 408.1417; found: 408.1390.

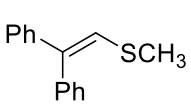

(*E*)-Phenyl(styryl)selane (3ai):[2] Yellow oil (0.109 g, 96%); eluent hexane; **^{1}H NMR (400 MHz, CDCl$_3$** δ 7.31 – 7.27 (m, 2H), 7.24 – 7.20 (m, 3H), 7.15 (s, 1H), 7.12 (m, 4H), 6.45 (s, 1H), 2.25 (s, 3H). **^{13}C{^{1}H} NMR (100 MHz, CDCl$_3$)** δ 141.7, 139.4, 138.3, 129.63 128.3, 128.2, 127.6, 127.5, 126.9, 126.8, 17.9.

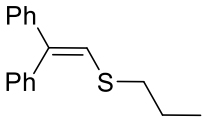

(2,2-Diphenylvinyl)(propyl)sulfane (3aj): Yellow liquid (0.12 g, 92%); eluent hexane; **^{1}H NMR (400 MHz, CDCl$_3$)** δ 7.51-7.48 (m, 1H), 7.47 (d, *J* = 2.0 Hz, 1H), 7.45 (d, *J* = 1.7 Hz, 1H), 7.43 (m, 1H), 7.40 (m, 1H), 7.37-7.35 (m, 2H), 7.34 – 7.30 (m, 3H), 6.70 (s, 1H), 2.86 – 2.81 (m, 2H), 1.81 (d, *J* = 7.3 Hz, 2H), 1.11 (t, *J* = 7.3 Hz, 3H). **^{13}C{^{1}H} NMR (100 MHz, CDCl$_3$)** δ 141.9, 139.5, 138.2, 129.62 128.2, 128.1, 127.3, 126.9, 126.7, 126.3, 36.8, 23.6, 13.2. **HRMS (ESI)**, m/z calcd for $C_{18}H_{19}S$ $[M + H]^+$: 255.1202; found: 255.1169.

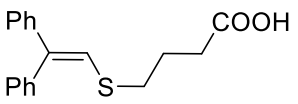

4-((2,2-Diphenylvinyl)thio)butanoic acid (3ak): Yellow viscous liquid (0.11 g, 76%); eluent hexane; **^{1}H NMR (400 MHz, CDCl$_3$)** δ 7.31-7.29 (m, 3H), 7.25 – 7.20 (m, 3H), 7.14 – 7.12 (m, 4H), 6.47 (s, 1H), 2.73 (t, *J* = 7.1 Hz, 2H), 2.42 (t, *J* = 7.2 Hz, 2H), 1.97 – 1.89 (m, 2H). **^{13}C NMR (100 MHz, CDCl$_3$)** δ 179.0,

141.7, 139.4, 139.3, 129.6, 128.3, 128.2, 127.5, 126.95, 126.9, 125.2, 33.8, 32.3, 25.1. **HRMS (ESI)**, m/z calcd for $C_{18}H_{18}O_2S$ [M]: 298.1028; found: 298.1053.

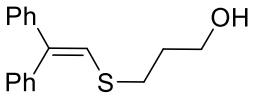

3-((2,2-Diphenylvinyl)thio)propan-1-ol (3al): Viscous liquid (0.084 g, 62%); eluent hexane; **^{1}H NMR (400 MHz, $CDCl_3$)** δ 7.30 – 7.28 (m, 2H), 7.24 – 7.22 (m, 3H), 7.19 – 7.17 (m, 2H), 7.16 – 7.11 (m, 3H), 6.59 (s, 1H), 2.88 – 2.80 (m, 1H), 1.96 (d, *J* = 2.9 Hz, 1H), 1.74 – 1.68 (m, 2H), 1.35-1.25 (m, 2H).**^{13}C{^{1}H} NMR (100 MHz, $CDCl_3$)** δ 178.6, 141.7, 139.5, 139.4, 129.7, 128.3, 128.2, 127.5, 127.0, 126.9, 125.2, 33.8, 32.2, 25.1. **Anal** calcd for $C_{17}H_{18}OS$: C, 75.52; H, 6.71; S, 11.86; found C, 75.40; H, 6.82; S, 11.79.

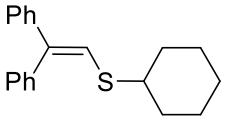

Cyclohexyl(2,2-diphenylvinyl)sulfane (3am): Colourless oil (0.097 g, 69%); eluent hexane; **^{1}H NMR (400 MHz, $CDCl_3$)** δ 7.30 – 7.28 (m, 3H), 7.23 (d, *J* = 7.4 Hz, 2H), 7.119 – 7.17 (m, 2H), 7.16 – 7.11 (m, 3H), 6.59 (s, 1H), 2.88 – 2.80 (m, 1H), 2.02 – 1.94 (m, 2H), 1.74 – 1.68 (m, 2H), 1.58 – 1.53 (m, 1H), 1.40 – 1.16 (m, 5H). **^{13}C{^{1}H} NMR (100 MHz, $CDCl_3$)** δ 142.2, 139.7, 138.2, 129.7, 128.2, 128.2, 127.3, 127.0, 126.7, 124.7, 46.8, 33.8, 26.1, 25.6. **HRMS (ESI)**, m/z calcd for $C_{20}H_{22}S$ [M]: 294.1442; found: 294.1437.

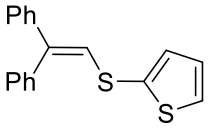

2-((2,2-Diphenylvinyl)thio)thiophene (3an):[2] White solid (0.109 g, 74%); eluent hexane; **^{1}H NMR (400 MHz, $CDCl_3$)** δ 7.37 – 7.32 (m, 2H), 7.31 – 7.25 (m, 4H), 7.20 – 7.14 (m, 3H), 7.13 – 6.91 (m, 4H), 6.63 (s, 1H). **^{13}C NMR (100 MHz, $CDCl_3$)** δ 141.0, 139.2, 138.8, 133.9, 132.7, 129.7, 129.3, 128.5, 128.3, 127.9, 127.6, 127.3, 127.1.

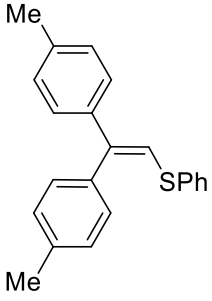

(2,2-Di-*p*-tolylvinyl)(phenyl)sulfane (3ba):[2] Colourless liquid (0.124 g, 78%); eluent hexane; **^{1}H NMR (400 MHz, $CDCl_3$)** δ 7.35 – 7.31 (m, 2H), 7.22 (t, *J* = 7.6 Hz, 2H), 7.15 – 7.14 (m, 5H), 7.07 (d, *J* = 8.2 Hz, 2H), 7.00 (d, *J* = 7.9 Hz, 2H), 6.68 (s, 1H), 2.30 (s, 3H), 2.24 (s, 3H). **^{13}C{^{1}H} NMR (100 MHz, $CDCl_3$)**, δ 141.4, 138.9, 137.5, 137.1, 136.8, 136.4, 129.6, 129.3, 129.03, 128.96, 128.2, 127.2, 126.6, 122.4, 21.3, 21.1.

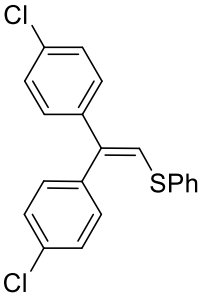

(2,2-Bis(4-chlorophenyl)vinyl)(phenyl)sulfane (3ca): White solid (0.16 g, 91%); eluent hexane; **^{1}H NMR (400 MHz, CDCl$_3$)** δ 7.38 – 7.33 (m, 3H), 7.31 – 7.26 (m, 3H), 7.22 – 7.16 (m, 5H), 7.08 – 7.06 (m, 2H), 6.76 (s, 1H). **^{13}C{^{1}H} NMR (100 MHz, CDCl$_3$)** δ 139.6, 138.2, 137.1, 135.7, 133.8, 133.3, 131.1, 129.8, 129.2, 128.8, 128.6, 128.34, 127.2, 125.7.**HRMS (ESI)**, m/z calcd for $C_{20}H_{15}Cl_2S$ $[M + H]^+$: 356.0193; found: 356.0160.

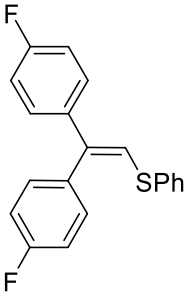

((2,2-Bis(4-fluorophenyl)vinyl)(phenyl)sulfane (3da): Yellow oil (0.126 g, 78%); eluent hexane; **^{1}H NMR (400 MHz, CDCl$_3$)** δ 7.31 (d, *J* = 7.4 Hz, 2H), 7.23 – 7.18 (m, 4H), 7.13 (d, *J* = 7.2 Hz, 1H), 7.09 – 7.05 (m, 2H), 6.99 (t, *J* = 8.7 Hz, 2H), 6.85 (t, *J* = 8.6 Hz, 2H), 6.66 (s, 1H). **^{13}C NMR (100 MHz, CDCl$_3$** δ 162.20 (d, $^{1}J_{C\text{-}F}$ = 246 Hz), 162.21 (d, $^{1}J_{C\text{-}F}$ = 246 Hz), 138.9, 137.5, 136.0, 134.9, 131.45 (d, $^{3}J_{C\text{-}F}$ = 8 Hz), 129.6, 129.2, 128.7 (d, $^{3}J_{C\text{-}F}$ = 8 Hz), 127.0, 124.3, 115.2 (d, $^{2}J_{C\text{-}F}$ = 21 Hz), 115.4 (d, $^{2}J_{C\text{-}F}$ = 21 Hz). **^{19}F NMR (376 MHz, CDCl$_3$)** δ -113.28 (s), -114.51 (s). **HRMS (ESI)**, m/z calcd for $C_{20}H_{15}F_2S$ $[M + H]^+$: 325.0857; found: 325.0811.

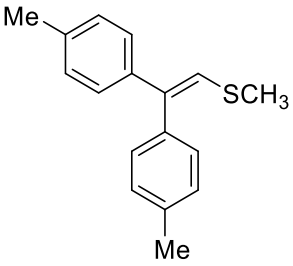

(2,2-Di-p-tolylvinyl)(methyl)sulfane (3bi): Yellow solid (0.12 g, 92%); eluent hexane; mp = 65 - 67 ^{o}C; **^{1}H NMR (400 MHz, CDCl$_3$)** δ 7.21 (s, 4H), 7.12 – 7.10 (m, 2H), 6.48 (s, 1H), 2.39 (s, 3H), 2.37 (s, 3H), 2.34 (s, 3H). **^{13}C{^{1}H} NMR (100 MHz, CDCl$_3$)** δ 139.1, 138.4, 137.1, 136.6, 136.5, 129.5, 128.9, 128.9, 126.9, 126.1, 21.3, 21.0, 18.0. **HRMS (ESI)**, m/z calcd for $C_{17}H_{18}S$ [M]: 254.1129; found: 254.1199. The assignment is also supported by an X-ray crystallographic structure determination (**CCDC 2261525**).

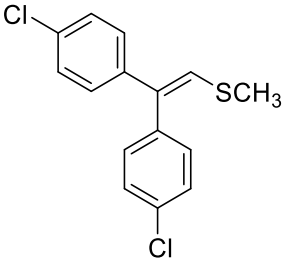

(2,2-Bis(4-chlorophenyl)vinyl)(methyl)sulfane (3ci):[2] Orange solid (011 g, 72%); eluent hexane; **^{1}H NMR (400 MHz, CDCl$_3$)** δ 7.27 (d, *J* = 8.6 Hz, 2H), 7.16 – 7.12 (m, 4H), 7.01 (d, *J* = 8.7 Hz, 2H), 6.46 (s, 1H), 2.29 (s, 3H). **^{13}C{^{1}H} NMR (100 MHz, CDCl$_3$)** δ 139.8, 137.4, 135.8, 133.4, 132.8, 131.0, 128.9, 128.7, 128.4, 128.1, 17.9.

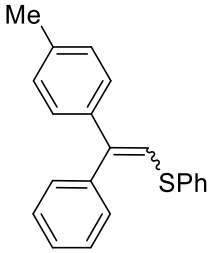

(Phenyl(2-phenyl-2-(p-tolyl)vinyl)sulfane (3ea): Colourless oil (0.114 g, 75%, Z:E = 55:45); eluent hexane; **^{1}H NMR (400 MHz, CDCl$_3$)** δ 7.39 – 7.35 (m, 5H), 7.33 – 7.25 (m, 9H), 7.22 – 7.19 (m, 10H), 7.07 (dd, J = 21.0, 5.0 Hz, 4H), 6.78 (s, 1H), 6.77 (s, 1H), 2.35 (s, 3H), 2.29 (s, 3H). **^{13}C{^{1}H} NMR (100 MHz, CDCl$_3$** δ 141.7, 141.4, 141.18, 139.3\3, 138.7, 137.6, 137.2, 136.7, 136.6, 136.2, 129.7, 129.6, 129.5, 129.4, 129.1, 129.0, 128.3, 128.3, 127.7, 127.3, 127.1, 126.7, 126.6, 123.6, 122.9 **Anal** calcd for $C_{21}H_{18}S$: C, 83.40; H, 6.00; S, 10.60; found C, 83.23; H, 5.82; S, 10.56.

.

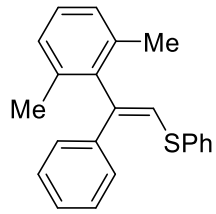

(*E*)-(2-(2,6-Dimethylphenyl)-2-phenylvinyl)(phenyl)sulfane (3fa): Colourless liquid (0.068 g, 43%); eluent hexane; **^{1}H NMR (400 MHz, CDCl$_3$)** δ 7.44 – 7.42 (m, 2H), 7.35 – 7.31 (m, 2H), 7.24 – 7.22 (m, 4H), 7.22 (s, 1H), 7.17 (d, *J* = 8.2 Hz, 2H), 7.10 (d, J = 8.0 Hz, 2H), 6.79 (s, 1H), 2.40 (s, 3H), 2.34 (s, 3H).**^{13}C{^{1}H} NMR (100 MHz, CDCl$_3$)** δ 141.4, 138.9, 137.5, 137.1, 136.8, 136.4, 129.6, 129.4, 129.04, 128.96, 128.2, 127.2, 126.6, 122.4, 21.3, 21.1. Anal calcd for $C_{22}H_{20}S$: C, 83.50; H, 6.37; S, 10.13; found C, 83.64; H, 6.31; S, 10.05.

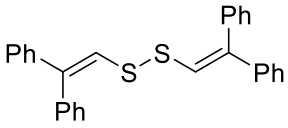

1,2-Bis(2,2-diphenylvinyl)disulfane (4): Yellow solid (0.13 g, 60%); eluent hexane; mp = 96 - 98 ^{o}C; **^{1}H NMR (400 MHz, CDCl$_3$** δ 7.49 – 7.45 (m, 8H), 7.42 – 7.40 (m, 5H), 7.37 (t, *J* = 4.3 Hz, 4H), 7.31 (d, *J* = 1.4 Hz, 3H), 6.91 (s, 2H). **^{13}C NMR (100 MHz, CDCl$_3$**) δ 141.7, 139.9, 139.0, 129.7, 128.4, 128.3, 127.7, 127.2, 124.5 (Overlapping peaks are present). **Anal** calcd for $C_{28}H_{22}S_2$: C, 79.58; H, 5.25; S, 15.17; found C, 79.40; H, 5.43; S, 15.33.

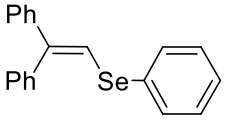

(2,2-Diphenylvinyl)(phenyl)selane (6aa):[7] Yellow solid (0.16 g, 96%); eluent hexane; **^{1}H NMR (400 MHz, CDCl$_3$)** δ 7.44 (dd, *J* = 7.5, 1.9 Hz, 2H), 7.32 – 7.19 (m, 5H), 7.19 – 7.02 (m, 8H), 7.00 (s, 1H). **^{13}C{^{1}H} NMR (100 MHz, CDCl$_3$)** δ 143.0, 141.5, 140.3, 132.4, 131.2, 129.2, 129.2, 128.4, 128.2, 127.8, 127.3, 127.2, 127.1, 122.5.

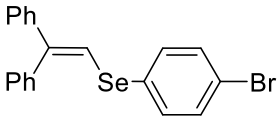

(4-Bromophenyl)(2,2-diphenylvinyl)selane (6ab):[7] White solid (0.16 g, 77%); eluent hexane; **^{1}H NMR (400 MHz, CDCl$_3$)** δ 7.32-7.31 (m, 5H), 7.30 – 7.26 (m, 2H), 7.22 – 7.19 (m, 2H), 7.16 – 7.13 (m, 5H), 6.93 (s, 1H). **^{13}C{^{1}H} NMR (100 MHz, CDCl$_3$)** δ 143.8, 141.3, 140.1, 134.0, 132.4, 130.5, 129.3, 128.5, 128.3, 128.1, 127.4, 127.2, 121.7, 121.5.

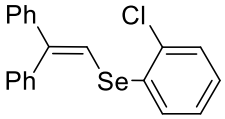

(2-Chlorophenyl)(2,2-diphenylvinyl)selane (6ac):[7] White solid (0.174 g, 94%); eluent hexane; **^{1}H NMR (400 MHz, CDCl$_3$)** δ 7.54 (dd, *J* = 7.7, 1.7 Hz, 2H), 7.40 – 7.37 (m, 4H), 7.34 – 7.30 (m, 6H), 7.19 – 7.16 (m, 1H), 7.15 – 7.13 (m, 1H), 7.10 (s, 1H).**^{13}C{^{1}H} NMR (100 MHz, CDCl$_3$)** δ 155.2, 141.5, 139.1, 135.4, 132.8, 130.3, 129.7, 128.9, 128.7, 128.7, 128.6, 128.3, 128.2, 128.0, 127.8, 127.6.

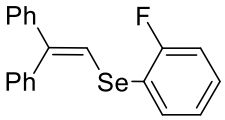

(2,2-Diphenylvinyl)(2-fluorophenyl)selane (6ad): Yellow solid (0.164 g, 93%); eluent hexane; mp = 58 - 60 ^{o}C; **^{1}H NMR (400 MHz, CDCl$_3$)** δ 7.65 – 7.60 (m, 1H), 7.51 – 7.46 (m, 2H), 7.42 (m, 3H), 7.34 – 7.28 (m, 6H), 7.18 – 7.10 (m, 3H). **^{13}C NMR (100 MHz, CDCl$_3$)** δ 161.3 (d, $^{1}J_{C\text{-}F}$ = 242Hz), 144.0, 141.4, 140.0, 133.9, 129.4, 129.3, 128.5, 128.3, 128.0, 127.4, 127.2, 124.9, 120.1, 118.2 (d, $^{2}J_{C\text{-}F}$ = 23 Hz), 115.7 (d, $^{2}J_{C\text{-}F}$ = 23 Hz). **^{77}Se NMR (76 MHz, CDCl$_3$)** δ 302.08 (s). **^{19}F NMR (376 MHz, CDCl$_3$)** δ -103.64 (s). **Anal** calcd for $C_{20}H_{15}FSe$ C, 67.99; H, 4.28 found C, 68.14; H, 4.16.

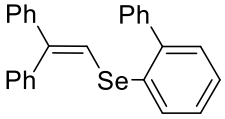

[1,1'-Biphenyl]-2-yl(2,2-diphenylvinyl)selane (6ae): Yellow solid (0.15 g, 75%); eluent hexane; mp = 87 - 89 ^{o}C; **^{1}H NMR (400 MHz, CDCl$_3$)** δ 7.74 – 7.71 (m, 1H), 7.39 – 7.33 (m, 11H), 7.28 (s, 3H), 7.24 – 7.22 (m, 2H), 7.21 – 7.19 (m, 2H), 7.06 (s, 1H). **^{13}C{^{1}H} NMR (100 MHz, CDCl$_3$)** δ 144.1, 143.9, 141.8, 141.6, 140.2, 134.2, 132.1, 132.0, 130.2, 129.4, 129.1, 128.3, 128.2, 128.1, 127.8, 127.5, 127.2, 127.0, 122.2 (Overlapping peaks are present). **^{77}Se NMR (76 MHz, CDCl$_3$)** δ 350.06 (s). **Anal** calcd for $C_{26}H_{20}Se$: C, 75.91; H, 4.90; found C, 75.80; H, 5.02.

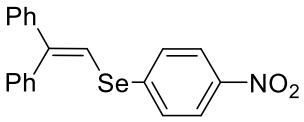

(2,2-Diphenylvinyl)(4-nitrophenyl)selane (6af): Yellow solid (0.071 g, 37%); eluent hexane; mp = 55 - 57 °C; **^{1}H NMR (400 MHz, $CDCl_3$)** δ 7.34 – 7.28 (m, 4H), 7.27 – 7.21 (m, 3H), 7.20 – 7.13 (m, 7H), 6.66 (s, 1H)·. **^{13}C{^{1}H} NMR (100 MHz, $CDCl_3$)** δ 142.1, 141.2, 138.9, 135.7, 132.1, 130.8, 129.7, 128.4, 128.3, 127.9, 127.5, 127.2, 122.9, 120.6.. **Anal** calcd for $C_{20}H_{15}NO_2Se$: C, 63.17; H, 3.98; N, 3.68; found C, 63.47; H, 3.56; N, 3.82.

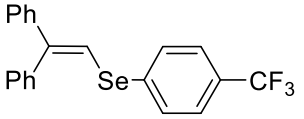

(2,2-Diphenylvinyl)(4-(trifluoromethyl)phenyl)selane (6ag):[7] White solid (0.13 g, 62%); eluent hexane; **^{1}H NMR (400 MHz, $CDCl_3$** δ 7.52 (d, *J* = 8.0 Hz, 2H), 7.42 (d, *J* = 8.1 Hz, 2H), 7.35 – 7.27 (m, 3H), 7.21 – 7.12 (m, 7H), 6.97 (s, 1H).**^{13}C NMR (100 MHz, $CDCl_3$)** δ 145.1, 141.2, 140.06, 137.0, 131.7, 129.2, 128.6, 128.4, 128.2, 127.6, 127.2, 126.0, 125.4, 124.0 (d, $^1J_{C\text{-}F}$ = 270 Hz), 120.0.

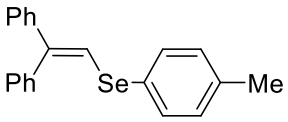

(2,2-Diphenylvinyl)(p-tolyl)selane (6ah):[7] Yellow solid (0.13 g, 73%); eluent hexane; **^{1}H NMR (400 MHz, $CDCl_3$)** δ 7.36 – 7.33 (m, 1H), 7.32 – 7.29 (m, 2H), 7.24 – 7.23 (m, 3H), 7.22 (s, 1H), 7.21 – 7.11 (m, 7H), 6.47 (s, 1H), 2.28 (s, 3H). **^{13}C NMR (100 MHz, $CDCl_3$** δ 141.7, 139.5, 138.4, 133.4, 132.9, 129.7, 128.6, 128.3, 128.2, 127.6, 127.5, 127.0, 126.8, 18.0.

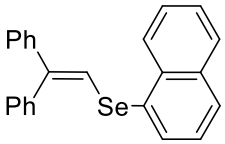

(2,2-Diphenylvinyl)(naphthalen-1-yl)selane (6ai):[7] Yellow solid (0.16 g, 84%); eluent hexane; **^{1}H NMR (400 MHz, $CDCl_3$)** δ 8.47 (d, *J* = 8.2 Hz, 1H), 8.03 (d, *J* = 7.1 Hz, 1H), 7.95 (t, *J* = 7.3 Hz, 2H), 7.69 – 7.60 (m, 3H), 7.59–7.57 (m, 3H), 7.55 – 7.49 (m, 2H), 7.33 (s, 5H), 7.21 (s, 1H). **^{13}C NMR (100 MHz, $CDCl_3$)** δ 142.9, 141.4, 140.3, 134.1, 134.0, 132.8, 130.4, 129.4, 128.9, 128.6, 128.5, 128.2, 127.9, 127.6, 127.1, 127.1, 126.8, 126.3, 125.8, 122.9.

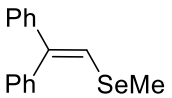

(2,2-Diphenylvinyl)(methyl)selane (6aj): White solid (0.126 g, 92%); eluent hexane; mp = 55 - 57 °C; **^{1}H NMR (400 MHz, $CDCl_3$)** δ 7.28 – 7.26 (m, 2H), 7.23 – 7.22 (m, 1H), 7.20 (d, *J* = 1.6 Hz, 1H), 7.18 (d, *J* = 1.4 Hz, 1H), 7.17 – 7.15 (m, 1H), 7.12 – 7.10 (m, 4H), 6.78 (s, 1H), 2.09 (s, 3H). **^{13}C NMR (100 MHz, $CDCl_3$)** δ 141.9, 141.8, 140.5, 129.2, 128.4, 128.2, 127.6, 126.9, 126.9, 123.0, 7.6. **Anal** calcd for $C_{15}H_{14}Se$: C, 65.94; H, 5.16 found C, 65.82; H, 5.32.

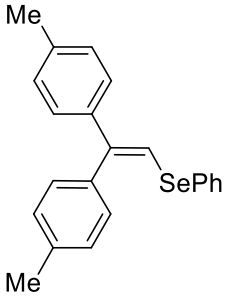

(2,2-Di-*p*-tolylvinyl)(phenyl)selane (6ba): Yellow solid (0.14 g, 78%); eluent hexane; mp = 85 - 87 °C; **^{1}H NMR (400 MHz, CDCl$_3$)** δ 7.49 – 7.46 (m, 2H), 7.23 – 7.17 (m, 3H), 7.13 (s, 4H), 7.05 (d, *J* = 8.2 Hz, 2H), 6.98 (d, *J* = 8.1 Hz, 2H), 6.94 (s, 1H), 2.30 (s, 3H), 2.23 (s, 3H). **^{13}C NMR (100 MHz, CDCl$_3$)** δ 143.2, 139.0, 137.6, 137.5, 137.0, 132.3, 131.8, 129.2, 129.2, 129.1, 128.9, 127.2, 127.1, 120.8, 21.3, 21.1. **^{77}Se NMR (76 MHz, CDCl$_3$)** δ 371.81 (s). **Anal** calcd for $C_{22}H_{20}Se$ C, 72.72; H, 5.55 found C, 72.96 ; H, 5.38.

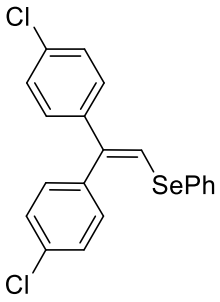

(2,2-Bis(4-chlorophenyl)vinyl)(phenyl)selane (6ca):[7] Yellow oil (0.15 g, 74%); eluent hexane; **^{1}H NMR (400 MHz, CDCl$_3$)** δ 7.50 – 7.47 (m, 2H), 7.33 – 7.30 (m, 2H), 7.25 – 7.22 (m, 3H), 7.18 (s, 1H), 7.17 – 7.15 (m, 2H), 7.14 (s, 1H), 7.05 (d, *J* = 2.1 Hz, 1H), 7.03 (d, *J* = 2.2 Hz, 2H).**^{13}C {^{1}H} NMR (100 MHz, CDCl$_3$)** δ 140.4, 139.7, 138.2, 133.9, 133.3, 132.7, 131.0, 130.7, 129.4, 128.9, 128.5, 128.3, 127.7, 124.2.

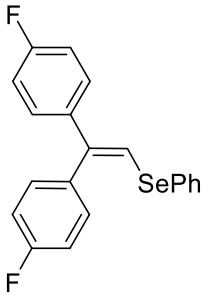

(2,2-Bis(4-fluorophenyl)vinyl)(phenyl)selane (6da): Yellow oil (0.169 g, 91%); eluent hexane; **^{1}H NMR (400 MHz, CDCl$_3$)** δ 7.65 – 7.56 (m, 2H), 7.36 – 7.32 (m, 5H), 7.25 – 7.18 (m, 2H), 7.15 (t, *J* = 8.7 Hz, 2H), 7.08 (s, 1H), 6.99 (t, *J* = 8.7 Hz, 2H). **^{13}C NMR (100 MHz, CDCl$_3$)** δ 162.3 (d, $^{1}J_{C\text{-}F}$ = 246 Hz), 162.2 (d, $^{1}J_{C\text{-}F}$ = 240 Hz), 140.9, 137.7, 136.0, 132.6, 131.2, 131.0 (d, $^{3}J_{C\text{-}F}$ = 8 Hz), 129.4, 128.5 (d, $^{3}J_{C\text{-}F}$ = 8 Hz), 127.6, 122.7, 115.5 (d, $^{2}J_{C\text{-}F}$ = 39 Hz), 115.3 (d, $^{2}J_{C\text{-}F}$ = 39 Hz),. **^{77}SeNMR (76 MHz, CDCl$_3$)** δ 378.00 (s). **^{19}F NMR (376 MHz, CDCl$_3$)** δ -113.14 (s), -114.63 (s). **HRMS (ESI)**, m/z calcd for $C_{20}H_{14}F_2Se$ [M]: 372.0229; found: 372.0237.

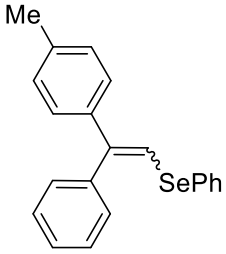

Phenyl(2-phenyl-2-(*p*-tolyl)vinyl)selane (6ea):[7] Colourless oil (0.11 g, 65%); eluent hexane; **^{1}H NMR (400 MHz, CDCl$_3$)** δ 7.51-7.46 (m, 4H), 7.38 – 7.23 (m, 6H), 7.22 – 7.17 (m, 5H), 7.16 (dd, *J* = 5.9, 2.1 Hz, 4H), 7.15 (d, *J* = 4.3 Hz, 4H), 7.11 (d, *J* = 3.8 Hz, 2H), 7.06 – 6.99 (m, 3H), 6.98 (s, 1H), 6.97 (s, 1H), 2.31 (s, 3H), 2.22 (s, 3H).**^{13}C{^{1}H} NMR (100 MHz, CDCl$_3$)** δ 143.2, 143.1, 141.7, 140.5, 138.8, 137.7, 137.4, 137.1, 132.4, 132.4, 131.7, 129.3, 129.2, 129.2, 129.0, 128.7, 128.4, 128.2, 127.8, 127.3, 127.3, 127.2, 127.1, 127.0, 122.0, 121.3, 21.3, 21.1.

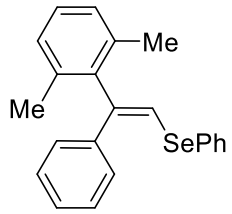

(*E*)-(2-(2,6-Dimethylphenyl)-2-phenylvinyl)(phenyl)selane (6fa): Pale yellow oil (0.1 g, 55%); eluent hexane; **^{1}H NMR (400 MHz, CDCl$_3$)** δ 7.53 – 7.42 (m, 2H), 7.21 (d, *J* = 7.0 Hz, 3H), 7.15 (s, 1H), 7.14 (s, 3H), 7.06 (d, *J* = 8.2 Hz, 2H), 6.99 (d, *J* = 8.1 Hz, 2H), 6.95 (s, 1H), 2.31 (s, 3H), 2.23 (s, 3H).**^{13}C{^{1}H} NMR (100 MHz, CDCl$_3$)** δ 143.2, 139.0, 137.6, 137.5, 137.0, 132.3, 131.8, 129.2, 129.2, 129.1, 128.9, 127.2, 127.1, 120.8, 21.3, 21.1. Anal calcd for $C_{22}H_{20}Se$: C, 72.72; H, 5.55; found C, 72.86; H, 5.38.

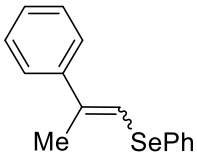

Phenyl(2-phenylprop-1-en-1-yl)selane (6ga): Yellow oil (0.042 g, 31%); eluent hexane; **^{1}H NMR (400 MHz, CDCl$_3$)** δ 7.62 – 7.57 (m, 4H), 7.44 (dd, J = 8.0, 6.6 Hz, 3H), 7.40 – 7.37 (m, 2H), 7.35 – 7.31 (m, 5H), 7.28 – 7.25 (m, 6H), 7.15 (s, 1H), 7.10 (s, 1H), 2.43 (s, 3H), 2.35 (s, 3H). **^{13}C{^{1}H} NMR (100 MHz, CDCl$_3$)** δ 143.1, 141.7, 140.5, 138.8, 137.7, 137.4, 137.1, 132.4, 132.4, 131.7, 129.2, 129.2, 129.0, 128.7, 128.4, 128.2, 127.8, 127.3, 127.3, 127.19, 127.2, 127.0, 21.3, 21.1. **Anal** calcd for $C_{15}H_{14}Se$: C, 65.94; H, 5.16; found C, 65.99; H, 5.04.

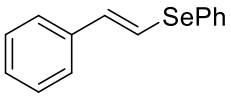

(*E*)-Phenyl(styryl)selane (6ia):[8] Yellow solid (0.032 g, 25%); eluent hexane; **^{1}H NMR (400 MHz, CDCl$_3$)** δ 7.67 – 7.49 (m, 2H), 7.43 (dd, *J* = 9.3, 5.6 Hz, 2H), 7.40 – 7.32 (m, 3H), 7.29 - 7.25 (m, 3H), 7.24 (d, *J* = 7.6 Hz, 1H), 7.16 (d, *J* = 7.8 Hz, 1H). **^{13}C{^{1}H} NMR (100 MHz, CDCl$_3$)** δ 143.1, 133.5, 132.3, 129.3, 129.0, 128.5, 128.2, 128.0, 127.7, 127.2.

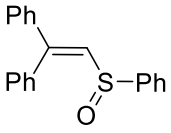

(2-(Phenylsulfinyl)ethene-1,1-diyl)dibenzene (7):[9] White solid (0.075 g, 82%); eluent hexane; **^{1}H NMR (400 MHz, CDCl$_3$)** δ 7.64 – 7.57 (m, 2H), 7.46 – 7.38 (m, 6H), 7.32 – 7.25 (m, 3H), 7.21 (dt, *J* = 10.8, 7.7 Hz, 4H), 6.75 (s, 1H). **^{13}C{^{1}H} NMR (100 MHz, CDCl$_3$)** δ 152.8, 144.8, 138.9, 136.9, 133.3, 130.8, 130.1, 129.8, 129.4, 129.2, 128.5, 128.4, 128.4, 124.6.

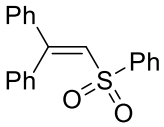

(2-(Phenylsulfinyl)ethene-1,1-diyl)dibenzene (8):[10] White solid (0.073 g, 76%); eluent hexane; **^{1}H NMR (400 MHz, CDCl$_3$)** δ 7.59 – 7.57 (m, 2H), 7.48 (t, *J* = 4.0 Hz, 1H), 7.40 – 7.34 (m, 4H), 7.33 – 7.29 (m, 4H), 7.23 – 7.20 (m, 2H), 7.10 – 7.06 (m, 2H), 7.03 (s, 1H). **^{13}C{^{1}H} NMR (100 MHz, CDCl$_3$)** δ 155.2, 141.4, 139.0, 135.4, 132.8, 130.3, 129.7, 128.9, 128.7, 128.6, 128.6, 128.2, 127.8, 127.6.

***N*-((2,2-diphenylvinyl)(phenyl)-λ_4-sulfanylidene)-4-methylbenzenesulfonamide (9):** White

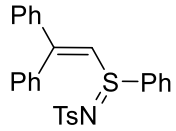

solid (0.11 g, 78%); eluent 20% ethyl acetate : hexane; mp = 96 - 98 ^{o}C; **^{1}H NMR (400 MHz, CDCl$_3$)** δ 7.71 – 7.65 (m, 4H), 7.51 – 7.46 (m, 4H), 7.40 – 7.36 (m, 3H), 7.31 (t, *J* = 7.5 Hz, 2H), 7.19 – 7.13 (m, 4H), 7.08 – 7.06 (m, 2H), 6.67 (s, 1H), 2.35 (s, 3H).**^{13}C{^{1}H} NMR (100 MHz, CDCl$_3$)** δ 155.5, 141.6, 141.4, 137.9, 136.9, 136.1, 131.8, 130.6, 129.8, 129.7, 129.7, 129.1, 128.7, 128.6, 128.5, 126.43, 126.4, 123.0, 21.4. **Anal** calcd for $C_{27}H_{23}NO_2S_2$: C, 70.87; H, 5.07; N, 3.06; S, 14.01; found C,70.99; H, 5.03; N, 3.02; S, 14.04.

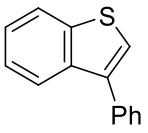

3-Phenylbenzo[b]thiophene (10):[11] White solid (0.018 g, 40%); eluent hexane; **^{1}H NMR (400 MHz, CDCl$_3$)** δ 7.78 (m, 2H), 7.45 (dd, *J* = 8.2, 1.3 Hz, 2H), 7.35 (dd, *J* = 8.1, 6.8 Hz, 2H), 7.25 – 7.18 (m, 2H), 7.16 – 7.08 (m, 2H). **^{13}C{^{1}H} NMR (100 MHz, CDCl$_3$)** δ 140.7, 138.1, 137.9, 136.0, 131.0, 129.2, 128.7, 127.5, 124.4, 124.3, 123.4, 122.9.

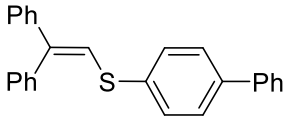

[1,1'-Biphenyl]-4-yl(2,2-diphenylvinyl)sulfane (11):[2] White solid (0.092 g, 84%); eluent hexane; **^{1}H NMR (400 MHz, CDCl$_3$)** δ 7.60 – 7.56 (m, 4H), 7.53 – 7.50 (m, 2H), 7.47 – 7.42 (m, 4H), 7.40 – 7.36 (m, 4H), 7.32 – 7.27 (m, 5H), 6.91 (s, 1H).**^{13}C{^{1}H} NMR (100 MHz, CDCl$_3$)** δ 141.4, 141.3, 140.3, 139.8, 139.2, 135.5, 129.8, 129.8, 128.9, 128.4, 128.3, 127.8, 127.8, 127.5, 127.3, 127.2, 126.9, 123.9.

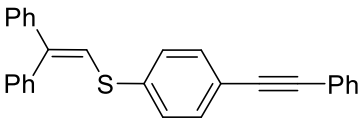

(2,2-Diphenylvinyl)(4-(phenylethynyl)phenyl)sulfane (12): Yellow viscous liquid (0.049 g, 42%); eluent hexane; **^{1}H NMR (400 MHz, CDCl$_3$)** δ 7.70 (m, 1H), 7.40 – 7.29 (m, 12H), 7.25

(d, *J* = 2.2 Hz, 1H), 7.24 (d, *J* = 2.2 Hz, 2H), 7.22 – 7.21 (m, 1H), 7.20 – 7.17 (m, 2H), 7.04 (s, 1H).**^{13}C{^{1}H} NMR (100 MHz, CDCl$_3$)** δ 143.4, 136.3, 132.3, 131.4, 131.2, 131.1, 131.0, 129.0, 128.1, 127.9, 127.8, 127.5, 127.24 125.9, 125.7, 125.4, 124.9, 124.2, 123.9, 122.9, 92.9, 89.1. **Anal** calcd for $C_{28}H_{20}S$: C, 86.56; H, 5.19; S, 8.25; found C, 86.65; H, 5.14; S, 8.21.

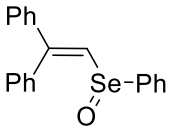

(2-(Phenylseleninyl)ethene-1,1-diyl)dibenzene (13): Colourless oil (0.081 g, 77%); eluent hexane; **^{1}H NMR (400 MHz, CDCl$_3$)** δ 7.66 (dd, *J* = 7.7, 1.8 Hz, 2H), 7.47 – 7.38 (m, 6H), 7.25-7.23 (m, 4H), 7.22 – 7.18 (m, 3H), 6.88 (s, 1H). **^{13}C NMR (100 MHz, CDCl$_3$)** δ 153.9, 142.0, 138.3, 137.7, 133.6, 131.1, 129.8, 129.7, 129.5, 128.7, 128.7, 128.5, 128.2, 126.4. **^{77}SeNMR (76 MHz, CDCl$_3$)** δ 848.85 (s). **Anal** calcd for $C_{20}H_{16}OSe$: C, 68.38; H, 4.59; found C, 68.49; H, 4.41.

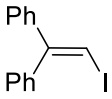

(2-Iodoethene-1,1-diyl)dibenzene (14):[12] Pale yellow oil (0.138 g, 90%); eluent hexane; **^{1}H NMR (400 MHz, CDCl$_3$)** δ 7.31 (d, J = 7.2 Hz, 3H), 7.20 – 7.14 (m, 5H), 7.12 (dd, J = 3.7, 1.6 Hz, 2H), 6.84 (s, 1H).**^{13}C{^{1}H} NMR (100 MHz, CDCl$_3$)** δ 152.7, 141.8, 141.1, 129.4, 128.3, 128.3, 128.1, 128.0, 127.5, 79.0.

^{1}H and ^{13}C NMR Spectra of Some Selected Diphenylvinyl Sulfanes and Selanes

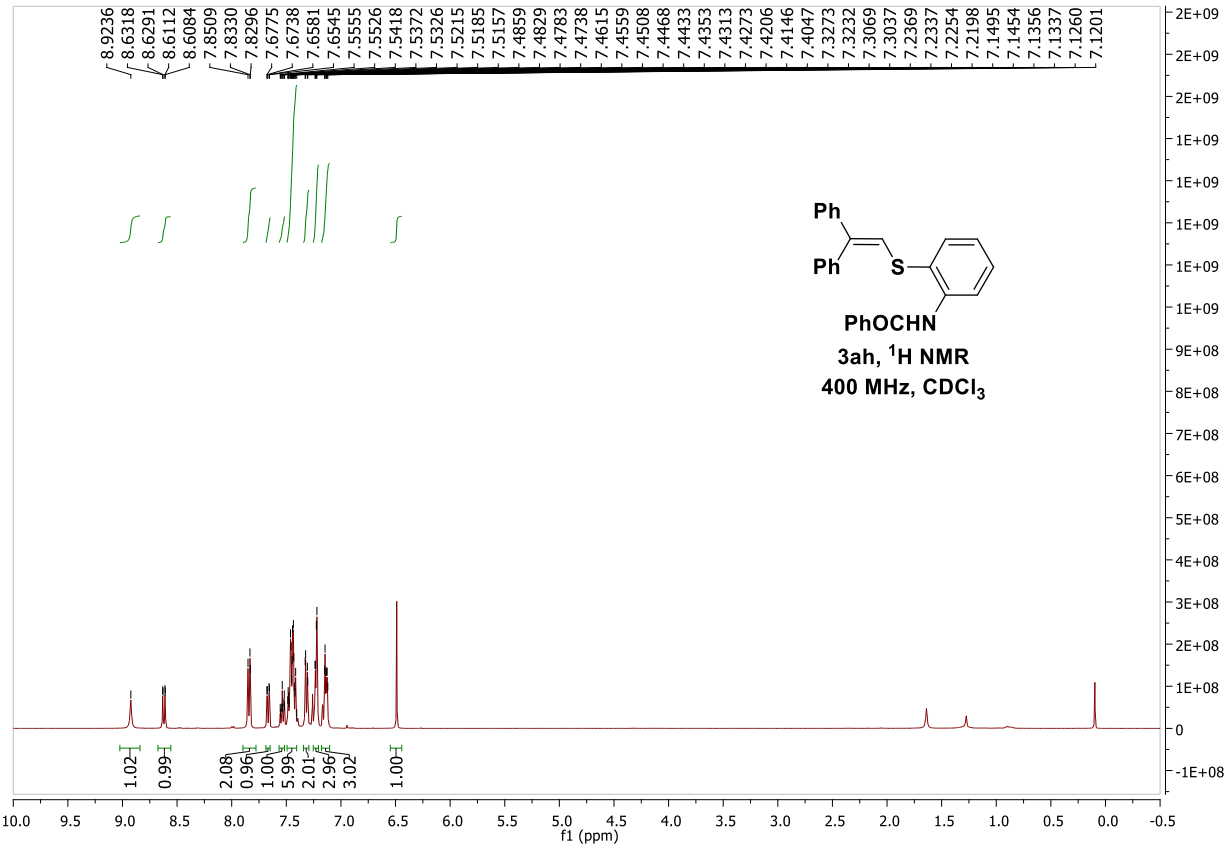
8.9236
8.6318
8.6291
8.6112
8.6084
7.8509
7.8330
7.8296
7.6775
7.6738
7.6581
7.6545
7.5555
7.5526
7.5418
7.5372
7.5326
7.5215
7.5185
7.5157
7.4859
7.4829
7.4783
7.4738
7.4615
7.4559
7.4508
7.4468
7.4433
7.4353
7.4313
7.4273
7.4206
7.4146
7.4047
7.3273
7.3232
7.3069
7.3037
7.2369
7.2337
7.2254
7.2198
7.1495
7.1454
7.1356
7.1337
7.1260
7.1201
Ph
Ph
S
PhOCHN
3ah, ^{1}H NMR
400 MHz, $CDCl_3$
1.02
0.99
2.08
0.96
1.00
5.99
2.01
2.96
3.02
1.00
f1 (ppm)

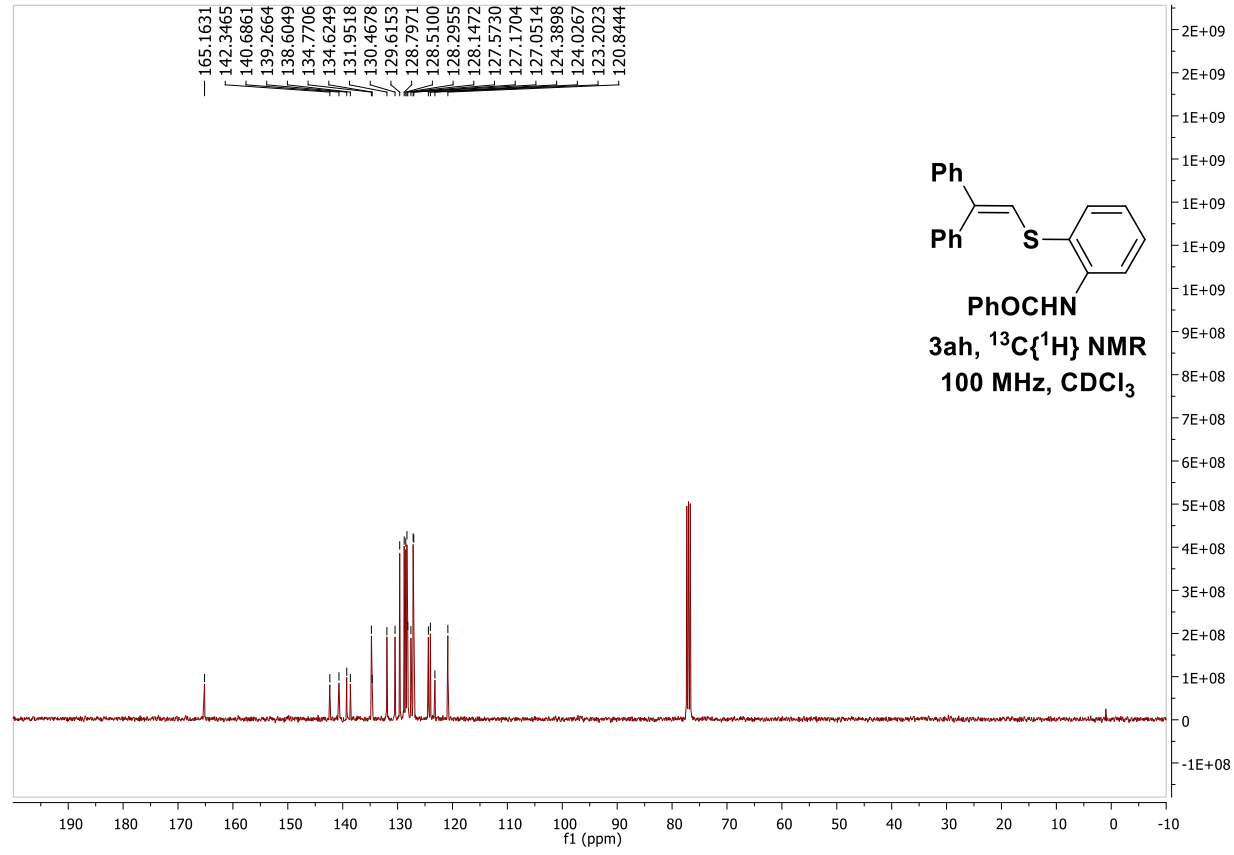
165.1631
142.3465
140.6861
139.2664
138.6049
134.7706
134.6249
131.9518
130.4678
129.6153
128.7971
128.5100
128.2955
128.1472
127.5730
127.1704
127.0514
124.3898
124.0267
123.2023
120.8444
Ph
Ph
S
PhOCHN
3ah, ^{13}C{^{1}H} NMR
100 MHz, $CDCl_3$
f1 (ppm)

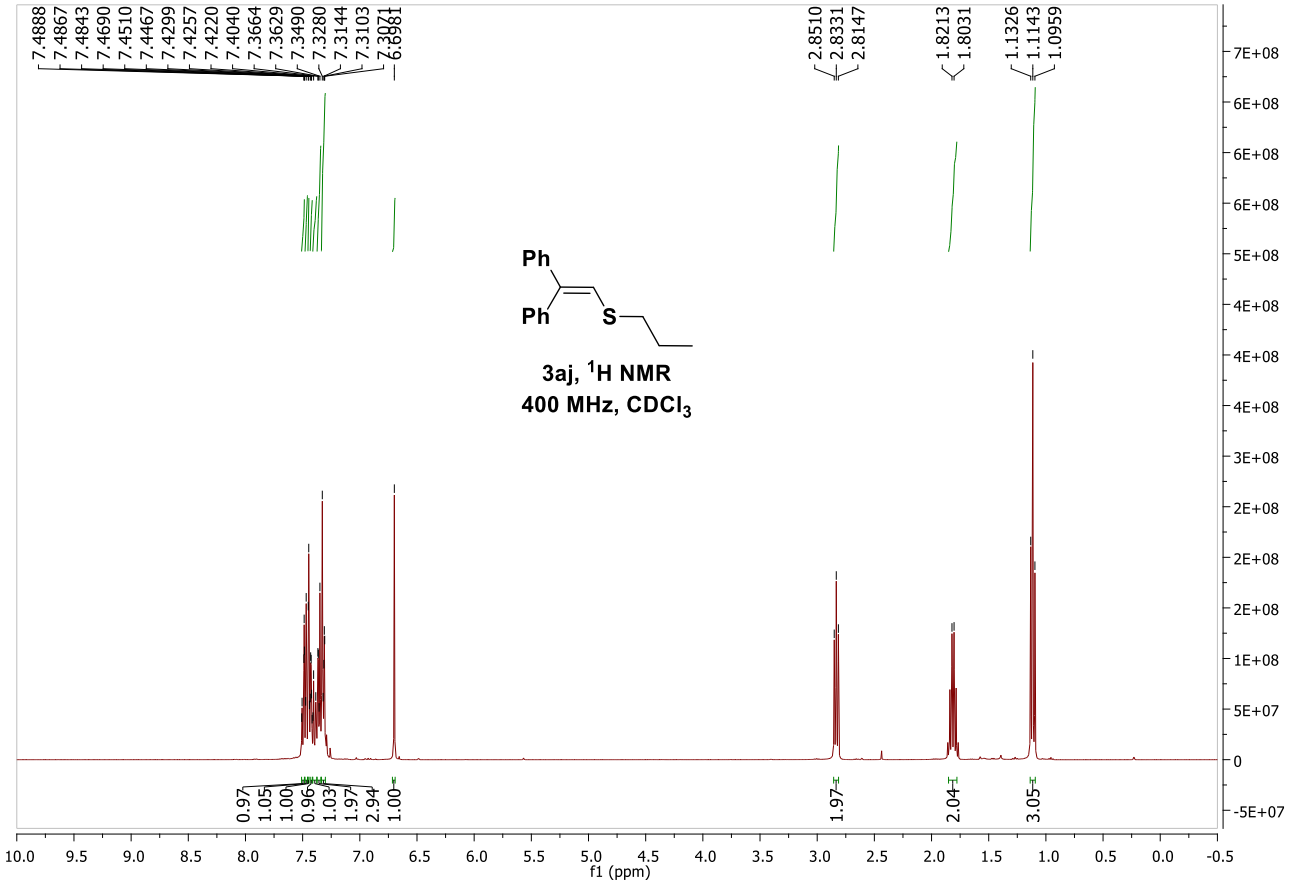
7.4888
7.4867
7.4843
7.4690
7.4510
7.4467
7.4299
7.4257
7.4220
7.4040
7.3664
7.3629
7.3490
7.3280
7.3144
7.3103
7.3071
6.6981
2.8510
2.8331
2.8147
1.8213
1.8031
1.1326
1.1143
1.0959
Ph
Ph
S
3aj, ^{1}H NMR
400 MHz, CDCl$_3$
0.97
1.05
1.00
0.96
1.03
1.97
2.94
1.00
1.97
2.04
3.05
f1 (ppm)

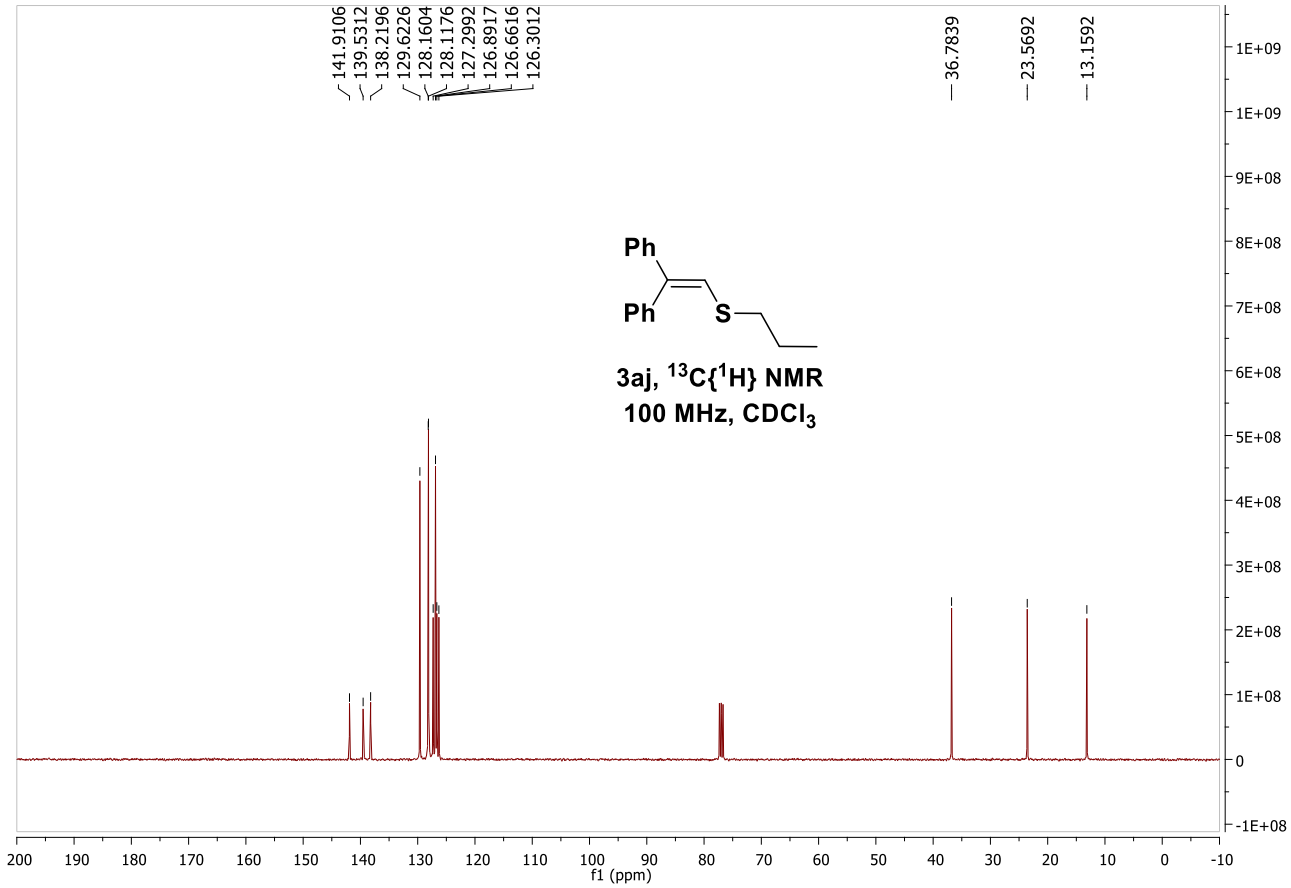
141.9106
139.5312
138.2196
129.6226
128.1604
128.1176
127.2992
126.8917
126.6616
126.3012
36.7839
23.5692
13.1592
Ph
Ph
S
3aj, ^{13}C{^{1}H} NMR
100 MHz, CDCl$_3$
f1 (ppm)

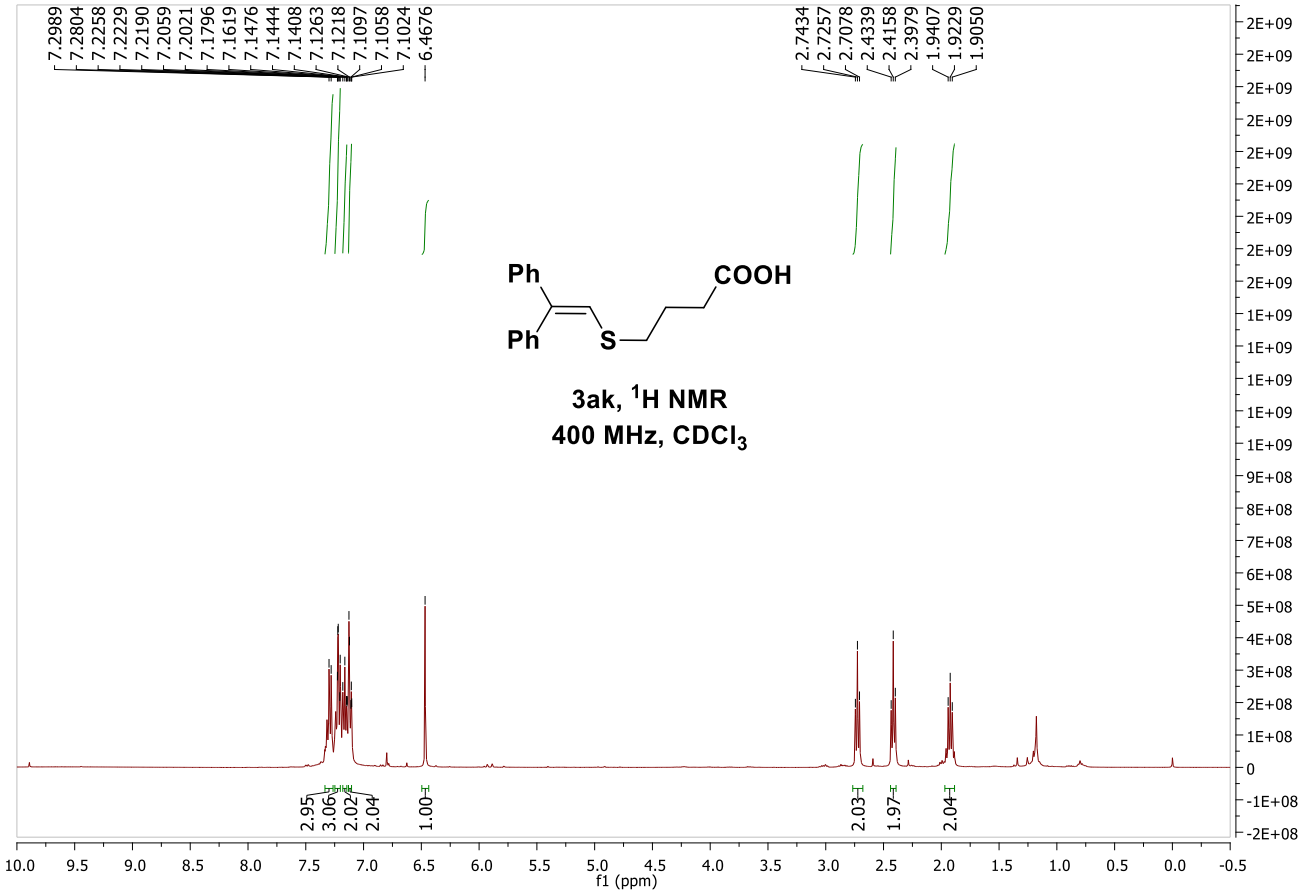
7.2989
7.2804
7.2258
7.2229
7.2190
7.2059
7.2021
7.1796
7.1619
7.1476
7.1444
7.1408
7.1263
7.1218
7.1097
7.1058
7.1024
6.4676
2.7434
2.7257
2.7078
2.4339
2.4158
2.3979
1.9407
1.9229
1.9050
Ph
Ph
S
COOH
3ak, 1H NMR
400 MHz, CDCl3
2.95
3.06
2.02
2.04
1.00
2.03
1.97
2.04
f1 (ppm)

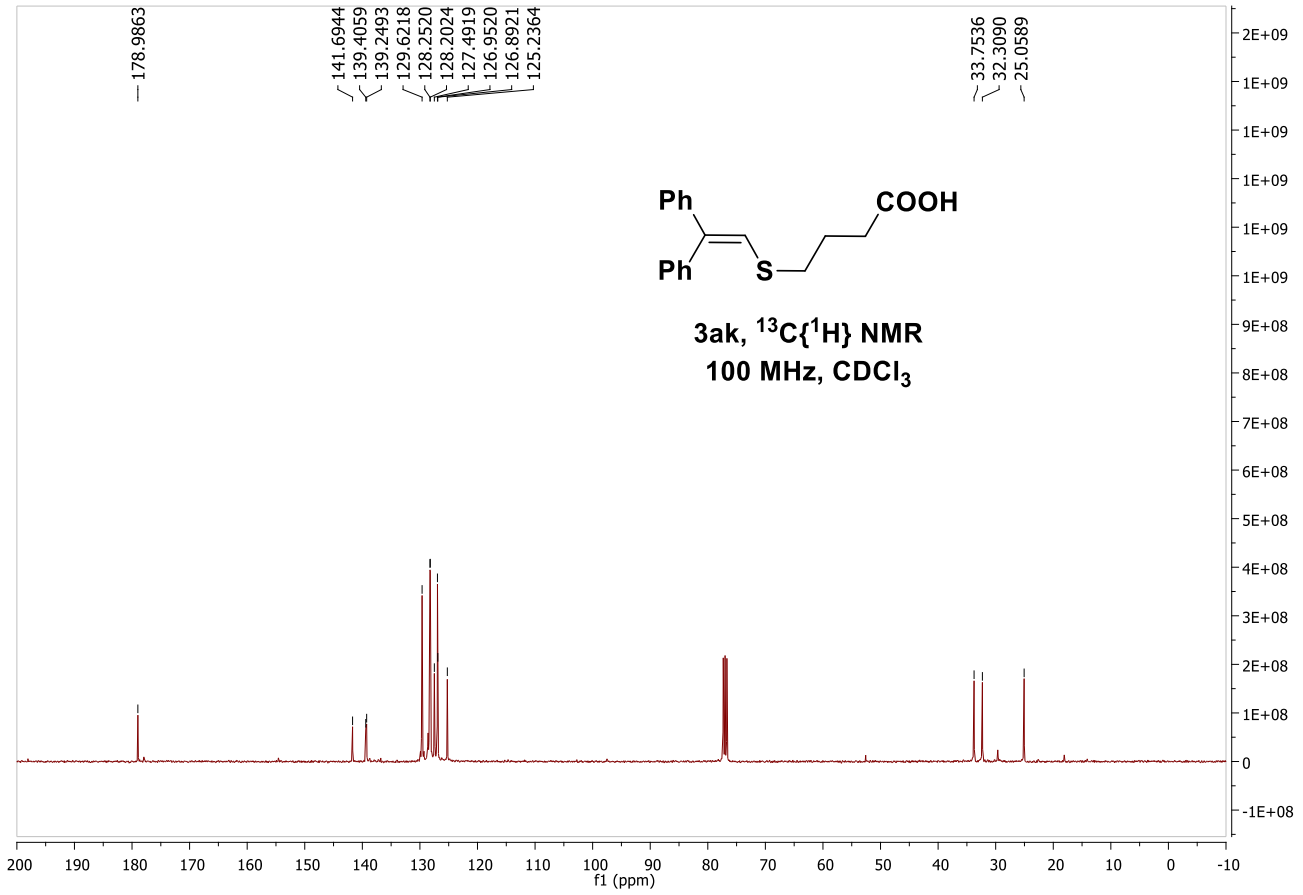
178.9863
141.6944
139.4059
139.2493
129.6218
128.2520
128.2024
127.4919
126.9520
126.8921
125.2364
33.7536
32.3090
25.0589
Ph
Ph
S
COOH
3ak, 13C{1H} NMR
100 MHz, CDCl3
f1 (ppm)

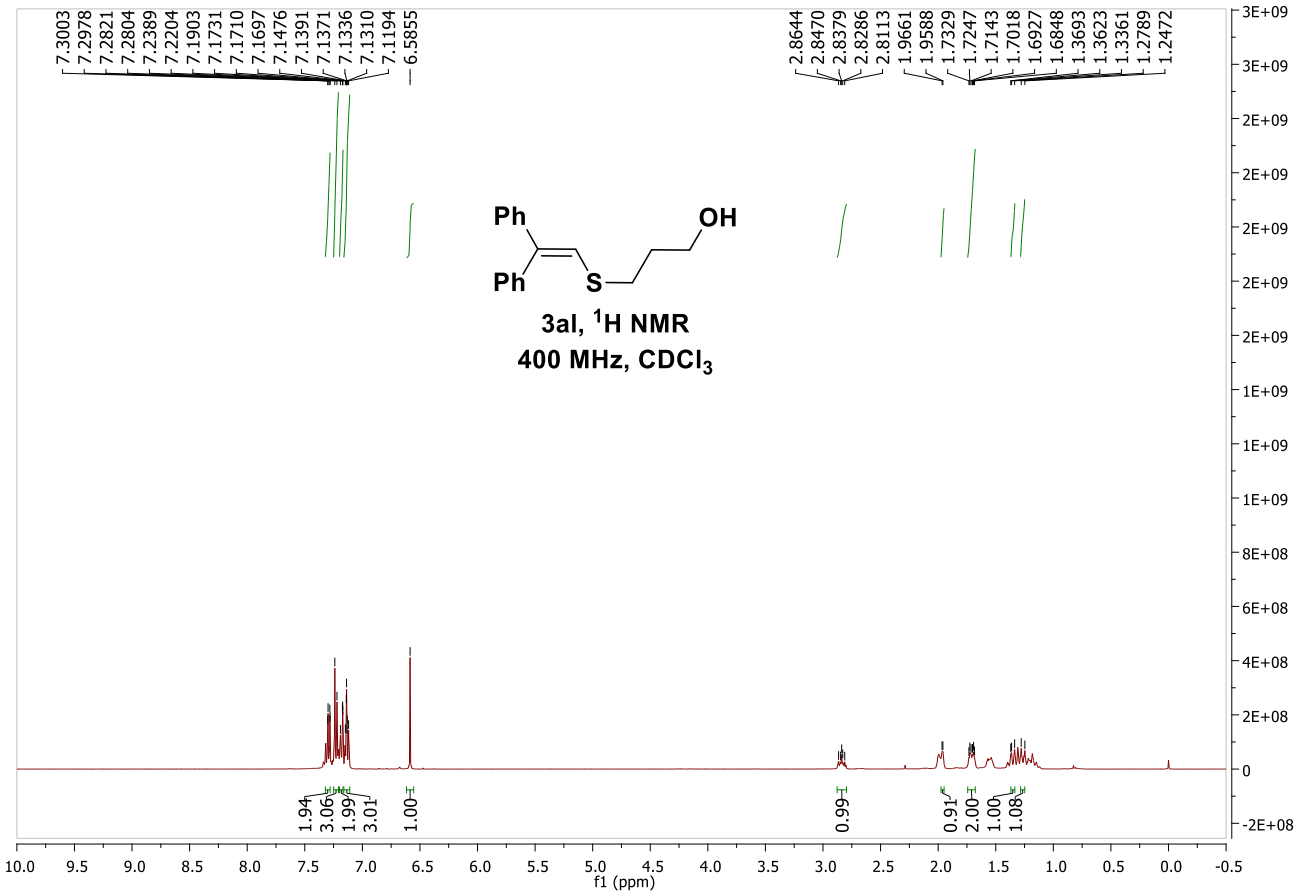
7.3003
7.2978
7.2821
7.2804
7.2389
7.2204
7.1903
7.1731
7.1710
7.1697
7.1476
7.1391
7.1371
7.1336
7.1310
7.1194
6.5855
2.8644
2.8470
2.8379
2.8286
2.8113
1.9661
1.9588
1.7329
1.7247
1.7143
1.7018
1.6927
1.6848
1.3693
1.3623
1.3361
1.2789
1.2472
Ph
OH
Ph
S
3al, 1H NMR
400 MHz, CDCl3
1.94
3.06
1.99
3.01
1.00
0.99
0.91
2.00
1.00
1.08
f1 (ppm)

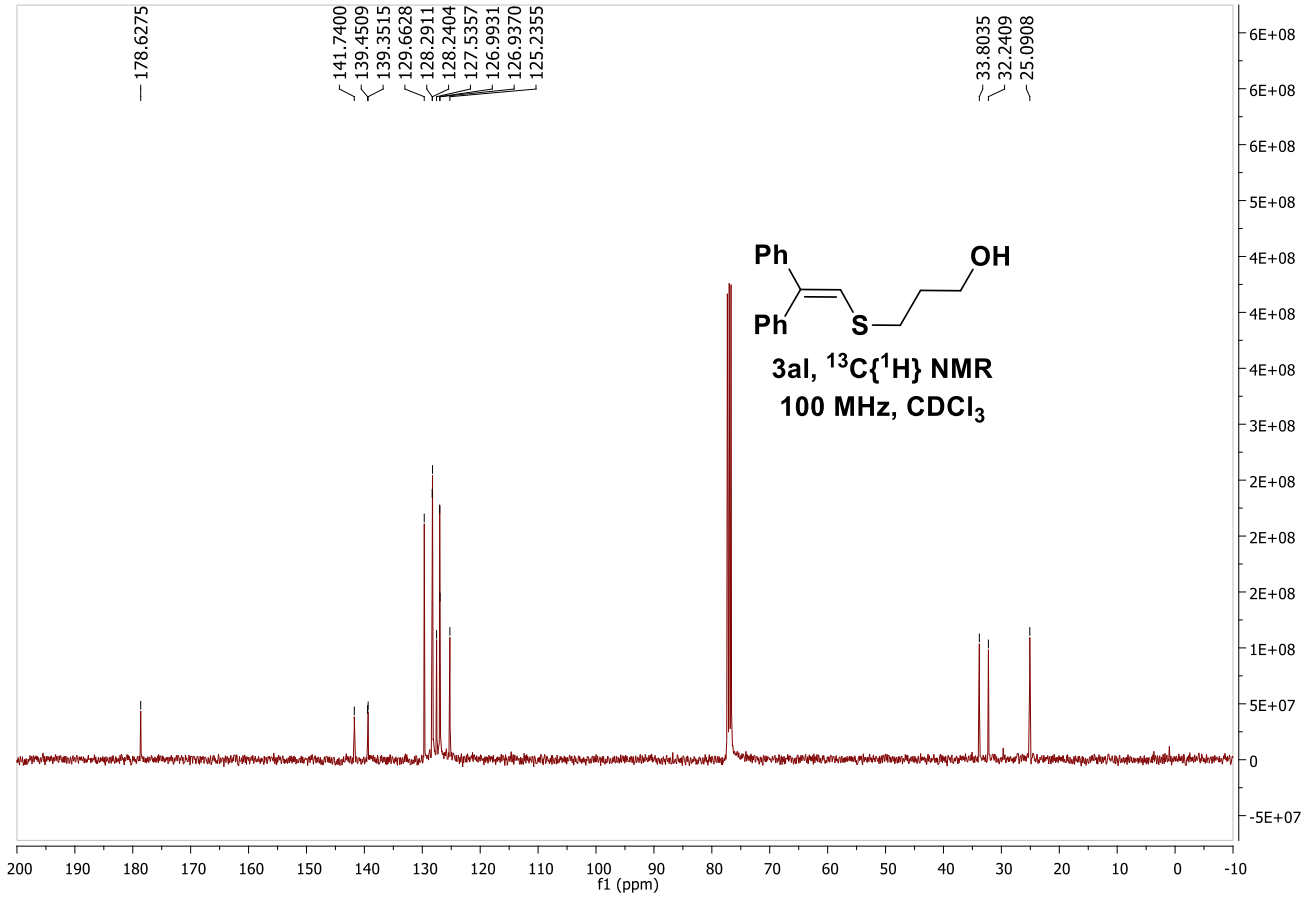
178.6275
141.7400
139.4509
139.3515
129.6628
128.2911
128.2404
127.5357
126.9931
126.9370
125.2355
33.8035
32.2409
25.0908
Ph
OH
Ph
S
3al, 13C{1H} NMR
100 MHz, CDCl3
f1 (ppm)

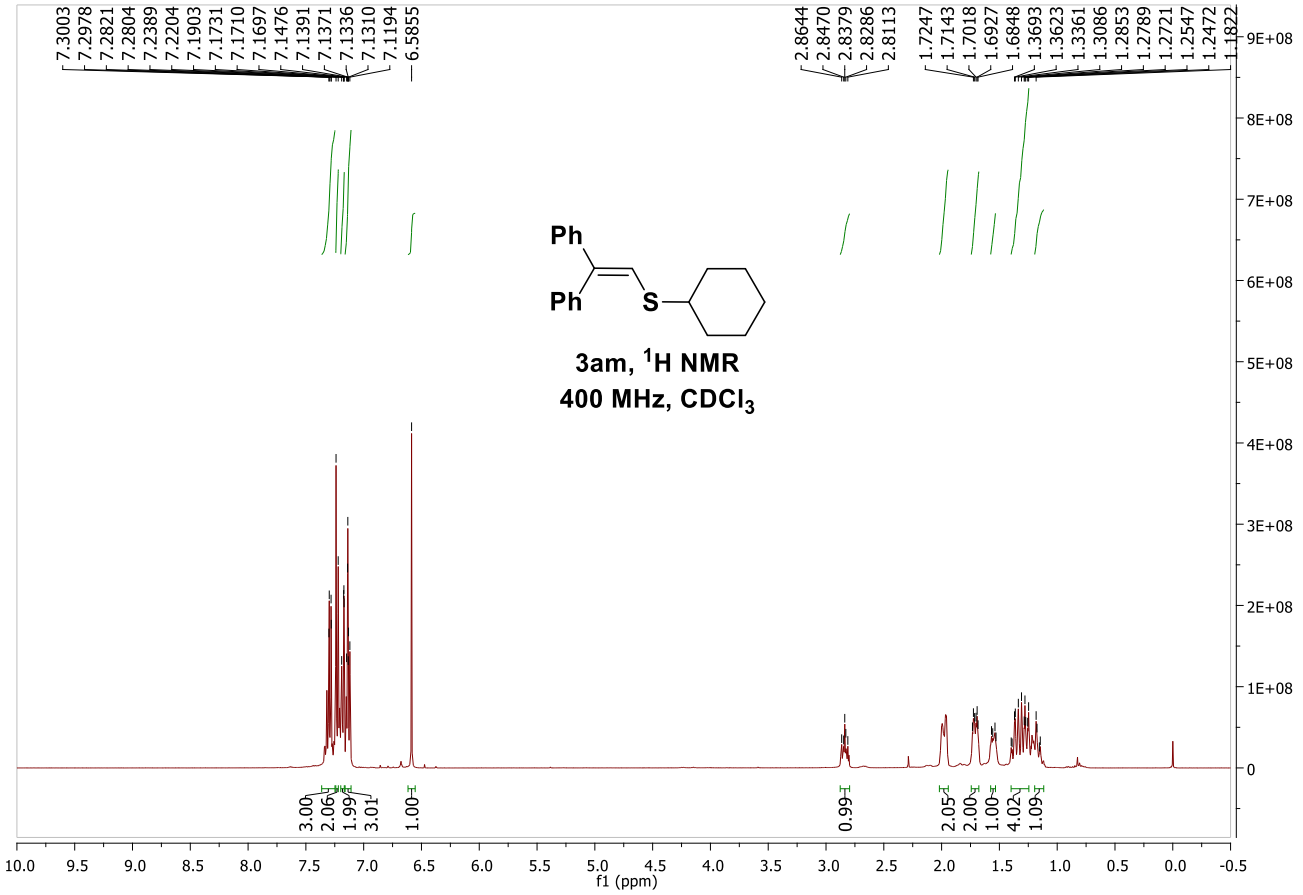
7.3003
7.2978
7.2821
7.2804
7.2389
7.2204
7.1903
7.1731
7.1710
7.1697
7.1476
7.1391
7.1371
7.1336
7.1310
7.1194
6.5855
2.8644
2.8470
2.8379
2.8286
2.8113
1.7247
1.7143
1.7018
1.6927
1.6848
1.3693
1.3623
1.3361
1.3086
1.2853
1.2789
1.2721
1.2547
1.2472
1.1822
Ph
Ph
S
3am, 1H NMR
400 MHz, CDCl3
3.00
2.06
1.99
3.01
1.00
0.99
2.05
2.00
1.00
4.02
1.09
f1 (ppm)

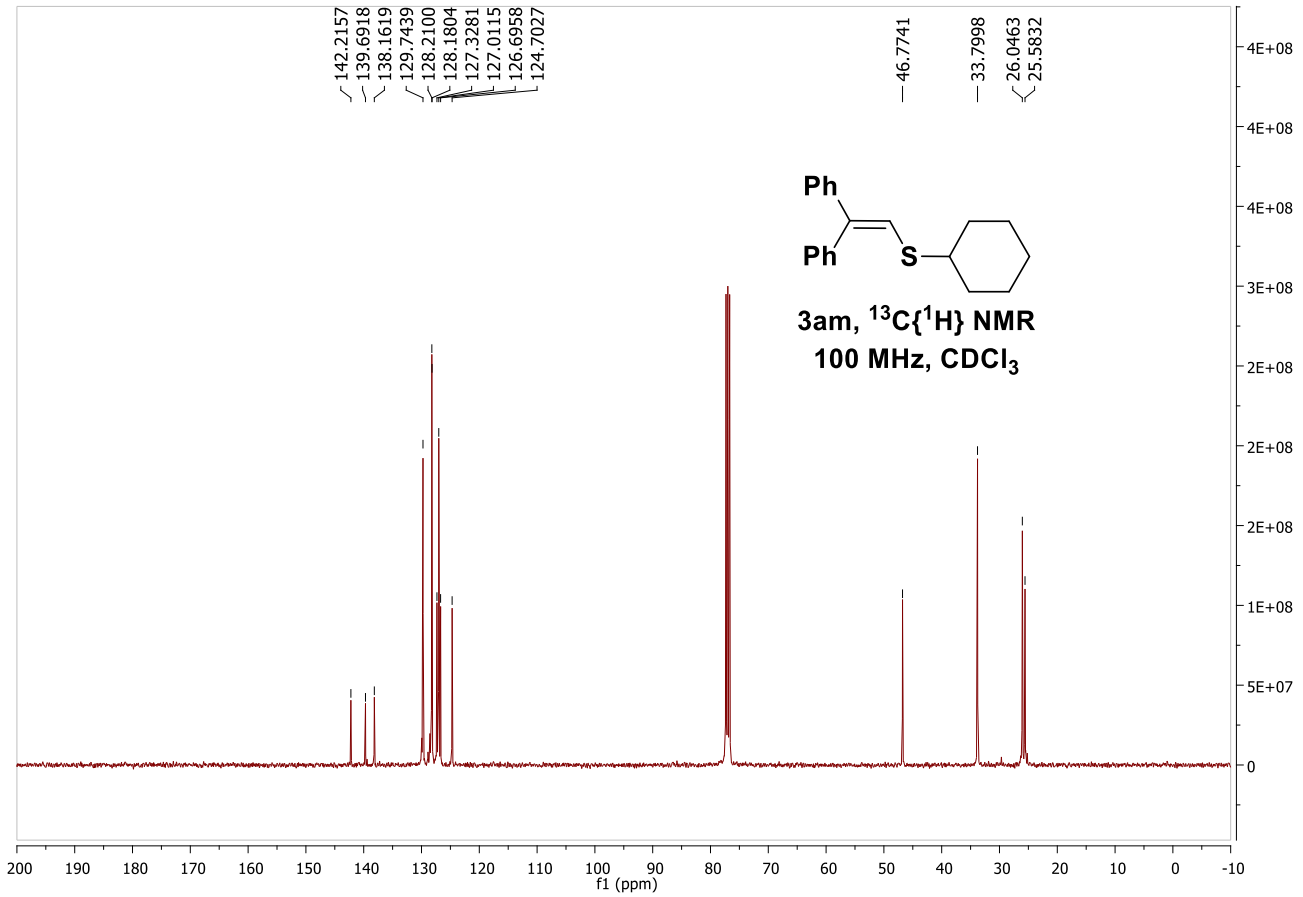
142.2157
139.6918
138.1619
129.7439
128.2100
128.1804
127.3281
127.0115
126.6958
124.7027
46.7741
33.7998
26.0463
25.5832
Ph
Ph
S
3am, 13C{1H} NMR
100 MHz, CDCl3
f1 (ppm)

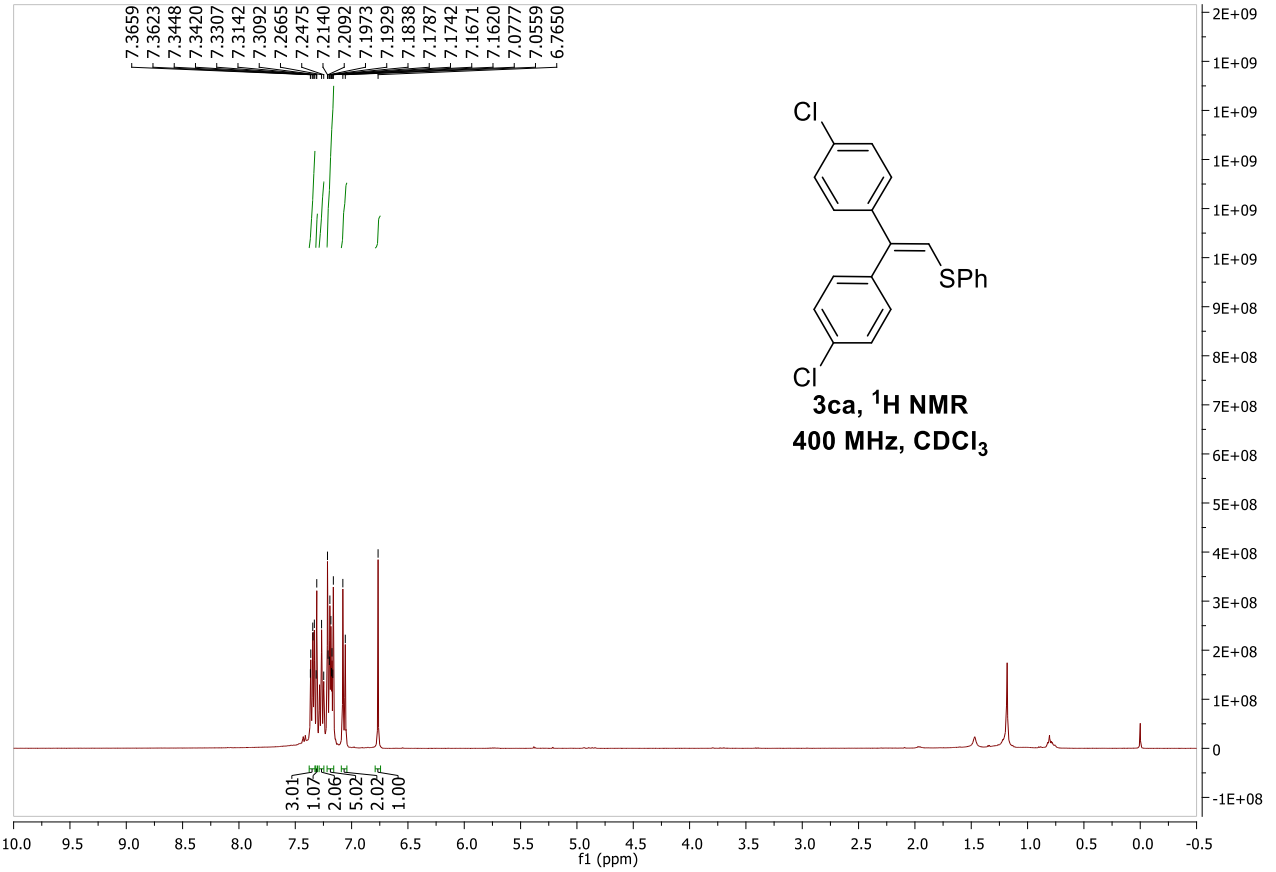
7.3659
7.3623
7.3448
7.3420
7.3307
7.3142
7.3092
7.2665
7.2475
7.2140
7.2092
7.1973
7.1929
7.1838
7.1787
7.1742
7.1671
7.1620
7.0777
7.0559
6.7650
Cl
SPh
Cl
3ca, ^{1}H NMR
400 MHz, $CDCl_3$
3.01
1.07
2.06
5.02
2.02
1.00
f1 (ppm)

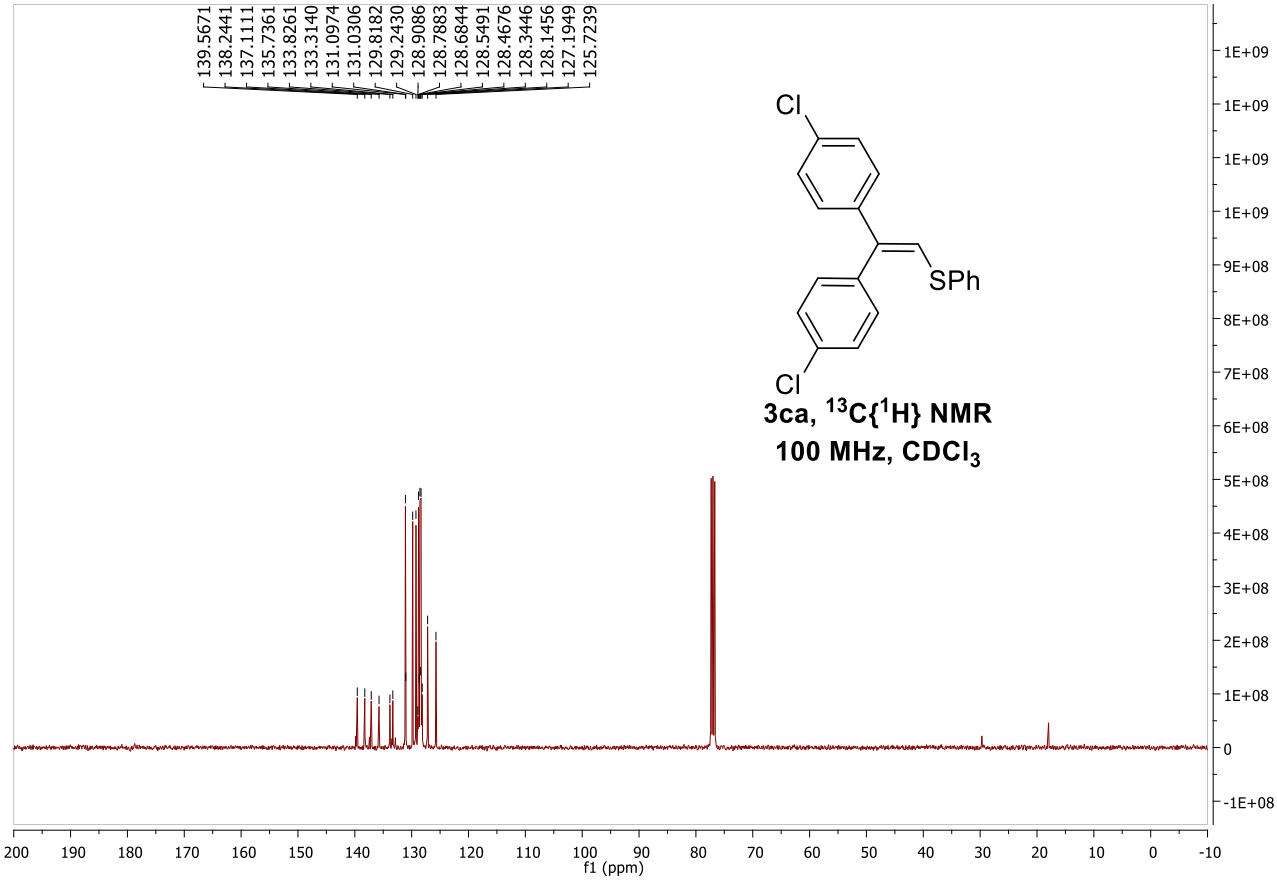
139.5671
138.2441
137.1111
135.7361
133.8261
133.3140
131.0974
131.0306
129.8182
129.2430
128.9086
128.7883
128.6844
128.5491
128.4676
128.3446
128.1456
127.1949
125.7239
Cl
SPh
Cl
3ca, $^{13}C\{^{1}H\}$ NMR
100 MHz, $CDCl_3$
f1 (ppm)

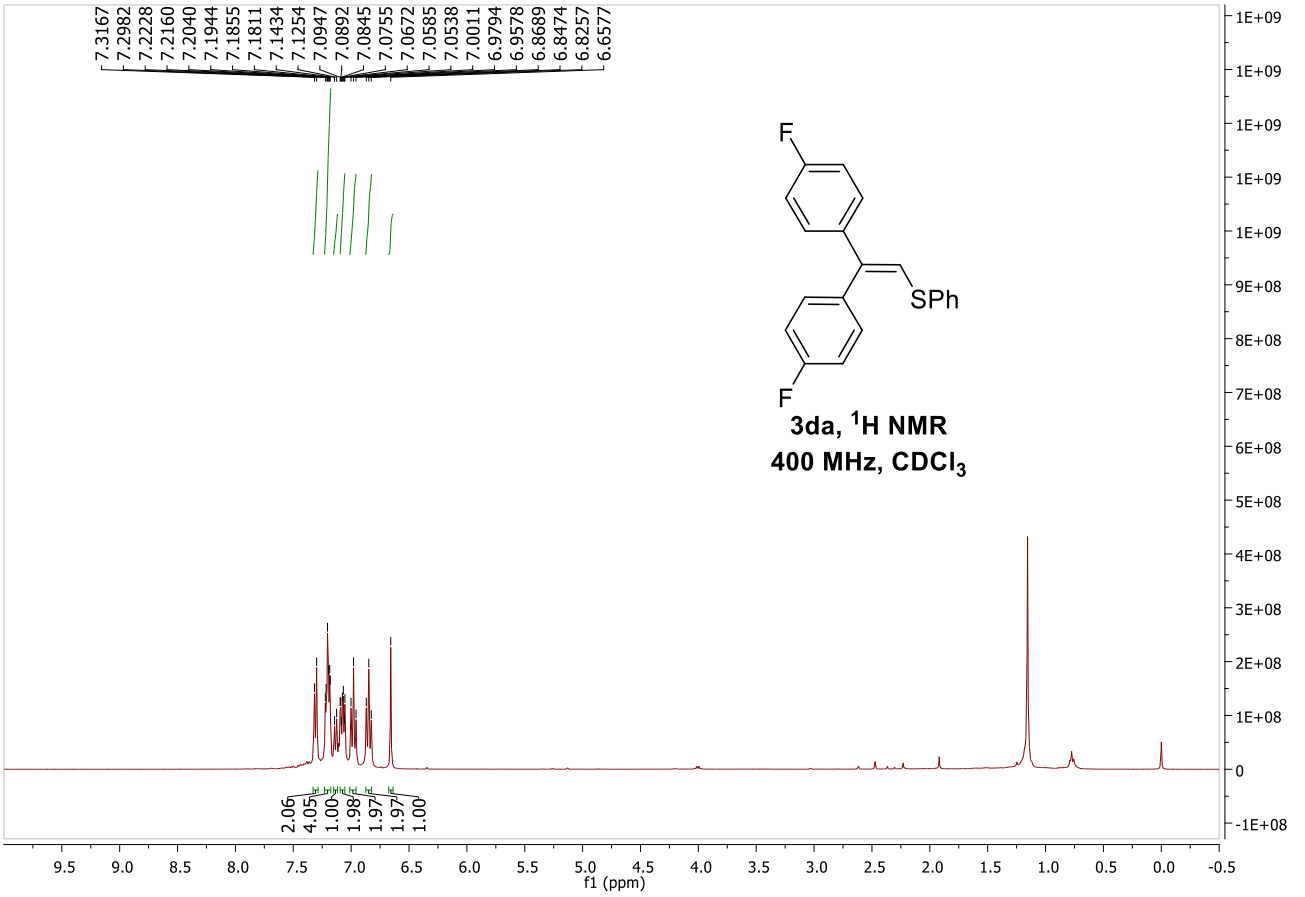
7.3167
7.2982
7.2228
7.2160
7.2040
7.1944
7.1855
7.1811
7.1434
7.1254
7.0947
7.0892
7.0845
7.0755
7.0672
7.0585
7.0538
7.0011
6.9794
6.9578
6.8689
6.8474
6.8257
6.6577
F
SPh
F
3da, ^{1}H NMR
400 MHz, $CDCl_3$
2.06
4.05
1.00
1.98
1.97
1.97
1.00
f1 (ppm)

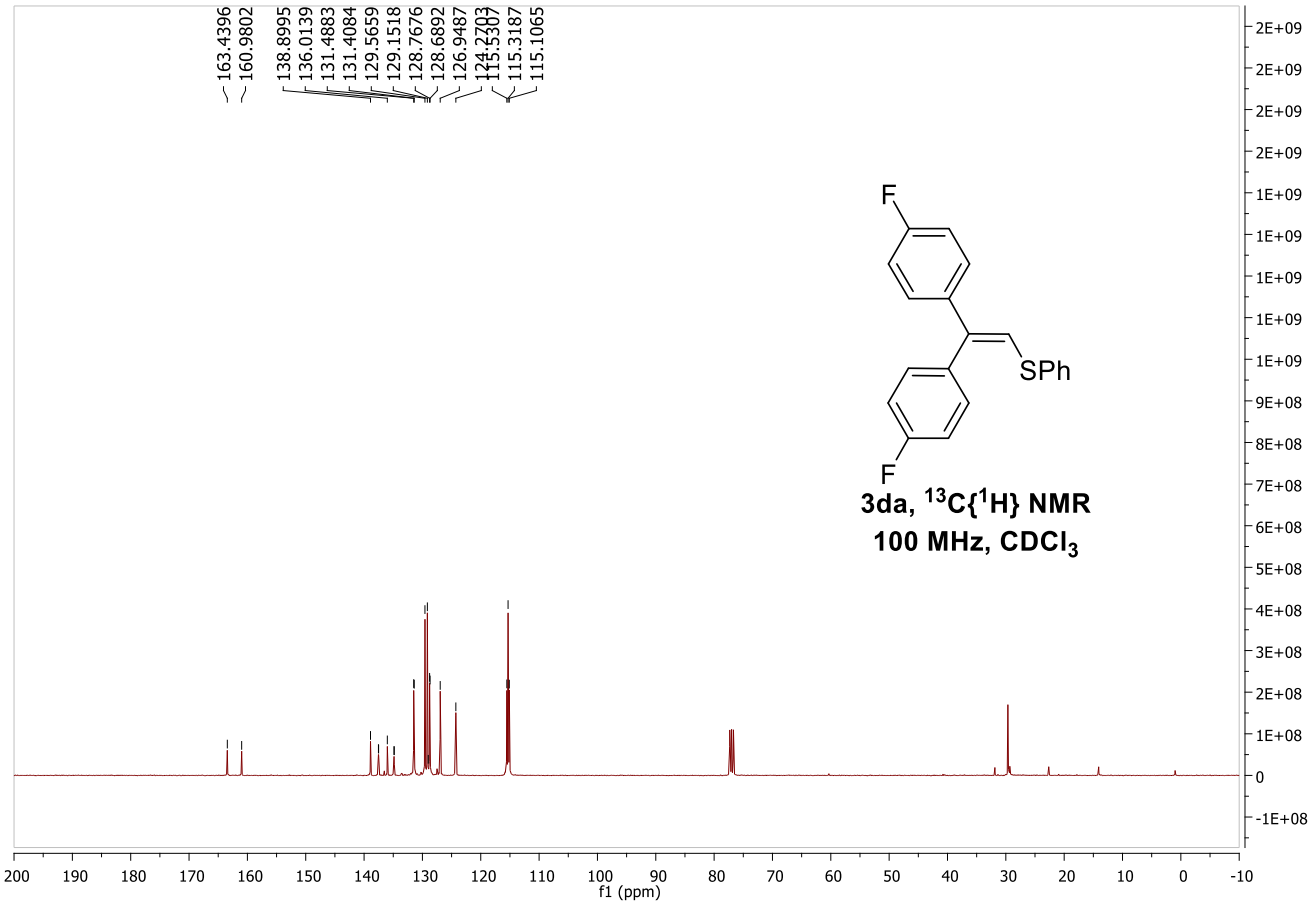
163.4396
160.9802
138.8995
136.0139
131.4883
131.4084
129.5659
129.1518
128.7676
128.6892
126.9487
124.2703
115.5307
115.3187
115.1065
F
SPh
F
3da, ^{13}C{^{1}H} NMR
100 MHz, $CDCl_3$
f1 (ppm)

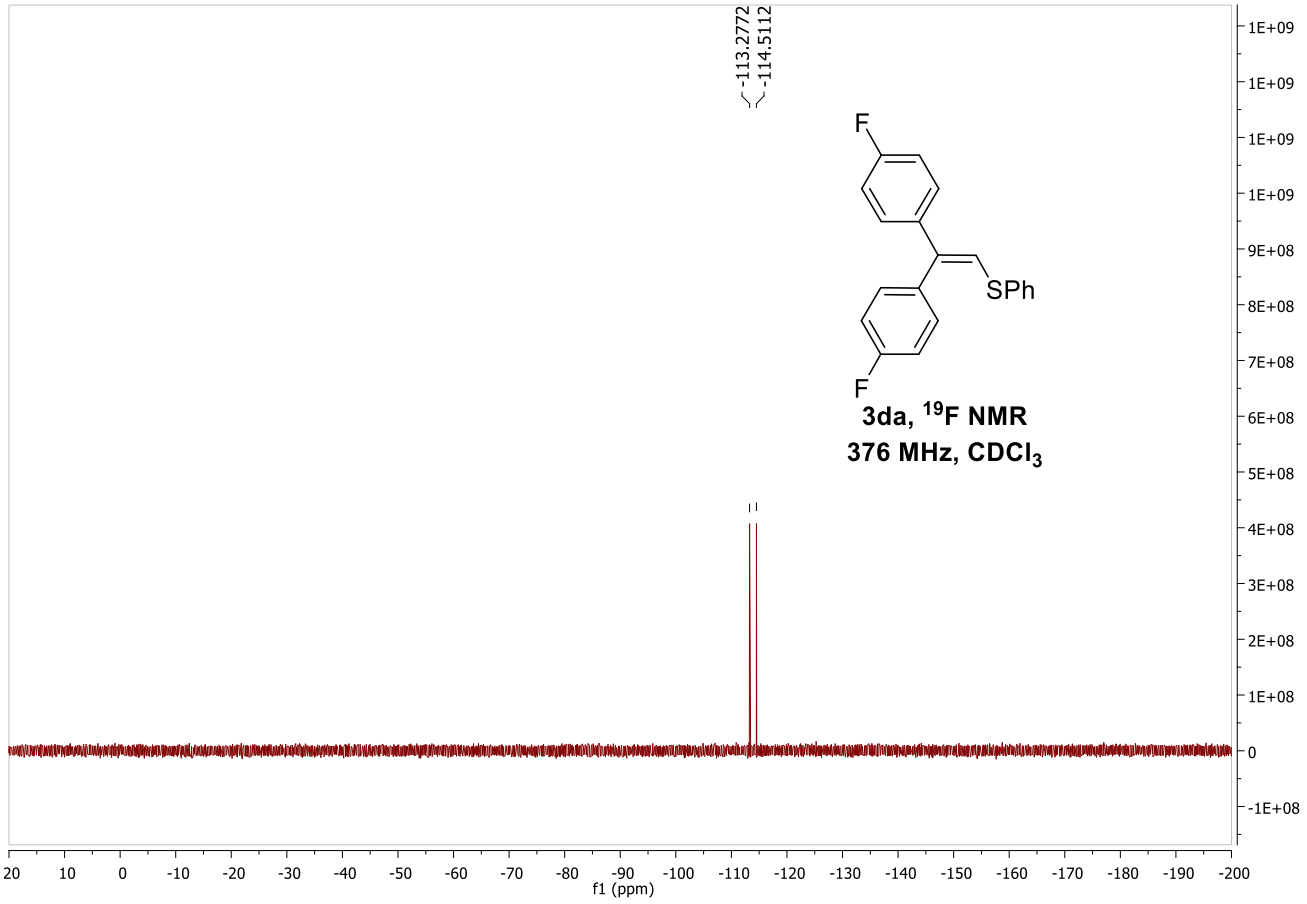
-113.2772
-114.5112
F
SPh
F
3da, 19F NMR
376 MHz, CDCl3
f1 (ppm)

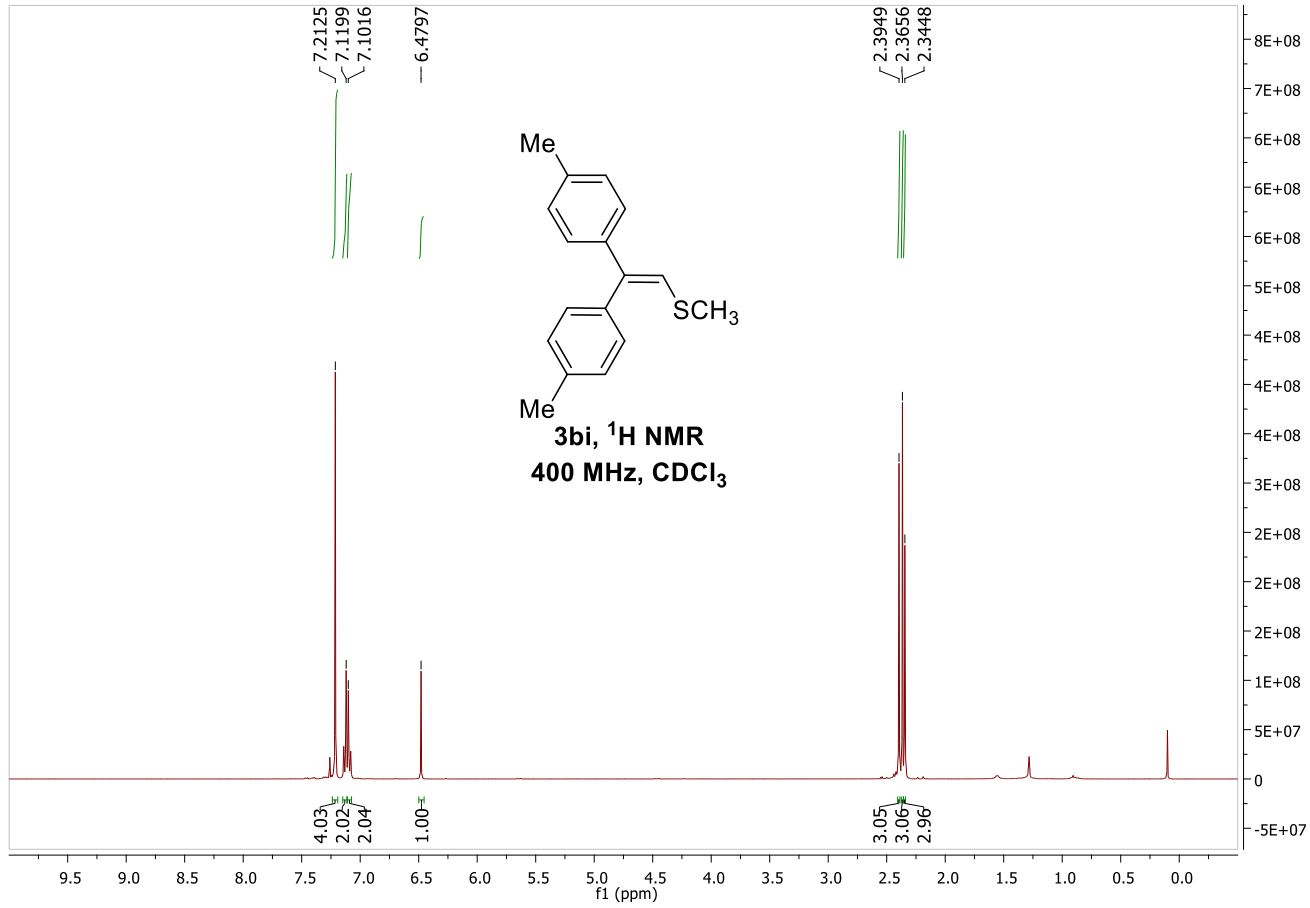
7.2125
7.1199
7.1016
6.4797
2.3949
2.3656
2.3448
Me
SCH3
Me
3bi, 1H NMR
400 MHz, CDCl3
4.03
2.02
2.04
1.00
3.05
3.06
2.96
f1 (ppm)

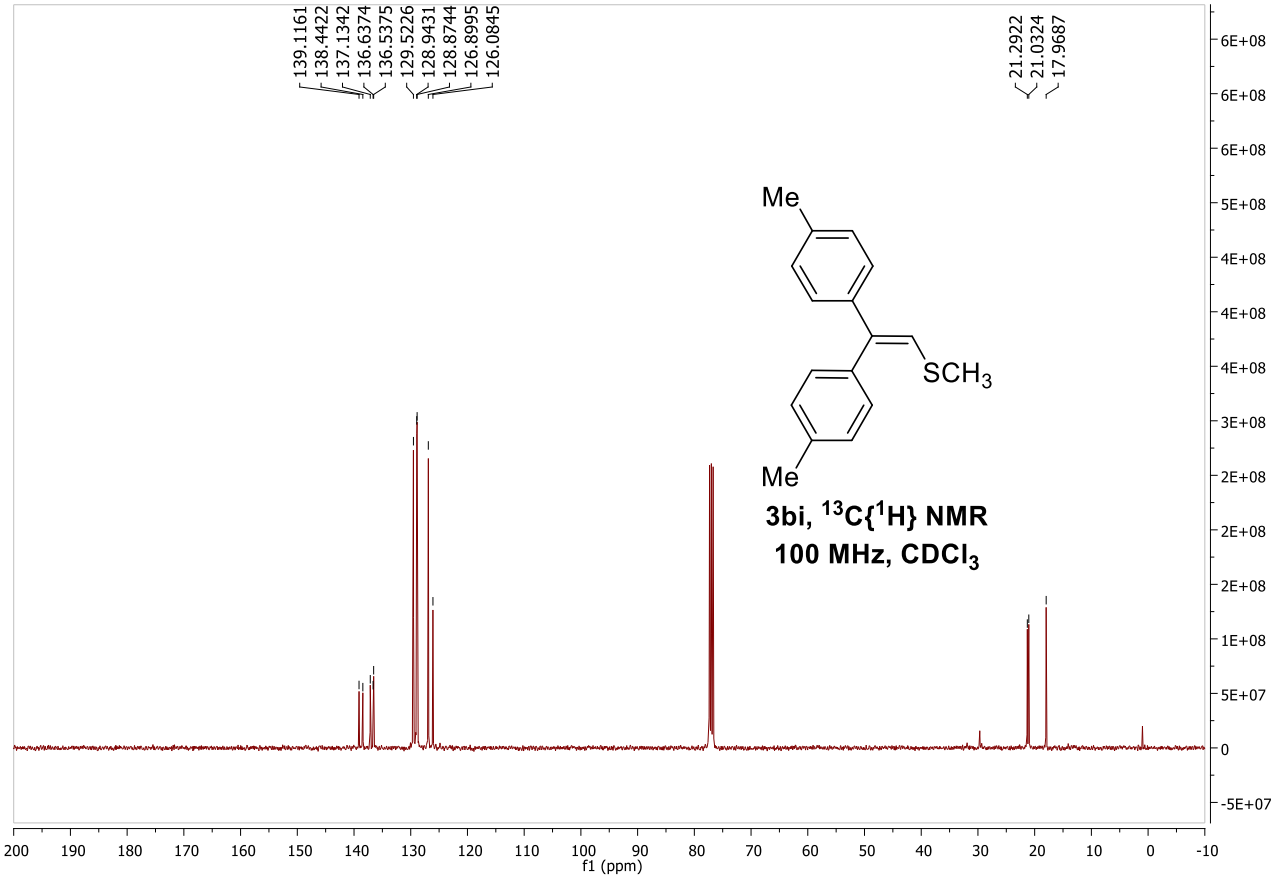
139.1161
138.4422
137.1342
136.6374
136.5375
129.5226
128.9431
128.8744
126.8995
126.0845
21.2922
21.0324
17.9687
Me
SCH3
Me
3bi, 13C{1H} NMR
100 MHz, CDCl3
f1 (ppm)

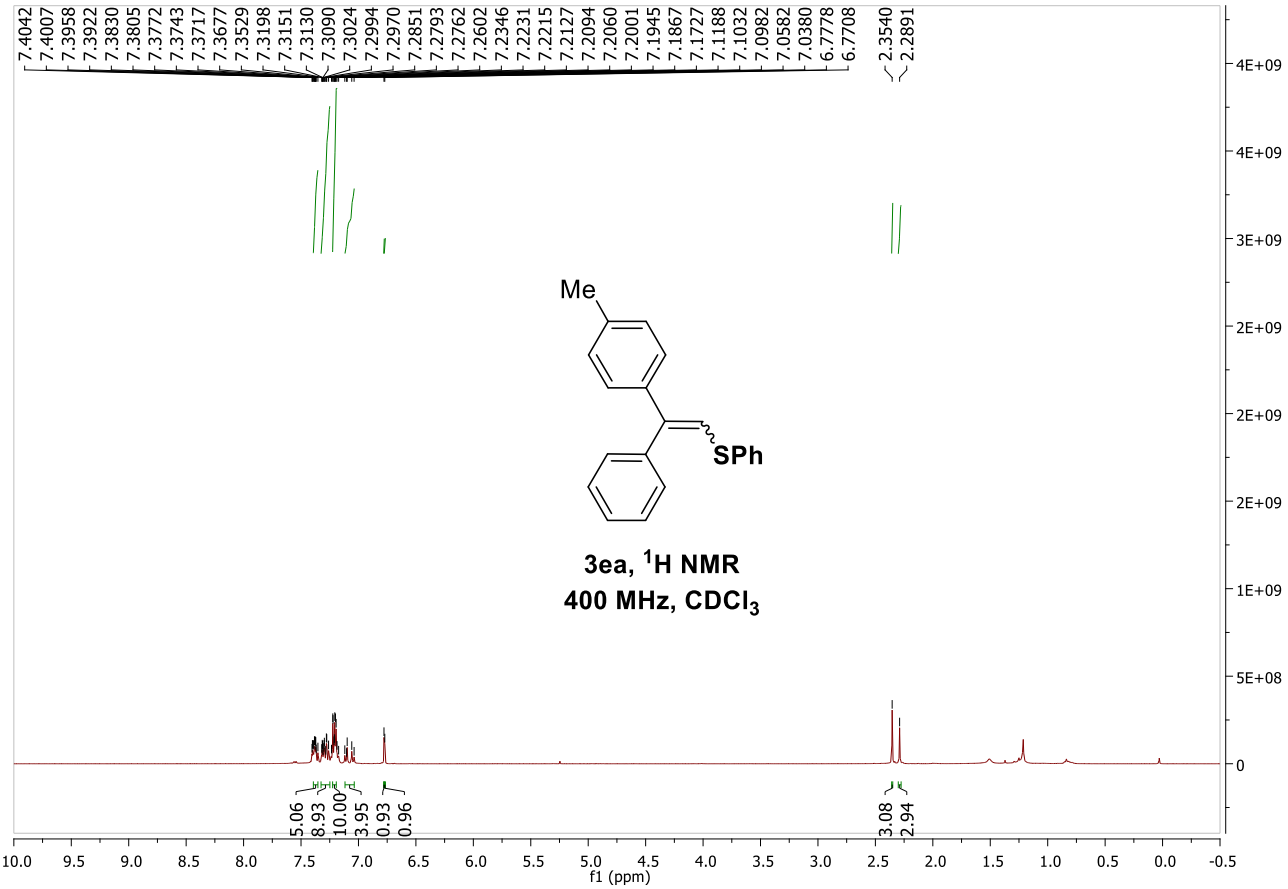
7.4042
7.4007
7.3958
7.3922
7.3830
7.3805
7.3772
7.3743
7.3717
7.3677
7.3529
7.3198
7.3151
7.3130
7.3090
7.3024
7.2994
7.2970
7.2851
7.2793
7.2762
7.2602
7.2346
7.2231
7.2215
7.2127
7.2094
7.2060
7.2001
7.1945
7.1867
7.1727
7.1188
7.1032
7.0982
7.0582
7.0380
6.7778
6.7708
2.3540
2.2891
Me
SPh
3ea, 1H NMR
400 MHz, CDCl3
5.06
8.93
10.00
3.95
0.93
0.96
3.08
2.94
f1 (ppm)

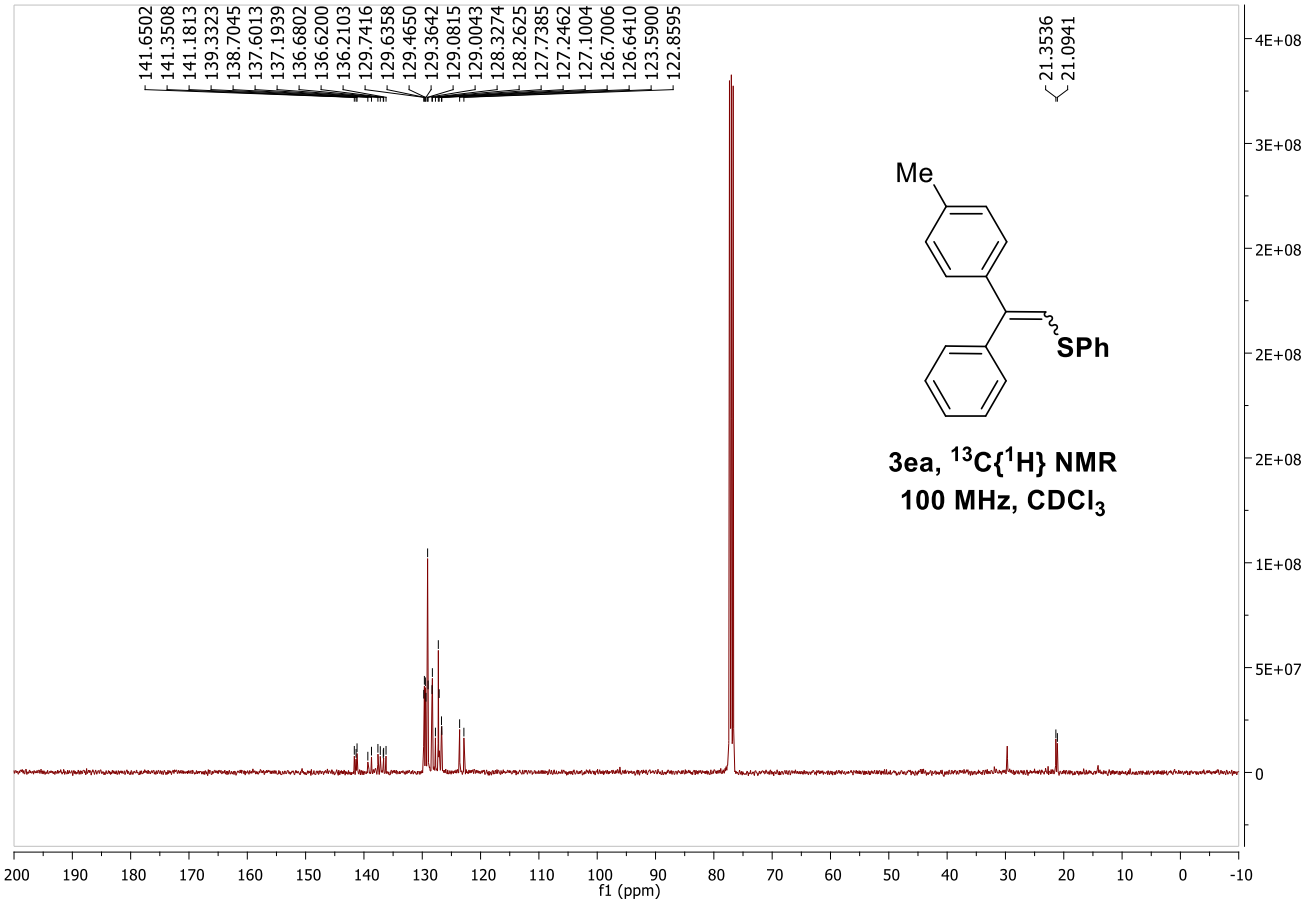
141.6502
141.3508
141.1813
139.3323
138.7045
137.6013
137.1939
136.6802
136.6200
136.2103
129.7416
129.6358
129.4650
129.3642
129.0815
129.0043
128.3274
128.2625
127.7385
127.2462
127.1004
126.7006
126.6410
123.5900
122.8595
21.3536
21.0941
Me
SPh
3ea, $^{13}C\{^{1}H\}$ NMR
100 MHz, $CDCl_3$
f1 (ppm)

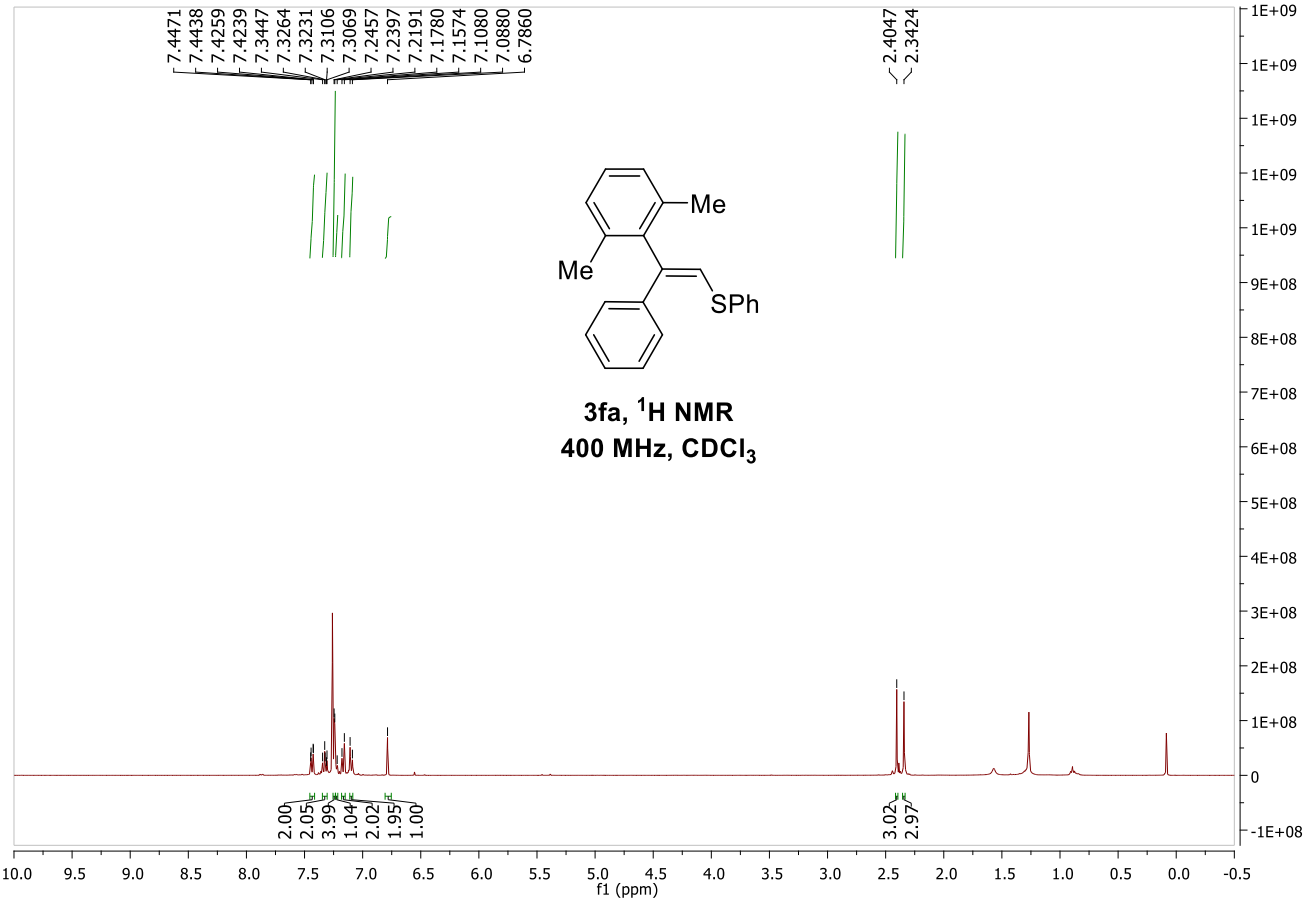
7.4471
7.4438
7.4259
7.4239
7.3447
7.3264
7.3231
7.3106
7.3069
7.2457
7.2397
7.2191
7.1780
7.1574
7.1080
7.0880
6.7860
2.4047
2.3424
Me
Me
SPh
2.00
2.05
3.99
1.04
2.02
1.95
1.00
3.02
2.97
3fa, ^{1}H NMR
400 MHz, $CDCl_3$
f1 (ppm)

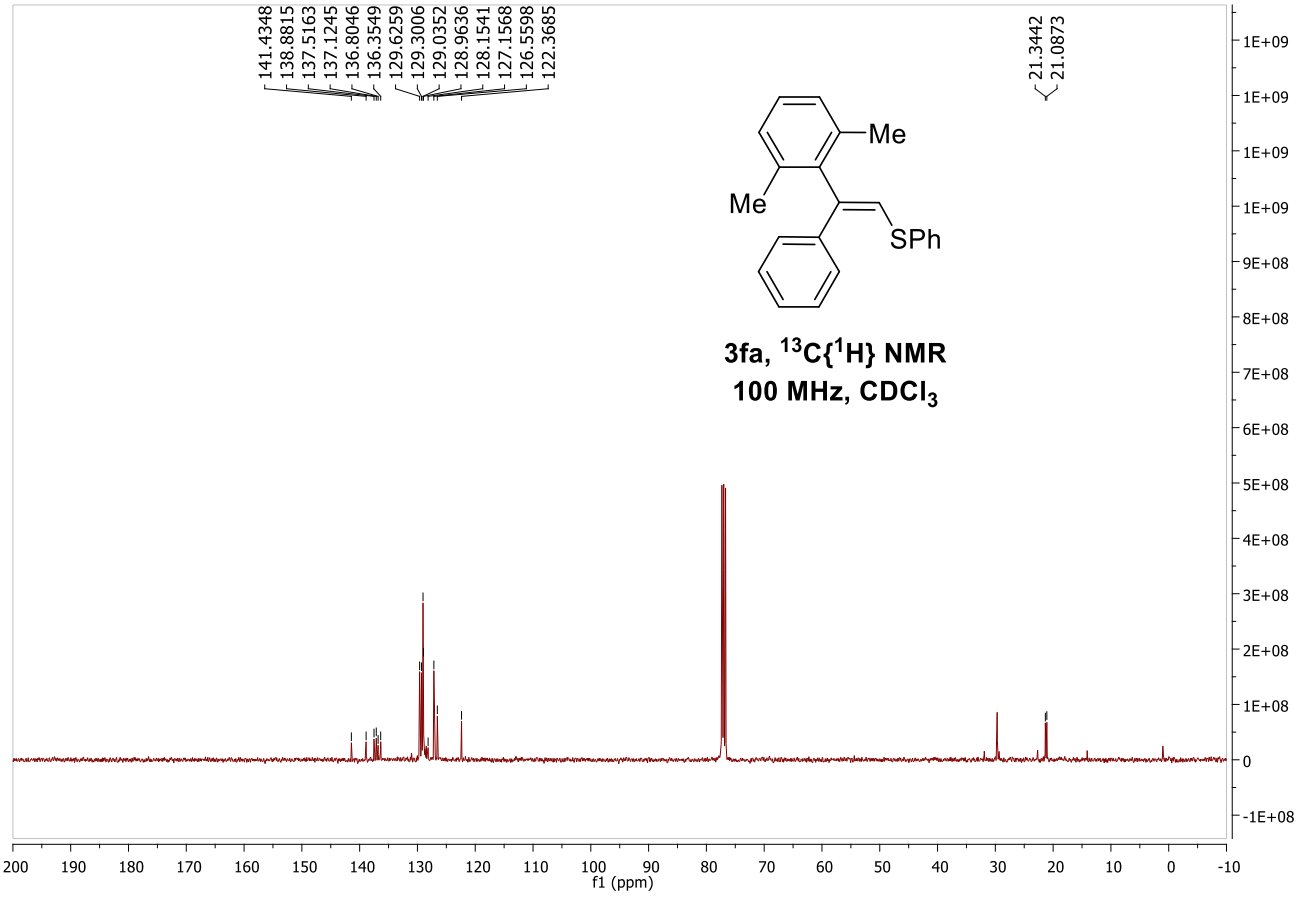
141.4348
138.8815
137.5163
137.1245
136.8046
136.3549
129.6259
129.3006
129.0352
128.9636
128.1541
127.1568
126.5598
122.3685
21.3442
21.0873
Me
Me
SPh
3fa, 13C{1H} NMR
100 MHz, CDCl3
f1 (ppm)

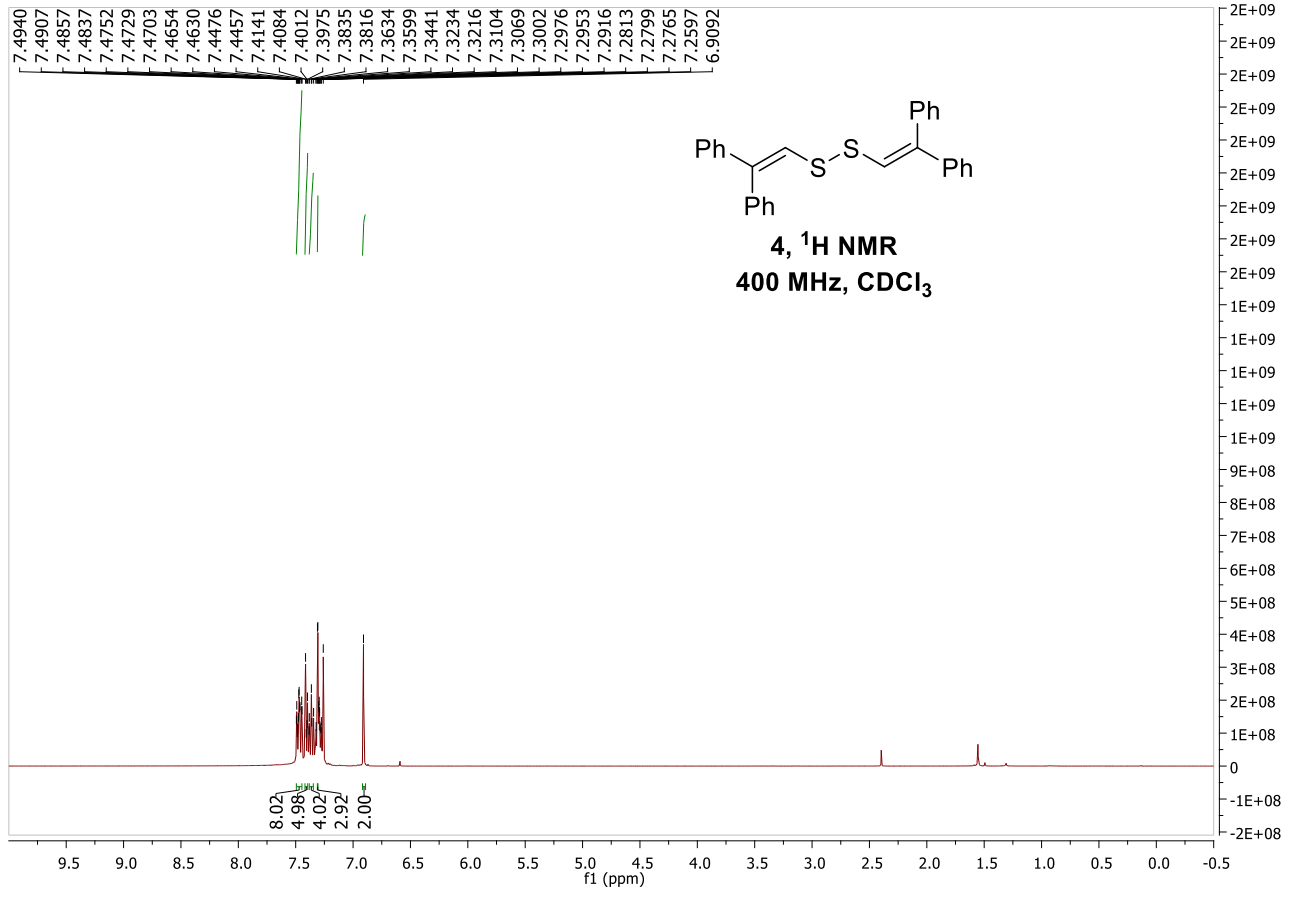
7.4940
7.4907
7.4857
7.4837
7.4752
7.4729
7.4703
7.4654
7.4630
7.4476
7.4457
7.4141
7.4084
7.4012
7.3975
7.3835
7.3816
7.3634
7.3599
7.3441
7.3234
7.3216
7.3104
7.3069
7.3002
7.2976
7.2953
7.2916
7.2813
7.2799
7.2765
7.2597
6.9092
Ph
Ph
S
S
Ph
Ph
4, 1H NMR
400 MHz, CDCl3
8.02
4.98
4.02
2.92
2.00
f1 (ppm)

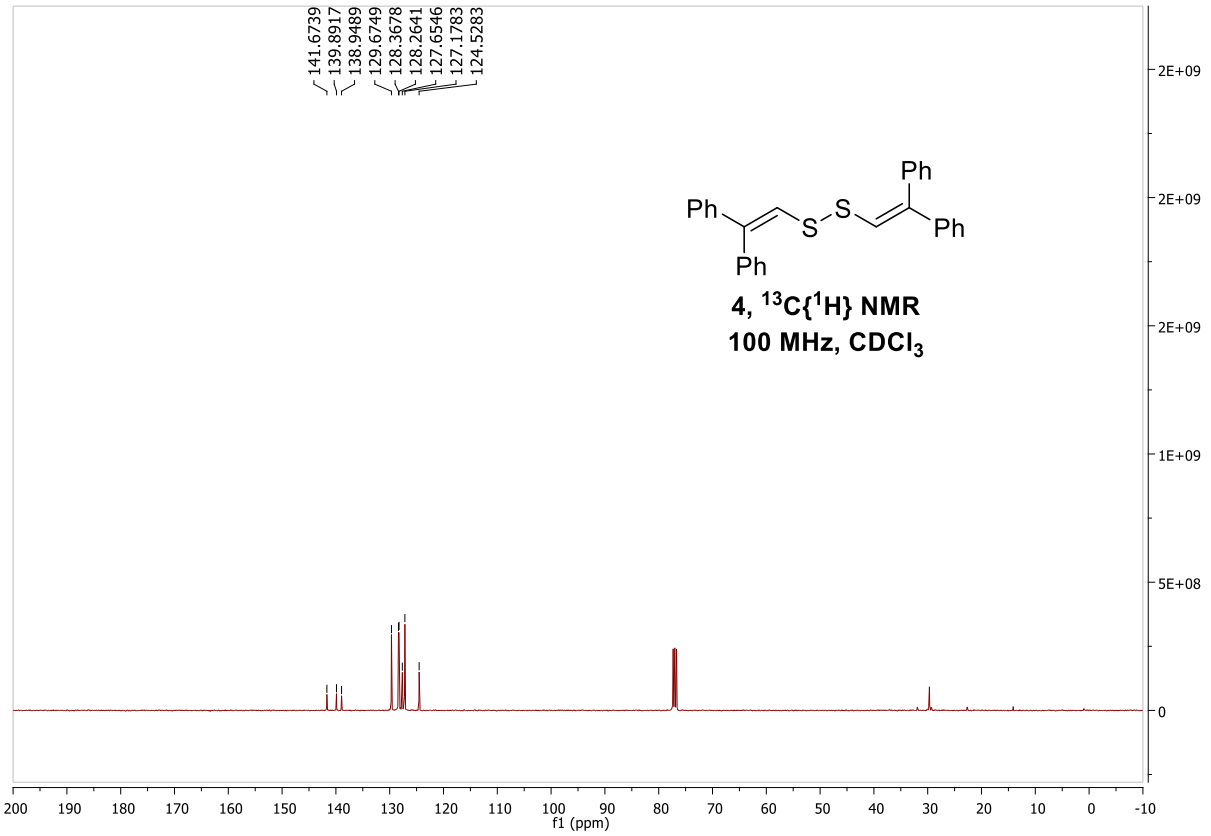
141.6739
139.8917
138.9489
129.6749
128.3678
128.2641
127.6546
127.1783
124.5283
Ph
Ph
S
S
Ph
Ph
4, 13C{1H} NMR
100 MHz, CDCl3
f1 (ppm)

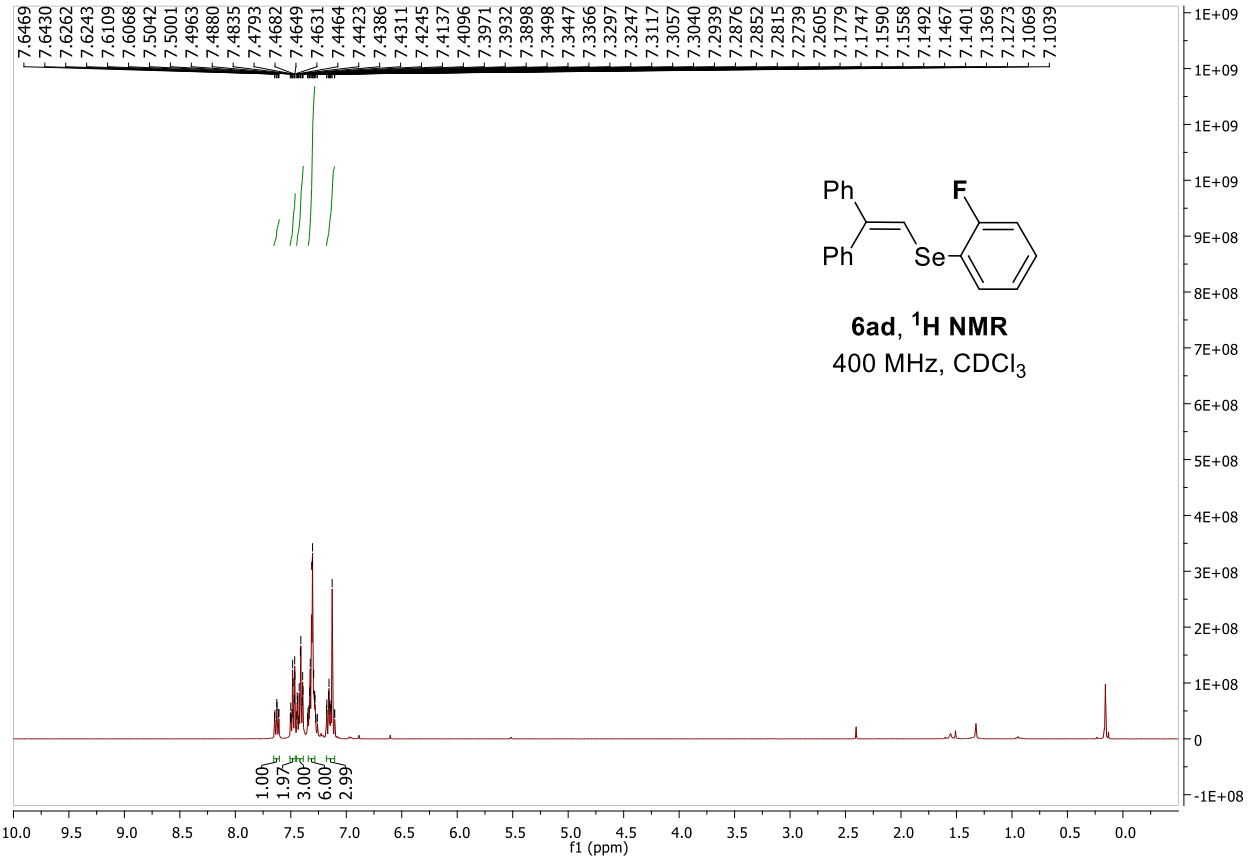
7.6469
7.6430
7.6262
7.6243
7.6109
7.6068
7.5042
7.5001
7.4963
7.4880
7.4835
7.4793
7.4682
7.4649
7.4631
7.4464
7.4423
7.4386
7.4311
7.4245
7.4137
7.4096
7.3971
7.3932
7.3898
7.3498
7.3447
7.3366
7.3297
7.3247
7.3117
7.3057
7.3040
7.2939
7.2876
7.2852
7.2815
7.2739
7.2605
7.1779
7.1747
7.1590
7.1558
7.1492
7.1467
7.1401
7.1369
7.1273
7.1069
7.1039
Ph
Ph
F
Se
6ad, 1H NMR
400 MHz, CDCl3
1.00
1.97
3.00
6.00
2.99
f1 (ppm)

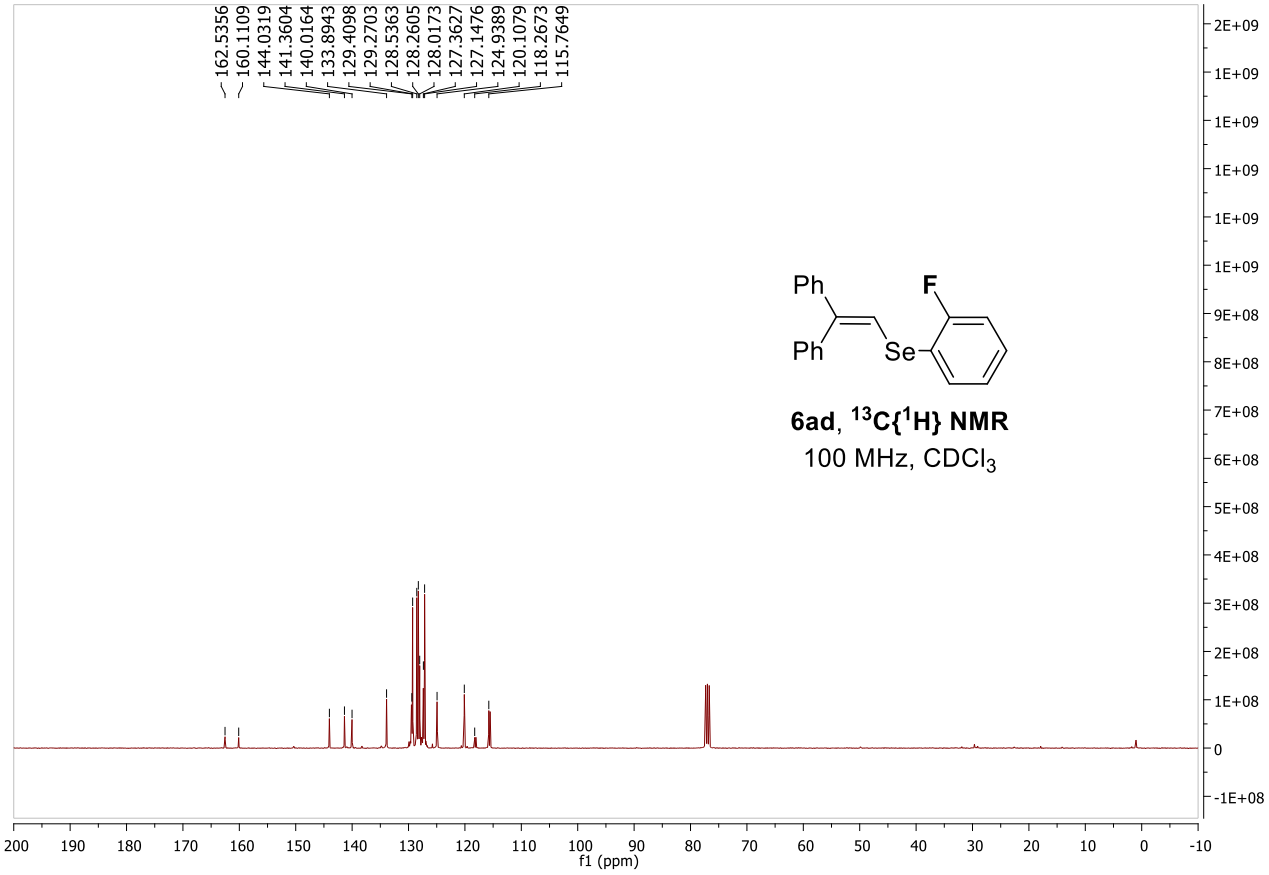
162.5356
160.1109
144.0319
141.3604
140.0164
133.8943
129.4098
129.2703
128.5363
128.2605
128.0173
127.3627
127.1476
124.9389
120.1079
118.2673
115.7649
Ph
F
Ph
Se
6ad, 13C{1H} NMR
100 MHz, CDCl3
f1 (ppm)

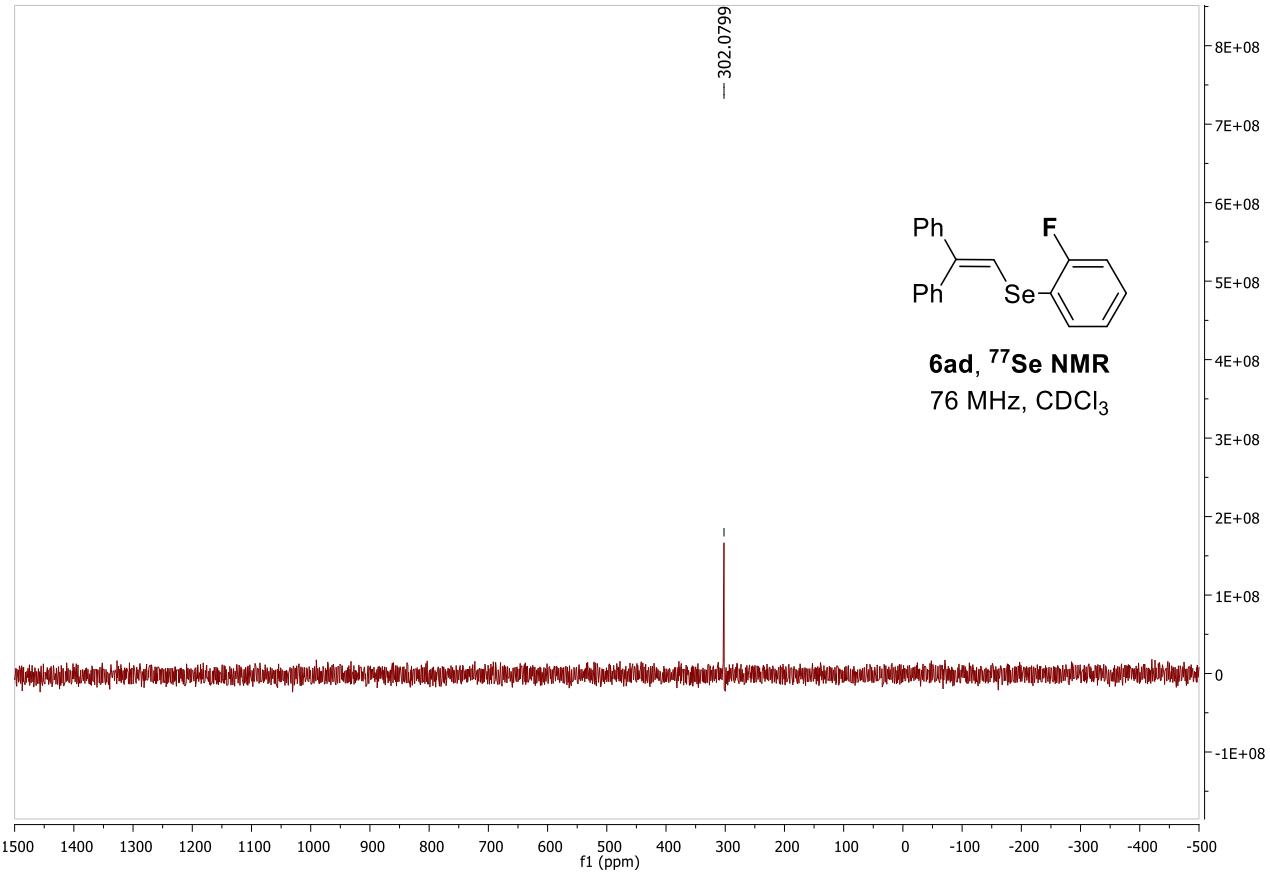
302.0799
Ph
F
Ph
Se
6ad, 77Se NMR
76 MHz, CDCl3
f1 (ppm)

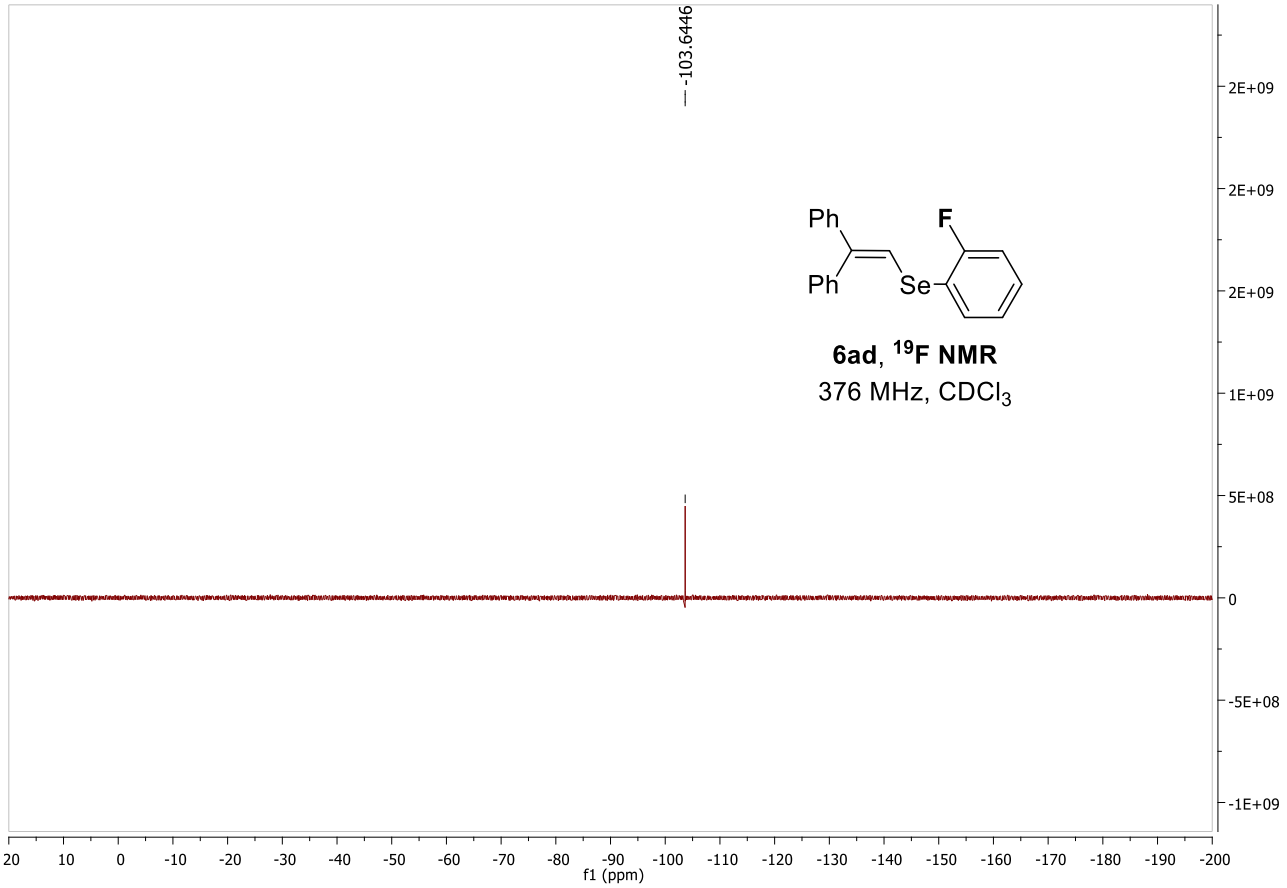
-103.6446
Ph
F
Ph
Se
6ad, 19F NMR
376 MHz, CDCl3
f1 (ppm)

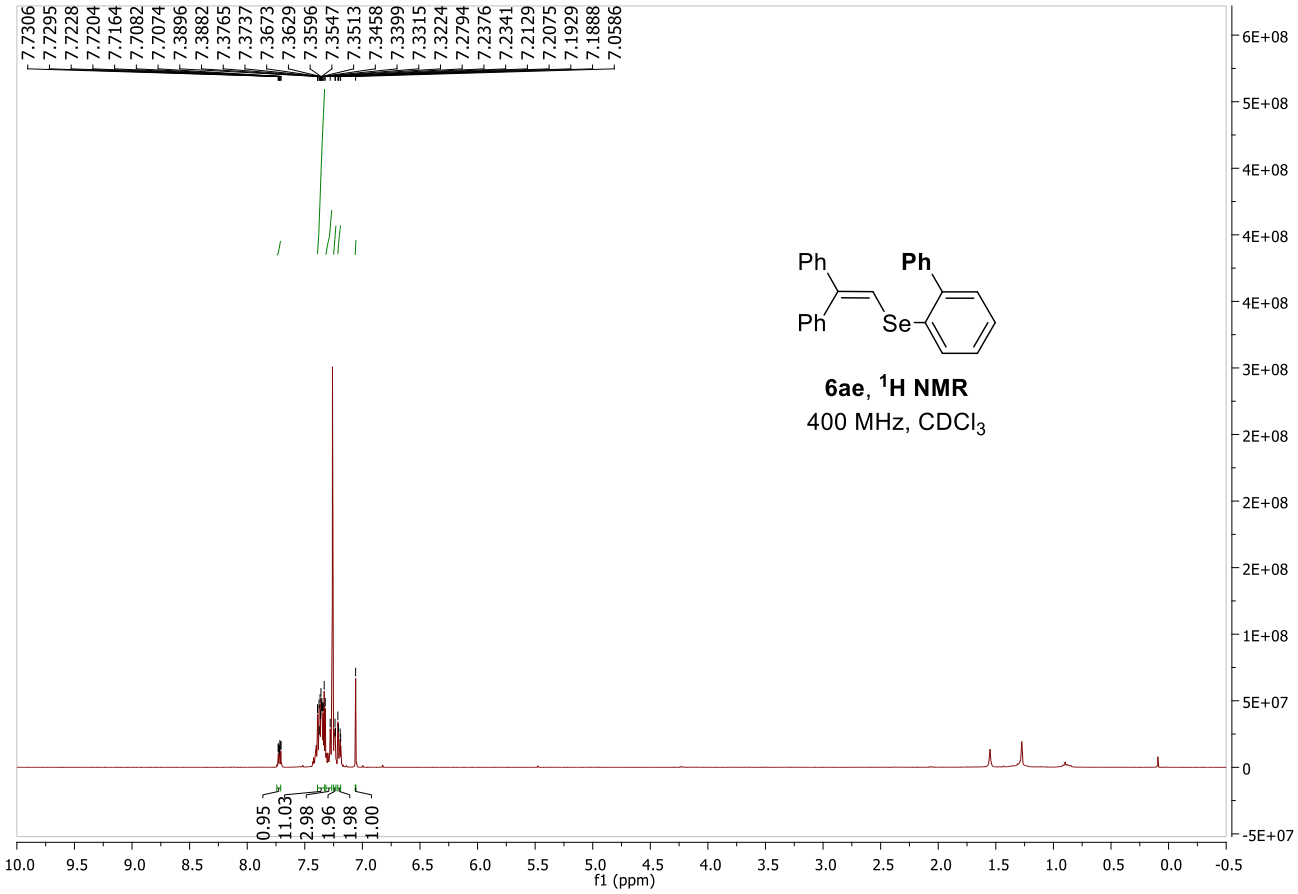
7.7306
7.7295
7.7228
7.7204
7.7164
7.7082
7.7074
7.3896
7.3882
7.3765
7.3737
7.3673
7.3629
7.3596
7.3547
7.3513
7.3458
7.3399
7.3315
7.3224
7.2794
7.2376
7.2341
7.2129
7.2075
7.1929
7.1888
7.0586
Ph
Ph
Ph
Se
6ae, 1H NMR
400 MHz, CDCl3
0.95
11.03
2.98
1.96
1.98
1.00
f1 (ppm)

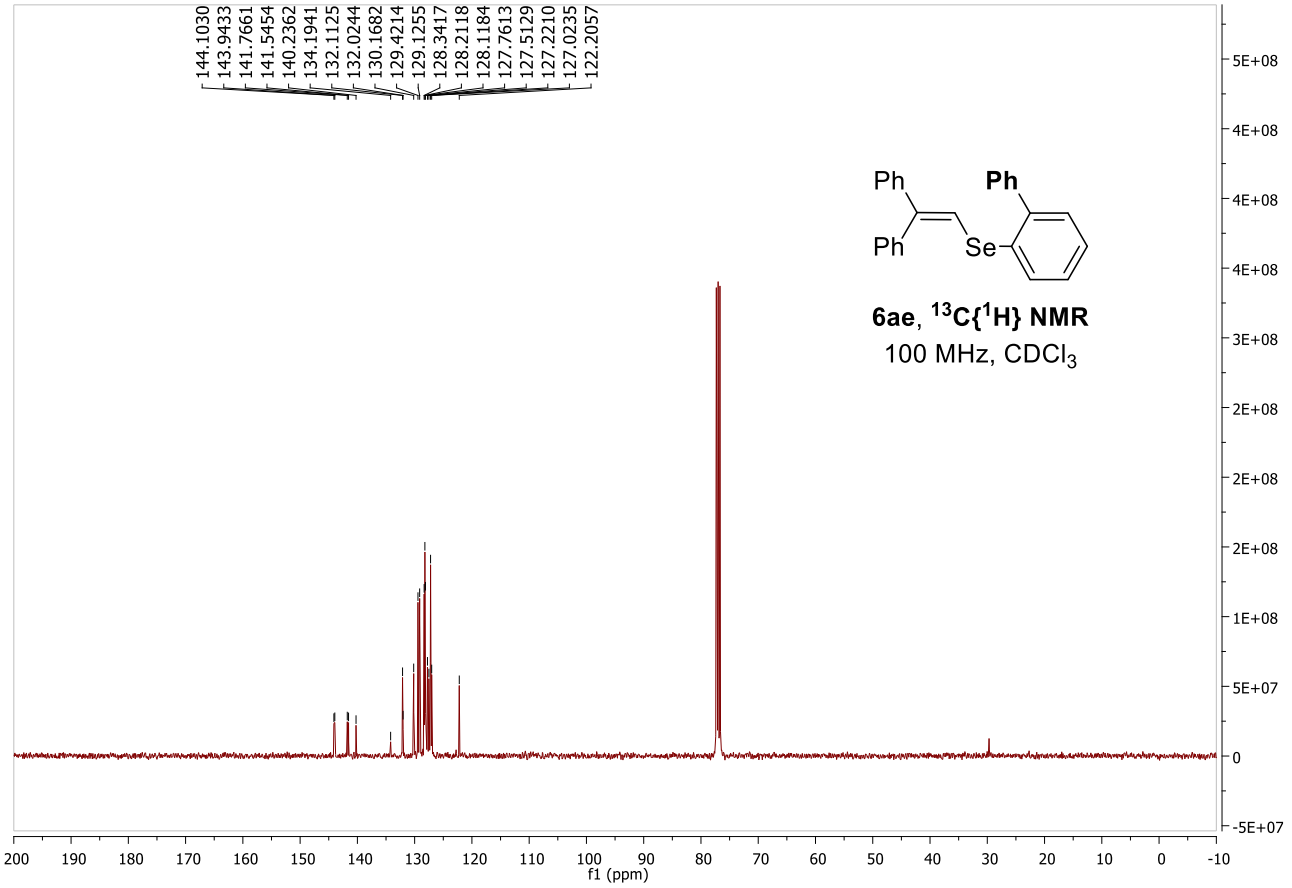
144.1030
143.9433
141.7661
141.5454
140.2362
134.1941
132.1125
132.0244
130.1682
129.4214
129.1255
128.3417
128.2118
128.1184
127.7613
127.5129
127.2210
127.0235
122.2057
Ph
Ph
Ph
Se
6ae, 13C{1H} NMR
100 MHz, CDCl3
f1 (ppm)

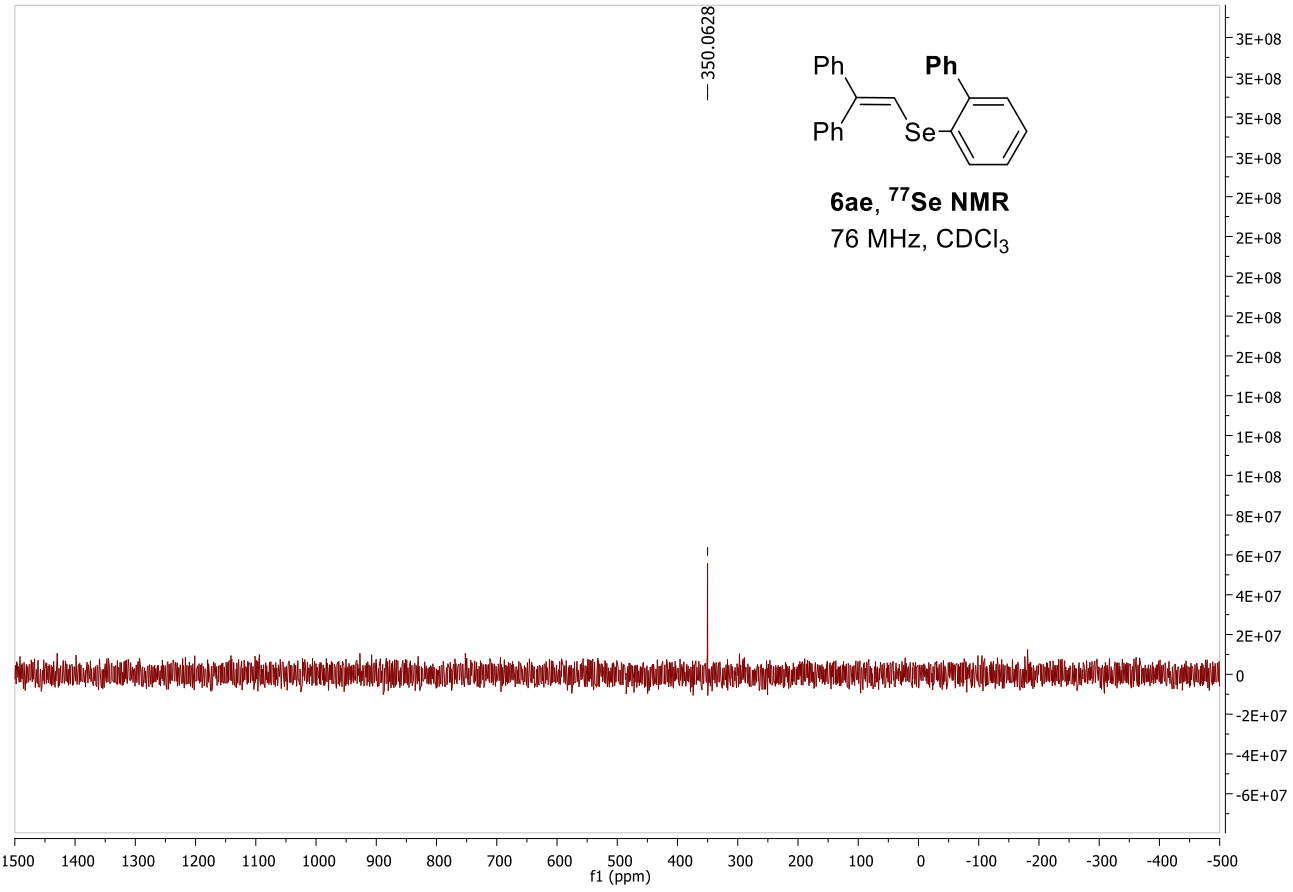
350.0628
Ph
Ph
Ph
Se
6ae, 77Se NMR
76 MHz, CDCl3
f1 (ppm)

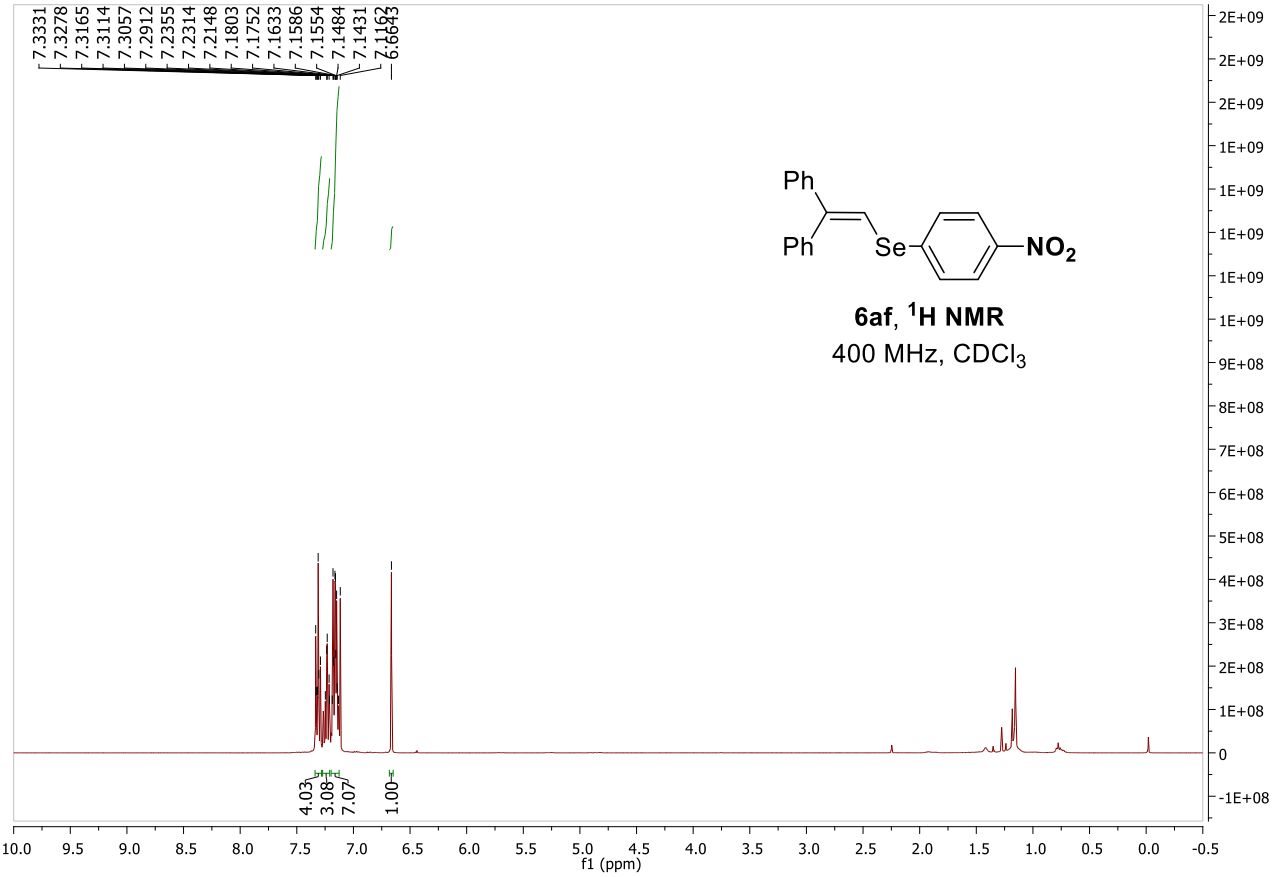
7.3331
7.3278
7.3165
7.3114
7.3057
7.2912
7.2355
7.2314
7.2148
7.1803
7.1752
7.1633
7.1586
7.1554
7.1484
7.1431
7.1162
6.6643
Ph
Ph
Se
NO2
6af, 1H NMR
400 MHz, CDCl3
4.03
3.08
7.07
1.00
f1 (ppm)

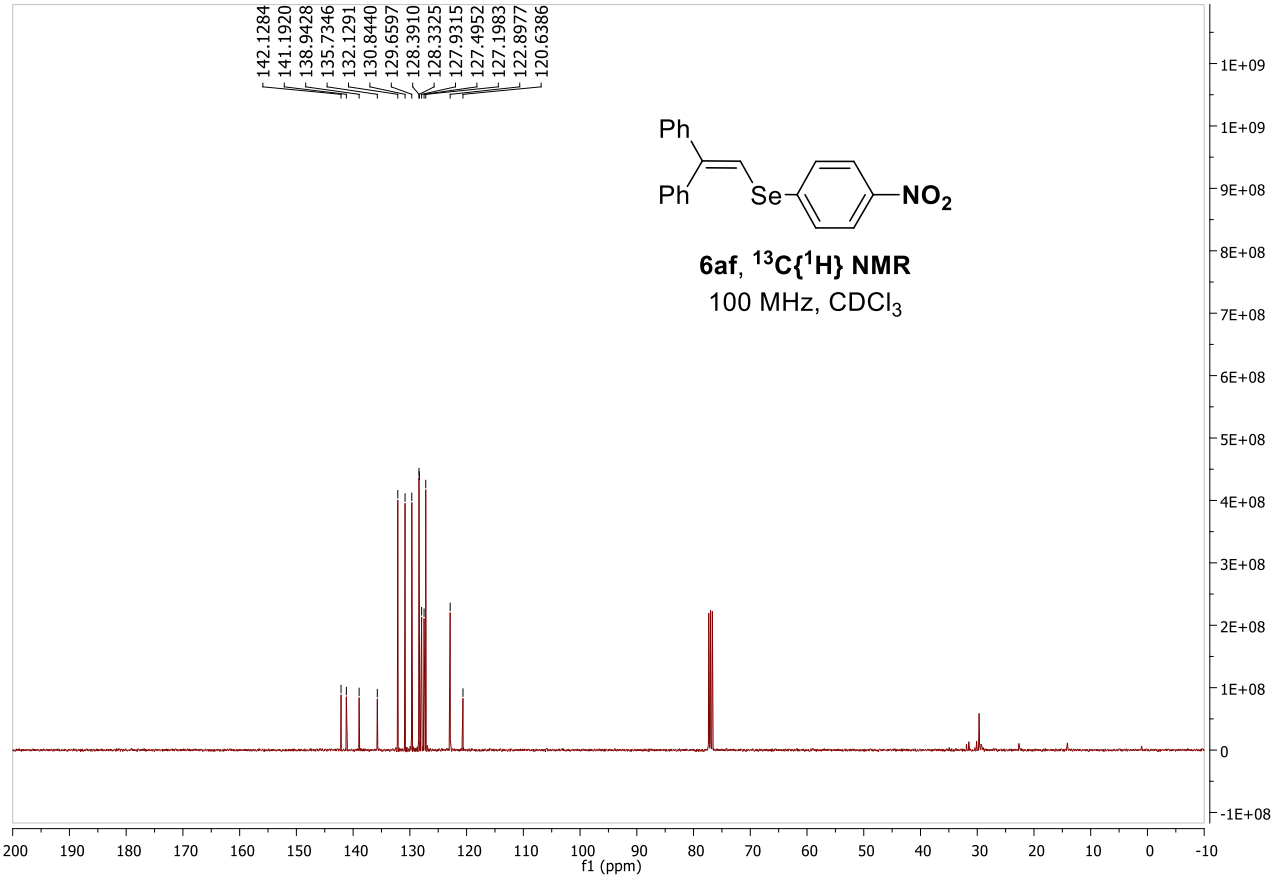
142.1284
141.1920
138.9428
135.7346
132.1291
130.8440
129.6597
128.3910
128.3325
127.9315
127.4952
127.1983
122.8977
120.6386
Ph
Ph
Se
NO2
6af, 13C{1H} NMR
100 MHz, CDCl3
f1 (ppm)

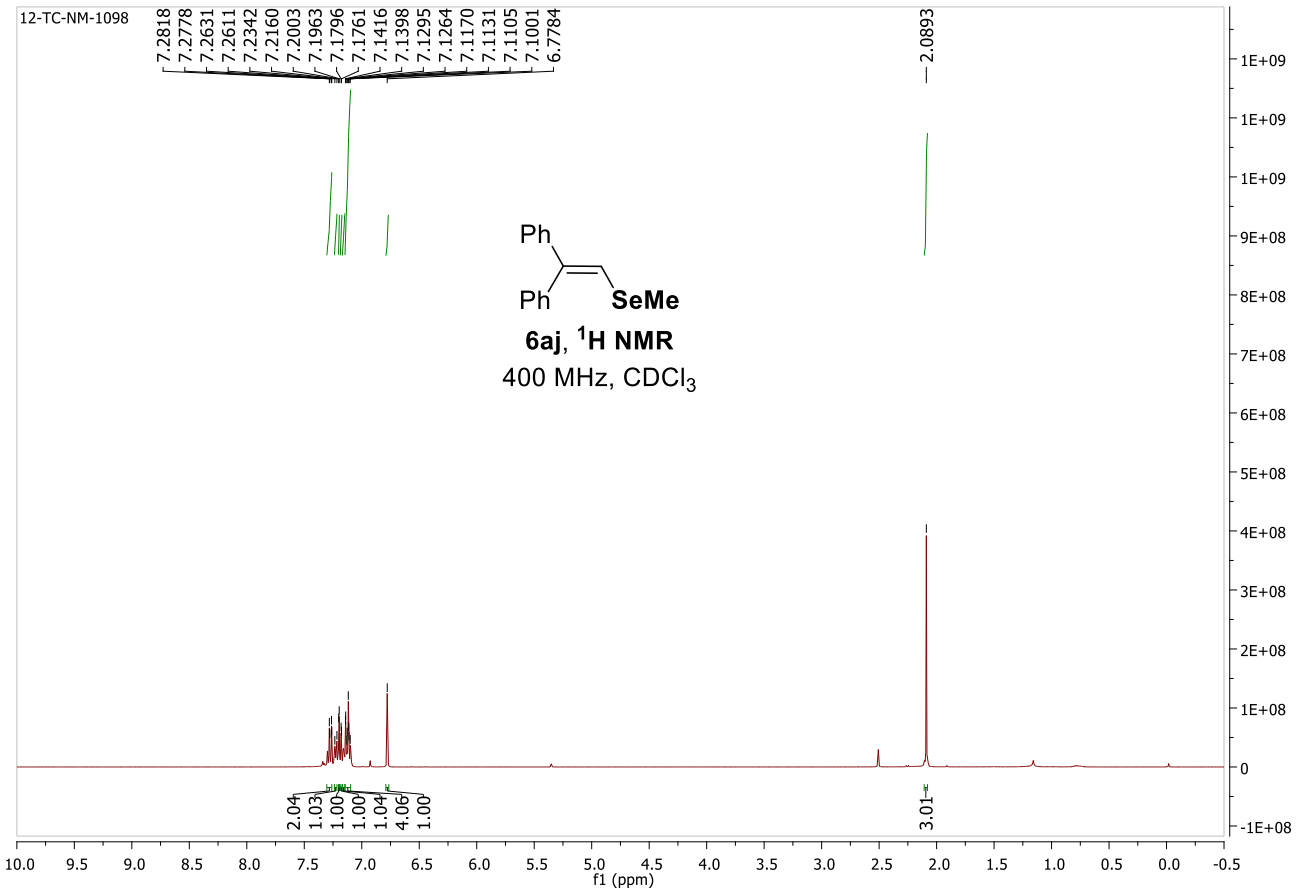
12-TC-NM-1098
7.2818
7.2778
7.2631
7.2611
7.2342
7.2160
7.2003
7.1963
7.1796
7.1761
7.1416
7.1398
7.1295
7.1264
7.1170
7.1131
7.1105
7.1001
6.7784
2.0893
Ph
Ph
SeMe
6aj, 1H NMR
400 MHz, CDCl3
2.04
1.03
1.00
1.00
1.04
4.06
1.00
3.01
f1 (ppm)

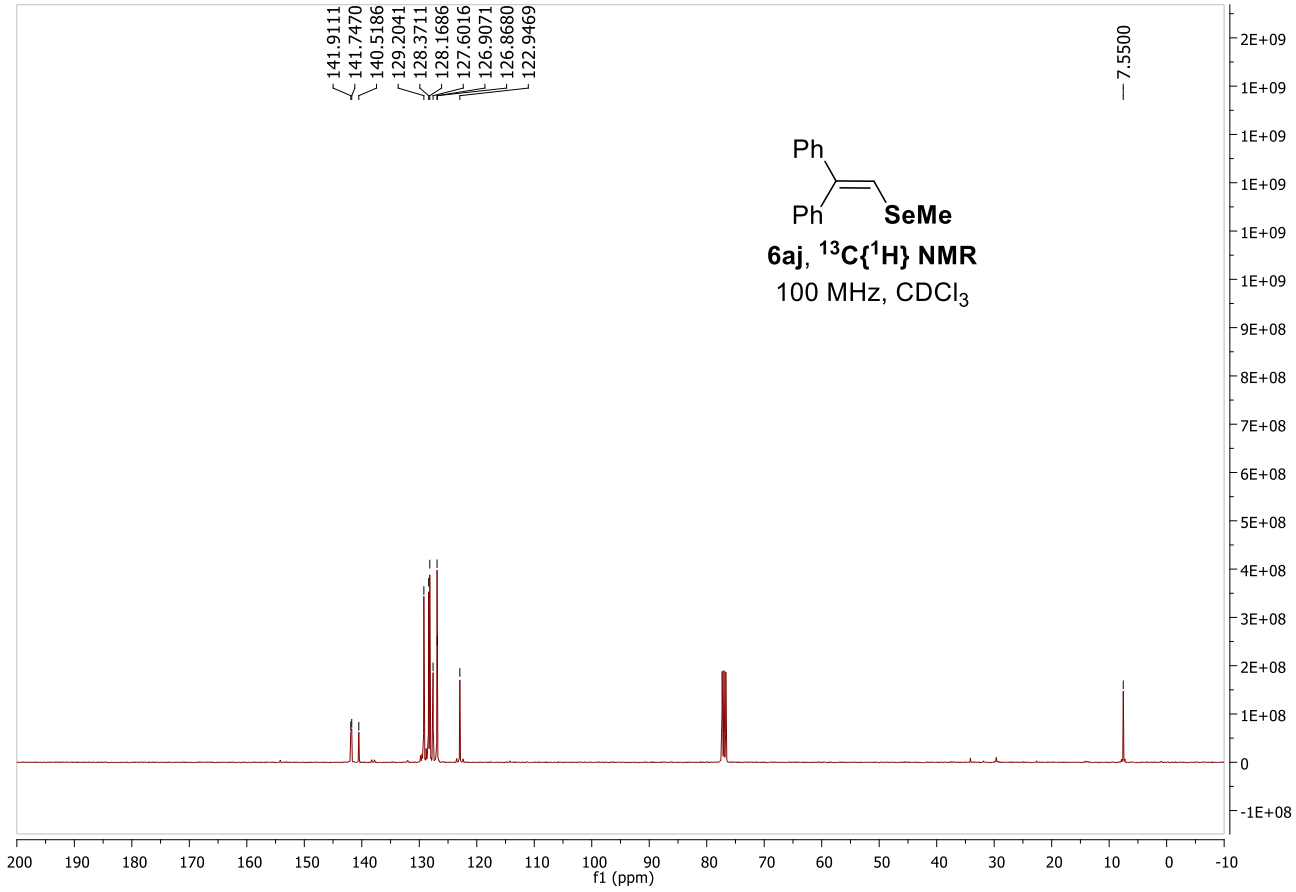
141.9111
141.7470
140.5186
129.2041
128.3711
128.1686
127.6016
126.9071
126.8680
122.9469
7.5500
Ph
Ph
SeMe
6aj, 13C{1H} NMR
100 MHz, CDCl3
f1 (ppm)

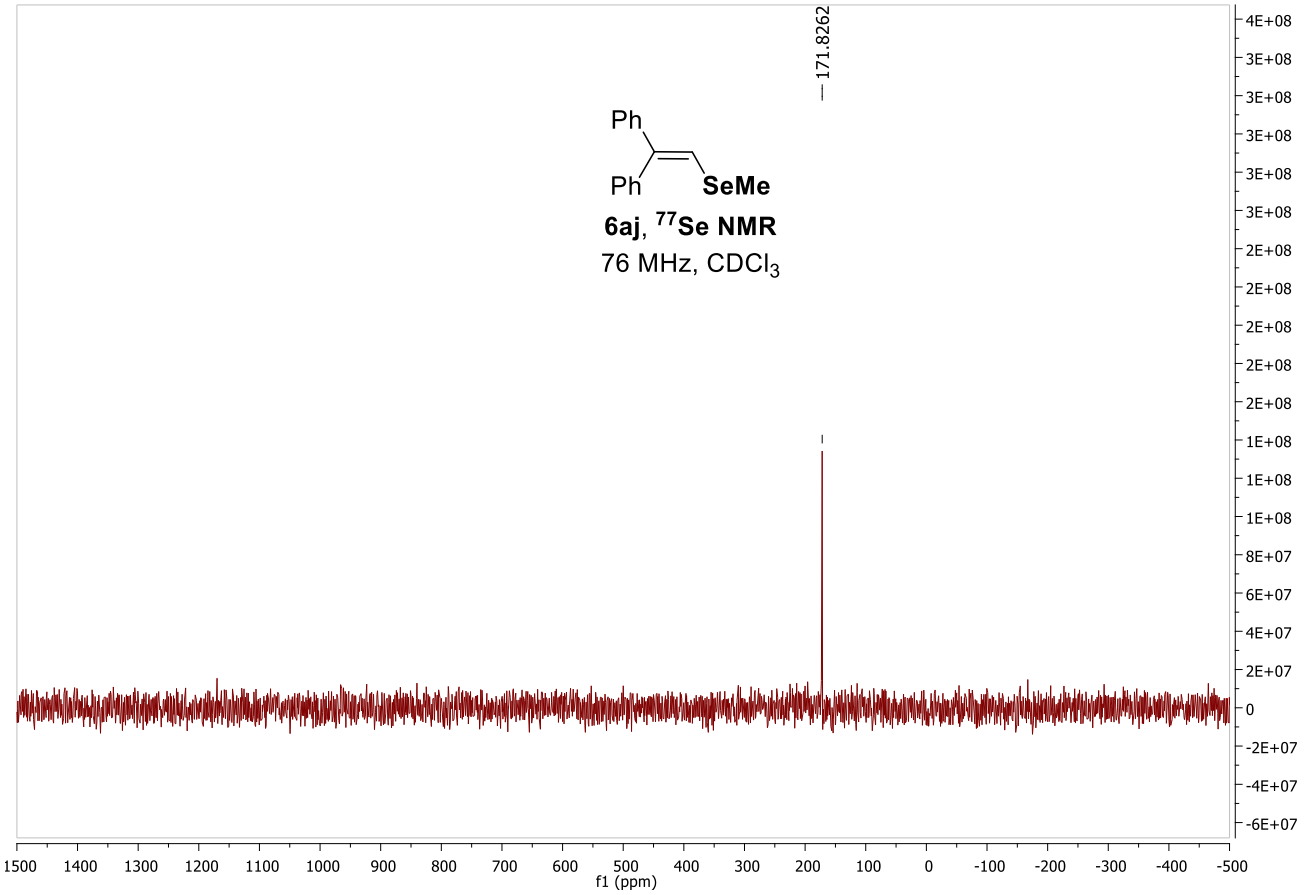
171.8262
Ph
Ph
SeMe
6aj, 77Se NMR
76 MHz, CDCl3
f1 (ppm)

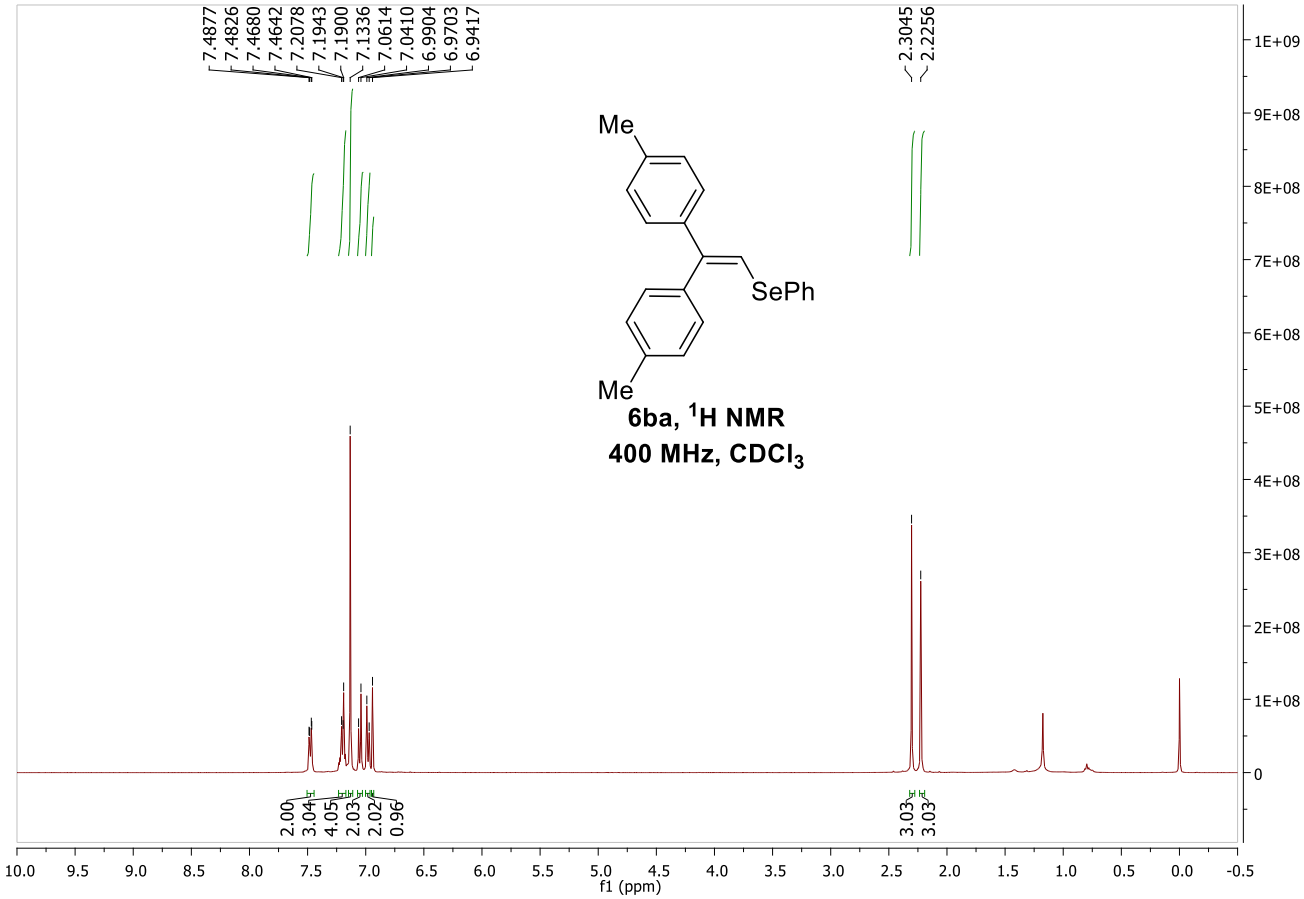
7.4877
7.4826
7.4680
7.4642
7.2078
7.1943
7.1900
7.1336
7.0614
7.0410
6.9904
6.9703
6.9417
2.3045
2.2256
Me
SePh
Me
6ba, 1H NMR
400 MHz, CDCl3
2.00
3.04
4.05
2.03
2.02
0.96
3.03
3.03
f1 (ppm)

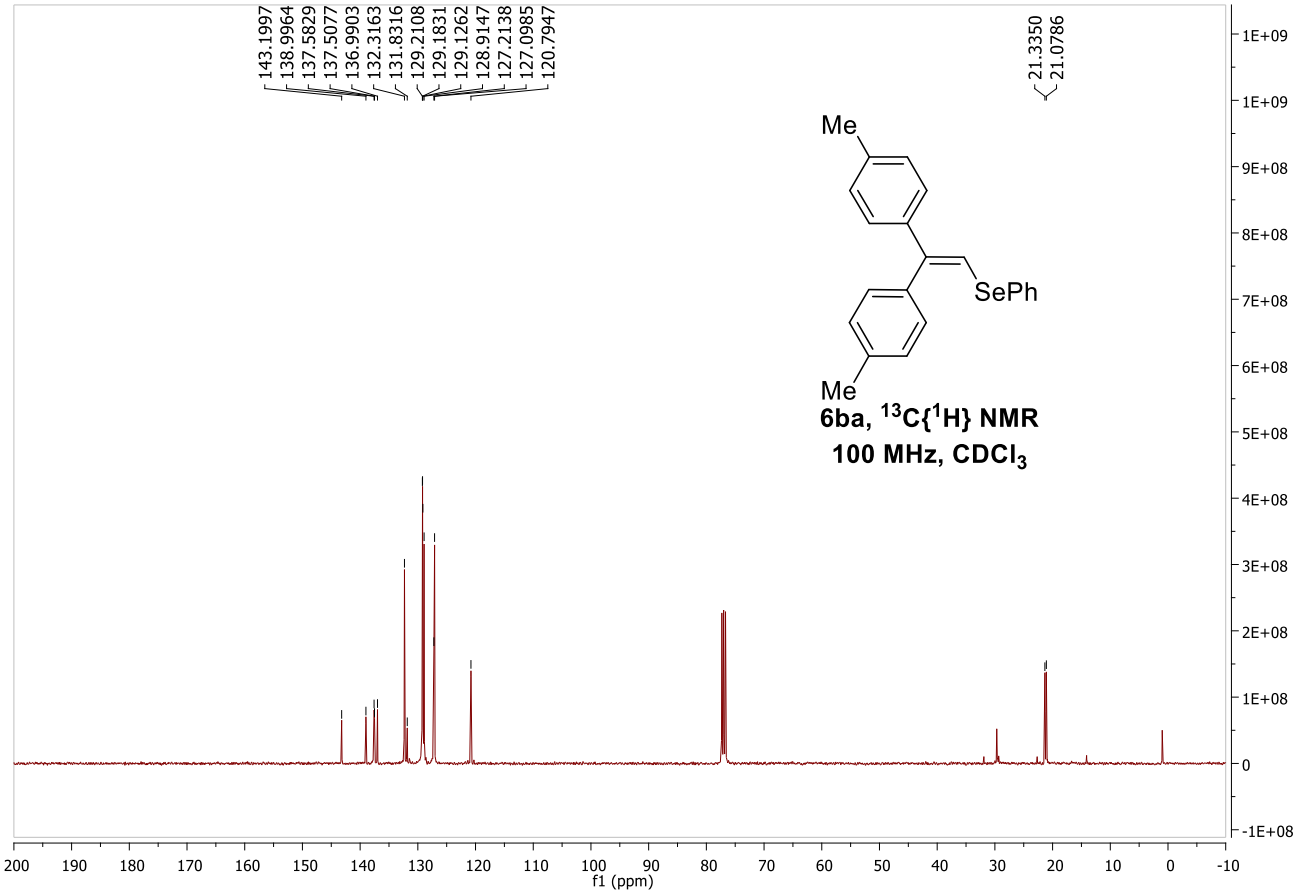
143.1997
138.9964
137.5829
137.5077
136.9903
132.3163
131.8316
129.2108
129.1831
129.1262
128.9147
127.2138
127.0985
120.7947
21.3350
21.0786
Me
SePh
Me
6ba, $^{13}C\{^{1}H\}$ NMR
100 MHz, $CDCl_3$
f1 (ppm)

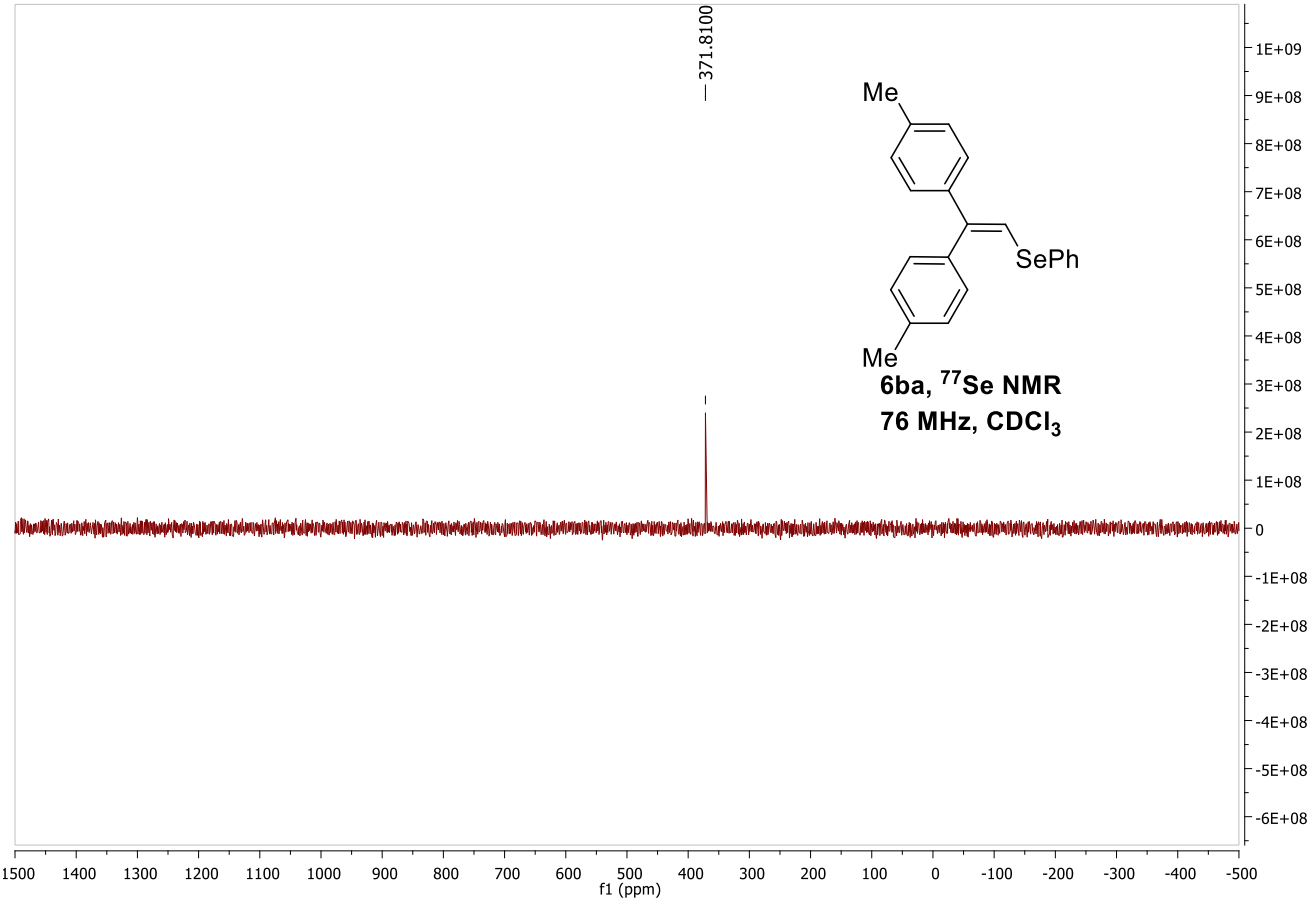
371.8100
Me
SePh
Me
6ba, ^{77}Se NMR
76 MHz, $CDCl_3$
f1 (ppm)

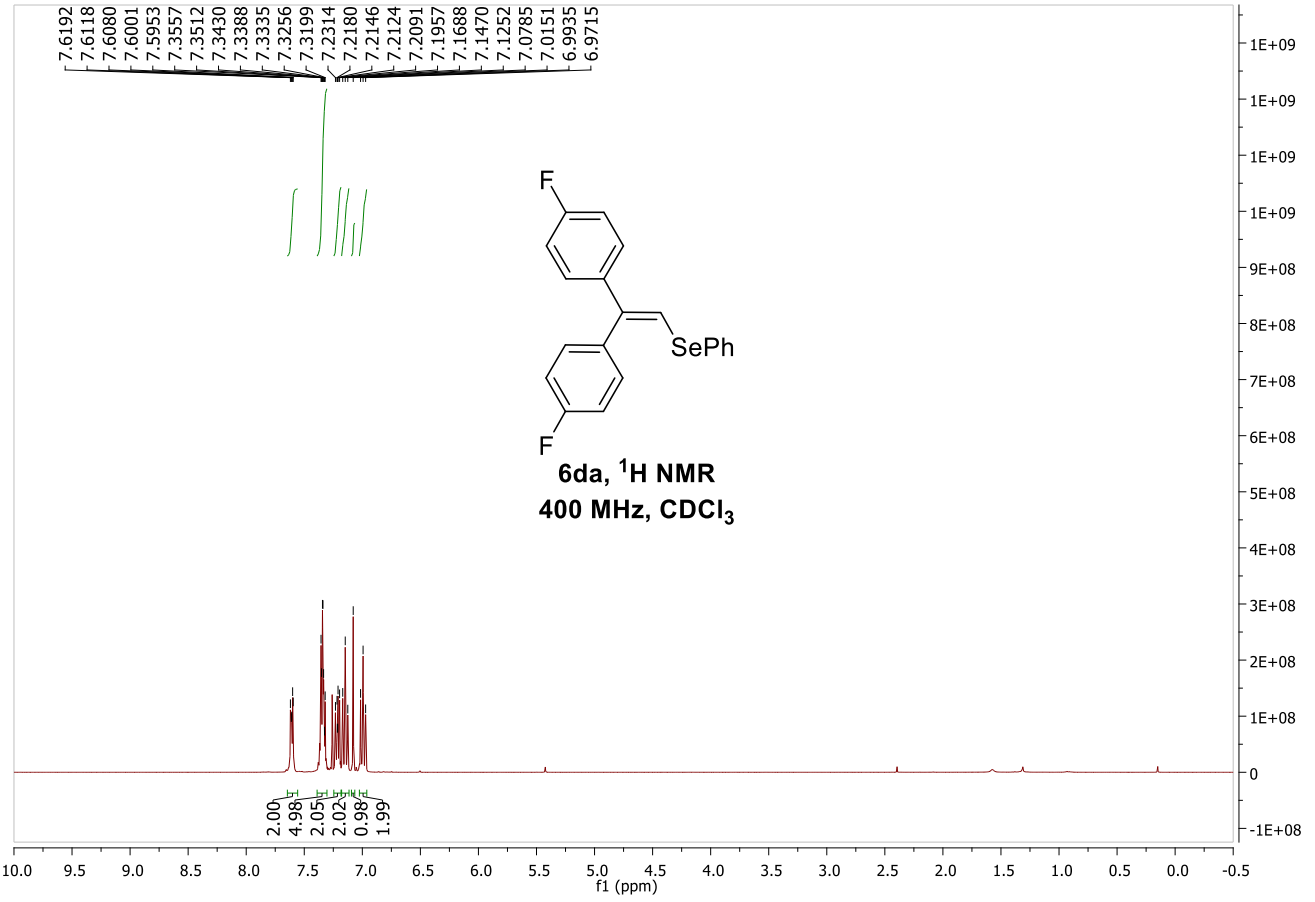
7.6192
7.6118
7.6080
7.6001
7.5953
7.3557
7.3512
7.3430
7.3388
7.3335
7.3256
7.3199
7.2314
7.2180
7.2146
7.2124
7.2091
7.1957
7.1688
7.1470
7.1252
7.0785
7.0151
6.9935
6.9715
F
SePh
F
6da, ^{1}H NMR
400 MHz, CDCl$_3$
2.00
4.98
2.05
2.02
0.98
1.99
f1 (ppm)

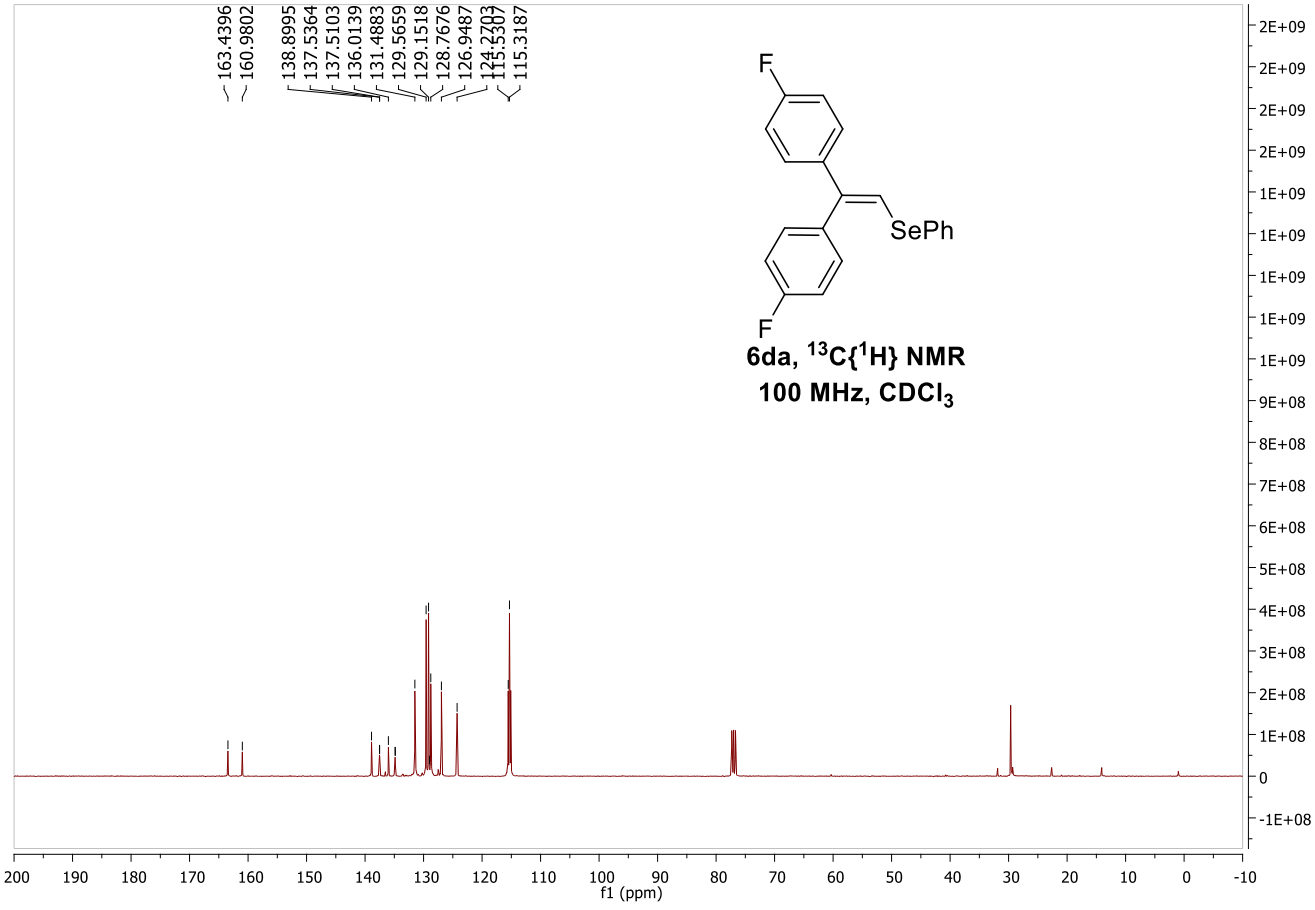
163.4396
160.9802
138.8995
137.5364
137.5103
136.0139
131.4883
129.5659
129.1518
128.7676
126.9487
115.5307
115.3187
F
SePh
F
6da, ^{13}C{^{1}H} NMR
100 MHz, CDCl$_3$
f1 (ppm)

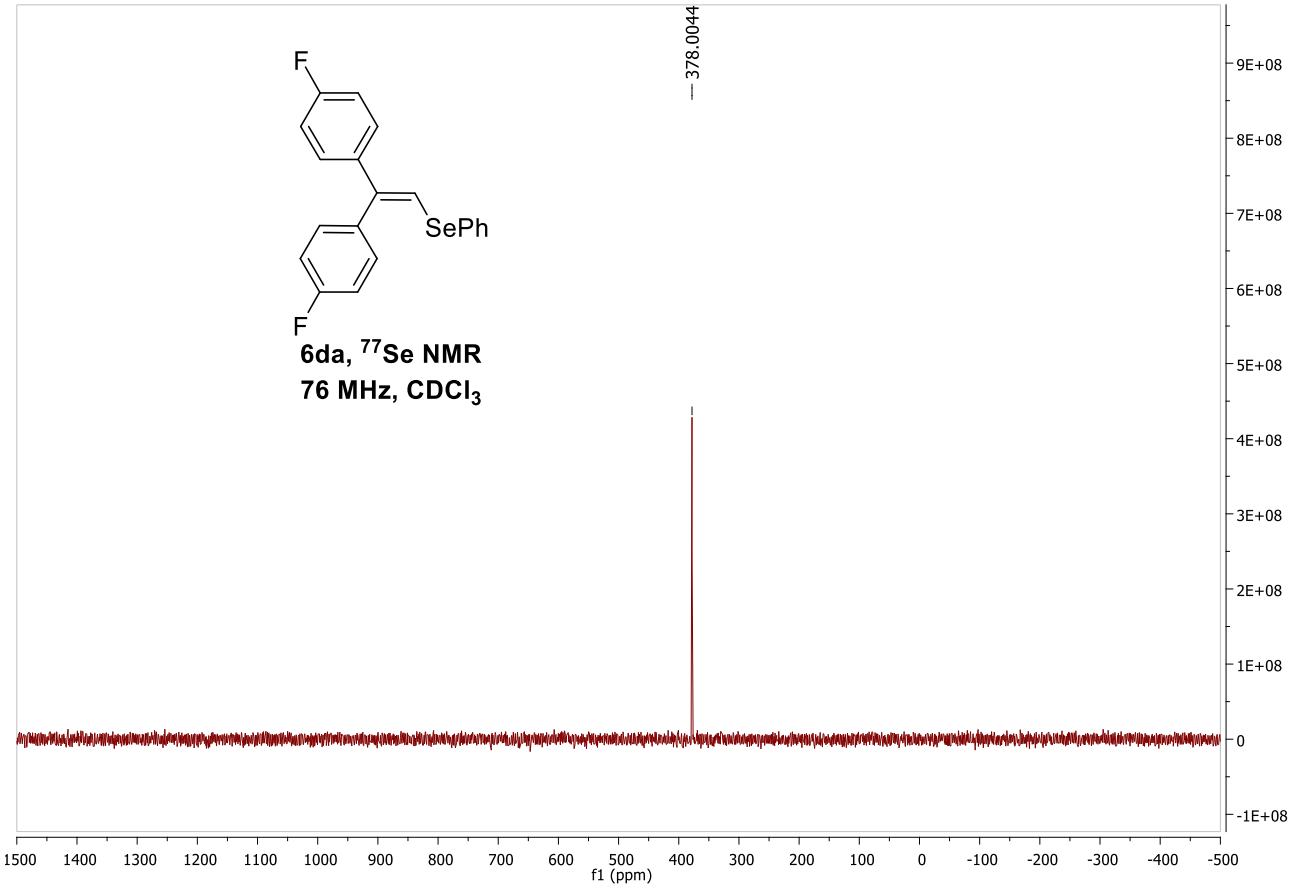
F
SePh
F
378.0044
6da, 77Se NMR
76 MHz, CDCl3
9E+08
8E+08
7E+08
6E+08
5E+08
4E+08
3E+08
2E+08
1E+08
0
-1E+08
1500 1400 1300 1200 1100 1000 900 800 700 600 500 400 300 200 100 0 -100 -200 -300 -400 -500
f1 (ppm)

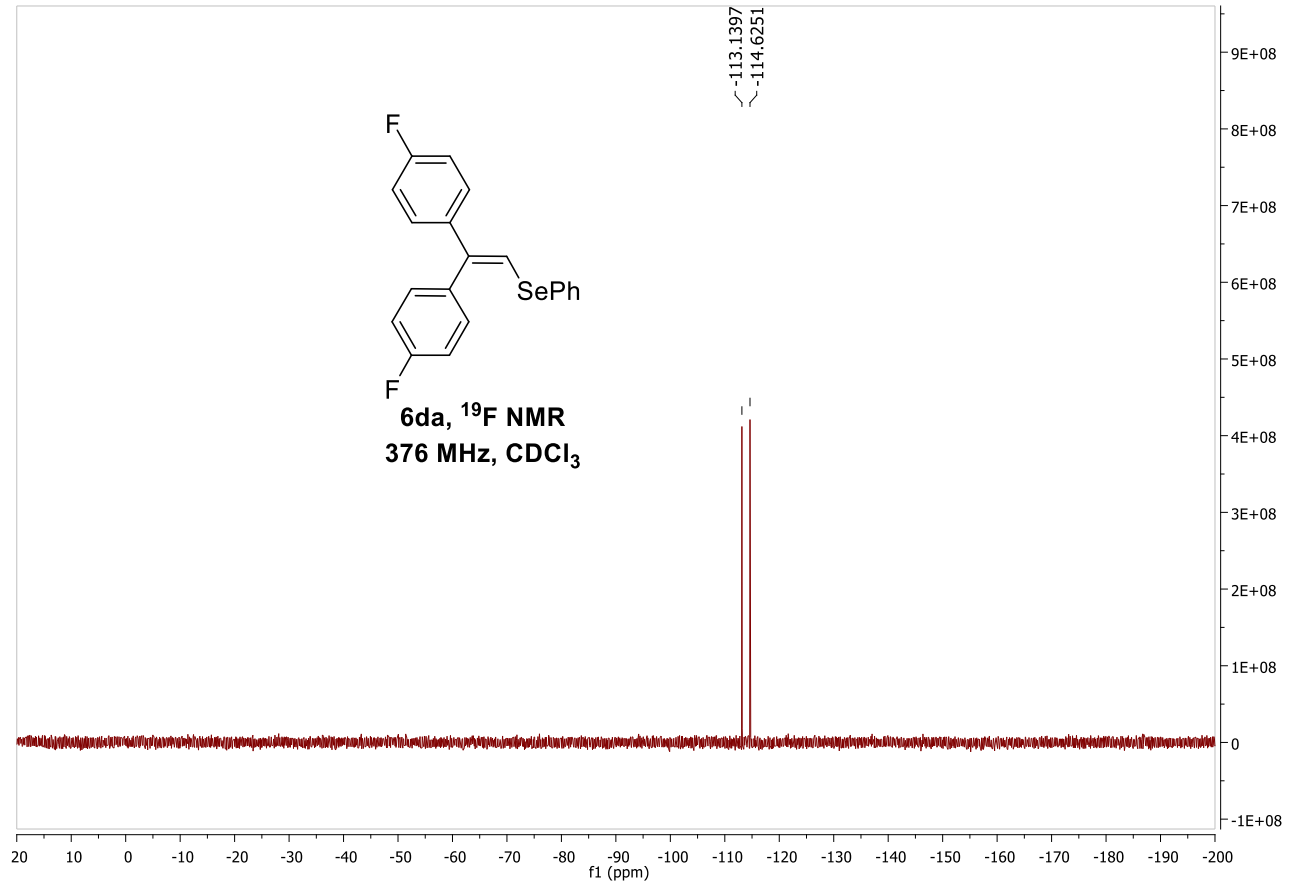
F
SePh
F
-113.1397
-114.6251
6da, 19F NMR
376 MHz, CDCl3
9E+08
8E+08
7E+08
6E+08
5E+08
4E+08
3E+08
2E+08
1E+08
0
-1E+08
20 10 0 -10 -20 -30 -40 -50 -60 -70 -80 -90 -100 -110 -120 -130 -140 -150 -160 -170 -180 -190 -200
f1 (ppm)

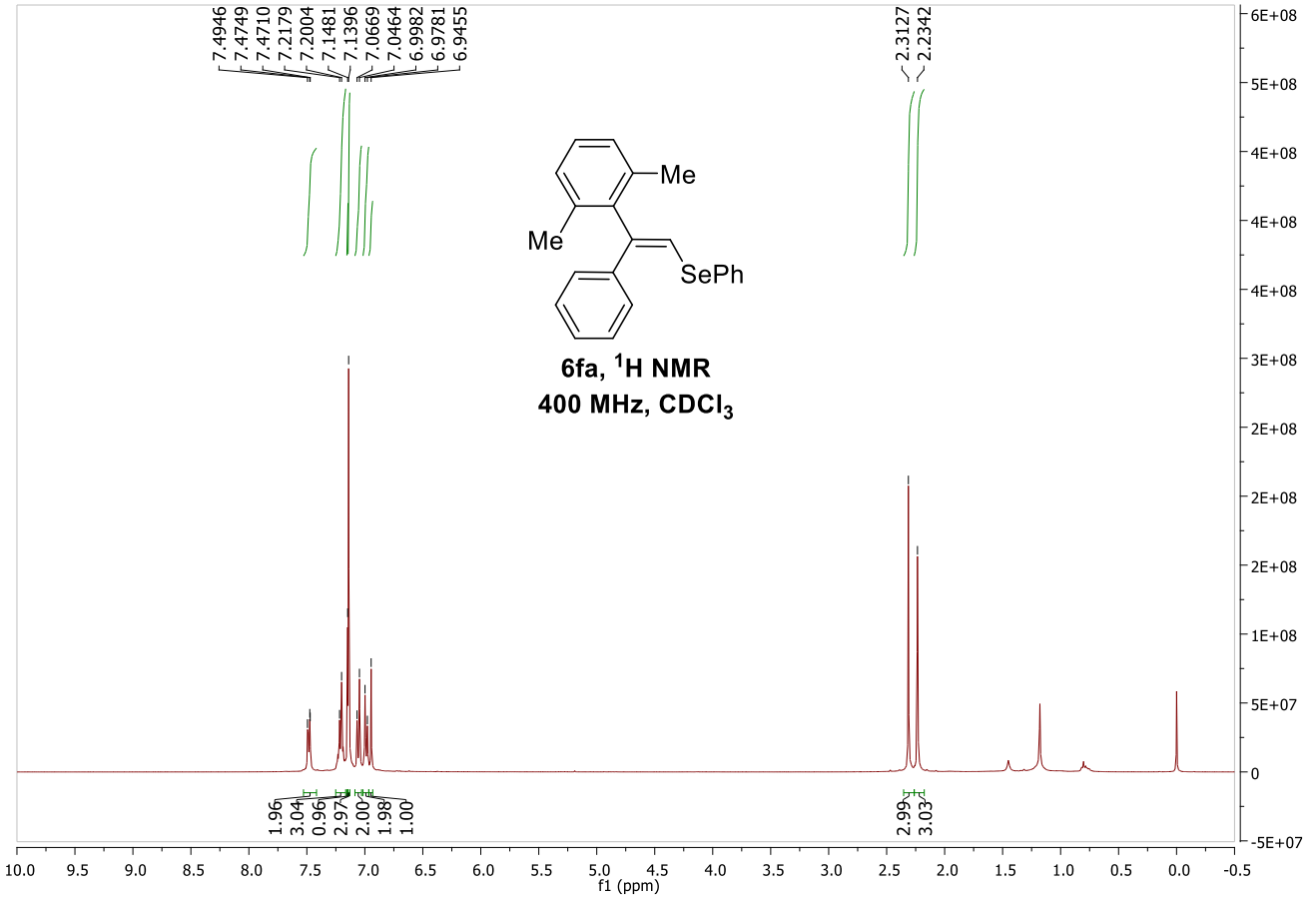
7.4946
7.4749
7.4710
7.2179
7.2004
7.1481
7.1396
7.0669
7.0464
6.9982
6.9781
6.9455
2.3127
2.2342
Me
Me
SePh
6fa, ^{1}H NMR
400 MHz, CDCl$_3$
1.96
3.04
0.96
2.97
2.00
1.98
1.00
2.99
3.03
f1 (ppm)

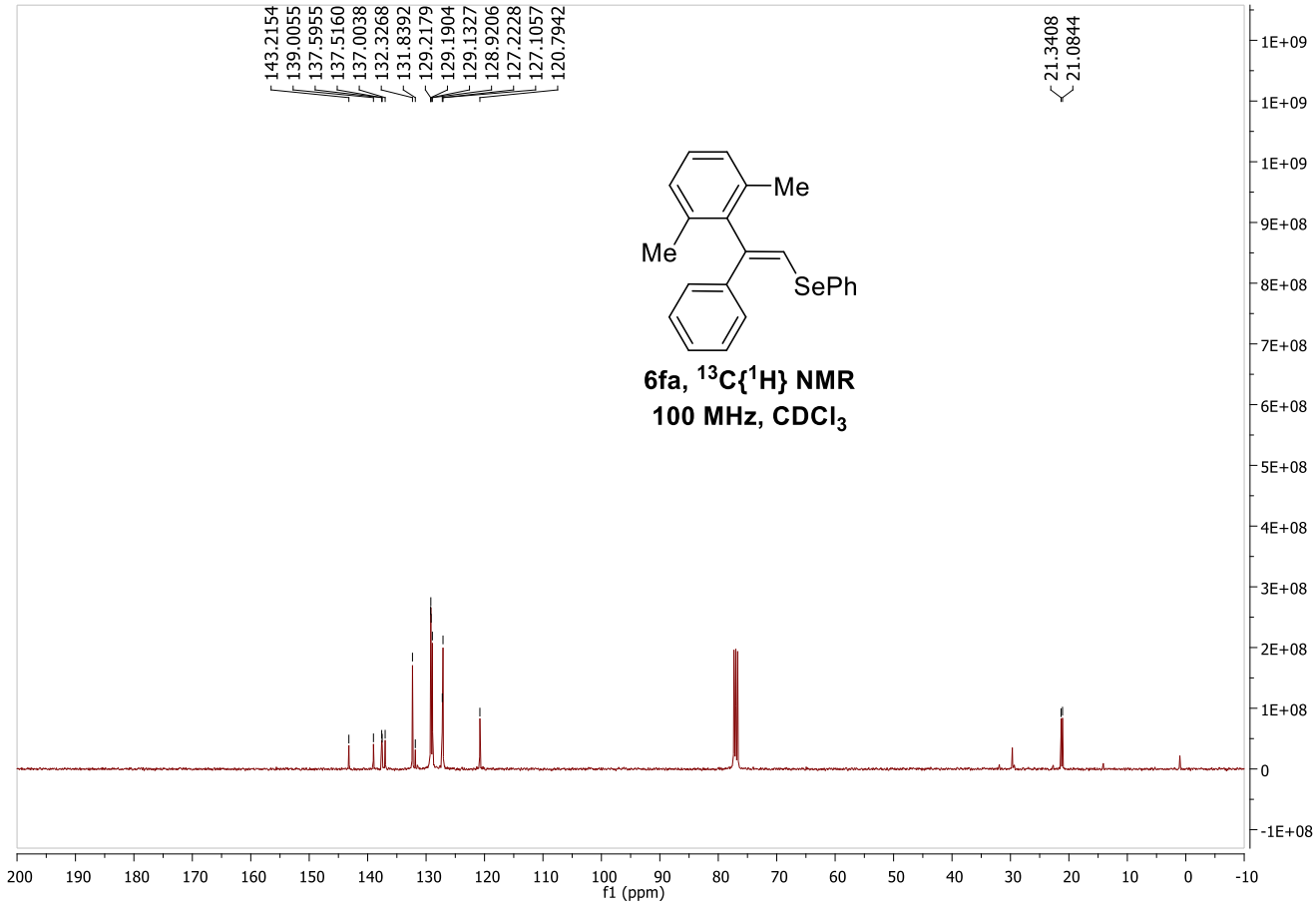
143.2154
139.0055
137.5955
137.5160
137.0038
132.3268
131.8392
129.2179
129.1904
129.1327
128.9206
127.2228
127.1057
120.7942
21.3408
21.0844
Me
Me
SePh
6fa, ^{13}C{^{1}H} NMR
100 MHz, CDCl$_3$
f1 (ppm)

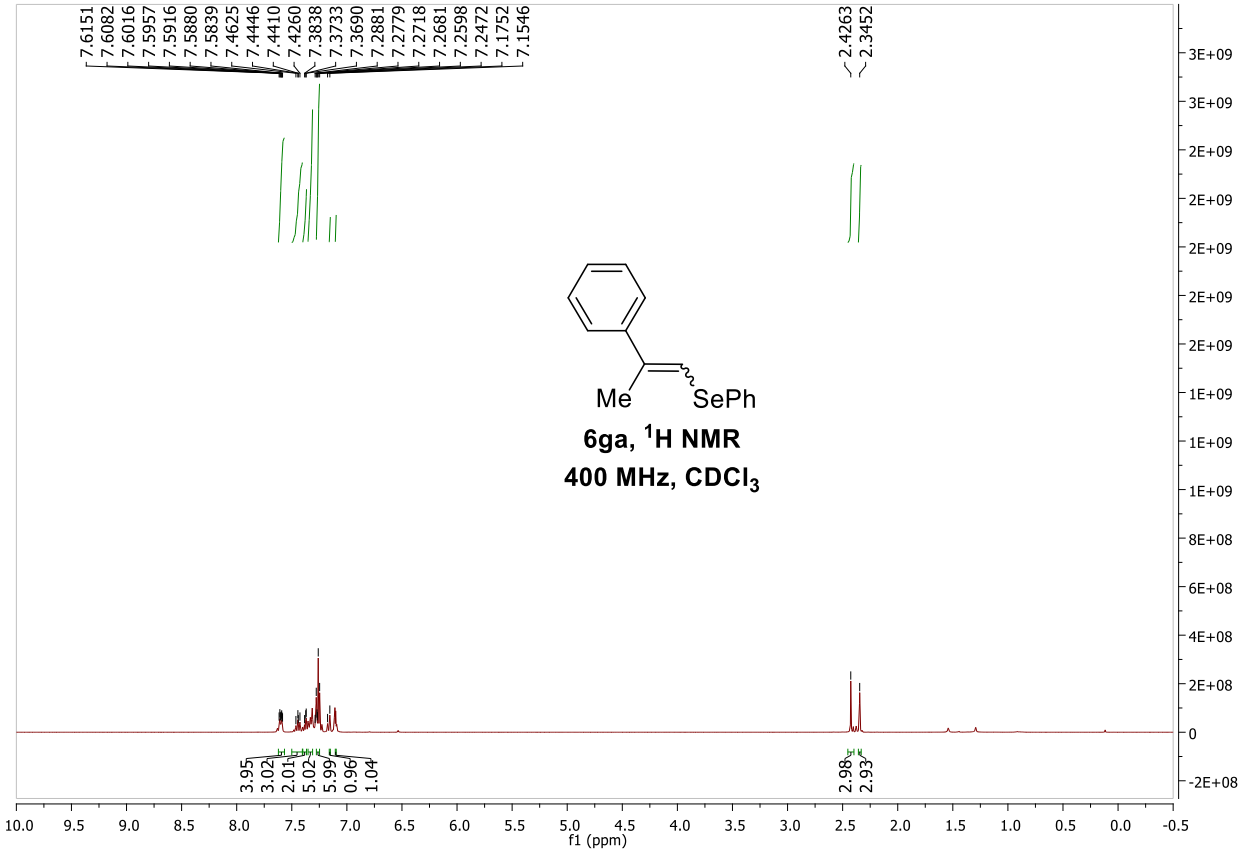
7.6151
7.6082
7.6016
7.5957
7.5916
7.5880
7.5839
7.4625
7.4446
7.4410
7.4260
7.3838
7.3733
7.3690
7.2881
7.2779
7.2718
7.2681
7.2598
7.2472
7.1752
7.1546
2.4263
2.3452
Me
SePh
6ga, 1H NMR
400 MHz, CDCl3
3.95
3.02
2.01
5.02
5.99
0.96
1.04
2.98
2.93
f1 (ppm)

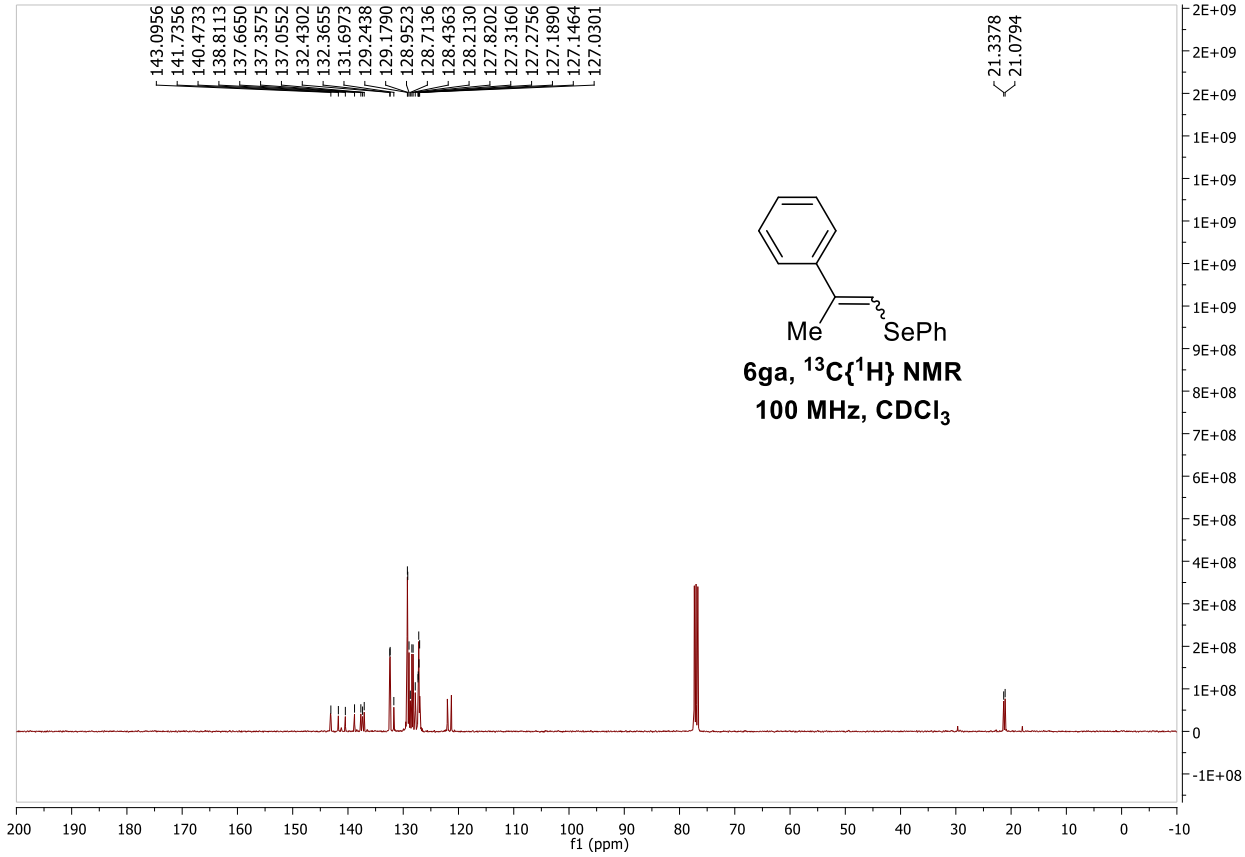
143.0956
141.7356
140.4733
138.8113
137.6650
137.3575
137.0552
132.4302
132.3655
131.6973
129.2438
129.1790
128.9523
128.7136
128.4363
128.2130
127.8202
127.3160
127.2756
127.1890
127.1464
127.0301
21.3378
21.0794
Me
SePh
6ga, 13C{1H} NMR
100 MHz, CDCl3
f1 (ppm)

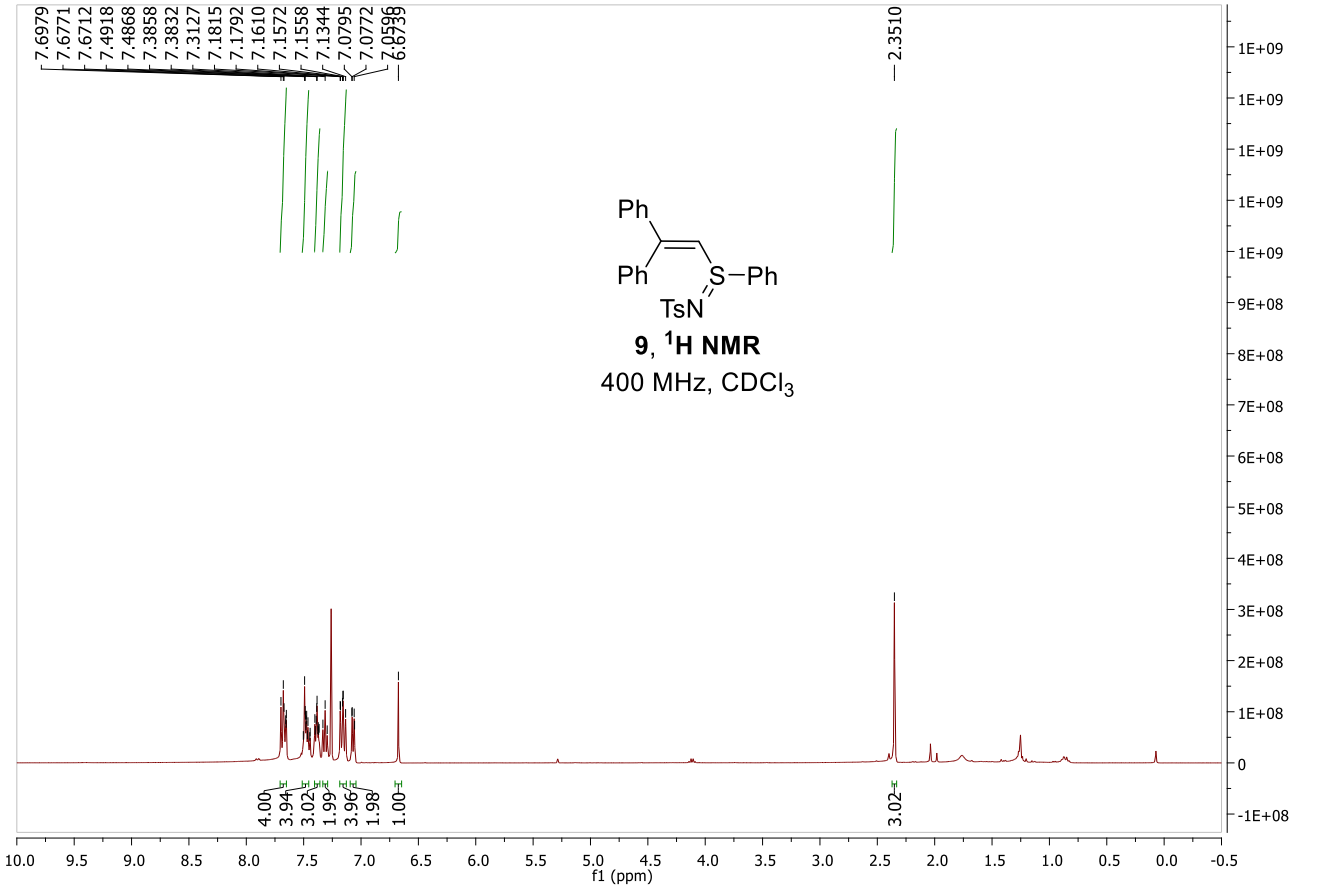
7.6979
7.6771
7.6712
7.4918
7.4868
7.3858
7.3832
7.3127
7.1815
7.1792
7.1610
7.1572
7.1558
7.1344
7.0795
7.0772
7.0598
6.6739
2.3510
Ph
Ph
S—Ph
TsN
9, 1H NMR
400 MHz, CDCl3
4.00
3.94
3.02
1.99
3.96
1.98
1.00
3.02
f1 (ppm)

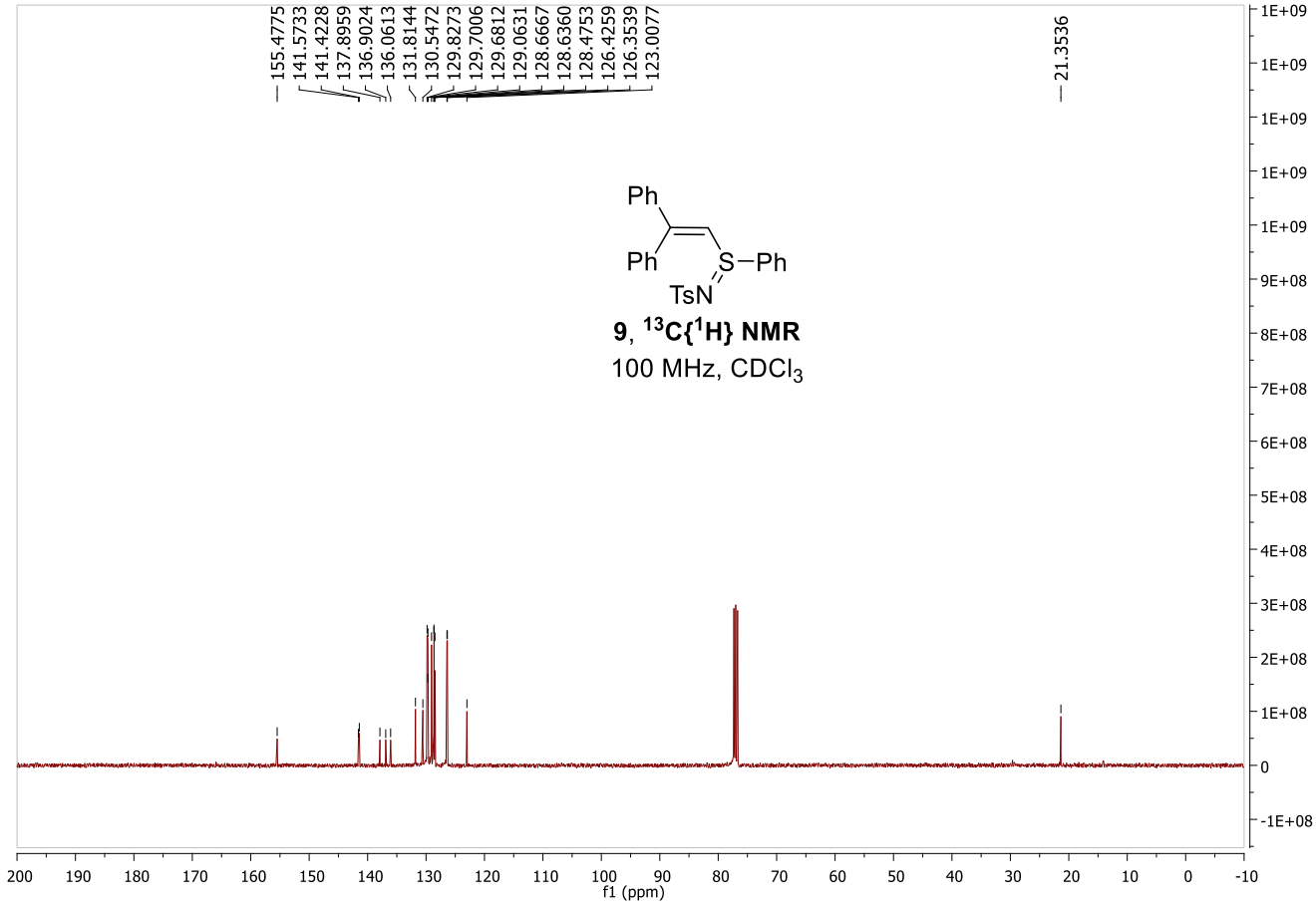
155.4775
141.5733
141.4228
137.8959
136.9024
136.0613
131.8144
130.5472
129.8273
129.7006
129.6812
129.0631
128.6667
128.6360
128.4753
126.4259
126.3539
123.0077
21.3536
Ph
Ph
S—Ph
TsN
9, 13C{1H} NMR
100 MHz, CDCl3
f1 (ppm)

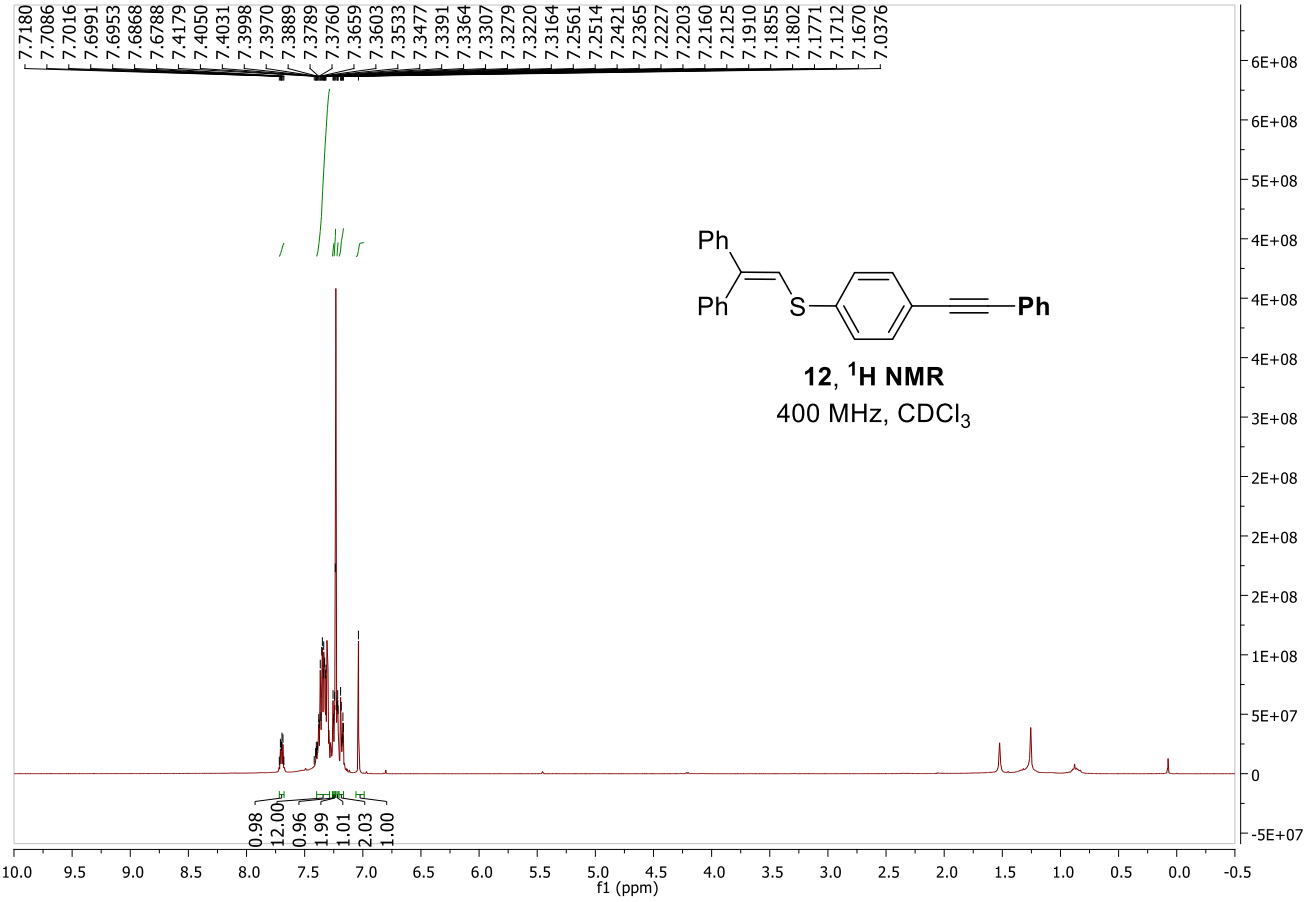
7.7180
7.7086
7.7016
7.6991
7.6953
7.6868
7.6788
7.4179
7.4050
7.4031
7.3998
7.3970
7.3889
7.3789
7.3760
7.3659
7.3603
7.3533
7.3477
7.3391
7.3364
7.3307
7.3279
7.3220
7.3164
7.2561
7.2514
7.2421
7.2365
7.2227
7.2203
7.2160
7.2125
7.1910
7.1855
7.1802
7.1771
7.1712
7.1670
7.0376
Ph
Ph
S
Ph
12, 1H NMR
400 MHz, CDCl3
0.98
12.00
0.96
1.99
1.01
2.03
1.00
f1 (ppm)

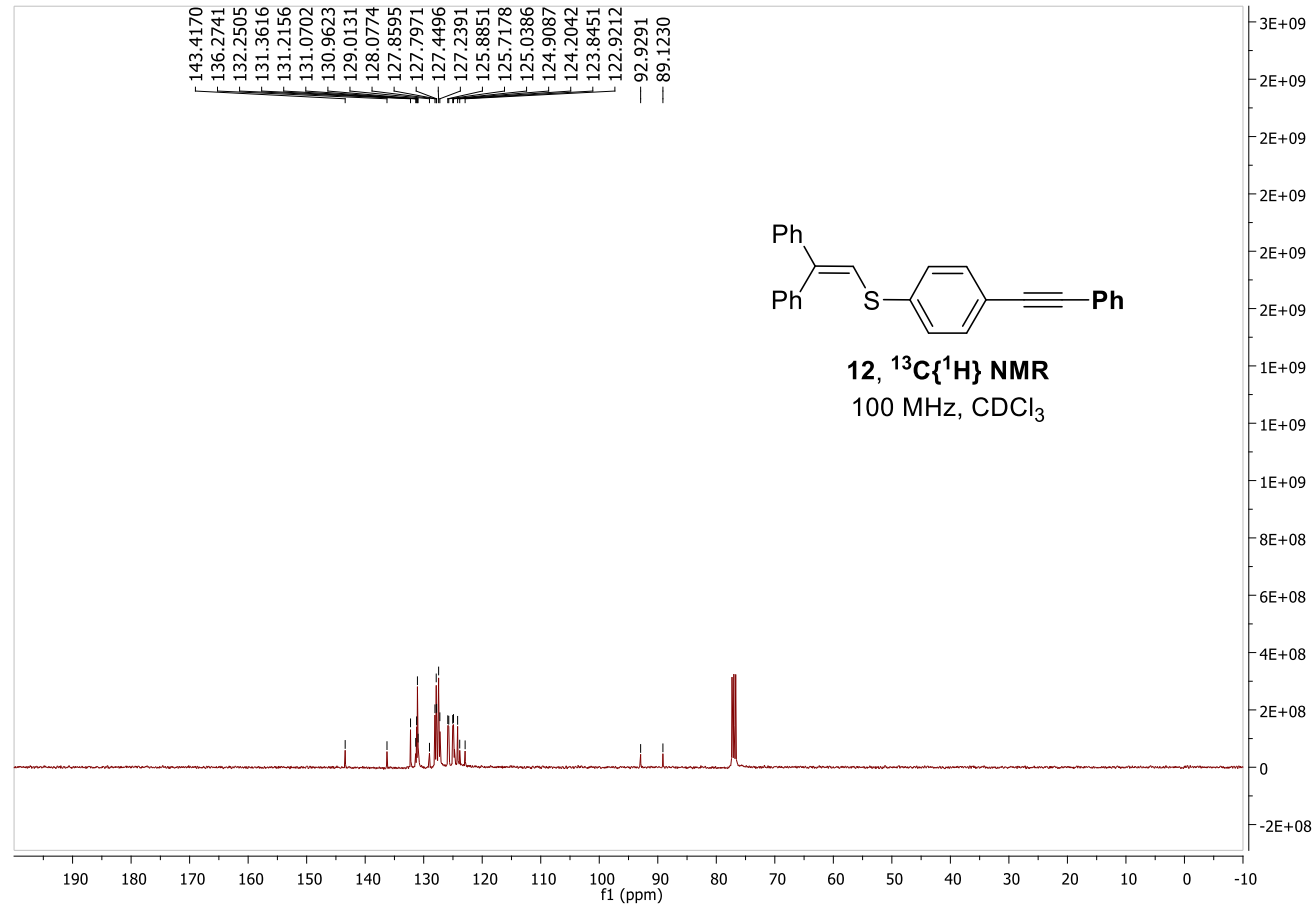
143.4170
136.2741
132.2505
131.3616
131.2156
131.0702
130.9623
129.0131
128.0774
127.8595
127.7971
127.4496
127.2391
125.8851
125.7178
125.0386
124.9087
124.2042
123.8451
122.9212
92.9291
89.1230
Ph
Ph
S
Ph
12, 13C{1H} NMR
100 MHz, CDCl3
f1 (ppm)

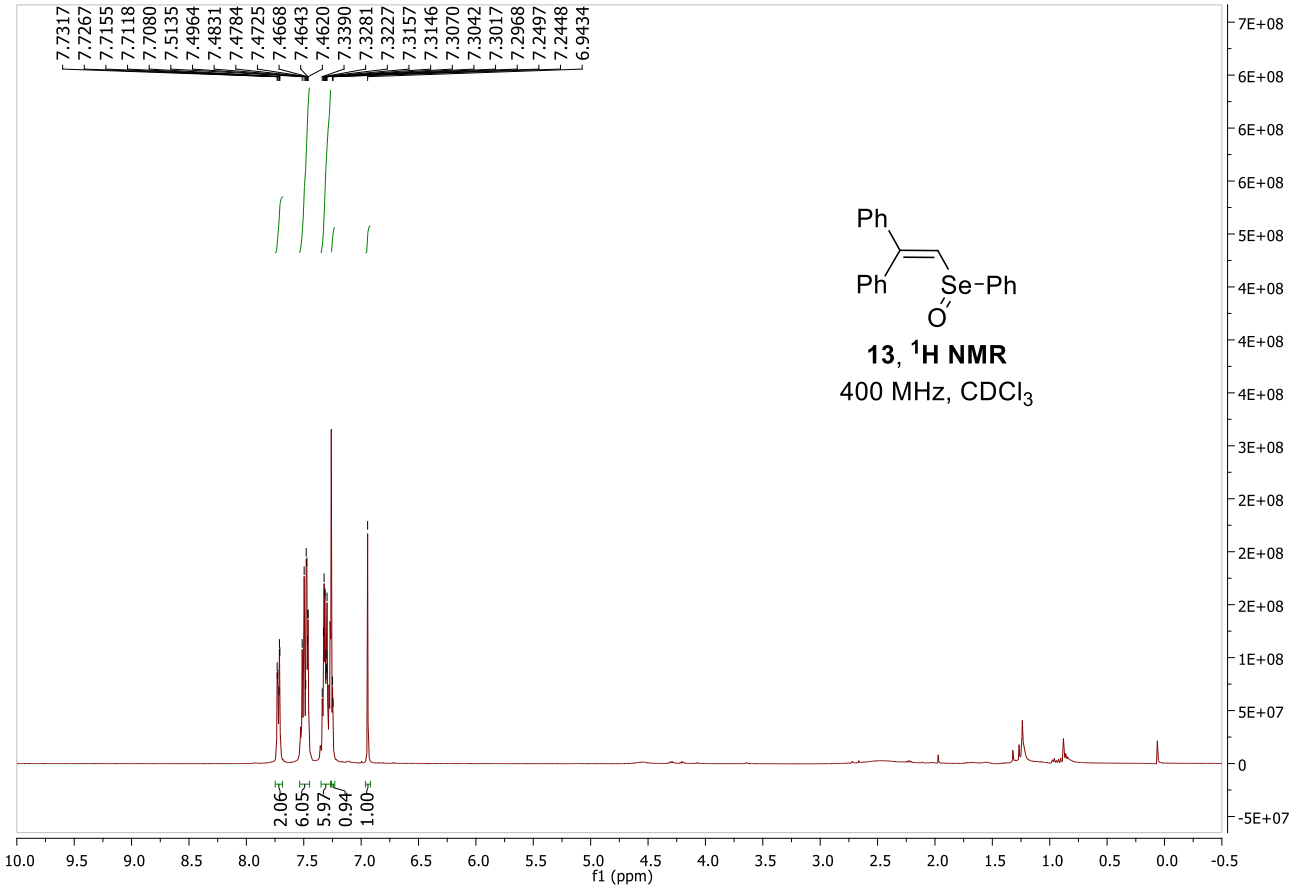
7.7317
7.7267
7.7155
7.7118
7.7080
7.5135
7.4964
7.4831
7.4784
7.4725
7.4668
7.4643
7.4620
7.3390
7.3281
7.3227
7.3157
7.3146
7.3070
7.3042
7.3017
7.2968
7.2497
7.2448
6.9434
Ph
Ph
Se-Ph
O
13, 1H NMR
400 MHz, CDCl3
2.06
6.05
5.97
0.94
1.00
f1 (ppm)

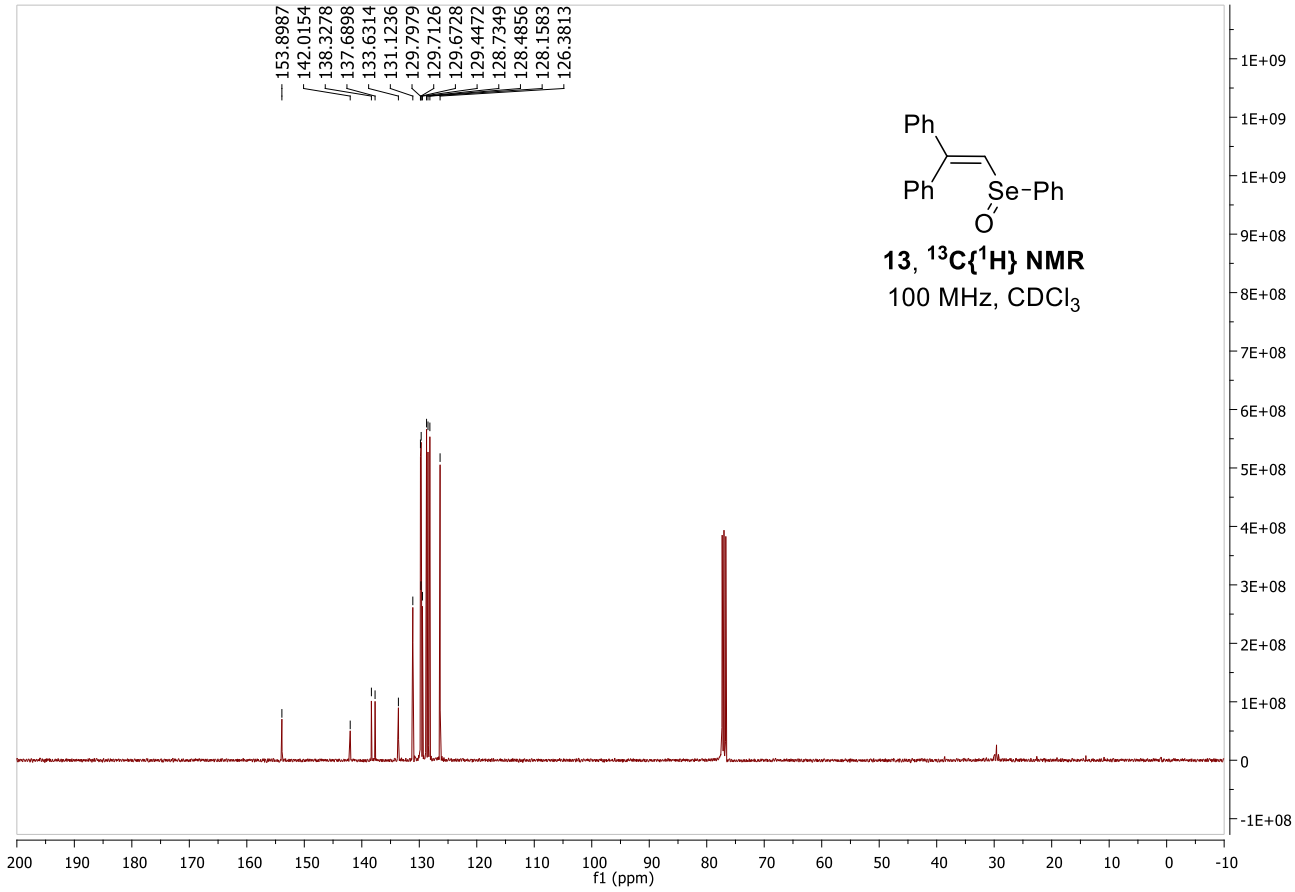
153.8987
142.0154
138.3278
137.6898
133.6314
131.1236
129.7979
129.7126
129.6728
129.4472
128.7349
128.4856
128.1583
126.3813
Ph
Ph
Se-Ph
O
13, 13C{1H} NMR
100 MHz, CDCl3
f1 (ppm)

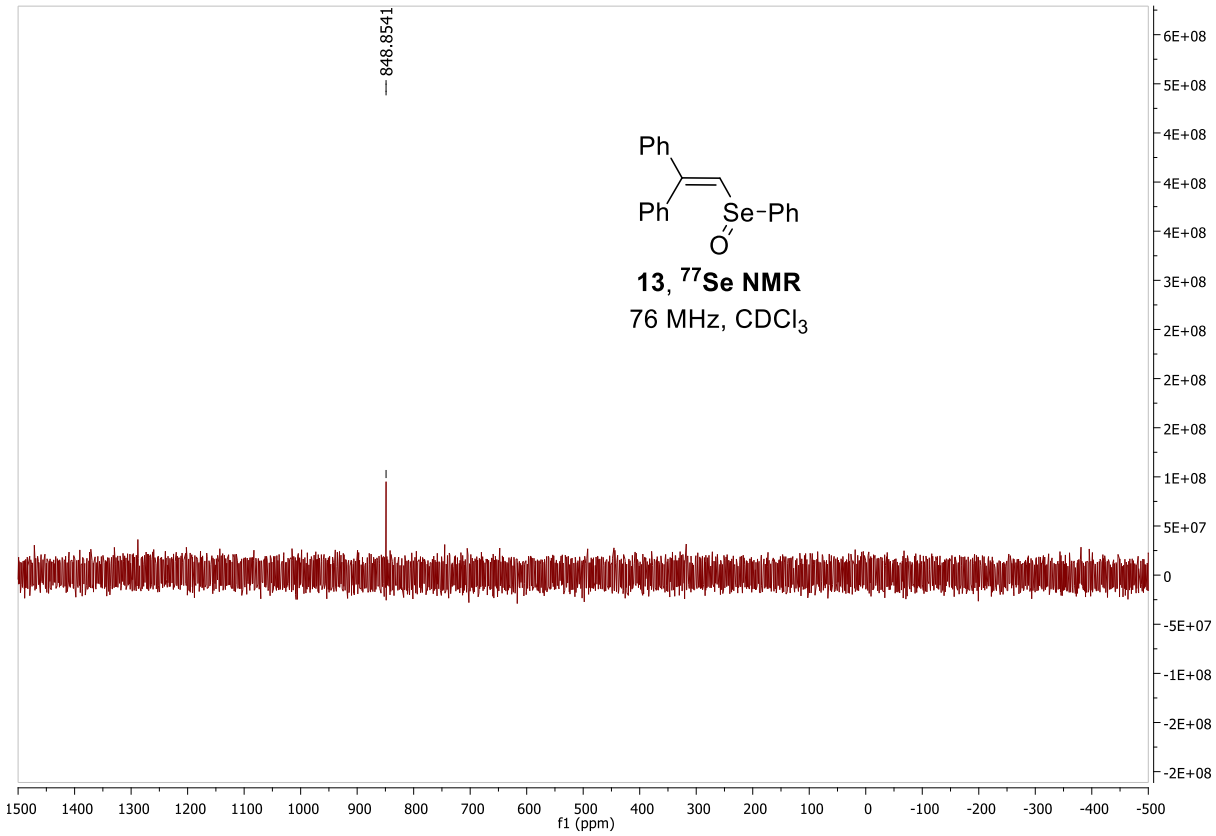
848.8541
Ph
Ph
Se-Ph
O
13, 77Se NMR
76 MHz, CDCl3
f1 (ppm)

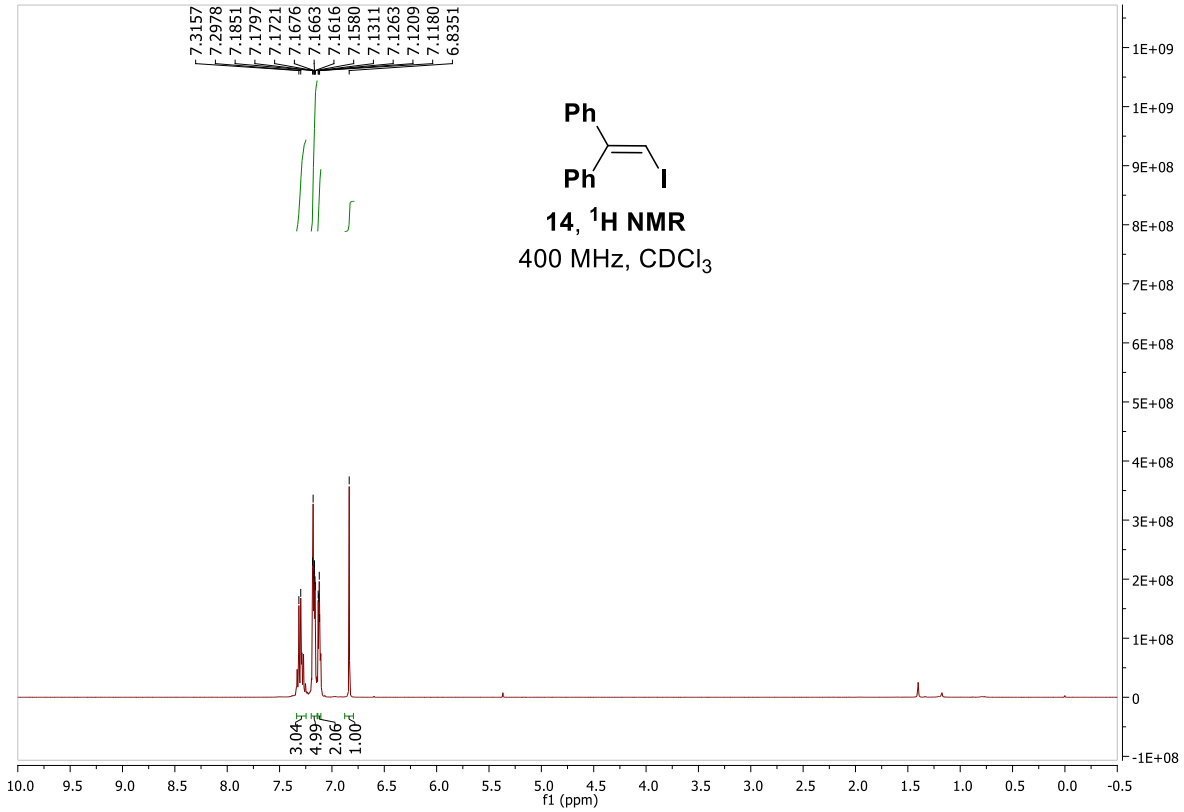
7.3157
7.2978
7.1851
7.1797
7.1721
7.1676
7.1663
7.1616
7.1580
7.1311
7.1263
7.1209
7.1180
6.8351
Ph
Ph
I
14, 1H NMR
400 MHz, CDCl3
3.04
4.99
2.06
1.00
f1 (ppm)

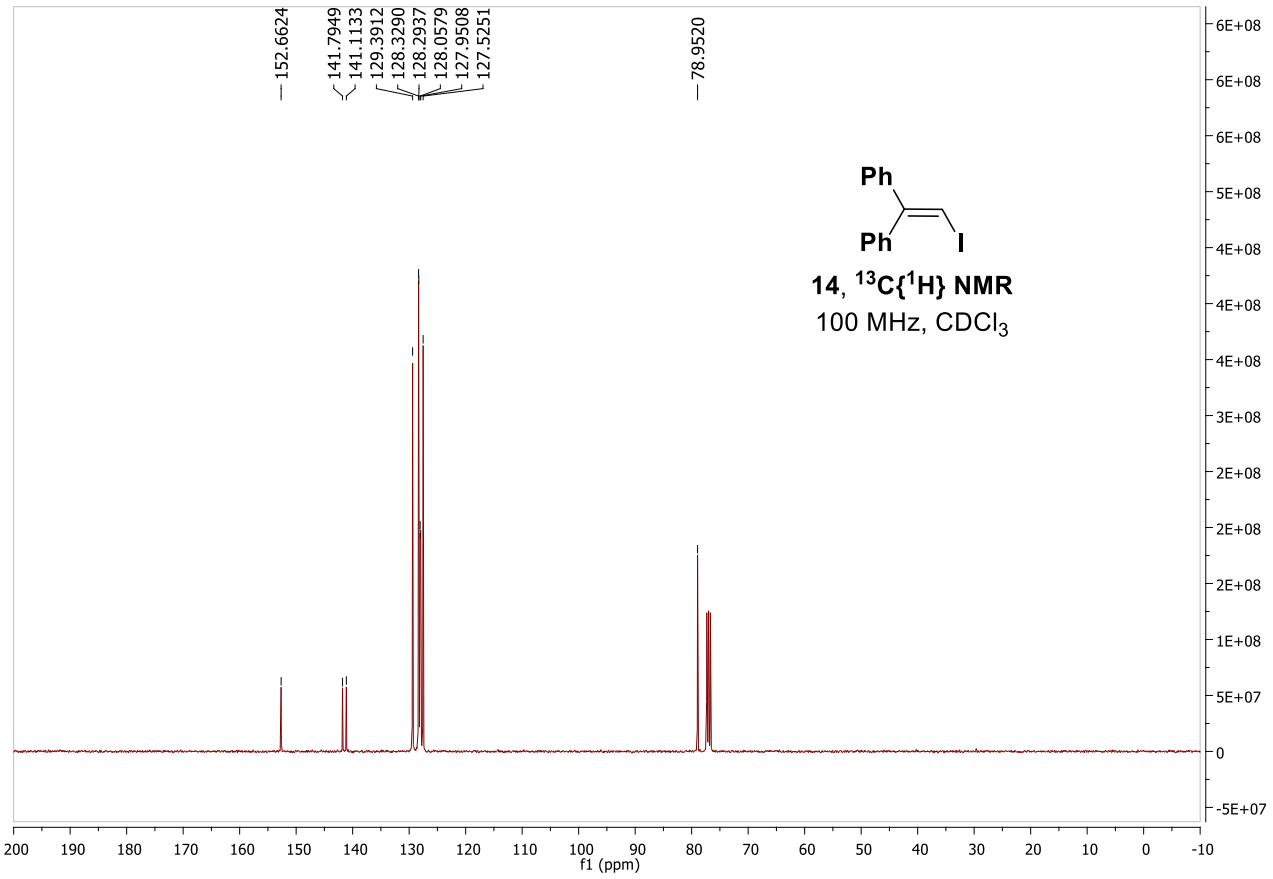
152.6624
141.7949
141.1133
129.3912
128.3290
128.2937
128.0579
127.9508
127.5251
78.9520
Ph
Ph
I
14, 13C{1H} NMR
100 MHz, CDCl3
f1 (ppm)

Check for updates

Green Chemistry

Cutting-edge research for a greener sustainable future

View Article Online
View Journal

Accepted Manuscript

This article can be cited before page numbers have been issued, to do this please use: N. Mukherjee and T. Chatterjee, *Green Chem.*, 2023, DOI: 10.1039/D3GC02999A.

ARTICLE

Recyclable iodine-catalyzed oxidative C-H chalcogenation of 1,1-diarylethenes in water: Green synthesis of trisubstituted vinyl sulfides and selenides

Received 00th January 20xx,
Accepted 00th January 20xx

DOI: 10.1039/x0xx00000x

Nilanjana Mukherjee[a] and Tanmay Chatterjee*[a]

We disclose a metal-free, iodine-catalyzed oxidative C-H sulfenylation and selenation of alkenes, particularly 1,1-diarylethenes with diorganyl dichalcogenides in water for the cost-effective, highly atom-economic, and sustainable synthesis of valuable vinyl sulfides and selenides including some aggregation-induced-emission (AIE) active molecules. The transformation required only 10 mol% iodine as the catalyst and a very small amount of a green oxidant, H_2O_2 (0.3 equiv) to afford the desired products in moderate to high yields up to 96% under mild reaction conditions, *i.e*, 50 °C and aerobic atmosphere. The products were further synthetically diversified to various novel classes of organic molecules. The notable advantages of this method over the previously developed ones for the C-H chalcogenation of 1,1-diarylalkenes are (a) a metal-free, energy-efficient, cost-effective and sustainable protocol for the synthesis of both vinyl sulfides and selenides, (b) use of inexpensive reagents such as iodine as the catalyst and H_2O_2 as the green oxidant, (c) water as green reaction medium and water as the only byproduct (d) straightforward scale-up process up to the gram scale without any compromisation in the reaction outcome, (c) very clean reactions (100% conversion) in multiple cases to afford pure vinyl sulfides/selenides without the requirement of huge organic-solvent consuming column chromatographic purification technique, (d) excellent green chemistry metrics such as atom-economy (>96%), atom-efficiency (>87%), carbon-efficiency (>88%), reaction-mass efficiency (>81%), very low E-factor (<5 g waste/g product) while the byproduct is nothing but water, and very high EcoScale score (>80) which revealed that this method is excellent in the context of green chemistry. Moreover, the catalyst, iodine could be recovered after the reaction and recycled without any compromization in the reaction outcome which makes the process highly sustainable. Mechanistic studies revealed a radical pathway for this transformation.

Introduction

Vinyl sulfides[1] and selenides[2] are valuable structural units in numerous biologically active compounds including drug molecules such as antibiotics and proliferation-inhibitor (Fig. 1).

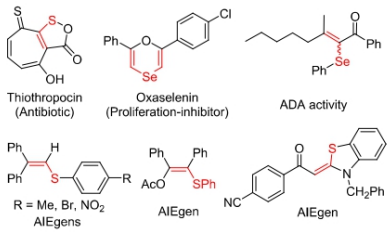

Figure 1 Examples of valuable vinyl sulfides and selenides.

Moreover, these classes of molecules also find useful applications as versatile intermediates or valuable building blocks in organic syntheses such as Michael acceptor,[3] olefin metathesis,[4] enol substitutes,[5] and vinyl or ethylene derivatives.[6] Vinyl sulfides possess various applications in materials science, such as aggregation-induced emission (AIE),[7] luminogens,[7b] polymers,[8] and molecular electronics (Fig. 1).[9] Consequently, several synthetic strategies have been developed to synthesize vinyl sulfides[10] and selenides,[11] and among them, the following two are employed most frequently *i.e.*, (a) transition-metal-catalyzed cross-coupling of vinyl halides or boronic acids with various organochalcogenides such as thiols/disulfides and selenols/diselenides[12] and (b) hydrothiolation/hydroselenation of alkynes.[13] However, these strategies suffered from one of the following limitations such as (a) the requirement of expensive and/or hazardous metallic or non-metallic reagents and/or ligands in catalytic or stoichiometric amounts, thus producing considerable waste, (b) the requirement of prefunctionalized starting materials leading to the generation of stoichiometric waste and resulting in poor atom-economy and (c) poor stereoselectivity.

Since the last few decades, developing the C-H functionalization strategy for synthesizing valuable classes of molecules has received tremendous attention from synthetic organic chemists owing to its high atom-economic feature and non-requirement of prefunctionalized substrates.[14] Consequently, several C-H chalcogenation strategies have also

[a] *Department of Chemistry, Birla Institute of Technology and Science, Pilani, Hyderabad Campus, Jawahar Nagar, Hyderabad – 500078, India. E-mail: tanmay@hyderabad.bits-pilani.ac.in*

Electronic Supplementary Information (ESI) available: [experimental procedures, x-ray data, analytical data, LC-MS spectra, and NMR spectra of the synthesized compounds]. See DOI: 10.1039/x0xx00000x

Future Aspects

The current studies revealed the successful utilization of a solvent, *i.e.*, DMSO in developing a C-H methylsulfenylative annulation reaction where DMSO itself played the role of a methylsulfenylating reagent and oxidant. This concept could be further utilized in the future in developing methylsulfenylative annulation reactions with other alkynes to access novel organosulfides. Moreover, as described in the thesis (Chapter 2, Section IV), one of our synthesized molecules, 9-methylsulfenyl-10-phenylphenanthrene nicely probed the micellization of various surfactants and also the binding isotherm of a surfactant with protein. Based on these results, a variety of novel fluorescent probes could be designed and synthesized for other potential applications. The present thesis described the utility of molecular iodine as a recyclable catalyst in developing green synthetic methods for the chalcogenylative C-H annulation and C-H chalcogenation reactions in water to access a wide variety of polycyclic aromatic hydrocarbons (PAHs), polycyclic heteroaromatics and vinyl chalcogenides. This green strategy could further be utilized in designing and developing more C-H chalcogenative annulations and C-H chalcogenation reactions with other alkynes or alkenes for the synthesis of valuable organochalcogenides.

The current studies also revealed that the electrochemical approach for the selenylative annulation is more efficient in comparison to that of the iodine-catalyzed conventional thermal approach. Thus, more chalcogenylative annulations including selenylative annulations of other alkyne substrates could be designed and developed under electrochemical conditions for the efficient synthesis of novel carbocyclic or heterocyclic molecules bearing a chalcogen functional group.

References:

Chapter-1

1. (a) Warner, J. C.; Stolte, S.; Sto, R.; Arning, J.; Jastorff, B.; Sommer, E.; Difiore, D.; Protection, U. S. E.; Maddux, B. L. S.; Hutchison, J. E.; Price, K. E.; Steinbacher, L.; Bogdan, A. R.; Mcquade, D. T.; Khetan, S. K.; Collins, T. J.; Choi, C.; Yasuda, H. Introduction : Green Chemistry. **2007**, *107*, 2167-2168. (b) Ganesh, K. N.; Zhang, D.; Miller, S. J.; Rossen, K.; Chirik, P. J.; Kozlowski, M. C.; Zimmerman, J. B.; Brooks, B. W.; Savage, P. E.; Allen, D. T.; Voutchkova-Kostal, A. M. Green Chemistry: A Framework for a Sustainable Future. *Org. Process Res. Dev.* **2021**, *25*, 1455–1459. (c) de Marco, B. A.; Rechelo, B. S.; Tótoli, E. G.; Kogawa, A. C.; Salgado, H. R. N. Evolution of Green Chemistry and Its Multidimensional Impacts: A Review. *Saudi Pharm. J.* **2019**, *27*, 1–8. (d) Anastas, P.; Eghbali, N. Green Chemistry: Principles and Practice. *Chem. Soc. Rev.* **2010**, *39*, 301–312.

2. (a) Meyer, S.; Glaser, B.; Quicker, P. Technical, Economical, and Climate-Related Aspects of Biochar Production Technologies: A Literature Review. *Environ. Sci. Technol.* **2011**, *45*, 9473–9483. (b) Singh, H.; Li, C.; Cheng, P.; Wang, X.; Liu, Q. A Critical Review of Technologies, Costs, and Projects for Production of Carbon-Neutral Liquid e-Fuels from Hydrogen and Captured CO_2. *Energy Adv.* **2022**, *1*, 580–605. (c) Chau, K.; Djire, A.; Khan, F. Review and Analysis of the Hydrogen Production Technologies from a Safety Perspective. *Int. J. Hydrogen Energy* **2022**, *47*, 13990–14007.

3. Anastas, P. T.; Zimmerman, J. B. The United Nations Sustainability Goals: How Can Sustainable Chemistry Contribute? *Curr. Opin. Green Sustain. Chem.* **2018**, *13*, 150–153. (b) Horváth, I. T. Introduction: Sustainable Chemistry. *Chem. Rev.* **2018**, *118* (2), 369–371. (b) Rosa, R.; Pini, M.; Cappucci, G. M.; Ferrari, A. M. Principles and Indicators for Assessing the Environmental Dimension of Sustainability within Green and Sustainable Chemistry. *Curr. Opin. Green Sustain. Chem.* **2022**, *37*, 100654. (c) Marr, P. C.; Marr, A. C. Ionic Liquid Gel Materials: Applications in Green and Sustainable Chemistry. *Green Chem.* **2015**, *18*, 105–128. (d) Jenck, J. F.; Agterberg, F.; Droescher, M. J. Products and Processes for a Sustainable Chemical Industry: A Review of Achievements and Prospects. *Green Chem.* **2004**, *6*, 544–556.

4. (a) Judson, R. S.; Martin, M. T.; Egeghy, P.; Gangwal, S.; Reif, D. M.; Kothiya, P.; Wolf, M.; Cathey, T.; Transue, T.; Smith, D.; Vail, J.; Frame, A.; Mosher, S.; Cohen Hubal, E. A.; Richard, A. M. Aggregating Data for Computational Toxicology Applications: The U.S. Environmental Protection Agency (EPA) Aggregated Computational Toxicology Resource (ACToR) System. *Int. J. Mol. Sci.* **2012**, *13*, 1805-1831. (b) Thayer, K. A.; Shaffer, R. M.; Angrish, M.; Arzuaga, X.; Carlson, L. M.; Davis, A.; Dishaw, L.; Druwe, I.; Gibbons, C.; Glenn, B.; Jones, R.; Kaiser, J. P.; Keshava, C.; Keshava, N.; Kraft, A.; Lizarraga, L.; Markey, K.; Persad, A.; Radke, E. G.; Rice, G.; Schulz, B.; Shannon, T.; Shapiro, A.; Thacker, S.; Vulimiri, S.; Woodall, G.; Yost, E. Use of Systematic Evidence Maps within the US Environmental Protection Agency (EPA) Integrated Risk Information System (IRIS) Program: Advancements to Date and Looking Ahead. *Environ. Int.* **2022**, *169*, 107363.

5. (a) Sepúlveda, A.; Schluep, M.; Renaud, F. G.; Streicher, M.; Kuehr, R.; Hagelüken, C.; Gerecke, A. C. A Review of the Environmental Fate and Effects of Hazardous Substances Released from Electrical and Electronic Equipments during Recycling: Examples from China and India. *Environ. Impact Assess. Rev.* **2010**, *30*, 28–41. (b) Huang, X.; Gong, Z.; Lv, Y. Advances in Metal-Organic Frameworks-Based Gas Sensors for Hazardous Substances. *TrAC - Trends Anal. Chem.* **2022**, *153*, 116644. (c) Peron, M.; Arena, S.; Paltrinieri, N.; Sgarbossa, F.; Boustras, G. Risk Assessment for Handling Hazardous Substances within the European Industry: Available Methodologies and Research Streams. *Risk Anal.* **2022**, *43*, 1434–1462.

6. (a) Binnemans, K.; Jones, P. T. The Twelve Principles of Circular Hydrometallurgy. *J. Sustain. Metall.* **2023**, *9*, 1–25. (b) Suárez-Eiroa, B.; Fernández, E.; Méndez, G. Integration of the Circular Economy Paradigm under the Just and Safe Operating Space Narrative: Twelve Operational Principles Based on Circularity, Sustainability and Resilience. *J. Clean. Prod.* **2021**, *322*, 129071 (c) Sajid, M.; Płotka-Wasylka, J. Green Analytical Chemistry Metrics: A Review. *Talanta.* **2022**, *238*, 123046 (d) Fantoni, T.; Tolomelli, A.; Cabri, W. A Translation of the Twelve Principles of Green Chemistry to Guide the Development of Cross-Coupling Reactions. *Catal. Today.* **2021**, *2022*, *397–399*. (e) Freschi, M.; Paniz, A.; Cerqueni, E.; Colella, G.; Dotelli, G. The Twelve Principles of Green Tribology: Studies, Research, and Case Studies—A Brief Anthology. *Lubricants* **2022**, *10*, 102433. (f) Ashok, M.; Madan, R.; Joha, A.; Sivarajah, U. Ethical Framework for Artificial Intelligence and Digital Technologies.

Int. J. Inf. Manage. **2022**, *62*, 102433.

7. (a) Aswathi, V. P.; Meera, S.; Maria, C. G. A.; Nidhin, M. Green Synthesis of Nanoparticles from Biodegradable Waste Extracts and Their Applications: A Critical Review. *Nanotechnol. Environ. Eng.* **2023**, *8*, 377–397. (b) Parmar, S.; Kaur, H.; Singh, J.; Matharu, A. S.; Ramakrishna, S.; Bechelany, M. Recent Advances in Green Synthesis of Ag NPs for Extenuating Antimicrobial Resistance. *Nanomaterials* **2022**, *12*, 1115 (c) Taha, R. H. Green Synthesis of Silver and Gold Nanoparticles and Their Potential Applications as Therapeutics in Cancer Therapy; a Review. *Inorg. Chem. Commun.* **2022**, *143*,109610 (d) Huq, M. A.; Ashrafudoulla, M.; Rahman, M. M.; Balusamy, S. R.; Akter, S. Green Synthesis and Potential Antibacterial Applications of Bioactive Silver Nanoparticles: A Review. *Polymers (Basel).* **2022**, *14*, 1–22. (e) Verma, V.; Al-Dossari, M.; Singh, J.; Rawat, M.; Kordy, M. G. M.; Shaban, M. A Review on Green Synthesis of TiO2 NPs: Synthesis and Applications in Photocatalysis and Antimicrobial. *Polymers (Basel).* **2022**, *14*, 1444.

8. (a) Sadiq, M. U.; Shah, A.; Haleem, A.; Shah, S. M.; Shah, I. Eucalyptus Globulus Mediated Green Synthesis of Environmentally Benign Metal Based Nanostructures: A Review. *Nanomaterials* **2023**, *13*, 2019 (b) Brandt, F.; Jacob, C. R. Efficient Automatic Construction of Atom-Economical QM Regions with Point-Charge Variation Analysis. *Phys. Chem. Chem. Phys.* **2023**, *25*, 14484–14495. (c) Jandial, T.; Gupta, A.; Jan, G.; Karuppasamy, M.; Nagarajan, S.; Maheswari, C. U.; Sridharan, V. A Microwave-Assisted Intramolecular Aminopalladation-Triggered Domino Sequence: An Atom Economical Route to 5,10-Dihydroindeno[1,2-*b*]Indoles. *Org. Biomol. Chem.* **2023**, *21*, 3121–3131.

9. Monga, A.; Bagchi, S.; Sharma, A. Iodine/DMSO Oxidations: A Contemporary Paradigm in C-N Bond Chemistry. *New J. Chem.* **2018**, *42*, 1551–1576.

10. (a) Biswas, T.; Biswas, S. K. Utility of Iodine Catalyzed Tandem Oxidation, Cross-Coupling and Cyclisation Reactions in Organic Synthesis. *Int. J. Exp. Res. Rev.* **2022**, *27*, 39–44. (b) Dhawan, S.; Kumar, V.; Girase, P. S.; Mokoena, S.; Karpoormath, R. Recent Progress in Iodine-Catalysed C−O/C−N Bond Formation of 1,3-Oxazoles: A Comprehensive Review. *ChemistrySelect* **2021**, *6*, 754–787.

11. Wang, J. Q.; Zuo, Z. Y.; He, W. Recent Advances of Green Catalytic System I_2/DMSO in C–C and C–Heteroatom Bonds Formation. *Catalysts* **2022**, *12*, 1–38.

12. (a) Bryan, M. C.; Dillon, B.; Hamann, L. G.; Hughes, G. J.; Kopach, M. E.; Peterson, E. A.; Pourashraf, M.; Raheem, I.; Richardson, P.; Richter, D.; Sneddon, H. F. Sustainable Practices in Medicinal Chemistry: Current State and Future Directions. *J. Med. Chem.* **2013**, *56*, 6007–6021. (b) Cernak, T.; Dykstra, K. D.; Tyagarajan, S.; Vachal, P.; Krska, S. W. The Medicinal Chemist's Toolbox for Late Stage Functionalization of Drug-like Molecules. *Chem. Soc. Rev.* **2016**, *45*, 546–576. (c) Kuttruff, C. A.; Eastgate, M. D.; Baran, P. S. Natural Product Synthesis in the Age of Scalability. *Nat. Prod. Rep.* **2014**, *31*, 419–432.

13. (a) Horn, E. J.; Rosen, B. R.; Baran, P. S. Synthetic Organic Electrochemistry: An Enabling and Innately Sustainable Method. *ACS Cent. Sci.* **2016**, *2*, 302–308. (b) Cardoso, D. S. P.; Šljukić, B.; Santos, D. M. F.; Sequeira, C. A. C. Organic Electrosynthesis: From Laboratorial Practice to Industrial Applications. *Org. Process Res. Dev.* **2017**, *21*, 1213–1226. (c) Kärkäs, M. D. Electrochemical Strategies for C-H Functionalization and C-N Bond Formation. *Chem. Soc. Rev.* **2018**, *47*, 5786–5865. (d) Martins, G. M.; Shirinfar, B.; Hardwick, T.; Murtaza, A.; Ahmed, N. Organic Electrosynthesis: Electrochemical Alkyne Functionalization. *Catal. Sci. Technol.* **2019**, *9*, 5868–5881.

Chapter-2: Section-I

1. (a) Chen, X. Y.; Zhang, X.; Wan, J. P. Recent Advances in Transition Metal-Free Annulation toward Heterocycle Diversity Based on the C-N Bond Cleavage of Enaminone Platform. *Org. Biomol. Chem.* **2022**, *20*, 2356–2369. (b) Poudel, T. N.; Tamargo, R. J. I.; Cai, H.; Lee, Y. R. Recent Progress in Transition-Metal-Free, Base-Mediated Benzannulation Reactions for the Synthesis of a Diverse Range of Aromatic and Heteroaromatic Compounds. *Asian J. Org. Chem.* **2018**, *7*, 985–1005. (c) Lam, H.; Abel-Snape, X.; Köllen, M. F.; Lautens, M. Recent Advances in Transition-Metal-Free (4+3)-Annulations. *Synth.* **2021**, *53*, 4134–4177. (d) Khan, I.; Zaib, S.; Ibrar, A. New Frontiers in the Transition-Metal-Free Synthesis of Heterocycles from Alkynoates: An Overview and Current Status. *Org. Chem. Front.* **2020**, *7*, 3734–3791. (e) Das, S. Indole Frameworks via Transition-Metal-Free Annulation: A Current Perspective. *New J. Chem.* **2023**, *47*, 13729–13775.

2. (a) Liu, D.; Lei, A. Iodine-Catalyzed Oxidative Coupling Reactions Utilizing C-H and

X-H as Nucleophiles. *Chem. - An Asian J.* **2015**, *10*, 806–823. (b) Jereb, M.; Vražič, D.; Zupan, M. Iodine-Catalyzed Transformation of Molecules Containing Oxygen Functional Groups. *Tetrahedron* **2011**, *67*, 1355–1387.

3. Suresh, S.; Kavala, V.; Yao, C. F. Iodine-Catalyzed Annulation Reaction of Ortho-Formylarylketones with Indoles: A General Strategy for the Synthesis of Indolylbenzo[*b*]Carbazoles. *J. Org. Chem.* **2023**, *88*, 3666–3677.

4. (a) Demmer, C. S.; Bunch, L. Benzoxazoles and Oxazolopyridines in Medicinal Chemistry Studies. *Eur. J. Med. Chem.* **2015**, *97*, 778–785. (b) Jiao, W. H.; Li, J.; Wang, D.; Zhang, M. M.; Liu, L. Y.; Sun, F.; Li, J. Y.; Capon, R. J.; Lin, H. W. Cinerols, Nitrogenous Meroterpenoids from the Marine Sponge Dysidea Cinerea. *J. Nat. Prod.* **2019**, *82*, 2586-2593. (c) Brown, R. N.; Cameron, R.; Chalmers, D. K.; Hamilton, S.; Luttick, A.; Krippner, G. Y.; McConnell, D. B.; Nearn, R.; Stanislawski, P. C.; Tucker, S. P.; Watson, K. G. 2-Ethoxybenzoxazole as a Bioisosteric Replacement of an Ethyl Benzoate Group in a Human Rhinovirus (HRV) Capsid Binder. *Bioorganic Med. Chem. Lett.* **2005**, *15*, 2051–2055.

5. Aboonajmi, J.; Panahi, F.; Hosseini, M. A.; Aberi, M.; Sharghi, H. Iodine-Catalyzed Synthesis of Benzoxazoles Using Catechols, Ammonium Acetate, and Alkenes/Alkynes/Ketones via C-C and C-O Bond Cleavage. *RSC Adv.* **2022**, *12*, 20968–20972.

6. Wu, Y. X.; Wu, S. Y.; Dong, Z. B. Green and Practical Synthesis of Thioenamines and Chromones *via* Iodine-Catalyzed Cross-Dehydrogenation Coupling Reaction. *J. Org. Chem.* **2022**, *87*, 15350–15357.

7. Liu, Y.; Wu, W.; Sang, X.; Xia, Y.; Fang, G.; Hao, W. I2-Mediated Csp2-P Bond Formation via Tandem Cyclization of o-Alkynylphenyl Isothiocyanates with Organophosphorus Esters. *RSC Adv.* **2022**, *12*, 18072–18076.

8. Pace, D. P.; Robidas, R.; Tran, U. P. N.; Legault, C. Y.; Nguyen, T. V. Iodine-Catalyzed Synthesis of Substituted Furans and Pyrans: Reaction Scope and Mechanistic Insights. *J. Org. Chem.* **2021**, *86*, 8154–8171.

9. Zhang, X. K.; Miao, X. Y.; Zhou, Y.; Wang, Y. M.; Song, Y. C.; Liu, H.; Xiong, Y. L.; Li, L. Y.; Wu, A. X.; Zhu, Y. P. Iodine-Catalyzed Oxidative Annulation: Facile Synthesis of Pyrazolooxepinopyrazolones: Via Methyl Azaarene sp^3-C-H

Functionalization. *Org. Biomol. Chem.* **2022**, *20*, 1236–1242.

10. Gui, Q. W.; Teng, F.; Li, Z. C.; Jin, X. F.; Zhang, M.; Dai, J. N.; Lin, Y. W.; Cao, Z.; He, W. M. Molecular Iodine-Catalyzed Multicomponent Synthesis of α-Cyanopyrrolines with Ambient Air as the Oxidant under Neat Conditions. *Org. Chem. Front.* **2020**, *7*, 4026–4030.

11. Panigrahi, A.; Dhineshkumar, J.; Prabhu, K. R. Iodine-Catalyzed C−H Functionalization of Cyclopentenedione with Benzamidine: A Double Dehydrogenative Oxidative Cyclization to Access Fused Imidazoles. *Adv. Synth. Catal.* **2020**, *362*, 2466–2473.

12. Zhu, J. N.; Wang, W. K.; Zheng, J.; Lin, H. P.; Deng, Y. X.; Zhao, S. Y. Iodine-Catalyzed Regioselective Oxidative Cyclization of Aldehyde Hydrazones with Electron-Deficient Olefins for the Synthesis of Mefenpyr-Diethyl. *J. Org. Chem.* **2019**, *84*, 11032–11041.

13. (a) Lhassani, M.; Chavignon, O.; Chezal, J. M.; Teulade, J. C.; Chapat, J. P.; Snoeck, R.; Andrei, G.; Balzarini, J.; De Clercq, E.; Gueiffier, A. Synthesis and Antiviral Activity of Imidazo[1,2-*a*]Pyridines. *Eur. J. Med. Chem.* **1999**, *34*, 271–274. (b) East, S. P.; White, C. B.; Barker, O.; Barker, S.; Bennett, J.; Brown, D.; Boyd, E. A.; Brennan, C.; Chowdhury, C.; Collins, I.; Convers-Reignier, E.; Dymock, B. W.; Fletcher, R.; Haydon, D. J.; Gardiner, M.; Hatcher, S.; Ingram, P.; Lancett, P.; Mortenson, P.; Papadopoulos, K.; Smee, C.; Thomaides-Brears, H. B.; Tye, H.; Workman, J.; Czaplewski, L. G. DNA Gyrase (GyrB)/Topoisomerase IV (ParE) Inhibitors: Synthesis and Antibacterial Activity. *Bioorganic Med. Chem. Lett.* **2009**, *19*, 894–899.

14. Ujwaldev, S. M.; Rohit, K. R.; Harry, N. A.; Anilkumar, G. Novel One Step Synthesis of Imidazo[1,2-*a*]Pyridines and Zolimidine via Iron/Iodine-Catalyzed Ortoleva-King Type Protocol. *Tetrahedron Lett.* **2019**, *60*, 150950.

15. Zhang, Y.; Su, J.; Lin, T.; Lin, Z.; Zhou, Z.; Li, Y. Iodine/K_2CO_3 -Catalyzed Synthesis of Multisubstituted Pyrrolidine-2-Carboxylates *via* a One-Pot Reaction between an Araldehyde, an Amino Acid Ester, and a Chalcone. *J. Chem. Res.* **2019**, *43*, 90-96

16. Debnath, S.; Das, T.; Gayen, S.; Ghosh, T.; Maiti, D. K. Iodine-Catalyzed Functionalization of Primary Aliphatic Amines to Oxazoles, 1,4-Oxazines, and

Oxazinones. *ACS Omega.* **2019**, *4*, 20410–20422.

17. Wan, J. P.; Cao, S.; Hu, C.; Wen, C. Iodine-Catalyzed, Ethyl-Lactate-Mediated Synthesis of 1,4-Benzothiazines via Metal-Free Cascade Enaminone Transamination and C−H Sulfenylation. *Asian J. Org. Chem.* **2018**, *7*, 328–331.

18. Liu, X.; Zhou, Y.; Chen, G.; Yang, Z.; Li, Q.; Liu, P. Iodine-Catalyzed Oxidative Annulation of 3-Cyanoacetylindoles with Benzylamines: Facile Access to 5-(3-Indolyl)Oxazoles. *Org. Biomol. Chem.* **2018**, *16*, 3572–3575.

19. Liu, J. Q.; Feng, B. Bin; Wang, X. S. Iodine-Catalyzed Synthesis of 5-Benzoyl-8*H*-Phthalazino[1,2-*b*]Quinazolin-8-One Derivatives via a Domino Reaction Involving a Benzyl Automatic Oxidation by Oxygen. *Tetrahedron* **2018**, *74*, 4746–4753.

20. Liu, Y.; Yuan, X.; Guo, X.; Zhang, X.; Chen, B.; Efficient 2-Aryl Benzothiazole Formation from Acetophenones, Anilines, and Elemental Sulfur by Iodine-Catalyzed Oxidative C(CO)-C(alkyl) Bond Cleavage. *Tetrahedron* **2018**, *74*, 6057-6062.

21. Chacko, P.; Shivashankar, K. I2-Catalyzed One-Pot Synthesis of Benzofuro/Thieno[2,3-*b*]Pyrrole Motifs. *Tetrahedron* **2018**, *74*, 1520–1526.

22. Shivashankar, K.; Chacko, P.; Nano Structured Spinel Co_3O_4-Catalyzed Four Component Reaction: A Novel Synthesis of Ugi Adducts from Aryl Alcohols As A Key Reagent. *Chin. Chem. Lett*. **2017**, *28*, 1619-1624.

23. Diana, P.; Martorana, A.; Barraja, P.; Montalbano, A.; Dattolo, G.; Cirrincione, G.; Dall'Acqua, F.; Salvador, A.; Vedaldi, D.; Basso, G.; Viola, G. Isoindolo[2,1-*a*]Quinoxaline Derivatives, Novel Potent Antitumor Agents with Dual Inhibition of Tubulin Polymerization and Topoisomerase I. *J. Med. Chem.* **2008**, *51*, 2387–2399.

24. Morales-Castellanos, J. J.; Ramírez-Hernández, K.; Gómez-Flores, N. S.; Rodas-Suárez, O. R.; Peralta-Cruz, J. Microwave-Assisted Solvent-Free Synthesis and *in Vitro* Antibacterial Screening of Quinoxalines and Pyrido[2, 3b]Pyrazines. *Molecules* **2012**, *17*, 5164–5176.

25. Burguete, A.; Pontiki, E.; Hadjipavlou-Litina, D.; Villar, R.; Vicente, E.; Solano, B.; Ancizu, S.; Pérez-Silanes, S.; Aldana, I.; Monge, A. Synthesis and Anti-Inflammatory/Antioxidant Activities of Some New Ring Substituted 3-Phenyl-1-(1,4-Di-*N*-oxide Quinoxalin-2-yl)-2-Propen-1-One Derivatives and of Their 4,5-Dihydro-

(1H)-Pyrazole Analogues. *Bioorganic Med. Chem. Lett.* **2007**, *17*, 6439–6443.

26. Rong, F.; Chow, S.; Yan, S.; Larson, G.; Hong, Z.; Wu, J. Structure-Activity Relationship (SAR) Studies of Quinoxalines as Novel HCV NS5B RNA-Dependent RNA Polymerase Inhibitors. *Bioorganic Med. Chem. Lett.* **2007**, *17*, 1663–1666.

27. Myers, M. R.; He, W.; Hanney, B.; Setzer, N.; Maguire, M. P.; Zulli, A.; Bilder, G.; Galzcinski, H.; Amin, D.; Needle, S.; Spada, A. P. Potent Quinoxaline-Based Inhibitors of PDGF Receptor Tyrosine Kinase Activity. Part 1: SAR Exploration and Effective Bioisosteric Replacement of a Phenyl Substituent. *Bioorganic Med. Chem. Lett.* **2003**, *13*, 3091–3095.

28. Zi, J.; Gu, D. W.; Zhang, Y.; Hu, Z. Y.; Zhang, X. Q.; Guo, X. X. Synthesis of Quinoxalines through Iodine-Catalyzed One-Pot Annulation of Alkynes with o-Phenylenediamines. *Synth. Commun.* **2018**, *48*, 915–920.

29. Bodhak, C.; Pramanik, A. One-Pot, Three-Component Synthesis of 5-Sulfenyl-2-Iminothiazolines by Cross-Dehydrogenative C-S Coupling Using I_2/DMSO in Open Air. *J. Org. Chem.* **2019**, *84*, 7265–7278.

30. Sun, P.; Yang, D.; Wei, W.; Sun, X.; Zhang, W.; Zhang, H.; Wang, Y.; Wang, H. Metal- and Solvent-Free, Iodine-Catalyzed Cyclocondensation and C-H Bond Sulphenylation: A Facile Access to C-4 Sulfenylated Pyrazoles *via* a Domino Multicomponent Reaction. *Tetrahedron* **2017**, *73*, 2022–2029.

Chapter-2: Section-II

1. (a) Tóth, B.; Hohmann, J.; Vasas, A. Phenanthrenes: A Promising Group of Plant Secondary Metabolites. *J. Nat. Prod.* **2018**, *81*, 661–678. (b) Kovács, A.; Vasas, A.; Hohmann, J. Natural Phenanthrenes and Their Biological Activity. *Phytochemistry* **2008**, *69* , 1084–1110.

2. Wang, K.; Hu, Y.; Liu, Y.; Mi, N.; Fan, Z.; Lieu, Y.; Wang, Q. Design, Synthesis, and Antiviral Evaluation of Phenanthrene-Based Tylophorine Derivatives as Potential Antiviral Agents. *J. Agric. Food Chem.* **2010**, *58*, 12337–12342.

3. (a) Hattori, T.; Shimazumi, Y.; Goto, H.; Yamabe, O.; Morohashi, N.; Kawai, W.; Miyano, S. Synthesis , Resolution , and Absolute Stereochemistry of (-) -Blestriarene

C. **2003**, *6*, 2099–2108. (b) Zhao, W.; Xu, L. L.; Zhang, Gong, X. W.; Zhu, D. L.; Xu, X. H.; Wang, F.; Yang, X. L. Three New Phenanthrenes with Antimicrobial Activities from the Aerial Parts of Juncus Effusus. *Fitoterapia* **2018**, *130*, 247–250.

4. Wilson, S.; Ruenitz, P. C. Structural Characterization and Biological Effects of Photocyclized Products of Tamoxifen Irradiation. *J. Pharm. Sci.* **1993**, *82*, 571–574.

5. Wei, L.; Shi, Q.; Bastow, K. F.; Brossi, A.; Morris-Natschke, S. L.; Nakagawa-Goto, K.; Wu, T. S.; Pan, S. L.; Teng, C. M.; Lee, K. H. Antitumor Agents 253. Design, Synthesis, and Antitumor Evaluation of Novel 9-Substituted Phenanthrene-Based Tylophorine Derivatives as Potential Anticancer Agents. *J. Med. Chem.* **2007**, *50*, 3674–3680.

6. Cernak, T.; Dykstra, K. D.; Tyagarajan, S.; Vachal, P.; Krska, S. W. The Medicinal Chemist's Toolbox for Late Stage Functionalization of Drug-like Molecules. *Chem. Soc. Rev.* **2016**, *45*, 546–576.

7. Rosenau, T.; Netscher, T.; Ebner, G.; Kosma, P. Facile Synthesis of *α,ω*-Bis(5-γ-Tocopheryl)Alkanes. *Synlett* **2005**, 243–246.

8. Omidi, A. R.; Dadsetani, M. Optical Properties of Phenanthrene: A DFT Study for Comparison between Linear and Nonlinear Regimes. *Solid State Commun.* **2016**, *234–235*, 1–9.

9. Tian, H.; Shi, J.; Dong, S.; Yan, D.; Wang, L.; Geng, Y.; Wang, F. Novel Highly Stable Semiconductors Based on Phenanthrene for Organic Field-Effect Transistors. *Chem. Commun.* **2006**, 3498–3500.

10. Kim, Y. A.; Hwang, K. Il; Kang, M.; Kim, N. K.; Jang, S. young; Kim, I. B.; Kim, J.; Kim, D. Y. Effect of Side Chains on Phenanthrene Based D-A Type Copolymers for Polymer Solar Cells. *Org. Electron.* **2017**, *44*, 238–246.

11. (a) Floyd, A. J.; Dyke, S. F.; Ward, S. E. The Synthesis of Phenanthrenes. *Chem. Rev.* **1976**, *76*, 509−562. (b) Del Tito, A.; Abdulla, H. O.; Ravelli, D.; Protti, S.; Fagnoni, M. Photocatalyzedsyntheses of phenanthrenes and their aza-analogues. A review.*Beilstein J. Org. Chem*. **2020**, *16*, 1476−1488.

12. (a) Yoshikawa, E.; Radhakrishnan, K. V.; Yamamoto,Y. Palladium-Catalyzed Controlled Carbopalladation of Benzyne. *J. Am.Chem. Soc*. **2000**, *122*, 7280−7286. (b)

Yoshikawa, E.; Yamamoto, Y.Palladium-Catalyzed Intermolecular Controlled Insertion of Benzyne-Benzyne-Alkene and Benzyne-Alkyne-Alkene-Synthesis of Phenan-threne and Naphthalene Derivatives. *Angew. Chem., Int. Ed*. **2000**, *39*, 173−175. (c) Mandal, A. B.; Lee, G.-H.; Liu, Y.-H.; Peng, S.-M.;Leung, M.-K. Formation of 4-Methylphenanthrenes in Palladium-Catalyzed Annulation of Diethyl 2,2′-Diiodo-4,4′-biphenyldicarbox-ylate with Internal Alkynes, Using Methyl Nitrobenzoates as theMethylating Agent. *J. Org. Chem*. **2000**, *65*, 332−336. (d) Catellani,M.; Motti, E.; Baratta, S. A Novel Palladium-Catalyzed Synthesis ofPhenanthrenes fromortho-Substituted Aryl Iodides and Diphenyl- orAlkylphenylacetylenes. *Org. Lett*. **2001**, *3*, 3611−3614. (e) Almeida, J.F.; Castedo, L.; Fernandez, D.; Neo, A. G.; Romero, V.; Tojo, G.Base-Induced Photocyclization of 1,2-Diaryl-1-tosylethenes. A Mech-anistically Novel Approach to Phenanthrenes and Phenanthrenoids. *Org. Lett*. **2003**, *5*, 4939−4941. (f) Iuliano, A.; Piccioli, P.; Fabbri, D.Ring-Closing Olefin Metathesis of 2,2′-Divinylbiphenyls: A Novel andGeneral Approach to Phenanthrenes. *Org. Let*t. **2004**, *6*, 3711−3714.(g) Kanno, K.-i.; Liu, Y.; Iesato, A.; Nakajima, K.; Takahashi, T.Chromium-Mediated Synthesis of Polycyclic Aromatic Compoundsfrom Halobiaryls. *Org. Lett*. **2005**, *7*, 5453−5456. (h) Zhao, Y.-B.;Mariampillai, B.; Candito, D. A.; Laleu, B.; Li, M.; Lautens, M.Exploiting the Divergent Reactivity of Aryl−Palladium Intermediatesfor the Rapid Assembly of Fluorene and Phenanthrene Derivatives. *Angew. Chem., Int. Ed*. **2009**, *48*, 1849−1852. (i) Bera, K.; Sarkar, S.;Jalal, S.; Jana, U. Synthesis of Substituted Phenanthrene by Iron(III)-Catalyzed Intramolecular Alkyne-Carbonyl Metathesis. *J. Org. Chem*. **2012**, *77*, 8780−8786. (j) Lin, Y.-D.; Cho, C.-L.; Ko, C.-W.; Pulte, A.;Wu, Y.-T. Palladium-Catalyzed Annulation of 2,2′-Diiodobiphenylswith Alkynes: Synthesis and Applications of Phenanthrenes. *J. Org.Chem*. **2012**, *77*, 9979−9988. (k) Fu, W. C.; Wang, Z.; Chan, W. T.K.; Lin, Z.; Kwong, F. Y. Regioselective Synthesis of Polycyclic and Heptagon-embedded Aromatic Compounds through a Versatile p-Extension of Aryl Halides. *Angew. Chem., Int. Ed*. **2017**, *56*, 7166−7170. (l) Zhong, Y.; Wu, W.-Y.; Yu, S.-P.; Fan, T.-Y.; Yu, H.-T.; Li,N.-G.; Shi, Z.-H.; Tang, Y.-P.; Duan, J.-A. A novel and efficient Synthesis of Phenanthrene Derivatives *via* Palladium/Norbornadiene-catalyzed domino one-pot reaction. *Beilstein J. Org. Chem*. **2019**, *15*, 291−298.

13. Wu, G.; Rheingold, A. L.; Geib, S. J.; Heck, R. F. Palladium-catalyzed Annulation of Aryl Iodides with Diphenylacetylene. *Organo*-metallics. **1987**, *6*, 1941−1946.

14. (a) Shen, H.-C.; Tang, J.-M.; Chang, H.-K.; Yang, C.-W.; Liu, R.-S. Short and Efficient Synthesis of CoroneneDerivatives via Ruthenium-Catalyzed Benzannulation Protocol. *J. Org.Chem*. **2005**, *70*, 10113−10116. (f) Zhang, Z.; He, P.; Du, H.;Xu, J.; Li, P. Sulfur-Mediated Electrophilic Cyclization of Aryl-Substituted Internal Alkynes. *J. Org. Chem.* **2019**, *84*, 4517−4524.

15. Chatterjee, T.; Lee, D. S.; Cho, E. J. Extended Study of Visible-Light-Induced Photocatalytic [4 + 2] Benzannulation: Synthesis of Polycyclic (Hetero)Aromatics. *J. Org. Chem.* **2017**, *82*, 4369–4378.

16. Nagata, T.; Satoh, T.; Nishii, Y.; Miura, M. Rhodium-Catalyzed Oxidative Annulation of (2-Arylphenyl)Boronic Acids with Alkynes: Selective Synthesis of Phenanthrene Derivatives. *Synlett* **2016**, *27*, 1707–1710.

17. Pati, K.; Michas, C.; Allenger, D.; Piskun, I.; Coutros, P. S.; Dos Passos Gomes, G.; Alabugin, I. V. Synthesis of Functionalized Phenanthrenes via Regioselective Oxidative Radical Cyclization. *J. Org. Chem.* **2015**, *80*, 11706–11717.

18. Nagata, T.; Hirano, K.; Satoh, T.; Miura, M. Iridium-Catalyzed Annulative Coupling of 2-Arylbenzoyl Chlorides with Alkynes: Selective Formation of Phenanthrene Derivatives. *J. Org. Chem.* **2014**, *79*, 8960–8967.

19. Matsumoto, A.; Ilies, L.; Nakamura, E. Phenanthrene Synthesis by Iron-Catalyzed [4 + 2] Benzannulation between Alkyne and Biaryl or 2-Alkenylphenyl Grignard Reagent. *J. Am. Chem. Soc.* **2011**, *133*, 6557–6559.

20. Wang, C.; Rakshit, S.; Glorius, F. Palladium-Catalyzed Intermolecular Decarboxylative Coupling of 2-Phenylbenzoic Acids with Alkynes via C-H and C-C Bond Activation. *J. Am. Chem. Soc.* **2010**, *132*, 14006–14008.

21. Komeyama, K.; Igawa, R.; Takaki, K. Cationic Iron-Catalyzed Intramolecular Alkyne-Hydroarylation with Electron-Deficient Arenes. *Chem. Commun.* **2010**, *46*, 1748–1750.

22. Mamane, V.; Hannen, P.; Fürstner, A. Synthesis of Phenanthrenes and Polycyclic Heteroarenes by Transition-Metal Catalyzed Cycloisomerization Reactions. *Chem. - A Eur. J.* **2004**, *10*, 4556–4575.

23. Fürstner, A.; Mamane, V. Flexible Synthesis of Phenanthrenes by a Reaction Rapidly Gaining Importance as a Convenient Catalyst for a Host of Skeletal Rearrangements of

Enynes and Related Ingly Quite Diverse in Nature , Substantial Evidence Has Accumulated That They Are Invariably. *J. Org. Chem.* **2002**, *67*, 6264–6267.

24. Larock, R. C.; Doty, M. J.; Tian, Q.; Zenner, J. M. Synthesis of Polycyclic Aromatic Hydrocarbons by the Pd-Catalyzed Annulation of Alkynes. *J. Org. Chem.* **1997**, *62*, 7536–7537.

Chapter-2: Section-III

1. (a) Palinkas, L.; Horwitz, S.; Green, C. Sulfur Containing Scaffolds in Drugs: Synthesis and Application in Medicinal Chemistry. *Curr. Top. Med. Chem.* **2016**, *16,* 1200-1216. (b) Gangjee, A.; Zeng, Y.; Talreja, T.; McGuire, J. J.; Kisliuk, R. L.; Queener, S. F. Design and Synthesis of Classical and Nonclassical 6-Arylthio-2,4-Diamino- 5-Ethylpyrrolo[2,3-*d*]Pyrimidines as Antifolates. *J. Med. Chem.* **2007**, *50*, 3046–3053. (c) Liu, G.; Link, J. T.; Pei, Z.; Reilly, E. B.; Leitza, S.; Nguyen, B.; Marsh, K. C.; Okasinski, G. F.; Von Geldern, T. W.; Ormes, M.; Fowler, K.; Gallatin, M. Discovery of Novel P-Arylthio Cinnamides as Antagonists of Leukocyte Function-Associated Antigen-1/Intracellular Adhesion Molecule-1 Interaction. 1. Identification of an Additional Binding Pocket Based on an Anilino Diaryl Sulfide Lead. *J. Med. Chem.* **2000**, *43*, 4025–4040.

2. (a) Dunbar, K. L.; Scharf, D. H.; Litomska, A.; Hertweck, C. Enzymatic Carbon-Sulfur Bond Formation in Natural Product Biosynthesis. *Chem. Rev.* **2017**, *117*, 5521–5577. (b) Nakazawa, T.; Xu, J.; Nishikawa, T.; Oda, T.; Fujita, A.; Ukai, K.; Mangindaan, R. E. P.; Rotinsulu, H.; Kobayashi, H.; Namikoshi, M. Lissoclibadins, Polysulfur Aromatic Alkaloids from the Indonesian Ascidian Lissoclinum Cf. Badium. *J. Nat. Prod.* **2007**, *70*, 439–442.

3. (a) Okamoto, T.; Mitsui, C.; Yamagishi, M.; Nakahara, K.; Soeda, J.; Hirose, Y.; Miwa, K.; Sato, H.; Yamano, A.; Matsushita, T.; Uemura, T.; Takeya, J. V-Shaped Organic Semiconductors with Solution Processability, High Mobility, and High Thermal Durability. *Adv. Mater.* **2013**, *25*, 6392–6397. (b) Mori, T.; Nishimura, T.; Yamamoto, T.; Doi, I.; Miyazaki, E.; Osaka, I.; Takimiya, K. Consecutive Thiophene-Annulation Approach to π-Extended Thienoacene-Based Organic Semiconductors with [1]Benzothieno[3,2-*b*][1]Benzothiophene (BTBT) Substructure. **2013**. (c) Takimiya,

K.; Shinamura, S.; Osaka, I.; Miyazaki, E. Thienoacene-Based Organic Semiconductors. *Adv. Mater.* **2011**, *23*, 4347–4370. (d) Hellberg, J.; Remonen, T.; Johansson, M.; Inganäs, O.; Theander, M.; Engman, L.; Eriksson, P. New Monomers for Polythiophenes. *Synth. Met.* **1997**, *84*, 251–252.

4. (a) Beletskaya, I. P.; Ananikov, V. P. Transition-Metal-Catalyzed C-S, C-Se, and C-Te Bond Formation via Cross-Coupling and Atom-Economic Addition Reactions. *Chem. Rev.* **2011**, *111*, 1596–1636. (b) Arisawa, M. Synthesis of Organosulfides Using Transition-Metal-Catalyzed Substitution Reactions: To Construct Exergonic Reactions Employing Metal Inorganic and Organic Co-Substrate/Co-Product Methods. *Tetrahedron Lett.* **2014**, *55*, 3391–3399. (c) Amri, N.; Wirth, T. Recent Advances in the Electrochemical Synthesis of Organosulfur Compounds. *Chem. Rec.* **2021**, *21*, 2526–2537. (d) Chatterjee, T.; Ranu, B. C. Synthesis of Organosulfur and Related Heterocycles under Mechanochemical Conditions. *J. Org. Chem.* **2021**, *86*, 13895–13910.

5. (a) Sundaravelu, N.; Sangeetha, S.; Sekar, G. Metal-Catalyzed C-S Bond Formation Using Sulfur Surrogates. *Org. Biomol. Chem.* **2021**, *19*, 1459–1482. (b) Desnoyer, A. N.; Love, J. A. Recent Advances in Well-Defined, Late Transition Metal Complexes That Make and/or Break C-N, C-O and C-S Bonds. *Chem. Soc. Rev.* **2017**, *46*, 197–238. (c) Pan, F.; Shi, Z. J. Recent Advances in Transition-Metal-Catalyzed C-S Activation: From Thioester to (Hetero)Aryl Thioether. *ACS Catal.* **2014**, *4*, 280–288.

6. Yao, T.; Campo, M. A.; Larock, R. C. Synthesis of Polycyclic Aromatics and Heteroaromatics via Electrophilic Cyclization. *J. Org. Chem.* **2005**, *70*, 3511–3517.

7. Hu, B. L.; Pi, S. S.; Qian, P. C.; Li, J. H.; Zhang, X. G. Palladium-Catalyzed Iodine-Mediated Electrophilic Annulation of 2-(1-Alkynyl)Biphenyls with Disulfides. *J. Org. Chem.* **2013**, *78*, 1300–1305.

Chapter-2: Section-IV

1. (a) Sharma, P.; Rohilla, S.; Jain, N. Copper Acetate-DMSO Promoted Methylthiolation of Arenes and Heteroarenes. *J. Org. Chem.* **2015**, *80*, 4116–4122. (b) Cui, X.; Liu, X.;

Wang, X.; Tian, W.; Wei, D.; Huang, G. Copper-Catalyzed ortho Thiomethylation of Benzamides via 8-Aminoquinoline-Assisted C-H Activation with Dimethyl Sulfoxide. *ChemistrySelect* **2017**, *2*, 8607–8611. (c) Luo, F.; Pan, C.; Li, L.; Chen, F.; Cheng, J. Copper-mediated methylthiolation of aryl halides with DMSO. *Chem. Commun.* **2011**, *47*, 5304–5306.

2. (a) For a recent review on DMSO mediated reactions, see: Tashrifi, Z.; Khanaposhtani, M. M.; Larijanic, B.; Mahdavic, M. DMSO: Yesterday's Solvent, Today's Reagent. *Adv. Synth. Catal.* **2020**, *362*, 65-86. (b) Rajasekar, S.; Krishna, T. P. A.; Tharmalingam, N.; Andivelu, I.; Mylonakis, E. Metal-Free C-H Thiomethylation of Quinones Using Iodine and DMSO and Study of Antibacterial Activity. *ChemistrySelect* **2019**, *4*, 2281–2287.

3. Hu, B.-L.; Pi, S.-S.; Qian, P.-C.; Li, J.-H.; Zhang, X.-G. Palladium-Catalyzed Iodine-Mediated Electrophilic Annulation of 2-(1-Alkynyl)biphenyls with Disulfides. *J. Org. Chem.* **2013**, *78*, 1300–1305.

4. Tasneem, K.; Khan, K. Z. Dimethyl Sulphoxide-Acetic Anhydride: An Excellent Source of Formaldehyde and Thiomethanol. *Asian J. Chem.* **2008**, *20*, 929–933.

5. Monga, A.; Bagchi, S.; Sharma, A. Iodine/DMSO oxidations: a contemporary p aradigm in C–N bond chemistry. *New J. Chem*, **2018**, *42*, 1551–1576.

6. Yu, B.; Liu, A.-H.; He, L.-N.; Li, B.; Diao, Z.-F.; Li, Y.-N. Catalyst-free approach for solvent-dependent selective oxidation of organic sulfides with oxone. *Green Chem.* **2012**, *14*, 957–962.

7. Wu, Y.; Peng, X.; Luo, B.; Wu, F.; Liu, B.; Song, F.; Huang, P.; Wen, S. Palladium catalyzed dual C–H functionalization of indoles with cyclic diaryliodoniums, an approach to ring fused carbazole derivatives. *Org. Biomol. Chem.* **2014**, *12*, 9777-9780.

8. Rodriguez, L.-I.; Linge, R.; Meyer, S.; Heil, H. *PCT Int. Appl.*, WO **2017**/036573 Al.

9. Yu, L.-Z; Wei, Y.; Shi, M. Copper-catalyzed trifluoromethylazidation and rearrangement of aniline-linked 1,7-enynes: access to CF_3-substituted azaspirocyclic dihydroquinolin-2-ones and furoindolines. *Chem. Commun*. **2017**, *53*, 8980-8983.

10. Shen, J.; Yuan, D.; Qiao, Y.; Shen, X.; Zhang, Z.; Zhong, Y.; Yi, Y.; Zhu, X. Diaceno[*a*,*e*]pentalenes from Homoannulations of *o*-Alkynylaryliodides Utilizing a Unique $Pd(OAc)_2$/*n*-Bu_4NOAc Catalytic Combination. *Org. Lett.* **2014**, *16*, 4924–4927.

11. Takahashi, I.; Fujita, T.; Shoji, N.; Ichikawa, J. Brønsted acid-catalysed hydroarylation of unactivated alkynes in a fluoroalcohol–hydrocarbon biphasic system: construction of phenanthrene frameworks. *Chem. Commun*. **2019**, *55*, 9267-9270.

12. Jiang, H.; Zhang, Y.; Chen, D.; Zhou, B.; Zhang, Y. An Approach to Tetraphenylenes via Pd-Catalyzed C–H Functionalization. *Org. Lett*. **2016**, *18*, 2032–2035.

13. Huang, Q.; Campo, M.A.; Yao, T.; Tian, Q.; Larock, R.C. Synthesis of Fused Polycycles by 1,4-Palladium Migration Chemistry. *J. Org. Chem.* **2004**, *69*, 8251–8257.

14. Liu, W.; Chen, J.; Jin, R.; Xu, D.; Li, Y.; Ba, F.; Gu, G.; Kuang, Y.; Guo, H. $CuBr_2$-Promoted Cyclization and Bromination of Arene–alkynes: C–Br Bond Formation *via* Reductive Elimination of Cu(III) Species. *Org. Chem. Front*. **2016**, *3*, 852-855.

15. Naveen, K.; Nikson, S.A.; Perumal, P.T. Palladium-Catalyzed Synthesis of Tetrasubstituted Olefins by Triple Domino Process. *Adv. Synth. Catal*. **2017**, *359*, 2407-2413.

16. Pati, K.; Michas, C.; Allenger, D.; Piskun, I.; Coutros, P. S.; Gomes, G. d. P.; Alabugin, I. V. Synthesis of Functionalized Phenanthrenes via Regioselective Oxidative Radical Cyclization. *J. Org. Chem.* **2015**, *80*, 11706–11717.

17. Yuan, Y.; Wu, F.-P.; Xu, J.-X.; Wu, X.-F. Four-Component Borocarbonylation of Vinylarenes Enabled by Cooperative Cu/Pd Catalysis: Access to β-Boryl Ketones and β-Boryl Vinyl Esters. *Angew. Chem., Int. Ed.* **2020**, *59*, 17055-17061.

Chapter-2: Section-V

1. Bahri, M. A.; Hoebeke, M.; Grammenos, A.; Delanaye, L.; Vandewalle, N.; Seret, A. Investigation of SDS, DTAB and CTAB Micelle Microviscosities by Electron Spin Resonance. *Colloids Surfaces A Physicochem. Eng. Asp.* **2006**, *290*, 206–212.

2. Chauhan, S.; Kaur, M.; Kumar, K.; Chauhan, M. S. Study of the Effect of Electrolyte and Temperature on the Critical Micelle Concentration of Dodecyltrimethylammonium Bromide in Aqueous Medium. *J. Chem. Thermodyn.* **2014**, *78*, 175–181.

3. Dharaiya, N.; Aswal, V. K.; Bahadur, P. Characterization of Triton X-100 and Its Oligomer (Tyloxapol) Micelles Vis-à-Vis Solubilization of Bisphenol A by Spectral and Scattering Techniques. *Colloids Surfaces A Physicochem. Eng. Asp.* **2015**, *470*, 230–239.

4. Sonu; Kumari, S.; Saha, S. K. Effect of Polymethylene Spacer of Cationic Gemini Surfactants on Solvation Dynamics and Rotational Relaxation of Coumarin 153 in Aqueous Micelles. *J. Phys. Chem. B.* **2015**, *119*, 9751–9763.

5. Halder, S.; Kumari, S.; Aggrawal, R.; Aswal, V. K.; Ray, D.; Study of Refolding of a Denatured Protein and Microenvironment Probed through FRET to a Twisted Intramolecular Charge Transfer Fluorescent Biosensor Molecule. *J. Mol. Liq.* **2021**, *322*, 114532.

6. Sonu; Halder, S.; Kumari, S.; Aggrawal, R.; Aswal, V. K.; Saha, S. K. Study on Interactions of Cationic Gemini Surfactants with Folded and Unfolded Bovine Serum Albumin: Effect of Spacer Group of Surfactants. *J. Mol. Liq.* **2017**, *243*, 369–379.

7. Akram, M.; Bhat, I. A.; Kabir-Ud-Din. New Insights into Binding Interaction of Novel Ester-Functionalized m-E2-m Gemini Surfactants with Lysozyme: A Detailed Multidimensional Study. *RSC Adv.* **2015**, *5*, 102780–102794.

8. Halder, S.; Aggrawal, R.; Saha, S. K. Concentration-Dependent β-Cyclodextrin-Promoted Refolding of Gold Nanoparticles-Conjugated Bovine Serum Albumin Complexed with Gemini Surfactants with Different Spacer Groups. *Colloids Surfaces A Physicochem. Eng. Asp.* **2022**, *644*. 128862.

9. Halder, S.; Aggrawal, R.; Aswal, V. K.; Ray, D.; Saha, S. K. Study of Refolding of a Denatured Protein and Microenvironment Probed through FRET to a Twisted Intramolecular Charge Transfer Fluorescent Biosensor Molecule. *J. Mol. Liq.* **2021**, *322*, 114532.

Chapter-3: Section-I

1. Dhawan, S.; Kumar, V.; Girase, P. S.; Mokoena, S.; Karpoormath, R. Recent Progress in Iodine-Catalysed C−O/C−N Bond Formation of 1,3-Oxazoles: A Comprehensive Review. *ChemistrySelect.* **2021**, *6*, 754–787.

2. (a) Qadir, T.; Amin, A.; Sharma, P. K.; Jeelani, I.; Abe, H. *A Review on Medicinally Important Heterocyclic Compounds*. **2022**, *16*, 1-33. (b) Kabir, E.; Uzzaman, M. A Review on Biological and Medicinal Impact of Heterocyclic Compounds. *Results Chem.* **2022**, *4*, 100606.

3. (a) Guo, Y.; Wang, G.; Wei, L.; Wan, J. P. Domino C-H Sulfonylation and Pyrazole Annulation for Fully Substituted Pyrazole Synthesis in Water Using Hydrophilic Enaminones. *J. Org. Chem.* **2019**, *84*, 2984–2990. (b) Cortes-Clerget, M.; Yu, J.; Kincaid, J. R. A.; Walde, P.; Gallou, F.; Lipshutz, B. H. Water as the Reaction Medium in Organic Chemistry: From Our Worst Enemy to Our Best Friend. *Chem. Sci.* **2021**, *12*, 4237–4266. (c) Debbarma, S.; Sk, M. R.; Modak, B.; Maji, M. S. On-Water Cp∗Ir(III)-Catalyzed C-H Functionalization for the Synthesis of Chromones through Annulation of Salicylaldehydes with Diazo-Ketones. *J. Org. Chem.* **2019**, *84*, 6207–6216.

4. Bürglová, K.; Moitra, N.; Hodačová, J.; Cattoën, X.; Wong Chi Man, M. Click Approaches to Functional Water-Sensitive Organotriethoxysilanes. *J. Org. Chem.* **2011**, *76*, 7326–7333.

5. Bera, D.; Sarkar, R.; Saha, P.; Ghosh, P.; Mukhopadhyay, C. Aqueous Mediated Iodine Catalyzed C-N Coupling Followed by C-C Coupling towards 5*H*-Pyrazino[2,3-*b*]Indoles. *Chem. Commun.* **2023**, *59*, 7771-7774.

6. Adhikary, S.; Majumder, L.; Pakrashy, S.; Srinath, R.; Mukherjee, K.; Mandal, C.; Banerji, B.; Banerji, B. Polysubstituted Imidazoles as LysoTracker Molecules: Their Synthesis *via* Iodine/H_2O and Cell-Imaging Studies. *ACS Omega* **2020**, *5*, 14394–14407.

7. Banerji, B.; Adhikary, S.; Majumder, L.; Ghosh, S. A Green Synthetic Approach towards Polyarylated Oxazoles via Iodine-Catalyzed One-Pot sp^3 C−H Functionalization in Water: From Natural Product Synthesis To Photophysical Studies.

Asian J. Org. Chem. **2019**, *8*, 514–525.

8. Singh, P. K.; Verma, F.; Bhardiya, S. R.; Singh, M.; Rai, V. K.; Rai, A. A Facile Iodine-Promoted Enals-Based *Cis*-Selective Construction of Aziridine-2-Aldehyde in Water. *ChemistrySelect.* **2019**, *4*, 1240–1243.

Chapter-3: Section-II

1. (a) Marion, P.; Bernela, B.; Piccirilli, A.; Estrine, B.; Patouillard, N.; Guilbot, J.; Jérôme, F. Sustainable Chemistry: How to Produce Better and More from Less? *Green Chem.* **2017**, *19*, 4973–4989. (b) Axon, S.; James, D. The UN Sustainable Development Goals: How Can Sustainable Chemistry Contribute? A View from the Chemical Industry. *Curr. Opin. Green Sustain. Chem.* **2018**, *13*, 140–145.
2. (a) Anastas, P.; Eghbali, N. Green Chemistry: Principles and Practice. *Chem. Soc. Rev.* **2010**, *39*, 301–312. (b) Zimmerman, J. B.; Anastas, P. T.; Erythropel, H. C.; Leitner, W. Julie B. Zimmerman Paul T. Anastas Hanno C. Erythopel Walter Leitner. *Science* . **2020**, *367*, 397–400.
3. Mukherjee, N.; Satyanarayana, A. N. V.; Singh, P.; Dixit, M.; Chatterjee, T. Recyclable Iodine-Catalyzed Radical Selenylative Annulation of 2-Alkynyl Biaryls with Diselenides in Water: A Green Approach to Selanyl Polycyclic Aromatic Hydrocarbons and Polycyclic Heteroaromatics. *Green Chem.* **2022**, *24*, 7029-7038.
4. Charpe, V. P.; Ragupathi, A.; Sagadevan, A.; Hwang, K. C. Photoredox Synthesis of Functionalized Quinazolinesviacopper-Catalyzed Aerobic Oxidative Csp2-H Annulation of Amidines with Terminal Alkynes. *Green Chem.* **2021**, *23*, 5024–5030.
5. Van Aken, K.; Strekowski, L.; Patiny, L. EcoScale, a Semi-Quantitative Tool to Select an Organic Preparation Based on Economical and Ecological Parameters. *Beilstein J. Org. Chem.* **2006**, *2*, 1–7.
6. Tobiszewski, M.; Marć, M.; Gałuszka, A.; Namieśnik, J. Green Chemistry Metrics with Special Reference to Green Analytical Chemistry. *Molecules* **2015**, *20*, 10928–10946.
7. Hu, B.-L.; Pi, S.-S.; Qian, P.-C.; Li, J.-H.; Zhang, X.-G. Palladium-Catalyzed Iodine-Mediated Electrophilic Annulation of 2-(1-Alkynyl)Biphenyls with Disulfides. *J. Org. Chem.* **2013**, *78*, 1300–1305.

8. Yi, R.; Liu, S.; Gao, H.; Liang, Z.; Xu, X.; Li, N. Iodine-Promoted Direct Thiolation (Selenylation) of Imidazole with Disulfides (Diselenide): A Convenient and Metal-Free Protocol for the Synthesis of 2-Arylthio(Seleno)Imidazole. *Tetrahedron* **2020**, *76*, 130951.

Chapter-4: Section-I

1. Nagata, T.; Hirano, K.; Satoh, T.; Miura, M. Iridium-Catalyzed Annulative Coupling of 2-Arylbenzoyl Chlorides with Alkynes: Selective Formation of Phenanthrene Derivatives. *J. Org. Chem.* **2014**, *79*, 8960–8967. (b) Mugesh, G.; Du Mont, W. W.; Sies, H. Chemistry of Biologically Important Synthetic Organoselenium Compounds. *Chem. Rev.* **2001**, *101*, 2125–2179. (c) Woods, J. A.; Hadfield, J. A.; McGown, A. T.; Fox, B. W. Bioactivity and Molecular Modelling of Diphenylsulfides and Diphenylselenides. *Bioorganic Med. Chem.* **1993**, *1*, 333–340. (d) Engman, L.; Stern, D.; Frisell, H.; Vessman, K.; Berglund, M.; Ek, B.; Andersson, C. M. Synthesis, Antioxidant Properties, Biological Activity and Molecular Modelling of a Series of Chalcogen Analogues of the 5-Lipoxygenase Inhibitor DuP 654. *Bioorganic Med. Chem.* **1995**, *3*, 1255–1262. (e) Millois, C.; Diaz, P. Solution-Phase Synthesis of Diaryl Selenides Using Polymer-Supported Borohydride. *Org. Lett.* **2000**, *2*, 1705–1708. (f) Chatterjee, T.; Ranu, B. C. Synthesis of Organosulfur and Related Heterocycles under Mechanochemical Conditions. *J. Org. Chem.* **2021**, *86*, 13895–13910.

2. (a) Nogueira, C. W.; Zeni, G.; Rocha, J. B. T. Organoselenium and Organotellurium Compounds: Toxicology and Pharmacology. *Chem. Rev.* **2004**, *104*, 6255–6285. (b) Manna, D.; Mugesh, G. Regioselective Deiodination of Thyroxine by Iodothyronine Deiodinase Mimics: An Unusual Mechanistic Pathway Involving Cooperative Chalcogen and Halogen Bonding. *J. Am. Chem. Soc.* **2012**, *134*, 4269–4279.

3. (a) Fürstner, A.; Mamane, V. Flexible Synthesis of Phenanthrenes by a Reaction Rapidly Gaining Importance as a Convenient Catalyst for a Host of Skeletal Rearrangements of Enynes and Related Ingly Quite Diverse in Nature , Substantial Evidence Has Accumulated That They Are Invariably. *J. Org. Chem.* **2002**, *67*, 6264–6267. (b) Mamane, V.; Hannen, P.; Fürstner, A. Synthesis of Phenanthrenes and Polycyclic Heteroarenes by Transition-Metal Catalyzed Cycloisomerization Reactions. *Chem. - A Eur. J.* **2004**, *10*, 4556–4575. (c) Komeyama, K.; Igawa, R.; Takaki, K.

Cationic Iron-Catalyzed Intramolecular Alkyne-Hydroarylation with Electron-Deficient Arenes. *Chem. Commun.* **2010**, *46*, 1748–1750. (d) Zhang, Z.; He, P.; Du, H.; Xu, J.; Li, P. Sulfur-Mediated Electrophilic Cyclization of Aryl-Substituted Internal Alkynes. *J. Org. Chem.* **2019**, *84*, 4517–4524. (e) Larock, R. C.; Doty, M. J.; Tian, Q.; Zenner, J. M. Synthesis of Polycyclic Aromatic Hydrocarbons by the Pd-Catalyzed Annulation of Alkynes. *J. Org. Chem.* **1997**, *62*, 7536–7537. (f) Wang, C.; Rakshit, S.; Glorius, F. Palladium-Catalyzed Intermolecular Decarboxylative Coupling of 2-Phenylbenzoic Acids with Alkynes via C-H and C-C Bond Activation. *J. Am. Chem. Soc.* **2010**, *132*, 14006–14008. (g) Matsumoto, A.; Ilies, L.; Nakamura, E. Phenanthrene Synthesis by Iron-Catalyzed [4 + 2] Benzannulation between Alkyne and Biaryl or 2-Alkenylphenyl Grignard Reagent. *J. Am. Chem. Soc.* **2011**, *133*, 6557–6559. (h) Chatterjee, T.; Lee, D. S.; Cho, E. J. Extended Study of Visible-Light-Induced Photocatalytic [4+2] Benzannulation: Synthesis of Polycyclic (Hetero)Aromatics. *J. Org. Chem.* **2017**, *82*, 4369–4378.

4. Mantovani, A. C.; Back, D. F.; Zeni, G. Chalcogenoalkynes: Precursors for the Regioselective Preparation of 2-Chalcogeno-1-Halonaphthalenes through [4+2] Cycloaddition. *Eur. J. Org. Chem.* **2012**, *24*, 4574–4579.

5. Zhang, Z.; Wang, S.; Tan, P.; Gu, X.; Sun, W.; Liu, C.; Chen, J.; Li, J.; Sun, K. K2S2O8/I2-Promoted Electrophilic Selenylative Cyclization to Access Seleno-Benzo[*b*]Azepines. *Org. Lett.* **2022**, *24*, 2288–2293.

6. Perin, G.; Araujo, D. R.; Nobre, P. C.; Lenardao, E. J.; Jacob, R. G.; Silva, M. S.; Roehrs, J. A. Ultrasound-Promoted Synthesis of 2-Organoselanyl-Naphthalenes Using Oxone in Aqueous Medium as an Oxidizing Agent. *PeerJ.* **2018**, *2018*, 1–15.

7. Nair, A. M.; Halder, I.; Volla, C. M. R. A Metal-Free Four-Component Sulfonylation, Giese Cyclization, Selenylation Cascade via Insertion of Sulfur Dioxide. *Chem. Commun.* **2022**, *58*, 6950–6953.

8. Hou, H.; Sun, Y.; Pan, Y.; Yu, H.; Han, Y.; Shi, Y.; Yan, C.; Zhu, S. Visible-Light Mediated Diarylselenylative Cyclization of 1,6-Enynes. *J. Org. Chem.* **2021**, *86*, 1273–1280.

9. Yao, H. F.; Li, F. H.; Li, J.; Wang, S. Y.; Ji, S. J. Iron(III) Chloride-Promoted Cyclization of α,-Alkynic Tosylhydrazones with Diselenides: Synthesis of 4-

(Arylselanyl)-1-*H*-Pyrazoles. *Org. Biomol. Chem.* **2020**, *18*, 1987–1993.

10. Sonawane, A. D.; Sonawane, R. A.; Win, K. M. N.; Ninomiya, M.; Koketsu, M. In Situ Air Oxidation and Photophysical Studies of Isoquinoline-Fused N-Heteroacenes. *Org. Biomol. Chem.* **2020**, *18*, 2129–2138.

11. Mutra, M. R.; Kudale, V. S.; Li, J.; Tsai, W. H.; Wang, J. J. Alkene: Versus Alkyne Reactivity in Unactivated 1,6-Enynes: Regio-And Chemoselective Radical Cyclization with Chalcogens under Metal-And Oxidant-Free Conditions. *Green Chem.* **2020**, *22*, 2288–2300.

12. Zhou, X. J.; Liu, H. Y.; Mo, Z. Y.; Ma, X. L.; Chen, Y. Y.; Tang, H. T.; Pan, Y. M.; Xu, Y. L. Visible-Light-Promoted Selenylative Spirocyclization of Indolyl-Ynones toward the Formation of 3-Selenospiroindolenine Anticancer Agents. *Chem. - An Asian J.* **2020**, *15*, 1536–1539.

13. Dutta, S.; Prabagar, B.; Vanjari, R.; Gandon, V.; Sahoo, A. K. An Unconventional Sulfur-to-Selenium-to-Carbon Radical Transfer: Chemo-and Regioselective Cyclization of Yne-Ynamides. *Green Chem.* **2020**, *22*, 1113–1118.

14. Reddy, C. R.; Ranjan, R.; Prajapti, S. K. Copper-Catalyzed Intramolecular Chalcogenoamination of Enynyl Azides: Synthesis of 5-Selenyl/Sulfenyl Nicotinates. *Org. Lett.* **2019**, *21*, 623–626.

15. Ma, X. L.; Wang, Q.; Feng, X. Y.; Mo, Z. Y.; Pan, Y. M.; Chen, Y. Y.; Xin, M.; Xu, Y. L. Metal-Free Visible-Light Induced Cyclization/Substitution Cascade Reaction of Alkyne-Tethered Cyclohexadienones and Diselenides: Access to 5-Hydroxy-3-Selenyl-4a,8a-Dihydro-2: H -Chromen-6(5-*H*)-Ones. *Green Chem.* **2019**, *21*, 3547–3551.

16. Goulart, H. A.; Neto, J. S. S.; Barcellos, A. M.; Barcellos, T.; Silva, M. S.; Alves, D.; Jacob, R. G.; Lenardão, E. J.; Perin, G. Synthesis of 5H-Selenopheno[3,2-c]Isochromen-5-Ones Promoted by Dialkyl Diselenides and Oxone. *Adv. Synth. Catal.* **2019**, *361*, 3403–3411.

17. Perin, G.; Soares, L. K.; Hellwig, P. S.; Silva, M. S.; Neto, J. S. S.; Roehrs, J. A.; Barcellos, T.; Lenardão, E. J. Synthesis of 2,3-Bis-Organochalcogenyl-Benzo[*b*]Chalcogenophenes Promoted by Oxone. *New J. Chem.* **2019**, *43*, 6323–6331..

18. Perin, G.; Nobre, P. C.; Mailahn, D. H.; Silva, M. S.; Barcellos, T.; Jacob, R. G.; Lenardão, E. J.; Santi, C.; Roehrs, J. A. Synthesis of 4-Organoselanyl-1*H*-Pyrazoles: Oxone-Mediated Electrophilic Cyclization of *α*,β-Alkynyl Hydrazones by Using Diorganyl Diselenides. *Synth.* **2019**, *51*, 2293–2304.

19. Sahoo, H.; Grandhi, G. S.; Ramakrishna, I.; Baidya, M. Metal-Free Switchable: *Ortho*/*Ipso* -Cyclization of *N* -Aryl Alkynamides: Divergent Synthesis of 3-Selenyl Quinolin-2-Ones and Azaspiro[4,5]Trienones. *Org. Biomol. Chem.* **2019**, *17*, 10163–10166.

20. An, C.; Li, C. Y.; Huang, X. B.; Gao, W. X.; Zhou, Y. B.; Liu, M. C.; Wu, H. Y. Selenium Radical Mediated Cascade Cyclization: Concise Synthesis of Selenated Benzofurans (Benzothiophenes). *Org. Lett.* **2019**, *21*, 6710–6714.

Chapter-4: Section-II

1. Hattori, T.; Shimazumi, Y.; Goto, H.; Yamabe, O.; Morohashi, N.; Kawai, W.; Miyano, S. Synthesis , Resolution , and Absolute Stereochemistry of (-) -Blestriarene C. **2003**, *68*, 2099–2108.

2. Wei, L.; Shi, Q.; Bastow, K. F.; Brossi, A.; Morris-Natschke, S. L.; Nakagawa-Goto, K.; Wu, T. S.; Pan, S. L.; Teng, C. M.; Lee, K. H. Antitumor Agents 253. Design, Synthesis, and Antitumor Evaluation of Novel 9-Substituted Phenanthrene-Based Tylophorine Derivatives as Potential Anticancer Agents. *J. Med. Chem.* **2007**, *50*, 3674–3680.

3. Sun, Z.; Zeng, Z.; Wu, J. Zethrenes, Extended p-Quinodimethanes, and Periacenes with a Singlet Biradical Ground State. *Acc. Chem. Res.* **2014**, *47*, 2582–2591.

4. Shen, Y.; Chen, C.; Reactions, D. À. A.; Reactions, F. À. C.; Cyclizations, M. Helicenes : Synthesis and Applications. *Chem.Rev*. **2012**, 1463–1535.

5. Yao, T.; Campo, M. A.; Larock, R. C. Synthesis of Polycyclic Aromatics and Heteroaromatics via Electrophilic Cyclization. *J. Org. Chem.* **2005**, *70*, 3511–3517.

6. Grimaldi, T. B.; Lutz, G.; Back, D. F.; Zeni, G. (Biphenyl-2-Alkyne) Derivatives as Common Precursors for the Synthesis of 9-Iodo-10-Organochalcogen-Phenanthrenes

and 9-Organochalcogen-Phenanthrenes. *Org. Biomol. Chem.* **2016**, *14*, 10415–10426.

7. Arsenyan, P.; Petrenko, A.; Belyakov, S. Selanyl and Tellanyl Electrophiles as a Driving Force in the Construction of Sophisticated Polyaromatic Hydrocarbons. *New J. Chem.* **2021**, *45*, 7247–7255.

8. An, S.; Zhang, Z.; Li, P. Metal-Free Synthesis of Selenodihydronaphthalenes by Selenoxide-Mediated Electrophilic Cyclization of Alkynes. *Eur. J. Org. Chem.* **2021**, *2021*, 3059–3070.

Chapter-4: Section-III

1. Mukherjee, N.; Chatterjee, T. Iodine-Catalyzed Methylthiolative Annulation of 2-Alkynyl Biaryls with DMSO: A Metal-Free Approach to 9-Sulfenylphenanthrenes. *J. Org. Chem.* **2021**, *86*, 7881–7890.

2. Mukherjee, N.; Chatterjee, T. Iodine-Catalyzed, Highly Atom-Economic Synthesis of 9-Sulfenylphenanthrenes and Polycyclic Heteroaromatics in Water. *Green Chem.* **2021**, *23*, 10006–10013.

3. Arsenyan, P.; Petrenko, A.; Belyakov, S. Selanyl and Tellanyl Electrophiles as a Driving Force in the Construction of Sophisticated Polyaromatic Hydrocarbons. *New J. Chem.* **2021**, *45*, 7247–7255.

4. (a) Van Aken, K.; Strekowski, L.; Patiny, L. EcoScale, a Semi-Quantitative Tool to Select an Organic Preparation Based on Economical and Ecological Parameters. *Beilstein J. Org. Chem.* **2006**, *2*, 1–7. (b) Constable, D. J. C.; Curzons, A. D.; Cunningham, V. L. Metrics to "green" Chemistry - Which Are the Best? *Green Chem.* **2002**, *4*, 521–527. (c) Tobiszewski, M.; Marć, M.; Gałuszka, A.; Namieśnik, J. Green Chemistry Metrics with Special Reference to Green Analytical Chemistry. *Molecules* **2015**, *20*, 10928–10946.

5. Yang, Y. F.; Li, C. Y.; Leng, T.; Huang, X. B.; Gao, W. X.; Zhou, Y. B.; Liu, M. C.; Wu, H. Y. Cu-Catalyzed Radical Selenylation of Olefin: A Direct Access to Vinyl Selenides. *Adv. Synth. Catal.* **2020**, *362*, 2168–2172.

6. Frisch, J. M. T. W. M.; Schlegel, B. H.; Scuseria, E. G.; Robb, A. M. C. R. J.; Scalmani, G.; Barone, V.; Mennucci, B.; Petersson, A. G. N. H.; Caricato, M.; Li, X.; Hratchian,

P. H.; Izmaylov, F. A. B. G.; Zheng, G.; Sonnenberg, L. J.; Hada, M. ; Ehara, M. T. K.; Fukuda, R.; Hasegawa, J.; Ishida, M. ; Nakajima, T.; Honda, Y. K. O.; Nakai, H.; Vreven, T.; Montgomery, A. J.; Jr., Peralta, E. J. O. F.; Bearpark, M.; Heyd, J. J. ; Brothers, E.; Kudin, N. K. S. N. V.; Keith, T.; Kobayashi, R.; Normand, J.; Raghavachari, K. R. A.; Burant, C. J.; Iyengar, S. S. ; Tomasi, J. ; Cossi, M. R. N.; Millam, M. J.; Klene, M.; Knox, E. K.; Cross, B. J.; Bakken, V. A. C.; Jaramillo, J. ; Gomperts, R. Stratmann, E. R.; Yazyev, O. A. J. A.; Cammi, R.; Pomelli, C.; Ochterski, W. J.; Martin, L. R. M. K.; Zakrzewski, G. V.; Voth, A. G.; Salvador, P. D. J. J.; Dapprich, S. ; Daniels, D. A.; Farkas, O. F. B. G.; Ortiz, V. J.; Cioslowski, J.; and Fox, J. D.; *Gaussian 09, Revision C.01, Gaussian, Inc., Wallingford CT,* **2010.**

6.. Baldassari, L. L.; Mantovani, A. C.; Jardim, M.; Maryasin, B.; Lüdtke, D. S. Meyer-Schuster-Type Rearrangement for the Synthesis of α-Selanyl-α,β-Unsaturated Thioesters. *Chem. Commun.* **2021**, *57*, 117–120.

7. Grimaldi, T. B.; Lutz, G.; Back, D. F.; Zeni, G. (Biphenyl-2-Alkyne) Derivatives as Common Precursors for the Synthesis of 9-Iodo-10-Organochalcogen-Phenanthrenes and 9-Organochalcogen-Phenanthrenes. *Org. Biomol. Chem.* **2016**, *14*, 10415–10426.

8. An, S.; Zhang, Z.; Li, P. Metal-Free Synthesis of Selenodihydronaphthalenes by Selenoxide-Mediated Electrophilic Cyclization of Alkynes. *Eur. J. Org. Chem.* **2021**, *2021*, 3059–3070.

Chapter-5: Section-I

1. (a) Kuttruff, C. A.; Eastgate, M. D.; Baran, P. S. Natural Product Synthesis in the Age of Scalability. *Nat. Prod. Rep.* **2014**, *31*, 419–432. (b) Bryan, M. C.; Dillon, B.; Hamann, L. G.; Hughes, G. J.; Kopach, M. E.; Peterson, E. A.; Pourashraf, M.; Raheem, I.; Richardson, P.; Richter, D.; Sneddon, H. F. Sustainable Practices in Medicinal Chemistry: Current State and Future Directions. *J. Med. Chem.* **2013**, *56*, 6007–6021. (c) Cernak, T.; Dykstra, K. D.; Tyagarajan, S.; Vachal, P.; Krska, S. W. The Medicinal Chemist's Toolbox for Late Stage Functionalization of Drug-like Molecules. *Chem. Soc. Rev.* **2016**, *45*, 546–576.

2. (a) Lodh, J.; Paul, S.; Sun, H.; Song, L.; Schöfberger, W.; Roy, S. Electrochemical Organic Reactions: A Tutorial Review. *Front. Chem.* **2023**, *10*, 1–24. (b) Yuan, Y.; Lei, A. Is Electrosynthesis Always Green and Advantageous Compared to Traditional Methods? *Nat. Commun.* **2020**, *11*, 2018–2020.

3. (a) Bairagi, A. S. Electro-Organic Conversions: A Review on Electrocatalysis of Heck Reactions. *Curr. Res. Green Sustain. Chem.* **2022**, *5*, 100313. (b) Meyer, T. H.; Choi, I.; Tian, C.; Ackermann, L. Powering the Future: How Can Electrochemistry Make a Difference in Organic Synthesis? *Chem.* **2020**, *6*, 2484–2496.

4. (a) Martins, G. M.; Shirinfar, B.; Hardwick, T.; Murtaza, A.; Ahmed, N. Organic Electrosynthesis: Electrochemical Alkyne Functionalization. *Catal. Sci. Technol.* **2019**, *9*, 5868–5881. (b) Horn, E. J.; Rosen, B. R.; Baran, P. S. Synthetic Organic Electrochemistry: An Enabling and Innately Sustainable Method. *ACS Cent. Sci.* **2016**, *2*, 302–308. (c) Cardoso, D. S. P.; Šljukić, B.; Santos, D. M. F.; Sequeira, C. A. C. Organic Electrosynthesis: From Laboratorial Practice to Industrial Applications. *Org. Process Res. Dev.* **2017**, *21*, 1213–1226. (d) Kärkäs, M. D. Electrochemical Strategies for C-H Functionalization and C-N Bond Formation. *Chem. Soc. Rev.* **2018**, *47*, 5786–5865.

5. (a) Ryczak, J.; Papini, M.; Lader, A.; Nasereddin, A.; Kopelyanskiy, D.; Preu, L.; Jaffe, C. L.; Kunick, C. 2-Arylpaullones Are Selective Antitrypanosomal Agents. *Eur. J. Med. Chem.* **2013**, *64*, 396–400. (b) Fordyce, E. A. F.; Brookes, D. W.; Lise-Ciana, C.; Coates, M. S.; Hunt, S. F.; Ito, K.; King-Underwood, J.; Onions, S. T.; Parra, G. F.; Rapeport, G.; Sherbukhin, V.; Stockwell, J. A.; Strong, P.; Thomas, J. C.; Murray, J. Discovery of Novel Benzothienoazepine Derivatives as Potent Inhibitors of Respiratory Syncytial Virus. *Bioorganic Med. Chem. Lett.* **2017**, *27*, 2201–2206.

6. Tan, P.; Lu, L.; Wang, S.; Wang, J.; Chen, J.; Zhang, Y.; Xie, L.; Yang, S.; Chen, J.; Zhang, Z. Photo- or Electrochemical Cyclization of Dienes with Diselenides to Access Seleno-Benzo[*b*]Azepines. *J. Org. Chem.* **2023**.

7. Doerner, C. V.; Scheide, M. R.; Nicoleti, C. R.; Durigon, D. C.; Idiarte, V. D.; Sousa, M. J. A.; Mendes, S. R.; Saba, S.; Neto, J. S. S.; Martins, G. M.; Rafique, J.; Braga, A. L. Versatile Electrochemical Synthesis of Selenylbenzo[*b*]Furan Derivatives Through the Cyclization of 2-Alkynylphenols. *Front. Chem.* **2022**, *10*, 1–10.

8. Li, H.; Lu, F.; Xu, J.; Hu, J.; Alhumade, H.; Lu, L.; Lei, A. Electrochemical Oxidative Selenocyclization of Olefinic Amides towards the Synthesis of Iminoisobenzofurans. *Org. Chem. Front.* **2022**, 2786–2791.

9. Huang, C.; Hu, J.; Chen, G.; Wu, M.; Cao, H.; Liu, X. Electrochemical Oxidative Cyclization of Alkenes, Boronic Acids, and Dichalcogenides to Access Chalcogenated Boronic Esters and 1,3-Diols. *Org. Chem. Front.* **2022**, *9*, 12–18.

10. Maiti, D.; Halder, A.; Sasidharan Pillai, A.; De Sarkar, S. Synthesis of Polysubstituted Furans through Electrochemical Selenocyclization of Homopropargylic Alcohols. *J. Org. Chem.* **2021**, *86*, 16084–16094.

11. Cheng, X.; Hasimujiang, B.; Xu, Z.; Cai, H.; Chen, G.; Mo, G.; Ruan, Z. Direct Electrochemical Selenylation/Cyclization of Alkenes: Access to Functionalized Benzheterocycles. *J. Org. Chem.* **2021**, *86*, 16045–16058.

12. Raji Reddy, C.; Kolgave, D. H. Electrochemical Selenylative Carbannulation of Biaryl Ynones to Seleno-Dibenzocycloheptenones/Spiro[5.5]Trienones. *J. Org. Chem.* **2021**, *86*, 17071–17081.

13. Kharma, A.; Jacob, C.; Bozzi, Í. A. O.; Jardim, G. A. M.; Braga, A. L.; Salomão, K.; Gatto, C. C.; Silva, M. F. S.; Pessoa, C.; Stangier, M.; Ackermann, L.; da Silva Júnior, E. N. Electrochemical Selenation/Cyclization of Quinones: A Rapid, Green and Efficient Access to Functionalized Trypanocidal and Antitumor Compounds. *European J. Org. Chem.* **2020**, *2020*, 4474–4486.

14. Pan, C.; Liu, P.; Wu, A.; Li, M.; Wen, L.; Guo, W. Electrochemical-Promoted Synthesis of 2-Thiazolines via Selenylation/Cyclization of N-Allylthioamides. *Chin. J. Org. Chem.* **2020**, *40*, 2855–2862.

15. Scheide, M. R.; Schneider, A. R.; Jardim, G. A. M.; Martins, G. M.; Durigon, D. C.; Saba, S.; Rafique, J.; Braga, A. L. Electrochemical Synthesis of Selenyl-Dihydrofurans via Anodic Selenofunctionalization of Allyl-Naphthol/Phenol Derivatives and Their Anti-Alzheimer Activity. *Org. Biomol. Chem.* **2020**, *18*, 4916–4921.

16. Hua, J.; Fang, Z.; Xu, J.; Bian, M.; Liu, C. K.; He, W.; Zhu, N.; Yang, Z.; Guo, K. Electrochemical Oxidative Cyclization of Activated Alkynes with Diselenides or

Disulfides: Access to Functionalized Coumarins or Quinolinones. *Green Chem.* **2019**, *21*, 4706–4711.

Chapter-5: Section-II

1. Mukherjee, N.; Satyanarayana, A. N. V.; Singh, P.; Dixit, M.; Chatterjee, T. Recyclable Iodine-Catalyzed Radical Selenylative Annulation of 2-Alkynyl Biaryls with Diselenides in Water: A Green Approach to Selanyl Polycyclic Aromatic Hydrocarbons and Polycyclic Heteroaromatics. *Green Chem.* **2022,** 7029-7038.

2. (a) Van Aken, K.; Strekowski, L.; Patiny, L. EcoScale, a Semi-Quantitative Tool to Select an Organic Preparation Based on Economical and Ecological Parameters. *Beilstein J. Org. Chem.* **2006**, *2*, 1–7. (b) Constable, D. J. C.; Curzons, A. D.; Cunningham, V. L. Metrics to "green" Chemistry - Which Are the Best? *Green Chem.* **2002**, *4*, 521–527. (c) Tobiszewski, M.; Marć, M.; Gałuszka, A.; Namieśnik, J. Green Chemistry Metrics with Special Reference to Green Analytical Chemistry. *Molecules* **2015**, *20*, 10928–10946.

3. Tobisu, M.; Masuya, Y.; Baba, K.; Chatani, N. Palladium(II)-Catalyzed Synthesis of Dibenzothiophene Derivatives via the Cleavage of Carbon-Sulfur and Carbon-Hydrogen Bonds. *Chem. Sci.* **2016**, *7*, 2587–2591.

4. a) Zhang, X.; Wang, C.; Jiang, H.; Sun, L.; *Chem. Commun*. **2018**, *54*, 8781–8784; b) Meirinho, G. A.; Pereira, F. V.; Martins, M. G.; Saba, S.; Rafique, J.; Braga, L. A.; Mendes, R. S.; *Eur. J. Org. Chem*. **2019**, *2019*, 6465–6469; c) Kim, J. Y.; Kim, Y. D.; *Tetrahedron Lett*. **2019**, *60*, 739–742; d) Liu, X.; Wang, Y.; Song, D.; Wang, Y.; Cao, H.; *Chem. Commun*. **2020**, *56*, 15325–15328; e) L. Sun, L. Wang, H. Alhumade, H. Yi, H. Cai, A. Lei, Org. Lett. 2021, 23, 7724–7729; f) Lin, S.; Cheng, X.; Hasimujiang, B.; Xu, Z.; Li, F.; Ruan, Z. *Org. Biomol. Chem*. **2022**, *20*, 117–121; g) Shi, J.; Wang, Z.; Teng, X.; Zhang, B.; Sun, K.; Wang, X.; *Molecules*. **2023**, *28*, 2206.

5. a) Hua, J.; Fang, J.; Xu, J.; Bian, M.; Liu, K. C.; He, W.; Zhu, N.; Yang, Z. Guo, K. *Green Chem*. **2019**, *21*, 4706– 4711; b) Yu, K.; Kong, X.; Yang, J.; Li, G.; Xu, B.; Chen, Q.; *J. Org. Chem*. **2021**, *86*, 917–928; c) Hasimujiang, B.; Lin, S.; Zheng, C.; Zeng, Y. ; Ruan, Z.; *Molecules*. **2022**, *27*, 6314; d) Cheng, X.; Hasimujiang, B.; Xu, Z. ; Cai, H.;

Chen, G.; Mo, G.; Ruan, Z. ; *J. Org. Chem*. **2021**, *86*, 16045–16058; e) Maiti, D.; Halder, A.; Pillai, S. A.; S. Sarkar, D.; *J. Org. Chem*. **2021**, *86*, 16084–16094; f) Wang, Y. X.; Zhong, F. Y.; Mo, Y. Z.; Wu, H. S.; Xu, L. Y.; Tang, T. H.; Pan, M. Y.; *Adv. Synth. Catal*. **2021**, *363*, 208–214; g) Reddy, R. C.; Kolgave, H. D.; *J. Org. Chem.* **2021**, *86*, 17071–17081; h) Doerner, V. C.; Scheide, R. M.; Nicoleti, R. C.; Durigon, C. D.; Idiarte, D. V.;. Sousa, A. J. M.; Mendes, R. S.; Saba, S.; Neto, S. S. J.; Martins, M. G.; Rafique, J.; Braga, L. A.; *Front. Chem*. **2022**, *10*, 1–10.

6. Zhou, J.; Ma, Y. Z.; Shonhe, C.; Jia, H. S.; Cai, R. Y.; *Green Chem*. **2021**, *23*, 8566–8570.

Chapter-6: Section-I

1. (a) Davies, H. M. L.; Morton, D. Recent Advances in C-H Functionalization. *J. Org. Chem.* **2016**, *81*, 343–350. (b) Davies, H. M. L.; Du Bois, J.; Yu, J. Q. C–H Functionalization in Organic Synthesis. *Chem. Soc. Rev.* **2011**, *40*, 1855–1856. (c) Abrams, D. J.; Provencher, P. A.; Sorensen, E. J. Recent Applications of C-H Functionalization in Complex Natural Product Synthesis. *Chem. Soc. Rev.* **2018**, *47*, 8925–8967. (d) Gutekunst, W. R.; Baran, P. S. C-- -H Functionalisation in Organic Synthesis Themed Issue. *Chem. Soc. Rev.* **2011**, *40*, 1976–1991. (e) Brückl, T.; Baxter, R. D.; Ishihara, Y.; Baran, P. S. Innate and Guided C-H Functionalization Logic. *Acc. Chem. Res.* **2012**, *45*, 826–839.

2. Junrong, H.; Min, Y.; Chuan, D.; Yajun, Z.; Fang, H.; Lizhi, Z.; Feng, Y.; Zigang, L.; Novel Strategies in C-H Oxidations for Natural Product Diversification—A Remote Functionalization Application Summary. *Front. Chem*. **2021**, *9*, 1-7.

3. Shi, L.; Li, T.; Mei, G. J. Recent Advances in Transition-Metal-Free C–H Functionalization of Imidazo[1,2-*a*]Pyridines. *Green Synth. Catal.* **2022**, *3*, 227–242. (b) Zhu, C.; Falck, J. R. Transition Metal-Free Ipso-Functionalization of Arylboronic Acids and Derivatives. *Adv. Synth. Catal.* **2014**, *356*, 2395–2410. (c) Liu, Y.; Xiong, J.; Wei, L. Recent Advances in the C(sp^2)-S Bond Formation Reactions by Transition Metal-Free C(Sp^2)-*H* Functionalization. *Chin. J. Org. Chem.* **2017**, *37*, 1667–1680. (c) Kaur, R.; Mandal, S.; Banerjee, D.; Kumar Yadav, A. Transition Metal Free A−C−H

Functionalization of Six Membered Heteroaromatic-*N*-Oxides. *ChemistrySelect* **2021**, *6*, 2832–2854.

4. Wang, J. Q.; Zuo, Z. Y.; He, W. Recent Advances of Green Catalytic System I_2/DMSO in C–C and C–Heteroatom Bonds Formation. *Catalysts.* **2022**, *12*, 1–38.

5. Ghosh, P.; Chhetri, G.; Das, S. Metal Free C-3 Chalcogenation (Sulfenylation and Selenylation) of 4H-Pyrido[1,2-*a*]Pyrimidin-4-Ones. *RSC Adv.* **2021**, *11*, 10258–10263.

6. Pandey, A. K.; Chand, S.; Singh, R.; Kumar, S.; Singh, K. N. Iodine-Catalyzed Synthesis of 3-Arylthioindoles Employing a 1-Aryltriazene/CS_2 Combination as a New Sulfenylation Source. *ACS Omega.* **2020**, *5*, 7627–7635.

7. Zhu, Y. S.; Xue, Y.; Liu, W.; Zhu, X.; Hao, X. Q.; Song, M. P. Temperature-Controlled Chalcogenation and Chalcogenocyanation of Imidazopyridines in Water under Transition Metal-Free Conditions. *J. Org. Chem.* **2020**, *85*, 9106–9116.

8. Muniraj, N.; Dhineshkumar, J.; Prabhu, K. R. *N*-Iodosuccinimide Catalyzed Oxidative Selenocyanation and Thiocyanation of Electron Rich Arenes. *ChemistrySelect.* **2016**, *1*, 1033–1038.

9. Dey, A.; Hajra, A. Iodine-Catalyzed Selenylation of 2 *H*-Indazole. *J. Org. Chem.* **2019**, *84*, 14904–14910.

10. Kumar, V.; Banert, K.; Ray, D.; Saha, B. An Atom-Economical and Regioselective Metal-Free C-5 Chalcogenation of 8-Aminoquinolines under Mild Conditions. *Org. Biomol. Chem.* **2019**, *17*, 10245–10250.

11. Liu, S.; Yang, H.; Jiao, L. Y.; Zhang, J. H.; Zhao, C.; Ma, Y.; Yang, X. Regioselective Deoxygenative Chalcogenation of 7-Azindole: *N*-Oxides Promoted by I_2/PEG-200. *Org. Biomol. Chem.* **2019**, *17*, 10073–10087.

12. Iida, H.; Demizu, R.; Ohkado, R. Tandem Flavin-Iodine-Catalyzed Aerobic Oxidative Sulfenylation of Imidazo[1,2- *a*]Pyridines with Thiols. *J. Org. Chem.* **2018**, *83*, 12291–12296.

Chapter-6: Section-II

1. Pasquini, S.; Mugnaini, C.; Tintori, C.; Botta, M.; Trejos, A.; Arvela, K. R.; Larhed, M.; Witvrouw, M.; Michiels, M. ; Christ, F.; Debyser, Z.; and Corelli, F. Investigations on the 4-Quinolone-3-carboxylic Acid Motif. 1. Synthesis and Structure−Activity Relationship of a Class of Human Immunodeficiency Virus type 1 Integrase Inhibitors. *J. Med. Chem.* **2008**, *51*, 5125–5129.

2. (a) Mugesh, G.; Du Mont, W.; and Sies, H. Chemistry of Biologically Important Synthetic Organoselenium Compounds. *Chem. Rev.* **2001**, *101*, 2125–2179. (b) Perin, G.; Lenardão, J. E.;. Jacob, G. R.; Panatieri, B. R. Synthesis of Vinyl Selenides. *Chem. Rev.* **2009**, *109*, 1177–1301. (c) Rezanka, T.; Sigler, K. Biologically Active Compounds Of Semi-Metals. S*tud. Nat. Prod. Chem.* **2008**, *35*, 835–921. (d) Bellé, P. L.; Bitencourt, E. R. P.; Abdalla, H. F.; Guerra, B. R.; Funchal C.; Moretto, B. M. An *in vitro* Comparison of a New Vinyl Chalcogenide and Sodium Selenate on Adenosine Deaminase Activity of Human Leukocytes. *Chem. Biol. Interact.,* **2011**, *189*, 141–145.

3. (a) Fei, W.; Xu, P.; Hou, J. Yao, W. Phosphine Catalyzed [3+2] Cyclization/Michael Addition of Allenoate with CS_2 to form 2-Thineyl Vinyl Sulfide. *Chem. Commun.* **2020**, *56*, 11669–11672. (b) Tanini, D.; Scarpelli, S;. Ermini E.; Capperucci, A. Seleno-Michael Reaction of Stable Functionalised Alkyl Selenols: A Versatile Tool for the Synthesis of Acyclic and Cyclic Unsymmetrical Alkyl and Vinyl Selenides. *Adv. Synth. Catal.* **2019**, *361*, 2337–2346. (c) Tanini, D.; Ermini E.; Capperucci, A. Thio- and Seleno-Michael addition: An Efficient Tool for the Delivery of Sulfur and Selenium Functionalities. *Phosphorus, Sulfur Silicon Relat. Elem.* **2019**, *194*, 720–722. (d) Nacca, G. F.; Monti, B.; Lenardão, J. E.; Evans, P.; Santi, C. A Simple Zinc-Mediated Method for Selenium Addition to Michael Acceptors. *Molecules*, **2020**, *25***,** 2018. (e) Wan, P. J.; Zhong, S.; Xie, L.; Cao, X.; Liu, Y.; Wei, L. KIO_3-Catalyzed Aerobic Cross-Coupling Reactions of Enaminones and Thiophenols: Synthesis of Polyfunctionalized Alkenes by Metal-Free C–H Sulfenylation. *Org. Lett.* **2016**, *18*, 584–587.

4. (a) Lin, A. Y.; J. M. Chalker, M. J.; Davis, G. B. Olefin Cross-Metathesis on Proteins: Investigation of Allylic Chalcogen Effects and Guiding Principles in Metathesis Partner Selection. *J. Am. Chem. Soc.* **2010**, *132*, 16805–16811. (b) Lin, A. Y.; Davis, G. B. Olefin Cross-Metathesis on Proteins: Investigation of Allylic Chalcogen Effects and Guiding Principles in Metathesis Partner Selection. *Beilstein J. Org. Chem.* **2010**, *6*,

1219–1228.

5. (a) Trost, M. B.; Lavoie, C. A. Enol Thioethers as Enol Substitutes. An Alkylation Sequence *J. Am. Chem. Soc.* **1983**, 5075–5090. (b) Reich, J. H.; lora, C.; Shah, K. S. Selenium Stabilized Carbanions. Preparation of .Alpha.-Lithio Selenides and Applications to the Synthesis of Olefins by Reductive Elimination of .Beta.-Hydroxy Selenides and Selenoxide *syn* Elimination. *J. Am. Chem. Soc.* **1979**, *101*, 6638–6648.

6. N. Velasco, N.; Virumbrales, C.; Sanz, R.; Suárez-Pantiga, S.; M. A. Fernández-Rodríguez, A. M.; General Synthesis of Alkenyl Sulfides by Palladium-Catalyzed Thioetherification of Alkenyl Halides and Tosylates. *Org. Lett.* **2018**, *20*, 2848–2852.

7. (a) Liu, S. X.; Tang, Z.; Li, Z.; Li, M.; Xu, L.; Liu, L. Modular and Stereoselective Synthesis of Tetrasubstituted Vinyl Sulfides Leading to a Library of AIEgens. *Nat. Commun.* **2021**, *12*, 1–(b) Wang, W. B.; Jiang, K.; Li, X. J.; Luo, H. S.; Z. Y. Wang, Y. Z.; H. F. Jiang, F. H. 1,1-Diphenylvinylsulfide as a Functional AIEgen Derived from the Aggregation-Caused-Quenching Molecule 1,1-Diphenylethene through Simple Thioetherification. *Angew.Chem.Int.Ed*. **2020**, *59*, 2338–2343. (c) Biesen, L. ; Nirmalananthan-Budau, N.; Hoffmann, K.; Resch-Genger U.; T. J. J. Müller, J. J. T. Solid-State Emissive Aroyl-*S,N*-Ketene Acetals with Tunable Aggregation-Induced Emission Characteristics. *Angew.Chem.Int.Ed.* **2020**, *59*, 10037–10041.

8. (a) Ziegenbalg, N.; Elbinger, L.; Schubert, S. U.; Brendel, C. J. Polymers from *S*-vinyl Monomers: Reactivities and Properties**.** *Polym. Chem.* **2022**, 5019–5041. (b) Cho, G. C. B. A. Feit, A. B.; Webster, W. O. Cationic Polymerization of Isobutyl Vinyl Ether: Livingness Enhancement by Dialkyl Sulfides. *Macromolecules*, **1990**, *23*, 1918–1923. (c) Nakabayashi, K.; Abiko, Y.; Mori, H. RAFT Polymerization of S-Vinyl Sulfide Derivatives and Synthesis of Block Copolymers Having Two Distinct Optoelectronic Functionalities. *Macromolecules*, **2013**, *46*, 5998–6012. (d) Kosai, J.; Masuda, Y.; Chikayasu, Y.; Takahashi, Y.; Sasabe, H.; Chiba, T.; Kido, J.; Mori, H. *S*-Vinyl Sulfide-Derived Pendant-Type Sulfone/Phenoxazine-Based Polymers Exhibiting Thermally Activated Delayed Fluorescence: Synthesis and Photophysical Property Characterization. *ACS Appl. Polym. Mater*. **2020**, *2*, 3310–3318.

9. (a) Bassaco, M. M.; Monçalves, M.; Rinaldi, F.; T. S. Kaufman, S. T.; Silveira, C. C. Synthesis and Photophysical Characterization of Novel π-Conjugated Vinyl Sulfides. *J. Photochem. Photobiol. A Chem.* **2014**, *290*, 1–10. (b) Pötzsch, R.; Komber, H.; B. C.

Stahl, C. B.; Hawker, J. C.; Voit, I. B. Radical Thiol-yne Chemistry on Diphenylacetylene: Selective and Quantitative Addition Enabling the Synthesis of Hyperbranched Poly(vinyl sulfides). *Macromol. Rapid Commun.* **2013**, *34*, 1772–1778.

10. (a) Zyk, V. N.; Beloglazkina, K. E.; M. A. Belova, A. M.; N. S. Dubinina, S. N. Methods for the Synthesis of Vinyl Sulfides. *Russ. Chem. Rev.* **2003**, *72*, 864–884. (b) Ledovskaya, S. M.; Voronin, V. V.; K. S. Rodygin, S. K. Methods for the synthesis of O-, S- and N-vinyl derivatives. *Russ. Chem. Rev.* **2018**, *87*, 167–191. (c) Y. Fang, Y.; Luo, Z.; Xu, X. Recent Advances in the Synthesis of Vinyl Sulfones. *RSC Adv.* **2016**, *6*, 59661–59676.

11. (a) Hellwig, S. P.; Goulart, A. H.; Abenante, L.; Lenardao J. Perin, G. Synthesis of Vinyl Selenides and Tellurides: An Updated Review. *Russ. Chem. Rev.* **2022**, *91*, 1–34 (b) Braverman, S.; Cherkinsky, M.; Kalendar, Y.; Jana, R.; Sprecher, M.; Goldberg, I. Synthesis of Water-Soluble Vinyl Selenides and Their High Glutathione Peroxidase (GPx)-Like Antioxidant Activity. *Synthesis* **2014**, *46*, 119–125. (c) Palomba, M.; Coelho Dias, F. I.; Rosati O.; and Marini, F. Modern Synthetic Strategies with Organoselenium Reagents: A Focus on Vinyl Selenones. *Molecules*, **2021**, *26*, 3148.

12. (a) (b) Chang, D.; Bao, W. Stereoselective Synthesis of Vinyl Selenides by Coupling of Vinyl Bromides with Diorgano Diselenides Catalyzed by Copper(I) in [Bmim]BF_4. *Synlett*, **2006**, 1786–1788. (c) Bates, G. C.; Saejueng, P.; Doherty Q. M.;. Venkataraman, D. Copper-Catalyzed Synthesis of Vinyl Sulfides. *Org. Lett.* **2004**, *6*, 5005–5008. (d) Sartori, G.; Neto, S. S. J.; Pesarico, P.A.; Back, F. D.; Nogueira, W. C.; Zeni, G. Bis-vinyl Selenides Obtained *via* Iron(III) Catalyzed Addition of PhSeSePh to Alkynes: Synthesis and Antinociceptive Activity. *Org. Biomol. Chem.* **2013**, *11*, 1199–1208 and references cited therein. (j) (e) Kundu, D.; Mukherjee, N.; Ranu, B. C. A General and Green Procedure for the Synthesis of Organochalcogenides by $CuFe_2O_4$ Nanoparticle Catalysed Coupling of Organoboronic Acids and Dichalcogenides in PEG-400. *RSC Adv.* **2013**, *3*, 117–125. (f) Saha, A.; Saha, D.; Ranu, C. B. Copper Nano-catalyst: Sustainable Phenyl-selenylation of Aryl Iodides and Vinyl Bromides in Water under Ligand free Conditions. *Org. Biomol. Chem.* **2009**, *7*, 1652–1657. (g). Gonçalves, C. C. L.; Lima, B. D.; Borba, Y. M. P.; G. Perin, G.; Alves, D.; Jacob, G. R.; Lenardão, J. E. Glycerol/CuI/Zn as a Recyclable Catalytic System for Synthesis of Vinyl Sulfides and Tellurides. *Tetrahedron Lett.* **2013**, *54*, 3475–3480. (h) Gonalves, C. L.; Fiss, F.

G.; Perin, G.; D. Alves, D.; Jacob, G. R.; Lenardão, J. E.. Glycerol as a Promoting Medium for Cross-coupling Reactions of Diaryl Diselenides with Vinyl Bromides. *Tetrahedron Lett.* **2010**, *51*, 6772–6775 and references cited therein.

13. (a) Wang, D. Peng, Y. H.; M. M. Yang, M. M.; Hao, J. E. Y. S. Li, S. Y.; Dong, B. Z. Cs_2CO_3-Promoted Hydrothiolation of Alkynes with Aryl Thioureas: Stereoselective Synthesis of (Z)-Vinyl Sulfides. *J. Org. Chem.* **2021**, *86*, 8457–8464 and references cited therein. (b) Weiss, J. C.; Wobser, D. S.; Marks, J. T. Organoactinide-Mediated Hydrothiolation of Terminal Alkynes with Aliphatic, Aromatic, and Benzylic Thiols. *J. Am. Chem. Soc.* **2009**, *131*, 2062–2063. (c) Di Giuseppe, A.;. Castarlenas, R; Pérez-Torrente, J. J.; Crucianelli, M.; Polo, V. Sancho, R.; Lahoz, J. F.; Oro, A. L. Ligand-Controlled Regioselectivity in the Hydrothiolation of Alkynes by Rhodium N-Heterocyclic Carbene Catalysts. *J. Am. Chem. Soc.* **2012**, *134*, 8171–8183. (d) Ikeda, T.; Tamai, T. ; Daitou, M. Minamida, Y.; Mitamura, T.; Kusano, H.; Nomoto, A.;. Ogawa, A. Highly Regioselective Palladium-catalyzed Double Hydroselenation of Terminal Alkynes with Benzeneselenol in the Presence of Acetic Acid. *Chem. Lett.* **2013**, *42*, 1383–1385. (e) Ozaki, T.; Kotani, M.; Kusano, H.; Nomoto, A.; Ogawa, A. Highly Regioselective Hydroselenation and Double-bond Isomerization of Terminal Alkynes with Benzeneselenol Catalyzed by Bis(triphenylphosphine)palladium(II) Dichloride. *J. Organomet. Chem.* **2011**, *696*, 450–455. (f) Santi, C.;. Battistelli, B.; Testaferri, L.; M. Tiecco, M. On Water Preparation of Phenylselenoesters. *Green Chem.* **2012**, *14*, 1277–1280. (g) S. I. Kawaguchi, I. S.; Kotani, M.; Atobe, S.; Nomoto, A.; Sonoda, M.; Ogawa, A. Rhodium-Catalyzed Highly Stereoselective Hydroselenation of Internal Alkynes Bearing an Electron-withdrawing Group. *Organometallics*, **2011**, *30*, 6766–6769.

14. (a) Ni, S.; Zhang, L.; Zhang, W.; Mei, H.; Han, J.; Pan, Y.; Synthesis of Trisubstituted Vinyl Sulfides via Oxidative Thiolation Initiated Cascade Reaction of Alkynoates with Thiols. *J. Org. Chem.* **2016**, *81*, 9470–9475. (b) Xinming, X.; Jiazhua, L.; Zuli, W. Recent Advances in Transition Metal-Free Sulfenylation of Indoles. *Chin. J. Org. Chem.* **2020**, *40*, 886-898. (c) Xinming, X.; Hanlina, Y.; Wenzhong, L. Transition Metal-Free Direct C—H Bond Sulfenylation of Alkenes and Arenes. *Chin. J. Org. Chem.* **2020**, *40*, 1912-1925 and references cited therein. (d) Saikia, B. S.; Borpatra, P. J.; Rahman, I.; Deb, M. L.; Baruah, P. K. Visible-light-promoted Sulfenylation of 6-Aminouracils under Catalyst-free Conditions. *New J. Chem.* **2022**, *46*, 16523–16529. (e) Saroha, M.;

Sindhu, J.; Kumar, S.; Bhasin, K. K.; Khurana, J. M.; Varma, R. S.; Tomar, D. *ChemistrySelect* **2021**, *6*, 13077-13208 and references cited therein.

15. (a) Verdegem, E. J. P.; Monnee, F. C. M.; Lugtenburg, J. Simple and Efficient Preparation of [10,20-13C2]- and [10-CH3,13-13C2]-10-Methylretinal: Introduction of Substituents at the 2-Position of 2,3-Unsaturated Nitriles. *J. Org. Chem.* **2001**, *66*, 1269–1282. (b) Brandsma, L.; Verkruijsse, D. H.; Schade, C.; Schleyer, R. V. P. The First Successful Direct Metallation of Ethene. *J. Chem. Soc. Chem. Commun.* **1986**, 260–261.

16. Yang, L.; Wen, Q.; Xiao, F.; Deng, J. G. Silver-mediated Oxidative Vinylic C–H Bond Sulfenylation of Enamides with Disulfides. *Org. Biomol. Chem.* **2014**, *12*, 9519–9523.

17. Liu, C.; Fang, Y.; Wang, Y. S.; Ji, J. S. Highly Regioselective Rh^{III}-Catalyzed Thiolation of N-Tosyl Acrylamides: General Access to (Z)-β-Alkenyl Sulfides. *Org. Lett.* **2018**, *20*, 6112–6116.

18. Tu, Y. H.; Hu, L. B.; Deng, L. C.; Zhang, G. X. Copper-mediated Stereospecific C–H Oxidative Sulfenylation of Terminal Alkenes with Disulfides. *Chem. Commun.* **2015**, *51*, 15558–15561.

19. Liu, S.; Wang, L.; Ma, Z.; X. Zeng, X.; Xu, B. Pyridine Hydrochloride-catalyzed Thiolation of Alkenes: Divergent Synthesis of Allyl and Vinyl Sulfides. *Org. Chem. Front.* **2020**, *7*, 3474–3479.

20. Yang, F. Y.; Li, Y. C.; Leng, T.; Huang, B. X.; Gao, X. W.; Y. B. Zhou, B. Y.; Liu, C. M.; and H. Y. Wu, Y. H. Cu-Catalyzed Radical Selenylation of Olefin: A Direct Access to Vinyl Selenides. *Adv. Synth. Catal.* **2020**, *362*, 2168–2172.

Chapter-6: Section-III

1. (a) Mukherjee, N.; Chatterjee, T. Iodine-Catalyzed Methylthiolative Annulation of 2-Alkynyl Biaryls with DMSO: A Metal-Free Approach to 9-Sulfenylphenanthrenes. *J. Org. Chem.* **2021**, *86*, 7881–7890. (b) Mukherjee, N.; Chatterjee, T. Iodine-catalyzed, Highly Atom-economic Synthesis of 9-Sulfenylphenanthrenes and Polycyclic Heteroaromatics in Water. *Green Chem.* **2021**, *23*, 10006–10013. (c) Mukherjee, N.;

Satyanarayana, A. N. V.; Singh, P.; Dixit M.; Chatterjee, T.; *Green Chem.* **2022**, 24, 7029-7038 (d) Satyanarayana, A. N. V.; Mukherjee N.; Chatterjee, T. Recyclable Iodine-catalyzed Radical Selenylative Annulation of 2-Alkynyl Biaryls with Diselenides in Water: A Green Approach to Selanyl Polycyclic Aromatic Hydrocarbons and Polycyclic Hheteroaromatics. *Green Chem.* **2023**, *25*, 779–788.

2. Wang, W. B.; Jiang, K.; Li, X. J.; Luo, H. S.; Z. Y. Wang, Y. Z.; H. F. Jiang, F. H. 1,1-Diphenylvinylsulfide as a Functional AIEgen Derived from the Aggregation-Caused-Quenching Molecule 1,1-Diphenylethene through Simple Thioetherification. *Angew. Chemie - Int. Ed*. **2020**, *59*, 2338–2343.

3. (a) Van Aken, K.; Strekowski, L.; Patiny, L. EcoScale, a Semi-Quantitative Tool to Select an Organic Preparation Based on Economical and Ecological Parameters. *Beilstein J. Org. Chem.* **2006**, *2*, 1–7. (b) Constable, D. J. C.; Curzons, A. D.; Cunningham, V. L. Metrics to "green" Chemistry - Which Are the Best? *Green Chem.* **2002**, *4*, 521–527. (c) Tobiszewski, M.; Marć, M.; Gałuszka, A.; Namieśnik, J. Green Chemistry Metrics with Special Reference to Green Analytical Chemistry. *Molecules* **2015**, *20*, 10928–10946.

4. Keri, S. R.; Chand, K.; Budagumpi, S.; Somappa, B. S.; Patil, S. A.; Nagaraja, M. B. An Overview of Benzo[*b*]thiophene-based Medicinal Chemistry. *Eur. J. Med. Chem.* **2017**, *138*, 1002–1033.

5. Tobisu, M.; Masuya, Y.; Baba, K.; Chatani, N. Palladium(ii)-catalyzed Synthesis of Dibenzothiophene Derivatives *via* the Cleavage of Carbon–sulfur and Carbon–Hydrogen Bonds**.** *Chem. Sci.* **2016**, *7*, 2587–2591.

6. Monga, A.; Bagchi, S.; Sharma, A. Iodine/DMSO oxidations: A Contemporary Paradigm in C–N bond Chemistry. *New J. Chem.* **2018**, *42*, 1551.

7. Yang, F. Y.; Li, Y. C.; Leng, T. ; Huang, B. X.; Gao, X. W.; Zhou, B. Y.; Liu, C. M.;.

   Wu, Y. H.; Cu-Catalyzed Radical Selenylation of Olefin: A Direct Access to Vinyl Selenides. *Adv. Synth. Catal*., **2020**, *362*, 2168–2172.

8. Sun, N.; Zheng, K.; Zhang, M.; Zheng, G.; Jin, L.; Hu, B.; Shen, Z.; Hu, X. Cu-Catalysed Chan–Lam Synthesis of Unsymmetrical Aryl Chalcogenides under Aqueous Micellar Conditions. *Green Chem.* **2023**, 25, 2782–2789.

9. Carey, A. F.; Hernanj, O. Silicon-containing carbanions. III. Synthesis of Vinyl Sulfoxides *via* 1-Trimethylsilyl-1-(phenylsulfinyl)methyllithium. *J. Org. Chem.* **1973**, 58, 2670–2675.

10. Zhang, G.; Fu, G. J.; Zhao, Q.; Zhang, S. G.; Li, Y. M.; Feng, G. C.; Lin, Q. G. Silver-Promoted Synthesis of Vinyl Sulfones from Vinyl Bromides and Sulfonyl Hydrazides in Water. *Chem. Commun.*, **2020**, *56***,** 4688.

11. Sang, R.; Noble, A.; Aggarwal, K. V. Chiral Benzothiophene Synthesis *via* Enantiospecific Coupling of Benzothiophene S-Oxides with Boronic Esters. *Angew. Chem. Int. Ed.* **2021**, *60*, 25313-25317.

12. Yang, M.; Hua, J.; Wang H.; Ma, T.; Liu, C.; He, W.; Zhu, N.; Hu, Y.; Fang, Z.; Guo, K. Photomediated Spirocyclization of *N*-Benzyl Propiolamide with *N*-Iodosuccinimide for Access to Azaspiro[*4.5*]deca-6,9-diene-3,8-dione. *J. Org. Chem.* **2022**, *87*, 8445–8457.

List of Publications

1. **Nilanjana Mukherjee** and Tanmay Chatterjee,* Iodine-Catalyzed Methylthiolative Annulation of 2-Alkynyl Biaryls with DMSO: A Metal-Free Approach to 9-Sulfenylphenanthrenes, *J. Org. Chem.* **2021**, *86*, 7881 - 7890.

2. **Nilanjana Mukherjee** and Tanmay Chatterjee**,*** Iodine-catalyzed, highly atom-economic synthesis of 9-sulfenylphenanthrenes and polycyclic heteroaromatics in water, *Green Chem.* **2021**, 23, 10006-10013.

3. Tanmay Chatterjee* and **Nilanjana Mukherjee**, Transition-Metal-Free Synthetic Strategies for the Cross-Coupling Reactions in Water: A Green Approach, *Curr. Green Chem*. **2021**, *8*, 70-91.

4. **Nilanjana Mukherjee**, Appanapalli N. V. Satyanarayana, Priti Singh, Mudit Dixit, and Tanmay Chatterjee**,*** Recyclable iodine-catalyzed radical selenylative annulation of 2-alkynyl biaryls with diselenides in water: A green approach to selanyl polycyclic aromatic hydrocarbons and polycyclic heteroaromatics, Green *Chem.* **2022**, 24, 7029-7038.

5. Appanapalli N. V. Satyanarayana, **Nilanjana Mukherjee** and Tanmay Chatterjee,* 100% Atom-economical and highly regio- and stereoselective iodosulfenylation of alkynes: A reagentless and sustainable approach to access (*E*)-β-iodoalkenyl sulfides and (Z)-tamoxifen, *Green Chem.* **2023**, 25, 779-788.

6. Tanmay Chatterjee**,*** Paramita Pattanayak, Appanapalli N. V. Satyanarayana and **Nilanjana Mukherjee**, Recent advances in developing highly atom-economic C-H annulation reactions in water, *Curr. Opin. Green Sustain. Chem.* **2023**, *41*, 100826.

7. **Nilanjana Mukherjee** and Tanmay Chatterjee,* Highly Atom-Economic and Efficient Electrochemical Selenylative Annulation of 2-Alkynyl Biaryls, *Adv. Synth. Catal*. **2023**, 365, 2255-2265.

8. **Nilanjana Mukherjee** and Tanmay Chatterjee,* Recyclable Iodine-catalyzed Oxidative C-H Chalcogenation of 1,1-Diarylethenes in Water: Green Synthesis of Trisubstituted Vinyl Sulfides and Selenides. *Green Chem*. **2023**, 10.1039/D3GC02999A**.**

9. Shalini Dyagala, Sayantan Halder, **Nilanjana Mukherjee**, Shamik Chakravorty, Dr. S. Murugesan, Tanmay Chatterjee and Subit Kumar Saha, Exploration of methyl(10-phenylphenanthren-9-yl)sulfane (MPPS) as an Efficient Fluorescent Probe to Study Self-assembly of Surfactants and Protein-surfactants Interactions. (Manuscript under Preparation).

List of National/International Conferences

1. **Nilanjana Mukherjee** and Tanmay Chatterjee,* Iodine Catalyzed Methylthiolative Annulation of 2-Alkynylbiaryls with DMSO: A Sustainable Approach to 9-Sulfenylphenanthrenes - Green Technologies for Sustainable Development (GTSD - 21), A Virtual International Conference Organized by Dharmsinh Desai University (DDU), Nadiad, Gujrat, India; March 9^{th} –11^{th}, 2021 (**Oral Presentation**)

2. **Nilanjana Mukherjee** and Tanmay Chatterjee,* Iodine Catalyzed, Highly Atom-Economic and Green Synthesis of 9-Sulfenylphenanthrenes and Polycyclic Heteroaromatics in Water - 27th International Conference of International Academy of Physical Sciences (CONIAPS XXVII) on Recent Advances in Catalysis Science & Engineering (RACSE), October 26^{th} – 28^{th}, 2021 (**Poster Presentation**)

3. **Nilanjana Mukherjee**, Appanapalli N. V. Satyanarayana, Priti Singh, Mudit Dixit, and Tanmay Chatterjee,* Iodine-catalyzed Selanylative Annulation of 2-Alkynyl Biaryls in Water to Access 9-Selanylphenanthrenes and Polycyclic Heteroaromatics-National Conference on Organic Chemistry NITT Organic Chemistry Conference'21 conducted from December 16^{th}–18^{th}, 2021 (**Oral Presentation**)

4. **Nilanjana Mukherjee** and Tanmay Chatterjee,* Iodine-catalyzed Thiolative Annulation of 2-Alkynyl Biaryls in Water to Access 9-Sulfenylphenanthrenes and Polycyclic Heteroaromatics-XVII JNOST Conference for Research Scholars, January 6^{th}–9^{th}, 2022, School of Chemistry, UoH (**Oral Presentation**)

5. **Nilanjana Mukherjee** and Tanmay Chatterjee,* Reagentless, Highly Atom-Economic and Efficient Selenylative Annulation of 2-Alkynyl Biaryls under Electrochemical Conditions, 2^{nd} National Conference on "Contemporary Facets in Organic Synthesis Conference (CFOS-2022)", December 1^{st} – 4^{th}, 2022, IIT Roorkee, India (**Poster Presentation**)

6. **Nilanjana Mukherjee** and Tanmay Chatterjee,* Reagentless, Highly Atom-Economic and Efficient Selenylative Annulation of 2-Alkynyl Biaryls under Electrochemical

Conditions National Symposium on ” Convergence of Chemistry and Materials (CCM-2023)”, January 6th–7th, 2023, BITS-Pilani, Hyderabad Campus (**Poster Presentation**)

7. **Nilanjana Mukherjee** and Tanmay Chatterjee,* Recyclable Iodine-catalyzed Oxidative C-H Chalcogenation of 1,1-Diarylethenes in Water: Green Synthesis of Trisubstituted Vinyl Sulfides and Selenides, International Conference on Recent Advances on Green and sustainable Developments (ICRAGSD 2023), September 6th–8th, 2023 (**Oral Presentation**)

Brief Bibliography of the Candidate

Mrs. Nilanjana Mukherjee

Research Scholar,

Department of Chemistry, BITS Pilani, Hyderabad Campus

Hyderabad, Telengana-500078, India

Mrs. N. Mukherjee obtained her M.Sc. degree in Organic Chemistry in 2018, from the Behala College (University of Calcutta), India. She worked as a project fellow in a project entitled as "Transition Metal Free Base Mediated C-Se Bond Formation at Room Temperature" under Prof. Brindaban C. Ranu at Indian Association for the Cultivation of Science (IACS), Kolkata. She joined the Ph.D. program of the Birla Institute of Technology & Science (BITS) Pilani, Hyderabad Campus at the Department of Chemistry, in January 2019 under the supervision of Dr. Tanmay Chatterjee. To Date, she has published seven papers in peer-reviewed international journals and has attended various international/national conferences and has also been awarded for best poster award in RSC-CFOS-2022, in IIT Roorkee.

Email id: p20180411@hyderabad.bits-pilani.ac.in

Brief Bibliography of the Supervisor

Dr. Tanmay Chattrerjee

Assisstant Professor

Department of Chemistry, BITS-Pilani, Hyderabad Campus

Hyderabad, Telangana-500078, India

Dr. Tanmay Chatterjee received M.Sc. degree in Chemistry from Indian Institute of Technology, Delhi in 2009. He obtained a Ph.D. degree in 2014 for his work on the "Green Synthesis using Benign Solvents, Reagents and Catalysts" under the supervision of Prof. Brindaban C. Ranu at Indian Association for the Cultivation of Science (IACS), Kolkata. Then he moved to South Korea and worked with Prof. E. J. Cho on visible-light photocatalysis during 2014−2017 at Hanyang University as a postdoctoral fellow and at Chung-Ang University as a research professor, respectively. He returned to India and started his independent career in 2018 as an Assistant Professor at Birla Institute of Technology and Science, Pilani (BITS-Pilani), Hyderabad campus. His research interest mainly lies on the development of metal-free, highly atom-economic and green synthetic methodologies under iodine-catalysis and electrochemical conditions and also metal-free, trifluoromethylation reactions for the synthesis of new classes of potential organic molecules. So far, Dr. Chatterjee has authored/co-authored 42 research papers published in various reputed international journals, 2 book chapters, and also published 2 patents which fetched 1860 citations with an H-index of 22. He successfully completed one major research project, sponsored by Chanceux Labs LLP, Hyderabad (Industry Project), and another project, sponsored by the Council of Scientific and Industrial Research (CSIR), Govt. of India, is currently underway. He is an editorial board member of an international journal, Current Green Chemistry (Impact Factor: 2.2) of Bentham Science Publishers. He is also serving as a reviewer of many reputed international journals. Currently, he is guiding five Ph.D. students. He received the "Best Researcher Award" in the International Scientist Awards on Engineering, Science, and Medicine, held on 12th November, 2021 in Chennai, India, organized by VDGOOD Professional Association.

Email id: tanmay@hyderabad.bits-pilani.ac.in